



THE UNIVERSITY OF QUEENSLAND
AUSTRALIA

Paleoenvironmental Evolution of Continental Landscapes Through Combined High-Resolution Geochronology and $\delta^{18}\text{O}$ Ion Microprobe Analysis of Goethite

Hevelyn da Silva Monteiro

B.Sc, M.Sc

A thesis submitted for the degree of Doctor of Philosophy at

The University of Queensland in 2017

School of Earth and Environmental Sciences

ABSTRACT

Goethite (α -FeOOH), the most common product of weathering of Fe-bearing minerals, is an attractive target for (U-Th)/He geochronology because of its abundance and relative stability in the surficial environment. Combined (U-Th)/He- $^4\text{He}/^3\text{He}$ geochronology of 24 goethite samples representative of different source rocks, precipitation mechanisms, solid-solution compositions, purity, and porosity provides information on the influence of these factors on U-Th-He contents, distribution, and retentivity in natural goethites. Measured activation energies (E) for He diffusion from goethites range from 11.2 ± 0.5 to 74.5 ± 3.2 kcal.mol $^{-1}$, with an average value at 36.2 ± 13.5 (1σ) kcal.mol $^{-1}$; and frequency factors ($\ln D_0/r_0^2$) range from -4.1 ± 0.5 to 62.8 ± 1.9 s $^{-1}$, with an average value of 24.1 ± 13 (1σ) s $^{-1}$. The average activation energy of ~ 35 kcal.mol $^{-1}$ indicates that He retentivity in goethite is comparable to other phases dated by the (U-Th)/He method. A major distinction between goethite and other phases used in (U-Th)/He geochronology is its large frequency factor, a possible consequence of the fact that supergene goethite is composed of masses of cryptocrystalline aggregates and not single crystals.

Armed with an improved understanding of goethite's He retentivity, and its suitability to (U-Th)/He and cosmogenic ^3He analyses, two field sites were investigated in detail to unravel the history of mineral precipitation, exhumation and erosion that created the characteristic plateau landscapes at the Quadrilátero Ferrífero and Carajás, Brazil. (U-Th)/He geochronology of goethite and cosmogenic ^3He in goethite and hematite reveal mineral precipitation ages as old as 55 Ma and apparent exposure ages > 5 Ma for canga-cemented plateaus at the Quadrilátero Ferrífero. Pebbles of hypogene hematite-magnetite from colluvia or shallow creeks draining the canga-cemented plateaus record a much longer exposure history than *in situ* canga blocks, showing that even older duricrusts, now eroded, once blanketed these plateaus. The long-term erosion history obtained from cosmogenic ^3He on BIF plateaus confirms that relic surfaces persist in the landscape for millions of years. Combined ^3He and (U-Th)/He dating shows that cangas are preferentially goethite cemented by biogeochemical reactions in the subsurface. Physically stable but biogeochemically dynamic, cangas armor the landscape by pervasive and recurrent iron cycling and cementation, slowing erosion of weathered BIF and friable hematite-magnetite ore. At Carajás, (U-Th)/He geochronology reveals a longer history of weathering, spanning from ca. 80 Ma to the present. Cosmogenic ^3He measurements for hematite blocks cemented onto the plateaus yield apparent exposure ages > 7 Ma and erosion rates as low as 0.08 m.Ma $^{-1}$, confirming that plateau surfaces are virtually immune to physical erosion for tens of millions of years. In contrast, (U-Th)/He geochronology of ferruginous duricrusts blanketing low elevation (250-100 m) plains surrounding the Carajás plateaus reveal that the low elevation plain is diachronous and range from ~ 10 Ma away from the plateau to ~ 1 Ma

next to it, having evolved by scarp retreat. The virtual cessation of scarp retreat at some sites suggests that metamorphosed banded iron-formations provide effective barriers to retreating escarpments, helping to preserve some of the oldest continuously exposed landsurfaces on Earth.

To derive paleoenvironmental information about these landsurfaces, new protocols were developed for high-spatial resolution $\delta^{18}\text{O}$ analysis of goethite with the Sensitive High Mass Resolution Ion Microprobe – Stable Isotopes (SHRIMP-SI). A natural sample from the Capão Mine, Minas Gerais, Brazil, was extensively characterized and now provides a working goethite reference material (RM) for ion microprobe analyses. A laser fluorination value of $-17.22 \pm 0.03 \text{ ‰}$ (1σ) was obtained for an aliquot of this RM. The repeatability of SHRIMP-SI measurements of the Capão L4 RM was often better than 1.5‰ (2σ). Using Capão L4 as a RM, several natural goethite samples were analysed to test the relationship between natural properties, preparation procedures, instrument conditions, and the overall reliability of the $\delta^{18}\text{O}_{\text{SIMS}}$ results.

Finally, combined laser-heating (U-Th)/He geochronology, SHRIMP-SI $\delta^{18}\text{O}$ measurements ($\delta^{18}\text{O}_{\text{SIMS-gth}}$), and electron microprobe analysis of goethites from the Quadrilátero Ferrífero and Carajás sites produced two extensive Cenozoic paleoclimatic records for the continental interior of Brazil, spanning from $\sim 70 \text{ Ma}$ to 900 ka at Carajás and from $\sim 40 \text{ Ma}$ to 600 ka at the QF. The results identify major climatic shifts in continental Brazil, compatible with global climatic changes observed in the $\delta^{18}\text{O}$ record of oceanic sediments. Periods of optimum climatic conditions (Early to Mid-Eocene, Late Oligocene, and Mid-Miocene) correspond to more frequent precipitation of weathering minerals, stoichiometrically pure goethites, and $\delta^{18}\text{O}_{\text{SIMS-gth}}$ shifts towards lighter isotopic values. These shifts are consistent with warm monsoonal conditions in the continental interior. Abrupt shifts in the $\delta^{18}\text{O}_{\text{SIMS-gth}}$ record towards more positive values occur during global glaciation (Oi-1 and Mi-1 glaciations), periods that also correspond to less frequent precipitation of Al-rich goethites suggestive of dryer continental environments. The combined goethite (U-Th)/He– $\delta^{18}\text{O}_{\text{SIMS-gth}}$ record provides a robust new way of investigating continental paleoclimates on Earth.

DECLARATION BY AUTHOR

This thesis is composed of my original work, and contains no material previously published or written by another person except where due reference has been made in the text. I have clearly stated the contribution by others to jointly-authored works that I have included in my thesis.

I have clearly stated the contribution of others to my thesis as a whole, including statistical assistance, survey design, data analysis, significant technical procedures, professional editorial advice, and any other original research work used or reported in my thesis. The content of my thesis is the result of work I have carried out since the commencement of my research higher degree candidature and does not include a substantial part of work that has been submitted to qualify for the award of any other degree or diploma in any university or other tertiary institution. I have clearly stated which parts of my thesis, if any, have been submitted to qualify for another award.

I acknowledge that an electronic copy of my thesis must be lodged with the University Library and, subject to the policy and procedures of The University of Queensland, the thesis be made available for research and study in accordance with the Copyright Act 1968 unless a period of embargo has been approved by the Dean of the Graduate School.

I acknowledge that copyright of all material contained in my thesis resides with the copyright holder(s) of that material. Where appropriate I have obtained copyright permission from the copyright holder to reproduce material in this thesis.

PUBLICATIONS DURING CANDIDATURE

Peer-Reviewed papers

Vasconcelos P. M., Heim J. A., Farley K. A., **Monteiro H. S.**, Waltenberg K. (2013) $^{40}\text{Ar}/^{39}\text{Ar}$ and (U-Th)/He - $^4\text{He}/^3\text{He}$ geochronology of landscape evolution and channel iron deposit genesis at Lynn Peak, Western, Australia. *Geochimica et Cosmochimica Acta* **117**, 283-312.

Monteiro, H. S., Vasconcelos, P. M. P., Farley, K. A., Spier, C. A., and Mello, C. L. (2014), (U-Th)/He geochronology of goethite and the origin and evolution of cangas, *Geochimica et Cosmochimica Acta*, **131**, 267-289.

Conference Abstracts

Gagen E., **Monteiro H.S.**, Tyson G., Vasconcelos P.M., and Southam G. (2014), Biogeochemical cycling of iron in canga ecosystems. *Australian Earth Sciences Convention*, Newcastle, NSW, 04RE-PO8, p. 315.

Monteiro, H. S., Vasconcelos, Ireland, T.P. M. P., Farley, K. A., Avila, J., Miller, H., Eiler, J., and Southam, G. (2015), SHRIMP-SI ($^{18}\text{O}/^{16}\text{O}$) analyses of goethite: Technical aspects and applications to paleoenvironmental studies. 25th *Goldschmidt Conference*, Prague, Czech Republic, p. 665.

Vasconcelos P.M., **Monteiro H.S.**, Ireland T., Farley, K.A., Avila J., and Holden P. (2015) Super Light Rain in Supercontinents. 25th *Goldschmidt Conference*, Prague, Czech Republic, p. 3246.

PUBLICATIONS INCLUDED IN THIS THESIS

No publications included.

CONTRIBUTIONS BY OTHERS TO THE THESIS

Prof. Paulo Vasconcelos provided financial support and assistance during fieldwork, gave me access to all drill-core samples from the Igarapé Bahia profile used in this thesis, and helped to design most of the experimental work accomplished in this project. This thesis greatly benefits from his intellectual insights and assistance during the writing of the manuscripts.

Prof. Kenneth Farley helped me carry out the $4\text{He}/3\text{He}$ diffusion experiments and cosmogenic 3He measurements. This thesis greatly benefits from his intellectual input, proofreading, and editing of manuscripts.

Dr. Albert Mostert patiently guided me (step-by-step) in the laboratory during my goethite precipitation experiments and instructed me on Rietveld refinement of goethites.

Dr. Kathryn Waltenberg carried some of the diffusion experiments presented in Chapter 2.

Dr. Janaína Ávila kindly analysed a batch of my goethite samples in the SHRIMP-SI (Run 4). Dr. Janaína Ávila and Dr. Peter Holden always provided invaluable assistance during my visits to the SHRIMP laboratory at ANU.

Hayden Miller carried laser fluorination analysis of all goethite reference material candidates investigated in this project.

STATEMENT OF PARTS OF THE THESIS SUBMITTED TO QUALIFY FOR THE AWARD OF ANOTHER DEGREE

None.

ACKNOWLEDGEMENTS

First, I must thank Prof. Paulo Vasconcelos for his dedication and creativity, encouragement, generosity, intellectual support and friendship throughout this undertaking. I am immensely grateful to you for the scientific opportunity and intellectual stimulation.

I would like to thank Prof. Ken Farley for the great opportunity to work in his laboratory. Without his patience and guidance, I'd not have been able to complete this work.

I also want to thank some very special collaborators for helping me in different aspects of this work: Ying Yu, Kim Sewell, and Ron Rash (Microscopy and Microanalysis); Colm Cahill and Cheryl Berquist (for promptly attending my requests to use the freeze-dryer and TGA); Anya Yago (XRD); Kim Baublys (for helping me with stable isotope analysis of my synthesis experiment solutions); Lindsey Hedges (for all your assistance with preparation of solutions for ICP-MS analysis and for taking me out for dinner during my visits to Caltech and for been such a wonderful person); Florian Hofmann (for doing ICP-MS analysis of goethite solutions I left behind); Gang Xia and Feliz Farrajota (for always saying *yes* to my last minute requests of sample preparation in the rock lab.); Dave Perkins and Alan Reid (to help with everything related to mechanical services); and David Thiede (for always attending my requests to buy supplies for the Argon laboratory).

Thanks to Pamela Cooper, Ashleigh Paroz, Tracy Paroz, Sue Hine, and Indira Jones for your dedication and hard work to make the School of Earth Sciences such a wonderful place for us.

I would like to thank friends and colleagues that supported me throughout my time at UQ. I want to say a special *thank you* to the Argon lab group: Tracey, Helen, Albert, Llyam, and Kristy. Also, I greatly appreciate Nicole's help with the formatting of Chapters 2 and 4 of this thesis.

I acknowledge the financial support of the Australian Research Council (ARC), the Brazilian Research Council (CNPq), and The University of Queensland - Argon Geochronology in Earth Sciences Laboratory.

Finally, I want to express my true gratitude to my family. Thanks, Mum (for your love and prayers for good health) and Dad (for your unconditional love), my sister Herica (for all words of wisdom and for sharing so many family photos), my brother Raphael, my sister Paula, and my precious treasures, Raphaela and João Guilherme. I also want to thank my aunt Meri for sharing her love via WhatsApp messages. I love you all.

Keywords

Goethite, (U-Th)/He geochronology, cosmogenic ^3He , SHRIMP-SI, paleoclimate, Quadrilátero Ferrífero, Carajás

Australian and New Zealand Standard Research Classifications (ANZSRC)

ANZSRC code: 040303, Geochronology, 50%

ANZSRC code: 040203, Isotope Geochemistry, 30%

ANZSRC code: 040605, Paleoclimatology, 20%

Fields of Research (FoR) Classification

FoR code: 0403, Geology, 40%

FoR code: 0402, Geochemistry, 30%

FoR code: 0406, Physical Geography and Environmental Geoscience, 30%

TABLE OF CONTENTS

Chapter 1: Thesis Structure and Introduction

1. THESIS STRUCTURE.....	1
2. INTRODUCTION.....	1
2.1. THE MINERALOGY-CRYSTALLOGRAPHY OF GOETHITE.....	4
2.2. THE COMBINED (U-TH)/HE - $^4\text{He}/^3\text{He}$ METHOD APPLIED TO GOETHITE.....	5
2.3. COSMOGENIC ^3He ACCUMULATION IN GOETHITE-HEMATITE.....	7
2.4. THE $\delta^{18}\text{O}$ RECORD OF GOETHITE.....	8
2.5. THE SENSITIVE HIGH RESOLUTION ION MICROPROBE FOR THE STABLE ISOTOPE ANALYSIS OF GOETHITE.....	10
REFERENCES.....	11

Chapter 2: On Goethite as a (U-Th)/He- $^4\text{He}/^3\text{He}$ Geochronometer..... 16

ABSTRACT.....	17
1. INTRODUCTION.....	18
1.1. Modes of Precipitation of Natural Goethites.....	20
2. SAMPLES INVESTIGATED.....	21
3. METHODS.....	26
3.1. Microscopy and Microanalysis.....	26
3.2. Optical and Scanning Electron Microscopy.....	26
3.3. Electron Microprobe Analysis (EPMA).....	26
3.4. X-ray Diffraction.....	26
3.5. Thermogravimetric Analysis.....	27
3.6. (U-Th)/He analysis.....	29
3.7. $^4\text{He}/^3\text{He}$ heating-step experiments.....	29
4. RESULTS.....	30
4.1. Goethite Composition.....	30
4.2. Goethite Crystallinity.....	34
4.2.1. XRD.....	34
4.2.2. TGA.....	34
4.3. (U-Th)/He Apparent Ages.....	34
4.4. $^4\text{He}/^3\text{He}$ results.....	42
4.4.1. Rstep/Rbulk and Incremental Heating Spectra.....	42
4.4.2. Arrhenius plots.....	45
4.4.3. Isothermal Retention Time Diagrams.....	46
5. DISCUSSION.....	46
5.1. The occurrence and purity of supergene goethite.....	46

5.2. Crystallinity and crystallite sizes in supergene goethite.....	52
5.3. The effects of purity and crystallinity on the thermal stability of supergene goethite.....	52
5.4. The effect of crystallinity on (U-Th)/He and $^4\text{He}/^3\text{He}$ results.....	53
5.5. The effects of mineral purity on (U-Th)/He and $^4\text{He}/^3\text{He}$ results.....	53
5.6. The effects of purity on $^4\text{He}/^3\text{He}$ spectra.....	55
5.7. The effect of crystallinity on $^4\text{He}/^3\text{He}$ spectra.....	56
5.8. The effect of multiple generation on (U-Th)/He and $^4\text{He}/^3\text{He}$ results.....	57
5.9. Rstep/Rbulk diagrams and He release from goethite.....	58
5.10. Arrhenius plots.....	59
5.11. Isothermal holding time.....	60
5.12. Interpreting $^4\text{He}/^3\text{He}$ incremental heating profiles.....	60
6. RECOMMENDED PROCEDURES.....	61
6.1. Before Geochronology.....	62
6.2. (U-Th)/He and $^4\text{He}/^3\text{He}$ Analysis.....	62
6.3. Presenting and Interpreting $^4\text{He}/^3\text{He}$ Incremental Heating Data.....	62
7. CONCLUSION.....	63
Acknowledgments.....	64
REFERENCES.....	65

Chapter 3: A combined (U-Th)/He and cosmogenic ^3He record of landscape armoring by biogeochemical iron cycling.....	70
--	----

ABSTRACT.....	71
1. INTRODUCTION.....	72
2. GEOLOGY AND GEOMORPHOLOGY OF THE QUADRILÁTERO FERRÍFERO.....	73
3. METHODS.....	75
4. RESULTS.....	80
4.1. Mineralogy.....	80
4.2. (U-Th)/He ages.....	80
4.3. Cosmogenic ^3He concentrations, minimum surface exposure ages, and erosion rates.....	80
5. DISCUSSION.....	88
5.1. The goethite (U-Th)/He record: chemical processes controlling the formation of saprolites and cangas.....	91
5.2. The cosmogenic ^3He record: mechanisms controlling the dismantling of cangas.....	94
5.3. Rates of erosion for canga plateaus.....	95
5.4. Age vs elevation relationships for canga plateaus.....	96
5.5. Cangas: self-healing biogeochemical conveyor belts.....	97
6. CONCLUSION.....	99
Acknowledgments.....	100
REFERENCES.....	101

Chapter 4: Ages and evolution of diachronous erosion surfaces in the Amazon: the (U-Th)/He and cosmogenic ^3He records.....	107
ABSTRACT.....	108
1. INTRODUCTION.....	109
2. GEOLOGY AND GEOMORPHOLOGY OF THE CARAJÁS PLATEAUS AND ADJACENT AREAS.....	111
3. SAMPLING STRATEGY AND ANALYTICAL METHODS.....	113
3.1. Optical and scanning electron microscopy.....	114
3.2. X-ray diffraction.....	115
3.3. Electron microprobe analysis (EMPA).....	115
3.4. (U-Th)/He geochronology and $^4\text{He}/^3\text{He}$	117
3.5. Cosmogenic ^3He	118
4. RESULTS.....	118
4.1. Microscopy.....	118
4.2. Mineralogy.....	119
4.3. Goethite composition.....	119
4.4. (U-Th)/He geochronology.....	123
4.5. Cosmogenic ^3He	127
5. DISCUSSION.....	128
5.1. The goethite (U-Th)/He record: chemical processes controlling the formation of saprolites and cangas	129
5.2. The (U-Th)/He age record.....	130
5.3. The cosmogenic ^3He record: the relative stability of duricrusts.....	132
5.4. Age vs elevation relationships for the Carajás and Itacaiunas Surfaces.....	132
5.5. Formation and evolution of the diachronous Itacaiunas erosion surface.....	133
6. CONCLUSION.....	139
Acknowledgments.....	139
REFERENCES.....	140
Chapter 5: Development and implementation of suitable protocols for in situ measurement of oxygen isotopes in goethite by ion microprobe.....	145
ABSTRACT.....	146
1. INTRODUCTION.....	147
2. SUITABLE SHRIMP-SI $^{18}\text{O}/^{16}\text{O}$ GOETHITE REFERENCE MATERIAL.....	149
3. ANALYTICAL TECHNIQUES.....	152
3.1. Optical and Scanning Electron Microscopy.....	152
3.2. Electron Microprobe Analysis (EPMA).....	152
3.3. X-ray Diffraction.....	153
3.4. Synthetic Goethite.....	153
3.5. (U-Th)/He analysis.....	153
3.6. Laser fluorination analysis	154

3.7. In situ analysis of oxygen isotopes by SHRIMP-SI	154
4. RESULTS	155
4.1. Electron microprobe analysis	155
4.2. XRD	157
4.3. (U-Th)/He ages	157
4.4. Laser fluorination analysis	158
4.5. SHRIMP-SI $^{18}\text{O}/^{16}\text{O}$ analysis	158
5. DISCUSSION	164
5.1. The effect of crystallographic orientation on $^{18}\text{O}/^{16}\text{O}$ ratios	164
5.2. Porosity control on $^{18}\text{O}/^{16}\text{O}$ ratios	168
5.3. The influence of texture and multiple generations on the $\delta^{18}\text{O}$ value of goethite	170
5.4. The influence of minor and trace elements on the $\delta^{18}\text{O}$ value of goethite	173
5.5. Evaluating the most suitable reference material	174
5.6. The Capão L4 SHRIMP-SI reference material	175
6. CONCLUSIONS	177
Acknowledgements	178
REFERENCES	179

Chapter 6: Cenozoic continental paleoclimatic record from combined (U-Th)/He dating and SHRIMP-SI $\delta^{18}\text{O}$ analysis of goethite	184
---	-----

ABSTRACT	185
1. INTRODUCTION	186
2. STUDY SITES AND SAMPLING APPROACH	189
3. RESULTS	191
4. DISCUSSION	192
4.1. Mineralogical Controls	192
4.2. Climatic Controls	197
4.3. The Climatic Record Trough Time	198
<i>The Carajás Record</i>	198
<i>The Quadrilátero Ferrífero Record</i>	202
5. THE WAY FOWARD	203
Acknowledgments	204
REFERENCES	205

Chapter 7: Conclusions	211
------------------------------	-----

Appendices

Chapter 2

EA1: Electron Microprobe Analysis

EA2a: $R_{\text{step}}/R_{\text{bulk}}$ Diagrams corrected for blank

EA2b: $R_{\text{step}}/R_{\text{bulk}}$ Diagrams not corrected for blank

EA3: Step-heating $^4\text{He}/^3\text{He}$ analysis

Chapter 4

EA1: Electron Microprobe Analysis

Chapter 5

EA1: SHRIMP-SI Disk

EA2: Electron Microprobe Analysis (SHRIMP-SI Reference Material)

EA2: Electron Microprobe Analysis (Brazilian and Australian Goethites)

EA3: SHRIMP-SI data for RM candidates

Chapter 6

EA1: Electron Microprobe Analysis (Carajás and QF)

EA2: SHRIMP-SI data for Carajás

EA2: SHRIMP-SI data for the QF

LIST OF FIGURES AND TABLES

Chapter 1

Figure 1: Digital Elevation Model (Amante and Eakins, 2009).....	3
Figure 2: (a) Typical colloform growth of goethite precipitated.....	5
Figure 3: The flux of primary cosmic rays (PCR).....	8

Chapter 2

Figure 1: Goethite samples illustrating different modes.....	25
Figure 2: Scanning electron microscopy images of representative.....	28
Figure 3: (a) Histogram illustrating chemical composition.....	31
Figure 4: Powder XRD patterns (A) for goethite.....	35
Figure 5: Thermogravimetric analyses for goethites investigated.....	36
Figure 6: $R_{\text{step}}/R_{\text{bulk}}$ versus Cum $F^3\text{He}$ plots.....	43
Figure 7: Plateau-age diagrams plotted for all samples with software Isoplot 4.15.....	44
Figure 8: Incremental heating (U-Th)/He- $^4\text{He}/^3\text{He}$ diagrams.....	45
Figure 9: ^4He and ^3He Arrhenius diagrams for all goethites.....	47
Figure 10: Activation energies and frequency factors derived.....	49
Figure 11: Figure 11 illustrates that total U and Th contents.....	54
Figure 12: A correlation between calculated E and $\text{Ln}(D_0/r_0^2)$ for 22.....	58
Table 1: Electron Microprobe Analysis of representative goethite grains.....	32
Table 2: (U-Th)/He ages.....	37
Table 3: Goethite diffusion parameters calculated from ^3He	48

Chapter 3

Figure 1: The (a) digital elevation model and (b) topographic cross-section.....	75
Figure 2: (a) Undulating plateau surfaces are underlain by canga.....	77
Figure 3: (a) The higher elevation and more extensive Gandarela.....	79
Figure 4: Photomicrographs of representative samples used in ^3He	85
Figure 5: (a) Diagrammatic illustration of the QF landscape.....	86

Figure 6: Histograms illustrating the frequency of goethite (U-Th)/He age	88
Figure 7: Cosmogenic ^3He and apparent exposure ages.....	89
Figure 8: Diagrammatic illustration that shows the most relevant processes.....	92
Figure 9: Erosion rates derived from in situ and detrital iron.....	96
Figure 10: A correlation between goethite precipitation and exposure ages.....	98
Table 1: (U-Th)/He results for the Quadrilátero Ferrífero goethite.....	81
Table 2: Cosmogenic ^3He results.....	87
Table 3: Chemical reactions illustrating the most important processes.....	92

Chapter 4

Figure 1: The digital elevation model illustrates the distinct landscape.....	110
Figure 2: Deep weathering profiles underlay the Carajás Plateau.....	114
Figure 3: (a, b) Deep weathering profiles developed on BIFs are also.....	116
Figure 4: (a) Field photo showing the topographic positions of the	117
Figure 5: Photomicrographs of representative goethite grains from.....	120
Figure 6: Electron microprobe analysis (1003 spots).....	121
Figure 7: Correlation diagrams for the elemental contents.....	122
Figure 8: The distribution of (U-Th)/He ages shows the large.....	123
Figure 9: Trends in Th/U vs depth illustrate the effective leaching of U.....	130
Figure 10: An age vs depth diagram for all goethites from the IB profile.....	131
Figure 11: Plate reconstruction for South America.....	134
Figure 12: The spatial and temporal distribution of dated duricrusts.....	136
Table 1: U, Th, He contents and (U-Th)/He ages.....	124
Table 2: Cosmogenic ^3He Analysis.....	128

Chapter 5

Figure 1: SEM image of goethite bands showing	148
Figure 2: Four natural samples selected as potential goethite.....	151
Figure 3: Electron microprobe analyses (a, c, e) for representative.....	156

Figure 4: X-ray diffraction analysis reveals that samples.....	158
Figure 5: Goethite is orthorhombic and preferentially elongated.....	166
Figure 6: SHRIMP-SI results obtained for three aliquots.....	167
Figure 7: Fragments of pressed pellets of synthetic goethites	169
Figure 8: (a, b) Reproducibility of SHRIMP-SI $\delta^{18}\text{O}$ results.....	172
Figure 9: $\delta^{18}\text{O}_{\text{SIMS}}$ vs Al+Si contents for all reference.....	174
Figure 10: All SHRIMP-SI results obtained for natural goethite.....	176
Figure 11: $\delta^{18}\text{O}_{\text{SIMS}}$ values obtained for our proposed reference.....	177
 Table 1: Elemental composition of SHRIMP-SI goethite reference.....	 157
Table 2: (U-Th)/He ages.....	160
Table 3: Summary of SHRIMP-SI oxygen isotope ratios and uncertainties.....	161

Chapter 6

Figure 1: (a) Lateritic weathering profiles, such as the Igarapé.....	187
Figure 2: The two continental sites investigated in this study.....	190
Figure 3: Multi-year monthly mean precipitation at the Belém,.....	191
Figure 4: (U-Th)/He Vs. $\delta^{18}\text{O}_{\text{SIMS-gth}}$ data for Carajás (b) and the QF.....	194
Figure 5: Correlation diagrams for the most important minor elements.....	196
Figure 6: Plate reconstructions using the Earthviewer software.....	201

LIST OF ABBREVIATIONS

CMM: Centre for Microscopy and Microanalysis

Cpm: Cryptomelane

DEM: Digital Elevation Model

DTA: Differential Thermal Analysis

E: Activation energy

EPMA: Electron probe microanalysis

Gibb: Gibbsite

Gth: Goethite

Hem: Hematite

HRD: High-retentivity domain

ICP-MS: Inductively coupled plasma mass spectrometer

Lep: Lepidrocrocite

LF: Laser Fluorination

LRD: Low-retentivity domain

Mag: Magnetite

PCR: Primary Cosmic Rays

QF: Cuadrilátero Ferrífero

Qtz: Quartz

RM: Reference Material

SEM: Scanning electron microscopy

SHRIMP-SI: Sensitive High Resolution Ion Micro Probe-Stable Isotope

Ma: million years ago

TGA: Thermogravimetric Analysis

Wt%: weight percent

XRD: X-ray diffraction

Chapter 1: Thesis Structure and Introduction

1. THESIS STRUCTURE

The document consists of seven chapters, where Chapter 1 (Introduction) and Chapter 7 (Conclusions) summarize the main objectives, approaches, and findings presented in Chapter 2 (“On Goethite as a (U-Th)/He- $^4\text{He}/^3\text{He}$ Geochronometer”); Chapter 3 (“A combined (U-Th)/He and cosmogenic ^3He record of landscape armoring by biogeochemical iron cycling”); Chapter 4 (“Ages and evolution of diachronous erosion surfaces in the Amazon: the (U-Th)/He and cosmogenic ^3He records”); Chapter 5 (“Development and implementation of suitable protocols for in situ measurement of oxygen isotopes in goethite by ion microprobe”); and Chapter 6 (“Cenozoic continental paleoclimatic record from combined (U-Th)/He dating and SHRIMP-SI $\delta^{18}\text{O}$ analysis of goethite”).

Chapters 2 to 6 consist of stand-alone scientific articles, some already submitted for publication or under submission to the journals identified at the first page of each chapter. To avoid repetition and to make the entire document more readable to the examiner, I provide in Chapter 1 only a cursory review of the main topics and analytical approaches utilized in each chapter. More in-depth review of each topic and pertinent literature reviews are provided within individual chapters. Similarly, as each chapter contains a comprehensive set of conclusions, I will very briefly summarize the main conclusions of the entire thesis in Chapter 7, and focus the attention of that chapter on recommendations and future studies that may follow from this contribution.

2. INTRODUCTION

The chemical and isotopic compositions of low-temperature minerals formed at the Earth’s surface can be used to reconstruct past environmental conditions at the time of mineral precipitation (Savin and Epstein, 1970). Supergene minerals, produced by mass and energy transfer processes at the near-surface environment, may be preserved in the geological record for tens of millions of years (Vasconcelos et al., 1994a, b; Shuster et al., 2005), providing a time capsule of paleoenvironmental conditions. In addition to information about paleoenvironmental conditions, the history of mineral precipitation in the surficial environment permits determining the timing and rate of processes shaping the Earth’s surface. Retrieving information from supergene minerals requires combining detailed mineralogy, accurate and precise geochronology with environmental isotope investigation at high temporal- and spatial- resolution scales. It also requires bringing all this information together into self-consistent models of surface evolution.

This thesis aims at improving the resolution and reliability of geochronological methods suitable for dating goethite (i.e., combined (U-Th)/He- $^4\text{He}/^3\text{He}$ complemented by cosmogenic ^3He analysis) and developing suitable analytical protocols to retrieve paleoenvironmental conditions from the $\delta^{18}\text{O}$ record preserved in this mineral. Therefore, the thesis has both a methodological development/improvement aspect and a number of application components.

The methodological development/improvement aspect has three sub-components:

1. to investigate mineralogical, crystallographic, and geological controls on the suitability of goethite to (U-Th)/He geochronology (Chapter 2), and apply this knowledge to investigate weathering profiles (Chapters 3 and 4);
2. to refine the application of cosmogenic ^3He accumulated in goethite and hematite to investigate exposure ages (or erosion rates) of long-lived land surfaces in cratonic environments (Chapters 3 and 4);
3. to refine a set of analytical protocols (e.g., find and characterize a suitable reference material, evaluate crystallographic controls, evaluate matrix effects, etc.) suitable for exploiting the high spatial resolution and speed of analysis of ion microprobes in the study of the $\delta^{18}\text{O}$ values of goethites (Chapter 5).

Upon successfully completing these methodological and general application aspects, the study aims at applying the improved analytical protocols to investigate the paleoenvironmental evolution of two sites in Brazil: the Quadrilátero Ferrífero (QF), Minas Gerais, and the Carajás-Marabá region, Pará (Figure 1) (Chapter 6). I will try to demonstrate that by combining (U-Th)/He dating and $^4\text{He}/^3\text{He}$ diffusion kinetics, cosmogenic ^3He exposure dating, and Sensitive High Resolution Ion Microprobe – Stable Isotopes (SHRIMP-SI) analyses of iron oxides and oxyhydroxides cementing relict surfaces in these cratonic regions, it is possible to determine ages and rates of erosion of different components of complex landscapes, it is possible to unravel the processes and sequence of events that helped shaping these landscapes, and it is possible to reconstruct the paleoenvironmental conditions prevailing during the evolution of long-lived cratonic landscapes. The approach illustrated here also demonstrates that long-lived landscapes in continental environments contain a paleoenvironmental record that, if resolved at the correct spatial and temporal scales, is directly comparable and complementary to the paleoenvironmental record preserved in oceanic sediments. Improved precision and application of the method on a large number of samples from across the planet will permit a direct comparison between continental and oceanic paleoenvironmental records at a global scale, potentially enabling a complete reconstruction – combining oceanic and

continental records – of the paleoenvironmental history of the Earth as far back as the age of the oldest preserved weathering profiles.



Figure 1: Digital Elevation Model (Amante and Eakins, 2009) shows the two study sites, Carajás and Quadrilátero Ferrífero, investigated in this project.

In order to reach these goals, it is important to understand some key aspects about the mineralogy-crystallography of goethites that make this mineral such a useful paleoenvironmental capsule; we need to assess some of the mineralogical issues associated with the use of goethite as a geochronometer; we must briefly review specific analytical aspects of the (U-Th)/He- $^4\text{He}/^3\text{He}$ method as it applies to goethite; we must briefly analyze methodological developments relevant to the production and measurement of cosmogenic ^3He in goethite-hematite; we must investigate the vast literature on environmental isotopes (O, H, and C) measurements on goethite; and we must

briefly summarize instrumental aspects of ion microprobes that may be relevant to in-situ $^{18}\text{O}/^{16}\text{O}$ analysis of goethites.

2.1. THE MINERALOGY-CRYSTALLOGRAPHY OF GOETHITE

Goethite ($\alpha\text{-FeOOH}$) precipitated at surficial conditions occurs as polycrystalline aggregates forming botryoidal, mammillary, radial, acicular, fibrous, and filamentous structures. The typical colloform growth (Figure 2a) of goethite indicates precipitation in open spaces created by the dissolution of primary minerals during weathering. Colloform growth produces cm-scale goethite masses containing several μm -scale growth bands (Figure 2b). Each micrometric layer records an event of mineral precipitation, while the colloform masses record the history of mineral precipitation through time. Therefore, by retrieving chemical and isotopic information from sequential growth bands in goethite we can reconstruct past ambient conditions and constrain the sequence of climatic shifts through time.

Goethite is a common mineral in soils and weathering profiles and it forms under diverse climatic regimes (Fitzpatrick and Schwertmann, 1982). Its chemistry, crystallinity, and rates of precipitation-dissolution are influenced by ambient conditions such as solution chemistry, temperature, pH, and availability of organic acids (Sposito, 2008). Cation substitution is an important process that takes place during goethite precipitation from weathering solutions. Fe^{3+} in goethite is commonly replaced by Al up to 0.33 mol%, where the amount of incorporation is affected by solution pH, temperature, and abundance of Al (Cornell and Schwertmann, 2003). Other common cations replacing Fe^{3+} in octahedral sites are: Ni, Zn, Cr, Mn, Co, and Cu (Manceau et al. 2000). The degree of cation replacement in goethite has direct implications to environmental studies. Importantly, fractionation of O isotopes between goethite and water depends on Al-substitution in goethites (Yapp, 2012). In addition, it greatly affects goethite crystallinity and crystallite size (Cornell and Schwertmann, 2003; Mostert, 2014), key properties to be considered when using goethite as a (U-Th)/He geochronometer.

Geological controls on goethite precipitation and elemental composition are addressed in Chapters 2, 3, and 4, and the effects of precipitation mechanisms and trace elements on the $\delta^{18}\text{O}$ signatures of goethites will be discussed in Chapters 5 and 6.

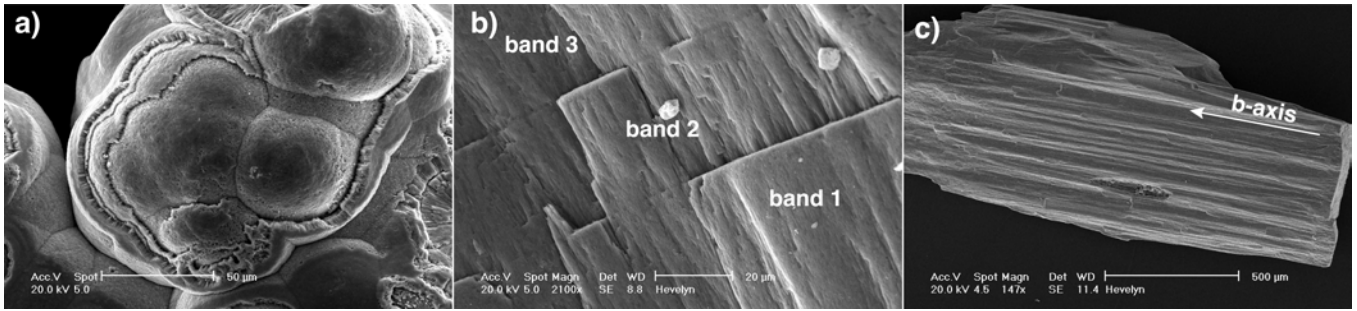


Figure 2: (a) Typical colloform growth of goethite precipitated in empty space. (b) Goethite growth-bands represent separate precipitation events. (c) Goethite crystallites tightly packed revealing preferential growth along the b-axis.

2.2. THE COMBINED (U-TH)/HE - $^4\text{He}/^3\text{He}$ METHOD APPLIED TO GOETHITE

The (U-Th)/He method is based on the decay series of ^{238}U , ^{235}U , ^{232}Th , and ^{147}Sm (the large majority of He is produced by actinide decay) (Farley, 2002). For most minerals, where the concentration of ^{147}Sm is negligible, He production is calculated from the equation:

$$^4\text{He} = 8^{238}\text{U}(\exp(\lambda_{238}t) - 1) + 7(^{238}\text{U}|137.88)(\exp(\lambda_{235}t) - 1) + 6^{232}\text{Th}(\exp(\lambda_{232}t) - 1)$$

where

^4He , U, Th are the present-day concentrations of each parent and daughter isotope;

t is the age of precipitation;

and λ 's are the decay constants for ^{238}U ($1.511 \times 10^{-10} \text{ yr}^{-1}$), ^{235}U ($9.849 \times 10^{-10} \text{ yr}^{-1}$), and ^{232}Th ($4.948 \times 10^{-11} \text{ yr}^{-1}$), respectively.

The major challenge in using the (U-Th)/He method in dating goethite is the possibility that goethite loses He by volume diffusion during its geological history (Strutt 1909; Lippolt et al., 1995, 1998). Since the work of Shuster et al. (2005) showing, through the combined (U-Th)/He- $^4\text{He}/^3\text{He}$ method, that goethite may retain He quantitatively and that He losses by volume diffusion can be quantified and corrected for, the (U-Th)/He method has been successfully applied to date goethite precipitated from weathering profiles around the world (Heim, et al., 2006; Lima, 2008; Waltenberg, 2012; Vasconcelos et al., 2013; Danišik et al., 2013; Monteiro et al., 2014; Riffel et al., 2015; Miller et al., 2017; Hofmann et al., 2017). These studies suggest that the major challenges to overcome when dating goethite by the (U-Th)/He method are: (1) selection, in the field, of suitable goethite for geochronology; (2) selection of pure, single-generation goethite in the laboratory; (3) assessing possible He losses over geological time; and (4) assessing possible incorporation or losses of U and/or Th after goethite precipitation. Selection of appropriate material for dating is a crucial

step for obtaining meaningful (U-Th)/He ages (Monteiro et al., 2014).

In nature, goethite does not form large euhedral crystals at the mm to cm scale, except perhaps for late-stage goethite precipitated in pegmatites (Berry, 2001). In most cases, individual crystallites in supergene goethites are only 10 to 50 μm long, with aspect ratios of 1:5 to 1:20 (Figure 2c). The long-distance ejection of α particles (^4He) during decay of U and Th (Farley, 2002 and references there in) would effectively preclude using the (U-Th)/He method to investigate individual crystals of supergene goethite. However, under the right conditions (slow precipitation directly from solution in open spaces) supergene goethite will form cm-scale cements or colloform masses composed of intimately intertwined individual crystallites which, in principle, eliminate the α ejection problem. Of course, α ejection may still occur if the individual crystallites are not closely packed. Fortunately, the degree of packing and the amount of pore space in natural goethites is directly proportional to the colour of natural samples; closely packed goethites free of pore space are black and vitreous, while poorly packed randomly oriented crystallites separated by a large volume of pore space forms friable and yellow goethite with an earthy luster. Simple visual identification of these macroscopic properties suffices to select, in the field, the most suitable goethites for geochronology. In this study, we targeted the interior of large masses of densely packed dark brown to black vitreous goethites for (U-Th)/He geochronology.

He release kinetics experiments have shown that well-crystallized goethite effectively retains helium for millions of years (Shuster et al., 2005; Waltenberg, 2012). Applying the (U-Th)/He method in combination with $^4\text{He}/^3\text{He}$ step-heating experiments permits correcting a sample's age for both He loss and excess ^4He from contaminants (Shuster et al., 2005; Vasconcelos et al., 2013). Despite previous quantification of He retentivity for well-crystallized goethites, the fact that goethite in nature varies in crystallinity, crystallite sizes, and density of polycrystalline aggregates demands a careful characterization of ^4He release behavior for various types of goethites (e.g., yellow and fine-grained goethites) frequently found in lateritic weathering profiles.

Shuster et al. (2005) propose the two domains model of He diffusion for goethites. More complete ^4He diffusion characterization indicates that goethites are composed of multiple diffusion domains (crystallites of different sizes) (Waltenberg, 2012). In well-crystallized goethites, high-retentive domains retain most of the gas relevant for calculating a sample's He age (Shuster et al., 2005; Vasconcelos et al., 2013). By carrying $^4\text{He}/^3\text{He}$ diffusion studies, the amount of He lost from low-retentive domains can be estimated and a correction factor can be applied to the calculated He age (Shuster et al., 2005).

In Chapter 2, the $^4\text{He}/^3\text{He}$ method is applied to conduct detail investigation of He release kinetics in goethites derived from a variety of geological environments, displaying both good and poor crystallization, complex chemistry and textures, and multiple generations.

2.3. COSMOGENIC ^3He ACCUMULATION IN GOETHITE-HEMATITE

Cosmic rays entering the Earth's atmosphere are composed primarily by protons (87%), and α -particles (12%) (Friedlander, 1989). Collision between primary cosmic rays and atomic nuclei in the atmosphere generates a cascade of secondary cosmic rays (e.g., neutrons, pions, muons) (Friedlander, 1989). Neutrons are the dominant secondary cosmic rays interacting with rocks at the upper 2 m of the Earth's surface, while muons are the most important cosmic rays driving reactions at depths greater than 2 m and down to ~ 20 m (Figure 3) (Stone et al., 1998; Dunai, 2010). Depending on the energy of the cosmic rays, spallation reactions and/or thermal neutron and negative muon capture may take place. (e.g., $^{16}\text{O}(n,4p3n)^{10}\text{Be}$) (Dunai, 2010). These atomic collisions happen in several ways, so the types of particles and energy produced are variable (Serber 1947; Masarik and Beer, 1999). Production of cosmogenic ^3He takes place during spallation reactions between secondary cosmic rays and atomic nuclei within minerals. Masarik (2002) calculated the total sea level high latitude (s.l.h.l.) production rate (atoms/g/year) of ^3He to be:

$$^3\text{He} = 128.7 [\text{O}] + 110.2 [\text{Mg}] + 102 [\text{Al}] + 106 [\text{Si}] + 57.7 [\text{Ca}] + 38.5 [\text{Fe}]$$

Shuster et al. (2012) calculated s.l.h.l. ^3He production rates in hematite and goethite to be 68.1 ± 8.1 and 72.5 ± 8.6 atoms/g/year, respectively. The hematite and goethite ^3He production rates of Shuster et al. (2012) are applied in this study.

Cosmogenic ^3He produced in goethite can potentially be used to determine the exposure ages of weathering profiles (Shuster et al., 2012). Unfortunately, goethite's propensity to undergo dissolution-precipitation in the near surface environment makes measuring cosmogenic isotopes in this mineral a challenge. On the other hand, primary hematite from banded iron-formations often survives during the formation of lateritic weathering profiles. Cosmogenic ^3He (Shuster et al., 2012) and ^{53}Mn (Fujioka et al., 2010) measured from such hematites from weathered banded iron-formations in Brazil were successfully used to calculate exposure ages for the ancient surfaces hosting the weathering profiles. The results of these studies suggest that high-elevation surfaces underlain by ancient weathering profiles in tropical Brazil erode at extreme low rates ($\sim 0.1 - 0.54$ m.Ma $^{-1}$) and are among the oldest continuously exposed surfaces on Earth.

This study takes advantage of the combined (U-Th)/He and ^3He cosmogenic isotope methods to retrieve both the precipitation and exposure ages of supergene goethites and co-existing hematites to determine the timing and depth of precipitation of goethite cements and speed of exhumation of the goethite cements and co-existing hematite. The combined approach reveals, in addition to timing, the mechanisms controlling the formation, exhumation, and destruction of ferruginous duricrusts overlying weathered banded iron-formations. This information can be combined with the environmental isotope composition of goethite cements to determine paleoclimatic controls on the formation and destruction of these duricrusts.

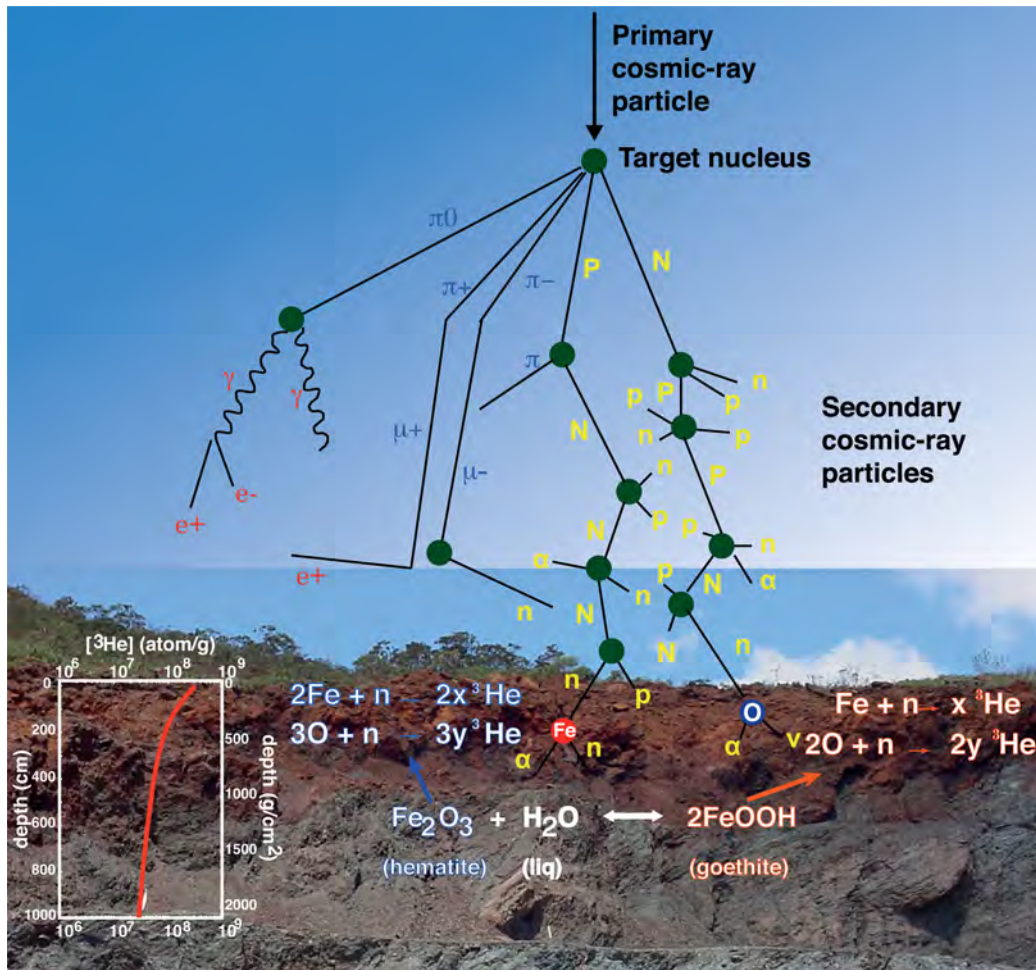


Figure 3: The flux of primary cosmic rays (PCR) change with latitude, altitude, and air pressure (Stone, 2000). A cascade is initiated when PCRs collide with atoms in the atmosphere. At the Earth's surface, neutrons dominate the cascade. They interact with nuclei in rock-forming minerals (e.g., goethite and hematite) via spallation reactions (Lal, 1991) to produce cosmogenic nuclides (e.g., ^3He). Cosmogenic nuclides are also produced at depth via muon reactions [inset] (Shuster et al., 2012).

2.4. THE $\delta^{18}\text{O}$ RECORD OF GOETHITE

$^{18}\text{O}/^{16}\text{O}$ (and D/H) measurements of natural goethites have been widely used to constrain paleotemperatures and isotopic composition of weathering solutions present at the time of mineral

precipitation (Yapp, 1987, 1993, 1997, 2001; Yapp and Shuster, 2011; Bao et al., 2000; Bird et al., 1992, 1993; Girard et al., 2000; Poage et al., 2000; Sjöström et al., 2004). To interpret variations in $^{18}\text{O}/^{16}\text{O}$ in natural goethites, it is necessary to determine the fractionation factors for equilibrium $^{18}\text{O}/^{16}\text{O}$ -exchange reactions between goethite and water ($\alpha_{\text{gth-water}}$) at various temperatures (Yapp, 1987, 1990, 2007; Müller, 1995; Bao and Koch, 1999). Discrepancies among fractionation factors derived from several experiments, carried out under various experimental conditions, show the dependence of $\alpha_{\text{gth-water}}$ on T is rather complex, as $\alpha_{\text{gth-water}}$ also depends on pH, solution composition, rates of precipitation, and post-precipitation reactions (Bao and Koch, 1999; Yapp, 2001). It is not the objective of this study to assess the fundamental aspects of goethite-water isotopic fractionation, and all the interpretations in this study rely on the fractionation factors derived by Yapp (1990):

$$1000 \ln ^{18}\alpha = \frac{1.63 \times 10^6}{T^2} - 12.3$$

where

$$\alpha_w^g = \frac{R_g}{R_w} = \frac{\left(\frac{^{18}\text{O}}{^{16}\text{O}}\right)_g}{\left(\frac{^{18}\text{O}}{^{16}\text{O}}\right)_w}$$

R_g is the ratio of the heavy isotope to the light isotope in goethite

R_w is the ratio of the heavy isotope to the light isotope in water

and T (K) is temperature of water-mineral interaction.

Major challenges also exist on the stable isotope characterization of natural goethites. For example, a major challenge in using traditional methodologies to investigate the isotopic composition of goethites from weathering profiles is the fact that large quantities of a single generation of goethite must be identified, retrieved, and analyzed. Unfortunately, pure, single-generation goethite in supergene environments is an elusive phase (Monteiro et al., 2014), and $^{18}\text{O}/^{16}\text{O}$ measurements performed in bulk samples of natural goethites may represent mixed-isotopic signatures extracted from various co-existing generations of goethite, precipitated at different times and from solutions with distinct isotopic compositions, or mixed-signatures associated with extraneous minerals included in goethite (hematite, gibbsite, quartz, Ti-oxides, phosphates, carbonates) in a sample. Bird

et al. (1992, 1993) obviate this problem by determining the $^{18}\text{O}/^{16}\text{O}$ of bulk-goethite and residual contaminants of chemically digested goethite masses, and calculating the isotopic composition of pure goethites by mass balance. This is a feasible but time consuming approach. In addition, it does not resolve the issue associated with intimately intergrown multiple generations of goethite. In this study, we focus on high spatial resolution approaches to obviate these problems.

2.5. THE SENSITIVE HIGH RESOLUTION ION MICROPROBE FOR THE STABLE ISOTOPE ANALYSIS OF GOETHITE

Natural pure goethites often occur as colloform masses composed of successively deposited growth bands that may span significant periods of time and may record information about solutions that were changing through time. The individual micrometric growth bands – typically 10-20 μm wide – are impossible to sample and analyze by traditional methods. The high spatial resolution of the method used in this study – SHRIMP stable isotope analysis – provides a clear advantage over previous attempts to measure the stable isotopic composition of minerals from weathering profiles, and it permit measuring the isotopic composition of each micrometric band in colloform goethite masses. This, in turn, permits resolving changes in isotopic compositions of weathering solutions through time.

The SHRIMP for stable isotopes is a recently developed instrument for the in-situ analysis of solid materials (Ireland et al., 2008). A few micrograms of material are sputtered from the sample surface with a focused ion beam (Cs^+ or O^-), transferred into a mass analyzer for separation of the masses of interest, and detected simultaneously in multiple collectors (Ireland et al., 2014). Precision at the order of 0.1-0.3 ‰ (2σ) can be obtained for some minerals (e.g., quartz) but different minerals behave differently in contact with the ion beam. Many of the potential obstacles to SHRIMP stable isotopes analyzes of goethite (e.g., matrix effect, crystal orientation) were investigated in this project (Chapter 5). The results presented and discussed in Chapters 5 and 6 clearly demonstrate that ion microprobe analysis of supergene goethite is an approach worth pursuing.

The results in Chapter 6 also shows the advantages of combining μm -scale investigation of the stable isotope composition with direct dating of goethite grains to derive constrained paleoenvironmental information from continental environments.

REFERENCES

- Amante C. and Eakins B.W. (2009) ETOPO1 1 Arc-Minute Global Relief Model: Procedures, Data Sources and Analysis. NOAA Technical Memorandum NESDIS NGDC-24. National Geophysical Data Center, NOAA. doi:10.7289/V5C8276M
- Bao H. and Koch P. L. (1999) Oxygen isotope fractionation in ferric oxide-water systems: Low temperature synthesis. *Geochimica et Cosmochimica Acta*, **55** (1999) 599-613.
- Bao H., Koch P. L. and Thiemens H. (2000) Oxygen isotopic composition of ferric oxides from recent soil, hydrologic, and marine environments. *Geochimica et Cosmochimica Acta*, **64** (2000) 2221-2231.
- Berry R. R. (2001) Goethite inclusions in Quartz from the Pikes Peak Granite. *Rocks & Minerals* 76 (4), 228-232.
- Bird M. I., Longstaffe F. J., Fyfe W. S., and Bildgen P. (1992) Oxygen-isotope systematics in a multiple weathering system in Haiti. *Geochimica et Cosmochimica Acta*, **56** (1992) 2831-2838.
- Bird M. I., Longstaffe F. J., Fyfe W. S., Kronberg B. I., and Kishida A. (1993) An oxygen-isotope study of weathering in the Eastern Amazon basin, Brazil. In: *Climate Change in Continental Isotopic Record*, *Geophysical Monograph* **78**, 295-307.
- Cornell R. M. and Schwertmann U. (2003) The iron oxides: structure, properties, reactions, occurrence and uses. Wiley-VCH Verlag GmbH & Co. KGaA, Weinheim.
- Danišík M., Evans N. J., Ramanaidou E. R., McDonald B. J., Mayers C., and McInnes, B. I. A. (2013) (U–Th)/He chronology of the Robe River channel iron deposits, Hamersley Province, Western Australia: *Chemical Geology* **354**, 150-162.
- Dunai T. J. (2010) *Cosmogenic nuclides: Principles, Concepts, and Application in the Earth Surface Sciences*. Cambridge University Press, 186 p.
- Hofmann F., Reichenbacher B., and Farley K.A. (2017) Evidence of >5Ma paleo-exposure of an Eocene-Miocene paleosol of the Bohnerz Formation, Switzerland. *Earth and Planetary Science Letters* **465**, 168-175.
- Fujioka T., Fifield L. K., Stone J. O., Vasconcelos P. M. P., Tims S. G., and Chappell J. (2010) In situ cosmogenic ⁵³Mn production rate from ancient low-denudation surface in tropic Brazil, *Nuclear Instruments and Methods in Physics Research B* **268**, 1209-1213.

- Farley K. A. (2002) (U-Th)/He dating: techniques, calibrations, and applications. *Reviews in Mineralogy and Geochemistry* **47**, 819-844.
- Fitzpatrick R. W. and Schwertmann U. (1982) Al-substituted goethite - An indicator of pedogenic and other weathering environments in South Africa. *Geoderma* **27**, 335-347.
- Friedlander M. W. (1989) Cosmic Rays. Harvard University Press, 160 p.
- Girard J. -P., Freyssinet P., and Chazot G. (2000) Unravelling climatic changes from intraprofile variation in oxygen and hydrogen isotopic composition of goethite and kaolinite in laterites: An integrated study from Yaou, French Guiana. *Geochimica et Cosmochimica Acta* **64** (3) 409-426.
- Heim J. A., Vasconcelos P. M. P., Shuster D. L., Farley K. A., and Broadbent G. (2006) Dating paleochannel iron ore by (U-Th)/He analysis of supergene goethite, Hamersley province, Australia. *Geology* **34**(3), 173-176.
- Ireland T. R., Clement S., Compston W., Foster J. J., Holden P., Jenkins B., Lanc P., Schram N., and Williams I. S. (2008) Development of SHRIMP, *Australian Journal of Earth Sciences* **55**, 937-954.
- Ireland T.R., Schram N., Holden P., Lanc P., Ávila J., Armstrong R., Amelin Y., Latimore A., Corrigan D., Clement S., Foster J.J., and Compston W. (2014) Charge-mode electrometer measurements of S-isotopic compositions on SHRIMP-SI. *International Journal of Mass Spectrometer* **359**, 26-37.
- Lal D. (1991) Cosmic ray labeling of erosion surfaces: in situ nuclide production rates and erosion models. *Earth and Planetary Science Letters* **104**, 424-439.
- Lima M. G. (2008) A história do intemperismo na província Borborema Oriental, Nordeste do Brasil: implicações paleoclimáticas e tectônicas. Tese de doutorado. Universidade Federal do Rio Grande do Norte, Brasil.
- Lippolt H. J., Wernicke R. S., and Bähr R. (1995) Paragenetic specularite and adularia (Elba, Italy): Concordant (U+Th)-He and K-Ar ages. *Earth and Planetary Science Letters* **132**, 43-51.
- Lippolt H. J., Brander T., and Mankopf N. R. (1998) An attempt to determine formation ages of goethites and limonites by (U+Th)-4He dating. *Neues Jahrbuch für Mineralogie - Monatshefte*, 505-528.

- Manceau A., Schlegel M. L., Musso M., Sole V. A., Gauthier C., Petit P. E., and Trolard F. (2000) Crystal chemistry of trace elements in natural and synthetic goethite. *Geochimica et Cosmochimica Acta* **64**, 3643-3661.
- Masarik J. (2002) Numerical simulation of in-situ production of cosmogenic nuclides. *Geochimica et Cosmochimica Acta* **66**, A491.
- Masarik J. and Beer (1999) Simulation of particle fluxes and cosmogenic nuclide production in the Earth's atmosphere. *Journal of Geophysical Research* **104D**, 12099-12111.
- Miller H. B. D., Vasconcelos P. M. P., Eiler J. M., and Farley K. A. (2017) An Australian Cenozoic terrestrial paleoclimate record from He dating and stable isotope geochemistry of goethites. *Geology*, doi: <https://doi.org/10.1130/G38989.1>.
- Monteiro H. S., Vasconcelos P. M. P., Farley K. A., Spier C. A. and Mello C. L. (2014) (U-Th)/He geochronology of goethite and the origin and evolution of cangas. *Geochimica et Cosmochimica Acta* **131**, 267-289.
- Mostert A. B. (2014) Variations in Goethite Crystallography with Reference to the Ravensthorpe Ni-Laterite, PhD Thesis, The University of Queensland, Brisbane, p. 290.
- Poage M. A., Sjostrom D. J., Goldberg J., Chamberlain C. P., and Furnnis G. (2000) Isotopic evidence for Holocene climate change in the northern Rockies from a goethite-rich ferricrete chronosequence. *Chemical Geology* **166**, 327-340.
- Riffel S. B., Vasconcelos P. M. P., Carmo I. O., and Farley K. A. (2015) Combined $^{40}\text{Ar}/^{39}\text{Ar}$ and (U-Th)/He geochronological constraints on the long-term landscape evolution of the Second Paraná Plateau and its ruiniform surface features, Paraná, Brazil. *Geomorphology* **23**, 52-63.
- Savin M. S. and Epstein S. (1970) The oxygen and hydrogen geochemistry of clay minerals. *Geochimica et Cosmochimica Acta* **34**, 25-42.
- Serber R. (1947) Nuclear reactions at high energies, *Physics Reviews* **72**, 1114-1115.
- Shuster D. L., Vasconcelos P. M. P., Heim J. A. and Farley K. A. (2005) Weathering geochronology by (U-Th)/He dating of goethite. *Geochimica et Cosmochimica Acta* **69(3)**, 659-673.
- Shuster D. L., Farley K. A., Vasconcelos P. M. P., Balco G., Monteiro H. S., Waltenberg K. M., and Stone J. O. (2012) Cosmogenic ^3He in hematite and goethite from Brazilian "canga" duricrust demonstrates the extreme stability of these surfaces. *Earth and Planetary Science Letters* **329-**

330, 41-50.

- Sjostrom D. J., Hren M. T. and Chamberlain C. P. (2004) Oxygen isotope records of goethite from ferricrete deposits indicate regionally varying Holocene climate change in the Rocky Mountain region, U.S.A.
- Sposito, G. (2008) The chemistry of soils. Oxford University Press, Inc., 329 p.
- Stone J. O., Evans J. M., Fifield L. K., Allan G. L., and Cresswell R.G. (1998) Cosmogenic chlorine-26 production in calcite by muons. *Geochimica et Cosmochimica Acta* **62**, 433-454.
- Stone J. O. (2000) Air pressure and cosmogenic isotope production, *Journal of Geophysical Research* **105(B10)**, 23,753-23,759.
- Strutt R. J. (1909) The Accumulation of Helium in Geological Time. *II Proceedings of the Royal Society of London Series A* **83**, 96-99.
- Vasconcelos P. M. P., Brimhall G. H., Becker T. A., and Renne P. R. (1994a) $^{40}\text{Ar}/^{39}\text{Ar}$ analysis of supergene jarosite and alunite: Implications to the paleoweathering history of the western USA and West Africa. *Geochimica et Cosmochimica Acta* **58**, 401-420.
- Vasconcelos P. M. P., Becker T. A., Renne P. R. and Brimhall G. H. (1994b) Direct dating of weathering phenomena by K-Ar and $^{40}\text{Ar}/^{39}\text{Ar}$ analysis of supergene K-Mn oxides. *Geochimica et Cosmochimica Acta* **58**, 1635-1665.
- Vasconcelos P. M. P., Heim J. A., Farley K. A., Monteiro H. S., Waltenberg K. M. (2013) $^{40}\text{Ar}/^{39}\text{Ar}$ and (U-Th)/He - $^4\text{He}/^3\text{He}$ geochronology of landscape evolution and channel iron deposit genesis at Lynn Peak, Western, Australia. *Geochimica et Cosmochimica Acta* **117**, 283-312.
- Yapp C. J. (1987) Oxygen and hydrogen isotope variations among goethites ($\alpha\text{-FeOOH}$) and the determination of paleotemperatures. *Geochimica et Cosmochimica Acta* **51**, 355-364.
- Yapp C. J. (1990) Oxygen isotopes in iron(III) oxides. 1. Mineral– water fractionation factors. *Chemical Geology* **85**, 329-335.
- Yapp C. J. (1993) The stable isotope geochemistry of low temperature Fe(III) and Al “oxide” with implications for continental paleoclimates. In: Climate Change in Continental Isotopic Record, *Geophysical Monograph* **78**, 285-294.
- Yapp C. J. (1997) An assessment of isotopic equilibrium in goethites from a bog iron deposit and a lateritic regolith. *Chemical Geology* **135**, 159-171.

- Yapp C. J. (2001) Rusty relics of Earth history: iron(III) oxides, isotopes and surficial environments. *Annual Review of Earth and Planetary Sciences* **29**, 165-199.
- Yapp C. J. (2007) Oxygen isotopes in synthetic goethite and a model for the apparent pH dependence of goethite-water $^{18}\text{O}/^{16}\text{O}$ fractionation. *Geochimica et Cosmochimica Acta* **71**, 1115-1129.
- Yapp C. J. (2012) Oxygen isotope effects associated with substitution of Al and Fe in synthetic goethite: Some experimental evidence and the criterion of oxygen yield. *Geochimica et Cosmochimica Acta* **97**, 200-212.
- Yapp C. J. and Shuster D. L. (2011) Environmental memory and a possible seasonal bias in the stable isotope composition of (U-Th)/He-dated goethite from the Canadian Arctic. *Geochimica et Cosmochimica Acta* **75**, 4194-4215.
- Waltenberg K. M. (2012) Mineral physics and crystal chemistry of minerals suitable for weathering geochronology: implications to $^{40}\text{Ar}/^{39}\text{Ar}$ and (U-Th)/He geochronology, PhD Thesis, The University of Queensland, Brisbane, p. 421.

Chapter 2: On Goethite as a (U-Th)/He-⁴He/³He Geochronometer

H. S. Monteiro¹, P.M.P Vasconcelos¹, K. A. Farley², and K. M. Waltenberg¹

¹ School of Earth and Environmental Sciences, University of Queensland, Brisbane, Queensland 4072, Australia

² Division of Geological and Planetary Sciences, California Institute of Technology, Pasadena, CA 91125

To be submitted to the American Journal of Science

** Corresponding author:*

H.S. Monteiro

The University of Queensland

Earth Sciences, Steele Building

Brisbane, Qld 4072

Phone: (61)(7) 3346-7636 (Office)

ABSTRACT

Goethite (αFeOOH), the most common product of weathering of iron-bearing minerals, is an excellent target for (U-Th)/He geochronology because of its abundance and relative stability in the surficial environment. New and previously published combined (U-Th)/He- $^4\text{He}/^3\text{He}$ geochronology of 24 goethite samples representative of different source rocks, precipitation mechanisms, solid-solution compositions, purity, and porosity provides information on the influence of these factors on U-Th-He contents, distribution, and retentivity in pure and impure natural goethites. The results reveal a complex pattern of He distribution, where U-Th-He may reside in the goethite itself and be released by volume diffusion from intra- and inter-crystalline sites. Alternatively, these elements may partially reside in mineral contaminants included within goethite, affecting (U-Th)/He results. Measured activation energies (E) for He diffusion from goethites range from 11.2 ± 0.5 to 74.5 ± 3.2 kcal.mol⁻¹, with an average value at 36.2 ± 13.5 (1 σ) kcal.mol⁻¹; and $\ln D_0/r_0^2$ ranges from -4.1 ± 0.5 to 62.8 ± 1.9 s⁻¹, with an average value of 24.1 ± 13 (1 σ) s⁻¹. Correlation between E and $\ln D_0/r_0^2$ ($y = 11.58 + 1.024x \pm 0.021$, $R^2 = .98$) reveals that goethite follows the compensation law closely. The mean in activation energy at ~ 35 kcal.mol⁻¹ indicates that He retentivity in goethite is comparable to other phases dated by the (U-Th)/He method. A major distinction between goethite and other phases used in (U-Th)/He geochronology is its large frequency factor, a possible consequence of the fact that supergene goethite is composed of masses of cryptocrystalline aggregates and not single crystals.

1. INTRODUCTION

(U-Th)/He geochronology of goethite (α -FeOOH) provides information on timing and rates of surficial processes that until recently could only be obtained from $^{40}\text{Ar}/^{39}\text{Ar}$ analysis of supergene Mn oxides and alunite-group sulfates (Vasconcelos, 1999). For example, (U-Th)/He dating of goethite permits dating old ($> 1\text{Ma}$) soils and weathering profiles (Lippolt et al., 1998; Shuster et al., 2005; Riffel, 2012; Riffel et al., 2015) and confirms the extreme antiquity ($> 70\text{ Ma}$) of continuously exposed lateritic surfaces in Brazil (Shuster et al., 2005) and Australia (Vasconcelos et al., 2013). Goethite (U-Th)/He shows that channel iron deposits (CIDs) in Western Australia are older (Heim et al., 2006; Vasconcelos et al., 2013) than previously assumed, while also demonstrating that CIDs undergo iron cementation during drawdown of the water table (Heim et al., 2006). It reveals that cangas (iron cemented duricrusts overlying banded iron formations) constitute some of the oldest continuously exposed landsurfaces on the planet (Shuster et al., 2005, 2012; Monteiro et al., 2014, 2017), and that the resilience of these duricrusts results from recurrent biologically mediated iron dissolution-reprecipitation (self-healing) through time (Monteiro et al., 2014). Finally, goethite (U-Th)/He also provides insights into the role of paleoclimates on the formation of supergene goethite (Yapp and Shuster, 2011; Danisik et al., 2013; Monteiro et al., 2017) and on fluid movement in sandstones and diagenetic reactions in the shallow crust in the Colorado Plateau, USA (Reiners et al., 2014). Despite the advances possible with modern (U-Th)/He geochronology of goethite, several aspects of the method are still being assessed.

An important aspect of investigating He retentivity is the behavior of goethite under vacuum. Unlike to phases commonly used in (U-Th)/He geochronology, goethite grains reveal variable outgassing behavior when placed in an ultra-high vacuum line, where some samples release a large amount of He at ambient temperature, increasing blanks in the mass spectrometer extraction line and suggesting that He may continuously leak from the sample under normal Earth's surface temperature. This outgassing behavior under ultra-high vacuum may not be relevant to gas retentivity in nature, but it raises suspicions that goethite, or at least some types of goethite, may be too vulnerable to He loss to be useful in geochronology. $^4\text{He}/^3\text{He}$ data (Shuster et al., 2005; Heim et al., 2006; Vasconcelos et al., 2013) show that goethites do indeed undergo some (2-20%) He loss during their geological histories, but the number and types of samples analyzed are too small to draw any general conclusion. In addition, the absence of clear correlations between the proportion of He loss and mechanisms of mineral precipitation, exposure histories, compositions, and goethite crystallinities makes it imprudent to extrapolate results from few experiments to predict the behavior of goethites in general. Improved predictability on the suitability of a specific type of goethite for geochronology is needed.

Another challenge in (U-Th)/He geochronology of goethite is the fact that FeOOH grains are opaque, preventing the visual detection of mineral inclusions. The only means of screening goethite (U-Th)/He results for the possible effects of contaminants is to carry out micro-CT scans in each aliquot before dating (Cooperdock and Stockli, 2016), an onerous task, or to analyze many replicate aliquots and eliminate apparent ages that are too discrepant from the mean (Monteiro et al., 2014). Any direct way of detecting the presence of contaminants prior to geochronology or quantifying the effect of contaminants after analysis will improve the reliability of goethite as a geochronometer.

$^4\text{He}/^3\text{He}$ vs $\sum^3\text{He}$ incremental heating profiles may display (1) well-defined plateaus; (2) progressively increasing spectra; (3) large increase in $^4\text{He}/^3\text{He}$ ratios in the last step (Vasconcelos et al., 2013); and (4) decreasing or variable $^4\text{He}/^3\text{He}$ throughout the experiment (Waltenberg, 2013). This variability of the $^4\text{He}/^3\text{He}$ vs $\sum^3\text{He}$ spectra also raise questions about the distribution and diffusivity of ^4He and ^3He in the various possible intercrystalline and intracrystalline reservoirs. Improved understanding of the physical parameters controlling the various shapes of $^4\text{He}/^3\text{He}$ incremental heating profiles will raise confidence in goethite as a geochronometer.

Understanding the behavior of U, Th, and He after goethite precipitation is important to improve our confidence on the geological history derived from (U-Th)/He results. A significant challenge is that goethites show more complex paragenesis, chemistry, and crystallinity than other minerals used in (U-Th)/He geochronology, a complexity related to goethite formation. In general, supergene goethites do not form single crystals at the mm- or cm-scale, but they are instead composed of aggregates of nm- to μm -size crystallites. In these masses, He (and possibly U and Th) may be hosted within the crystallites (intracrystalline sites) or in between crystallites (intercrystalline sites), similar to Ar distribution in supergene hollandite-group Mn oxides (Vasconcelos et al., 1994, 1995). In addition, some authors suggest that interstitial U- or Th-rich phases may co-precipitate between hematite (in our case, goethite) crystallites (Evenson et al., 2014). Therefore, it is reasonable to expect that ^4He should be more effectively retained in pure and dense masses of well-cemented goethites, where α -particles generated within goethite crystallites have high probabilities of being implanted into nearby crystallites. Porous goethites, where microcrystallites are surrounded by air and water, should be more prone to ^4He losses, as ejected α -particle may not be readily re-implanted in nearby crystallites and may reside in intercrystalline spaces. In those cases, closely bound crystallites may tightly hold He (and U or Th) residing in intercrystalline sites, while large and interconnected void spaces in porous goethite may allow relatively easy exchange of He (and U or Th) with the external environment. In the case of coexistence of interstitial U-Th-rich minerals with goethite, the removal of those phases during sample preparation or dissolution chemistry would generate parentless He, which will affect the final He age. Characterizing the relationship between

crystallinity/crystallite size, porosity, extraneous co-precipitated interstitial phases, and He, Th, and U retentivities is necessary to properly interpret geochronology results.

The composition of supergene goethite may also affect U and Th contents and ^4He retentivity. For example, Al-rich goethites often form less crystalline porous precipitates where individual crystallites are stubby and randomly oriented (Schwertmann and Carlson, 1994; Mostert, 2014); these goethites may be more prone to He losses. Alternatively, substitution of divalent (Ni, Co, Cu) cations for Fe^{3+} or PO_4^{3-} for OH^- in the goethite structure may help accommodating tetravalent U and Th ions elsewhere in the structure, and coupled substitution may potentially increase U and Th contents in goethites, also increasing the ^4He contents. Lastly, some authors have interpreted variable ages obtained from replicate goethite grains as evidence for U or Th gain or loss (Reiners et al., 2014), which also needs addressing.

Here we explore the effects of mineral precipitation mechanisms, crystallinity and crystallite size, chemical composition, and the effects of mineral inclusions on goethite (U-Th)/He data. We use field geology, hand sample and thin section petrography, SEM, XRD, TGA, and electron microprobe analysis, (U-Th)/He age distributions, He diffusivity and $^4\text{He}/^3\text{He}$ measurements to show that well crystallized goethites are as He retentive as apatite or some hematites and that Al-rich and less crystallized goethites may lose large amounts of He during their life time and need to be investigated with the combined (U-Th)/He – $^4\text{He}/^3\text{He}$ method.

1.1. Modes of Precipitation of Natural Goethites

Goethite is a ubiquitous supergene mineral forming in several distinct environments. These different environments yield goethites which differ in bulk chemistry, crystallinity, crystallite size, and characteristic mineral impurities. Each of these in turn is a factor in goethite He geochronology.

At the outset it is important to point out that goethite exhibits diverse textures and varying crystallite sizes and packaging, from very fine powdery yellow soil, to dense, hard and vitreous masses. Although (U-Th)/He dating may have some applicability to the former, the denser and more crystalline material (Figure 1) has been the focus of all geochronology efforts to date (Shuster et al., 2005; Heim et al., 2006; Waltenberg, 2012; Vasconcelos et al., 2013; Danisík et al., 2013; Monteiro et al., 2014, 2017; Riffel et al., 2015).

Supergene goethite often precipitates in situ during the dissolution of iron-bearing minerals. For example, during weathering of Fe-bearing sulfides or carbonates, leaching of $\text{SO}_4^{2-}(\text{aq})$ and $\text{CO}_3^{2-}(\text{aq})$ creates cavities where iron released by mineral dissolution may immediately reprecipitate, resulting in mineralogically pure colloform, mammillary, botryoidal, or stalagmitic masses of crypto- to

microcrystalline parallel-oriented acicular goethite crystals growing from the cavity walls into empty space (Figure 1a). Incongruent dissolution of Fe-Mg-silicates (e.g., olivine, pyroxene) in ultramafic rocks also results in relatively pure goethite masses, but goethite precipitated under those conditions typically forms porous powdery masses of randomly oriented crystallites. If this porous goethite undergoes recurrent dissolution-reprecipitation through time, colloform goethite concretions and pisoids may form (Figure 1b), eventually evolving into Fe-cemented duricrusts that often blanket deeply weathered ultramafic rocks (Millot, 1970; Samama, 1986). Pyrite in sulfide-facies banded iron formations, framboidal pyrite in sediments, or pyrite porphyroclasts in slates, schists, quartzites or marbles often weather pseudomorphically to goethite (Figure 1c). The resulting goethite pseudomorph is frequently cavernous in the center, and it can be very pure and devoid of mineral contaminants. Alternatively, it may contain inherited inclusions of quartz, rutile, ilmenite, muscovite, etc. Weathering of Fe-Al-bearing silicates (e.g., amphibole, biotite), on the other hand, invariably results in impure porous finely crystalline goethite masses intergrown with clay minerals and primary oxides, particularly magnetite and ilmenite.

Goethite may also result from the dissolution and transport of aqueous iron species ($\text{Fe}^{3+}_{(\text{aq})}$ in acid oxidizing conditions or $\text{Fe}^{2+}_{(\text{aq})}$ in acid reducing conditions), and the subsequent precipitation of iron minerals filling cavities, pore spaces, or replacing other minerals away from the source (Blanchard, 1968; Alpers and Brimhall, 1988). If Fe precipitates in void spaces, mineralogically pure colloform goethite may form; if weathering solutions contain other cations, goethite may alternate with bands of Mn-oxides, gibbsite, malachite, azurite, or other supergene phases (Blanchard, 1968), depending on solution composition and evolving environmental conditions. Where supergene goethite fills small pores or replaces primary minerals, it is often contaminated with fragments of weathering-resistant hypogene phases (e.g., hematite, magnetite, ilmenite, quartz, zircon, tourmaline, etc.) or with the products of incongruent dissolution of the mineral undergoing replacement (e.g., kaolinite in weathering of feldspars, amphiboles or biotites). Pore-filling and replacement goethite often grows in three-dimensional concentric bands (e.g., Liesegang bands), suggesting a protracted period of fluid influx and mineral precipitation (Figure 1d). Thus precipitation mechanisms control the crystallinity, purity and composition of goethite.

2. SAMPLES INVESTIGATED

Goethite specimens investigated in this study come from weathering profiles in Brazil and Australia (Shuster et al., 2005; Heim et al., 2006; Vasconcelos et al., 2013; Waltenberg, 2013; Monteiro et al., 2014; Vasconcelos et al., 2015). A summary of sources, compositions, and physical properties of each goethite occurrence is outlined below.

Winsor

The Winsor goethite (Win-06-01B) is a dense, well crystallized, wood-like colloform goethite pebble (~6 cm in diameter) collected from an alluvial plain at the foot of Prism Hill, Flinders Ranges, South Australia. Its original source is uncertain, but it was most likely eroded from an ancient weathering profile blanketing deeply weathered plateaus in the region. The sample shows multiple nucleation sites from which goethite bands grow in a concentric and radiating pattern (Figure 1d). Goethite bands vary in color from black to golden yellow indicating variable porosity, crystallinity, or composition. Crosscutting veins filled with opal are identified by optical and electron microscopy.

Roy Hill

The Roy Hill goethite (Roy 02 02 Ca and Roy 02 02 C3b) has a botryoidal, radiating fan-shaped texture (Figure 1e) of elongated fibrous crystals that are mineralogically very pure and suggest precipitation in open space, possibly during weathering of carbonate or sulfide horizons in BIF (Heim, 2006). It originates from a detrital deposit on low relief ridges (~ 400m elevation) at the foot of the Chinchester Ranges, Hamersley Province, Northwestern Australia. Veins of late-stage goethite (Figure 2c-f) suggest some partial recrystallization.

Igarapé Bahia

Goethites from the Igarapé Bahia Cu-Au mine, Carajás, Pará, Brazil, come from different horizons in a 100-150 m deep weathering profile (Vasconcelos et al., 2015). Samples BAH-F124-114 and BAH-F124-111.2 (Figure 1f, g) come from ~ 80 m below the modern surface, while goethite IBH 13 09h (Figure 1h) originates from ~ 10 m below the surface. The two BAH-F124 goethites precipitated from solution into empty cavities created by the dissolution of sulfides and carbonates (Shuster et al., 2005). Both BAH-124 goethites are vitreous, colloform, and may occur intergrown with Cu-rich Mn oxides. The IBH-13-09h goethite is Al-rich (6 wt% on average), has extremely complex texture, and cements fragments of primary minerals (e.g., quartz, ilmenite, magnetite, tourmaline), suggesting precipitation by Fe-cementation and pseudomorphic replacement of primary minerals during pedogenesis.

Capão

The Capão goethite (Capão L2, Capão L3, Capão L4, Capão L5) is a dense, well crystallized, colloform, mushroom-shaped ~ 10 cm mostly brown pebble (Figure 1i) collected in colluvia close to the Capão topaz mine, Rodrigo Silva, Minas Gerais, Brazil. Its habit and purity suggests precipitation in a cavity. The outermost layer contains black vitreous goethite intergrown with

hematite (interpreted as a late-stage recrystallization). Rare veins (mm-scale) filled with (Pb,Ba)-rich Mn-oxide occur along and cross-cutting goethite grains.

Gandarela

The Gandarela goethites (Pic 21, Pic 22, Pic 24) precipitated in a weathering profile overlying BIF in the Quadrilátero Ferrífero region, Minas Gerais, Brazil (Monteiro et al., 2014; Monteiro et al., 2017). Samples Pic 21 and Pic 24 represent the iron duricrust, while sample Pic 22 comes from ~15 m depth in the saprolite. Goethite replaces primary magnetite-hematite or fills empty cavities. Sample Pic 21 is dense, massive, mostly black, and cryptocrystalline (Figure 1j); crosscutting veins of μm -size crystals of reddish black acicular goethite intergrown with hematite occur in this sample. Sample Pic 24 is dark-brown, vitreous, and botryoidal (Figure 1k) and results from weathering of dolomitic BIF; it contains kaolinite and gibbsite inclusions. Pic 22 is a mixture of dense, black, and well-crystallized pure goethite with porous, dark-brown to yellow, and impure goethite (Figure 1l).

Lynn Peak

The Lynn Peak channel iron deposit (CID) is located in the Hamersley Province, Northwestern Australia. Ancient lateritic weathering profiles forming high-elevation plateaus were likely the source of ferruginized sediments filling the palaeochannel (Vasconcelos et al., 2013). Lynn Peak goethites (LynP0209-A1, -A2, -A3) may occur as detrital fragments, pisoliths, ferruginized clay and wood fragments, and authigenic cements (Figure 1m). Brown to black vitreous colloform goethite cements form continuous layers enclosing CID clasts, suggesting partial dissolution of detrital particles and in situ reprecipitation of Fe and some Al and Si.

Yandicoogina (Yandi)

The Yandi CID goethites (Yan-02-01-A, -D), Hamersley Province, Northwestern Australia, occur as nuclei and rims of ooids (<2 mm) and pisoids (>2 mm), replacement for primary rock and wood fragments, and botryoidal vitreous pure dark brown late-stage cements (Figure 1n) (Ramanaidou et al., 2003; Heim et al., 2006); these late-stage goethite cements are very mineralogically pure. Heim et al. (2006) envisaged precipitation of the botryoidal vitreous goethite cement at the groundwater-atmosphere interface, after palaeoriver infill, as the water table moved downward through time.

Ravensthorpe

The Ravensthorpe Ni-laterite deposit is located in Western Australia, approximately 550 km southeast of Perth. The laterite results from weathering of a sequence of komatiites, minor felsic volcanic rocks, and metasediments. The Ravensthorpe goethites (RS 3.4 TLcM) were collected

from the limonite horizon, which hosts the majority of the Ni mineralization (Mostert, 2014). It is postulated that these goethites precipitated under alkaline conditions (Mostert, 2014). They occur as massive, vitreous dark brown to black bands and lumps in a softer orange to brown friable goethite matrix (Figure 1b).



Figure 1: Goethite samples illustrating different modes of precipitation and from which goethite grains were selected for $^4\text{He}/^3\text{He}$ studies. (a) Botryoidal mass of crypto- to microcrystalline parallel-oriented acicular goethite crystals growing from the cavity walls into empty space. (b) Colloform, vitreous goethite concretions intermixed with brown powdering goethite. (c) Goethite pseudomorph to pyrite. (d) Goethite pebble from Flinders Rangers, South Australia. The concentric growth pattern is indicative of protracted precipitation in an open space. (e) Roy Hill goethite showing centimeter-thick layers of acicular crystals very tightly packed. (f) Cu-rich goethite coexisting with Mn-oxide. (g) Goethite precipitated in cavity after dissolution of sulfide minerals. (h) Goethite cemented duricrust from the soil-laterite boundary. (i) Alternate bands of yellow and dark-brown goethite and a late-stage black-vitreous goethite layer containing densely packed needle-shape crystallites. (j) Massive, black-vitreous cryptocrystalline goethite crosscut by μm -scale Al-poor goethite veins. The patchy appearance of the massive goethite suggests it was subjected to several events of recrystallization. (k) Canga sample containing Al-rich (~ 3.5 wt% on average) black-vitreous goethite cement. (l) Massive-black and yellow goethite in saprolite close to the canga-saprolite contact. (m) CID hand-specimen showing well crystallized goethite precipitated in veins and cementing ferruginized detrital material. (n) Rounded to angular fragments of hematite, goethite, and ferruginized wood rimmed by thin goethite layers cemented together by late-stage well-crystallized goethite.

3. METHODS

3.1. Microscopy and Microanalysis

Hand-specimens were photographed and sampled for optical and scanning electron microscopy (SEM), microprobe analysis (EMPA), X-ray diffractometry (XRD), thermogravimetric analysis (TGA), (U-Th)/He geochronology, and goethite $^4\text{He}/^3\text{He}$ diffusion experiments. Goethite fragments were directly broken from the samples or micro-drilled from slabs of selected hand-specimens. Sample fragments or micro-cores (2 cm long and 4 mm in diameter) were crushed to 0.1 – 2 mm grains, ultrasonicated in tap water for ~ 30 min, then in distilled water for 5 – 10 min, rinsed in ethanol, and air-dried. Clean goethite grains were mounted in 2.6 cm ID acrylic disks, filled with epoxy, polished, and imaged by optical and electron microscopy and analyzed in an EMP. Carbon- and iridium-coated grains were investigated for crystal morphology by SEM. Separate aliquots of hundreds of grains from each sample were powdered for X-ray diffractometry. Finally, clean goethite grains were sieved (825-425, 425-150 μm , <150 μm) for thermo-gravimetric analysis.

3.2. Optical and Scanning Electron Microscopy

Polished blocks and thin-sections were investigated in transmitted and reflected light to determine mineral textures, assemblages, paragenetic relationships, and modes of precipitation. Scanning electron microscopy (Figure 2) aided in documenting mineral paragenesis, the presence of relic primary minerals (e.g., hematite, magnetite, ilmenite, zircon), the size and morphology of goethite crystals, mineral textures, and goethite precipitation mechanisms (including microbial and root pseudomorphic replacement).

3.3. Electron Microprobe (EPMA)

Electron microprobe analyses were performed with a JEOL JXA-8200 EPMA at the Centre for Microscopy and Microanalysis (CMM) of the University of Queensland, Brisbane, Australia. The EPMA is fitted with secondary and backscattered electron detectors, one ED (Energy Dispersive) spectrometer, and 5 WD (Wavelength Dispersive) spectrometers. All runs were performed using a beam current of 15 nA, accelerating voltage of 15 kV, and highly focused spot size (except for more volatile elements; spot size = 10 μm). Mineral standards of known compositions were analyzed together with our samples in order to ascertain the accuracy of the results.

3.4. X-ray Diffraction

Bench-top powder XRD was performed in a Bruker D8 Advance X-ray diffractometer equipped with either a Cu- (1.5405 \AA) or a Co-source (1.7889 \AA) operated at 40 kV and 40 mA. Scans were

collected from 5° to $90^\circ 2\theta$. LaB6 standard was analyzed before and after each run. Rietveld refinement (Rietveld, 1969) using Fullprof (Rodriguez-Carvajal, 2001) was used to determine crystallite sizes and unit-cell volumes for selected samples.

Synchrotron X-ray diffraction were carried out for some samples at the Australian National Beamline Facility (ANBF) at the Photon Factory, National Laboratory for High Energy Physics (KEK), Tsukuba, Japan, following the sample preparation and analytical procedures outlined in Vasconcelos et al. (2013).

3.5. Thermogravimetric Analysis

Aliquots (7-32 mg) of clean goethite grains were loaded in 70 μL alumina crucibles and heated in air (flow rate of 20 ml/min) from 25 to 900 $^\circ\text{C}$ at a rate of 10 $^\circ\text{C}/\text{min}$. The system was allowed to equilibrate for 20 min at 25 and 900 $^\circ\text{C}$ and cooled down to 25 $^\circ\text{C}$ at a rate of 10 $^\circ\text{C}/\text{min}$. An empty crucible was heated/cooled under the same analytical conditions at the beginning and end of each run to correct for instrumental drift. Thermogravimetric analyses were carried on 10 goethites investigated for noble gas release kinetics, except samples from Lynn Peak, Yandi, Ravensthorpe, and Igarapé Bahia.

3.6. (U-Th)/He analysis

Goethite grains were analyzed following standard practices at Caltech (Monteiro et al., 2014). Briefly, goethite was prepared by crushing, with a mortar and pestle, large fragments down to 0.2-2 mm grain size. Grains selected for geochronology (typically 300 μ m x 500 μ m) were inserted in Pt-capsules and placed in a copper disk, loaded in a vacuum chamber, and pumped down for at least 3 h. Helium was extracted by heating individual capsules with a diode laser at 900 °C during 6 min. Evolved He was purified by passage through a charcoal trap held at liquid nitrogen temperature. A pure ^3He spike, calibrated against a precisely known amount of ^4He , was then introduced. He was cryofocussed on charcoal held 14K, cryopurified by release at 34 K, and analyzed in a Pfeiffer Prisma quadrupole mass spectrometer. Re-heating the capsules at 900 °C for 6 min after gas extraction confirmed complete degassing of each goethite grain. ^4He blanks were measured repeatedly over the course of a session of goethite measurements, and were typically very small compared to the He evolved from the sample.

Degassed Pt capsules containing the goethite grains were removed from the vacuum chamber and transferred to 1.5 ml Teflon containers. 25 μ l of spike solution containing known concentrations of ^{235}U and ^{230}Th , and 100 μ l of concentrated SeastarTM HCl, were added to the Teflon vials. Capped vials were placed in an oven at 90 °C overnight to promote goethite dissolution. Pt capsules were removed and the Teflon vials placed on a hot plate at 95 °C until solution evaporated completely. 50 μ l of concentrated SeastarTM HNO₃ was added to bring the salt back into solution. 1000 μ l of Milli-Q water was added to the Teflon beakers and the diluted solutions were decanted into a 1.5 ml ICP-MS cup. Homogenization of the solutions was done by vigorously shaking the closed ICP-MS vials. A procedural blank was prepared following the same steps outlined above. Unknown, procedural blank, acid blank, and calibrated normal solutions were analyzed using the Agilent 8800 ICP-MS in the Environmental Analysis Center at Caltech.

3.7. $^4\text{He}/^3\text{He}$ heating-step experiments

Goethite separates selected for $^4\text{He}/^3\text{He}$ experiments were proton irradiated at the Frances H. Burr proton Beam Therapy Center at Massachusetts General Hospital (Shuster et al., 2003). After irradiation, a few goethite grains were weighed, wrapped in degassed copper foil, suspended on a chromel-alumel thermocouple, placed in a diffusion-cell, and pumped until the blank level was deemed low enough to start measurements. Copper foil packets were incrementally heated up to ~ 500 °C with a halogen lamp. After each heating step, purified He was analyzed on either a MAP-215-50 or GV-SFT mass spectrometer using standard procedures (Shuster and Farley, 2005).

Copper foil packets were then removed from the diffusion-cell, wrapped in Sn foil, and transferred to a resistance furnace for complete degassing of the sample at ~ 1200 °C.

System blanks were measured at the beginning of each run (also throughout the run for samples containing small amounts of gas) and measured values subtracted from gas released in each heating step. To obviate problems associated with gas released by the sample during pumping under ultra-high vacuum, Waltenberg (2013) applied a slightly different blank correction procedure by measuring the gas in an empty sample chamber before the start of the heating-experiment. Standard gas aliquots were measured several times during an incremental heating experiment. Temperature cycling was applied to all samples.

4. RESULTS

4.1. Goethite Composition

Stoichiometric goethite should contain 62.86 wt% Fe, 36.02 wt% O, and 1.13 wt% H, and EM results should add to ~ 98.9 wt%, as H is not measured. Our totals range from 97.0 to 101.9 wt%, suggesting some elemental deficits and apparent excesses. As electron microprobe results were frequently standardized, and standards analyzed as unknowns yield results indistinguishable from their accepted values, we conclude that the excesses and deficiencies are real features in our samples. Iron contents are consistent with a goethite composition, although some grains also appear to contain minor hematite, kaolinite, and gibbsite. Excesses probably reflect analysis at the boundary between goethite and contaminants (gibbsite, kaolinite, hematite, etc.) (Maaskant and Kaper, 1991).

Natural goethites are solid solutions incorporating divalent and trivalent cations, particularly Al, V, Ti, Cr, Mn, Cu, Zn and Pb substituting for Fe^{3+} (Schwertmann et al. 1989; Cornell, 1991; Cornell and Schwertmann, 1996; Manceau et al., 2000; Schroth and Parnell, 2005). The positively skewed Al+V+Ti+Cr+Mn+Si+Cu+Pb and the negatively skewed Fe distributions (Figure 3a) in our data are consistent with this model. The most abundant substituting metal in our samples is Al (Figure 3b), followed by Mn, Cu, Ni, Cr, Pb, and minor Ti (Table 1). These minor and trace metals provide useful environmental fingerprints. Al-rich goethites (Table 1; EA1) form in proximity to clay minerals in soil horizons and detrital deposits, and they often also contain Ti (e.g., Lynn Peak samples). Cu-rich goethites precipitate in the oxidation zone overlying Cu-Au deposits (e.g., Igarapé Bahia samples). Ni- and Cr-rich goethites originate from weathered ultramafic rocks in Ni-laterite deposits (Ravensthorpe samples).

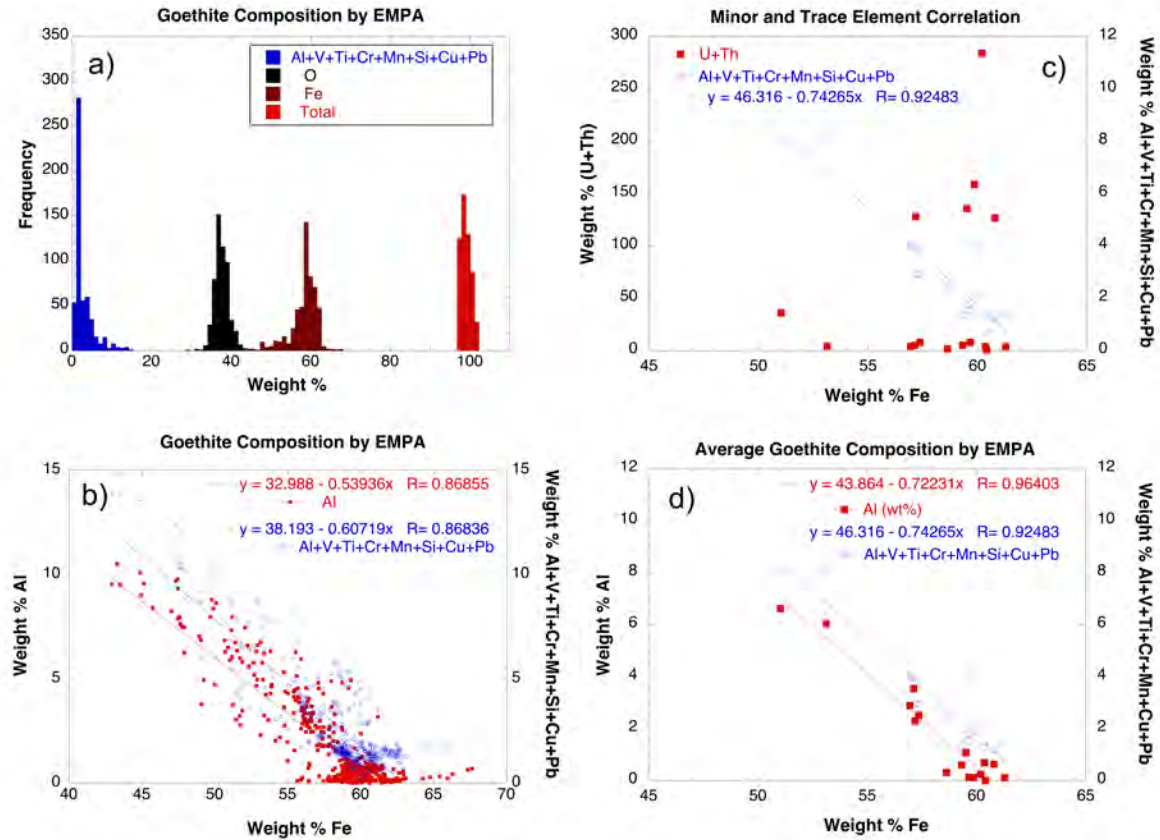


Figure 3: (a) Histogram illustrating chemical composition variation for all goethites analyzed in this study. (b) The strong correlation between Al+V+Ti+Cr+Mn+Si+Cu+Pb with Fe suggests incorporation of these elements in the goethite structure.

Table 1 - Electron Microprobe Analyses of representative goethite grains from each sample investigated.

Sample Name	O	Na	P	V	Ti	Mg	S	Cr	Mn	Al	K	Ni	Fe	Si	Ca	Cu	Co	Sr	Ba	Zn	Pb	Total	# of analysis
Capão L4 (G1)	35.25	0.02	0.01	-	0.01	0.12	0.02	0.01	0.05	0.15	0.01	0.01	62.29	1.24	0.00	0.02	0.07	0.01	0.03	0.02	0.25	99.59	15
±	0.89	0.02	0.01	-	0.02	0.02	0.01	0.02	0.02	0.02	0.01	0.02	0.49	0.06	0.00	0.03	0.01	0.02	0.03	0.02	0.07	1.26	
Capão L4 (G2)	36.77	0.02	0.01	0.01	0.00	0.10	0.01	0.01	0.05	0.11	0.01	0.01	60.79	1.13	0.00	0.03	0.07	-	-	0.01	0.26	99.40	6
±	1.07	0.03	0.01	0.02	0.00	0.01	0.01	0.01	0.02	0.02	0.01	0.01	0.54	0.08	0.00	0.02	0.01	-	-	0.02	0.04	1.00	
Capão L4 (G3)	36.33	0.08	0.02	0.00	0.01	0.10	0.00	0.00	0.04	0.10	0.00	0.00	60.31	1.17	0.00	0.03	0.06	-	-	0.02	0.26	98.53	6
±	1.16	0.06	0.02	0.00	0.01	0.01	0.01	0.00	0.02	0.01	0.01	0.01	0.31	0.09	0.00	0.02	0.02	-	-	0.02	0.04	1.37	
Capão L4 (G4)	35.54	-0.02	0.02	-0.01	-0.01	0.10	0.05	0.00	0.05	0.13	0.00	0.01	61.77	1.08	-0.05	0.01	0.07	-	-	0.03	0.24	99.01	20
±	0.31	0.02	0.04	0.03	0.02	0.02	0.14	0.01	0.03	0.01	0.01	0.03	0.48	0.05	0.01	0.03	0.02	-	-	0.05	0.06	0.74	
Capão L5 (G1)	37.64	0.02	0.02	0.02	0.01	0.30	0.02	0.00	0.10	0.32	0.00	0.01	58.64	1.81	0.05	0.10	0.09	0.00	0.02	0.04	0.24	99.45	8
±	0.51	0.02	0.01	0.03	0.02	0.04	0.01	0.01	0.03	0.06	0.00	0.01	0.33	0.10	0.01	0.03	0.05	0.01	0.02	0.03	0.07	0.50	
IBH-13-09h (G1)_Goe a	38.57	0.01	0.10	0.03	0.05	0.01	0.09	0.02	0.01	3.08	0.00	0.00	56.26	0.23	0.00	0.02	0.07	0.01	0.01	0.03	0.03	98.62	3
±	0.31	0.01	0.02	0.04	0.03	0.01	0.00	0.02	0.01	0.46	0.00	0.00	0.19	0.02	0.00	0.03	0.03	0.00	0.01	0.02	0.05	0.65	
IBH-13-09h (G1)_Goe b	40.73	0.00	0.15	0.07	0.14	0.00	0.09	0.02	0.03	7.22	0.00	0.01	48.70	1.77	0.00	0.03	0.04	0.01	0.01	0.02	0.04	99.11	15
±	0.95	0.01	0.04	0.06	0.12	0.01	0.02	0.02	0.02	1.32	0.01	0.01	3.02	1.18	0.00	0.03	0.03	0.01	0.02	0.03	0.05	0.51	
IBH-13-09h (G2)	39.25	-	0.11	0.09	0.15	0.00	0.10	0.03	0.02	5.84	-	-	50.23	0.44	-	0.02	0.04	-	-	-	0.04	96.38	10
±	0.49	-	0.02	0.03	0.08	0.01	0.02	0.03	0.02	0.67	-	-	1.44	0.41	-	0.03	0.02	-	-	-	0.04	0.36	
IBH-13-09h (G3)	40.21	0.01	0.16	-	0.15	0.01	0.12	0.02	0.02	7.80	0.01	0.00	49.83	1.77	0.00	0.02	0.04	0.01	0.04	0.01	0.02	100.24	19
±	1.16	0.01	0.04	-	0.09	0.01	0.02	0.03	0.02	1.90	0.01	0.01	3.56	1.13	0.00	0.02	0.03	0.01	0.04	0.02	0.03	0.93	
IBH-13-09h (G4)	40.25	0.01	0.11	0.10	0.11	0.01	0.13	0.03	0.01	6.23	-	0.00	53.07	1.05	0.00	0.03	0.05	-	-	0.02	0.03	101.24	10
±	0.78	0.02	0.03	0.02	0.08	0.01	0.01	0.02	0.01	1.32	-	0.01	2.58	0.71	0.00	0.02	0.03	-	-	0.02	0.05	0.95	
Win-06-01B (G1)	36.73	-	0.07	0.00	0.01	0.04	0.01	0.01	0.26	0.20	-	-	58.54	1.01	-	0.05	0.07	-	-	-	0.06	97.06	15
±	1.04	-	0.02	0.01	0.02	0.03	0.01	0.01	0.03	0.05	-	-	0.60	0.05	-	0.04	0.03	-	-	-	0.05	1.53	
Win-06-01B (G2)	36.15	-	0.06	0.01	0.01	0.04	0.02	0.00	0.23	0.11	-	-	58.78	0.99	-	0.02	0.10	-	-	-	0.04	96.55	14
±	0.96	-	0.03	0.01	0.02	0.02	0.01	0.01	0.05	0.06	-	-	0.29	0.08	-	0.03	0.04	-	-	-	0.04	1.13	
Win-06-01B (G3)	36.28	-	0.05	0.01	0.02	0.04	0.01	0.01	0.24	0.13	-	-	59.07	0.90	-	0.02	0.09	-	-	-	0.04	96.90	15
±	0.59	-	0.03	0.01	0.02	0.02	0.01	0.01	0.06	0.07	-	-	0.53	0.26	-	0.03	0.04	-	-	-	0.03	0.61	
Win-06-01B (G4)	36.76	-	0.04	0.02	0.01	0.03	0.01	0.02	0.23	0.12	-	-	58.70	1.10	-	0.03	0.06	-	-	-	0.03	97.16	15
±	0.56	-	0.02	0.02	0.01	0.02	0.01	0.02	0.04	0.01	-	-	0.38	0.04	-	0.03	0.04	-	-	-	0.04	0.73	
Win-06-01B (G5)	36.65	-	0.05	0.01	0.02	0.02	0.02	0.01	0.25	0.13	-	-	58.29	1.20	-	0.01	0.06	-	-	-	0.04	96.76	15
±	0.43	-	0.02	0.01	0.02	0.02	0.01	0.01	0.03	0.04	-	-	0.35	0.05	-	0.02	0.04	-	-	-	0.05	0.53	
Win-06-01B (G6)	37.06	-	0.06	0.01	0.01	0.03	0.01	0.01	0.24	0.16	-	-	58.48	1.07	-	0.03	0.07	-	-	-	0.02	97.26	15
±	0.73	-	0.03	0.02	0.02	0.01	0.01	0.02	0.04	0.02	-	-	0.20	0.13	-	0.03	0.04	-	-	-	0.04	0.86	
Win-06-01B (G7)	36.37	-	0.06	0.01	0.02	0.03	0.01	0.02	0.25	0.17	-	-	58.33	1.07	-	0.01	0.08	-	-	-	0.03	96.45	15
±	0.19	-	0.02	0.01	0.02	0.01	0.01	0.02	0.02	0.02	-	-	0.33	0.07	-	0.02	0.03	-	-	-	0.04	0.37	
Win-06-01B (G8)	37.01	0.02	0.05	-	0.02	0.07	0.02	0.01	0.25	0.15	0.01	0.01	62.50	1.02	0.12	0.02	0.08	0.01	0.03	0.01	0.05	101.45	15
±	0.58	0.02	0.02	-	0.02	0.04	0.02	0.02	0.07	0.06	0.01	0.02	0.40	0.15	0.31	0.02	0.03	0.02	0.04	0.03	0.05	0.63	
Win-06-01B (G9)	36.96	0.02	0.05	-	0.02	0.03	0.01	0.01	0.25	0.09	0.01	0.01	62.28	0.92	0.00	0.02	0.08	0.01	0.04	0.02	0.02	100.86	10
±	0.46	0.02	0.02	-	0.03	0.01	0.01	0.02	0.03	0.01	0.01	0.03	0.26	0.01	0.00	0.02	0.04	0.01	0.04	0.03	0.03	0.50	
Win-06-01B (G10)	36.98	0.02	0.05	-	0.02	0.04	0.01	0.01	0.29	0.10	0.00	0.00	62.06	1.12	0.00	0.02	0.08	0.01	0.04	0.05	0.04	100.93	10
±	0.30	0.01	0.02	-	0.03	0.01	0.01	0.01	0.03	0.01	0.01	0.01	0.48	0.02	0.00	0.03	0.03	0.01	0.04	0.05	0.03	0.65	
S 3.4 TLcM_BG grain 1	36.99	0.10	0.01	0.03	0.16	0.17	0.03	0.26	0.01	6.04	0.02	0.57	53.14	1.59	0.00	0.02	0.07	-	0.01	0.02	0.01	99.25	9
±	1.96	0.05	0.01	0.02	0.03	0.03	0.01	0.04	0.01	0.62	0.01	0.17	2.56	0.30	0.00	0.02	0.02	-	0.02	0.02	0.02	1.13	
S 3.4 TLcM_BG grain 2	36.72	0.65	0.00	0.02	0.03	0.12	0.03	0.20	0.02	2.89	0.01	0.56	56.95	0.79	0.00	0.02	0.05	-	0.02	0.03	0.04	99.14	10
±	0.63	1.10	0.01	0.02	0.03	0.04	0.02	0.11	0.01	0.59	0.01	0.28	0.93	0.17	0.00	0.02	0.02	-	0.03	0.03	0.05	0.87	
Pic-06-21 (G1)†	39.16	0.01	0.10	-	0.03	0.00	0.13	0.02	0.01	3.42	0.00	0.00	57.52	0.23	0.00	0.01	0.05	0.01	0.02	0.02	0.01	100.75	15
±	0.32	0.01	0.02	-	0.03	0.00	0.03	0.03	0.02	0.36	0.00	0.00	0.67	0.06	0.00	0.03	0.03	0.02	0.03	0.03	0.03	0.43	
Pic-06-21 (G2)‡	38.60	0.02	0.06	0.01	0.02	0.01	0.05	0.01	0.00	2.34	0.00	0.01	57.35	0.32	0.00	0.01	0.05	-	-	0.01	0.02	98.91	11
±	0.36	0.03	0.02	0.01	0.02	0.01	0.01	0.01	0.01	0.83	0.00	0.01	1.06	0.07	0.00	0.02	0.02	-	-	0.02	0.03	0.81	
Pic-06-21 (G3)†	38.89	0.05	0.12	0.01	0.13	0.01	0.03	0.01	0.00	1.81	0.01	0.02	57.25	0.27	0.00	0.01	0.06	-	-	0.03	0.03	98.73	10
±	0.15	0.06	0.03	0.01	0.01	0.01	0.01	0.01	0.01	0.03	0.01	0.02	0.14	0.01	0.00	0.02	0.02	-	-	0.02	0.03	0.21	
Pic-06-21-Al-poor (G4)*	37.34	0.02	0.01	0.00	0.00	0.00	0.01	0.01	0.00	0.01	0.00	0.00	60.42	0.61	0.00	0.00	0.06	-	-	0.01	0.02	98.56	6
±	0.45	0.02	0.02	0.01	0.00	0.01	0.01	0.01	0.01	0.01	0.01	0.01	1.16	0.06	0.00	0.01	0.02	-	-	0.02	0.04	1.33	
Pic-06-22-BG (G1)**	37.01	0.01	0.12	0.02	0.02	0.01	0.03	0.01	0.02	0.61	0.00	0.01	59.33	0.61	0.00	0.02	0.06	-	-	0.02	0.04	97.95	50
±	0.67	0.02	0.03	0.02	0.02	0.02	0.02	0.01	0.03	0.19	0.01	0.01	0.55	0.16	0.00	0.02	0.03	-	-	0.03	0.05	0.75	
Pic-06-22-YG (G1)+	35.66	0.03	0.10	0.01	0.02	0.02	0.05	0.01	0.02	0.70	0.00	0.01	60.36	0.42	0.00	0.03	0.07	-	-	0.02	0.05	97.60	49
±	0.68	0.04	0.03	0.02	0.03	0.02	0.02	0.02	0.03	0.19	0.01	0.02	0.91	0.12	0.00	0.03	0.03	-	-	0.03	0.05	0.64	
Pic-06-24 (G1)	38.30	0.05	0.44	0.02	0.06	0.04	-	0.01	0.02	3.55	0.01	0.01	57.14	0.19	0.00	0.03	0.06	-	0.02	0.02	0.05	100.01	45
±	1.44	0.05	0.11	0.03	0.09	0.04	-	0.02	0.02	0.79	0.01	0.02	1.60	0.09	0.0								

Elemental substitution for Fe often correlates with Th and U abundances. For example, Al-Ti-rich goethites are preferentially enriched in Th (Vasconcelos et al., 2013; Monteiro et al., 2014) because dissolution of primary minerals and leaching of more soluble elements progressively enrich the near-surface environment with Al, Ti, and Th. Our summary results do not show any clear correlation between Al+Ti vs U+Th for our entire sample set, but for individual weathering profiles, Al, Ti, and Th simultaneously enrich towards the surface. For example, sample IBH-13-09h, a fragment of ferruginous duricrust from a deep soil profile (~10 m depth) in the Igarapé Bahia gold deposit, contains patchy impure colloform Al-Ti-Th-rich goethite (Figure 2ak), and it is relatively enriched in Th (23.9 ppm) as compared to U (12.2 ppm). In contrast, U is relatively depleted near the surface and enriched at depth. Samples BAH-F124-111.2 and 114, from the same profile, occur as cavity-fills at ~ 70-80 m below the surface, and they are extremely rich in U (150-300 ppm) and poor in Th (0.01 to 0.03 ppm), confirming the effective transport of U as $\text{UO}_2^{+2}(\text{aq})$ in the oxidizing solutions and the residual enrichment of virtually insoluble Th at the surface. These goethites are rich in P, which correlates positively with U. Interestingly, analytical results for our entire sample set shows a direct correlation between U and P content. It is unclear whether U is bound to nano-inclusions of phosphates in goethite, or whether PO_4^{-3} replaces OH^- sites in the goethite structure, possibly increasing goethite's tendency to incorporate U.

Enrichment in Al, Ti, and Th also occurs at Lynn Peak (Table 1), where goethite forms by recurrent dissolution-precipitation of detrital minerals in a channel iron deposit. Ravensthorpe goethites, on the other hand, formed by in situ weathering of olivine and pyroxene, are preferentially enriched in Al, Ni, Cr, and Ti, where some of these elements are directly inherited from refractory spinels, particularly chromite, derived from the ultramafic bedrock.

The persistence and incorporation of some of refractory mineral contaminants inherited from the bedrock, such as ilmenite, hematite, chromite, rutile, or zircon, will have a significant effect on the (U-Th)/He and $^4\text{He}/^3\text{He}$ results, as discussed below.

A curious aspect of all goethites is their consistent enrichment in Si, independently of mode of precipitation, geological environment, or position within the weathering profile. As the small and highly charged Si^{4+} ion does not easily fit into Fe^{3+} -sites in goethite, it is likely that Si occurs in a separate phase intimately intergrown with goethite (Glasauer et al., 1999). The absence of any measurable SiO_2 polymorph in XRD diffraction patterns (even high-sensitivity synchrotron XRD) and the homogeneous distribution of Si throughout the sample suggest an amorphous silica thin film coating goethite microcrystallites.

4.2. Goethite Crystallinity

4.2.1. XRD

X-ray diffractometry reveals a direct correlation between goethite crystallinity, as determined by the height and width of major peaks, and Al content. The most crystalline goethites (BAH, Capão, Roy and Winsor) are Al-poor (Figure 4). As Al contents increase, crystallinity decreases. Al-rich goethites often coexist with gibbsite and kaolinite (Figure 4). Minor hematite is also present in some samples, but hematite occurs both in well-crystallized and poorly crystalline goethite. Despite the presence of Si in all samples, no quartz or SiO₂ polymorphs are detectable in the XRD results.

4.2.2. TGA

Thermogravimetric analysis shows that our goethite samples undergo phase transformation to hematite over a wide temperature range (from 250 to 400 °C) (Figure 5). The most crystalline and pure Fe goethites (e.g., samples Capão L2, L3, or L4) undergo phase transformations at higher temperatures and within narrower ranges, while poorly crystalline Al-rich goethites display broader ranges of phase transformation temperatures (Figure 5).

4.3. (U-Th)/He Ages

In addition to varying in modes of precipitation, composition, crystallinity, and temperatures of phase transformation, the samples investigated also range widely in (U-Th)/He ages (from 1 to 300 Ma) and in U (0.1 to ~ 300 ppm) and Th (0.02 to ~ 100 ppm) contents (Table 2). Many samples analyzed multiple times yield reproducible results (e.g., BAH-F124-111.2B, Capão L2, IBH-13-09h), but some samples yield discrepant (U-Th)/He ages for distinct aliquots (e.g., Capão L3, Pic 06 24; Table 2). We will discuss the possible causes for variability in (U-Th)/He ages below. An important observation is that (U-Th)/He ages for individual samples or study sites cluster within discrete age ranges [e.g., all Capão samples are old (~ 300 Ma), all Roy Hill samples are intermediate (~70-55 Ma), while all Ravensthorpe samples are young (~ 8-4 Ma) revealing a high degree of internal consistency in the results.

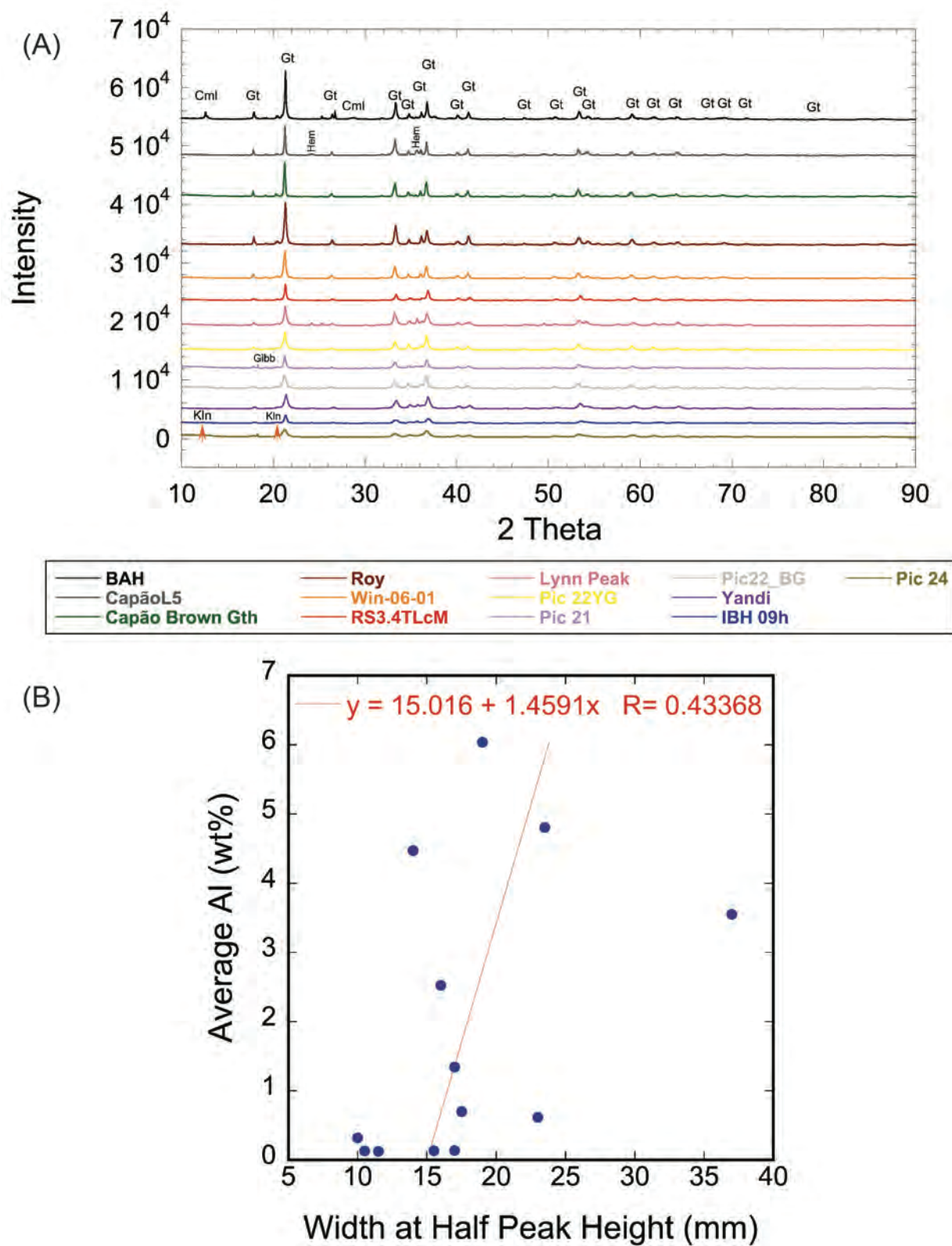


Figure 4: Powder XRD patterns (A) for goethite samples investigated in this study show a positive correlation (B) between Al contents and the decrease in goethite crystallinity/crystallite size.

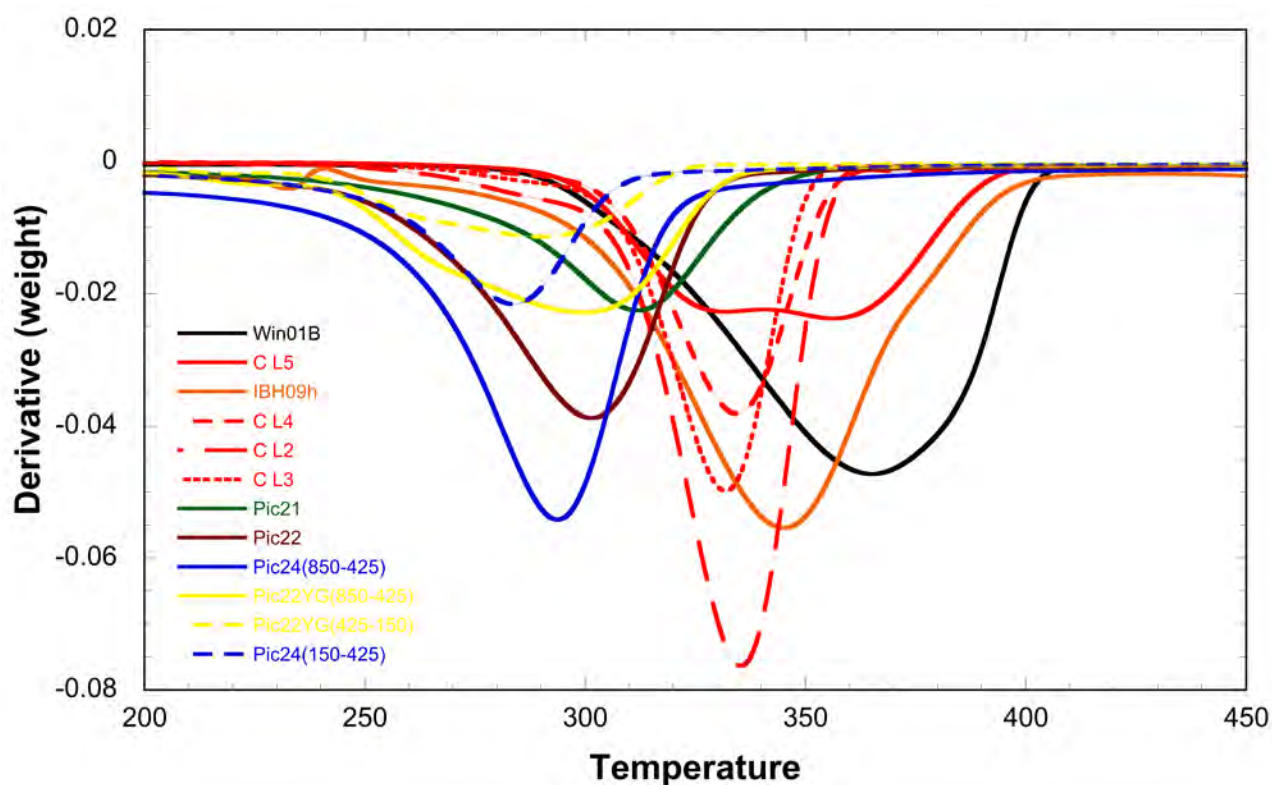


Figure 5: Thermogravimetric analyses for goethites investigated in this study reveal a wide range in temperatures of phase transformation. There are two clear distinct groups, pure well-crystallized goethites that undergo phase transformation at ~ 330 °C or greater and poorly crystalline porous often Al-rich goethites that undergo phase transformations below 300 °C.

Table 2: (U-Th)/He ages

Sample Name	Corr Age (Ma)	$\pm 1 \sigma$	U ppm	$\pm 1 \sigma$	Th ppm	$\pm 1 \sigma$	He nmol/g	$\pm 1 \sigma$	Th/U
BAH-F124-111.2B	41.7	0.5	28.24		0.14		6.44		0.0050
BAH-F124-111.2B	41.6	0.5	59.67		0.20		13.54		0.0034
BAH-F124-111.2B	41.2	0.5	77.69		0.02		17.45		0.0003
BAH-F124-111.2B	43.2	0.5	96.97		0.05		22.88		0.0005
BAH-F124-111.2B	43.7	0.5	103.44		0.05		24.66		0.0005
BAH-F124-111.2B	44.4	0.7	70.29		0.02		17.02		0.0003
Average	42.6		72.7		0.1				
2 σ	2.6		54.5		0.1				
BAH-F124-114	9.7	0.1	149.53		0.05		7.85		0.0003
BAH-F124-114	10.0	0.1	152.79		0.03		8.33		0.0002
BAH-F124-114	11.7	0.1	120.30		0.00		7.63		0.0000
BAH-F124-114	10.1	0.1	156.17		0.00		8.56		0.0000
BAH-F124-114	9.9	0.1	154.71		0.01		8.31		0.0001
BAH-F124-114	10.1	0.1	162.31				8.95		
BAH-F124-114	9.9	0.1	155.80				8.39		
BAH-F124-114	10.8	0.1	15.79				0.93		
BAH-F124-114	10.3	0.1	160.46				9.02		
BAH-F124-114	10.2	0.1	325.63		0.03		18.02		0.0001
BAH-F124-114	10.7	0.1	368.81		0.05		21.47		0.0001
BAH-F124-114	10.95	0.1	329.83		0.02		19.64		0.0001
BAH-F124-114	11.36	0.1	288.13		0.01		17.80		0.0000
BAH-F124-114	11.86	0.1	250.95		0.02		16.18		0.0001
BAH-F124-114	10.63	0.2	312.68		0.03		18.08		0.0001
BAH-F124-114	10.81	0.1	265.29		0.06		15.60		0.0002
BAH-F124-114	11.74	0.2	246.92				15.77		
BAH-F124-114	13.89	0.1	260.23		0.03		19.67		0.0001
BAH-F124-114	10.17	0.1	280.50		0.01		15.51		0.0000
BAH-F124-114	10.26	0.1	269.60		0.03		15.05		0.0001
BAH-F124-114	10.69	0.1	282.26		0.02		16.41		0.0001
BAH-F124-114	10.79	0.1	272.72		0.02		16.00		0.0001
BAH-F124-114	8.97	0.1	265.23		0.02		12.93		0.0001
Average	10.7		228.1		0.02				
2 σ	2.0		169.3		0.03				
Capao L2	268.8	6.9	5.50	0.09	0.62	0.04	8.50	0.19	0.11
Capao L2	270.2	7.1	5.18	0.09	0.59	0.04	8.06	0.17	0.11
Capao L2	275.1	6.6	5.70	0.08	0.63	0.03	9.03	0.27	0.11
Capao L2	282.3	7.2	5.33	0.09	0.63	0.04	8.69	0.20	0.12
Capao L2	276.5	6.5	5.59	0.07	0.59	0.03	8.88	0.29	0.10
Average	274.6		5.5		0.61				
2 σ	10.7		0.4		0.04				

Table 2: (U-Th)/He ages

Sample Name	Corr Age (Ma)	$\pm 1 \sigma$	U ppm	$\pm 1 \sigma$	Th ppm	$\pm 1 \sigma$	He nmol/g	$\pm 1 \sigma$	Th/U
Capão L3	304.5	7.9	3.83	0.06	0.41	0.03	6.74	0.20	0.11
Capão L3	272.3	9.6	2.78	0.08	0.12	0.06	4.30	0.05	0.04
Capão L3	266.0	7.8	2.68	0.06	0.13	0.03	4.04	0.10	0.05
Capão L3	267.2	7.4	2.54	0.05	0.12	0.02	3.85	0.13	0.05
Capão L3	302.6	7.8	3.34	0.05	0.24	0.02	5.79	0.21	0.07
Capão L3	330.2	8.0	4.19	0.06	0.53	0.03	8.05	0.31	0.13
Capão L3	273.4	6.5	5.31	0.07	0.45	0.03	8.30	0.28	0.09
Average	288.0		3.5		0.29				
2σ	49.3		2.0		0.35				
Capão L4	285.9	7.9	3.44	0.07	0.32	0.03	5.64	0.14	0.09
Capão L4	292.3	7.7	3.70	0.06	0.38	0.03	6.23	0.18	0.10
Capão L4	286.5	7.6	3.56	0.06	0.33	0.03	5.85	0.17	0.09
Capão L4	289.7	7.0	4.70	0.06	0.40	0.02	7.81	0.28	0.09
Capão L4	274.2	6.3	5.06	0.06	0.46	0.02	7.94	0.32	0.09
Capão L4	275.6	6.7	3.07	0.04	0.27	0.02	4.86	0.26	0.09
Capão L4	278.8	6.7	4.04	0.05	0.37	0.02	6.46	0.26	0.09
Average	283.3		3.9		0.36				
2σ	14.1		1.4		0.12				
Capão L5	205.7	6.6	2.37	0.06	0.11	0.03	2.75	0.06	0.05
Capão L5	217.2	7.2	1.69	0.04	0.07	0.03	2.07	0.05	0.04
Capão L5	261.1	7.2	1.85	0.04	0.08	0.02	2.75	0.13	0.04
Capão L5	244.3	7.3	1.56	0.03	0.03	0.02	2.15	0.09	0.02
Capão L5	209.9	5.3	2.16	0.03	0.06	0.01	2.55	0.16	0.03
Capão L5	259.2	5.7	7.03	0.06	0.81	0.03	10.48	0.42	0.11
Capão L5	220.0	5.9	1.85	0.03	0.04	0.01	2.30	0.13	0.02
Capão L5	253.6	6.0	6.65	0.08	0.73	0.03	9.67	0.28	0.11
Average	233.9		3.1		0.24				
2σ	46.1		4.6		0.66				
IBH-13-09h gr1	34.2	0.8	15.97	0.16	26.35	0.36	4.14	0.06	1.65
IBH-13-09h gr2	38.6	0.9	12.09	0.17	23.35	0.34	3.70	0.05	1.93
IBH-13-09h gr3	35.2	0.9	8.64	0.13	22.02	0.31	2.65	0.04	2.55
Average	36.0		12.2		23.91				
2σ	4.6		7.3		4.44				

Table 2: (U-Th)/He ages

Sample Name	Corr Age (Ma)	$\pm 1 \sigma$ U ppm	$\pm 1 \sigma$ Th ppm	$\pm 1 \sigma$ He nmol/g	$\pm 1 \sigma$ Th/U
Lynn Peak-9-A1 ⁺	32.4	34.95	81.92	9.58	2.34
Lynn Peak-9-A1 ⁺	29.2	41.37	93.43	10.07	2.26
Lynn Peak-9-A1 ⁺	30.4	38.64	90.82	9.94	2.35
Lynn Peak-9-A2 ⁺	30.2	38.32	86.93	9.67	2.27
Lynn Peak-9-A2 ⁺	31.1	36.34	102.19	10.23	2.81
Lynn Peak-9-A2 ⁺	30.7	35.72	85.20	9.33	2.39
Lynn Peak-9-A3 ⁺	29.2	38.60	98.65	9.82	2.56
Lynn Peak-9-A4 ⁺	30.3	39.96	91.51	10.15	2.29
Lynn Peak-9-A5 ⁺	32.7	40.21	98.09	11.27	2.44
Lynn Peak-9-A6 ⁺	29.2	29.53	64.04	7.08	2.17
Lynn Peak-9-A7 ⁺	28.0	27.53	54.58	6.15	1.98
Lynn Peak-9-A8 ⁺	26.8	37.32	70.72	7.87	1.89
Average	30.0	36.5	84.84		
2 σ	3.4	8.4	29.43		

Pic-06-24/1 [‡]	14.7	0.5	4.56	0.08	3.39	0.07	0.43	0.01	0.74
Pic-06-24/2 [‡]	6.7	0.3	4.43	0.08	0.84	0.04	0.17	0.01	0.19
Pic-06-24/4 [‡]	10.4	0.4	4.53	0.08	0.77	0.04	0.27	0.01	0.17
Pic-06-24/5 [‡]	20.7	0.9	2.24	0.05	0.52	0.04	0.27	0.01	0.23
Average	13.1	3.9	1.38						
2 σ	12.0	2.3	2.69						

Pic 06 22 gr1_black	18.5	0.4	5.02	0.07	0.16	0.02	0.51	0.02	0.03
Pic 06 22 gr2_black	22.2	0.5	3.86	0.05	0.37	0.02	0.48	0.02	0.10
Pic 06 22 gr3_black	14.5	0.3	5.84	0.04	0.16	0.01	0.47	0.03	0.03
Pic 06 22 gr4_black	15.8	0.4	5.80	0.06	0.18	0.02	0.50	0.02	0.03
Average	17.8	5.1	0.22						
2 σ	6.8	1.9	0.20						

Pic 06 22 gr5_yellow	15.9	0.4	4.02	0.06	0.44	0.03	0.36	0.01	0.11
Pic 06 22 gr6_yellow	10.5	0.3	5.21	0.07	0.43	0.03	0.30	0.01	0.08
Pic 06 22 gr7_yellow	12.8	0.3	2.84	0.05	0.29	0.02	0.20	0.01	0.10
Pic 06 22 gr8_yellow	13.9	0.3	3.02	0.04	0.19	0.01	0.23	0.01	0.06
Average	13.2	3.8	0.33						
2 σ	4.5	2.2	0.24						

Table 2: (U-Th)/He ages

Sample Name	Corr Age (Ma)	$\pm 1 \sigma$ U ppm	$\pm 1 \sigma$ Th ppm	$\pm 1 \sigma$ He nmol/g	$\pm 1 \sigma$ Th/U				
Pic-06-21 AlPoor Goe	27.4	1.8	0.23	0.01	0.11	0.02	0.04	0.00	0.49
Pic-06-21 AlPoor Goe	21.3	1.4	0.32	0.01	0.11	0.03	0.04	0.00	0.36
Pic-06-21 AlPoor Goe	24.3	0.8	0.63	0.02	2.57	0.05	0.16	0.01	4.11
Pic-06-21 AlPoor Goe	21.8	0.8	0.29	0.01	1.12	0.03	0.07	0.00	3.83
Pic-06-21 AlPoor Goe	27.5	1.7	0.21	0.01	0.02	0.02	0.03	0.00	0.12
Pic-06-21 AlPoor Goe	27.1	2.1	0.17	0.01	0.07	0.02	0.03	0.00	0.43
Pic-06-21 AlPoor Goe	28.8	1.1	0.26	0.01	1.90	0.04	0.11	0.01	7.27
Pic-06-21 AlPoor Goe	26.9	1.2	0.38	0.02	1.60	0.05	0.11	0.00	4.20
Pic-06-21 AlPoor Goe	32.3	1.6	0.26	0.01	0.47	0.02	0.07	0.00	1.78
Pic-06-21 AlPoor Goe	26.8	1.0	0.38	0.01	1.32	0.03	0.10	0.01	3.44
Pic-06-21 AlPoor Goe	26.8	1.6	0.24	0.01	0.14	0.02	0.04	0.00	0.59
Pic-06-21 AlPoor Goe	27.4	1.7	0.24	0.01	0.62	0.04	0.06	0.00	2.61
Pic-06-21 AlPoor Goe	31.6	2.6	0.11	0.01	0.09	0.02	0.02	0.00	0.84
Pic-06-21 AlPoor Goe	29.7	1.4	0.15	0.01	0.22	0.01	0.03	0.00	1.47
Pic-06-21 AlPoor Goe	48.3	3.0	0.09	0.00	0.10	0.01	0.03	0.00	1.12
Average	27.1	0.3	0.74						
2 σ	6.2	0.3	1.65						
Pic-06-21 FwVG	17.2	0.4	7.61	0.08	28.62	0.31	1.34	0.04	3.76
Pic-06-21 FwVG	16.2	0.4	4.68	0.09	19.35	0.28	0.82	0.01	4.13
Pic-06-21 FwVG	14.3	0.4	4.61	0.09	16.84	0.25	0.66	0.01	3.66
Pic-06-21 FwVG	19.2	0.5	6.00	0.09	25.51	0.31	1.25	0.03	4.25
Pic-06-21 FwVG	17.7	0.5	3.73	0.08	18.47	0.27	0.78	0.01	4.95
Pic-06-21 FwVG	17.7	0.4	4.79	0.08	21.98	0.27	0.96	0.03	4.58
Average	17.0	5.2	21.79						
2 σ	3.3	2.7	9.04						
Pic-06-21_frostedGt	20.6	0.6	2.54	0.06	10.08	0.16	0.55	0.01	3.97
Pic-06-21_frostedGt	25.9	0.8	1.52	0.04	7.32	0.12	0.46	0.01	4.82
Pic-06-21_frostedGt	30.6	0.8	3.95	0.08	16.46	0.25	1.30	0.02	4.16
Pic-06-21_frostedGt	32.1	1.0	1.02	0.03	2.62	0.06	0.29	0.01	2.58
Pic-06-21_frostedGt	30.5	1.2	1.11	0.04	3.79	0.10	0.33	0.01	3.42
Average	27.9	2.0	8.05						
2 σ	9.4	2.5	11.09						
Pic-06-21_vitreousGt	9.7	0.3	5.36	0.10	38.32	0.46	0.75	0.01	7.15
Pic-06-21_vitreousGt	9.6	0.3	5.26	0.10	28.73	0.38	0.62	0.01	5.47
Pic-06-21_vitreousGt	11.3	0.3	3.40	0.07	31.66	0.38	0.67	0.01	9.30
Pic-06-21_vitreousGt	9.5	0.2	6.49	0.06	22.05	0.23	0.60	0.03	3.40
Pic-06-21_vitreousGt	10.0	0.2	8.10	0.11	39.00	0.44	0.94	0.02	4.82
Pic-06-21_vitreousGt	11.7	0.3	5.34	0.10	32.45	0.41	0.82	0.01	6.08
Average	10.3	5.7	32.04						
2 σ	1.9	3.1	12.61						

Table 2: (U-Th)/He ages

Sample Name		Corr Age (Ma)	$\pm 1 \sigma$ U ppm	$\pm 1 \sigma$ Th ppm	$\pm 1 \sigma$ He nmol/g	$\pm 1 \sigma$ Th/U				
Pic-06-21_yellowGt		19.1	0.5	7.59	0.12	20.95	0.30	1.30	0.02	2.76
Pic-06-21_yellowGt		25.5	0.8	2.42	0.06	7.87	0.15	0.59	0.01	3.26
Pic-06-21_yellowGt		29.5	0.8	3.76	0.08	15.51	0.23	1.19	0.02	4.13
Average		24.7		4.6		14.78				
2 σ		10.6		5.4		13.14				
Roy-02-02-B1(a)	+	65.5								0.14
Roy-02-02-B1(b)	+	64.8								0.13
Roy-02-02-B2(a)	+	62.0								0.09
Roy-02-02-B2(a)	+	63.4								0.10
Roy-02-02-B2(a)	+	61.3								0.12
Roy-02-02-B2(a)	+	62.4								0.23
Roy-02-02-B2(a)	+	62.1								0.12
Roy-02-02-B2(a)	+	59.3								0.30
Roy-02-02-B2(a)	+	63.7								0.11
Roy-02-02-B2(a)	+	53.5								0.15
Roy-02-02-B2(a)	+	66.1								0.36
Average		62.2								
2 σ		7.0								
RS 3.4 TLcM gr1		4.0	0.2	0.67	0.02	2.11	0.05	0.03	0.00	3.16
RS 3.4 TLcM gr2		8.2	0.3	1.79	0.04	3.45	0.07	0.12	0.00	1.93
RS 3.4 TLcM gr3		3.7	0.1	1.87	0.04	2.66	0.06	0.05	0.00	1.42
Average		5.3		1.4		2.74				
2 σ		5.0		1.3		1.35				
Winsor		209.7	4.5	8.10	0.06	0.08	0.02	9.47	0.39	0.01
Winsor		202.6	4.5	8.04	0.08	0.07	0.02	9.08	0.29	0.01
Winsor		202.9	4.3	7.94	0.06	0.04	0.02	8.97	0.37	0.01
Winsor		203.5	4.7	7.94	0.09	0.18	0.03	9.03	0.24	0.02
Winsor		187.1	4.4	7.85	0.09	0.09	0.03	8.17	0.21	0.01
Average		201.1		8.0		0.09				
2 σ		16.8		0.2		0.10				
Yan02-01-A(a)	°	10.0	0.3							1.08
Yan02-01-D1(a)	°	13.6	0.4							0.29
Yan02-01-D1(d)	°	13.3	0.4							0.29
Yan02-01-D2(c)	°	10.7	0.3							0.47
Yan02-01-D2(d)	°	11.0	0.3							0.47
Average		11.7								
2 σ		3.2								

* (U-Th)/He ages from Shuster et al. (2005)

‡ (U-Th)/He ages from Monteiro et al. (2014)

+ (U-Th)/He ages from Vasconcelos et al. (2013)

° (U-Th)/He ages from Heim et al. (2006)

4.4 $^4\text{He}/^3\text{He}$ results

4.4.1. $R_{\text{step}}/R_{\text{bulk}}$ and Incremental Heating Spectra

The $^4\text{He}/^3\text{He}$ data are presented as $R_{\text{step}}/R_{\text{bulk}}$ profiles for each sample (Figure 6; EA2), and all the results (EA3) are illustrated as incremental heating spectra (Figure 7) following the procedures of Shuster and Farley (2004). The spectra are organized in increasing degree of complexity, as discussed below.

We plot $R_{\text{step}}/R_{\text{bulk}}$ diagrams with and without blank correction to determine a sample's sensitivity to measured blank. The diagrams illustrate that well crystallized He retentive samples are not sensitive to blank correction. In contrast, the $R_{\text{step}}/R_{\text{bulk}}$ diagrams with or without blank correction differ markedly for poorly crystalline porous goethite (Figure 6; EA2). We conclude that, for these samples, the steps analyzed before the start of the heating procedure are not true blanks as they contain significant amounts of ^3He and ^4He extracted from the pore spaces by pumping under ultra-high vacuum. Accepting these steps as true blanks and subtracting their values from subsequent steps result in erroneous interpretation of a sample's He retention properties, yielding incorrect diffusion parameters. It will also result in $R_{\text{step}}/R_{\text{bulk}}$ diagrams that fail to identify the magnitude of He loss experienced during the sample's geological history. Figure 6 provides the most suitable $R_{\text{step}}/R_{\text{bulk}}$ diagrams for our samples (some with or some without blank corrections) while EA2a and EA2b illustrate $R_{\text{step}}/R_{\text{bulk}}$ diagrams for all samples with and without blanks corrections, respectively.

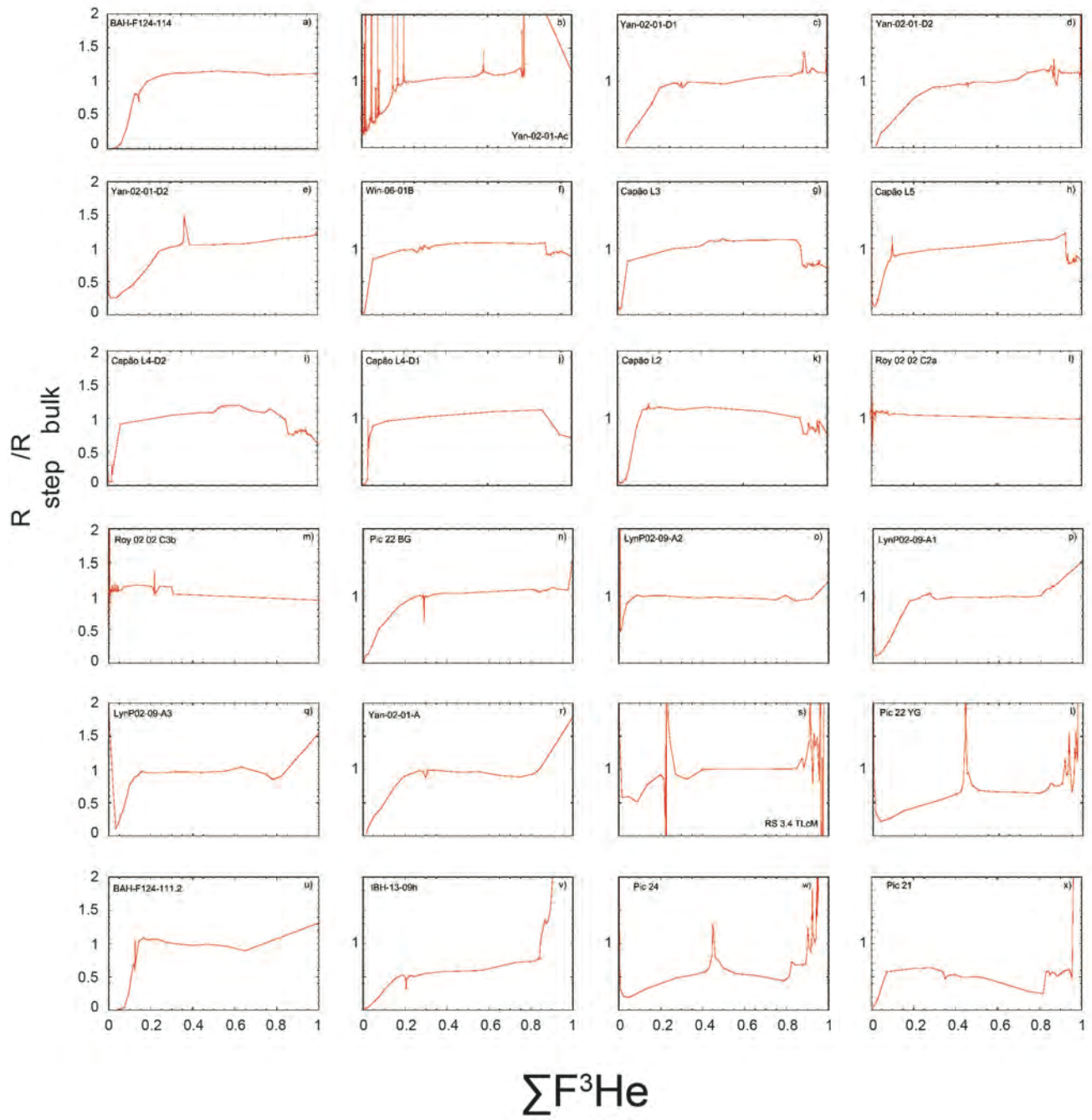


Figure 6: $R_{\text{step}}/R_{\text{bulk}}$ versus Cum F^3He plots illustrate that most samples investigated display ascending spectra that reach relatively well defined plateaus with $R_{\text{step}}/R_{\text{bulk}} \sim 1$. Only poorly crystalline/small crystallite goethites plot significantly below 1, suggesting that these samples display a significantly different He production-release behavior.

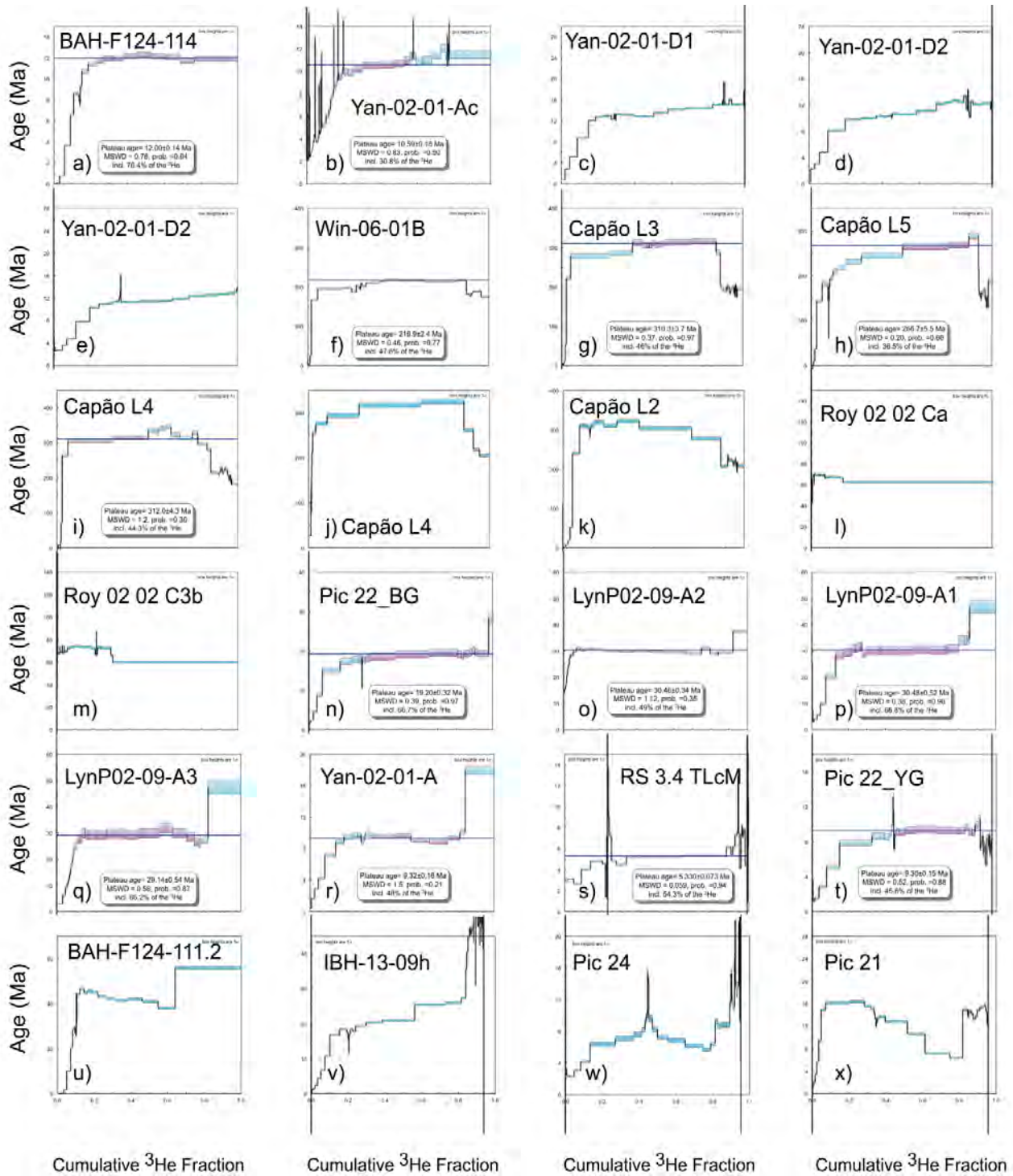


Figure 7: Plateau-age diagrams plotted for all samples with software Isoplot 4.15. Apparent ages for each step in the incremental-heating experiments were calculated by multiplying the average (U-Th)/He age by the $R_{\text{step}}/R_{\text{bulk}}$ ratio for each step. A plateau-age is defined as that part of a spectrum containing, in two or more contiguous steps, $\geq 30\%$ of the total amount of gas released by the sample. Errors for each step are at the 1σ confidence level. Samples in this study yield well-defined flat plateaus (a), identifying pure well crystallized single generation goethite free of contaminants. Figure 7b-e show that all Yandi samples display similar ascending spectra that may or may not reach a plateau. None of these samples show markedly increases in apparent ages in the last step, suggesting that the grains analyzed do not contain significant contents of older contaminants. All Winsor, Capão, and Roy samples (Figure 7f-m) show hump-shaped spectra indicative of grains containing two or more generations of intergrown goethite. Figure 7n-r and u identify samples that define plateaus (or plateau-like segments – 7u) at the intermediate to high temperature steps, but which also show a significant age increase in

the last high-T (1200 °C) step, interpreted as evidence of significant masses of older detrital contaminants. Figures 7s-t illustrate samples that reach plateaus in the intermediate to high temperature steps, possibly contain multiple generations of goethite, and contain very small amounts of much older hypogene contaminants that only release their He budgets in the last high-T (1200 °C) step. Finally, Figures 7v-x show complex spectra for samples that contain many generations of goethite of variable ages and present in different proportions, each releasing their He contents at different temperatures throughout the experiment; these samples also show evidence for significant amounts of old hypogene contaminants in the last step. Plateau ages for samples that contain significant amounts of contaminant must be recalculated by plotting the incremental heating spectra without accounting for the contaminants' contribution (without the last step), as illustrated in Figure 8.

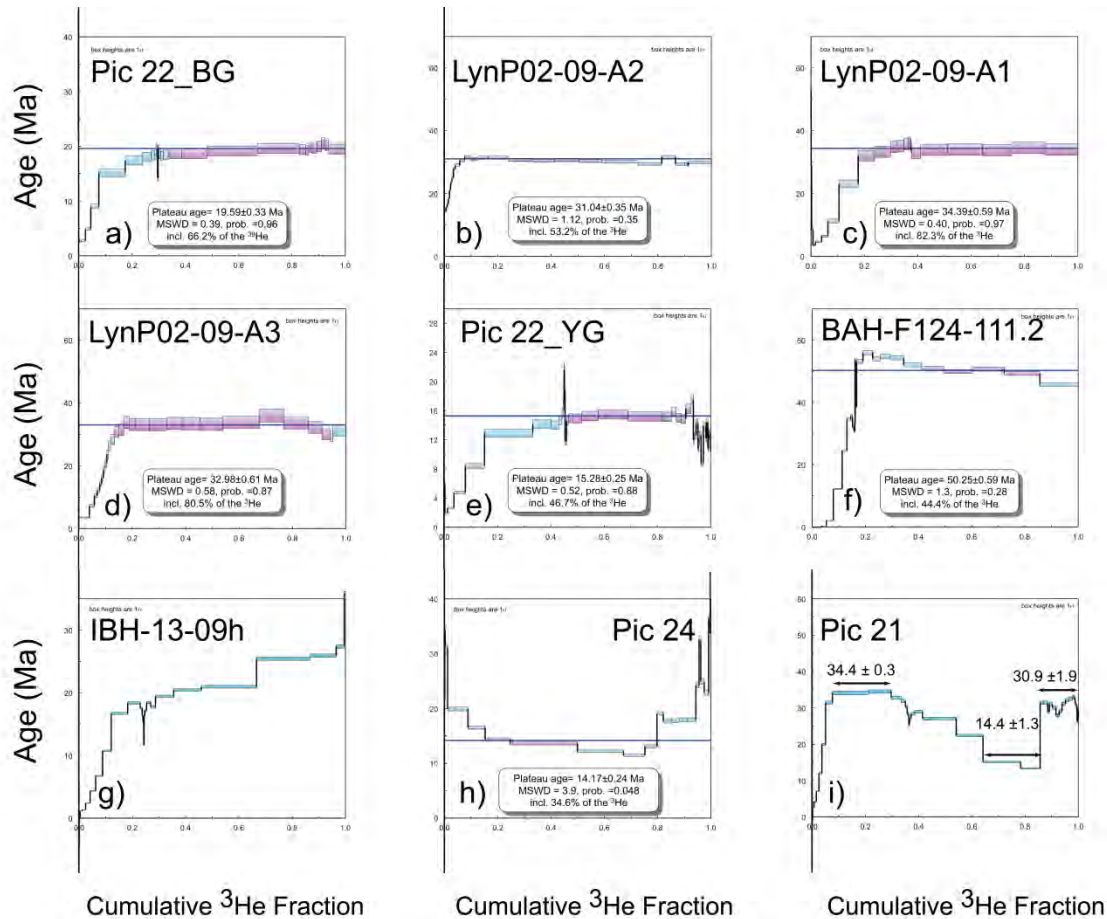


Figure 8: Incremental heating (U-Th)/He-⁴He/³He diagrams plotted for some of the samples illustrated in Figure 7. Samples that showed significant age increases in the last high-T step in Figure 7 were replotted in Figure 8 after deleting the last step and re-calculating the plateau age. Figure 8a-d, f show small increases in plateau ages, while Figure 8e, h-i reveal significant increases in the recalculated plateau ages. The magnitude of the effect of the last step is dependent on the differences in ages between the goethite host and the contaminant. Very old contaminants will significantly affect the plateau age and must be removed before a correct age for the goethite host can be calculated.

4.4.2. Arrhenius plots

Incremental heating ⁴He and ³He experiments were cast in Arrhenius diagrams using the cumulative fraction of each isotope and applying the gas loss equations of Fechtig and Kalbitzer (1966) to derive D/a^2 for each fraction of gas released. The activation energy and frequency factor for the lowest retentivity domain in a sample were calculated from the slope and intercept of a reference line through the low-T steps (Lovera et al., 1991). Additional least-squares straight lines were

drawn through retrograde-prograde step-series at progressively higher temperatures (Figure 9). Arrhenius parameters were derived from the ^3He component since loss of ^4He during a sample's history would induce incorrect parameters (Shuster et al., 2005).

4.4.3. Isothermal Retention Time Diagrams

The Arrhenius parameters were used to calculate isothermal retention times (Figure 10) for all samples following procedures outlined in Wolf et al. (1998) and introduced for goethites by Shuster et al. (2005). Calculations are performed for every domain identified for each sample. All samples show significant amounts of He loss from the low retentivity domains, but most samples (except for PIC-22 YG, PIC-22-BG, PIC 24) reveal that $\geq 80\%$ of the He hosted in the high retentivity domains is retained through a sample lifetime.

5. Discussion

5.1. The occurrence and purity of supergene goethite

Iron is the most abundant element on Earth (32.1%), the fourth most abundant element in the Earth's crust (5-6 wt%), and the third or fourth most abundant element in soils and weathering profiles (1-10 wt%). Therefore, common iron minerals (hematite, magnetite, and goethite) provide an attractive target for geochronology. Goethite typically precipitates as a supergene mineral in soils and weathering profiles. It may also occur as a hypogene phase in hydrothermal veins (Scholten et al., 1991; Iizasa et al., 1998; Dill et al., 2008; Dekov et al., 2009) and pegmatites (Dawns, 2006; Young et al., 2006), but hypogene goethite is rare when compared to weathering-related occurrences. Unfortunately, pure stoichiometric supergene goethite is also rare. Most natural goethites in soils and weathering profiles form by iron metasomatism of other minerals, or by local dissolution-reprecipitation of primary Fe-Mn-Ni-Cu-Al-bearing phases, leading to goethite masses rich in inclusions of other minerals or containing minor and trace elements in solid solution (Figures 1 and 2).

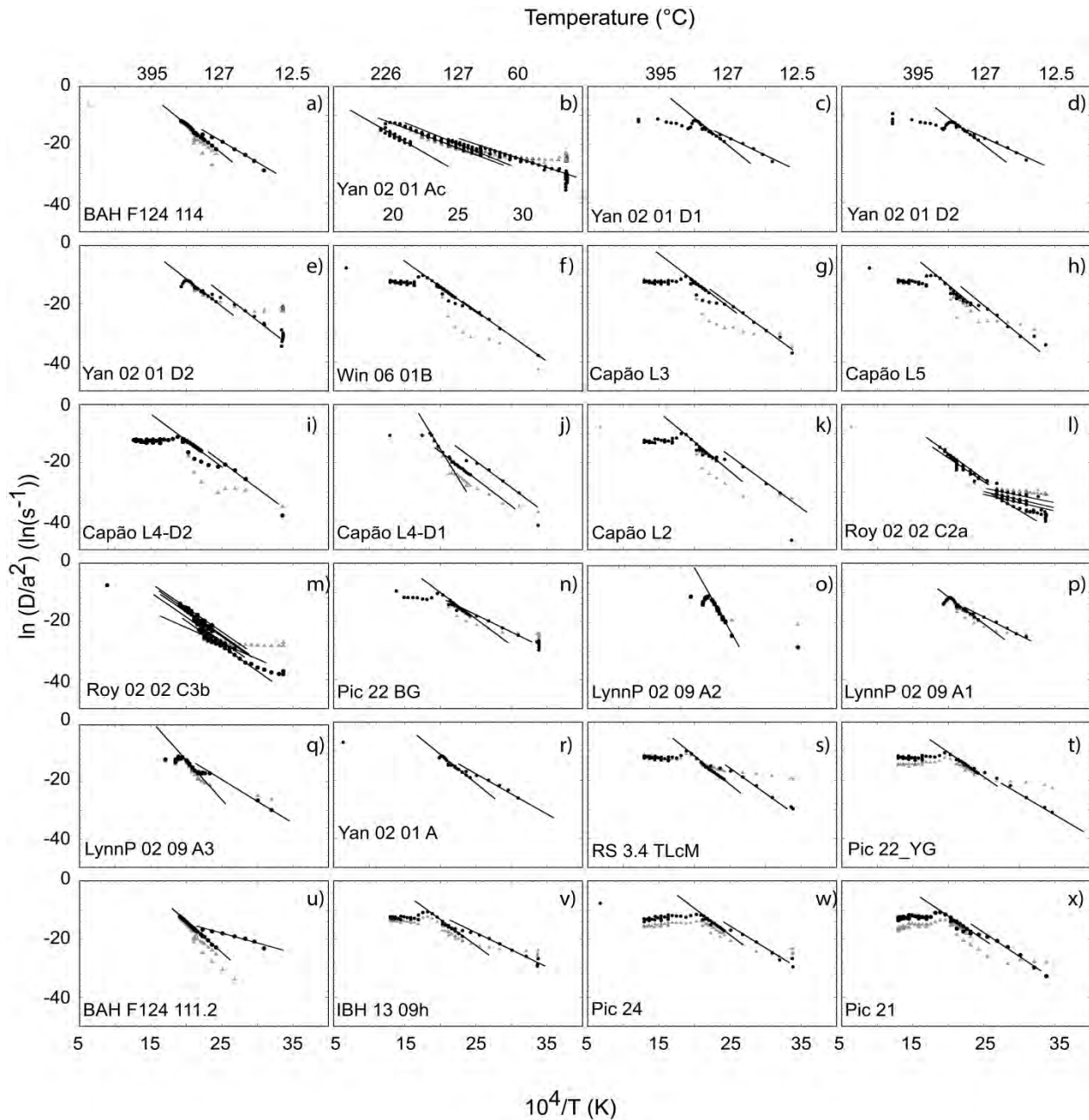
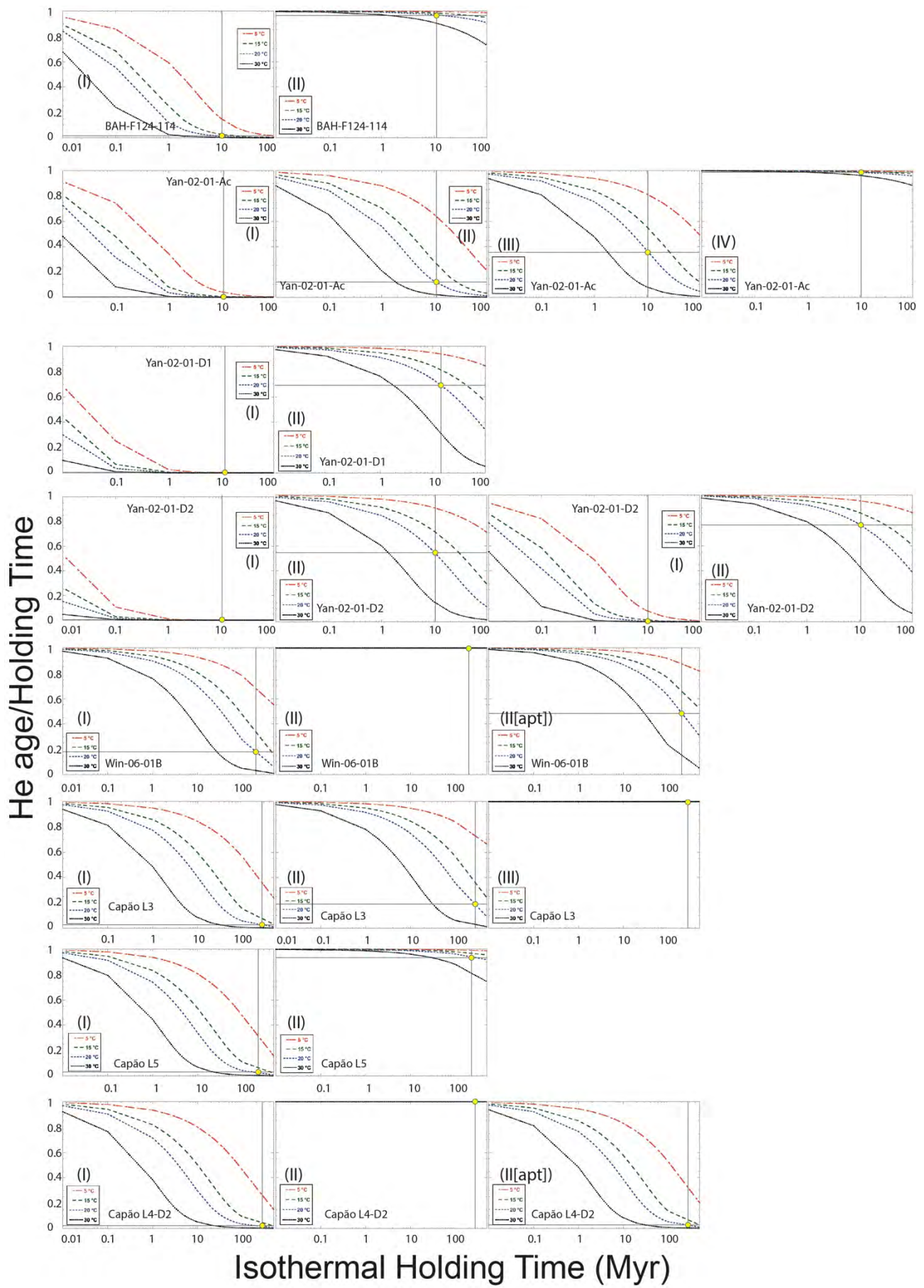


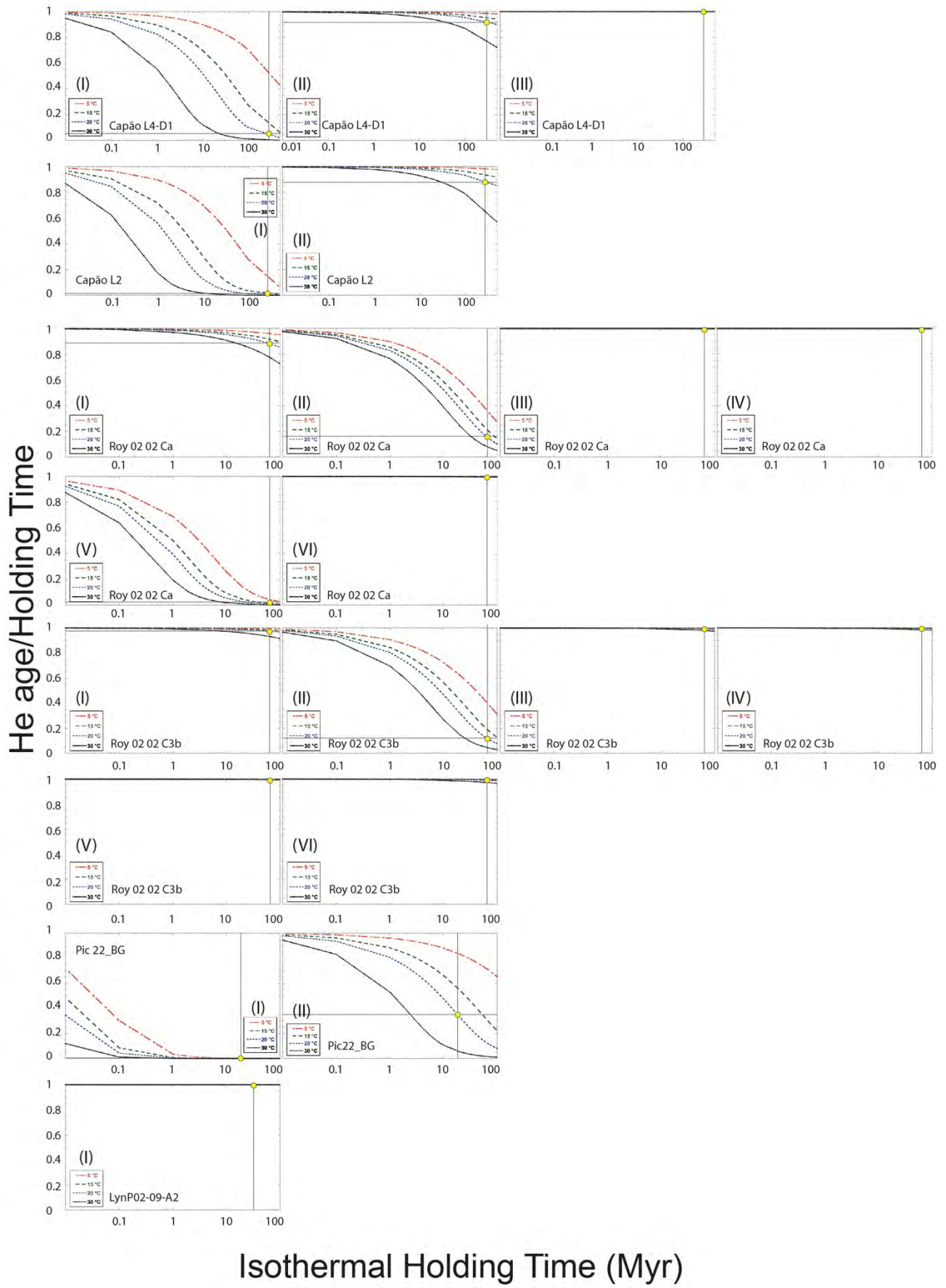
Figure 9: ^4He (gray triangles) and ^3He (black circles) Arrhenius diagrams for all goethites samples. Lines of best-fit through low-T and retrograde-prograde steps define domains of different retentivity in each sample. Arrhenius parameters (E and $\ln(D_0/a_0^2)$) were derived from the fraction of gas represented by the points defining each curve (Table 3). The amount of gas derived from low retentivity domains (intercrystalline sites) ranges from ~ 0.1 to 7.5% of the total ^3He budgets, while gas released from higher retentivity domains (intracrystalline sites) accounts for more than 90 to nearly 100% of the total ^3He . Most experiments only detect two domains in each sample investigated, but samples analyzed in much greater detail (e.g, Figure 9b) reveal the presence of several high retentivity domains, which we interpret as He release from progressively larger crystallites as we probe the samples at progressively higher temperatures. Two samples (Figure 9 l-m) released more than 70 - 80% of their total ^3He in the last step, and their Arrhenius diagrams are uninterpretable. One sample (Figure 9 x, PIC-21) contains so many generations of intergrown goethites that its derived Arrhenius parameters are not reliable.

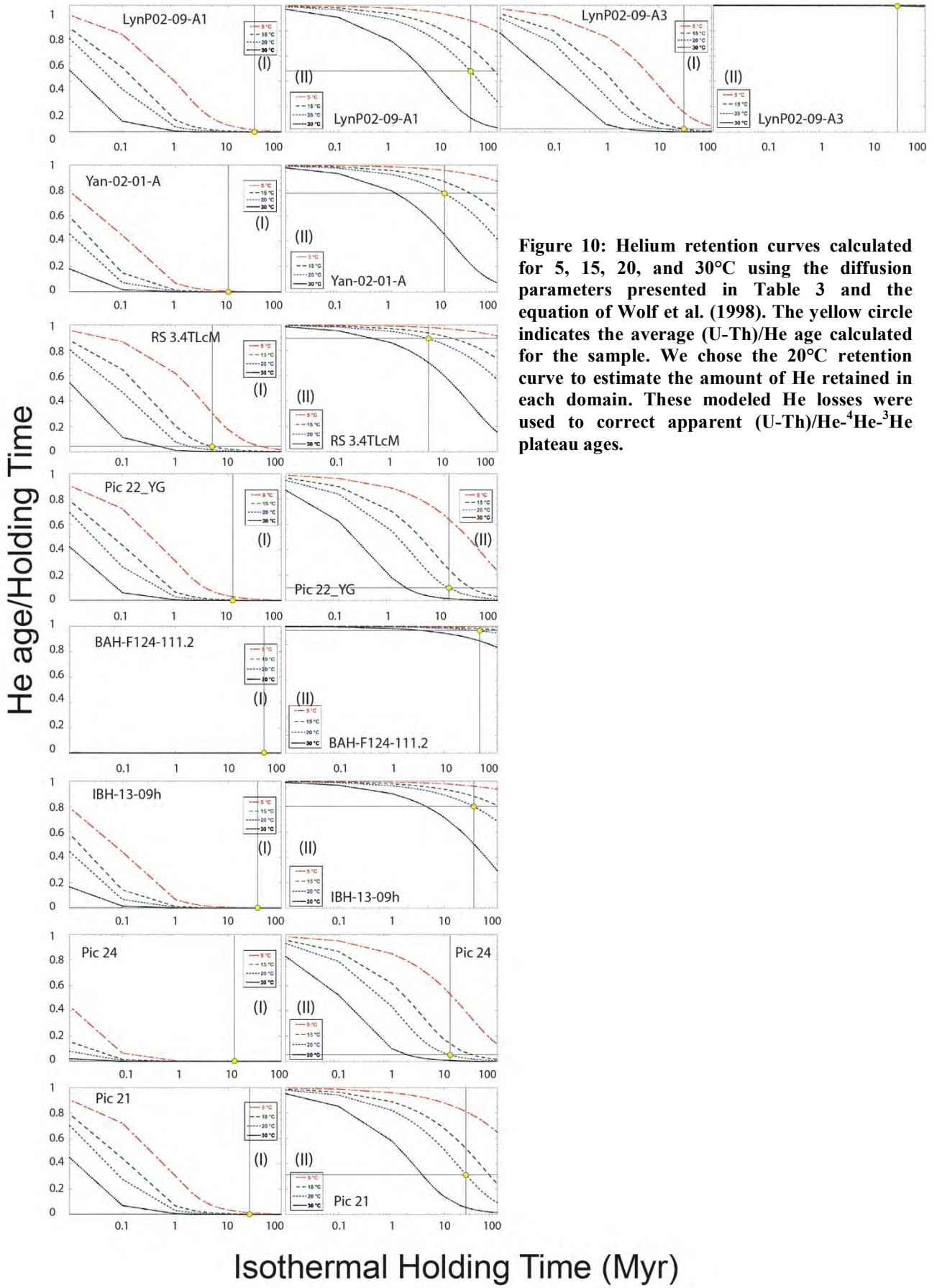
Table 3: Goethite diffusion parameters calculated from ^3He

Sample	Domain	Ea (kJ/mol)	Ea (kcal/mol)	\pm	$\ln D_0/a^2$ ($\ln(s^{-1})$)	\pm	% of gas	Starting Temp.	Ending Temp.	Heating Schedule	Source
Win 06 01B	I	134.4	32.1	2.2	18.0	2.9	0.5	79	139	prograde	This study
	II	263.2	62.9	4.1	47.8	4.2		199	238	prograde	
	II [apt]	146.1	34.9	0.4	21.0	0.4	99.5	229	277	retrograde/prograde	
Roy 02 02 2ca	I	99.8	23.9	0.3	-0.1	0.4		70	90	prograde	Waltenberg, 2012
	II	49.0	11.7	0.7	-16.0	1.1		80	50	retrograde/prograde	
	III	42.3	10.1	1.1	-33.9	1.8	0.1	100	50	retrograde/prograde	
	IV	34.1	8.2	1.9	-44.8	2.9		50	100	retrograde/prograde	
	V	74.2	17.7	1.9	-2.7	2.5		140	199	retrograde/prograde	
	VI	147.2	35.2	0.3	10.4	0.3	99.9	160	259	retrograde/prograde	
Roy 02 02 3cb	I	143.2	34.2	0.4	14.6	0.6		80	120	prograde	Waltenberg, 2012
	II	70.4	16.8	0.4	-6.9	0.6	0.1	140	110	trograde/prograde/retrograde	
	III	132.9	31.8	0.4	8.1	0.5		150	180	retrograde/prograde	
	IV	138.5	33.1	0.4	9.7	0.4		190	200	retrograde/prograde	
	V	145.1	34.7	0.1	10.7	0.1	99.9	160	239	retrograde/prograde	
	VI	138.1	33.0	0.2	10.8	0.2		229	229	retrograde/prograde	
BAH F124 111.2	I	46.8	11.2	0.5	-4.1	0.5	7.4	50	175	prograde	Shuster et al., 2005
	II	175.9	42.0	0.5	28.2	0.5	92.6	200	250	othermal/retrograde/prograde	
BAH F 124 114	I	114.4	27.3	1.0	15.2	1.4	3.9	65	150	prograde	Shuster et al., 2005
	II	170.2	40.7	0.9	27.8	1.0	96.1	200	240	othermal/retrograde/prograde	
Capão L2	I	144.1	34.4	0.8	25.1	1.1	0.4	39	99	prograde	This study
	II	174.8	41.8	0.8	29.1	0.9	99.6	189	257	retrograde/prograde	
Capão L3	I	140.3	33.5	1.5	22.0	2.1	0.6	59	119	prograde	This study
	II	147.8	35.3	0.8	23.0	0.8		219	259	retrograde/prograde	
	III	286.1	68.4	###	53.6	###	99.4	199	239	prograde	
Capão L4 (D1)	I	155.7	37.2	0.5	27.8	0.8	0.9	49	124	prograde	This study
	II	160.6	38.4	1.5	22.4	1.7		179	195	retrograde/prograde	
	III	311.5	74.5	3.2	59.6	3.1	99.1	218	266	prograde	
Capão L4 (D2)	I	139.4	33.3	0.8	22.2	1.2	0.7	25	119	prograde	This study
	II	299.2	71.5	###	57.2	###		199	239	prograde	
	II [apt]	135.4	32.4	0.8	20.1	0.8	99.3	229	238	retrograde/prograde	
Capão L5	I	132.9	31.8	1.4	19.3	2.1	0.2	59	119	prograde	This study
	II	175.7	42.0	0.9	28.2	1.0	99.8	199	277	retrograde/prograde	
Pic 06 21	I	109.8	26.2	0.9	14.7	1.3	1.5	39	119	prograde	This study
	II	140.9	33.7	0.9	21.8	0.9	98.5	209	219	retrograde/prograde	
Pic 06 22_BG	I	95.1	22.7	0.7	10.7	0.9	2.5	50	125	prograde	This study
	II	149.4	35.7	1.4	25.4	1.6	97.5	180	218	retrograde/prograde	
LynnP 02 09 A1	I	97.3	23.3	1.3	10.6	1.8	4.7	65	151	prograde	Vasconcelos et a. 2013
	II	147.5	35.3	1.2	23.5	1.3	95.3	190	205	retrograde/prograde	
LynnP 02 09 A2	I	310.6	74.2	1.8	62.8	1.9	99.9	178	227	prograde	Vasconcelos et a. 2013
LynnP 02 09 A3	I	121.5	29.0	1.2	17.2	1.7	3.3	39	156	prograde	Vasconcelos et a. 2013
	II	215.5	51.5	2.1	39.3	2.2	96.7	186	226	prograde	
Yan 02 01 A	I	101.4	24.2	0.5	12.7	0.7	1.6	65.0	125.0	prograde	Heim, 2006
	II	156.6	37.4	0.8	26.4	0.8	98.4	160.0	225.0	rograde/retrograde/prograde	
Yan 02 01 Ac	I	111.2	26.6	0.2	15.1	0.3	1.4	29	84	rograde/retrograde/prograde	Waltenberg, 2012
	II	129.2	30.9	0.4	19.0	0.6		129	114	rograde/retrograde/prograde	
	III	131.2	31.4	0.5	18.5	0.6	98.6	100	140	rograde/retrograde/prograde	
	IV	153.7	36.7	2.2	19.5	2.2		259	229	rograde/retrograde/prograde	
Yan 02 01 D1	I	93.2	22.3	1.4	10.1	1.8	6.4	65	150	prograde	Heim, 2006
	II	154.0	36.8	1.1	25.7	1.2	93.6	180	220	retrograde/prograde	
Yan 02 01 D2	I	87.4	20.9	1.1	8.5	1.5	1.0	65	150	prograde	Heim, 2006
	II	148.9	35.6	0.6	24.8	0.6	99.0	200	205	retrograde/prograde	
Yan 02 01 D2	I	119.8	28.6	1.2	18.1	1.7	4.0	50	130	prograde	Waltenberg, 2012
	II	154.0	36.8	0.8	25.4	0.8	96.0	189	224	retrograde/prograde	
Pic 06 22_YG	I	122.1	29.2	0.8	19.8	1.3	3.7	16	75	prograde	This study
	II	137.6	32.9	0.4	22.5	0.4	96.3	140	220	retrograde/prograde	
IBH 13 09h	I	97.9	23.4	0.7	11.8	1.0	1.1	59	99	prograde	This study
	II	153.3	36.6	0.9	23.5	1.0	98.9	159	257	retrograde/prograde	
Pic 06 24	I	95.1	22.7	0.1	12.4	0.2	2.3	50	100	prograde	This study
	II	137.3	32.8	0.9	23.0	1.0	97.7	189	205	retrograde/prograde	
RS 3.4 TLcM	I	141.4	33.8	1.4	26.8	3.7	1.1	50	100	prograde	This study
	II	156.9	37.5	0.7	25.7	0.5	98.9	190	257	prograde	

[apt]: after phase transformation







Inclusions in goethite may affect the content, distribution and release of U, Th, and He in the small (100-500 μm) sample fragments used in geochronology. Mineral inclusions will be particularly problematic when they are much older or much richer in U, Th, and He than the goethite hosts, as discussed below. Substituting elements in solid solution also influence goethite's crystallinity, thermodynamic stability, and crystallite size and shape, possibly affecting its He retentivity. A particularly important element, Al is present in many of our goethites, and Al-rich goethites are demonstrably less crystalline than pure Fe-goethite or goethite containing other elements (Mn, Ni, Cu, or Pb) in solid solution. The effect of solid solution on crystallinity, U-Th contents, and He retentivity will be discussed below. Importantly, minor Ti and Cr contents (Table 1; EA1) appear to correlate with the presence of mineral inclusions (Figure 2w, x), affecting the geochronological results, as discussed below.

5.2. Crystallinity and crystallite sizes in supergene goethite

XRD patterns alone are not sufficient to differentiate between the effects of crystallinity versus crystallite size (Mostert, 2014). Therefore, we attribute the broadening of the XRD peaks to the collective effects of lower crystallinity and smaller crystallite sizes. Figure 4 illustrates that samples with the lowest Al contents are the most crystalline/larger crystallites, and that crystallinity/crystallite size decreases progressively with increasing Al contents. Lower goethite crystallinity/crystallite size is also accompanied by increases in mineral impurities, particularly kaolinite, gibbsite and hematite (Figure 2ak-an). Silica content does not correlate with increases or decreases in crystallinity/crystallite size or with the appearance of any minor silica phase, perpetuating the mystery associated with the relatively high (up to ~ 1.8 wt%) SiO_2 contents in most natural supergene goethites we investigated.

5.3. The effects of purity and crystallinity on the thermal stability of supergene goethite

The TGA results (Figure 5) reveal that the purest and most crystalline goethites undergo phase transformations at higher temperatures than poorly crystalline and impure samples. Sample IBH09h (Table 1), an Al-rich goethite, shows a surprising behavior, as its broad phase transformation curve peaks at ~ 345 $^{\circ}\text{C}$, higher than most other samples.

The wide range of temperatures under which various goethites undergo phase transformations implies that incremental heating geochronology of goethites, particularly the analysis of retrograde steps, requires careful programing, as it is difficult to predict a priori temperatures at which each sample may start phase transition. Comparisons between TGA results and incremental heating $^4\text{He}/^3\text{He}$ analyses helps to predict approximate temperatures of phase transitions, but TGA is carried out under normal atmospheric pressures while incremental heating experiments take place under

ultra-high vacuum. Therefore, TGA experiments could underestimate temperatures of phase transition by ~ 50 - 100 °C. Knowing phase transition T is crucial for optimizing incremental heating analysis and temperature cycling in order to differentiate He release by diffusion from He lost during phase transformation. Understanding heating-induced phase transitions under vacuum is also necessary to explain why some samples appear to retain He beyond the temperature of phase transition, when opening of the goethite structure should result in complete He release.

5.4. The effect of crystallinity on (U-Th)/He and $^4\text{He}/^3\text{He}$ results

Assuming pure volume diffusion, increased crystallinity/crystallite size would most likely result in greater He retentivity simply because the diffusing He atom would encounter a longer and tighter path in highly crystalline samples with larger diffusion domains. In addition, more crystalline larger domain samples should, in principle, undergo phase transformation at a higher and narrower temperature range. XRD patterns (Figure 4) show that Capão and Winsor samples are more crystalline/contain larger crystallites. TGA results (Figure 5) show that these samples undergo phase transformations at higher temperatures. Several dated aliquots show great reproducibility, which suggest near quantitative He retention. Incremental-heating $^4\text{He}/^3\text{He}$ profiles (Figure 7) confirm that these samples display the lowest ^4He deficits, and isothermal holding time diagrams (Figure 10) demonstrate that these samples are retentive to He for 10's to 100's of millions of years.

5.5. The effects of mineral purity on (U-Th)/He and $^4\text{He}/^3\text{He}$ results

Despite great efforts to select only visually pure goethites for geochronology, optical and electron microscopy (Figure 2), electron microprobe analysis (Figure 3), and $^4\text{He}/^3\text{He}$ profiles (Figure 7) suggest that many of the samples selected for geochronology contain inclusions of other phases (primarily hematite, gibbsite, and kaolinite and other clays, but also rutile, ilmenite, and even zircon). These impurities are present in small concentrations (relict minerals), and some of the mineral inclusions (e.g., gibbsite) should not influence the geochronology results because they do not host significant U or Th and they are not retentive of He. However, even small amounts of hematite, ilmenite or zircon (Figure 2w-ab, ag-al) contaminants may potentially affect the geochronology results.

The influence of these contaminant minerals in (U-Th)/He dating may be minor. The reason is that hematite, ilmenite, and zircon retain most of their He contents beyond the maximum temperature used for He extraction in our experiments (~ 900 °C for (U-Th)/He dating); therefore, they may not directly contribute to the He concentrations computed in age calculations. In addition, these minerals are not soluble (except for hematite) in the concentrated HCl solutions used for goethite

dissolution prior to U-Th-Sm analysis, and consequently they do not contribute to the budget of parent nuclides included in age calculations, either.

The most significant contribution of these mineral inclusions may be in the production of parentless He implanted into the surrounding goethite, artificially increasing its (U-Th)/He age. This effect is real, but it is relatively small given the small inclusion volumes and the large U and Th contents (Figure 11) of > 900 goethites aliquots analyzed by (U-Th)/He. For example, if a 20 Ma spherical goethite grain ($r = 250 \mu\text{m}$) with 5 ppm U and 1 ppm Th contains 10 fragments of 1 Ga zircon ($r = 5 \mu\text{m}$) with 200 ppm U and 100 ppm Th, the total mass of ^4He ejected from the zircon into the goethite would be less than 0.5% of the total He budget of the goethite grain, an insignificant contribution to the measured age. On the other hand, the total amount of He contained in the 10 fragments of 1 Ga zircon would amount to $\sim 30\%$ of the total amount of He in the goethite host. In order to obviate contributions from these contaminants, it is necessary to extract He from goethite at the lowest possible temperatures (600-900 °C), below the temperatures at which the contaminants typically released their He contents. Low temperature He extraction, if combined with HCl-only dissolution to avoid contaminant-derived U, Th, and Sm contributions, may permit obtaining reliable ages for goethites, even if they host contaminants. The incremental-heating $^4\text{He}/^3\text{He}$ method is even more appropriate for detecting and obviating the effects of contaminants. In our incremental heating $^4\text{He}/^3\text{He}$ experiments, He is extracted from goethite up to 500-550 °C, while He derived from contaminants such as zircon, rutile, or ilmenite is only released in the last high-temperature (1200°C) step. $^4\text{He}/^3\text{He}$ incremental heating profiles will clearly detect contributions from contaminants, when present, and this contribution can be obviated as outlined below.

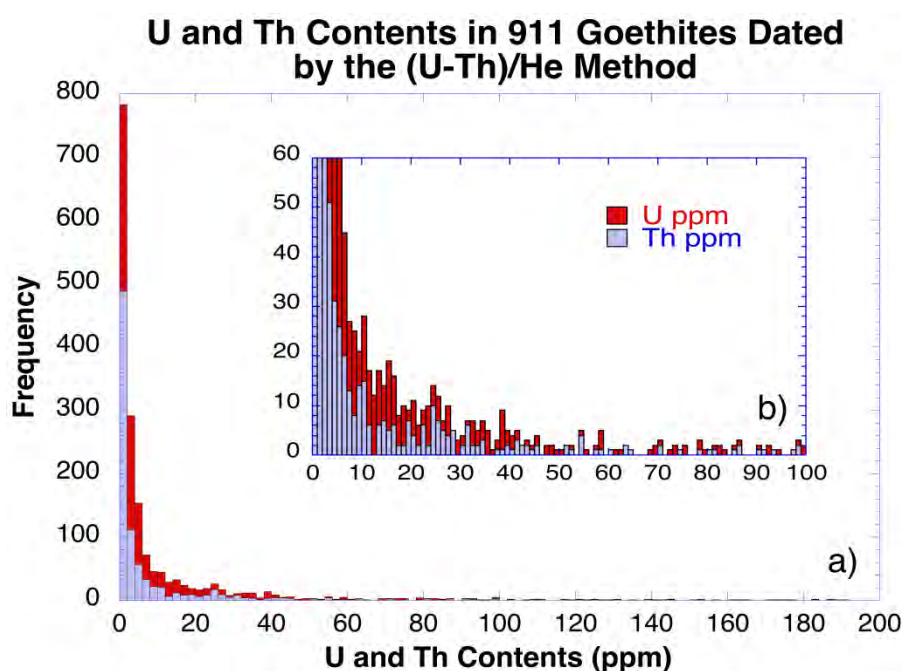


Figure 11: Total U and Th contents of more than 900 goethite samples dated by the (U-Th)/He method, showing that natural goethites generally contain less than ~ 20 -40 ppm U+Th, but that some samples may contain as much as several hundred ppm of these radioactive nuclides. In fact, some of the samples investigated in this study contain > 300 ppm U.

5.6. The effects of purity on $^4\text{He}/^3\text{He}$ spectra

Significant contaminant-derived He contributions are detected in some $^4\text{He}/^3\text{He}$ age-spectra (Figure 7). These profiles record ^3He and ^4He released by incremental heating up to 500-520 °C in a diffusion cell, complemented by a last step obtained by total extraction at 1200 °C in a resistance furnace. Pure single generation goethite samples show flat or slightly ascending or descending spectra without a significant apparent age increase in the last step (Figure 7a-e). Impure goethites show a noticeable increase in the apparent age for the last step (Figure 7n-x). The increase in $^4\text{He}/^3\text{He}$ ratio can be large and correspond to a significant amount of the total ^3He released (e.g., LynnP-02-09-A1, A3, BAH-F124-111.2) or it can be very large but represent only a small fraction of the total ^3He released (e.g., Pic22 BG and YG). These differences reflect the relative amounts of total contaminant and the differences in ^4He content between the contaminants and the goethite host. Most samples do not show an increase in apparent age until the last step, suggesting that the old and He retentive contaminant does not contribute to the He budget attributed to the goethite, while some samples (e.g., IBH-13-09h) reveal a progressive contribution of He from the contaminant(s) from temperatures as low as ~ 250-300 °C. This difference reflects the nature of the contaminant.

The Lynn Peak samples (Figure 7o-q) provide an excellent case study for the influence of contaminants on $^4\text{He}/^3\text{He}$ results. These samples represent authigenic goethite cements partially replacing detrital hematite (Figure 2w-ab). The rise in apparent age at the high-temperature end of the $^4\text{He}/^3\text{He}$ experiment corresponds to about 15-20% of the total ^3He budget in the sample, revealing a significant mass of the contaminant. However, this contaminant is not as old as the underlying Archean bedrock because the increase in apparent age in the last step only reaches ~ 60-40 Ma. These apparent ages for the contaminants correspond to independently determined ages of detrital phases eroded from ancient (~ 60 Ma) weathering profiles that once blanketed the source areas for the Lynn Peak channel (Vasconcelos et al., 2013). Therefore, we interpret the contaminant to be supergene hematite or martite eroded from previously formed weathering profiles. The flat low-T plateau (presumably from gas derived from goethite only) and the old last step (representing gas derived from detrital hematite) suggest that the Lynn Peak $^4\text{He}/^3\text{He}$ incremental-heating spectra simultaneously retrieve ages for the authigenic cements (low age plateau) and the detritus aggraded into the channels (last step).

If the contaminating phase only contributes to the He budget in the last step of $^4\text{He}/^3\text{He}$ incremental heating profiles, and if the U-Th-Sm contents from contaminants are not being accounted in deriving a (U-Th)/He age for the sample (as discussed above), then an age spectra that exclude the last step should faithfully represent the age of the goethite. Since individual plateau apparent ages

depend on $R_{\text{step}}/R_{\text{bulk}}$ [or $(^4\text{He}/^3\text{He})_{\text{step}} / (^4\text{He}/^3\text{He})_{\text{bulk}}$], removing the last step from the computation will increase the apparent age for individual steps and for the plateau age calculated for the remaining steps (Figure 8). The increase in apparent age will depend on the overall contribution from the last step, but it can be significant (e.g., Figure 8e). Given the strong evidence that the last step represents He released primarily from contaminants, a recommended procedure is to plot incremental heating $^4\text{He}/^3\text{He}$ spectra with and without the last step in order to determine the magnitude of the contribution from contaminants, but only to compute an age from spectra that omit the last (contaminant-contribution) step when calculating the age for the authigenic goethite.

5.7. The effect of crystallinity on $^4\text{He}/^3\text{He}$ spectra

Crystallinity/crystallite size undoubtedly affects (U-Th)/He results, but this contribution is not apparent from (U-Th)/He data alone. The effect of crystallinity/crystallite size, however, is transparent in $^4\text{He}/^3\text{He}$ spectra. Well-crystallized goethites devoid of contaminants show flat (Figure 7a) or nearly flat (Figure 7b) $^4\text{He}/^3\text{He}$ spectra consistent with a He-retentive medium. Deviations from flat spectra in well crystallized goethites results from contaminants (discussed above); sample recrystallization after initial goethite formation (discussed below), where two or more coexisting generations of pure-crystalline-He-retentive goethites of distinct ages will yield complex profiles (Figure 7f-m, x); or low crystallinity. Low crystallinity/crystallite size, as shown by the decrease in peak intensity and increase in peak width in the XRD patterns (Figure 4), is accompanied by a progressive rounding of the $^4\text{He}/^3\text{He}$ spectra (Figure 7c-e, t, v, w). Less crystalline/smaller crystallite goethites display the most rounded $^4\text{He}/^3\text{He}$ profiles (Figure 7c-e, t, v, w), suggesting significant ^4He losses. Data for He release kinetics, when plotted in isothermal holding time diagrams, illustrate that the intracrystalline domains (HRD) for most of our well-crystallized goethites retain He quantitatively during their life-time, and maximum He losses determined for those samples is $< 20\%$, as previously determined (Shuster et al., 2005). On the other hand, He diffusivity data for poorly crystalline/small crystallite goethites reveal up to 85-90 % He losses (e.g., samples Pic 22 and Pic 24, Figures 6t,w, 7t,w and 10) during the sample's lifetime. These results strongly suggest that He retentivity does indeed depend on crystallinity/crystallite size. Fortunately, applying age corrections (Shuster et al., 2005) for He diffusive losses yield encouraging results, even for samples showing these significant ^4He losses.

Samples PIC-22 BG (black goethite) and PIC-22-YG (yellow goethite), derived from the same hand specimen, provide a useful example. Textural relationships in the hand specimen suggest that the two types of goethites are coeval. EMP analysis show that BG and YG have comparable compositions, and petrographic and XRD data show that they differ based on the crystallinity and density of the interlocking goethite crystallites, where BG is denser and more crystalline, while YG

is less dense, porous, and poorly crystalline. Uncorrected (U-Th)/He- $^4\text{He}/^3\text{He}$ plateau ages for these samples reveal apparent ages of 19.20 ± 0.32 and 9.30 ± 0.15 Ma for BG and YG, respectively. Correcting these plateau ages for the contribution of contaminants yields new apparent ages: 19.59 ± 0.33 Ma for BG and 15.28 ± 0.25 Ma for YG. Further correcting these apparent ages for the He losses quantified by isothermal holding time modeling yields apparent ages of 32.3 ± 0.63 (1σ) Ma (65% correction; calculated from the 20°C isothermal holding time curve) for BG and 29.0 ± 0.47 (1σ) Ma (90% correction; calculated from the 20°C isothermal holding time curve) for YG. These ages are very close to each other, and, we estimate, close to the true precipitation ages of the goethites, suggesting that BG and YG are indeed coeval, that both samples underwent significant He losses, and that the more poorly and finely crystalline porous YG underwent much greater He losses than the coexisting BG. These results are particularly encouraging because the internally consistent corrected ages correspond to a main peak of goethite precipitation independently determined for the same study site by Monteiro et al. (2017). The results suggest that proper interpretation of combined (U-Th)/He and $^4\text{He}/^3\text{He}$ data may indeed lead to reliable and geologically meaningful geochronological data if appropriate age corrections are implemented. But these results also provide a cautionary note to researchers interested in dating porous, poorly crystalline powdery soil goethites, which are likely to have undergone significant He losses.

5.8. The effect of multiple generations on (U-Th)/He and $^4\text{He}/^3\text{He}$ results

Similarly to crystallinity/crystallite size, the effect of intimately intergrown multiple generations of goethite is not obvious from (U-Th)/He data alone, unless a large number of mineral fragments are separately analyzed (e.g., Pic 21; Table 2). The lack of reproducibility in apparent ages, without petrographic evidence for significant amounts of hypogene contaminants, can often be traced to multiple generations of intergrown goethites of disparate ages (Monteiro et al., 2014).

Fortunately, the incremental-heating $^4\text{He}/^3\text{He}$ method is also suitable for identifying aliquots composed of multiple generations. Multiple-generation goethites produce complex spectra, where apparent ages for individual steps may vary up-or-down with progressive heating, depending on the relative abundances, ages, crystallinities, and retentivities of the various generations of the intergrown goethites (Figure 7f-m, t, x). Often, the latest goethite generation is also the most crystalline and He retentive, resulting in incremental-heating $^4\text{He}/^3\text{He}$ age spectra that define lower apparent-age plateaus at the highest temperatures (Figure 7f-k). When the two or more distinct generations of intergrown goethites release their He contents at distinct temperatures, ages for each generation may be independently determined (e.g., Figure 7l, m).

On the other hand, less crystalline or less He retentive late generations will release their He contents at various temperatures, increasing the complexity of the incremental-heating spectrum (Figure 7x). This type of sample poses serious challenges in geochronology, where the most reasonable conclusion derived from a $^4\text{He}/^3\text{He}$ spectrum is that the lowest and highest apparent age for an individual step record the maximum age for the youngest generation and the minimum age for the oldest generation, respectively (Figure 8i), and that the number of plateau-like segments records the minimal possible number of distinct generations of goethite in the grain (Figure 8i). It is particularly reassuring if these youngest and oldest apparent ages also match the youngest and oldest (U-Th)/He ages obtained for the various individual aliquots analyzed from the same sample (Table 2).

5.9. $R_{\text{step}}/R_{\text{bulk}}$ diagrams and He release from goethite

There is some redundancy in $R_{\text{step}}/R_{\text{bulk}}$ diagrams and the $^4\text{He}/^3\text{He}$ age spectra derived from them, but $R_{\text{step}}/R_{\text{bulk}}$ diagrams provide one piece of information not obvious from age spectra. The $R_{\text{step}}/R_{\text{bulk}}$ diagrams (Figure 6) reveal that samples prone to significant He losses invariably plot below the 1-ratio line, in the forbidden zone (Shuster et al., 2005) of the method if we assume uniform production-diffusion in a dense close-packed medium. Therefore, $R_{\text{step}}/R_{\text{bulk}}$ diagrams clearly identify samples that violate the assumption that He is being generated in the interior of a crystalline and densely packed medium that only allows He to reach the external environment via volume diffusion. Goethite grains that plot well below the 1-ratio line in $R_{\text{step}}/R_{\text{bulk}}$ diagrams (e.g., Pic 22YG; Figure 6t) are much more porous, with a distinct crystallite packing that allows

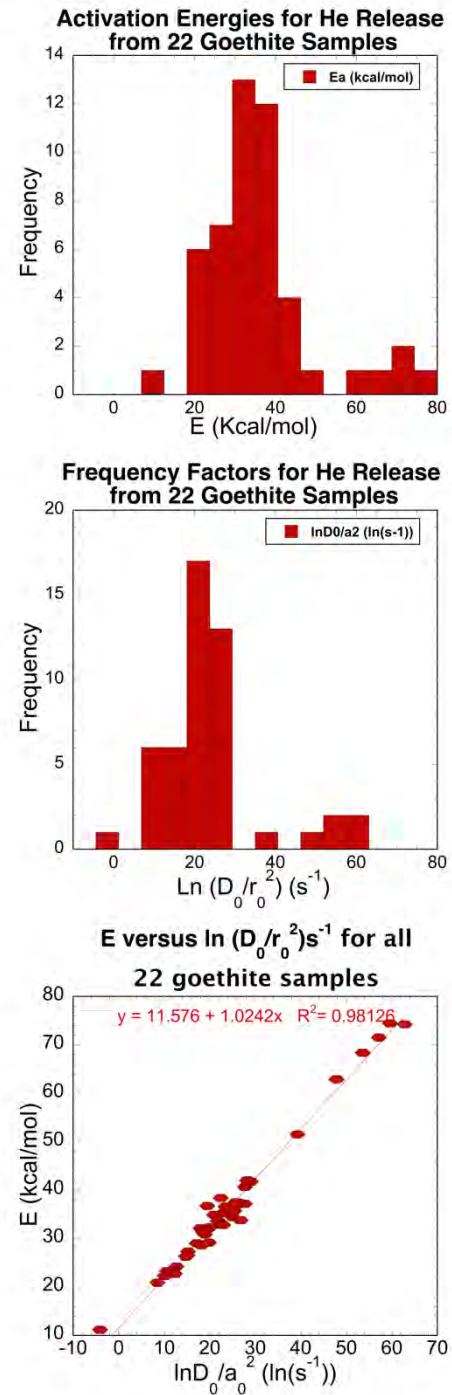


Figure 12: A correlation between calculated E and $\ln(D_0/r_0^2)$ for 22 of the goethites investigated in this study reveal that Arrhenius parameters for goethites follow closely the compensation law, and that the rate of release of He from goethite crystallites converges at $\sim 242^\circ\text{C}$.

He release via alternative routes. A useful analogy is to view these porous, friable, and poorly crystalline goethite grains as sponge fragments where the innermost part of the grain may be as close to the outside environment as any other part of the sample because the pathway of He release is a network of interconnected and readily available pore spaces.

Fortunately, as we show above, combined information derived from the $R_{\text{step}}/R_{\text{bulk}}$ diagrams, Arrhenius parameters, and isothermal holding time modeling leads to positive identification of the “spongy” samples showing anomalous He retention and release behaviors.

5.10. Arrhenius plots

Interpreting and extracting diffusivity data from Arrhenius diagrams requires understanding the physical processes controlling the release of He from goethite aliquots during stepwise heating. Slightly different heating-schedules were applied in the various $^4\text{He}/^3\text{He}$ experiments. In most experiments, the sample was progressively heated and retrograde procedures started at relatively low temperatures ($\leq 200^\circ\text{C}$), before phase transformation. In these samples, prograde and retrograde steps plot along a single straight line, suggesting He release by volume diffusion. In some experiments, however, the retrograde steps appear to have been carried out after the initiation of phase transformation. In these experiments, the slope of prograde steps immediately preceding the retrograde experiments define a different and much steeper straight line (Figure 9 c,d) than the one describe by the retrograde experiment. A puzzling result, however, is the fact that prograde steps that follow the retrograde experiment define a single line with the retrograde steps. If phase breakdown did occur before the start of the retrograde experiment, it must have occurred rapidly and resulted in the formation of a new phase that is also He retentive. This newly formed and homogeneous phase releases He by volume diffusion during both retrograde and subsequent prograde steps.

As illustrated in Figure 9, straight lines defined from the He release experiments were used to calculate activation energies (E) and frequency factors ($\ln D_0/r_0^2$) for low and high retentivity domains (summarized in Table 3). Plots of E (Figure 12a) and $\ln D_0/r_0^2$ (Figure 12b) calculated for 22 goethite samples show that E ranges from 11.2 ± 0.5 to 74.5 ± 3.2 kcal.mol $^{-1}$, with an average value at $\sim 36.2 \pm 13.5$ (1 σ) kcal/mol; and $\ln D_0/r_0^2$ ranges from -4.1 ± 0.5 to 62.8 ± 1.9 s $^{-1}$, with an average value of 24.1 ± 13 (1 σ) s $^{-1}$. A correlation diagram for these parameters (Figure 12c) defines a straight line ($y = 11.58 + 1.024x \pm 0.021$, $R^2 = .98$). The tight correlation between E and $\ln D_0/r_0^2$ suggests that data for He release from the 22 out of the 24 goethites investigated in this study (we excluded Roy02 01 C2a and Roy 02 01 C3b because most of the gas in these samples was released in a single step, resulting in uninterpretable Arrhenius diagrams) follow the compensation law

closely (Lasaga, 1998; McDougall and Harrison, 1999). The peak in activation energy at ~ 35 kcal.mol⁻¹ indicates that He retentivity in goethite is comparable to other phases dated by the (U-Th)/He method (e.g., apatite, with $E \sim 32$ -38 kcal/mol; Farley, 2000). On the other hand, the higher frequency factors observed clearly show that massive aggregates of goethite nano- and microcrystallites have very peculiar He retention and release properties that demands further investigation.

Despite prevailing uncertainties about the meaning of the compensation law, by applying the values derived from ($y = 11.58 + 1.024 x$) to the relationship $T^* = m/R$, we calculate “the temperature at which all species diffuse at the same rate” (McDougall and Harrison, 1999), which is ~ 242 °C for our samples. This temperature is very close to our estimate of the temperature of initiation of goethite breakdown to hematite under vacuum, suggesting that the release of noble gases from some of our samples may have coincided with or taken place after phase transformation.

5.11. Isothermal holding time

Derived kinetic parameters for He release from goethite were used to calculate isothermal holding times for the various samples, and to estimate the proportion of ⁴He loss for a sample of a given age during its lifetime. The isothermal holding time diagrams for the gases hosted in the low retentivity domains, which we interpret to be the pore spaces in between individual goethite crystallites, suggest that these sites lose their entire helium budget in a very short time. However, the very small proportion of He residing in these sites in most samples (1-7%), as compared to the He hosted within crystallites, indicates that loss of helium from pore spaces has no noticeable effect in ages derived from most samples.

This conclusion breaks down for porous and friable goethite samples, where a large proportion of the ⁴He generated within goethite masses may end up in the intercrystalline spaces and readily travel out of the mineral mass. These samples lose all of their He from the intercrystalline sites in a very short period and a significant proportion of He from the intracrystalline sites during their geological lifetimes. These samples are readily identifiable in our ⁴He/³He experiments and in the $R_{\text{step}}/R_{\text{bulk}}$ graphs, as discussed above. Fortunately, retrieval of Arrhenius parameters for these samples and application of these parameters in the isothermal holding time equation permits correcting for He loss during geological history even in cases where these losses reach 90%.

5.12. Interpreting ⁴He/³He incremental heating profiles

The combined (U-Th)/He – ⁴He/³He method is to (U-Th)/He geochronology what the ⁴⁰Ar/³⁹Ar method is to K-Ar dating. The K-Ar method may produce very reliable ages for a sample, but the

reliability of the results can only be ascertained through the application of incremental heating $^{40}\text{Ar}/^{39}\text{Ar}$ analyses, where possible excess Ar, Ar loss, the presence of mixed generations or contaminants can be clearly identified or ruled out. Similarly, (U-Th)/He ages may be correct, but only through the combined (U-Th)/He – $^4\text{He}/^3\text{He}$ method can the reliability of that age and the suitability of the material analyzed be confirmed.

Incremental-heating profiles for 24 goethite samples analyzed or re-interpreted in this study (where two were previously investigated by Shuster et al. 2005, two by Heim et al. 2006, and three by Vasconcelos et al. 2013) represent a diverse range of mechanisms of precipitation, compositions, crystallinities, and purity that permits drawing general conclusions about the suitability of goethite to geochronology. The incremental heating spectra reveal that pure crystalline 100% He retentive goethites are elusive phases in nature, but, when found, these samples are excellent for geochronology (e.g., sample BAH-F124-114 reveals close to 100% He retention; Figure 7a). Most natural goethites, however, are composed of partially recrystallized mixed phases possibly containing various amounts of contaminants and subject to variable proportions of ^4He losses during the sample's lifetime. Despite these challenges, the results summarized here are encouraging because they clearly reveal that the combined (U-Th)/He – $^4\text{He}/^3\text{He}$ method can identify and obviate most of these problems. The example from Lynn Peak, discussed above, clearly demonstrates the power of the method in detecting and correcting for the contribution of contaminants. Similarly, the examples for the black and yellow goethites from Gandarela also reveal that even in worst-case scenarios, where samples are poorly crystalline, partially contaminated, and subject to extreme He losses, age corrections using the combined (U-Th)/He – $^4\text{He}/^3\text{He}$ method permit retrieving meaningful geochronological results.

6. RECOMMENDED PROCEDURES

Given the challenges and promising conclusions outlined above, we recommend a set of procedures, from sampling to final interpretation of results, in order to make geochronology of goethite a more reliable technique.

Sample selection should always aim at targeting large masses of visually pure goethites. Even in areas where most goethites are porous and finally disseminated through the soil or weathering profile, time in the field searching for areas where natural processes concentrated goethite in dense coherent masses will save a very large amount of laboratory and interpretation time.

Natural goethites range from black, brown, orange, and bright yellow, where color reflects grain size and packing. Large crystals and densely packed crystallites are dark-brown to black and vitreous (Figure 1a, d, e, I, j). As crystallites became smaller and less densely packed, the color

lightens to light brown, orange, yellow, and finally intense yellow but dull (Figure 1b). Any goethite, independently of color, will be intense yellow if ground into a fine powder. Therefore, natural yellow goethites tend to be less crystalline, more porous, and – as we hypothesized at the beginning of this study – less He retentive. The $^4\text{He}/^3\text{He}$ incremental heating studies confirm that yellow goethites have lower activation energies in both intercrystalline and intracrystalline sites (Figure 9; Table 3), lose a significant amount of He during their geological histories (Figure 10), and, when black and yellow goethite co-exist in a hand specimen, the black goethite yield older (U-Th)/He apparent ages than the neighboring yellow goethite (Figure 8a, e; Table 3). This observation may be helpful in selecting goethite for (U-Th)/He dating by preferentially targeting darker grains more likely to have quantitatively retained He throughout their entire geological history. Conversely, when possible, powdery yellow goethite should be avoided in geochronology or be analyzed by the combined (U-Th)/He – $^4\text{He}/^3\text{He}$ method, which permits quantifying and correcting for He loss.

6.1. Before Geochronology

Thorough sample characterization (optical and electron microscopy, EMPA, XRD, and TGA) is required to sound interpretation of geochronological results. Pure, stoichiometric well crystallized goethite is suitable for dating by the (U-Th)/He method, and it does not necessary require further characterization by $^4\text{He}/^3\text{He}$ analysis. Goethites containing elevated concentrations of Ti, Cr, or Al may suggest the presence of contaminants, and both (U-Th)/He and $^4\text{He}/^3\text{He}$ experiments should be designed to detect and obviate the effects of these contaminants. Goethites that show high Al contents and low crystallinity when analyzed by XRD should only be analyzed by the combined (U-Th)/He – $^4\text{He}/^3\text{He}$ methods, as these samples will likely required significant age corrections.

6.2. (U-Th)/He and $^4\text{He}/^3\text{He}$ Analysis

For each sample to be investigated by geochronology, a minimum of six grains need to be dated to provide a solid knowledge of the variability and range of ages to be expected for the sample. Ideally, each sample should also be analyzed by the $^4\text{He}/^3\text{He}$ method.

6.3. Presenting and Interpreting $^4\text{He}/^3\text{He}$ Incremental Heating Data

The most effective approach for presenting and interpreting combined (U-Th)/He – $^4\text{He}/^3\text{He}$ method results is to plot the $R_{\text{step}}/R_{\text{bulk}}$ versus Cumulative Fractions of ^3He spectra, apply (U-Th)/He ages derived from several (≥ 3) aliquots to produce incremental heating apparent age spectra, extract Arrhenius parameters from the ^3He data, plot isothermal holding time diagrams using the derived Arrhenius parameters, replot incremental heating spectra eliminating high-T steps that detect the

contribution of contaminants, calculate plateau apparent ages for the goethite from the diagrams excluding contributions from contaminants, and apply ^4He loss age corrections to these contaminant-free plateau apparent ages or to the average of (U-Th)/He ages if a plateau apparent age is not obtained. This procedure should lead to the most reliable and precisely determined age for the goethite sample.

If geochronology of goethite is to be applied without the aid of the $^4\text{He}/^3\text{He}$ method, a large number of samples (>50) must be analyzed if a cursory understanding of the weathering history of a sample profile or landsurface is to be obtained. Concocting elaborate geological histories from a few (U-Th)/He ages is unwarranted as it portrays an understanding not substantiated by sound analytical data and interpretation.

7. CONCLUSION

Combined new and previously published (U-Th)/He – $^4\text{He}/^3\text{He}$ geochronology of 24 goethite samples representing different environments, modes of precipitation, compositions, crystallinities, age ranges, and U-Th contents reveals that most goethites are suitable for geochronology as long as appropriate analytical and interpretation methods are employed. Our results reveal that He retention in goethite varies with crystallinity, and that choosing dense highly crystalline goethite is the most reliable way of ensuring correct geochronological results. The results also reveal that activation energies (E) for goethites range from 11.2 ± 0.5 to 74.5 ± 3.2 kcal.mol $^{-1}$, with an average value at $\sim 36.2 \pm 13.5$ (1 σ) kcal.mol $^{-1}$; and $\ln D_0/r_0^2$ ranges from -4.1 ± 0.5 to 62.8 ± 1.9 s $^{-1}$, with an average value of 24.1 ± 13 (1 σ) s $^{-1}$. Activation energies peak at ~ 35 kcal.mol $^{-1}$, indicating that He retentivity in goethite is comparable to that of apatite. The higher frequency factors clearly show that goethites have very peculiar He retention and release properties, still requiring further characterization. Despite the early efforts of Strutt (1905) more than 110 years ago, we are still at the early stages of unraveling the geochronological potential of goethite. And despite the 17 years since we started our investigations, the limited access to laboratory facilities, the lengthy duration of individual experiments, the need to collate mineralogical, crystallographic, geochronological, and thermochronological information and the need to integrate and model the results for several aliquots from a same sample to derive general conclusions about the behavior of He, U, and Th, has slowed down progress in the field. On a positive note, the results presented and interpreted here provide a hopeful outlook for the prospects of goethite as a geochronometer. The results show that the combined (U-Th)/He - $^4\text{He}/^3\text{He}$ approaches permit determining the U, Th, and He budgets in natural goethites; identifying, quantifying and correcting for ^4He losses during the samples geological history; determining the presence of contaminants and obviating their effects in age determination

for most cases; and identifying samples that have witnessed complex histories of mineral dissolution-reprecipitation through time, but which still provide valuable information if each generation of goethite can be identified and probed individually. Encouraging, diffusion parameters (activation energies and frequency factors) for goethite reveal a phase just as helium retentive as apatite, but much more variable and dependent on mode of mineral precipitation. Also encouraging, the application of the combined (U-Th)/He - $^4\text{He}/^3\text{He}$ methods yield reliable ages for goethites as young as ~ 5 Ma and as old as ~ 350 Ma, suggesting that goethites are valuable time capsules that record reliable long-term information on the surficial history of terrestrial planets.

Acknowledgments

This project was funded by the Australian Research Council (ARC Discovery DP160104988) grant to Paulo Vasconcelos and Kenneth Farley, and the Brazilian Research Council (CNPq) Science Without Borders scholarship to HM.

REFERENCES

- Alpers C. N. and Brimhall G. H. (1988) Middle Miocene climatic change in the Atacama desert, northern Chile: evidence from supergene mineralization at La Escondida. *Geological Society of America Bulletin* 100, 1640-1656.
- Blanchard R., (1968) Interpretation of leached outcrops: Nevada Bur. of Mines Bull. 66, 196 p.
- Chan, M.A., Parry, W.T., Petersen, E.U., and Hall, C.M., (2001) ^{40}Ar - ^{39}Ar age and chemistry of manganese mineralization in the Moab to Lisbon fault systems, southeastern Utah. *Geology* **29**, p. 331–334.
- Cooperdock, E. H. G. and Stockli, D. F. (2016) Unraveling alteration histories in serpentinites and associated ultramafic rocks with magnetite (U-Th)/He geochronology. *Geology* 44(11): 967-970. doi: 10.1130/G38587.1
- Cornell, R.M. (1991) Simultaneous incorporation of manganese, nickel, and cobalt in the goethite (-Fe(OOH) structure. *Clay Minerals* 26, 427-430.
- Cornell, R.M., Schwertmann, U. (1996) The iron oxides: structure, properties, reactions, occurrence and uses. Weinheim, New York.
- Danišík, M., Evans, N. J., Ramanaidou, E. R., McDonald, B. J., Mayers, C., and McInnes, B. I. A. (2013) (U-Th)/He chronology of the Robe River channel iron deposits, Hamersley Province, Western Australia: *Chemical Geology*, v. 354, p. 150-162.
- Evenson, N. S., Reiners, P. W., Spencer, J. E., and Shuster, D. L. (2014) Hematite and Mn oxide (U-Th)/He dates from the Buckskin-Rawhide detachment system, Western Arizona: gaining insights into hematite (U-Th)/He systematics. *American Journal of Science*, **314**, 1373-1435.
- Farley K. A. (2002) (U-Th)/He dating: techniques, calibrations, and applications. *Rev Mineral Geochem* **47**: 819-844.
- Glasauer, S., Friedl, J., Schwertmann, U. (1999) Properties of Goethites Prepared under Acidic and Basic conditions in the Presence of Silica. *Journal of Colloid and Interface Science* 216, 9.
- Heim J. A., Vasconcelos P. M., Farley K. A., Shuster D. L. and Broadbent G. C. (2006) Dating paleochannel iron ore by (U-Th)/He analysis of supergene goethite, Hamersley Province, Australia. *Geology* **34**, 173-176.
- Heim J. A. (2007) Geochronology of weathering and landscape evolution, Hamersley Iron

Province, Australia. PhD Thesis, University of Queensland, Brisbane.

- Lasaga A. C. (1998) Kinetic Theory in earth sciences: Princeton Series in Geochemistry. Princeton University Press. 811 p.
- Lippolt H. J., Brander T., and Mankopf N. R. (1998) An attempt to determine formation ages of goethites and limonites by (U+Th)-4He dating. *Neues Jahr. Mineral.-Monat.* **11**, 505–528.
- Lovera O., Richter F., and Harrison T. (1989) The $^{40}\text{Ar}/^{39}\text{Ar}$ thermochronometry for slowly cooled samples having a distribution of diffusion domain sizes. *J. Geophys. Res.* **94**, 17917–17935.
- Lovera O., Richter F., and Harrison T. (1991) Diffusion domains determined by ^{39}Ar released during step heating. *J. Geophys. Res.* **96**, 2057–2069.
- McDougall I. and Harrison T. M. (1999) Geochronology and Termochronology by the $^{40}\text{Ar}/^{39}\text{Ar}$ Method. Oxford Univ. Press.
- Manceau A., Schlegel M. L., Musso M., Sole V. A., Gauthier C., Petit P. E., and Trolard F. (2000) Crystal chemistry of trace elements in natural goethite. *Geochimica et Cosmochimica Acta* **64**, 3643-3661.
- Millot, G. (1970) Geology of Clays: Weathering, Sedimentology, Geochemistry. Springer-Verlag, New York.
- Monteiro, H. S., Vasconcelos, P. M. P., Farley, K. A., Spier, C. A., and Mello, C. L. (2014), (U-Th)/He geochronology of goethite and the origin and evolution of cangas, *Geochimica et Cosmochimica Acta*, **131**, 267-289.
- Monteiro, H. S., Vasconcelos, P. M. P., and Farley K.A. (2017) A combined (U-Th)/He and cosmogenic ^3He record of landscape armoring by biogeochemical iron cycling. *JGR Earth Surface*, submitted.
- Mostert A. B. (2014) Variations in Goethite Crystallography with Reference to the Ravensthorpe Ni-Laterite, PhD Thesis, The University of Queensland, Brisbane, p. 290.
- Reiners, P. W., Chan, M. A., and Evenson, N. S., 2014, (U-Th)/He geochronology and chemical compositions of diagenetic cement, concretions, and fracture-filling oxide minerals in Mesozoic sandstones of the Colorado Plateau: *Geological Society of America Bulletin*.

- Ramanaidou, E.R., Morris, R.C., and Horwitz, R.C. (2003) Channel iron deposits of the Hamersley province, Western Australia: *Australian Journal of Earth Sciences*, v. 50, p. 669–690, doi: 10.1111/j.1440-0952.2003.01019.x.
- Riffel S. B. (2012) $^{40}\text{Ar}/^{39}\text{Ar}$ and (U-Th)/He Dating of Weathered Landsurfaces on the Rifted Continental Margin of Southern Brazil, PhD Thesis, The University of Queensland, Brisbane, p. 292.
- Riffel S. B., Vasconcelos P. M., Carmo I. O., and Farley K. A. (2015) Combined $^{40}\text{Ar}/^{39}\text{Ar}$ and (U-Th)/He geochronological constraints on the long-term landscape evolution of the Second Paraná Plateau and its ruiniform surface features, Paraná, Brazil. *Geomorphology* **23**, 52-63.
- Rietveld H. M. (1969) Profile refinement method for nuclear and magnetic structures. *Journal of Applied Crystallography* **2**, 65-71.
- Rodriguez-Carvajal J. (2001) An introduction to the Program Fullprof 2000 (version July 2001).
- Samama, J. C. (1986) Ore fields and continental weathering, Van Nostrand Reinhold Co.
- Schulze, D.G. (1984) The influence of aluminium on iron oxides. VIII. Unit-cell dimensions of Al-substituted goethites and estimation of Al from them. *Clays and Clay Minerals* **32**, 8.
- Schwertmann, U. (1971) Transformation of hematite to goethite in soils. *Nature* **232**, 624 - 625.
- Schwertmann, U. (1984) The double dehydroxylation peak of goethite. *Thermochimica Acta* **78**, 39 - 46.
- Schwertmann, U., 1985. Occurrence and formation of iron oxides in various pedoenvironments, in: Stucki, J.W., Goodman, B.A., Schwertmann, U. (Eds.), *Iron in soils and clay minerals*. D. Reidel, Dordrecht, pp. 267 - 308.
- Schwertmann, U., 1991. Solubility and dissolution of iron oxides. *Plant Soil FIELD Full Journal Title:Plant and Soil* **130**, 1-25.
- Schwertmann, U., Carlson, L., 1994. Aluminum influence on iron oxides: XVII. Unit-cell parameters and aluminum substitution of natural goethites. *Soil Science Society of America Journal* **58**, 256-261.
- Schwertmann, U., Gasser, U., Sticher, H., 1989. Chromium-for-iron substitution in synthetic goethites. *Geochimica et Cosmochimica Acta* **53**, 1293-1297.

- Schwertmann, U., Murad, E., 1983. Effect of pH on the formation of goethite and hematite from ferrihydrite. *Clays and Clay Minerals* 31, 277 - 284.
- Shuster, D. L., and Farley, K. A., (2004) $^4\text{He}/^3\text{He}$ thermochronometry: Earth and Planetary Science Letters, v. 217, no. 1–2, p. 1-17.
- Shuster D. L., Farley K. A., Sisterson J. M., and Burnett D. S. (2004) Quantifying the diffusion kinetics and spatial distributions of radiogenic ^4He in minerals containing proton-induced ^3He . *Earth Planet. Sci. Lett.* **217** (1–2), 19–32.
- Shuster D. L. and Farley K. A. (2005) $^4\text{He}/^3\text{He}$ Thermochronology: Theory, Practice, and Potential Complications. *Reviews in Mineralogy and Geochemistry* **58**, 181-203.
- Shuster D. L., Vasconcelos P. M., Heim J. A. and Farley K. A. (2005) Weathering geochronology by (U-Th)/He dating of goethite. *Geochimica et Cosmochimica Acta* **69**(3), 659-673.
- Strutt R. J. (1905) On the radioactive of minerals. *Proceedings of the Royal Society* A76, 88-101.
- Vasconcelos P. M. P., Rene P. R., Becker T. A., and Wenk H. –R. (1995) mechanism and Kinetics of atmospheric, radiogenic, and nucleogenic argon release from cryptomelane during $^{40}\text{Ar}/^{39}\text{Ar}$ analysis. *Geochimica et Cosmochimica Acta* **59**, 2057-2070.
- Vasconcelos P. M. (1999) $^{40}\text{Ar}/^{39}\text{Ar}$ geochronology of supergene processes in ore deposits. *Economic Geology* **12**, 73–113.
- Vasconcelos P. M., Heim J. A., Farley K. A., Monteiro H. S., Waltenberg K. (2013) $^{40}\text{Ar}/^{39}\text{Ar}$ and (U-Th)/He - $^4\text{He}/^3\text{He}$ geochronology of landscape evolution and channel irondeposit genesis at LynnPeak, Western, Australia. *Geochimica et Cosmochimica Acta* **117**, 283-312.
- Vasconcelos P.M., Reich M., Shuster D. (2015) Supergene metal deposits and paleoclimates. *Elements* **11**, 317-322.
- Waltenberg K. M. (2012) Mineral physics and crystal chemistry of minerals suitable for weathering geochronology: implications to $^{40}\text{Ar}/^{39}\text{Ar}$ and (U-Th)/He geochronology, PhD Thesis, The University of Queensland, Brisbane, p. 421.
- Wolf R. A., Farley K. A., and Kass D. M. (1998) Modeling of the temperature sensitivity of the apatite (U-Th)/He thermochronometer. *Chem. Geol.* **148**, 105–114.

Yapp C. J. and Shuster D. L. (2011) Environmental memory and a possible seasonal bias in the stable isotope composition of (U-Th)/He-dated goethite from the Canadian Arctic. *Geochimica et Cosmochimica Acta* **75**, 4194-4215.

Chapter 3: A combined (U-Th)/He and cosmogenic ^3He record of landscape armoring by biogeochemical iron cycling

H. S. Monteiro¹, P.M.P. Vasconcelos^{1,2}, and K.A. Farley²

¹School of Earth and Environmental Sciences, The University of Queensland, Brisbane, Queensland 4072, Australia.

²Division of Geological and Planetary Sciences, California Institute of Technology, Pasadena, CA 91125.

Submitted to the Journal of Geophysical Research – Earth Sciences

Corresponding author: Hevelyn Monteiro (h.monteiro@uq.edu.au)

Key Points:

- We combine (U-Th)/He dating and cosmogenic ^3He measurements in supergene iron oxides to study relic banded iron formation (BIF) landscapes
- We confirm that cangas are long-lasting features of BIF landscapes
- Precipitation of goethite cements takes place primarily in the subsurface

ABSTRACT

(U-Th)/He geochronology and cosmogenic ^3He in iron oxides reveal mineral precipitation ages as old as 55 Ma and exposure ages greater than 5 Ma for canga-cemented plateaus in the Quadrilátero Ferrífero (QF), Brazil, showing that lateritic profiles overlying banded iron-formation (BIF) landscapes in tropical regions have a long history of surface exposure. The long-term erosion history obtained from cosmogenic ^3He on BIF plateaus confirms that relic surfaces persist in the landscape for millions of years. Combined ^3He and (U-Th)/He dating shows that cangas are preferentially goethite cemented by biogeochemical reactions in the subsurface. Importantly, pebbles of hematite-magnetite in colluvia or shallow creeks draining the canga-cemented plateaus record a much longer exposure history than *in situ* canga blocks, showing that even older duricrusts, now eroded, once blanketed these plateaus. Physically stable but biogeochemically dynamic, cangas armor the landscape by pervasive and recurrent iron cycling and cementation, slowing down the delivery of weathered BIF or friable hematite-magnetite ore to erosion.

1. INTRODUCTION

In geomorphology, weathering is often portrayed as the combination of physical, chemical, and biological processes that turn bedrock into erodible material [e.g., *Tucker and Singerland*, 1994; *Tucker and Hancock*, 2010; *Braun et al.*, 2016]. The rate of delivery of this erodible material to drainage systems ultimately controls landscape evolution [*Carlson and Kirby*, 1972]. In fast evolving landscapes, the weathered blanket is quickly eroded, and this effective transfer of physical and chemical sediments to the drainage system is particularly pronounced in active tectonic environments (e.g. Himalaya [*Vance et al.*, 2003], San Gabriel Mountains, CA [*DiBiase et al.*, 2010 and references therein]). The role of chemical and physical weathering in shielding landscapes against erosion is less well-appreciated.

Canga, an iron duricrust that caps weathered banded iron-formations (BIFs), is essentially a shallow karstic breccia derived from significant mass loss during BIF weathering. This breccia is shaped by biologically- and gravity-driven mechanical processes that allow material to move up-and-down the profile. In addition, biologically-driven mineral dissolution-reprecipitation allows the brecciated material to be re-cemented over-and-over through time [*Monteiro et al.*, 2014]. Field inferences [*King*, 1956; *Twidale*, 1956], $^{40}\text{Ar}/^{39}\text{Ar}$ geochronology [*Vasconcelos et al.*, 1994; *Carmo and Vasconcelos*, 2004; *Spier et al.*, 2006], and (U-Th)/He geochronology [*Shuster et al.*, 2005, 2012; *Monteiro et al.*, 2014] show that cangas blanketing weathered BIFs in cratonic landscapes constitute some of the longest-lived continuously exposed land surfaces on Earth. The chemical and physical weathering processes that form these duricrusts may impede erosion instead of helping the delivery of disaggregated bedrock to the drainage system [*Vasconcelos*, 1999]. If true, physical and chemical weathering may function in exactly the opposite way as portrayed in physical landscape models [e.g., *Tucker and Singerland*, 1994; *Tucker and Hancock*, 2010]. Therefore, understanding this moderating effect of weathering in sediment production is essential in quantifying and modeling landscape evolution in cratonic environments.

Cosmogenic ^3He concentrations generated by spallation reactions on Fe and O in Fe-oxyhydroxides and (U-Th)/He precipitation ages (*pAs*) for those minerals may help to unravel the role of supergene iron cycling in slowing down erosion and armoring landscapes [*Shuster et al.*, 2012; *Monteiro et al.*, 2014]. For example, (U-Th)/He *pAs* for supergene goethite cementing cangas at Carajás, Pará, and the Quadrilátero Ferrífero (QF), Minas Gerais, Brazil, reveal that duricrusts began forming some time before ~60 Ma [*Shuster et al.*, 2005, 2012; *Monteiro et al.*, 2014]. Canga longevity is independently confirmed by cosmogenic isotope results [*Fujioka et al.*, 2010; *Shuster et al.*, 2012]. At Carajás, cosmogenic ^3He concentrations in hypogene hematite fragments and associated supergene goethite cements show that canga-blanketed surfaces erode very slowly (0.13–0.46

m.Ma⁻¹) over tens of millions of years [Shuster *et al.*, 2012]. Cosmogenic ⁵³Mn concentrations in these iron oxides also suggest a long exposure history under very low rates of erosion [Fujioka *et al.*, 2010].

These previous (U-Th)/He and cosmogenic isotope results confirm the longevity of iron duricrusts, but they do not provide information on the mechanisms linking the advance of weathering fronts at depth to the delivery of clastic material to the drainage system at the surface. Measuring both (U-Th)/He ages and cosmogenic ³He concentrations is a powerful way of determining when, where (surface *vs* subsurface), and how goethite cementation takes place. This information permits resolving age, depth of precipitation, and history of burial and exhumation of goethite cements, improving our understanding of the processes controlling canga evolution and armoring of landscapes.

In this study, we measure concentrations of cosmogenic ³He in supergene goethite cements, in hematite-magnetite clasts embedded in duricrusts, and in hematite-magnetite±goethite pebbles eroded from canga-armored plateaus at Serras da Moeda, Serrinhas and Gandarela, Quadrilátero Ferrífero, Minas Gerais, Brazil (Figure 1). We also combine previously determined *pAs* for goethite veins in saprolites, fragments of goethite veins cemented into cangas, and goethite cementing the cangas (n=157) with new ages for additional cements (n=138). The combined (U-Th)/He and cosmogenic ³He methods reveal a history of BIF partial dissolution, fragmentation, translocation, local transport, re-cementation, possible shallow re-burial and re-exhumation, and very slow physical erosion by surface degradation and scarp retreat.

2. GEOLOGY AND GEOMORPHOLOGY OF THE QUADRILÁTERO FERRÍFERO

The Quadrilátero Ferrífero (QF), an ~ 7000 km² region within the São Francisco craton, southeastern Brazil, comprises deeply weathered Archean and Proterozoic metavolcanics, metapelites, metaconglomerates, quartzites, BIFs, and carbonates [Alkmim and Marshak, 1998]. Paleoproterozoic (*Transamazonian*) and Neoproterozoic to Cambrian (*Brasiliano*) tectonism [Chemale *et al.*, 1994] promoted magmatism, greenschist to amphibolite grade metamorphism, and deformation of the supracrustal rocks into large-scale synclines and anticlines [Dorr, 1969]. Tectonic activity after ~ 500 Ma is only detectable by thermochronology [Carmo *et al.*, 2004] or surficial features (e.g., abrupt changes in drainage profiles) [Magalhães Jr. and Saadi, 1994], suggesting that this is a relatively stable part of the São Francisco craton. Apatite fission track thermochronology reveals that regional exhumation started at ~ 180 Ma, before the opening of the Atlantic Ocean [Carmo *et al.*, 2004; Kohn *et al.*, 2016].

Geomorphologically, the QF is bounded by elevated quartzite and BIF plateaus and ridges (Caraça, Gandarela, Moeda, Curral, Serrinhas, and Ouro Branco) ranging from 2100 – 1100 m, incised by steep valleys, and surrounded by lower elevation (500 – 800 m) convex hills (the “Mar de Morros” or “Sea of Hills” of *Ab’Saber* [1966]) (Figure 1a). The highest elevations in the QF are underlain by quartzites on the eastern margin (Serra do Caraça), but we focus our investigation on plateaus and ridges formed primarily on BIFs in the central and western (Gandarela, Moeda, and Serrinhas) parts of the QF (Figure 1). Modern drainage in the QF (e.g., Rio das Velhas) preferentially incises into schists, phyllites, granites, and gneisses, while granitic-gneissic units underlay the surrounding “Mar de Morros” landscape (Figure 1a).

Climate in the QF is humid subtropical (ranging from Cwa to Cwb in Köppen-Geiger’s classification) with annual rainfall between 1300-1600 mm [*Alvares et al.*, 2013], a wet season from November to April and a dry season from May to October. All rivers in the region are perennial, except for small creeks draining the highest elevation plateaus, which are intermittent and flow torrentially only during and immediately after summer storms. Water analysis for a natural spring (“Nascente da Mina”) at the Pico Mine (Serra das Serrinhas, Figure 1) shows neutral (pH=7.12), moderate salinity (TDS = 197 mg.L⁻¹), low dissolved oxygen (3.7 mg.L⁻¹), Ca- and Mg-rich (78 and 20 mg.L⁻¹, respectively), and bicarbonate-buffered (68.9 mg.L⁻¹) waters devoid of dissolved Fe (<0.01 mg.L⁻¹). Vegetation ranges from tropical to subtropical rainforest in most of the region, except areas underlain by iron duricrusts or deeply weathered quartzites, which host endemic epilithic (“rupestre”) vegetation [*Jacobi et al.*, 2007].

⁴⁰Ar/³⁹Ar ages obtained for the deeply weathered profiles in the QF [*Carmo and Vasconcelos*, 2004; *Spier et al.*, 2006] suggest a surface exposure and weathering history already on-going by the end of the Cretaceous (~ 70 Ma). These ancient weathering profiles are overlain by Fe-duricrusts, which probably began armouring the landscape with the onset of weathering [*Shuster et al.*, 2012; *Monteiro et al.*, 2014]. Depth and lateral continuity of the duricrusts vary across the region, where the highest elevation plateaus are capped by the deepest (up to 70 m according to *Carlos et al.*, [2014]) and most continuous canga blankets (e.g., Serra do Gandarela, Figure 1b) [*Baltazar et al.*, 2005a]. Low elevation plateaus are overlain by intermittent and shallower cangas (up to 30 m) (e.g., Serra da Moeda, Figure 1b) [*Baltazar et al.*, 2005b, c], whereas the narrowest and mostly discontinuous ridges are blanketed by intermittent cangas (e.g., Serra das Serrinhas, Figure 1b) [*Baltazar et al.*, 2005b, c]. Rills incised into plateaus and carving their shoulders contain transported fragments of eroded duricrusts (Figure 2a-e). Saddles between plateaus contain colluvia hosting fragments of ancient duricrusts that were eroded, transported to lower parts of the landscape, and re-cemented (Figure 2f).

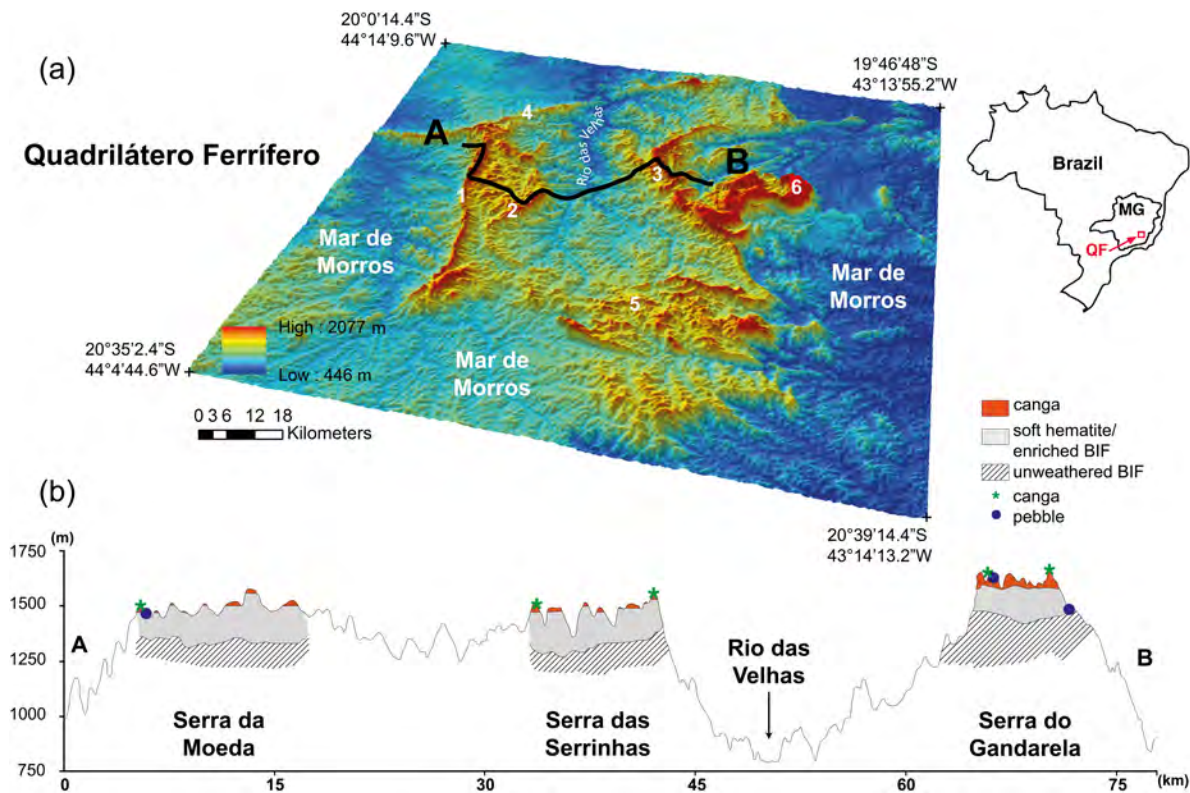


Figure 1: The (a) digital elevation model and (b) topographic cross-section (A-B) depicts the BIF-landscape and shows the most prominent regional landscape features (1 – Serra da Moeda; 2 – Serra das Serrinhas; 3 – Serra do Gandarela; 4 – Serra do Curral; 5 – Serra do Ouro Branco; and 6 – Serra do Caraça) in the Quadrilátero Ferrífero (QF) and adjacent regions, Minas Gerais, Brazil. The interior of the QF is dissected by the das Velhas river and its tributaries, and low-elevation convex hills dominate the surrounding “Mar de Morros” landscape. Schematic and simplified geological cross-sections [Spier *et al.*, 2003, 2006, 2008; Carlos *et al.*, 2014] plotted on the topographic profile illustrate that weathering profiles as deep as 250 m are capped by continuous or intermittent cangas. The approximate location of cangas and hematite-magnetite pebbles investigated in this study is shown.

3. METHODS

Fragments of canga and hematite-magnetite \pm goethite clasts and pebbles were collected at the surface from eight (8) pristine sites, unaffected by mining, along the Serras da Moeda, Serrinhas, and Gandarela (Figures 1, 2, 3). Goethite veins were collected from mine sites or road-cuts exposing saprolites at lower elevations (Figure 3f). Canga blocks and goethite and hematite-magnetite \pm goethite pebbles were collected *in situ* and from colluvia, transported cangas, or shallow channels draining the plateaus (Figures 1, 2, 3). In order to test the reproducibility of results for duplicate samples and to test the distribution of cosmogenic ^3He with depth, two canga blocks ($\sim 15 \times 15$ cm), collected at ~ 5 km from each other at slightly different elevations on the Gandarela plateau (Figures 1, 3a-d), were drilled (2-cm (ID) \times 7-cm long drill bit) and the cores sliced every half or one centimeter.

Goethite grains for (U-Th)/He geochronology were selected, prepared, and analyzed following procedures outlined in Monteiro *et al.* [2014]. Samples for ^3He measurements were prepared in

three ways: (1) crushing canga blocks and picking massive goethite and hematite fragments; (2) micro-drilling (5-mm (ID) diamond drill bit) canga-cemented hematite clasts; and (3) micro-drilling rounded loose pebbles of hematite collected from plateau surfaces or within small channels draining the plateaus. Canga fragments and drill-cores were crushed, sieved, ultrasonically cleaned, washed with acetone or absolute ethanol, and air-dried. For the micro-drilled samples, magnetic separation was used to isolate magnetic from non-magnetic fractions. The magnetic fraction, composed mostly of hypogene magnetite-hematite, was preferentially selected for ^3He analyses. Representative aliquots of goethites selected for geochronology and cosmogenic ^3He measurements were mounted in epoxy disks, polished, and investigated by optical and electron microscopy. A separate aliquot was powdered and studied by X-ray diffractometry (XRD). Mineralogical investigation followed procedures outlined in *Monteiro et al.* [2014].

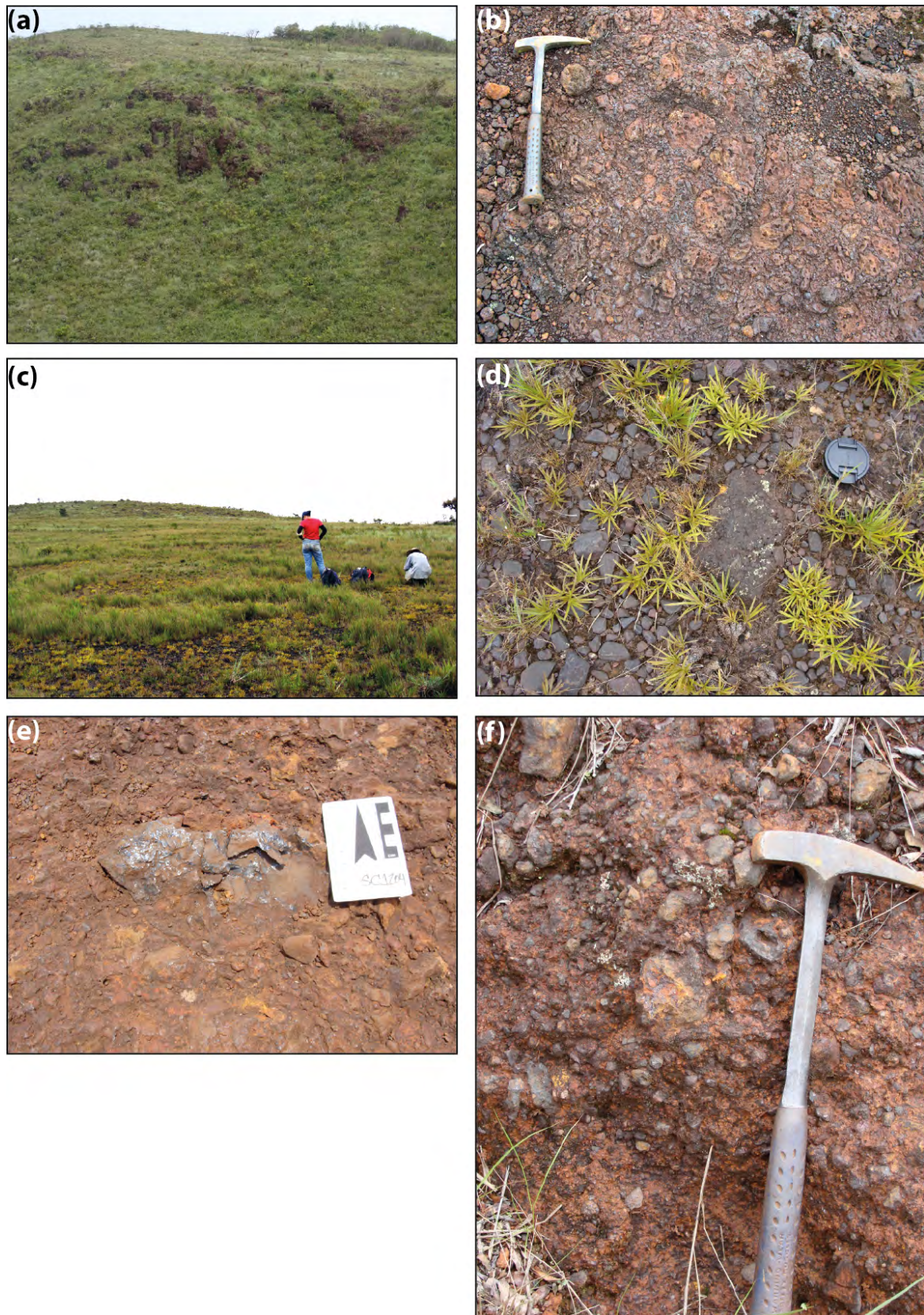


Figure 2: (a) Undulating plateau surfaces are underlain by canga blankets that undergo erosion by rill incision and scarp retreat at plateau edges. (b) The canga blanket shows a complex history of goethite cementation, fragmentation, and recementation. (c) Partial dismantling of the canga blanket generates a (d) colluvial layer composed of loose fragments of hematite-magnetite ore and transported canga blocks that provide useful material for cosmogenic ^3He quantification. (e) Fragments of massive goethite veins cemented into canga and (f) fragments of canga in colluvium yield some of the oldest (U-Th)/He results in this study.

(U-Th)/He geochronology followed procedures outlined in *Shuster et al.* [2005], *Vasconcelos et al.* [2013] and *Monteiro et al.* [2014]. Isothermal holding time modeling confirms that most goethites retain more than 80% of their radiogenic He budget throughout their lifetime [*Heim, et al.* 2006; *Waltenberg, 2012*; *Vasconcelos, et al., 2013*], suggesting that the error propagation used in this study (adding 10% to the age and imposing a $\pm 10\%$ uncertainty) provides a reasonable estimation of the precipitation ages for the grains analyzed. Dating multiple aliquots may help to identify and eliminate obvious outliers associated with the possible presence of hypogene contaminants [*Monteiro, et al., 2014*], further suggesting that the (U-Th)/He results record ages of mineral precipitation. The coexistence of several goethite generations in a single grain may result in mixed ages, a difficult problem to obviate.

Between ~ 5 and 50 mg of sample were loaded in Sn foil packets and degassed at 1200 °C in a resistance furnace. Re-extracts were performed to assure complete gas extraction. Analytical procedures are described elsewhere [*Patterson and Farley, 1998*; *Amidon and Farley, 2011*].

To calculate apparent exposure ages for each sample, we used a sea level high latitude ^3He production rate of $68.1 \pm 8.1 \text{ atoms g}^{-1} \text{ yr}^{-1}$ for hematite, $71.5 \pm 8.5 \text{ atoms g}^{-1} \text{ yr}^{-1}$ for goethite [*Shuster et al., 2012*], and $64.7 \pm 7 \text{ atoms g}^{-1} \text{ yr}^{-1}$ for magnetite ($\sim 5\%$ less than P ^3He for hematite, as suggested by *Masarik* [2002]) corrected for latitude and elevation following procedures outlined in *Stone* [2000]. For samples containing more than one mineral, we estimated the relative proportions of each species by petrographic observation of representative aliquots and calculated total ^3He production based on the proportions of each mineral phase. As some samples show evidence for continuous exposure (discussed below), we cast the same results in terms of erosion rates by using an average density of 2.88 g/cm^3 [*Santos, 2006*] for cangas, and calculate erosion rates ($\dot{\epsilon}$ in $\text{g/cm}^2/\text{yr}$) as $\dot{\epsilon} = P\Lambda/N$, where P is the production rate (atoms/g/yr), Λ is an attenuation lengthscale (160 g/cm^2), and N is the nuclide concentration (atom/g) measured at the surface [*Lal, 1991*]. For goethite samples where (U-Th)/He ages suggest recrystallization in the more recent past, only the oldest exposure ages (or slowest erosion rates) are relevant. Similarly, magnetite-hematite grains may contain areas partially recrystallized to goethite, which potentially results in partial ^3He loss. Therefore, we interpret all results as minimum values and refer to all results as apparent exposure ages (*aEA*).

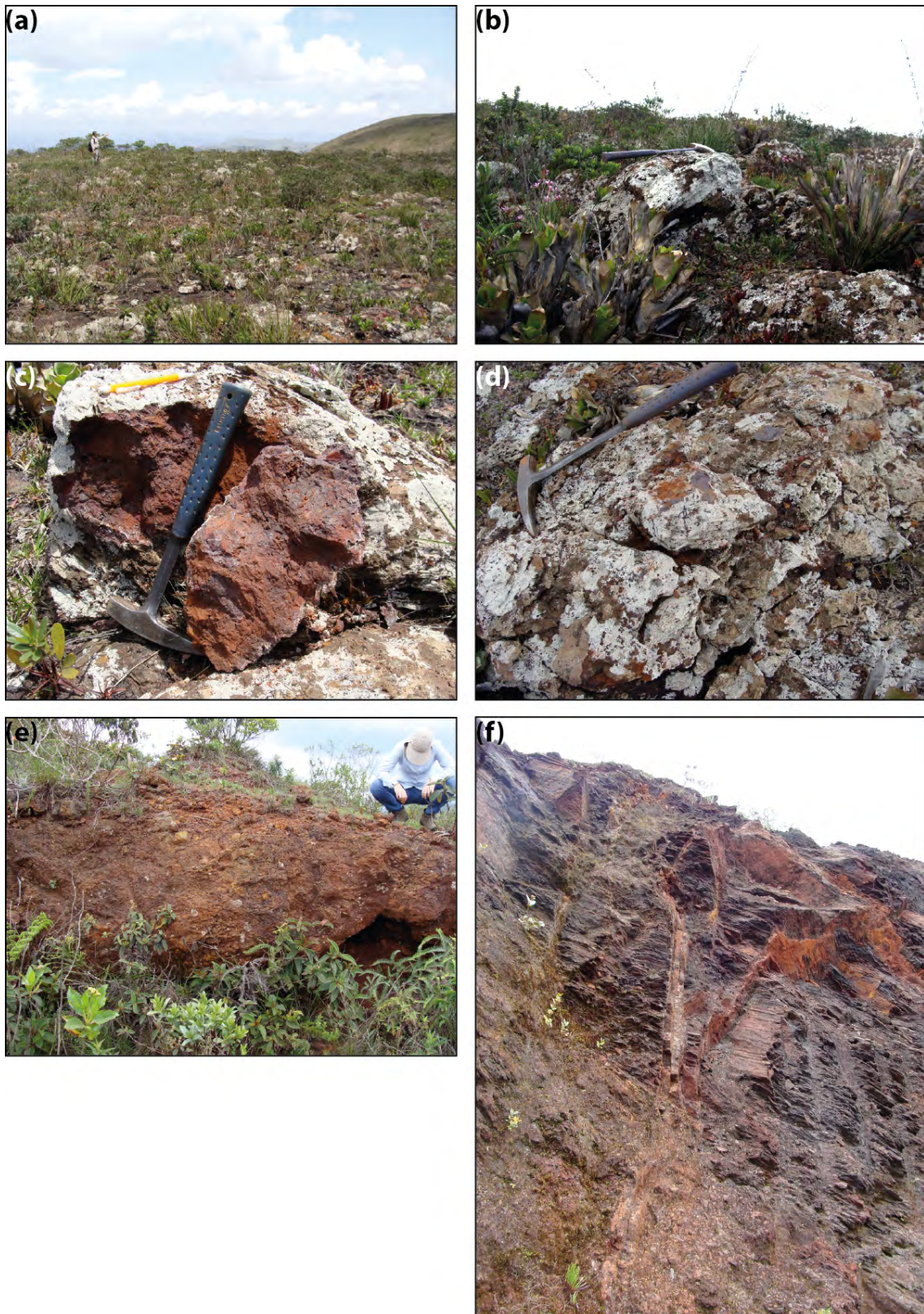


Figure 3: (a) The higher elevation and more extensive Gandarela plateau is underlain by the thickest and most continuous canga blanket in the region [Baltazar *et al.*, 2005a; Carlos *et al.*, 2014]. (b) Boulders of canga covered in lichen and protruding 20-50 cm from the surface reveal the mechanisms (biogeochemical dissolution and physical disaggregation) partially responsible for the very slow destruction of cangas. (c) Fragments of canga or (d) hematite-magnetite ore cemented in cangas were micro-drilled for quantifying the vertical concentration of ^3He . (e) Cobbles and pebbles of hematite-magnetite ore in transported cangas on top of the Gandarela plateau suggest the existence of a paleo drainage system above the present topographic level. (f) Veins of goethite in saprolite provide some of the oldest goethites dated in this study.

4. RESULTS

4.1. Mineralogy

Goethite, hematite, martite (hematite pseudomorph after magnetite), and magnetite are the Fe-bearing phases identified by optical microscopy, XRD, and SEM investigation of samples used in this study. Hematite and magnetite are often partially altered to goethite (Figure 4a,b). Pure goethite masses commonly show evidence of several generations intimately intergrown (Figure 4c,d); goethite masses may also contain small amounts of supergene gibbsite and rarely quartz. Goethite often shows evidence of ferruginized tree roots and bacterial fossils, attesting to the strong role of the biota in iron cementation [Monteiro *et al.*, 2014; Levett *et al.*, 2016].

4.2. (U-Th)/He ages

We report new and previously published [Monteiro *et al.*, 2014] (U-Th)/He goethite precipitation ages (*pAs*) ($n = 157$). New goethite (U-Th)/He results come from plateau surfaces ($n = 86$), detrital canga fragments deposited in colluvia ($n = 19$), and saprolites ($n = 30$) (Table 1; Figures 5, 6). Goethites cementing cangas at Serra do Gandarela yield, on average, older results (53.2-0.8 Ma, $n = 104$) than those obtained for goethites from Serra da Moeda (37.9-0.4 Ma, $n = 49$) and Serra das Serrinhas (24.3-0.4 Ma, $n = 77$) (Table 1; Figure 5a). Goethites from saprolites at the three sites are, on average, older than goethite cements from cangas (Table 1; Figures 5a, 6).

4.3. Cosmogenic ^3He concentrations, *minimum surface exposure ages*, and erosion rates

Fifteen goethite samples previously dated by (U-Th)/He and 60 hematite-magnetite-martite samples were analyzed for cosmogenic ^3He . Most samples yield significant concentrations of ^3He (Table 2), which we interpret to be cosmogenic [Shuster *et al.*, 2012]. Hematite-magnetite and martite grains yield higher ^3He contents than coexisting goethite cements (e.g., samples 1A, 1B, 1C; Table 2), but significant ^3He concentrations also occur in goethite grains (e.g., sample 21; Table 2). Interestingly, a single canga block may display a significant range of ^3He concentrations, as illustrated by the results obtained along 7cm-long 2cm-wide drill cores from samples G1201 and G1209 (Table 2; Figure 7). Detrital fragments and pebbles show ^3He concentrations larger than or equal to those measured from immediately adjacent and partially dismantled canga blocks (Figure 5a,c; Table 2).

Table 1: Published and new (U-Th)/He results for Quadrilátero Ferrífero goethite cements from regional duricrusts, saprolites and colluvia.

Site	Sample Name	Weathering Stage	Latitude/ Longitude	Elevation (m)	Depth (m)	Measured He Age (Ma)	Corrected He Age (Ma)	±	He (nmol/g)	±	U (ppm)	±	Th (ppm)	±	Th/U	Mass (µg)
Serra das Serpinhas	Pic-06-01A/1	duricrust	20° 15' 23.72"S 43° 52' 43.88"W	1495	0	1.7	1.8	0.2	0.0058	0.0021	0.30	0.01	1.45	0.05	4.83	199.70
	Pic-06-01A/1a	duricrust		1495	0	4.2	4.7	0.5	0.0306	0.0013	0.47	0.02	3.68	0.08	7.83	50.64
	Pic-06-01A/1b*	duricrust		1495	0	1.6	1.8	0.2	0.0115	0.0007	0.46	0.02	3.63	0.11	7.88	29.02
	Pic-06-01A/2*	duricrust		1495	0	0.7	0.8	0.2	0.0039	0.0020	0.49	0.02	2.06	0.05	4.20	52.94
	Pic-06-01A/3	duricrust		1495	0	2.7	2.9	0.3	0.0098	0.0022	0.31	0.01	1.58	0.05	5.10	175.25
	Pic-06-01A/4	duricrust		1495	0	3.0	3.3	0.3	0.0145	0.0023	0.31	0.01	2.51	0.06	8.10	119.79
	Pic-06-01A/4a*	duricrust		1495	0	0.6	0.7	0.1	0.0037	0.0008	0.30	0.01	3.32	0.07	11.18	76.26
	Pic-06-01A/4b*	duricrust		1495	0	0.5	0.6	0.1	0.0022	0.0006	0.20	0.01	2.32	0.05	11.37	81.61
	Pic-06-01A/4c*	duricrust		1495	0	0.4	0.4	0.1	0.0028	0.0007	0.36	0.01	4.16	0.08	11.66	83.06
	Pic-06-01A/5b*	duricrust		1495	0	1.6	1.7	0.3	0.0027	0.0007	0.12	0.01	0.80	0.03	6.50	106.22
	Pic-06-01A/5c*	duricrust		1495	0	0.5	0.6	0.1	0.0017	0.0006	0.14	0.01	1.96	0.04	13.88	128.49
	Pic-06-01A/6a*	duricrust		1495	0	1.2	1.4	0.2	0.0053	0.0007	0.31	0.02	2.03	0.06	6.45	48.13
	Pic-06-01A/6b*	duricrust		1495	0	0.7	0.8	0.4	0.0019	0.0004	0.18	0.01	1.33	0.05	7.36	51.32
	Pic-06-01A/6c	duricrust		1495	0	2.5	2.7	0.3	0.0163	0.0010	0.41	0.02	3.41	0.08	8.29	56.33
	Pic-06-01A/7a*	duricrust		1495	0	0.8	0.9	0.5	0.0018	0.0004	0.17	0.01	0.90	0.05	5.26	49.43
	Pic-06-01A/7b*	duricrust		1495	0	0.6	0.7	0.2	0.0019	0.0005	0.15	0.01	1.72	0.05	11.09	72.24
	Pic-06-01A/7c*	duricrust		1495	0	0.4	0.4	0.2	0.0013	0.0004	0.20	0.01	2.05	0.05	10.49	68.16
	Pic-06-01A/8a	duricrust		1495	0	1.9	2.1	0.2	0.0285	0.0012	0.61	0.02	9.06	0.15	14.97	54.63
	Pic-06-01A/8b*	duricrust		1495	0	0.4	0.5	0.2	0.0016	0.0005	0.23	0.01	2.06	0.05	9.15	68.43
	Pic-06-01A/8c	duricrust		1495	0	3.4	3.7	0.4	0.0178	0.0010	0.31	0.01	2.81	0.07	8.98	52.93
	Pic-06-01B/1	duricrust	20° 15' 23.72"S 43° 52' 43.88"W	1495	0	1.4	1.5	0.2	0.0051	0.0020	0.30	0.01	1.62	0.05	5.40	119.53
	Pic-06-01B/3	duricrust		1495	0	2.7	2.9	0.3	0.0214	0.0025	0.64	0.02	3.55	0.07	5.55	139.68
	Pic-06-01B/3a	duricrust		1495	0	2.3	2.6	0.3	0.0136	0.0023	0.38	0.02	2.94	0.07	7.84	54.94
	Pic-06-01B/3b	duricrust		1495	0	2.3	2.5	0.3	0.0160	0.0024	0.50	0.02	3.29	0.07	6.63	84.29
	Pic-06-01B/3c	duricrust		1495	0	2.2	2.5	0.2	0.0101	0.0022	0.35	0.02	2.08	0.06	5.97	63.26
	Pic-06-01B/4	duricrust		1495	0	1.3	1.5	0.1	0.0080	0.0021	0.50	0.02	2.60	0.06	5.20	72.78
	Pic-06-01B/5a	duricrust		1495	0	1.9	2.1	0.2	0.0069	0.0021	0.19	0.01	2.00	0.05	10.30	90.85
	Pic-06-01B/5b*	duricrust		1495	0	1.3	1.4	0.2	0.0054	0.0021	0.22	0.01	2.36	0.06	10.58	69.01
	Pic-06-01B/5c	duricrust		1495	0	1.3	1.4	0.1	0.0074	0.0021	0.37	0.01	2.95	0.05	8.06	126.01
	Pic-06-01C/2	duricrust	20° 15' 23.72"S 43° 52' 43.88"W	1495	0	3.3	3.6	0.4	0.0568	0.0036	1.30	0.03	8.09	0.12	6.22	187.83
	Pic-06-01C/2a	duricrust		1495	0	3.1	3.4	0.3	0.1070	0.0050	2.66	0.06	15.89	0.23	5.97	51.04
	Pic-06-01C/2b	duricrust		1495	0	2.7	2.9	0.3	0.0297	0.0028	0.78	0.03	5.39	0.10	6.90	68.87
	Pic-06-01C/2c	duricrust		1495	0	5.1	5.6	0.6	0.0554	0.0035	0.81	0.02	5.01	0.09	6.22	87.64
	Pic-06-01C/3	duricrust		1495	0	2.6	2.8	0.3	0.0345	0.0029	0.96	0.02	6.37	0.10	6.64	75.99
	Pic-06-01C/5	duricrust		1495	0	2.5	2.8	0.3	0.0230	0.0026	0.76	0.02	3.87	0.07	5.09	109.29
	Pic-06-01C/6a	duricrust		1495	0	5.5	6.1	0.6	0.3310	0.0115	3.61	0.07	31.45	0.36	8.72	58.05
	Pic-06-01C/6b	duricrust		1495	0	6.0	6.6	0.7	0.0711	0.0040	0.71	0.02	6.19	0.10	8.73	91.73
	Pic-06-01C/6c	duricrust		1495	0	1.8	2.0	0.2	0.0117	0.0022	0.75	0.02	1.91	0.04	2.55	121.47
	Pic-06-02/1	duricrust	20° 15' 23.47"S 43° 52' 43.50"W	1490	5	0.8	0.9	0.1	0.0038	0.0020	0.47	0.02	1.79	0.05	3.81	119.04
	Pic-06-02/2	duricrust		1490	5	0.9	0.9	0.1	0.0055	0.0021	0.57	0.02	2.55	0.06	4.47	96.24
	Pic-06-02/4*	duricrust		1490	5	1.5	1.7	0.2	0.0066	0.0021	0.37	0.01	1.79	0.05	4.84	62.97
	Pic-06-02/5*	duricrust		1490	5	1.3	1.4	0.2	0.0108	0.0022	0.83	0.02	3.15	0.06	3.80	31.83
	Pic-06-02/6	duricrust		1490	5	1.0	1.1	0.1	0.0066	0.0021	0.75	0.02	2.19	0.05	2.92	81.32
	Pic-06-02/7	duricrust		1490	5	1.9	2.1	0.2	0.0159	0.0024	0.76	0.02	3.24	0.07	4.26	103.08
	Pic-06-02/8	duricrust		1490	5	1.6	1.8	0.2	0.0128	0.0023	0.79	0.02	2.86	0.06	3.62	74.56
	Pic-06-02/9*	duricrust		1490	5	0.7	0.7	0.2	0.0037	0.0020	0.49	0.02	2.12	0.05	4.33	45.06
	Pic-06-02/10a*	duricrust		1490	5	1.9	2.0	0.3	0.0033	0.0020	0.14	0.01	0.81	0.03	5.76	95.55
	Pic-06-02/10b*	duricrust		1490	5	1.6	1.8	0.3	0.0053	0.0021	0.24	0.01	1.49	0.05	6.15	57.54
	Pic-06-02/10c*	duricrust		1490	5	1.6	1.7	0.3	0.0044	0.0020	0.18	0.01	1.40	0.04	7.75	69.47
	Pic-06-02/11a*	duricrust		1490	5	0.4	0.5	0.1	0.0012	0.0019	0.16	0.01	1.58	0.03	9.68	184.89
	Pic-06-02/11b*	duricrust		1490	5	1.7	1.9	0.2	0.0046	0.0020	0.19	0.01	1.29	0.04	6.80	78.73
	Pic-06-02/11c*	duricrust		1490	5	1.0	1.1	0.2	0.0027	0.0020	0.15	0.01	1.54	0.04	10.48	106.33
	Pic-06-03/1	duricrust	20° 15' 23.79"S 43° 52' 43.88"W	1480	15	14.3	15.7	1.6	0.4367	0.0146	2.44	0.05	13.53	0.17	5.55	103.64
	Pic-06-03/2	duricrust		1480	15	9.9	10.8	1.1	0.3537	0.0122	5.64	0.10	4.09	0.07	0.73	67.91
	Pic-06-03/3	duricrust		1480	15	3.0	3.3	0.3	0.0713	0.0040	2.06	0.04	9.68	0.13	4.70	102.81
	Pic-06-03/4	duricrust		1480	15	12.7	14.0	1.4	0.3097	0.0109	2.30	0.05	9.25	0.13	4.02	125.88
	Pic-06-03/5	duricrust		1480	15	18.3	20.1	2.0	0.4459	0.0149	3.62	0.07	3.68	0.07	1.02	146.97
	Pic-06-03/6a	duricrust		1480	15	22.1	24.4	2.4	0.3463	0.0120	2.22	0.04	2.79	0.05	1.26	112.38
	Pic-06-03/6b	duricrust		1480	15	17.6	19.3	1.9	0.5129	0.0168	2.83	0.05	10.77	0.15	3.80	78.05
	Pic-06-03/6c	duricrust		1480	15	6.7	7.4	0.7	0.3630	0.0125	2.57	0.04	31.30	0.28	12.18	122.47
	Pic-06-07/1*	duricrust	20° 12' 38.52"S 43° 51' 10.76"W	1554	1	0.4	0.4	0.1	0.0040	0.0020	1.35	0.03	2.07	0.05	1.53	95.20
	Pic-06-07/1a*	duricrust		1554	1	0.7	0.8	0.1	0.0065	0.0004	1.22	0.04	2.00	0.06	1.64	47.90
	Pic-06-07/1b	duricrust		1554	1	1.7	1.9	0.2	0.0323	0.0007	2.60	0.07	3.83	0.10	1.47	37.23
	Pic-06-07/1c	duricrust		1554	1	0.7	0.8	0.1	0.0157	0.0005	2.95	0.07	4.47	0.10	1.51	39.64
	Pic-06-07/5a	duricrust		1554	1	1.2	1.3	0.1	0.0147	0.0005	1.67	0.05	2.47	0.07	1.48	42.38
	Pic-06-07/5b	duricrust		1554	1	0.8	0.9	0.1	0.0177	0.0008	3.48	0.06	2.80	0.06	0.80	81.79
	Pic-06-07/5c	duricrust		1554	1	2.8	3.1	0.3	0.2400	0.0036	9.66	0.15	24.85	0.35	2.57	33.18
	Pic-06-08/2*	duricrust	20° 12' 38.09"S 43° 51' 11.17"W	1555	0	1.2	1.3	0.1	0.0045	0.0020	0.54	0.02	0.62	0.04	1.15	89.85
	Pic-06-08/6b	duricrust		1555	0	3.9	4.2	0.4	0.1007	0.0018	3.37	0.08	6.08	0.13	1.80	39.36
	Pic-06-08/6c	duricrust		1555	0	3.2	3.5	0.4	0.0879	0.0014	3.60	0.09	6.01	0.14	1.67	32.06
	Pic-06-08/7a	duricrust		1555	0	1.9	2.0	0.2	0.0189	0.0009	1.29	0.03	2.48	0.05	1.93	92.08
	Pic-06-08/7b	duricrust		1555	0	1.7	1.8	0.2	0.0117	0.0008	0.91	0.02	1.61	0.04	1.77	116.39
	Pic-06-08/7c	duricrust		1555	0	2.4	2.7	0.3	0.0146	0.0010	0.82	0.02	1.25	0.03	1.53	125.01
Pic-06-08/9a	duricrust	1555		0	2.4	2.6	0.3	0.0114	0.0006	0.59	0.02	1.19	0.04	2.01	60.49	
Pic-06-08/9b	duricrust	1555		0	5.0	5.5	0.6	0.1174	0.0033							

Table 1: Published and new (U-Th)/He results for Quadrilátero Ferrífero goethite cements from regional duricrusts, saprolites and colluvia.

Site	Sample Name	Weathering Stage	Latitude/ Longitude	Elevation (m)	Depth (m)	Measured He Age (Ma)	Corrected He Age (Ma)	±	He (nmol/g)	±	U (ppm)	±	Th (ppm)	±	Th/U	Mass (µg)
Serra do Gandarela	Pic-06-21/5	duricrust		1651	0	8.3	9.1	0.9	0.0740	0.0041	0.80	0.02	3.59	0.07	4.49	137.77
	Pic-06-21/6 a	duricrust		1651	0	27.0	29.7	3.0	0.6569	0.0260	2.62	0.05	7.87	0.12	3.01	88.32
	Pic-06-21/6 b	duricrust		1651	0	16.0	17.6	1.8	0.5454	0.0180	2.55	0.05	15.79	0.20	6.20	73.72
	Pic-06-21/6 c	duricrust		1651	0	17.7	19.4	1.9	0.7843	0.0324	3.20	0.05	21.08	0.23	6.59	92.08
	Pic-06-21/6 d	duricrust		1651	0	10.7	11.8	1.2	0.3641	0.0202	3.54	0.04	11.44	0.14	3.23	123.72
	Pic-06-21/6 e	duricrust		1651	0	20.0	21.9	2.2	0.4772	0.0160	1.74	0.04	11.30	0.16	6.51	74.54
	Pic-06-21/6 f	duricrust		1651	0	26.5	29.2	2.9	0.7024	0.0201	2.51	0.05	10.01	0.15	3.99	63.76
	Pic-06-21/6 g	duricrust		1651	0	23.6	25.9	2.6	0.4419	0.0218	1.83	0.04	6.87	0.10	3.76	110.01
	Pic-06-21/6 h	duricrust		1651	0	21.4	23.5	2.3	0.3645	0.0134	1.57	0.04	6.66	0.11	4.25	81.98
	Pic-06-21/6 i	duricrust		1651	0	18.0	19.8	2.0	0.4401	0.0147	1.61	0.04	12.24	0.17	7.60	73.41
	Pic-06-21/6 j	duricrust		1651	0	12.7	13.9	1.4	0.6244	0.0156	3.26	0.07	24.67	0.30	7.57	55.57
	Pic-06-21/6 l	duricrust		1651	0	18.1	20.0	2.0	0.1975	0.0126	0.90	0.02	4.69	0.07	5.23	142.10
	Pic-06-21/6 m	duricrust		1651	0	15.6	17.1	1.7	0.5978	0.0212	2.94	0.05	17.49	0.21	5.96	79.19
	Pic-06-21/6 n	duricrust		1651	0	20.4	22.5	2.2	0.4532	0.0215	1.77	0.04	9.83	0.13	5.57	105.87
	Pic-06-21/6 o	duricrust		1651	0	14.5	15.9	1.6	0.5587	0.0203	2.57	0.05	19.20	0.23	7.47	81.03
	Pic-06-21/6 p	duricrust		1651	0	13.6	15.0	1.5	0.4487	0.0217	2.83	0.04	13.67	0.16	4.83	107.86
	Pic-06-21/6 q	duricrust		1651	0	17.5	19.2	1.9	0.5468	0.0188	2.17	0.05	15.22	0.19	7.03	76.47
	Pic-06-21/6 r	duricrust		1651	0	21.9	24.1	2.4	0.8249	0.0284	2.98	0.05	16.72	0.21	5.61	76.79
	Pic-06-21/6 s	duricrust		1651	0	15.1	16.6	1.7	0.3735	0.0180	2.62	0.04	8.19	0.11	3.12	107.70
	Pic-06-21/6 t	duricrust		1651	0	20.9	23.0	2.3	0.4029	0.0148	1.68	0.04	7.95	0.12	4.74	82.01
	Pic-06-21/6 u	duricrust		1651	0	18.4	20.2	2.0	0.4516	0.0194	2.23	0.04	9.74	0.13	4.37	95.99
	Pic-06-21-1G-1a	duricrust		1651	0	26.3	28.9	2.9	0.4039	0.0247	1.20	0.02	6.90	0.09	5.77	136.28
	Pic-06-21-1G-1b	duricrust		1651	0	26.6	29.3	2.9	0.5166	0.0313	1.29	0.03	9.66	0.12	7.47	135.10
	Pic-06-21-1G-1c	duricrust		1651	0	43.7	48.1	4.8	0.4620	0.0128	0.30	0.01	6.96	0.12	23.16	61.62
	Pic-06-21-1G-2a	duricrust		1651	0	30.2	33.2	3.3	0.2254	0.0107	0.76	0.02	2.59	0.05	3.41	105.64
	Pic-06-21-1G-2b	duricrust		1651	0	28.9	31.8	3.2	0.2939	0.0214	0.97	0.02	3.81	0.06	3.93	162.42
	Pic-06-21-1G-3a	duricrust		1651	0	41.6	45.8	4.6	0.2269	0.0076	0.45	0.02	2.33	0.05	5.14	74.50
	Pic-06-21-1G-3b	duricrust		1651	0	25.9	28.5	2.8	0.2176	0.0134	0.84	0.02	3.01	0.05	3.60	136.95
	Pic-06-21-1G-3c	duricrust		1651	0	23.4	25.8	2.6	0.5254	0.0087	2.51	0.07	6.85	0.14	2.73	36.26
	Pic-06-21-1G-4a	duricrust		1651	0	19.0	20.9	2.1	0.4119	0.0075	2.22	0.06	7.54	0.14	3.40	39.17
	Pic-06-21-1G-4b	duricrust		1651	0	21.3	23.5	2.3	0.5630	0.0133	2.68	0.06	9.24	0.15	3.45	52.14
	Pic21_FG	duricrust		1651	0	20.6	22.6	2.3	0.5498	0.0136	2.54	0.06	10.08	0.16	3.97	54.98
	Pic21_FG	duricrust		1651	0	25.9	28.5	2.8	0.4575	0.0147	1.52	0.04	7.32	0.12	4.82	71.83
	Pic21_FG	duricrust		1651	0	30.6	33.6	3.4	1.3034	0.0232	3.95	0.08	16.46	0.25	4.16	39.81
	Pic-06-21_frostedGt	duricrust		1651	0	32.1	35.3	3.5	0.2858	0.0029	1.02	0.03	2.62	0.06	2.58	96.65
	Pic-06-21_frostedGt	duricrust		1651	0	30.5	33.5	3.4	0.3315	0.0221	1.11	0.04	3.79	0.10	3.42	43.98
	Pic21_VG	duricrust	20° 07' 5.48"S 43° 39' 38.02"W	1651	0	9.7	10.6	1.1	0.7544	0.0127	5.36	0.10	38.32	0.46	7.15	37.37
	Pic21_VG	duricrust		1651	0	9.6	10.5	1.1	0.6240	0.0100	5.26	0.10	28.73	0.38	5.47	35.30
	Pic21_VG	duricrust		1651	0	11.3	12.5	1.2	0.6682	0.0133	3.40	0.07	31.66	0.38	9.30	44.38
	Pic21_VG	duricrust		1651	0	9.5	10.5	1.0	0.6035	0.0269	6.49	0.06	22.05	0.23	3.40	99.33
	Pic21_VG	duricrust		1651	0	10.0	11.0	1.1	0.9361	0.0187	8.10	0.11	39.00	0.44	4.82	44.52
	Pic21_VG	duricrust		1651	0	11.7	12.8	1.3	0.8223	0.0141	5.34	0.10	32.45	0.41	6.08	38.11
	Pic21_FwVG	duricrust		1651	0	17.2	18.9	1.9	1.3388	0.0410	7.61	0.08	28.62	0.31	3.76	68.28
	Pic21_FwVG	duricrust		1651	0	16.2	17.9	1.8	0.8160	0.0142	4.68	0.09	19.35	0.28	4.13	38.56
	Pic21_FwVG	duricrust		1651	0	14.3	15.7	1.6	0.6645	0.0129	4.61	0.09	16.84	0.25	3.66	43.15
	Pic21_FwVG	duricrust		1651	0	19.2	21.1	2.1	1.2544	0.0298	6.00	0.09	25.51	0.31	4.25	52.94
	Pic21_FwVG	duricrust		1651	0	17.7	19.4	1.9	0.7766	0.0130	3.73	0.08	18.47	0.27	4.95	37.13
	Pic21_FwVG	duricrust		1651	0	17.7	19.5	2.0	0.9613	0.0266	4.79	0.08	21.98	0.27	4.58	61.71
	Pic-06-21-2G-1	duricrust		1651	0	21.0	23.1	2.3	0.0208	0.0014	0.11	0.01	0.30	0.03	2.64	55.16
	Pic-06-21-2G-2	duricrust		1651	0	22.9	25.2	2.5	0.0243	0.0025	0.13	0.01	0.27	0.01	2.01	162.84
	Pic-06-21-2G-3	duricrust		1651	0	28.6	31.5	3.1	0.0299	0.0022	0.11	0.01	0.35	0.02	3.17	103.00
	Pic-06-21-2G-4	duricrust		1651	0	10.8	11.9	1.2	0.0228	0.0019	0.21	0.01	0.75	0.04	3.61	61.89
	Pic-06-21-2G-5	duricrust		1651	0	27.6	27.6	5.8	0.0150	0.0018	0.09	0.01	0.05	0.02	0.61	72.40
	Pic-06-21-2G-6	duricrust		1651	0	16.8	18.5	1.8	0.0557	0.0034	0.39	0.01	0.92	0.03	2.34	114.41
	Pic-06-21-2G-7	duricrust		1651	0	19.8	21.7	2.2	0.0350	0.0025	0.19	0.01	0.57	0.02	2.99	105.37
	Pic-06-21-2G-8	duricrust		1651	0	16.5	18.1	1.8	0.0386	0.0027	0.21	0.01	0.95	0.03	4.55	120.71
	Pic-06-21-2G-9	duricrust		1651	0	43.3	47.7	4.8	0.0265	0.0024	0.10	0.005	0.07	0.01	0.72	140.29
	Pic-06-21-2G-10	duricrust		1651	0	22.0	22.0	5.8	0.0141	0.0016	0.10	0.01	0.05	0.04	0.52	46.08
	Pic21_AlPoor Goe	duricrust		1651	0	27.4	30.1	3.0	0.0383	0.0019	0.23	0.01	0.11	0.02	0.49	78.54
	Pic21_AlPoor Goe	duricrust		1651	0	21.3	23.5	2.3	0.0401	0.0017	0.32	0.01	0.11	0.03	0.36	59.12
	Pic21_AlPoor Goe	duricrust		1651	0	24.3	26.7	2.7	0.1628	0.0067	0.63	0.02	2.57	0.05	4.11	90.53
	Pic21_AlPoor Goe	duricrust		1651	0	21.8	23.9	2.4	0.0660	0.0037	0.29	0.01	1.12	0.03	3.83	117.58
	Pic21_AlPoor Goe	duricrust		1651	0	27.5	30.3	3.0	0.0319	0.0020	0.21	0.01	0.02	0.02	0.12	101.66
	Pic21_AlPoor Goe	duricrust		1651	0	27.1	29.8	3.0	0.0271	0.0010	0.17	0.01	0.07	0.02	0.43	78.60
	Pic21_AlPoor Goe	duricrust		1651	0	28.8	31.7	3.2	0.1112	0.0054	0.26	0.01	1.90	0.04	7.27	108.25
	Pic21_AlPoor Goe	duricrust		1651	0	26.9	29.6	3.0	0.1112	0.0027	0.38	0.02	1.60	0.05	4.20	53.29
	Pic21_AlPoor Goe	duricrust		1651	0	32.3	35.5	3.5	0.0658	0.0030	0.26	0.01	0.47	0.02	1.78	89.83
	Pic21_AlPoor Goe	duricrust		1651	0	26.8	29.4	2.9	0.1008	0.0054	0.38	0.01	1.32	0.03	3.44	115.55
	Pic21_AlPoor Goe	duricrust		1651	0	26.8	29.5	2.9	0.0396	0.0020	0.24	0.01	0.14	0.02	0.59	84.44
	Pic21_AlPoor Goe	duricrust		1651	0	27.4	30.1	3.0	0.0570	0.0020	0.24	0.01	0.62	0.04	2.61	60.78
	Pic21_AlPoor Goe	duricrust		1651	0	31.6	34.7	3.5	0.0232	0.0017	0.11	0.01	0.09	0.02	0.84	104.16
	Pic21_AlPoor Goe	duricrust		1651	0	29.7	32.7	3.3	0.0333	0.0031	0.15	0.01	0.22	0.01	1.47	189.21
	Pic21_AlPoor Goe	duricrust		1651	0	48.3	53.2	5.3	0.0301	0.0023	0.09	0.00	0.10	0.01	1.12	172.82
	Pic-06-24/1	duricrust		1506	5	14.7	16.1	1.6	0.4344	0.0145	4.56	0.08	3.39	0.07	0.74	90.85
	Pic-06-24/2	duricrust		1506	5	6.7	7.4	0.7	0.1682	0.0068	4.43	0.08	0.84	0.04	0.19	70.73
	Pic-06-24/3*	duricrust	20° 06' 45.50"S	1506	5	5.8	6.3	6.4	0.2750	0.0099	7.55	0.13	5.23	0.09	0.69	0.16</

Table 1: Published and new (U-Th)/He results for Cuadrilátero Ferrífero goethite cements from regional duricrusts, saprolites and colluvia.

Site	Sample Name	Weathering Stage	Latitude/ Longitude	Elevation (m)	Depth (m)	Measured He Age (Ma)	Corrected He Age (Ma)	±	He (nmol/g)	±	U (ppm)	±	Th (ppm)	±	Th/U	Mass (µg)
Serrado Gandra	G-12-04A_black	duricrust	20° 06' 0.53"S 43° 40' 39.2"W	1670	0	8.12	8.9	0.9	0.120	0.0038	1.95	0.04	3.30	0.07	1.69	66.98
	G-12-04A_black	duricrust		1670	0	7.21	7.9	0.8	0.074	0.0039	1.39	0.03	2.16	0.05	1.55	112.31
	G-12-04A_black	duricrust		1670	0	10.68	11.7	1.2	0.099	0.0060	1.37	0.03	1.45	0.04	1.06	132.06
	G-12-04A_brown	duricrust		1670	0	18.79	20.7	2.1	0.192	0.0090	1.02	0.03	3.62	0.07	3.53	103.76
	G-12-04A_brown	duricrust		1670	0	21.72	23.9	2.4	0.233	0.0154	1.14	0.03	3.55	0.06	3.12	146.88
	G-12-04A_brown	duricrust		1670	0	17.86	19.6	2.0	0.285	0.0091	1.69	0.04	5.31	0.09	3.15	70.78
	G-12-05 vitreous black	duricrust	20° 06' 0.21"S 43° 40' 39.37"W	1659	0	0.76	0.8	0.1	0.028	0.0024	1.01	0.02	24.77	0.22	24.52	166.44
	G-12-05 vitreous black	duricrust		1659	0	1.54	1.7	0.2	0.039	0.0036	0.36	0.01	18.34	0.17	50.44	195.87
	G-12-05	duricrust		1659	0	3.45	3.8	0.4	0.185	0.0040	1.72	0.05	34.56	0.40	20.06	45.41
	G-12-05	duricrust		1659	0	5.06	5.6	0.6	0.265	0.0070	1.39	0.04	34.94	0.37	25.21	58.30
	G-12-06	duricrust	20° 06' 0.21"S 43° 40' 39.37"W	1659	0	31.43	34.6	3.5	0.040	0.0042	0.20	0.01	0.12	0.01	0.60	228.55
	G-12-06	duricrust		1659	0	47.98	52.8	5.3	0.074	0.0080	0.24	0.01	0.17	0.01	0.69	240.08
	G-12-06 (drill-core)	duricrust		1659	0	16.84	18.5	1.9	0.350	0.0199	2.73	0.04	4.66	0.08	1.71	126.73
	G-12-06 (drill-core)	duricrust		1659	0	23.72	26.1	2.6	0.187	0.0174	1.15	0.02	1.29	0.03	1.13	206.41
	G-12-06 (drill-core)	duricrust		1659	0	44.30	48.7	4.9	0.376	0.0461	0.92	0.02	2.70	0.04	2.92	273.24
	G-12-06 (reddish)	duricrust		1659	0	8.15	9.0	0.9	0.232	0.0188	3.32	0.04	8.10	0.10	2.44	180.57
	G-12-06 vitreous black	duricrust		1659	0	7.13	7.8	0.8	0.246	0.0166	4.11	0.04	9.49	0.11	2.31	181.68
	G-12-06 vitreous black	duricrust		1659	0	7.18	7.9	0.8	0.217	0.0200	3.95	0.04	6.81	0.09	1.72	170.52
	G-12-08	duricrust	20° 06' 59.02"S	1644		13.91	15.3	1.5	0.416	0.0239	4.679	0.053	3.455	0.061	0.74	127.87
	G-12-08	duricrust	43° 39' 40.32"W	1644		14.78	16.3	1.6	0.520	0.0292	4.086	0.051	10.084	0.131	2.47	125.44
	G-12-09	duricrust	20° 07' 3.88"S 43° 39' 38.97"W	1658	0	6.69	7.4	0.7	0.185	0.0137	4.221	0.042	3.723	0.060	0.88	164.78
	G-12-09	duricrust		1658	0	7.03	7.7	0.8	0.185	0.0130	4.297	0.044	2.325	0.044	0.54	156.00
	GA-13-04 Type1	duricrust	20° 01' 00.1"S 43° 34' 43.1"W	1134	0	5.18	5.7	0.6	0.051		1.296	0.035	2.208	0.055	1.70	87.86
	GA-13-04 Type1	duricrust		1134	0	9.85	10.8	1.1	0.045		0.692	0.026	0.664	0.041	0.96	66.29
	Pic-06-22/5	saprolite	20° 06' 42.94"S 43° 39' 2.69"W	1490	10	48.6	53.5	5.4	0.1162	0.0053	0.41	0.02	0.10	0.03	0.24	107.54
	Pic-06-22/5a	saprolite		1490	10	29.0	31.9	3.2	0.0683	0.0033	0.42	0.01	0.04	0.02	0.10	105.64
	Pic-06-22/5b	saprolite		1490	10	27.1	29.8	3.0	0.0627	0.0027	0.42	0.02	0.04	0.02	0.09	93.19
	Pic-06-22/5c	saprolite		1490	10	37.6	41.4	4.1	0.0830	0.0055	0.40	0.01	0.04	0.01	0.09	148.13
	Pic 06 22 gr1_black	saprolite		1490	10	18.49	20.3	2.0	0.5096	0.0180	5.02	0.07	0.16	0.02	0.03	78.62
	Pic 06 22 gr2_black	saprolite		1490	10	22.24	24.5	2.4	0.4781	0.0220	3.86	0.05	0.37	0.02	0.10	102.48
	Pic 06 22 gr3_black	saprolite		1490	10	14.54	16.0	1.6	0.4653	0.0270	5.84	0.04	0.16	0.01	0.03	129.57
	Pic 06 22 gr4_black	saprolite		1490	10	15.83	17.4	1.7	0.5036	0.0227	5.80	0.06	0.18	0.02	0.03	100.28
	Pic 06 23 gr1	saprolite	20° 06' 42.80"S 43° 39' 2.64"W	1517		10.10	11.1	1.1	0.1493	0.0040	2.68	0.06	0.17	0.03	0.06	55.80
	Pic 06 23 gr2	saprolite		1517		8.61	9.5	0.9	0.1011	0.0062	2.13	0.03	0.12	0.01	0.06	133.00
	Pic 06 23 gr3	saprolite		1517		20.15	22.2	2.2	0.1930	0.0073	1.73	0.04	0.14	0.02	0.08	82.52
	Pic 06 23 gr4	saprolite		1517		11.04	12.1	1.2	0.1582	0.0064	2.59	0.05	0.19	0.02	0.07	88.64
	G-12-10	saprolite	20° 06' 42.20"S	1533	5	16.53	18.2	1.8	0.188	0.0133	1.414	0.028	2.870	0.050	2.03	157.32
	G-12-10	saprolite	43° 39' 5.75"W	1533	5	18.14	20.0	2.0	0.133	0.0058	0.877	0.026	1.985	0.048	2.26	95.58
	G-12-10	saprolite		1533	5	18.32	20.2	2.0	0.225	0.0080	1.626	0.041	2.691	0.064	1.65	78.41
	G-12-11 botryoidal gt	saprolite	20° 07' 5.96"S 43° 38' 55.84"W	1441	15	32.72	36.0	3.6	0.135	0.0113	0.731	0.018	0.116	0.012	0.16	184.69
	G-12-11 botryoidal gt	saprolite		1441	15	35.87	39.5	3.9	0.133	0.0140	0.660	0.016	0.082	0.009	0.12	234.42
	G-12-11 botryoidal gt	saprolite		1441	15	36.72	40.4	4.0	0.133	0.0058	0.645	0.019	0.075	0.018	0.12	95.33
	G-12-11 layered gt	saprolite		1441	15	28.27	31.1	3.1	0.195	0.0058	1.242	0.034	0.111	0.026	0.09	65.05
	G-12-11 layered gt	saprolite		1441	15	27.35	30.1	3.0	0.191	0.0080	1.249	0.030	0.148	0.020	0.12	91.98
	G-12-12	saprolite	20° 07' 5.96"S 43° 38' 55.84"W	1441	15	16.09	17.7	1.8	0.124	0.0063	1.287	0.040	0.554	0.045	0.43	40.21
	G-12-12	saprolite		1441	15	28.87	31.8	3.2	0.185	0.0087	1.144	0.030	0.119	0.021	0.10	77.01
	G-12-12	saprolite		1441	15	22.28	24.5	2.5	0.129	0.0091	1.022	0.024	0.167	0.015	0.16	156.30
	G-12-12	saprolite		1441	15	26.24	28.9	2.9	0.122	0.0131	0.844	0.018	0.026	0.008	0.03	239.97
	G-12-07a	colluvium	20° 06' 3.07"S 43° 40' 31.82"W	1654		0.48	0.5	0.1	0.003	0.0013	0.337	0.013	2.620	0.050	7.79	138.04
	G-12-07a	colluvium		1654		1.27	1.4	0.1	0.001	0.0014	0.129	0.009	0.326	0.021	2.51	115.82
	G-12-07b (cement)	colluvium		1654		0.79	0.9	0.1	0.008	0.0014	0.770	0.019	4.575	0.066	5.95	186.52
	G-12-07b (cement)	colluvium		1654		0.99	1.1	0.1	0.012	0.0014	0.817	0.023	5.871	0.091	7.19	115.96
	G-12-07b (massive)	colluvium		1654		7.69	8.5	0.8	0.135	0.0139	2.510	0.029	3.012	0.046	1.20	229.78
	G-12-07b (massive)	colluvium		1654		20.30	22.3	2.2	0.084	0.0065	0.630	0.017	0.538	0.019	0.85	170.58
	G-12-07c	colluvium		1654		21.74	23.9	2.4	0.213	0.0194	1.697	0.027	0.446	0.016	0.26	202.88
	G-12-07c	colluvium		1654		28.86	31.8	3.2	0.205	0.0094	1.209	0.031	0.395	0.025	0.33	101.91

Table 1: Published and new (U-Th)/He results for Quadrilátero Ferrífero goethite cements from regional duricrusts, saprolites and colluvia.

Site	Sample Name	Weathering Stage	Latitude/ Longitude	Elevation (m)	Depth (m)	Measured He Age (Ma)	Corrected He Age (Ma)	±	He (nmol/g)	±	U (ppm)	±	Th (ppm)	±	Th/U	Mass (µg)
Serra da Moeda	Pic-06-25A/1	duricrust		1460	0	9.2	10.1	1.0	0.7314	0.0232	13.32	0.23	5.49	0.09	0.41	89.13
	Pic-06-25A/2	duricrust		1460	0	7.7	8.4	0.8	0.5468	0.0178	12.55	0.21	2.54	0.06	0.20	126.39
	Pic-06-25A/4	duricrust		1460	0	6.3	6.9	0.7	0.1988	0.0077	5.56	0.10	1.22	0.04	0.22	166.17
	Pic-06-25A/5	duricrust		1460	0	7.5	8.2	0.8	0.5002	0.0165	11.71	0.20	2.69	0.06	0.23	43.60
	Pic-06-25A/6	duricrust		1460	0	7.1	7.8	0.8	0.6373	0.0204	15.88	0.27	2.50	0.06	0.16	64.09
	Pic-06-25A/8	duricrust		1460	0	8.8	9.6	1.0	0.4113	0.0139	7.88	0.14	3.22	0.07	0.41	138.56
	Pic-06-25B/2	duricrust	20° 08' 28.10"S	1460	0	11.2	12.3	1.2	0.7130	0.0226	11.23	0.19	1.93	0.05	0.17	126.52
	Pic-06-25B/4	duricrust	43° 58' 35.12"W	1460	0	5.9	6.5	0.6	0.4110	0.0139	12.54	0.21	1.12	0.04	0.09	155.92
	Pic-06-25C/1	duricrust		1460	0	9.5	10.4	1.0	0.6144	0.0198	10.99	0.19	3.98	0.07	0.36	104.01
	Pic-06-25C/2	duricrust		1460	0	13.6	15.0	1.5	1.3144	0.0401	15.99	0.27	7.53	0.11	0.47	45.48
	Pic-06-25C/3	duricrust		1460	0	6.7	7.4	0.7	0.5642	0.0183	14.37	0.24	4.69	0.08	0.33	112.33
	Pic-06-25C/4	duricrust		1460	0	10.4	11.5	1.1	0.4578	0.0152	7.15	0.13	3.97	0.07	0.56	195.85
	Pic-06-25C/6	duricrust		1460	0	12.2	13.4	1.3	0.3409	0.0118	4.18	0.08	4.10	0.07	0.98	67.22
	Pic-06-25C/7	duricrust		1460	0	11.1	12.2	1.2	0.6943	0.0221	10.52	0.18	4.36	0.08	0.41	196.44
	Pic-06-26A/1	duricrust		1411	0	7.7	8.4	0.8	0.3828	0.0130	6.75	0.12	10.31	0.14	1.53	126.35
	Pic-06-26A/2	duricrust	20° 05' 9.81"S 43° 58' 45.16"W	1411	0	2.1	2.3	0.2	0.0612	0.0037	4.22	0.08	4.97	0.08	1.18	404.08
	Pic-06-26A/3	duricrust		1411	0	3.8	4.2	0.4	0.0574	0.0036	2.26	0.05	2.16	0.05	0.96	256.46
	Pic-06-26B/3	duricrust		1411	0	1.0	1.1	0.1	0.0269	0.0027	2.27	0.05	10.73	0.14	4.73	220.37
	Pic-06-27/4	duricrust		1426	0.5	1.5	1.7	0.2	0.0034	0.0020	0.36	0.01	0.27	0.03	0.75	191.78
	Pic-06-27/5	duricrust		1426	0.5	1.8	1.9	0.2	0.0084	0.0021	0.74	0.02	0.61	0.04	0.82	205.45
	Pic-06-27	duricrust	20° 02' 45.11"S	1426	0.5	2.0	2.2	0.2	0.011	0.0260	0.901	0.026	0.587	0.029	0.65	76.04
	Pic-06-27	duricrust	43° 58' 55.35"W	1426	0.5	2.8	3.1	0.3	0.025	0.0362	1.399	0.036	1.156	0.040	0.83	67.17
	Pic-06-27	duricrust		1426	0.5	0.4	0.4	0.0	0.002	0.0258	0.875	0.026	0.567	0.030	0.65	73.68
	Pic-06-27	duricrust		1426	0.5	1.5	1.7	0.2	0.010	0.0322	1.088	0.032	0.659	0.037	0.61	58.36
	SC-12-01-dark brown	duricrust		1485		27.7	30.4	3.0	0.290	0.0249	1.542	0.028	1.620	0.033	1.05	191.09
	SC-12-01_ dark brown	duricrust		1485		25.6	28.2	2.8	0.270	0.0187	1.559	0.031	1.609	0.036	1.03	153.77
	SC-12-04(A)	duricrust		1474		8.3	9.1	0.9	0.359	0.0207	6.181	0.060	7.517	0.108	1.22	127.90
	SC-12-04(A)	duricrust		1474		5.4	6.0	0.6	0.266	0.0063	3.174	0.075	24.927	0.332	7.85	51.18
	SC-12-04(A)	duricrust	20° 05' 55.45"S	1474		6.1	6.7	0.7	0.297	0.0089	2.783	0.062	26.434	0.322	9.50	65.78
	SC-12-04(A)	duricrust	43° 59' 01.86"W	1474		21.0	23.1	2.3	0.459	0.0326	2.454	0.039	6.655	0.093	2.71	158.51
	SC-12-04(B)	duricrust		1474		24.7	27.2	2.7	0.128	0.0102	0.558	0.016	1.681	0.035	3.01	173.79
	SC-12-04(B)	duricrust		1474		34.5	37.9	3.8	0.159	0.0078	0.521	0.018	1.390	0.040	2.67	104.78
	SC-12-05	duricrust	20° 06' 18.60"S	1480		26.7	29.3	2.9	0.400	0.0175	1.882	0.042	3.698	0.072	1.96	97.18
	SC-12-05	duricrust	43° 59' 0.34"W	1480		28.8	31.7	3.2	0.255	0.0392	1.166	0.018	1.951	0.031	1.67	342.45
	SC-12-05	duricrust		1480		21.5	23.7	2.4	0.594	0.0344	3.839	0.052	5.240	0.084	1.37	129.34
	SC-12-06(A)	duricrust		1477		3.8	4.2	0.4	0.19	0.0042	2.77	0.06	27.03	0.33	9.77	47.67
	SC-12-06(A)	duricrust	20° 06' 20.49"S	1477		2.7	3.0	0.3	0.26	0.0039	4.40	0.10	54.75	0.62	12.44	31.80
	SC-12-06(B)	duricrust	43° 58' 60"W	1477		23.86	26.2	2.6	1.56	0.0143	6.19	0.14	24.71	0.40	3.99	20.39
	SC-12-06(B)	duricrust		1477		20.18	22.2	2.2	1.19	0.0176	4.95	0.10	25.24	0.35	5.10	32.74
	SC-12-07(A)	duricrust		1468		6.19	6.8	0.7	0.54	0.0196	15.88	0.06	1.04	0.03	0.07	80.36
	SC-12-07(A)	duricrust	20° 06' 23.64"S	1468		7.11	7.8	0.8	0.68	0.0277	17.25	0.06	1.18	0.03	0.07	91.02
	SC-12-07(B)	duricrust	43° 59' 0.57"W	1468		21.05	23.2	2.3	0.46	0.0243	2.96	0.03	4.63	0.07	1.56	116.67
	SC-12-15	duricrust	20° 06' 6.12"S 43° 59' 01.23"W	1439	-	5.53	6.1	0.6	0.47	0.0083	11.78	0.14	16.39	0.24	1.39	38.93
	SC-12-15	duricrust		1439	-	5.50	6.1	0.6	0.42	0.0063	10.65	0.15	14.72	0.24	1.38	32.81
	SC-12-17(d)	duricrust	20° 06' 4.91"S 43° 59' 1.07"W	1469		1.8	1.9	0.2	0.01	0.0035	0.69	0.02	2.83	0.05	4.10	117.01
	SC-12-17(d)	duricrust		1469		9.0	9.9	1.0	0.08	0.0047	0.80	0.02	3.93	0.06	4.94	85.36
	SC-12-22(B)	duricrust	20° 06' 43.01"S	1493		4.91	5.4	0.5	0.48	0.0053	16.31	0.21	6.69	0.16	0.41	24.21
	SC-12-22(B)	duricrust	43° 58' 55.72"W	1493		3.11	3.4	0.3	0.38	0.0088	14.40	0.11	33.37	0.37	2.32	51.97
	SC-12-20(A)	saprolite		1389		17.82	19.6	2.0	0.35	0.0265	3.55	0.04	0.01	0.01	0.00	170.84
	SC-12-20(A)	saprolite	20° 05' 53.63"S	1389		15.97	17.6	1.8	0.30	0.0251	3.49	0.04	0.00	-0.01	0.00	183.99
	SC-12-20(A)	saprolite	43° 58' 49.26"W	1389		25.61	28.2	2.8	0.25	0.0227	1.79	0.03	0.01	0.01	0.00	200.50
	SC-12-20(A)	saprolite		1389		24.04	26.4	2.6	0.18	0.0147	1.35	0.03	0.02	0.01	0.01	181.73
	SM-13-01	saprolite	20° 16' 14.55"S	1491	2.5	27.13	29.8	3.0	0.29	0.0168	1.93	0.03	0.10	0.01	0.05	129.72
	SM-13-01	saprolite	43° 57' 24.17"W	1491	2.5	27.59	30.4	3.0	0.27	0.0116	1.78	0.04	0.11	0.02	0.06	94.80
	SM-13-02	saprolite	20° 16' 14.84" S	1493	2.5	40.05	44.1	4.4	0.125	0.0073	0.571	0.018	0.010	0.017	0.02	125.96
	SM-13-02	saprolite	43° 57' 24.13"W	1493	2.5	28.13	30.9	3.1	0.113	0.0058	0.734	0.023	0.016	0.020	0.02	107.67
	SM-13-07	saprolite	20° 15' 20.4"S 43° 57' 57.3"W	1478		26.40	29.0	2.9	0.146	0.0116	1.006	0.023	0.009	0.012	0.01	176.07
	SM-13-07	saprolite		1478		23.56	25.9	2.6	0.146	0.0117	1.126	0.024	0.018	0.012	0.02	178.21
	SC-12-16(B)_black	rubble		1439		36.2	39.9	4.0	0.55	0.0391	1.87	0.02	3.94	0.05	2.11	158.05
	SC-12-16(B)_black	rubble	20° 06' 5.84"S 43° 59' 1.12"W	1439		36.0	39.6	4.0	0.67	0.0149	2.42	0.05	4.25	0.08	1.76	49.28
	SC-12-16(B)_brown	rubble		1439		13.5	14.9	1.5	0.44	0.0159	3.47	0.05	10.72	0.13	3.09	79.77
	SC-12-16(B)_brown	rubble		1439		11.1	12.2	1.2	0.36	0.0159	3.29	0.04	11.07	0.13	3.37	99.27
	SC-12-21(A)	colluvium		1470		48.54	53.4	5.3	0.08	0.0050	0.26	0.01	0.13	0.01	0.50	133.72
	SC-12-21(A)	colluvium		1470		47.36	52.1	5.2	0.08	0.0059	0.19	0.01	0.45	0.01	2.42	161.86
	SC-12-21(A)	colluvium	20° 06' 19.85"S	1470		22.94	25.2	2.5	0.04	0.0044	0.17	0.01	0.61	0.01	3.52	227.63
	SC-12-21(B)	colluvium	43° 59' 04.37"W	1470		8.6	9.5	1.0	0.61	0.0414	9.83	0.03	13.57	0.13	1.38	150.83
	SC-12-21(B)	colluvium		1470		10.59	11.7	1.2	0.62	0.0234	8.48	0.04	9.55	0.12	1.13	84.17
	SC-12-21(D)	colluvium		1470		13.27	14.6	1.5	1.65	0.0417	16.35	0.09	27.53	0.32	1.68	56.46
	SC-12-21(D)	colluvium		1470		15.19	16.7	1.7	1.82	0.0331	11.86	0.13	43.36	0.48	3.66	40.52

(1*) Samples for which blanks exceed 10% of the measured He. An error >10% was applied for those samples.

(Italic) Data from Monteiro et al. [2014].

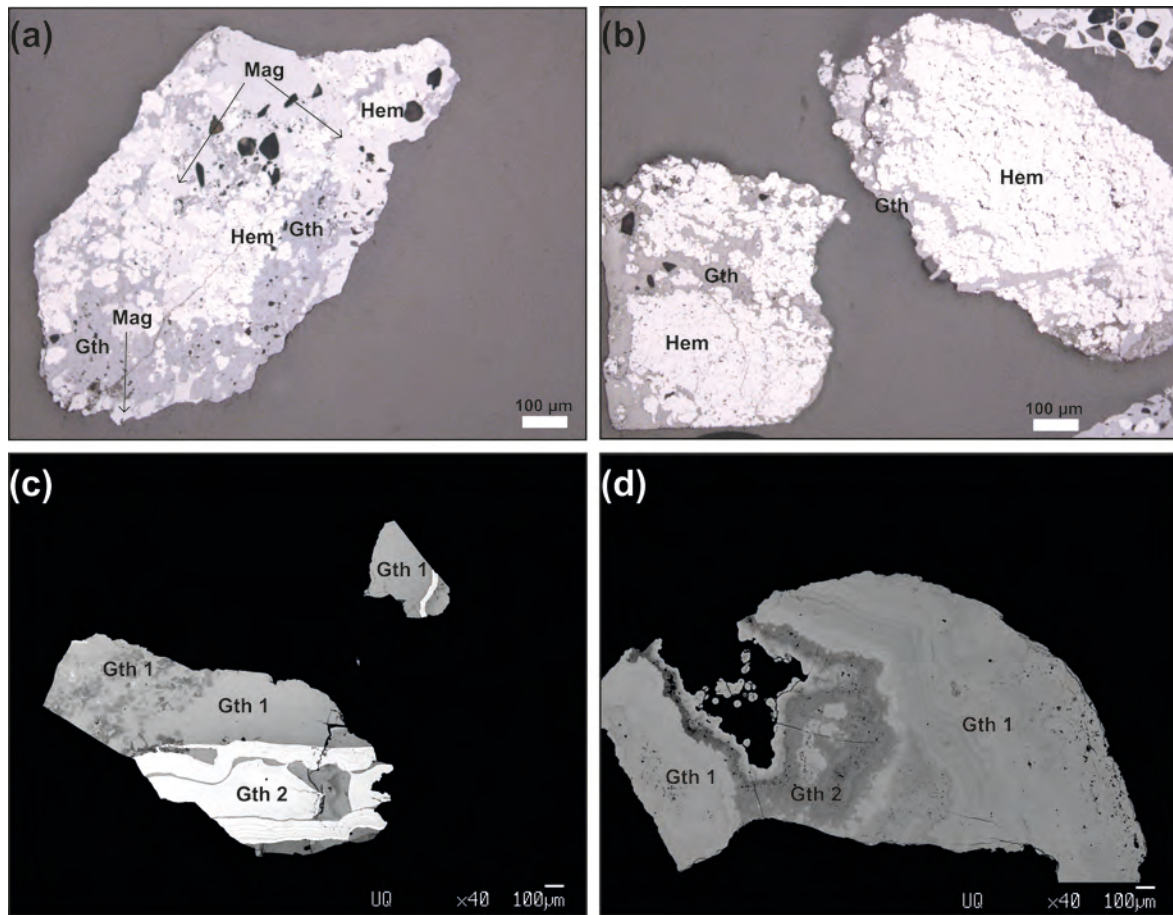


Figure 4: Photomicrographs of representative samples used in ^3He measurements (a, b) reveal the complex mineralogy (Hem – hematite, Mag – magnetite, and Gth – goethite) and (c, d) several generations of goethite (Gth 1, Gth 2) showing BSE contrast between first-generation dark cryptocrystalline Al-rich and porous goethite and bright bands of microcrystalline (20-30 μm long) Al-poor densely packed goethite. The colloform nature of the goethite cements (c, d) record the duration of mineral precipitation.

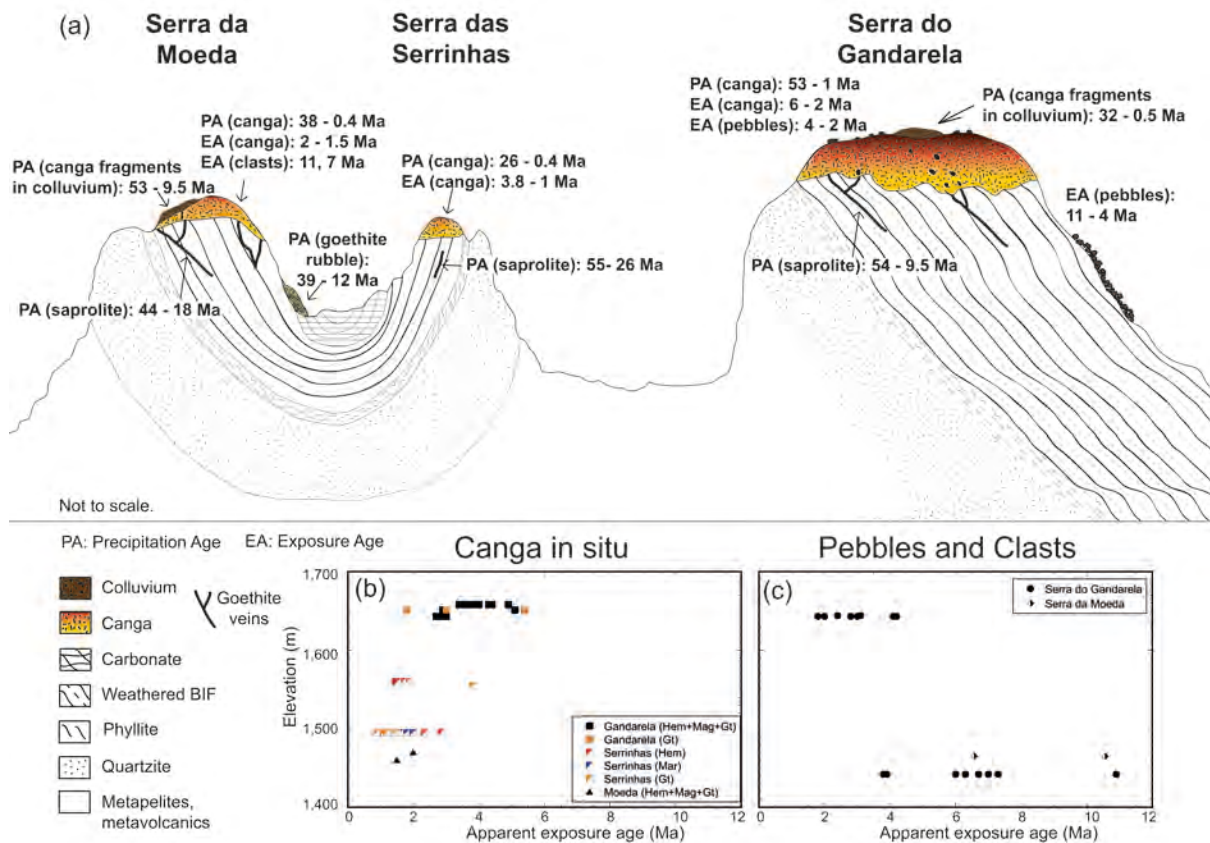


Figure 5: (a) Diagrammatic illustration of the QF landscape show that ridges and plateaus are blanketed by deeper and more continuous (Gandarela) or shallower (Moeda) and discontinuous (Serrinhas) canga blankets. Veins within saprolites and transported canga and colluvia on plateau surfaces and shoulders host some of the most ancient goethite cements dated in this study. **(a-b)** Apparent exposure ages (*aEAs*) measured from cosmogenic ^3He concentrations show that higher elevation plateaus (Gandarela) have a longer history of exposure than lower elevation plateaus (Serrinhas and Moeda). **(c)** Pebbles collected on plateau summits and in streams draining the plateaus show the longest exposure histories, revealing that erosion of hematite blocks from the plateaus is a very slow process.

Table 2: Cosmogenic ^3He analysis

Sample	Rock type	Mineralogy ^(a)	Location ^(b)	Lat./Long.	Elevation (m)	Depth (cm)	Aliquot weight (mg)	³ He (ppcc.g ⁻¹)	³ He (Mat.g ⁻¹) ±	Production rate (at.g ⁻¹ .a ⁻¹)	Exposure age (Ma)	±	Erosion rate (m.Ma ⁻¹)	±	Average erosion rate (m.Ma ⁻¹)	Average (U-Th)/He age (Ma)	±
G1201	canga	sem (85%)+mag (5%)+gth (10%)	SG		1643	0		14.9	401	140	2.9	0.3	0.19	0.02	0.20		
G1201	canga	sem (85%)+mag (5%)+gth (10%)	SG		1643	0.5		14.3	383	140	2.7	0.3	0.20	0.02			
G1201	canga	sem (85%)+mag (5%)+gth (10%)	SG		1643	1		15.5	417	140	3.0	0.4	0.19	0.02			
G1201	canga	sem (85%)+mag (5%)+gth (10%)	SG	20°5'25.39"S/	1643	1.5		15.3	411	140	2.9	0.4	0.19	0.02			
G1201	canga	sem (85%)+mag (5%)+gth (10%)	SG	43°41'2.453"W	1643	2		15.2	408	140	2.9	0.4	0.19	0.02			
G1201	canga	sem (85%)+mag (5%)+gth (10%)	SG		1643	3		15.0	403	140	2.9	0.3	0.19	0.02			
G1201	canga	sem (85%)+mag (5%)+gth (10%)	SG		1643	4		14.9	400	140	2.9	0.3	0.19	0.02			
G1201	canga	sem (85%)+mag (5%)+gth (10%)	SG		1643	5		14.4	387	140	2.8	0.3	0.20	0.02			
G1201	canga	sem (85%)+mag (5%)+gth (10%)	SG		1643	6		13.8	371	140	2.7	0.3	0.21	0.03			
21-2	canga	mag	SG		1651	0	21.7	25.5	686	41	134	5.1	0.6	0.11	0.01	0.15	
21-3	canga	mag	SG	20°7'5.257"S/	1651	0	36.7	14.6	392	23	134	2.9	0.3	0.19	0.02		
21-5	canga	gth	SG	43°39'38.048"W	1651	0	52.3	9.9	266	16	148	1.8	0.2	0.31	0.04	0.20	9.1
21-5	canga	gth	SG		1651	0	52.5	29.8	801	28	148	5.4	0.6	0.10	0.01		0.9
21-6	canga	gth	SG		1651	0	56.3	16.6	447	20	148	3.0	0.3	0.18	0.02	24.6	9.0
G1209	hematite blocksem (85%)+mag (5%)+gth (10%)	SG			1658	0		19.8	532	142	3.7	0.4	0.15	0.02	0.14		
G1209	hematite blocksem (85%)+mag (5%)+gth (10%)	SG			1658	0.5		19.4	522	142	3.7	0.4	0.15	0.02			
G1209	hematite blocksem (85%)+mag (5%)+gth (10%)	SG			1658	1		18.1	486	142	3.4	0.4	0.16	0.02			
G1209	hematite blocksem (85%)+mag (5%)+gth (10%)	SG			1658	1.5		25.8	692	142	4.9	0.6	0.11	0.01			
G1209	hematite blocksem (85%)+mag (5%)+gth (10%)	SG	20°7'3.888"S/		1658	2		22.5	604	142	4.3	0.5	0.13	0.02			
G1209	hematite blocksem (85%)+mag (5%)+gth (10%)	SG	43°39'38.972"W		1658	2.5		22.8	613	142	4.3	0.5	0.13	0.02			
G1209	hematite blocksem (85%)+mag (5%)+gth (10%)	SG			1658	3.5		23.1	620	142	4.4	0.5	0.13	0.02			
G1209	hematite blocksem (85%)+mag (5%)+gth (10%)	SG			1658	4.5		19.9	534	142	3.8	0.5	0.15	0.02			
G1209	hematite blocksem (85%)+mag (5%)+gth (10%)	SG			1658	5.5		19.0	511	142	3.6	0.4	0.15	0.02			
G1209	hematite blocksem (85%)+mag (5%)+gth (10%)	SG			1658	6.4		21.4	574	142	4.0	0.5	0.14	0.02			
G1202 (1) r1	pebble	hem (90%)+mag (5%)+gth (5%)	SG		1643	0	50.6	22.1	595	2	140	4.2	0.5	0.13	0.02	0.13	
G1202 (1) r2	pebble	hem (90%)+mag (5%)+gth (5%)	SG		1643	0	25.0	21.8	585	3	140	4.2	0.4	0.13	0.02		
G1202 (1) r3	pebble	hem (90%)+mag (5%)+gth (5%)	SG		1643	0	25.1	21.4	576	3	140	4.1	0.4	0.14	0.02	0.19	
G1202 (2) r2	pebble	hem (90%)+mag (5%)+gth (5%)	SG	20°5'25.39"S/	1643	0	25.7	15.5	416	2	140	3.0	0.3	0.19	0.02		
G1202 (2) r3	pebble	hem (90%)+mag (5%)+gth (5%)	SG	43°41'2.453"W	1643	0	25.4	14.6	392	3	140	2.8	0.3	0.20	0.02	0.30	
G1202 (3) r1	pebble	hem (90%)+mag (5%)+gth (5%)	SG		1643	0	50.3	9.2	246	1	140	1.8	0.2	0.32	0.04		
G1202 (3) r2	pebble	hem (90%)+mag (5%)+gth (5%)	SG		1643	0	25.0	9.5	254	2	140	1.8	0.2	0.31	0.04		
G1202 (3) r3	pebble	hem (90%)+mag (5%)+gth (5%)	SG		1643	0	25.1	10.4	278	1	140	2.0	0.2	0.28	0.03		
G1202 (3) r4	pebble	hem (90%)+mag (5%)+gth (5%)	SG		1643	0	13.6	10.3	276	1	140	2.0	0.2	0.28	0.03		
GA1302	pebble	hem (90%)+mag (5%)+gth (5%)	SG	20°5'36.48"S/	1644	0	17.2	12.5	335	140	2.4	0.3	0.23	0.03	0.21		
GA1302	pebble	hem (90%)+mag (5%)+gth (5%)	SG	43°40'59.07"W	1644	0	13.4	16.1	432	140	3.1	0.3	0.18	0.02			
GA1301 A (1) r2	pebble	hem (90%)+mag (5%)+gth (5%)	SG		1442	0	25.0	30.4	817	3	122	6.7	0.7	0.08	0.01	0.08	
GA1301 A (1) r3	pebble	hem (90%)+mag (5%)+gth (5%)	SG		1442	0	25.6	31.5	846	4	122	7.0	0.7	0.08	0.01		
GA1301 A (1) r4	pebble	hem (90%)+mag (5%)+gth (5%)	SG		1442	0	17.0	28.4	763	4	122	6.3	0.7	0.09	0.01		
GA1301 A (2) r2	pebble	hem (90%)+mag (5%)+gth (5%)	SG	20°7'06.37"S/	1442	0	25.4	27.0	727	3	122	6.0	0.6	0.09	0.01	0.07	
GA1301 A (2) r3	pebble	hem (90%)+mag (5%)+gth (5%)	SG	43°38'56.64"W	1442	0	25.4	49.6	1332	6	122	10.9	1.2	0.05	0.01		
GA1301 A (2) r4	pebble	hem (90%)+mag (5%)+gth (5%)	SG		1442	0	13.8	33.0	888	5	122	7.3	0.8	0.08	0.01		
GA1301 A (3) r1	pebble	hem (90%)+mag (5%)+gth (5%)	SG		1442	0	52.2	17.5	472	2	122	3.9	0.4	0.14	0.02	0.15	
GA1301 A (3) r2	pebble	hem (90%)+mag (5%)+gth (5%)	SG		1442	0	25.4	17.3	465	3	122	3.8	0.4	0.15	0.02		
GA1301 A (3) r3	pebble	hem (90%)+mag (5%)+gth (5%)	SG		1442	0	25.2	17.2	461	2	122	3.8	0.4	0.15	0.02		
01A4	canga	gth	SS		1495	0	4.14	1.3	36	21	133	0.3	0.2	2.05	0.25	2.05	1.2
01A5	canga	gth	SS		1495	0	8.96	5.6	149	31	133	1.1	0.2	0.49	0.06	0.43	1.2
01A5	canga	gth	SS		1495	0	16.8	7.4	198	26	133	1.5	0.2	0.37	0.04		0.8
01A5	canga	hem	SS		1495	0	17.4	6.4	172	22	126	1.4	0.2	0.41	0.05	0.41	
01A6	canga	gth	SS		1495	0	22.3	4.4	117	17	133	0.9	0.2	0.63	0.08	0.63	1.6
01A7	canga	gth	SS		1495	0	4.28	1.1	30	21	133	0.2	0.1	2.46	0.30	0.43	0.7
01A7	canga	gth	SS	20°15'23.7240"S/	1495	0	21.2	7.0	187	22	133	1.4	0.2	0.39	0.05		0.3
01A7	canga	mt	SS	43°52'43.8816"W	1495	0	22.4	8.4	224	21	126	1.8	0.2	0.31	0.04		
01A8	canga	gth	SS		1495	0	23.4	6.1	164	20	133	1.2	0.2	0.45	0.05	0.45	2.1
01A8	canga	hem	SS		1495	0	31.3	11.0	295	20	126	2.3	0.3	0.24	0.03	0.24	1.6
01A8	canga	mt	SS		1495	0	37.2	7.5	201	16	126	1.6	0.2	0.35	0.04	0.35	
01B2	canga	mt	SS		1495	0	29.4	9.3	251	21	126	2.0	0.3	0.28	0.03	0.28	
01B5	canga	gth	SS		1495	0	8.43	1.0	26	12	133	0.2	0.1	2.82	0.34	2.82	1.6
01C6	canga	gth	SS		1495	0	6.02	5.8	157	33	133	1.2	0.3	0.47	0.06	0.47	4.9
01C6	canga	hem	SS		1495	0	13.8	13.4	360	40	126	2.8	0.4	0.20	0.02	0.20	2.5
08-6	canga	gth	SS	20°12'38.0880"S/	1555	0	3.06	1.3	35	25	138	0.2	0.2	2.22	0.27	2.23	3.9
08-9a	canga	gth	SS	43°51'11.1743"W	1555	0	22.7	19.7	529	38	138	3.8	0.5	0.15	0.02	1.13	0.5
08-9b	canga	gth	SS		1555	0	28.8	1.4	36	9	138	0.3	0.1	2.11	0.25	2.11	1.4
Pic-06-12Ab ^(b)	hematite block	hem	SS		1560	0	20.5	7.2	193	17	132	1.5	0.2	0.38	0.05	0.35	
Pic-06-12Ac ^(b)	hematite block	hem	SS		1560	0	23.3	7.3	195	18	132	1.5	0.2	0.38	0.05		
Pic-06-12Ad ^(b)	hematite block	hem	SS		1560	0	3.8	8.9	239	42	132	1.8	0.4	0.31	0.04		
Pic-06-12Ae ^(b)	hematite block	hem	SS	20°8'59.28"S/	1560	0	5.2	7.5	201	29	132	1.5	0.3	0.36	0.04		
Pic-06-12Af ^(b)	hematite block	hem	SS	43°52'34.1292"W	1560	0	5.2	8.0	214	38	132	1.6	0.4	0.34	0.04		
Pic-06-12Ag ^(b)	hematite block	hem	SS		1560	0	27.3	8.2	220	25	132	1.7	0.3	0.33	0.04		
Pic-06-12Ba ^(b)	hematite block	hem	SS		1560	0	20.3	7.3	197	19	132	1.5	0.2	0.37	0.04		
Pic-06-12Bb ^(b)	hematite block	hem	SS		1560	0	22.8	7.5	201	16	132	1.5	0.2	0.36	0.04		
25B r3	canga	sem (85%)+mag (5%)+gth (10%)	SM	20°8'27"S/	1460	0	5.29	6.9	184	2	123	1.5	0.2	0.37	0.04	0.37	
SC1217 d1	canga	hem (90%)+mag (5%)+gth (5%)	SM	20°5'56.46"S/	1470	0	9.97	9.2	247	124	2.0	0.2	0.28	0.03	0.28		
SC1217 d2	canga	hem (90%)+mag (5%)+gth (5%)	SM	43°58'59.6"W	1470	0	10.16	9.2	247	124	2.0	0.2	0.28	0.03			
SC1218a	clast	hem (90%)+mag (5%)+gth (5%)	SM	20°5'56.46"S/	1465	0		48.6	1306	124	10.6	1.3	0.05	0.01	0.07		
SC1218b	clast	hem (90%)+mag (5%)+gth (5%)	SM	43°58'59.6"W	1465	0		30.2	812	124	6.6	0.8	0.08	0.01			

(a) Abbreviations: hematite (hem), magnetite (mag), goethite (gth), martite (mt), Serra do Gandarela (SG), Serra das Serrinhas (SS), Serra da Moeda (SM).

(b) Shuster et al. [2012]

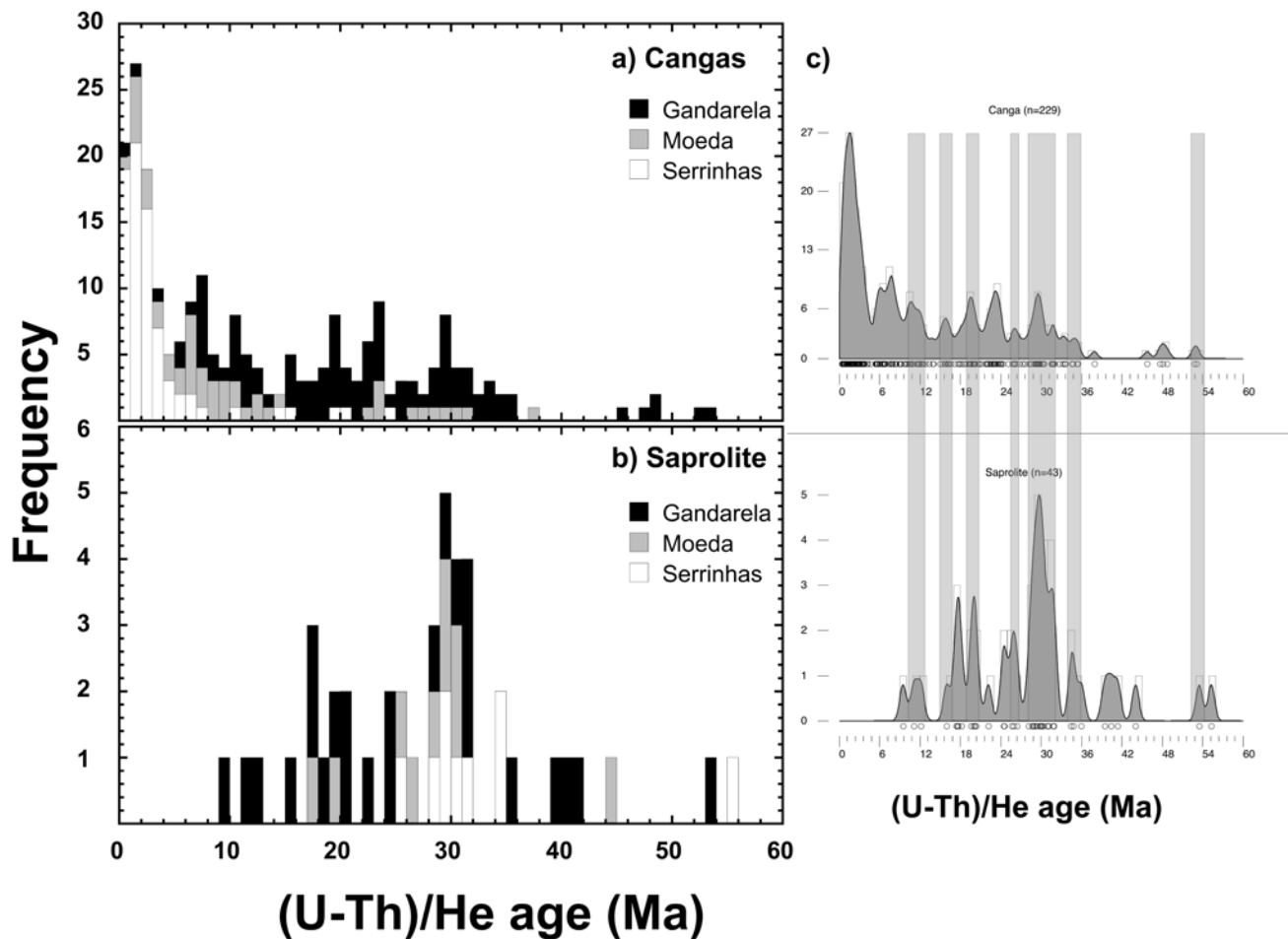


Figure 6: Histograms illustrating the frequency of goethite (U-Th)/He age distribution in (a) cangas and (b) saprolites reveal the more active and recent history of goethite cementation in cangas. The correspondence in some of the (c) major peaks in age distribution suggests that cangas and saprolites have weathered in tandem for a long time.

When cast in terms of apparent exposure ages (*aEA*), the ^3He results reveal that the thicker and more laterally continuous canga blankets at Gandarela record a longer exposure history than the thinner and intermittent cangas at Serras da Moeda and das Serrinhas (Figure 5; Table 2). But the longest *aEAs* were obtained for hematite-magnetite clast eroded from cangas and pebbles collected in colluvia or creeks draining the plateaus (Figure 5a,c; Table 2).

5. DISCUSSION

We interpret all (U-Th)/He data in this study as precipitation ages, with age variability for a sample indicating the presence of multiple goethite generations [Monteiro *et al.*, 2014]. The relatively large sample population (291 (U-Th)/He *pAs* and 75 cosmogenic ^3He *aEAs*) provides a robust dataset that allows addressing the histories of weathering, exposure, and erosion of the three distinct Quadrilátero Ferrífero landsurfaces (Gandarela, Moeda, and Serrinhas).

Cangas on the Gandarela plateau (Figures 1, 3a, 5a), which are much deeper (up to 70m) and more continuous [Baltazar *et al.*, 2005a] than cangas on other plateaus, record significantly longer

exposure (average $aEAs = 3.5 \pm 0.9$ Ma, max = 5.4 ± 0.6 Ma, $n = 24$) and weathering (pAs of 53.2 to 0.8 Ma, $n = 102$) histories. Detrital grains collected on top of the Gandarela plateau, next to in situ cangas, yield aEA results compatible with those obtained from coexisting cangas (e.g., average = 2.8 ± 1.0 Ma, max = 4.2 ± 0.5 Ma, $n = 11$). Pebbles from creeks draining the plateau, at lower elevation sites, yield much longer $aEAs$ (average = 6.2 ± 2.3 Ma, max = 10.9 ± 1.2 Ma, $n = 9$). The results suggest that, once released from the canga, hematite-magnetite clasts travel very slowly through and out of the plateau.

At Serra da Moeda, the canga blanket is thinner and discontinuous relative to Gandarela [Baltazar *et. al.*, 2005b, c]. The $aEAs$ (average = 1.8 ± 0.3 and max = 2.0 ± 0.2 Ma, $n = 3$) and (U-Th)/He pAs (38-0.4 Ma, $n = 48$) reveal the relatively recent exposure of an old canga blanket. Detrital hematite blocks accumulated on scree wash surrounding the canga outcrops, only ~ 5 m topographically below the summits underlain by cangas, yield much larger $aEAs$ (average = 8.6 ± 2.8 Ma, max = 10.6 ± 1.3 Ma, $n = 2$).

At Serra das Serrinhas, the fragmentary canga on the narrow and isolated ridges are young ((U-Th)/He pAs of 24.3-0.4 Ma, $n = 78$) and more recently exposed (average $aEA = 1.8 \pm 0.8$ Ma, max = 3.8 ± 0.5 Ma, $n = 13$).

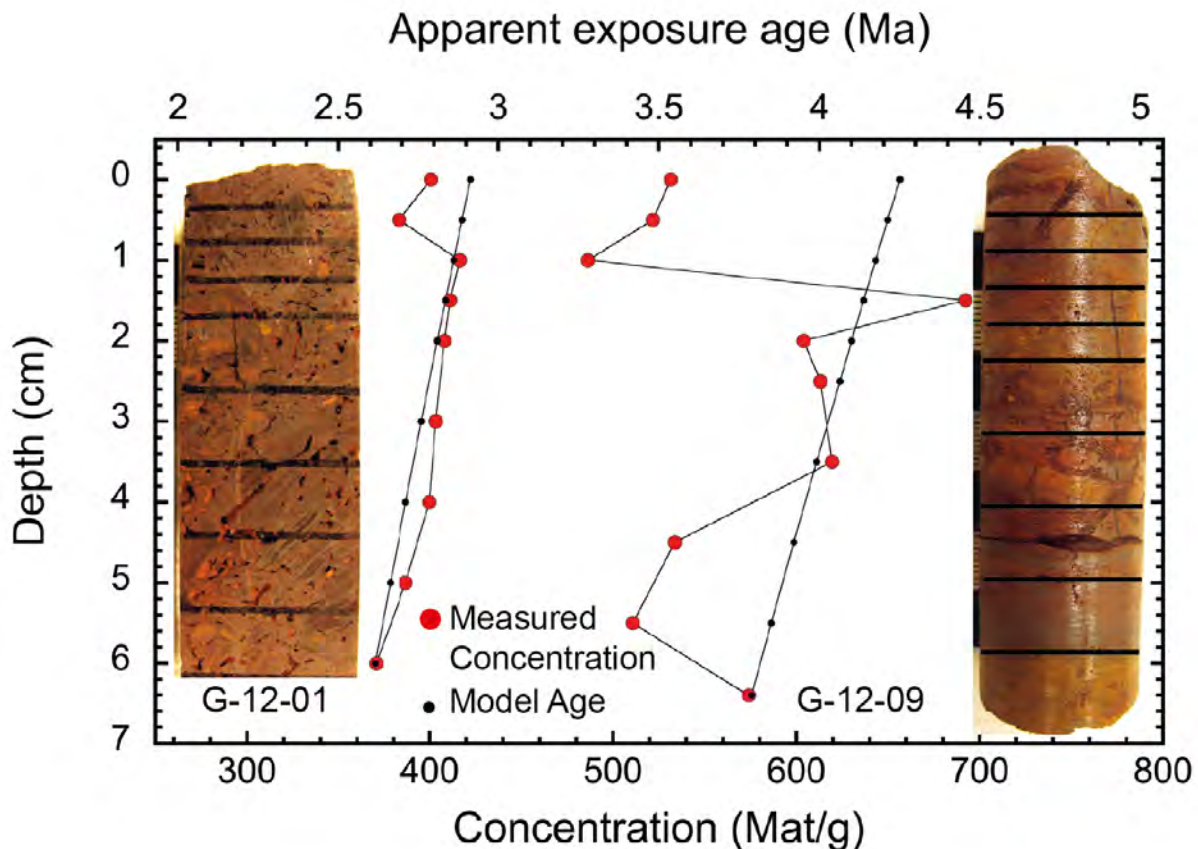


Figure 7: Cosmogenic ^3He and apparent exposure ages with depth for two drill cores from hematite-magnetite-rich cores in cangas reveal vertical distributions compatible with a continuous history of surface exposure (modeled results in black) for the two blocks. The scatter in the results and lower ^3He concentrations in the near-surface environment reveals partial ^3He loss during hydration of hematite-magnetite to goethite.

The cumulative concentration of cosmogenic isotopes in a canga sample probably does not record uniform exhumation, but it records a minimum exposure history as a mineral grain is uncovered and released (possibly several times) by partial mechanical breakdown of the canga, translocates back down into the profile, and eventually returns to the surface by physical erosion of the overlying material (e.g., *Shuster et al.*, [2012]). This complex history of exposure and shielding from cosmic rays suggest that our *aEAs*, which assume continuous exposure at the surface and no erosion, most likely underestimates the amount of time a sample has interacted with cosmic rays within the uppermost two meters. Therefore, cosmogenic ^3He results (Table 2) suggest that the canga-covered plateaus at the QF have been exposed at the surface for at least 5.5 Ma, probably much longer.

Another important result is that cosmogenic ^3He concentrations for a given surface or even a single canga block may display a large range (Table 2). Two canga blocks (Figure 7) collected at slightly different elevations on the Gandarela plateau, approximately 5 km apart (Figures 1b, 3d, 5a; Table 2), yield quite distinct ^3He concentrations but similar depth profiles, which suggest that the two blocks share a relatively simple history of continuous and protracted exposure at the surface. The block from the higher elevation site (G1209) shows a longer exposure history and greater scatter in measured ^3He than the second block. ^3He scatter may reflect partial recrystallization of hematite-magnetite to goethite (Figure 4a, b). The coarser grained (425-850 μm) magnetic fraction analyzed from block G1209 (Table 2) may contain a greater proportion of grains composed of mixtures of hematite-magnetite \pm goethite than the finer grained (150-425 μm) magnetic fraction analyzed for block G1201. The better-behaved ^3He profile for block G1201 suggests that targeting the finer grained magnetic fraction is the most suitable approach for quantifying cosmogenic ^3He in Fe-duricrusts.

In addition to some scatter, both vertical profiles show a slight depletion in the expected ^3He concentrations for the grains closest to the surface, suggesting possible ^3He loss by partial mineral dissolution-reprecipitation or by diffusive ^3He loss during bush fires. Petrographic observation and XRD analysis confirm that goethite is more abundant in the samples closest to the surface (35-45 % as opposed to 25-30 % in the middle of the core) and show that hydration of hematite-magnetite to goethite near the surface is partially responsible for ^3He loss (Figure 7). Lichens growing on the surface of canga blocks (Figure 3b-d) facilitate weathering [*Banfield et al.*, 1999] and near-surface water retention, driving the biogeochemical reactions that transform hematite-magnetite into goethite and partially release cosmogenic ^3He . Fractures that allow the preferential penetration of

weathering solutions may also lead to partial hydration of hematite-magnetite to goethite (e.g., sample G1209, Figure 7). Other factors that may account for the variability in cosmogenic ^3He concentrations in individual canga blocks, such as complexities of canga block geometry with respect to the surface and cosmic ray flux, or the possible rotation of the block during its weathering history, must also be considered.

It is not our intention to address each of these issues in detail here, but some sampling and analytical approaches may help to obviate some of these problems. For example, to obtain a representative exposure history for a canga plateau we sample and analyze, by both (U-Th)/He and cosmogenic ^3He , as many samples as possible, of known mineralogical composition (i.e., pure hematite, magnetite, goethite) that represent different parts of the canga (detrital blocks, cements, cemented blocks, etc.). Although more samples would be desirable, our record is comprehensive enough to reveal some of the most important aspects of the weathering and erosion histories of the QF plateaus.

5.1. The goethite (U-Th)/He record: chemical processes controlling the formation of saprolites and cangas

Weathering geochronology by (U-Th)/He analysis dates the chemical reactions and processes depicted in Figure 8 and Table 3. As summarized in those reactions, banded iron-formations weather through mass loss during dissolution of interbedded carbonates, sulfides, silicates, and silica minerals, producing saprolites essentially composed of residual concentrations of friable and indurated hematite±magnetite (martite) ore. Alkali-earth elements and Si are leached from the system, since the reprecipitation of these elements is not energetically favored (Table 3). The scarcity of goethite suggests that iron is relatively insoluble under the conditions prevailing in saprolites, promoting the effective leaching of all other minerals and the residual concentration of hematite±magnetite (or martite). The presence of sporadic goethite horizons or veins (Figures 3f, 5a, 8) in saprolites suggests that soluble iron minerals (siderite or sulfides) dissolve releasing Fe^{2+} , which is then locally re-precipitated as goethite. (U-Th)/He ages for goethite veins in saprolites (Figure 3f, 5a, 6; Table 1, e.g., SC-12-20(A)) and fragments of goethite veins in cangas (Figure 2e, 5a; Table 1, e.g., SC-12-04(B)) record, on average, older results than those obtained for goethite cement in cangas (Figures 5a, 6; Table 1). The results show that saprolites are older than the overlying cangas and suggest that cangas evolve by the slow transformation of the underlying saprolite.

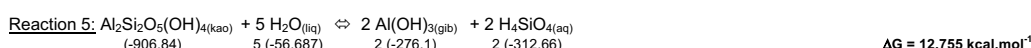
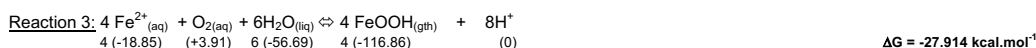
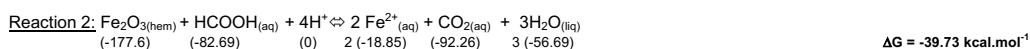
Legend



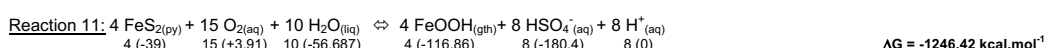
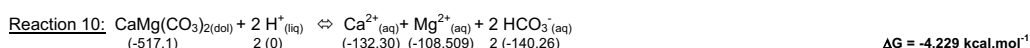
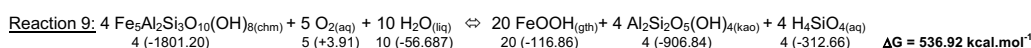
Figure 8: Diagrammatic illustration that shows the most relevant processes and reactions (Table 3) during weathering of BIF to saprolite and saprolite to canga. The dashed lines illustrate the depth of erosion recorded by the weathering profiles at Gandarela, Moeda, and Serrinhas.

Table 3 – Chemical reactions illustrating the most important processes during weathering of BIFs

Saprolite to canga



Banded iron formation to saprolite



The transformation from saprolite to canga is both chemical (quartz and carbonate dissolution and leaching) and mechanical (collapse and translocation associated with mass losses during silica and carbonate dissolution) (Figure 8). It is also strongly influenced by biological processes [Monteiro *et al.*, 2014; Levett *et al.*, 2016]. The most important chemical processes are the dissolution and

leaching of silica, carbonates, and minor sulfides, and the reductive dissolution of hematite and magnetite with subsequent precipitation of goethite. Significant mass loss during leaching of silica and carbonates creates cavities where hematite-magnetite beds, blocks, and loose grains fall and rotate, generating a collapse breccia. Sometimes these cavities are not filled, resulting in vugs, caves, and karstic pipes common in cangas [Auler *et al.*, 2014]. Direct oxidation and/or hydration of magnetite to goethite is common and energetically favored, while the direct hydration of hematite to goethite is thermodynamically inhibited (Table 3). Reductive dissolution of hematite and magnetite occurs throughout the history of canga formation, and it is aided by organic acids exuded by plants and generated by the decaying biota. Soluble iron reprecipitates locally as goethite cements (Figure 8; Table 3). Slowly, the BIF saprolite becomes devoid of silica minerals (quartz, chalcedony) and carbonates and evolves into a duricrust composed of fragments of BIF, fragments of goethite veins, blocks of hypogene hematite±magnetite ore, and fine grains of hypogene hematite and magnetite all cemented by supergene goethite (and minor supergene hematite, gibbsite, and rarely chalcedony/opal) (Figure 8). Translocation of surface material into caves and pipes contributes to the vertical mobility of iron minerals in the weathering profile. Translocated particles may be fine grained and follow pathways created by plant roots and insect (termites, ants) burrows [Shuster *et al.*, 2012], or, more rarely, they involve cm- to m-sized blocks collapsed into caves and pipes. If erosion of the canga at the surface is slow, the canga horizon grows with time at the expense of the underlying saprolite. If erosion surpasses the rate of propagation of the canga front, cangas are slowly eroded and eventually disappear from the landscape.

(U-Th)/He results (Figures 5, 6) reveal that the history of mineral precipitation in cangas and the underlying saprolites is roughly coeval, and some of the most frequent goethite precipitation ages (e.g., 32-30 Ma) measured in saprolites also occur in cangas (Figure 6). The coeval events of mineral dissolution-reprecipitation in the duricrust and saprolite suggest that the saprolite-canga consortium has existed for a long time and has evolved together. Goethite precipitation events detected by geochronology are likely driven by changing climates [Vasconcelos, 1999; Carmo and Vasconcelos, 2004; Spier *et al.*, 2006], as they are strongly dependent on an active biota at the surface to generate the organic acids necessary to promote the redox-driven dissolution-reprecipitation of iron species (Figure 8; Table 3). Peaks in the goethite (U-Th)/He record (e.g., at 32-30 Ma) likely record periods under paleoclimatic conditions conducive to weathering. The link between paleoclimate and the history of mineral precipitation in weathering profiles has been explored by several authors (e.g., Vasconcelos *et al.*, 1994; Hénocque *et al.*, 1998; Carmo and Vasconcelos, 2004; Colin *et al.*, 2005; Vasconcelos *et al.*, 2015), and we will not focus on this topic here.

5.2 The cosmogenic ^3He record: mechanisms controlling the dismantling of cangas

The combined *aEAs* and *pAs* reveal a dynamic history of evolution for the three profiles investigated. Gandarela, the plateau at highest elevation, most laterally extensive, and covered by the most continuous canga blanket, records the longest exposure and goethite precipitation histories (Figure 5; Table 2). Detrital material derived from erosion of this plateau suggests that slow degradation of the plateau is occurring through the breakdown of the canga and the release of hematite clasts that record an even longer ($> \sim 10.5$ Ma) history of exposure (Figure 5a, c; Table 2). The geometry of canga blocks on the surface of the Gandarela plateau (Figure 3a-d) hints at the likely processes leading to plateau degradation.

Typically, canga slabs protrude 20 to 50 cm from the surface and are surrounded by rills paved with detrital canga fragments and hematite-magnetite clasts (Figure 3b-d). These geomorphic features suggest that the canga blanket undergoes slow in situ erosion by a combination of biogeochemical dissolution of goethite cements and mechanical disaggregation of the brecciated material, with local release of fragments of hematite±magnetite that slowly undergo hydration, partial dissolution, and transport towards the edges of the plateaus (Figures 2a, 3 a-d, 5a). These clasts must be laterally transported by intermittently surface wash during major storms and must overcome barriers provided by surface protruding canga blocks. The clasts must surmount traps produced by vertical cracks in the duricrust, and they must also escape re-cementation. Clasts that overcome these barriers may arrive at the shoulders of the plateaus and be carried downward by diffusive processes. Ultimately, these lag fragments fall off the edges of the plateaus and supply detrital material to the shallow streams draining the plateaus or are incorporated into colluvia or transported cangas shouldering the plateaus. The old *aEA* results for the detrital blocks eroded from the plateaus (> 10.5 Ma) confirm that dismantling, re-cementation, and ultimately erosion of cangas supplies the detritus surrounding the plateaus and that clasts released by canga fragmentation travel very slowly through and out of the system. It also suggests that the current canga blanket has slowly lost some of its upper horizons by slow chemical and physical erosion (Figures 5, 8).

At Serra da Moeda, faster erosion of the duricrust is indicated by a thinner and discontinuous canga with younger cements (< 38 Ma) than at Gandarela. The *aEAs* here are relatively short (~ 2 Ma), also suggesting a more active degradation of the duricrust and explaining the abundance of hematite detritus surrounding the exposed canga surfaces (Figure 2d, 5). A similar history of canga breakdown to that proposed for Gandarela occurs here, but the erosion history is more advanced and the current surface represents a deeper zone of a partially eroded canga (Figures 5, 8). The abundant detrital material travels very slowly out of the system through rills (on plateau surfaces and shoulders, Fig. 2a, 3a) and colluvia (on slopes and terraces, Fig. 2c, 3e), as indicated by the

average (8.6 ± 2.8 Ma) and maximum (10.6 ± 1.3 Ma) *aEAs* obtained for detrital hematite (Figure 5; Table 2). The even greater ages (pAs of 53 to 9 Ma) of goethite cements in detrital canga fragments from a colluvium derived from the Moeda plateau (Figures 2f, 5a) confirm the hypothesis that an older canga layer once blanketed the plateau and that this blanket has now been eroded and its detrita redeposited locally.

The lowest elevation and most discontinuous canga blanket at Serrinhas is cemented by the youngest goethites and also has a recent history of exposure (average *aEAs* ~ 2 Ma), suggesting that this plateau has been eroded to the lowest levels of the duricrust, close to the saprolite-canga interface, when compared to cangas at Moeda and Gandarela (Figures 5, 8).

5.3. Rates of erosion for canga plateaus

Since we have evidence that at least some of the canga blocks have undergone a history of protracted and continuous exposure at the surface, without reburial, it is reasonable that ^3He concentrations in cm-size hematite-magnetite clasts, the mineral less likely to have undergone dissolution-reprecipitation or to have translocated up and down the profile (except where caves occurs), be cast in terms of erosion rates. Calculated erosion rates are: 0.17 m.Ma^{-1} for Gandarela, 0.31 m.Ma^{-1} for Serra da Moeda, and 0.28 m.Ma^{-1} for Serra das Serrinhas. These differences suggest that erosion rates greater than $\sim 0.25\text{-}0.30 \text{ m.Ma}^{-1}$ may exceed the self-healing capacity of canga-cemented plateaus, leading to their eventual destruction (Figure 8). When a surface becomes too narrow and steep (Figures 1a, 5, 8), running surface water and gravitational forces may drive erosion beyond the kinetic threshold of iron re-cementation. The eroded canga fragments may be either removed from the system or remain as detrital aprons on hill slopes (Figure 2a-d, 5).

The erosion rates measured for cangas and detrital hematite-magnetite clasts are of similar magnitude as shorter-term rates measured from quartz sands in rivers draining quartzites in the QF [Salgado *et al.*, 2006, 2008] (Figure 9). But at a regional scale, long-term erosion rates obtained from ^3He concentrations in situ and in detrital iron oxyhydroxides are much lower than erosion rates obtained from ^{10}Be in quartz (Figure 9), suggesting that plateaus blanketed by cangas are more effectively shielded from erosion than plateaus underlain by quartzites and other lithologies. This interpretation is consistent with the fact that the summits at Serras do Gandarela, Moeda, and Serrinhas are mostly underlain by BIFs and not other lithologies (Figures 1, 5; Baltazar *et al.*, [2005]).

5.4. Age vs elevation relationships for canga plateaus

Monteiro *et al.* [2014] postulated that differences in (U-Th)/He ages for high- and low-elevation canga-cemented plateaus in the QF originate from two possible models of landscape evolution: (1) the QF was once equally leveled and progressively eroded forming canga-plateaus at different elevations, or (2) the QF was never leveled and cangas at higher and lower elevations evolved simultaneously. Differences in erosion rates for low- and high-elevation surfaces ($<0.17 \text{ m.Ma}^{-1}$ for Gandarela and 0.31 m.Ma^{-1} for Moeda) if extrapolated back in time would require an unreasonable period of $\sim 600 \text{ Ma}$ for the two plateaus to share a same elevation. Therefore, the plateaus at Gandarela, Moeda, and Serrinhas probably evolved simultaneously on a landscape already showing moderate relief. More rapid physical erosion of the canga blanket as the plateaus became progressively narrower at Moeda and Serrinhas (Figure 1) likely accounts for the differences in ages, elevations, and lateral continuity for the canga blankets overlying the various plateaus.

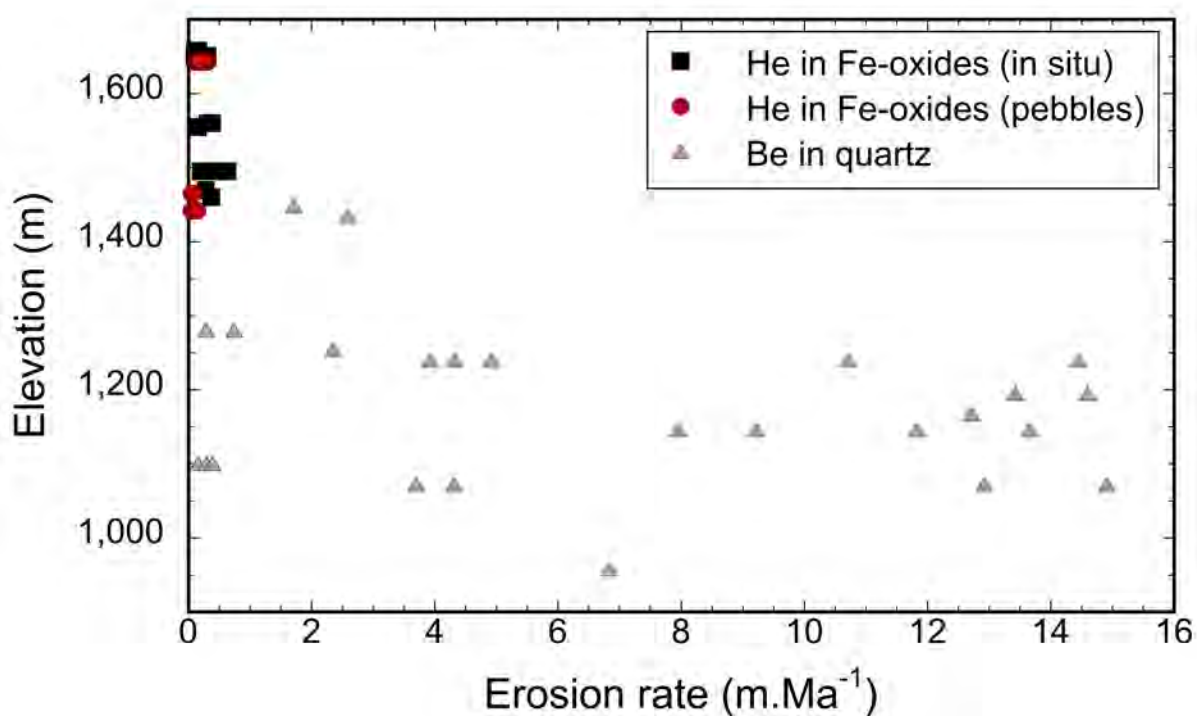


Figure 9: Erosion rates derived from in situ and detrital iron oxyhydroxides (this study) are much lower than similar rates derived from quartz [Salgado *et al.*, 2006, 2007, 2008], consistent with the observation that the plateaus and ridges in the areas investigated are underlain by iron-duricrusts overlying banded iron-formations.

The mechanisms envisaged for the evolution of landscapes in the QF (plateau cementation by canga, slow surface erosion, scarp retreat, etc.) implies that erosion is differential and that the relief increases with time [Vasconcelos, 1998, 1999]. The narrowing of plateaus suggests that the entire landscape was once covered by a more extensive and interconnected but undulating land surface.

Rounded hematite-magnetite cobbles and pebbles in colluvia and detrital cangas imply effective material transport in a mature drainage system, which is presently absent from the plateaus because of their limited catchment area. These river sediments are relics of an ancient drainage system that once existed on a now mostly eroded undulating palaeosurface that blanketed the entire region.

Despite the active histories of chemical and mechanical weathering and erosion, canga-blanketed plateaus evolve very slowly. Slow rates of erosion elsewhere are commonly attributed to rainfall deficiency in semi-arid or arid conditions [Nishiizumi *et al.*, 2005; Dunai *et al.*, 2005; Summerfield *et al.*, 1999]. The results in this study suggest that deeply weathered BIF in tropical landscapes erode at rates equivalent to or lower than those measured in arid or semi-arid environments. The joint application of ^3He and (U-Th)/He age measurements reveal that weathering-driven armoring of the landscape by goethite cementation and re-cementation in iron duricrusts offers a plausible explanation for the low rates of erosion and the preservation of continuously exposed landsurfaces in tropical humid conditions. Investigating the long-term evolution of these landscapes must consider the role of weathering as an inhibitor to physical erosion, and not solely as the process that makes erodible material from bedrock.

5.5. Cangas: self-healing biogeochemical conveyor belts

Determining both (U-Th)/He precipitation ages and ^3He exposure ages for the same sample permits addressing some of the complexities in a sample's history as it is exhumed through erosion. For example, exposure ages for goethite cements are either equal to or less than their precipitation ages (Figure 10), suggesting that most goethite cementation occurs in the subsurface, where the cements reside before slowly ascending to the surface. The biogenic processes interpreted to control the self-healing properties of cangas [Monteiro *et al.*, 2014; Levett *et al.*, 2016] may occur both at the surface and the subsurface, but a key ingredient in goethite cementation is reduced and acidic water. Since cangas are very porous and water readily infiltrates into a network of tubules, vugs, and fractures, it is likely that this infiltrating water carries organic acids leached from the surface, accumulates in subsurface void spaces, and establishes a reducing environment that can dissolve iron from hematite±magnetite±goethite (Figure 8; Table 3). Iron reprecipitation from these solutions may occur in the subsurface by direct oxidation of aqueous Fe^{2+} into insoluble Fe^{3+} -oxyhydroxides during the periodic influx of oxygenated meteoric waters, by neutralization of the organic acids during reaction with wall rock, or by microbially induced Fe^{2+} oxidation [Weber *et al.*, 2006 and references therein].

The difference in (U-Th)/He pA and cosmogenic ^3He aEA for a fragment of goethite cement reveals how far from the surface goethite cementation may have taken place and how long it took for the

cement to be brought to the surface. An alternative explanation – that cements form at the surface, translocate down into the profile, and return to the surface at a later date – is also plausible. For example, large pores, fractures, and tubules in canga permit the downward transport of mineral grains, and geopetal textures in root and insect burrows reveal that downward translocation of mineral particles does occur. However, the translocated particles are usually small (mm-size) and wholesale transport of large canga blocks up and down the profile, although possible where caves and karstic pipes exist, is less likely than the downward movement of weathering solutions.

Further evidence that goethite cementation takes place at depth is the presence of old goethite veins within saprolites and the extensive iron cementation that characterize the “goethite cementation-front” at the canga-saprolite interface. A strong piece of evidence for the precipitation of goethite cements at depth is provided by the (U-Th)/He goethite *pAs* from block G1209 (Figure 7). These *pAs* are ~ 2-4 Ma greater than the cosmogenic ^3He *aEAs* for the same block suggesting that goethite cementation took place at depth, below the zone of accumulation of cosmogenic ^3He (< ~2 m). The 2-4 Ma difference between the goethite precipitation age and ^3He exposure ages reveals that it took ~2-4 Ma for a sample formed at > 2 m depth to reach the surface, suggesting a sample exhumation rate of ~ 0.5-1 m.Ma⁻¹, compatible with the average erosion rates estimated above. The exhumation rate of ~0.5-1 m.Ma⁻¹ is the net rate of transfer of friable and erodible material from the saprolite through the canga and to the drainage system. In other words, ~0.5-1 m.Ma⁻¹ is the net rate of mass transfer through the canga biogeochemical conveyor belt.

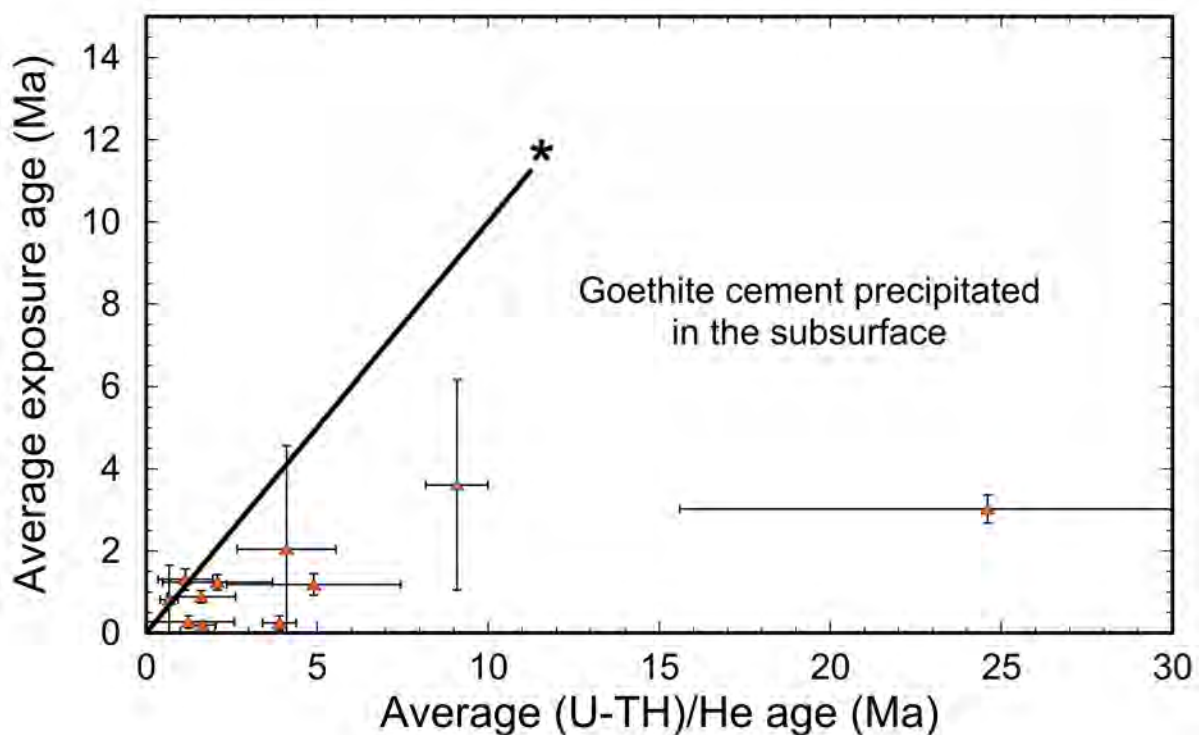


Figure 10: A correlation between goethite precipitation and exposure ages suggest that the majority of the goethite cementing cangas is precipitated and remains below the surface, suggesting that Fe-cementation is primarily occurring in the subsurface, where water rich in organic acids accumulate and promote iron reductive dissolution, local transport, and reprecipitation. The 1:1 line (*) identifies goethite cements that precipitated and remained at the surface during their entire history.

6. CONCLUSION

The history of weathering and erosion discussed here show that cangas are long-lasting features of banded iron-formation (BIF) landscapes. The more extensive and continuous the canga cover, the more stable it is and the more effective its protective power. Similarities in apparent exposure ages (*aEAs*) for in situ canga blocks and adjacent detrital fragments suggest that cangas evolve by fragmentation and Fe-re-cementation in situ (self-healing). Exposure ages for goethite cements are either equal to or younger than their precipitation ages, suggesting either that goethite cements formed at the surface are rapidly buried after precipitation, only returning to the surface very slowly, or, alternatively, that most of the cementation of canga occurs in the sub-surface. The difference in (U-Th)/He precipitation age (*pA*) and cosmogenic ^3He *aEA* for a fragment of goethite cement reveals how far from the surface goethite cementation may have taken place and how long it took for the cement to be brought to the surface. The combined ^3He and (U-Th)/He results suggest that biogeochemical processes interpreted to control the self-healing properties of cangas occur both at the surface but primarily at the subsurface. The history of weathering and erosion derived from the combined (U-Th)/He and cosmogenic ^3He records reveals that surface armoring by weathering and erosion is the primarily mechanism shaping landscapes in ancient and deeply weathered BIF terrains.

The ultimate effect of canga in BIF landscapes is to provide a very stable and protracted transfer mechanism, slowly converting friable and easily erodible BIF saprolite into physically resilient goethite-cemented breccias that slowly ascends to the surface to be eventually dismantled and eroded. In that sense, cangas act as natural conveyor belts that stabilize fragments of friable weathered BIF between their break down at depth until their eventual delivery to the drainage system. A transfer rate of $\sim 0.5\text{-}1 \text{ m.Ma}^{-1}$ implies that a 70 m canga cover would need about 70-140 Ma to bring a cement formed at depth to the surface and deliver it to the drainage system. Therefore, while the role of chemical and physical weathering in BIF landscapes is to transform bedrock into material to be delivered to erosion, internal biogeochemical reactions in these systems slow this transfer down to a level where the transfer mechanism itself becomes the main force shaping the landscape.

Acknowledgments

We thank Shirley Barros, Carolina Silva, MBR and Vale for logistic support; UQ-CMM staff for help during microanalysis; and, particularly, the late Lindsey Hedges for help and guidance during (U-Th)/He analyses. We also thank D. Granger, A. Ault, M. Schulz, and two editors from JGR for their constructive comments and suggestions. This project was supported by the Australian Research Council (ARC Discovery Grant DP160104988) grant to Paulo Vasconcelos and Kenneth Farley and the Brazilian Research Council (CNPq), which sponsored Hevelyn Monteiro's PhD studies. Geochronological dataset is available at <http://dx.doi.org/10.1594/IEDA/100730>

References

- Ab'Saber, A. N. (1966), O domínio de mares de morros no Brasil, *Geomorfologia*, 2, 9 p.
- Alkmim, F. F., and S. Marshak (1998), Transamazonian orogeny in the Southern São Francisco craton region, Minas Gerais, Brazil: evidence for Paleoproterozoic collision and collapse in the Quadrilátero Ferrífero, *Precambrian Res.*, 90, 29-58.
- Alvares, C. A., J. L. Stape, P. C. Sentelhas, J. L. de M. Gonçalves, and G. Sparovek (2013) Köppen's climate classification map for Brazil. *Meteorol. Z.*, 22(6), 711-728.
- Amidon, W. H., and K. A. Farley (2011), Cosmogenic ^3He production rates in apatites, zircon and pyroxene inferred from Bonneville flood erosional surfaces, *Quaternary Geo.*, 6, 10-21.
- Auler, A. S., L. B. Piló, C. W. Parker, J. M. Senko, I. D. Sasowsky, and H. A. Barton (2014), Hypogene cave patterns in iron ore caves: convergence of forms or processes? in Hypogene cave Morphologies, Selected papers and abstracts of the symposium held February 2 through 7, San Salvador Island, Bahamas, Karst Water Institute Special Publication 18, edited by A. Klimchouk, I. Sasowsky, J. Mylroie, S. A. Engel, and A. S. Engel, pp. 15-19, Karst Water Institute, Leesburg, Virginia.
- Baltazar, O. F., F. J. Baars, L. M. Lobato, L. B. Reis, A. B. Achtschin, G. V. Berni, V. D. Silveira (2005a), Mapa geológico Gandarela na escala 1:50.000 com nota explicativa, In: Projeto Geologia do Quadrilátero Ferrífero - Integração e correção cartográfica em SIG com nota explicativa, Lobato et al., (2005) CODEMIG, Belo Horizonte.
- Baltazar, O. F., F. J. Baars, L. M. Lobato, L. B. Reis, A. B. Achtschin, G. V. Berni, V. D. Silveira (2005b), Mapa geológico Itabirito na escala 1:50.000 com nota explicativa, In: Projeto Geologia do Quadrilátero Ferrífero - Integração e correção cartográfica em SIG com nota explicativa, Lobato et al., (2005) CODEMIG, Belo Horizonte.
- Baltazar, O. F., F. J. Baars, L. M. Lobato, L. B. Reis, A. B. Achtschin, G. V. Berni, V. D. Silveira (2005c), Mapa geológico Casa de Pedra na escala 1:50.000 com nota explicativa, In: Projeto Geologia do Quadrilátero Ferrífero - Integração e correção cartográfica em SIG com nota explicativa, Lobato et al., (2005) CODEMIG, Belo Horizonte.
- Banfield, J. F., W. W. Barker, S. A. Welch and A. Taunton (1999), Biological impact on mineral dissolution: Application of the lichen model to understanding mineral weathering in the rhizosphere. *Proc. Natl. Acad. Sci. USA*, 96(7), 3404-3011.

- Bierman, P. R., and M. Caffee (2001), Slow rates of rock surface erosion and sediment production across the Namib desert and escarpment, Southern Africa, *Am. J. Sci.*, *301*, 326-358.
- Braun, J., J. Mercier, F. Guillocheau and C. Robin (2016), A simple model for regolith formation by chemical weathering, *J. Geophys. Res.-ES*, *121*, 2140 - 2171.
- Carlos, D. U., L. Uieda, and V. C. F. Basbosa (2014), Imaging iron ore from the Quadrilátero Ferrífero (Brazil) using geophysical inversion and drill hole data, *Ore Geol. Rev.*, *61*, 268-285.
- Carmo, I. O. and P. M. P. Vasconcelos (2004), Geochronological evidence for pervasive Miocene weathering, Minas Gerais, Brazil, *Earth Surf. Processes Landforms*, *29*, 1303-1320.
- Carmo, I. O., P. M. P. Vasconcelos, and B. Kohn (2004), Geocronologia de intemperismo, termocronologia por traços de fissão em apatita e preservação de antigas superfícies geomorfológicas, Quadrilátero Ferrífero, SE Brasil, Congresso Brasileiro de Geologia 42, p. 17-22.
- Carson, M. A. and M. J. Kirkby (1972), Hillslope Form and Process. Cambridge University Press, Cambridge, UK.
- Chemale Jr., F., C. A. Rosière, and I. Endo (1994), The tectonic evolution of the Quadrilátero Ferrífero, Minas Gerais, Brazil, *Precambrian Res.*, *65*, 25-54.
- Colin, F., A. Beauvais, G. Ruffet, and O. Hénocque (2005), First $^{40}\text{Ar}/^{39}\text{Ar}$ geochronology of lateritic manganiferous pisolites: Implications for the Paleogeone history of a West Africa landscape. *Earth Planet. Sci. Lett.*, *238*, 172-188.
- DiBiase, R. A., K. X. Whipple, A. M. Heimsath, and W. B. Ouimet (2010), Landscape form and millennial erosion rates in the San Gabriel Mountains, CA. *Earth Planet. Sci. Lett.*, *289*, 134-144.
- Dorr II, J. V. N. (1964), Supergene iron ores of Minas Gerais, Brazil, *Econ. Geol.*, *59*(7), 1203-1240.
- Dorr II J. V. N. (1969), Physiographic, stratigraphic and structural development of the Quadrilátero Ferrífero, Minas Gerais, Brazil, U.S.G.S. Prof. Paper, 614-A, Washington, DC, 110 pp.
- Dunai, T. J., G. A. G. López, and J. Juez-Larré (2005), Oligocene-Miocene age of aridity in the Atacama Desert revealed by exposure dating of erosion-sensitive landforms, *Geology*, *33*(4), 321 - 324.

- Fujioka, T., L. K. Fifield, J. O. Stone, P. M. P. Vasconcelos, S. G. Tims, and J. Chappell (2010), In situ cosmogenic ^{53}Mn production rate from ancient low-denudation surface in tropic Brazil, *Nucl. Instrum. Meth. Phys. Res. B*, 268, 1209-1213.
- Hénocque, O., G. Ruffet, F. Colin, and G. Féraud (1998), $^{40}\text{Ar}/^{39}\text{Ar}$ dating of West Africa lateritic cryptomelanes. *Geochim. Cosmochim. Acta*, 62(16), 2739-2756.
- Jacobi, C. M., F. F. do Carmo, R. C. Vincent, and J. R. Stehmann (2007), Plant communities on ironstone outcrops: a diverse and endangered Brazilian ecosystem. *Biodivers. Conserv.*, 16(7), 2185-2200.
- King, L. C. (1956), A Geomorfologia do Brasil Oriental. *Rev. Bras. Geografia*, 2, 147-265.
- Kohn, B., I. O. Carmo, and P. M. P. Vasconcelos (2016), Denudation history of the SE Brazil margin from combined low temperature thermochronology and $^{40}\text{Ar}/^{39}\text{Ar}$ weathering geochronology: implications for landscape evolution, 15th International Conference on Thermochronology, Maresias, Brazil, 88-89.
- Lal, D. (1991), Cosmic ray labeling of erosion surfaces: in situ nuclide production rates and erosion models, *Earth Planet. Sci. Lett.*, 104, 424-439.
- Levett, A., E. Gagen, J. Shuster, L. Rintoul, M. Tobin, J. Vongsivut, K. Bamberg, P. Vasconcelos, and G. Southam (2016), Evidence of biogeochemical processes in iron duricrust formation, *J. S. Am. Earth Sci.*, 71, 131-142.
- Masarik, J. (2002), Numerical simulation of in-situ production of cosmogenic nuclides. *Geochim. Cosmochim. Acta*, 66, A491.
- Magalhães Jr., A. and A. Saadi (1994), Ritmos da dinâmica fluvial Neo-Cenozóica controlados por soerguimento regional e falhamento: o vale do rio das Velhas na região de Belo Horizonte, Minas Gerais, Brasil, *Geonomos*, 2, 42-54.
- Monteiro, H. S., P. M. P. Vasconcelos, K. A. Farley, C. A. Spier, and C. L. Mello (2014), (U-Th)/He geochronology of goethite and the origin and evolution of cangas, *Geochim. Cosmochim. Acta*, 131, 267-289.
- Nishiizumi, K., M. W. Caffee, R. C. Finkel, G. Brimhall, and T. Mote (2005), Remnants of a fossil alluvial fan landscape of Miocene age in the Atacama Desert of northern Chile using cosmogenic nuclide exposure dating, *Earth Planet. Sci. Lett.*, 237, 499 - 507.

- Patterson, D. B., and K. A. Farley (1998), Extraterrestrial ^3He in seafloor sediments: Evidence for correlated 100 kyr periodicity in the accretion rate of interplanetary dust, orbital parameters, and Quaternary climate, *Geochim. Cosmochim. Acta*, 62(23/24), 3669-3682.
- Salgado, A. A. R., R. Braucher, F. Colin, H. A. Nalini Jr., A. F. D. C. Varajão and C. A. C. Varajão (2006), Denudation rates of the Quadrilátero Ferrífero (Minas Gerais, Brazil): preliminary results from measurements of solute fluxes in rivers and in situ-produced cosmogenic ^{10}Be , *J. Geochem. Explor.*, 88, 313–317.
- Salgado, A. A. R., C. A. C. Varajão, F. Colin, R. Braucher, A. F. D. C. Varajão, and H. A. Nalini Jr. (2007), Study of the erosion rates in the upper Maracujá Basin (Quadrilátero Ferrífero/MG, Brazil) by the in situ produced cosmogenic ^{10}Be method, *Earth Surf. Processes Landforms*, 32(6), 905–911.
- Salgado, A. A. R., R. Braucher, C. A. C. Varajão, A. F. D. C. Varajão, and H. A. Nalini Jr. (2008), Relief evolution of the Quadrilátero Ferrífero (Minas Gerais, Brazil) by means of (^{10}Be) cosmogenic nuclei, *Zeitschrift Geomorphol.* 52, 317–323.
- Santos, P. A. dos (2006) Estudo de densidades de rochas e comparação de técnicas de medição, Região do Quadrilátero Ferrífero, Minas Gerais, Brasil, Dissertação de Mestrado, ISEI: p. 58.
- Shuster, D. L., P. M. P. Vasconcelos, J. A. Heim, and K. A. Farley (2005), Weathering geochronology by (U-Th)/He dating of goethite, *Geochim. Cosmochim. Acta*, 69(3), 659-673.
- Shuster, D. L., K. A. Farley, P. M. P. Vasconcelos, G. Balco, H. S. Monteiro, K. Waltenberg, and J. O. Stone (2012), Cosmogenic ^3He in hematite and goethite from Brazilian "canga" duricrust demonstrates the extreme stability of these surfaces, *Earth Planet. Sci. Lett.*, 329-330, 41-50.
- Spier, C. A., S. M. B. Oliveira, and C. A. Rosière (2003), Geology and geochemistry of the Águas Claras and Pico Iron mines, Quadrilátero Ferrífero, Minas Gerais, Brazil, *Miner. Deposita*, 38, 751-774, doi: 10.1007/s00126-003-0371-2
- Spier, C. A., P. M. P. Vasconcelos, and S. M. B. Oliveira (2006), $^{40}\text{Ar}/^{39}\text{Ar}$ geochronological constraints on the evolution of lateritic iron deposits in the Quadrilátero Ferrífero, Minas Gerais, Brazil, *Chem. Geol.*, 234, 79-104.
- Spier, C. A., S. M. B. Oliveira, C. A. Rosière, and J. D. Ardisson (2008), Mineralogy and trace-element geochemistry of the high-grade iron ores of the Águas Claras mine and comparison

with the Capão Xavier and Tamanduá iron ore deposits, Quadrilátero Ferrífero, Brazil, *Miner Deposita*, 43, 229-254, doi: 10.1007/s00126-007-0157-z

Stone, J. O. (2000), Air pressure and cosmogenic isotope production, *J. Geophys. Res.*, 105(B10), 23,753-723,759.

Summerfield, M. A., F. M. Stuart, H. A. P. Cockburn, D. E. Sugden, G. H. Denton, T. Dunai, and D. R. Marchant (1999), Long-term rates of denudation in the Dry Valleys, Transantarctic Mountains, southern Victoria Land, Antarctica based on in-situ-produced ^{21}Ne , *Geomorphology*, 27, 113 - 129.

Tucker, G. E. and R. Singerland (1994), Erosional dynamics, flexural isostasy, and long-lived escarpments: A numerical modeling study, *J. Geophys. Res.*, 99(136), 12,229 - 12,243.

Tucker, G. E. and G. R. Hancock (2010), Modelling landscape evolution: *Earth Surf. Process. Landf.*, 35, 28 - 50.

Twidale, C. R. (1956), Chronology of denudation in northwest Queensland: *Bull. Geol. Soc. Am.*, 67(7), 867 - 882.

Twidale, C. R., R. C. Horwitz, and E. M. Campbell (1985), Hamersley landscapes of the northwest of Western Australia, *Rev. Geol. Dyn. Geogr. Phys.*, 26, 173-186.

Vasconcelos, P. M. P., P. R. Rene, G. H. Brimhall, and T. A. Becker (1994), Direct dating of weathering phenomena by $^{40}\text{Ar}/^{39}\text{Ar}$ and K-Ar analysis of supergene K-Mn oxides, *Geochim. Cosmochim. Ac.*, 58(6), 1635-1665.

Vasconcelos, P. M. (1999), $^{40}\text{Ar}/^{39}\text{Ar}$ geochronology of supergene processes in ore deposits. *Econ. Geol.*, 12, 73-113.

Vasconcelos, P. M. (1998), Geochronology of weathering in the Mt Isa and Charters Towers regions, northern Queensland, Restricted Report 68R/E&M Rep. 452R, Perth, Australia, CRC LEME.

Vasconcelos, P. M. P., M. Reich, and D. L. Shuster (2015), The paleoclimatic signatures of supergene metal deposits. *Elements*, 11, 317-322.

Vance, D., M. Bickle, S. Ivy-Ochs, and P. W. Kubik (2003), Erosion and exhumation of the Himalaya from cosmogenic isotope inventories of river sediments. *Earth Planet. Sci. Lett.*, 206, 273-288.

- Waltenberg K. M. (2012) Mineral physics and crystal chemistry of minerals suitable for weathering geochronology: implications to $^{40}\text{Ar}/^{39}\text{Ar}$ and (U-Th)/He geochronology, PhD Thesis, The University of Queensland, Brisbane, p. 421.
- Weber, K. A., L. A. Achenback, and J. D. Coates (2006), Microorganisms pumping iron: anaerobic microbial iron oxidation and reduction. *Nature Rev. Microbiol.*, 4, 752-764.

Chapter 4: Ages and evolution of diachronous erosion surfaces in the Amazon: the (U-Th)/He and cosmogenic ^3He records

H.S. Monteiro^{1*}, P.M.P. Vasconcelos^{1,2}, K.A. Farley², and C.A.M. Lopes³

¹School of Earth and Environmental Sciences, The University of Queensland, Brisbane, Queensland 4072, Australia.

²Division of Geological and Planetary Sciences, California Institute of Technology, Pasadena, CA 91125. ³Geosistemas Ltda.

Submitted to Geochimica et Cosmochimica Acta

Corresponding author: Hevelyn Monteiro (h.monteiro@uq.edu.au)

Key Points:

- (U-Th)/He geochronology of goethites in stepped landscapes shows that older surfaces are higher and younger surfaces are lower.
- Cosmogenic ^3He in hematites from the Carajás Plateau show extremely low rates of erosion.
- (U-Th)/He geochronology of goethites shows that low-lying surfaces are diachronous, younging towards receding escarpments surrounding older plateaus.

ABSTRACT

(U-Th)/He geochronology of two weathered plateaus (Igarapé Bahia and N1) on top of the Carajás Mountains, Pará, Brazil, reveals a history of protected weathering spanning from ca. 80 Ma to the present for this high elevation (~ 700 m) landsurface. Cosmogenic ^3He measurements for hematite blocks cemented onto the plateaus at two sites, N1 and S11D, yield erosion rates as low as 0.09 and 0.08 $\text{m}\cdot\text{Ma}^{-1}$ for each plateau, respectively, confirming that the plateau surfaces are immune to physical erosion for tens of millions of years. (U-Th)/He geochronology for ferruginous duricrusts blanketing the low elevation (250-100 m) plains surrounding the Carajás Mountains yield results consistently younger than ~ 10 Ma. The geochronology results also reveal that the low elevation plain is diachronous, becoming progressively younger towards the receding plateaus. The spatial distribution of (U-Th)/He ages permits reconstructing the history of scarp retreat for the Carajás landscape, showing that scarp retreat along major river valleys may have been as fast as 20 $\text{km}\cdot\text{Ma}^{-1}$ during tectonically active and humid periods in the Cenozoic. The cessation of scarp retreat at some sites suggests that metamorphosed banded iron formations and quartzites provide effective barriers to retreating escarpments, helping to preserve some of the oldest continuously exposed landsurfaces on Earth.

1. INTRODUCTION

Ancient landscapes in relatively stable cratonic areas in Australia, Africa, and Brazil host deeply weathered plateaus surrounded by undulating lowland that are blanketed by shallower and less evolved soils and weathering profiles (King, 1956). Classical landscape evolution models often attribute ages to these distinct elevation landsurfaces, where the higher elevation deeply weathered plateaus are purportedly older than the surrounding low elevation plains (King, 1956). These higher elevation plateaus are interpreted as remnants of old erosion surfaces now undergoing destruction by scarp retreat.

$^{40}\text{Ar}/^{39}\text{Ar}$ geochronology of supergene Mn oxides from both high and low elevation surfaces in Australia (Vasconcelos, 2002), Brazil (Carmo and Vasconcelos, 2006; Vasconcelos and Carmo, 2017), Africa (Beauvais et al., 2008; Colin et al., 2005), and India (Beauvais et al., 2016; Bonnet et al., 2016) confirms that weathering profiles on the elevated plateaus are older than those in lower elevation surfaces. $^{40}\text{Ar}/^{39}\text{Ar}$ geochronology also shows that weathering profiles on the highest elevation plateaus are as old as ~ 70 Ma, suggesting that remnant plateaus erode very slowly (Vasconcelos et al., 1994; Vasconcelos, 2002; Vasconcelos and Carmo, 2017). These results and conclusions are confirmed by completely independent methods. For example, the combination of (U-Th)/He geochronology of supergene goethites (Shuster et al., 2005) with cosmogenic ^3He (Shuster et al., 2012) measurements at Carajás confirm the longevity of the surfaces overlying the plateaus and their low rates of erosion. Low rates of erosion are confirmed by cosmogenic ^{53}Mn analysis (Fujioka et al., 2010). (U-Th)/He geochronology of supergene goethites and cosmogenic ^3He measurements for plateaus at the Quadrilátero Ferrífero, Minas Gerais, corroborate the low rates of erosion for the ancient (> 50 Ma) plateaus.

Here, we expand on those studies and apply a similar approach to that used by Monteiro et al. (2014, 2017a) for the Quadrilátero Ferrífero, Minas Gerais, Brazil, to investigate, in addition to ages, possible mechanisms controlling the formation and preservation of ancient weathering profiles at Carajás. We take advantage of iron cementation and duricrust formation to investigate whether the low-lying undulating plains surrounding the ancient Carajás plateaus are indeed younger than the surfaces defining the plateaus. Lastly, we test the hypothesis that the low elevation surface evolves by scarp retreat, expanding at the expense of the receding plateaus. If that hypothesis is correct, the low-lying surface should be diachronous, becoming progressively younger in the direction of scarp retreat. If Fe-cementation started on these surfaces shortly after their formation, goethite cemented duricrusts in the low-lying surfaces should be older away from the escarpment and they should become progressively younger as one approaches the receding plateaus.

We dated Fe-cemented weathering profiles at two sites, N1 and Igarapé Bahia (IB) (Figure 1). We also measured ^3He concentrations from N1 and S11D (Figure 1) to determine erosion rates for the high elevation plateaus. Finally, we dated goethite cements from four weathering profiles distributed along a traverse from Marabá through Curionópolis to near Canaã dos Carajás (Figure 1) to evaluate whether rates of scarp retreat could be retrieved from the ages of the weathering profiles in the low elevation undulating plains.

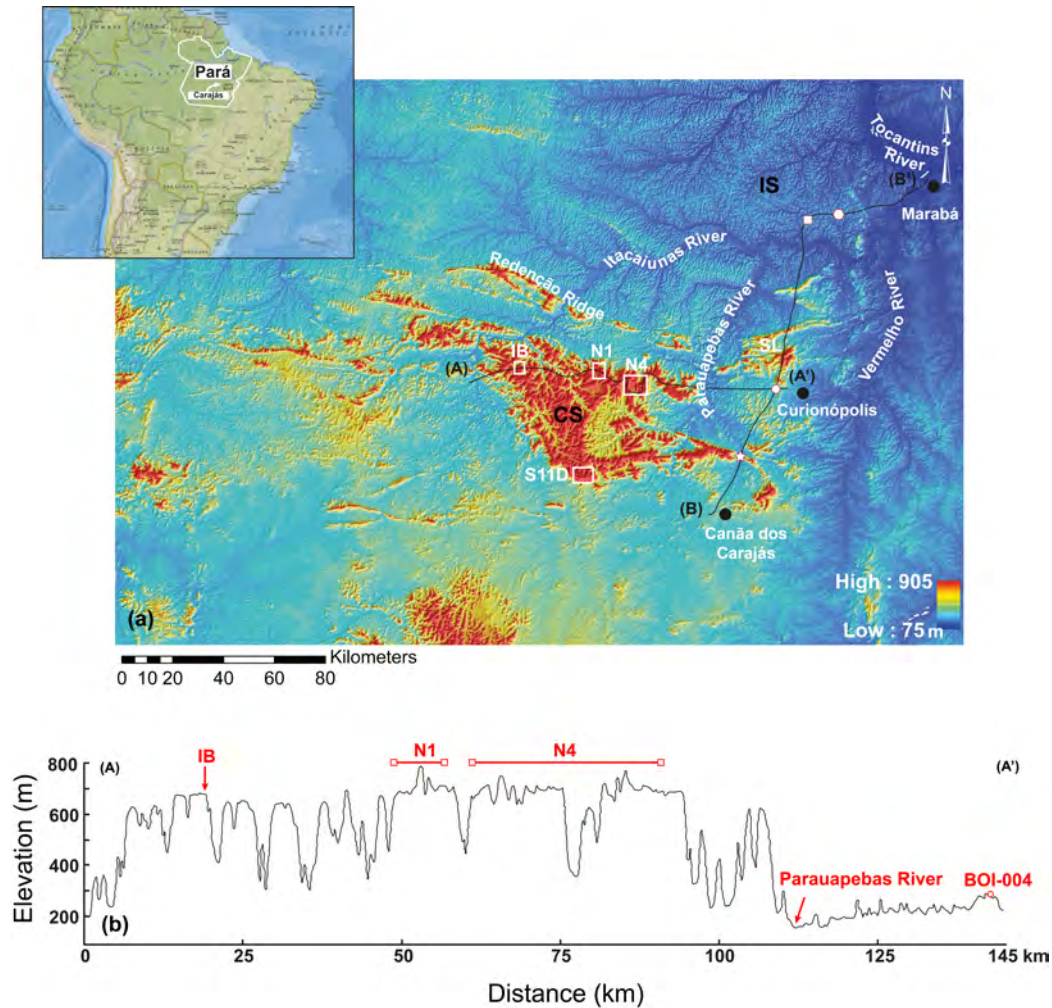


Figure 1: (a) An GMTED2010 image illustrates the stepped landscape of this part of the Amazon region, Pará, Brazil. The highlands of the Carajás Surface (CS) (900-600 m asl) (red in the DEM) contrasts with the surrounding low-lying Itacaiunas Surface (IS) (250-100 m asl). The CS is dissected to the north by the Itacaiunas and Parauapebas rivers and to the east by the Vermelho River. Three sites at the CS (Igarapé Bahia (IB), N1, and S11D) and four localities on the IS (BOI-002, BOI-004, BOI-013, BOI-014) were investigated in this study. A-A' and B-B' identify the Google Earth topographic transects presented in (b) and Figure 4, respectively.

2. GEOLOGY, CLIMATE, AND GEOMORPHOLOGY OF THE CARAJÁS PLATEAUS AND ADJACENT AREAS

The Carajás plateaus are located on the southeastern margin of the Amazon Craton ~ 540 km inland from the mouth of the Amazon River, Pará, Brazil. They comprise Archean granitoid-greenstone units (*Andorinhas Supergroup* [2.9 Ga]; (Docegeo, 1988; Araújo et. al., 1988; Huhn et. al., 1988a, b) and metavolcano and metasedimentary sequences, including banded iron-formations (BIFs) (*Itacaiúnas Supergroup* [2.73-2.84 Ga], (Machado et. al. 1991, Trendall et. al., 1998)) intruded by granitic and ultramafic to mafic magmas of distinct ages (2.76-2.56 Ga alkaline and calc-alkaline granites and mafic dykes; and 1.88 Ga anorogenic granites). The most recent granitic intrusive event in the area occurred ~ 600 Ma during the formation of the Neoproterozoic Araguaia Fold Belt (Grainger et al., 2008). Unpublished $^{40}\text{Ar}/^{39}\text{Ar}$ geochronology reveals the presence of coarse grained mafic dykes ~ 250-200 Ma, suggesting that magmatism persisted in the area until the Mesozoic (Vasconcelos, unpublished results). These results suggest that the area was exhumed after ~ 250-200 Ma.

Climate in Carajás is tropical monsoonal (Am in Köppen-Geiger's classification) with annual rainfall ranging from 1700 to 2800 mm (Alvares et al., 2013), a wet period from December to May and a dry season from June to November. The area is drained by the Itacaiúnas, Parauapebas, and Vermelho rivers and many small creeks that ultimately deliver their water and sediment loads to the Tocantins River, near Marabá (Figure 1). There are no perennial rivers or creeks on the Carajás Surface, but iron-cemented channels drain the plateau surfaces. These iron-cemented channels turn into intermittent creeks flowing torrentially during and immediately after major storms. Rainfall also accumulates in lakes associated with internal collapse basins on the Carajás Surface. Water analysis from natural springs (Bahia, Sumidouro, Bacelar, and Vizinho) draining the Igarapé Bahia plateau are slightly acid (pH = 4.6 to 6.3), show low salinity (TDS = 8.75 – 16.64 mg.L⁻¹), contain low dissolved oxygen loads (2.1 – 8.3 mg.L⁻¹), and very low concentrations of dissolved Ca, Mg, and Fe (0.43-1.62, 0.40-2.40, and <0.2 mg.L⁻¹, respectively). Lush tropical rainforest used to blanket most of the region until the uncontrolled deforestation that started in the 1970s and denuded most of the region turning it into cattle pasture, except for some protected areas (indigenous reservations and national parks, mostly). Tropical rainforest, however, remain in parts of the Carajás Surface, except for areas underlain by BIFs, where iron duricrusts – cangas – host endemic epilithic (“rupestre”) vegetation (Viana et al., 2016 and references therein). Climatic conditions are (at least were until the 1970s) conducive to deep weathering throughout the entire region.

Deep weathering on the Carajás Plateau has resulted in karstic landscapes, particularly over weathered BIFs, where caves form by significant mass loss during leaching of quartz and

carbonates; internal lakes fill collapse basins. The plateaus are thoroughly covered by iron duricrusts, which range in thickness and mineralogical complexity depending on the underlying lithology. In some areas, the duricrust is exposed at the surface (e.g., plateaus blanketing weathered BIFs), while throughout most of the Carajás plateau duricrusts sit below soils and sedimentary layers of variable thicknesses (0-15 m). The duricrust is not horizontal, and local depressions in duricrusts may be filled with sediments containing pebbles and cobbles, suggesting that an ancient paleodrainage once drained the plateaus. This ancient paleodrainage, possibly Mesozoic or Cenozoic, is presently unrecognizable under a thick layer of very fine grained soil (Sombroek, 1966; Klammer, 1971; Truckenbrodt and Kotschoubey, 1981; Lucas, 1989) that attenuates any previous undulation of the Carajás Surface. Late Cenozoic sediments, mostly Quaternary, also fill karstic lakes (Sahoo et al., 2016).

In addition to its geomorphic significance, weathering in the region has a major economic impact. The Itacaiúnas Supergroup hosts Cu-Au (e.g., Igarapé Bahia, Salobo, Sossego) (Figure 2 a, b), Cu-Zn (e.g., Pojuca), Mn (e.g., Azul), and Fe (e.g., N1, N4, N5) mineralization (Figure 3a-c). On top of the Carajás Plateau, mineralized areas are covered by thick (100 to > 500 m) weathering profiles and supergene enrichment blankets, forming classic lateritic Fe (Tolbert et al., 1971), Mn (Coelho and Rodrigues, 1986), Au (Netuno Villas and Santos, 2001), Ni (Alves et al., 1986), and Al (Costa et al., 1997) deposits. These mineralized areas constitute some of the largest open pit mining operations on the planet today, and they offer access to the entire stratigraphy of the deep weathering profiles.

While lateritic ore deposits are common on the Carajás Plateau, they are absent in the surrounding low elevation plains of the Itacaiunas Surface. In these areas, weathering profiles are relatively shallow (commonly < 30 m), and they contain saprolites directly below soils or, locally, ferruginized sediments. The sediments are intermittent, generally < 10 m thick and composed of strongly weathered alternating sand and gravel layers, often capped by a goethite-cemented duricrust (Figure 4). The sediments are afossiliferous and their ages are unknown, but they are interpreted as Cenozoic, and have been informally grouped as the Monte Lopes Formation (cacamedeirosfilho.blogspot.com.au). The low elevation Fe-cemented sediments or bedrocks are identifiable from a distance by their tabular aspect (Figure 4). Iron cementation in these sediments make them potentially datable by the (U-Th)/He method.

Throughout this publication, we will refer to the high elevation (~ 900-600 m) plateaus hosting deeply weathered lateritic profiles as the Carajás Surface (CS) (Figures 1, 2, 3), and the low elevation (~250-100 m,) undulating plains hosting intermittent duricrusts as the Itacaiunas Surface (IS) (Figure 4). We investigated several weathering profiles blanketing both surfaces.

3. SAMPLING AND ANALYTICAL METHODS

The most extensively sampled weathering profile is the Igarapé Bahia (IB) lateritic gold deposit, which was mined from 1989-2002 and produced ~ 110 tons of gold metal. The deposit was first visited and sampled by one of the authors (PV) during the exploration phase in 1988, and visited and sampled yearly until 1993, as open pit operations progressed. The IB deposit was subsequently visited and sampled in 1999, 2002, 2003, 2004, and 2013. In addition to the samples collected from different stages of the open pit mining operations, we collected representative samples from each meter of a suite of drill cores illustrated in Figure 2c. These drill-core samples were crushed, homogenized, and split into representative aliquots, which were further split for mineralogical investigations (sample fragments) and pulped for major and trace element analysis. Additional pure goethite from selected depths were sampled for petrographic analysis, mineralogical investigation, and geochronology. A total of > 900 individual samples from the IB profile were available for this investigation. But only a limited number of these samples could undergo geochronological analysis.

The N1 iron plateau was also sampled in 1988-1993, 1999, 2002, 2003, and 2013. The main samples used for this investigation were collected along NW-SE traverses on the plateau (Figure 3d). The plateau surface itself is not flat along our traverse, ranging from ~ 780 m in the NW to about ~ 650 m in the SE. Several karstic lakes along the traverse provided samples for mineralogical, geochronological, and geomicrobiological investigation. The sampling exercise at the N1 plateau focused solely on surface samples. Similarly, a N-S traverse along the S11D plateau provided the few samples from Serra Sul investigated here (Figure 1).

The samples from the dissected plains and rolling hills between Carajás and the Tocantins river (Figure 1) were collected along a traverse from Carajás to Marabá, when four sites were targeted: a ferruginized low elevation duricrust near Canaã dos Carajás (Figures 1, 4a, b); a duricrust along the state highway PA275, near Curionópolis (Figures 1, 4a, c); and two ferruginized sedimentary deposits near Marabá (Figures 1, 4a, d).

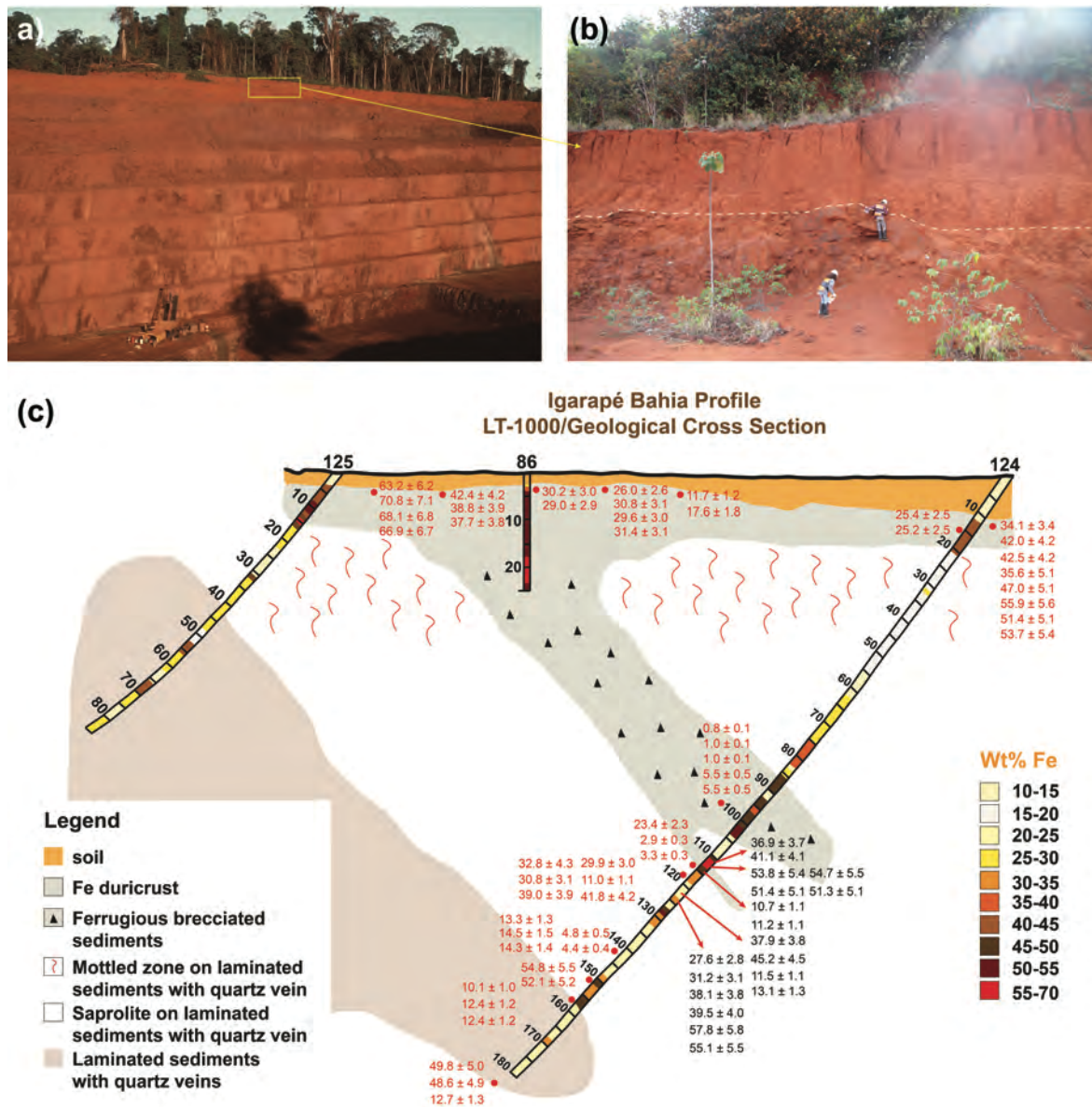


Figure 2: Deep weathering profiles underlay the Carajás Plateau. At Igarapé Bahia (IB), (a) the 150 m thick weathering profile is covered by a ~ 0-15 m thick soil layer. (b) A duricrust delimits the contact (dashed line) between goethite-gibbsite-quartz-rich soils and sediments and the underlying mottled zone and gossan. (c) Major element analyses of drill core samples from the IB profile reveal that Fe is preferentially enriched within the duricrust and gossans. (U-Th)/He ages obtained for goethites selected from 5 drill cores are presented in (c). Ages obtained for core F124 are in black, while ages of goethites from adjacent drill holes (not in the plane of this cross section) are in red. Goethites from the duricrust and saprolite are commonly older than 30 Ma, while younger goethite generations (He ages < 5 Ma) were only found at great depths. The results imply that the weathering profile had already reached its currently depths at ~ 60 Ma.

3.1. Optical and scanning electron microscopy

Mineralogical investigation followed procedures outlined in Monteiro et al. (2014). Polished thin-sections and grain mounts were investigated to determine mineralogy, texture, paragenesis, and modes of goethite precipitation (e.g., pseudomorphic replacement, pore space fill, empty cavity precipitation). We paid particular attention to the identification of potential primary mineral contaminants within goethite.

3.2. X-ray diffraction

Hundreds of aliquots from each sample were powdered using an agate mortar and pestle. Powder XRD was performed in a Bruker D8 Advance X-ray diffractometer equipped with either a Cu- (1.5405 Å) or a Co-source (1.7889 Å) operated at 40 kV and 40 mA. Scans were collected from 5° to 90° 2θ at 0.02° intervals.

3.3. Electron microprobe analysis (EMPA)

Electron microprobe analyses of mounts of visually pure grains (similar to ones selected for geochronology) were performed with a JEOL JXA-8200 EPMA at the Centre for Microscopy and Microanalysis (CMM) of the University of Queensland, Brisbane, Australia. All runs were performed using a beam current of 15 nA, accelerating voltage of 15 kV, and highly focused spot sizes (except for Na, K, Ca, and S, for which spot size = 10 μm). Samples and standards were carbon coated together before EPMA sessions. During sample analysis, some spots were programed on mineral standards to ascertain the accuracy of the results. Between 14 and 21 elements were measured in each individual analytical session using the following standards and calculated detection limits: **O** (fayalite ORNL-263 std.; 601-255 ppm), **Na** (Cazadero albite std.; 293-138 ppm), **Mg** (diopside Checterman-358 std.; 133-83 ppm), **Al** (Al₂O₃-913 std.; 91-64 ppm), **Si** (fayalite ORNL-263 std.; 124-90 ppm); **P** (Cl-apatite synthetic-283 std.; 220-130 ppm), **S** (chalcopyrite UC-1232 std.; 149-75 ppm), **K** (orthoclase MAD10-374 std.; 146-98 ppm), **Ca** (diopside Checterman-358 std.; 494-140 ppm), **Ti** (TiO₂-922 std.; 506-251 ppm), **V** (V₂O₃-923 std.; 758-212 ppm), **Cr** (Cr metal-524 std.; 730-174 ppm), **Mn** (MnO-925 std.; 373-168 ppm); **Fe** (fayalite ORNL-263 std.; 416-198 ppm), **Co** (CoO-927 std.; 397-178 ppm), **Ni** (NiO-928 std.; 452-202 ppm), **Cu** (Cu metal-529 std.; 517-241 ppm), **Zn** (ZnO-930 std.; 646-306 ppm), **Pb** (galena UC-7400 std.; 656-324 ppm), **Ba** (barite std.; 555-368 ppm), and **Sr** (Sr titanite std.; 287-285 ppm).

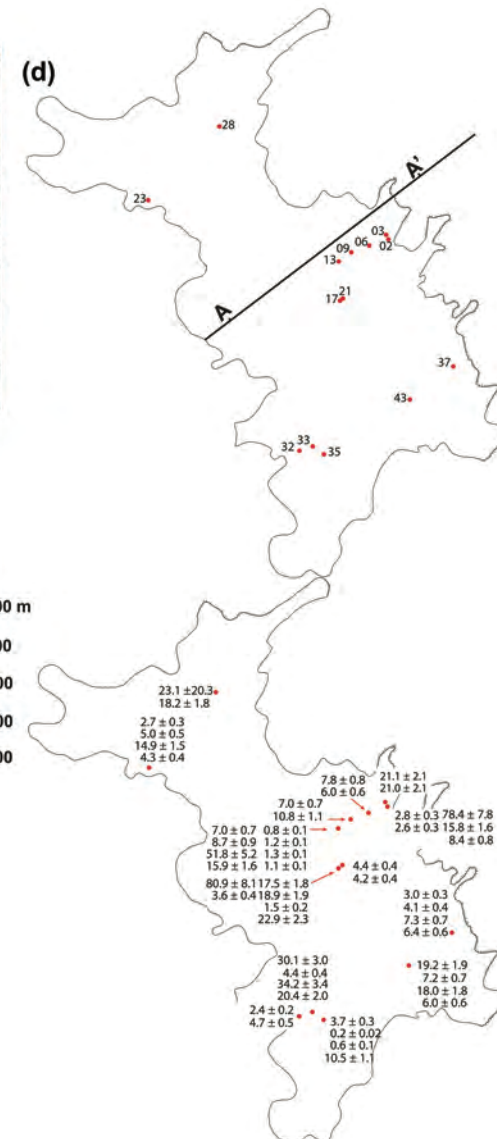
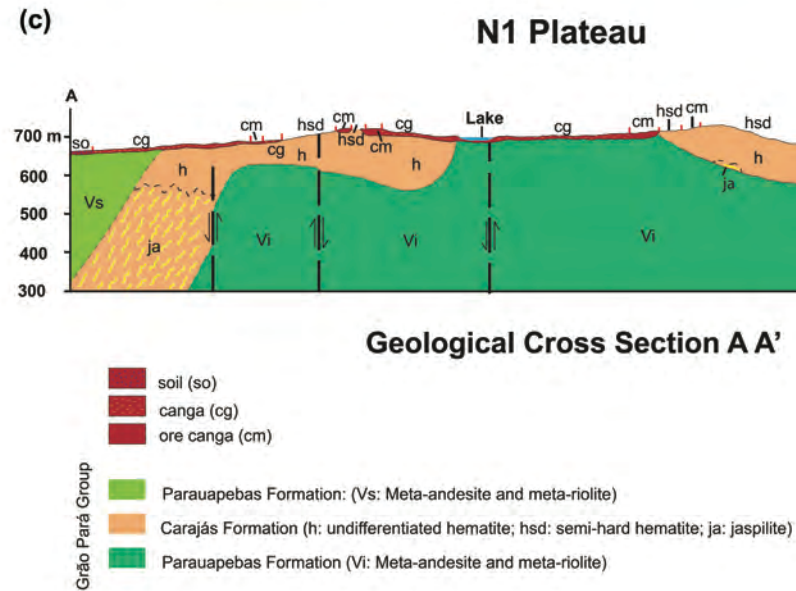
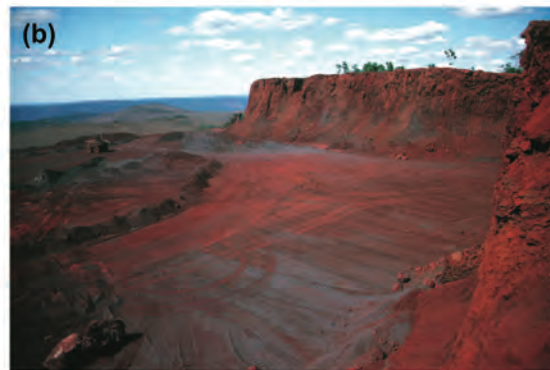


Figure 3: (a, b) Deep weathering profiles developed on BIFs are also found in the N1, N4, N5, and S11D plateaus. (c) The plateaus are blanketed by a thick canga that varies in composition depending on the rocks underneath [BIF or volcanic units] (Rezende and Barbosa, 1972). (d) Samples for geochronology and cosmogenic studies were collected at the surface along NE-SW transects. There is no clear pattern in the distribution of ages on the plateau surface, a direct effect of biogeochemical processes driving iron dissolution-cementation in these crusts.

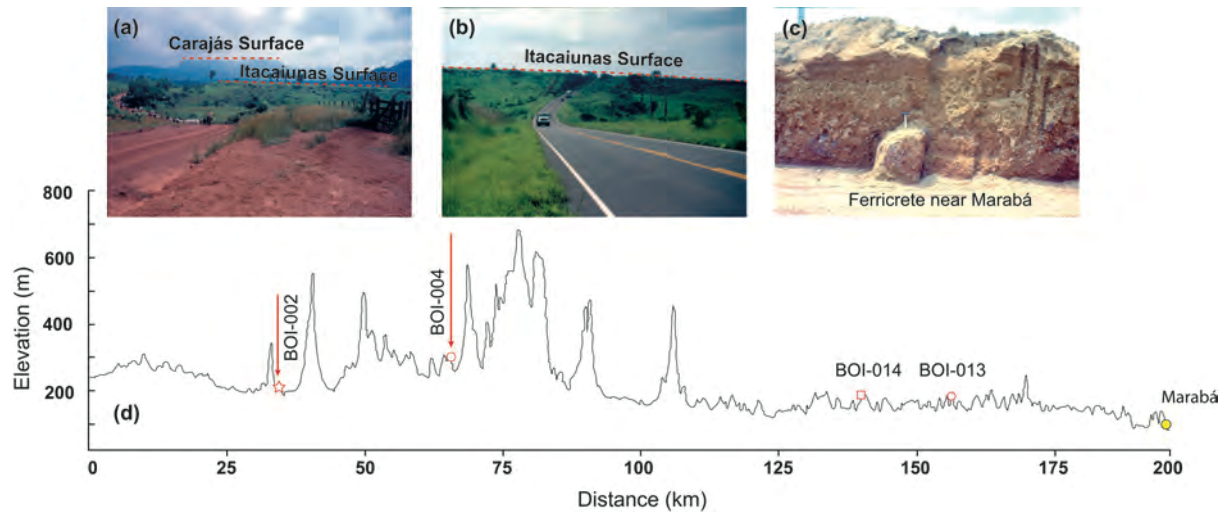


Figure 4: (a) Field photo showing the topographic positions of the Carajás (background) and the Itacaiunas Surfaces (foreground) near the city of Canãa dos Carajás. (b) Basement rocks and Cenozoic continental sediments (Monte Lopes Formation) are overlain by shallow weathering profiles covered by an iron-cemented duricrust. This indurated, ferruginous horizon forms small and discontinuous plateaus at 200-285 m elevation widely distributed throughout the Itacaiunas Surface (c, d).

3.4. (U-Th)/He geochronology and $^4\text{He}/^3\text{He}$

Goethite grains for (U-Th)/He geochronology were selected, photographed, encapsulated, and analyzed following procedures outlined in Monteiro et al. (2014). Helium extractions were performed by heating encapsulated goethite with a diode laser at 900 °C for 6 minutes. Cleaned gas was spiked with pure ^3He , calibrated against ^4He standard, and analyzed in a Pfeiffer Prisma quadrupole mass spectrometer. A second extract was performed for all samples to ensure complete degassing.

After helium extraction, degassed goethite grains were transferred to Teflon vials and pipetted with 100 μl of concentrated SeastarTM HCl solution and 25 μl of spike solution (containing known amounts of ^{235}U and ^{230}Th). Closed vials were placed in the oven at 90 °C overnight. The solutions were allowed to evaporate completely in a hot plate at 95 °C. 50 μl of concentrated SeastarTM HNO₃ was added to each Teflon container to dissolve the golden salt accumulated at the bottom. 1000 μl of Milli-Q water was added to the Teflon beakers and the diluted solutions were decanted into a 1.5 ml ICP-MS cup. Measurements of U and Th were carried in an Agilent 8800 ICP-MS in the Environmental Analysis Center, Caltech, USA.

Three samples from the IB profile were also investigated by the $^4\text{He}/^3\text{He}$ method (Shuster et al., 2005; Monteiro et al., 2017b). Goethite grains selected for $^4\text{He}/^3\text{He}$ experiments were proton irradiated at the Harvard Cyclotron as outlined in Shuster et al. (2003). Helium extraction by incremental heating is described in Monteiro et al. (2017b).

3.5. Cosmogenic ^3He

Samples for ^3He measurements were prepared in two ways: (1) crushing hematite fragments extracted from duricrusts, and (2) micro-drilling loose pebbles of hematite scattered on plateau surfaces. Canga fragments and drill-cores were crushed, sieved, ultrasonicated in distilled water, absolute ethanol or acetone, and air-dried. For the micro-drilled samples, magnetic separation was used to isolate magnetic from non-magnetic fractions. Approximately 15 mg of sample were loaded into Sn foil packets and degassed at 1200 °C in a resistance furnace. Re-heating to 1200°C was performed to assure complete gas extraction. Analytical procedures are described elsewhere (Patterson and Farley, 1998; Amidon and Farley, 2011).

To calculate apparent exposure ages for each sample, we used a sea level high latitude ^3He production rate of 68.1 ± 8.1 atoms $\text{g}^{-1} \text{yr}^{-1}$ for hematite (Shuster et al., 2012) corrected for latitude and elevation following procedures outlined in Stone (2000). We cast the same results in terms of erosion rates by using an average density of 2.88 g/cm^3 (Santos, 2006) for duricrusts, and calculate erosion rates (\dot{e} in $\text{g/cm}^2/\text{yr}$) as $\dot{e} = P\Lambda/N$, where P is the production rate (atoms/g/yr); Λ is an attenuation length scale (160 g/cm^2); and N is the nuclide concentration (atom/g) measured at the surface (Lal, 1991). Hematite grains may contain areas partially recrystallized to goethite, which potentially results in partial ^3He loss. Therefore, we interpret all results as minimum values and refer to all results as apparent exposure ages (*aEA*).

4. RESULTS

4.1. Microscopy

The purest and most crystalline goethites (Figure 5a,b) occur in the Igarapé Bahia gossan. Goethite often occur in association with other supergene phases (e.g., Mn oxides, cuprite, native Cu, supergene gold) but are devoid of relict hypogene contaminants, making them ideally suited for geochronology. In contrast, goethites from the duricrust reveal complex textures (Figure 5c) where several generations of intergrown goethites occur intermixed with gibbsite, anatase, rutile, hematite, tourmaline, and clay minerals.

Similarly, vitreous goethites cementing N1 plateau duricrusts are Al-rich (Figure 5d) and often contain relict primary hematite, quartz, ilmenite, and rutile (Figure 5e). Goethite also occurs as

pisoliths cemented by a mixture of poorly crystallized porous yellow goethite and gibbsite. Goethite comprising ferruginized organic material (e.g., plant roots) (Figure 5f) and microbial mats (Levett et al., 2016) occurs in these samples.

Goethite cementing sediments and duricrusts from the Itacaiunas Surface are porous, less crystalline and host significant amounts of kaolinite, quartz, and hematite (Figure 5g-i).

4.2. Mineralogy

X-ray diffraction patterns reveal that goethite varies in crystallinity and purity, depending on underlying lithology, mode of precipitation, and proximity to the surface. Goethites from the gossans at the Igarapé Bahia deposit are purest and most crystalline, where mm to cm-wide goethite bands alternate with μm to mm bands of cryptomelane, or contain minor inclusions of cuprite and native Cu and Au. In contrast, goethites from the duricrust contain goethite, hematite, gibbsite, kaolinite, and minor anatase. Goethites from the N1 plateau host minor hematite, gibbsite, quartz, lepidocrocite, and anatase. Finally, duricrust samples from the Itacaiunas Surface contain goethite partially contaminated with minor quartz, hematite, and kaolinite.

Broadening of the main goethite peaks in X-ray diffraction patterns reveals distinct goethite crystallinities. For most goethites, except IBH-13-09h, there is a strong correlation between decrease in crystallinity and increase in Al contents ($R^2 = 0.83$).

4.3. Goethite composition

Most goethites investigated here are not stoichiometric FeOOH but contain a significant amount of minor and trace elements (Al+Si+Mn+Cu+V+Co+Cr+Ni+Ti+Zn+Pb) substituting for iron (Figures 6, 7). Electron microprobe analyses showing low totals (< 90 wt%) correspond to analyses of porous goethite, while high totals (100-104 wt%) are associated with the analysis of grain interfaces in contaminated goethite cements (Maaskant and Kaper, 1991). Minor and trace element contents vary inversely with Fe-contents, and the nature and amount of trace elements are distinct for the three types of weathering profiles investigated (Figure 7). Igarapé Bahia goethites are the most complex, hosting significant amounts of Al, Mn, and Cu and low Si and P contents. Goethites from the N1 profile and from the four sites on the Itacaiunas Surface contain large amounts of Al and Si. The N1 goethites also contain significant Ti, suggesting contamination with ilmenite or rutile (now weathered to anatase) inherited from the underlying volcanic units (Fig. 3c). Itacaiunas Surface goethites also contain some Ti (Figure 7c), suggesting contamination by detrital ilmenite or rutile.

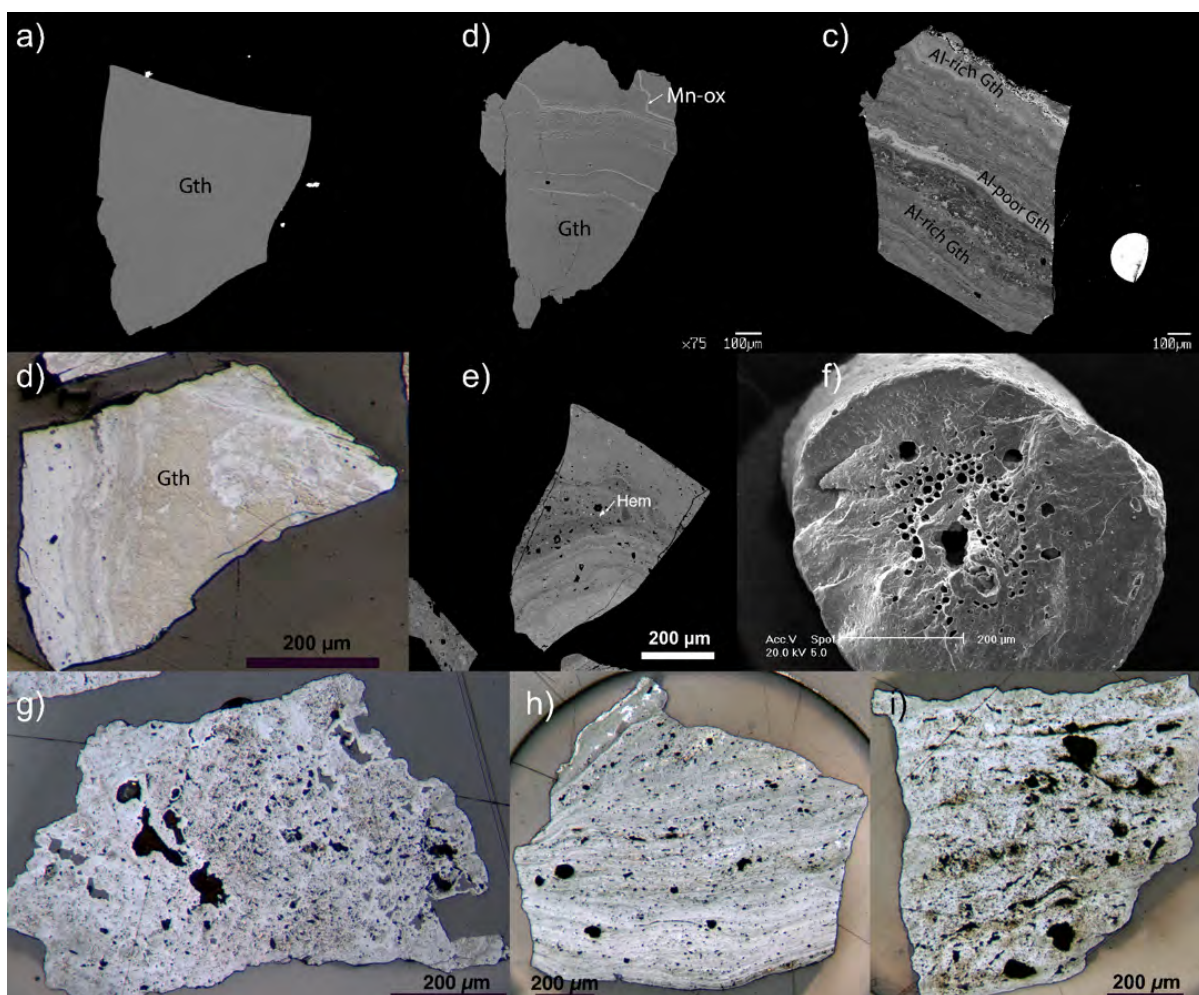


Figure 5: Photomicrographs of representative goethite grains from the IB, N1, and Itacaiunas Surface weathering profiles. (a) At the IB profile, pure colloform goethite occurs throughout the profile, particularly below the duricrust. This type of goethite is commonly devoid of contaminants and ideal for geochronology. **(b)** Pure, botryoidal goethite may also coexist with other supergene phases (e.g., Mn-oxides). **(c)** Goethites from the duricrust occur as complex layers of Al-rich and Al-poor goethites, intergrown with hematite and cementing gibbsite-rich pisoliths. They usually contain relict primary minerals. **(d)** The coexistence of multiple goethite generations reveals the very dynamic nature of goethite cements in cangas of the N1 plateau. **(e)** Primary mineral (arrow), possibly containing significant amounts of ^4He , survives weathering and are incorporated within goethite masses. Degassing of goethites at temperatures above 900°C will release ^4He from these relic phases and generate discrepant ages. **(f)** During iron cementation, goethite replaces root fragment in the duricrust. **(g-i)** Typical goethite cements in sediments from the Itacaiunas Surface. They are usually less crystalline and impure.

Goethite compositions are strongly dependent on mechanisms of precipitation and depth within the profile. At the IB deposit, goethites precipitated in the duricrust are usually enriched in Al, while those precipitated at depth are commonly depleted in Al (< 1 wt%). Mn and Cu-concentrations are high for goethites precipitated at depth (2-7 wt% Mn, 2-5 wt% Cu), suggesting effective leaching of these elements from the upper parts of the profile and their enrichment at depth (EA1). In addition to Mn and Cu, P also becomes significantly enriched in goethites precipitated at depth (1.5-3.2 wt% P).

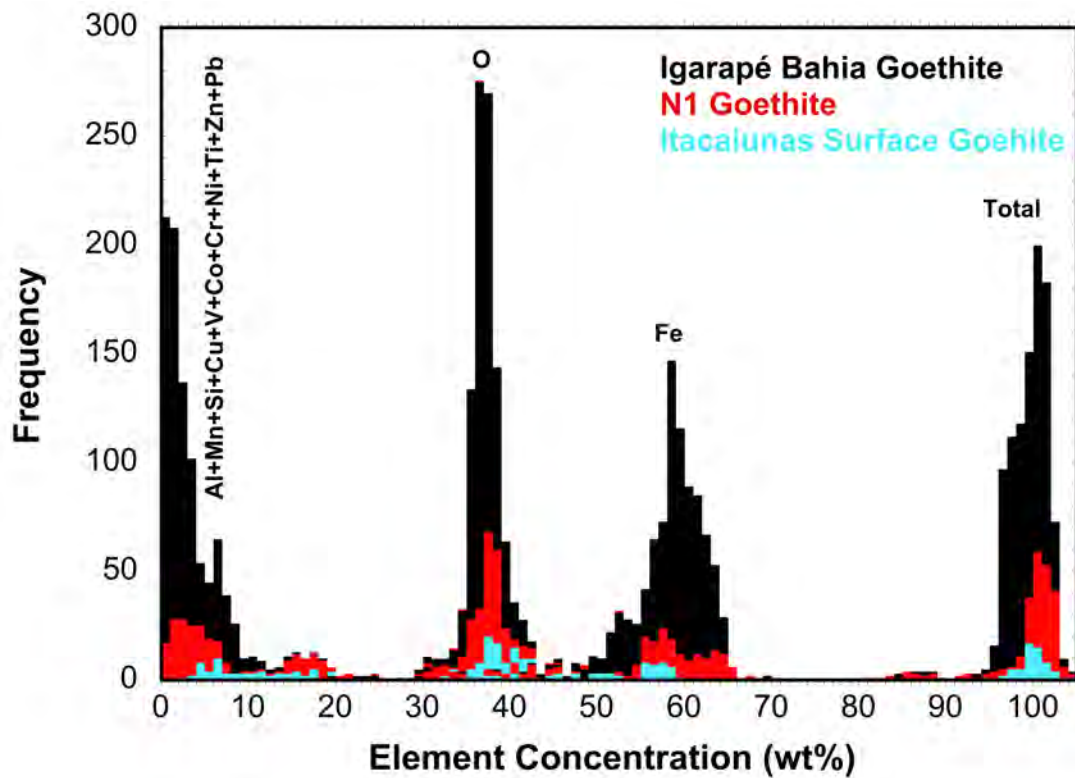


Figure 6: Electron microprobe analysis (1003 spots) for the Fe-oxyhydroxides investigated reveal that most goethites show some degree of elemental substitution. For example, well-crystallized IB goethites may incorporate high concentrations of Mn, Cu, and P (EA1). N1 goethites show large Al contents, while all Itacaiunas Surface goethites significant Al and Si contents.

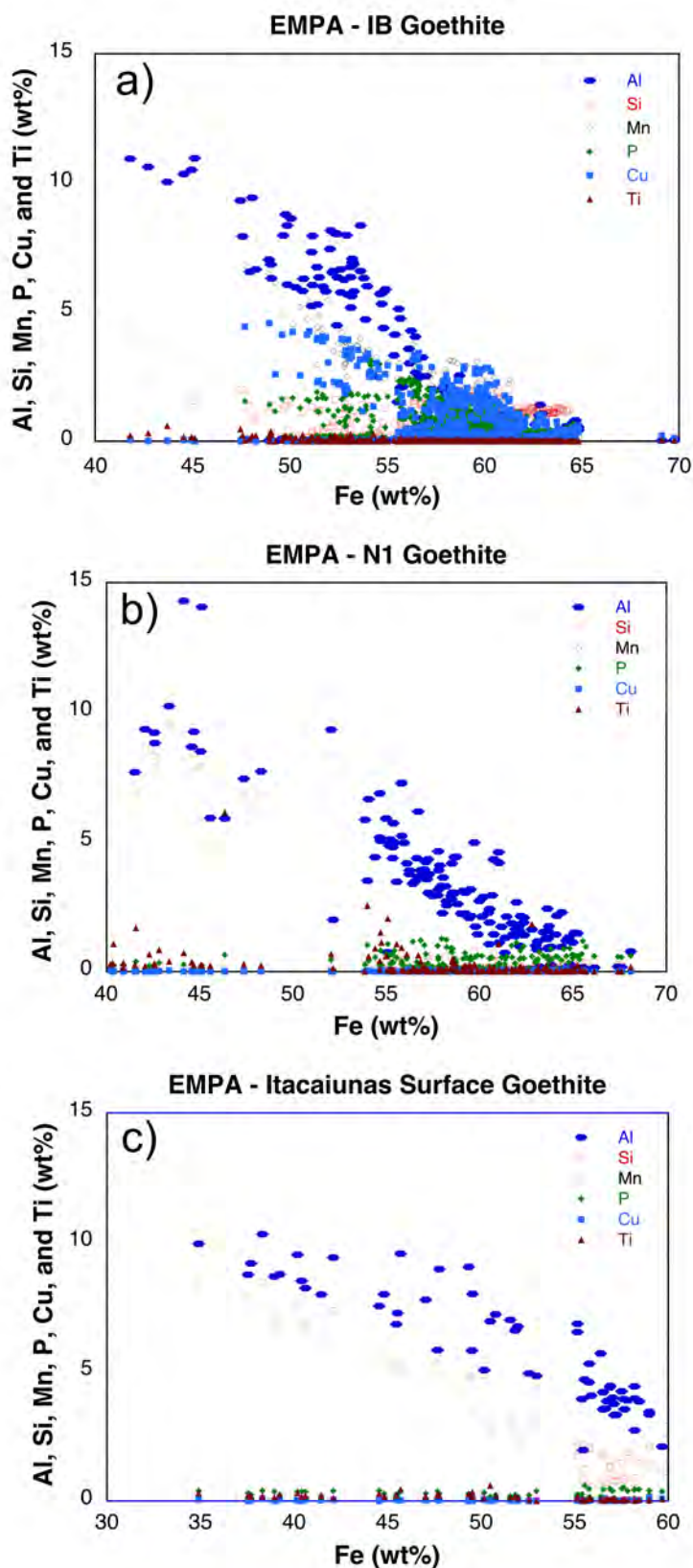


Figure 7: Correlation diagrams for the elemental contents of goethite cements, as determined by EMPA, for the three distinct sites (IB, N1, and IS) illustrates goethite's propensity to reflect the composition of the underlying bedrock, as discussed in the text.

4.4. (U-Th)/He geochronology

Table 1 lists U, Th, and ^4He contents and (U-Th)/He precipitation ages (*pAs*) for goethites from the IB, N1, and Itacaiunas Surface sites. Age distributions for these sites are illustrated in Figure 8. [U], [Th], and [He] concentrations vary from 1.5 to 1640 ppm [U], 0 to 109 ppm [Th], and 0.04 to 336 nmol/g [He] for the IB profile; from 0.05 to 35 ppm [U], 0.2 to 232 ppm [Th], and 0.001 to 6.6 nmol/g [He] for the N1 plateau; and from 3 to 24 ppm [U], 2.5 to 59 ppm [Th], and 0.1 to 1.1 nmol/g [He] for the Itacaiunas Surface. Th/U ratios range between 0 - 5.4 (usually < 1 ; 80 out of 107) for the IB, 0.5 - 12.7 (~ 5 on average) for the N1P, and 0.8 - 6.7 (~ 3 on average) for the Itacaiunas Surface. The oldest (U-Th)/He results (~ 80 -70 Ma) were obtained for the IB and N1 sites. (U-Th)/He ages for the four sites on the Itacaiunas Surface vary from 7.5 ± 0.8 to 9.4 ± 0.9 Ma for site BOI 014, 7.4 ± 0.8 to 8.5 ± 0.8 Ma for site BOI 013, 2.0 ± 0.2 to 4.3 ± 0.4 Ma for site BOI 002, and 0.5 ± 0.1 to 1.3 ± 0.1 Ma for site BOI 004. Replicate (U-Th)/He analyses of IB and Itacaiunas Surface goethites usually yield reproducible results, while ages obtained for replicates of N1 goethites show large variability (Table 1).

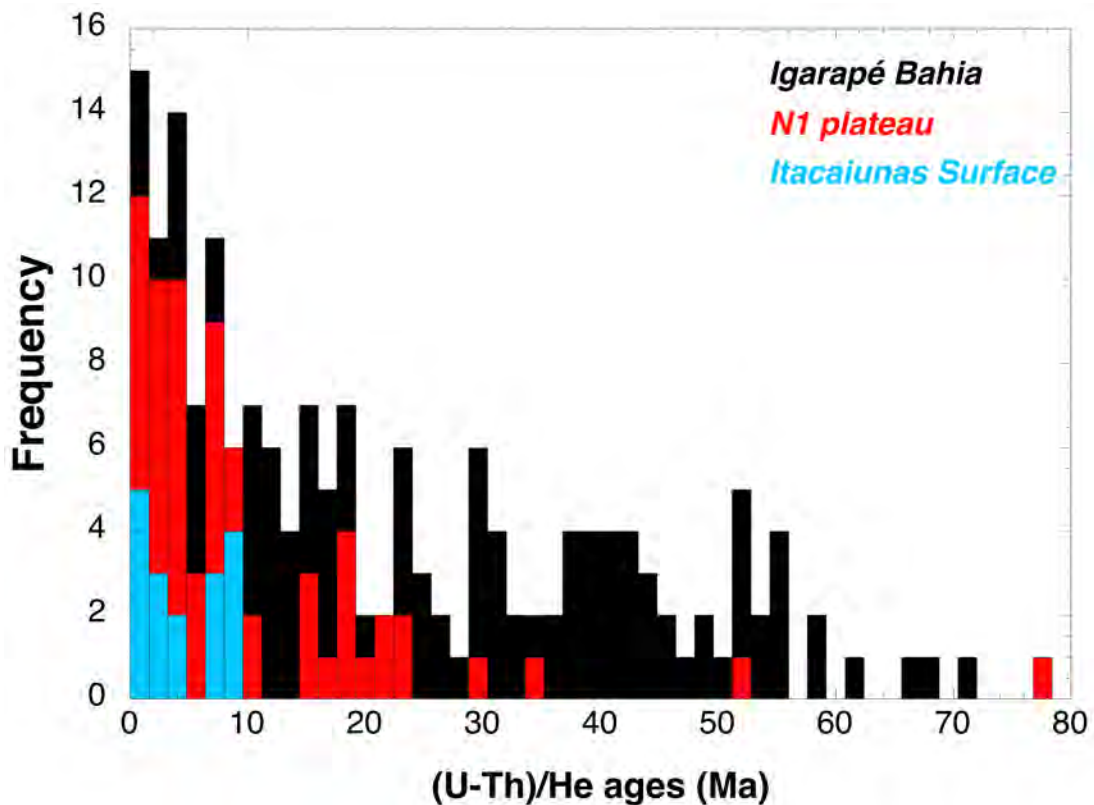


Figure 8: The distribution of (U-Th)/He ages shows the large discrepancy between the older results obtained for goethites from the IB and N1 sites (as old as ~ 80 Ma) and the < 10 Ma results obtained for all four sites on the Itacaiunas Surface.

Table 1: U, Th, He contents and (U-Th)/He ages for goethites from the different weathering profiles in the Carajás region, Brazil

Site	Sample Name	Calculated Age (Ma)	$\pm 1\sigma$ (Ma)	Age + 10% (Ma)	$\pm 10\%$ (Ma)	U (ppm)	$\pm 1\sigma$ (ppm)	Th (ppm)	$\pm 1\sigma$ (ppm)	He (nmol/g)	$\pm 1\sigma$ (nmol/g)	Th/U
Igarapé Bahia	B-93-01	56.6	1.1	62.3	6.2	27.91	0.10	0.00	0.02	8.64	0.40	0.000
	B-93-01	64.3	1.3	70.8	7.1	8.46	0.04	0.01	0.01	2.98	0.23	0.001
	BA-P010-surface	61.9	1.3	68.1	6.8	123.19	0.45	0.13	0.01	41.74	3.51	0.001
	BA-P010-surface	60.8	1.2	66.9	6.7	111.34	0.39	0.10	0.03	37.02	1.13	0.001
	BAH 3 cml 7 3 bottom layers	14.0	0.3	15.5	1.5	141.69	0.51	0.02	0.02	10.83	0.48	0.000
	BAH 3 cml 7 3 bottom layers	13.2	0.3	14.5	1.5	153.01	0.55	0.03	0.02	10.98	0.50	0.000
	BAH 3 cml 7 3 bottom layers	12.3	0.3	13.6	1.4	117.61	0.42	0.01	0.01	7.90	0.44	0.000
	BAH 3 cml 7 3 bottom layers	10.1	0.2	11.1	1.1	176.01	0.63	0.10	0.03	9.70	0.24	0.001
	BAH 3 cml 7 3 bottom layers	10.3	0.2	11.4	1.1	117.50	0.42	0.04	0.01	6.60	0.37	0.000
	BAH 3 cml 7 3 bottom layers	14.9	0.3	16.4	1.6	99.30	0.35	0.19	0.02	8.04	0.30	0.002
	BAH 3 cml 7 large goethite layer	15.4	0.3	16.9	1.7	75.35	0.27	0.05	0.02	6.30	0.22	0.001
	BAH 3 cml 7 large goethite layer	14.2	0.3	15.6	1.6	81.71	0.29	0.06	0.02	6.31	0.25	0.001
	BAH-03 cml 6 LT100_black	4.3	0.1	4.8	0.5	135.48	0.49	0.03	0.02	3.18	0.17	0.000
	BAH-03 cml 6 LT100_black	4.3	0.1	4.7	0.5	126.22	0.45	0.00	-0.03	2.96	0.10	0.000
	BAH-03 cml 6 LT100_brown	7.0	0.1	7.7	0.8	52.99	0.19	-0.01	-0.03	2.02	0.06	0.000
	BAH-03 cml 6 LT100_brown	7.0	0.1	7.8	0.8	38.33	0.13	0.02	0.04	1.47	0.04	0.001
	BAH-100_black	31.0	0.6	34.1	3.4	1133.15	4.98	0.08	0.01	191.61	12.56	0.000
	BAH-100_black	38.2	0.8	42.0	4.2	311.65	1.28	0.04	0.01	64.92	7.83	0.000
	BAH-100_black	38.7	0.8	42.5	4.3	401.41	1.70	0.13	0.01	84.64	10.60	0.000
	BAH-100_black gt	32.4	0.7	35.6	3.6	1640.39	7.17	0.42	0.03	289.69	10.23	0.000
	BAH-100_black gt	42.7	0.9	47.0	4.7	1439.42	6.22	0.22	0.02	335.61	12.03	0.000
	BAH-100_brown gt	50.8	1.0	55.9	5.6	351.77	1.29	0.15	0.03	97.71	2.53	0.000
	BAH-100_brown gt	46.7	1.0	51.4	5.1	368.53	1.42	0.16	0.02	94.00	4.39	0.000
	BAH-100_brown gt	48.9	1.0	53.7	5.4	431.10	1.73	0.10	0.01	115.01	6.81	0.000
	BAH-99-01 gr1	23.5	0.5	25.9	2.6	111.59	0.39	0.07	0.04	14.30	0.25	0.001
	BAH-99-01 gr2	18.5	0.4	20.3	2.0	83.29	0.29	0.01	0.02	8.37	0.29	0.000
	BAH-99-01 gr3	26.4	0.5	29.0	2.9	70.57	0.25	0.06	0.03	10.13	0.26	0.001
	BAH-F115-15-16G	23.1	0.5	25.4	2.5	162.94	0.61	0.19	0.01	20.47	1.36	0.001
	BAH-F115-15-16G	22.9	0.5	25.2	2.5	160.24	0.57	0.09	0.03	19.96	0.48	0.001
	BAH-F124-111.2B	33.6	0.7	36.9	3.7	187.00	0.68	0.03	0.02	34.24	1.25	0.000
	BAH-F124-111.2B	37.3	0.8	41.1	4.1	130.93	0.47	0.02	0.01	26.65	1.26	0.000
	BAH-F124-112	48.9	1.0	53.8	5.4	38.80	0.14	-0.04	-0.02	10.36	0.49	-0.001
	BAH-F124-112	46.7	0.9	51.4	5.1	57.10	0.20	-0.06	-0.02	14.57	0.61	-0.001
	BAH-F124-112	49.8	1.0	54.7	5.5	35.90	0.13	0.00	-0.01	9.76	0.70	0.000
	BAH-F124-112	46.6	0.9	51.3	5.1	69.65	0.25	0.24	0.02	17.73	0.94	0.003
	BAH-F124-114	9.8	0.2	10.7	1.1	295.67	1.10	0.04	0.02	15.67	0.62	0.000
	BAH-F124-114	10.2	0.2	11.2	1.1	272.69	1.01	0.02	0.02	15.08	0.54	0.000
	BAH-F124-123.1 (black)	34.5	0.7	37.9	3.8	86.36	0.31	0.00	-0.02	16.24	0.88	0.000
	BAH-F124-123.1 (black)	41.1	0.8	45.2	4.5	94.40	0.34	-0.02	-0.01	21.18	2.21	0.000
	BAH-F124-123.1 (sparkling)	10.4	0.2	11.5	1.1	27.13	0.10	-0.03	-0.01	1.54	0.13	-0.001
	BAH-F124-123.1 (sparkling)	11.9	0.2	13.1	1.3	20.45	0.07	-0.03	-0.02	1.32	0.07	-0.001
	BAH-F124-123.2 (weird gt)	25.1	0.5	27.6	2.8	32.09	0.11	-0.03	-0.01	4.38	0.33	-0.001
	BAH-F124-123.2 (weird gt)	28.3	0.6	31.2	3.1	18.45	0.06	-0.01	-0.01	2.85	0.23	-0.001
	BAH-F124-123.2 (black)	34.6	0.7	38.1	3.8	128.83	0.46	-0.06	-0.02	24.30	1.21	0.000
	BAH-F124-123.2 (black)	35.9	0.7	39.5	4.0	145.27	0.53	0.02	0.01	28.47	2.19	0.000
	BAH-F124-123.7	52.6	1.1	57.8	5.8	211.21	0.78	0.01	0.01	60.64	3.79	0.000
	BAH-F124-123.7	50.1	1.0	55.1	5.5	174.04	0.64	0.03	0.01	47.59	3.40	0.000
	BAH-F177-115	2.7	0.1	2.9	0.3	187.30	0.71	0.02	0.01	2.70	0.27	0.000
	BAH-F177-115	3.0	0.1	3.3	0.3	173.76	0.64	0.02	0.01	2.87	0.21	0.000
	BAH-F177-115 (brown)	21.3	0.4	23.4	2.3	33.40	0.12	0.56	0.04	3.89	0.12	0.017
	BAH-F226-142.7_black	4.4	0.1	4.8	0.5	119.16	0.43	0.01	0.01	2.83	0.19	0.000
	BAH-F226-142.7_black	4.0	0.1	4.4	0.4	108.00	0.38	0.04	0.02	2.33	0.12	0.000
	BAH-F226-142.7_brown	12.1	0.2	13.3	1.3	58.22	0.20	0.07	0.02	3.82	0.15	0.001
	BAH-F226-142.7_brown	13.2	0.3	14.5	1.5	62.65	0.22	0.08	0.01	4.50	0.37	0.001
	BAH-F226-142.7_sparkling	13.0	0.3	14.3	1.4	38.58	0.14	0.00	0.01	2.73	0.24	0.000
	BAH-F226-152.67	49.8	1.0	54.8	5.5	82.65	0.32	0.03	0.00	22.47	3.21	0.000
	BAH-F226-152.67	47.4	1.0	52.1	5.2	85.94	0.33	0.09	0.00	22.24	3.20	0.001
	BAH-F226-157.6_black	9.1	0.2	10.1	1.0	99.15	0.35	0.03	0.02	4.93	0.23	0.000

Table 1: U, Th, He contents and (U-Th)/He ages for goethites from the different weathering profiles in the Carajás region, Brazil

Site	Sample Name	Calculated Age (Ma)	$\pm 1\sigma$ (Ma)	Age + 10% (Ma)	$\pm 10\%$ (Ma)	U (ppm)	$\pm 1\sigma$ (ppm)	Th (ppm)	$\pm 1\sigma$ (ppm)	He (nmol/g)	$\pm 1\sigma$ (nmol/g)	Th/U
Igarapé Bahia	BAH-F226-157.6_brown	11.3	0.2	12.4	1.2	49.80	0.18	0.01	0.02	3.06	0.15	0.000
	BAH-F226-157.6_brown	11.2	0.2	12.4	1.2	41.86	0.15	0.86	0.03	2.57	0.11	0.020
	BAH-F226-182.2_stalagmite	74.9	2.3	82.3	8.2	3.51	0.08	0.04	0.05	1.44	0.03	0.012
	BAH-F226-182.2_stalagmite	22.1	0.5	24.3	2.4	10.21	0.06	0.03	0.02	1.23	0.06	0.003
	BAH-F226-182.2_stalagmite	4.4	0.1	4.9	0.5	1.52	0.03	0.09	0.01	0.04	0.00	0.060
	BAH-F226-186.8 (dark grey)	45.3	0.9	49.8	5.0	585.80	2.29	7.60	0.12	145.26	6.33	0.013
	BAH-F226-186.8 (dark grey)	44.2	0.9	48.6	4.9	710.66	2.78	4.48	0.09	171.64	6.25	0.006
	BAH-F226-186.8	11.6	0.2	12.7	1.3	44.17	0.16	1.29	0.03	2.80	0.23	0.029
	BAH-F226-193.5	30.1	0.6	33.1	3.3	48.41	0.17	0.65	0.02	7.97	0.58	0.013
	BAH-F226-193.5	21.0	0.4	23.1	2.3	10.74	0.04	-0.01	-0.01	1.23	0.09	-0.001
	BAH-F282-118.2_black	27.2	0.6	29.9	3.0	39.34	0.14	-0.01	-0.01	5.83	0.67	0.000
	BAH-F282-118.2_black	10.0	0.2	11.0	1.1	21.41	0.08	-0.02	-0.01	1.16	0.10	-0.001
	BAH-F282-118.2_brown	38.0	0.8	41.8	4.2	72.84	0.26	-0.04	-0.01	15.08	1.21	-0.001
	BAH-F282-118.2_brown	29.8	0.6	32.8	3.3	58.84	0.21	-0.01	-0.01	9.56	1.61	0.000
	BAH-F282-118.4_brown	28.0	0.6	30.8	3.1	75.43	0.27	0.02	0.01	11.52	0.57	0.000
	BAH-F282-118.4_brown	35.4	0.7	39.0	3.9	108.36	0.40	0.02	0.01	20.93	1.72	0.000
	BAH-F282-118.4_brown&black	17.1	0.3	18.8	1.9	164.75	0.60	0.05	0.01	15.32	0.94	0.000
	BAH-F282-118.4_black	32.4	0.7	35.6	3.6	98.85	0.36	0.02	0.01	17.44	1.65	0.000
	BAH-F282-118.4_sparkling	21.4	0.4	23.5	2.4	32.02	0.11	0.07	0.01	3.73	0.28	0.002
	BAH-F282-120.5 (brown)	41.9	0.9	46.1	4.6	516.33	1.94	0.19	0.03	118.08	2.83	0.000
	BAH-F282-120.5 (brown)	40.4	0.8	44.5	4.4	526.89	1.99	0.13	0.03	116.23	2.89	0.000
	BAH-F282-120.5 (black)	37.4	0.8	41.1	4.1	1014.77	4.48	0.07	0.01	206.99	16.15	0.000
	BAH-F282-120.5 (black)	37.2	0.8	41.0	4.1	1135.51	4.96	0.43	0.02	230.64	14.09	0.000
	BAH-F282-124.9_stalag.	39.9	0.8	43.9	4.4	26.86	0.09	0.01	0.01	5.85	0.47	0.001
	BAH-F282-124.9_stalag.	35.7	0.7	39.3	3.9	40.08	0.14	-0.04	-0.01	7.80	0.51	-0.001
	BAH-F282-126.3	53.2	1.1	58.5	5.9	92.71	0.35	0.99	0.02	27.02	4.20	0.011
	BAH-F282-126.3	39.3	0.8	43.3	4.3	388.71	1.59	4.61	0.06	83.66	4.76	0.012
	BAH-F282-94.3	44.0	0.9	48.4	4.8	152.16	0.57	0.01	0.01	36.54	3.61	0.000
	BAH-F282-94.3	37.2	0.8	40.9	4.1	138.12	0.54	0.02	0.01	28.04	4.84	0.000
	IBH-03-8 2nd bench/3.5m	21.2	0.5	23.4	2.3	6.12	0.07	19.73	0.23	1.24	0.05	3.224
	IBH-03-8 2nd bench/3.5m	15.3	0.4	16.8	1.7	6.99	0.08	24.64	0.27	1.07	0.05	3.523
	IBH-13-03 Top Crust	0.7	0.0	0.8	0.1	483.66	1.91	0.03	0.02	1.95	0.11	0.000
	IBH-13-03 Top Crust	0.9	0.0	1.0	0.1	422.95	1.61	0.01	0.02	2.04	0.10	0.000
	IBH-13-03 under TC_black	0.9	0.0	1.0	0.1	684.52	2.69	0.00	-0.02	3.38	0.14	0.000
	IBH-13-03 under TC_reddish	5.0	0.1	5.5	0.5	69.21	0.25	0.00	-0.01	1.87	0.13	0.000
	IBH-13-03 under TC_reddish	5.0	0.1	5.5	0.5	79.94	0.28	0.00	0.01	2.17	0.16	0.000
	IBH-13-08c	27.4	0.7	30.2	3.0	20.23	0.29	109.44	1.21	6.87	0.05	5.409
	IBH-13-08c	26.3	0.7	29.0	2.9	15.00	0.28	74.27	0.96	4.65	0.03	4.951
	IBH-13-09b(1) gt filling cav.	23.7	0.6	26.0	2.6	7.06	0.08	19.85	0.24	1.51	0.06	2.813
	IBH-13-09b(1) gt filling cav.	28.0	0.7	30.8	3.1	6.08	0.09	19.60	0.26	1.63	0.05	3.221
	IBH-13-09b(2) gt cement	26.9	0.6	29.6	3.0	6.72	0.09	23.82	0.28	1.81	0.07	3.542
	IBH-13-09b(2) gt cement	28.6	0.7	31.4	3.1	5.36	0.07	17.37	0.21	1.47	0.07	3.238
	IBH-13-09e	10.6	0.3	11.7	1.2	6.70	0.07	30.18	0.31	0.80	0.04	4.502
	IBH-13-09e	16.0	0.4	17.6	1.8	5.70	0.08	25.93	0.30	1.03	0.04	4.548
	IBH-13-09h	34.2	0.8	37.7	3.8	15.97	0.16	26.35	0.36	4.14	0.06	1.650
	IBH-13-09h	38.6	0.9	42.4	4.2	12.09	0.17	23.35	0.34	3.70	0.05	1.931
	IBH-13-09h	35.2	0.9	38.8	3.9	8.64	0.13	22.02	0.31	2.65	0.04	2.550
	IBH-13-12	16.4	0.4	18.0	1.8	2.78	0.05	3.27	0.06	0.32	0.02	1.179
	IBH-13-12	16.3	0.4	17.9	1.8	2.77	0.05	3.52	0.07	0.32	0.02	1.272
N1 Plateau	N1P1302	2.6	0.3	2.8	0.3	0.13	0.00	0.43	0.01	0.00	0.00	3.301
	N1P1302	2.4	0.3	2.6	0.3	0.21	0.01	0.60	0.02	0.00	0.00	2.846
	N1P1302	71.3	3.0	78.4	7.8	0.79	0.03	3.63	0.11	0.64	0.01	4.571
	N1P1302	14.4	0.7	15.8	1.6	0.75	0.04	7.90	0.20	0.20	0.00	10.493
	N1P1302	7.6	0.9	8.4	0.8	0.31	0.02	1.69	0.09	0.03	0.00	5.457
	N1P1303	19.2	0.5	21.1	2.1	3.00	0.06	8.60	0.14	0.52	0.01	2.862
	N1P1303	19.1	0.5	21.0	2.1	3.08	0.06	9.88	0.16	0.56	0.01	3.207
	N1P1306	7.1	0.3	7.8	0.8	0.73	0.03	4.34	0.10	0.07	0.00	5.963
	N1P1306	5.4	0.3	6.0	0.6	0.38	0.02	2.04	0.06	0.03	0.00	5.421

Table 1: U, Th, He contents and (U-Th)/He ages for goethites from the different weathering profiles in the Carajás region, Brazil

Site	Sample Name	Calculated Age (Ma)	$\pm 1\sigma$ (Ma)	Age + 10% (Ma)	$\pm 10\%$ (Ma)	U (ppm)	$\pm 1\sigma$ (ppm)	Th (ppm)	$\pm 1\sigma$ (ppm)	He (nmol/g)	$\pm 1\sigma$ (nmol/g)	Th/U
N1 Plateau	NIP1309	6.4	0.6	7.0	0.7	0.36	0.02	0.40	0.04	0.02	0.00	1.110
	NIP1309	9.8	0.3	10.8	1.1	1.01	0.03	0.83	0.03	0.06	0.00	0.815
	NIP1313	0.7	0.3	0.8	0.1	0.44	0.02	0.88	0.04	0.00	0.00	1.993
	NIP1313	1.1	0.6	1.2	0.1	0.21	0.01	0.60	0.03	0.00	0.00	2.860
	NIP1313b	1.2	0.4	1.3	0.1	0.20	0.01	0.57	0.02	0.00	0.00	2.833
	NIP1313b	1.0	0.4	1.1	0.1	0.21	0.01	0.46	0.02	0.00	0.00	2.195
	NIP1314	6.3	0.4	7.0	0.7	0.28	0.01	1.07	0.03	0.02	0.00	3.763
	NIP1314	7.9	0.3	8.7	0.9	0.37	0.01	1.62	0.03	0.03	0.00	4.329
	NIP1314	47.1	1.9	51.8	5.2	0.67	0.03	3.94	0.10	0.41	0.01	5.871
	NIP1314	14.5	1.1	15.9	1.6	0.26	0.01	1.32	0.07	0.04	0.00	5.184
	NIP1317	15.9	0.6	17.5	1.7	0.60	0.02	4.81	0.10	0.15	0.00	8.073
	NIP1317	17.2	0.5	18.9	1.9	3.13	0.06	19.85	0.25	0.73	0.01	6.349
	NIP1317	1.4	0.1	1.5	0.2	2.75	0.08	14.87	0.25	0.05	0.00	5.402
	NIP1317	20.8	0.5	22.9	2.3	18.60	0.36	125.30	1.52	5.44	0.03	6.737
	NIP1317 Pisolith	73.5	2.1	80.9	8.1	4.36	0.10	17.84	0.28	3.43	0.05	4.095
	NIP1317 Pisolith	3.2	0.1	3.6	0.4	2.00	0.06	8.03	0.17	0.07	0.00	4.025
	NIP1318 lake	2.7	0.1	2.9	0.3	1.00	0.04	9.39	0.18	0.05	0.00	9.429
	NIP1318 lake	2.0	0.1	2.2	0.2	0.73	0.03	5.30	0.10	0.02	0.00	7.237
	NIP1321b	4.0	0.5	4.4	0.4	0.15	0.01	1.39	0.05	0.01	0.00	9.073
	NIP1321b	3.8	0.8	4.2	0.4	0.13	0.01	1.02	0.05	0.01	0.00	7.681
	NIP1323	2.5	0.2	2.7	0.3	0.35	0.01	4.42	0.08	0.02	0.00	12.696
	NIP1323	4.5	0.2	5.0	0.5	0.64	0.02	5.05	0.09	0.04	0.00	7.879
	NIP1323	13.6	0.3	14.9	1.5	34.94	0.51	232.30	2.41	6.61	0.03	6.649
	NIP1323	3.9	0.2	4.3	0.4	1.20	0.04	4.03	0.11	0.05	0.00	3.362
	NIP1328	21.0	0.6	23.1	2.3	4.86	0.10	20.05	0.30	1.09	0.02	4.121
	NIP1328	16.5	0.5	18.2	1.8	2.79	0.06	5.79	0.11	0.37	0.01	2.076
	NIP1332	2.2	0.2	2.4	0.2	0.90	0.03	4.24	0.11	0.02	0.00	4.718
	NIP1332	4.3	0.2	4.7	0.5	1.32	0.04	5.15	0.12	0.06	0.00	3.916
	NIP1333	27.3	0.8	30.1	3.0	1.29	0.03	6.97	0.10	0.44	0.01	5.414
	NIP1333	4.0	0.1	4.4	0.4	1.89	0.04	10.38	0.13	0.09	0.00	5.508
	NIP1333	31.1	0.9	34.2	3.4	8.88	0.22	51.91	0.78	3.57	0.02	5.845
	NIP1333	18.5	0.6	20.4	2.0	6.10	0.18	32.73	0.59	1.39	0.01	5.363
	NIP1335	3.4	0.4	3.7	0.4	0.36	0.01	0.37	0.02	0.01	0.00	1.025
	NIP1335	0.1	0.4	0.2	0.0	0.39	0.01	1.96	0.03	0.00	0.01	5.079
	NIP1335	0.6	0.5	0.6	0.1	0.20	0.01	1.14	0.05	0.00	0.00	5.623
	NIP1335	9.6	1.9	10.5	1.1	0.06	0.01	0.38	0.04	0.01	0.00	5.960
	NIP1337_bIV Gt	2.7	1.5	3.0	0.3	0.09	0.01	0.40	0.05	0.00	0.00	4.671
	NIP1337_bIV Gt	3.7	0.5	4.1	0.4	0.10	0.01	0.59	0.03	0.00	0.00	5.892
	NIP1337_brown Gt	6.7	0.4	7.3	0.7	0.65	0.03	3.37	0.09	0.05	0.00	5.162
	NIP1337_brown Gt	5.8	0.2	6.4	0.6	1.69	0.06	9.25	0.20	0.12	0.00	5.478
Itacaiunas Surface	NIP1343	17.4	1.7	19.2	1.9	0.13	0.01	0.41	0.03	0.02	0.00	3.288
	NIP1343	6.6	1.8	7.2	0.7	0.05	0.00	0.21	0.01	0.00	0.00	4.573
	NIP1343	16.4	1.8	18.0	1.8	0.16	0.01	0.70	0.06	0.03	0.00	4.301
	NIP1343	5.5	0.6	6.0	0.6	0.20	0.01	0.63	0.03	0.01	0.00	3.107
	BOI-002	3.4	0.1	3.7	0.4	16.81	0.09	10.56	0.16	0.35	0.01	0.628
	BOI-002	2.4	0.1	2.7	0.3	27.56	0.10	20.03	0.25	0.43	0.01	0.727
	BOI-002	3.9	0.1	4.3	0.4	10.86	0.11	5.19	0.10	0.26	0.01	0.478
	BOI-002	1.8	0.0	2.0	0.2	29.12	0.26	86.58	0.93	0.48	0.00	2.973
	BOI-002	2.4	0.1	2.6	0.3	23.99	0.20	16.07	0.26	0.36	0.00	0.670
	BOI-004	0.5	0.0	0.6	0.1	15.62	0.15	26.18	0.34	0.06	0.00	1.676
	BOI-004	1.2	0.0	1.3	0.1	8.65	0.16	15.82	0.27	0.08	0.00	1.828
	BOI-004	0.7	0.0	0.8	0.1	8.66	0.17	16.14	0.29	0.05	0.00	1.864
	BOI-004	0.5	0.0	0.5	0.1	15.91	0.17	19.64	0.29	0.06	0.00	1.234
	BOI-004	0.7	0.0	0.8	0.1	13.36	0.16	22.33	0.31	0.07	0.00	1.671
	BOI-013	6.9	0.2	7.6	0.8	3.24	0.05	2.53	0.05	0.15	0.01	0.780
	BOI-013	6.8	0.2	7.4	0.7	3.03	0.05	3.89	0.07	0.15	0.01	1.281
	BOI-013	7.7	0.2	8.5	0.8	2.96	0.06	3.99	0.08	0.16	0.00	1.347
	BOI-014	8.5	0.2	9.4	0.9	10.09	0.08	58.83	0.48	1.11	0.04	5.830
	BOI-014	6.8	0.2	7.5	0.8	7.18	0.11	45.27	0.48	0.66	0.01	6.305
	BOI-014	8.5	0.2	9.3	0.9	8.18	0.10	54.57	0.53	0.97	0.02	6.668
	BOI-014	7.9	0.2	8.7	0.9	9.42	0.11	54.39	0.53	0.96	0.02	5.772

4.5. Cosmogenic ^3He

Cosmogenic ^3He concentrations in hematites from the N1 and S11D plateaus are shown in Table 2. All samples yield significant amounts of ^3He , with minimum and maximum ^3He concentrations ranging from 100 to 495 Mat.g⁻¹ for surface hematites. Maximum apparent exposure ages (*aEAs*) of 7.3 ± 0.9 Ma and 6.5 ± 0.8 Ma were calculated for the canga plateaus at S11D and N1, respectively. When cosmogenic isotopes are cast in terms of erosion rates, values obtained from S11D and N1 are as low as 0.08 and 0.09 m.Ma⁻¹, respectively (Table 2).

Table 2: Cosmogenic ^3He analysis

Sample	Rock type	Mineralogy	Location	Latitude	Longitude	Elevation (m)	Depth (cm)	Aliquot weight (mg)	^3He (pcc.g $^{-1}$)	^3He (Mat.g $^{-1}$)	Production rate (at.g $^{-1}$.a $^{-1}$)	Exposure age (Ma)	Erosion rate (m.Ma $^{-1}$)	\pm
NIP-13-08	canga	hem	N1 Plateau	S 06° 01' 30.9"	W 50° 16' 47.8"	784	0	14.80	6.3	170	73	2.3	0.24	0.03
NIP-13-20	canga	hem	N1 Plateau	S 06° 01' 45.9"	W 50° 17' 01.8"	724	0	19.28	8.9	241	70	3.4	0.4	0.02
SS-03-01 o/c	canga	hem	Serra Sul	S 06° 24' 26.87"	W 50° 19' 38.46"	678	0	19.28	18.4	495	21	7.3	0.3	0.003
SS-03-02 o/c	canga	hem	Serra Sul	S 06° 24' 26.87"	W 50° 19' 38.46"	836	0	7.4	7.4	199	10	2.6	0.1	0.01
SS-03-03 o/c	canga	hem	Serra Sul	S 06° 24' 26.87"	W 50° 19' 38.46"	884	0	15.04	3.7	100	13	1.3	0.2	0.06
NIP-13-01 (1)	pebble	hem	N1 Plateau	S 06° 01' 27.3"	W 50° 16' 45.1"	776	0	14.41	10.6	286	73	3.9	0.5	0.02
NIP-13-01 (2)	pebble	hem	N1 Plateau	S 06° 01' 27.3"	W 50° 16' 45.1"	776	0	14.41	7.3	197	73	2.7	0.3	0.02
NIP-13-16 (1)	pebble	hem	N1 Plateau	S 06° 01' 33.1"	W 50° 17' 02.8"	726	0	17.03	16.7	449	70	6.4	0.8	0.01
NIP-13-16 (2)	pebble	hem	N1 Plateau	S 06° 01' 33.1"	W 50° 17' 02.8"	726	0	16.83	16.9	455	70	6.5	0.8	0.01

5. DISCUSSION

The significant sample population in this study (177 (U-Th)/He *pAs* and 9 cosmogenic ^3He *aEAs*), combined with additional results from Shuster et al. (2005, 2012) (55 (U-Th)/He *pAs*, 2 $^4\text{He}/^3\text{He}$ profiles, and 25 cosmogenic ^3He erosion rate) and Monteiro et al. (chapter 2) (1 $^4\text{He}/^3\text{He}$ age profile), provide a comprehensive dataset suitable for addressing the histories of weathering, exposure, and erosion of the Carajás plateaus and surrounding plains. The results provide useful constraints on the ages of the various landsurfaces and on the rates and mechanisms involved in the evolution of long-term landscapes in the region. Thus, the results help resolve long-standing questions about the hierarchy of landsurfaces and the mechanisms involved in their formation and destruction. However, the results also reveal an extreme complex surficial history in these old landscapes, suggesting that additional sites and samples are required to identify all the processes shaping these continental land forms, quantify rates of weathering and erosion through time, unravel the influence of climate in accelerating or decelerating these processes, and properly determine the controls imposed by tectonics on the formation and preservation of stepped landscapes in cratonic settings.

Before presenting and discussing the main conclusions in this study, we will address some issues related to the types of samples analyzed; their mineralogical complexities and suitability to (U-Th)/He dating; issues related to U, Th, and He incorporation, mobility, and retentivity in goethite and hematite; and factors associated with bedrock controls on the precipitation and preservation of iron oxyhydroxides suitable for geochronology.

5.1. The goethite (U-Th)/He record: chemical processes controlling the formation of saprolites and cangas

The Igarapé Bahia profile provides a comprehensive goethite dataset, where samples were collected at the surface, within the duricrust immediately beneath the thick soil that blankets most of the plateau, at various depths within the saprolite, and at the contact between the weathering-bedrock interface (Figure 2).

The Igarapé Bahia lateritic profile results from the oxidation of massive hydrothermal Fe-Cu sulfide orebodies, which released large quantities of sulfuric acid and iron in solution. Iron reprecipitated as massive colloform and essentially monomineralic goethite bands, sometimes alternating with bands of Cu-cryptomelane, and containing variable amounts of Al, Mn, Cu, Si, and P. Some of these elements replace Fe in solid solution. Some of these elements are possibly present as nano-scale mineral contaminants not yet identified (e.g., iron phosphates). These massive colloform goethites are the purest and most suitable samples for geochronology. Exotic mineral phases intergrown with colloform goethites (Cu-cryptomelane, native Cu, cuprite, Au) also precipitated during weathering. These phases may precede, be coeval, or postdate goethite precipitation, but they all formed during weathering and, fortunately, do not contain any isotopic or He memory from the underlying Archean bedrock. Concentric growth patterns in the colloform samples permits identifying, selectively sampling, and separately dating distinct generations of these supergene minerals (Vasconcelos et al., 1995; Shuster et al., 2005).

In contrast, goethites from duricrusts (Figure 2b), the result of several events of iron dissolution-reprecipitation or Fe-metasomatism of soils and previously formed weathered material (Monteiro et al., 2014), contain a diverse range of primary and supergene minerals re-cemented by supergene Fe and Al oxyhydroxides. The presence of minerals inherited from the bedrock may influence the (U-Th)/He ages (Vasconcelos et al., 2013; Monteiro et al., 2014). These goethites also show evidence for biological control in iron cycling, where relatively pure Al-rich goethite surrounds root cavities or replaces roots (Figure 5f) and microorganisms (Levett et al., 2015). These goethites are relatively enriched in Th with respect to U (Figure 9), suggesting that both U and Th enter solution by complexation with organic ligands, but that Th readily reprecipitates while U remains in solution and is leached towards the bottom of the weathering profiles. The clear enrichment in Th and depletion of U for goethites from near surface sites at Igarapé Bahia are similar to the relative U-Th enrichment/depletion previously observed for Fe-duricrusts at the QF, Minas Gerais (Monteiro et al., 2014; 2017a).

A similar trend is noticeable for goethite samples from N1 (Figure 9). As all N1 samples investigated in this study are derived from the present surface, they probably reflect a protracted history of iron dissolution-reprecipitation, leading to the observed U depletion and Th enrichment. Samples with high Th/U values are more complex, contain multiple generations intimately intergrown, and show greater variability in (U-Th)/He apparent ages for replicate grains from a same sample. N1 goethites are also compositionally complex because the plateau is underlain by both BIF and volcanic units, leading to high Al and Ti contents in the supergene Fe and Al oxyhydroxides (Figure 7b). Results for the nearby N4 plateau (Shuster et al., 2012) show similar trends in U and Th distribution with depth in the profile.

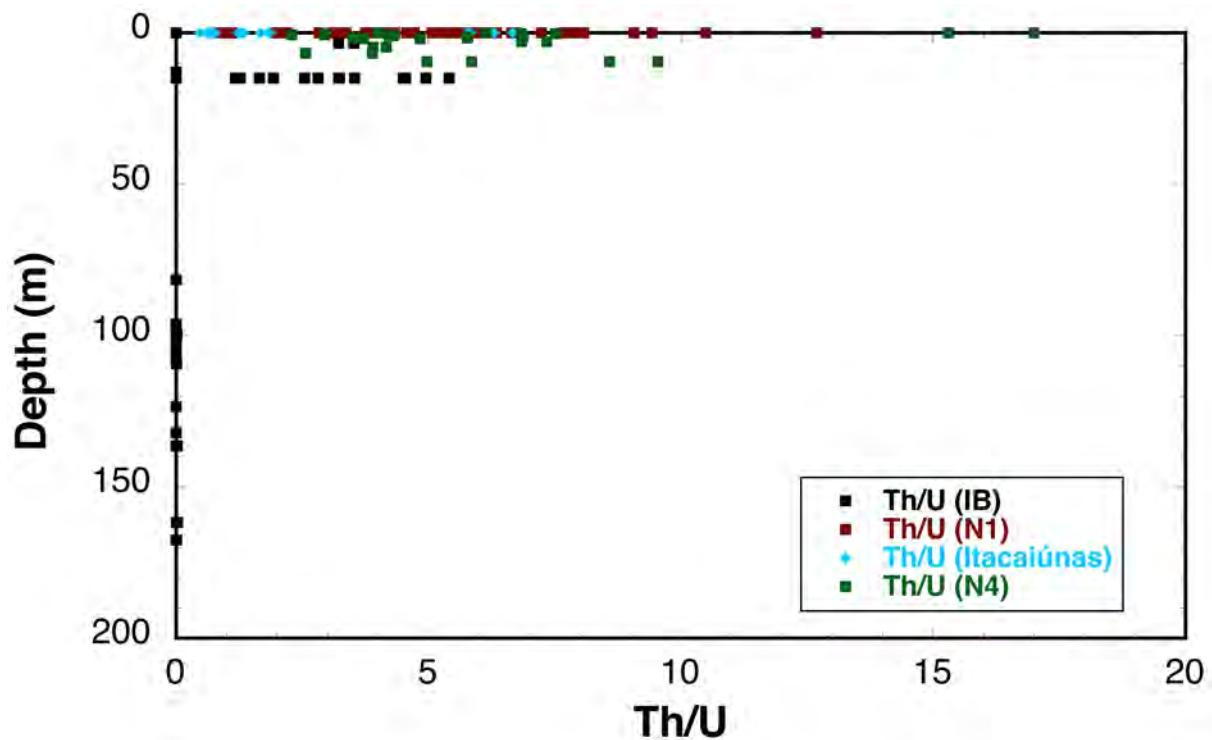


Figure 9: Trends in Th/U vs depth illustrate the effective leaching of U from surface sites and the progressive enrichment of Th towards the surface.

Finally, goethites from the Itacaiunas Surface display the preferential enrichment in Th vs U observed in the IB duricrusts and in the N1 cangas, common for goethites formed by cementation and pseudomorphic replacement of other minerals (Vasconcelos et al., 2013; Monteiro et al., 2014; Riffel et al. 2015). They are also rich in Al and Ti, which is consistent with their mode of formation.

5.2. The (U-Th)/He age record

The (U-Th)/He record for the Igarapé Bahia profile reveals a complex age pattern, but two distinct features are obvious from the record. First, on average, samples collected from the upper parts of the weathering profile, mostly from the duricrust, are older than samples collected at the bottom of the profile (Figure 10). The oldest result (70.8 ± 7.1 Ma) occurs in the duricrust and the youngest

result (0.82 ± 0.08 Ma) comes from a sample at 100 m below the surface (Figure 10, Table 1). Interestingly, samples as old as ~ 58 Ma occur at depth, suggesting that the oxidation front that formed the lateritic gold deposit had reached great depths early in the history of weathering. The geometry of the profile (Figure 2c), where depth of weathering appears to follow mineralization, suggests that, early in the history of exhumation, the oxidation of sulfides generated acid-oxidizing solutions that carved a preferential path downward into the bedrock along the mineralized zone, allowing the oxidation front to reach great depths rapidly. This deeply oxidized and mineralized breccia zone (gossan) focused subsequent percolation of weathering solutions. The descending meteoric solutions that traversed less mineralized, less reactive, and probably less permeable lithologies supplied, slowly through time, dissolved species that added to the complexity of the weathering assemblages at depth. An age vs depth relationship for the IB profile shows a minimum rate of penetration of the oxidation front from ~ 70 to 58 Ma of ~ 8.5 m.Ma⁻¹ (Figure 10). This rate is indistinguishable from that obtained for weathering profiles in SE Brazil (8.9 ± 1.1 m.Ma⁻¹) (Carmo and Vasconcelos, 2006), but $>$ twice the rate calculated for advancing weathering fronts in Australia (Vasconcelos and Conroy, 2003; Heim et al., 2006).

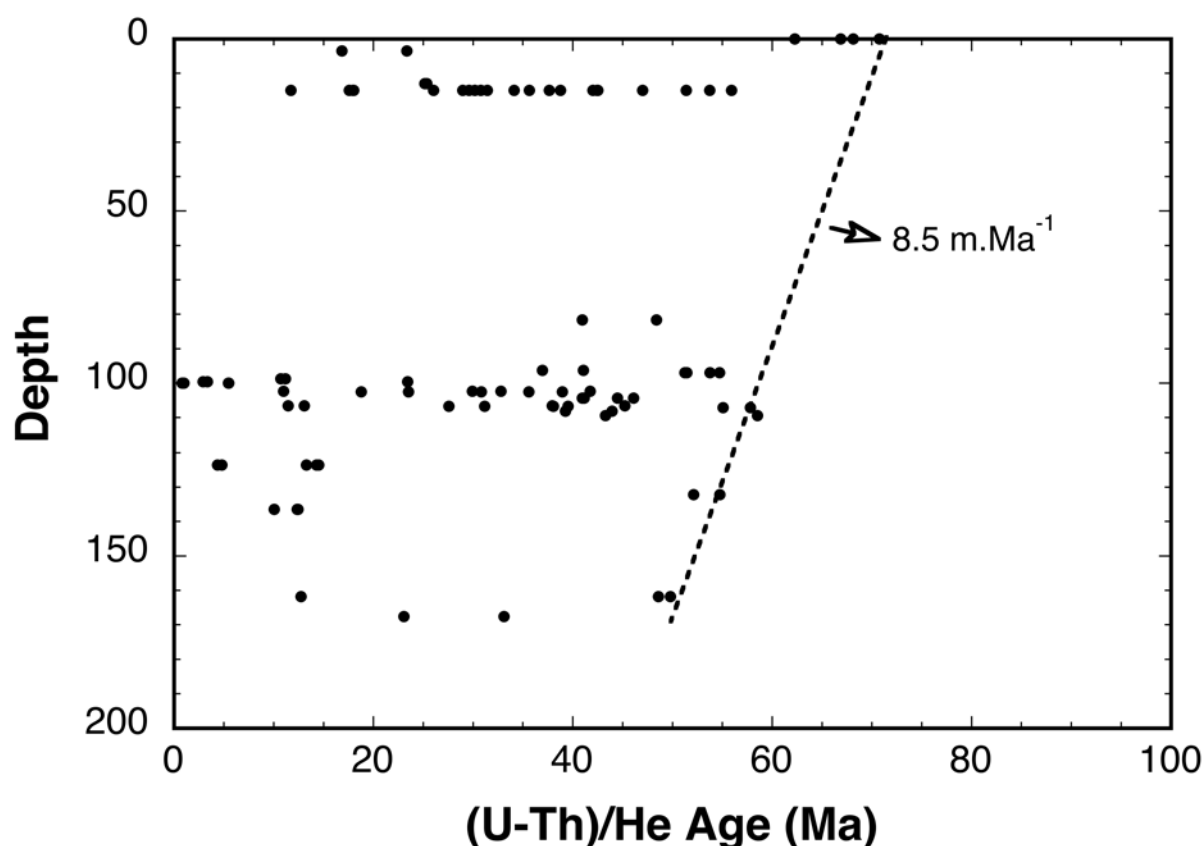


Figure 10: An age vs depth diagram for all goethites from the IB profile reveals that, on average, goethites are older near the surface, while younger generations are more frequent at depth. The results also show that the weathering profile had already reached depths of ~ 100 m by ~ 58 Ma. The calculated rate for weathering front propagation yield rates similar to those obtained for Miocene weathering profiles in SE Brazil (Carmo and Vasconcelos, 2006), and twice as fast as similar rates obtained for weathering profiles in Australia (Vasconcelos and Conroy, 2003; Heim et al., 2006).

The distribution of ages for the N1 plateau also reveals that weathering started at the end of the Mesozoic (~ 80 Ma) and continued throughout the entire Cenozoic. The paucity of results and the fact that all samples come from the surface precludes determining whether the weathering history (as recorded by mineral dissolution-reprecipitation, which should reflect in the age frequency through time) preserved at N1 is continuous or episodic, but the combined results from N1 and IB (this study) and N4C (Shuster et al., 2005, 2012) suggest a history of continuous surface exposure of the Carajás surface throughout the entire Cenozoic.

Significantly, all the results obtained for the Itacaiunas Surface goethites are younger than 10 Ma, suggesting a much shorter history of exposure and weathering for this low elevation landscape. This shorter history of weathering is consistent with the shallower and less evolved weathering profiles devoid of significant supergene enrichment in the undulating plains (Figure 4). This shorter history is also consistent with the thin, immature, and intermittent nature of the duricrusts distributed throughout the Itacaiunas Surface (Figure 4c).

5.3. The cosmogenic ^3He record: the relative stability of duricrusts

Cosmogenic ^3He concentrations were measured for surface samples from the N1 and S11D plateaus (Figure 1, Table 2). The results for exhumed hematite blocks presently cemented in cangas and for loose hematite pebbles yield compatible average rates of erosion of 0.20 ± 0.05 (1σ) m.Ma^{-1} for N1 and 0.24 ± 0.18 (1σ) m.Ma^{-1} for S11D, confirming that the plateaus are indeed impervious to physical erosion for tens of millions of years. The relatively higher erosion rates (0.44 m.Ma^{-1}) obtained for partially hydrated and goethite-rich cements (Table 2) suggests that the plateaus evolve by slow hydration and dissolution-reprecipitation, with some mass loss resulting from downward leaching of soluble species. These chemical processes are very slow, and the plateau suffers very little chemical and physical erosion.

5.4. Age vs elevation relationships for the Carajás and Itacaiunas Surfaces

The geochronological results clearly show that the Carajás Surface started its history of exposure and weathering before the end of the Mesozoic, and that it has been stable, emergent, and undergoing weathering and minimal erosion since ~ 80 Ma. The long history of exposure and weathering obtained from the (U-Th)/He record is entirely compatible with the history of weathering obtained from the $^{40}\text{Ar}/^{39}\text{Ar}$ Mn oxide geochronological record (Vasconcelos et al., 1994, 2015; Ruffet et al., 1996) confirming that the Carajás surface is indeed one the oldest continuously exposed landsurfaces on Earth. The low erosion rates implied by the long history of surface exposure revealed by the two independent weathering geochronology records ($^{40}\text{Ar}/^{39}\text{Ar}$ on

Mn oxides and (U-Th)/He on Fe oxyhydroxides) are confirmed by the cosmogenic ^3He (Shuster et al., 2012; this study) and ^{53}Mn (Fujioka et al., 2010) records. By targeting the magnetic fraction of hematite pebbles, we were able to obviate the effects of partial ^3He loss during hydration of hematite to goethite, and are able to demonstrate that erosion rates at N1 and S11D are compatible with but even lower than that obtained from a 10m deep profile at the nearby N4C iron deposit (Figures 1, 2; Shuster et al., 2012).

The long history of exposure and weathering and the extreme resilience of the Carajás surface contrasts with the much shorter history of weathering and exposure derived from the more recent weathering geochronology results obtained for the four sites investigated on the Itacaiunas Surface. If we take these results at face value, they imply that the Itacaiunas Surface was exhumed and has been exposed to weathering and erosion for less than ~ 10 Ma.

5.5. Formation and evolution of the diachronous Itacaiunas erosion surface

The differences in elevation, depth of weathering, complexity of weathering profiles, and ages of weathering for the Carajás and Itacaiunas Surfaces lead to the conclusion that these land surfaces represent different stages of the geomorphological evolution of the Carajás region. The physical and chronological differences and the topographic relationships between the two surfaces (~ 700 m elevation average for the Carajás Surface and ~ 250 m for the Itacaiunas Surface) also suggest that the Itacaiunas Surface must have evolved at the expense of the Carajás Surface. Since to destroy a land surface it is necessary to erode it, and since both the weathering geochronology and the cosmogenic isotope ^3He records indicate that the surface of the Carajás plateaus undergo negligible erosion (for example, in 80 Ma the surface of the N1 and S11D plateaus would have been lowered less than 30 m), it is also an important conclusion that the process that forms the Itacaiunas Surface at the expense of the Carajás Surface is scarp retreat. In fact, landslides are commonly observed in the major gullies and steep escarpments after the raining season, suggesting that scarp retreat is the most active landscape evolution processes modifying the Carajás Surface today and, most likely, throughout the Cenozoic.

Given the longevity of the Carajás Surface revealed by the weathering geochronology and cosmogenic isotope records, it is also reasonable to conclude that scarp retreat of a proto –Carajás Surface, presumably much more extensive than the present surface, has been ongoing since the beginning of the Cenozoic. Plate reconstructions show that the Carajás plateau region has been emergent for a long time, certainly since 160 Ma (Figure 11; Amante and Eakins, 2009). Plate reconstructions also show that the entire Amazon plain has been intermittently submerged by advancing seas. Until about 15 Ma the sea occupied areas close to Marabá (Figure 11), as evident

from fossiliferous calcareous units from the Pirabas Formation that crop out in this area (Petri and Fúlfaro, 1983). Renewed tectonic activity (Hoorn, 1993; Hoorn et al., 2010 and references there in) in the Andes at the time likely promoted uplift of the Brazilian shield, marine regression, and the onset of the scarp retreat that shaped the present Carajás landscape.

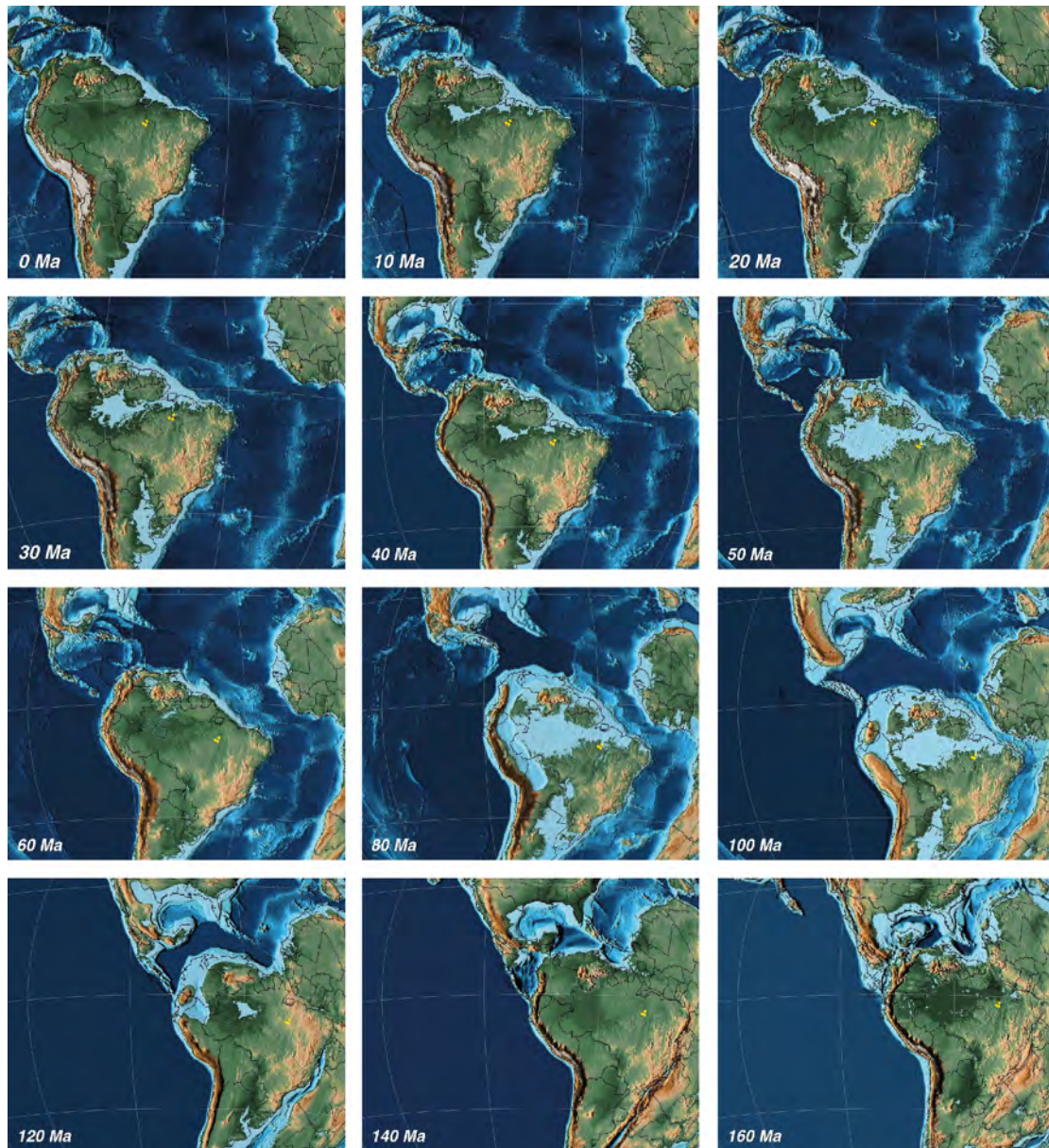


Figure 11: Plate reconstruction for South America (Scotese, 2001) shows that the Carajás region has been continuously emergent since 160 Ma, and that the sea has flooded areas adjacent to the Carajás Plateaus intermittently throughout the Mesozoic and Cenozoic, and as late as ~20-15 Ma. Yellow dots indicate sites investigated in this study.

Weathering geochronology may help in the reconstruction of the history of scarp retreat and slow destruction of the Carajás Surface, and consequent formation of the Itacaiunas Surface if we consider that a freshly exposed landsurface, or the sediments deposited on them by a retreating

scarp, will be immediately subject to weathering and erosion. Under favorable conditions (low relief, abundant vegetation cover, humid climate, active biota), weathering will be more effective than erosion, and stratified weathering profiles blanketed by iron duricrusts will start to develop locally. As the scarp retreats, a new surface is exposed, and the process repeats itself, forming a new duricrust. Therefore, the age of ferruginisation and duricrust formation on the Itacaiunas Surface should track the receding escarpment.

Another important inference is that scarp retreat will proceed from the coastline and along major drainages inward into the continent. Since the sea was near Marabá at ~ 15 Ma, sea level drop initiated at that time, possibly linked to the tectonic uplift event that tilted the continent towards the NE and drove the Amazon drainage into the Marajó graben (Shepard et al., 2010 and references therein), would have triggered the onset of the scarp retreat event that formed the Itacaiunas Surface. Using our geochronological results as markers of when the Itacaiunas Surface was exposed and stabilized at a given point, it is possible to reconstruct the patterns and retreat rates for the receding scarp (Figure 12).

The reconstruction on Figure 12 illustrates the possible sequence of events, and the rates of scarp retreat that shaped the present landscape at Carajás and adjacent areas. Assuming that the scarp initiated at the margins of the present Tocantins river at Marabá (Figures 1, 12a), it would have reached and exposed our sites BOI 013 and BOI 014 by ~ 10 -8 Ma (Figure 12b), implying a rate of scarp retreat of 5 -7 km.Ma⁻¹. From sites BOI 013 and BOI 014, the scarp retreats towards the Carajás plateau along the two major drainages, the Itacaiunas and the Parauapebas rivers (Figure 1). The old duricrust at our BOI 002 site suggests that the Parauapebas river had eroded into approximately its present level by ~ 3 Ma. Given that the duricrust at this site is very close to escarpments to the east and west (Figure 4d, 12e), it suggests that only a narrow valley needed to have formed for the duricrusted surface to evolve and be stabilized. The rate of downward incision of the proto-Parauapebas river would have been 150 m.Ma⁻¹ at the site of the duricrust near Canaã dos Carajás, and the rate of scarp retreat along the valley, from sites BOI 013 and BOI 014 to site BOI 002, would have been ~ 20 km.Ma⁻¹. Finally, westward scarp retreat from the Vermelho River and eastward retreat from the Parauapebas River or vicinity would have partially consumed a then more extensive proto Serra Leste (SL), and the retreating escarpment would have exposed our BOI 004 site at ~ 1 Ma (Fig.12d).

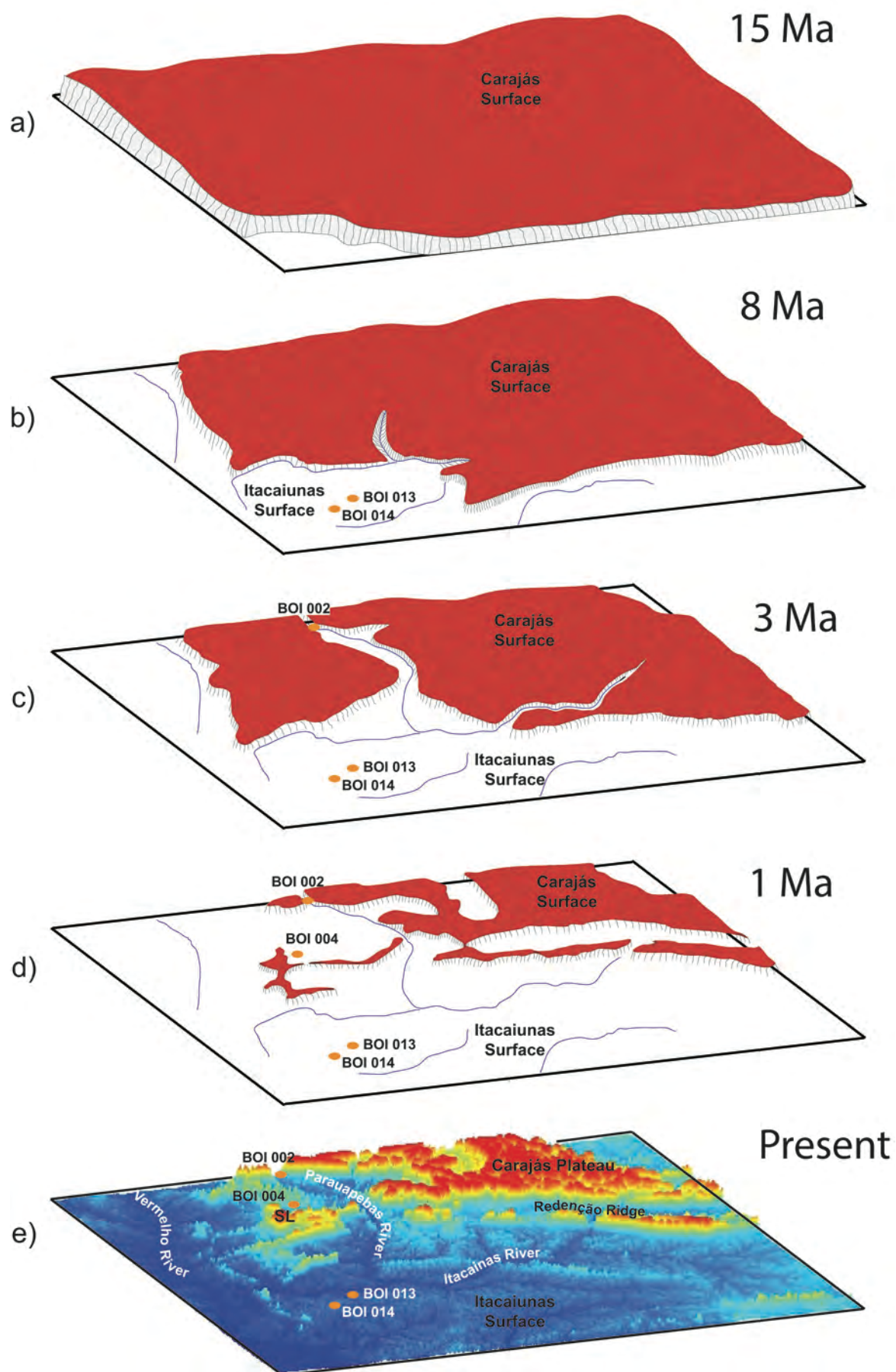


Figure 12: The spatial and temporal distribution of dated duricrusts on the Itacaiunas Surface can be used as time markers of the relative positions of the receding escarpment that now surrounds the Carajás Plateaus and nearby ridges. Initiation of scarp retreat occurred ~ 10 Ma (BOI 013: $7.4 \pm 0.7 - 8.5 \pm 0.8$ Ma; BOI 014: $7.5 \pm 0.8 - 9.4 \pm 0.9$ Ma). At ~ 3 Ma, the scarp had retreated along the main drainage system and reached the Carajás Plateau near the city of Canaã dos Carajás (BOI 002: $2.0 \pm 0.2 - 4.3 \pm 0.4$ Ma). Lateral down-cutting by mainstream channels and their tributaries resulted in the advanced destruction of the Carajás Surface reaching the BOI 004 site between $0.5 \pm 0.1 - 1.3 \pm 0.1$ Ma. Rates of scarp retreat and nickpoint propagation appear to vary through time (from $5\text{--}20 \text{ km.Ma}^{-1}$), and they are greater than similar rates calculated for retreating bedrock escarpments in more arid landscapes. The rapid rates of scarp retreat derived from dated weathering profiles in this study are consistent with the fact that the Carajás Surface was already deeply weathered before the onset of scarp retreat.

Independent of assumptions about the time of initiation of marine regression and possible uplift that would have triggered scarp retreat, the minimum and maximum scarp retreat rates estimated here are greater than rates of retreat of bedrock escarpment in East Australia ($3\text{--}35 \text{ m.Ma}^{-1}$; Heimsath et al., 2006), the Drakensberg in West Africa ($50\text{--}95 \text{ m.Ma}^{-1}$; Fleming et al., 1999), or the Serra do Mar escarpment in southeastern Brazil ($13\text{--}90 \text{ m.Ma}^{-1}$; Gonzalez et al., 2016), but they are comparable to rates estimated for the scarp retreat in the Colorado Plateau (Schmidt, 1999). If rates of scarp retreat at Carajás appear fast, it is relevant to consider that deep weathering profiles already blanketed the Carajás Surface by about 50 Ma, and that rivers and the receding scarps were eroding into deeply weathered bedrock. Deeply weathered granites, gneisses, schists, and other mineralogically complex lithologies would erode relatively easily. But when strong silica-cemented quartzites or iron-cemented banded iron-formations were encountered by the receding escarpment, scarp retreat rates decreased. The remnant quartzite ridge at “Serra da Redenção” and the proximity between the ferruginous duricrust at the Canaã dos Carajás and nearby Carajás Surface BIF plateaus (Figure 1) suggest that these resistive lithologies slowed or nearly stopped the receding scarp.

Scarp retreat from Marabá to Carajás would have generated the volume of weathered material, mostly derived from granitic-granodioritic lithologies, to account for the volume and types of sediments (quartz + clays + oxides) deposited to the north (Petri and Fúlfaro, 1983). Re-weathering of these sediments after deposition would have generated the bauxite deposits of Paragominas and adjacent areas (Kotschoubey et al., 1997). The age of this “re-weathering” process that formed these large bauxite deposits could be easily determined through the application of the methods illustrated here.

An important conclusion from this study is that the landscapes in the Carajás region are not in steady state, as steady-state landscape evolution models (Hack et al., 1960) require mountains and valleys to erode at the same rate, which is incompatible with our geochronological results. On the other hand, the preservation of topographic summits completely immune to erosion for tens of millions of years (e.g., the Carajás Surface) is incompatible with a Davisian perspective on landscape evolution where the highest divides would progressively erode to a peneplain (Davis,

1899). Preservation of the Carajás Surface for > 70 Ma is also incompatible with Penck's model of landscape ablation towards an endrumpf in mature landscapes (Penck 1924, 1953). Therefore, the distribution of ages of weathering profiles at the Carajás-Marabá landscape is only compatible with King's scarp retreat model (King, 1956), where the Itacaiunas Surface is the pediplain that will ultimately consume the retreating Carajás Plateaus, erasing any memory of a preterious event of uplift.

This tentative landscape evolution history, informed by our weathering geochronology record, clearly needs refinement and a more comprehensive reconstruction through geochronology of many more sites. It would also benefit from cosmogenic isotope measurements at these same sites. Nevertheless, using the distribution of dated weathering profiles to infer processes and rates of landscape evolution is a novel, informative, and powerful new and quantitative way of tracking the evolution of landscapes through time. Expansion of this approach at Carajás and other similar land surfaces elsewhere will certainly improve our understanding of the climatic and tectonic history that shaped long-lived continental landscapes.

6. CONCLUSION

The weathering profiles of the Carajás Plateau record goethite precipitation from ~ 80 Ma to 1 Ma. Cosmogenic ^3He concentrations suggest that the plateau surfaces have been essentially immune ($<0.1 \text{ m.Ma}^{-1}$) to physical erosion throughout its Cenozoic history of exposure. The paleosurface that was carved by scarp retreat to form the present Carajás Plateaus landscape may have extended at least to the Tocantins River in the Miocene. Sea level drop and tectonic uplift at ~ 15 Ma may have initiated the river incision and scarp retreat. Apparent exposure ages as old as ~ 7 Ma suggest that the Carajás Plateau has eroded very slowly since the Mesozoic. The landscape investigated in this study developed through scarp retreat since the end of the Lower Miocene. Our (U-Th)/He results suggest at least two phases (different rates) of erosion. Retreat of the scarp at rates of 5-7 Km.Ma^{-1} initiated the destruction of the Carajás Surface. Exposure of fresh or partially weathered bedrock and fluvial sediments filling river channels to intense weathering led to the formation of incipient weathering mantles in the landscape. Between 8 – 3 Ma the scarp continued to retreat, now at an average rate of 20 Km.Ma^{-1} , along the Itacaiúnas river and its tributaries. Ferruginization of the low-lying surface at the foot of the Carajás Plateau started around 3 Ma. Therefore, the low-lying surfaces surrounding the plateaus of Carajás formed diachronously.

Acknowledgments

We thank present and past colleagues from Vale, particularly Carlos Monte Lopes, Luzimar Rego, Clovis Maurity, Paulo Sérgio, Fernando Greco, Fernando Martins, Henrique Meireles, Carlos Augusto de Medeiros Filho, Augusto Kishida, and Felipe Porto for field support and heated discussions on the evolution of Carajás region. This project was funded by the Australian Research Council (ARC Discovery Grant DP160104988) grant to Paulo Vasconcelos and Kenneth Farley and the Brazilian Research Council (CNPq), which sponsored Hevelyn Monteiro's PhD studies.

REFERENCES

- Amante C. and Eakins B.W. (2009) ETOPO1 1 Arc-Minute Global Relief Model: Procedures, Data Sources and Analysis. NOAA Technical Memorandum NESDIS NGDC-24. National Geophysical Data Center, NOAA. doi:10.7289/V5C8276M.
- Alves, C. A., Bernardelli, A. L., and Beisegel, V. de R. (1986) A Jazida de níquel laterítico do Vermelho, Serra dos Carajás, In: Principais Depósitos Minerais do Brasil Vol. II, 325-334, Ed. Schobbenhaus, C. and Coelho, C. E. S., DNPM.
- Andrade W. O., Machesy, M. L., and Rose Arthur (1991) God distribution and mobility in the surficial environment, Carajás region, Brazil, *Journal of Geochemical Exploration*, 40, 95-114.
- Araújo, O.J.B., Maia, R.G.N., 1991. Serra dos Carajás, folha SB.22-Z- A, Estado do Pará. Programa Levantamentos Geológicos Básicos do Brasil. Companhia de Pesquisa de Recursos Mimerais. 136 pp.
- Amidon, W. H., and Farley, K. A. (2011), Cosmogenic ^3He production rates in apatites, zircon and pyroxene inferred from Bonneville flood erosional surfaces, *Quaternary Geochronology*, 6, 10-21.
- Beauvais, A., Ruffet, G., Hénocque, O., and Colin, F., 2008, Chemical and physical erosion rhythms of the West African Cenozoic morphogenesis: The ^{39}Ar - ^{40}Ar dating of supergene K-Mn oxides: *Journal of Geophysical Research*, v. 113, F04007, doi:10.1029/2008JF000996.
- Beauvais, A., Bonnet, N. J., Chardon D., Arnaud N., and Jayananda M. (2016) Very long-term stability of passive margin escarpment constrained by $^{40}\text{Ar}/^{39}\text{Ar}$ dating of K-Mn oxides, *Geology* 44, 299-302.
- Bonnet, N. J., Beauvais, A., Arnaud N., Chardon D., Jayananda M. (2016) Cenozoic lateritic weathering and erosion history of Peninsular India from $^{40}\text{Ar}/^{39}\text{Ar}$ dating of supergene K-Mn oxides, *Chemical Geology*, 446, 33-53.
- Carmo, I. O., and Vasconcelos, P. M. P. (2006) $^{40}\text{Ar}/^{39}\text{Ar}$ geochronology constraints on late Miocene weathering, Minas Gerais, Brazil, *Earth Surface Processes and Landforms* 29, 1303-1320.
- Coelho, C. E. S. and Rodrigues, O. B. (1986) Jazida de Mnaganês do Azul, Serra dos Carajás, Pará. In: Principais Depósitos Minerais do Brasil Vol. II, 145-152, Ed. Schobbenhaus, C. and Coelho, C. E. S., DNPM.

- Colin, F., Beauvais, A., Ruffet, G., Hénocque, O., (2005) First $^{40}\text{Ar}/^{39}\text{Ar}$ geochronology of lateritic manganiferous pisolites: implications for the Palaeogene history of a West African landscape. *Earth Planet. Sci. Lett.* 238, 172–188. <http://dx.doi.org/10.1016/j.epsl.2005.06.052>.
- Costa M. L., Lemos V. P., and Villas R. N. N. (1997) The bauxite of Carajás Mineral Province. In: *Brazilian Bauxites*, A. Carvalho, B. Boulangé, A. J. Melfi, Y. Lucas (eds), - São Paulo: USP, FAPESP; Paris: Orstom, 1997, 331p.
- DOCEGEO (Rio Doce Geologia e Mineração S.A.) (1988) *Província Mineral de Carajás. Litoestratigrafia e principais depósitos minerais*. 35 Congresso Brasileiro de Geologia, vol. 165.
- Fleming A., Summerfield, M. A., Stone, J. O., Fifield, L. K., and Cresswell, R. G. (1999) Denudation rates for the southern Drakensberg escarpment, SE Africa, derived from in-situ-produced cosmogenic ^{36}Cl : initial results. *Journal of the Geological Society, London*, 156, 209-212.
- Fujioka, T., Fifield, L. K., Stone, J. O., Vasconcelos, P. M. P., Tims, S. G., and Chappell, J. (2010), In situ cosmogenic ^{53}Mn production rate from ancient low-denudation surface in tropic Brazil, *Nuclear Instruments and Methods in Physics Research B*, 268, 1209-1213.
- Grainger, C. J., Groves, D. I., Tallarico F. H.B., and Fletcher I. R. (2008) Metallogenesis of the Carajás Mineral Province, Southern Amazon Craton, Brazil: Varying styles of Archean through Paleoproterozoic to Neoproterozoic base- and precious-metal mineralisation, *Ore Geology Review* 33, 451-489.
- Heim, J.A., Vasconcelos, P.M., Shuster, D.L., Farley, K.A. and Broadbent, G.C., 2006d. Dating palaeochannel iron ore by (U-Th)/He analysis of supergene goethite. *Geology*, 34(3): 173-176.
- Heimsath, A. M., Chappell, J., Finkel, R. C., Fifield, K., and Alimanovic, A. (2006) Escarpment erosion and landscape evolution in southeastern Australia, in Willet, S. D., Hovius, N., Brandon, M. T., and Fisher, D. M., eds., *Tectonics, Climate, and Landscape Evolution: Geological Society of America Special Paper 398, Penrose Conference Series*, p. 173-190.
- Hoorn, C. (1993), Marine incursions and the influence of Andean tectonics on the Miocene depositional history of northwestern Amazonia: results of a palynostratigraphic study, *Palaeogeography, Paleoclimatology, Paleoecology*, 105, 267-309.
- Hoorn, C., Wesselingh, F. P., ter Steege, H., Bermudez, M. A., Mora, A., Sevink, J., Sanmartín, I., Sanchez-Meseguer, A., Anderson, C. L., Figueiredo, J. P., Jaramillo, C., Riff, D., Negri, F. R., Hooghiemstra, H., Lundberg, J., Stadler, T., Sarkinen, T., and Antonelli, A. (2010) Amazonia

trough time: Andean uplift, Climate change, Landscape evolution, and Biodiversity, *Science*, 330, 927-931.

Huhn, S.R.B., Santos, A.B.S., Amaral, A.F., Ledsham, E.J., Gouveia, L.J., Martins, L.P.B., Montavo, R.M.G., Costa, V.C., (1988a), O terreno granite greenstone da regioao de Rio Maria — Sul do Pará. Congresso Brasileiro de Geologia, Belém, Anais, vol. 35, pp. 1438–1452.

Huhn, S.R.B., Santos, A.B.S., Amaral, A.F., Ledsham, E.J., Gougêa, J.L., Martins, L.P., Montalvão, R.G.M., Costa, V.G., (1988b), O terreno “granito greenstone” da região de Rio Maria — Sul do Pará. XXXV Congresso Brasileiro de Geologia, vol. 3, pp. 1438–1452.

King, L. C. (1956), A Geomorfologia do Brasil Oriental *Revista Brasileira de Geografia*, 2, 147-265.

Kotschoubey, B., Truckenbrodt, W., Hieronymus, B. (1997), Bauxite deposits of Paragominas. In: A. Carvalho, B. Boulangé, A.J. Melfi, Y. Lucas (eds.) *Brazilian Bauxites*. USP, FAPESP, ORSTOM, pp.: 75-106.

Lal, D. (1991), Cosmic ray labeling of erosion surfaces: in situ nuclide production rates and erosion models, *Earth and Planetary Science Letters*, 104, 424-439.

Levett, A., Gagen, E., Shuster, J., Rintoul, L., Tobin, M., Vongsivut, J., Bamberg, K., Vasconcelos, P., and Southam, G. (2016), Evidence of biogeochemical processes in iron duricrust formation, *Journal of South America Earth Sciences*, 71, 131-142.

Machado, N., Lindenmayer, Z., Krogh, T.E., Lindenmayer, D., 1991. U–Pb geochronology of Archean magmatism and basement reactivation in the Carajás area, Amazon Shield, Brazil. *Precambrian Research* 49, 329–354.

Maaskant P. and Kaper H. (1991) Fluorescence effects at phase boundaries: petrological implications for Fe-Ti oxides. *Mineral. Mag.* 55, 277-9.

Monteiro, H. S., Vasconcelos, P. M. P., Farley, K. A., Spier, C. A., and Mello, C. L. (2014), (U-Th)/He geochronology of goethite and the origin and evolution of cangas, *Geochimica et Cosmochimica Acta*, 131, 267-289.

Monteiro, H. S., Vasconcelos, P. M. P., and Farley K.A. (2017a) A combined (U-Th)/He and cosmogenic ^3He record of landscape armoring by biogeochemical iron cycling. *JGR Earth Surface*, submitted.

- Monteiro, H. S., Vasconcelos, P. M. P., and Farley K. A. (2017b) On goethite as a (U-Th)/He and $^4\text{He}/^3\text{He}$ geochronometer, Chapter 3 (this thesis).
- Netuno Villas, R., and Santos, M. D. (2001) Gold deposits of the Carajás mineral province: deposit types and metallogenesis, *Mineralium Deposita*, 36, 300-331.
- Patterson, D. B., and Farley, K.A. (1998), Extraterrestrial ^3He in seafloor sediments: Evidence for correlated 100 kyr periodicity in the accretion rate of interplanetary dust, orbital parameters, and Quaternary climate, *Geochimica et Cosmochimica Acta*, 62(23/24), 3669-3682.
- Petri, S. and Fúlfaro, V. J. (1983) *Geologia do Brasil (Fanerozóico)*, - São Paulo: T. A. Queiroz: Ed. da Universidade de São Paulo, p. 631.
- Rezende, N. P. and Barbosa, L. M. (Eds.) (1972), *Relatório de Pesquisa de Minério de Ferro, Distrito Ferrífero da Serra dos Carajás, Estado do Pará - Brasil - Volume II*.
- Riffel, S.B., Vasconcelos, P.M., Carmo, I.O., Farley, K.A., 2015. Combined $^{40}\text{Ar}/^{39}\text{Ar}$ and (U-Th)/He geochronological constraints on long-term landscape evolution of the Second Paraná Plateau and its ruiniform surface features, Paraná, Brazil. *Geomorphology* 233, 52–63. <http://dx.doi.org/10.1016/j.geomorph.2014.10.041>.
- Ruffet, G., Innocent, C., Michard, A., Féraud, G., Beauvais, A., Nahon, D., Hamelin, B., 1996. A geochronological $^{40}\text{Ar}/^{39}\text{Ar}$ and $^{87}\text{Rb}/^{81}\text{Sr}$ study of K–Mn oxides from the weathering sequence of Azul, Brazil. *Geochim. Cosmochim. Acta* 60, 2219–2232. [http://dx.doi.org/10.1016/0016-7037\(96\)00080-4](http://dx.doi.org/10.1016/0016-7037(96)00080-4).
- Santos, P. A. dos (2006) Estudo de densidades de rochas e comparação de técnicas de medição, Região do Quadrilátero Ferrífero, Minas Gerais, Brasil, Dissertação de Mestrado, ISEI: p. 58.
- Schmidt, K.-H. (1999) The significance of scarp retreat for Cenozoic landform evolution on the Colorado Plateau, U.S.A. *Earth Surface Processes and Landforms* 14, 93-105.
- Scotese, C. R. (2001) *Atlas of Earth History, Volume 1, Paleogeography, PALEOMAP Project*, Arlington, Texas, 52 pp.
- Shepard, G. E., Müller, R. D., Liu, L., and Gurnis, M. (2010) Miocene drainage reversal of the Amazon river driven by plate-mantle interaction. *Nature Geosciences*, vol. 3, 870-875.
- Shuster, D. L., Vasconcelos, P. M. P., Heim, J. A., and Farley, K. A. (2005), Weathering geochronology by (U-Th)/He dating of goethite, *Geochimica et Cosmochimica Acta*, 69(3), 659-673.

- Shuster, D. L., Farley, K. A., Vasconcelos, P. M. P., Balco, G., Monteiro, H. S., Waltenberg, K., and Stone, J. O. (2012), Cosmogenic ^3He in hematite and goethite from Brazilian "canga" duricrust demonstrates the extreme stability of these surfaces, *Earth and Planetary Science Letters*, 329-330, 41-50.
- Stone, J. O. (2000), Air pressure and cosmogenic isotope production, *Journal of Geophysical Research*, 105(B10), 23,753-723,759.
- Trendall, A.F., Basei, M.A.S., Laeter, J.R., Nelson, D.R., 1998. SHRIMP zircon U–Pb constraints on the age of the Carajás formation, Grão Pará Group, Amazon Craton. *Journal of South American Earth Sciences* 11, 265–277.
- Tolbert, G.E., Tremaine, J.W., Melcher, G.C., Gomes, C.B., 1971. The recently discovered Serra dos Carajás iron deposit, northern Brazil. *Economic Geology* 66, 985–994.
- Truckenbrodt, W. and Kotschoubey, B. (1981), Argila de Belterra - Cobertura terciária das bauxitas Amozônicas, *Revista Brasileira de Geociências* 11 (3): 203-208.
- Vasconcelos, P. M. P., Rene P. R., Brimhall G. H., and Becker T. A. (1994), Direct dating of weathering phenomena by $^{40}\text{Ar}/^{39}\text{Ar}$ and K-Ar analysis of supergene K-Mn oxides, *Geochimica et Cosmochimica Acta*, 58(6), 1635-1665.
- Vasconcelos, P. M. P (2002), $^{40}\text{Ar}/^{39}\text{Ar}$ geochronology of supergene processes in ore deposits, *Reviews in Economic Geology*, 12, 73-113.
- Vasconcelos, P. M. P and Conroy, M. (2003) Geochronology of weathering and landscapes evolution, Dugald River valley, NW Queensland, Australia, *Geochimica et Cosmochimica Acta*, 67, 2913-2930.

Chapter 5: Development and implementation of suitable protocols for *in situ* measurement of oxygen isotopes in goethite by ion microprobe

Monteiro, H.S.^{1*}, Vasconcelos, P.M.^{1,3}, Ávila, J.N.², Holden, P.², Miller H.³, Ireland, T.R.², and Farley, K.A.³

¹*School of Earth and Environmental Sciences, The University of Queensland, Brisbane, Queensland 4072, Australia*

²*Research School of Earth Sciences, The Australian National University, Canberra, ACT 2601, Australia*

³*Division of Geological and Planetary Sciences, California Institute of Technology, Pasadena, CA 91125, USA*

To be submitted to Chemical Geology

** Corresponding author:*

H.S. Monteiro

The University of Queensland

Earth and Environmental Sciences, Steele Building

Brisbane, Qld 4072

Phone: (61)(7) 3346-7636 (Office)

ABSTRACT

We present new protocols for high-spatial resolution measurement of oxygen isotope ratios of goethite (α -FeOOH) with the Sensitive High Mass Resolution Ion Microprobe – Stable Isotopes (SHRIMP-SI) and propose a natural sample as a potential goethite reference material (RM) for the ion microprobe. We assess the effects of crystallographic orientation, goethite texture, and composition on the accuracy and reproducibility of SHRIMP-SI $\delta^{18}\text{O}$ ($\delta^{18}\text{O}_{\text{SIMS}}$) results. Synthetic goethites evaluated as potential $\delta^{18}\text{O}_{\text{SIMS}}$ RM are powdery, porous, and finely crystalline; they do not yield reproducible results. A dense colloform stoichiometric goethite from the Capão Mine, Minas Gerais, Brazil, fulfills major prerequisites: it is relatively pure, yields reproducible results, and occurs in large enough abundance to produce RM for long-term use. A laser fluorination $\delta^{18}\text{O}$ value of $-17.22 \pm 0.03 \text{ ‰}$ (1σ) was obtained for an aliquot of this RM. Multiple $\delta^{18}\text{O}_{\text{SIMS}}$ analyses of individual grains of the Capão L4 RM yield an average precision of $\pm 0.6 \text{ ‰}$ (2σ). Grain-to-grain variability of $\delta^{18}\text{O}_{\text{SIMS}}$ measurements of the Capão L4 RM was often better than $\pm 1.5 \text{ ‰}$ (2σ). Natural variability [$\pm 0.6 \text{ ‰}$ on average (2σ)] and crystal orientation effect [$\sim 2 \text{ ‰}$ (2σ)] are the main reasons for the worsening of precision of the $\delta^{18}\text{O}_{\text{SIMS}}$ results. Using Capão L4 as RM, goethite samples were analysed to test the relationship between natural properties (e.g., porosity, minor element content), preparation procedures (e.g., polish and relief), instrument conditions, and the overall reproducibility and reliability of the $\delta^{18}\text{O}_{\text{SIMS}}$ results. Porous samples are unsuitable for SHRIMP-SI $\delta^{18}\text{O}$ analysis, and samples containing $> 2\text{wt\% Al}$ may require significant matrix corrections. Dense colloform samples yield reproducible results for individual growth bands, showing that the high spatial resolution, moderate precision, and speed of analysis of the SHRIMP-SI can resolve variations in oxygen isotope composition acquired during sample growth. (U-Th)/He dating of equivalent aliquots from the same goethite samples reveal that the combination of the two methods permits extracting temporal variation in the isotopic compositions of meteoric solutions in the geological past.

1. INTRODUCTION

The oxygen isotope composition of goethite (α -FeOOH) is a useful environmental indicator applied in the reconstruction of the isotopic signature of ancient waters and past surface temperatures on Earth (Yapp, 1987, 1993, 1997, 2000, 2008; Bird et al., 1992, 1993; Girard et al., 1997, 2000, 2002; Poage et al., 2000; Sjöström et al., 2004; Yapp and Shuster, 2011; Miller et al., 2017). The basic assumption of goethite as an environmental indicator is that it precipitates in isotopic equilibrium with water carrying the dissolved oxygen species, and that the goethite-water $^{18}\text{O}/^{16}\text{O}$ fractionation factor $\alpha_{(\text{gth-water})}$ – determined from mineral precipitation experiments, calculated theoretically, or derived from mineral-water exchange reactions – is well known. Fractionation factors depend on temperature, and there are a number of competing equations derived for the $\alpha_{(\text{gth-water})}$ –temperature dependence (Yapp, 1990, 2012; Müller, 1995; Bao and Koch, 1999; Zheng, 1998). The discrepant regression lines proposed for the $\alpha_{(\text{gth-water})}$ –temperature dependence reflect the fact that $\alpha_{(\text{gth-water})}$ also depends on pH, solution composition, and rate of precipitation, posing challenges in recovering environmental information from the oxygen isotope composition of natural goethites.

Determining the isotopic composition of natural goethites is not without its own challenges. Traditional methods for stable isotope analysis using fluorination and carbon reduction require ~ 20 mg of material (Yapp, 1987). Modern laser fluorination techniques offer the advantage of requiring < 2 mg of pure sample (Girard et al., 1997). Both approaches have been successfully used in measuring the $\delta^{18}\text{O}$ value of natural goethites from diverse settings, and they permit deriving relevant information about paleoenvironments (e.g., Bird et al., 1992; Poage et al., 2000; Bao et al., 2000; Miller et al., 2017).

Despite these successes, a major challenge in determining the isotopic composition of goethites is the fact that most natural goethites form colloform aggregates of finely distributed crystals oriented parallel to the direction of mineral precipitation (Figure 1a). Colloform goethites form sequential bands that may span millions of years (Heim, 2016; Vasconcelos et al., 2013). Parental solutions change in composition through time, as revealed by the variations in minor and trace element compositions of the various goethite bands. In addition, goethite masses often show evidence for partial dissolution before resumption of colloform growth (Figure 1b), contain cross-cutting veins of late-stage goethite generations (Figure 1b), and may be intimately intergrown with hypogene or supergene mineral phases (quartz, kaolinite, gibbsite, cryptomelane, cuprite, malachite, etc.) (Figure 1b) with drastically distinct isotopic compositions. Bulk analysis of these samples produces a composite $\delta^{18}\text{O}$ value for the distinct generations of goethite plus the potential mineral contaminants likely present within the goethite masses (chemical analysis and material balance

calculations must be applied to derive the $\delta^{18}\text{O}$ value of the end-member goethite; Yapp, 1987). Therefore, to determine the $\delta^{18}\text{O}$ value of a single generation of goethite that may have precipitated in equilibrium with a particular meteoric solution in the past, the isotopic composition of the goethite must be determined at the scale (μm to mm) of the colloform growth bands typical of natural samples.

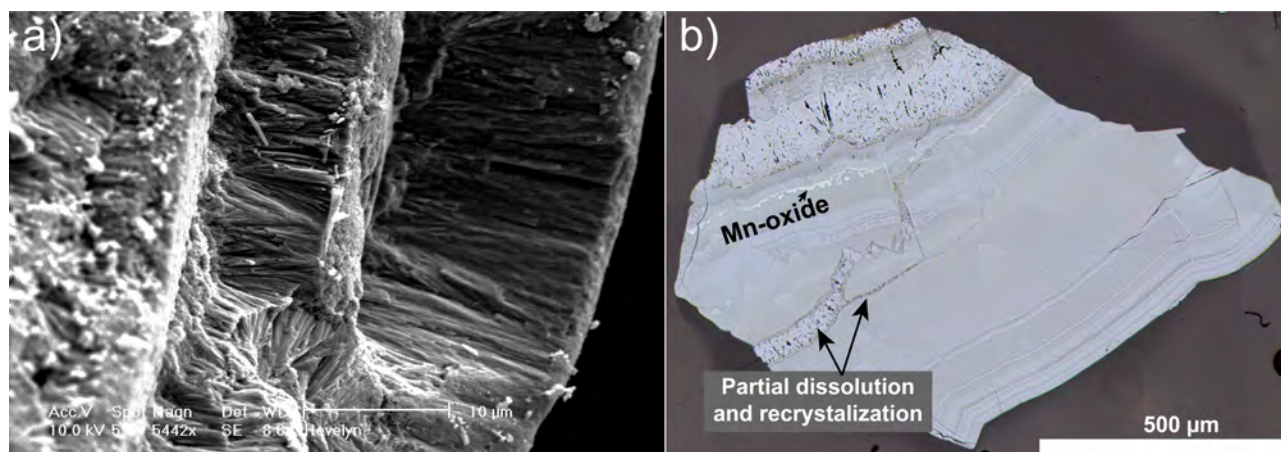


Figure 1: a) SEM image of goethite bands showing μm -size crystals orientated parallel to the direction of growth. b) Goethite grain showing partial dissolution and recrystallization features. Bulk $\delta^{18}\text{O}$ analysis will only retrieve average results for these samples. *In situ* SHRIMP-SI measurement resolves the $\delta^{18}\text{O}$ value of each generation, and permits retrieving environmental information for specific periods of mineral precipitation.

Access to the Sensitive High Resolution Ion Microprobe – Stable Isotopes (SHRIMP-SI) (Ireland et al., 2008) at the Research School of Earth Sciences, Australian National University, offers a unique opportunity to determine the oxygen isotope composition of goethite at scales necessary to resolve single mineral precipitation events, potentially resolving the isotopic composition of single rainfall events in the geological past. The additional advantage of the approach illustrated in this study is that, by combining SHRIMP-SI $^{18}\text{O}/^{16}\text{O}$ measurements with laser-heating (U-Th)/He dating of the same goethite sample, it may be possible to produce time-calibrated goethite $\delta^{18}\text{O}$ values. The spatial resolution of the (U-Th)/He method ($\sim 400 \mu\text{m}$), when combined with the spatial resolution of SHRIMP-SI $^{18}\text{O}/^{16}\text{O}$ analysis ($\sim 25 \mu\text{m}$), offers the opportunity to study, at previously unattainable scales, environmental conditions during mineral precipitation at specific times in the geological past.

Oxygen isotopic measurements of goethite with the SHRIMP-SI bring its own challenges. Probably the greatest challenge is the need for, and lack of, a well-characterized reference material (RM). Other challenges are sample- and instrument-related, such as the potential dependence of ionization efficiency and instrumental mass fractionation on crystallographic orientation, sample porosity, texture, polishing (e.g., relief), and minor and trace element contents (e.g., Kita et al., 2009, 2010; Eiler et al., 1997; Vielzeuf et al., 2005; Ickert and Stern, 2013). We will first address these four

issues: the characterization and validation of a suitable goethite reference material for *in situ* measurements of oxygen isotopes by the SHRIMP-SI; the investigation of crystallographic effects on measured $\delta^{18}\text{O}$ values, with suggestions on suitable approaches for obviating this problem; the characterization of sample-related parameters that may affect isotopic analysis with the SHRIMP-SI and guidelines on sample selection criteria to maximize the chance of successful $\delta^{18}\text{O}_{\text{SIMS}}$ analysis; and sample preparation procedures that will ensure reliable analytical results.

2. SUITABLE SHRIMP-SI $^{18}\text{O}/^{16}\text{O}$ GOETHITE REFERENCE MATERIAL

A suitable reference material (RM) must show homogenous chemical and isotopic compositions, and exist in large enough quantity to yield material that, once characterized and validated, can be made available to the wider scientific community for independent comparisons. The greatest difficulty in finding a suitable goethite RM lies in the fact that supergene goethites either precipitate as (1) cements metasomatically replacing previously existing phases, which potentially host large amounts of mineral contaminants and variable minor/trace element composition, at the μm to cm scale, inherited from the replaced phases; (2) they occur as replacement of wood and organic matter, forming porous goethites mimicking the cellular structure of the replaced organic matter; and, when (3) pure and precipitated directly from solution in empty cavities, they form colloform masses that change chemical and possibly isotopic composition at the μm -, mm-, or cm-scale and in the direction of growth. We focussed on the third genetic type, the most likely to yield sufficient quantities of pure, massive, and compositionally homogeneous goethite. From a suite of several hundred goethite samples collected over two decades from various weathering profiles in Brazil, Australia, New Caledonia, Africa, China, and the USA, we targeted four suitable candidates, from which we had previous information on age and compositional homogeneity, to test whether these samples were also isotopically homogeneous and potentially suitable as reference materials. These four RM candidates are briefly described below.

Capão

The Capão goethite is dense, massive, colloform, and well crystallized (Figure 2 a-c). This goethite sample is a ~ 10 cm pebble collected from a colluvium near the Capão Topaz Deposit, Minas Gerais, Brazil. Its chemical and mineralogical purity, as determined by electron microprobe analysis and X-ray diffractometry, its colloform habit, and the absence of primary mineral contaminants suggest precipitation in an empty cavity. Acicular goethite crystals are closely packed with the b-axis oriented in the direction of sample growth. Rare late-stage veins of (Pb,Ba)-rich Mn-oxide (coronadite) may be present. Several of the visually distinct growth bands (Figure 2a, 1-5) were

selected as potential standard material, micro-sampled with a 5-mm ID diamond drill-bit, crushed, homogenized, and analysed as described below.

Roy Hill

The Roy Hill goethite is also dense, massive, and well crystallized (Figure 2 d-f). It was sampled from colluvia at the foot of the Chichester Ranges, Hamersley Province, Western Australia (Heim, 2006; Vasconcelos et al., 2013). Its habit and purity also suggest precipitation in open cavities (Vasconcelos et al., 2013). The Roy Hill goethite shows a radiating fan-shaped texture of elongated fibrous crystals.

Winsor

The Winsor goethite is a dense, massive visually pure colloform goethite band deposited on a detrital fragment of strongly ferruginised metasedimentary rock from the Winsor Ridge, Flinders Ranges, South Australia (Figure 2g). The relatively large mass of pure goethite and previously reproducible (U-Th)/He results for several grains from this sample (Waltenberg, 2012) suggest that the selected band from the Winsor sample could provide a suitable RM.

Stop-1-D1

The Stop-1-D1 goethite occurs as stalactitic and stalagmitic cavity fills in a deeply weathered banded iron formation horizon from the Metawandy Valley, Hamersley Province, Western Australia (Figure 2j) (Heim, 2006). Amalgamation of different stalactites and stalagmites during growth creates a complex pattern in crystal orientation (Figure 2k), but the mode of precipitation suggests that this goethite should be pure and potentially suitable as a RM.

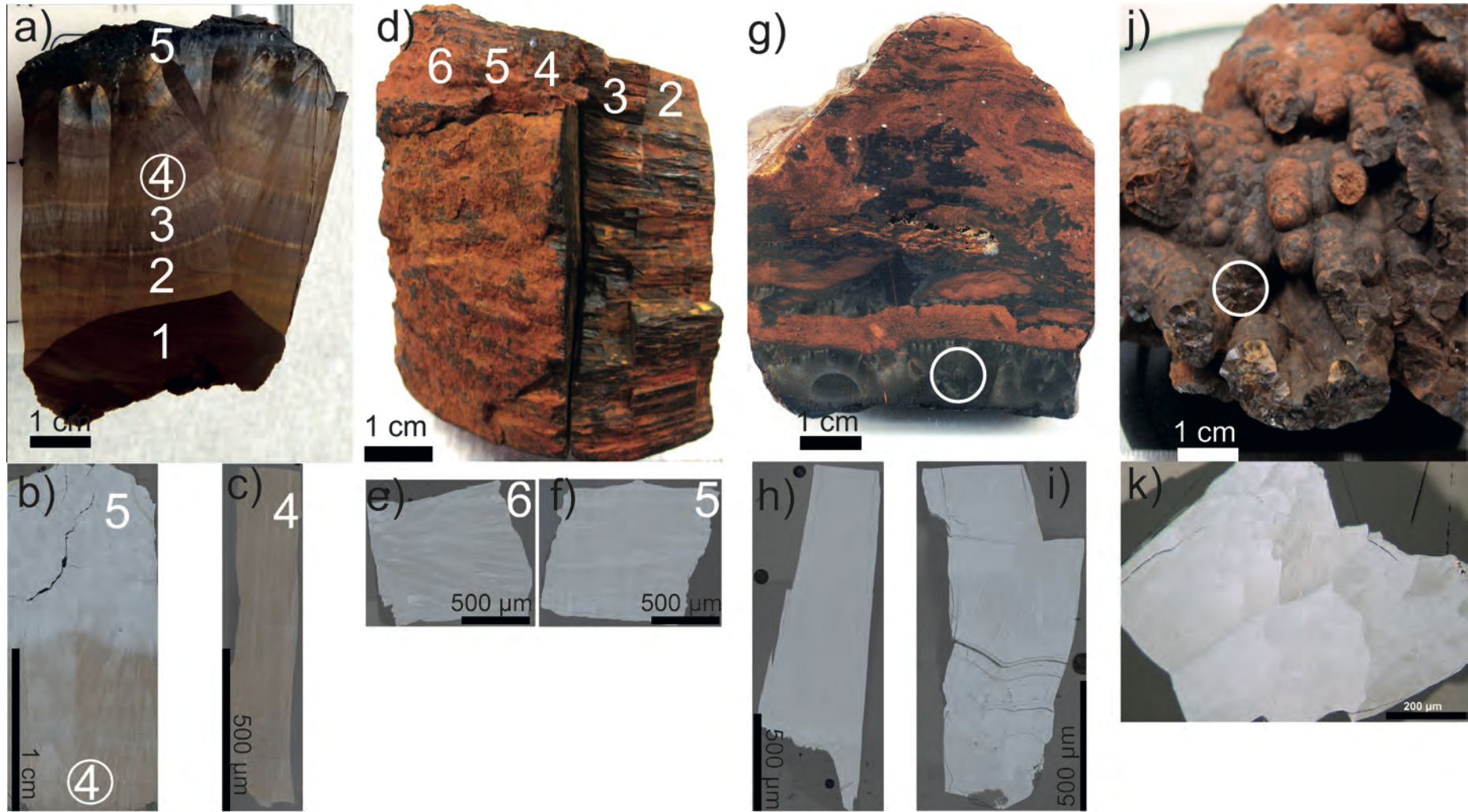
**Capão****Roy Hill****Winsor****Stop-1-D1**

Figure 2: Four natural samples selected as potential goethite $^{18}\text{O}/^{16}\text{O}$ reference material for the SHRIMP-SI. These samples all share some common features: they are colloform, appear to have precipitated in empty cavities, they are relatively pure (as previously determined by electron microprobe analyses), and (U-Th)/He ages for distinct bands from these samples are reproducible, suggesting a narrow interval of mineral precipitation. SEM photomicrographs for the samples reveal individual goethite crystallites with the long axis (b-axis) oriented in the direction of colloform growth, suggesting that sample fragments mounted for SHRIMP-SI analysis will have similar crystallographic orientations. Sample Stop-1-D1, precipitated by stalagmitic and stalactitic growth into a cavity, is an exception and it displays crystals in random orientations (Fig. 2k).

3. ANALYTICAL TECHNIQUES

Hand samples were photographed and selected areas were targeted for optical and scanning electron microscopy (SEM), electron microprobe analysis (EPMA), X-ray diffraction (XRD), (U-Th)/He geochronology, laser fluorination, and SHRIMP-SI oxygen isotope analysis. Visually pure goethite fragments were micro-drilled from selected growth bands or physically broken from the samples. Micro-cores (~1-2 cm long and 5 mm internal diameter (ID)) and fragments were crushed to 0.1 – 2 mm grains, ultrasonicated in tap water (~ 30 min), distilled water (5 – 10 min), rinsed in ethanol, and air-dried. Clean goethite grains were mounted in 2.6 cm ID acrylic disks specially designed for the SHRIMP-SI during this study (EA1), filled with epoxy, polished, imaged by optical and electron microscopy, and investigated by EPMA before or after ion microprobe analysis. In addition to goethite aliquots, cm-size fragments from selected samples were also mounted in epoxy and analyzed by ion microprobe.

3.1. Optical and Scanning Electron Microscopy

Polished blocks and thin-sections were investigated by transmitted- and reflected-light optical microscopy and by SEM to determine goethite textures, mineral assemblages, paragenetic relationships, modes of precipitation, and sample purity. Only samples deemed pure and devoid of contaminants were selected for further consideration.

3.2. Electron Microprobe Analysis

Electron microprobe analyses were performed with a JEOL JXA-8200 at the Centre for Microscopy and Microanalysis (CMM) of the University of Queensland, Brisbane, Australia. Standards and unknowns were carbon coated under the same conditions. Analyses were performed using a beam current of 15 nA, accelerating voltage of 15 kV, and highly focused spot size (except for more volatile elements, for which spot size was 10 μm). Between 14 and 21 elements were measured in each individual analytical session using the following standards and calculated detection limits: **O** (fayalite ORNL-263 std.; 601-255 ppm), **Na** (Cazadero albite std.; 293-138 ppm), **Mg** (diopside Checterman-358 std.; 133-83 ppm), **Al** (Al_2O_3 -913 std.; 91-64 ppm), **Si** (fayalite ORNL-263 std.; 124-90 ppm); **P** (Cl-apatite synthetic-283 std.; 220-130 ppm), **S** (chalcopyrite UC-1232 std.; 149-75 ppm), **K** (orthoclase MAD10-374 std.; 146-98 ppm), **Ca** (diopside Checterman-358 std.; 494-140

ppm), **Ti** (TiO₂-922 std.; 506-251 ppm), **V** (V₂O₃-923 std.; 758-212 ppm), **Cr** (Cr metal-524 std.; 730-174 ppm), **Mn** (MnO-925 std.; 373-168 ppm), **Fe** (fayalite ORNL-263 std.; 416-198 ppm), **Co** (CoO-927 std.; 397-178 ppm), **Ni** (NiO-928 std.; 452-202 ppm), **Cu** (Cu metal-529 std.; 517-241 ppm), **Zn** (ZnO-930 std.; 646-306 ppm), **Pb** (galena UC-7400 std.; 656-324 ppm), **Ba** (barite std.; 555-368 ppm), and **Sr** (Sr titanite std.; 287-285 ppm).

3.3. X-ray Diffraction

Candidates for reference material were analysed by bench-top powder XRD, following analytical and data reduction procedures outlined in Monteiro et al. (2017b), to ascertain that goethites were indeed pure and well crystallized. Some of the samples (Roy Hill and Winsor) were also analysed by synchrotron X-ray diffractometry at the Australian National Beamline Facility (ANBF), Photon Factory, National Laboratory for High Energy Physics (KEK), Tsukuba, Japan, as outlined in Heim (2006), Waltenberg (2012), Vasconcelos et al. (2013).

3.4. Synthetic Goethite

Goethite powders were precipitated at various temperatures (22, 30, and 40°C) and distinct pHs (<2 and >12) (Mostert 2014). For the high pH experiments, solutions were prepared by adding 125 ml of 1 M Fe(NO₃)₃·9H₂O to 125 ml of 5 M KOH into high density polyethylene (HDP) bottles. For the low pH experiments, 350 ml of 1 M Fe(NO₃)₃·9H₂O plus 175 ml 2 M HNO₃ were diluted with 175 ml H₂O. 140 ml of this bulk solution was then mixed to 140 ml of 1 M NaOH in a HDP bottle. The solutions were stored in 500 ml bottles for a minimum period of 74 days. Goethite precipitates were split in three or more 50 ml falcon tubes, topped up with clean H₂O, and centrifuged for 28 min. The supernatant was then decanted, the falcon tube filled with clean H₂O a second time, and sonicated for 15 min. The falcon tube containing the goethite residue and clean water was once again centrifuged for the same period. This procedure was repeated at least three times to ensure that all unwanted salts were removed. All precipitates were dried in air and stored in closed falcon tubes (Mostert 2014).

3.5. (U-Th)/He analysis

Several aliquots of goethite extracted from the potential RM were analysed by (U-Th)/He geochronology at Caltech, USA, following the procedures outlined in Monteiro et al. (2014). For He extraction, individual goethite aliquots were encapsulated in Pt tubes, loaded into wells in a copper disk, placed in a sample chamber, and heated (900 °C) with a diode laser under vacuum. To ensure total He extraction, Pt capsules were heated a second time for the same amount. After He extraction was completed, degassed samples were carefully transferred to Teflon containers where

they were dissolved in concentrated Seastar™ HCl (closed vials were placed in the oven at 90°C for 12h), spiked with known concentrations of ^{235}U and ^{230}Th , evaporated and re-dissolved in concentrated Seastar™ HNO_3 , diluted in Milli-Q water and analysed by ICP-MS.

3.6. Laser fluorination analysis

Reference material candidates (except for Roy-L5 and Roy-L6) were analysed by laser fluorination at the Stable Isotope Laboratory at Caltech following procedures outlined in Miller et al. (2017). The reported $\delta^{18}\text{O}$ values are single measurements carried in 1-2 mg of sample. Total yield varied between 93 and 108% (except for sample Win-06-01B for which yield was 36.7%). Several aliquots of the UWG-2 garnet standard measured throughout the runs yield average $\delta^{18}\text{O}_{\text{vsmow}}$ values of $5.4 \pm 0.1 \text{ ‰}$ (1σ) and $5.51 \pm 0.01 \text{ ‰}$ (1σ). $\delta^{18}\text{O}$ values of unknowns were corrected for the difference between measured and accepted values (5.8‰) of the UWG-2 garnet standard (Valley et al., 1995).

3.7. *In situ* analysis of oxygen isotopes by SHRIMP-SI

To improve efficiency in sample preparation and polish, avoid sample identification errors, ensure that samples were placed only within the area where mount geometry effects are negligible, and enable the analysis of the same grains in different instruments, we designed and manufactured a special SHRIMP acrylic disk sample holder for this study (EA1). Clean goethite aliquots from individual samples, subsampled from the same aliquots used for (U-TH)/He geochronology, were placed in individual pits in the 37-pit disk mount. Loaded disks were filled with epoxy under vacuum to minimize air bubbles. Sample mounts were lapped, polished to $.25 \text{ }\mu\text{m}$, and imaged with a Leica DM6000M automated microscope. Some samples, for which standard petrographic microscope slides had been previously prepared, had selected areas of the slide micro-drilled with an ultrasonic disk cutter. Glasses were then mounted in epoxy together with reference materials. All mounts were cleaned with detergent and ethanol, dried in vacuum at $60 \text{ }^\circ\text{C}$, coated with gold, and kept under vacuum at $60 \text{ }^\circ\text{C}$ for at least two days before analysis. Unknowns were analysed in sequences of 10-12 analyses intercalating with primary and secondary reference materials to correct for instrumental drift. In addition, in five sessions, the in-house magnetite RM was also analysed for monitoring the stability of the instrument.

Oxygen stable isotope measurements were carried out during nine analytical sessions, from October 2014 to September 2017, at the SHRIMP Laboratory, The Australian National University, Canberra, Australia. All measurements were performed using the SHRIMP-SI (Ireland et al., 2008, 2014). Sputtering of goethite grains was done with a Cs^+ primary beam operating with acceleration potential of +5 kV. At the sample surface, the acceleration potential was held at $\sim -10 \text{ kV}$,

producing the final collision energy of 15 keV at the target (Ireland et al., 2014). An elliptical beam spot of $\sim 20 \times 25 \mu\text{m}$ was used for all sessions. The low and high mass head detectors equipped with Faraday cups were used for simultaneous detection of $^{16}\text{O}^-$ and $^{18}\text{O}^-$. The electrometers measuring $^{16}\text{O}^-$ and $^{18}\text{O}^-$ were set to $10^{11} \Omega$ (50V range) and $10^{11} \Omega$ (5V range), respectively. For the oxygen isotope measurements presented here the collector slit widths were set at 400 μm for $^{16}\text{O}^-$ and 300 μm for $^{18}\text{O}^-$. Potential isobaric interferences on $^{18}\text{O}^-$ from $^{17}\text{OH}^-$ and $^{16}\text{OD}^-$ were well resolved. Oxygen measurements consisted of five or six acquisition cycles of 20s, each corresponding to 10 repeats of 2s for a total acquisition time of about 2 min on peak. The $^{18}\text{O}/^{16}\text{O}$ ratio is the weighted average of five or six sets. $\delta^{18}\text{O}_{\text{SIMS}}$ values were calibrated (i.e., corrected for instrumental bias) against our goethite RM of known oxygen isotope composition. Data reduction was carried using the ANU in house software “POXY”.

4. RESULTS

4.1. Electron microprobe analysis

Figure 3 and Table 1 illustrate the elemental composition of representative goethite grains analysed in this study; complete analytical results are available in EA2. For comparison purposes, we illustrate the composition of the goethites selected as potential candidates for SHRIMP-SI RMs (a, c, e) against the compositions of several goethite samples from many sites in Australia and Brazil (b, d, f) for which we have electron microprobe analysis. The goethite samples selected as SHRIMP-SI RMs show stoichiometric concentrations of Fe and O (Figure 3a) and usually less than $\sim 2 \text{ wt}\%$ total minor and trace element contents (Figure 3b). Compared to the other natural samples, the goethites selected as potential reference material are the most homogeneous and purest stoichiometric natural goethites that we have been able to identify.

To avoid matrix effect uncertainties associated with the effect of trace elements on the $\delta^{18}\text{O}_{\text{SIMS}}$ value of a goethite RM, we precipitated pure stoichiometric synthetic goethite at various temperatures following the procedures of Mostert (2014) and investigated their potential suitability as SHRIMP-SI RM. Given their purity, known temperature of precipitation, and the known composition of the water from which the FeOOH precipitated, we thought that these synthetic samples would provide an appropriate reference material for the SHRIMP-SI. As discussed below, the finely crystalline texture of the synthetic material, its porous nature, and the heterogeneous nature of pellets produced when the synthetic powders were agglomerated under a 10-30-ton/cm² hydraulic press demonstrated that synthetic goethite is not suitable as a SHRIMP-SI RM.

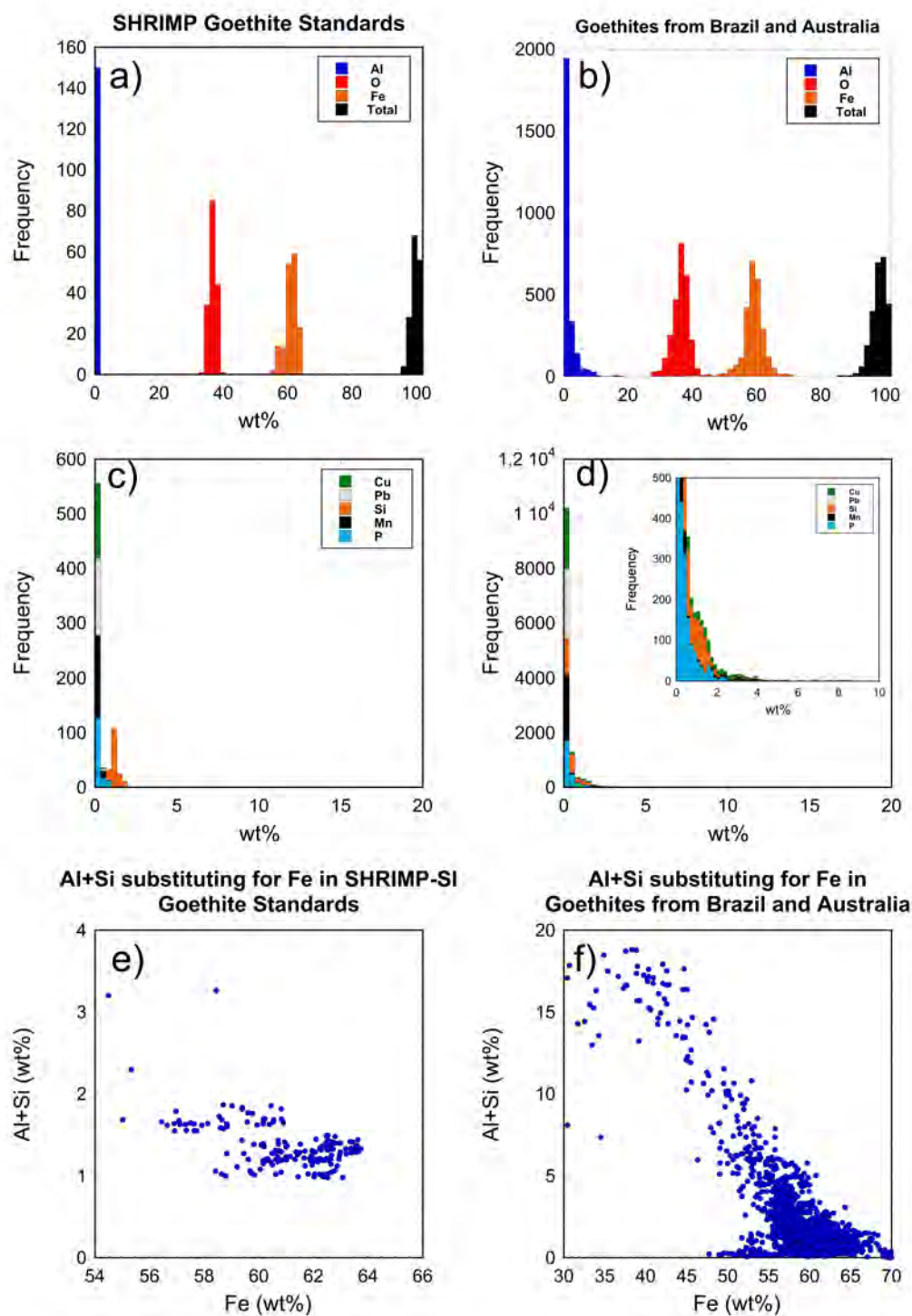


Figure 3: Electron microprobe analyses (a, c, e) for representative grains from each sample illustrated in Figure 2 reveal a population compatible with relatively pure stoichiometric goethite, except for a slight Si enrichment (and consequent Fe depletion) in some of the analysis. The samples selected as potential reference material show lower minor element contents than that observed for a large population of natural goethites (b, d, f) from weathering profiles in Brazil (Carajás and Quadrilátero Ferrífero) and Australia (Hamersley Province).

Table 1: Elemental composition of SHRIMP goethite standard candidates

	Capao L4	Roy L5	Roy L6	Win 06 03A	Win 06 01B	Stop 1 D1
Element	(wt%)	(wt%)	(wt%)	(wt%)	(wt%)	(wt%)
O	35.78	37.44	37.59	36.94	36.99	37.73
Na	0.01	0.04	0.02	0.01	0.02	0.07
K	0.00	0.01	0.00	0.02	0.01	0.00
V	0.00	0.00	0.01	0.03	-	0.01
Co	0.07	0.05	0.06	0.08	0.08	0.00
Mg	0.11	0.02	0.00	0.16	0.05	0.16
P	0.02	0.01	0.02	0.26	0.05	0.76
Cr	0.01	0.00	0.01	0.00	0.01	-0.01
Fe	61.21	60.04	60.65	57.77	62.41	58.44
Al	0.12	0.11	0.13	0.34	0.12	0.02
S	0.03	0.03	0.01	0.01	0.02	0.01
Ni	0.01	0.00	0.00	0.02	0.01	-0.01
Mn	0.05	0.55	0.62	0.21	0.25	0.09
Si	1.12	1.08	1.08	1.57	0.98	1.37
Pb	0.26	0.02	0.02	0.05	0.04	-0.01
Cu	0.02	0.01	0.00	0.14	0.02	0.00
Ti	0.00	0.03	0.01	0.02	0.02	0.00
Ca	0.00	0.00	0.00	0.11	0.07	0.20
Zn	0.03	0.01	0.03	0.38	0.01	0.02
Ba	-	-	-	0.03	0.04	-
Sr	-	-	-	-	0.01	-
Cl	-	-	-	0.01	-	-
Total	98.83	99.44	100.25	98.14	101.21	98.85

4.2. XRD

Figure 4 illustrates XRD patterns for samples selected as potential SHRIMP-SI RM to show that the samples are composed of crystalline goethite devoid of significant amounts of contaminants within the resolution of the method. XRD patterns for Roy and Win-01B goethites reveal small quartz peaks. Rietveld refinement for a representative aliquot of the CAPÃO sample indicates that goethite is the only identifiable mineral. Trace veins of Mn oxides, detectable by reflected-light optical microscopy, are not detectable by XRD (Figure 4).

4.3. (U-Th)/He ages

(U-Th)/He ages for replicate aliquots of our goethite SHRIMP-SI RM candidates are summarized in Table 2. The samples yield reproducible or very narrow ranges of results for the replicates, suggesting that, at least within the spatial and chronological resolution of the (U-Th)/He method, they are homogeneous and potentially suitable as SHRIMP-SI RM. Most SHRIMP-SI goethite RM candidates show low U (< 10 ppm) and Th (< 1 ppm) contents (sample Win 06 03A is an exception for which U and Th concentrations range between 150 – 317 ppm and 9 – 18 ppm, respectively). (U-Th)/He ages range from ~ 284 to ~ 3 Ma. Th/U ratios are low for all goethite SHRIMP-SI RM candidates.

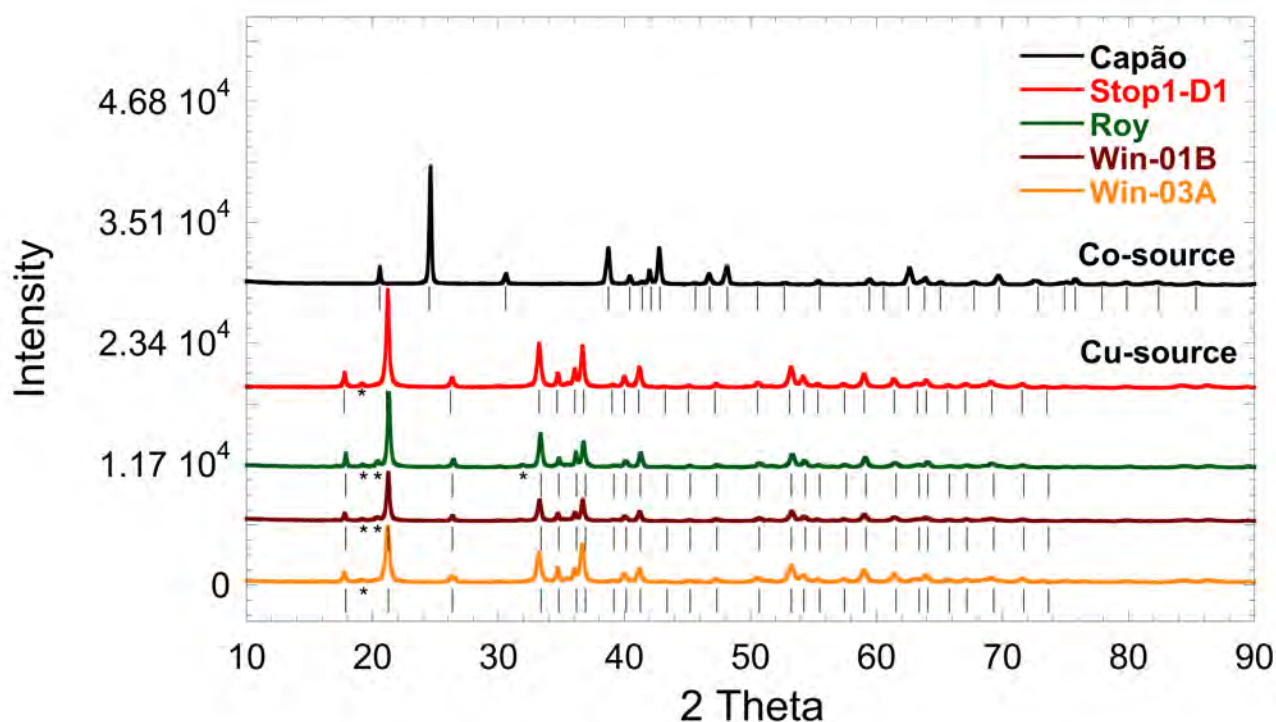


Figure 4: X-ray diffraction analysis reveals that samples considered as RM consist of pure α -FeOOH (lines indicate goethite x-ray diffraction peaks) and are free from any detectable amounts of contaminants, except perhaps for some silica polymorph (*).

4.4. Laser fluorination analysis

SHRIMP-SI RMs Capão L4, Capão L2, Win-06-03A, and Stop1-6-D1 yield laser fluorination $\delta^{18}\text{O}$ values of $-17.22 \pm 0.03 \text{ ‰}$ (1σ), $-17.90 \pm 0.01 \text{ ‰}$ (1σ), $-2.21 \pm 0.02 \text{ ‰}$ (1σ), and $-0.96 \pm 0.04 \text{ ‰}$ (1σ), respectively. Unfortunately, laser fluorination $\delta^{18}\text{O}$ value obtained for sample Win-06-01B is not well-known due to the low oxygen yield of the measurement.

4.5. SHRIMP-SI $^{18}\text{O}/^{16}\text{O}$ analysis

A summary of the oxygen isotopic measurements and their relative uncertainties for all RM candidates investigated in this study are presented in Table 3; the complete dataset is given in the supplementary resource (EA3). The reproducibility of $\delta^{18}\text{O}_{\text{SIMS}}$ values, calculated as the standard deviation of several spot analysis during a single analytical session, for individual aliquots of the RM candidates is: $\pm 1.2 \text{ ‰}$ (2 SD) for the Win-01B RM, $\pm 0.8 \text{ ‰}$ (2 SD) for Roy L5 and Roy L6 RMs, $\pm 0.7 \text{ ‰}$ (2 SD) for Win-03A RM, and $\pm 0.6 \text{ ‰}$ (2 SD) for Stop1-6-D1, Capão L4, and Capão L2 RMs. The average grain-to-grain scatter of $^{18}\text{O}/^{16}\text{O}$ ratios for goethite RMs across the runs is usually better than: **Capão L4** = $\pm 1.5 \text{ ‰}$ (2 SD), $n=1599$; **Win-01B** = $\pm 1.5 \text{ ‰}$ (2 SD), $n=33$; **Capão L2** = $\pm 1.8 \text{ ‰}$ (2 SD), $n=145$; **Stop1-6-D1** = $\pm 2.2 \text{ ‰}$ (2 SD), $n=102$; **Win-03A** = $\pm 2.4 \text{ ‰}$ (2 SD), $n=123$; **Roy L5** = $\pm 2.4 \text{ ‰}$ (2 SD), $n=316$; and **Roy L6** = $\pm 2.6 \text{ ‰}$ (2 SD), $n=352$. Isotopic ratios

shown in Table 3 have been normalized to Capão L4 ($\delta^{18}\text{O}_{\text{LF}} = -17.22 \pm 0.03 \text{ ‰}$), our best goethite SHRIMP-SI RM so far.

In parallel, issues related to crystallographic orientation, porosity, and compositional variations that could potentially influence $\delta^{18}\text{O}_{\text{SIMS}}$ determinations were further assessed. These results, and special features associated with crystal orientation, sample position in the disk, porosity, composition, instrument variability, and ultimate reliability of the $\delta^{18}\text{O}_{\text{SIMS}}$ determinations are illustrated in Figures 5 to 11 below.

Table 2: (U-Th)/He ages

Sample	(U-Th)/He age (Ma)	$\pm 1\sigma$	U ppm	$\pm 1\sigma$	Th ppm	$\pm 1\sigma$	He nmol/g	$\pm 1\sigma$	Th/U
Capao L2	268.8	6.9	5.50	0.09	0.62	0.04	8.50	0.19	0.11
Capao L2	270.2	7.1	5.18	0.09	0.59	0.04	8.06	0.17	0.11
Capao L2	275.1	6.6	5.70	0.08	0.63	0.03	9.03	0.27	0.11
Capao L2	282.3	7.2	5.33	0.09	0.63	0.04	8.69	0.20	0.12
Capao L2	276.5	6.5	5.59	0.07	0.59	0.03	8.88	0.29	0.10
<i>Average</i>	<i>274.6</i>		<i>5.46</i>		<i>0.61</i>		<i>8.63</i>		<i>0.11</i>
<i>S.D. (1 σ)</i>	<i>5.4</i>		<i>0.21</i>		<i>0.02</i>		<i>0.38</i>		
Capao L4	285.9	7.9	3.44	0.07	0.32	0.03	5.64	0.14	0.09
Capao L4	292.3	7.7	3.70	0.06	0.38	0.03	6.23	0.18	0.10
Capao L4	286.5	7.6	3.56	0.06	0.33	0.03	5.85	0.17	0.09
Capao L4	289.7	7.0	4.70	0.06	0.40	0.02	7.81	0.28	0.09
Capão L4	274.2	6.3	5.06	0.06	0.46	0.02	7.94	0.32	0.09
Capão L4	275.6	6.7	3.07	0.04	0.27	0.02	4.86	0.26	0.09
Capão L4	278.8	6.7	4.04	0.05	0.37	0.02	6.46	0.26	0.09
<i>Average</i>	<i>283.3</i>		<i>3.94</i>		<i>0.36</i>		<i>6.40</i>		<i>0.09</i>
<i>S.D. (1 σ)</i>	<i>7.1</i>		<i>0.71</i>		<i>0.06</i>		<i>1.13</i>		
Win 01B	209.7	4.5	8.10	0.06	0.08	0.02	9.47	0.39	0.01
Win 01B	202.6	4.5	8.04	0.08	0.07	0.02	9.08	0.29	0.01
Win 01B	202.9	4.3	7.94	0.06	0.04	0.02	8.97	0.37	0.01
Win 01B	203.5	4.7	7.94	0.09	0.18	0.03	9.03	0.24	0.02
Win 01B	187.1	4.4	7.85	0.09	0.09	0.03	8.17	0.21	0.01
<i>Average</i>	<i>201.1</i>		<i>7.98</i>		<i>0.09</i>		<i>8.94</i>		<i>0.01</i>
<i>S.D. (1 σ)</i>	<i>8.4</i>		<i>0.10</i>		<i>0.05</i>		<i>0.47</i>		
Roy L5	66.6	1.8	3.18	0.06	0.21	0.02	1.18	0.04	0.07
Roy L5	67.5	1.9	3.24	0.06	0.30	0.03	1.22	0.03	0.09
<i>Average</i>	<i>67.1</i>		<i>3.21</i>		<i>0.26</i>		<i>1.20</i>		<i>0.08</i>
<i>S.D. (1 σ)</i>	<i>0.7</i>		<i>0.04</i>		<i>0.06</i>		<i>0.03</i>		
Roy L6	78.9	2.0	3.66	0.06	0.12	0.02	1.59	0.06	0.03
Roy L6	77.9	2.2	3.52	0.07	0.13	0.03	1.52	0.03	0.04
<i>Average</i>	<i>78.4</i>		<i>3.59</i>		<i>0.12</i>		<i>1.56</i>		<i>0.03</i>
<i>S.D. (1 σ)</i>	<i>0.7</i>		<i>0.10</i>		<i>0.002</i>		<i>0.06</i>		
WIN 03A(b)*	37.7	-	150.48		8.96		31.34		0.06
WIN 03A(c)*	37.8	-	150.53		2.71		31.13		0.02
WIN 03A(d)*	36.8	-	317.35		18.24		64.61		0.06
<i>Average</i>	<i>37.4</i>		<i>206.12</i>		<i>9.97</i>		<i>42.36</i>		<i>0.05</i>
<i>S.D. (1 σ)</i>	<i>0.5</i>		<i>96.33</i>		<i>7.81</i>		<i>19.27</i>		
STOP1-6-D1 [‡]	2.8	0.2	3.11		0.21		0.05		0.07
STOP1-6-D1 [‡]	4.1	0.2	3.33		0.11		0.08		0.03
<i>Average</i>	<i>3.5</i>		<i>3.22</i>		<i>0.16</i>		<i>0.07</i>		<i>0.05</i>
<i>S.D. (1 σ)</i>	<i>0.9</i>		<i>0.16</i>		<i>0.07</i>		<i>0.02</i>		

* He age from Waltenberg (2012)

‡ He age from Heim (2006)

Table 3: Summary of SHRIMP-SI oxygen isotope ratios and uncertainties. RM = reference material.

Session	$\delta^{18}\text{O}_{\text{SIMS}}$	\pm Internal error _{sample} (σ 95%)	Standard deviation (1 σ)	MSWD	no. spots	no. outliers	Internal error _{spot} average (σ 95%)	External error _{spot} average (σ 95%)	$\delta^{18}\text{O}_{\text{F}}$	Bias (absolute)
Session #2: HM-1										
Capão L4 - normalizing RM	- 17.22	0.16	0.10	0.64	4	0	0.12	0.11		
Capão L2	- 19.53	0.15	0.16	1.56	10	3	0.12	0.11	-17.90	1.63
Win0601B	- 11.90	0.21	0.33	8.46	15	3	0.12	0.11	-	-
Session #2: HM-4										
Capão L4 - normalizing RM	- 17.22	0.17	0.35	7.15	19	0	0.13	0.26		
Capão L2	- 16.72	0.61	0.85	77.83	10	0	0.11	0.26	-17.90	1.18
Win0601B	- 11.80	0.78	0.87	61.45	8	1	0.13	0.26	-	-
Session#3: HM-4										
Capão L4 - normalizing RM	- 17.22	0.27	0.49	21.84	16	1	0.12	0.36		
Session#3: HM-9										
Capão L4 - normalizing RM	- 17.22	0.59	1.38	137.65	24	1	0.13	0.98		
Session#3: HM-11										
Capão L4 - normalizing RM	- 17.22	0.31	1.09	38.60	51	4	0.20	0.79		
Capão L2	- 16.70	0.35	0.36	7.21	6	0	0.20	0.79	-17.90	1.20
Roy L5	1.13	0.37	0.45	5.37	8	1	0.20	0.79	-	-
Roy L6	2.41	0.32	0.53	7.97	13	1	0.19	0.78	-	-
Session#4: JA-1										
Capão L4 - normalizing RM	- 17.22	0.09	0.35	4.44	63	1	0.21	0.29		
Capão L2	- 17.82	0.20	0.90	27.80	79	2	0.22	0.29	-17.90	0.08
Session#5: HM-14										
Capão L4 - normalizing RM	- 17.22	0.23	0.27	2.16	16	0	0.21	0.24		
Session#5: HM-14B										
Capão L4 - normalizing RM	- 17.22	0.21	0.43	10.11	26	2	0.21	0.33		
Session#5: HM-15										
Capão L4 - normalizing RM	- 17.22	0.16	0.35	4.53	20	3	0.19	0.28		
Session#5: HM-13										
Capão L4 - normalizing RM	- 17.22	0.25	0.50	18.47	18	2	0.19	0.38		
Capão L2	- 21.49	0.38	0.33	2.08	3	0	0.21	0.38	-17.90	3.59
Roy L5	0.29	0.22	0.35	7.07	12	0	0.17	0.37	-	-
Roy L6	1.12	0.24	0.38	5.04	12	0	0.19	0.38	-	-
Stop1-6-D1	1.29	0.23	0.44	9.27	16	0	0.18	0.37	-0.96	2.25
Win0603A	0.92	0.37	0.37	7.54	6	1	0.17	0.37	-2.21	3.13
Win0601B	- 11.98	0.55	0.87	29.04	12	0	0.19	0.38	-	-
Session#6: HM-16A										
Capão L4 - normalizing RM	- 17.22	0.20	0.44	10.89	22	0	0.16	0.33		
Roy L5	1.80	0.67	0.40	17.69	5	1	0.16	0.33	-	-
Roy L6	2.66	0.47	0.41	6.57	5	0	0.17	0.34	-	-
Session#6: HM-16B										
Capão L4 - normalizing RM	- 17.22	0.27	0.71	24.82	28	0	0.21	0.52		
Session#6: HM-16C										
Capão L4 - normalizing RM	- 17.22	0.33	0.70	24.87	25	2	0.18	0.51		
Session#6: HM-17A										
Capão L4 - normalizing RM	- 17.22	0.23	0.74	24.97	43	2	0.22	0.55		
Roy L5	2.17	0.43	0.78	16.03	9	1	0.23	0.55	-	-
Roy L6	2.67	0.32	0.45	10.89	10	1	0.22	0.54	-	-
Session#6: HM-17B										
Capão L4 - normalizing RM	- 17.22	0.21	0.57	16.15	31	1	0.20	0.43		

Table 3: Summary of SHRIMP-SI oxygen isotope ratios and uncertainties. RM = reference material.

Session	$\delta^{18}\text{O}_{\text{SMS}}$	\pm Internal error _{sample} (σ 95%)	Standard deviation (1 σ)	MSWD	no. spots	no. outliers	Internal error _{spot} average (σ 95%)	External error _{spot} average (σ 95%)	$\delta^{18}\text{O}_{\text{LF}}$	Bias (absolute)
Session#6: HM-18A										
Capão L4 - normalizing RM	- 17.22	0.51	0.89	21.74	14	0	0.23	0.65		
Session#6: HM-18B										
Capão L4 - normalizing RM	- 17.22	1.04	1.04	32.00	6	0	0.21	0.75		
Roy L5	1.36	0.74	0.64	17.26	5	0	0.18	0.75	-	-
Roy L6	1.56	0.29	0.25	2.40	5	0	0.22	0.75	-	-
Session#6: HM-18C										
Capão L4 - normalizing RM	- 17.22	0.22	1.19	153.21	78	4	0.27	0.85		
Roy L5	1.95	0.21	0.41	16.40	16	1	0.14	0.85	-	-
Roy L6	1.99	0.23	0.47	17.44	18	0	0.14	0.85	-	-
Stop1-6-D1	2.48	0.17	0.36	13.79	23	3	0.13	0.85	-0.96	3.44
Session#6: HM-19 20A										
Capão L4 - normalizing RM	- 17.22	0.43	1.42	190.85	49	5	0.15	1.01		
Roy L5	2.27	0.46	0.63	72.31	27	5	0.17	1.01	-	-
Roy L6	2.45	0.39	0.81	60.32	21	2	0.13	1.01	-	-
Stop1-6-D1	4.08	0.40	0.60	24.74	14	4	0.14	1.01	-0.96	5.04
Session#6: HM-19 20B										
Capão L4 - normalizing RM	- 17.22	0.17	0.66	24.62	62	4	0.16	0.48		
Roy L5	2.69	0.41	0.82	51.62	19	1	0.16	0.48	-	-
Roy L6	2.54	0.20	0.48	19.55	25	1	0.16	0.48	-	-
Stop1-6-D1	3.55	0.24	0.49	14.59	18	0	0.15	0.48	-0.96	4.51
Session#6: HM-20 BAH										
Capão L4 - normalizing RM	- 17.22	0.12	0.34	7.97	36	4	0.16	0.27		
Roy L5	1.92	0.46	0.99	83.76	19	0	0.15	0.27	-	-
Roy L6	3.02	0.26	0.56	18.30	20	0	0.16	0.27	-	-
Stop1-6-D1	3.41	0.20	0.41	11.23	19	0	0.16	0.27	-0.96	4.37
Session#7: HM-16										
Capão L4 - normalizing RM	- 17.22	0.11	0.65	29.76	35	3	0.12	0.47		
Roy L5	1.86	0.16	0.43	8.07	8	1	0.13	0.47	-	-
Roy L6	2.69	0.13	0.39	8.95	10	1	0.13	0.47	-	-
Session#7: HM-18B										
Capão L4 - normalizing RM	- 17.22	0.25	0.39	11.39	20	3	0.13	0.29		
Roy L5	1.95	0.33	0.77	7.09	8	2	0.12	0.29	-	-
Roy L6	1.98	0.36	0.84	7.18	8	2	0.13	0.29	-	-
Session#7: HM-17										
Capão L4 - normalizing RM	- 17.22	0.16	0.46	23.84	53	2	0.13	0.34		
Roy L5	2.72	0.26	0.51	12.63	15	1	0.13	0.34	-	-
Roy L6	2.90	0.19	0.52	5.95	14	1	0.13	0.34	-	-
Session#7: HM-17D										
Capão L4 - normalizing RM	- 17.22	0.18	0.57	18.31	43	2	0.13	0.42		
Roy L5	1.60	0.45	0.78	38.15	15	1	0.13	0.42	-	-
Roy L6	2.27	0.28	0.43	11.30	12	1	0.13	0.42	-	-
Session#7: HM-21										
Capão L4 - normalizing RM	- 17.22	0.14	0.42	10.49	38	2	0.14	0.31		
Roy L5	2.20	0.16	0.54	12.84	13	2	0.14	0.31	-	-
Roy L6	1.53	0.41	0.59	14.77	12	2	0.15	0.31	-	-
Stop1-6-D1	2.72	0.29	0.42	9.23	11	1	0.13	0.31	-0.96	3.68
Session#7: HM-23										
Capão L4 - normalizing RM	- 17.22	0.13	0.55	16.82	66	3	0.15	0.40		
Roy L5	1.71	0.30	0.89	39.06	41	2	0.15	0.40	-	-
Roy L6	1.95	0.21	0.64	18.12	41	4	0.15	0.40	-	-
Win0603A	2.24	0.13	0.47	12.46	59	3	0.14	0.40	-2.21	4.45
Session#7: HM-23 27										
Capão L4 - normalizing RM	- 17.22	0.18	0.44	16.82	28	1	0.16	0.33		
Roy L5	1.39	0.54	0.59	16.40	10	3	0.16	0.33	-	-
Roy L6	1.69	0.46	0.43	10.04	8	2	0.16	0.34	-	-
Win0603A	2.11	0.37	0.40	7.67	8	1	0.17	0.33	-2.21	4.32
Capão L2	- 17.62	0.31	0.48	6.73	12	0	0.19	0.34	-17.90	0.28
Session#7: HM-23										
Capão L4 - normalizing RM	- 17.22	0.18	0.48	11.98	31	2	0.15	0.36		
Roy L5	1.35	0.74	1.11	46.50	12	1	0.16	0.36	-	-
Roy L6	1.56	0.30	0.64	9.68	15	1	0.16	0.36	-	-
Win0603A	2.51	0.29	0.50	10.28	19	1	0.15	0.36	-2.21	4.72

Table 3: Summary of SHRIMP-SI oxygen isotope ratios and uncertainties. RM = reference material.

Session	$\delta^{18}\text{O}_{\text{SAMS}}$	\pm Internal error _{sample} (σ 95%)	Standard deviation (1 σ)	MSWD	no. spots	no. outliers	Internal error _{spot} average (σ 95%)	External error _{spot} average (σ 95%)	$\delta^{18}\text{O}_{\text{LF}}$	Bias (absolute)
Session#8: HM-22&JA										
Capão L4 HM-22 - normalizing RM	-17.22	0.23	0.25	4.63	7	0	0.11	0.19		
Capão L4 JA	-19.18	0.27	0.43	11.71	13	1	0.10	0.31	-17.22	1.96
Session#8: HM-22&JA										
Capão L4 HM-22 - normalizing RM	-17.22	0.17	0.37	15.78	19	0	0.10	0.27		
Capão L4 JA	-17.15	0.27	0.39	18.65	38	0	0.10	0.29	-17.22	0.07
Roy L5	-0.52	0.56	0.35	17.24	11	0	0.10	0.25	-	-
Roy L6	-0.44	0.92	0.59	30.89	11	1	0.10	0.42	-	-
Session#8: BAH&JA										
Capão L4 - normalizing RM	-17.22	0.18	0.28	6.82	48	0	0.11	0.21		
Capão L2	-18.26	0.61	0.61	44.14	21	1	0.10	0.44	-17.90	0.36
Session#8: HM-23&JA										
Capão L4 JA - normalizing RM	-17.22	0.23	0.34	13.27	37	1	0.10	0.25		
Capão L4 HM 23	-20.26	0.29	0.41	19.56	33	2	0.09	0.29	-17.22	3.04
Roy L6	-1.50	0.87	0.59	38.22	11	0	0.09	0.42	-	-
Roy L6	0.04	0.59	0.43	22.02	11	0	0.10	0.31	-	-
Win0603A	-0.53	0.66	0.59	48.52	18	1	0.10	0.42	-2.21	1.68
Session#9: HM-27 HM-16										
Capão L4 - normalizing RM	-17.22	0.13	0.28	5.72	64	1	0.11	0.21		
Capão L2	-18.26	0.50	0.29	6.51	9	0	0.12	0.22	-17.90	0.36
Roy L5	-0.05	0.31	0.28	5.57	14	0	0.10	0.21	-	-
Roy L6	-0.36	0.53	0.45	17.06	16	0	0.11	0.33	-	-
Session#9: HM-27 HM22										
Capão L4 - normalizing RM	-17.22	0.18	0.29	7.68	43	1	0.11	0.22		
Roy L5	0.38	1.08	0.40	13.67	6	0	0.11	0.29	-	-
Roy L6	0.32	0.71	0.25	7.49	6	0	0.11	0.19	-	-
Session#9: HM-27 HM22										
Capão L4 - normalizing RM	-17.22	0.18	0.32	9.96	53	0	0.11	0.24		
Session#9: HM-27										
Capão L4 - normalizing RM	-17.22	0.53	0.43	17.15	14	0	0.10	0.31		
Session#10: HM-27 HM-17										
Capão L4 - normalizing RM	-17.22	0.18	0.46	27.19	125	4	0.10	0.33		
Roy L5	0.32	0.62	0.64	47.71	20	0	0.10	0.46	-	-
Roy L6	0.71	0.26	0.26	8.83	20	0	0.10	0.20	-	-
Session#10: HM-27 HM-18										
Capão L4 - normalizing RM	-17.22	0.33	0.74	64.38	80	0	0.10	0.52		
Roy L5	-0.84	0.48	0.31	9.95	10	0	0.10	0.23	-	-
Roy L6	-0.68	0.33	0.20	4.57	10	0	0.10	0.16	-	-
Stop1-6-D1	0.88	0.33	0.26	4.61	10	0	0.10	0.20	-0.96	1.84
Session#10: HM-27 HM-23										
Capão L4 - normalizing RM	-17.22	0.16	0.37	15.66	92	0	0.10	0.27		
Roy L5	0.47	0.26	0.23	4.54	13	0	0.10	0.18	-	-
Roy L5	-0.43	0.42	0.25	7.16	10	0	0.10	0.19	-	-
Roy L6	1.06	0.36	0.36	14.07	18	0	0.10	0.27	-	-
Roy L6	-1.14	0.80	0.44	27.71	10	1	0.10	0.32	-	-
Win0603A	0.27	0.25	0.26	9.74	25	1	0.10	0.20	-2.21	2.48

5. DISCUSSION

5.1. The effect of crystallographic orientation on $^{18}\text{O}/^{16}\text{O}$ ratios

Crystallographic orientation has been recognized as an important feature affecting the ionization efficiency during the isotopic analysis of oxides (e.g., hematite, magnetite) by ion microprobes (Lyon et al., 1998; Huberty et al., 2010; Kita et al., 2011). This effect may result in instrument-determined isotopic variability as large as 5 ‰, masking any potential variation in natural isotopic compositions acquired by mineral-water exchange during mineral precipitation. To test whether goethite is subject to the crystallographic effects previously detected for other oxides, we mounted between 2 and 8 aliquots where the b-axis was both parallel (Figure 5 c, d) and perpendicular (Figure 5e) to the plane of the sample mount. Fortunately, for goethites this is easily achieved because natural goethites grow preferentially along the b-axis, forming elongated needles, blades, or prismatic microcrystallites with aspect ratios of 5-1000 (Figure 5a, b). These samples preferentially break into grains elongated along the b-axis, which will sit flat when placed at the bottom of the pit in the sample mount.

SHRIMP-SI spot analysis for two aliquots of the Win-01B RM illustrated in Figure 5c-e are individually shown in Figure 5f. The results, -11.66 ± 0.65 ‰ (2σ , $n=6$) for aliquots where the b-axis is parallel to the surface ablated by the Cs^+ -beam, and -12.13 ± 0.56 ‰ (2σ , $n=6$) for aliquots where the b-axis is perpendicular to that plane, show a small difference in apparent isotopic composition with crystal orientation. Similar tests carried out on other samples show an isotopic fractionation of ~ 2 ‰. For example, two aliquots of the Capão L4 RM mounted with b-axis parallel and one aliquot mounted with b-axis perpendicular to the polished surface yielded an average instrumental bias of ~ 2 ‰.

Another test for the sensitivity of SHRIMP-SI results to crystallographic orientation is provided in the experiment illustrated in Figure 6. In this case, three aliquots from the Capão L4 RM, showing the b-axis parallel to the surface to be bombarded by the Cs^+ -beam, were analysed as illustrated in Figure 6a,d, yielding the results plotted in Figure 6f. In the same run, the same sample disk was rotated 90° clockwise with respect to the Cs^+ -beam and reanalysed, as illustrated in Figure 6b,e. The three aliquots yield average $\delta^{18}\text{O}_{\text{SIMS}}$ values of -16.9 ± 0.2 [G1] (1σ), -17.0 ± 0.3 [G2] (1σ), and -17.6 ± 0.3 ‰ [G3] (1σ) before 90° rotation, and -19.3 ± 0.1 [G1_R] (1σ), -18.2 ± 0.2 [G2_R] (1σ), and -19.2 ± 0.1 ‰ [G3_R] (1σ) after 90° rotation, suggesting that instrumental fractionation related to crystallographic orientation could introduce an instrumental bias of approximately 1.5‰ on $\delta^{18}\text{O}_{\text{SIMS}}$ values.

The test results above reveal a maximum isotopic shift of $\sim 2\text{‰}$ when goethite aliquots are analysed in different crystallographic orientations. And, fortuitously, the fact that most goethite samples tend to break into elongated fragments with the direction of elongation parallel to b-axis ensures that most aliquots analysed in the SHRIMP-SI can be mounted in similar crystallographic orientations, and their similarities or differences in $\delta^{18}\text{O}$ values should faithfully reflect the isotopic compositions of the solutions from which the minerals precipitated.

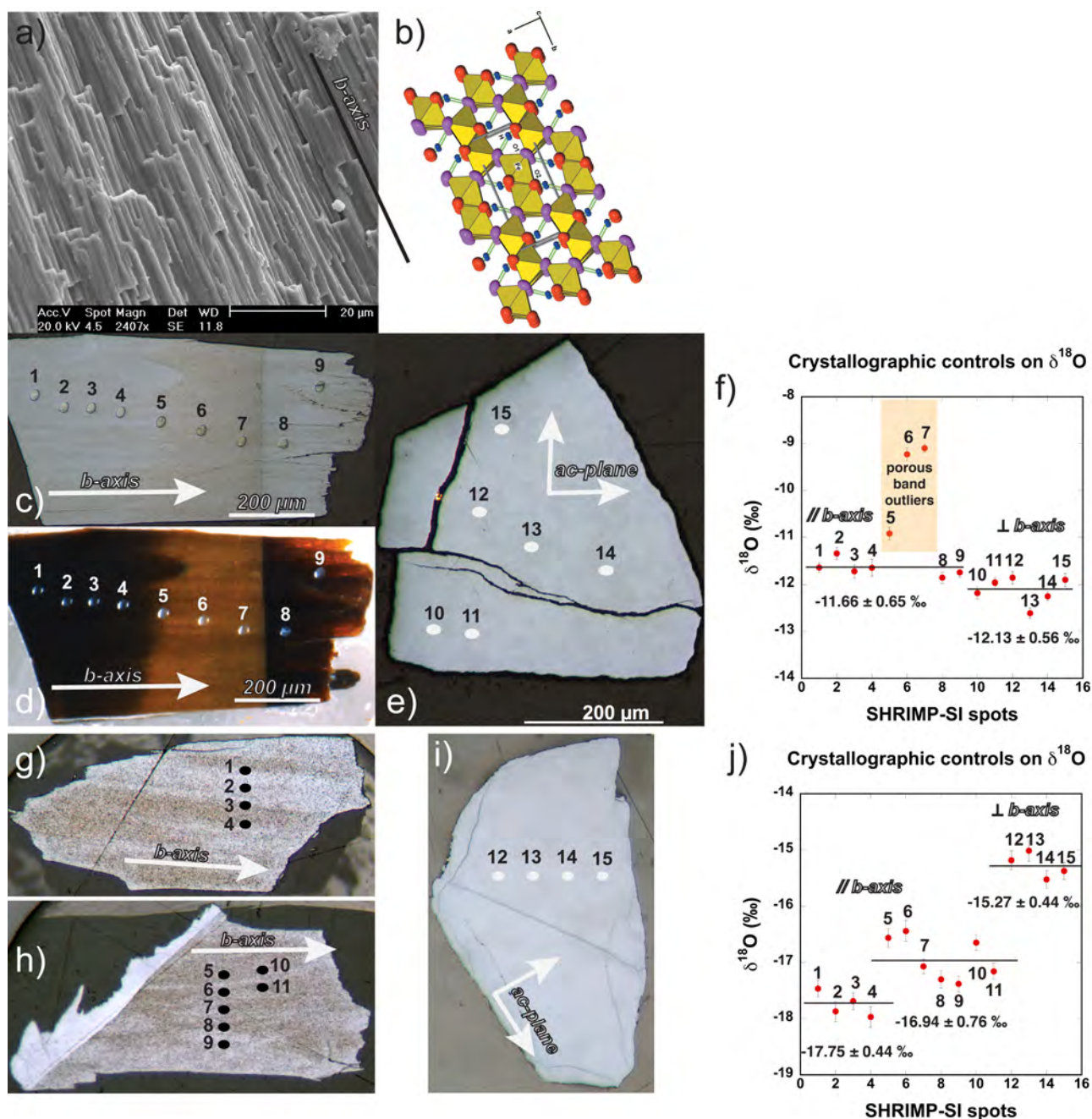


Figure 5: Goethite is orthorhombic and preferentially elongated along the b-axis (a, b; Yang et al., 2006). Fragments of large bands of colloform goethite fracture along the b-axis. To test the dependency of $\delta^{18}\text{O}_{\text{SIMS}}$ values on crystal orientation, we analysed two aliquots for sample Winsor 06 01B in distinct crystallographic positions (c-e). The results (f) show a slight difference in measured $\delta^{18}\text{O}_{\text{SIMS}}$ values for the crystals oriented with the b-axis parallel and perpendicularly to the disk surface, but the results for each orientation are within error from the average value for all analysis for this sample (-11.9 ± 0.3 ‰). However, the goethite aliquot in c, d shows increased porosity in one of the bands (yellow band in d), and porosity appears to play a major influence in the measured $\delta^{18}\text{O}$ values (EMPA does not detect any difference in composition between the yellow and brown layers shown in d). In another experiment using sample Capão L4 (g-i), aliquots were mounted in a similar fashion as the Winsor test. The results (j) reveal a crystal orientation bias $\sim 2\%$ for this sample.

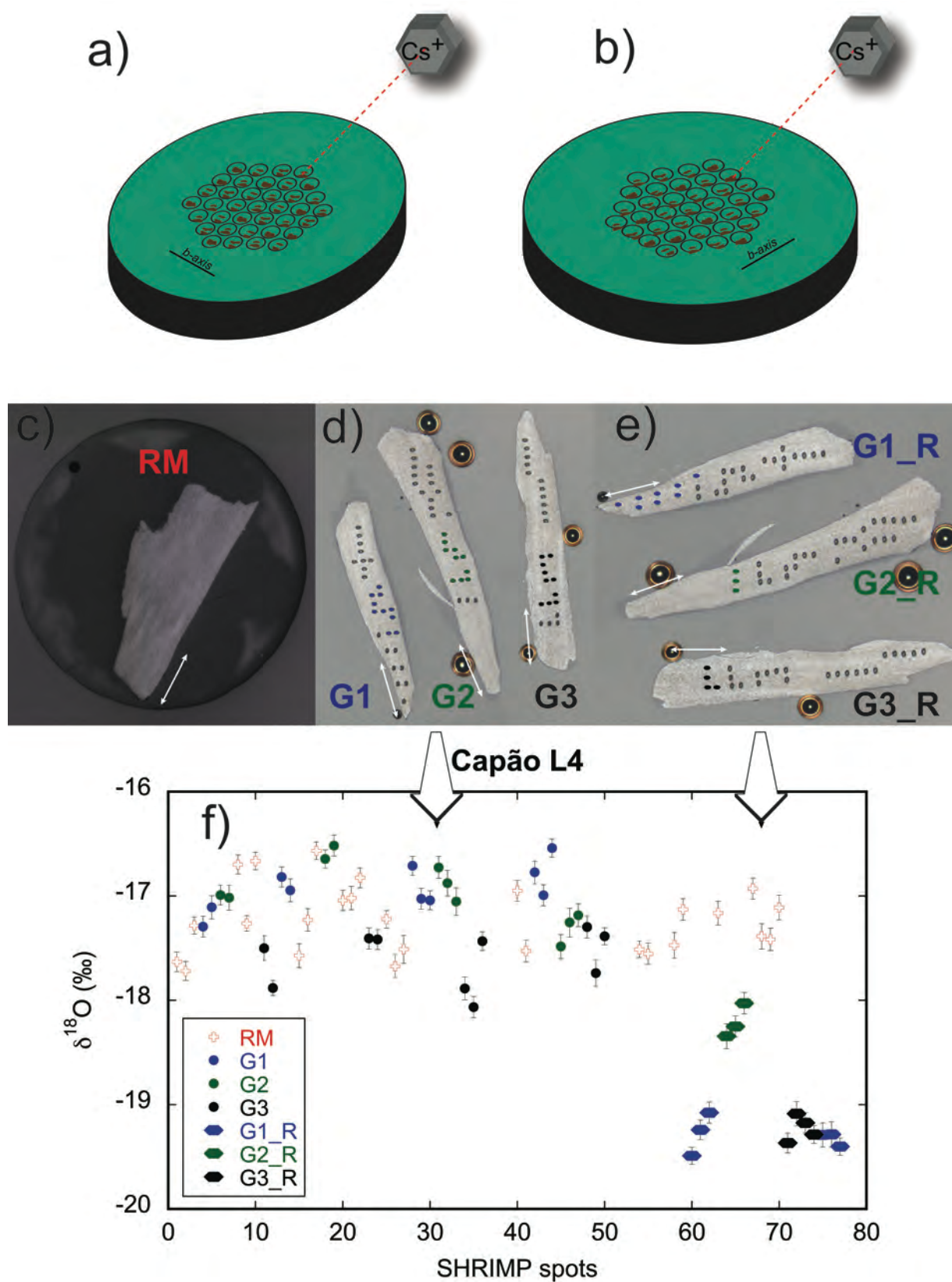
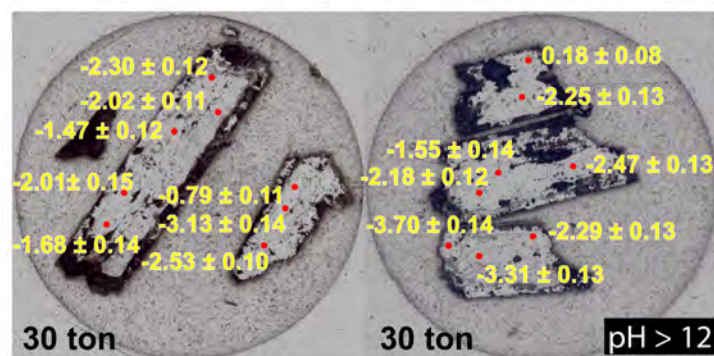


Figure 6: SHRIMP-SI results obtained for three aliquots from Capão L4 RM, where the aliquots have b-axes parallel to the disk surface. With the disk oriented as shown in (a), the three aliquots in (d) were analysed yielding the results shown in f. When the disk is rotated 90° clockwise and reanalysed (b, e), the results show larger discrepancies from the RM values.

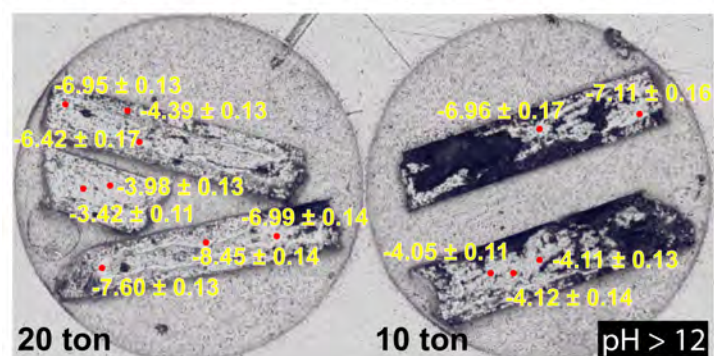
5.2. Porosity control on $^{18}\text{O}/^{16}\text{O}$ ratios

Porosity is another sample-related factor that may affect the measured $^{18}\text{O}/^{16}\text{O}$ ratios determined in the SHRIMP-SI. This feature was particularly noticeable in our first attempt to analyse synthetic stoichiometric goethites (Figure 7). Successful analysis of these synthetic samples would permit the development of stoichiometrically pure reference material (and metal doped goethites), and it would also permit calibrating mineral-water isotopic fractionation factors at various temperatures. Attempts to eliminate pore spaces by agglomerating the finely crystalline goethite masses into pellets using a hydraulic press ($\sim 10\text{-}30\text{ tons/cm}^2$) were unsuccessful. The pressed pellets still showed variable porosity after polishing (Figure 7), and the isotopic results from more porous areas varied from those of the less porous segments of the pellet (-3.42 to -8.45 ‰), suggesting that it was not possible to overcome the porosity barrier for a successful SHRIMP-SI analysis. Various fragments of the pressed pellets also showed large variations in isotopic composition when analysed by laser fluorination, suggesting that during sample agglomeration under pressure the goethite grains may change composition or acquire different water contents, ultimately affecting the isotopic signature of the sample fraction analysed.

Precipitation Temperature: 22°C



Precipitation Temperature: 30°C



Precipitation Temperature: 40°C

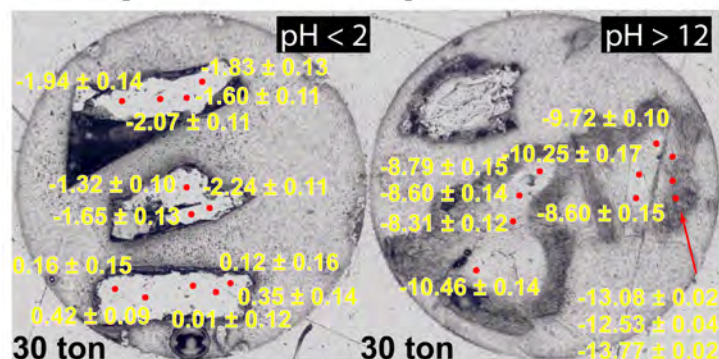


Figure 7: Fragments of pressed pellets of synthetic goethite analysed by ion microprobe. $\delta^{18}\text{O}_{\text{SIMS}}$ results are shown in yellow. The scattered results prevent the use of these synthetic samples as SHRIMP-SI goethite $\delta^{18}\text{O}$ RM. However, despite the large scatter, trends in the data (e.g., goethite precipitated a pH>12 shows progressively lighter isotopic composition with temperature, while goethites precipitated at the same temperature but at pH<2 show drastically different $\delta^{18}\text{O}$ values) suggest that broad trends in $\delta^{18}\text{O}$ values for synthetic samples may be resolved with the SHRIMP-SI, even if results precision are partially compromised by sample porosity.

Porosity also alters SHRIMP-SI $\delta^{18}\text{O}$ results for natural samples. For example, the grain illustrated in Figure 5c,d yields relatively reproducible results except for spots 6 and 7, which are discrepant by about +2‰ from the mean. Petrographic observation shows that the two spots that yield discrepant results occur in a (yellow) porous zone in the grain. Spot 5, sitting at the boundary between brown (nonporous) and yellow (porous) goethite yields an intermediate result. The re-

occurrence of this feature in several samples, where spot analysis of porous areas in a grain yield results largely discrepant from the mean results obtained from the analysis of other areas in the same grain, leads to the conclusion that areas of high porosity should be avoided when selecting positions for SHRIMP-SI spot $\delta^{18}\text{O}$ analysis in goethite. As porosity is a difficult feature to quantify, it is difficult to ascertain how much of the measured variability of $\delta^{18}\text{O}_{\text{SIMS}}$ results for a sample may arise from variations in porosity not readily discernible by visual inspection.

5.3. The influence of texture and multiple generations on the $\delta^{18}\text{O}$ value of goethite

We use grain texture as a selection and vetting criterion when choosing samples to be analysed and when interpreting results obtained from goethite analyses by the SHRIMP-SI. Figure 8 illustrates three goethite grains displaying drastically different textures. We will show below the effect of these textures on SHRIMP-SI results.

Grain BAH-F124-111.2B (Figure 8a) represents a typical colloform goethite symmetrically precipitated from the walls towards the center of an open cavity. After the cavity was completely sealed by the precipitating goethite (with minor alternating bands of Cu-rich cryptomelane), the sample continued to grow in the direction illustrated by the arrows in Figure 8a. SHRIMP-SI analysis of spots on same-generation symmetrical bands from opposite sides of the cavity wall yield the results illustrated in Figure 8b. The entire dataset reveals a relatively homogeneous population of $1.3 \pm 0.6 \text{ ‰}$ (1σ). Average results for individual bands show they are isotopically symmetrical: Band I: $0.7 \pm 0.2 \text{ ‰}$ (1σ) for spots 27-30, and $1.3 \pm 0.4 \text{ ‰}$ (1σ) for spots 39-45; Band II: $1.2 \pm 0.1 \text{ ‰}$ (1σ) for spots 21-25, and $1.5 \pm 0.4 \text{ ‰}$ (1σ) for spots 46-53; Band III: $2.1 \pm 0.5 \text{ ‰}$ (1σ) for spots 34-37, and $1.6 \pm 0.3 \text{ ‰}$ (1σ) for spots 54-61; Band IV: $1.2 \pm 0.4 \text{ ‰}$ (1σ) for spots 11-16, and $0.1 \pm 0.7 \text{ ‰}$ (1σ) for spots 17-20, and $1.0 \pm 0.1 \text{ ‰}$ (1σ) for spots 31 and 33; Band V: $1.6 \pm 0.5 \text{ ‰}$ (1σ) for spots 8-10; Band VI: $1.6 \pm 0.6 \text{ ‰}$ (1σ) for spots 4-7; and Band VII: $1.5 \pm 0.1 \text{ ‰}$ (1σ) for spots 1-3. The greater scatter observed for Band IV could result from: i) instrument shifts during analysis; ii) it could reflect a true isotopic difference between the symmetrical growth bands, possibly reflecting non-equilibrium conditions during mineral precipitation; iii) it could suggest differences in band porosity on the opposite sides of the vein; or iv) it could reflect large isotopic variations across the inner growth band. Further analysis of additional samples displaying similar textures will be needed to resolve the possible scenarios above; but an important conclusion from this study is that individual growth bands in colloform goethites are excellent samples for SHRIMP-SI $\delta^{18}\text{O}$ analysis: they are well crystallized, the crystals are parallel and elongated along the b-axis avoiding possible variability related to crystallographic orientation, the results are relatively well constrained and reproducible, and the spatial resolution of the SHRIMP-SI resolves the history of mineral

precipitation through time, making full use of the advantages provided by in situ analysis with the ion microprobe.

The very homogeneous goethite mass illustrated in Figure 8c and the results summarized in Figure 8d also help to illustrate the effect of goethite density and textural homogeneity on the relatively good reproducibility of SHRIMP-SI $\delta^{18}\text{O}$ results ($0.8 \pm 0.6 \text{ ‰}$ (1σ), $n=7$). In contrast, the porous, prismatic and randomly oriented grains illustrated in Figure 8e yield discrepant data: $0.2 \pm 1.0 \text{ ‰}$ (1σ), $n=7$ for one aliquot; and $-1.1 \pm 1.1 \text{ ‰}$ (1σ), $n=7$ for the second aliquot; and, for the entire population, $-0.2 \pm 1.4 \text{ ‰}$ (1σ), $n=14$. The scatter in $\delta^{18}\text{O}_{\text{SIMS}}$ values may be a function of true variability in the sample, a function of crystallographic orientation (individual crystallites appear to grow aligned in different directions), a function of porosity, or the combined result of all these effects. These data suggest that sample texture should be used as a vetting criterion for the selection of the best grains or the best areas in a grain to undergo stable isotope analysis with the SHRIMP-SI.

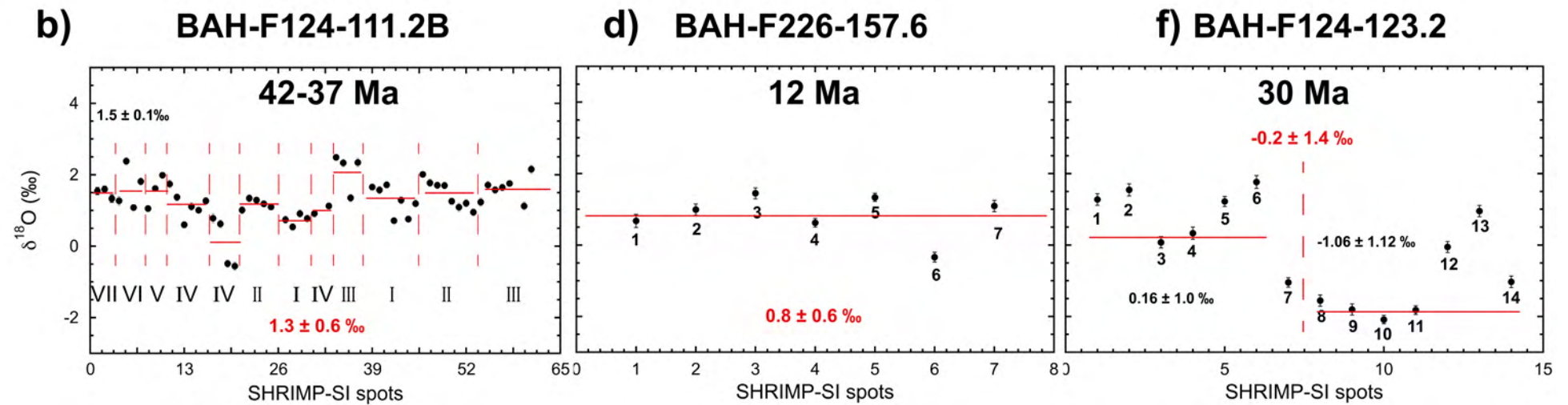
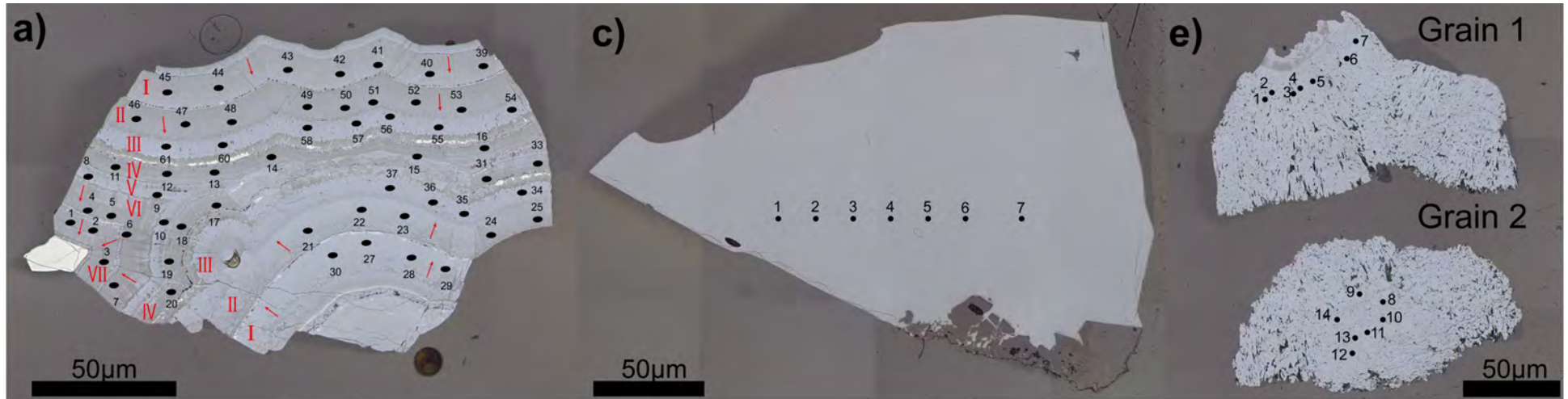


Figure 8: (a, b) Reproducibility of SHRIMP-SI $\delta^{18}\text{O}$ results for symmetrical colloform bands on opposite walls of a cavity infilled with goethite. The entire population yields a relatively narrow $\delta^{18}\text{O}$ range (1.3 ± 0.6 ‰). Figure 8c,d illustrates the reproducibility of SHRIMP-SI $\delta^{18}\text{O}$ results for an optically homogeneous sample, while 8e,f illustrates much larger scatter obtained for goethite masses composed of randomly oriented and poorly packed crystals.

5.4. The influence of minor and trace elements on the $\delta^{18}\text{O}$ value of goethite

A potential source of uncertainty in measuring $\delta^{18}\text{O}$ values for goethite is the fact $\alpha\text{-FeOOH}$ is notorious for containing elements substituting for Fe^{+3} in solid solution, particularly Al^{+3} (Schulze, 1984; Schwertmann, 1994). In addition, natural goethites often contain Si as a minor or trace element, and it is unclear whether Si occurs in solid solution or as a mineral contaminant (Glasauer and Schwertmann, 1999). Evidence against Si being present as a mineral contaminant is the fact that XRD patterns for Si-bearing goethites do not show the presence of quartz or other crystalline silica polymorph, even when goethite powders are analysed by high-resolution Rietveld refinement of synchrotron X-ray diffraction data (Mostert, 2014). It has been proposed that some of the silica may occur as thin films of amorphous silica (opal) coating individual goethite fibers (Glasauer and Schwertmann, 1999), a difficult feature to assess.

Independent of whether silica occurs in solid solution or as a trace phase not detectable by XRD, the fact that natural $\alpha\text{-FeOOH}$ may contain elevated Al and Si contents requires quantifying the potential effect (also known as the matrix effect) of these elements on measured $\delta^{18}\text{O}_{\text{SIMS}}$ values for goethite. This is particularly important for natural goethite samples under consideration as potential reference material for the SHRIMP-SI. Figure 4a,c illustrates the major and minor/trace element composition, respectively, of the goethites being investigated as potential SHRIMP-SI $\delta^{18}\text{O}$ RMs in this study. For comparison purposes, we also plot the elemental compositions determined by more than 2,000 individual electron microprobe analyses of several hundred aliquots of goethite samples from Brazil and Australia. The results clearly show that goethites do indeed contain up to a few percent Al and Si (and also Mn, P, and Cu) as dopants or contaminants (Figure 4b). The goethites investigated as potential RMs also show an increase in Si (Figure 4c) and a corresponding decrease in Fe contents (Figure 4e). A plot of total Al + Si content versus $\delta^{18}\text{O}_{\text{SIMS}}$ values (Figure 9) for goethites under consideration as possible RM shows only a very slight increase in the $\delta^{18}\text{O}$ values with increasing Al + Si contents. We should highlight, however, that the Al+Si content of the potential RMs analysed here has a narrow range compared to other natural goethite samples from Australia and South America (Figure 3b,d,f). Although noticeable, this trend is too subtle to play a major role in the isotopic composition of the sample we selected as a suitable SHRIMP-SI RMs.

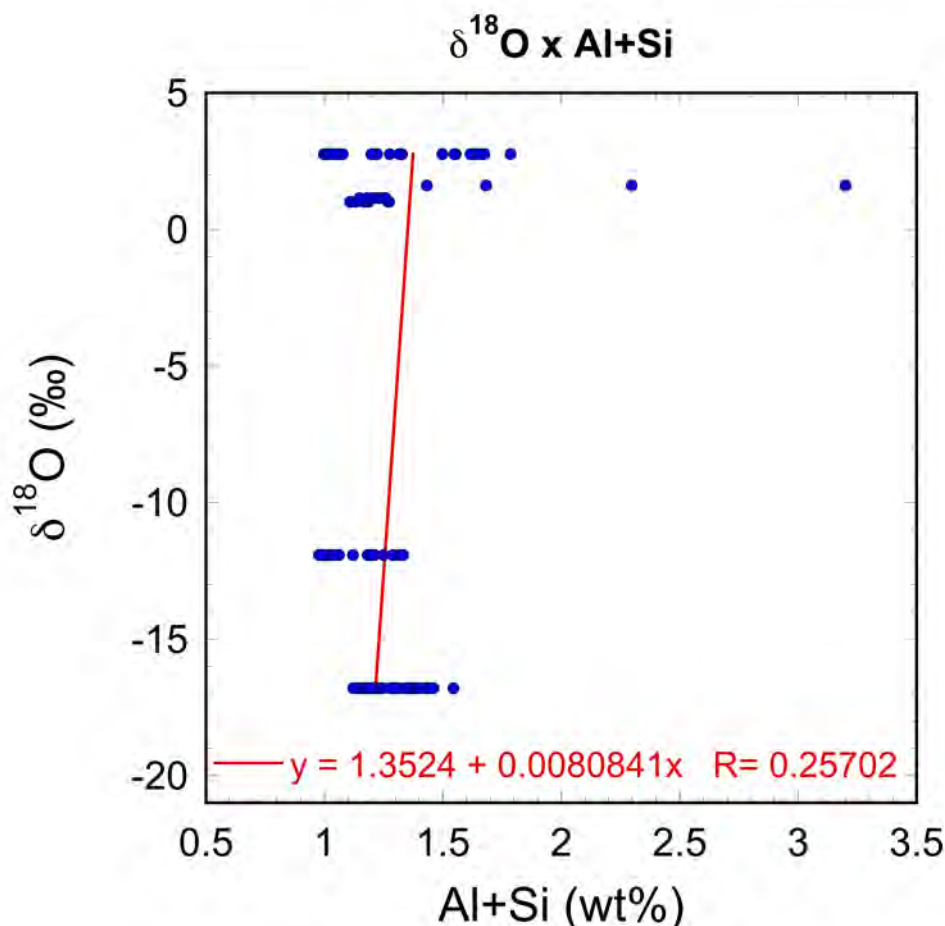


Figure 9: $\delta^{18}\text{O}_{\text{SIMS}}$ vs Al+Si contents for all RM candidates shows a weak positive correlation. This result indicates that sample chemistry will probably not be responsible for any instrumental mass fractionation in this Al+Si range.

5.5. Evaluating the most suitable reference material

The LF and $\delta^{18}\text{O}_{\text{SIMS}}$ values obtained for all aliquots from the various goethites previously selected as potential candidates for RMs (Figure 2) are illustrated in Figure 10. A cursory examination of all results reveals that samples Roy L5 ($1.3 \pm 2.4\text{‰}$ (2σ)), Roy L6 ($1.5 \pm 2.6\text{‰}$ (2σ)), Win 06 3a ($1.4 \pm 2.4\text{‰}$ (2σ)), and Stop D1 ($2.6 \pm 2.2\text{‰}$ (2σ)) show variability in measured $\delta^{18}\text{O}$ incompatible with that expected for a homogeneous and reproducible RM. The only samples that yielded promising results are Capão L4 ($16.9 \pm 1.5\text{‰}$ (2σ)), Capão L2 ($-17.9 \pm 1.8\text{‰}$ (2σ)) and Win 06 01B ($-11.9 \pm 1.5\text{‰}$ (2σ)). Of these three samples, we chose to focus on Capão L4 because it was a larger sample, showed lower variability than all other samples during the runs where instrument-induced uncertainties were not significant (R2, R4, R5, R7, R8, R9, R10), and showed very low Al and relatively low Si contents (Table 1).

Noticeably, the LF results for five other potential goethite RM differ from the results obtained by the SHRIMP-SI when using Capão L4 as the RM. The LF and SHRIMP-SI results are concordant for sample Capão L2. The discrepancy between LF and SHRIMP-SI results vary between runs, and it is larger for runs 6 and 7 (Figure 10; Table 3). For those runs, results by the two methods differ by $3.5 \pm 1.8\text{‰}$ and $3.3 \pm 1.8 \text{‰}$ for Roy L5, 3.9 and 3.5 ‰ for Roy L6, 4.1 and 3.6 ‰ for Stop1-6-D1, and 4.5 ‰ for Win-06-03A. An important observation is that most aliquots of the Capão L4 RM analysed during runs 6 and 7 were positioned with b-axis oriented as shown in Figure 6b. In other runs, the Capão L4 RM aliquots were positioned with the b-axis oriented as shown in Figure 6a, resulting in $\delta^{18}\text{O}_{\text{SIMS}}$ values closer to the known LF values for the secondary reference materials. Therefore, part of the discrepancy between the two methods arises from instrumental fractionation due to crystal orientation, confirming the existence of $\sim 2\text{‰}$ bias when analysing the Capão L4 RM in different orientations. However, the $\sim 2\text{‰}$ bias cannot explain the $>2\text{‰}$ difference between LF and $\delta^{18}\text{O}_{\text{SIMS}}$ values. Therefore, this discrepancy must be resolved by reanalysing all samples by laser fluorination or by traditional methods as well.

5.6. The Capão L4 SHRIMP-SI reference material

Sample Capão L4 constitutes, at this stage and in the absence of a better candidate, a suitable RM for stable isotope analysis of natural goethites with the SHRIMP-SI. To derive a suitable reference value for Capão L4, we eliminated analyses from Runs 3 and 6 (Figure 10) because both runs were fraught with instrument malfunctions. We also only use results from runs for which we analysed the in-house magnetite RM for monitoring of instrument drift. $\delta^{18}\text{O}_{\text{SIMS}}$ -magnetite values were calculated for each session using the LF value of $-17.22 \pm 0.03 \text{‰}$ (1σ) for the Capão L4 RM. Figure 11 illustrates the complete set of $\delta^{18}\text{O}_{\text{SIMS}}$ values calculated for the Capão L4 RM.

We caution potential users of Capão L4 as a RM for a source of uncertainty that we will be addressing in the near future, but which must be carefully considered. The $\delta^{18}\text{O}_{\text{SIMS}}$ value of $-16.9 \pm 1.5 \text{‰}$ (2σ) for Capão L4 is predicated on the laser fluorination value of -17.22 ± 0.03 (1σ) obtained by one analysis of an aliquot from this sample carried out at the Stable Isotope Laboratory, Caltech, USA. As this value plays a crucial role in $\delta^{18}\text{O}_{\text{SIMS}}$ values calculated using the Capão L4 RM, it is useful and necessary that this absolute value be validated by replicate analyses at independent laboratories. It is our intention to carry out these independent analyses before openly proposing to the scientific community the value outlined above.

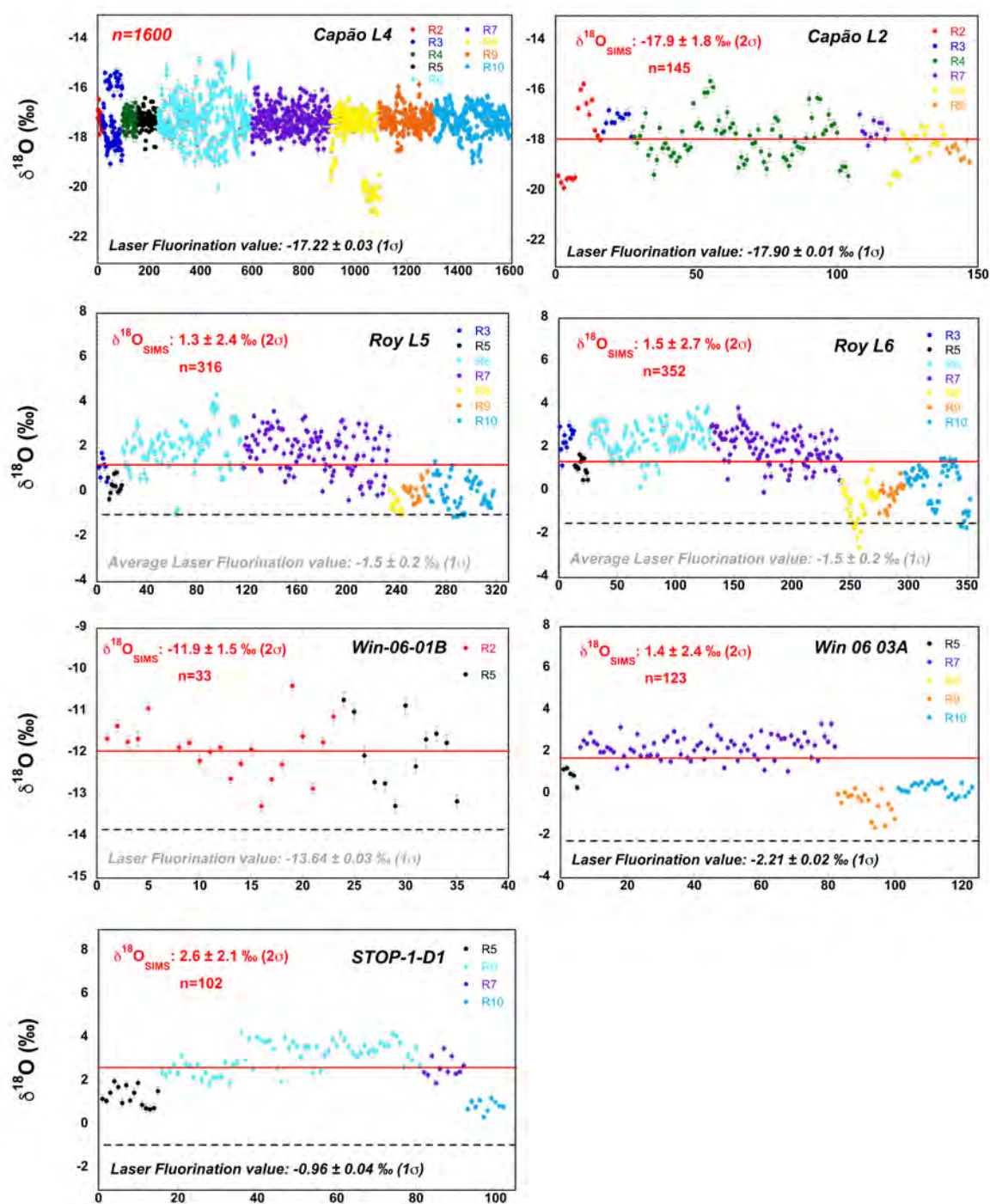


Figure 10: All SHRIMP-SI results obtained for natural goethite samples potentially suitable as reference material.

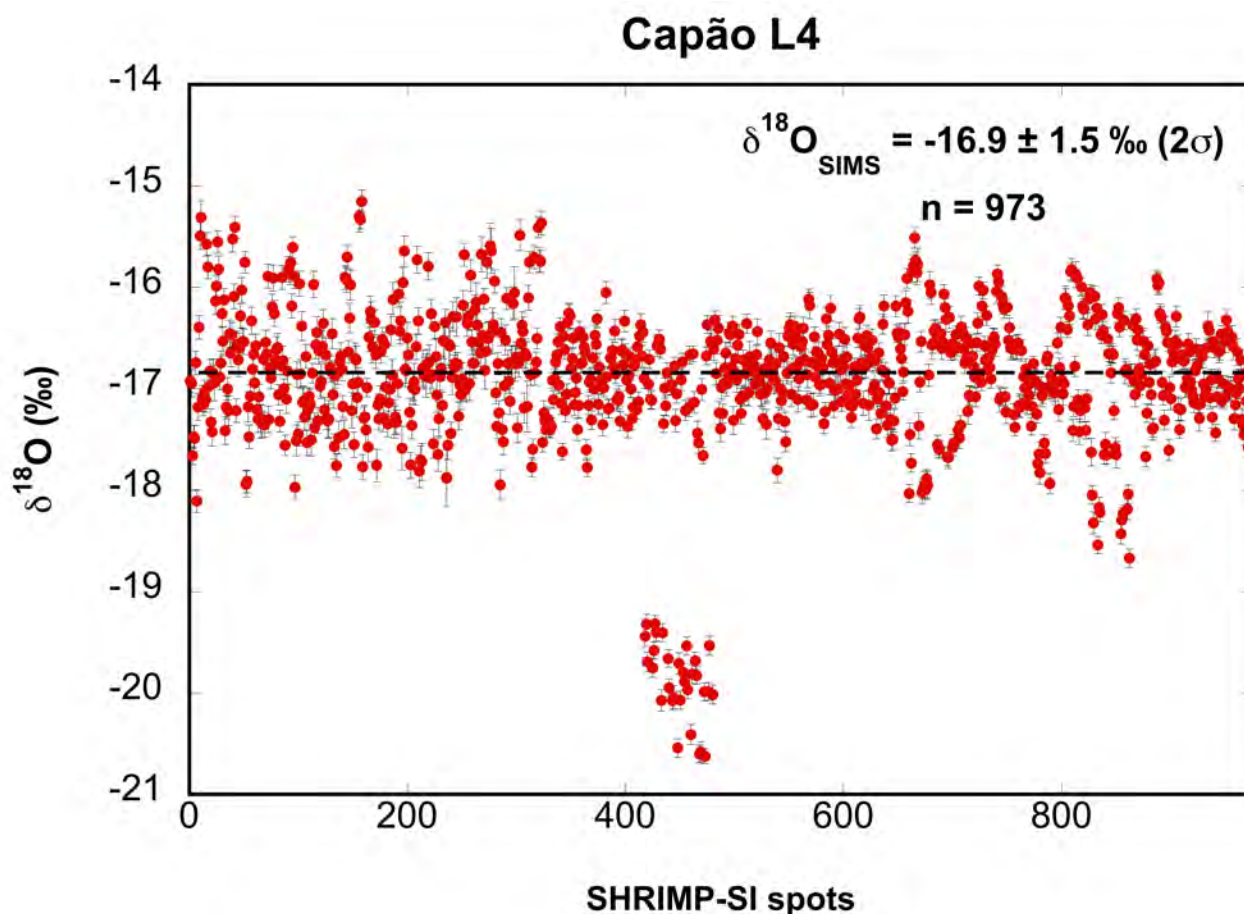


Figure 11: $\delta^{18}\text{O}_{\text{SIMS}}$ values obtained for our proposed reference material, Capão L4. $\delta^{18}\text{O}_{\text{SIMS}}$ values plotting between -19.4 and -21.0 (Run 8) represent two aliquots of the Capão L4 mounted perpendicular to the Capão L4 aliquot used as RM.

6. CONCLUSIONS

The Sensitive High Resolution Ion Microprobe for Stable Isotopes (SHRIMP-SI) is a unique platform for investigating the stable isotope composition preserved in supergene goethites (FeOOH) retrieved from continental weathering profiles. The comprehensive record of mineral precipitation preserved in these profiles, when combined with the fact that goethite can yield both age (by the (U-Th)/He method) and $\delta^{18}\text{O}$ signatures of minerals (and paleo-solutions from which these minerals precipitated), make the combined (U-Th)/He - SHRIMP-SI $\delta^{18}\text{O}$ approach an excellent tool to investigate the paleoclimatic record of terrestrial planets. In order to make this approach feasible, a suitable SHRIMP-SI $\delta^{18}\text{O}$ goethite reference material was identified and characterized. After evaluating several possible candidates, we concluded that a sample of dense colloform detrital goethite (Capão L4) from the Capão Mine, Minas Gerais, Brazil, provides a suitable goethite RM. Additional SHRIMP-SI tests show that crystallographic orientation plays a small role in measured $\delta^{18}\text{O}$ values, but sample porosity, relief, and minor element contents also affect the results significantly. The high spatial resolution possible with the SHRIMP-SI permits resolving the

isotopic composition of single growth bands in colloform samples, possibly resolving the temporal $\delta^{18}\text{O}$ record preserved in natural goethites.

Acknowledgements

We thank present and past colleagues from Vale, particularly Carlos Monte Lopes, Luzimar Rego, Clovis Maurity, Paulo Sérgio, Fernando Greco, Fernando Martins, Henrique Meireles, Carlos Augusto de Medeiros Filho, Augusto Kishida, and Felipe Porto for field support in the Carajás region. This project was funded by the Australian Research Council (ARC Discovery DP160104988) grant to Paulo Vasconcelos and Kenneth Farley, Australian Research Council (ARC LP1401008005) grant to Gordon Southam et al., Australian Research Council (ARC LE0560868) grant to Trevor Ireland, and the Brazilian Research Council (CNPq) Science Without Borders scholarship to HM.

REFERENCES

- Bao H. and Koch P. L. (1999) Oxygen isotope fractionation in ferric oxide-water systems: Low temperature synthesis. *Geochimica et Cosmochimica Acta*, **55** (1999) 599-613.
- Bao H., Koch P. L. and Thiemens H. (2000) Oxygen isotopic composition of ferric oxides from recent soil, hydrologic, and marine environments. *Geochimica et Cosmochimica Acta*, **64** (2000) 2221-2231.
- Bird M. I., Longstaffe F. J., Fyfe W. S., and Bildgen P. (1992) Oxygen-isotope systematics in a multiphase weathering system in Haiti. *Geochim. Cosmochim. Acta* **56**, 2831–2838.
- Bird M. I., Longstaffe F. J., Fyfe W. S., Kronberg B. I., and Kishida A. (1993) An oxygen-isotope study of weathering in the eastern Amazon Basin, Brazil. In *Climate Change in Continental Isotopic Records* (ed. P. K. Swart et al.), Vol. 78, pp. 295–307, Geophysical Monograph, American Geophysical Union.
- Eiler J. M., Graham C. and Valley J. W. (1997) SIMS analysis of oxygen isotopes: matrix effects in complex minerals and glasses. *Chemical Geology* 138, 221-244.
- Girard J.-P., Razanadranoro D. and Freyssinet P. (1997) Laser oxygen isotope analysis of weathering goethite from the lateritic profile of Yaou, French Guiana: paleoweathering and paleoclimatic implications. *Applied Geochemistry* 12, 163-174.
- Girard J.-P., Freyssinet P., and Chazot G. (2000) Unraveling climatic changes from intraprofile variation in oxygen and hydrogen isotopic composition of goethite and kaolinite in laterites: An integrated study from Yaou, French Guiana. *Geochim. Cosmochim. Acta* **64**, 409–426.
- Girard J.-P., Freyssinet P., and Morillon A.-C. (2002) Oxygen isotope study of Cayenne duricrust paleosurfaces: implications for past climate and laterization processes over French Guiana. *Chemical Geology* 191, 329-343.
- Glasauer, S., Friedl, J., and Schwertmann, U. (1999) Properties of Goethites Prepared under Acidic and Basic conditions in the Presence of Silicate. *Journal of Colloid and Interface Science* **216**, 106-115.
- Huberty J. M., Kita N. T., Kozdon R., Heck P. R., Fournelle J. H., Spicuzza M. J., Xu H., and Valley J. W. (2010) Crystal orientation effects in $\delta^{18}\text{O}$ for magnetite and hematite by SIMS. *Chemical Geology* 276, 269-283.
- Ickert R. B., Hiess, J., Williams, I. S., Holden, P., Ireland, T. R., Lanc, P., Schram, N., Foster, J. J.,

- and Clement, S.W. (2008) Determining the high precision, in situ, oxygen isotope ratios with a SHRIMP II: Analyses of MPI-DING silicate-glass reference materials and zircon from contrasting granites. *Chemical Geology* **257**, 114-128.
- Ickert R. B. and Stern R. A. Matrix (2013) Corrections and Error Analysis in High Precision SIMS $^{18}\text{O}/^{16}\text{O}$ Measurements of Ca–Mg–Fe Garnet. *Geostandards and Geoanalytical Research* XX, 1-20.
- Ireland T. R. (1995) Ion microprobe mass spectrometry: Techniques and applications in cosmochemistry, geochemistry, and geochronology. In: *Advances in analytical geochemistry*. M. Hyman & M. Rowe (eds.). JAI Press, Vol. 2: 1-118.
- Ireland T. (2004) SIMS Measurements of Stable Isotopes. *Handbook of Stable Isotope Analytical Tecqniques*, Volume-I, 654-691
- Ireland, T. R., Clement, S., Compston, W., Foster, J. J., Holden, P., Jenkins, B., Lanc, P., Schram, N., and Williams, I. S. (2008) Development of SHRIMP, *Australian Journal of Earth Sciences*, **55**: 6 – 7, 937 – 954.
- Ireland T.R., Schram N., Holden P., Lanc P., Ávila J., Armstrong R., Amelin Y., Latimore A., Corrigan D., Clement S., Foster J.J., and Compston W. (2014) Charge-mode electrometer measurements of S-isotopic compositions on SHRIMP-SI. *International Journal of Mass Spectrometer* 359, 26-37.
- Kita N. T., Ushikubo T., Fu B., Valley J. W. (2009) High precision SIMS oxygen isotope analysis and the effect of sample topography. *Chemical Geology* 264, 43-57
- Lyon, I.C., Saxton, J.M., Cornah, S.J., 1998. Isotopic fractionation during secondary ionisation mass spectrometry: crystallographic orientation effects in magnetite. *International Journal of Mass Spectrometry and Ion Processes* 172 (1–2), 115–122.
- Miller H. B. D., Vasconcelos P. M. P., Eiler J. M., and Farley K. A. (2017) An Australian Cenozoic terrestrial paleoclimate record from He dating and stable isotope geochemistry of goethites. *Geology*, doi: <https://doi.org/10.1130/G38989.1>.
- Monteiro H. S., Vasconcelos P. M., Farley K. A., Spier C. A. and Mello C. L. (2014) (U-Th)/He geochronology of goethite and the origin and evolution of cangas. *Geochimica et Cosmochimica Acta* **131**, 267-289.
- Monteiro H. S., Vasconcelos P. M., and Farley K. A. (2017a) A combined (U-Th)/He and

cosmogenic ^3He record of landscape armoring by biogeochemical iron cycling. Submitted to the *Journal of Geophysical Research – Earth Surface*.

Monteiro H. S., Vasconcelos P. M., Farley K. A., and Waltenberg, K. M. (2017b) On goethite as (U-Th)/He and $^4\text{He}/^3\text{He}$ geochronometer. To be submitted to the *American Journal of Sciences*.

Mostert A. B. (2014) Variations in Goethite Crystallography with Reference to the Ravensthorpe Ni-Laterite, PhD Thesis, The University of Queensland, Brisbane, p. 290.

Poage M. A., Sjöström D. J., Goldberg J., Chamberlain C. P., Furniss G. (2000) Isotopic evidence for Holocene climate change in the northern Rockies from a goethite-rich ferricrete chronosequence. *Chemical Geology* 166, 327-340.

Schulze, D.G. (1984) The influence of aluminium on iron oxides. VIII. Unit-cell dimensions of Al-substituted goethites and estimation of Al from them. *Clays and Clay Minerals* 32, 8.

Schwertmann, U. (1994) Aluminum influence on iron oxides: XVII. Unit-cell parameters and aluminium substitution in natural goethites. *Soil Science Society of American Journal* 58, 256-261.

Sjöström D. J., Hren M. T. and Chamberlain C. P. (2004) Oxygen isotope records of goethite from ferricrete deposits indicate regionally varying Holocene climate change in the Rocky Mountain region, U.S.A.

Valley, J.W., Kitchen, N., Kohn, M.J., Niendorf, C.R., Spicuzza, M.J. (1995) UWG-2, a garnet standard for oxygen isotope ratios: strategies for high precision and accuracy with laser heating. *Geochimica et Cosmochimica Acta* 59, 5223–5231.

Vasconcelos P. M., Heim J. A., Farley K. A., Monteiro H. S., Waltenberg K. (2013) $^{40}\text{Ar}/^{39}\text{Ar}$ and (U-Th)/He - $^4\text{He}/^3\text{He}$ geochronology of landscape evolution and channel iron deposit genesis at LynnPeak, Western, Australia. *Geochimica et Cosmochimica Acta* 117, 283-312.

Vielzeuf D., Champenois M., Valley J. W., Brunet F., and Devidal J. L. (2005) SIMS analyses of oxygen isotopes: Matrix effects in Fe-Mg-Ca garnets. *Chemical Geology* 223, 208-226.

Waltenberg K. M. (2014). Mineral physics and crystal chemistry of minerals suitable for weathering geochronology: implications to $^{40}\text{Ar}/^{39}\text{Ar}$ and (U-Th)/He geochronology. PhD Thesis, School of Earth Sciences, The University of Queensland, 421p.

Yang, H., Lu, R., Downs, R.T., Costin, G., 2006. Goethite, $\alpha\text{-FeO(OH)}$, from single-crystal data. *Acta Crystallographica*, Section E: Structure Reports Online E62, i250-i252.

- Yapp C. J. (1987) Oxygen and hydrogen isotope variations among goethites (α -FeOOH) and the determination of paleotemperatures. *Geochim. Cosmochim. Acta* 51, 355–364.
- Yapp C. J. (1990) Oxygen isotopes in iron(III) oxides. 1. Mineral– water fractionation factors. *Chem. Geol.* 85, 329–335.
- Yapp C. J. (1993) The stable isotope geochemistry of low temperature Fe(III) and Al “oxides” with implications for continental paleoclimates. *Clim. Change Cont. Isotopic Records Geophys. Monograph* 78, 285–294.
- Yapp C. J. (1997) An assessment of isotopic equilibrium in goethites from a bog iron deposit and a lateritic regolith. *Chem. Geol.* 135, 159–171.
- Yapp C. J. (1998) Paleoenvironmental interpretations of oxygen isotope ratios in oolitic ironstones. *Geochim. Cosmochim. Acta* 62, 2409–2420.
- Yapp C. J. (2000) Climatic implications of surface domains in arrays of δD and $\delta^{18}O$ from hydroxyl minerals: goethite as an example. *Geochim. Cosmochim. Acta* 64, 2009–2025.
- Yapp C. J. (2001) Rusty relics of Earth history: iron(III) oxides, isotopes and surficial environments. *Ann. Rev. Earth Plan. Sci.* 29, 165–199.
- Yapp C. J. (2007) Oxygen isotopes in synthetic goethite and a model for the apparent pH dependence of goethite–water $^{18}O/^{16}O$ fractionation. *Geochim. Cosmochim. Acta* 71, 1115–1129.
- Yapp C. J. (2008) $^{18}O/^{16}O$ and D/H in goethite from a North American Oxisol of the Early Eocene climatic optimum. *Geochim. Cosmochim. Acta* 72, 5838–5851.
- Yapp C. J. and Pedley M. D. (1985) Stable hydrogen isotopes in iron oxides-II. D/H variations among natural goethites. *Geochim. Cosmochim. Acta* 49, 487–495.
- Yapp C. J. and Poths H. (1995) Stable hydrogen isotopes in iron oxides: III. Nonstoichiometric hydrogen in goethite. *Geochim. Cosmochim. Acta* 59, 3405–3412.
- Yapp C. J. and Shuster D. L. (2011) Environmental memory and a possible seasonal bias in the stable isotope composition of (UTh)/ He-dated goethite from the Canadian Arctic. *Geochim. Cosmochim. Acta* 75, 4194–4215.

Yapp, C. J. (2012) Oxygen isotope effects associated with substitution of Al and Fe in synthetic goethite: Some experimental evidence and the criterion of oxygen yield. *Geochim. Cosmochim. Acta* 97, 200–212.

Chapter 6: Cenozoic continental paleoclimatic record from combined (U-Th)/He dating and SHRIMP-SI $\delta^{18}\text{O}$ analysis of goethite

Monteiro, H.S.^{1*}, Vasconcelos, P.M.^{1,3}, Ávila, J.N.², Farley, K.A.³, and Ireland, T.R.²

¹*School of Earth and Environmental Sciences, The University of Queensland, Brisbane, Queensland 4072, Australia*

²*Research School of Earth Sciences, The Australian National University, Canberra, ACT 2601, Australia*

³*Division of Geological and Planetary Sciences, California Institute of Technology, Pasadena, CA 91125, USA*

To be submitted to Nature (after shortening, of course)

** Corresponding author:*

H.S. Monteiro

The University of Queensland

Earth and Environmental Sciences, Steele Building

Brisbane, Qld 4072

Phone: (61)(7) 3346-7636 (Office)

ABSTRACT

We combined laser-heating (U-Th)/He geochronology, Sensitive High Resolution Ion Microprobe Stable Isotope (SHRIMP-SI) $\delta^{18}\text{O}$ analysis ($\delta^{18}\text{O}_{\text{SIMS-gth}}$), and electron microprobe analysis of goethites from lateritic weathering profiles to produce two near continuous Cenozoic paleoclimatic records for the continental interior of Brazil. The continental $\delta^{18}\text{O}$ goethite records span from ~ 70 Ma to 900 ka at Carajás and from ~ 40 Ma to 600 ka at the Quadrilátero Ferrífero. The results identify major climatic shifts in continental Brazil compatible with global climatic shifts observed in the $\delta^{18}\text{O}$ record of oceanic sediments. Periods of optimum climatic conditions (Early to Mid-Eocene, Late Oligocene, and Mid-Miocene) are characterized by more frequent precipitation of weathering minerals, stoichiometrically pure goethites, and $\delta^{18}\text{O}_{\text{SIMS-gth}}$ shifts towards lighter isotopic values. These shifts are consistent with warm monsoonal conditions in the continental interior. Abrupt shifts in the $\delta^{18}\text{O}_{\text{SIMS-gth}}$ record towards more positive values occur during global glaciation (Oi-1 and Mi-1 glaciations), periods that also correspond to less frequent precipitation of Al-rich goethites suggestive of dryer continental environments. The combined goethite (U-Th)/He- $\delta^{18}\text{O}_{\text{SIMS-gth}}$ record provides a robust new way of investigating continental paleoclimates on Earth.

1. INTRODUCTION

Much of what we know about the Earth's past climate and environmental conditions comes from ocean sediments (Holland, 1984; Veizer et al., 1999; Zachos et al., 2001), as we still lack a continuous and long-term paleoenvironmental record for exposed landmasses. The continental climatic history, crucial for understanding direct effects of future climate changes on human activity on Earth, is poorly resolved (Koch, 1998; Mosbrugger et al., 2005). The lack of such data makes the reconciliation between continental and oceanic records difficult. A traditional route to continental paleoenvironmental reconstruction is the paleoecological interpretation of the fossil record, a robust approach but one that is fragmentary and incomplete (e.g., Wolfe, 1994; White, 1994). Soils and weathering profiles provide useful information, but data traditionally retrieved from these systems are often qualitative and based on interpreting mineral assemblages and stratigraphic relationships (Retallack, 2001). Notable efforts to use the isotopic composition of pedogenic phases to infer quantitative paleoenvironmental conditions (Lawrence & Taylor, 1972; Bird & Chivas, 1988, 1989, 1993; Koch, 1998; Gilg, 2000; Poage et al., 2000; Poage & Chamberlain, 2005; Sheldon & Tabor, 2009) yield valuable insights; but a great uncertainty in this approach is the lack of direct information on the timing of precipitation of the phases analysed. A promising solution to this problem resides in the joint application of geochronology, elemental analysis, and stable isotope geochemistry to minerals precipitated and preserved in long-lived chemically stratified weathering profiles, i.e., lateritic profiles (Vasconcelos et al., 2015) (Figure 1).

Lateritic profiles, common on cratonic landmasses, have a history of surface exposure spanning as far back as ~ 70 Ma, potentially hosting a continuous continental paleoenvironmental record (Vasconcelos, 1999a). This continuous history of exposure results in deep profiles (> 100 m sometimes exceeding 500 m) hosting complex mineral assemblages precipitated by weathering reactions (Vasconcelos, 1999b) (Figure 1). Some of these minerals, particularly oxides and hydroxides of Fe, Al, and Mn, may form throughout the entire history of weathering. Supergene oxides and hydroxides precipitated during profile evolution may continue to exist, in metastable equilibrium, from the time of mineral precipitation to the present (Vasconcelos et al., 2015). If these minerals can be individually identified, dated, and analyzed for their elemental and environmental isotope compositions (O, H, C, etc.), a complete history of weathering is potentially recoverable. As continental weathering is directly linked to the magnitude and seasonal variations in surface temperature and rainfall (Slessarev et al. 2016), ancient lateritic weathering profiles may provide the long-term land-based record needed to reconcile ocean- and continent-based paleoenvironmental histories.

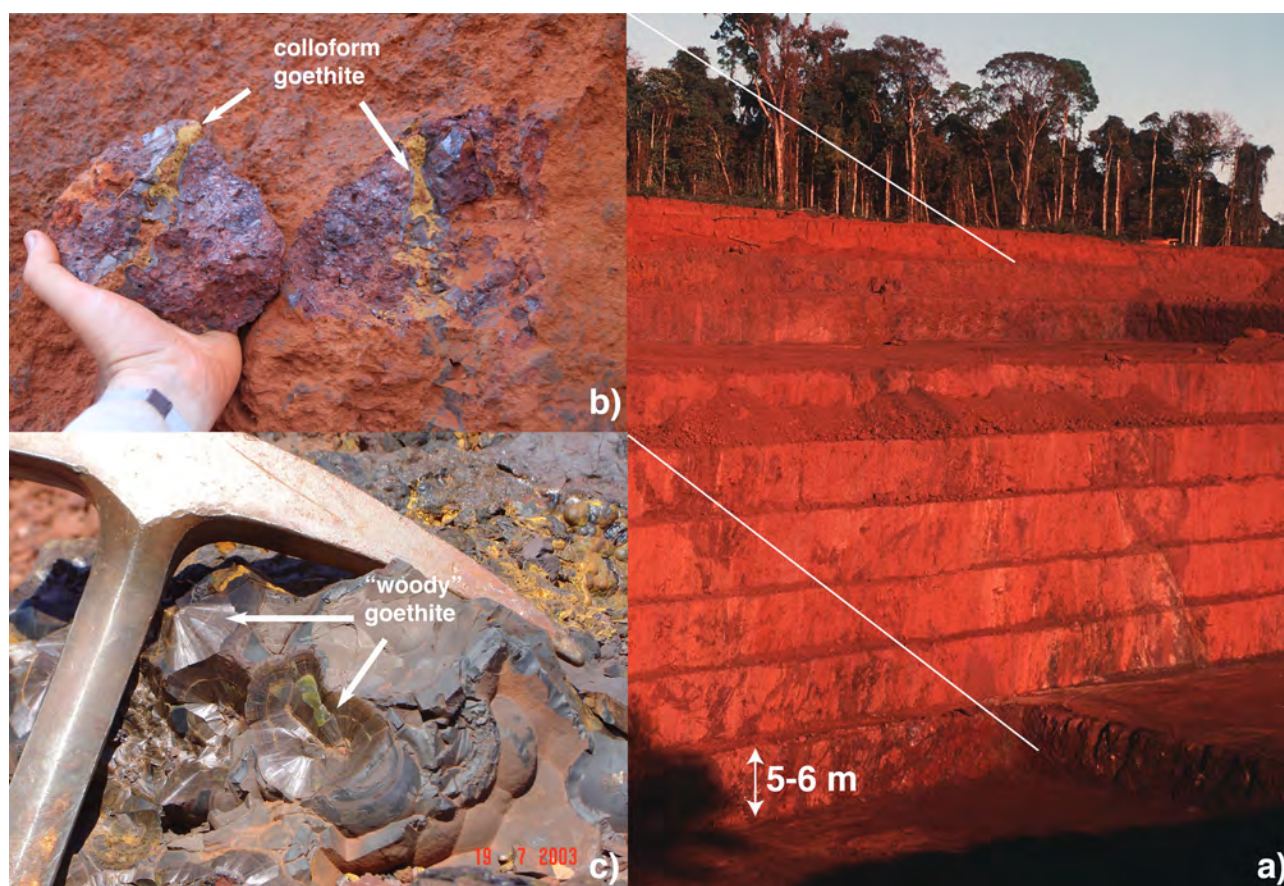


Figure 1. (a) Lateritic weathering profiles, such as the Igarapé Bahia lateritic gold deposit in the Carajás Mountains, Pará, Brazil, host supergene goethites precipitated throughout the evolution of the profile (b-c). These supergene goethites are colloform, often showing a woody texture where each individual growth band potentially records the elemental and isotopic compositions of weathering solutions (meteoric water) during mineral precipitation in the remote past. Electron microprobe combined with (U-Th)/He- $\delta^{18}\text{O}_{\text{SIMS-gth}}$ analysis of each growth band yields a history of meteoric water composition through time, and it permits the generation of a nearly continuous record of paleoenvironmental conditions for continental landscapes.

A major obstacle in retrieving ages and isotopic signatures from minerals formed by weathering is their fine-grained nature, which requires high spatial resolution analytical methods. Fortunately, developments in microanalysis have greatly improved our ability to date these phases: $^{40}\text{Ar}/^{39}\text{Ar}$ dating of supergene K-bearing oxides and sulfates (Vasconcelos et al., 1994; Vasconcelos, 1999; Vasconcelos & Conroy, 2003); (U-Th)/He dating of supergene goethite and hematite (Shuster et al., 2005; Heim et al., 2006; Farley and Flowers, 2008; Vasconcelos et al., 2013; Monteiro et al., 2014; Miller et al., 2017); micro-sampling and U-series dating of pedogenic carbonates (Sharp et al., 2003); *in situ* LA-MC-ICP MS U-series dating of supergene Fe-oxyhydroxides (Bernal *et al.* 2005, 2006) or carbonates; and U-Pb dating of speleothems (Woodhead *et al.*, 2006). Similarly, improvements in the theoretical understanding of O-isotope systematics in supergene Fe oxyhydroxides (e.g., Yapp, 2001) accompanied by developments in $\delta^{18}\text{O}$ analysis by laser methodologies (Girard et al., 1997; Bao et al., 1999; Sharp et al., 2001) and ion probes (Ireland et al., 2008) have provided a more robust approach for retrieving paleoenvironmental information from the isotopic analysis of minerals precipitated by weathering.

The missing component in most of these studies, with rare exceptions (Sjostrom et al., 2004; Yapp & Shuster, 2011; Miller et al., 2017), is tying high-resolution geochronology to high-spatial resolution elemental and stable isotope analysis. A difficulty in this combined approach is that most elemental and isotopic analyses are destructive and require large sample masses, challenging our ability to retrieve complementary data from that exact same aliquot of a hand sample potentially containing several generations of the same mineral. Even more important is the need to apply geochronology and environmental isotope analysis to a single mineral phase (e.g., goethite) that may have precipitated throughout the entire history of weathering and which may host a nearly continuous record of continental water-rock interactions through time.

Both of these challenges can be overcome if we take advantage of natural textural features in supergene minerals (i.e., minerals precipitated by weathering solutions). An advantage of some supergene oxides and hydroxides is their tendency to form sequential growth bands – i.e., colloform textures – that can lead to pure and homogenous generations of a same mineral phase, where each individual band was precipitated from the same solution, at the same time, under the exact same environmental conditions (Figure 1). These bands, which can range for μm to mm , and form masses spanning tens of centimetres, are analogous to growth bands in trees or stalagmites-stalactites. Sampling and analysing these individual bands provides a sequential environmental record spanning significant time periods (Vasconcelos et al., 1994; Monteiro et al., 2017d). By targeting colloform mineral masses, it is possible to analyse, by various methods, several fragments from a coeval growth band. We can date several aliquots from each band; carry out electron microprobe analyses on equivalent aliquots to determine elemental compositions and mineral stoichiometry; and analyse the oxygen stable isotope compositions of these very same aliquots by in situ ion microprobe. This approach, key to successful continental paleoenvironmental reconstructions, requires fully automated high-resolution geochronological and stable isotope systems to enable quick and cost-effective analysis of multiple aliquots from a sample and to produce a statistically significant time-series of mineral elemental and isotopic compositions.

Here we combine (U-Th)/He geochronology, electron microprobe analysis, and SHRIMP-SI $\delta^{18}\text{O}$ investigation of colloform goethites to determine continental environmental histories preserved in weathering profiles from the Serra dos Carajás, Pará, and the Quadrilátero Ferrífero (QF), Minas Gerais, Brazil (Figure 2). These two sites are located in continental areas that have been continuously emergent and exposed at the surface at least since the Mesozoic (Figure 2) (and possibly since the Permo-Triassic transition) (Müller, et al., 2008 and references therein). They also contain deep, long-lived, and previously dated weathering profiles with a history of episodic mineral precipitation spanning the entire Cenozoic (Vasconcelos et al., 1994; Ruffet et al., 1996;

Shuster et al., 2005; Spier et al., 2006; Vasconcelos and Carmo, 2017, *submitted*; Monteiro et al., 2017c). Exploration and mining activities at these sites enable access to entire profiles, where deeply weathered banded iron-formation and sulfide ore bodies host an abundance of pure and colloform supergene goethites. The relative locations of Carajás and the QF permit assessing the influence of local, regional, and global weather patterns on the temporal and environmental evolution of weathering profiles. South America's relatively stationary Cenozoic latitudinal position ($\sim 10\text{-}11^\circ$ northward migration) during the past 70 Ma suggest that continental weathering profiles should record changing regional or global climates through time, as opposed to the continent's changing position with respect to climatic zones, as is the case for Australia (e.g. Bird et al., 1988; Miller et al., 2017).

2. STUDY SITES AND SAMPLING APPROACH

The Carajás sampling sites are located 6° S and ~ 550 km inland south of the Amazon delta on top of 700-800m plateaus blanketed by deeply weathered profiles developed on banded iron formations (N1 site) and lateritic gold deposits formed over iron-oxide copper-gold deposits (Igarapé Bahia site) (Figure 2). The climate in the region is tropical monsoon (Köppen and Geiger, 1961), with mean annual temperature of 25°C , $\sim 2000\text{-}2400\text{mm}$ average annual precipitation, with most of the precipitation concentrated in the Dec-May period and a dry season from Jun-Nov (Figure 3) (WORLD METEOROLOGICAL ORGANIZATION).

The Quadrilátero Ferrífero sites are in southeastern Brazil, $\sim 20^\circ\text{S}$ 43°W , and are also associated with deeply weathered banded iron-formation plateaus ranging from 1200 to 1800 m elevation (Figure 2). The sites are ~ 350 km inland from the Atlantic coast, with mean annual temperature of $\sim 20^\circ\text{C}$ and rainfall of ~ 1500 mm, also seasonal, with a rainy season from Oct-Mar and a dry season from Apr-Sep (Figure 3) (WORLD METEOROLOGICAL ORGANIZATION).

Eighty-three (83) samples selected from surface sites, open mining pits, and drill-cores were sectioned, and suitable goethites were micro-sampled, crushed, cleaned, and analyzed by mineralogical (SEM, EMPA, XRD, TGA), geochronological ((U-Th)/He) and isotopic ($^{18}\text{O}/^{16}\text{O}$ by Laser Fluorination and SHRIMP-SI) methods following the procedures presented in Monteiro et al. (2017a-d) and summarized in EA1 and EA2.

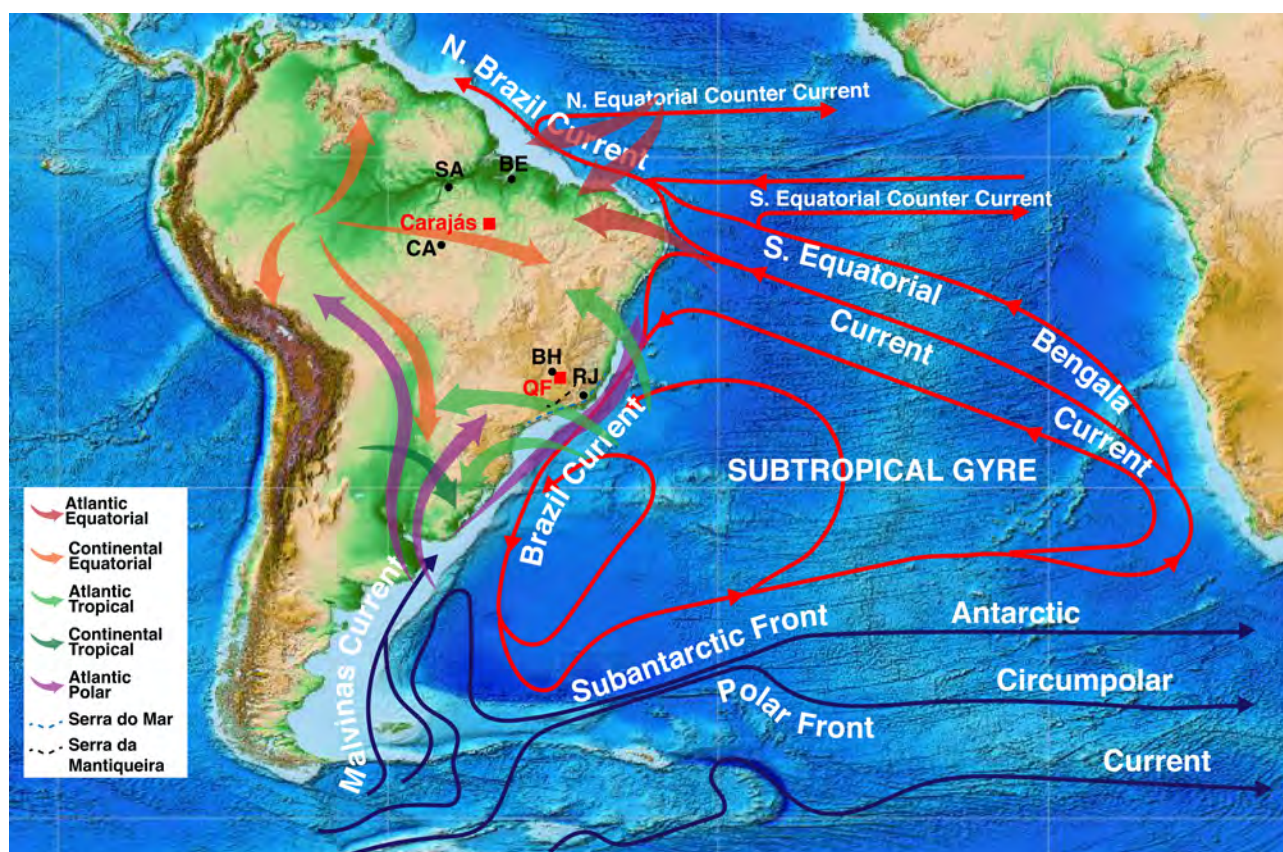


Figure 2. The two continental sites investigated in this study (Carajás and QF) are located in strategic positions in South America (Amante and Eakins, 2009) with respect to the equator, wind patterns, and oceanic currents that may affect the supply and isotopic composition of rainfall at each site. We also illustrate the locations of International Atomic Energy Agency stations for meteoric water collection and isotopic analysis (BE-Belém, SA-Santarém, CA-Cachimbo; BH-Belo Horizonte; RJ-Rio de Janeiro). Potential orographic barriers to moisture delivery to the QF (Serras do Mar and da Mantiqueira) are also illustrated. The interplay between the Subtropical Gyre and the Subantarctic Front in the geological past may have played a pivotal role in the isotopic composition of precipitation at the QF.

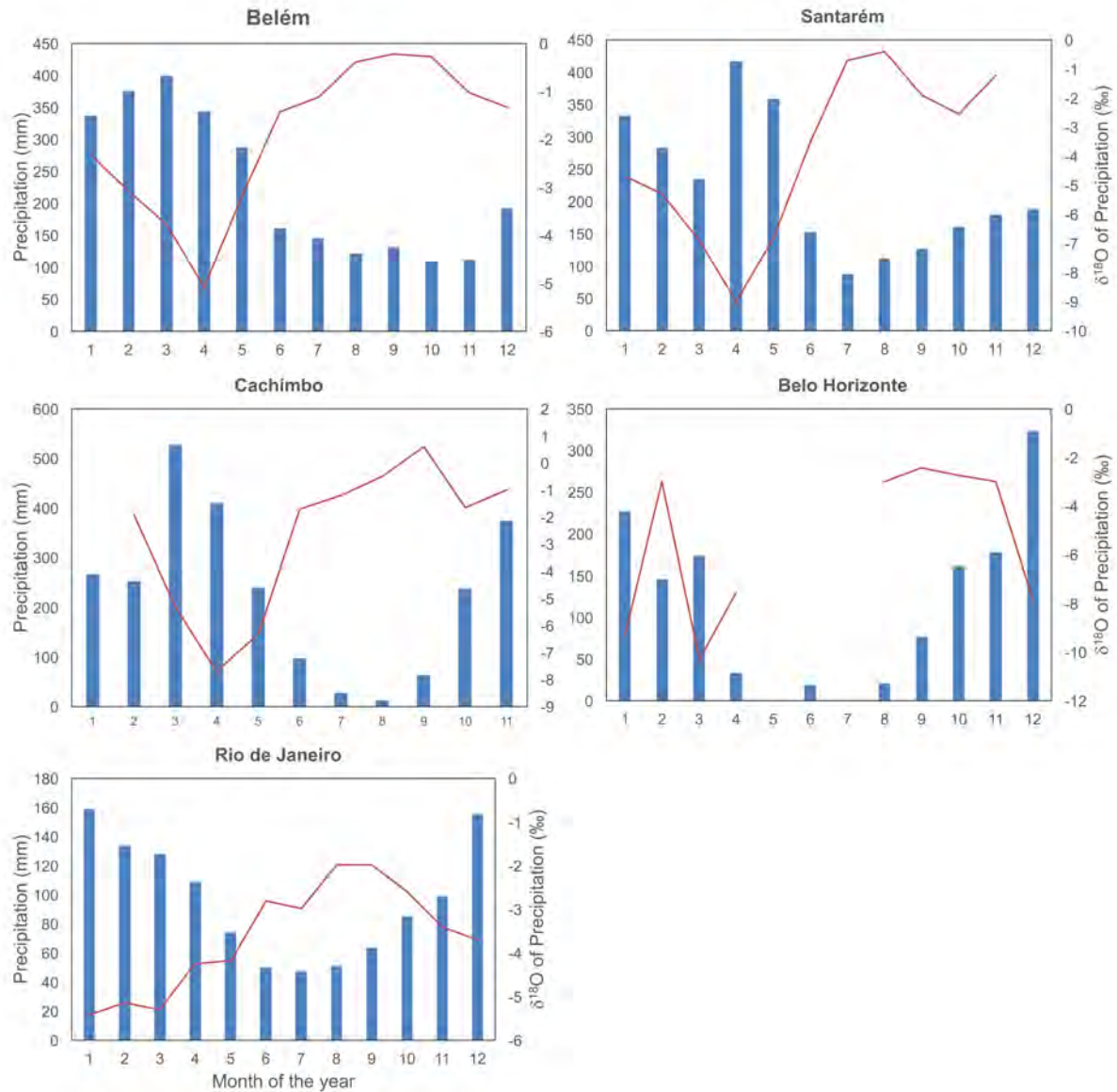


Figure 3: Multi-year monthly mean precipitation at the Belém, Santarém, Cachimbo, Belo Horizonte, and Rio de Janeiro sites show the irregular distribution and monsoonal character of rainfall at these sites, and the strong influence of precipitation intensity on the $\delta^{18}\text{O}$ value of rainfall (WORLD METEOROLOGICAL ORGANIZATION; INTERNATIONAL ATOMIC ENERGY AGENCY). These data suggest that the isotopic composition of surface and groundwater (including soil and weathering solutions) at these sites primarily reflect the isotopically light precipitation delivered during the wet seasons at each of these sites.

3. RESULTS

A total of 107 and 280 goethite (U-Th)/He ages and 1429 (34 samples) and 557 (32 samples) individual $\delta^{18}\text{O}_{\text{SIMS-gth}}$ results from Carajás and the QF, respectively, provide an extensive database for reconstructing the paleoclimatic history at these two sites (EA2). The results are complemented by 2400 electron microprobe analyses. The continental $\delta^{18}\text{O}_{\text{SIMS-gth}}$ record is remarkably complete, spanning from ~ 70 Ma to 900 ka at Carajás and from ~ 40 Ma to 600 ka (the lower limit of the (U-Th)/He method) at the QF (Figure 4).

$\delta^{18}\text{O}_{\text{SIMS-gth}}$ values range from -4.7 ± 0.1 to 26.8 ± 0.2 ‰ (95% CI) for the Igarapé Bahia site, from -2.0 ± 0.1 to 14.5 ± 0.1 ‰ (95% CI) for the N1 site, and from -7.3 ± 0.3 to 16.7 ± 0.2 ‰ (95% CI) for the QF site. Extreme positive $\delta^{18}\text{O}_{\text{SIMS-gth}}$ values correspond to Al-rich goethites. The $\delta^{18}\text{O}_{\text{SIMS-gth}}$ data were smoothed using a 5-point moving average, and curve-fitted using a smooth function. Long-term shifts of the $\delta^{18}\text{O}_{\text{SIMS-gth}}$ record intensification and decline in precipitation. The most noticeable wetting trends (and global warming trends from the benthic isotopic record) occurred from the Mid-Paleocene to Mid-Eocene, Late Oligocene (the QF $\delta^{18}\text{O}_{\text{SIMS-gth}}$ record show an opposite trend for this interval), and Mid-Miocene, while the most pronounced drying trends (and global cooling trends from the benthic isotopic record) appeared near the Eocene-Oligocene boundary, Early Miocene, and at the Miocene-Pliocene transition (the QF $\delta^{18}\text{O}_{\text{SIMS-gth}}$ record also display an opposite trend for this interval). The most noticeable peaks appear at the Paleocene-Eocene boundary (~ 54 Ma), Early to Middle Oligocene (~ 30 Ma), and Mid-Miocene (~ 16-8 Ma) for Carajás and the QF.

4. DISCUSSION

An important feature, and potential difficulty, in both records is that the distribution of minerals through time is not homogeneous. There are periods when mineral precipitation is more frequent (e.g., Mid-Miocene), while other periods (Late Oligocene-Early Miocene) show gaps in mineral precipitation. This irregular distribution may simply reflect a sampling bias; alternatively, it may reflect a real variation in the intensity of mineral precipitation through time (Vasconcelos, 1999a). Intensification of rainfall or large drawdowns of the water table may enhance water-rock interaction, leading to large volumes of minerals precipitated (Vasconcelos et al., 1994, 2015). In this case, random sampling of the weathering profiles will invariably be biased by the preferential recovery of overrepresented minerals.

4.1. Mineralogical Controls

In addition to variable distribution through time, goethites show periodic variation in elemental and isotopic composition. As these changes may be interdependent (e.g., $\delta^{18}\text{O}$ value of goethite depends both on the isotopic composition of the weathering solution and on the elemental composition of the goethite), it is necessary to differentiate between these two effects. Furthermore, the isotopic composition of goethite measured in situ by ion microprobe – $\delta^{18}\text{O}_{\text{SIMS-gth}}$ – may also suffer from matrix effects (Eiler et al., 1997; Vielzeuf et al., 2005), and matrix corrections for the various trace elements in goethite were not applied in this study (correction for matrix effects requires goethite reference materials with various trace element contents analyzed by both laser fluorination and ion microprobe, and these reference materials are not yet available) (Monteiro et al, 2017d). Therefore,

we need to independently assess the magnitude of the matrix effects in this study to confidently assess that our $\delta^{18}\text{O}_{\text{SIMS-gth}}$ curves indeed map the variation of goethite isotopic composition through time.

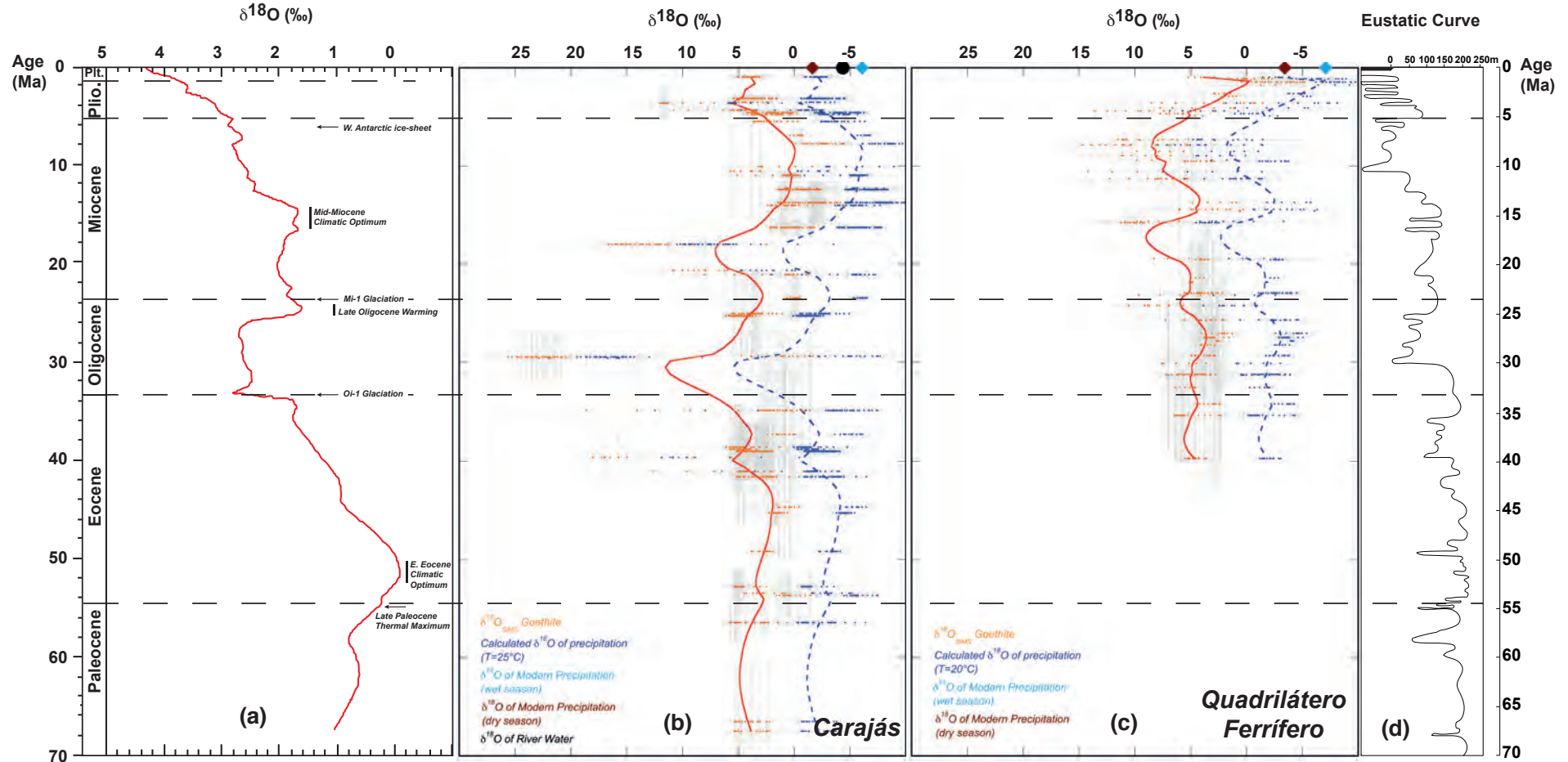


Figure 4. (U-Th)/He Vs. $\delta^{18}\text{O}_{\text{SIMS-gth}}$ data for Carajás (b) and the QF (c) are plotted against the $\delta^{18}\text{O}$ data of ocean sediments of Zachos et al. (2001) (a) and the eustatic sea level curve of Haq et al. (1987). Also shown are major Cenozoic climatic events. The continental $\delta^{18}\text{O}$ goethite record spans from ~70 Ma to 900 ka at Carajás and from ~40 Ma to 600 ka at the QF. Also plotted are estimated compositions of rainwater through time (assuming a constant temperature of 25 and 20°C and goethite-water fractionation factors of 1.0061 and 1.0067 for the Carajás, and QF sites, respectively), the isotopic composition of present rainwater in nearby sites during the wet and dry seasons, and the isotopic composition of river water near Carajás.

Correlation diagrams (Figure 5) show that trace elements known to replace Fe in (Fe-X)OOH solid solutions (where X = Al, Mn, Cu) affect to greater or lesser extents our measured $\delta^{18}\text{O}_{\text{SIMS-gth}}$ values. For example, Al appears to influence $\delta^{18}\text{O}_{\text{SIMS-gth}}$ while Mn and Cu do not. Elements that show elevated concentrations in our goethites (Si and P) but whose crystallographic positions are undetermined (EA1) also appear to have no influence on measured $\delta^{18}\text{O}_{\text{SIMS-gth}}$. Therefore, our data confirm that enrichment in Mn, Cu, Si (samples containing Al > 4wt% are not plotted), and P do not affect measured $\delta^{18}\text{O}_{\text{SIMS-gth}}$ results. Similarly, up to 2 wt% Al contents do not appear to influence the measured $\delta^{18}\text{O}_{\text{SIMS-gth}}$ values; on the other hand, goethites containing more than 4 wt% Al in solid solution show a noticeable increase in measured $\delta^{18}\text{O}_{\text{SIMS-gth}}$. This increase can result from matrix effects; from larger goethite-water $^{18}\text{O}/^{16}\text{O}$ fractionation factors with increasing Al contents (Yapp, 2012); and from the fact that lower water-rock ratios may lead to heavier waters and more alkaline solutions, leading to the precipitation of Al-rich goethites (Mostert, 2014) enriched in ^{18}O .

The correlation plot between wt% Al and $\delta^{18}\text{O}_{\text{SIMS-gth}}$ defines a line with slope of ~ 2 . Two important features in that correlation suggest that matrix effects cannot entirely account for the shift in $\delta^{18}\text{O}$. First, the largest Al contents do not correspond to the highest measured $\delta^{18}\text{O}_{\text{SIMS-gth}}$ values. Second, matrix effects alone could not explain the high ^{18}O enrichments in some the goethites containing moderate average (4-7 wt%) Al-contents. High $\delta^{18}\text{O}_{\text{SIMS-gth}}$ values could result from the added contributions of matrix effects (an analytical feature) and larger $^{18}\text{O}/^{16}\text{O}$ fractionation factors for Al-rich goethites (a sample dependent factor). However, the maximum shift in measured $\delta^{18}\text{O}$ from goethites containing up to 9 mol% Al is ~ 1 ‰ (Yapp, 1997), which is too low to explain the extreme ^{18}O enrichments in some of our samples.

Therefore, we tentatively conclude that the high measured $\delta^{18}\text{O}_{\text{SIMS-gth}}$ values indeed identify ^{18}O -rich goethites from our study sites, which most likely reveal goethite precipitation from waters enriched in ^{18}O . Goethite $\delta^{18}\text{O}$ values depend on the isotopic composition of the water from which it precipitates (Savin and Epstein, 1970; Lawrence and Taylor, 1971), temperature (Yapp, 1990), pH (Yapp, 2001 and references therein), rate of precipitation (Bao and Koch, 1999), post-precipitation recrystallization of poorly crystalline phases (Bao and Koch, 1999), Al substitution for Fe in the goethite structure (Yapp, 2012), and, in this study, matrix effects in the SHRIMP-SI. We have already presented evidence that matrix effects, although likely present in our results, do not completely explain the $\delta^{18}\text{O}$ enrichment of our Al-rich goethites. The effect of precipitation rates and post-precipitation recrystallization of poorly crystalline phases are important in experimental studies (Bao and Koch, 1999), but they are likely averaged out in the much longer-term natural

processes. The effects of trace elements other than Al (and maybe Si) appear negligible for the Carajás and QF samples. Temperature effects on goethite oxygen isotopic composition are relatively minor (Yapp, 2001). The fact that our study sites have always resided near the tropics, where temperature variations during the past 70 Ma should have been moderate, suggests that temperature may not have played a significant role on the isotopic compositions of our goethites. Temperature is also a minor factor in the isotopic composition of the meteoric waters from which our goethites precipitated, because its influence on the isotopic composition of rainwater near the tropics is negligible (Dansgaard, 1964; Rozanski et al., 1993; Salati et al., 1979).

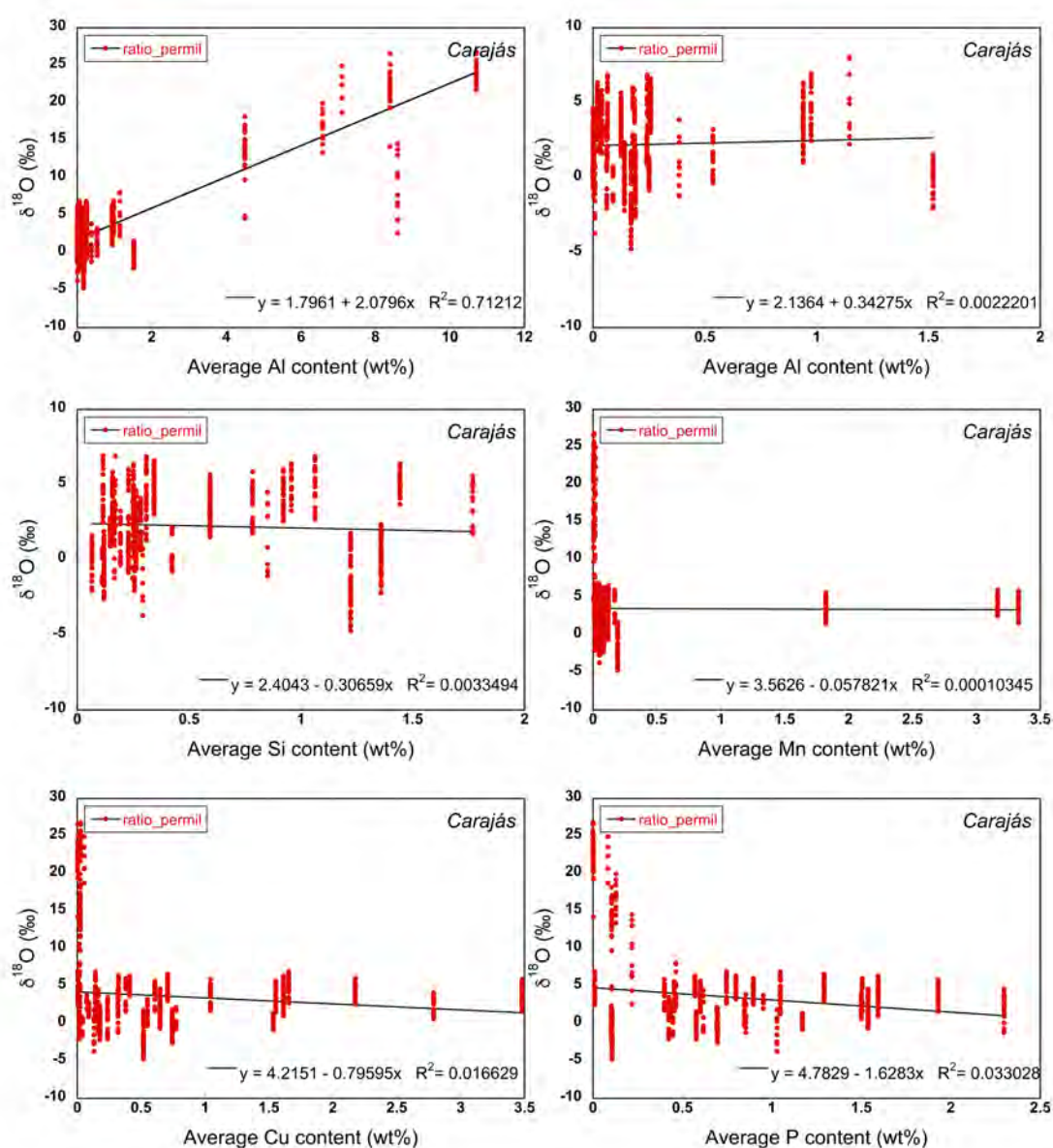


Figure 5. Correlation diagrams for the most important minor elements detected in our goethites and measured $\delta^{18}\text{O}_{\text{SIMS-gth}}$ values show that Mn, Cu, Si, and P do not affect the ion microprobe results. Al-contents up to $\sim 2\text{wt}\%$ also show no effect on the measured $\delta^{18}\text{O}_{\text{SIMS-gth}}$ values. However, goethites containing more than $\sim 2\text{wt}\%$ Al are enriched in ^{18}O . This enrichment is a function of a larger goethite-water fractionation factor for Al-rich

goethite (Yapp, 2012), it may result from matrix effects during $\delta^{18}\text{O}_{\text{SIMS-gth}}$ analysis, and it may also be a function of isotopically heavier and alkaline waters favoring the precipitation of Al-rich goethites during more arid conditions in our study sites.

4.2. Climatic Controls

The $\delta^{18}\text{O}$ values of rainwater in tropical regions is dependent on seasonality (wet and dry), where periods of intense rainfall correspond to isotopically light rain, and periods of less intense precipitation are marked by isotopically heavier precipitation (Figure 3). In the Amazon, most of the rainwater today originates from westward transported atmospheric moisture generated in the tropical Atlantic by Atlantic Equatorial winds (Figure 2), and precipitation is isotopically light during the rainy season (Dec-May), becoming progressively heavier in the dry season (Jun-Nov) (Figure 3) (WORLD METEOROLOGICAL ORGANIZATION; INTERNATIONAL ATOMIC ENERGY AGENCY). An additional effect, associated with recycling of rainwater by the vegetation, has been implicated in the progressively lighter composition of rainfall towards the interior of the continent (Salatti et al., 1979), an effect that is also enhanced during the rainy season. Rain and river waters near Carajás (Figures 3, 4), and probably the weathering solutions at Carajás, have isotopic compositions that are primarily controlled by the intense and isotopically light rain that falls in the wet season. Therefore, rainfall intensity, as opposed to continentality or temperature, poses the greatest influence on the isotopic compositions of weathering solutions at Carajás. The low elevations between Carajás and the Atlantic margin also suggest that there are no meaningful orographic effects. Plate reconstructions (Figure 6) reveal that orographic effects did not exist in the past either, suggesting that seasonality has possibly controlled the isotopic composition of weathering solutions at Carajás as far back as 70 Ma. The same variations in rainfall isotopic composition associated with seasonality should be observable in longer term climate cycles, when isotopic composition would be heavier during arid periods and become progressively lighter during wet and monsoonal paleoclimates. An additional feature that must be considered in long-term reconstructions, however, is the fact that the Amazon has been periodically occupied by large bodies of water during periods of high sea-level (Räsänen et al., 1995; Lovejoy et al., 1998). These continental water bodies were likely fed by continental precipitation flowing into the Amazon basin and were most probably extensive fresh water lakes with isotopic compositions strongly influenced by recycled isotopically light meteoric waters. If these continental lakes acted as local sources of moisture, driven easternward by enhanced Continental Equatorial winds, rainfall would be more abundant and even lighter during periods of high sea stand.

Similarly, at the QF seasonality also controls the isotopic composition of rainfall and weathering solutions, with isotopically lighter rainfall in the wet season and isotopically heavier precipitation during the dry season. But orographic effects associated with the barriers imposed by the Serras do

Mar and da Mantiqueira (Figure 2), which reach elevations exceeding 2,000 m, may also impact the isotopic composition of rainfall at the QF. Another effect, which we will discuss below, is the possible temporal variation in the isotopic composition, salinity, and temperature of ocean water along the southern coast of South America during periods of advancing or waning glaciation in Antarctica, with consequent intensification and northward incursion or southward regression of the Subantarctic Front and the Malvinas Current (Figure 2).

4.3. The Climatic Record Trough Time

We explore the significance and implications of the (U-Th)/He age vs $\delta^{18}\text{O}$ records for Carajás and the Quadrilátero Ferrífero, plotted in Figure 4 together with the $\delta^{18}\text{O}$ curve for ocean sediments of Zachos et al. (2001) and the sea-level curve of Haq et al. (1987). Also shown are estimated compositions of meteoric water through time (assuming a constant temperature and goethite-water fractionation factors of 1.0061 and 1.0067 for the Carajás and QF sites, respectively), the isotopic composition of present rainwater in nearby sites during the wet and dry seasons, and the isotopic composition of river water near Carajás. Even though our $\delta^{18}\text{O}_{\text{SIMS-gth}}$ record only extends until ~ 900 ka at Carajás and 600 ka at the QF, the goethite $\delta^{18}\text{O}$ values (and the calculated isotopic compositions of the weathering solutions at the time of goethite precipitation) are compatible with the isotopic composition of present river and rainwater at both sites. With the reassurance that our measured $\delta^{18}\text{O}_{\text{SIMS-gth}}$ values may indeed record the isotopic compositions of weathering solutions at present, we will now attempt to interpret the $\delta^{18}\text{O}_{\text{SIMS-gth}}$ record through time. Our interpretation is strongly based on the premise that variations in the isotopic composition of goethite through time primarily records the isotopic composition of rainfall, which is itself primarily dependent on the sources of moisture and on the intensity of precipitation (Salati et al., 1979), and relatively insensitive to mean surface temperature (Dansgaard, 1964; Rozanski et al., 1993).

The Carajás Record

The 70 Ma record for Carajás shows major trends and, particularly, shifts in the (U-Th)/He age vs $\delta^{18}\text{O}$ curve that are roughly consistent with global trends observed in the benthic foraminifera $\delta^{18}\text{O}$ record. Particularly noticeable are the shifts towards lighter isotopic compositions in the Eocene, Late Oligocene, and Mid-Miocene. Also noticeable are the trends towards heavier isotopic compositions near the Eocene-Oligocene boundary, the lower Miocene (~ 20 Ma), and at the Miocene-Pliocene transition. Discrepancies between the continental record at Carajás and the global marine record are the pronounced and persistent light $\delta^{18}\text{O}$ period throughout most of the Mid- and Late-Miocene and the tendency towards lighter isotopic values since the Mid-Pliocene on the continental record, showing exact opposite isotopic trends from the global oceanographic record.

The peaks in lighter isotopic compositions in the Eocene, Late Oligocene, and Mid-Miocene correspond to warmer periods in the global δO^{18} ocean record. Warmer oceans would result in enhanced evaporation and rainfall, intensifying plant growth, enhancing continental weathering, and promoting effective mineral/dissolution precipitation (Vasconcelos et al., 1994; Vasconcelos, 1999). This is suggested by distribution of dated goethites through time, which appear more frequent during these warm, wet intervals. Increased frequency of mineral precipitation, reflecting greater water-rock interaction, is independently substantiated by the $\delta^{18}\text{O}$ signatures of goethites precipitated at those times, which are isotopically lighter, independently suggesting intensification of rainfall.

Increases in the $\delta^{18}\text{O}$ values of supergene goethites at Carajás correspond to periods of enhanced global glaciation in the Eocene-Oligocene boundary, the lower Miocene (~ 20 Ma), and at the Miocene-Pliocene transition. Global glaciation results in colder oceans, less evaporation and precipitation, and dryer continental climates. Weathering conditions likely changed during these times. Less precipitation resulted in less vegetation cover, evaporation would drive lowering of the water table, meteoric waters would become isotopically heavier (due to lighter precipitation and higher evapotranspiration) and be stored deeper in the weathering profile; lower water-rock ratios would result in less mineral dissolution-reprecipitation. The (U-Th)/He- $\delta^{18}\text{O}_{\text{SIMS-gth}}$ record shows that periods of major global glaciation correspond to periods of less frequent mineral precipitation and isotopically heavier goethites. These periods also correspond to Al-rich goethites, which also record drier continental climates. This interpretation is entirely compatible with present understanding of the role of climate on weathering (Slessarev et al., 2016).

Water balance controls soil pH, and, by consequence, the pH of weathering solutions, at a global scale (Slessarev et al., 2016). Wet conditions, when mean annual precipitation (MAP) minus potential evaporation (PET) is greater than 0, lead to acid soils buffered by gibbsite [$\text{Al}(\text{OH})_3$] dissolution-reprecipitation. Drier conditions, when $\text{MAP}-\text{PET} < 0$, results in alkaline soils buffered by calcite (CaCO_3) dissolution-reprecipitation. Acid weathering solutions result in the precipitation of both goethite and gibbsite because low pHs hinder the incorporation of Al into the structure of goethite (Mostert, 2014) and those are the conditions conducive to the formation of the bauxite deposits that abound throughout the Amazon. During dry periods, less precipitation would lead to alkaline soils and, by analogy weathering solutions, buffered by bicarbonate. Goethite precipitated under alkaline conditions will effectively incorporate Al in solid solution in the $\alpha\text{-FeOOH}$ structure, promoting the precipitation of Al-rich goethites (Mostert, 2014). Our (U-Th)/He- $\delta^{18}\text{O}_{\text{SIMS-gth}}$ confirm that isotopically heavier Al-rich goethites are more common in periods of intensified global glaciation, consistent with continental aridification, isotopically heavier rainfall and surface waters,

and the establishment of alkaline weathering conditions leading to less frequent precipitation of Al-rich and isotopically heavier goethites.

Prolonged periods of isotopically light goethites throughout the Eocene and mid to late Miocene are anomalous. Although the oceanic and continental records at these times are not antagonistic, humid conditions associated with isotopically light precipitation over Carajás appear to have lasted longer than would be expected from the duration of optimum global climatic conditions as recorded in the ocean record. An important consideration is the sources of meteoric water at these times. Presently, and most likely intermittently throughout the Cenozoic, rainwaters over the Amazon are generated by evaporation in the tropical Atlantic and blown westward by “Eastern Trade Winds” (Nimer, 1989) (Figure 2). Throughout the Eocene, the Amazon basin was occupied by a large continental lake likely fed by freshwater captured from rainfall in the basin. This large body of shallow water would have provided a significant local supply of isotopically light moisture that would have been blown easternward by Continental Equatorial winds (Figure 2), feeding isotopically light rain to the vegetation and weathering profiles at Carajás. Similar conditions of widespread flooding persisted throughout the mid to late Miocene in the Amazon (Figure 6). Therefore, we interpret that isotopically light local water sources during high sea stands most likely account for the abundance of isotopically light goethites in these periods. Importantly, the isotopically heavy and Al-rich goethites at ~ 30 Ma correspond to a rapid sea level drop, when fresh continental lakes in the Amazon essentially dried out (Figure 6).

The last notable difference between the ocean and the Carajás continental record is the trend towards lighter isotopic compositions of post ~ 4 Ma goethites. This trend is likely real because it converges towards goethite in isotopic equilibrium with present rainfall. The lighter isotopic composition may reflect increase in seasonality in the Amazon from ~4 Ma to the Present and it may also record a greater influence of the tropical rainforest in the water cycle.

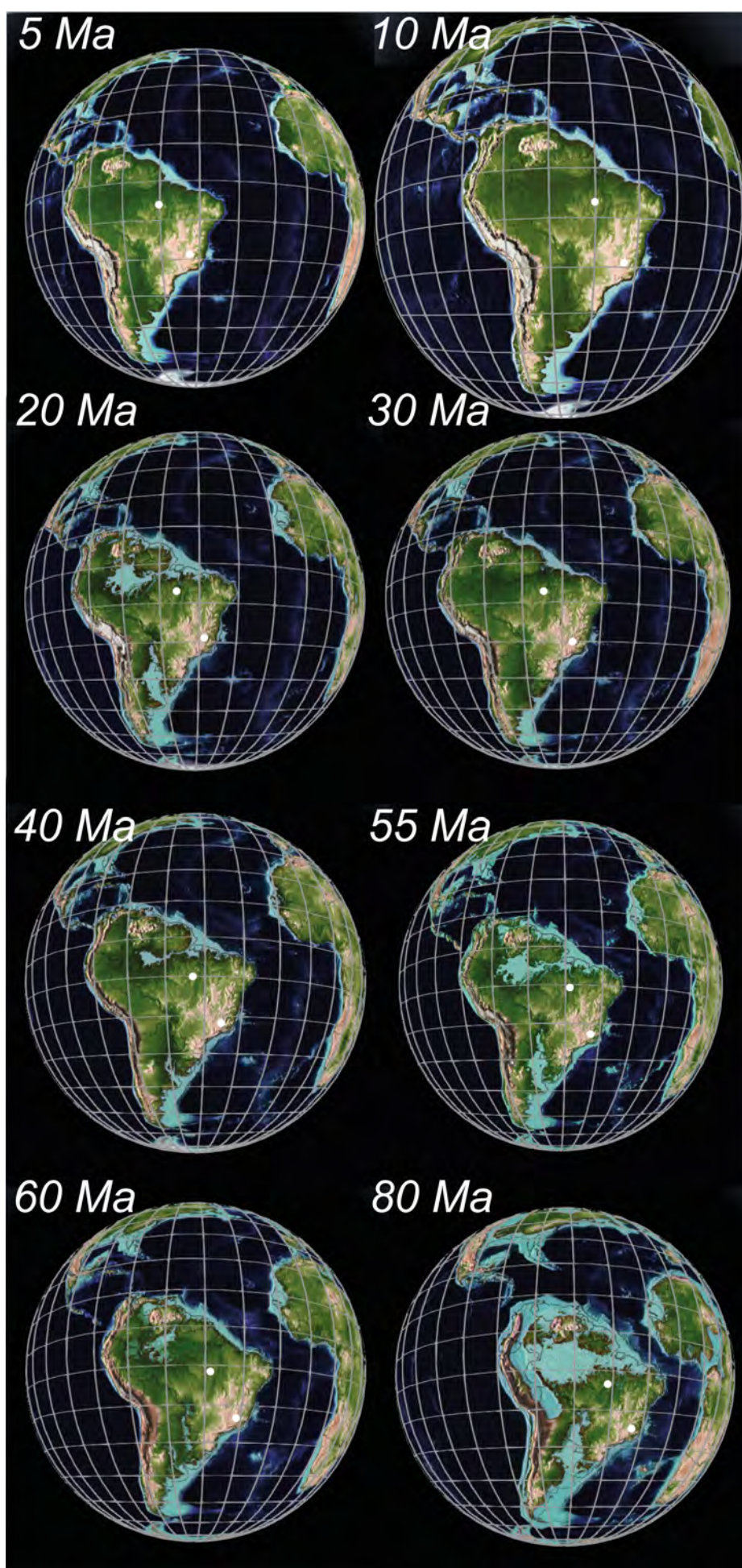


Figure 6. Plate reconstructions using the Earthviewer software (Scotese 2012) illustrates that our study sites have been continuously emergent and subject to surface weathering since the Mesozoic. It also illustrates that South America has remained relatively stationary with respect to the equator throughout the entire Cenozoic, suggesting that changes in weathering conditions at our study sites most likely record changing climates through time, and that these changes are likely to be primarily driven by variations in rainfall distribution and do not record changing surface temperatures. A final important observation is the intermittent presence of large bodies of standing water (freshwater lakes?) in the Amazon basin during the Cenozoic, which may have affected the source, intensity, distribution, and isotopic composition of rainfall at our Carajás study sites.

The Quadrilátero Ferrífero Record

Similarly to Carajás, our youngest goethites in the QF show isotopic compositions compatible with the composition of modern regional rainfall. Unfortunately, the QF $\delta^{18}\text{O}$ record only extends to ~ 40 Ma. Despite the shorter history, the record in the QF shows some trends entirely compatible with those observed in the ocean and the Carajás $\delta^{18}\text{O}$ curves: progression towards goethites with heavier $\delta^{18}\text{O}$ values near the Eocene-Oligocene boundary and in the early to mid-Miocene, and lighter $\delta^{18}\text{O}$ values for Eocene and mid-Miocene (Figure 4). This record also shows major discrepancies from the Carajás and benthic foraminifera records, particularly in the Oligocene and late Miocene, when goethites in the QF become isotopically lighter and heavier, respectively (Figure 4).

Similarly to Carajás, the $\delta^{18}\text{O}$ values of QF goethites should also be dominated by rainfall seasonality (Figure 3) or variation through time, and it should be relatively independent of surface temperature. But unlike from Carajás, global climatic cycles, particularly advance or retreat of glacial ice in Antarctica, may have played a major role in influencing the isotopic composition of rainfall in this region. The isotopic composition of rainfall along the southeastern margin of South America should reflect the intensification or weakening of the Subtropical Gyre and the Antarctic Circumpolar Current (Figure 2). Intensification of the latter would promote a northward shift in the Subantarctic Front and the Malvinas Current, bringing colder and isotopically lighter waters further north along the coast and pushing the warmer, more saline, and isotopically heavier Brazil current northward. Colder and isotopically lighter southern waters would result in slower evaporation and in the production of isotopically lighter sea moisture blowing into the continent by the easterly Atlantic Tropical winds, producing isotopically lighter rainfall in the continental interior, as observed in the Oligocene (U-Th)/He- $\delta^{18}\text{O}_{\text{SIMS-gth}}$ QF record. Further fractionation by Rayleigh distillation and orographic effects would make rainfall even lighter.

Pronounced and prolonged warming during the Miocene may result in southward shift of the Subtropical Gyre, allowing the Brazilian Current to bring warmer, more saline, and isotopically heavier waters further south, enhancing seawater evaporation, producing isotopically heavier sea moisture, and generating isotopically heavier rain along the coast and in the continental interior (Figures 2-4).

Finally, Pliocene-Present intensification of glaciation in Antarctica would reverse this trend, and rainfall would, once again, become lighter in the continental interior. In addition, a proposed reactivation of tectonic uplift at Serras do Mar and da Mantiqueira in the Neogene (Cogné et al. 2011) may intensify orographic effects and explain the trend towards lighter rainfall in the QF from ~ 10 Ma to the Present. A more comprehensive and continuous paleorainfall isotopic record for continental areas in southeastern Brazil will eventually yield the dataset needed for properly evaluating those orographic effects through time.

5. THE WAY FOWARD

The (U-Th)/He age vs $\delta^{18}\text{O}_{\text{SIMS-gth}}$ curves for the two sites show that it is possible to retrieve long-term paleoenvironmental records from continental lateritic weathering profiles. Of course, the scenarios outlined above are drawn from an incipient and still incomplete (U-Th)/He- $\delta^{18}\text{O}_{\text{SIMS-gth}}$ record. But some of the considerations presented clearly demonstrate the value of combining high-resolution geochronology with *in situ* $\delta^{18}\text{O}_{\text{SIMS}}$ analysis of datable supergene minerals (goethite, hollandite, hematite, etc.) from lateritic weathering profiles to retrieve a time-calibrated paleoclimatic curve for continental interiors. Widespread application of this approach will permit reconstructing the paleoclimatic history of continents and reconciling that history with the global oceanic climatic record, potentially creating a much sounder understanding of climate change through time.

In the tropics, seasonality (wet and dry periods) is the main process affecting $\delta^{18}\text{O}$ values of meteoric waters participating in weathering reactions. Long-term shifts toward lighter or heavier $\delta^{18}\text{O}_{\text{SIMS-gth}}$ also appears to record increase (during warm and wet periods) and decrease (during cold and dry periods) in the amount of rainfall. Other possible controls on climate in the tropics are vegetation cover and ephemeral continental water bodies that feed the cloud systems with isotopically light moisture. In the Quadrilátero Ferrífero, southeastern Brazil, orographic barriers may also affect the isotopic composition of rainfall, specially during events of tectonic reactivation in the Neogene. Our $\delta^{18}\text{O}_{\text{SIMS-gth}}$ results roughly match the benthic foraminifera $\delta^{18}\text{O}$ record. The $\delta^{18}\text{O}_{\text{SIMS-gth}}$ results reveal increasing rainfall trends at the Paleocene-Eocene boundary, Mid-Eocene, Oligocene-Miocene boundary, and Mid-Miocene, while light rainfall trends in the Early Oligocene, Early Miocene, and Late Miocene.

Acknowledgments

We thank present and past colleagues from Vale, particularly Carlos Monte Lopes, Luzimar Rego, Clovis Maurity, Paulo Sérgio, Fernando Greco, Fernando Martins, Henrique Meireles, Carlos Augusto de Medeiros Filho, Augusto Kishida, and Felipe Porto for field support in the Carajás region. This project was funded by the Australian Research Council (ARC Discovery DP160104988) grant to Paulo Vasconcelos and Kenneth Farley, Australian Research Council (ARC LE0560868) grant to Trevor Ireland, National Science Foundation grant to KF, and the Brazilian Research Council (CNPq) Science Without Borders scholarship to HM.

REFERENCES

- Bao H. and Koch P. L. (1999) Oxygen isotope fractionation in ferric oxide-water systems: Low temperature synthesis. *Geochimica et Cosmochimica Acta*, **55** (1999) 599-613.
- Bao H., Koch P., and Rumble III D. (1999) Paleocene-Eocene climatic variation in western North America: Evidence from the $\delta^{18}\text{O}$ of pedogenic hematite. *GSA Bull.* 111, 1405-1415
- Bernal J.P., Eggins S.M. and McCulloch M.T. (2005) Accurate in situ ^{238}U – ^{234}U – ^{232}Th – ^{230}Th analysis of silicate glasses and iron oxides by laser-ablation MC-ICP-MS. *J. Anal. Atom. Spectrom.* 20, 1240–1249;
- Bernal J.P., Eggins S.M., McCulloch M.T., Grün R. and Eggleton RA (2006) Dating of chemical weathering processes by in situ measurement of U-series disequilibria in supergene Fe-oxy/hydroxides using LA-MC-ICPMS. *Chem. Geol.* 235, 76–94;
- Bird, M.I., and Chivas, A.R. (1988) Oxygen-isotope dating of the Australian regolith. *Nature* 331: 513-516; 332: 568.
- Bird, M.I., and Chivas, A.R. (1989) Stable-isotopes geochronology of the Australia regolith. *Geochim. Cosmochim. Acta* 53, 3239-3256.
- Bird, M.I., and Chivas, A.R. (1993) Geomorphic and palaeoclimatic implications of an oxygen-isotope chronology for Australian deeply weathered profiles. *Australia Journal of Earth Sciences* 40:4, 345-358.
- Cogné, N., Gallagher, K., and Cobbold, P.R. (2011) Post-rift reactivation of the onshore margin of southeast Brazil: evidence from apatite (U-Th)/He and fission-track data. *Earth and Planetary Science Letters* 309, 118-130.
- Eiler J. M., Graham C. and Valley J. W. (1997) SIMS analysis of oxygen isotopes: matrix effects in complex minerals and glasses. *Chemical Geology* 138, 221-244.
- Dansgaard, W. (1964) Stable isotope in precipitation. *Tellus* 16, 436-468.
- Farley, K.A., Flowers, R.M. (2008) (U-Th)/Ne and multidomain (U-Th)/He systematics of a hydrothermal hematite from eastern Grand Canyon. *Earth and Planetary Science Letters* 359-360, 131-140.
- Gilg, H.A. (2000) D–H evidence for the timing of kaolinitization in Northeast Bavaria, Germany. *Chemical Geology* 170, 5–18.

- Girard J.-P., Razanadrano D. and Freyssinet P. (1997) Laser oxygen isotope analysis of weathering goethite from the lateritic profile of Yaou, French Guiana: paleoweathering and paleoclimatic implications. *Applied Geochemistry* 12, 163-174.
- Haq, B. U., Hardenbol, J., and Vail, P.R. (1987) Chronology of fluctuating sea levels since the Triassic (250 million years ago to present). *Science* 235: 1156–1167.
- Heim J. A., Vasconcelos P. M., Farley K. A., Shuster D. L. and Broadbent G. C. (2006) Dating paleochannel iron ore by (U-Th)/He analysis of supergene goethite, Hamersley Province, Australia. *Geology* 34, 173-176.
- Holland, H. (1984) The chemical evolution of the atmosphere and oceans / Heinrich D. Holland. (Princeton series in geochemistry). Princeton, N.J.: Princeton University Press.
- INTERNATIONAL ATOMIC ENERGY AGENCY. Environmental Isotope Data No. 1-10: World Survey of Isotope Concentration in Precipitation.
- Ireland, T. R., Clement, S., Compston, W., Foster, J. J., Holden, P., Jenkins, B., Lanc, P., Schram, N., and Williams, I. S. (2008) Development of SHRIMP, *Australian Journal of Earth Sciences*, 55: 6 – 7, 937 – 954.
- Koch, P.L. (1998) Isotopic reconstruction of past environments. *Annu. Rev. Earth Planet. Sci.* 26, 573-613.
- Lawrence, J.R. and Taylor, H.P. Jr. (1971) Deuterium and oxygen-18 correlation: clay minerals and hydroxides in Quaternary soils compared to meteoric waters. *Geochim. Cosmochim. Acta* 35, 993 –1003.
- Lawrence, J.R. and Taylor, H.P. Jr. (1972) Hydrogen and oxygen systematics in weathering profiles. *Geochim. Cosmochim. Acta* 36, 1377 –1393.
- Lovejoy, N.R., Bermingham, E., and Martin, A.P. (1988) Marine incursion into South America. *Nature* 336, 421-422.
- Miller, H.B.D., Eiler, J., Vasconcelos, P., and Farley K. (2017) An Australian Cenozoic terrestrial paleoclimate record from He dating and stable isotope geochemistry of goethites. *Geology*. Accepted.
- Monteiro H. S., Vasconcelos P. M., Farley K. A., Spier C. A. and Mello C. L. (2014) (U-Th)/He geochronology of goethite and the origin and evolution of cangas. *Geochimica et Cosmochimica Acta* 131, 267-289.

- Monteiro H. S., Vasconcelos P. M., and Farley K. A. (2017a) A combined (U-Th)/He and cosmogenic ^3He record of landscape armoring by biogeochemical iron cycling. Submitted to the *Journal of Geophysical Research – Earth Surface*.
- Monteiro H. S., Vasconcelos P. M., Farley K. A., and Waltenberg, K. M. (2017b) On goethite as (U-Th)/He and $4\text{He}/3\text{He}$ geochronometer. To be submitted to the *American Journal of Sciences*.
- Monteiro H. S., Vasconcelos P. M., and Farley K. A. (2017c) Ages and evolution of diachronous erosion surfaces in the Amazon: the (U-Th)/He and cosmogenic ^3He records. *To be submitted*.
- Monteiro, H. S., Vasconcelos, P.M., and Farley, K.A. (2017d) Ages and evolution of diachronous erosion surfaces in the Amazon: the (U-Th)/He and cosmogenic ^3He records. *To be submitted*.
- Mostert A. B. (2014) Variations in Goethite Crystallography with Reference to the Ravensthorpe Ni-Laterite, PhD Thesis, The University of Queensland, Brisbane, p. 290.
- Mosbrugger, V., Utescher, T., and Dilcher, D. (2005) Cenozoic continental climatic evolution of Central Europe. *Proceedings of the National Academy of Sciences* 102 (42), 14964-14969.
- Müller, R.D., Sdrolias, M., Gaina, C., and Roest, W.R. (2008) Age, spreading rates, and spreading asymmetry of the world's ocean crust. *Geochemistry, Geophysics, Geosystems* 9(4), Q04006, doi:10.1029/2007GC001743.
- Nimer, E. (1989) *Climatologia do Brasil*. IBGE, Departamento de Recursos Minerais e Estudos Ambientais, 421p.
- Poage, M.A., Sjöström, D.J., Goldberg, J., Chamberlain, C.P., and Furnnis, G. (2000) Isotopic evidence for Holocene climate change in the northern Rockies from a goethite-rich ferricrete chronosequence. *Chemical Geology* 166, 327-340.
- Poage, M.A., and Chamberlain, C.P. (2001) Empirical relationships between elevation and the stable isotope composition of precipitation and surface waters: considerations for studies of paleoelevation change. *American Journal of Science* 301, 1-15.
- Räsänen, M.E., Linna, A.M., Santos, and Negri, F.R. (1995) Late Miocene tidal deposits in the Amazon foreland basin. *Science* 269, 386-390.
- Retallack, G.J. (2001) A 300-million-year record of atmospheric carbon dioxide from fossil plant cuticles. *Nature* 411, 287-290.

- Rozanski, K., Araguás-Araguás, L., and Gonfiantini, R. (1993) Isotopic patterns in modern global precipitation. *Climate Change in continental isotopic record*: P.K. Swart, K.C. Lohmann, J. Mackenzie, S. Savin (eds) – Geophysical Monograph: 78, 1-36.
- Ruffet, G., Innocent, C., Michard, A., Féraud, G., Beauvais, A., Nahon, D., Hamelin, B., (1996) A geochronological $^{40}\text{Ar}/^{39}\text{Ar}$ and $^{87}\text{Rb}/^{81}\text{Sr}$ study of K–Mn oxides from the weathering sequence of Azul, Brazil. *Geochim. Cosmochim. Acta* 60, 2219–2232. [http://dx.doi.org/10.1016/0016-7037\(96\)00080-4](http://dx.doi.org/10.1016/0016-7037(96)00080-4).
- Salati, E., Dall'Olio, A., Matsui, E., and Gat, J. (1979) Recycling of water in the Amazon basin: and isotopic study. *Water Resources Research* 15, 1250-1258.
- Savin, M.S. and Epstein, S. (1970) The oxygen and hydrogen geochemistry of clay minerals. *Geochimica et Cosmochimica Acta* 34, 25-42.
- Sharp, Z.D., Atudorei, V., and Durakiewicz, T. (2001) A rapid method for determination of hydrogen and oxygen isotope ratios from water and hydrous minerals. *Chemical Geology* 178, 197-210.
- Sharp WD, Ludwig, KR, Chadwick, OA, Amundson, R & Glaser LL, 2003. Dating fluvial terraces by $^{230}\text{Th}/\text{U}$ on pedogenic carbonate, Wind River Basin, Wyoming. *Quat. Res.* 59, 139-150
- Sheldon, N. D., and Tabor, N.J. (2009) Quantitative paleoenvironmental and paleoclimatic reconstruction using paleosols. *Earth-Sciences Review* 95, 1-52.
- Shuster D. L., Vasconcelos P. M., Heim J. A. and Farley K. A. (2005) Weathering geochronology by (U-Th)/He dating of goethite. *Geochimica et Cosmochimica Acta* **69(3)**, 659-673.
- Sjostrom D. J., Hren M. T. and Chamberlain C. P. (2004) Oxygen isotope records of goethite from ferricrete deposits indicate regionally varying Holocene climate change in the Rocky Mountain region, U.S.A.
- Spier, C. A., Vasconcelos, P. M. P., and Oliveira, S. M. B. (2006) $^{40}\text{Ar}/^{39}\text{Ar}$ geochronological constraints on the evolution of lateritic iron deposits in the Quadrilátero Ferrífero, Minas Gerais, Brazil, *Chemical Geology*, 234, 79-104.
- Slessarev, E.W., Lin, Y., Bingham, N.L., Johnson, J.E., Dai, Y., Schimel, J.P., and Chadwick, O.A. (2016) Water balance creates a threshold in soil pH at the global scale. *Nature* 540, 567-569.

- Vasconcelos P. M., Becker T. A., Renne P. R. and Brimhall G. H. (1994) Direct dating of weathering phenomena by K-Ar and $^{40}\text{Ar}/^{39}\text{Ar}$ analysis of supergene K-Mn oxides. *Geochimica et Cosmochimica Acta* **58**, 1635-65.
- Vasconcelos P. M. (1999a) K-Ar and $^{40}\text{Ar}/^{39}\text{Ar}$ geochronology of weathering processes. *Annual Reviews Earth and Planetary Sciences* **27**, 183-229.
- Vasconcelos P. M. (1999b) $^{40}\text{Ar}/^{39}\text{Ar}$ geochronology of supergene processes in ore deposits. *Economic Geology* **12**, 73-113.
- Vasconcelos P. M. and Conroy M. (2003) Geochronology of weathering and landscape evolution, Dugald River Valley, NW Queensland, Australia. *Geochimica et Cosmochimica Acta* **67**, 2913-2930.
- Vasconcelos P. M., Heim J. A., Farley K. A., Monteiro H. S., Waltenberg K. (2013) $^{40}\text{Ar}/^{39}\text{Ar}$ and (U-Th)/He - $^4\text{He}/^3\text{He}$ geochronology of landscape evolution and channel iron deposit genesis at LynnPeak, Western, Australia. *Geochimica et Cosmochimica Acta* **117**, 283-312.
- Vasconcelos P.M., Reich M., Shuster D. (2015) Supergene metal deposits and paleoclimates. *Elements* **11**, 317-322.
- Vasconcelos, P.M. and Carmo, I.O. (2017) Calibrating Denudation Chronology through $^{40}\text{Ar}/^{39}\text{Ar}$ Weathering Geochronology. *Earth-Science Reviews*. Submitted.
- Veizer, J., Ala, D., Azmy, K., Bruckschen, P., Buhl, D., Bruhn, F., Carden, G.A.F., Diener, A., Ebner, S., Godderis, Y., Jasper, T., Korte, C., Pawellek, F., Podlaha, O.G., and Strauss, H. (1999) $^{87}\text{Sr}/^{86}\text{Sr}$, $\delta^{13}\text{C}$, and $\delta^{18}\text{O}$ evolution of Phanerozoic seawater. *Chemical Geology* **161**, 59-88.
- Vielzeuf D., Champenois M., Valley J. W., Brunet F., and Devidal J. L. (2005) SIMS analyses of oxygen isotopes: Matrix effects in Fe-Mg-Ca garnets. *Chemical Geology* **223**, 208-226.
- White M.E. (1994) After the Greening: The Browning of Australia. Kangaroo Press, Kenthurst, NSW.
- Wolfe, J.A. (1994) Tertiary climate changes at middle latitudes of western North America. *Palaeogeography, Palaeoclimatology, Palaeoecology* **108**, 195-205.
- WORLD METEOROLOGICAL ORGANIZATION, Climatological Normals (Climo) for climate and climate ship stations for the period 1932-1960, WMO/OMM No. 17, TP.52.

WORLD METEOROLOGICAL ORGANIZATION, Weather Reporting, Volume A: Observing Stations, WMO/OMM No. 9, TP.4.

WORLD METEOROLOGICAL ORGANIZATION in Co-operation with Environmental Science Services Administration USA, Monthly Climatic Data for the World, United States Government Printing Office, monthly editions.

Woodhead J, Hellstrom J, Maas R, Drysdale R, Zanchetta G, Devine P & Taylor E (2006). U–Pb geochronology of speleothems by MC-ICPMS. *Quaternary Geochronology* 1, 208–221.

Yapp C. J. (1990) Oxygen isotopes in iron(III) oxides. 1. Mineral– water fractionation factors. *Chem. Geol.* 85, 329–335.

Yapp C. J. (2001) Rusty relics of Earth history: iron(III) oxides, isotopes and surficial environments. *Ann. Rev. Earth Plan. Sci.* 29, 165–199.

Yapp C. J. and Shuster D. L. (2011) Environmental memory and a possible seasonal bias in the stable isotope composition of (UTh)/ He-dated goethite from the Canadian Arctic. *Geochim. Cosmochim. Acta* 75, 4194–4215.

Yapp, C. J. (2012) Oxygen isotope effects associated with substitution of Al and Fe in synthetic goethite: Some experimental evidence and the criterion of oxygen yield. *Geochim. Cosmochim. Acta* 97, 200–212.

Zachos, J., Pagani, M., Sloan, L., Thomas, E., and Billups, K. (2001) Trends, Rythms, and Aberrations in Global Climate 65 Ma to Present. *Science* 292, 686-693.

Chapter 7: Conclusions

The main objectives of this study were: (1) to evaluate the state-of-the-art of the various microanalytical tools suitable for investigating the timing and environmental conditions controlling the precipitation and preservation of supergene goethites; (2) to refine or to develop additional methodologies that could contribute to a better understanding of paleoenvironmental controls on goethite precipitation; (3) and to apply the various reference materials and improved tools to generate a continental paleoclimatic curve with the necessary detail to be comparable to the paleoclimatic curves obtained by the isotopic compositions of ocean sediments.

Several important conclusions can be drawn from the analytical aspects of the project. Helium kinetics studies on goethites displaying distinct crystallinities, chemical compositions, mechanisms of precipitation, and coexisting generations show that goethite mineralogy plays a fundamental role on He retentivity. The investigations also suggest that samples deviating from an ideal goethite stoichiometry should undergo diffusivity studies by the $^4\text{He}/^3\text{He}$ method to improve the confidence of the geochronological results obtained from this mineral. Therefore, the simultaneous application of the (U-Th)/He– $^4\text{He}/^3\text{He}$ methods on the same sample to determine both age of precipitation and He retentivity is the most suitable approach when determining ages of complex goethites.

This study also shows that the combination of (U-Th)/He and cosmogenic ^3He in goethite and coexisting hematite is a powerful way to unveil the history of weathering and erosion of long-lived cratonic landscapes. Iron cementation at the surface and at the subsurface slows erosion down and allows the preservation of relic surface for millions of years. More importantly, by deriving precipitation and exposure ages for goethites and combining these measurements with the exposure ages of co-existing hypogene hematite, it is possible to unravel the chemical and mechanical processes controlling the transformation of bedrock into weathered material and the delivery of the weathered product to erosional transport. It is also possible to quantify scarp retreat rates for weathered continental landscapes, a measurement that has been elusive until this study.

This contribution was the first, as far as I know, to successfully attempt to develop an ion microprobe reference material for stable isotope analysis of goethite. Much remains to be done in terms of further characterization of this reference material to finally produce a widely-accepted ion-microprobe goethite reference material, but this thesis has made a major contribution in that direction. The thesis also shows the importance of measuring oxygen stable isotope compositions at the appropriate μm -scale to extract the complete environmental history recorded in supergene phases.

Finally, we show examples of this environmental history by combining electron microprobe analysis, (U-Th)/He geochronology, and ion microprobe $\delta^{18}\text{O}$ measurements – the combined EPMA-(U-Th)/He- $\delta^{18}\text{O}_{\text{SIMS-gth}}$ method – to determine the paleoenvironmental evolution, from 70 Ma – 900 ka at Carajás and from ~40 Ma – 600 ka at the Quadrilátero Ferrífero, of two continental sites in Brazil. The results reveal a nearly continuous environmental isotope record that can be compared with the $\delta^{18}\text{O}$ curve for ocean sediments. The history demonstrates the power of the proposed combined methodology, it provides exciting new insights into the paleoenvironmental – particularly the paleoprecipitation – history of continental settings, and it reveals that further studies that complete the record at Carajás, the Quadrilátero Ferrífero, and other continental sites across the planet will enable a comprehensive reconciliation of ocean and continental environmental conditions throughout the entire Cenozoic, and possibly extending into the Mesozoic, at an unprecedented scale.

Appendices

EA1: Electron Microprobe Analysis

EA2a: Blank-corrected $R_{\text{step}}/R_{\text{bulk}}$ diagrams

EA2b: Not blank-corrected $R_{\text{step}}/R_{\text{bulk}}$ diagrams

EA3: Step-Heating $^4\text{He}/^3\text{He}$ analysis

Appendix 1: Electron Microprobe analyses

Index	O	Na	P	V	Ti	Mg	S	Cr	Mn	Al	K	Ni	Fe	Si	Ca	Cu	Co	Sr	Ba	Zn	Pb	Total	Comment	Spot#	Run Date
1	35.65	0.15	0.69	0.01	0.00	0.06	-	0.00	0.03	3.17	0.01	0.02	61.17	0.27	0.00	0.00	0.00	-	0.02	0.00	0.04	101.28	Line 5 Pic 06 24/2	136	14/5/10
2	39.10	0.00	0.43	0.01	0.03	0.04	-	0.01	0.00	2.46	0.00	0.03	56.59	0.34	0.00	0.00	0.05	-	0.00	0.00	0.08	99.16	Line 6 Pic 06 24/2	137	14/5/10
3	35.68	0.06	0.61	0.04	0.28	0.14	-	0.00	0.02	4.83	0.00	0.00	58.72	0.12	0.01	0.02	0.06	-	0.03	0.06	0.09	100.75	Line 7 Pic 06 24/2	138	14/5/10
4	37.27	0.02	0.64	0.02	0.00	0.00	-	0.01	0.06	2.67	0.02	0.04	58.70	0.38	0.00	0.04	0.09	-	0.10	0.00	0.10	100.14	Line 8 Pic 06 24/2	139	14/5/10
5	34.87	0.11	0.61	0.06	0.17	0.05	-	0.02	0.00	4.94	0.00	0.00	59.33	0.20	0.01	0.04	0.07	-	0.00	0.04	0.00	100.48	Line 10 Pic 06 24/2	141	14/5/10
6	33.46	0.00	0.64	0.03	0.12	0.11	-	0.03	0.00	4.88	0.00	0.01	57.98	0.18	0.01	0.01	0.12	-	0.00	0.00	0.02	97.57	Line 13 Pic 06 24/2	144	14/5/10
7	36.23	0.07	0.42	0.02	0.00	0.01	-	0.01	0.05	1.39	0.00	0.00	60.58	0.34	0.00	0.00	0.04	-	0.00	0.06	0.07	99.29	Line 14 Pic 06 24/2	145	14/5/10
8	36.77	0.00	0.59	0.03	0.15	0.08	-	0.01	0.04	4.54	0.01	0.01	57.10	0.16	0.00	0.05	0.07	-	0.00	0.01	0.00	99.59	Line 15 Pic 06 24/2	146	14/5/10
9	38.37	0.12	0.60	0.00	0.08	0.06	-	0.02	0.00	4.56	0.00	0.00	56.25	0.15	0.00	0.00	0.14	-	0.01	0.01	0.14	100.51	Line 16 Pic 06 24/2	147	14/5/10
10	39.81	0.05	0.70	0.00	0.04	0.00	-	0.00	0.01	4.29	0.03	0.00	55.00	0.21	0.00	0.00	0.01	-	0.00	0.04	0.12	100.33	Line 17 Pic 06 24/2	148	14/5/10
11	39.50	0.13	0.36	0.08	0.04	0.00	-	0.00	0.00	2.86	0.01	0.00	55.99	0.13	0.00	0.03	0.06	-	0.00	0.03	0.15	99.36	Line 18 Pic 06 24/2	149	14/5/10
12	38.44	0.16	0.36	0.00	0.07	0.04	-	0.00	0.00	3.00	0.00	0.00	56.59	0.12	0.00	0.00	0.06	-	0.00	0.00	0.06	98.89	Line 19 Pic 06 24/2	150	14/5/10
13	38.99	0.00	0.37	0.02	0.06	0.02	-	0.00	0.03	3.03	0.02	0.03	56.44	0.11	0.00	0.08	0.06	-	0.03	0.00	0.03	99.32	Line 20 Pic 06 24/2	151	14/5/10
14	38.90	0.03	0.38	0.02	0.07	0.06	-	0.00	0.04	3.04	0.00	0.06	56.10	0.12	0.00	0.08	0.00	-	0.01	0.00	0.00	98.90	Line 21 Pic 06 24/2	152	14/5/10
15	38.55	0.00	0.33	0.01	0.24	0.01	-	0.04	0.00	2.75	0.00	0.03	56.87	0.17	0.00	0.05	0.04	-	0.00	0.05	0.05	99.19	Line 22 Pic 06 24/2	153	14/5/10
16	40.06	0.05	0.41	0.05	0.45	0.00	-	0.05	0.00	2.87	0.01	0.03	56.27	0.15	0.00	0.05	0.16	-	0.03	0.06	0.00	100.69	Line 23 Pic 06 24/2	154	14/5/10
17	38.99	0.06	0.38	0.04	0.00	0.00	-	0.00	0.03	2.66	0.00	0.00	56.98	0.14	0.00	0.00	0.11	-	0.00	0.00	0.01	99.38	Line 24 Pic 06 24/2	155	14/5/10
18	39.06	0.04	0.32	0.00	0.03	0.06	-	0.00	0.04	2.74	0.01	0.00	56.30	0.17	0.00	0.00	0.08	-	0.00	0.00	0.00	98.85	Line 25 Pic 06 24/2	156	14/5/10
19	39.05	0.08	0.34	0.08	0.00	0.11	-	0.00	0.03	2.96	0.00	0.00	56.65	0.14	0.00	0.00	0.08	-	0.03	0.02	0.07	99.64	Line 26 Pic 06 24/2	157	14/5/10
20	38.96	0.03	0.33	0.04	0.04	0.07	-	0.00	0.02	2.76	0.00	0.00	56.30	0.15	0.00	0.05	0.09	-	0.00	0.07	0.00	98.90	Line 27 Pic 06 24/2	158	14/5/10
21	38.14	0.00	0.32	0.00	0.06	0.05	-	0.00	0.00	2.97	0.00	0.00	57.20	0.09	0.00	0.00	0.07	-	0.00	0.00	0.00	98.91	Line 29 Pic 06 24/2	160	14/5/10
22	38.15	0.00	0.42	0.07	0.05	0.01	-	0.04	0.02	3.40	0.03	0.02	56.14	0.26	0.00	0.04	0.02	-	0.00	0.01	0.02	98.70	Line 30 Pic 06 24/2	161	14/5/10
23	39.04	0.00	0.35	0.00	0.00	0.00	-	0.06	0.05	3.46	0.02	0.01	55.93	0.18	0.00	0.08	0.11	-	0.07	0.05	0.07	99.47	Line 31 Pic 06 24/2	162	14/5/10
24	39.16	0.02	0.36	0.07	0.06	0.00	-	0.00	0.00	3.40	0.00	0.06	56.11	0.18	0.00	0.10	0.10	-	0.05	0.05	0.04	99.75	Line 32 Pic 06 24/2	163	14/5/10
25	39.19	0.01	0.38	0.00	0.02	0.02	-	0.00	0.04	3.43	0.01	0.00	56.07	0.17	0.00	0.00	0.11	-	0.00	0.00	0.00	99.45	Line 33 Pic 06 24/2	164	14/5/10
26	39.58	0.07	0.42	0.00	0.00	0.00	-	0.01	0.04	4.46	0.00	0.00	55.48	0.15	0.00	0.05	0.09	-	0.00	0.02	0.12	100.49	Line 34 Pic 06 24/2	165	14/5/10
27	39.73	0.00	0.36	0.08	0.08	0.09	-	0.04	0.00	3.67	0.00	0.00	56.29	0.16	0.00	0.02	0.07	-	0.01	0.05	0.11	100.74	Line 35 Pic 06 24/2	166	14/5/10
28	38.87	0.00	0.39	0.00	0.01	0.02	-	0.00	0.00	3.87	0.01	0.00	55.77	0.16	0.00	0.00	0.00	-	0.04	0.05	0.03	99.22	Line 36 Pic 06 24/2	167	14/5/10
29	39.22	0.05	0.41	0.02	0.00	0.00	-	0.01	0.00	3.88	0.00	0.00	56.33	0.19	0.00	0.00	0.03	-	0.00	0.00	0.00	100.14	Line 37 Pic 06 24/2	168	14/5/10
30	35.42	0.00	0.43	0.00	0.03	0.08	-	0.04	0.06	4.55	0.00	0.02	59.16	0.16	0.00	0.02	0.05	-	0.06	0.00	0.04	100.14	Line 38 Pic 06 24/2	169	14/5/10
31	39.09	0.20	0.42	0.01	0.08	0.06	-	0.00	0.00	4.27	0.00	0.04	57.42	0.16	0.00	0.00	0.07	-	0.00	0.00	0.00	101.81	Line 39 Pic 06 24/2	170	14/5/10
32	38.83	0.00	0.50	0.01	0.03	0.01	-	0.00	0.05	3.27	0.00	0.00	58.22	0.35	0.00	0.10	0.05	-	0.00	0.00	0.00	101.43	Line 40 Pic 06 24/2	171	14/5/10
33	38.05	0.13	0.43	0.00	0.02	0.07	-	0.00	0.00	4.79	0.01	0.00	57.08	0.17	0.00	0.00	0.08	-	0.01	0.03	0.10	100.98	Line 41 Pic 06 24/2	172	14/5/10
34	39.23	0.00	0.43	0.03	0.04	0.07	-	0.03	0.01	3.97	0.00	0.01	55.51	0.14	0.00	0.00	0.00	-	0.00	0.00	0.00	99.47	Line 42 Pic 06 24/2	173	14/5/10
35	39.45	0.09	0.36	0.00	0.01	0.00	-	0.01	0.00	3.63	0.02	0.02	55.95	0.16	0.00	0.04	0.03	-	0.00	0.03	0.00	99.78	Line 43 Pic 06 24/2	174	14/5/10
36	38.69	0.00	0.34	0.01	0.04	0.04	-	0.00	0.01	3.33	0.00	0.02	56.40	0.15	0.00	0.01	0.05	-	0.00	0.07	0.11	99.27	Line 44 Pic 06 24/2	175	14/5/10
37	39.32	0.03	0.39	0.06	0.08	0.02	-	0.02	0.00	4.12	0.00	0.00	55.68	0.16	0.00	0.06	0.02	-	0.05	0.07	0.07	100.14	Line 45 Pic 06 24/2	176	14/5/10
38	39.39	0.07	0.40	0.00	0.00	0.08	-	0.00	0.02	4.07	0.00	0.03	55.79	0.15	0.00	0.00	0.10	-	0.00	0.01	0.07	100.18	Line 46 Pic 06 24/2	177	14/5/10
39	39.14	0.00	0.37	0.00	0.06	0.06	-	0.00	0.00	3.37	0.00	0.01	56.63	0.17	0.00	0.09	0.05	-	0.02	0.12	0.00	100.09	Line 47 Pic 06 24/2	178	14/5/10
40	38.68	0.00	0.39	0.03	0.13	0.03	-	0.00	0.00	3.34	0.00	0.00	56.18	0.14	0.00	0.03	0.08	-	0.00	0.00	0.00	99.04	Line 48 Pic 06 24/2	179	14/5/10
41	38.91	0.12	0.42	0.00	0.02	0.05	-	0.01	0.00	3.69	0.00	0.00	56.61	0.13	0.00	0.00	0.07	-	0.00	0.00	0.11	100.13	Line 49 Pic 06 24/2	180	14/5/10
42	38.37	0.05	0.42	0.05	0.00	0.06	-	0.00	0.00	3.66	0.00	0.00	58.02	0.15	0.00	0.00	0.05	-	0.00	0.00	0.00	100.83	Line 50 Pic 06 24/2	181	14/5/10
43	36.51	0.00	0.13	0.02	0.00	0.04	0.03	0.01	0.02	0.57	0.00	0.02	59.13	0.73	0.00	0.00	0.04	-	-	0.00	0.04	97.28	Line 1 Pic 06 22 BDG	571	20/11/10
44	36.58	0.00	0.07	0.08	0.00	0.03	0.01	0.00	0.00	0.50	0.00	0.00	59.28	0.61	0.00	0.02	0.03	-	-	0.00	0.06	97.26	Line 2 Pic 06 22 BDG	572	20/11/10
45	35.43	0.00	0.12	0.00	0.06	0.02	0.09	0.01	0.01	0.76	0.01	0.02	59.75	0.56	0.00	0.04	0.11	-	-	0.00	0.07	97.04	Line 3 Pic 06 22 BDG	573	20/11/10
46	37.13	0.00	0.12	0.00	0.03	0.01	0.08	0.02	0.00	0.64	0.00	0.00	58.75	0.84	0.00	0.00	0.10	-	-	0.07	0.00	97.78	Line 4 Pic 06 22 BDG	574	20/11/10
47	37.92	0.02	0.17	0.00	0.00	0.00	0.00	0.02	0.00	0.72	0.01	0.06	58.24	0.87	0.00	0.00	0.03	-	-	0.00	0.00	98.05	Line 5 Pic 06 22 BDG	575	20/11/10
48	37.69	0.00	0.15	0.04	0.01	0.01	0.02	0.00	0.11	0.71	0.00	0.00	59.14	0.81	0.00	0.02	0.03	-	-	0.05	0.08	98.86	Line 6 Pic 06 22 BDG	576	20/11/10
49	37.22	0.00	0.13	0.04	0.02	0.02	0.03	0.01	0.00	0.50	0.00	0.00	58.69	0.80	0.00	0.05	0.06	-	-	0.00	0.02	97.58	Line 7 Pic 06 22 BDG	577	20/11/10
50	37.26	0.00	0.13	0.00	0.00	0.00	0.07	0.00	0.07	0.62	0.01	0.00	58.08	0.82	0.00	0.00	0.00	-	-	0.00	0.02	97.08	Line 8 Pic 06 22 BDG	578	20/11/10
51	37.94	0.00	0.14	0.00	0.00	0																			

Appendix 1: Electron Microprobe analyses

Index	O	Na	P	V	Ti	Mg	S	Cr	Mn	Al	K	Ni	Fe	Si	Ca	Cu	Co	Sr	Ba	Zn	Pb	Total	Comment	Spot#	Run Date
76	37.98	0.02	0.08	0.00	0.00	0.02	0.01	0.00	0.00	0.78	0.02	0.02	59.17	0.52	0.00	0.03	0.09	-	-	0.00	0.05	98.79	Line 34 Pic 06 22 BD	604	20/11/10
77	36.45	0.00	0.09	0.02	0.00	0.00	0.03	0.02	0.07	0.37	0.00	0.00	59.57	0.35	0.00	0.02	0.06	-	-	0.00	0.14	97.17	Line 35 Pic 06 22 BD	605	20/11/10
78	36.93	0.01	0.11	0.01	0.00	0.05	0.04	0.02	0.05	0.58	0.00	0.00	59.57	0.38	0.00	0.04	0.06	-	-	0.00	0.00	97.84	Line 36 Pic 06 22 BD	606	20/11/10
79	36.25	0.06	0.10	0.00	0.00	0.00	0.05	0.02	0.03	0.48	0.00	0.00	59.83	0.36	0.00	0.00	0.06	-	-	0.00	0.06	97.29	Line 37 Pic 06 22 BD	607	20/11/10
80	36.94	0.11	0.03	0.00	0.05	0.00	0.04	0.02	0.00	0.40	0.00	0.00	59.86	0.34	0.00	0.04	0.08	-	-	0.04	0.00	97.96	Line 38 Pic 06 22 BD	608	20/11/10
81	37.09	0.00	0.16	0.02	0.00	0.00	0.03	0.01	0.02	0.75	0.00	0.00	60.77	0.55	0.00	0.02	0.11	-	-	0.00	0.00	99.53	Line 39 Pic 06 22 BD	609	20/11/10
82	36.93	0.03	0.09	0.00	0.02	0.00	0.04	0.02	0.02	0.45	0.00	0.00	59.94	0.38	0.00	0.00	0.01	-	-	0.00	0.00	97.91	Line 40 Pic 06 22 BD	610	20/11/10
83	36.64	0.00	0.14	0.01	0.03	0.00	0.04	0.03	0.02	0.70	0.02	0.01	59.70	0.52	0.00	0.02	0.03	-	-	0.00	0.00	97.89	Line 41 Pic 06 22 BD	611	20/11/10
84	36.52	0.00	0.12	0.02	0.09	0.01	0.03	0.01	0.00	0.47	0.01	0.00	59.80	0.37	0.00	0.00	0.08	-	-	0.02	0.00	97.56	Line 42 Pic 06 22 BD	612	20/11/10
85	36.71	0.00	0.07	0.02	0.01	0.04	0.02	0.00	0.00	0.46	0.00	0.04	59.07	0.56	0.00	0.00	0.07	-	-	0.00	0.06	97.12	Line 43 Pic 06 22 BD	613	20/11/10
86	36.62	0.00	0.15	0.04	0.00	0.01	0.03	0.00	0.00	0.73	0.00	0.00	60.27	0.71	0.00	0.10	0.03	-	-	0.03	0.06	98.77	Line 45 Pic 06 22 BD	615	20/11/10
87	36.66	0.02	0.10	0.02	0.00	0.02	0.03	0.01	0.00	0.29	0.01	0.00	59.39	0.37	0.00	0.00	0.03	-	-	0.03	0.02	97.00	Line 46 Pic 06 22 BD	616	20/11/10
88	35.98	0.01	0.11	0.00	0.00	0.04	0.06	0.00	0.05	0.63	0.01	0.03	59.94	0.55	0.00	0.00	0.05	-	-	0.00	0.00	97.45	Line 47 Pic 06 22 BD	617	20/11/10
89	37.50	0.03	0.07	0.00	0.00	0.00	0.01	0.00	0.00	0.32	0.00	0.00	59.24	0.36	0.00	0.03	0.02	-	-	0.00	0.04	97.63	Line 48 Pic 06 22 BD	618	20/11/10
90	37.24	0.00	0.11	0.00	0.00	0.00	0.05	0.01	0.02	0.59	0.01	0.00	59.87	0.53	0.00	0.00	0.01	-	-	0.00	0.02	98.46	Line 50 Pic 06 22 BD	620	20/11/10
91	34.89	0.07	0.10	0.00	0.03	0.00	0.05	0.00	0.05	0.82	0.00	0.00	60.80	0.35	0.00	0.00	0.10	-	-	0.00	0.06	97.32	Line 1 Pic 06 22 VYG	621	20/11/10
92	35.08	0.03	0.10	0.00	0.04	0.03	0.04	0.00	0.04	0.84	0.00	0.00	61.01	0.36	0.00	0.02	0.05	-	-	0.09	0.15	97.86	Line 2 Pic 06 22 VYG	622	20/11/10
93	34.93	0.05	0.13	0.00	0.08	0.05	0.02	0.01	0.00	0.89	0.00	0.01	60.79	0.31	0.00	0.01	0.04	-	-	0.00	0.13	97.44	Line 3 Pic 06 22 VYG	623	20/11/10
94	35.00	0.06	0.08	0.00	0.08	0.00	0.03	0.01	0.00	0.80	0.01	0.00	60.90	0.31	0.00	0.02	0.10	-	-	0.00	0.09	97.48	Line 4 Pic 06 22 VYG	624	20/11/10
95	36.05	0.14	0.11	0.03	0.09	0.00	0.05	0.03	0.05	0.81	0.00	0.00	60.80	0.50	0.00	0.00	0.09	-	-	0.00	0.00	97.78	Line 5 Pic 06 22 VYG	625	20/11/10
96	36.57	0.07	0.08	0.00	0.00	0.01	0.04	0.04	0.00	0.83	0.00	0.03	58.75	1.05	0.00	0.03	0.06	-	-	0.00	0.01	97.58	Line 6 Pic 06 22 VYG	626	20/11/10
97	36.07	0.02	0.07	0.00	0.05	0.01	0.05	0.02	0.00	0.61	0.00	0.02	59.47	0.44	0.00	0.01	0.07	-	-	0.07	0.08	97.06	Line 7 Pic 06 22 VYG	627	20/11/10
98	35.59	0.19	0.12	0.02	0.01	0.00	0.05	0.00	0.00	0.91	0.02	0.04	60.42	0.39	0.00	0.05	0.07	-	-	0.00	0.03	97.90	Line 9 Pic 06 22 VYG	629	20/11/10
99	35.21	0.07	0.12	0.03	0.07	0.00	0.08	0.00	0.03	1.04	0.00	0.00	60.70	0.34	0.00	0.01	0.10	-	-	0.00	0.01	97.79	Line 10 Pic 06 22 VY	630	20/11/10
100	35.78	0.03	0.17	0.02	0.01	0.05	0.07	0.02	0.04	1.00	0.00	0.00	60.32	0.37	0.00	0.08	0.06	-	-	0.02	0.00	98.03	Line 11 Pic 06 22 VY	631	20/11/10
101	36.23	0.05	0.14	0.01	0.00	0.01	0.04	0.02	0.00	0.87	0.01	0.00	60.51	0.39	0.00	0.02	0.11	-	-	0.00	0.00	98.41	Line 16 Pic 06 22 VY	636	20/11/10
102	35.99	0.00	0.07	0.00	0.05	0.04	0.05	0.03	0.07	0.73	0.00	0.00	59.99	0.39	0.00	0.00	0.11	-	-	0.00	0.00	97.52	Line 17 Pic 06 22 VY	637	20/11/10
103	35.63	0.06	0.12	0.03	0.06	0.03	0.06	0.00	0.02	0.75	0.00	0.00	60.55	0.43	0.00	0.09	0.13	-	-	0.07	0.06	98.08	Line 18 Pic 06 22 VY	638	20/11/10
104	35.19	0.00	0.08	0.05	0.02	0.04	0.03	0.05	0.01	0.74	0.00	0.00	60.95	0.41	0.00	0.05	0.15	-	-	0.06	0.00	97.81	Line 19 Pic 06 22 VY	639	20/11/10
105	35.79	0.00	0.13	0.01	0.06	0.05	0.02	0.00	0.04	0.65	0.01	0.00	60.21	0.38	0.00	0.06	0.11	-	-	0.00	0.00	97.52	Line 20 Pic 06 22 VY	640	20/11/10
106	35.17	0.06	0.13	0.00	0.00	0.01	0.05	0.06	0.04	0.75	0.00	0.11	60.52	0.42	0.00	0.00	0.09	-	-	0.06	0.05	97.51	Line 21 Pic 06 22 VY	641	20/11/10
107	35.05	0.00	0.12	0.09	0.05	0.03	0.06	0.02	0.01	0.78	0.01	0.00	60.44	0.48	0.00	0.07	0.07	-	-	0.00	0.01	97.27	Line 23 Pic 06 22 VY	643	20/11/10
108	35.58	0.01	0.10	0.03	0.06	0.02	0.04	0.01	0.09	0.73	0.00	0.00	60.44	0.51	0.00	0.06	0.04	-	-	0.00	0.01	97.70	Line 24 Pic 06 22 VY	644	20/11/10
109	34.61	0.00	0.11	0.00	0.00	0.00	0.06	0.00	0.03	0.81	0.02	0.00	61.06	0.50	0.00	0.03	0.02	-	-	0.00	0.00	97.24	Line 25 Pic 06 22 VY	645	20/11/10
110	36.22	0.02	0.13	0.01	0.01	0.03	0.07	0.00	0.10	0.80	0.01	0.00	59.95	0.66	0.00	0.08	0.09	-	-	0.10	0.11	98.35	Line 26 Pic 06 22 VY	646	20/11/10
111	36.52	0.00	0.08	0.00	0.00	0.00	0.05	0.00	0.01	0.47	0.00	0.03	60.52	0.42	0.00	0.13	0.00	-	-	0.00	0.00	98.22	Line 27 Pic 06 22 VY	647	20/11/10
112	36.59	0.00	0.08	0.00	0.00	0.03	0.05	0.04	0.01	0.60	0.00	0.05	59.94	0.47	0.00	0.05	0.09	-	-	0.00	0.04	98.03	Line 28 Pic 06 22 VY	648	20/11/10
113	35.82	0.00	0.11	0.00	0.08	0.04	0.05	0.02	0.06	0.73	0.02	0.00	59.98	0.43	0.00	0.00	0.09	-	-	0.04	0.00	97.46	Line 29 Pic 06 22 VY	649	20/11/10
114	35.95	0.04	0.08	0.04	0.01	0.03	0.06	0.01	0.05	0.58	0.00	0.04	60.61	0.40	0.00	0.00	0.06	-	-	0.00	0.04	97.98	Line 30 Pic 06 22 VY	650	20/11/10
115	35.65	0.00	0.12	0.00	0.03	0.03	0.05	0.00	0.01	0.69	0.00	0.00	60.65	0.41	0.00	0.07	0.11	-	-	0.05	0.10	97.96	Line 31 Pic 06 22 VY	651	20/11/10
116	35.03	0.05	0.08	0.03	0.02	0.03	0.04	0.04	0.05	0.70	0.00	0.00	60.79	0.39	0.00	0.05	0.00	-	-	0.00	0.01	97.30	Line 32 Pic 06 22 VY	652	20/11/10
117	35.28	0.00	0.10	0.00	0.01	0.02	0.08	0.00	0.00	0.74	0.00	0.04	61.26	0.39	0.00	0.00	0.07	-	-	0.00	0.05	98.04	Line 33 Pic 06 22 VY	653	20/11/10
118	35.18	0.00	0.11	0.00	0.05	0.05	0.05	0.00	0.02	0.69	0.00	0.04	60.69	0.37	0.00	0.00	0.09	-	-	0.05	0.13	97.50	Line 34 Pic 06 22 VY	654	20/11/10
119	37.17	0.03	0.03	0.00	0.00	0.01	0.03	0.00	0.03	0.31	0.00	0.00	59.37	0.31	0.00	0.00	0.10	-	-	0.00	0.01	97.40	Line 35 Pic 06 22 VY	655	20/11/10
120	34.66	0.06	0.09	0.00	0.00	0.00	0.05	0.00	0.01	0.68	0.00	0.02	61.00	0.37	0.00	0.00	0.04	-	-	0.00	0.09	97.06	Line 36 Pic 06 22 VY	656	20/11/10
121	36.20	0.00	0.09	0.02	0.00	0.05	0.03	0.00	0.00	0.64	0.00	0.00	60.75	0.42	0.00	0.01	0.09	-	-	0.09	0.00	98.40	Line 37 Pic 06 22 VY	657	20/11/10
122	35.40	0.08	0.13	0.00	0.00	0.02	0.05	0.03	0.05	0.77	0.00	0.00	60.59	0.42	0.00	0.05	0.08	-	-	0.00	0.15	97.80	Line 38 Pic 06 22 VY	658	20/11/10
123	35.02	0.07	0.10	0.01	0.00	0.01	0.08	0.02	0.04	0.79	0.00	0.00	60.95	0.37	0.00	0.00	0.09	-	-	0.11	0.05	97.72	Line 39 Pic 06 22 VY	659	20/11/10
124	36.17	0.00	0.06	0.00	0.02	0.03	0.05	0.02	0.00	0.61	0.00	0.00	60.17	0.40	0.00	0.05	0.05	-	-	0.00	0.03	97.67	Line 40 Pic 06 22 VY	660	20/11/10
125	35.11	0.00	0.09	0.00	0.00	0.01	0.06	0.00	0.00	0.84	0.01	0.06	61.40	0.45	0.00	0.02	0.02	-	-	0.00	0.13	98.19	Line 41 Pic 06 22 VY	661	20/11/10
126																									

Appendix 1: Electron Microprobe analyses

Index	O	Na	P	V	Ti	Mg	S	Cr	Mn	Al	K	Ni	Fe	Si	Ca	Cu	Co	Sr	Ba	Zn	Pb	Total	Comment	Spot#	Run Date
151	37.41	0.00	0.04	0.06	0.11	0.02	0.07	0.01	0.00	0.59	0.00	0.01	60.59	0.23	0.00	0.00	0.11	-	0.00	0.00	0.13	99.37	Line 37 LynP-02-09-A1	65	6/12/10
152	37.71	0.00	0.04	0.02	0.28	0.00	0.08	0.01	0.00	0.58	0.00	0.00	59.87	0.21	0.00	0.01	0.07	-	0.00	0.00	0.02	98.89	Line 42 LynP-02-09-A1	70	6/12/10
153	37.86	0.00	0.00	0.04	0.07	0.04	0.12	0.01	0.00	0.57	0.03	0.05	59.09	0.31	0.00	0.03	0.12	-	0.00	0.01	0.02	98.35	Line 44 LynP-02-09-A1	72	6/12/10
154	37.58	0.10	0.01	0.03	0.12	0.01	0.09	0.01	0.00	0.43	0.00	0.00	61.52	0.24	0.00	0.02	0.07	-	0.01	0.04	0.03	100.30	Line 46 LynP-02-09-A1	74	6/12/10
155	37.99	0.00	0.02	0.00	0.16	0.01	0.11	0.00	0.00	0.53	0.03	0.00	60.82	0.23	0.00	0.02	0.06	-	0.00	0.03	0.02	100.04	Line 48 LynP-02-09-A1	76	6/12/10
156	37.84	0.07	0.03	0.05	0.06	0.00	0.10	0.01	0.00	0.75	0.00	0.00	60.79	0.23	0.00	0.00	0.03	-	0.07	0.05	0.08	100.15	Line 49 LynP-02-09-A1	77	6/12/10
157	37.72	0.00	0.02	0.01	0.04	0.01	0.09	0.04	0.00	0.76	0.01	0.00	60.15	0.17	0.00	0.06	0.13	-	0.02	0.10	0.04	99.34	Line 50 LynP-02-09-A1	78	6/12/10
158	38.09	0.00	0.04	0.08	0.12	0.00	0.23	0.00	0.02	2.87	0.01	0.00	58.18	0.69	0.00	0.00	0.10	-	0.02	0.00	0.11	100.56	Line 1 LynP-02-09-A2	79	6/12/10
159	40.10	0.00	0.07	0.13	0.25	0.03	0.18	0.05	0.00	4.62	0.00	0.00	53.87	1.36	0.00	0.04	0.01	-	0.06	0.04	0.00	100.81	Line 2 LynP-02-09-A2	80	6/12/10
160	40.04	0.02	0.12	0.02	0.13	0.01	0.16	0.04	0.00	4.96	0.00	0.00	53.29	1.65	0.00	0.05	0.08	-	0.07	0.05	0.16	100.83	Line 3 LynP-02-09-A2	81	6/12/10
161	39.22	0.09	0.12	0.13	0.04	0.00	0.18	0.00	0.00	3.36	0.01	0.00	55.39	0.69	0.00	0.07	0.09	-	0.01	0.00	0.11	99.49	Line 4 LynP-02-09-A2	82	6/12/10
162	39.56	0.00	0.11	0.07	0.06	0.02	0.19	0.01	0.00	4.29	0.00	0.00	53.81	0.83	0.00	0.05	0.03	-	0.05	0.00	0.09	99.16	Line 5 LynP-02-09-A2	83	6/12/10
163	40.12	0.00	0.16	0.20	0.36	0.00	0.28	0.00	0.00	5.90	0.00	0.00	51.03	0.34	0.00	0.00	0.13	-	0.04	0.03	0.05	98.65	Line 6 LynP-02-09-A2	84	6/12/10
164	40.26	0.09	0.15	0.13	0.03	0.00	0.26	0.02	0.00	4.96	0.00	0.05	52.89	0.54	0.00	0.09	0.13	-	0.00	0.04	0.00	99.64	Line 7 LynP-02-09-A2	85	6/12/10
165	40.04	0.05	0.14	0.05	0.02	0.01	0.20	0.00	0.00	4.24	0.00	0.00	53.50	0.26	0.00	0.00	0.07	-	0.00	0.00	0.00	98.60	Line 8 LynP-02-09-A2	86	6/12/10
166	40.70	0.04	0.10	0.00	0.34	0.01	0.25	0.01	0.03	5.58	0.00	0.00	56.12	0.45	0.00	0.04	0.06	-	0.00	0.08	0.01	99.99	Line 9 LynP-02-09-A2	87	6/12/10
167	38.11	0.00	0.09	0.05	0.06	0.00	0.12	0.01	0.00	1.87	0.00	0.00	57.88	0.19	0.00	0.01	0.11	-	0.00	0.00	0.00	98.49	Line 10 LynP-02-09-A2	88	6/12/10
168	37.43	0.06	0.06	0.02	0.08	0.00	0.11	0.04	0.00	1.40	0.00	0.00	59.02	0.22	0.00	0.00	0.03	-	0.00	0.02	0.00	98.47	Line 11 LynP-02-09-A2	89	6/12/10
169	38.42	0.00	0.09	0.11	0.06	0.00	0.10	0.00	0.00	2.13	0.00	0.01	57.38	0.18	0.00	0.00	0.11	-	0.00	0.00	0.00	98.61	Line 13 LynP-02-09-A2	91	6/12/10
170	39.34	0.00	0.11	0.02	0.12	0.01	0.16	0.03	0.00	3.09	0.00	0.00	56.17	0.28	0.00	0.02	0.04	-	0.00	0.00	0.00	99.40	Line 14 LynP-02-09-A2	92	6/12/10
171	40.77	0.00	0.25	0.09	0.10	0.05	0.19	0.04	0.00	4.67	0.00	0.00	52.84	0.42	0.00	0.01	0.10	-	0.00	0.00	0.03	99.57	Line 15 LynP-02-09-A2	93	6/12/10
172	37.50	0.00	0.04	0.00	0.04	0.01	0.06	0.05	0.00	0.50	0.01	0.00	59.86	0.12	0.00	0.00	0.09	-	0.00	0.05	0.02	98.34	Line 17 LynP-02-09-A2	95	6/12/10
173	38.57	0.07	0.10	0.03	0.06	0.00	0.11	0.06	0.00	1.59	0.02	0.00	58.26	0.18	0.00	0.02	0.09	-	0.00	0.03	0.05	99.24	Line 18 LynP-02-09-A2	96	6/12/10
174	37.54	0.06	0.05	0.01	0.07	0.00	0.06	0.00	0.00	0.25	0.02	0.00	61.63	0.12	0.00	0.04	0.07	-	0.00	0.00	0.00	99.93	Line 20 LynP-02-09-A2	98	6/12/10
175	37.81	0.03	0.13	0.03	0.05	0.00	0.14	0.01	0.00	0.84	0.00	0.00	58.69	0.18	0.00	0.04	0.11	-	0.01	0.00	0.05	98.09	Line 21 LynP-02-09-A2	99	6/12/10
176	36.38	0.08	0.01	0.05	0.08	0.00	0.05	0.00	0.00	0.46	0.00	0.00	59.77	0.10	0.00	0.00	0.06	-	0.00	0.03	0.00	97.06	Line 23 LynP-02-09-A2	101	6/12/10
177	37.12	0.00	0.11	0.05	0.13	0.00	0.08	0.01	0.00	1.02	0.00	0.00	59.19	0.13	0.00	0.03	0.12	-	0.00	0.00	0.00	97.99	Line 25 LynP-02-09-A2	103	6/12/10
178	37.20	0.09	0.03	0.00	0.01	0.05	0.08	0.00	0.00	0.84	0.01	0.06	58.80	0.16	0.00	0.00	0.09	-	0.08	0.00	0.00	97.50	Line 26 LynP-02-09-A2	104	6/12/10
179	37.25	0.03	0.05	0.00	0.13	0.00	0.10	0.01	0.00	0.85	0.00	0.00	59.64	0.14	0.00	0.00	0.04	-	0.03	0.05	0.00	98.32	Line 28 LynP-02-09-A2	106	6/12/10
180	37.15	0.00	0.06	0.00	0.11	0.00	0.07	0.04	0.00	0.85	0.01	0.00	60.61	0.10	0.00	0.00	0.11	-	0.06	0.04	0.00	99.19	Line 29 LynP-02-09-A2	107	6/12/10
181	37.94	0.00	0.09	0.03	0.12	0.03	0.07	0.06	0.00	0.89	0.00	0.03	59.40	0.12	0.00	0.01	0.02	-	0.00	0.00	0.00	98.79	Line 30 LynP-02-09-A2	108	6/12/10
182	37.61	0.11	0.14	0.08	0.15	0.00	0.10	0.04	0.00	2.45	0.00	0.00	56.22	0.66	0.00	0.00	0.03	-	0.00	0.00	0.00	97.58	Line 31 LynP-02-09-A2	109	6/12/10
183	37.68	0.00	0.07	0.06	0.11	0.02	0.08	0.05	0.00	1.02	0.01	0.00	59.38	0.12	0.00	0.03	0.09	-	0.06	0.02	0.04	98.84	Line 32 LynP-02-09-A2	110	6/12/10
184	37.63	0.00	0.03	0.01	0.04	0.00	0.08	0.00	0.00	1.14	0.00	0.02	58.97	0.11	0.00	0.02	0.06	-	0.04	0.11	0.00	98.26	Line 33 LynP-02-09-A2	111	6/12/10
185	37.37	0.00	0.09	0.03	0.06	0.00	0.07	0.01	0.00	1.10	0.01	0.00	59.01	0.15	0.00	0.00	0.08	-	0.00	0.07	0.06	98.10	Line 34 LynP-02-09-A2	112	6/12/10
186	40.09	0.08	0.18	0.13	0.18	0.00	0.22	0.13	0.00	5.18	0.01	0.00	52.70	0.92	0.00	0.05	0.02	-	0.02	0.03	0.00	99.91	Line 36 LynP-02-09-A2	114	6/12/10
187	38.83	0.00	0.09	0.12	0.11	0.03	0.11	0.07	0.00	2.67	0.01	0.03	57.18	0.31	0.00	0.00	0.05	-	0.08	0.00	0.03	99.70	Line 37 LynP-02-09-A2	115	6/12/10
188	39.14	0.01	0.13	0.05	0.15	0.00	0.17	0.04	0.00	3.63	0.00	0.00	54.74	0.42	0.00	0.00	0.10	-	0.00	0.00	0.10	98.66	Line 38 LynP-02-09-A2	116	6/12/10
189	38.03	0.01	0.08	0.01	0.09	0.01	0.14	0.13	0.00	2.22	0.00	0.00	53.38	0.27	0.00	0.06	0.04	-	0.00	0.03	0.00	98.95	Line 39 LynP-02-09-A2	117	6/12/10
190	37.46	0.02	0.07	0.06	0.11	0.00	0.07	0.06	0.00	0.81	0.02	0.00	59.74	0.13	0.00	0.00	0.02	-	0.02	0.03	0.00	98.61	Line 44 LynP-02-09-A2	122	6/12/10
191	39.10	0.00	0.12	0.00	0.24	0.04	0.15	0.02	0.00	2.75	0.00	0.00	54.77	0.56	0.00	0.01	0.09	-	0.12	0.09	0.00	98.04	Line 45 LynP-02-09-A2	123	6/12/10
192	38.29	0.00	0.08	0.03	0.30	0.00	0.09	0.00	0.00	1.00	0.00	0.00	58.99	0.14	0.00	0.08	0.03	-	0.01	0.05	0.00	99.08	Line 47 LynP-02-09-A2	125	6/12/10
193	38.04	0.08	0.07	0.03	0.09	0.00	0.08	0.00	0.00	1.15	0.00	0.00	58.81	0.14	0.00	0.00	0.08	-	0.01	0.10	0.00	98.67	Line 48 LynP-02-09-A2	126	6/12/10
194	36.81	0.08	0.00	0.00	0.15	0.00	0.08	0.00	0.00	0.28	0.00	0.05	61.27	0.18	0.00	0.00	0.09	-	0.00	0.13	0.00	99.10	Line 49 LynP-02-09-A2	127	6/12/10
195	37.57	0.02	0.01	0.02	0.07	0.00	0.03	0.00	0.00	0.15	0.01	0.00	60.19	0.13	0.00	0.00	0.08	-	0.07	0.00	0.00	98.35	Line 50 LynP-02-09-A2	128	6/12/10
196	35.84	0.03	0.02	0.01	0.14	0.00	0.10	0.00	0.00	0.26	0.01	0.00	60.77	0.21	0.00	0.00	0.08	-	0.00	0.06	0.04	97.57	Line 3 LynP-02-09-A3	131	6/12/10
197	39.69	0.06	0.09	0.04	0.23	0.02	0.10	0.07	0.00	3.24	0.01	0.00	53.38	2.79	0.00	0.03	0.04	-	0.00	0.00	0.00	99.80	Line 6 LynP-02-09-A3	134	6/12/10
198	37.26	0.00	0.01	0.06	0.08	0.01	0.05	0.00	0.00	0.38	0.01	0.03	61.22	0.23	0.00	0.04	0.08	-	0.00	0.06	0.00	99.51	Line 9 LynP-02-09-A3	137	6/12/10
199	37.18	0.00	0.04	0.01	0.09	0.00	0.10	0.00	0.00	0.86	0.00	0.00	59.79	0.22	0.00	0.00	0.07	-	0.01	0.00	0.00	98.37	Line 11 LynP-02-09-A3	139	6/12/10
200	37.50	0.06	0.05	0.0																					

Appendix 1: Electron Microprobe analyses

Index	O	Na	P	V	Ti	Mg	S	Cr	Mn	Al	K	Ni	Fe	Si	Ca	Cu	Co	Sr	Ba	Zn	Pb	Total	Comment	Spot#	Run Date	
226	42.12	0.01	0.10	0.08	0.09	0.00	0.08	0.03	0.01	9.50	0.00	0.00	43.50	4.04	0.00	0.00	0.05	0.00	0.02	0.06	0.03	99.69	Line 1 IBH-13-09h	106	22/2/14	
227	40.78	0.00	0.16	0.07	0.18	0.00	0.12	0.03	0.03	7.03	0.01	0.02	48.94	1.16	0.00	0.00	0.09	0.00	0.02	0.11	0.11	98.86	Line 2 IBH-13-09h	107	22/2/14	
228	41.59	0.00	0.14	0.11	0.08	0.00	0.10	0.06	0.03	8.39	0.00	0.03	45.75	2.86	0.00	0.07	0.04	0.02	0.04	0.02	0.09	99.41	Line 3 IBH-13-09h	108	22/2/14	
229	41.28	0.00	0.10	0.01	0.10	0.00	0.07	0.00	0.02	7.63	0.02	0.02	47.61	2.56	0.00	0.01	0.02	0.04	0.00	0.02	0.00	99.51	Line 4 IBH-13-09h	109	22/2/14	
230	40.33	0.00	0.13	0.06	0.06	0.00	0.09	0.03	0.07	6.30	0.00	0.03	50.70	1.12	0.00	0.00	0.03	0.00	0.00	0.00	0.05	99.00	Line 5 IBH-13-09h	110	22/2/14	
231	40.64	0.00	0.18	0.02	0.37	0.04	0.09	0.02	0.01	6.85	0.00	0.00	49.04	1.36	0.00	0.00	0.05	0.01	0.02	0.00	0.00	98.70	Line 6 IBH-13-09h	111	22/2/14	
232	40.72	0.00	0.12	0.07	0.10	0.01	0.09	0.03	0.00	7.96	0.00	0.00	47.53	2.26	0.00	0.01	0.04	0.00	0.00	0.02	0.11	99.08	Line 7 IBH-13-09h	112	22/2/14	
233	40.84	0.02	0.17	0.12	0.05	0.00	0.10	0.02	0.04	7.47	0.00	0.02	47.90	2.42	0.00	0.06	0.00	0.00	0.00	0.04	0.00	99.27	Line 8 IBH-13-09h	113	22/2/14	
234	38.56	0.00	0.08	0.00	0.03	0.02	0.09	0.03	0.01	3.02	0.00	0.00	56.16	0.25	0.00	0.00	0.10	0.00	0.03	0.04	0.00	98.43	Line 9 IBH-13-09h	114	22/2/14	
235	41.43	0.02	0.12	0.00	0.23	0.00	0.13	0.00	0.02	7.93	0.00	0.01	47.58	2.00	0.00	0.08	0.01	0.01	0.03	0.00	0.00	99.58	Line 10 IBH-13-09h	115	22/2/14	
236	39.77	0.00	0.20	0.09	0.03	0.00	0.10	0.00	0.03	5.81	0.01	0.00	51.86	0.53	0.00	0.00	0.08	0.00	0.00	0.00	0.00	98.51	Line 11 IBH-13-09h	116	22/2/14	
237	41.11	0.01	0.11	0.05	0.36	0.00	0.07	0.01	0.02	7.88	0.00	0.00	47.44	2.66	0.00	0.00	0.05	0.05	0.00	0.00	0.01	0.02	99.85	Line 12 IBH-13-09h	117	22/2/14
238	41.44	0.00	0.14	0.04	0.19	0.00	0.08	0.04	0.00	9.01	0.00	0.04	44.94	3.02	0.00	0.04	0.04	0.00	0.00	0.07	0.06	99.13	Line 13 IBH-13-09h	118	22/2/14	
239	38.26	0.00	0.12	0.03	0.03	0.00	0.09	0.00	0.00	2.66	0.00	0.00	56.48	0.24	0.00	0.06	0.07	0.01	0.02	0.04	0.00	98.10	Line 14 IBH-13-09h	119	22/2/14	
240	42.70	0.01	0.09	0.05	0.18	0.00	0.11	0.00	0.05	9.52	0.01	0.00	42.94	3.99	0.00	0.10	0.06	0.00	0.04	0.00	0.00	99.85	Line 16 IBH-13-09h	121	22/2/14	
241	38.88	0.01	0.10	0.07	0.08	0.00	0.09	0.02	0.03	3.58	0.01	0.00	56.13	0.21	0.00	0.00	0.05	0.01	0.00	0.00	0.09	99.34	Line 17 IBH-13-09h	122	22/2/14	
242	39.50	0.00	0.20	0.12	0.00	0.00	0.08	0.02	0.05	5.99	0.00	0.00	51.71	0.36	0.00	0.05	0.02	0.02	0.00	0.00	0.06	98.17	Line 18 IBH-13-09h	123	22/2/14	
243	38.99	0.00	0.21	0.07	0.00	0.00	0.12	0.00	0.01	4.72	0.00	0.01	53.90	0.17	0.00	0.00	0.01	0.03	0.05	0.00	0.11	98.40	Line 19 IBH-13-09h	124	22/2/14	
244	39.79	0.00	0.24	0.23	0.15	0.00	0.09	0.05	0.06	5.77	0.00	0.00	52.63	0.15	0.00	0.03	0.09	0.00	0.03	0.01	0.02	99.33	Line 20 IBH-13-09h	125	22/2/14	
245	36.67	-	0.08	0.00	0.00	0.09	0.01	0.00	0.29	0.18	-	-	58.71	1.07	-	0.01	0.02	-	-	-	-	0.00	97.13	Line 2 Win0601B_1	10	28/3/14
246	36.48	-	0.09	0.01	0.00	0.04	0.00	0.00	0.22	0.17	-	-	59.21	1.01	-	0.10	0.05	-	-	-	-	0.01	97.40	Line 3 Win0601B_1	11	28/3/14
247	36.62	-	0.07	0.00	0.00	0.06	0.00	0.00	0.22	0.18	-	-	59.02	0.99	-	0.00	0.11	-	-	-	-	0.07	97.35	Line 5 Win0601B_1	13	28/3/14
248	37.04	-	0.06	0.00	0.00	0.03	0.00	0.03	0.21	0.19	-	-	58.68	0.97	-	0.00	0.08	-	-	-	-	0.00	97.29	Line 6 Win0601B_1	14	28/3/14
249	37.37	-	0.08	0.00	0.00	0.03	0.00	0.00	0.27	0.19	-	-	58.29	1.04	-	0.00	0.08	-	-	-	-	0.10	97.44	Line 7 Win0601B_1	15	28/3/14
250	37.12	-	0.06	0.00	0.03	0.03	0.02	0.03	0.28	0.19	-	-	58.38	1.03	-	0.03	0.03	-	-	-	-	0.05	97.26	Line 8 Win0601B_1	16	28/3/14
251	37.49	-	0.07	0.02	0.00	0.01	0.01	0.00	0.28	0.18	-	-	58.65	1.07	-	0.05	0.07	-	-	-	-	0.17	98.07	Line 9 Win0601B_1	17	28/3/14
252	37.89	-	0.07	0.00	0.07	0.03	0.00	0.01	0.26	0.19	-	-	58.86	1.04	-	0.01	0.09	-	-	-	-	0.08	98.58	Line 10 Win0601B_1	18	28/3/14
253	37.61	-	0.06	0.00	0.03	0.05	0.00	0.00	0.28	0.19	-	-	58.38	0.97	-	0.08	0.09	-	-	-	-	0.10	97.83	Line 11 Win0601B_1	19	28/3/14
254	36.69	-	0.06	0.00	0.08	0.05	0.01	0.00	0.22	0.08	-	-	58.88	0.95	-	0.04	0.12	-	-	-	-	0.00	97.16	Line 2 Win0601B_2	25	28/3/14
255	37.12	-	0.05	0.03	0.01	0.04	0.00	0.01	0.26	0.07	-	-	58.67	0.96	-	0.00	0.06	-	-	-	-	0.01	97.29	Line 3 Win0601B_2	26	28/3/14
256	37.09	-	0.05	0.00	0.00	0.01	0.00	0.00	0.24	0.09	-	-	59.29	0.97	-	0.00	0.04	-	-	-	-	0.12	97.90	Line 10 Win0601B_2	33	28/3/14
257	36.94	-	0.09	0.00	0.00	0.05	0.02	0.02	0.22	0.08	-	-	59.20	1.00	-	0.02	0.11	-	-	-	-	0.02	97.76	Line 11 Win0601B_2	34	28/3/14
258	36.63	-	0.09	0.00	0.00	0.02	0.03	0.00	0.26	0.10	-	-	58.69	1.11	-	0.06	0.04	-	-	-	-	0.01	97.04	Line 15 Win0601B_2	38	28/3/14
259	35.98	-	0.01	0.00	0.00	0.06	0.02	0.01	0.16	0.13	-	-	60.30	0.43	-	0.05	0.05	-	-	-	-	0.07	97.27	Line 1 Win0601B_3	39	28/3/14
260	36.97	-	0.03	0.00	0.03	0.03	0.00	0.00	0.29	0.07	-	-	59.09	1.04	-	0.05	0.15	-	-	-	-	0.04	97.78	Line 7 Win0601B_3	45	28/3/14
261	36.65	-	0.09	0.00	0.00	0.03	0.00	0.00	0.26	0.06	-	-	59.07	1.01	-	0.00	0.10	-	-	-	-	0.00	97.25	Line 9 Win0601B_3	47	28/3/14
262	37.48	-	0.05	0.02	0.04	0.04	0.02	0.00	0.25	0.08	-	-	58.87	0.94	-	0.00	0.11	-	-	-	-	0.10	98.00	Line 10 Win0601B_3	48	28/3/14
263	36.70	-	0.02	0.00	0.00	0.05	0.01	0.03	0.26	0.10	-	-	58.70	1.13	-	0.03	0.07	-	-	-	-	0.03	97.12	Line 13 Win0601B_3	51	28/3/14
264	37.04	-	0.03	0.04	0.01	0.03	0.01	0.01	0.22	0.14	-	-	58.74	1.10	-	0.00	0.06	-	-	-	-	0.00	97.45	Line 2 Win0601B_4	55	28/3/14
265	36.89	-	0.00	0.03	0.00	0.05	0.01	0.06	0.28	0.12	-	-	58.54	1.10	-	0.00	0.05	-	-	-	-	0.03	97.16	Line 3 Win0601B_4	56	28/3/14
266	37.41	-	0.06	0.05	0.00	0.01	0.01	0.06	0.30	0.12	-	-	58.15	1.15	-	0.09	0.08	-	-	-	-	0.00	97.47	Line 5 Win0601B_4	58	28/3/14
267	37.44	-	0.02	0.01	0.00	0.03	0.01	0.03	0.16	0.13	-	-	59.10	1.09	-	0.03	0.05	-	-	-	-	0.00	98.11	Line 7 Win0601B_4	60	28/3/14
268	37.46	-	0.08	0.04	0.00	0.06	0.01	0.02	0.25	0.11	-	-	59.21	1.08	-	0.06	0.11	-	-	-	-	0.13	98.60	Line 8 Win0601B_4	61	28/3/14
269	37.06	-	0.05	0.00	0.00	0.04	0.00	0.02	0.24	0.13	-	-	58.99	1.07	-	0.00	0.11	-	-	-	-	0.03	97.74	Line 9 Win0601B_4	62	28/3/14
270	36.69	-	0.06	0.00	0.00	0.05	0.02	0.03	0.20	0.12	-	-	59.11	1.07	-	0.02	0.03	-	-	-	-	0.00	97.40	Line 10 Win0601B_4	63	28/3/14
271	36.82	-	0.01	0.00	0.01	0.00	0.01	0.00	0.27	0.12	-	-	58.75	1.06	-	0.02	0.12	-	-	-	-	0.07	97.25	Line 11 Win0601B_4	64	28/3/14
272	36.65	-	0.00	0.00	0.00	0.05	0.03	0.00	0.21	0.12	-	-	59.10	1.06	-	0.01	0.08	-	-	-	-	0.00	97.30	Line 15 Win0601B_4	68	28/3/14
273	36.91	-	0.01	0.00	0.04	0.01	0.01	0.00	0.27	0.14	-	-	58.24	1.22	-	0.00	0.11	-	-	-	-	0.06	97.03	Line 1 Win0601B_5	69	28/3/14
274	37.10	-	0.03	0.00	0.03	0.00	0.01	0.00	0.20	0.14	-	-	58.34	1.14	-	0.00	0.09	-	-	-	-	0.00	97.07	Line 2 Win0601B_5	70	28/3/14
275	37.17	-	0.06	0.01	0.00	0.04	0.03	0.03	0.23	0.14	-	-	58.60	1.22	-	0.00	0.10	-	-	-	-	0.10	97.71	Line 6 Win0601B_5	74	28/3/14
276	36.62	-	0.00	0.02	0.04	0.00	0.01	0.00	0.28	0.04	-	-	58.71	1.29	-	0.00	0.06	-	-	-	-	0.00	97.06	Line 11 Win0601B_5	79	28/3/14
277	36.71	-	0.06	0.00	0.06	0.03	0.02	0.02	0.26	0.10	-	-	58.67	1.23	-	0.00	0.07	-	-	-	-	0.16	97.3			

Appendix 1: Electron Microprobe analyses

Index	O	Na	P	V	Ti	Mg	S	Cr	Mn	Al	K	Ni	Fe	Si	Ca	Cu	Co	Sr	Ba	Zn	Pb	Total	Comment	Spot#	Run Date
301	37.51	0.03	0.02		0.00	0.02	0.03	0.00	0.23	0.10	0.00	0.00	62.52	0.93	0.00	0.02	0.10	0.02	0.06	0.00	0.08	101.66	Line 2 SHRIMP HM1 Win 06 01B	213	18/7/14
302	36.40	0.06	0.05		0.00	0.03	0.01	0.00	0.25	0.10	0.00	0.00	62.50	0.91	0.00	0.00	0.17	0.01	0.04	0.03	0.00	100.56	Line 3 SHRIMP HM1 Win 06 01B	214	18/7/14
303	37.49	0.06	0.08		0.02	0.05	0.02	0.02	0.29	0.10	0.00	0.00	62.04	0.93	0.00	0.00	0.10	0.00	0.08	0.09	0.03	101.37	Line 4 SHRIMP HM1 Win 06 01B	215	18/7/14
304	36.84	0.00	0.06		0.01	0.02	0.00	0.00	0.22	0.10	0.00	0.00	62.35	0.92	0.00	0.02	0.10	0.03	0.00	0.00	0.02	100.67	Line 5 SHRIMP HM1 Win 06 01B	216	18/7/14
305	36.21	0.03	0.04		0.00	0.04	0.02	0.04	0.26	0.08	0.02	0.00	62.23	0.94	0.00	0.03	0.02	0.00	0.02	0.00	0.00	99.97	Line 6 SHRIMP HM1 Win 06 01B	217	18/7/14
306	37.08	0.00	0.07		0.04	0.04	0.00	0.00	0.29	0.08	0.00	0.00	62.34	0.91	0.00	0.04	0.07	0.00	0.10	0.03	0.02	101.10	Line 7 SHRIMP HM1 Win 06 01B	218	18/7/14
307	36.95	0.02	0.05		0.09	0.03	0.00	0.00	0.27	0.10	0.01	0.09	61.81	0.92	0.00	0.00	0.05	0.01	0.06	0.00	0.00	100.44	Line 8 SHRIMP HM1 Win 06 01B	219	18/7/14
308	36.56	0.00	0.07		0.02	0.03	0.01	0.00	0.20	0.10	0.00	0.00	62.66	0.94	0.00	0.07	0.10	0.01	0.00	0.00	0.00	100.77	Line 9 SHRIMP HM1 Win 06 01B	220	18/7/14
309	37.43	0.01	0.04		0.00	0.02	0.01	0.00	0.25	0.08	0.00	0.00	62.38	0.91	0.00	0.01	0.09	0.02	0.00	0.00	0.00	101.25	Line 10 SHRIMP HM1 Win 06 01B	221	18/7/14
310	39.31	0.00	0.11		0.02	0.01	0.12	0.00	0.00	4.14	0.01	0.00	55.40	0.69	0.00	0.06	0.06	0.02	0.09	0.00	0.03	100.06	Line 1 SHRIMP HM3 IBH 13 09h	222	18/7/14
311	39.80	0.00	0.13		0.15	0.02	0.12	0.02	0.02	7.96	0.00	0.00	51.18	0.39	0.00	0.02	0.06	0.00	0.12	0.04	0.00	100.03	Line 2 SHRIMP HM3 IBH 13 09h	223	18/7/14
312	40.21	0.01	0.15		0.10	0.00	0.10	0.02	0.01	7.33	0.00	0.00	51.12	1.33	0.00	0.00	0.05	0.06	0.00	0.01	0.01	100.50	Line 3 SHRIMP HM3 IBH 13 09h	224	18/7/14
313	39.46	0.04	0.18		0.13	0.00	0.12	0.04	0.02	6.35	0.00	0.00	51.51	1.22	0.00	0.03	0.02	0.01	0.05	0.03	0.04	99.23	Line 4 SHRIMP HM3 IBH 13 09h	225	18/7/14
314	41.94	0.00	0.16		0.16	0.01	0.13	0.04	0.00	10.09	0.02	0.05	44.87	3.17	0.00	0.00	0.09	0.00	0.03	0.00	0.00	100.77	Line 6 SHRIMP HM3 IBH 13 09h	227	18/7/14
315	39.58	0.02	0.16		0.17	0.00	0.13	0.00	0.00	7.97	0.00	0.01	49.68	1.23	0.00	0.07	0.05	0.00	0.00	0.02	0.00	99.08	Line 7 SHRIMP HM3 IBH 13 09h	228	18/7/14
316	40.64	0.00	0.23		0.09	0.00	0.15	0.00	0.04	6.74	0.01	0.00	51.40	1.16	0.00	0.00	0.01	0.01	0.04	0.09	0.00	100.62	Line 8 SHRIMP HM3 IBH 13 09h	229	18/7/14
317	40.74	0.00	0.11		0.13	0.00	0.08	0.04	0.04	9.56	0.00	0.00	45.12	3.61	0.00	0.01	0.02	0.00	0.03	0.00	0.09	99.59	Line 9 SHRIMP HM3 IBH 13 09h	230	18/7/14
318	39.71	0.00	0.14		0.17	0.02	0.13	0.00	0.01	9.69	0.01	0.00	47.30	2.53	0.00	0.00	0.01	0.01	0.00	0.00	0.01	99.74	Line 10 SHRIMP HM3 IBH 13 09h	231	18/7/14
319	41.09	0.00	0.20		0.16	0.01	0.14	0.00	0.00	8.63	0.00	0.00	50.06	1.55	0.00	0.05	0.04	0.00	0.00	0.00	0.05	101.98	Line 11 SHRIMP HM3 IBH 13 09h	232	18/7/14
320	42.18	0.01	0.14		0.23	0.00	0.15	0.00	0.00	10.50	0.02	0.00	50.50	4.04	0.00	0.03	0.04	0.01	0.07	0.00	0.00	100.69	Line 12 SHRIMP HM3 IBH 13 09h	233	18/7/14
321	41.62	0.00	0.16		0.17	0.02	0.11	0.00	0.04	8.36	0.00	0.00	49.87	1.58	0.00	0.00	0.00	0.01	0.00	0.02	0.03	101.99	Line 13 SHRIMP HM3 IBH 13 09h	234	18/7/14
322	38.13	0.00	0.19		0.16	0.01	0.13	0.04	0.05	9.77	0.02	0.00	47.45	2.44	0.00	0.00	0.02	0.00	0.00	0.00	0.00	98.40	Line 14 SHRIMP HM3 IBH 13 09h	235	18/7/14
323	41.67	0.00	0.11		0.47	0.01	0.11	0.04	0.03	9.32	0.00	0.00	47.47	2.00	0.00	0.00	0.00	0.00	0.00	0.00	0.00	101.23	Line 15 SHRIMP HM3 IBH 13 09h	236	18/7/14
324	39.17	0.03	0.15		0.11	0.00	0.11	0.00	0.02	6.84	0.00	0.00	50.68	2.42	0.00	0.02	0.02	0.01	0.00	0.03	0.12	99.71	Line 16 SHRIMP HM3 IBH 13 09h	237	18/7/14
325	40.94	0.01	0.13		0.14	0.02	0.10	0.00	0.00	8.24	0.01	0.00	47.02	2.99	0.00	0.03	0.04	0.00	0.09	0.00	0.00	99.74	Line 17 SHRIMP HM3 IBH 13 09h	238	18/7/14
326	39.94	0.00	0.14		0.09	0.00	0.14	0.02	0.00	5.32	0.03	0.00	54.73	0.44	0.00	0.00	0.08	0.00	0.00	0.00	0.06	100.99	Line 18 SHRIMP HM3 IBH 13 09h	239	18/7/14
327	39.38	0.00	0.24		0.14	0.00	0.16	0.10	0.00	7.45	0.00	0.03	52.07	0.55	0.00	0.05	0.00	0.00	0.12	0.00	0.02	100.30	Line 19 SHRIMP HM3 IBH 13 09h	240	18/7/14
328	38.51	0.00	0.14		0.14	0.01	0.13	0.02	0.07	4.05	0.00	0.00	56.46	0.30	0.00	0.00	0.05	0.00	0.04	0.00	0.00	99.90	Line 20 SHRIMP HM3 IBH 13 09h	241	18/7/14
329	37.13	0.02	0.05		0.00	0.05	0.00	0.01	0.27	0.10	0.00	0.01	61.64	1.10	0.00	0.00	0.07	0.00	0.00	0.16	0.05	100.65	Line 1 SHRIMP HM3 Win 06 01B	272	18/7/14
330	37.42	0.03	0.08		0.00	0.05	0.02	0.00	0.29	0.07	0.01	0.00	62.04	1.10	0.00	0.00	0.08	0.00	0.10	0.06	0.00	101.33	Line 2 SHRIMP HM3 Win 06 01B	273	18/7/14
331	36.88	0.00	0.03		0.01	0.03	0.01	0.00	0.26	0.11	0.00	0.00	62.57	1.10	0.00	0.00	0.08	0.00	0.03	0.00	0.05	101.17	Line 3 SHRIMP HM3 Win 06 01B	274	18/7/14
332	37.17	0.00	0.04		0.09	0.04	0.02	0.05	0.34	0.10	0.01	0.00	62.49	1.13	0.00	0.06	0.08	0.00	0.04	0.01	0.06	101.73	Line 4 SHRIMP HM3 Win 06 01B	275	18/7/14
333	36.70	0.03	0.03		0.07	0.05	0.00	0.01	0.27	0.10	0.03	0.00	61.70	1.08	0.00	0.00	0.09	0.01	0.00	0.00	0.10	100.27	Line 5 SHRIMP HM3 Win 06 01B	276	18/7/14
334	36.74	0.01	0.06		0.00	0.01	0.04	0.00	0.28	0.10	0.00	0.00	62.65	1.10	0.00	0.01	0.10	0.02	0.10	0.09	0.08	101.38	Line 6 SHRIMP HM3 Win 06 01B	277	18/7/14
335	37.42	0.00	0.05		0.02	0.05	0.00	0.00	0.26	0.12	0.00	0.02	62.67	1.14	0.01	0.00	0.07	0.00	0.02	0.00	0.04	101.87	Line 7 SHRIMP HM3 Win 06 01B	278	18/7/14
336	36.59	0.04	0.03		0.00	0.05	0.01	0.03	0.26	0.11	0.00	0.00	61.64	1.15	0.00	0.00	0.04	0.00	0.00	0.06	0.06	100.05	Line 8 SHRIMP HM3 Win 06 01B	279	18/7/14
337	36.68	0.02	0.06		0.01	0.04	0.02	0.00	0.29	0.11	0.00	0.00	61.57	1.13	0.00	0.06	0.12	0.00	0.06	0.06	0.00	100.23	Line 9 SHRIMP HM3 Win 06 01B	280	18/7/14
338	37.05	0.01	0.03		0.03	0.06	0.02	0.01	0.34	0.10	0.00	0.00	61.61	1.13	0.00	0.03	0.02	0.02	0.11	0.04	0.00	100.61	Line 10 SHRIMP HM3 Win 06 01B	281	18/7/14
339	35.46	-0.03	-0.01	-0.03	0.00	0.11	0.09	0.02	0.04	0.12	-0.01	0.04	61.66	1.09	-0.03	0.06	0.09	-	-	-0.06	0.33	98.93	Capao L4 Vertical-1	207	22/6/16
340	35.43	0.00	-0.01	0.01	0.03	0.13	0.30	-0.02	0.08	0.16	-0.01	-0.01	61.88	1.03	-0.05	-0.03	0.03	-	-	0.07	0.21	99.24	Capao L4 Vertical-1	208	22/6/16
341	35.36	-0.05	0.01	-0.01	0.02	0.12	0.06	-0.02	0.05	0.12	-0.02	0.00	60.99	1.11	-0.06	-0.01	0.05	-	-	0.01	0.11	97.85	Capao L4 Vertical-1	209	22/6/16
342	35.61	-0.02	-0.06	-0.03	-0.01	0.05	0.27	0.01	-0.01	0.12	-0.01	0.01	61.96	1.04	-0.05	-0.02	0.09	-	-	0.08	0.25	99.28	Capao L4 Vertical-1	210	22/6/16
343	36.13	-0.04	0.06	0.00	-0.05	0.12	-0.06	-0.01	0.05	0.13	0.01	0.08	61.49	1.16	-0.06	0.05	0.06	-	-	0.01	0.25	99.40	Capao L4 Vertical-1	211	22/6/16
344	35.24	-0.03	-0.03	0.00	-0.02	0.07	0.01	0.00	0.05	0.12	0.00	-0.03	60.83	1.07	-0.05	-0.01	0.06	-	-	0.01	0.13	97.42	Capao L4 Vertical-1	212	22/6/16
345	35.18	0.01	0.05	-0.02	-0.01	0.10	0.01	0.01	0.07	0.13	0.00	-0.03	61.32	1.07	-0.07	0.00	0.11	-	-	0.06	0.21	98.22	Capao L4 Vertical-1	213	22/6/16
346	35.18	-0.07	0.05	-0.02	-0.01	0.11	-0.18	0.04	0.01	0.11	0.01	0.03	61.01	1.08	-0.04	0.04	0.09	-	-	0.00	0.30	97.72	Capao L4 Vertical-1	214	22/6/16
347	35.76	0.01	0.07	0.03	-0.01	0.13	-0.07	0.02	0.06	0.12	-0.01	0.01	61.93	1.12	-0.04	0.01	0.04	-	-	0.09	0.31	99.59	Capao L4 Vertical-1	215	22/6/16
348	35.35	-0.06	0.01	0.02	0.01	0.09	0.22	0.02	0.07	0.13	0.01	-0.02	61.36	1.16	-0.05	0.01	0.06	-	-	0.10	0.22	98.71	Capao L4 Vertical-1	216	22/6/16
349	35.38	-0.02	0.05	0.05	-0.04	0.10	-0.03	0.01	0.04	0.14	0.00	0.03	61.87	1.07	-0.04	-0.01	0.09	-	-	0.03	0.28	99.00	Capao L4 Vertical-1	217	22/6/16
350	35.34	-0.02	0.10	0.02	-0.01	0.10	0.0																		

Appendix 1: Electron Microprobe analyses

Index	O	Na	P	V	Ti	Mg	S	Cr	Mn	Al	K	Ni	Fe	Si	Ca	Cu	Co	Sr	Ba	Zn	Pb	Total	Comment	Spot#	Run Date
376	38.10	0.00	0.06	0.00	0.01	0.01	0.03	0.02	0.00	1.53	0.01	0.02	58.29	0.37	0.00	0.00	0.08	-	-	0.00	0.08	98.62	Hm-19_Pic6-21-6-VG-7	56	6/7/16
377	38.71	0.02	0.03	0.02	0.04	0.00	0.03	0.00	0.02	1.67	0.00	0.01	59.54	0.38	0.00	0.03	0.01	-	-	0.00	0.05	100.57	Hm-19_Pic6-21-6-VG-8	57	6/7/16
378	38.46	0.00	0.07	0.00	0.01	0.00	0.03	0.02	0.03	1.57	0.00	0.01	57.04	0.38	0.00	0.00	0.07	-	-	0.00	0.04	97.72	Hm-19_Pic6-21-6-VG-9	58	6/7/16
379	38.06	0.04	0.05	0.00	0.00	0.00	0.06	0.02	0.00	1.37	0.00	0.00	57.78	0.37	0.00	0.00	0.05	-	-	0.01	0.00	97.81	Hm-19_Pic6-21-6-VG-10	59	6/7/16
380	38.49	0.00	0.01	0.03	0.03	0.00	0.05	0.00	0.00	1.77	0.00	0.00	57.77	0.35	0.00	0.04	0.06	-	-	0.00	0.00	98.62	Hm-19_Pic6-21-6-VG-11	60	6/7/16
381	38.72	0.16	0.16	0.04	0.15	0.01	0.04	0.00	0.00	1.84	0.00	0.00	57.20	0.27	0.00	0.01	0.06	-	-	0.00	0.00	98.66	Line 1 HM-19_Pic6-21-6-Black-Dull-Gt	61	6/7/16
382	38.96	0.03	0.10	0.00	0.15	0.00	0.02	0.01	0.00	1.82	0.02	0.00	57.14	0.26	0.00	0.00	0.06	-	-	0.06	0.02	98.66	Line 2 HM-19_Pic6-21-6-Black-Dull-Gt	62	6/7/16
383	38.79	0.01	0.09	0.01	0.13	0.00	0.05	0.00	0.00	1.83	0.00	0.03	57.27	0.26	0.00	0.01	0.05	-	-	0.05	0.00	98.59	Line 3 HM-19_Pic6-21-6-Black-Dull-Gt	63	6/7/16
384	39.24	0.00	0.14	0.00	0.13	0.01	0.03	0.03	0.00	1.78	0.01	0.05	57.27	0.27	0.00	0.00	0.05	-	-	0.00	0.04	99.06	Line 4 HM-19_Pic6-21-6-Black-Dull-Gt	64	6/7/16
385	38.98	0.01	0.11	0.01	0.12	0.01	0.04	0.00	0.02	1.77	0.01	0.02	57.38	0.27	0.00	0.01	0.04	-	-	0.01	0.09	98.88	Line 5 HM-19_Pic6-21-6-Black-Dull-Gt	65	6/7/16
386	38.84	0.02	0.08	0.00	0.12	0.01	0.02	0.01	0.00	1.77	0.01	0.06	57.40	0.28	0.00	0.00	0.06	-	-	0.02	0.00	98.71	Line 6 HM-19_Pic6-21-6-Black-Dull-Gt	66	6/7/16
387	38.81	0.12	0.13	0.00	0.12	0.00	0.05	0.00	0.00	1.83	0.01	0.00	57.14	0.27	0.00	0.01	0.04	-	-	0.02	0.02	98.56	Line 7 HM-19_Pic6-21-6-Black-Dull-Gt	67	6/7/16
388	38.89	0.13	0.11	0.00	0.13	0.01	0.02	0.00	0.01	1.83	0.00	0.03	57.28	0.28	0.00	0.03	0.09	-	-	0.04	0.06	98.92	Line 8 HM-19_Pic6-21-6-Black-Dull-Gt	68	6/7/16
389	38.74	0.00	0.15	0.01	0.13	0.00	0.04	0.00	0.00	1.80	0.00	0.03	56.99	0.27	0.00	0.06	0.08	-	-	0.05	0.01	98.37	Line 9 HM-19_Pic6-21-6-Black-Dull-Gt	69	6/7/16
390	38.91	0.00	0.13	0.01	0.11	0.00	0.03	0.02	0.00	1.80	0.01	0.00	57.47	0.26	0.00	0.00	0.07	-	-	0.03	0.08	98.93	Line 10 HM-19_Pic6-21-6-Black-Dull-Gt	70	6/7/16
391	38.01	0.00	0.01	0.00	0.00	0.00	0.01	0.01	0.00	0.00	0.00	0.00	59.49	0.70	0.00	0.00	0.10	-	-	0.00	0.10	98.42	HM-19_Pic6-21-6-Alpoor-Gt-1	71	6/7/16
392	36.70	0.00	0.04	0.00	0.00	0.00	0.02	0.01	0.00	0.01	0.02	0.00	59.61	0.61	0.00	0.00	0.07	-	-	0.00	0.00	97.10	HM-19_Pic6-21-6-Alpoor-Gt-2	72	6/7/16
393	37.28	0.06	0.03	0.01	0.00	0.00	0.01	0.02	0.00	0.00	0.00	0.00	60.58	0.57	0.00	0.02	0.05	-	-	0.00	0.00	98.63	HM-19_Pic6-21-6-Alpoor-Gt-3	73	6/7/16
394	37.53	0.03	0.00	0.00	0.00	0.01	0.01	0.00	0.00	0.02	0.00	0.00	62.11	0.57	0.00	0.00	0.05	-	-	0.04	0.00	100.38	HM-19_Pic6-21-6-Alpoor-Gt-4	74	6/7/16
395	37.03	0.00	0.00	0.00	0.00	0.01	0.00	0.00	0.00	0.02	0.00	0.00	59.29	0.68	0.00	0.00	0.07	-	-	0.00	0.02	97.12	HM-19_Pic6-21-6-Alpoor-Gt-5	75	6/7/16
396	37.51	0.04	0.00	0.02	0.01	0.00	0.01	0.00	0.02	0.02	0.00	0.01	61.44	0.54	0.00	0.00	0.04	-	-	0.02	0.02	99.69	HM-19_Pic6-21-6-Alpoor-Gt-6	76	6/7/16
397	35.91	0.00	0.04	0.00	0.00	0.12	0.00	0.00	0.04	0.13	0.01	0.00	60.09	1.25	0.00	0.07	0.05	-	-	0.06	0.39	98.15	HM-16-CapaoL4_5-3	202	6/7/16
398	34.85	0.00	0.03	0.01	0.00	0.15	0.01	0.00	0.05	0.14	0.00	0.06	61.03	1.22	0.00	0.02	0.08	-	-	0.00	0.32	97.98	HM-16-CapaoL4_5-5	204	6/7/16
399	35.27	0.05	0.00	0.00	0.00	0.13	0.01	0.02	0.08	0.13	0.00	0.00	60.71	1.30	0.00	0.01	0.10	-	-	0.05	0.27	98.12	HM-16-CapaoL4_5-6	205	6/7/16
400	36.11	0.00	1.39	0.00	0.00	0.02	0.00	0.01	0.04	0.29	0.00	0.02	60.43	0.26	0.00	2.20	0.08	-	-	0.10	0.05	101.00	HM-16 BAH-F124-114-1	301	6/7/16
401	36.76	0.00	1.38	0.01	0.00	0.01	0.02	0.00	0.03	0.41	0.01	0.02	60.15	0.26	0.00	2.21	0.04	-	-	0.01	0.03	101.35	HM-16 BAH-F124-114-2	302	6/7/16
402	36.29	0.00	1.35	0.00	0.00	0.01	0.01	0.00	0.03	0.42	0.00	0.04	60.53	0.26	0.00	2.19	0.08	-	-	0.04	0.00	101.24	HM-16 BAH-F124-114-3	303	6/7/16
403	36.60	0.00	1.38	0.05	0.02	0.01	0.00	0.00	0.03	0.34	0.01	0.04	60.63	0.27	0.00	2.27	0.06	-	-	0.05	0.01	101.77	HM-16 BAH-F124-114-4	304	6/7/16
404	37.01	0.00	0.74	0.01	0.00	0.02	0.00	0.00	0.03	0.01	0.01	0.01	60.03	0.15	0.00	0.05	0.02	-	-	0.02	0.05	98.15	HM-16 BAH-F124-114-5	305	6/7/16
405	36.16	0.00	0.79	0.00	0.00	0.00	0.00	0.00	0.04	0.00	0.01	0.03	59.74	0.18	0.00	0.01	0.06	-	-	0.02	0.02	97.05	HM-16 BAH-F124-114-6	306	6/7/16
406	36.66	0.00	1.36	0.02	0.00	0.01	0.00	0.00	0.04	0.34	0.03	0.04	60.45	0.25	0.00	2.19	0.10	-	-	0.00	0.00	101.47	HM-16 BAH-F124-114-2-1	308	6/7/16
407	36.42	0.00	1.42	0.00	0.00	0.01	0.00	0.00	0.07	0.32	0.00	0.05	60.11	0.26	0.00	2.14	0.06	-	-	0.05	0.00	100.89	HM-16 BAH-F124-114-2-2	309	6/7/16
408	36.55	0.00	1.29	0.02	0.04	0.00	0.02	0.00	0.07	0.35	0.01	0.00	59.76	0.26	0.00	2.09	0.09	-	-	0.05	0.00	100.58	HM-16 BAH-F124-114-2-3	310	6/7/16
409	36.37	0.00	0.60	0.00	0.05	0.05	0.01	0.01	2.08	0.17	0.00	0.02	60.51	0.21	0.00	1.55	0.08	-	-	0.07	0.03	101.80	HM17-BAH-F124-111.2_2	143	20/7/16
410	36.10	0.00	0.46	0.00	0.01	0.05	0.00	0.02	2.75	0.14	0.00	0.00	59.81	0.48	0.00	1.46	0.07	-	-	0.01	0.00	101.36	HM17-BAH-F124-111.2_4	145	20/7/16
411	36.75	0.00	0.49	0.00	0.00	0.02	0.01	0.00	1.93	0.11	0.00	0.02	59.96	0.30	0.00	1.35	0.02	-	-	0.03	0.03	101.01	HM17-BAH-F124-111.2_5	146	20/7/16
412	36.53	0.00	0.57	0.00	0.01	0.03	0.04	0.03	0.82	0.04	0.00	0.00	61.68	0.20	0.00	0.70	0.09	-	-	0.06	0.04	100.86	HM17-BAH-F124-111.2_7	148	20/7/16
413	35.95	0.00	0.61	0.00	0.00	0.01	0.01	0.01	2.47	0.15	0.00	0.00	60.51	0.29	0.00	1.64	0.07	-	-	0.02	0.00	101.73	HM17-BAH-F124-111.2_8	149	20/7/16
414	36.99	0.00	0.23	0.00	0.02	0.04	0.01	0.00	1.86	0.09	0.00	0.00	58.65	1.42	0.00	1.60	0.05	-	-	0.06	0.03	101.07	HM17-BAH-F124-111.2_10	151	20/7/16
415	37.35	0.00	0.30	0.01	0.00	0.03	0.00	0.00	1.95	0.12	0.01	0.00	58.50	1.32	0.00	1.75	0.05	-	-	0.01	0.03	101.40	HM17-BAH-F124-111.2_11	152	20/7/16
416	37.70	0.00	0.85	0.02	0.00	0.04	0.00	0.00	1.04	0.13	0.00	0.00	59.95	0.55	0.00	1.49	0.07	-	-	0.04	0.00	101.88	HM17-BAH-F124-111.2_12	153	20/7/16
417	37.72	0.00	0.87	0.04	0.03	0.02	0.00	0.00	0.93	0.12	0.01	0.06	58.51	0.57	0.00	1.60	0.06	-	-	0.02	0.09	100.63	HM17-BAH-F124-111.2_13	154	20/7/16
418	37.10	0.00	0.82	0.00	0.00	0.02	0.00	0.01	1.10	0.15	0.00	0.01	59.22	0.58	0.00	1.57	0.13	-	-	0.00	0.04	100.75	HM17-BAH-F124-111.2_15	156	20/7/16
419	38.22	0.00	0.84	0.00	0.04	0.04	0.01	0.00	1.13	0.11	0.00	0.00	59.14	0.63	0.00	1.62	0.09	-	-	0.00	0.00	101.89	HM17-BAH-F124-111.2_16	157	20/7/16
420	36.62	0.00	0.59	0.01	0.00	0.01	0.01	0.04	2.93	0.16	0.01	0.02	59.08	0.25	0.00	1.86	0.07	-	-	0.00	0.02	101.66	HM17-BAH-F124-111.2_21	162	20/7/16
421	37.88	0.00	0.31	0.02	0.02	0.04	0.00	0.01	0.04	0.00	0.00	0.00	59.45	0.96	0.00	0.02	0.09	-	-	0.00	0.00	98.84	HM17-BAH-F124-111.2_22	163	20/7/16
422	41.85	0.00	0.08	0.07	0.05	0.02	0.11	0.03	0.01	7.51	0.00	0.00	47.73	2.82	0.00	0.02	0.04	-	-	0.07	0.05	100.46	HM17-IBH-13-09h_1	164	20/7/16
423	39.81	0.00	0.10	0.10	0.04	0.02	0.13	0.01	0.00	6.32	0.00	0.00	53.81	1.13	0.00	0.04	0.08	-	-	0.02	0.12	101.72	HM17-IBH-13-09h_4	167	20/7/16
424	39.96	0.04	0.12	0.12	0.14	0.00	0.12	0.02	0.00	4.38	0.01	0.00	54.82	0.54	0.00	0.00	0.06	-	-	0.01	0.00	100.33	HM17-IBH-13-09h_5	168	20/7/16
425	39.95	0.01	0.14	0																					

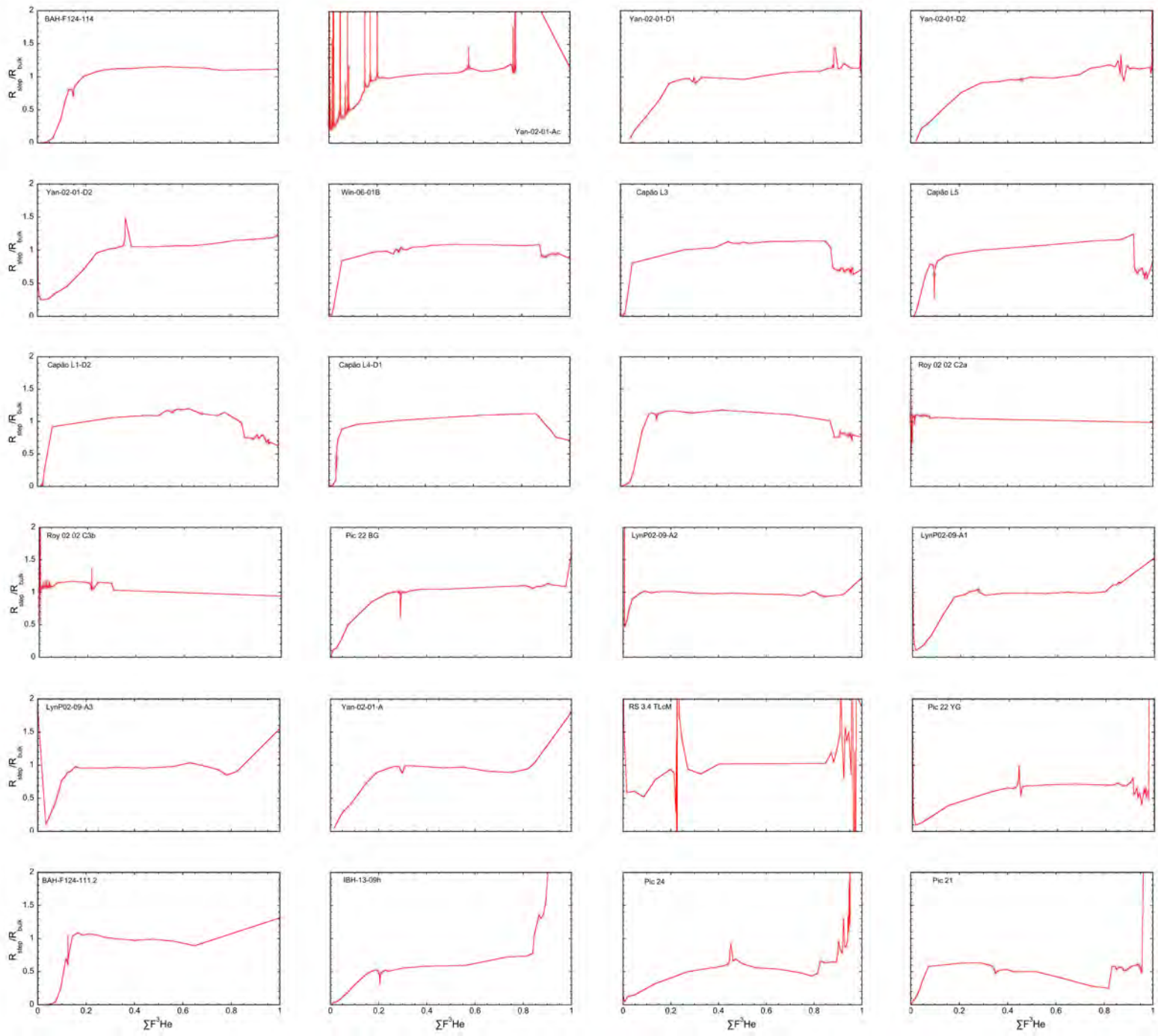
Appendix 1: Electron Microprobe analyses

Index	O	Na	P	V	Ti	Mg	S	Cr	Mn	Al	K	Ni	Fe	Si	Ca	Cu	Co	Sr	Ba	Zn	Pb	Total	Comment	Spot#	Run Date
451	34.34	0.17	0.00	0.02	0.18	0.13	0.05	0.25	0.02	5.94	0.03	0.68	55.90	1.34	0.00	0.04	0.04	-	0.01	0.02	0.00	99.15	RS 3.4 TLcM_BG 4	202	20/12/16
452	37.24	0.09	0.00	0.02	0.13	0.14	0.03	0.26	0.00	5.76	0.02	0.66	53.24	1.25	0.00	0.04	0.07	-	0.06	0.03	0.00	99.03	RS 3.4 TLcM_BG 5	203	20/12/16
453	37.66	0.00	0.02	0.04	0.13	0.19	0.03	0.26	0.02	4.54	0.03	0.17	55.67	1.78	0.00	0.02	0.07	-	0.00	0.00	0.00	100.62	RS 3.4 TLcM_BG 6	204	20/12/16
454	37.60	0.07	0.01	0.04	0.13	0.22	0.03	0.35	0.00	6.61	0.01	0.67	52.95	1.57	0.00	0.01	0.09	-	0.00	0.02	0.01	100.39	RS 3.4 TLcM_BG 7	205	20/12/16
455	38.19	0.09	0.01	0.04	0.15	0.14	0.02	0.22	0.00	6.20	0.00	0.45	53.36	1.19	0.00	0.00	0.08	-	0.00	0.07	0.00	100.20	RS 3.4 TLcM_BG 8	206	20/12/16
456	38.73	0.13	0.00	0.08	0.18	0.21	0.03	0.21	0.00	6.50	0.03	0.67	50.89	1.87	0.00	0.00	0.06	-	0.01	0.00	0.01	99.59	RS 3.4 TLcM_BG 9	207	20/12/16
457	39.37	0.06	0.00	0.06	0.20	0.18	0.02	0.24	0.04	6.26	0.01	0.55	47.90	1.98	0.00	0.00	0.09	-	0.01	0.04	0.03	97.03	RS 3.4 TLcM_BG 10	208	20/12/16
458	36.28	0.16	0.01	0.00	0.16	0.13	0.04	0.27	0.03	6.32	0.02	0.73	52.84	1.91	0.00	0.02	0.06	-	0.02	0.01	0.06	99.05	RS 3.4 TLcM_BG 11	209	20/12/16
459	36.54	0.00	0.00	0.01	0.03	0.12	0.04	0.25	0.00	3.38	0.01	0.74	56.76	0.92	0.00	0.06	0.04	-	0.01	0.00	0.02	98.93	Line 1 RS 3.4 TLcM_BG grain 2	210	20/12/16
460	35.26	1.33	0.02	0.01	0.02	0.10	0.03	0.28	0.03	2.68	0.02	0.38	57.46	0.69	0.00	0.00	0.07	-	0.00	0.06	0.00	98.42	Line 2 RS 3.4 TLcM_BG grain 2	211	20/12/16
461	36.91	0.09	0.00	0.00	0.06	0.09	0.04	0.15	0.00	2.71	0.01	0.44	57.88	0.69	0.00	0.03	0.02	-	0.09	0.04	0.00	99.22	Line 3 RS 3.4 TLcM_BG grain 2	212	20/12/16
462	36.81	1.25	0.00	0.01	0.02	0.12	0.05	0.15	0.03	2.91	0.02	0.38	56.31	0.69	0.00	0.00	0.07	-	0.03	0.00	0.00	98.83	Line 4 RS 3.4 TLcM_BG grain 2	213	20/12/16
463	36.74	0.13	0.00	0.02	0.00	0.10	0.02	0.13	0.00	2.57	0.01	0.36	57.82	0.70	0.00	0.01	0.04	-	0.00	0.08	0.08	98.79	Line 5 RS 3.4 TLcM_BG grain 2	214	20/12/16
464	37.14	3.42	0.01	0.00	0.08	0.10	0.00	0.11	0.02	2.61	0.03	0.39	55.91	0.69	0.00	0.03	0.05	-	0.04	0.01	0.03	100.66	Line 6 RS 3.4 TLcM_BG grain 2	215	20/12/16
465	37.77	0.00	0.01	0.06	0.07	0.21	0.06	0.44	0.03	4.39	0.03	1.16	55.39	0.96	0.00	0.05	0.06	-	0.00	0.07	0.02	100.76	Line 7 RS 3.4 TLcM_BG grain 2	216	20/12/16
466	36.68	0.05	0.01	0.07	0.02	0.14	0.03	0.23	0.02	2.85	0.02	0.92	56.36	1.17	0.00	0.00	0.07	-	0.00	0.00	0.10	98.73	Line 8 RS 3.4 TLcM_BG grain 2	217	20/12/16
467	36.74	0.09	0.00	0.02	0.00	0.08	0.02	0.14	0.00	2.44	0.01	0.38	57.46	0.72	0.00	0.00	0.05	-	0.00	0.03	0.13	98.28	Line 9 RS 3.4 TLcM_BG grain 2	218	20/12/16
468	36.58	0.13	0.00	0.00	0.00	0.08	0.02	0.12	0.02	2.43	0.00	0.43	58.14	0.72	0.00	0.04	0.06	-	0.00	0.04	0.00	98.81	Line 10 RS 3.4 TLcM_BG grain 2	219	20/12/16
469	36.32	0.02	0.01	0.04	0.00	0.14	0.02	0.00	0.04	0.13	0.00	0.00	60.07	1.21	0.00	0.01	0.07	-	0.00	0.00	0.32	98.41	Capao L4	265	20/12/16
470	35.33	0.00	0.02	0.00	0.02	0.13	0.01	0.00	0.05	0.14	0.01	0.02	60.68	1.28	0.00	0.06	0.02	-	0.01	0.01	0.30	98.09	Capao L4	268	20/12/16
471	35.14	0.02	0.02	0.00	0.04	0.14	0.00	0.00	0.09	0.14	0.01	0.00	59.74	1.30	0.00	0.05	0.09	-	0.00	0.04	0.35	97.17	Capao L4	269	20/12/16
472	34.41	0.05	0.02	0.05	0.00	0.11	0.02	0.00	0.09	0.16	0.00	0.04	60.63	1.12	0.00	0.09	0.06	-	0.00	0.00	0.36	97.21	Capao L4	270	20/12/16
473	35.08	0.02	0.00	0.00	0.01	0.14	0.00	0.00	0.08	0.13	0.00	0.08	59.95	1.42	0.00	0.07	0.06	-	0.00	0.01	0.35	97.40	Capao L4	271	20/12/16
474	36.06	0.02	0.00	0.08	0.00	0.15	0.02	0.00	0.08	0.15	0.00	0.00	60.58	1.25	0.00	0.07	0.08	-	0.02	0.00	0.26	98.81	Capao L4	272	20/12/16
475	35.32	0.01	0.00	0.01	0.07	0.13	0.03	0.00	0.05	0.11	0.01	0.00	60.07	1.28	0.00	0.10	0.07	-	0.00	0.04	0.32	97.64	Capao L4	273	20/12/16
476	40.29	0.13	0.11	0.17				0.00	0.01	4.94		0.01	49.23	2.13		0.00	0.09			0.01	0.00	97.11	Yan-02-01-A (2)	-	-
477	40.11	0.14	0.08	0.00				0.00	0.02	2.03		0.00	54.14	0.86		0.00	0.09			0.00	0.09	97.57	Yan-02-01-A (2)	-	-
478	40.03	0.13	0.02	0.04				0.03	0.04	2.19		0.00	54.46	0.81		0.00	0.08			0.06	0.05	97.94	Yan-02-01-A (2)	-	-
479	40.70	0.12	0.06	0.00				0.00	0.00	1.96		0.00	54.96	0.81		0.01	0.14			0.00	0.06	98.81	Yan-02-01-A (2)	-	-
480	39.55	0.08	0.00	0.00				0.00	0.00	0.17		0.03	55.90	1.52		0.01	0.12			0.00	0.00	97.38	Yan-02-01-A (2)	-	-
481	38.70	0.05	0.03	0.00				0.00	0.00	0.33		0.00	57.13	1.67		0.00	0.08			0.00	0.00	97.99	Yan-02-01-A (2)	-	-
482	39.16	0.04	0.08	0.00				0.00	0.00	0.31		0.00	57.82	1.42		0.00	0.13			0.04	0.02	99.01	Yan-02-01-A (2)	-	-
483	39.94	0.02	0.01	0.05				0.01	0.02	1.06		0.00	54.98	1.34		0.00	0.09			0.01	0.05	97.59	Yan-02-01-D2 (4)	-	-
484	39.96	0.05	0.05	0.12				0.03	0.00	1.57		0.01	55.45	1.20		0.02	0.08			0.00	0.00	98.55	Yan-02-01-D2 (4)	-	-
485	39.42	0.02	0.00	0.00				0.00	0.00	0.26		0.02	55.99	2.41		0.00	0.09			0.00	0.00	98.23	Yan-02-01-D2 (4)	-	-
486	39.81	0.02	0.00	0.00				0.00	0.05	0.71		0.00	56.39	1.18		0.00	0.11			0.03	0.06	98.37	Yan-02-01-D2 (4)	-	-
487	39.12	0.02	0.00	0.00				0.00	0.00	0.11		0.00	56.45	1.84		0.03	0.12			0.00	0.00	97.70	Yan-02-01-D2 (4)	-	-
488	39.63	0.03	0.00	0.08				0.00	0.03	0.86		0.04	56.46	1.41		0.00	0.15			0.05	0.04	98.80	Yan-02-01-D2 (4)	-	-
489	39.01	0.05	0.02	0.05				0.00	0.04	0.93		0.00	56.48	1.50		0.04	0.18			0.02	0.00	98.34	Yan-02-01-D2 (4)	-	-
490	40.07	0.01	0.03	0.03				0.00	0.01	0.08		0.00	57.42	1.59		0.00	0.10			0.00	0.00	99.34	Yan-02-01-D2 (4)	-	-
491	39.34	0.01	0.01	0.00				0.00	0.06	0.09		0.00	57.86	1.30		0.00	0.12			0.04	0.00	98.83	Yan-02-01-D2 (4)	-	-
492	33.10	0.01	0.00	0.00				0.00	0.00	0.22		0.00	62.43	1.59		0.04	0.10			0.01	0.00	97.51	Yan-02-01-D2 (4)	-	-
493	32.85	0.01	0.03	0.01				0.00	0.02	0.21		0.04	64.25	1.48		0.02	0.11			0.00	0.03	99.09	Yan-02-01-D2 (4)	-	-
494	33.74	0.01	0.01	0.00				0.00	0.01	0.28		0.03	64.75	1.37		0.00	0.13			0.00	0.07	100.41	Yan-02-01-D2 (4)	-	-
495	31.88	0.01	0.02	0.09				0.00	0.03	0.31		0.00	65.41	1.05		0.00	0.11			0.00	0.06	98.97	Yan-02-01-D2 (4)	-	-
496	33.20	0.02	0.03	0.00				0.03	0.03	0.23		0.00	65.95	1.27		0.06	0.11			0.05	0.10	101.11	Yan-02-01-D2 (4)	-	-
497	33.06	0.04	0.00	0.16				0.02	0.03	0.42		0.02	66.30	0.97		0.00	0.10			0.00	0.08	101.22	Yan-02-01-D2 (4)	-	-
498	41.73	0.15	0.06	0.20				0.01	0.00	4.71		0.05	50.00	1.05		0.03	0.07			0.02	0.01	98.09	Yan-02-D1 (1)	-	-
499	41.39	0.11	0.02	0.05				0.00	0.01	3.22		0.03	51.70	1.03		0.01	0.08			0.05	0.07	97.79	Yan-02-D1 (1)	-	-
500	41.15	0.09	0.04	0.11				0.02	0.01	2.77		0.00	51.75	0.97		0.00	0.12			0.06	0.06	97.15	Yan-02-D1 (1)	-	-
501	41.01	0.12	0.04	0.10				0.02	0.02	3.47		0.00	51.87	0.88		0.00	0.10			0.01	0.15	97.78	Yan-02-D1 (1)	-	-
502	40.91	0.10	0.08	0.07				0.04	0.01	2.29		0.00	53.12	0.95		0.03	0.11			0.01	0.00	97.74	Yan-02-D1 (1)	-	-
503	41.26	0.11	0.02	0.03				0.00	0.02	3.02		0.01	53.65	0.84		0.03	0.06			0.03	0.07	99.15	Yan-02-D1 (1)	-	-
504	41.82	0.17	0.04	0.12				0.03	0.03	3.77		0.02	49.07	2.00		0.00	0.14			0.00	0.00	97.22	Yan-02-D1 (2)	-	-
505	42.30	0.12	0.06	0.12				0.02	0.03	3.74		0.0													

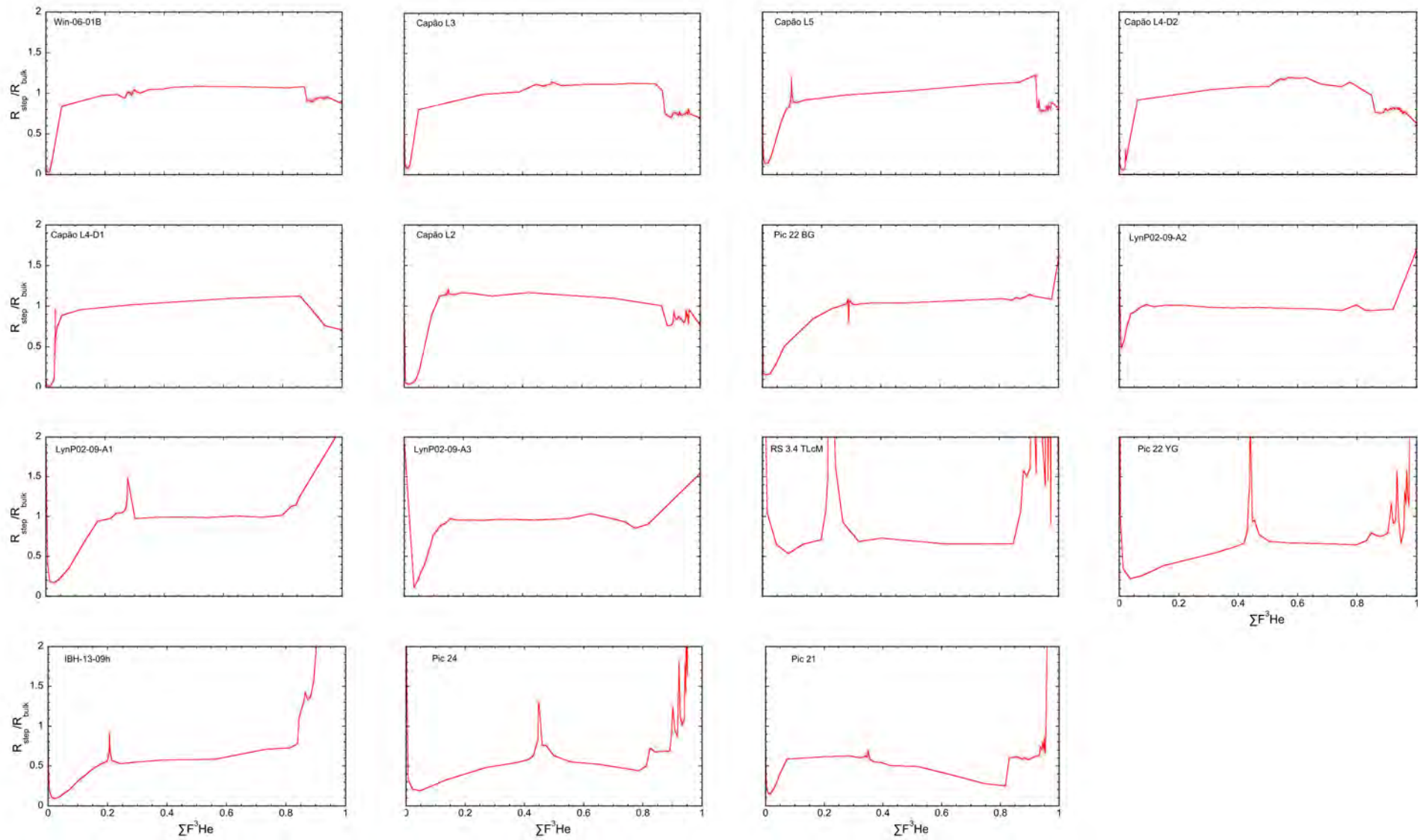
Appendix 1: Electron Microprobe analyses

Index	O	Na	P	V	Ti	Mg	S	Cr	Mn	Al	K	Ni	Fe	Si	Ca	Cu	Co	Sr	Ba	Zn	Pb	Total	Comment	Spot#	Run Date
526	38.65		0.02	0.00	0.00			0.00	0.35	0.11		0.01	58.78	0.82		0.01	0.09			0.01	0.05	98.90	Roy02-02-Cy4 (4a)	-	-
527	38.13		0.01	0.01	0.02			0.03	0.34	0.15		0.00	58.45	0.81		0.03	0.10			0.02	0.09	98.19	Roy02-02-Cy4 (4a)	-	-
528	38.66		0.01	0.02	0.00			0.01	0.44	0.13		0.00	59.24	0.84		0.00	0.00			0.00	0.07	99.43	Roy02-02-Cy4 (4a)	-	-
529	38.68		0.03	0.01	0.00			0.01	0.42	0.13		0.04	59.07	0.80		0.05	0.05			0.00	0.03	99.29	Roy02-02-Cy4 (4a)	-	-
530	38.85		0.01	0.02	0.00			0.00	0.38	0.11		0.00	58.80	0.86		0.00	0.05			0.00	0.03	99.11	Roy02-02-Cy4 (4a)	-	-
531	38.41		0.06	0.03	0.00			0.02	0.33	0.15		0.04	58.58	0.80		0.02	0.04			0.00	0.01	98.49	Roy02-02-Cy4 (4a)	-	-
532	39.02		0.01	0.06	0.00			0.05	0.39	0.13		0.00	58.92	0.86		0.01	0.09			0.01	0.00	99.54	Roy02-02-Cy4 (4a)	-	-
533	38.39		0.04	0.00	0.00			0.03	0.37	0.14		0.06	58.66	0.87		0.03	0.03			0.06	0.00	98.68	Roy02-02-Cy4 (4a)	-	-
534	38.22		0.03	0.00	0.00			0.00	0.34	0.13		0.00	58.76	0.87		0.00	0.01			0.09	0.07	98.51	Roy02-02-Cy4 (4a)	-	-
535	38.00		0.02	0.00	0.00			0.00	0.38	0.13		0.00	58.62	0.77		0.04	0.07			0.05	0.09	98.15	Roy02-02-Cy4 (4a)	-	-
536	38.65		0.02	0.04	0.00			0.01	0.38	0.15		0.00	58.87	0.82		0.03	0.05			0.00	0.00	99.02	Roy02-02-Cy4 (4a)	-	-
537	38.05		0.04	0.00	0.00			0.01	0.35	0.13		0.07	59.34	0.83		0.00	0.09			0.02	0.01	98.92	Roy02-02-Cy4 (4a)	-	-
538	38.87		0.03	0.03	0.00			0.00	0.35	0.14		0.00	58.80	0.88		0.00	0.00			0.01	0.04	99.17	Roy02-02-Cy4 (4a)	-	-
539	38.18		0.04	0.01	0.00			0.00	0.37	0.12		0.01	58.94	0.89		0.01	0.04			0.03	0.05	98.69	Roy02-02-Cy4 (4a)	-	-
540	38.30		0.04	0.00	0.00			0.02	0.34	0.14		0.00	58.86	0.94		0.00	0.09			0.01	0.05	98.80	Roy02-02-Cy4 (4a)	-	-
541	38.77		0.03	0.00	0.00			0.01	0.33	0.13		0.02	58.49	0.92		0.00	0.02			0.00	0.07	98.78	Roy02-02-Cy4 (4a)	-	-
542	39.06		0.03	0.06	0.00			0.01	0.37	0.13		0.00	58.71	0.89		0.00	0.07			0.10	0.06	99.49	Roy02-02-Cy4 (4a)	-	-
543	38.46		0.01	0.04	0.00			0.00	0.38	0.13		0.04	58.47	0.86		0.01	0.02			0.00	0.02	98.43	Roy02-02-Cy4 (4a)	-	-
544	38.31		0.01	0.00	0.03			0.00	0.35	0.14		0.06	58.89	0.83		0.00	0.02			0.04	0.02	98.67	Roy02-02-Cy4 (4a)	-	-
545	39.34		0.01	0.00	0.00			0.01	0.34	0.15		0.02	58.95	0.93		0.01	0.10			0.04	0.06	99.95	Roy02-02-Cy4 (4a)	-	-
546	39.34		0.05	0.00	0.00			0.00	0.35	0.15		0.04	58.36	0.88		0.00	0.07			0.12	0.00	99.38	Roy02-02-Cy4 (4a)	-	-
547	38.12		0.03	0.04	0.01			0.00	0.38	0.14		0.05	58.44	0.94		0.02	0.06			0.00	0.00	98.24	Roy02-02-Cy4 (4a)	-	-
548	38.86		0.03	0.00	0.00			0.00	0.31	0.19		0.00	58.67	1.02		0.01	0.07			0.02	0.00	99.18	Roy02-02-Cy4 (4a)	-	-
549	39.20		0.05	0.02	0.00			0.00	0.25	0.23		0.00	58.73	1.10		0.02	0.03			0.00	0.08	99.69	Roy02-02-Cy4 (4a)	-	-

Electronic appendix 2a: Blank-corrected $R_{\text{step}}/R_{\text{bulk}}$ diagrams.



Electronic appendix 2b: Not blank-corrected $R_{\text{step}}/R_{\text{bulk}}$ diagrams



Appendix: $^4\text{He}/^3\text{He}$ incremental heating results

Yan0201D2b		2.42 mg					
Step	T (°C)	time (min)	^3He (CPS)	\pm	^4He (CPS)	\pm	
0	26	60	1.88E-01	8.53E-02	1.09E+04	2.80E+01	
1	25.35	60	2.82E-01	3.04E-02	6.16E+03	7.03E+00	
2	24.87	60	2.89E-01	2.52E-02	4.75E+03	6.49E+00	
3	24	60	3.46E-01	2.52E-02	3.81E+03	4.87E+00	
4	24.19	60	3.91E-01	2.94E-02	3.06E+03	1.18E+01	
5	24	60	3.49E-01	3.46E-02	2.43E+03	1.44E+01	
6	24	60	3.96E-01	2.97E-02	1.88E+03	1.07E+01	
7	24	60	3.48E-01	2.89E-02	1.47E+03	8.41E+00	
8	24	60	3.35E-01	2.82E-02	1.14E+03	7.63E+00	
9	24	60	3.26E-01	2.89E-02	9.45E+02	6.41E+00	
10	24	60	3.26E-01	2.97E-02	7.42E+02	5.22E+00	
11	24	60	3.59E-01	2.63E-02	5.95E+02	6.36E+00	
12	24	60	2.67E-01	6.67E-02	5.07E+02	6.82E+00	
13	24	60	3.57E-01	2.72E-02	4.50E+02	4.84E+00	
14	49.33	30	2.26E+00	8.08E-02	3.68E+02	5.37E+00	
15	26.07	60	6.61E-01	4.19E-02	3.76E+02	3.81E+00	
16	49.9	300	1.54E+01	1.68E-01	1.33E+03	1.05E+01	
17	64.9	300	5.04E+01	7.83E-01	1.63E+03	1.05E+01	
18	79.88	240	1.06E+02	4.29E-01	2.20E+03	1.29E+01	
19	99.77	120	2.08E+02	7.39E-01	3.42E+03	1.44E+01	
20	129.78	120	8.17E+02	2.74E+00	1.42E+04	2.81E+01	
21	149.55	60	6.43E+02	1.27E+00	1.45E+04	3.84E+01	
22	174.44	60	1.25E+03	3.39E+00	3.69E+04	6.92E+01	
23	199.16	60	1.97E+03	2.48E+00	9.45E+04	9.38E+01	
24	199.1	60	1.29E+03	1.77E+00	8.19E+04	9.68E+01	
25	199.14	60	1.33E+03	3.47E+00	8.95E+04	9.11E+01	
26	189.16	60	6.55E+02	2.50E+00	4.45E+04	4.93E+01	
27	179.8	120	5.29E+02	2.49E+00	3.68E+04	4.83E+01	
28	169.86	180	3.20E+02	1.72E+00	2.25E+04	3.61E+01	
29	159.86	180	1.36E+02	5.55E-01	1.00E+04	9.89E+00	
30	149.89	240	7.09E+01	3.32E-01	5.71E+03	6.34E+00	
31	139.92	300	3.11E+01	2.99E-01	3.06E+03	1.22E+01	
32	174.89	240	6.48E+02	2.48E+00	4.51E+04	7.01E+01	
33	194.74	180	1.95E+03	3.79E+00	1.35E+05	1.71E+02	
34	204.57	120	2.69E+03	6.32E+00	1.89E+05	2.41E+02	
35	209.16	60	1.94E+03	5.39E+00	1.37E+05	1.36E+02	
36	214.12	60	2.31E+03	4.46E+00	1.68E+05	2.15E+02	
37	219.08	60	2.26E+03	7.11E+00	1.71E+05	2.18E+02	
38	224.08	60	1.91E+03	2.57E+00	1.47E+05	1.46E+02	
39	229.1	60	1.44E+03	3.61E+00	1.12E+05	1.00E+02	
40	234.07	60	8.03E+02	2.39E+00	6.33E+04	6.10E+01	
41	239.23	60	3.40E+02	6.96E-01	2.75E+04	5.24E+01	
42	244.5	60	1.18E+02	4.86E-01	9.90E+03	2.96E+01	
43	53.72	30	2.76E-01	4.71E-02	2.06E+02	3.26E+00	
44	29.61	60	1.72E-01	2.37E-02	2.63E+02	4.90E+00	
45	24.73	120	3.64E-01	6.07E-02	3.87E+02	6.36E+00	

Step	T (°C)	time (min)	³ He (CPS)	±	⁴ He (CPS)	±
46	24	30	1.81E-01	2.10E-02	1.66E+02	3.85E+00
Last Step			4.30E+03		3.70E+05	
Total		77.5 hr	3.01E+04		2.08E+06	

Yan0201Ac **13.9 mg**

Step	T (°C)	time (min)	³ He (CPS)	±	⁴ He (CPS)	±
0	23.97	60	6.34E-01	4.32E-02	1.95E+04	3.63E+01
1	24	60	6.10E-01	2.87E-02	1.17E+04	1.18E+01
2	24	60	7.81E-01	4.15E-02	1.02E+04	1.68E+01
3	24	60	6.19E-01	3.39E-02	6.16E+03	8.79E+00
4	23.88	60	7.24E-01	3.43E-02	5.04E+03	7.04E+00
5	23.02	60	8.27E-01	6.76E-02	4.19E+03	5.71E+00
6	23	720	4.73E+00	9.48E-02	2.05E+04	4.47E+01
7	23	60	6.42E-01	3.17E-02	1.32E+03	9.48E+00
8	23.45	60	6.81E-01	4.77E-02	1.26E+03	6.96E+00
9	23.7	60	7.28E-01	3.77E-02	1.20E+03	9.21E+00
10	23.74	60	8.50E-01	3.80E-02	1.09E+03	7.55E+00
11	23.96	120	1.32E+00	5.28E-02	1.82E+03	1.28E+01
12	23.42	120	1.37E+00	4.93E-02	1.59E+03	1.12E+01
13	23	120	1.39E+00	5.17E-02	1.42E+03	1.02E+01
14	23	120	1.20E+00	4.63E-02	1.31E+03	8.46E+00
15	23	120	1.38E+00	5.46E-02	1.19E+03	8.55E+00
16	23	180	1.91E+00	5.24E-02	1.56E+03	9.83E+00
17	23.16	180	1.97E+00	6.36E-02	1.36E+03	8.32E+00
18	23.67	180	1.99E+00	7.27E-02	1.23E+03	1.05E+01
19	23.97	180	1.97E+00	5.76E-02	1.09E+03	7.40E+00
20	23.28	240	2.49E+00	6.63E-02	1.22E+03	6.80E+00
21	23	240	2.54E+00	7.64E-02	1.09E+03	8.35E+00
22	23	240	2.45E+00	6.96E-02	9.63E+02	5.68E+00
23	23.09	300	3.18E+00	7.54E-02	1.07E+03	7.36E+00
24	24	300	3.29E+00	6.92E-02	9.93E+02	8.25E+00
25	23.74	300	3.25E+00	8.29E-02	9.25E+02	6.60E+00
26	23	360	3.66E+00	6.86E-02	1.03E+03	9.01E+00
27	23.34	360	3.61E+00	8.07E-02	9.78E+02	6.88E+00
28	23.59	420	4.30E+00	9.05E-02	1.11E+03	1.02E+01
29	24	1380	1.48E+01	1.72E-01	4.92E+03	6.01E+00
30	23.28	600	5.52E+00	8.86E-02	1.77E+03	9.73E+00
31	23.24	600	5.80E+00	2.07E-01	1.60E+03	9.05E+00
32	23.49	600	5.50E+00	9.64E-02	1.54E+03	1.04E+01
33	23	600	5.29E+00	9.22E-02	1.50E+03	8.91E+00
34	23	600	5.29E+00	9.22E-02	1.50E+03	8.91E+00
35	23.95	600	5.41E+00	8.04E-02	1.60E+03	7.02E+00
36	23.12	600	5.04E+00	1.16E-01	1.67E+03	8.39E+00
37	23.67	600	5.49E+00	1.09E-01	1.70E+03	9.06E+00
38	23.37	600	5.47E+00	7.67E-02	1.68E+03	8.35E+00
39	24	300	2.71E+00	6.55E-02	8.70E+02	9.35E+00
40	24	18	2.12E-02	1.38E-02	1.09E+00	2.28E+00

Step	T (°C)	time (min)	³ He (CPS)	±	⁴ He (CPS)	±
41	28.54	18	7.42E-01	4.50E-02	2.00E+02	3.94E+00
42	29.27	60	1.39E+00	6.08E-02	2.51E+02	4.48E+00
43	34.35	60	2.32E+00	6.57E-02	2.55E+02	4.53E+00
44	39.37	60	4.37E+00	7.97E-02	2.68E+02	3.22E+00
45	44.42	60	7.80E+00	1.24E-01	3.18E+02	3.97E+00
46	49.38	60	1.30E+01	1.56E-01	3.82E+02	6.59E+00
47	44.34	60	6.42E+00	1.18E-01	3.27E+02	4.78E+00
48	40	300	6.11E+00	1.11E-01	4.48E+02	6.65E+00
49	23.69	30	4.19E-01	3.23E-02	1.59E+02	3.00E+00
50	34.32	60	1.85E+00	6.34E-02	2.47E+02	4.06E+00
51	29.35	60	1.07E+00	5.41E-02	2.45E+02	4.80E+00
52	23	180	1.50E+00	4.74E-02	5.32E+02	7.12E+00
53	29.31	60	9.75E-01	3.95E-02	2.27E+02	3.70E+00
54	29.36	60	9.86E-01	4.18E-02	2.29E+02	4.59E+00
55	34.33	60	1.79E+00	4.37E-02	2.41E+02	4.33E+00
56	39.36	60	3.01E+00	7.88E-02	2.63E+02	5.04E+00
57	44.43	60	5.82E+00	9.55E-02	2.97E+02	4.34E+00
58	49.37	60	1.07E+01	3.01E-01	3.38E+02	3.59E+00
59	44.35	60	5.32E+00	1.10E-01	2.81E+02	4.15E+00
60	39.35	60	2.88E+00	6.91E-02	2.64E+02	4.73E+00
61	34.32	60	1.58E+00	5.88E-02	2.53E+02	3.89E+00
62	29.35	60	8.70E-01	3.54E-02	2.36E+02	3.07E+00
63	29.35	60	8.52E-01	3.75E-02	2.29E+02	4.73E+00
64	29.35	60	7.19E-01	1.09E-01	2.28E+02	2.99E+00
65	34.36	60	1.51E+00	5.68E-02	2.38E+02	3.55E+00
66	39.35	60	2.76E+00	7.53E-02	2.67E+02	5.68E+00
67	44.4	60	4.91E+00	1.01E-01	2.89E+02	4.35E+00
68	49.39	60	9.21E+00	1.46E-01	3.39E+02	4.77E+00
69	54.41	60	1.61E+01	1.78E-01	4.13E+02	5.56E+00
70	59.4	60	2.71E+01	2.18E-01	5.27E+02	5.01E+00
71	59.4	60	2.71E+01	2.18E-01	5.27E+02	5.01E+00
72	64.41	60	4.28E+01	3.29E-01	7.20E+02	8.47E+00
73	59.42	60	1.98E+01	1.67E-01	4.58E+02	5.20E+00
74	54.37	60	1.03E+01	1.29E-01	3.39E+02	6.72E+00
75	49.41	60	5.62E+00	8.95E-02	2.85E+02	5.28E+00
76	44.35	60	2.99E+00	8.43E-02	2.54E+02	4.53E+00
77	39.35	60	1.63E+00	5.64E-02	2.51E+02	4.48E+00
78	39.38	60	1.62E+00	6.04E-02	2.38E+02	3.59E+00
79	39.35	60	1.66E+00	6.49E-02	2.39E+02	5.12E+00
80	44.42	60	2.96E+00	7.73E-02	2.56E+02	3.51E+00
81	49.4	60	5.56E+00	1.01E-01	2.92E+02	4.93E+00
82	54.35	60	9.83E+00	1.22E-01	3.40E+02	4.79E+00
83	59.4	60	1.82E+01	1.71E-01	4.44E+02	5.64E+00
84	64.4	60	3.14E+01	6.13E-01	5.90E+02	6.23E+00
85	69.4	60	4.94E+01	2.78E-01	8.13E+02	6.16E+00
86	64.38	60	2.46E+01	2.08E-01	5.28E+02	4.32E+00
87	59.4	60	1.37E+01	1.49E-01	3.95E+02	4.77E+00
88	54.37	60	7.37E+00	1.12E-01	3.25E+02	5.12E+00

Step	T (°C)	time (min)	³ He (CPS)	±	⁴ He (CPS)	±
89	49.32	60	4.11E+00	9.45E-02	2.83E+02	4.55E+00
90	49.39	60	4.47E+00	1.89E-01	2.68E+02	4.09E+00
91	49.37	60	3.97E+00	6.93E-02	2.81E+02	5.36E+00
92	54.42	60	6.84E+00	1.14E-01	3.06E+02	4.67E+00
93	59.4	60	1.32E+01	1.53E-01	3.86E+02	4.99E+00
94	64.38	60	2.30E+01	1.58E-01	5.10E+02	5.28E+00
95	69.39	60	3.93E+01	3.01E-01	7.01E+02	6.76E+00
96	74.4	60	6.76E+01	3.87E-01	1.08E+03	5.56E+00
97	79.43	60	9.78E+01	4.67E-01	1.44E+03	1.04E+01
98	74.41	60	5.49E+01	6.30E-01	8.70E+02	5.82E+00
99	69.38	60	2.78E+01	2.12E-01	5.77E+02	5.91E+00
100	64.4	60	1.46E+01	1.56E-01	4.13E+02	6.20E+00
101	59.32	60	7.92E+00	1.31E-01	3.27E+02	5.03E+00
102	59.32	60	8.07E+00	1.29E-01	3.25E+02	4.36E+00
103	64.36	60	1.44E+01	1.48E-01	4.11E+02	4.91E+00
104	69.34	60	2.85E+01	4.39E-01	5.73E+02	5.14E+00
105	74.41	60	4.61E+01	2.93E-01	8.38E+02	7.16E+00
106	79.41	60	7.77E+01	3.60E-01	1.27E+03	8.02E+00
107	84.35	60	1.21E+02	4.56E-01	1.82E+03	1.39E+01
108	89.3	60	1.76E+02	6.49E-01	2.56E+03	1.41E+01
109	94.46	60	2.50E+02	1.20E+00	3.52E+03	1.13E+01
110	99.36	60	3.45E+02	1.70E+00	4.90E+03	6.07E+00
111	94.4	60	1.62E+02	6.10E-01	2.48E+03	7.92E+00
112	89.32	60	8.94E+01	3.81E-01	1.47E+03	7.89E+00
113	84.39	60	4.85E+01	3.08E-01	9.15E+02	7.16E+00
114	79.39	60	2.76E+01	2.59E-01	6.22E+02	4.48E+00
115	74.37	60	1.52E+01	1.79E-01	4.33E+02	5.45E+00
116	69.39	60	8.75E+00	1.29E-01	3.49E+02	4.24E+00
117	64.36	60	4.89E+00	1.12E-01	3.04E+02	3.76E+00
118	59.38	60	2.58E+00	6.48E-02	2.66E+02	4.54E+00
119	59.38	60	2.73E+00	6.56E-02	2.71E+02	3.00E+00
120	64.39	60	5.15E+00	1.10E-01	3.01E+02	5.47E+00
121	69.4	60	8.22E+00	1.32E-01	3.48E+02	4.88E+00
122	74.41	60	1.45E+01	1.53E-01	4.40E+02	5.95E+00
123	79.38	60	2.75E+01	2.41E-01	6.22E+02	5.39E+00
124	84.4	60	4.80E+01	3.45E-01	9.58E+02	7.66E+00
125	89.44	60	8.27E+01	3.15E-01	1.46E+03	8.79E+00
126	94.39	60	1.35E+02	1.05E+00	2.23E+03	4.54E+00
127	99.44	60	2.02E+02	5.14E-01	3.25E+03	1.37E+01
128	89.39	60	6.27E+01	2.84E-01	1.19E+03	8.03E+00
129	79.4	60	2.07E+01	1.90E-01	5.31E+02	7.77E+00
130	69.4	60	6.41E+00	8.76E-02	3.25E+02	5.45E+00
131	59.34	60	2.11E+00	6.55E-02	2.58E+02	4.28E+00
132	49.35	60	8.06E-01	3.68E-02	2.26E+02	4.67E+00
133	24	900	3.06E+00	1.74E-01	2.13E+03	1.22E+01
134	99.88	300	7.57E+02	2.60E+00	1.22E+04	1.07E+01
135	99.86	300	5.24E+02	2.10E+00	9.02E+03	1.12E+01
136	99.87	300	4.07E+02	1.73E+00	7.41E+03	7.75E+00

Step	T (°C)	time (min)	³ He (CPS)	±	⁴ He (CPS)	±
137	99.87	300	3.58E+02	9.71E-01	6.88E+03	7.53E+00
138	99.89	300	3.20E+02	8.93E-01	6.41E+03	7.35E+00
139	99.88	300	2.73E+02	7.18E-01	5.76E+03	7.34E+00
140	99.9	300	2.51E+02	6.76E-01	5.42E+03	1.64E+01
141	99.86	300	2.36E+02	6.17E-01	5.29E+03	6.06E+00
142	99.91	480	3.30E+02	8.80E-01	7.70E+03	6.00E+00
143	99.93	480	3.00E+02	8.04E-01	7.36E+03	9.03E+00
144	99.92	480	2.64E+02	7.87E-01	7.04E+03	8.48E+00
145	99.91	480	2.42E+02	7.22E-01	6.82E+03	7.39E+00
146	99.93	480	2.19E+02	5.24E-01	6.17E+03	1.88E+01
147	0	0	1.00E+02	4.50E-01	1.15E+04	1.16E+01
148	23.98	60	3.91E-01	2.67E-02	2.07E+02	3.93E+00
149	24	60	3.92E-01	2.93E-02	2.13E+02	4.61E+00
150	99.88	300	1.01E+02	4.56E-01	2.85E+03	1.18E+01
151	99.85	300	1.04E+02	1.02E+00	2.96E+03	1.32E+01
152	99.87	300	1.00E+02	4.87E-01	2.96E+03	1.02E+01
153	99.87	300	9.75E+01	4.44E-01	2.95E+03	1.32E+01
154	49.87	300	1.20E+00	1.04E-01	6.95E+02	9.05E+00
155	49.88	300	1.41E+00	4.99E-02	6.87E+02	6.67E+00
156	59.82	300	2.05E+00	6.30E-02	7.06E+02	7.50E+00
157	69.78	180	2.61E+00	7.08E-02	4.78E+02	5.93E+00
158	79.8	180	6.67E+00	1.31E-01	5.69E+02	6.75E+00
159	89.79	180	1.96E+01	1.90E-01	8.85E+02	8.44E+00
160	99.77	180	6.14E+01	3.83E-01	1.92E+03	9.26E+00
161	99.71	120	3.94E+01	3.17E-01	1.27E+03	6.80E+00
162	99.7	120	4.03E+01	2.57E-01	1.29E+03	9.01E+00
163	89.64	120	1.30E+01	1.50E-01	6.24E+02	7.55E+00
164	79.7	120	5.01E+00	8.23E-02	4.12E+02	4.29E+00
165	69.64	120	1.78E+00	6.00E-02	3.41E+02	7.01E+00
166	59.69	180	1.28E+00	5.78E-02	4.34E+02	5.02E+00
167	49.72	180	9.55E-01	4.43E-02	4.32E+02	6.36E+00
168	49.76	180	9.59E-01	4.28E-02	4.35E+02	6.78E+00
169	49.76	180	8.39E-01	4.32E-02	4.72E+02	5.07E+00
170	59.7	120	9.25E-01	3.73E-02	3.41E+02	4.34E+00
171	69.71	120	1.85E+00	6.16E-02	3.42E+02	5.81E+00
172	79.4	60	2.23E+00	7.81E-02	2.33E+02	4.65E+00
173	89.4	60	5.65E+00	7.25E-02	3.19E+02	3.70E+00
174	99.4	60	1.76E+01	1.73E-01	6.06E+02	6.95E+00
175	99.4	60	1.78E+01	1.67E-01	6.22E+02	6.51E+00
176	99.4	60	1.68E+01	4.33E-01	6.24E+02	6.61E+00
177	99.42	60	1.78E+01	1.90E-01	6.25E+02	6.86E+00
178	24	4560	1.46E+01	1.58E-01	1.00E+04	2.99E+01
179	99.54	60	2.08E+01	2.40E-01	6.73E+02	7.82E+00
180	104.39	60	3.53E+01	2.78E-01	1.07E+03	8.10E+00
181	109.46	60	6.28E+01	3.40E-01	1.78E+03	9.35E+00
182	114.37	60	1.05E+02	4.56E-01	2.81E+03	1.68E+01
183	119.41	60	1.58E+02	5.08E-01	4.15E+03	6.28E+00
184	124.54	60	2.60E+02	1.32E+00	6.56E+03	7.97E+00

Step	T (°C)	time (min)	³ He (CPS)	±	⁴ He (CPS)	±
185	129.58	60	3.57E+02	8.75E-01	8.97E+03	1.18E+01
186	134.51	60	5.06E+02	1.05E+00	1.27E+04	1.26E+01
187	139.53	60	6.61E+02	1.09E+00	1.67E+04	3.33E+01
188	139.57	60	5.26E+02	2.42E+00	1.34E+04	1.46E+01
189	134.56	60	3.08E+02	8.07E-01	8.26E+03	8.66E+00
190	129.46	60	1.72E+02	5.96E-01	4.90E+03	6.35E+00
191	124.4	60	9.57E+01	4.19E-01	2.82E+03	4.58E+00
192	119.5	60	5.51E+01	2.98E-01	1.73E+03	9.50E+00
193	114.45	60	3.21E+01	2.93E-01	1.09E+03	7.49E+00
194	109.43	60	1.92E+01	1.82E-01	7.33E+02	5.66E+00
195	104.43	60	1.15E+01	1.30E-01	5.04E+02	5.10E+00
196	99.34	60	6.96E+00	1.38E-01	4.00E+02	4.66E+00
197	99.51	60	7.23E+00	9.97E-02	4.29E+02	5.64E+00
198	99.45	60	7.02E+00	1.15E-01	4.09E+02	4.97E+00
199	104.57	60	1.18E+01	1.45E-01	5.43E+02	3.98E+00
200	109.49	60	1.97E+01	1.76E-01	7.75E+02	8.87E+00
201	114.39	60	3.31E+01	2.72E-01	1.14E+03	1.10E+01
202	119.51	60	5.75E+01	3.10E-01	1.87E+03	1.23E+01
203	124.5	60	9.51E+01	4.43E-01	2.96E+03	1.11E+01
204	129.51	60	1.52E+02	4.66E-01	4.69E+03	6.38E+00
205	134.5	60	2.33E+02	1.32E+00	6.95E+03	7.00E+00
206	139.46	60	3.59E+02	1.70E+00	1.08E+04	1.01E+01
207	139.33	60	3.14E+02	8.73E-01	9.52E+03	2.81E+01
208	139.41	60	2.87E+02	7.63E-01	8.83E+03	8.16E+00
209	37.88	60	5.07E-01	5.61E-02	2.24E+02	4.87E+00
210	24.78	60	5.87E-01	3.52E-02	3.78E+02	5.69E+00
211	24	6	8.26E-01	3.94E-02	5.97E+02	6.60E+00
212	23.68	60	3.66E-01	2.66E-02	2.04E+02	3.29E+00
213	23.6	300	1.13E+00	4.31E-02	7.49E+02	5.77E+00
214	24	6	1.83E-01	2.15E-02	9.26E+01	2.46E+00
215	23.87	60	3.60E-01	2.95E-02	2.08E+02	3.47E+00
216	99.75	120	1.13E+01	1.45E-01	6.87E+02	6.93E+00
217	129.65	60	1.14E+02	5.73E-01	3.76E+03	1.29E+01
218	139.51	60	2.78E+02	6.97E-01	8.91E+03	8.96E+00
219	139.54	60	2.64E+02	6.55E-01	8.56E+03	2.57E+01
220	129.54	60	9.18E+01	3.51E-01	3.13E+03	5.30E+00
221	119.37	60	3.34E+01	2.52E-01	1.29E+03	8.27E+00
222	109.7	90	1.71E+01	1.96E-01	7.91E+02	6.56E+00
223	99.76	120	7.76E+00	1.07E-01	5.90E+02	5.95E+00
224	99.76	120	8.10E+00	1.16E-01	6.19E+02	7.52E+00
225	99.76	120	7.81E+00	1.18E-01	5.87E+02	8.88E+00
226	109.66	90	1.70E+01	1.85E-01	8.38E+02	7.56E+00
227	119.54	60	3.06E+01	2.73E-01	1.18E+03	7.71E+00
228	129.57	60	8.74E+01	4.21E-01	3.11E+03	1.02E+01
229	139.58	60	2.40E+02	1.34E+00	8.23E+03	1.86E+01
230	149.4	60	5.49E+02	9.63E-01	1.84E+04	2.75E+01
231	159.35	60	1.13E+03	3.70E+00	3.82E+04	5.86E+01
232	168.86	60	1.87E+03	1.89E+00	6.67E+04	5.83E+01

Step	T (°C)	time (min)	³ He (CPS)	±	⁴ He (CPS)	±
233	178.89	60	2.60E+03	2.44E+00	1.03E+05	1.03E+02
234	178.91	60	1.69E+03	2.06E+00	7.37E+04	6.70E+01
235	178.87	60	1.45E+03	5.62E+00	7.20E+04	8.18E+01
236	169.48	120	1.10E+03	1.32E+00	5.73E+04	6.30E+01
237	159.24	60	2.52E+02	7.67E-01	1.39E+04	2.41E+01
238	149.45	60	1.03E+02	3.94E-01	5.92E+03	9.22E+00
239	139.61	60	4.14E+01	2.19E-01	2.52E+03	1.02E+01
240	129.4	60	1.52E+01	1.33E-01	1.06E+03	7.01E+00
241	119.4	60	5.77E+00	8.71E-02	5.27E+02	5.71E+00
242	109.7	90	3.56E+00	8.01E-02	4.65E+02	5.80E+00
243	99.65	120	2.08E+00	5.46E-02	4.46E+02	4.43E+00
244	99.76	120	1.95E+00	5.74E-02	4.39E+02	4.83E+00
245	99.71	120	1.88E+00	6.21E-02	4.36E+02	5.77E+00
246	119.52	60	5.83E+00	1.11E-01	5.07E+02	6.05E+00
247	139.56	60	4.46E+01	3.15E-01	2.74E+03	8.49E+00
248	159.45	60	2.78E+02	7.23E-01	1.60E+04	2.65E+01
249	179.02	60	1.34E+03	3.11E+00	7.49E+04	7.18E+01
250	179.02	60	1.20E+03	1.81E+00	6.98E+04	8.93E+01
251	169.21	60	5.34E+02	8.50E-01	3.23E+04	4.33E+01
252	159.36	60	2.35E+02	7.19E-01	1.46E+04	2.05E+01
253	149.4	60	9.58E+01	4.56E-01	6.11E+03	5.26E+00
254	139.5	60	3.90E+01	2.45E-01	2.60E+03	1.37E+01
255	24	6	2.39E+00	7.74E-02	1.95E+03	8.06E+00
256	24	60	3.77E-01	2.61E-02	2.58E+02	3.63E+00
257	99.92	240	4.09E+00	9.05E-02	8.18E+02	7.51E+00
258	99.84	240	3.26E+00	9.58E-02	7.80E+02	6.52E+00
259	99.84	240	3.35E+00	7.15E-02	7.77E+02	8.83E+00
260	119.74	120	9.02E+00	2.70E-01	9.01E+02	9.84E+00
261	119.78	120	1.06E+01	1.41E-01	9.60E+02	6.40E+00
262	139.6	60	4.26E+01	3.03E-01	2.85E+03	1.45E+01
263	139.54	60	4.47E+01	2.75E-01	3.01E+03	6.26E+00
264	139.65	60	4.34E+01	2.86E-01	2.93E+03	1.15E+01
265	159.4	60	2.75E+02	1.57E+00	1.71E+04	2.86E+01
266	159.37	60	2.65E+02	7.16E-01	1.67E+04	2.29E+01
267	178.94	60	1.16E+03	1.81E+00	7.20E+04	7.18E+01
268	179.09	60	1.17E+03	1.53E+00	7.37E+04	4.76E+01
269	178.98	60	1.15E+03	1.79E+00	7.36E+04	6.35E+01
270	159.4	60	2.36E+02	6.76E-01	1.57E+04	3.05E+01
271	159.38	60	2.43E+02	8.11E-01	1.61E+04	3.43E+01
272	139.81	120	7.31E+01	4.01E-01	5.14E+03	7.01E+00
273	139.74	120	7.47E+01	3.40E-01	5.29E+03	6.57E+00
274	119.91	180	1.48E+01	1.72E-01	1.42E+03	8.84E+00
275	119.85	180	1.51E+01	3.80E-01	1.37E+03	8.48E+00
276	99.85	240	2.87E+00	5.22E-02	7.74E+02	7.61E+00
277	99.86	240	2.91E+00	7.65E-02	7.59E+02	9.21E+00
278	99.81	240	2.84E+00	7.06E-02	7.66E+02	6.37E+00
279	27.69	6	3.52E-01	2.98E-02	1.86E+02	4.55E+00
280	24.78	60	3.26E-01	3.24E-02	2.08E+02	3.50E+00

Step	T (°C)	time (min)	³ He (CPS)	±	⁴ He (CPS)	±
281	139.73	120	7.50E+01	3.60E-01	5.29E+03	8.99E+00
282	159.51	90	3.83E+02	7.68E-01	2.54E+04	4.29E+01
283	178.87	60	1.21E+03	3.27E+00	7.90E+04	6.86E+01
284	188.88	60	2.38E+03	6.22E+00	1.56E+05	1.42E+02
285	198.91	60.6	4.65E+03	1.03E+01	3.01E+05	5.08E+02
286	208.7	60	8.79E+03	7.33E+00	5.88E+05	6.54E+02
287	218.65	60	1.58E+04	4.06E+01	1.09E+06	1.37E+03
288	218.52	60	1.29E+04	1.84E+01	8.95E+05	6.97E+02
289	218.52	60	1.02E+04	1.65E+01	7.13E+05	8.44E+02
290	208.66	60	4.08E+03	5.06E+00	2.95E+05	1.75E+03
291	198.8	60	1.78E+03	7.62E+00	1.33E+05	8.31E+01
292	189.01	60	8.23E+02	1.87E+00	6.10E+04	6.37E+01
293	179.2	60	3.66E+02	1.04E+00	2.76E+04	3.90E+01
294	169.48	60	1.57E+02	5.52E-01	1.20E+04	2.81E+01
295	159.67	90	1.01E+02	4.57E-01	7.86E+03	5.82E+00
296	149.75	120	5.25E+01	3.22E-01	4.35E+03	4.78E+00
297	139.78	120	2.05E+01	2.13E-01	1.93E+03	9.94E+00
298	139.75	120	2.05E+01	1.93E-01	1.96E+03	8.92E+00
299	159.6	90	1.08E+02	1.06E+00	8.27E+03	1.75E+01
300	179.44	60	4.13E+02	9.76E-01	3.09E+04	4.23E+01
301	198.82	60	1.84E+03	3.03E+00	1.37E+05	1.03E+02
302	218.67	60	6.23E+03	7.21E+00	4.47E+05	7.37E+02
303	228.54	60	8.38E+03	1.34E+01	6.08E+05	9.70E+02
304	238.47	60	8.00E+03	1.14E+01	6.01E+05	9.94E+02
305	248.47	60	4.58E+03	6.26E+00	3.62E+05	1.58E+03
306	248.65	60	1.00E+03	2.04E+00	7.50E+04	7.54E+01
307	238.85	60	2.76E+02	9.56E-01	1.94E+04	3.13E+01
308	229.11	60	1.08E+02	4.58E-01	7.82E+03	9.93E+00
309	219.41	60	4.33E+01	2.70E-01	3.35E+03	5.67E+00
310	209.51	60	1.79E+01	2.01E-01	1.54E+03	1.31E+01
311	199.51	60	7.37E+00	2.40E-01	8.55E+02	8.55E+00
312	199.5	60	7.79E+00	1.17E-01	8.00E+02	6.31E+00
313	199.5	60	7.04E+00	2.27E-01	8.01E+02	6.96E+00
314	219.46	60	4.20E+01	3.10E-01	3.15E+03	9.48E+00
315	238.96	60	1.95E+02	4.97E-01	1.39E+04	1.13E+01
316	258.56	60	6.76E+02	1.10E+00	4.79E+04	4.39E+01
317	238.93	60	1.16E+02	4.89E-01	8.52E+03	2.61E+01
318	219.31	60	2.18E+01	1.91E-01	1.78E+03	1.04E+01
319	199.44	60	4.20E+00	8.63E-02	5.79E+02	5.30E+00
320	229.25	60	4.44E+01	3.16E-01	3.48E+03	6.81E+00
321	258.74	60.6	4.04E+02	8.51E-01	2.92E+04	4.94E+01
322	249.07	60	1.54E+02	6.90E-01	1.14E+04	2.18E+01
323	239.29	60	6.08E+01	3.80E-01	4.66E+03	1.51E+01
324	229.42	60	2.74E+01	2.23E-01	2.25E+03	1.15E+01
325	219.51	60	1.17E+01	1.55E-01	1.11E+03	8.33E+00
326	209.47	60	5.23E+00	9.79E-02	6.38E+02	7.09E+00
327	199.51	60	2.61E+00	1.85E-01	4.88E+02	5.25E+00
328	199.49	60	2.45E+00	6.93E-02	4.42E+02	5.54E+00

Step	T (°C)	time (min)	³ He (CPS)	±	⁴ He (CPS)	±
Last Step			3.78E+04		2.86E+06	
Total		748.5 hr	1.68E+05		1.12E+07	

Roy0202C2a 15.2 mg

Step	T (°C)	time (min)	³ He (CPS)	±	⁴ He (CPS)	±
0	24	60	1.68E-01	2.31E-02	1.12E+03	8.49E+00
1	24	60	1.31E-01	2.16E-02	4.33E+02	5.36E+00
2	24	60	9.63E-02	1.86E-02	3.55E+02	4.77E+00
3	24	60	9.67E-02	1.73E-02	3.10E+02	4.03E+00
4	24	60	1.04E-01	2.01E-02	2.68E+02	4.68E+00
5	24	60	8.16E-02	1.74E-02	2.61E+02	5.96E+00
6	23.5	60	1.53E-01	1.64E-02	2.44E+02	3.66E+00
7	23.04	60	1.07E-01	1.41E-02	2.19E+02	4.47E+00
8	23	60	1.03E-01	2.22E-02	2.14E+02	5.42E+00
9	23.01	60	1.00E-01	1.79E-02	2.07E+02	3.81E+00
10	23	60	7.75E-02	1.70E-02	1.93E+02	3.09E+00
11	23.08	60	1.15E-01	1.77E-02	1.90E+02	3.47E+00
12	24	60	1.04E-01	1.80E-02	2.00E+02	4.77E+00
13	24.77	30	1.22E-01	2.14E-02	1.22E+02	3.64E+00
14	29.47	72	1.16E-01	1.72E-02	2.29E+02	5.28E+00
15	34.46	60	1.41E-01	2.59E-02	2.14E+02	3.78E+00
16	39.5	60	1.84E-01	2.15E-02	2.21E+02	4.92E+00
17	44.59	60	1.62E-01	2.64E-02	2.55E+02	4.16E+00
18	49.65	60	1.67E-01	1.67E-01	2.65E+02	6.79E+00
19	44.43	60	1.62E-01	2.42E-02	2.28E+02	3.74E+00
20	24	1080	4.03E-01	2.70E-02	1.34E+03	9.82E+00
21	39.83	60	1.23E-01	2.27E-02	1.75E+02	4.16E+00
24	24	60	3.46E+00	7.80E-02	7.14E+03	2.45E+01
25	24	60	1.74E-01	2.35E-02	1.47E+02	3.75E+00
26	24	60	2.36E-01	2.65E-02	1.40E+02	3.49E+00
27	24	60	1.13E-01	4.45E-02	1.34E+02	2.91E+00
28	24	60	8.71E-02	3.95E-02	1.36E+02	3.67E+00
29	24	60	1.22E-01	3.93E-02	1.42E+02	4.45E+00
30	24	60	1.49E-01	1.88E-02	1.33E+02	3.25E+00
31	24	60	1.74E-01	1.87E-02	1.32E+02	2.75E+00
32	29.42	60	2.46E-01	1.88E-02	1.47E+02	3.48E+00
33	39.57	60	2.14E-01	2.29E-02	1.82E+02	3.55E+00
34	49.76	120	4.03E-01	2.42E-02	3.71E+02	3.85E+00
35	59.85	120	5.94E-01	3.71E-02	4.79E+02	5.75E+00
36	69.88	120	9.76E-01	4.09E-02	5.88E+02	5.35E+00
37	79.88	120	1.95E+00	6.21E-02	7.06E+02	4.66E+00
38	89.77	60	1.91E+00	1.39E-01	4.79E+02	5.07E+00
39	99.63	60	4.35E+00	7.97E-02	5.68E+02	5.46E+00
40	89.75	60	2.60E+00	7.27E-02	3.71E+02	4.86E+00
41	79.87	120	2.60E+00	7.57E-02	4.46E+02	6.95E+00
42	69.85	120	1.41E+00	6.21E-02	3.32E+02	4.81E+00
43	59.82	120	9.51E-01	4.25E-02	2.66E+02	4.85E+00

Step	T (°C)	time (min)	³ He (CPS)	±	⁴ He (CPS)	±
44	49.81	180	8.51E-01	4.24E-02	2.85E+02	3.69E+00
45	49.86	180	7.52E-01	3.59E-02	2.75E+02	4.17E+00
46	49.85	180	5.26E-01	8.78E-02	2.81E+02	4.23E+00
47	69.91	180	1.73E+00	5.71E-02	3.96E+02	6.47E+00
48	79.91	180	2.88E+00	7.95E-02	4.89E+02	4.85E+00
49	89.88	120	3.68E+00	7.23E-02	4.34E+02	5.66E+00
50	99.88	120	6.76E+00	2.48E-01	5.67E+02	5.38E+00
51	89.87	120	4.67E+00	8.48E-02	4.19E+02	4.80E+00
52	79.86	120	2.94E+00	8.81E-02	3.10E+02	4.79E+00
53	69.85	120	1.68E+00	6.59E-02	2.56E+02	4.32E+00
54	59.86	180	1.59E+00	4.10E-02	2.91E+02	4.52E+00
55	49.83	180	9.15E-01	4.01E-02	2.47E+02	5.36E+00
56	49.86	180	9.57E-01	4.17E-02	2.58E+02	4.50E+00
57	49.86	180	8.89E-01	4.90E-02	2.69E+02	5.45E+00
58	59.9	180	1.08E+00	1.04E-01	2.84E+02	4.88E+00
59	69.87	120	1.45E+00	5.12E-02	2.36E+02	3.63E+00
60	79.88	120	2.06E+00	7.12E-02	2.74E+02	4.57E+00
61	89.88	120	3.49E+00	9.38E-02	3.49E+02	4.72E+00
62	99.9	120	7.19E+00	2.23E-01	4.61E+02	6.23E+00
63	100	4560	2.13E+02	5.68E-01	1.03E+04	1.02E+01
64	99.9	120	4.43E+00	8.68E-02	2.85E+02	4.72E+00
65	33.34	60	2.44E-01	6.79E-02	1.25E+02	2.59E+00
66	24.15	300	8.52E-01	3.87E-02	3.28E+02	5.19E+00
67	49.88	120	8.09E-01	3.64E-02	1.72E+02	3.14E+00
68	49.86	180	1.07E+00	4.04E-02	2.54E+02	4.46E+00
69	49.9	240	1.33E+00	5.28E-02	2.85E+02	3.10E+00
70	49.9	300	1.51E+00	5.70E-02	3.64E+02	4.97E+00
71	59.9	180	1.27E+00	4.92E-02	2.36E+02	3.26E+00
72	69.88	120	1.25E+00	4.29E-02	2.13E+02	3.73E+00
73	79.9	120	1.79E+00	5.75E-02	2.38E+02	3.45E+00
74	89.84	120	2.59E+00	7.17E-02	2.46E+02	3.67E+00
75	99.9	120	3.50E+00	7.43E-02	2.52E+02	5.56E+00
76	24	6	1.29E+00	5.03E-02	5.31E+02	6.12E+00
77	24	60	2.53E-01	2.25E-02	1.21E+02	2.90E+00
78	24	300	4.66E-01	8.38E-02	3.10E+02	5.14E+00
79	99.87	120	3.70E+00	9.31E-02	2.62E+02	2.99E+00
80	99.88	120	3.91E+00	9.36E-02	2.78E+02	5.41E+00
81	99.85	120	3.84E+00	8.82E-02	2.59E+02	2.73E+00
82	99.88	120	4.00E+00	8.06E-02	2.79E+02	5.04E+00
83	99.92	120	3.83E+00	9.73E-02	2.47E+02	3.92E+00
84	99.87	120	3.68E+00	8.52E-02	2.50E+02	3.91E+00
85	99.89	120	3.75E+00	8.54E-02	2.41E+02	3.38E+00
86	99.88	120	4.12E+00	3.79E-01	2.38E+02	3.55E+00
87	99.88	120	3.82E+00	8.68E-02	2.34E+02	3.04E+00
88	99.87	120	3.52E+00	7.58E-02	2.31E+02	4.66E+00
89	99.88	120	3.50E+00	7.44E-02	2.31E+02	3.94E+00
90	99.89	120	3.56E+00	8.64E-02	2.44E+02	4.67E+00
91	99.79	120	3.37E+00	8.29E-02	2.39E+02	3.52E+00

Step	T (°C)	time (min)	³ He (CPS)	±	⁴ He (CPS)	±
92	99.88	120	3.45E+00	9.21E-02	2.46E+02	4.95E+00
93	99.88	120	3.43E+00	7.73E-02	2.46E+02	5.71E+00
94	99.87	120	3.31E+00	6.56E-02	2.45E+02	4.70E+00
95	99.89	120	3.32E+00	8.73E-02	2.59E+02	4.73E+00
96	99.94	300	7.83E+00	1.24E-01	5.03E+02	5.96E+00
97	99.95	300	7.65E+00	1.24E-01	4.98E+02	6.07E+00
98	99.95	300	7.47E+00	1.18E-01	4.85E+02	5.98E+00
99	99.95	300	7.33E+00	1.08E-01	4.91E+02	6.20E+00
100	99.95	300	6.84E+00	1.01E-01	4.80E+02	4.68E+00
101	99.95	300	6.44E+00	2.45E-01	4.71E+02	6.55E+00
102	99.95	300	6.58E+00	9.92E-02	4.71E+02	5.46E+00
103	99.95	300	6.56E+00	1.04E-01	4.55E+02	4.66E+00
104	99.95	300	6.51E+00	1.02E-01	4.59E+02	5.28E+00
105	99.95	300	6.18E+00	1.13E-01	4.48E+02	4.88E+00
106	24	6	7.59E-01	3.78E-02	3.57E+02	5.47E+00
107	24	60	2.65E-01	2.24E-02	1.07E+02	3.33E+00
108	24	300	5.70E-01	3.45E-02	3.07E+02	5.31E+00
109	99.95	300	5.57E+00	2.35E-01	4.76E+02	4.95E+00
110	99.92	300	6.18E+00	9.57E-02	4.73E+02	4.82E+00
111	99.92	300	5.51E+00	1.95E-01	4.50E+02	5.50E+00
112	99.92	300	5.89E+00	7.97E-02	4.38E+02	4.57E+00
113	99.95	300	5.74E+00	9.84E-02	4.57E+02	5.27E+00
114	99.94	300	5.65E+00	9.85E-02	4.41E+02	5.87E+00
115	99.95	300	5.47E+00	9.72E-02	4.67E+02	5.27E+00
116	149.76	60	2.80E+01	4.91E-01	6.66E+02	5.05E+00
117	199.73	60	7.55E+02	1.35E+00	3.96E+04	4.69E+01
118	199.7	60	9.75E+02	2.21E+00	6.24E+04	7.06E+01
119	179.74	60	2.83E+02	8.31E-01	1.77E+04	2.75E+01
120	159.76	60	6.48E+01	7.81E-01	3.60E+03	1.61E+01
121	139.76	60	1.75E+01	3.95E-01	8.21E+02	1.19E+01
122	119.89	120	1.30E+01	1.58E-01	5.64E+02	7.12E+00
123	99.92	180	7.88E+00	2.51E-01	4.80E+02	4.77E+00
124	119.89	120	1.01E+01	1.24E-01	4.64E+02	5.48E+00
125	139.79	60.6	1.43E+01	1.39E-01	7.43E+02	7.28E+00
126	159.69	60	6.49E+01	3.36E-01	4.02E+03	7.47E+00
127	179.76	60	3.16E+02	8.19E-01	2.14E+04	4.13E+01
128	199.1	60	1.16E+03	1.70E+00	8.03E+04	7.31E+01
129	199.23	60	1.17E+03	1.86E+00	8.15E+04	8.00E+01
130	199.23	60	1.18E+03	1.80E+00	8.25E+04	7.46E+01
131	179.71	60	2.95E+02	8.61E-01	2.03E+04	4.00E+01
132	159.74	60	5.86E+01	3.38E-01	3.83E+03	5.89E+00
133	149.88	120	4.88E+01	3.75E-01	3.03E+03	1.07E+01
134	149.88	120	4.77E+01	3.07E-01	3.06E+03	1.09E+01
135	199.05	60	1.18E+03	2.39E+00	8.37E+04	7.51E+01
136	209.22	60	2.07E+03	8.47E+00	1.48E+05	1.28E+02
137	219.14	60	3.54E+03	6.61E+00	2.51E+05	2.08E+02
138	219.17	60	3.18E+03	5.37E+00	2.24E+05	1.87E+02
139	219.13	60	2.99E+03	4.60E+00	2.11E+05	1.77E+02

Step	T (°C)	time (min)	³ He (CPS)	±	⁴ He (CPS)	±
140	199.62	60	7.85E+02	1.44E+00	5.53E+04	6.14E+01
141	179.73	60	1.68E+02	5.52E-01	1.18E+04	2.79E+01
142	159.88	120	6.05E+01	3.39E-01	4.33E+03	5.06E+00
143	159.88	120	5.94E+01	3.21E-01	4.23E+03	5.59E+00
144	199.68	60	8.22E+02	1.56E+00	5.84E+04	4.51E+01
145	229.03	60	4.95E+03	4.79E+00	3.48E+05	2.83E+02
146	219.16	60	2.51E+03	3.38E+00	1.76E+05	1.49E+02
147	209.12	60	1.30E+03	4.91E+00	9.18E+04	9.17E+01
148	199.63	60	6.65E+02	1.14E+00	4.71E+04	4.93E+01
149	199.7	60	6.77E+02	1.29E+00	4.78E+04	5.39E+01
150	199.69	60	6.66E+02	1.34E+00	4.70E+04	5.20E+01
151	219.2	60	2.60E+03	8.03E+00	1.76E+05	1.50E+02
152	239.02	60	8.26E+03	1.07E+01	5.68E+05	4.54E+02
153	258.86	60	2.48E+04	9.30E+01	1.70E+06	1.33E+03
154	238.95	60	7.95E+03	1.34E+01	5.39E+05	4.32E+02
Last Step			3.57E+05		2.27E+07	
Total		361.2 hr	4.33E+05		2.80E+07	

Roy0202C3b 8.4 mg

Step	T (°C)	time (min)	³ He (CPS)	±	⁴ He (CPS)	±
0	24	6	1.18E-01	2.09E-02	1.17E+03	7.49E+00
1	24	60	1.34E-01	2.09E-02	1.22E+03	6.51E+00
2	29.46	60	9.21E-02	1.69E-02	7.49E+02	6.48E+00
3	39.54	60	1.16E-01	1.75E-02	5.97E+02	5.24E+00
4	49.66	60	2.14E-01	2.14E-02	5.32E+02	5.10E+00
5	59.72	60	2.98E-01	2.35E-02	5.06E+02	4.38E+00
6	69.72	60	6.83E-01	7.40E-02	5.16E+02	5.30E+00
7	79.75	60	6.55E-01	1.01E-01	5.01E+02	6.15E+00
8	89.77	60	1.66E+00	5.34E-02	5.13E+02	4.37E+00
9	99.76	60	3.35E+00	6.68E-02	5.24E+02	5.52E+00
10	109.79	60	6.19E+00	1.17E-01	5.45E+02	6.65E+00
11	119.78	60	9.94E+00	1.33E-01	5.99E+02	7.67E+00
12	129.77	60	1.51E+01	1.73E-01	6.60E+02	6.41E+00
13	139.76	60	2.10E+01	1.97E-01	7.27E+02	5.16E+00
14	149.77	60	2.80E+01	2.14E-01	8.15E+02	7.43E+00
15	139.76	60	1.30E+01	1.40E-01	4.68E+02	6.12E+00
16	129.76	60	6.31E+00	1.02E-01	3.21E+02	5.38E+00
17	119.77	60	3.73E+00	9.26E-02	2.40E+02	4.18E+00
18	119.77	60	3.73E+00	9.26E-02	2.40E+02	4.18E+00
19	109.78	60	2.05E+00	5.33E-02	1.93E+02	3.73E+00
20	99.77	60	1.17E+00	4.74E-02	1.77E+02	3.74E+00
21	109.78	60	1.83E+00	6.89E-02	1.89E+02	3.49E+00
22	119.77	60	2.91E+00	6.36E-02	2.21E+02	3.94E+00
23	129.75	60	4.81E+00	9.68E-02	2.60E+02	5.20E+00
24	139.78	60	7.90E+00	1.33E-01	3.24E+02	5.90E+00
25	149.78	60	1.39E+01	1.75E-01	4.65E+02	5.15E+00

Step	T (°C)	time (min)	³ He (CPS)	±	⁴ He (CPS)	±
26	139.77	60	7.58E+00	1.26E-01	3.14E+02	6.43E+00
27	129.76	60	4.20E+00	1.08E-01	2.38E+02	6.10E+00
28	119.77	60	2.40E+00	7.38E-02	1.94E+02	3.96E+00
29	109.75	60	1.29E+00	4.41E-02	1.67E+02	4.04E+00
30	99.77	60	9.91E-01	9.07E-02	1.51E+02	3.65E+00
31	109.76	60	1.27E+00	4.36E-02	1.68E+02	3.06E+00
32	119.75	60	2.08E+00	5.79E-02	1.77E+02	3.32E+00
33	129.74	60	3.17E+00	7.54E-02	2.07E+02	3.36E+00
34	139.76	60	5.69E+00	9.29E-02	2.66E+02	3.54E+00
35	149.76	60	9.83E+00	1.50E-01	3.67E+02	5.44E+00
36	139.75	60	5.55E+00	1.03E-01	2.59E+02	3.78E+00
37	129.75	60	3.33E+00	8.28E-02	2.04E+02	4.24E+00
38	119.76	60	2.10E+00	1.38E-01	1.71E+02	2.98E+00
39	109.75	60	1.07E+00	3.53E-02	1.53E+02	3.88E+00
40	99.75	60	8.38E-01	3.73E-02	1.56E+02	4.17E+00
41	109.77	60	1.07E+00	4.29E-02	1.53E+02	4.30E+00
42	119.77	60	1.68E+00	5.98E-02	1.69E+02	3.10E+00
43	129.75	60	2.75E+00	6.96E-02	1.86E+02	3.42E+00
44	139.74	60	4.27E+00	9.00E-02	2.28E+02	4.30E+00
45	149.74	60	7.34E+00	2.46E-01	3.16E+02	5.73E+00
46	159.76	60	1.33E+01	1.62E-01	4.70E+02	4.22E+00
47	169.75	60	2.63E+01	1.86E-01	9.61E+02	7.21E+00
48	159.76	60	1.32E+01	1.51E-01	5.46E+02	6.63E+00
49	149.75	60	7.23E+00	1.41E-01	3.48E+02	5.11E+00
50	139.75	60	3.81E+00	8.23E-02	2.39E+02	5.21E+00
51	129.75	60	2.31E+00	7.12E-02	1.77E+02	4.40E+00
52	119.78	60	1.41E+00	5.40E-02	1.59E+02	3.69E+00
53	129.75	60	2.04E+00	5.88E-02	1.74E+02	3.75E+00
54	139.75	60	3.59E+00	8.11E-02	2.30E+02	3.41E+00
55	149.74	60	5.63E+00	1.03E-01	3.16E+02	5.25E+00
56	159.74	60	1.10E+01	1.41E-01	5.37E+02	4.86E+00
57	169.73	60	2.39E+01	2.18E-01	1.22E+03	9.57E+00
58	159.76	60	1.38E+01	1.48E-01	7.39E+02	7.56E+00
59	149.74	60	7.04E+00	1.17E-01	4.12E+02	5.44E+00
60	139.74	60	3.42E+00	9.37E-02	2.45E+02	3.57E+00
61	129.75	60	1.78E+00	5.61E-02	1.80E+02	2.83E+00
62	119.76	60	1.18E+00	5.65E-02	1.61E+02	3.40E+00
63	129.76	60	1.89E+00	7.36E-02	1.87E+02	3.62E+00
64	139.74	60	3.10E+00	7.21E-02	2.48E+02	3.53E+00
65	149.74	60	6.35E+00	1.21E-01	4.03E+02	3.03E+00
66	159.74	60	1.37E+01	1.46E-01	7.78E+02	7.21E+00
67	169.75	60	3.05E+01	2.22E-01	1.75E+03	8.81E+00
68	179.73	60	9.10E+01	9.24E-01	5.39E+03	6.00E+00
69	184.74	60	1.76E+02	1.28E+00	1.10E+04	1.10E+01
70	179.74	60	1.36E+02	5.46E-01	8.86E+03	8.83E+00
71	169.74	60	6.42E+01	3.90E-01	4.28E+03	6.15E+00
72	159.71	60	2.50E+01	4.03E-01	1.68E+03	1.14E+01
73	149.75	60	1.23E+01	1.46E-01	8.46E+02	5.82E+00

Step	T (°C)	time (min)	³ He (CPS)	±	⁴ He (CPS)	±
74	139.76	60	5.09E+00	8.80E-02	4.01E+02	5.49E+00
75	129.75	60	2.25E+00	6.60E-02	2.36E+02	4.35E+00
76	119.74	60	1.01E+00	3.21E-02	1.62E+02	3.17E+00
77	129.75	60	1.90E+00	6.82E-02	2.19E+02	3.75E+00
78	139.74	60	4.33E+00	9.32E-02	3.50E+02	4.54E+00
79	149.74	60	1.10E+01	1.36E-01	7.56E+02	6.03E+00
80	159.75	60	3.02E+01	2.19E-01	2.05E+03	9.46E+00
81	169.76	60	7.65E+01	3.71E-01	5.12E+03	7.04E+00
82	179.6	60	1.59E+02	5.92E-01	1.06E+04	1.03E+01
83	189.75	60	4.64E+02	6.84E-01	3.11E+04	4.19E+01
84	199.7	60	1.01E+03	1.41E+00	6.73E+04	7.20E+01
85	189.56	60	4.93E+02	1.72E+00	3.32E+04	4.08E+01
86	179.75	60	2.43E+02	1.27E+00	1.63E+04	2.59E+01
87	169.76	60	1.05E+02	9.87E-01	7.22E+03	9.02E+00
88	159.55	60	4.36E+01	3.37E-01	3.05E+03	1.28E+01
89	149.78	60	1.83E+01	1.93E-01	1.33E+03	7.38E+00
90	159.85	60	4.70E+01	2.29E-01	3.26E+03	1.38E+01
91	169.75	60	1.03E+02	4.34E-01	7.09E+03	2.39E+01
92	179.77	60	2.62E+02	7.41E-01	1.78E+04	3.55E+01
93	189.74	60	4.84E+02	1.01E+00	3.32E+04	3.73E+01
94	199.54	60	9.50E+02	2.92E+00	6.43E+04	6.64E+01
95	189.73	60	4.52E+02	8.79E-01	3.10E+04	3.70E+01
96	179.74	60	2.35E+02	5.55E-01	1.62E+04	3.50E+01
97	169.56	60	1.01E+02	4.13E-01	6.89E+03	1.94E+01
98	159.76	60	4.21E+01	2.58E-01	2.93E+03	1.41E+01
99	149.74	60	1.69E+01	1.74E-01	1.22E+03	1.01E+01
100	24	480	3.19E-01	2.45E-02	4.53E+02	6.29E+00
101	24	60	1.59E-01	1.84E-02	1.10E+02	3.13E+00
102	149.76	60	1.54E+01	1.66E-01	1.10E+03	1.01E+01
103	149.76	60	1.76E+01	1.97E-01	1.30E+03	9.27E+00
104	159.76	60	3.97E+01	2.51E-01	2.73E+03	1.52E+01
105	169.59	60	1.14E+02	4.61E-01	7.82E+03	8.46E+00
106	179.74	60	2.21E+02	5.72E-01	1.50E+04	1.45E+01
107	189.73	60	4.66E+02	2.28E+00	3.13E+04	4.44E+01
108	199.71	60	8.81E+02	3.05E+00	5.96E+04	4.66E+01
109	189.55	60	4.66E+02	9.86E-01	3.19E+04	5.08E+01
110	179.76	60	1.80E+02	6.36E-01	1.25E+04	3.31E+01
111	169.75	60	7.94E+01	4.20E-01	5.47E+03	6.03E+00
112	159.55	60	4.14E+01	2.81E-01	2.91E+03	5.21E+00
113	149.65	60	1.38E+01	1.46E-01	1.01E+03	6.30E+00
114	149.78	60	1.51E+01	1.52E-01	1.10E+03	9.60E+00
115	159.75	60	3.93E+01	6.88E-01	2.83E+03	1.36E+01
116	169.57	60	1.07E+02	4.85E-01	7.40E+03	2.18E+01
117	179.75	60	2.56E+02	1.63E+00	1.72E+04	4.32E+01
118	189.71	60	5.10E+02	2.10E+00	3.47E+04	4.35E+01
119	199.69	60	8.93E+02	1.48E+00	6.12E+04	5.80E+01
120	208.95	60	1.73E+03	4.42E+00	1.18E+05	2.91E+02
121	219.2	60	3.03E+03	3.77E+00	2.17E+05	2.00E+02

Step	T (°C)	time (min)	³ He (CPS)	±	⁴ He (CPS)	±
122	229.12	60	4.96E+03	1.28E+01	3.59E+05	3.24E+02
123	239.04	60	7.79E+03	6.19E+00	5.70E+05	5.08E+02
124	248.93	60	1.29E+04	8.92E+00	9.39E+05	8.30E+02
125	229.14	60	3.98E+03	9.30E+00	2.83E+05	2.58E+02
126	209.62	60	9.74E+02	1.14E+00	6.42E+04	6.68E+01
127	189.74	60	2.38E+02	1.35E+00	1.55E+04	3.90E+01
128	169.75	60	4.26E+01	3.10E-01	2.99E+03	7.12E+00
129	149.76	60	8.84E+00	1.19E-01	7.58E+02	7.62E+00
130	169.59	60	4.47E+01	3.00E-01	3.05E+03	1.17E+01
131	189.74	60	2.69E+02	7.03E-01	1.79E+04	2.33E+01
132	209.44	60	1.22E+03	1.65E+00	8.06E+04	6.83E+01
133	229.15	60	3.93E+03	8.29E+00	2.85E+05	2.59E+02
134	248.76	60	1.17E+04	1.22E+01	8.37E+05	7.41E+02
135	219.2	60	1.99E+03	2.29E+00	1.30E+05	1.01E+02
136	189.72	60	2.15E+02	1.23E+00	1.40E+04	1.26E+01
Last Step			1.47E+05		8.70E+06	
Total		32.1 hr	2.13E+05		1.34E+07	

Pic 24

Step	T (°C)	time (h)	³ He *(CPS)	±	⁴ He *(CPS)	±
1	22	1	-4.72E-01	-1.02E-01	-1.20E+03	
2	23	1	1.38E-01	1.03E-01	1.34E+02	
3	23	1	3.74E-01	1.10E-02	1.08E+03	
4	39	1	1.52E+00	6.05E-02	5.64E+02	
5	50	1	4.02E+00	7.17E-02	1.23E+02	
6	75	1	2.87E+01	9.85E-02	2.61E+02	
7	100	1	9.32E+01	1.12E-01	2.32E+03	
8	125	1	1.61E+02	1.10E-01	4.63E+03	
9	150	1	2.15E+02	1.02E-01	9.17E+03	
10	175	1	3.13E+02	4.77E-01	1.95E+04	
11	199	1	8.46E+02	1.73E+00	8.33E+04	
12	189	1	5.99E+02	1.31E+00	6.54E+04	
13	180	1	2.72E+02	5.98E-01	3.11E+04	
14	170	1	1.14E+02	2.70E-01	1.35E+04	
15	160	1	4.60E+01	1.40E-01	5.59E+03	
16	150	2	3.72E+01	1.51E-01	4.79E+03	
17	140	2	1.26E+01	4.74E-02	2.02E+03	
18	145	2	2.18E+01	1.31E-01	3.95E+03	
19	155	2	5.54E+01	1.33E-01	7.19E+03	
20	165	1	7.03E+01	1.98E-01	9.56E+03	
21	175	1	1.65E+02	3.47E-01	2.01E+04	
22	185	1	3.49E+02	8.05E-01	3.83E+04	
23	195	1	5.80E+02	1.21E+00	6.14E+04	
24	205	1	5.78E+02	1.09E+00	5.47E+04	
25	219	0.5	2.68E+02	5.29E-01	2.29E+04	
26	239	0.5	1.51E+02	2.23E-01	1.41E+04	
27	258	0.5	7.77E+01	1.78E-01	1.02E+04	

Step	T (°C)	time (min)	³ He (CPS)	±	⁴ He (CPS)	±
	28	279	0.5	1.01E+02	3.29E-01	1.27E+04
	29	299	0.5	9.86E+01	2.86E-01	1.24E+04
	30	319	0.5	1.01E+02	2.14E-01	1.29E+04
	31	339	0.5	1.03E+02	2.62E-01	1.31E+04
	32	340	0.5	3.85E+01	1.72E-01	5.88E+03
	33	340	0.5	2.07E+01	7.52E-02	3.91E+03
	34	358	0.5	4.23E+01	1.40E-01	6.82E+03
	35	380	0.5	5.44E+01	2.23E-01	8.33E+03
	36	379	0.5	1.83E+01	8.04E-02	3.90E+03
	37	378	0.5	1.05E+01	-8.95E-03	2.68E+03
	38	399	0.5	2.51E+01	-2.19E-02	4.36E+03
	39	416	0.5	3.71E+01	1.34E-01	6.36E+03
	40	420	2	4.35E+01	1.42E-01	8.29E+03
	41	440	0.5	1.20E+01	5.65E-02	3.16E+03
	42	459	0.5	1.78E+01	3.02E-02	3.88E+03
	43	459	0.5	6.84E+00	2.96E-02	2.50E+03
	44	477	0.5	1.07E+01	9.64E-02	2.92E+03
	45	499	0.5	1.24E+01	1.09E-01	2.92E+03
	46	499	0.5	4.33E+00	8.70E-02	1.91E+03
Last step (guess)		2	4.93E-01		2.62E+02	
Total		42.50	5.82E+03		6.04E+05	

* blank corrected - ³He blank: 1.4 cps, ⁴He blank: 1790 cps

Win-06-01B

Step	T (°C)	time (h)	³ He *(CPS)	±	⁴ He *(CPS)	±
<i>1</i>	<i>23.00</i>	<i>1</i>	<i>8.93E-03</i>		<i>1.87E+00</i>	
2	78.92	1	9.77E-01	5.55E-02	2.25E+02	7.27E+00
3	98.90	1	3.65E+00	1.41E-01	1.94E+02	6.95E+00
4	119.12	1	1.05E+01	2.41E-01	7.41E+02	9.33E+00
5	139.03	1	1.84E+01	3.31E-01	8.59E+02	9.23E+00
6	159.21	1	2.41E+01	3.34E-01	1.07E+03	1.01E+01
7	179.24	1	3.21E+01	3.92E-01	1.92E+03	1.33E+01
8	199.27	1	4.75E+01	5.57E-01	1.41E+04	2.40E+01
9	219.29	1	2.41E+02	1.69E+00	4.23E+05	
10	238.42	1	9.58E+02	2.83E+00	1.95E+06	
11	229.27	1	3.67E+02	1.52E+00	7.56E+05	
12	219.28	1	1.75E+02	1.70E+00	3.44E+05	
13	209.28	1	7.76E+01	7.21E-01	1.65E+05	2.06E+02
14	199.25	1	3.54E+01	4.16E-01	7.39E+04	7.56E+01
15	189.63	2	3.13E+01	4.15E-01	6.58E+04	5.41E+01
16	179.61	2	1.37E+01	2.69E-01	2.78E+04	3.70E+01
17	184.63	2	2.08E+01	3.20E-01	4.31E+04	3.63E+01
18	194.62	2	4.60E+01	5.65E-01	1.01E+05	8.33E+01
19	204.28	1	5.15E+01	4.99E-01	1.09E+05	6.09E+01
20	214.29	1	1.05E+02	6.77E-01	2.19E+05	
21	224.29	1	1.94E+02	9.76E-01	4.24E+05	
22	234.29	1	3.38E+02	2.07E+00	7.43E+05	

Step	T (°C)	time (min)	³ He (CPS)	±	⁴ He (CPS)	±
23	238.58	0.5	2.03E+02	1.14E+00	4.54E+05	
24	257.83	0.5	5.57E+02	1.92E+00	1.26E+06	
25	276.84	0.5	1.01E+03	3.31E+00	2.28E+06	
26	296.07	0.5	1.19E+03	3.67E+00	2.67E+06	
27	317.4	0.5	4.07E+02	2.79E+00	9.22E+05	
28	338.36	0.5	5.81E+01	5.13E-01	1.11E+05	1.53E+02
29	338.82	0.5	2.38E+01	3.66E-01	4.50E+04	9.75E+01
30	338.81	0.5	1.52E+01	2.93E-01	2.89E+04	4.71E+01
31	358.88	0.5	3.43E+01	4.02E-01	6.50E+04	8.04E+01
32	378.61	0.5	5.42E+01	5.04E-01	1.01E+05	8.22E+01
33	378.5	0.5	2.62E+01	3.31E-01	5.03E+04	4.43E+01
34	378.57	0.5	1.74E+01	3.18E-01	3.36E+04	5.69E+01
35	398.63	0.5	3.71E+01	4.29E-01	7.16E+04	5.61E+01
36	418.38	0.5	5.35E+01	4.76E-01	1.06E+05	7.96E+01
37	419.58	2	6.97E+01	5.63E-01	1.37E+05	8.97E+01
38	438.18	0.5	2.44E+01	3.85E-01	4.82E+04	3.55E+01
39	458.05	0.5	3.92E+01	4.80E-01	7.66E+04	5.84E+01
40	457.53	0.5	2.03E+01	3.56E-01	3.98E+04	3.70E+01
41	477.8	0.5	3.35E+01	4.30E-01	6.63E+04	5.51E+01
42	497.6	0.5	4.09E+01	5.13E-01	8.13E+04	6.17E+01
43	497.81	0.5	1.92E+01	3.21E-01	3.79E+04	4.15E+01
Last step	850.00	2.0	3.23E+02	1.21E+00	5.90E+05	
Total		40	7.05E+03		1.47E+07	

* blank corrected - ³He blank: 0.1 cps, ⁴He black: 390 cps

Capao L3

Step	T (°C)	time (h)	³ He *(CPS)	±	⁴ He *(CPS)	±
1	23.21	1	4.69E-03	2.09E-02	1.71E+01	1.74E+01
2	38.64	1	6.64E-02	2.55E-02	1.48E+02	3.00E+01
3	58.84	1	1.55E-01	3.20E-02	-7.64E+00	1.93E+01
4	79.05	1	7.13E-01	6.73E-02	6.60E+01	2.15E+01
5	99.14	1	3.75E+00	1.65E-01	8.78E+01	2.01E+01
6	119.20	1	9.27E+00	2.35E-01	2.58E+02	2.54E+01
7	139.10	1	1.08E+01	2.20E-01	1.47E+02	2.18E+01
8	159.20	1	1.02E+01	2.11E-01	3.55E+02	2.01E+01
9	179.20	1	1.07E+01	2.51E-01	6.92E+02	2.51E+01
10	199.24	1	1.41E+01	2.40E-01	3.36E+03	9.16E+01
11	219.27	1	5.62E+01	5.32E-01	5.45E+04	1.66E+02
12	239.29	1	5.19E+02	2.60E+00	6.28E+05	1.64E+03
13	229.29	1	2.96E+02	1.86E+00	3.70E+05	1.09E+03
14	219.28	1	1.35E+02	8.76E-01	1.84E+05	1.78E+02
15	209.26	1	6.24E+01	5.43E-01	8.27E+04	1.44E+02
16	199.25	1	2.78E+01	4.12E-01	3.70E+04	1.11E+02
17	189.62	2	2.49E+01	3.35E-01	3.30E+04	1.19E+02
18	180.00	2	1.04E+01	1.95E-01	1.39E+04	5.67E+01
19	195.11	2	3.79E+01	4.64E-01	5.13E+04	1.43E+02
20	204.26	1	3.94E+01	5.17E-01	5.22E+04	1.37E+02
21	214.26	1	7.91E+01	6.82E-01	1.06E+05	2.14E+02

Step	T (°C)	time (min)	³ He (CPS)	±	⁴ He (CPS)	±
22	224.26	1	1.43E+02	8.06E-01	1.94E+05	1.89E+02
23	234.29	1	2.14E+02	1.34E+00	2.92E+05	1.09E+03
24	238.59	0.5	1.13E+02	7.18E-01	1.56E+05	1.42E+02
25	258.50	0.5	2.14E+02	1.32E+00	2.93E+05	1.09E+03
26	278.62	0.5	5.44E+01	5.20E-01	6.80E+04	9.83E+01
27	298.64	0.5	2.14E+01	3.14E-01	1.90E+04	5.77E+01
28	318.68	0.5	2.42E+01	3.72E-01	2.08E+04	7.05E+01
29	338.74	0.5	2.76E+01	3.70E-01	2.30E+04	7.57E+01
30	338.74	0.5	1.12E+01	2.42E-01	9.48E+03	3.78E+01
31	338.79	0.5	7.05E+00	1.68E-01	5.81E+03	2.43E+01
32	358.81	0.5	1.35E+01	2.73E-01	1.19E+04	3.10E+01
33	378.60	0.5	1.90E+01	3.13E-01	1.65E+04	4.66E+01
34	378.64	0.5	8.94E+00	2.31E-01	7.22E+03	2.35E+01
35	378.77	0.5	5.50E+00	1.82E-01	4.46E+03	1.75E+01
36	398.50	0.5	1.10E+01	2.04E-01	9.13E+03	2.59E+01
37	418.52	0.5	1.49E+01	2.86E-01	1.28E+04	3.76E+01
38	419.61	2	1.78E+01	3.18E-01	1.55E+04	3.94E+01
39	438.32	0.5	6.26E+00	1.83E-01	5.04E+03	1.58E+01
40	458.24	0.5	9.39E+00	1.97E-01	8.12E+03	2.86E+01
41	458.20	0.5	5.35E+00	1.50E-01	4.11E+03	1.28E+01
42	478.05	0.5	7.65E+00	2.31E-01	6.84E+03	2.02E+01
43	497.79	0.5	9.90E+00	2.28E-01	8.32E+03	2.63E+01
44	497.84	0.5	5.06E+00	1.67E-01	3.87E+03	1.75E+01
Laste step	850.00	2	8.02E+01	2.47E-01	6.81E+04	
Total		40	2.39E+03		2.88E+06	

* blank corrected - ³He blank: 0.03 cps, ⁴He black: 800 cps

Capao L5

Step	T (°C)	time (h)	³ He *(CPS)	±	⁴ He *(CPS)	±
1	23.91	1	4.65E-02	4.92E-02	2.75E+01	4.54E+01
2	38.65	1	-2.57E-01	2.96E-02	-3.82E+02	3.14E+01
3	58.82	1	-8.19E-02	4.13E-02	-5.56E+02	2.42E+01
4	79.48	1	1.41E+00	9.10E-02	-5.81E+02	2.10E+01
5	99.26	1	6.75E+00	1.88E-01	-6.33E+02	1.17E+01
6	119.03	1	1.58E+01	2.33E-01	-4.52E+02	1.62E+01
7	139.05	1	2.45E+01	3.76E-01	-2.70E+02	1.88E+01
8	159.18	1	3.04E+01	4.41E-01	1.13E+02	3.02E+01
9	179.17	1	4.01E+01	4.40E-01	9.63E+02	4.48E+01
10	199.24	1	6.03E+01	5.89E-01	5.01E+03	4.47E+01
11	219.2	1	1.90E+02	9.87E-01	5.85E+04	1.66E+02
12	209.17	1	1.14E+02	7.02E-01	4.43E+04	1.07E+02
13	199.2	1	5.64E+01	5.85E-01	2.18E+04	5.66E+01
14	189.19	1	2.55E+01	3.43E-01	9.56E+03	2.86E+01
15	179.16	1	1.12E+01	2.65E-01	3.48E+03	1.35E+01
16	169.59	2	9.46E+00	2.16E-01	2.90E+03	1.58E+01
17	159.59	2	3.72E+00	1.27E-01	4.93E+02	1.36E+01
18	169.59	2	9.01E+00	2.22E-01	2.74E+03	1.38E+01
19	179.66	2	2.25E+01	3.69E-01	8.46E+03	1.87E+01

Step	T (°C)	time (min)	³ He (CPS)	±	⁴ He (CPS)	±
20	189.59	2	5.41E+01	5.10E-01	2.23E+04	3.61E+01
21	199.2	1	5.99E+01	4.56E-01	2.53E+04	2.92E+01
22	209.2	1	1.30E+02	7.95E-01	5.87E+04	5.44E+01
23	219.18	1	2.87E+02	1.18E+00	1.34E+05	1.47E+02
24	238.61	0.5	5.21E+02	1.52E+00	2.56E+05	4.66E+02
25	257.63	0.5	1.37E+03	4.01E+00	7.17E+05	1.40E+03
26	276.94	0.5	1.54E+03	4.27E+00	8.64E+05	1.40E+03
27	297.19	0.5	6.71E+02	3.07E+00	3.83E+05	4.66E+02
28	317.87	0.5	3.20E+02	1.14E+00	1.96E+05	4.66E+02
29	318.6	0.5	1.17E+01	2.34E-01	5.44E+03	8.27E+01
30	318.64	0.5	7.43E+00	2.22E-01	2.76E+03	5.18E+01
31	338.56	0.5	1.73E+01	3.01E-01	5.92E+03	4.38E+01
32	358.57	0.5	2.71E+01	3.68E-01	9.40E+03	5.08E+01
33	358.38	0.5	1.30E+01	2.58E-01	4.22E+03	2.68E+01
34	378.57	0.5	2.60E+01	4.12E-01	8.28E+03	2.39E+01
35	397.93	0.5	3.43E+01	4.63E-01	1.19E+04	2.76E+01
36	418.02	0.5	3.87E+01	4.79E-01	1.34E+04	3.23E+01
37	419.53	2	4.70E+01	4.67E-01	1.69E+04	6.06E+01
38	437.68	0.5	1.59E+01	3.41E-01	5.02E+03	1.67E+01
39	458.5	0.5	2.41E+01	3.33E-01	7.76E+03	2.26E+01
40	458.31	0.5	1.20E+01	2.25E-01	3.33E+03	1.44E+01
41	477.67	0.5	1.86E+01	3.09E-01	5.95E+03	1.66E+01
42	497.83	0.5	2.30E+01	3.16E-01	7.52E+03	1.93E+01
43	497.87	0.5	1.06E+01	2.34E-01	2.96E+03	1.48E+01
Last step	850.00	2	1.50E+02	5.35E-01	6.02E+04	8.34E+02
Total		41.5	6.05E+03		2.98E+06	

* blank corrected - ³He blank: 0.4 cps, ⁴He blank: 2000 cps

Capao L4-D2

Step	T (°C)	time (h)	³ He *(CPS)	±	⁴ He *(CPS)	±
1	25.07	1	2.86E-03	1.66E-02	2.27E+01	3.03E+01
2	79.18	1	1.49E+00	9.47E-02	-4.39E+02	1.66E+01
3	98.95	1	5.49E+00	1.61E-01	-2.40E+02	2.16E+01
4	119.19	1	1.25E+01	2.57E-01	-1.71E+02	2.56E+01
5	135.18	16	3.48E+01	5.05E-01	2.13E+03	4.68E+01
6	158.92	1	2.53E+00	1.07E-01	-3.21E+01	3.38E+01
7	179.23	1	7.39E+00	2.20E-01	7.67E+02	2.55E+01
8	199.25	1	1.60E+01	2.93E-01	6.53E+03	4.45E+01
9	219.26	1	8.93E+01	5.83E-01	1.34E+05	1.82E+02
10	238.72	1	6.83E+02	2.75E+00	1.18E+06	2.22E+03
11	229.23	1	3.67E+02	1.71E+00	6.54E+05	1.11E+03
12	219.19	1	1.67E+02	1.48E+00	2.98E+05	1.11E+03
13	209.24	1	7.68E+01	6.67E-01	1.46E+05	1.55E+02
14	199.24	1	3.39E+01	4.25E-01	6.46E+04	1.50E+02
15	189.62	2	3.08E+01	3.91E-01	5.79E+04	1.70E+02
16	179.54	2	1.30E+01	2.50E-01	2.40E+04	9.13E+01
17	184.62	2	1.93E+01	3.78E-01	3.68E+04	1.16E+02
18	194.61	2	4.27E+01	4.95E-01	8.27E+04	2.02E+02

Step	T (°C)	time (min)	³ He (CPS)	±	⁴ He (CPS)	±
19	204.22	1	4.38E+01	4.99E-01	8.44E+04	2.11E+02
20	214.31	1	8.31E+01	7.07E-01	1.62E+05	3.19E+02
21	224.26	1	1.37E+02	1.47E+00	2.51E+05	1.67E+03
22	234.27	1	1.88E+02	1.32E+00	3.34E+05	1.67E+03
23	238.44	0.5	8.15E+01	6.29E-01	1.52E+05	1.54E+02
24	258.61	0.5	1.41E+02	1.07E+00	2.36E+05	1.11E+03
25	278.63	0.5	5.63E+01	5.26E-01	8.95E+04	9.34E+01
26	298.62	0.5	3.47E+01	4.34E-01	4.27E+04	8.82E+01
27	318.64	0.5	3.76E+01	4.27E-01	4.58E+04	1.04E+02
28	338.72	0.5	3.69E+01	4.41E-01	4.49E+04	1.05E+02
29	338.80	0.5	1.39E+01	3.07E-01	1.68E+04	4.31E+01
30	338.40	0.5	8.40E+00	1.96E-01	1.00E+04	2.73E+01
31	358.76	0.5	1.91E+01	3.08E-01	2.34E+04	5.26E+01
32	378.55	0.5	2.62E+01	3.55E-01	3.41E+04	6.39E+01
33	378.64	0.5	1.24E+01	2.83E-01	1.50E+04	4.26E+01
34	378.63	0.5	7.63E+00	2.04E-01	9.21E+03	2.57E+01
35	398.40	0.5	1.56E+01	3.03E-01	1.94E+04	3.71E+01
36	418.36	0.5	2.04E+01	3.34E-01	2.64E+04	5.17E+01
37	419.64	2	2.19E+01	3.63E-01	2.76E+04	5.05E+01
38	438.44	0.5	7.13E+00	1.86E-01	8.49E+03	2.48E+01
39	458.20	0.5	1.20E+01	2.93E-01	1.41E+04	3.26E+01
40	458.18	0.5	6.48E+00	1.78E-01	7.16E+03	2.39E+01
41	478.00	0.5	1.07E+01	2.54E-01	1.19E+04	2.06E+01
42	497.90	0.5	1.27E+01	2.87E-01	1.50E+04	2.69E+01
43	497.89	0.5	6.53E+00	2.05E-01	6.92E+03	1.77E+01
44	517.69	0.5	9.09E+00	2.09E-01	1.01E+04	2.25E+01
Last step	850.00	2	9.83E+01	1.78E-01	1.01E+05	
Total		55.5	2.75E+03		4.48E+06	

* blank corrected - ³He blank: 0.02 cps, ⁴He black: 1300 cps

Capao L4-D1

Step	T (°C)	time (h)	³ He *(CPS)	±	⁴ He *(CPS)	±
1	23.10	1	-2.44E-03	4.63E-02	4.37E+01	6.63E+00
2	48.60	1	6.49E-01	6.03E-02	7.89E+01	8.60E+00
3	73.79	1	4.49E+00	1.55E-01	1.01E+02	9.63E+00
4	99.06	1	2.87E+01	3.97E-01	6.61E+02	9.50E+00
5	124.13	1	7.58E+01	6.12E-01	1.45E+03	1.37E+01
6	149.26	1	8.67E+01	6.20E-01	2.09E+03	1.44E+01
7	196.92	1	1.62E+02	9.22E-01	2.58E+04	4.01E+01
8	189.36	1	2.33E+01	3.62E-01	1.41E+04	2.32E+01
9	179.49	1	1.07E+01	2.43E-01	7.92E+03	2.05E+01
10	169.36	1	4.29E+00	1.34E-01	3.39E+03	1.47E+01
11	159.08	1	2.12E+00	1.10E-01	1.22E+03	8.09E+00
12	149.65	2	1.23E+00	7.83E-02	8.69E+02	8.67E+00
13	139.68	2	5.31E-01	5.13E-02	2.47E+02	7.68E+00
14	144.68	2	7.60E-01	6.45E-02	5.46E+02	7.43E+00
15	154.77	2	2.31E+00	1.19E-01	1.51E+03	1.06E+01
16	164.30	1	2.88E+00	1.25E-01	2.29E+03	1.09E+01

Step	T (°C)	time (min)	³ He (CPS)	±	⁴ He (CPS)	±
17	174.21	1	7.66E+00	2.05E-01	7.07E+03	1.64E+01
18	184.44	1	2.01E+01	3.54E-01	2.12E+04	2.77E+01
19	194.55	1	5.28E+01	5.21E-01	6.46E+04	5.76E+01
20	218.21	0.5	2.06E+02	1.85E+00	3.04E+05	5.88E+02
21	234.31	0.5	7.81E+02	2.81E+00	1.24E+06	5.88E+02
22	248.30	0.5	2.20E+03	4.84E+00	3.73E+06	2.94E+03
23	258.80	0.5	4.30E+03	7.45E+00	7.84E+06	2.94E+03
24	265.80	0.5	2.93E+03	7.03E+00	5.47E+06	2.35E+03
25	300.00	0.5	6.51E+02	2.88E+00	9.81E+05	5.88E+02
26	500.00	0.5	4.19E+02	1.91E+00	5.28E+05	5.88E+02
Last step	850.00	2	7.27E+02	2.33E-01	8.56E+05	5.88E+02
Total		28.5	1.27E+04		2.11E+07	

* blank corrected - ⁴He black: 600 cps

Capao L2

Step	T (°C)	time (h)	³ He *(CPS)	±	⁴ He *(CPS)	±
<i>1</i>	<i>23.85</i>	<i>1</i>	<i>4.00E-05</i>	<i>8.77E-03</i>	<i>8.39E+01</i>	<i>5.99E+00</i>
2	38.61	1	1.35E-01	3.27E-02	7.89E+01	1.16E+01
3	58.82	1	5.48E-01	5.20E-02	-9.10E+01	7.75E+00
4	99.12	1	1.17E+01	2.47E-01	6.12E+01	7.32E+00
5	138.80	1	3.29E+01	4.15E-01	9.49E+02	2.41E+01
6	159.10	1	3.28E+01	4.04E-01	1.83E+03	5.82E+01
7	179.00	1	3.13E+01	4.32E-01	3.46E+03	8.21E+01
8	199.30	1	3.37E+01	4.01E-01	9.58E+03	1.01E+02
9	219.10	1	1.10E+02	8.00E-01	1.39E+05	3.17E+02
10	208.90	1	7.82E+01	6.83E-01	1.28E+05	2.78E+02
11	199.20	1	4.16E+01	4.88E-01	6.81E+04	1.23E+02
12	189.20	1	1.97E+01	2.99E-01	3.18E+04	3.51E+01
13	179.10	1	8.51E+00	2.40E-01	1.37E+04	2.51E+01
14	169.60	2	7.42E+00	2.00E-01	1.17E+04	2.83E+01
15	159.60	2	3.08E+00	1.28E-01	4.58E+03	1.30E+01
16	169.60	2	7.41E+00	1.59E-01	1.15E+04	1.57E+01
17	179.60	2	1.77E+01	3.12E-01	2.88E+04	3.94E+01
18	189.50	2	4.17E+01	4.39E-01	6.87E+04	7.74E+01
19	198.90	1	4.51E+01	4.82E-01	7.57E+04	6.00E+01
20	209.20	1	9.83E+01	6.86E-01	1.66E+05	1.36E+02
21	219.20	1	1.99E+02	1.15E+00	3.26E+05	4.70E+02
22	237.70	0.5	3.39E+02	2.03E+00	5.77E+05	4.70E+02
23	257.30	0.5	7.95E+02	2.79E+00	1.27E+06	1.88E+03
24	277.40	0.5	4.43E+02	1.57E+00	6.50E+05	1.41E+03
25	297.90	0.5	5.50E+01	5.73E-01	6.01E+04	1.48E+02
26	317.90	0.5	4.09E+01	4.81E-01	4.50E+04	1.29E+02
27	318.40	0.5	1.24E+01	2.30E-01	1.37E+04	6.33E+01
28	318.60	0.5	6.87E+00	1.79E-01	8.51E+03	7.25E+01
29	338.10	0.5	1.37E+01	2.50E-01	1.61E+04	1.07E+02
30	358.00	0.5	1.89E+01	2.82E-01	2.22E+04	1.38E+02
31	358.20	0.5	8.69E+00	2.07E-01	1.02E+04	7.35E+01
32	377.40	0.5	1.40E+01	3.23E-01	1.67E+04	9.48E+01

Step	T (°C)	time (min)	³ He (CPS)	±	⁴ He (CPS)	±	
	33	397.60	0.5	1.83E+01	3.03E-01	2.14E+04	1.09E+02
	34	417.80	0.5	1.82E+01	3.57E-01	2.01E+04	3.62E+01
	35	419.50	2	1.70E+01	2.97E-01	1.98E+04	1.09E+02
	36	438.00	0.5	4.54E+00	1.28E-01	5.44E+03	5.35E+01
	37	457.70	0.5	6.70E+00	1.67E-01	7.64E+03	4.06E+01
	38	457.70	0.5	3.75E+00	1.21E-01	4.10E+03	1.82E+01
	39	477.00	0.5	5.77E+00	1.55E-01	6.56E+03	2.04E+01
	40	497.10	0.5	7.85E+00	2.05E-01	8.02E+03	1.99E+01
	41	497.30	0.5	3.53E+00	1.21E-01	4.05E+03	1.75E+01
Last step		850.00	2	1.05E+02	5.64E-01	1.16E+05	
Total			40	2.76E+03		3.99E+06	

* blank corrected - ³He blank: 0.0009 cps, ⁴He black: 900 cps

Pic 22 BG

Step	T (°C)	time (h)	³ He *(CPS)	±	⁴ He *(CPS)	±
	1	22.00	1	-6.50E-02	3.85E-03	7.53E+01
	2	22.00	1	-1.17E-01	2.79E-03	-5.76E+01
	3	22.00	1	1.37E-01	-1.80E-02	-3.03E+01
	4	22.00	1	1.58E-01	8.31E-02	-2.90E+01
	5	22.00	1	6.64E-01	1.49E-02	8.98E+01
	6	24.43	1	7.31E-03	2.39E-02	-4.85E+01
	7	50.00	1	3.72E+00	-2.54E-02	-3.97E+01
	8	74.78	1	1.92E+01	2.58E-02	4.00E-02
	9	100.00	1	6.85E+01	3.33E-02	9.34E+02
	10	125.02	1	1.37E+02	4.73E-02	2.43E+03
	11	149.97	1	1.81E+02	6.03E-02	6.07E+03
	12	174.97	1	2.73E+02	2.99E-01	1.73E+04
	13	199.01	1	8.98E+02	2.01E+00	9.66E+04
	14	189.13	1	5.93E+02	1.40E+00	7.32E+04
	15	179.84	1	2.85E+02	6.89E-01	3.62E+04
	16	170.00	1	1.26E+02	3.23E-01	1.61E+04
	17	159.94	1	5.17E+01	1.23E-01	6.43E+03
	18	150.02	2	4.08E+01	7.05E-02	5.31E+03
	19	139.99	2	1.52E+01	-3.42E-02	1.17E+03
	20	145.00	2	2.58E+01	7.57E-02	3.19E+03
	21	154.99	2	6.72E+01	1.58E-01	8.55E+03
	22	164.97	1	8.10E+01	1.11E-01	1.02E+04
	23	174.90	1	1.88E+02	4.50E-01	2.44E+04
	24	184.97	1	4.43E+02	1.14E+00	5.85E+04
	25	193.62	1	8.47E+02	2.11E+00	1.12E+05
	26	218.18	0.5	1.71E+03	4.24E+00	2.33E+05
	27	236.88	0.5	1.43E+03	3.81E+00	1.99E+05
	28	258.97	0.5	2.11E+02	4.65E-01	2.87E+04
	29	278.98	0.5	1.10E+02	2.89E-01	1.46E+04
	30	297.87	0.5	1.17E+02	2.08E-01	1.61E+04
	31	323.44	0.5	1.58E+02	4.41E-01	2.16E+04
	32	345.98	0.5	1.50E+02	3.88E-01	2.10E+04
	33	373.84	0.5	1.31E+02	3.58E-01	1.88E+04

Step	T (°C)	time (min)	³ He (CPS)	±	⁴ He (CPS)	±
	34	397.92	0.5	1.19E+02	2.56E-01	1.68E+04
	35	450.48	0.5	5.72E+02	1.38E+00	7.89E+04
Last step		850.00	2	2.16E+02	2.91E-01	4.36E+04
Total		36	9.27E+03		1.17E+06	

* blank corrected - ³He blank: 0.7 cps, ⁴He blank: 445 cps

RS 3.4 TLcM

Step	T (°C)	time (h)	³ He *(CPS)	±	⁴ He *(CPS)	±
1	22.00	1	2.11E-01	1.08E-01	5.37E+02	
2	24.35	1	1.51E-02	-3.26E-02	-4.87E+02	
3	50.00	1	3.41E+00	2.13E-02	3.43E+02	
4	75.02	1	3.22E+01	7.80E-02	7.79E+02	
5	99.97	1	1.34E+02	8.60E-02	1.17E+03	
6	125.03	1	3.24E+02	8.07E-02	2.93E+03	
7	149.99	1	4.18E+02	4.81E-02	3.24E+03	
8	174.94	1	5.10E+02	7.10E-02	5.94E+03	
9	199.48	1	6.45E+02	2.29E-01	9.00E+03	
10	189.96	1	1.67E+02	6.65E-02	2.20E+03	
11	179.98	1	6.98E+01	4.92E-02	2.96E+02	
12	169.98	1	3.18E+01	5.12E-02	6.53E+02	
13	159.99	1	1.32E+01	8.66E-02	-3.17E+01	
14	150.00	2	1.02E+01	6.28E-02	6.60E+02	
15	140.00	2	3.85E+00	1.24E-02	-3.96E+02	
16	145.01	2	6.28E+00	-4.52E-02	6.39E+02	
17	155.00	2	1.70E+01	3.19E-02	6.89E+02	
18	165.02	1	2.14E+01	7.84E-02	8.36E+02	
19	174.99	1	4.79E+01	4.95E-02	1.25E+03	
20	184.97	1	1.19E+02	1.23E-01	2.46E+03	
21	194.90	1	2.57E+02	1.30E-01	3.60E+03	
22	203.95	1	5.62E+02	1.59E-01	7.26E+03	
23	218.74	0.5	8.02E+02	3.21E-01	1.22E+04	
24	237.41	0.5	2.27E+03	8.48E-01	3.45E+04	
25	256.62	0.5	2.38E+03	7.77E-01	3.64E+04	
26	278.75	0.5	2.60E+02	9.24E-02	4.60E+03	
27	298.21	0.5	9.71E+01	3.82E-02	1.51E+03	
28	318.93	0.5	1.18E+02	1.05E-01	2.10E+03	
29	338.57	0.5	1.20E+02	9.86E-02	2.52E+03	
30	337.13	0.5	4.18E+01	1.09E-01	9.08E+02	
31	339.77	0.5	2.65E+01	2.03E-02	9.78E+02	
32	358.98	0.5	5.45E+01	6.33E-02	1.17E+03	
33	378.93	0.5	8.68E+01	6.16E-02	1.03E+03	
34	378.77	0.5	4.00E+01	6.45E-02	8.48E+02	
35	379.80	0.5	2.73E+01	8.97E-02	6.37E+02	
36	398.97	0.5	5.96E+01	4.97E-02	1.22E+03	
37	417.10	0.5	8.79E+01	-7.63E-03	1.98E+03	
38	419.59	2	1.06E+02	4.02E-02	1.34E+03	
39	439.59	0.5	3.68E+01	-2.23E-03	2.33E+03	
40	458.74	0.5	5.51E+01	4.90E-02	-2.97E+02	

Step	T (°C)	time (min)	³ He (CPS)	±	⁴ He (CPS)	±
	41	457.95	0.5	2.36E+01	7.47E-02	-1.10E+03
	42	479.46	0.5	3.86E+01	1.08E-02	6.89E+02
	43	498.70	0.5	4.19E+01	1.07E-01	-1.35E+03
	44	499.23	0.5	1.93E+01	7.07E-02	5.90E+02
Last step		850.00	2	2.48E+02	1.17E+00	6.98E+03
Total		40.5	1.04E+04		1.55E+05	

* blank corrected - ³He blank: 0.5 cps, ⁴He blank: 2300 cps

Pic 22 YG

Step	T (°C)	time (h)	³ He *(CPS)	±	⁴ He *(CPS)	±
	1	16.00	1	-3.95E-02	1.50E-01	9.91E+01
	2	25.00	1	1.96E-01	3.22E-02	-6.07E+00
	3	50.02	1	4.23E+00	5.40E-02	1.07E+03
	4	75.04	1	3.87E+01	3.02E-02	1.22E+03
	5	100.04	1	1.19E+02	1.27E-01	1.29E+03
	6	124.98	1	2.88E+02	1.52E-01	4.14E+03
	7	150.03	1	5.12E+02	3.24E-01	1.30E+04
	8	174.06	1	8.60E+02	8.13E-01	3.80E+04
	9	198.66	1	2.17E+03	2.97E+00	1.47E+05
	10	188.92	1	8.18E+02	1.28E+00	6.08E+04
	11	179.80	1	3.53E+02	5.65E-01	2.59E+04
	12	170.00	1	1.41E+02	2.87E-01	1.08E+04
	13	160.04	1	5.26E+01	2.40E-01	4.31E+03
	14	150.03	2	4.35E+01	1.69E-01	3.81E+03
	15	140.00	2	1.64E+01	1.60E-01	1.85E+03
	16	145.00	2	2.57E+01	1.15E-01	2.51E+03
	17	155.00	2	6.76E+01	2.05E-01	4.18E+03
	18	165.00	1	8.45E+01	2.62E-01	6.46E+03
	19	175.03	1	1.91E+02	3.33E-01	1.50E+04
	20	184.94	1	4.14E+02	7.39E-01	3.24E+04
	21	194.08	1	7.28E+02	1.23E+00	5.82E+04
	22	218.28	0.5	1.34E+03	2.25E+00	1.08E+05
	23	237.51	0.5	1.55E+03	2.60E+00	1.23E+05
	24	258.57	0.5	4.13E+02	6.76E-01	3.27E+04
	25	278.41	0.5	2.09E+02	3.65E-01	1.74E+04
	26	298.88	0.5	2.17E+02	3.46E-01	1.70E+04
	27	318.51	0.5	2.14E+02	4.72E-01	1.67E+04
	28	337.08	0.5	2.43E+02	4.80E-01	2.07E+04
	29	338.90	0.5	9.89E+01	2.42E-01	9.07E+03
	30	338.92	0.5	4.49E+01	1.05E-01	2.82E+03
	31	359.13	0.5	7.66E+01	1.41E-01	5.04E+03
	32	378.10	0.5	8.65E+01	1.87E-01	6.48E+03
	33	379.57	0.5	4.33E+01	5.25E-02	2.45E+03
	34	379.46	0.5	2.76E+01	-5.72E-02	1.70E+03
	35	397.64	0.5	6.54E+01	1.36E-01	4.34E+03
	36	418.72	0.5	1.02E+02	2.15E-01	4.72E+03
	37	418.74	2	1.17E+02	2.26E-01	8.50E+03
	38	438.62	0.5	3.69E+01	1.07E-01	2.36E+03

Step	T (°C)	time (min)	³ He (CPS)	±	⁴ He (CPS)	±
	39	456.43	0.5	5.35E+01	1.44E-01	4.03E+03
	40	459.23	0.5	2.61E+01	1.50E-01	1.49E+03
	41	475.30	0.5	3.99E+01	1.59E-01	2.65E+03
	42	498.62	0.5	5.07E+01	2.02E-01	3.45E+03
	43	497.51	0.5	2.14E+01	-5.03E-02	1.17E+03
Last step	850.00	2	2.94E+02	1.17E+00	5.66E+05	
Total		39.5	1.23E+04		1.39E+06	

* blank corrected - ³He blank: 0.5 cps, ⁴He blank: 3900 cps

IBH 13 09h

Step	T (°C)	time (h)	³ He *(CPS)	±	⁴ He *(CPS)	±
1	24.00	1	1.07E+02	6.74E-01	2.24E+04	4.12E+01
2	24.00	1	-1.71E-01	5.98E-02	-6.41E+01	2.13E+01
3	23.60	1	-3.05E-01	5.37E-02	-2.86E+02	1.26E+01
4	23.00	1	4.75E-01	6.66E-02	3.48E+02	3.75E+01
5	38.68	1	7.54E-01	6.87E-02	-4.51E+02	1.21E+01
6	59.02	1	4.52E+00	1.33E-01	-3.94E+02	9.35E+00
7	79.39	1	1.61E+01	2.66E-01	-1.01E+02	1.28E+01
8	98.94	1	3.89E+01	4.38E-01	4.56E+02	1.18E+01
9	119.03	1	6.22E+01	6.50E-01	9.56E+02	1.73E+01
10	138.84	1	8.43E+01	5.68E-01	2.38E+03	3.80E+01
11	158.96	1	1.02E+02	6.89E-01	5.21E+03	7.12E+01
12	179.22	1	1.30E+02	7.33E-01	1.03E+04	8.12E+01
13	199.22	1	1.62E+02	9.12E-01	2.03E+04	1.15E+02
14	219.10	1	3.07E+02	1.27E+00	5.97E+04	2.00E+02
15	209.26	1	1.55E+02	9.16E-01	3.32E+04	1.27E+02
16	199.27	1	7.81E+01	6.75E-01	1.67E+04	6.68E+01
17	189.22	1	3.54E+01	3.83E-01	7.24E+03	2.78E+01
18	179.25	1	1.52E+01	2.79E-01	2.87E+03	1.55E+01
19	169.62	2	1.35E+01	2.60E-01	2.40E+03	1.11E+01
20	159.44	2	4.50E+00	1.60E-01	5.72E+02	1.14E+01
21	169.43	2	1.28E+01	2.31E-01	2.43E+03	1.19E+01
22	179.66	2	3.36E+01	4.29E-01	6.70E+03	1.98E+01
23	189.52	2	7.74E+01	6.68E-01	1.66E+04	3.10E+01
24	199.29	1	8.83E+01	6.17E-01	1.82E+04	2.99E+01
25	219.07	1	3.38E+02	1.35E+00	7.63E+04	1.89E+02
26	237.68	0.5	5.17E+02	1.92E+00	1.23E+05	2.19E+02
27	256.90	0.5	1.03E+03	3.17E+00	2.52E+05	4.47E+02
28	276.40	0.5	1.00E+03	2.72E+00	2.96E+05	8.94E+02
29	296.84	0.5	4.88E+02	2.00E+00	1.47E+05	2.05E+02
30	317.55	0.5	1.49E+02	9.35E-01	4.75E+04	1.07E+02
31	318.20	0.5	2.82E+01	3.69E-01	1.18E+04	6.84E+01
32	338.20	0.5	4.17E+01	4.22E-01	1.97E+04	1.13E+02
33	358.33	0.5	5.31E+01	5.33E-01	2.78E+04	1.22E+02
34	358.28	0.5	2.61E+01	3.87E-01	1.45E+04	6.07E+01
35	377.52	0.5	4.46E+01	5.39E-01	2.37E+04	6.99E+01
36	397.88	0.5	5.89E+01	5.34E-01	3.24E+04	1.22E+02
37	417.55	0.5	6.19E+01	5.70E-01	3.94E+04	1.51E+02

Step	T (°C)	time (min)	³ He (CPS)	±	⁴ He (CPS)	±	
	38	419.52	2	6.72E+01	6.00E-01	5.82E+04	1.60E+02
	39	437.84	0.5	2.39E+01	3.79E-01	2.02E+04	4.57E+01
	40	457.95	0.5	3.78E+01	4.21E-01	3.30E+04	6.43E+01
	41	457.96	0.5	2.00E+01	3.57E-01	1.96E+04	2.85E+01
	42	477.97	0.5	3.70E+01	4.22E-01	3.52E+04	4.18E+01
	43	478.00	0.5	1.98E+01	2.53E-01	2.08E+04	3.15E+01
	44	497.95	0.5	3.35E+01	3.94E-01	3.36E+04	3.58E+01
	45	497.22	0.5	1.82E+01	3.02E-01	2.06E+04	3.46E+01
Last step	850.00	2.0	3.71E+02	9.33E-01	8.50E+05	1.44E+03	
Total		42.5	5.90E+03		2.41E+06		

* blank corrected - ³He blank: 0.7 cps, ⁴He blank: 1435 cps

Pic 21

Step	T (°C)	time (h)	³ He *(CPS)	±	⁴ He *(CPS)	±
1	23.00	1	6.68E+01	6.69E-01	1.25E+04	3.35E+01
2	23.00	1	1.69E-01	5.58E-02	3.84E+02	2.57E+01
3	23.00	1	-5.03E-02	4.41E-02	-6.63E+01	1.85E+01
4	23.00	1	-1.86E-01	3.17E-02	-3.16E+02	1.18E+01
5	38.69	1	8.00E-01	7.43E-02	-4.71E+02	8.40E+00
6	58.88	1	5.56E+00	1.75E-01	-3.18E+02	1.24E+01
7	79.41	1	1.97E+01	3.57E-01	-6.14E+01	1.18E+01
8	99.13	1	5.18E+01	5.96E-01	5.50E+02	1.79E+01
9	119.28	1	8.71E+01	6.04E-01	1.47E+03	2.60E+01
10	139.18	1	1.02E+02	8.32E-01	2.86E+03	3.94E+01
11	159.20	1	1.13E+02	7.52E-01	5.29E+03	7.27E+01
12	179.21	1	1.41E+02	8.53E-01	1.09E+04	9.83E+01
13	198.82	1	2.63E+02	1.15E+00	3.18E+04	7.60E+01
14	218.07	1	1.39E+03	4.73E+00	1.82E+05	9.20E+02
15	208.85	1	8.53E+02	2.84E+00	1.13E+05	1.78E+02
16	199.23	1	3.81E+02	1.40E+00	4.80E+04	1.30E+02
17	189.16	1	1.64E+02	8.50E-01	2.01E+04	1.05E+02
18	179.22	1	6.95E+01	5.58E-01	8.09E+03	5.11E+01
19	169.62	2	5.94E+01	5.87E-01	6.45E+03	2.65E+01
20	159.60	2	2.43E+01	3.92E-01	2.36E+03	1.41E+01
21	169.56	2	6.07E+01	5.93E-01	6.33E+03	2.01E+01
22	179.58	2	1.41E+02	8.44E-01	1.54E+04	3.28E+01
23	189.62	2	3.00E+02	1.29E+00	3.35E+04	7.57E+01
24	199.28	1	3.10E+02	1.21E+00	3.22E+04	5.07E+01
25	218.76	1	9.79E+02	3.03E+00	1.02E+05	2.12E+02
26	237.50	0.5	1.02E+03	2.64E+00	8.83E+04	1.54E+02
27	257.33	0.5	1.43E+03	3.77E+00	8.42E+04	1.29E+02
28	277.29	0.5	7.50E+02	2.13E+00	3.90E+04	7.41E+01
29	297.54	0.5	1.45E+02	8.96E-01	1.74E+04	7.44E+01
30	317.60	0.5	1.45E+02	1.02E+00	1.76E+04	1.01E+02
31	318.31	0.5	6.37E+01	5.40E-01	7.08E+03	3.88E+01
32	338.18	0.5	1.13E+02	7.08E-01	1.34E+04	9.44E+01
33	357.79	0.5	1.37E+02	7.04E-01	1.58E+04	1.01E+02
34	358.39	0.5	6.21E+01	5.33E-01	6.69E+03	5.13E+01

Step	T (°C)	time (min)	³ He (CPS)	±	⁴ He (CPS)	±	
	35	358.39	0.5	6.21E+01	5.33E-01	6.69E+03	5.13E+01
	36	377.50	0.5	1.08E+02	6.28E-01	1.21E+04	6.48E+01
	37	397.50	0.5	1.36E+02	8.19E-01	1.63E+04	9.83E+01
	38	417.47	0.5	1.30E+02	9.50E-01	1.61E+04	9.64E+01
	39	419.49	2	1.28E+02	6.68E-01	1.59E+04	1.13E+02
	40	437.87	0.5	3.90E+01	4.37E-01	4.94E+03	4.23E+01
	41	457.79	0.5	5.62E+01	5.60E-01	7.13E+03	4.15E+01
	42	457.90	0.5	2.62E+01	3.34E-01	3.23E+03	2.66E+01
	43	477.86	0.5	4.09E+01	4.07E-01	4.82E+03	3.67E+01
	44	477.90	0.5	1.97E+01	2.88E-01	2.31E+03	1.88E+01
	45	497.66	0.5	3.24E+01	3.83E-01	3.28E+03	2.13E+01
	46	497.90	0.5	1.65E+01	2.89E-01	1.85E+03	1.81E+01
	47	497.36	0.5	1.11E+01	2.08E-01	1.18E+03	1.47E+01
Last step	850.00	2	4.74E+02	1.69E+00	1.22E+06	9.71E+02	
Total		43.5	1.07E+04		2.22E+06		

* blank corrected - ³He blank: 0.4 cps, ⁴He blank: 1335 cps

LynP02-09-A1

Step	T (°C)	time (h)	³ He *(CPS)	±	⁴ He *(CPS)	±	
	1	50.12	5	2.44E+01	1.36E+00	1.65E+04	1.47E+02
	2	65.28	5	2.36E+01	9.22E-01	8.73E+03	2.06E+02
	3	80.75	4	5.92E+01	1.83E+00	6.71E+03	1.47E+02
	4	101.24	2	1.12E+02	7.96E-01	5.36E+03	3.18E+02
	5	127.00	2	2.86E+02	4.44E+00	1.79E+04	1.62E+02
	6	150.91	1	2.91E+02	3.58E+00	2.48E+04	2.63E+02
	7	174.05	1	5.09E+02	8.62E+00	7.45E+04	4.71E+02
	8	198.93	1	8.83E+02	5.79E+00	2.62E+05	2.72E+02
	9	199.71	1	7.62E+02	5.99E+00	3.13E+05	
	10	199.80	1	7.34E+02	8.31E+00	3.13E+05	
	11	189.78	1	3.15E+02	5.62E+00	1.41E+05	4.26E+02
	12	179.94	2	3.01E+02	3.15E+00	1.35E+05	3.80E+02
	13	169.96	3	2.15E+02	3.61E+00	9.84E+04	4.06E+02
	14	159.96	3	8.20E+01	1.64E+00	3.80E+04	9.97E+01
	15	149.97	4	3.84E+01	1.24E+00	1.75E+04	5.63E+01
	16	139.98	5	1.74E+01	6.69E-01	7.69E+03	8.10E+01
	17	174.97	4	4.16E+02	2.93E+00	1.75E+05	5.52E+02
	18	194.94	3	1.25E+03	7.05E+00	5.42E+05	
	19	204.71	2	1.61E+03	1.14E+01	7.04E+05	
	20	209.40	1	1.33E+03	8.68E+00	5.77E+05	
	21	214.41	1	1.54E+03	6.14E+00	6.80E+05	
	22	219.38	1	1.54E+03	1.08E+01	6.70E+05	
	23	224.50	1	1.11E+03	8.76E+00	4.96E+05	
	24	229.69	1	5.20E+02	2.69E+00	2.56E+05	
	25	234.70	1	2.80E+02	2.08E+00	1.38E+05	2.77E+02
	26	239.85	1	1.37E+02	2.10E+00	6.99E+04	1.36E+02
	27	244.84	1	7.31E+01	2.12E+00	3.66E+04	9.56E+01
Last step				2.40E+03		1.62E+06	

Step	T (°C)	time (min)	³ He (CPS)	±	⁴ He (CPS)	±
Total		58.0	1.69E+04		7.44E+06	

* blank corrected - ³He blank: 0.05 cps, ⁴He black: 3800 cps

LynP02-09-A2

Step	T (°C)	time (h)	³ He *(CPS)	±	⁴ He *(CPS)	±
1	22.69	1	6.84E+00	1.24E+00	9.67E+04	2.06E+04
2	158.36	0.62	3.44E+01	1.93E+00	8.53E+04	6.99E+02
3	168.83	0.67	-3.67E-02	2.93E-02	-6.96E+02	8.13E-01
4	178.16	0.42	3.06E+02	2.60E+00	3.36E+04	2.80E+02
5	178.13	0.58	2.46E+02	4.19E+00	2.94E+04	2.93E+02
6	186.19	0.29	1.89E+02	3.05E+00	2.41E+04	2.25E+02
7	187.64	0.36	2.02E+02	1.33E+00	2.82E+04	3.18E+02
8	187.42	0.43	1.99E+02	3.44E+00	3.20E+04	2.75E+02
9	188.07	0.49	2.41E+02	3.54E+00	4.30E+04	2.14E+02
10	187.63	0.56	2.74E+02	1.85E+00	5.18E+04	3.61E+02
11	188.29	0.62	3.32E+02	4.16E+00	7.00E+04	3.56E+02
12	197.99	0.64	8.20E+02	6.07E+00	1.80E+05	3.49E+02
13	205.23	0.33	8.83E+02	4.93E+00	2.04E+05	3.64E+02
14	202.17	0.39	1.04E+03	1.11E+01	2.49E+05	3.41E+02
15	205.74	0.44	1.42E+03	4.23E+00	3.32E+05	5.65E+02
16	207.37	0.51	1.84E+03	9.25E+00	4.37E+05	
17	216.55	0.53	3.62E+03	1.20E+01	8.59E+05	
18	217.79	0.65	4.48E+03	1.99E+01	1.04E+06	
19	224.23	0.36	3.98E+03	1.31E+01	9.16E+05	
20	226.45	0.42	4.48E+03	1.68E+01	1.04E+06	
21	226.8	0.5	4.14E+03	1.60E+01	9.50E+05	
22	244.59	0.36	6.50E+03	1.78E+01	1.48E+06	
23	245.46	0.52	4.38E+03	7.61E+00	9.75E+05	
24	254.49	0.37	2.49E+03	2.17E+01	5.96E+05	1.21E+03
25	257.73	0.56	1.68E+03	7.64E+00	3.73E+05	7.04E+02
26	266.13	0.51	4.74E+02	3.28E+00	1.05E+05	1.69E+02
27	267.27	0.51	2.04E+02	2.83E+00	4.46E+04	1.32E+02
28	329.6	1	4.21E+03	1.26E+01	9.54E+05	
Last step			4.16E+03	8.70E+00	1.19E+06	
Total		14.6	5.28E+04		1.24E+07	

* blank corrected - ⁴He black: 700 cps

LynP02-09-A3

Step	T (°C)	time (h)	³ He *(CPS)	±	⁴ He *(CPS)	±
1	39.22	1	3.71E+00	5.03E-01	7.88E+03	2.26E+02
2	59.4	1	1.66E+01	8.58E-01	9.56E+03	1.31E+02
3	155.65	0.62	1.80E+03	9.08E+00	6.10E+04	7.59E+02
4	168.38	0.67	8.30E+02	5.91E+00	5.65E+04	3.86E+02
5	174.76	0.42	4.79E+02	6.32E+00	4.65E+04	1.50E+02
6	177.18	0.58	4.24E+02	4.23E+00	4.77E+04	3.04E+02
7	186.17	0.29	3.11E+02	2.76E+00	4.09E+04	3.15E+02
8	186.07	0.36	2.87E+02	3.18E+00	4.27E+04	2.69E+02
9	187.94	0.43	2.99E+02	8.63E-01	5.12E+04	1.73E+02

Step	T (°C)	time (min)	³ He (CPS)	±	⁴ He (CPS)	±
10	187.92	0.49	2.92E+02	1.35E+00	5.56E+04	3.03E+02
11	187.97	0.56	2.98E+02	4.31E+00	6.41E+04	2.71E+02
12	188.31	0.62	3.25E+02	3.78E+00	7.82E+04	2.00E+02
13	197.79	0.64	6.99E+02	5.72E+00	1.81E+05	3.43E+02
14	205.32	0.33	6.69E+02	3.94E+00	1.87E+05	3.37E+02
15	206.06	0.39	8.47E+02	5.97E+00	2.43E+05	2.15E+02
16	205.65	0.44	9.43E+02	4.18E+00	2.90E+05	4.21E+02
17	205.97	0.51	1.07E+03	6.30E+00	3.22E+05	
18	215.47	0.53	2.28E+03	1.12E+01	6.88E+05	
19	215.52	0.65	2.90E+03	1.36E+01	8.71E+05	
20	221.46	0.36	2.58E+03	3.52E+00	7.84E+05	
21	223.47	0.42	3.08E+03	1.25E+01	9.36E+05	
22	225.72	0.5	3.82E+03	1.24E+01	1.15E+06	
23	240.84	0.36	6.13E+03	3.01E+01	1.89E+06	
24	245.08	0.52	4.02E+03	1.78E+02	1.32E+06	
25	255.58	0.37	4.19E+03	1.03E+01	1.28E+06	
26	256.5	0.56	2.28E+03	1.10E+01	6.69E+05	
27	266.68	0.51	1.36E+03	1.23E+01	3.71E+05	6.25E+02
28	267.36	0.51	4.76E+02	1.70E+00	1.28E+05	1.66E+02
29	311.94	1	2.23E+03	8.05E+00	6.36E+05	
Last step			9.68E+03	7.22E+01	4.72E+06	
Total		15.6	5.46E+04		1.72E+07	

* blank corrected - ⁴He black: 700 cps

BAH F124 114

Step	T (°C)	time (h)	³ He (CPS)	±	⁴ He (CPS)	±
1	50.00	5	2.90E-01	2.00E-02	BDL	BDL
2	65.00	5	1.20E+00	3.00E-02	BDL	BDL
3	80.00	4	2.50E+00	3.00E-02	BDL	BDL
4	100.00	2	3.93E+00	4.00E-02	BDL	BDL
5	125.00	2	1.81E+01	9.00E-02	3.20E+00	0.00E+00
6	150.00	1	2.02E+01	9.00E-02	1.41E+01	1.00E-01
7	175.00	1	3.05E+01	1.30E-01	1.11E+02	1.00E-01
8	200.00	1	3.72E+01	1.30E-01	6.11E+02	1.00E-01
9	200.00	1	2.16E+01	1.00E-01	6.35E+02	1.00E-01
10	200.00	1	1.88E+01	1.00E-01	7.20E+02	1.00E-01
11	190.00	1	8.97E+00	6.00E-02	3.44E+02	1.00E-01
12	180.00	2	7.51E+00	5.00E-02	2.84E+02	1.00E-01
13	170.00	3	4.42E+00	4.00E-02	1.55E+02	0.00E+00
14	160.00	3	1.77E+00	3.00E-02	5.91E+01	0.00E+00
15	150.00	4	8.20E-01	2.00E-02	2.85E+01	0.00E+00
16	140.00	5	3.00E-01	2.00E-02	1.15E+01	0.00E+00
17	175.00	4	9.75E+00	5.00E-02	4.03E+02	1.00E-01
18	195.00	3	3.94E+01	1.50E-01	1.87E+03	2.00E-01
19	205.00	2	5.78E+01	1.60E-01	2.93E+03	1.00E-01
20	210.00	1	4.18E+01	1.10E-01	2.18E+03	1.00E-01
21	215.00	1	5.69E+01	1.60E-01	3.02E+03	1.00E-01

Step	T (°C)	time (min)	³ He (CPS)	±	⁴ He (CPS)	±	
	22	220.00	1	7.12E+01	1.80E-01	3.79E+03	2.00E-01
	23	225.00	1	8.27E+01	1.90E-01	4.47E+03	2.00E-01
	24	230.00	1	9.11E+01	2.00E-01	4.97E+03	2.00E-01
	25	235.00	1	9.35E+01	1.90E-01	5.05E+03	2.00E-01
	26	240.00	1	9.51E+01	2.00E-01	5.09E+03	2.00E-01
	27	245.00	1	8.93E+01	1.90E-01	4.64E+03	2.00E-01
Last step		1300	0.5	2.78E+02	3.30E-01	1.47E+04	4.00E-01
Total			59	1.18E+03		5.61E+04	

BAH F124 111.2

Step	T (°C)	time (h)	³ He (CPS)	±	⁴ He (CPS)	±	
1	50	5	9.50E-01	2.00E-02	BDL	BDL	
2	65	5	2.27E+00	3.00E-02	BDL	BDL	
3	80	4	2.29E+00	3.00E-02	BDL	BDL	
4	100	2	1.79E+00	2.00E-02	8.00E-01	0.00E+00	
5	125	2	3.50E+00	4.00E-02	3.10E+00	0.00E+00	
6	150	1	2.66E+00	3.00E-02	8.10E+00	0.00E+00	
7	175	1	3.78E+00	5.00E-02	4.08E+01	0.00E+00	
8	200	1	4.77E+00	5.00E-02	2.64E+02	1.00E-01	
9	200	1	2.61E+00	3.00E-02	2.86E+02	1.00E-01	
10	200	1	2.08E+00	4.00E-02	3.19E+02	1.00E-01	
11	190	1	9.50E-01	2.00E-02	1.50E+02	0.00E+00	
12	180	2	7.90E-01	2.00E-02	1.13E+02	1.00E-01	
13	170	3	4.70E-01	1.00E-02	6.43E+01	0.00E+00	
14	160	3	1.40E-01	1.00E-02	2.10E+01	0.00E+00	
15	150	4	4.00E-02	1.00E-02	9.50E+00	0.00E+00	
16	140	5	2.00E-02	1.00E-02	3.00E+00	0.00E+00	
17	175	4	7.50E-01	2.00E-02	1.29E+02	1.00E-01	
18	195	3	3.49E+00	3.00E-02	8.22E+02	1.00E-01	
19	205	2	5.31E+00	4.00E-02	1.32E+03	1.00E-01	
20	210	1	4.02E+00	4.00E-02	9.61E+02	1.00E-01	
21	215	1	5.45E+00	5.00E-02	1.32E+03	1.00E-01	
22	220	1	7.26E+00	5.00E-02	1.75E+03	2.00E-01	
23	225	1	9.69E+00	6.00E-02	2.24E+03	1.00E-01	
24	230	1	1.24E+01	6.00E-02	2.79E+03	1.00E-01	
25	235	1	1.52E+01	8.00E-02	3.36E+03	1.00E-01	
26	240	1	1.75E+01	9.00E-02	3.93E+03	2.00E-01	
27	245	1	1.94E+01	8.00E-02	4.23E+03	2.00E-01	
28	250	1	2.10E+01	9.00E-02	4.26E+03	2.00E-01	
Last step		1300	0.5	8.15E+01	2.00E-01	2.43E+04	5.00E-01
Total			0.5	2.32E+02		5.26E+04	

**Chapter 4: Ages And Evolution Of Diachronous Erosion Surfaces In The Amazon: The
(U-Th)/He And Cosmogenic ^3He Records**

Appendix

EA1: Electron Microprobe Analysis

Appendix 1: Electron Microprobe Analyses of goethites from Carajás																										
INDEX	No.	O	Na	K	V	Co	Mg	P	Cr	Fe	Al	S	Ni	Mn	Si	Pb	Cu	Ti	Ca	Zn	Ba	Sr	Total	Date	Sample	
1	16	37.34	0.00	0.00	0.05	0.09	0.00	1.02	0.01	58.34	0.06	0.03	0.00	0.02	0.97	0.05	2.17	0.00	0.00	0.02			100.16	20-07-16	BAH-100 black gt	
2	17	37.54	0.00	0.00	0.00	0.02	0.03	0.96	0.04	58.73	0.05	0.00	0.02	0.02	0.98	0.00	1.97	0.02	0.00	0.02			100.38	20-07-16	BAH-100 black gt	
3	18	37.64	0.00	0.00	0.00	0.12	0.01	1.01	0.00	59.04	0.05	0.01	0.00	0.05	0.79	0.07	1.58	0.00	0.00	0.03			100.39	20-07-16	BAH-100 black gt	
4	19	37.01	0.00	0.00	0.00	0.03	0.01	0.68	0.01	58.04	0.06	0.00	0.00	0.00	1.27	0.00	2.56	0.00	0.00	0.00			99.67	20-07-16	BAH-100 black gt	
5	20	36.45	0.01	0.01	0.02	0.01	0.00	0.38	0.03	60.64	0.00	0.00	0.04	0.02	0.38	0.02	0.84	0.01	0.00	0.00			98.85	20-07-16	BAH-100 black gt	
6	21	36.73	0.00	0.00	0.00	0.05	0.00	0.63	0.00	58.77	0.01	0.01	0.04	0.00	0.85	0.00	1.73	0.03	0.00	0.04			98.88	20-07-16	BAH-100 black gt	
7	22	37.62	0.00	0.00	0.02	0.05	0.00	0.89	0.03	59.74	0.05	0.02	0.00	0.01	1.08	0.04	2.01	0.05	0.00	0.00			101.60	20-07-16	BAH-100 black gt	
8	23	37.19	0.00	0.00	0.00	0.08	0.02	0.95	0.00	60.75	0.14	0.02	0.00	0.01	0.93	0.00	1.44	0.00	0.00	0.00			101.52	20-07-16	BAH-100 black gt	
9	24	37.13	0.00	0.00	0.00	0.07	0.02	0.80	0.00	59.11	0.10	0.03	0.00	0.04	1.22	0.03	2.08	0.00	0.00	0.01			100.63	20-07-16	BAH-100 black gt	
10	25	38.05	0.00	0.00	0.04	0.05	0.00	1.01	0.02	59.77	0.15	0.03	0.00	0.04	0.86	0.07	1.33	0.00	0.00	0.00			101.43	20-07-16	BAH-100 black gt	
11	5511	34.03	0.00	0.00	0.02	0.00	0.10	1.65	0.01	57.89	2.10	0.08	0.02	1.83	0.24	0.03	2.34	0.02	0.18	0.08			100.63	10/11/16	BA-93-07	
12	5512	34.17	0.02	0.00	0.01	0.03	0.07	1.62	0.04	58.58	1.89	0.05	0.02	1.72	0.25	0.00	2.36	0.00	0.16	0.01			101.02	10/11/16	BA-93-07	
13	5517	33.13	0.07	0.00	0.00	0.00	0.06	1.65	0.00	58.10	1.87	0.07	0.02	1.82	0.25	0.09	2.35	0.02	0.14	0.13			99.76	10/11/16	BA-93-07 (continued)	
14	5518	32.56	0.02	0.00	0.00	0.05	0.07	1.61	0.00	57.83	2.00	0.07	0.00	1.82	0.27	0.00	2.08	0.00	0.17	0.17			98.72	10/11/16	BA-93-07 (continued)	
15	5519	39.08	0.01	0.03	0.00	0.03	0.00	5.61	0.00	30.46	8.06	0.19	0.00	0.80	0.03	0.14	1.84	0.02	0.63	0.00			86.93	10/11/16	BA-93-07 (continued)	
16	5520	33.45	0.03	0.00	0.01	0.00	0.09	1.69	0.00	58.04	1.80	0.07	0.00	2.27	0.32	0.02	1.81	0.02	0.19	0.22			100.02	10/11/16	BA-93-07 (continued)	
17	5521	32.16	0.07	0.02	0.00	0.03	0.07	1.48	0.00	57.35	1.57	0.10	0.00	2.64	0.38	0.02	1.98	0.01	0.18	0.17			98.24	10/11/16	BA-93-07 (continued)	
18	5522	29.76	0.05	0.00	0.02	0.00	0.06	1.61	0.00	55.54	1.52	0.09	0.00	2.41	0.36	0.03	1.91	0.00	0.18	0.03			93.57	10/11/16	BA-93-07 (continued)	
19	5523	38.37	0.05	0.00	0.00	0.03	0.00	5.18	0.00	34.50	7.29	0.15	0.00	1.11	0.06	0.13	2.02	0.00	0.45	0.08			89.41	10/11/16	BA-93-07 (continued)	
20	5524	38.95	0.03	0.04	0.00	0.01	0.01	6.48	0.00	24.84	9.38	0.19	0.00	1.48	0.05	0.07	2.10	0.00	0.54	0.00			84.15	10/11/16	BA-93-07 (continued)	
21	5525	33.34	0.06	0.01	0.05	0.00	0.05	1.58	0.02	58.46	1.61	0.08	0.00	2.09	0.44	0.02	2.01	0.00	0.18	0.16			100.17	10/11/16	BA-93-07 (continued)	
22	255	39.07	0.03	0.00	0.01	0.08	0.02	0.05	0.02	58.84	0.74	0.06	0.04	0.22	1.99	0.05	0.25	0.00	0.00	0.00			101.47	20-07-16	BA-HS-001_1	
23	258	38.36	0.03	0.00	0.07	0.08	0.03	0.06	0.00	60.07	0.75	0.05	0.01	0.17	1.98	0.05	0.19	0.00	0.00	0.02			101.91	20-07-16	BA-HS-001_4	
24	259	39.04	0.00	0.00	0.00	0.11	0.01	0.04	0.01	59.17	0.77	0.04	0.01	0.21	1.97	0.00	0.27	0.00	0.00	0.00			101.64	20-07-16	BA-HS-001_5	
25	261	37.89	0.00	0.00	0.00	0.04	0.00	0.06	0.00	58.80	0.78	0.05	0.00	0.22	1.98	0.07	0.26	0.00	0.00	0.04			100.18	20-07-16	BA-HS-001_7	
26	262	37.86	0.00	0.00	0.07	0.08	0.00	0.06	0.03	59.38	0.75	0.06	0.01	0.18	2.00	0.08	0.26	0.00	0.00	0.07			100.89	20-07-16	BA-HS-001_8	
27	263	37.51	0.00	0.00	0.04	0.06	0.02	0.02	0.01	61.22	0.27	0.03	0.00	0.26	1.96	0.00	0.13	0.03	0.00	0.00			101.54	20-07-16	BA-HS-001_9	
28	213	31.19			0.03	0.06	0.00	0.03	0.00	53.74	0.05	0.02		0.07	1.42	0.00	1.17	0.00					87.78	28-03-14	BAH 03 cml S850 SW	
29	214	37.00			0.00	0.06	0.00	0.12	0.02	57.84	0.12	0.01		0.06	1.29	0.07	1.01	0.00					97.59	28-03-14	BAH 03 cml S850 SW	
30	215	36.39			0.00	0.14	0.00	0.20	0.00	58.40	0.22	0.00		0.09	1.07	0.00	0.68	0.00					97.18	28-03-14	BAH 03 cml S850 SW	
31	216	36.58			0.02	0.09	0.00	0.13	0.03	58.92	0.21	0.02		0.03	1.03	0.06	0.60	0.03					97.75	28-03-14	BAH 03 cml S850 SW	
32	217	36.51			0.00	0.08	0.00	0.15	0.00	58.27	0.20	0.02		0.03	1.07	0.04	0.52	0.02					96.90	28-03-14	BAH 03 cml S850 SW	
33	218	37.02			0.00	0.03	0.00	0.14	0.00	58.71	0.20	0.02		0.08	1.20	0.10	0.40	0.00					97.88	28-03-14	BAH 03 cml S850 SW	
34	219	36.49			0.00	0.10	0.02	0.10	0.00	58.11	0.18	0.00		0.11	1.41	0.00	0.45	0.02					96.97	28-03-14	BAH 03 cml S850 SW	
35	220	36.88			0.05	0.03	0.00	0.13	0.03	58.15	0.18	0.00		0.02	1.42	0.01	0.42	0.00					97.32	28-03-14	BAH 03 cml S850 SW	
36	221	36.13			0.00	0.02	0.01	0.13	0.01	57.88	0.19	0.00		0.06	1.16	0.07	0.43	0.05					96.11	28-03-14	BAH 03 cml S850 SW	
37	222	36.56			0.03	0.12	0.02	0.14	0.04	58.98	0.20	0.02		0.07	1.12	0.03	0.29	0.00					97.61	28-03-14	BAH 03 cml S850 SW	
38	223	36.43			0.02	0.14	0.01	0.14	0.00	58.74	0.20	0.02		0.04	1.08	0.12	0.31	0.06					97.31	28-03-14	BAH 03 cml S850 SW	
39	224	36.65			0.00	0.06	0.00	0.17	0.01	58.56	0.20	0.00		0.08	1.06	0.10	0.31	0.00					97.20	28-03-14	BAH 03 cml S850 SW	
40	225	36.48			0.00	0.08	0.00	0.17	0.00	58.86	0.20	0.01		0.05	1.17	0.04	0.23	0.00					97.29	28-03-14	BAH 03 cml S850 SW	
41	226	36.19			0.04	0.08	0.00	0.10	0.00	58.12	0.15	0.01		0.05	1.34	0.00	0.30	0.00					96.37	28-03-14	BAH 03 cml S850 SW	
42	227	36.00			0.04	0.08	0.02	0.15	0.02	58.80	0.21	0.02		0.10	1.15	0.00	0.22	0.00					96.80	28-03-14	BAH 03 cml S850 SW	
43	117	36.90	0.00	0.00		0.09	0.00	0.15	0.00	62.08	0.19	0.00	0.00	0.16	1.19	0.00	0.64	0.00	0.00	0.00	0.02	0.01	101.436	18-07-14	BAH 3 cml7 3bott lay	
44	108	36.67	0.00	0.00		0.00	0.00	0.15	0.00	61.47	0.20	0.02	0.00	0.26	1.11	0.02	0.58	0.06	0.00	0.00	0.04	0.02	100.596	18-07-14	BAH 3 cml7 3bott lay	
45	109	36.68	0.00	0.01		0.10	0.00	0.16	0.02	61.73	0.21	0.01	0.01	0.20	1.10	0.06	0.60	0.01	0.00	0.00	0.02	0.00	100.906	18-07-14	BAH 3 cml7 3bott lay	
46	110	36.33	0.02	0.00		0.13	0.00	0.13	0.00	61.81	0.19	0.00	0.00	0.19	1.12	0.00	0.52	0.01	0.00	0.02	0.08	0.00	100.556	18-07-14	BAH 3 cml7 3bott lay	
47	111	37.22	0.00	0.00		0.07	0.00	0.17	0.00	61.64	0.20	0.00	0.00	0.26	1.11	0.14	0.64	0.00	0.00	0.00	0.00	0.02	101.471	18-07-14	BAH 3 cml7 3bott lay	
48	112	37.35	0.00	0.00		0.06	0.01	0.13	0.00	61.98	0.22	0.03	0.00	0.18	1.12	0.05	0.55	0.00	0.00	0.00	0.04	0.00	101.698	18-07-14	BAH 3 cml7 3bott lay	
49	113	36.70	0.00	0.00		0.04	0.01	0.11	0.00	61.57	0.21	0.00	0.00	0.21	1.10	0.00	0.60	0.00	0.00	0.03	0.06	0.04	100.687	18-07-14	BAH 3 cml7 3bott lay	
50	114	36.88	0.00	0.01		0.03	0.00	0.14	0.00	61.86	0.19	0.00	0.02	0.23	1.13	0.00	0.54	0.00	0.00	0.00	0.02	0.01	101.073	18-07-14	BAH 3 cml7 3bott lay	
51	115	36.54	0.00	0.00		0.10	0.00	0.18	0.00	61.93	0.20	0.01	0.00	0.26	1.14	0.02	0.67	0.05	0.00	0.00	0.00	0.00	101.083	18-07-14	BAH 3 cml7 3bott lay	
52	116	36.87	0.03	0.00		0.04	0																			

INDEX	No.	O	Na	K	V	Co	Mg	P	Cr	Fe	Al	S	Ni	Mn	Si	Pb	Cu	Ti	Ca	Zn	Ba	Sr	Total	Date	Sample
108	394	36.35	0.02	0.02		0.07	0.02	0.11	0.02	63.42	0.19	0.00	0.00	0.08	1.23	0.00	0.16	0.00	0.00	0.09	0.00	0.05	101.839	18-07-14	BAH cml7 large goe la
109	63	38.32	0.01	0.02		0.06	0.02	0.03	0.02	61.95	0.18	0.02	0.00	0.46	1.12	0.03	0.00	0.00	0.00	0.00	0.00	0.00	102.252	18-07-14	BAH cml7... 3 bottom
110	64	37.21	0.00	0.01		0.07	0.00	0.00	0.00	61.57	0.18	0.00	0.00	0.40	1.13	0.00	0.02	0.00	0.00	0.02	0.00	0.00	100.61	18-07-14	BAH cml7... 3 bottom
111	65	36.95	0.05	0.01		0.03	0.03	0.05	0.01	62.14	0.15	0.03	0.00	0.44	1.13	0.00	0.01	0.00	0.00	0.00	0.00	0.02	101.064	18-07-14	BAH cml7... 3 bottom
112	66	38.13	0.02	0.02		0.10	0.00	0.02	0.00	61.36	0.17	0.03	0.00	0.46	1.17	0.00	0.00	0.02	0.00	0.00	0.03	0.00	101.519	18-07-14	BAH cml7... 3 bottom
113	67	36.88	0.00	0.04		0.13	0.01	0.02	0.00	61.74	0.16	0.01	0.02	0.51	1.13	0.00	0.05	0.01	0.00	0.00	0.00	0.01	100.707	18-07-14	BAH cml7... 3 bottom
114	68	36.77	0.00	0.04		0.07	0.01	0.05	0.00	61.07	0.20	0.01	0.00	0.52	1.16	0.00	0.00	0.03	0.00	0.00	0.00	0.00	99.915	18-07-14	BAH cml7... 3 bottom
115	69	36.83	0.03	0.00		0.05	0.01	0.05	0.00	61.42	0.20	0.00	0.00	0.46	1.10	0.00	0.00	0.02	0.00	0.13	0.03	0.00	100.343	18-07-14	BAH cml7... 3 bottom
116	70	37.49	0.02	0.02		0.07	0.00	0.07	0.00	61.37	0.18	0.03	0.00	0.36	1.06	0.04	0.05	0.04	0.00	0.00	0.01	0.02	100.824	18-07-14	BAH cml7... 3 bottom
117	71	37.84	0.02	0.00		0.08	0.01	0.01	0.00	62.07	0.18	0.04	0.03	0.39	1.11	0.00	0.00	0.00	0.00	0.00	0.06	0.02	101.849	18-07-14	BAH cml7... 3 bottom
118	72	37.91	0.00	0.01		0.06	0.02	0.03	0.00	61.62	0.20	0.05	0.00	0.48	1.08	0.09	0.00	0.00	0.00	0.00	0.01	0.02	101.588	18-07-14	BAH cml7... 3 bottom
119	73	37.29	0.02	0.01		0.07	0.02	0.03	0.01	61.94	0.22	0.03	0.00	0.47	1.10	0.00	0.00	0.00	0.00	0.00	0.00	0.00	101.189	18-07-14	BAH cml7... 3 bottom
120	74	38.21	0.02	0.01		0.06	0.00	0.00	0.00	61.41	0.18	0.03	0.03	0.42	1.10	0.00	0.00	0.00	0.00	0.03	0.00	0.01	101.513	18-07-14	BAH cml7... 3 bottom
121	75	38.00	0.00	0.01		0.10	0.00	0.04	0.00	61.78	0.20	0.01	0.00	0.48	1.12	0.00	0.05	0.05	0.00	0.00	0.00	0.00	101.836	18-07-14	BAH cml7... 3 bottom
122	76	38.05	0.03	0.01		0.05	0.00	0.05	0.07	61.58	0.18	0.01	0.00	0.42	1.09	0.00	0.00	0.00	0.00	0.00	0.00	0.00	101.54	18-07-14	BAH cml7... 3 bottom
123	77	38.20	0.04	0.03		0.05	0.02	0.05	0.00	61.87	0.21	0.02	0.02	0.38	1.09	0.00	0.00	0.03	0.00	0.00	0.07	0.00	102.057	18-07-14	BAH cml7... 3 bottom
124	273	36.81	0.00	0.02	0.02	0.08	0.04	0.48	0.01	57.59	0.05	0.02	0.04	0.03	1.47	0.00	0.09	0.04	0.00	0.00			96.78	6/7/16	BAH F124 112-1
125	274	35.41	0.00	0.00	0.00	0.06	0.00	0.94	0.01	58.66	0.04	0.01	0.06	0.09	0.83	0.00	0.43	0.00	0.00	0.05			96.58	6/7/16	BAH F124 112-2
126	277	36.54	0.00	0.00	0.02	0.08	0.04	0.33	0.00	59.63	0.00	0.02	0.01	0.08	1.46	0.05	0.40	0.00	0.00	0.06			98.70	6/7/16	BAH F124 112-5
127	278	37.76	0.00	0.00	0.00	0.09	0.01	0.71	0.00	56.98	0.08	0.01	0.00	0.10	1.61	0.03	0.08	0.02	0.03	0.04			97.52	6/7/16	BAH F124 112-6
128	279	37.09	0.00	0.00	0.00	0.06	0.02	0.72	0.00	57.65	0.00	0.00	0.01	0.05	0.99	0.03	0.08	0.01	0.00	0.00			96.73	6/7/16	BAH F124 112-7
129	280	37.08	0.07	0.00	0.02	0.05	0.02	0.45	0.00	56.39	0.00	0.00	0.01	0.05	1.70	0.07	0.10	0.03	0.00	0.00			96.02	6/7/16	BAH F124 112-8
130	281	36.90	0.00	0.01	0.00	0.07	0.01	1.01	0.01	57.67	0.01	0.00	0.00	0.04	0.52	0.01	0.05	0.02	0.00	0.00			96.32	6/7/16	BAH F124 112-9
131	86	36.74	0.00	0.00	0.00	0.07	0.04	0.80	0.00	60.68	0.03	0.02	0.06	0.06	0.92	0.02	0.33	0.00	0.00	0.01			99.79	20-07-16	BAH F124 123_1_1
132	95	37.48	0.00	0.00	0.00	0.09	0.00	1.24	0.00	58.60	0.00	0.00	0.00	0.10	0.23	0.02	0.11	0.00	0.00	0.08			97.94	20-07-16	BAH F124 123_1_10
133	96	37.16	0.00	0.00	0.00	0.13	0.00	1.01	0.00	58.76	0.07	0.00	0.06	0.09	0.26	0.11	0.44	0.00	0.00	0.05			98.13	20-07-16	BAH F124 123_1_11
134	97	36.73	0.00	0.01	0.00	0.06	0.02	1.08	0.00	58.44	0.01	0.00	0.03	0.08	0.34	0.07	0.16	0.00	0.00	0.09			97.10	20-07-16	BAH F124 123_1_12
135	98	38.44	0.00	0.00	0.00	0.05	0.00	1.00	0.01	59.05	0.00	0.00	0.02	0.05	0.39	0.03	0.13	0.00	0.00	0.09			99.26	20-07-16	BAH F124 123_1_13
136	99	37.21	0.00	0.01	0.00	0.08	0.00	0.93	0.00	59.59	0.00	0.01	0.00	0.01	0.25	0.03	0.07	0.00	0.00	0.07			98.24	20-07-16	BAH F124 123_1_14
137	87	36.68	0.00	0.00	0.02	0.06	0.01	0.88	0.00	58.57	0.00	0.00	0.00	0.00	1.07	0.00	0.24	0.02	0.00	0.00			97.56	20-07-16	BAH F124 123_1_2
138	88	37.77	0.00	0.01	0.00	0.09	0.02	0.86	0.00	58.21	0.00	0.00	0.03	0.06	1.14	0.10	0.38	0.00	0.00	0.00			98.67	20-07-16	BAH F124 123_1_3
139	89	37.50	0.00	0.00	0.00	0.09	0.00	0.83	0.00	57.50	0.00	0.01	0.01	0.03	1.43	0.02	0.40	0.03	0.00	0.06			97.90	20-07-16	BAH F124 123_1_4
140	94	38.07	0.00	0.00	0.03	0.10	0.00	0.87	0.01	59.80	0.00	0.01	0.04	0.03	0.25	0.00	0.16	0.01	0.00	0.07			99.45	20-07-16	BAH F124 123_1_9
141	113	37.12	0.00	0.00	0.01	0.06	0.03	0.82	0.01	58.23	0.34	0.00	0.00	0.10	1.16	0.13	0.29	0.00	0.00	0.03			98.31	20-07-16	BAH F124 123_2_1
142	123	38.08	0.00	0.00	0.00	0.06	0.00	0.85	0.00	57.28	0.00	0.00	0.04	0.03	1.09	0.06	0.22	0.00	0.00	0.04			97.73	20-07-16	BAH F124 123_2_11
143	124	37.71	0.00	0.00	0.01	0.06	0.02	0.82	0.01	56.77	0.01	0.01	0.02	0.08	1.43	0.02	0.35	0.04	0.01	0.04			97.38	20-07-16	BAH F124 123_2_12
144	125	37.50	0.03	0.00	0.01	0.06	0.01	0.72	0.00	56.44	0.24	0.00	0.01	0.03	1.58	0.08	0.46	0.00	0.00	0.03			97.18	20-07-16	BAH F124 123_2_13
145	126	37.59	0.00	0.00	0.02	0.08	0.02	0.75	0.00	56.36	0.37	0.00	0.01	0.09	1.56	0.06	0.48	0.00	0.00	0.00			97.40	20-07-16	BAH F124 123_2_14
146	114	38.45	0.00	0.01	0.02	0.03	1.97	0.72	0.00	56.81	0.66	0.00	0.02	0.06	1.25	0.08	0.49	0.01	0.00	0.02			100.59	20-07-16	BAH F124 123_2_2
147	115	37.76	0.00	0.00	0.08	0.05	0.08	0.59	0.02	57.76	1.10	0.00	0.00	0.12	0.93	0.03	0.79	0.01	0.00	0.01			99.34	20-07-16	BAH F124 123_2_3
148	116	37.51	0.00	0.00	0.01	0.07	0.04	0.81	0.01	58.60	0.78	0.02	0.00	0.06	0.89	0.00	0.58	0.04	0.00	0.01			99.43	20-07-16	BAH F124 123_2_4
149	117	37.07	0.00	0.00	0.00	0.04	0.03	1.15	0.00	59.16	0.00	0.00	0.02	0.10	0.15	0.00	0.11	0.00	0.00	0.06			97.89	20-07-16	BAH F124 123_2_5
150	118	37.81	0.00	0.00	0.00	0.08	0.00	1.04	0.02	59.97	0.00	0.02	0.04	0.02	0.17	0.03	0.02	0.01	0.00	0.06			99.28	20-07-16	BAH F124 123_2_6
151	119	38.22	0.00	0.02	0.00	0.05	0.00	0.83	0.05	59.75	0.00	0.00	0.01	0.07	0.29	0.07	0.10	0.01	0.00	0.04			99.52	20-07-16	BAH F124 123_2_7
152	120	38.04	0.00	0.00	0.08	0.09	0.00	0.96	0.02	59.07	0.01	0.00	0.04	0.05	0.32	0.07	0.16	0.00	0.00	0.01			98.90	20-07-16	BAH F124 123_2_8
153	121	38.54	0.00	0.00	0.00	0.00	0.01	1.08	0.02	58.78	0.01	0.00	0.02	0.07	0.33	0.10	0.20	0.00	0.00	0.03			99.19	20-07-16	BAH F124 123_2_9
154	127	38.33	0.00	0.01	0.00	0.08	0.02	1.13	0.00	58.38	0.34	0.00	0.00	0.06	0.28	0.03	0.20	0.00	0.00	0.02			98.88	20-07-16	BAH F124 123_7-1
155	128	36.92	0.00	0.00	0.01	0.08	0.01	0.98	0.02	59.07	0.01	0.01	0.00	0.04	0.34	0.13	0.20	0.00	0.00	0.11			97.93	20-07-16	BAH F124 123_7-2
156	129	37.64	0.00	0.00	0.01	0.07	0.00	1.04	0.00	58.57	0.01	0.00	0.05	0.08	0.35	0.01	0.19	0.00	0.00	0.00			98.02	20-07-16	BAH F124 123_7-3
157	130	38.23	0.00	0.00	0.02	0.05	0.01	1.06	0.01	58.62	0.00	0.00	0.03	0.04	0.34	0.11	0.06	0.00	0.00	0.01			98.58	20-07-16	BAH F124 123_7-4
158	131</																								

INDEX	No.	O	Na	K	V	Co	Mg	P	Cr	Fe	Al	S	Ni	Mn	Si	Pb	Cu	Ti	Ca	Zn	Ba	Sr	Total	Date	Sample
216	161	35.65			0.06	0.05	0.01	0.59	0.00	59.76	0.00	0.01		0.11	0.25	0.00	0.26	0.03					96.79	28-03-14	BAH F282 118.2
217	162	35.75			0.05	0.12	0.06	0.52	0.05	59.72	0.02	0.00		0.04	0.30	0.00	0.22	0.01					96.84	28-03-14	BAH F282 118.2
218	163	35.35			0.02	0.06	0.02	0.51	0.01	59.35	0.00	0.00		0.10	0.27	0.00	0.28	0.00					95.98	28-03-14	BAH F282 118.2
219	164	34.78			0.00	0.01	0.03	0.49	0.00	59.59	0.02	0.00		0.09	0.26	0.01	0.18	0.05					95.50	28-03-14	BAH F282 118.2
220	165	35.59			0.00	0.06	0.03	0.51	0.00	59.19	0.01	0.00		0.04	0.26	0.09	0.24	0.00					96.01	28-03-14	BAH F282 118.2
221	166	35.63			0.02	0.09	0.00	0.57	0.00	59.68	0.00	0.00		0.03	0.25	0.09	0.22	0.00					96.58	28-03-14	BAH F282 118.2
222	167	35.52			0.00	0.04	0.03	0.52	0.00	59.48	0.01	0.02		0.05	0.28	0.00	0.17	0.00					96.11	28-03-14	BAH F282 118.2
223	189	36.23			0.00	0.06	0.00	0.71	0.00	59.42	0.00	0.00		0.04	0.27	0.00	0.11	0.00					96.84	28-03-14	BAH F282 118.2 grain 3
224	190	37.54			0.00	0.08	0.02	1.12	0.03	58.20	0.01	0.02		0.12	0.24	0.05	0.00	0.00					97.42	28-03-14	BAH F282 118.2 grain 3
225	191	36.25			0.00	0.06	0.00	0.83	0.08	60.13	0.02	0.00		0.05	0.20	0.09	0.14	0.00					97.85	28-03-14	BAH F282 118.2 grain 3
226	192	36.62			0.00	0.06	0.04	0.76	0.01	59.30	0.11	0.01		0.09	0.29	0.03	0.11	0.00					97.42	28-03-14	BAH F282 118.2 grain 3
227	193	36.91			0.01	0.02	0.03	1.13	0.00	57.22	0.02	0.01		0.12	0.50	0.00	0.72	0.00					96.68	28-03-14	BAH F282 118.2 grain 3
228	194	36.28			0.12	0.03	0.05	0.78	0.07	56.80	0.89	0.03		0.03	0.89	0.08	0.15	0.00					96.19	28-03-14	BAH F282 118.2 grain 3
229	195	37.19			0.07	0.05	0.06	1.21	0.04	55.85	0.34	0.01		0.18	0.46	0.00	1.18	0.00					96.62	28-03-14	BAH F282 118.2 grain 3
230	196	37.35			0.00	0.06	0.02	1.11	0.02	56.45	0.01	0.00		0.14	0.63	0.00	0.92	0.00					96.70	28-03-14	BAH F282 118.2 grain 3
231	197	37.31			0.00	0.09	0.04	1.07	0.00	55.95	0.02	0.00		0.10	0.66	0.00	1.08	0.04					96.34	28-03-14	BAH F282 118.2 grain 3
232	168	36.85			0.00	0.06	0.02	0.66	0.00	59.10	0.00	0.00		0.03	0.54	0.00	0.04	0.00					97.29	28-03-14	BAH F282 118.2 grain2
233	169	36.15			0.00	0.14	0.00	0.73	0.00	58.29	0.03	0.03		0.03	0.41	0.06	1.09	0.00					96.96	28-03-14	BAH F282 118.2 grain2
234	170	35.99			0.06	0.04	0.04	0.73	0.02	57.72	0.03	0.00		0.13	0.41	0.00	1.13	0.06					96.36	28-03-14	BAH F282 118.2 grain2
235	171	36.14			0.02	0.08	0.01	0.78	0.04	58.04	0.04	0.00		0.09	0.42	0.09	1.21	0.00					96.96	28-03-14	BAH F282 118.2 grain2
236	172	35.95			0.00	0.05	0.04	0.84	0.00	57.83	0.06	0.00		0.12	0.45	0.00	1.19	0.05					96.57	28-03-14	BAH F282 118.2 grain2
237	173	36.02			0.06	0.13	0.02	0.90	0.03	57.60	0.06	0.00		0.10	0.44	0.03	1.14	0.00					96.52	28-03-14	BAH F282 118.2 grain2
238	174	35.98			0.00	0.04	0.03	0.95	0.01	57.60	0.06	0.00		0.10	0.47	0.00	1.38	0.03					96.64	28-03-14	BAH F282 118.2 grain2
239	175	36.00			0.01	0.03	0.04	0.89	0.00	57.20	0.05	0.00		0.07	0.46	0.00	1.21	0.00					95.96	28-03-14	BAH F282 118.2 grain2
240	176	36.17			0.00	0.03	0.01	0.95	0.01	57.13	0.05	0.03		0.05	0.46	0.09	1.15	0.08					96.20	28-03-14	BAH F282 118.2 grain2
241	177	35.76			0.02	0.04	0.00	0.94	0.00	57.16	0.06	0.01		0.00	0.46	0.04	1.12	0.00					95.60	28-03-14	BAH F282 118.2 grain2
242	178	35.43			0.01	0.10	0.04	1.09	0.04	56.25	0.08	0.01		0.08	0.46	0.02	1.20	0.03					94.84	28-03-14	BAH F282 118.2 grain2
243	179	36.57			0.00	0.06	0.05	1.12	0.00	56.84	0.00	0.00		0.13	0.64	0.03	0.60	0.03					96.08	28-03-14	BAH F282 118.2 grain2
244	180	36.69			0.01	0.07	0.02	0.74	0.05	59.04	0.11	0.00		0.04	0.34	0.00	0.01	0.04					97.15	28-03-14	BAH F282 118.2 grain2
245	181	36.13			0.05	0.05	0.00	0.91	0.00	59.17	0.00	0.01		0.07	0.30	0.10	0.06	0.01					96.84	28-03-14	BAH F282 118.2 grain2
246	182	36.80			0.00	0.14	0.01	0.97	0.03	58.42	0.01	0.00		0.07	0.30	0.03	0.00	0.00					96.77	28-03-14	BAH F282 118.2 grain2
247	106	36.15	0.00	0.00	0.01	0.06	0.04	0.80	0.02	61.41	0.00	0.00	0.03	0.07	0.50	0.03	0.99	0.00	0.00	0.05			100.17	20-07-16	BAH F282 118.2-brown
248	107	36.32	0.00	0.00	0.03	0.07	0.03	0.81	0.04	60.82	0.00	0.00	0.01	0.09	0.52	0.08	0.90	0.00	0.00	0.07			99.77	20-07-16	BAH F282 118.2-brown
249	108	36.57	0.00	0.00	0.03	0.09	0.03	0.77	0.00	61.79	0.01	0.00	0.05	0.09	0.49	0.00	0.98	0.00	0.00	0.02			100.92	20-07-16	BAH F282 118.2-brown
250	109	36.48	0.03	0.00	0.00	0.08	0.04	0.80	0.00	61.37	0.00	0.03	0.02	0.06	0.51	0.02	1.01	0.00	0.00	0.06			100.51	20-07-16	BAH F282 118.2-brown
251	110	36.64	0.00	0.00	0.03	0.04	0.03	0.74	0.02	61.78	0.00	0.01	0.00	0.09	0.51	0.00	1.08	0.00	0.00	0.10			101.08	20-07-16	BAH F282 118.2-brown
252	111	36.55	0.00	0.00	0.00	0.10	0.04	0.77	0.00	61.49	0.01	0.01	0.00	0.06	0.51	0.05	1.04	0.00	0.00	0.09			100.70	20-07-16	BAH F282 118.2-brown
253	112	36.36	0.02	0.00	0.01	0.03	0.05	0.77	0.00	61.47	0.01	0.00	0.04	0.07	0.51	0.00	0.96	0.00	0.00	0.07			100.37	20-07-16	BAH F282 118.2-brown
254	100	35.06	0.00	0.00	0.02	0.05	0.02	0.54	0.00	59.66	0.02	0.01	0.07	0.03	0.30	0.00	0.03	0.00	0.00	0.04			95.86	20-07-16	BAH F282 118.4_1
255	101	35.26	0.00	0.00	0.02	0.06	0.02	0.45	0.02	60.73	0.07	0.00	0.06	0.02	0.25	0.00	0.17	0.00	0.00	0.00			97.13	20-07-16	BAH F282 118.4_2
256	102	35.64	0.00	0.01	0.08	0.05	0.03	0.44	0.00	60.82	0.22	0.01	0.11	0.00	0.26	0.05	0.30	0.00	0.00	0.07			98.09	20-07-16	BAH F282 118.4_3
257	103	37.36	0.00	0.00	0.02	0.14	0.02	0.51	0.00	60.25	0.00	0.00	0.03	0.00	0.30	0.05	0.00	0.00	0.00	0.00			98.68	20-07-16	BAH F282 118.4_4
258	104	35.97	0.00	0.00	0.02	0.09	0.01	0.46	0.02	60.89	0.13	0.00	0.02	0.04	0.27	0.07	0.18	0.05	0.00	0.09			98.31	20-07-16	BAH F282 118.4_5
259	105	36.15	0.01	0.00	0.04	0.08	0.03	0.50	0.04	61.54	0.23	0.00	0.03	0.04	0.28	0.00	0.53	0.00	0.00	0.03			99.52	20-07-16	BAH F282 118.4_6
260	38	36.66	0.01	0.00	0.01	0.06	0.00	0.39	0.01	63.03	0.12	0.01	0.02	0.02	0.12	0.00	0.07	0.00	0.00	0.00			100.52	20-07-16	BAH F282 120.5_brown
261	39	35.23	0.01	0.00	0.02	0.08	0.00	0.39	0.05	64.37	0.21	0.03	0.01	0.02	0.14	0.02	0.09	0.00	0.00	0.00			100.67	20-07-16	BAH F282 120.5_brown
262	40	34.70	0.00	0.00	0.00	0.06	0.00	0.42	0.01	63.99	0.22	0.01	0.00	0.02	0.13	0.02	0.06	0.00	0.00	0.00			99.65	20-07-16	BAH F282 120.5_brown
263	41	35.75	0.00	0.00	0.00	0.06	0.00	0.40	0.00	63.75	0.11	0.01	0.03	0.00	0.13	0.11	0.04	0.05	0.00	0.02			100.45	20-07-16	BAH F282 120.5_brown
264	42	35.28	0.00	0.01	0.00	0.07	0.00	0.41	0.02	63.25	0.11	0.02	0.00	0.02	0.11	0.01	0.04	0.02	0.00	0.00			99.37	20-07-16	BAH F282 120.5_brown
265	43	35.46	0.04	0.00	0.00	0.06	0.00	0.47	0.03	63.28	0.13	0.02	0.00	0.00	0.12	0.04	0.08	0.00	0.00	0.00			99.73	20-07-16	BAH F282 120.5_brown
266	44	34.93	0.02	0.00	0.01	0.08	0.02	0.39	0.01	63.61	0.15	0.03	0.06	0.04	0.13	0.04	0.10	0.00	0.00	0.03			99.65	20-07-16	BAH F282 120.5_brown
267	45	35.60	0.02	0.00	0.03	0.08	0.02	0.53	0.00	64.22	0.58	0.06	0.02	0.09	0.23	0.08	0.18	0.01	0.00	0.00			101.75	20-07-16	BAH F282 120.5_brown
268	46	32.37	0.00	0.00	0.00	0.08	0.00	0.48	0.00	64.69	0.53	0.03	0.00	0.06	0.17	0.06	0.15	0.00	0.00	0.01			98.63	20-07-16	BAH F282 120.5_brown
269	47	35.89	0.03	0.01	0.00	0.04	0.01	0.46	0.00	63.90	0.26														

INDEX	No.	O	Na	K	V	Co	Mg	P	Cr	Fe	Al	Si	Ni	Mn	Sr	Pb	Cu	Ti	Ca	Zn	Ba	Sr	Total	Date	Sample	
324	226	36.80	0.05	0.00	0.01	0.11	0.00	0.60	0.03	58.07	0.07	0.00	0.01	0.00	1.41	0.06	2.33	0.02	0.00	0.01			99.55	6/7/16	BAH-100-BI-2.5	
325	227	36.78	0.00	0.00	0.01	0.10	0.00	0.94	0.00	60.28	0.12	0.03	0.01	0.03	0.91	0.01	1.46	0.00	0.00	0.02			100.71	6/7/16	BAH-100-BI-2.6	
326	228	36.54	0.00	0.01	0.00	0.05	0.00	0.93	0.00	59.16	0.04	0.00	0.05	0.05	0.31	0.04	0.15	0.00	0.00	0.02			97.34	6/7/16	BAH-100-BI-2.7	
327	229	37.06	0.00	0.00	0.03	0.05	0.01	0.90	0.00	61.36	0.28	0.02	0.00	0.03	0.84	0.01	1.22	0.00	0.00	0.00			101.80	6/7/16	BAH-100-BI-2.8	
328	230	36.75	0.00	0.00	0.00	0.04	0.00	0.89	0.03	59.72	0.14	0.03	0.02	0.04	1.12	0.00	1.73	0.02	0.00	0.03			100.56	6/7/16	BAH-100-BI-2.9	
329	236	35.99	0.00	0.00	0.03	0.04	0.00	0.40	0.00	62.73	0.08	0.02	0.00	0.03	0.11	0.01	0.01	0.00	0.00	0.06			99.51	6/7/16	BAH-100-Brown-2-1	
330	237	34.45	0.00	0.01	0.02	0.07	0.02	0.50	0.01	62.73	0.10	0.02	0.01	0.02	0.11	0.03	0.04	0.02	0.00	0.07			98.22	6/7/16	BAH-100-Brown-2-2	
331	238	35.10	0.00	0.00	0.00	0.07	0.00	0.45	0.00	62.48	0.05	0.00	0.03	0.01	0.11	0.05	0.00	0.00	0.00	0.04			98.40	6/7/16	BAH-100-Brown-2-3	
332	239	34.50	0.00	0.01	0.00	0.08	0.04	0.43	0.01	62.34	0.10	0.02	0.03	0.01	0.13	0.02	0.03	0.00	0.00	0.02			97.77	6/7/16	BAH-100-Brown-2-4	
333	240	34.83	0.00	0.00	0.02	0.09	0.00	0.52	0.00	62.05	0.07	0.00	0.06	0.00	0.10	0.01	0.02	0.00	0.00	0.00			97.78	6/7/16	BAH-100-Brown-2-5	
334	241	33.23	0.00	0.01	0.02	0.06	0.00	0.47	0.01	61.56	0.06	0.00	0.04	0.02	0.10	0.00	0.00	0.00	0.00	0.05			95.61	6/7/16	BAH-100-Brown-2-6	
335	242	35.36	0.01	0.01	0.03	0.08	0.02	0.44	0.02	62.23	0.05	0.01	0.05	0.00	0.11	0.05	0.01	0.03	0.00	0.00			98.52	6/7/16	BAH-100-Brown-2-7	
336	243	34.82	0.00	0.00	0.01	0.10	0.02	0.17	0.00	64.06	0.20	0.02	0.01	0.18	1.22	0.07	0.45	0.00	0.00	0.07			101.38	6/7/16	BAH-3cml-3BL-1	
337	244	34.71	0.00	0.00	0.00	0.08	0.01	0.13	0.01	64.01	0.18	0.03	0.01	0.18	1.23	0.04	0.39	0.00	0.00	0.10			101.12	6/7/16	BAH-3cml-3BL-2	
338	245	35.19	0.00	0.01	0.00	0.06	0.02	0.13	0.00	64.38	0.19	0.01	0.01	0.19	1.24	0.00	0.45	0.00	0.00	0.03			101.90	6/7/16	BAH-3cml-3BL-3	
339	246	35.39	0.00	0.00	0.04	0.08	0.02	0.13	0.00	63.89	0.17	0.02	0.00	0.18	1.29	0.06	0.41	0.00	0.00	0.07			101.73	6/7/16	BAH-3cml-3BL-4	
340	247	35.19	0.00	0.00	0.00	0.07	0.02	0.13	0.01	63.77	0.18	0.03	0.00	0.20	1.32	0.01	0.49	0.02	0.00	0.00			101.43	6/7/16	BAH-3cml-3BL-5	
341	248	36.62	0.00	0.00	0.00	0.10	0.01	0.15	0.00	63.63	0.17	0.03	0.00	0.05	1.28	0.04	0.35	0.01	0.00	0.08			102.52	6/7/16	BAH-3cml-LGt-1	
342	249	35.67	0.00	0.00	0.00	0.08	0.01	0.15	0.03	63.83	0.15	0.00	0.00	0.08	1.29	0.00	0.41	0.00	0.00	0.00			101.69	6/7/16	BAH-3cml-LGt-2	
343	250	35.78	0.03	0.00	0.00	0.06	0.00	0.12	0.00	64.25	0.17	0.00	0.00	0.06	1.22	0.01	0.29	0.00	0.00	0.06			102.06	6/7/16	BAH-3cml-LGt-3	
344	251	35.63	0.05	0.00	0.00	0.04	0.01	0.12	0.02	63.95	0.17	0.00	0.00	0.06	1.21	0.03	0.29	0.05	0.00	0.03			101.64	6/7/16	BAH-3cml-LGt-4	
345	252	35.88	0.06	0.02	0.00	0.03	0.02	0.12	0.00	64.05	0.17	0.01	0.00	0.04	1.15	0.00	0.32	0.01	0.00	0.16			102.03	6/7/16	BAH-3cml-LGt-5	
346	253	36.35	0.01	0.00	0.01	0.09	0.02	0.10	0.00	64.23	0.17	0.01	0.00	0.07	1.13	0.05	0.27	0.00	0.00	0.00			102.50	6/7/16	BAH-3cml-LGt-6	
347	246	37.20	0.02	0.00	0.00	0.07	0.00	0.09	0.00	60.82	0.10	0.01	0.04	0.12	1.72	0.03	0.20	0.00	0.00	0.00			100.40	20-07-16	BAH-3cml7-alongC-axis_1	
348	247	37.28	0.01	0.00	0.00	0.09	0.00	0.10	0.00	59.76	0.09	0.00	0.01	0.10	1.68	0.14	0.18	0.00	0.00	0.01			99.45	20-07-16	BAH-3cml7-alongC-axis_2	
349	248	36.97	0.00	0.00	0.00	0.08	0.00	0.11	0.00	59.60	0.10	0.00	0.01	0.09	1.67	0.10	0.18	0.00	0.00	0.04			98.94	20-07-16	BAH-3cml7-alongC-axis_3	
350	249	36.73	0.02	0.01	0.00	0.08	0.02	0.11	0.00	58.55	0.09	0.01	0.02	0.05	1.64	0.09	0.22	0.00	0.00	0.05			97.68	20-07-16	BAH-3cml7-alongC-axis_4	
351	250	36.72	0.00	0.02	0.02	0.05	0.02	0.12	0.01	60.45	0.08	0.01	0.03	0.21	1.78	0.15	0.09	0.00	0.00	0.05			99.78	20-07-16	BAH-3cml7-alongC-axis_5	
352	251	37.20	0.03	0.00	0.00	0.08	0.00	0.12	0.00	59.39	0.08	0.01	0.00	0.22	1.74	0.08	0.20	0.01	0.00	0.02			99.18	20-07-16	BAH-3cml7-alongC-axis_6	
353	252	36.73	0.00	0.00	0.00	0.07	0.00	0.09	0.00	59.39	0.09	0.00	0.00	0.29	1.75	0.00	0.16	0.00	0.00	0.08			98.65	20-07-16	BAH-3cml7-alongC-axis_7	
354	253	37.31	0.00	0.01	0.00	0.07	0.00	0.08	0.01	59.02	0.08	0.02	0.00	0.23	1.77	0.08	0.13	0.02	0.00	0.00			98.84	20-07-16	BAH-3cml7-alongC-axis_8	
355	254	37.05	0.05	0.00	0.01	0.05	0.00	0.11	0.02	58.70	0.10	0.00	0.01	0.26	1.77	0.02	0.21	0.00	0.00	0.01			98.35	20-07-16	BAH-3cml7-alongC-axis_9	
356	285	37.48	0.00	0.00	0.00	0.08	0.01	0.51	0.01	59.61	0.48	0.01	0.00	0.22	1.10	0.01	0.82	0.01	0.00	0.06			100.40	6/7/16	BAH-93-01-1	
357	286	37.59	0.00	0.01	0.04	0.08	0.01	1.38	0.01	58.86	0.57	0.02	0.06	0.27	0.09	0.08	1.06	0.00	0.01	0.07			100.18	6/7/16	BAH-93-01-2	
358	287	37.53	0.00	0.00	0.00	0.04	0.03	1.46	0.02	60.04	0.44	0.02	0.00	0.27	0.12	0.07	0.89	0.00	0.00	0.00			100.93	6/7/16	BAH-93-01-3	
359	288	36.31	0.00	0.01	0.01	0.07	0.01	1.52	0.02	58.91	0.11	0.00	0.00	0.16	0.11	0.04	0.59	0.00	0.00	0.02			97.90	6/7/16	BAH-93-01-4	
360	289	36.26	0.00	0.00	0.00	0.05	0.00	1.75	0.00	58.35	0.00	0.01	0.00	0.11	0.16	0.00	0.02	0.00	0.00	0.05			96.75	6/7/16	BAH-93-01-5	
361	290	37.64	0.00	0.01	0.00	0.05	0.00	1.77	0.00	57.29	0.00	0.01	0.01	0.11	0.28	0.05	0.00	0.03	0.00	0.04			97.29	6/7/16	BAH-93-01-6	
362	291	37.21	0.00	0.00	0.00	0.08	0.02	1.60	0.01	57.86	0.00	0.00	0.00	0.14	0.25	0.00	0.03	0.00	0.00	0.05			97.25	6/7/16	BAH-93-01-7	
363	292	37.62	0.00	0.00	0.00	0.07	0.01	1.39	0.00	57.63	0.00	0.01	0.04	0.12	0.49	0.04	0.02	0.00	0.00	0.00			97.44	6/7/16	BAH-93-01-8	
364	293	36.62	0.00	0.00	0.00	0.10	0.01	1.17	0.00	58.17	0.00	0.00	0.00	0.14	0.46	0.00	0.00	0.03	0.00	0.05			96.76	6/7/16	BAH-93-01-9	
365	91	37.48	0.00	0.04	0.00	0.08	0.00	1.20	0.00	51.98	0.05	0.02	0.00	0.46	0.34	0.04	3.05	0.00	0.00	0.03	0.05	0.00	0.00	99.81	22-02-14	BAH-99-01
366	92	37.46	0.00	0.00	0.00	0.10	0.02	0.98	0.04	54.22	0.00	0.04	0.00	0.27	0.93	0.05	2.60	0.00	0.00	0.00	0.02	0.00	0.00	99.25	22-02-14	BAH-99-01
367	94	38.16	0.00	0.00	0.03	0.00	0.01	0.83	0.00	53.47	0.07	0.00	0.00	0.372	0.97	0.03	2.93	0.00	0.00	0.00	0.00	0.00	0.00	100.20	22-02-14	BAH-99-01
368	95	38.00	0.00	0.00	0.00	0.11	0.00	0.55	0.02	54.16	0.01	0.01	0.01	2.45	1.37	0.01	2.58	0.00	0.00	0.05	0.00	0.03	0.00	99.37	22-02-14	BAH-99-01
369	96	37.99	0.00	0.00	0.00	0.03	0.03	0.54	0.00	54.91	0.00	0.02	0.00	2.48	1.28	0.00	2.61	0.04	0.00	0.02	0.00	0.00	0.00	99.95	22-02-14	BAH-99-01
370	97	38.04	0.05	0.03	0.00	0.03	0.00	0.57	0.01	54.16	0.00	0.04	0.00	3.22	1.37	0.00	2.71	0.00	0.00	0.00	0.00	0.07	0.00	100.29	22-02-14	BAH-99-01
371	98	37.83	0.00	0.00	0.03	0.10	0.00	1.64	0.00	54.56	0.00	0.03	0.00	2.42	0.33	0.12	2.79	0.01	0.00	0.03	0.00	0.00	0.00	99.87	22-02-14	BAH-99-01
372	99	38.11	0.00	0.03	0.00	0.05	0.00	1.23	0.00	53.61	0.13	0.00	0.00	3.99	0.23	0.00	3.18	0.08	0.00	0.10	0.03	0.00	0.00	100.76	22-02-14	BAH-99-01
373	100	37.99	0.00	0.02	0.01	0.02	0.00	1.37	0.00	53.91	0.09	0.00	0.07	3.43	0.28	0.05	3.29	0.01	0.00	0.15	0.12	0.00	0.00	100.81	22-02-14	BAH-99-01
374	101	37.87	0.00	0.00	0.00	0.00	0.00	1.35	0.00</																	

INDEX	No.	O	Na	K	V	Co	Mg	P	Cr	Fe	Al	S	Ni	Mn	Si	Pb	Cu	Ti	Ca	Zn	Ba	Sr	Total	Date	Sample
432	146	36.75	0.00	0.00	0.00	0.12	0.03	0.49	0.00	59.96	0.11	0.01	0.02	1.93	0.30	0.03	1.35	0.00	0.00	0.03			101.01	20-07-16	BAH-F124-111.2_5
433	147	36.46	0.00	0.00	0.00	0.12	0.03	0.65	0.00	60.17	0.15	0.01	0.03	2.75	0.25	0.02	1.79	0.03	0.00	0.01			102.47	20-07-16	BAH-F124-111.2_6
434	148	36.53	0.00	0.00	0.00	0.09	0.03	0.57	0.03	61.68	0.04	0.04	0.00	0.82	0.20	0.04	0.70	0.01	0.00	0.06			100.86	20-07-16	BAH-F124-111.2_7
435	149	35.95	0.00	0.00	0.00	0.07	0.01	0.61	0.01	60.51	0.15	0.01	0.00	2.47	0.29	0.00	1.64	0.00	0.00	0.02			101.73	20-07-16	BAH-F124-111.2_8
436	150	37.30	0.00	0.00	0.03	0.08	0.01	0.59	0.00	59.72	0.14	0.00	0.01	1.85	0.78	0.00	1.62	0.02	0.00	0.00			102.15	20-07-16	BAH-F124-111.2_9
437	301	36.11	0.00	0.00	0.00	0.08	0.02	1.39	0.01	60.43	0.29	0.00	0.02	0.04	0.26	0.05	2.20	0.00	0.00	0.10			101.00	6/7/16	BAH-F124-114-1
438	302	36.76	0.00	0.01	0.01	0.04	0.01	1.38	0.00	60.15	0.41	0.02	0.02	0.03	0.26	0.03	2.21	0.00	0.00	0.01			101.35	6/7/16	BAH-F124-114-2
439	308	36.66	0.00	0.03	0.02	0.10	0.01	1.36	0.00	60.45	0.34	0.00	0.04	0.04	0.25	0.00	2.19	0.00	0.00	0.00			101.47	6/7/16	BAH-F124-114-2-1
440	309	36.42	0.00	0.00	0.00	0.06	0.01	1.42	0.00	60.11	0.32	0.00	0.05	0.07	0.26	0.00	2.14	0.00	0.00	0.05			100.89	6/7/16	BAH-F124-114-2-2
441	310	36.55	0.00	0.01	0.02	0.09	0.00	1.29	0.00	59.76	0.35	0.02	0.00	0.07	0.26	0.00	2.09	0.04	0.00	0.05			100.58	6/7/16	BAH-F124-114-2-3
442	303	36.29	0.00	0.00	0.00	0.08	0.01	1.35	0.00	60.53	0.42	0.01	0.04	0.03	0.26	0.00	2.19	0.00	0.00	0.04			101.24	6/7/16	BAH-F124-114-3
443	304	36.60	0.00	0.01	0.05	0.06	0.01	1.38	0.00	60.63	0.34	0.00	0.04	0.03	0.27	0.01	2.27	0.02	0.00	0.05			101.77	6/7/16	BAH-F124-114-4
444	305	37.01	0.00	0.01	0.01	0.02	0.02	0.74	0.00	60.03	0.01	0.00	0.01	0.03	0.15	0.05	0.05	0.00	0.00	0.02			98.15	6/7/16	BAH-F124-114-5
445	306	36.16	0.00	0.01	0.00	0.06	0.00	0.79	0.00	59.74	0.00	0.00	0.03	0.04	0.18	0.02	0.01	0.00	0.00	0.02			97.05	6/7/16	BAH-F124-114-6
446	307	35.58	0.00	0.00	0.00	0.08	0.01	0.62	0.00	60.21	0.03	0.01	0.03	0.03	0.15	0.01	0.01	0.00	0.00	0.03			96.78	6/7/16	BAH-F124-114-7
447	215	36.98	0.00	0.00	0.00	0.11	0.00	1.20	0.00	59.30	0.02	0.00	0.01	0.06	0.12	0.00	0.05	0.00	0.00	0.08			97.92	6/7/16	BAH-F124-123.1-10
448	216	37.49	0.01	0.00	0.02	0.09	0.00	0.87	0.00	59.11	0.01	0.02	0.02	0.01	0.29	0.03	0.04	0.00	0.00	0.00			98.00	6/7/16	BAH-F124-123.1-11
449	217	36.63	0.03	0.00	0.00	0.08	0.00	1.05	0.00	59.47	0.00	0.01	0.00	0.04	0.25	0.03	0.03	0.00	0.00	0.01			97.62	6/7/16	BAH-F124-123.1-12
450	218	37.44	0.05	0.01	0.02	0.06	0.01	0.86	0.00	58.72	0.00	0.02	0.04	0.03	0.28	0.03	0.08	0.00	0.00	0.06			97.68	6/7/16	BAH-F124-123.1-13
451	219	35.81	0.01	0.00	0.00	0.08	0.02	0.93	0.00	59.57	0.00	0.00	0.03	0.06	0.79	0.01	0.28	0.00	0.00	0.00			97.60	6/7/16	BAH-F124-123.1-14
452	220	36.98	0.02	0.00	0.00	0.06	0.02	0.89	0.03	56.40	0.00	0.00	0.00	0.01	1.45	0.03	0.44	0.00	0.01	0.00			96.33	6/7/16	BAH-F124-123.1-15
453	221	37.42	0.00	0.01	0.00	0.08	0.01	0.91	0.00	56.85	0.00	0.00	0.01	0.01	1.36	0.04	0.39	0.00	0.00	0.00			97.10	6/7/16	BAH-F124-123.1-16
454	208	37.02	0.00	0.00	0.02	0.06	0.01	0.29	0.00	59.55	0.05	0.01	0.00	0.05	1.94	0.02	0.83	0.01	0.00	0.05			99.90	6/7/16	BAH-F124-123.1-3
455	209	37.12	0.01	0.00	0.00	0.05	0.02	0.32	0.02	59.05	0.06	0.00	0.00	0.11	1.74	0.01	0.54	0.03	0.00	0.03			99.10	6/7/16	BAH-F124-123.1-4
456	212	37.35	0.00	0.02	0.09	0.08	0.00	0.28	0.00	59.32	0.06	0.01	0.00	0.08	1.91	0.03	0.92	0.00	0.00	0.04			100.19	6/7/16	BAH-F124-123.1-7
457	213	36.74	0.00	0.00	0.01	0.09	0.00	1.22	0.00	58.11	0.01	0.00	0.06	0.06	0.22	0.01	0.06	0.00	0.02	0.05			96.65	6/7/16	BAH-F124-123.1-8
458	214	36.55	0.03	0.01	0.01	0.09	0.00	1.15	0.00	59.64	0.00	0.01	0.05	0.01	0.15	0.01	0.08	0.00	0.00	0.00			97.78	6/7/16	BAH-F124-123.1-9
459	236	35.53	0.00	0.04	0.03	0.04	0.00	1.59	0.04	58.93	0.91	0.01	0.00	0.07	0.23	0.00	1.53	0.00	0.00	0.00	0.03		98.97	20-12-16	BAH-F177-115_CavityFilling
460	237	36.12	0.03	0.03	0.05	0.07	0.01	1.58	0.04	58.44	0.91	0.02	0.01	0.07	0.25	0.03	1.59	0.00	0.00	0.00	0.00		99.22	20-12-16	BAH-F177-115_CavityFilling
461	238	36.07	0.00	0.05	0.04	0.09	0.00	1.53	0.06	58.30	0.93	0.02	0.00	0.05	0.26	0.01	1.61	0.00	0.00	0.00	0.00		99.01	20-12-16	BAH-F177-115_CavityFilling
462	239	36.04	0.00	0.03	0.03	0.05	0.00	1.55	0.01	58.43	0.90	0.02	0.07	0.02	0.25	0.04	1.57	0.03	0.00	0.00	0.00		99.03	20-12-16	BAH-F177-115_CavityFilling
463	240	36.14	0.02	0.05	0.04	0.03	0.00	1.61	0.00	58.46	0.96	0.01	0.00	0.05	0.25	0.04	1.62	0.00	0.00	0.01	0.04		99.34	20-12-16	BAH-F177-115_CavityFilling
464	241	35.84	0.00	0.06	0.07	0.05	0.00	1.65	0.01	58.64	0.91	0.01	0.04	0.08	0.25	0.03	1.59	0.01	0.00	0.06	0.00		99.29	20-12-16	BAH-F177-115_CavityFilling
465	242	36.13	0.00	0.03	0.07	0.03	0.00	1.59	0.00	58.37	0.98	0.01	0.06	0.10	0.28	0.02	1.52	0.00	0.00	0.00	0.00		99.17	20-12-16	BAH-F177-115_CavityFilling
466	243	36.18	0.00	0.04	0.02	0.06	0.00	1.55	0.05	58.90	0.91	0.00	0.03	0.04	0.25	0.00	1.65	0.00	0.00	0.00	0.00		99.67	20-12-16	BAH-F177-115_CavityFilling
467	244	37.26	0.00	0.03	0.04	0.03	0.05	1.62	0.01	59.43	0.88	0.03	0.02	0.06	0.26	0.12	1.65	0.00	0.00	0.01	0.00		101.51	20-12-16	BAH-F177-115_CavityFilling
468	245	36.34	0.00	0.04	0.05	0.07	0.01	1.59	0.00	58.54	0.99	0.01	0.00	0.00	0.26	0.06	1.66	0.00	0.00	0.00	0.01		99.63	20-12-16	BAH-F177-115_CavityFilling
469	246	35.60	0.00	0.04	0.09	0.06	0.01	1.68	0.03	59.73	1.06	0.03	0.03	0.10	0.25	0.07	1.78	0.00	0.00	0.00	0.04		100.58	20-12-16	BAH-F177-115_CavityFilling
470	332	36.58	0.08	0.01	0.00	0.05	0.01	0.65	0.02	64.52	0.37	0.04	0.00	0.04	0.35	0.00	0.46	0.03	0.00	0.00			103.20	6/7/16	BAH-F226-120.5-B1-1
471	341	36.48	0.00	0.01	0.02	0.06	0.00	0.34	0.00	60.26	0.12	0.02	0.00	0.02	0.85	0.00	1.37	0.00	0.00	0.00			99.55	6/7/16	BAH-F226-120.5-B1-10
472	342	37.08	0.01	0.00	0.02	0.10	0.00	0.29	0.01	60.27	0.29	0.01	0.00	0.03	0.98	0.00	0.86	0.00	0.00	0.00			99.95	6/7/16	BAH-F226-120.5-B1-11
473	343	36.58	0.09	0.01	0.01	0.19	0.00	0.41	0.01	60.60	0.10	0.01	0.03	0.02	0.74	0.00	1.22	0.01	0.00	0.05			99.97	6/7/16	BAH-F226-120.5-B1-12
474	344	34.62	0.00	0.01	0.01	0.07	0.02	0.60	0.01	64.56	0.74	0.05	0.00	0.11	0.26	0.02	0.22	0.00	0.00	0.02			101.31	6/7/16	BAH-F226-120.5-B1-13
475	345	34.32	0.00	0.02	0.00	0.08	0.02	0.59	0.00	64.69	0.82	0.07	0.03	0.06	0.28	0.00	0.31	0.00	0.00	0.00			101.29	6/7/16	BAH-F226-120.5-B1-14
476	333	35.91	0.00	0.00	0.00	0.06	0.03	0.50	0.00	64.07	0.35	0.01	0.01	0.01	0.30	0.02	0.44	0.00	0.00	0.00			101.70	6/7/16	BAH-F226-120.5-B1-2
477	334	36.01	0.00	0.01	0.01	0.07	0.00	0.69	0.00	64.60	0.38	0.01	0.00	0.01	0.39	0.02	0.54	0.02	0.00	0.04			102.78	6/7/16	BAH-F226-120.5-B1-3
478	335	35.30	0.02	0.01	0.04	0.08	0.02	0.62	0.00	64.84	0.44	0.03	0.02	0.03	0.30	0.00	0.37	0.01	0.00	0.00			102.11	6/7/16	BAH-F226-120.5-B1-4
479	336	35.33	0.00	0.01	0.02	0.08	0.01	0.56	0.04	64.42	0.41	0.03	0.05	0.01	0.34	0.05	0.43	0.00	0.00	0.06			101.84	6/7/16	BAH-F226-120.5-B1-5
480	337	36.35	0.00	0.00	0.00	0.08	0.01	0.43	0.00	60.22	0.11	0.01	0.03	0.01	0.78	0.00	1.19	0.04	0.00	0.02			99.27	6/7/16	BAH-F226-120.5-B1-6
481	338	36.53	0.03	0.00	0.00	0.06	0.00	0.56	0.04	60.86	0.10	0.03	0.00	0.01	0.49	0.00	0.83	0.03	0.00	0.05			99.62	6/7/16	BAH-F226-120.5-B1-7
482	339	36.19																							

INDEX	No.	O	Na	K	V	Co	Mg	P	Cr	Fe	Al	S	Ni	Mn	Si	Pb	Cu	Ti	Ca	Zn	Ba	Sr	Total	Date	Sample
540	5585	38.04	0.00	0.00	0.03	0.01	0.03	0.59	0.01	60.90	0.01	0.00	0.01	0.05	0.34	0.00	0.58	0.00	0.03	0.03			100.66	10/11/16	BAH-F282-118.2_brown
541	5586	38.41	0.00	0.00	0.03	0.03	0.03	0.59	0.03	60.90	0.00	0.00	0.06	0.00	0.34	0.00	0.72	0.00	0.06	0.00			101.19	10/11/16	BAH-F282-118.2_brown
542	5593	38.17	0.04	0.02	0.00	0.00	0.04	0.64	0.00	61.64	0.00	0.00	0.03	0.08	0.35	0.00	0.54	0.00	0.05	0.08			101.65	10/11/16	BAH-F282-118.2_brown
543	5594	38.07	0.01	0.00	0.00	0.01	0.02	0.56	0.00	61.03	0.00	0.00	0.04	0.06	0.33	0.02	0.43	0.01	0.04	0.03			100.65	10/11/16	BAH-F282-118.2_brown
544	5595	38.38	0.00	0.00	0.00	0.02	0.02	0.58	0.00	61.19	0.00	0.00	0.05	0.04	0.32	0.00	0.46	0.02	0.03	0.09			101.21	10/11/16	BAH-F282-118.2_brown
545	5596	38.12	0.00	0.01	0.00	0.00	0.04	0.62	0.00	61.00	0.00	0.00	0.06	0.02	0.33	0.00	0.50	0.00	0.04	0.00			100.74	10/11/16	BAH-F282-118.2_brown
546	5597	38.13	0.03	0.00	0.01	0.02	0.03	0.64	0.01	61.37	0.00	0.00	0.03	0.01	0.38	0.00	0.63	0.00	0.06	0.00			101.35	10/11/16	BAH-F282-118.2_brown
547	5598	38.45	0.01	0.00	0.00	0.02	0.01	0.64	0.00	60.64	0.00	0.00	0.01	0.04	0.35	0.05	0.56	0.00	0.04	0.08			100.90	10/11/16	BAH-F282-118.2_brown
548	5599	37.59	0.05	0.00	0.00	0.01	0.02	0.61	0.00	60.86	0.00	0.00	0.03	0.06	0.36	0.02	0.63	0.00	0.05	0.08			100.37	10/11/16	BAH-F282-118.2_brown
549	5600	37.74	0.01	0.00	0.02	0.00	0.01	0.64	0.02	61.22	0.00	0.01	0.07	0.03	0.37	0.00	0.69	0.00	0.06	0.04			100.91	10/11/16	BAH-F282-118.2_brown
550	5484	36.52	0.00	0.00	0.02	0.00	0.01	0.38	0.01	61.38	0.02	0.00	0.06	0.03	0.25	0.00	0.44	0.01	0.01	0.06			99.19	10/11/16	BAH-F282-118.4
551	5485	36.45	0.01	0.01	0.00	0.00	0.01	0.36	0.00	61.49	0.01	0.00	0.05	0.03	0.24	0.08	0.31	0.00	0.02	0.02			99.09	10/11/16	BAH-F282-118.4
552	5486	36.60	0.00	0.00	0.00	0.00	0.02	0.36	0.00	61.08	0.01	0.00	0.04	0.04	0.24	0.07	0.32	0.01	0.02	0.00			98.79	10/11/16	BAH-F282-118.4
553	5487	36.42	0.00	0.01	0.02	0.00	0.04	0.35	0.01	60.97	0.01	0.00	0.06	0.08	0.22	0.07	0.35	0.00	0.02	0.04			98.70	10/11/16	BAH-F282-118.4
554	5488	36.49	0.00	0.00	0.00	0.00	0.01	0.36	0.00	61.32	0.01	0.01	0.07	0.06	0.24	0.00	0.23	0.00	0.02	0.07			98.89	10/11/16	BAH-F282-118.4
555	5489	36.47	0.01	0.00	0.01	0.02	0.02	0.36	0.01	60.19	0.01	0.00	0.00	0.05	0.23	0.03	0.14	0.00	0.02	0.00			97.58	10/11/16	BAH-F282-118.4
556	5490	36.36	0.00	0.00	0.01	0.00	0.03	0.38	0.00	60.58	0.02	0.01	0.07	0.03	0.22	0.00	0.26	0.01	0.02	0.01			98.00	10/11/16	BAH-F282-118.4
557	5491	36.42	0.01	0.00	0.01	0.03	0.01	0.38	0.00	60.57	0.02	0.01	0.04	0.04	0.24	0.00	0.16	0.00	0.03	0.07			98.05	10/11/16	BAH-F282-118.4
558	282	36.48	0.01	0.00	0.01	0.06	0.01	0.87	0.02	59.19	0.17	0.01	0.01	0.03	0.20	0.09	0.10	0.00	0.00	0.03			97.27	6/7/16	BAH-F282-94.3-1
559	283	37.05	0.00	0.01	0.00	0.06	0.00	1.04	0.02	58.78	0.25	0.00	0.03	0.04	0.26	0.08	0.08	0.00	0.00	0.02			97.71	6/7/16	BAH-F282-94.3-2
560	284	36.06	0.00	0.00	0.05	0.07	0.02	0.66	0.00	58.55	0.74	0.00	0.05	0.09	0.29	0.02	0.31	0.02	0.00	0.02			96.94	6/7/16	BAH-F282-94.3-3
561	5560	35.73	0.00	0.02	0.02	0.03	0.03	0.39	0.00	62.21	0.14	0.01	0.03	0.03	0.09	0.11	0.01	0.00	0.02	0.08			98.97	10/11/16	BAH100_Gibb+Goe
562	5561	35.73	0.04	0.00	0.00	0.01	0.02	0.42	0.00	62.70	0.21	0.01	0.03	0.02	0.12	0.02	0.00	0.01	0.03	0.01			99.39	10/11/16	BAH100_Gibb+Goe
563	5562	35.70	0.01	0.01	0.00	0.02	0.02	0.41	0.01	62.18	0.16	0.02	0.00	0.03	0.10	0.00	0.07	0.00	0.04	0.06			98.86	10/11/16	BAH100_Gibb+Goe
564	5563	35.68	0.04	0.01	0.00	0.00	0.02	0.47	0.00	62.20	0.15	0.02	0.03	0.05	0.11	0.00	0.02	0.00	0.03	0.01			98.84	10/11/16	BAH100_Gibb+Goe
565	5564	35.52	0.00	0.01	0.00	0.02	0.00	0.44	0.01	62.24	0.16	0.00	0.01	0.00	0.09	0.00	0.02	0.00	0.04	0.02			98.59	10/11/16	BAH100_Gibb+Goe
566	5565	35.67	0.05	0.00	0.02	0.04	0.00	0.45	0.00	62.57	0.16	0.01	0.03	0.06	0.11	0.00	0.03	0.00	0.04	0.02			99.27	10/11/16	BAH100_Gibb+Goe
567	5566	35.49	0.03	0.01	0.00	0.04	0.00	0.39	0.00	61.40	0.06	0.02	0.02	0.01	0.07	0.00	0.00	0.01	0.01	0.00			97.56	10/11/16	BAH100_Gibb+Goe
568	5567	35.95	0.01	0.01	0.00	0.03	0.01	0.41	0.01	61.66	0.12	0.02	0.01	0.01	0.08	0.01	0.05	0.00	0.04	0.02			98.45	10/11/16	BAH100_Gibb+Goe
569	5568	36.07	0.06	0.00	0.02	0.04	0.00	0.42	0.00	61.32	0.09	0.00	0.05	0.04	0.08	0.01	0.05	0.04	0.03	0.01			98.34	10/11/16	BAH100_Gibb+Goe
570	127	35.54	0.00	0.00		0.09	0.00	0.06	0.00	60.01	0.04	0.00	0.00	0.07	1.98	0.00	1.63	0.04	0.00	0.03	0.00	0.06	99.545	18-07-14	BAH3 cm17 3 bott lay
571	129	36.46	0.04	0.01		0.09	0.00	0.07	0.00	59.75	0.07	0.01	0.00	0.00	1.99	0.00	1.77	0.04	0.00	0.00	0.04	0.00	100.331	18-07-14	BAH3 cm17 3 bott lay
572	130	35.19	0.04	0.00		0.02	0.00	0.06	0.03	59.96	0.05	0.00	0.00	0.02	1.67	0.00	1.45	0.06	0.00	0.08	0.07	0.01	98.684	18-07-14	BAH3 cm17 3 bott lay
573	131	34.22	0.01	0.00		0.07	0.02	0.05	0.00	58.56	0.03	0.02	0.00	0.09	1.94	0.06	1.90	0.01	0.00	0.00	0.00	0.04	97.009	18-07-14	BAH3 cm17 3 bott lay
574	132	33.98	0.00	0.02		0.06	0.00	0.09	0.03	58.86	0.04	0.01	0.00	0.03	1.27	0.09	1.53	0.02	0.00	0.00	0.02	0.00	96.03	18-07-14	BAH3 cm17 3 bott lay
575	118	35.51	0.02	0.00		0.04	0.01	0.13	0.00	62.60	0.19	0.01	0.00	0.05	1.04	0.10	0.66	0.01	0.00	0.01	0.03	0.00	100.39	18-07-14	BAH3 cm17 3 bott lay
576	119	35.97	0.00	0.01		0.11	0.01	0.14	0.00	63.21	0.20	0.00	0.00	0.09	1.04	0.06	0.61	0.04	0.00	0.00	0.00	0.00	101.476	18-07-14	BAH3 cm17 3 bott lay
577	120	35.36	0.02	0.00		0.06	0.02	0.11	0.00	63.20	0.18	0.00	0.00	0.03	1.10	0.00	0.77	0.07	0.00	0.00	0.01	0.00	100.926	18-07-14	BAH3 cm17 3 bott lay
578	121	36.61	0.00	0.00		0.03	0.00	0.13	0.00	62.79	0.14	0.01	0.00	0.07	1.17	0.03	0.74	0.00	0.00	0.02	0.00	0.00	101.731	18-07-14	BAH3 cm17 3 bott lay
579	122	36.41	0.00	0.00		0.05	0.01	0.13	0.11	62.09	0.15	0.00	0.00	0.06	1.34	0.00	0.87	0.01	0.00	0.02	0.00	0.00	101.262	18-07-14	BAH3 cm17 3 bott lay
580	123	36.12	0.00	0.01		0.07	0.00	0.16	0.00	61.70	0.13	0.01	0.00	0.06	1.31	0.00	1.03	0.00	0.00	0.00	0.02	0.00	100.597	18-07-14	BAH3 cm17 3 bott lay
581	124	36.54	0.00	0.01		0.05	0.01	0.06	0.00	61.02	0.06	0.01	0.00	0.03	1.65	0.02	1.32	0.01	0.00	0.00	0.01	0.02	100.8	18-07-14	BAH3 cm17 3 bott lay
582	125	38.01	0.01	0.02		0.07	0.00	0.06	0.03	60.18	0.06	0.02	0.00	0.06	1.85	0.08	1.60	0.00	0.00	0.02	0.00	0.00	102.067	18-07-14	BAH3 cm17 3 bott lay
583	126	36.90	0.00	0.01		0.09	0.00	0.08	0.00	60.70	0.01	0.00	0.00	0.00	1.92	0.02	1.53	0.00	0.00	0.00	0.01	0.00	101.275	18-07-14	BAH3 cm17 3 bott lay
584	152	35.61	0.03	0.00		0.05	0.00	0.08	0.00	63.20	0.19	0.01	0.00	0.09	1.08	0.03	0.19	0.00	0.00	0.00	0.09	0.02	100.67	18-07-14	BAH3 cm17 large goe
585	153	36.05	0.01	0.00		0.08	0.03	0.11	0.00	63.60	0.21	0.01	0.00	0.05	1.08	0.02	0.23	0.05	0.00	0.00	0.07	0.02	101.6	18-07-14	BAH3 cm17 large goe
586	154	36.10	0.00	0.01		0.10	0.01	0.15	0.00	62.98	0.21	0.00	0.00	0.00	1.08	0.00	0.24	0.00	0.00	0.00	0.04	0.01	100.927	18-07-14	BAH3 cm17 large goe
587	155	35.39	0.00	0.00		0.04	0.01	0.10	0.00	63.53	0.18	0.01	0.00	0.14	1.10	0.03	0.25	0.00	0.00	0.06	0.00	0.02	100.865	18-07-14	BAH3 cm17 large goe
588	156	35.80	0.03	0.00		0.09	0.00	0.10	0.00	63.67	0.19	0.01	0.00	0.00	1.11	0.00	0.30	0.00	0.00	0.01	0.14	0.03	101.482	18-07-14	BAH3 cm17 large goe
589	157	36.27	0.01	0.00		0.08	0.00	0.09	0.00	63.18	0.20	0.03	0.00	0.07	1.13	0.03	0.22	0.03	0.00	0.03	0.00	0.06	101.439	18-07-14	BAH3 cm17 large goe
590	143	36.40																							

INDEX	No.	O	Na	K	V	Co	Mg	P	Cr	Fe	Al	S	Ni	Mn	Si	Pb	Cu	Ti	Ca	Zn	Ba	Sr	Total	Date	Sample
648	141	35.44	0.00	0.03	0.00	0.09	0.02	1.73	0.00	55.03	0.05	0.00	0.03	3.05	0.16	0.05	2.94	0.00	0.03	0.12	0.02		98.79	20-12-16	IBH-13-03-TC
649	142	36.09	0.05	0.03	0.02	0.00	0.01	1.75	0.00	54.46	0.05	0.02	0.00	3.26	0.14	0.11	3.03	0.00	0.04	0.00	0.04		99.09	20-12-16	IBH-13-03-TC
650	143	35.59	0.00	0.03	0.00	0.05	0.03	1.82	0.00	55.63	0.06	0.02	0.00	3.01	0.15	0.00	2.84	0.00	0.07	0.04	0.01		99.33	20-12-16	IBH-13-03-TC
651	144	34.95	0.00	0.03	0.00	0.06	0.04	1.65	0.00	56.67	0.07	0.01	0.02	3.18	0.14	0.00	2.87	0.04	0.06	0.03	0.00		99.81	20-12-16	IBH-13-03-TC
652	145	36.15	0.00	0.03	0.05	0.08	0.01	1.55	0.01	47.70	0.08	0.00	0.00	6.80	0.15	0.12	4.44	0.03	0.01	0.02	0.00		97.24	20-12-16	IBH-13-03-TC
653	146	35.08	0.00	0.02	0.05	0.05	0.01	1.73	0.03	56.32	0.07	0.08	0.05	3.75	0.17	0.00	3.14	0.00	0.10	0.04	0.00		100.68	20-12-16	IBH-13-03-TC
654	147	35.59	0.06	0.03	0.03	0.06	0.05	1.91	0.00	56.52	0.06	0.00	0.00	2.83	0.17	0.00	3.28	0.00	0.03	0.03	0.04		100.66	20-12-16	IBH-13-03-TC
655	148	35.82	0.00	0.03	0.02	0.07	0.02	1.95	0.00	56.40	0.05	0.01	0.00	2.93	0.16	0.00	3.35	0.00	0.06	0.03	0.00		100.87	20-12-16	IBH-13-03-TC
656	149	35.85	0.00	0.03	0.04	0.07	0.01	1.96	0.00	56.63	0.08	0.01	0.00	3.05	0.13	0.00	3.42	0.00	0.07	0.06	0.02		101.42	20-12-16	IBH-13-03-TC
657	150	36.47	0.00	0.02	0.02	0.06	0.00	1.82	0.00	53.50	0.03	0.00	0.01	3.70	0.14	0.07	3.54	0.00	0.02	0.01	0.00		99.41	20-12-16	IBH-13-03-TC
658	151	36.95	0.00	0.02	0.00	0.11	0.00	1.81	0.00	52.96	0.04	0.01	0.03	3.40	0.15	0.08	3.50	0.05	0.02	0.08	0.00		99.20	20-12-16	IBH-13-03-TC
659	152	36.68	0.00	0.01	0.02	0.03	0.03	1.87	0.03	53.14	0.03	0.02	0.04	3.71	0.13	0.02	3.57	0.00	0.01	0.05	0.02		99.40	20-12-16	IBH-13-03-TC
660	153	36.27	0.00	0.02	0.01	0.04	0.00	1.43	0.00	48.95	0.04	0.01	0.00	6.48	0.13	0.00	4.57	0.01	0.00	0.08	0.01		98.05	20-12-16	IBH-13-03-TC
661	154	35.90	0.00	0.03	0.03	0.04	0.02	1.67	0.00	51.86	0.04	0.00	0.02	4.12	0.16	0.00	4.02	0.00	0.00	0.01	0.05		97.96	20-12-16	IBH-13-03-TC
662	155	36.26	0.00	0.02	0.01	0.05	0.00	1.80	0.02	51.69	0.02	0.00	0.00	3.92	0.16	0.05	3.87	0.00	0.00	0.09	0.03		97.99	20-12-16	IBH-13-03-TC
663	156	36.68	0.00	0.03	0.02	0.11	0.02	1.61	0.00	50.88	0.02	0.01	0.00	4.72	0.15	0.08	4.13	0.00	0.00	0.09	0.00		98.53	20-12-16	IBH-13-03-TC
664	157	36.64	0.00	0.03	0.04	0.01	0.02	1.66	0.01	51.43	0.04	0.01	0.00	4.20	0.17	0.00	4.00	0.01	0.03	0.05	0.06		98.40	20-12-16	IBH-13-03-TC
665	158	36.12	0.04	0.02	0.00	0.07	0.03	1.69	0.02	51.68	0.01	0.01	0.00	4.36	0.16	0.08	4.06	0.00	0.01	0.03	0.06		98.46	20-12-16	IBH-13-03-TC
666	196	39.31	0.00	0.00	0.08	0.00	0.00	0.04	0.01	56.24	4.28	0.10	0.03	0.01	0.18	0.04	0.07	0.05	0.00	0.02	0.03	0.00	100.47	22-02-14	IBH-13-08c
667	200	39.11	0.00	0.00	0.04	0.05	0.01	0.16	0.03	55.37	3.33	0.12	0.00	0.04	0.21	0.00	0.10	0.05	0.00	0.01	0.00	0.00	98.63	22-02-14	IBH-13-08c
668	201	38.58	0.02	0.01	0.01	0.03	0.01	0.08	0.06	56.98	2.52	0.13	0.00	0.00	0.22	0.15	0.06	0.04	0.00	0.01	0.02	0.00	98.93	22-02-14	IBH-13-08c
669	292	43.94	0.00	0.00	0.05	0.01	0.01	0.05	0.05	24.26	25.90	0.07	0.00	0.00	1.01	0.01	0.02	0.47	0.00	0.04	0.04	0.00	95.93	20-12-16	IBH-13-09d
670	293	46.63	0.00	0.00	0.00	0.00	0.00	0.05	0.01	22.40	29.13	0.07	0.06	0.01	0.88	0.00	0.04	0.65	0.00	0.02	0.02	0.00	99.97	20-12-16	IBH-13-09d
671	294	45.85	0.03	0.02	0.05	0.03	0.02	0.06	0.04	23.24	27.59	0.06	0.00	0.01	0.82	0.00	0.01	0.21	0.00	0.08	0.00	0.00	98.09	20-12-16	IBH-13-09d
672	295	35.51	0.00	0.01	0.02	0.07	0.00	0.02	0.01	60.99	0.34	0.05	0.00	0.00	0.25	0.01	0.02	0.00	0.00	0.00	0.00	0.00	97.29	20-12-16	IBH-13-09d
673	296	37.03	0.00	0.01	0.00	0.04	0.00	0.01	0.01	59.88	0.63	0.05	0.00	0.00	0.22	0.00	0.02	0.00	0.00	0.01	0.06	0.00	97.96	20-12-16	IBH-13-09d
674	297	38.29	0.05	0.01	0.00	0.05	0.00	0.01	0.03	61.01	1.09	0.08	0.00	0.00	0.25	0.05	0.00	0.07	0.00	0.00	0.00	0.00	100.98	20-12-16	IBH-13-09d
675	298	42.25	0.00	0.02	0.10	0.04	0.02	0.14	0.11	38.86	13.44	0.09	0.07	0.00	3.92	0.03	0.03	0.23	0.00	0.05	0.01	0.00	99.40	20-12-16	IBH-13-09d
676	299	41.59	0.00	0.02	0.07	0.06	0.07	0.10	0.07	44.56	10.35	0.10	0.02	0.00	3.12	0.00	0.05	0.17	0.00	0.01	0.00	0.00	100.35	20-12-16	IBH-13-09d
677	300	41.11	0.01	0.03	0.06	0.02	0.02	0.05	0.03	43.71	10.04	0.13	0.09	0.00	3.53	0.00	0.02	0.60	0.00	0.04	0.00	0.00	99.47	20-12-16	IBH-13-09d
678	301	45.54	0.00	0.04	0.02	0.05	0.01	0.09	0.04	30.65	12.86	0.09	0.03	0.00	9.52	0.00	0.02	0.40	0.00	0.03	0.00	0.00	99.38	20-12-16	IBH-13-09d
679	302	40.91	0.01	0.02	0.03	0.08	0.00	0.05	0.00	42.73	10.61	0.07	0.04	0.01	3.67	0.00	0.01	0.32	0.00	0.00	0.00	0.00	98.57	20-12-16	IBH-13-09d
680	303	40.62	0.00	0.03	0.02	0.00	0.00	0.05	0.01	29.74	20.23	0.06	0.05	0.01	2.38	0.00	0.05	0.38	0.00	0.00	0.00	0.00	93.62	20-12-16	IBH-13-09d
681	304	41.56	0.00	0.02	0.06	0.00	0.01	0.07	0.02	41.81	10.94	0.10	0.00	0.02	4.00	0.00	0.07	0.23	0.00	0.04	0.02	0.00	98.95	20-12-16	IBH-13-09d
682	305	36.19	0.00	0.00	0.03	0.06	0.00	0.04	0.02	59.58	0.76	0.05	0.02	0.01	0.17	0.13	0.00	0.04	0.00	0.00	0.00	0.00	97.10	20-12-16	IBH-13-09d
683	306	37.62	0.06	0.02	0.07	0.06	0.00	0.03	0.00	61.50	0.74	0.05	0.00	0.02	0.23	0.01	0.06	0.01	0.00	0.09	0.00	0.00	100.57	20-12-16	IBH-13-09d
684	307	36.79	0.00	0.01	0.07	0.08	0.02	0.04	0.00	61.28	0.71	0.03	0.06	0.00	0.18	0.03	0.09	0.02	0.00	0.09	0.00	0.00	99.50	20-12-16	IBH-13-09d
685	183	41.16	0.01	0.03	0.11	0.03	0.01	0.04	0.43	48.07	9.43	0.17	0.03	0.00	0.77	0.04	0.08	0.22	0.00	0.00	0.00	0.02	100.63	22-02-14	IBH-13-09g
686	186	42.94	0.01	0.01	0.11	0.07	0.00	0.04	0.09	44.96	10.51	0.13	0.03	0.08	1.56	0.22	0.06	0.16	0.00	0.04	0.03	0.00	101.03	22-02-14	IBH-13-09g
687	187	37.66	0.03	0.00	0.02	0.09	0.00	0.00	0.09	60.47	1.11	0.04	0.00	0.00	0.20	0.00	0.07	0.01	0.00	0.00	0.03	0.04	99.86	22-02-14	IBH-13-09g
688	188	38.02	0.01	0.00	0.22	0.05	0.01	0.02	0.04	53.21	7.07	0.12	0.05	0.06	0.94	0.00	0.06	0.15	0.00	0.08	0.00	0.00	100.09	22-02-14	IBH-13-09g
689	190	38.74	0.02	0.01	0.11	0.05	0.00	0.06	0.02	52.32	8.06	0.10	0.02	0.00	1.61	0.00	0.00	0.24	0.00	0.00	0.00	0.01	101.34	22-02-14	IBH-13-09g
690	191	42.40	0.01	0.00	0.09	0.05	0.00	0.00	0.02	45.12	10.96	0.12	0.00	0.08	1.32	0.00	0.00	0.12	0.00	0.03	0.01	0.04	100.37	22-02-14	IBH-13-09g
691	192	38.15	0.02	0.00	0.00	0.03	0.00	0.00	0.00	60.88	1.00	0.06	0.00	0.00	0.20	0.02	0.04	0.03	0.00	0.00	0.04	0.00	100.46	22-02-14	IBH-13-09g
692	107	40.78	0.00	0.01	0.07	0.09	0.00	0.16	0.03	48.94	7.03	0.12	0.02	0.03	1.16	0.11	0.00	0.18	0.00	0.11	0.02	0.00	98.86	22-02-14	IBH-13-09h
693	110	40.33	0.00	0.00	0.06	0.03	0.00	0.13	0.03	50.70	6.30	0.09	0.03	0.07	1.12	0.05	0.00	0.06	0.00	0.00	0.00	0.00	99.00	22-02-14	IBH-13-09h
694	111	40.64	0.00	0.00	0.02	0.05	0.04	0.18	0.02	49.04	6.85	0.09	0.00	0.01	1.36	0.00	0.00	0.37	0.00	0.00	0.02	0.01	98.70	22-02-14	IBH-13-09h
695	114	38.56	0.00	0.00	0.00	0.10	0.02	0.08	0.03	56.16	3.02	0.09	0.00	0.01	0.25	0.00	0.00	0.03	0.00	0.04	0.03	0.00	98.43	22-02-14	IBH-13-09h
696	115	41.43	0.02	0.00	0.00	0.01	0.00	0.12	0.00	47.58	7.93	0.13	0.01	0.02	2.00	0.00	0.08	0.23	0.00	0.00	0.03	0.01	99.58	22-02-14	IBH-13-09h
697	116	39.77	0.00	0.01	0.09	0.08	0.00	0.20	0.00	51.86															

INDEX	No.	O	Na	K	V	Co	Mg	P	Cr	Fe	Al	S	Ni	Mn	Si	Pb	Cu	Ti	Ca	Zn	Ba	Sr	Total	Date	Sample
756	67	37.44	0.00	0.01	0.16	0.06	0.01	0.23	0.00	57.28	3.77	0.02	0.00	0.00	0.12	0.00	0.04	0.00	0.00	0.00	0.00	0.00	99.14	30-09-14	NIP 13 28 Gt+Hem+Gibb
757	68	38.21	0.00	0.02	0.13	0.15	0.00	0.23	0.00	57.17	3.58	0.01	0.00	0.00	0.14	0.11	0.00	0.00	0.00	0.00	0.00	0.00	99.75	30-09-14	NIP 13 28 Gt+Hem+Gibb
758	69	38.18	0.00	0.01	0.21	0.12	0.00	0.21	0.01	56.25	3.90	0.03	0.06	0.06	0.12	0.08	0.00	0.01	0.00	0.00	0.00	0.00	99.26	30-09-14	NIP 13 28 Gt+Hem+Gibb
759	70	38.34	0.00	0.00	0.17	0.01	0.00	0.19	0.01	56.23	3.77	0.02	0.03	0.02	0.15	0.00	0.09	0.05	0.00	0.01	0.00	0.00	99.08	30-09-14	NIP 13 28 Gt+Hem+Gibb
760	71	38.24	0.01	0.00	0.19	0.03	0.00	0.23	0.00	57.80	3.92	0.00	0.01	0.04	0.13	0.00	0.03	0.07	0.00	0.00	0.04	0.00	100.74	30-09-14	NIP 13 28 Gt+Hem+Gibb
761	72	48.03	0.02	0.00	0.07	0.03	0.01	0.20	0.01	19.68	33.74	0.02	0.00	0.05	0.09	0.04	0.00	0.04	0.00	0.06	0.02	0.00	102.11	30-09-14	NIP 13 28 Gt+Hem+Gibb
762	73	52.54	0.00	0.00	0.08	0.00	0.01	0.16	0.06	14.96	32.83	0.02	0.03	0.00	0.09	0.04	0.03	0.12	0.00	0.00	0.02	0.00	101.01	30-09-14	NIP 13 28 Gt+Hem+Gibb
763	74	37.70	0.00	0.01	0.17	0.11	0.00	0.14	0.07	58.00	2.26	0.00	0.00	0.00	0.14	0.10	0.05	0.07	0.00	0.00	0.00	0.00	98.81	30-09-14	NIP 13 28 Gt+Hem+Gibb
764	76	38.87	0.00	0.00	0.07	0.08	0.00	0.63	0.00	55.16	4.86	0.06	0.00	0.01	0.03	0.00	0.06	0.05	0.00	0.00	0.00	0.00	99.90	30-09-14	NIP 13 33 Gt
765	77	39.34	0.00	0.00	0.06	0.02	0.00	0.66	0.07	55.33	4.81	0.05	0.04	0.05	0.04	0.00	0.03	0.02	0.00	0.00	0.02	0.00	100.54	30-09-14	NIP 13 33 Gt
766	78	38.98	0.00	0.00	0.08	0.08	0.01	0.56	0.01	57.78	4.65	0.04	0.11	0.05	0.06	0.00	0.00	0.11	0.00	0.04	0.00	0.00	102.55	30-09-14	NIP 13 33 Gt
767	79	40.05	0.00	0.00	0.24	0.00	0.00	0.81	0.02	54.69	5.05	0.03	0.01	0.00	0.10	0.00	0.05	1.51	0.00	0.09	0.00	0.00	102.64	30-09-14	NIP 13 33 Gt
768	80	38.83	0.00	0.00	0.16	0.06	0.01	0.75	0.00	58.52	4.18	0.05	0.02	0.00	0.07	0.00	0.00	0.38	0.00	0.00	0.00	0.00	103.03	30-09-14	NIP 13 33 Gt
769	81	37.15	0.01	0.02	0.41	0.14	0.01	1.07	0.01	55.08	5.03	0.07	0.00	0.00	0.07	0.07	0.00	2.05	0.00	0.00	0.02	0.00	101.22	30-09-14	NIP 13 33 Gt
770	82	38.45	0.00	0.00	0.12	0.06	0.01	0.77	0.00	58.49	2.79	0.05	0.00	0.05	0.06	0.08	0.00	0.11	0.00	0.00	0.04	0.00	101.07	30-09-14	NIP 13 33 Gt
771	83	38.34	0.00	0.00	0.54	0.00	0.07	1.03	0.02	53.98	3.51	0.08	0.00	0.00	0.10	0.00	0.02	2.54	0.00	0.00	0.03	0.00	100.26	30-09-14	NIP 13 33 Gt
772	84	38.63	0.00	0.00	0.09	0.05	0.01	1.23	0.04	58.21	2.72	0.09	0.00	0.00	0.07	0.02	0.00	0.13	0.00	0.00	0.03	0.00	101.31	30-09-14	NIP 13 33 Gt
773	85	36.57	0.00	0.02	0.12	0.05	0.02	0.98	0.00	62.35	1.90	0.04	0.05	0.06	0.05	0.01	0.03	0.00	0.00	0.00	0.02	0.00	102.28	30-09-14	NIP 13 33 Gt
774	86	36.88	0.00	0.00	0.03	0.06	0.00	1.00	0.01	61.72	1.87	0.02	0.00	0.00	0.06	0.00	0.00	0.11	0.00	0.00	0.02	0.00	101.76	30-09-14	NIP 13 06 Vitreous gt
775	87	37.37	0.00	0.00	0.08	0.06	0.00	0.81	0.00	62.18	1.82	0.03	0.00	0.00	0.07	0.09	0.02	0.08	0.00	0.00	0.00	0.00	102.61	30-09-14	NIP 13 06 Vitreous gt
776	88	37.30	0.00	0.01	0.08	0.09	0.01	0.53	0.01	59.23	3.05	0.00	0.00	0.05	0.10	0.00	0.02	0.24	0.00	0.00	0.02	0.00	100.74	30-09-14	NIP 13 06 Vitreous gt
777	89	37.95	0.00	0.01	0.09	0.01	0.00	0.52	0.00	60.53	2.41	0.02	0.00	0.00	0.14	0.00	0.03	0.18	0.00	0.14	0.04	0.00	102.06	30-09-14	NIP 13 06 Vitreous gt
778	90	37.65	0.00	0.02	0.04	0.07	0.00	0.49	0.03	59.12	3.12	0.01	0.01	0.01	0.09	0.00	0.02	0.18	0.00	0.02	0.00	0.00	100.86	30-09-14	NIP 13 06 Vitreous gt
779	91	37.33	0.00	0.02	0.07	0.10	0.00	0.56	0.04	59.51	3.17	0.00	0.00	0.07	0.11	0.04	0.00	0.19	0.00	0.00	0.02	0.00	101.23	30-09-14	NIP 13 06 Vitreous gt
780	92	37.71	0.00	0.00	0.09	0.08	0.01	0.49	0.00	58.68	3.04	0.02	0.00	0.03	0.11	0.00	0.00	0.33	0.00	0.00	0.02	0.00	100.59	30-09-14	NIP 13 06 Vitreous gt
781	93	37.92	0.00	0.00	0.03	0.11	0.01	0.54	0.01	60.66	2.95	0.01	0.00	0.00	0.12	0.03	0.00	0.00	0.00	0.06	0.00	0.00	102.45	30-09-14	NIP 13 06 Vitreous gt
782	94	36.77	0.00	0.01	0.04	0.06	0.01	0.36	0.00	64.77	1.32	0.03	0.03	0.00	0.21	0.08	0.01	0.03	0.00	0.02	0.02	0.00	103.75	30-09-14	NIP 13 06 Vitreous gt
783	95	38.01	0.00	0.00	0.03	0.12	0.00	0.32	0.00	61.89	1.37	0.02	0.03	0.00	0.27	0.02	0.04	0.08	0.00	0.02	0.02	0.00	102.24	30-09-14	NIP 13 06 Vitreous gt
784	109	36.81	0.00	0.00	0.03	0.09	0.02	0.15	0.00	62.65	0.11	0.02	0.00	0.00	0.11	0.11	0.00	0.05	0.00	0.03	0.04	0.00	100.21	30-09-14	NIP 13 02
785	110	36.52	0.00	0.02	0.03	0.05	0.01	0.55	0.00	61.16	1.73	0.01	0.00	0.00	0.07	0.08	0.06	0.00	0.00	0.07	0.00	0.00	100.35	30-09-14	NIP 13 02
786	111	38.16	0.00	0.00	0.07	0.06	0.00	0.51	0.03	59.45	2.07	0.02	0.00	0.04	0.08	0.00	0.03	0.27	0.00	0.00	0.00	0.00	100.78	30-09-14	NIP 13 02
787	112	38.45	0.00	0.01	0.06	0.11	0.00	0.61	0.01	60.12	2.12	0.05	0.03	0.00	0.07	0.00	0.00	0.03	0.00	0.01	0.00	0.00	101.68	30-09-14	NIP 13 02
788	113	38.04	0.00	0.01	0.03	0.04	0.00	0.53	0.00	59.33	2.14	0.03	0.01	0.03	0.07	0.00	0.01	0.00	0.00	0.00	0.00	0.00	100.26	30-09-14	NIP 13 02
789	114	38.00	0.00	0.00	0.06	0.07	0.01	0.56	0.00	59.77	1.73	0.02	0.08	0.02	0.07	0.01	0.00	0.18	0.00	0.02	0.00	0.00	100.60	30-09-14	NIP 13 02
790	115	39.16	0.00	0.00	0.15	0.06	0.00	0.54	0.00	55.55	3.47	0.04	0.00	0.00	0.06	0.00	0.00	1.06	0.00	0.00	0.00	0.00	100.09	30-09-14	NIP 13 02
791	116	38.32	0.00	0.00	0.03	0.02	0.01	0.62	0.00	59.89	1.44	0.00	0.02	0.00	0.04	0.02	0.00	0.05	0.00	0.00	0.04	0.00	100.48	30-09-14	NIP 13 02
792	117	39.52	0.00	0.00	0.17	0.01	0.00	0.56	0.02	54.40	4.42	0.00	0.00	0.00	0.08	0.00	0.01	0.89	0.00	0.00	0.01	0.00	100.08	30-09-14	NIP 13 02
793	118	37.28	0.01	0.01	0.01	0.04	0.00	0.20	0.00	60.51	1.06	0.00	0.00	0.00	0.18	0.19	0.01	0.02	0.00	0.00	0.07	0.00	99.59	30-09-14	NIP 13 02
794	119	35.12	0.00	0.00	0.04	0.06	0.02	0.59	0.00	64.07	1.43	0.00	0.03	0.01	0.06	0.01	0.02	0.00	0.00	0.00	0.00	0.00	101.46	30-09-14	NIP 13 03
795	120	35.99	0.01	0.00	0.06	0.01	0.00	0.56	0.00	63.57	1.30	0.02	0.00	0.01	0.07	0.08	0.03	0.19	0.00	0.00	0.02	0.00	101.90	30-09-14	NIP 13 03
796	121	35.49	0.00	0.00	0.01	0.06	0.00	0.59	0.02	63.64	1.26	0.00	0.00	0.01	0.09	0.00	0.00	0.08	0.00	0.01	0.04	0.00	101.32	30-09-14	NIP 13 03
797	122	35.49	0.00	0.00	0.02	0.03	0.01	0.60	0.00	64.64	1.19	0.02	0.00	0.01	0.07	0.01	0.10	0.06	0.00	0.00	0.00	0.00	102.25	30-09-14	NIP 13 03
798	123	36.26	0.04	0.01	0.01	0.13	0.02	0.51	0.01	62.37	2.09	0.03	0.01	0.00	0.09	0.00	0.00	0.14	0.00	0.02	0.00	0.00	101.73	30-09-14	NIP 13 03
799	124	35.46	0.00	0.01	0.02	0.08	0.01	0.52	0.00	64.98	1.12	0.00	0.00	0.00	0.11	0.01	0.00	0.05	0.00	0.00	0.00	0.00	102.37	30-09-14	NIP 13 03
800	125	35.05	0.00	0.00	0.13	0.02	0.00	0.59	0.05	62.80	1.63	0.01	0.00	0.05	0.06	0.12	0.00	1.83	0.00	0.08	0.00	0.00	102.42	30-09-14	NIP 13 03
801	126	29.91	0.03	0.01	0.01	0.09	0.02	0.58	0.00	61.43	2.12	0.03	0.02	0.00	0.08	0.03	0.04	0.13	0.00	0.00	0.00	0.00	94.54	30-09-14	NIP 13 03
802	127	35.01	0.00	0.00	0.02	0.01	0.01	0.62	0.00	63.41	1.52	0.01	0.00	0.04	0.05	0.00	0.00	0.10	0.00	0.00	0.00	0.00	100.80	30-09-14	NIP 13 03
803	128	34.64	0.00	0.00	0.02	0.11	0.02	0.60	0.01	65.25	1.48	0.00	0.01	0.00	0.04	0.00	0.05	0.25	0.00	0.06	0.07	0.00	102.60	30-09-14	NIP 13 03
804	129	35.41	0.00	0.00	0.02	0.06	0.01	0.59	0.02	63.64	1.58	0.00	0.00	0.06	0.05	0.07	0.01	0.09	0.00	0.04	0.05				

INDEX	No.	O	Na	K	V	Co	Mg	P	Cr	Fe	Al	S	Ni	Mn	Si	Pb	Cu	Ti	Ca	Zn	Ba	Sr	Total	Date	Sample
864	191	39.78	0.00	0.00	0.07	0.06	0.00	0.35	0.00	55.38	5.73	0.08	0.00	0.00	0.51	0.06	0.00	0.02	0.00	0.01	0.00	0.00	102.03	30-09-14	NIP 13 18 lake
865	192	38.80	0.00	0.01	0.04	0.04	0.00	0.19	0.00	58.17	3.30	0.03	0.01	0.08	0.59	0.00	0.00	0.00	0.00	0.03	0.03	0.00	101.30	30-09-14	NIP 13 18 lake
866	193	38.15	0.00	0.01	0.04	0.03	0.00	0.17	0.04	60.75	1.44	0.01	0.00	0.02	0.55	0.05	0.00	0.01	0.00	0.00	0.00	0.00	101.26	30-09-14	NIP 13 18 lake
867	13	38.34	0.03	0.01		0.07	0.00	0.04	0.03	43.35	10.23	0.02	0.00	0.06	9.51	0.00	0.04	0.39	0.00	0.00	0.01	0.07	102.21	18-07-14	NIP-13-26 Pisolith
868	14	32.77	0.00	0.00		0.09	0.03	0.06	0.08	47.36	7.43	0.07	0.00	0.00	6.80	0.00	0.00	0.28	0.03	0.00	0.05	0.04	95.10	18-07-14	NIP-13-26 Pisolith
869	15	32.98	0.00	0.00		0.03	0.01	0.05	0.00	44.68	9.25	0.02	0.00	0.02	8.39	0.10	0.00	0.26	0.00	0.00	0.00	0.04	95.84	18-07-14	NIP-13-26 Pisolith
870	16	36.11	0.02	0.02		0.03	0.00	0.05	0.01	41.52	7.68	0.04	0.00	0.07	6.92	0.00	0.00	0.26	0.00	0.00	0.00	0.00	92.73	18-07-14	NIP-13-26 Pisolith
871	17	36.92	0.00	0.01		0.07	0.00	0.08	0.05	45.56	5.93	0.06	0.00	0.01	4.79	0.00	0.00	0.22	0.00	0.09	0.00	0.00	93.78	18-07-14	NIP-13-26 Pisolith
872	18	38.12	0.00	0.02		0.03	0.04	0.07	0.04	39.74	9.07	0.04	0.00	0.08	8.18	0.00	0.00	0.19	0.00	0.06	0.00	0.06	95.73	18-07-14	NIP-13-26 Pisolith
873	19	37.93	0.01	0.01		0.02	0.02	0.06	0.05	42.57	9.21	0.02	0.00	0.10	8.31	0.02	0.02	0.29	0.00	0.01	0.00	0.03	98.65	18-07-14	NIP-13-26 Pisolith
874	20	38.60	0.00	0.00		0.06	0.00	0.10	0.00	42.60	8.81	0.05	0.00	0.06	7.83	0.09	0.01	0.27	0.00	0.00	0.00	0.05	98.52	18-07-14	NIP-13-26 Pisolith
875	21	38.27	0.00	0.02		0.06	0.00	0.04	0.00	42.07	9.34	0.00	0.01	0.03	8.57	0.15	0.00	0.21	0.00	0.00	0.00	0.06	98.83	18-07-14	NIP-13-26 Pisolith
876	22	40.47	0.02	0.00		0.02	0.00	0.03	0.00	38.98	9.29	0.02	0.00	0.05	8.51	0.12	0.05	0.26	0.00	0.00	0.01	0.03	97.86	18-07-14	NIP-13-26 Pisolith
877	23	38.22	0.01	0.01		0.00	0.02	0.03	0.11	36.65	9.03	0.02	0.00	0.07	8.15	0.08	0.03	0.28	0.00	0.00	0.04	0.06	92.80	18-07-14	NIP-13-26 Pisolith
878	24	38.98	0.00	0.00		0.00	0.03	0.04	0.00	30.68	9.34	0.02	0.00	0.01	8.51	0.08	0.00	0.32	0.01	0.02	0.04	0.03	88.09	18-07-14	NIP-13-26 Pisolith
879	25	37.91	0.00	0.00		0.07	0.02	0.04	0.01	30.45	8.86	0.01	0.02	0.02	8.21	0.00	0.06	0.22	0.00	0.04	0.11	0.12	86.17	18-07-14	NIP-13-26 Pisolith
880	26	35.49	0.00	0.00		0.06	0.02	0.06	0.10	31.15	7.02	0.01	0.00	0.05	6.42	0.10	0.01	0.22	0.01	0.08	0.01	0.02	80.80	18-07-14	NIP-13-26 Pisolith
881	27	36.66	0.01	0.00		0.04	0.02	0.07	0.04	31.46	8.26	0.03	0.03	0.05	7.32	0.00	0.01	0.19	0.00	0.07	0.00	0.05	84.32	18-07-14	NIP-13-26 Pisolith
882	28	40.12	0.00	0.00		0.00	0.03	0.04	0.00	29.63	9.43	0.02	0.00	0.01	8.85	0.10	0.01	0.25	0.00	0.00	0.01	0.07	88.58	18-07-14	NIP-13-26 Pisolith
883	29	40.61	0.00	0.00		0.08	0.02	0.04	0.13	21.02	10.31	0.00	0.00	0.01	10.04	0.00	0.00	0.20	0.05	0.03	0.00	0.04	82.57	18-07-14	NIP-13-26 Pisolith
884	30	37.42	0.01	0.00		0.12	0.01	0.09	0.02	32.56	7.86	0.02	0.00	0.08	6.57	0.02	0.00	0.32	0.00	0.08	0.04	0.02	85.24	18-07-14	NIP-13-26 Pisolith
885	31	37.71	0.00	0.00		0.05	0.00	0.07	0.15	30.13	7.75	0.01	0.00	0.01	7.41	0.00	0.02	0.28	0.00	0.00	0.00	0.00	83.59	18-07-14	NIP-13-26 Pisolith
886	32	36.98	0.02	0.00		0.07	0.02	0.05	0.11	33.18	7.90	0.03	0.00	0.02	7.56	0.06	0.00	0.24	0.00	0.00	0.00	0.02	86.25	18-07-14	NIP-13-26 Pisolith
887	33	37.73	0.03	0.01		0.00	0.00	0.03	0.00	33.44	6.84	0.03	0.03	0.15	6.15	0.00	0.00	2.83	0.00	0.00	0.00	0.01	87.27	18-07-14	NIP-13-26 Pisolith
888	34	36.19	0.01	0.02		0.04	0.00	0.06	0.00	30.50	8.72	0.02	0.00	0.06	7.57	0.00	0.00	0.15	0.00	0.01	0.00	0.00	83.34	18-07-14	NIP-13-26 Pisolith
889	36	37.56	0.01	0.00		0.01	0.00	0.03	0.00	52.15	2.00	0.06	0.00	0.00	0.60	0.01	0.00	0.13	0.00	0.00	0.00	0.03	92.57	18-07-14	NIP-13-26 Pisolith
890	37	37.08	0.00	0.00		0.00	0.01	0.13	0.04	33.94	8.64	0.02	0.00	0.04	7.65	0.07	0.00	0.23	0.00	0.00	0.09	0.03	87.98	18-07-14	NIP-13-26 Pisolith
891	38	36.17	0.00	0.00		0.05	0.01	0.05	0.00	39.18	7.13	0.04	0.00	0.05	6.09	0.02	0.00	0.17	0.00	0.00	0.00	0.01	88.97	18-07-14	NIP-13-26 Pisolith
892	39	25.22	0.02	0.00		0.05	0.00	0.04	0.03	55.06	7.75	0.10	0.00	0.00	0.34	0.00	0.02	0.05	0.00	0.00	0.03	0.00	81.70	18-07-14	NIP-13-26 Pisolith
893	40	36.49	0.00	0.01		0.08	0.00	0.04	0.14	33.65	8.00	0.06	0.07	0.03	7.25	0.00	0.01	0.15	0.00	0.05	0.05	0.04	86.12	18-07-14	NIP-13-26 Pisolith
894	41	38.01	0.00	0.01		0.03	0.01	0.06	0.00	31.71	7.49	0.03	0.00	0.07	6.79	0.00	0.00	1.33	0.03	0.00	0.07	0.02	85.67	18-07-14	NIP-13-26 Pisolith
895	42	37.11	0.01	0.02		0.03	0.03	0.09	0.00	34.29	7.31	0.04	0.01	0.07	6.26	0.11	0.02	0.29	0.00	0.00	0.03	0.03	85.75	18-07-14	NIP-13-26 Pisolith
896	43	38.03	0.00	0.03		0.05	0.00	0.07	0.00	35.39	9.04	0.03	0.00	0.06	8.46	0.00	0.05	0.22	0.00	0.00	0.02	0.02	91.47	18-07-14	NIP-13-26 Pisolith
897	44	30.72	0.01	0.01		0.00	0.01	0.05	0.02	37.29	8.29	0.04	0.00	0.06	8.16	0.00	0.00	0.35	0.00	0.00	0.05	0.07	85.14	18-07-14	NIP-13-26 Pisolith
898	45	38.58	0.01	0.00		0.03	0.00	0.09	0.01	44.57	8.67	0.02	0.00	0.08	7.71	0.00	0.02	0.36	0.00	0.02	0.08	0.05	100.27	18-07-14	NIP-13-26 Pisolith
899	46	31.08	0.00	0.00		0.06	0.00	0.09	0.03	48.28	7.71	0.03	0.00	0.09	6.86	0.00	0.01	0.23	0.00	0.00	0.07	0.02	94.55	18-07-14	NIP-13-26 Pisolith
900	47	33.81	0.01	0.01		0.15	0.02	0.10	0.00	45.05	8.48	0.03	0.07	0.03	7.91	0.04	0.00	0.25	0.00	0.00	0.00	0.00	95.94	18-07-14	NIP-13-26 Pisolith
901	242	38.95	0.00	0.00		0.08	0.02	0.18	0.00	56.71	6.18	0.02	0.00	0.01	0.16	0.00	0.00	0.63	0.00	0.00	0.00	0.00	102.95	18-07-14	NIP 13 28
902	243	41.37	0.01	0.00		0.10	0.01	0.39	0.00	41.58	15.99	0.03	0.00	0.00	0.14	0.09	0.00	1.68	0.00	0.13	0.12	0.00	101.63	18-07-14	NIP 13 28
903	244	39.25	0.00	0.00		0.05	0.01	0.34	0.04	42.83	16.45	0.02	0.00	0.04	0.23	0.00	0.02	0.84	0.00	0.02	0.02	0.00	100.15	18-07-14	NIP 13 28
904	245	37.30	0.01	0.01		0.02	0.00	0.28	0.00	44.15	14.30	0.02	0.00	0.00	0.15	0.00	0.00	0.72	0.00	0.01	0.00	0.00	96.97	18-07-14	NIP 13 28
905	246	36.47	0.00	0.00		0.08	0.02	0.34	0.00	54.64	6.89	0.03	0.00	0.00	0.14	0.00	0.00	0.41	0.00	0.00	0.03	0.00	99.06	18-07-14	NIP 13 28
906	247	37.75	0.00	0.01		0.08	0.00	0.25	0.00	54.73	5.06	0.01	0.01	0.00	0.17	0.02	0.03	1.13	0.00	0.00	0.05	0.00	99.29	18-07-14	NIP 13 28
907	248	35.80	0.00	0.00		0.08	0.01	0.23	0.00	57.86	4.10	0.03	0.00	0.00	0.10	0.04	0.00	0.00	0.00	0.00	0.00	0.00	98.25	18-07-14	NIP 13 28
908	249	37.44	0.01	0.01		0.00	0.00	0.14	0.03	60.45	2.28	0.02	0.00	0.02	0.13	0.00	0.00	0.03	0.00	0.00	0.05	0.00	100.61	18-07-14	NIP 13 28
909	250	37.25	0.01	0.01		0.06	0.00	0.10	0.00	62.38	1.41	0.03	0.00	0.06	0.17	0.01	0.01	0.05	0.00	0.02	0.02	0.01	101.59	18-07-14	NIP 13 28
910	251	35.14	0.00	0.00		0.06	0.01	0.13	0.00	61.92	1.64	0.04	0.00	0.01	0.19	0.01	0.02	0.05	0.00	0.00	0.01	0.00	99.21	18-07-14	NIP 13 28
911	253	37.12	0.00	0.00		0.09	0.00	0.15	0.00	60.18	2.88	0.03	0.00	0.03	0.17	0.00	0.00	0.04	0.00	0.00	0.00	0.03	100.71	18-07-14	NIP 13 28
912	254	34.68	0.00	0.00		0.07	0.00	0.29	0.02	58.03	3.64	0.01	0.00	0.00	0.16	0.00	0.01	0.00	0.00	0.00	0.00	0.05	96.95	18-07-14	NIP 13 28
913	255	37.92	0.00	0.01		0.05	0.01	0.20	0.00	59.98	2.73	0.02	0.00	0.00	0.16	0.14	0.00	0.00	0.00	0.05	0.03	0.00	101.29	18-07-14	NIP 13 28
914	256	37.45	0.00	0.01		0.07	0.00	0.14	0.04																

INDEX	No.	O	Na	K	V	Co	Mg	P	Cr	Fe	Al	S	Ni	Mn	Si	Pb	Cu	Ti	Ca	Zn	Ba	Sr	Total	Date	Sample
972	5452	36.91	0.04	0.00	0.31	0.01	0.01	0.39	0.00	57.83	3.89	0.02	0.00	0.00	1.90	0.00	0.04	0.04	0.04	0.05			101.46	10/11/16	BOI-014
973	5453	36.75	0.03	0.00	0.35	0.00	0.01	0.45	0.00	58.44	3.85	0.03	0.00	0.01	1.45	0.00	0.03	0.06	0.03	0.00			101.48	10/11/16	BOI-014
974	5454	37.43	0.10	0.02	0.14	0.00	0.06	0.18	0.02	55.15	6.52	0.04	0.02	0.02	2.09	0.00	0.01	0.16	0.11	0.01			102.08	10/11/16	BOI-004
975	5455	37.84	0.02	0.01	0.11	0.00	0.04	0.25	0.01	55.15	6.85	0.03	0.02	0.03	1.76	0.00	0.03	0.09	0.11	0.00			102.35	10/11/16	BOI-004
976	5456	38.60	0.00	0.02	0.14	0.00	0.00	0.17	0.00	56.39	5.70	0.02	0.00	0.00	1.83	0.00	0.04	0.08	0.08	0.00			103.06	10/11/16	BOI-004
977	5457	38.39	0.04	0.01	0.11	0.03	0.03	0.19	0.00	51.56	7.00	0.04	0.00	0.00	2.91	0.01	0.02	0.14	0.07	0.02			100.57	10/11/16	BOI-004
978	5459	37.38	0.05	0.01	0.08	0.00	0.07	0.38	0.00	45.69	9.56	0.06	0.00	0.02	5.10	0.00	0.03	0.44	0.17	0.14			99.18	10/11/16	BOI-004
979	5460	38.46	0.05	0.00	0.10	0.00	0.05	0.28	0.00	49.34	9.05	0.05	0.00	0.00	4.76	0.05	0.00	0.26	0.15	0.15			102.74	10/11/16	BOI-004
980	5461	35.96	0.06	0.01	0.08	0.00	0.04	0.23	0.03	50.78	7.21	0.05	0.00	0.01	3.45	0.03	0.05	0.19	0.14	0.01			98.34	10/11/16	BOI-004
981	5462	37.32	0.03	0.01	0.06	0.00	0.04	0.15	0.00	55.79	5.30	0.05	0.00	0.00	2.06	0.00	0.03	0.13	0.09	0.00			101.07	10/11/16	BOI-004
982	5463	38.36	0.00	0.02	0.09	0.00	0.04	0.23	0.01	51.82	6.59	0.03	0.00	0.03	2.82	0.04	0.05	0.18	0.09	0.00			100.41	10/11/16	BOI-004
983	5464	39.33	0.02	0.01	0.11	0.00	0.05	0.22	0.00	49.54	8.00	0.02	0.00	0.01	3.53	0.00	0.02	0.33	0.07	0.05			101.33	10/11/16	BOI-004
984	5465	38.81	0.02	0.02	0.12	0.00	0.03	0.15	0.03	50.49	6.94	0.02	0.00	0.00	2.72	0.04	0.00	0.59	0.06	0.04			100.08	10/11/16	BOI-004
985	5467	39.45	0.02	0.01	0.16	0.00	0.02	0.16	0.00	51.97	6.74	0.04	0.00	0.04	2.32	0.00	0.01	0.11	0.07	0.05			101.18	10/11/16	BOI-004
986	5468	38.18	0.00	0.04	0.09	0.00	0.06	0.29	0.00	47.77	8.96	0.08	0.00	0.02	4.79	0.00	0.02	0.21	0.27	0.08			100.86	10/11/16	BOI-004
987	5469	36.30	0.02	0.01	0.09	0.00	0.05	0.29	0.05	47.04	7.78	0.04	0.01	0.00	2.86	0.00	0.03	0.18	0.13	0.10			94.97	10/11/16	BOI-004
988	5540	41.60	0.03	0.02	0.04	0.02	0.02	0.23	0.22	37.69	9.19	0.02	0.01	0.03	7.44	0.03	0.03	0.18	0.02	0.03			96.85	10/11/16	BOI-002_G2
989	5541	40.75	0.03	0.02	0.07	0.02	0.01	0.25	0.22	45.47	6.83	0.02	0.00	0.03	5.08	0.04	0.07	0.22	0.04	0.02			99.19	10/11/16	BOI-002_G2
990	5542	40.59	0.00	0.02	0.08	0.02	0.01	0.25	0.21	45.53	7.26	0.01	0.00	0.06	5.42	0.05	0.04	0.19	0.04	0.10			99.89	10/11/16	BOI-002_G2
991	5543	41.96	0.01	0.04	0.04	0.00	0.03	0.23	0.18	39.24	8.76	0.02	0.04	0.02	6.94	0.01	0.06	0.23	0.03	0.08			97.93	10/11/16	BOI-002_G2
992	5544	41.59	0.03	0.03	0.08	0.00	0.01	0.21	0.19	41.46	7.98	0.03	0.00	0.13	6.27	0.04	0.03	0.19	0.03	0.09			98.40	10/11/16	BOI-002_G2
993	5545	38.47	0.02	0.01	0.15	0.03	0.01	0.23	0.55	58.99	3.35	0.02	0.03	0.02	2.10	0.04	0.11	0.05	0.04	0.02			104.24	10/11/16	BOI-002_G2
994	5546	40.36	0.05	0.02	0.01	0.02	0.03	0.29	0.03	49.51	5.81	0.01	0.04	0.15	4.83	0.06	0.00	0.16	0.04	0.00			101.43	10/11/16	BOI-002_G2
995	5551	39.35	0.02	0.03	0.02	0.07	0.03	0.33	0.03	50.16	5.06	0.03	0.05	0.16	4.86	0.00	0.05	0.10	0.05	0.06			100.44	10/11/16	BOI-002_G2 (continued)
996	5552	39.50	0.02	0.04	0.03	0.01	0.03	0.36	0.02	47.67	5.83	0.02	0.00	0.15	5.27	0.04	0.06	0.25	0.05	0.07			99.44	10/11/16	BOI-002_G2 (continued)
997	5553	33.69	0.02	0.00	0.10	0.03	0.00	0.36	0.15	59.67	2.10	0.02	0.04	0.06	1.11	0.03	0.08	0.07	0.03	0.04			97.62	10/11/16	BOI-002_G2 (continued)
998	5554	36.74	0.02	0.02	0.24	0.02	0.00	0.26	0.01	55.39	3.94	0.02	0.00	0.02	2.19	0.00	0.00	0.04	0.02	0.06			98.99	10/11/16	BOI-014
999	5555	38.38	0.03	0.00	0.22	0.03	0.00	0.22	0.00	52.57	4.92	0.03	0.01	0.01	3.26	0.04	0.00	0.05	0.04	0.06			99.89	10/11/16	BOI-014
1000	5556	37.47	0.02	0.01	0.45	0.03	0.00	0.60	0.00	55.53	4.69	0.03	0.01	0.05	1.23	0.21	0.02	0.02	0.04	0.00			100.41	10/11/16	BOI-014
1001	5557	36.56	0.05	0.03	0.33	0.04	0.00	0.45	0.00	56.91	4.45	0.02	0.02	0.00	1.33	0.00	0.03	0.05	0.03	0.01			100.31	10/11/16	BOI-014
1002	5558	37.07	0.03	0.01	0.37	0.04	0.01	0.47	0.03	56.89	4.40	0.04	0.00	0.00	1.30	0.00	0.02	0.05	0.03	0.00			100.75	10/11/16	BOI-014
1003	5559	35.90	0.03	0.00	0.45	0.00	0.01	0.43	0.00	58.20	4.43	0.02	0.00	0.01	0.49	0.04	0.00	0.04	0.04	0.01			100.11	10/11/16	BOI-014

**Chapter 5: Development and implementation of suitable protocols for *in situ*
measurement of oxygen isotopes in goethite by ion microprobe**

Appendices

EA1: SHRIMP-SI Disk

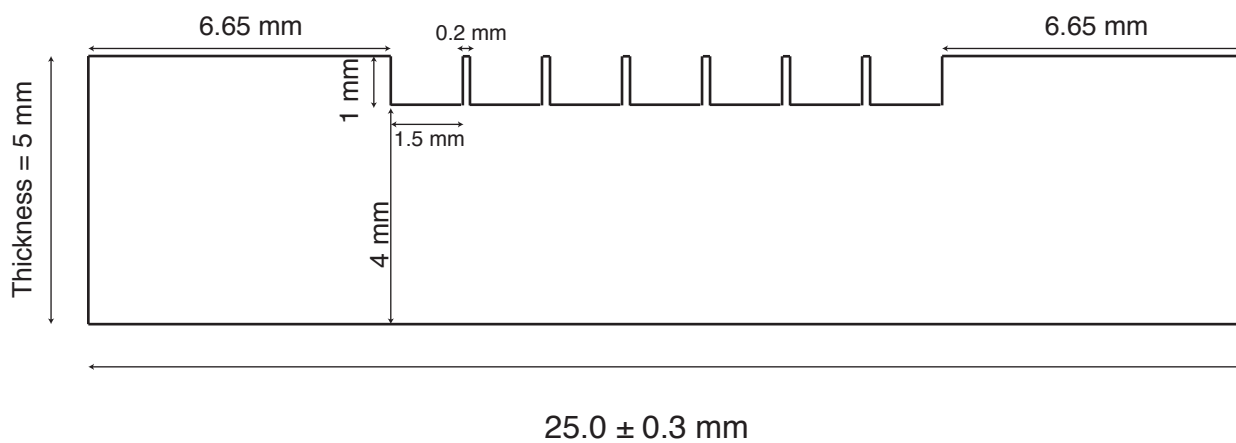
EA2: Electron Microprobe Analysis

EA3: SHRIMP-SI $^{18}\text{O}/^{16}\text{O}$ Analysis

Technical drawing of a circular plate with a 5x5 grid of holes. The plate has a diameter of 25.0 ± 0.3 mm. The grid of holes has a diameter of 1.5 mm. The center hole is marked with an asterisk. Dimensions for hole positions and plate size are provided in millimeters.

Key dimensions shown:

- Plate diameter: 25.0 ± 0.3 mm
- Hole diameter: 1.5 mm
- Grid dimensions: 10.2 mm (width), 11.7 mm (height)
- Center hole position: 5.1 mm from left and bottom edges, 0.75 mm from right and top edges.
- Other hole positions: 1.7 mm, 3.4 mm, and 5.1 mm from the left and bottom edges.



Appendix: Electron Microprobe Analysis of SHRIMP-Si Goethite Reference Material																										
INDEX	No.	O	Na	K	V	Co	Mg	P	Cr	Fe	Al	S	Ni	Mn	Si	Pb	Cu	Ti	Ca	Zn	Ba	Sr	Total	Date	Comment	
1	39	36.84	0.00	0.01	0.00	0.11	0.00	0.13	0.00	59.94	0.05	0.01	0.04	0.11	1.57	0.01	0.07	0.02	0.00	0.01	0.01	0.00	98.93	22-02-14	BAH LGB	
2	30	37.71	0.05	0.00	0.00	0.07	0.00	0.10	0.04	60.17	0.11	0.00	0.01	0.02	1.57	0.00	0.15	0.01	0.00	0.01	0.07	0.00	100.10	22-02-14	BAH LGB	
3	31	37.39	0.00	0.00	0.01	0.09	0.00	0.13	0.05	60.16	0.10	0.00	0.01	0.06	1.53	0.00	0.11	0.00	0.00	0.07	0.00	0.02	99.73	22-02-14	BAH LGB	
4	32	36.92	0.00	0.01	0.00	0.08	0.00	0.12	0.00	60.38	0.08	0.00	0.00	0.07	1.55	0.00	0.13	0.04	0.00	0.00	0.00	0.00	99.37	22-02-14	BAH LGB	
5	33	37.27	0.00	0.00	0.04	0.00	0.01	0.12	0.06	60.22	0.08	0.02	0.05	0.13	1.62	0.01	0.15	0.02	0.00	0.00	0.00	0.00	99.80	22-02-14	BAH LGB	
6	34	36.45	0.00	0.01	0.01	0.02	0.00	0.11	0.03	60.52	0.06	0.00	0.00	0.14	1.60	0.00	0.12	0.00	0.00	0.00	0.00	0.00	99.07	22-02-14	BAH LGB	
7	35	37.06	0.00	0.01	0.01	0.06	0.01	0.08	0.04	60.54	0.06	0.01	0.00	0.07	1.62	0.00	0.10	0.04	0.00	0.03	0.04	0.00	99.80	22-02-14	BAH LGB	
8	36	36.82	0.02	0.00	0.05	0.07	0.00	0.10	0.03	60.91	0.05	0.00	0.03	0.09	1.60	0.09	0.17	0.09	0.00	0.03	0.01	0.00	100.16	22-02-14	BAH LGB	
9	37	36.57	0.00	0.00	0.00	0.02	0.00	0.09	0.02	60.83	0.04	0.02	0.01	0.07	1.66	0.00	0.11	0.04	0.00	0.04	0.03	0.04	99.58	22-02-14	BAH LGB	
10	38	37.19	0.00	0.00	0.02	0.03	0.00	0.12	0.03	60.18	0.05	0.00	0.00	0.09	1.65	0.00	0.18	0.00	0.00	0.04	0.10	0.00	99.68	22-02-14	BAH LGB	
11	87	36.11	0.01	0.00		0.06	0.09	0.04	0.04	62.30	0.14	0.01	0.00	0.07	1.22	0.15	0.00	0.02	0.00	0.00	0.01	0.04	100.31	18-07-14	BAH LGB	
12	88	34.42	0.00	0.00		0.04	0.14	0.01	0.00	62.55	0.16	0.00	0.00	0.07	1.15	0.25	0.07	0.04	0.00	0.01	0.00	0.04	98.97	18-07-14	BAH LGB	
13	89	34.68	0.03	0.03		0.07	0.12	0.02	0.08	61.95	0.16	0.00	0.00	0.08	1.15	0.23	0.02	0.00	0.00	0.02	0.05	0.00	98.68	18-07-14	BAH LGB	
14	90	34.27	0.05	0.02		0.04	0.10	0.02	0.00	62.28	0.14	0.01	0.00	0.02	1.17	0.18	0.10	0.03	0.00	0.02	0.04	0.00	98.47	18-07-14	BAH LGB	
15	91	35.21	0.00	0.01		0.05	0.12	0.00	0.00	62.53	0.15	0.02	0.03	0.04	1.34	0.25	0.01	0.04	0.00	0.02	0.06	0.00	99.88	18-07-14	BAH LGB	
16	92	34.77	0.00	0.00		0.07	0.11	0.00	0.00	62.44	0.14	0.03	0.00	0.04	1.22	0.27	0.00	0.00	0.00	0.00	0.05	0.00	99.13	18-07-14	BAH LGB	
17	78	36.67	0.03	0.00		0.06	0.12	0.02	0.00	62.09	0.14	0.03	0.00	0.03	1.31	0.31	0.00	0.01	0.00	0.02	0.00	0.00	100.83	18-07-14	BAH LGB	
18	79	33.43	0.03	0.03		0.09	0.16	0.03	0.00	60.95	0.18	0.00	0.00	0.02	1.24	0.11	0.05	0.00	0.00	0.00	0.04	0.03	96.36	18-07-14	BAH LGB	
19	80	35.16	0.05	0.03		0.07	0.13	0.00	0.03	62.72	0.18	0.03	0.00	0.07	1.15	0.26	0.00	0.03	0.00	0.04	0.03	0.00	99.95	18-07-14	BAH LGB	
20	81	35.54	0.06	0.01		0.07	0.11	0.01	0.00	62.45	0.12	0.03	0.00	0.02	1.28	0.22	0.00	0.00	0.00	0.03	0.02	0.00	99.96	18-07-14	BAH LGB	
21	82	35.78	0.00	0.03		0.07	0.13	0.00	0.00	62.48	0.13	0.01	0.00	0.07	1.25	0.36	0.00	0.00	0.00	0.00	0.03	0.00	100.34	18-07-14	BAH LGB	
22	83	35.97	0.01	0.00		0.09	0.11	0.01	0.00	62.53	0.13	0.04	0.07	0.07	1.30	0.35	0.00	0.00	0.00	0.00	0.00	0.02	100.71	18-07-14	BAH LGB	
23	84	35.01	0.01	0.02		0.06	0.10	0.03	0.00	62.70	0.14	0.02	0.00	0.06	1.27	0.25	0.00	0.00	0.00	0.00	0.01	0.03	99.71	18-07-14	BAH LGB	
24	85	36.59	0.02	0.00		0.07	0.11	0.02	0.00	62.79	0.17	0.02	0.06	0.07	1.31	0.30	0.03	0.02	0.00	0.04	0.00	0.06	101.67	18-07-14	BAH LGB	
25	86	35.14	0.00	0.03		0.08	0.11	0.01	0.00	61.52	0.14	0.01	0.00	0.03	1.24	0.32	0.05	0.00	0.00	0.08	0.10	0.00	98.86	18-07-14	BAH LGB	
26	386	36.69	0.00	0.01		0.17	0.03	0.14	0.00	62.47	0.19	0.00	0.00	0.02	1.30	0.00	0.21	0.00	0.00	0.00	0.00	0.01	101.24	18-07-14	BAH LGB	
27	387	36.46	0.00	0.01		0.10	0.04	0.15	0.00	62.82	0.18	0.00	0.00	0.08	1.22	0.00	0.13	0.00	0.00	0.03	0.05	0.04	101.30	18-07-14	BAH LGB	
28	388	37.66	0.01	0.00		0.10	0.01	0.15	0.00	62.97	0.18	0.00	0.01	0.07	1.22	0.01	0.15	0.00	0.00	0.00	0.08	0.02	102.63	18-07-14	BAH LGB	
29	389	36.30	0.02	0.01		0.02	0.01	0.15	0.02	62.98	0.19	0.00	0.00	0.05	1.21	0.00	0.17	0.00	0.00	0.00	0.00	0.04	101.17	18-07-14	BAH LGB	
30	390	36.82	0.00	0.00		0.05	0.02	0.15	0.04	63.34	0.20	0.02	0.00	0.08	1.22	0.03	0.09	0.00	0.00	0.00	0.00	0.02	102.06	18-07-14	BAH LGB	
31	391	36.69	0.02	0.00		0.11	0.01	0.13	0.07	63.59	0.19	0.02	0.00	0.12	1.18	0.00	0.05	0.00	0.00	0.00	0.00	0.00	102.18	18-07-14	BAH LGB	
32	392	36.32	0.00	0.00		0.08	0.01	0.17	0.03	63.74	0.18	0.01	0.05	0.05	1.15	0.05	0.14	0.00	0.00	0.00	0.10	0.00	102.05	18-07-14	BAH LGB	
33	393	36.18	0.01	0.01		0.11	0.01	0.14	0.00	63.62	0.19	0.01	0.00	0.07	1.25	0.00	0.13	0.07	0.00	0.00	0.03	0.04	101.86	18-07-14	BAH LGB	
34	394	36.35	0.02	0.02		0.07	0.02	0.11	0.02	63.42	0.19	0.00	0.00	0.08	1.23	0.00	0.16	0.00	0.00	0.09	0.00	0.05	101.84	18-07-14	BAH LGB	
35	152	35.61	0.03	0.00		0.05	0.00	0.08	0.00	63.20	0.19	0.01	0.00	0.09	1.08	0.03	0.19	0.00	0.00	0.00	0.09	0.02	100.67	18-07-14	BAH LGB	
36	153	36.05	0.01	0.00		0.08	0.03	0.11	0.00	63.60	0.21	0.01	0.00	0.05	1.08	0.02	0.23	0.05	0.00	0.00	0.07	0.02	101.60	18-07-14	BAH LGB	
37	154	36.10	0.00	0.01		0.10	0.01	0.15	0.00	62.98	0.21	0.00	0.00	0.00	1.08	0.00	0.24	0.00	0.00	0.00	0.04	0.01	100.93	18-07-14	BAH LGB	
38	155	35.39	0.00	0.00		0.04	0.01	0.10	0.00	63.53	0.18	0.01	0.00	0.14	1.10	0.03	0.25	0.00	0.00	0.06	0.00	0.02	100.87	18-07-14	BAH LGB	
39	156	35.80	0.03	0.00		0.09	0.00	0.10	0.00	63.67	0.19	0.01	0.00	0.00	1.11	0.00	0.30	0.00	0.00	0.01	0.14	0.03	101.48	18-07-14	BAH LGB	
40	157	36.27	0.01	0.00		0.08	0.00	0.09	0.00	63.18	0.20	0.03	0.00	0.07	1.13	0.03	0.22	0.03	0.00	0.03	0.00	0.06	101.44	18-07-14	BAH LGB	
41	143	36.40	0.00	0.02		0.08	0.01	0.14	0.00	62.66	0.19	0.00	0.00	0.09	1.18	0.09	0.19	0.01	0.00	0.00	0.00	0.03	101.08	18-07-14	BAH LGB	
42	144	36.24	0.00	0.00		0.07	0.01	0.13	0.08	63.51	0.19	0.02	0.00	0.04	1.12	0.03	0.20	0.01	0.00	0.00	0.03	0.06	101.73	18-07-14	BAH LGB	
43	145	36.03	0.00	0.00		0.05	0.00	0.14	0.00	63.53	0.22	0.03	0.01	0.11	1.14	0.07	0.16	0.00	0.00	0.00	0.04	0.01	101.54	18-07-14	BAH LGB	
44	146	36.13	0.00	0.01		0.08	0.02	0.12	0.00	63.63	0.18	0.00	0.03	0.05	1.12	0.00	0.23	0.01	0.00	0.00	0.13	0.00	101.73	18-07-14	BAH LGB	
45	147	35.77	0.00	0.00		0.10	0.00	0.14	0.00	63.59	0.22	0.01	0.00	0.04	1.10	0.03	0.19	0.02	0.00	0.08	0.02	0.00	101.30	18-07-14	BAH LGB	
46	148	35.57	0.00	0.00		0.06	0.01	0.15	0.02	63.37	0.19	0.02	0.00	0.04	1.09	0.00	0.17	0.00	0.00	0.05	0.02	0.05	100.81	18-07-14	BAH LGB	
47	149	36.20	0.00	0.00		0.01	0.00	0.11	0.02	62.95	0.19	0.00	0.00	0.08	1.06	0.08	0.26	0.00	0.00	0.05	0.00	0.00	101.00	18-07-14	BAH LGB	
48	150	36.18	0.00	0.01		0.12	0.01	0.09	0.00	63.37	0.21	0.02	0.00	0.08	1.12	0.06	0.31	0.00	0.00	0.04	0.08	0.00	101.68	18-07-14	BAH LGB	
49	151	35.29	0.05	0.00		0.05	0.01	0.12	0.00	63.55	0.20	0.03	0.00	0.10	1.09	0.09	0.29	0.00	0.00	0.00	0.07	0.00	100.95	18-07-14	BAH LGB	
50	246	37.20	0.02	0.00	0.00	0.07	0.00	0.09	0.00	60.82	0.10	0.01	0.04	0.12	1.72	0.03	0.20	0.00	0.00	0.00			100.40	20-07-16	BAH LGB-baxis	
51	247	37.28	0.01	0.00	0.00	0.09	0																			

INDEX	No.	O	Na	K	V	Co	Mg	P	Cr	Fe	Al	S	Ni	Mn	Si	Pb	Cu	Ti	Ca	Zn	Ba	Sr	Total	Date	Comment
102	219	35.12	-0.02	0.01	-0.01	0.05	0.11	-0.02	0.02	61.91	0.12	0.01	0.01	0.06	1.11	0.27	-0.04	0.02	-0.03	0.08	-	-	98.77	22-06-16	Capao L4 Vertical-1
103	215	35.76	0.01	-0.01	0.03	0.04	0.13	0.07	0.02	61.93	0.12	-0.07	0.01	0.06	1.12	0.31	0.01	-0.01	-0.04	0.09	-	-	99.59	22-06-16	Capao L4 Vertical-1
104	226	35.70	-0.04	0.00	-0.05	0.07	0.09	-0.03	0.01	61.95	0.13	0.03	-0.01	0.05	1.00	0.18	0.02	-0.05	-0.07	-0.02	-	-	98.97	22-06-16	Capao L4 Vertical-1
105	210	35.61	-0.02	-0.01	-0.03	0.09	0.05	-0.06	0.01	61.96	0.12	0.27	0.01	-0.01	1.04	0.25	-0.02	-0.01	-0.05	0.08	-	-	99.28	22-06-16	Capao L4 Vertical-1
106	218	35.34	-0.02	0.01	0.02	0.05	0.10	0.10	0.01	62.04	0.15	0.04	0.02	0.01	1.05	0.33	0.00	-0.01	-0.04	0.12	-	-	99.33	22-06-16	Capao L4 Vertical-1
107	222	35.92	0.00	0.01	-0.03	0.08	0.10	0.05	-0.01	62.11	0.15	-0.03	0.05	0.08	1.05	0.22	0.02	-0.01	-0.06	0.01	-	-	99.69	22-06-16	Capao L4 Vertical-1
108	224	35.65	0.00	0.01	-0.02	0.06	0.09	0.00	0.00	62.15	0.13	-0.03	-0.01	0.07	1.04	0.20	0.05	0.03	-0.04	0.05	-	-	99.44	22-06-16	Capao L4 Vertical-1
109	221	35.20	-0.05	-0.03	0.01	0.09	0.13	0.03	0.00	62.24	0.14	-0.10	0.01	0.10	1.07	0.25	-0.02	0.00	-0.06	-0.08	-	-	98.91	22-06-16	Capao L4 Vertical-1
110	225	35.91	0.00	0.02	-0.01	0.08	0.13	0.00	0.00	62.39	0.17	0.22	-0.01	0.04	1.02	0.23	0.04	-0.06	-0.05	0.04	-	-	100.15	22-06-16	Capao L4 Vertical-1
111	223	35.87	-0.02	0.01	-0.03	0.04	0.11	0.03	0.01	62.63	0.13	0.00	-0.03	0.03	1.01	0.29	0.00	-0.01	-0.07	0.04	-	-	100.02	22-06-16	Capao L4 Vertical-1
112	201	34.35	0.05	0.01	0.00	0.05	0.15	0.00	0.00	60.17	0.13	0.01	0.01	0.06	1.26	0.28	0.01	0.03	0.00	0.00	-	-	96.57	6/7/16	CapaoL4_5-2
113	202	35.91	0.00	0.01	0.00	0.05	0.12	0.04	0.00	60.09	0.13	0.00	0.00	0.04	1.25	0.39	0.07	0.00	0.00	0.06	-	-	98.15	6/7/16	CapaoL4_5-3
114	203	34.05	0.01	0.00	0.02	0.07	0.13	0.02	0.01	60.71	0.14	0.00	0.00	0.05	1.25	0.35	0.04	0.00	0.00	0.07	-	-	96.91	6/7/16	CapaoL4_5-4
115	204	34.85	0.00	0.00	0.01	0.08	0.15	0.03	0.00	61.03	0.14	0.01	0.06	0.05	1.22	0.32	0.02	0.00	0.00	0.00	-	-	97.98	6/7/16	CapaoL4_5-5
116	205	35.27	0.05	0.00	0.00	0.10	0.13	0.00	0.02	60.71	0.13	0.01	0.00	0.08	1.30	0.27	0.01	0.00	0.00	0.05	-	-	98.12	6/7/16	CapaoL4_5-6
117	21	35.43	0.17	0.00	0.00	0.05	0.11	0.02	0.00	59.82	0.09	0.00	0.00	0.05	1.29	0.23	0.03	0.00	0.00	0.03	-	-	97.33	6/7/16	CapaoL4-1
118	23	36.85	0.12	0.00	0.00	0.06	0.08	0.04	0.01	60.19	0.10	0.00	0.00	0.01	1.25	0.30	0.04	0.00	0.00	0.02	-	-	99.08	6/7/16	CapaoL4-1
119	20	36.69	0.01	0.01	0.00	0.09	0.08	0.02	0.00	60.28	0.08	0.00	0.02	0.04	1.11	0.21	0.06	0.03	0.00	0.03	-	-	98.75	6/7/16	CapaoL4-1
120	22	34.78	0.03	0.02	0.00	0.07	0.10	0.00	0.00	60.29	0.10	0.00	0.00	0.05	1.10	0.24	0.01	0.00	0.00	0.00	-	-	96.78	6/7/16	CapaoL4-1
121	24	38.07	0.07	0.00	0.00	0.04	0.11	0.01	0.00	60.61	0.11	0.02	0.00	0.03	1.20	0.33	0.03	0.02	0.00	0.00	-	-	100.64	6/7/16	CapaoL4-1
122	19	36.14	0.06	0.00	0.01	0.05	0.11	0.03	0.00	60.69	0.10	0.00	0.00	0.06	1.07	0.25	0.01	0.00	0.00	0.05	-	-	98.63	6/7/16	CapaoL4-1
123	13	37.51	0.09	0.00	0.02	0.06	0.08	0.02	0.00	60.24	0.09	0.00	0.01	0.07	1.10	0.22	0.05	0.00	0.00	0.06	-	-	99.60	6/7/16	CapaoL4-2
124	18	36.39	0.00	0.00	0.01	0.08	0.11	0.00	0.03	60.26	0.09	0.01	0.00	0.05	1.11	0.32	0.05	0.00	0.00	0.00	-	-	98.51	6/7/16	CapaoL4-2
125	15	36.21	0.03	0.01	0.00	0.07	0.10	0.01	0.01	60.76	0.14	0.01	0.01	0.04	1.17	0.23	0.02	0.00	0.00	0.00	-	-	98.81	6/7/16	CapaoL4-2
126	14	37.77	0.00	0.00	0.04	0.07	0.11	0.00	0.00	60.83	0.13	0.02	0.00	0.05	1.16	0.30	0.02	0.00	0.00	0.00	-	-	100.51	6/7/16	CapaoL4-2
127	17	37.66	0.00	0.03	0.00	0.08	0.11	0.02	0.01	60.99	0.11	0.00	0.00	0.06	1.24	0.27	0.03	0.00	0.00	0.00	-	-	100.61	6/7/16	CapaoL4-2
128	16	35.06	0.00	0.01	0.00	0.07	0.08	0.00	0.00	61.69	0.11	0.00	0.03	0.02	1.01	0.22	0.00	0.00	0.00	0.03	-	-	98.35	6/7/16	CapaoL4-2
129	29	37.27	0.05	0.02	0.00	0.07	0.01	0.02	0.00	59.20	0.10	0.03	0.00	0.54	1.01	0.01	0.02	0.00	0.00	0.02	-	-	98.38	6/7/16	RoyL5-1
130	25	37.55	0.04	0.00	0.00	0.03	0.00	0.03	0.00	59.45	0.13	0.02	0.00	0.59	1.14	0.00	0.00	0.06	0.00	0.00	-	-	99.04	6/7/16	RoyL5-1
131	28	36.72	0.10	0.00	0.00	0.02	0.01	0.00	0.00	60.19	0.10	0.02	0.00	0.56	1.09	0.02	0.00	0.03	0.00	0.01	-	-	98.87	6/7/16	RoyL5-1
132	26	38.40	0.00	0.00	0.00	0.07	0.04	0.00	0.02	60.44	0.09	0.04	0.00	0.57	1.07	0.02	0.02	0.02	0.00	0.01	-	-	100.82	6/7/16	RoyL5-1
133	27	36.76	0.03	0.02	0.00	0.06	0.02	0.00	0.00	60.48	0.13	0.03	0.00	0.55	1.15	0.03	0.00	0.04	0.00	0.02	-	-	99.30	6/7/16	RoyL5-1
134	30	37.97	0.00	0.00	0.00	0.04	0.02	0.01	0.00	60.50	0.10	0.02	0.00	0.48	1.04	0.05	0.01	0.00	0.00	0.00	-	-	100.22	6/7/16	RoyL5-1
135	31	37.24	0.00	0.00	0.05	0.07	0.01	0.02	0.00	60.15	0.13	0.00	0.00	0.64	1.05	0.00	0.00	0.00	0.00	0.02	-	-	99.38	6/7/16	RoyL6-1
136	34	38.37	0.02	0.01	0.00	0.05	0.00	0.03	0.00	60.16	0.13	0.00	0.00	0.53	1.02	0.06	0.00	0.00	0.00	0.00	-	-	100.40	6/7/16	RoyL6-1
137	33	37.27	0.00	0.00	0.00	0.07	0.00	0.00	0.01	60.34	0.13	0.01	0.00	0.62	1.07	0.03	0.00	0.01	0.00	0.02	-	-	99.58	6/7/16	RoyL6-1
138	32	37.05	0.03	0.00	0.00	0.06	0.01	0.02	0.00	60.70	0.12	0.01	0.01	0.63	1.10	0.00	0.00	0.00	0.00	0.06	-	-	99.80	6/7/16	RoyL6-1
139	35	38.03	0.00	0.00	0.00	0.07	0.01	0.02	0.00	61.15	0.14	0.02	0.00	0.61	1.09	0.00	0.00	0.03	0.00	0.03	-	-	101.20	6/7/16	RoyL6-1
140	36	37.57	0.05	0.00	0.00	0.06	0.06	0.00	0.04	0.03	61.42	0.13	0.00	0.68	1.13	0.00	0.00	0.00	0.00	0.02	-	-	101.13	6/7/16	RoyL6-1
141	197	37.39	0.00	0.03		0.09	0.04	0.09	0.00	62.31	0.10	0.02	0.00	0.30	1.09	0.00	0.00	0.04	0.00	0.00	0.13	0.02	101.64	18-07-14	Win 06 018
142	198	36.75	0.04	0.00		0.06	0.02	0.05	0.00	62.40	0.11	0.01	0.00	0.27	1.08	0.00	0.00	0.00	0.00	0.03	0.10	0.07	100.97	18-07-14	Win 06 018
143	199	37.21	0.00	0.00		0.12	0.03	0.03	0.07	62.93	0.10	0.02	0.00	0.23	1.11	0.11	0.04	0.00	0.01	0.00	0.05	0.00	102.06	18-07-14	Win 06 018
144	200	36.60	0.00	0.03		0.10	0.05	0.01	0.00	62.48	0.11	0.02	0.00	0.24	1.10	0.00	0.01	0.00	0.00	0.00	0.01	0.00	100.76	18-07-14	Win 06 018
145	201	36.73	0.02	0.03		0.08	0.04	0.04	0.00	62.66	0.12	0.04	0.00	0.30	1.13	0.02	0.00	0.04	0.00	0.00	0.00	0.00	101.24	18-07-14	Win 06 018
146	202	36.37	0.00	0.02		0.09	0.05	0.07	0.01	62.50	0.15	0.00	0.00	0.27	1.17	0.03	0.04	0.00	0.00	0.00	0.00	0.02	100.79	18-07-14	Win 06 018
147	203	37.80	0.05	0.02		0.12	0.07	0.01	0.00	62.07	0.12	0.00	0.01	0.37	1.17	0.11	0.05	0.03	0.00	0.00	0.07	0.00	102.05	18-07-14	Win 06 018
148	204	37.85	0.02	0.02		0.12	0.08	0.05	0.00	62.23	0.16	0.00	0.00	0.25	1.17	0.00	0.00	0.04	0.03	0.00	0.02	0.00	102.05	18-07-14	Win 06 018
149	205	37.47	0.04	0.01		0.07	0.12	0.06	0.01	62.58	0.20	0.02	0.00	0.26	0.99	0.00	0.00	0.06	0.02	0.11	0.00	0.00	102.01	18-07-14	Win 06 018
150	206	36.72	0.02	0.00		0.10	0.12	0.08	0.02	62.87	0.19	0.04	0.07	0.08	0.93	0.04	0.07	0.00	0.11	0.00	0.00	0.00	101.47	18-07-14	Win 06 018
151	207	36.66	0.00	0.02		0.05	0.10	0.06	0.00	63.07	0.22	0.02	0.00	0.19	0.76	0.10	0.00	0.03	0.06	0.00	0.01	0.00	101.35	18-07-14	Win 06 018
152	208	36.60	0.01	0.01		0.07	0.09	0.03	0.00	62.52	0.23	0.05	0.00	0.20	0.75	0.00	0.06	0.03	0.43	0.01	0.00	0.00	101.07	18-07-14	Win 06 018
153	209	36.00	0.00	0.00		0.05																			

Appendix: Electron Microprobe Analysis of Brazilian and Australian Goethites																										
INDEX	No.	O	Na	K	V	Co	Mg	P	Cr	Fe	Al	S	Ni	Mn	Si	Pb	Cu	Ti	Ca	Zn	Ba	Sr	Total	Year	Sample	
1	30	36.87	0.11	0.00	0.00	0.05	0.00	0.00	61.54	0.33	0.10	0.00	0.00	0.21	0.02	0.00	0.19	0.00	0.00	0.00	-	-	-	9946	2010	Lynp-02-09-A1
2	31	37.21	0.11	0.00	0.01	0.12	0.00	0.08	0.00	58.42	1.96	0.14	0.00	0.00	0.96	0.04	0.04	0.60	0.00	0.00	0.02	-	-	9970	2010	Lynp-02-09-A1
3	33	35.02	0.00	0.01	0.05	0.10	0.03	0.03	0.04	62.75	0.47	0.07	0.06	0.00	0.25	0.00	0.00	0.15	0.00	0.05	0.00	-	-	9912	2010	Lynp-02-09-A1
4	38	37.14	0.03	0.00	0.06	0.10	0.00	0.03	0.01	61.65	0.39	0.10	0.04	0.00	0.25	0.08	0.00	0.15	0.00	0.00	0.00	-	-	10002	2010	Lynp-02-09-A1
5	39	37.75	0.04	0.00	0.02	0.04	0.00	0.00	0.01	60.34	0.33	0.09	0.06	0.00	0.24	0.04	0.00	0.12	0.00	0.06	0.01	-	-	9915	2010	Lynp-02-09-A1
6	41	36.47	0.02	0.00	0.01	0.10	0.02	0.02	0.00	62.59	0.48	0.09	0.03	0.00	0.25	0.05	0.00	0.13	0.00	0.03	0.01	-	-	10033	2010	Lynp-02-09-A1
7	42	34.35	0.00	0.01	0.11	0.11	0.01	0.07	0.02	60.00	2.37	0.15	0.04	0.01	0.97	0.00	0.00	0.43	0.00	0.02	0.02	-	-	9870	2010	Lynp-02-09-A1
8	45	38.01	0.00	0.00	0.03	0.03	0.03	0.03	0.00	59.64	0.64	0.10	0.00	0.00	0.21	0.02	0.00	0.14	0.00	0.02	0.02	-	-	9890	2010	Lynp-02-09-A1
9	48	38.15	0.06	0.00	0.00	0.01	0.00	0.01	0.01	60.89	0.53	0.10	0.00	0.00	0.25	0.05	0.01	0.09	0.00	0.00	0.00	-	-	10017	2010	Lynp-02-09-A1
10	49	37.56	0.02	0.03	0.03	0.06	0.02	0.00	0.00	60.18	0.11	0.05	0.05	0.00	0.15	0.00	0.00	0.11	0.00	0.00	0.00	-	-	9836	2010	Lynp-02-09-A1
11	50	35.68	0.01	0.00	0.08	0.09	0.02	0.04	0.07	62.91	0.57	0.09	0.00	0.00	0.27	0.00	0.00	0.19	0.00	0.00	0.00	-	-	10034	2010	Lynp-02-09-A1
12	56	35.78	0.12	0.00	0.01	0.12	0.00	0.04	0.00	62.24	0.67	0.08	0.04	0.00	0.24	0.10	0.00	0.16	0.00	0.00	0.05	-	-	9966	2010	Lynp-02-09-A1
13	58	36.64	0.02	0.01	0.05	0.03	0.03	0.03	0.00	61.08	0.41	0.07	0.03	0.00	0.17	0.00	0.01	0.12	0.00	0.00	0.02	-	-	9867	2010	Lynp-02-09-A1
14	59	37.53	0.07	0.01	0.00	0.04	0.00	0.01	0.01	60.36	0.21	0.05	0.00	0.00	0.18	0.00	0.00	0.13	0.00	0.00	0.00	-	-	9859	2010	Lynp-02-09-A1
15	61	35.99	0.08	0.01	0.00	0.03	0.00	0.05	0.00	61.00	0.59	0.09	0.00	0.00	0.23	0.06	0.13	0.06	0.00	0.02	0.00	-	-	9832	2010	Lynp-02-09-A1
16	62	37.62	0.00	0.00	0.01	0.10	0.02	0.00	0.00	60.72	0.91	0.08	0.00	0.00	0.13	0.15	0.00	0.08	0.00	0.01	0.00	-	-	9885	2010	Lynp-02-09-A1
17	65	37.41	0.00	0.00	0.06	0.11	0.02	0.04	0.01	60.59	0.59	0.07	0.01	0.00	0.23	0.13	0.00	0.11	0.00	0.00	0.00	-	-	9937	2010	Lynp-02-09-A1
18	70	37.71	0.00	0.00	0.02	0.07	0.00	0.04	0.01	59.87	0.58	0.08	0.00	0.00	0.21	0.02	0.01	0.28	0.00	0.00	0.00	-	-	9889	2010	Lynp-02-09-A1
19	72	37.86	0.00	0.03	0.04	0.12	0.04	0.00	0.01	59.09	0.57	0.12	0.05	0.00	0.31	0.02	0.03	0.07	0.00	0.01	0.00	-	-	9835	2010	Lynp-02-09-A1
20	74	37.58	0.10	0.00	0.03	0.07	0.01	0.01	0.01	61.52	0.43	0.09	0.00	0.00	0.24	0.03	0.02	0.12	0.00	0.04	0.01	-	-	10030	2010	Lynp-02-09-A1
21	76	37.99	0.00	0.03	0.00	0.06	0.00	0.02	0.00	60.82	0.39	0.16	0.00	0.00	0.23	0.02	0.02	0.16	0.00	0.00	0.00	-	-	10004	2010	Lynp-02-09-A1
22	77	37.84	0.07	0.00	0.05	0.03	0.00	0.03	0.01	60.79	0.75	0.10	0.00	0.00	0.23	0.08	0.00	0.06	0.00	0.05	0.07	-	-	10015	2010	Lynp-02-09-A1
23	78	37.72	0.00	0.01	0.01	0.13	0.01	0.02	0.04	60.15	0.76	0.09	0.00	0.00	0.17	0.04	0.06	0.04	0.00	0.10	0.02	-	-	9934	2010	Lynp-02-09-A1
24	79	38.09	0.00	0.01	0.08	0.10	0.00	0.04	0.00	58.18	0.28	0.23	0.00	0.02	0.69	0.11	0.00	0.12	0.00	0.00	0.02	-	-	10056	2010	Lynp-02-09-A2
25	80	40.10	0.00	0.00	0.13	0.01	0.03	0.07	0.05	53.87	4.62	0.18	0.00	0.00	1.36	0.00	0.04	0.25	0.00	0.04	0.06	-	-	10081	2010	Lynp-02-09-A2
26	81	40.04	0.02	0.00	0.01	0.08	0.01	0.12	0.04	52.39	4.96	0.15	0.00	0.00	1.65	0.00	0.00	0.13	0.00	0.00	0.00	-	-	10083	2010	Lynp-02-09-A2
27	82	39.22	0.09	0.01	0.13	0.09	0.00	0.12	0.00	55.39	3.36	0.18	0.00	0.00	0.69	0.11	0.07	0.04	0.00	0.00	0.01	-	-	9949	2010	Lynp-02-09-A2
28	83	39.56	0.00	0.00	0.07	0.03	0.02	0.11	0.01	53.81	4.29	0.19	0.00	0.00	0.83	0.09	0.05	0.06	0.00	0.00	0.05	-	-	9916	2010	Lynp-02-09-A2
29	84	40.12	0.00	0.00	0.20	0.13	0.00	0.16	0.00	51.03	5.90	0.28	0.00	0.00	0.34	0.05	0.00	0.36	0.00	0.03	0.04	-	-	9865	2010	Lynp-02-09-A2
30	85	40.26	0.09	0.00	0.13	0.13	0.00	0.15	0.02	52.89	4.96	0.26	0.05	0.00	0.54	0.00	0.09	0.03	0.03	0.04	0.00	-	-	9964	2010	Lynp-02-09-A2
31	86	40.04	0.07	0.01	0.14	0.00	0.32	0.24	0.00	51.30	4.24	0.20	0.00	0.00	0.26	0.00	0.00	0.11	0.00	0.00	0.00	-	-	9919	2010	Lynp-02-09-A2
32	87	40.70	0.04	0.00	0.00	0.06	0.01	0.10	0.01	52.32	5.58	0.25	0.00	0.03	0.45	0.01	0.04	0.34	0.00	0.08	0.00	-	-	9999	2010	Lynp-02-09-A2
33	88	38.11	0.00	0.00	0.05	0.11	0.00	0.09	0.01	57.88	1.87	0.12	0.00	0.00	0.19	0.00	0.01	0.06	0.00	0.00	0.00	-	-	9849	2010	Lynp-02-09-A2
34	89	37.43	0.06	0.00	0.02	0.03	0.00	0.06	0.04	59.02	1.40	0.11	0.00	0.00	0.22	0.00	0.00	0.08	0.00	0.02	0.00	-	-	9847	2010	Lynp-02-09-A2
35	91	38.42	0.00	0.00	0.11	0.11	0.00	0.09	0.00	57.38	2.13	0.10	0.01	0.00	0.18	0.00	0.00	0.06	0.00	0.00	0.00	-	-	9861	2010	Lynp-02-09-A2
36	92	39.34	0.00	0.01	0.03	0.08	0.00	0.01	0.11	0.57	1.09	0.07	0.00	0.00	0.15	0.06	0.00	0.06	0.00	0.07	0.00	-	-	9940	2010	Lynp-02-09-A2
37	93	40.77	0.00	0.00	0.09	0.10	0.05	0.25	0.04	52.84	4.67	0.19	0.00	0.00	0.42	0.03	0.01	0.10	0.00	0.00	0.00	-	-	9957	2010	Lynp-02-09-A2
38	95	37.50	0.00	0.01	0.00	0.09	0.01	0.04	0.05	59.86	0.50	0.06	0.00	0.00	0.12	0.02	0.00	0.04	0.00	0.05	0.00	-	-	9834	2010	Lynp-02-09-A2
39	96	38.57	0.07	0.02	0.03	0.09	0.00	0.10	0.06	58.26	1.59	0.11	0.00	0.00	0.18	0.05	0.02	0.06	0.00	0.03	0.00	-	-	9924	2010	Lynp-02-09-A2
40	98	37.54	0.06	0.02	0.01	0.07	0.00	0.05	0.00	61.63	0.25	0.06	0.00	0.00	0.12	0.00	0.04	0.07	0.00	0.00	0.00	-	-	9993	2010	Lynp-02-09-A2
41	99	37.81	0.03	0.00	0.03	0.11	0.00	0.13	0.01	58.69	0.84	0.04	0.00	0.00	0.18	0.05	0.04	0.05	0.00	0.00	0.00	-	-	9888	2010	Lynp-02-09-A2
42	101	36.38	0.08	0.00	0.05	0.06	0.00	0.01	0.00	59.77	0.46	0.05	0.00	0.00	0.10	0.00	0.00	0.08	0.00	0.03	0.00	-	-	9706	2010	Lynp-02-09-A2
43	103	37.12	0.00	0.00	0.05	0.12	0.00	0.11	0.01	59.19	1.02	0.08	0.00	0.00	0.13	0.00	0.03	0.13	0.00	0.00	0.00	-	-	9799	2010	Lynp-02-09-A2
44	104	37.20	0.09	0.01	0.00	0.09	0.05	0.03	0.00	58.80	0.84	0.08	0.06	0.00	0.16	0.00	0.00	0.01	0.00	0.00	0.08	-	-	9750	2010	Lynp-02-09-A2
45	106	37.25	0.03	0.00	0.00	0.04	0.00	0.05	0.01	59.64	0.85	0.10	0.00	0.00	0.14	0.00	0.00	0.13	0.00	0.05	0.03	-	-	9832	2010	Lynp-02-09-A2
46	107	37.15	0.00	0.00	0.01	0.11	0.00	0.06	0.04	60.61	0.85	0.07	0.00	0.00	0.10	0.00	0.00	0.11	0.00	0.04	0.06	-	-	9918	2010	Lynp-02-09-A2
47	108	37.94	0.00	0.00	0.03	0.02	0.03	0.09	0.06	59.40	0.89	0.07	0.03	0.00	0.12	0.00	0.01	0.12	0.00	0.00	0.00	-	-	9879	2010	Lynp-02-09-A2
48	109	37.61	0.11	0.00	0.08	0.03	0.00	0.14	0.04	56.22	2.45	0.10	0.00	0.00	0.66	0.00	0.00	0.15	0.00	0.00	0.00	-	-	9758	2010	Lynp-02-09-A2
49	110	37.68	0.00	0.01	0.06	0.09	0.02	0.07	0.05	59.38	1.02	0.08	0.00	0.00	0.12	0.04	0.03	0.11	0.00	0.02	0.06	-	-	9884	2010	Lynp-02-09-A2
50	111	37.63	0.00	0.00	0.01																					

INDEX	No.	O	Na	K	V	Co	Mg	P	Cr	Fe	Al	S	Ni	Mn	Si	Pb	Cu	Ti	Ca	Zn	Ba	Sr	Total	Year	Sample
150	55	37.00	0.00	0.02	0.02	0.01	0.07	0.07	0.01	0.00	60.04	0.46	0.01	0.05	0.71	0.02	0.00	0.00	0.00	0.01	0.01		98.58	2010	Pic 06 04/3
151	56	35.10	0.13	0.00	0.00	0.03	0.00	0.06	0.05	0.57	0.67	0.34	0.01	0.00	1.11	0.00	0.08	0.00	0.00	0.00	0.01	0.01	94.59	2010	Pic 06 04/3
152	57	35.09	0.06	0.02	0.07	0.06	0.00	0.04	0.00	59.88	0.18		0.00	0.00	1.43	0.01	0.00	0.06	0.00	0.00	0.00	0.03	96.93	2010	Pic 06 04/3
153	58	35.82	0.08	0.02	0.00	0.05	0.00	0.04	0.02	59.93	0.11		0.00	0.00	1.67	0.03	0.04	0.00	0.00	0.00	0.00	0.00	97.82	2010	Pic 06 04/3
154	59	35.55	0.00	0.00	0.06	0.07	0.06	0.01	0.00	59.53	0.09		0.00	0.03	1.69	0.12	0.07	0.00	0.00	0.00	0.00	0.01	97.28	2010	Pic 06 04/3
155	60	36.85	0.00	0.00	0.12	0.05	0.03	0.01	0.03	60.05	0.14	1.51	0.01	1.55	0.00	0.00	0.04	0.00	0.00	0.00	0.00	0.05	98.93	2010	Pic 06 04/3
156	61	35.65	0.00	0.00	0.00	0.06	0.00	0.05	0.00	59.68	0.22	0.08	0.01	1.39	0.00	0.00	0.08	0.00	0.07	0.00	0.00		97.28	2010	Pic 06 04/3
157	62	36.67	0.00	0.00	0.02	0.02	0.05	0.07	0.02	59.97	0.32		0.00	0.05	1.25	0.00	0.01	0.08	0.00	0.00	0.00		98.51	2010	Pic 06 04/3
158	63	35.69	0.02	0.00	0.01	0.09	0.00	0.05	0.00	59.12	0.36		0.00	0.00	0.63	0.00	0.02	0.05	0.00	0.02	0.04		96.08	2010	Pic 06 04/3
159	64	36.56	0.08	0.00	0.00	0.07	0.00	0.07	0.03	59.02	0.33		0.00	0.04	0.63	0.04	0.02	0.03	0.00	0.00	0.00	0.02	96.99	2010	Pic 06 04/3
160	65	37.55	0.19	0.00	0.00	0.00	0.00	0.13	0.00	59.04	0.91	0.00	0.02	0.81	0.03	0.00	0.04	0.00	0.06	0.00	0.00		98.78	2010	Pic 06 04/3
161	66	37.82	0.09	0.01	0.00	0.03	0.09	0.11	0.03	58.68	0.99	0.00	0.01	0.75	0.13	0.00	0.00	0.00	0.08	0.00	0.00		98.81	2010	Pic 06 04/3
162	67	36.95	0.00	0.02	0.01	0.06	0.04	0.10	0.01	57.00	1.03		0.00	0.03	0.80	0.00	0.06	0.00	0.00	0.00	0.00	0.03	96.13	2010	Pic 06 04/3
163	68	37.97	0.00	0.00	0.05	0.04	0.05	0.16	0.00	58.14	1.18		0.01	0.03	0.68	0.04	0.02	0.00	0.00	0.04	0.00		98.40	2010	Pic 06 04/3
164	69	36.79	0.06	0.01	0.00	0.06	0.02	0.12	0.00	57.38	0.93		0.00	0.03	0.72	0.04	0.02	0.01	0.00	0.10	0.02		96.36	2010	Pic 06 04/3
165	70	37.94	0.00	0.00	0.09	0.00	0.09	0.01	0.01	57.84	0.95		0.00	0.05	0.82	0.02	0.04	0.06	0.00	0.04	0.01		97.95	2010	Pic 06 04/3
166	71	37.83	0.18	0.01	0.05	0.06	0.04	0.10	0.02	58.73	0.83		0.00	0.00	0.86	0.01	0.00	0.00	0.01	0.00	0.00		98.73	2010	Pic 06 04/3
167	72	38.01	0.00	0.00	0.00	0.09	0.06	0.08	0.00	58.45	1.19		0.01	0.01	0.68	0.00	0.02	0.00	0.00	0.00	0.05		98.64	2010	Pic 06 04/3
168	73	37.76	0.00	0.00	0.01	0.03	0.03	0.11	0.01	58.28	1.32		0.02	0.00	0.55	0.00	0.07	0.00	0.00	0.08	0.00		98.26	2010	Pic 06 04/3
169	74	38.12	0.00	0.00	0.00	0.02	0.02	0.10	0.00	58.16	1.30		0.03	0.01	0.59	0.00	0.00	0.06	0.00	0.12	0.00		98.61	2010	Pic 06 04/3
170	75	37.17	0.00	0.00	0.01	0.10	0.00	0.11	0.06	57.65	1.22		0.00	0.00	0.64	0.00	0.00	0.05	0.00	0.01	0.03		97.05	2010	Pic 06 04/3
171	76	38.09	0.00	0.00	0.00	0.09	0.09	0.12	0.00	58.71	1.31		0.03	0.00	0.56	0.00	0.00	0.00	0.00	0.00	0.00		99.01	2010	Pic 06 04/3
172	77	37.37	0.00	0.00	0.00	0.06	0.03	0.09	0.02	58.92	0.98		0.02	0.02	0.58	0.00	0.00	0.00	0.00	0.00	0.00		98.07	2010	Pic 06 04/3
173	78	32.76	0.00	0.00	0.02	0.08	0.00	0.14	0.00	63.46	1.14		0.05	0.03	0.61	0.10	0.04	0.00	0.00	0.00	0.00		98.43	2010	Pic 06 04/3
174	79	35.67	0.00	0.00	0.00	0.00	0.00	0.09	0.03	62.97	1.03		0.01	0.02	0.60	0.00	0.02	0.06	0.00	0.00	0.00		100.59	2010	Pic 06 04/3
175	80	36.64	0.00	0.00	0.03	0.06	0.08	0.01	0.00	58.70	0.70		0.01	0.02	0.59	0.05	0.01	0.03	0.00	0.00	0.00		96.92	2010	Pic 06 04/3
176	81	36.27	0.01	0.00	0.01	0.05	0.07	0.05	0.05	60.95	0.86		0.00	0.04	0.59	0.10	0.00	0.01	0.00	0.00	0.00		99.05	2010	Pic 06 04/3
177	82	32.66	0.14	0.00	0.00	0.10	0.00	0.11	0.03	60.73	0.59		0.00	0.01	0.60	0.07	0.00	0.02	0.00	0.00	0.00		95.06	2010	Pic 06 04/3
178	83	37.37	0.00	0.00	0.00	0.09	0.00	0.09	0.00	61.46	0.76		0.00	0.00	0.67	0.00	0.04	0.03	0.00	0.00	0.05		100.55	2010	Pic 06 04/3
179	84	37.30	0.00	0.00	0.00	0.06	0.03	0.10	0.00	58.78	0.80		0.00	0.00	0.60	0.00	0.04	0.00	0.00	0.00	0.00		97.85	2010	Pic 06 04/3
180	85	36.54	0.00	0.00	0.00	0.06	0.00	0.09	0.01	59.39	0.79		0.01	0.00	0.56	0.03	0.00	0.00	0.00	0.00	0.01		97.49	2010	Pic 06 04/3
181	86	37.34	0.06	0.00	0.03	0.08	0.00	0.08	0.02	58.66	0.66		0.00	0.00	0.64	0.00	0.00	0.02	0.00	0.00	0.00		97.59	2010	Pic 06 04/3
182	88	37.74	0.07	0.00	0.01	0.04	0.46	0.63	0.00	58.59	1.56		0.00	0.18	0.97	0.05	0.00	0.03	0.02	0.02	0.04		100.40	2010	Pic 06 05B/2
183	89	33.12	0.02	0.00	0.02	0.04	0.12	0.30	0.01	61.40	1.19		0.00	0.13	0.56	0.05	0.00	0.00	0.00	0.00	0.02		96.96	2010	Pic 06 05B/2
184	91	35.15	0.00	0.00	0.00	0.00	0.11	0.32	0.00	62.12	1.79		0.00	0.20	0.47	0.07	0.00	0.05	0.00	0.00	0.02		100.24	2010	Pic 06 05B/2
185	92	35.74	0.00	0.00	0.06	0.07	0.10	0.35	0.00	61.02	1.84		0.00	0.19	0.49	0.05	0.04	0.00	0.00	0.00	0.02		99.98	2010	Pic 06 05B/2
186	94	37.10	0.00	0.02	0.05	0.04	0.02	0.03	0.00	60.60	0.12		0.00	0.04	0.84	0.12	0.05	0.01	0.00	0.00	0.02		99.05	2010	Pic 06 05B/2
187	95	36.70	0.00	0.01	0.00	0.04	0.00	0.05	0.02	60.07	0.13		0.00	0.00	0.95	0.00	0.00	0.00	0.00	0.00	0.02		97.99	2010	Pic 06 05B/2
188	96	37.70	0.15	0.00	0.00	0.03	0.01	0.06	0.00	60.02	0.09		0.00	0.00	1.15	0.00	0.00	0.03	0.00	0.00	0.00		99.27	2010	Pic 06 05B/2
189	97	36.86	0.02	0.02	0.05	0.12	0.00	0.02	0.00	60.04	0.07		0.00	0.07	0.15	0.00	0.00	0.00	0.00	0.00	0.00		98.34	2010	Pic 06 05B/2
190	98	36.73	0.18	0.01	0.00	0.09	0.00	0.06	0.00	59.86	0.14		0.01	0.01	0.86	0.17	0.03	0.02	0.00	0.00	0.00		98.16	2010	Pic 06 05B/2
191	99	36.13	0.00	0.00	0.04	0.10	0.00	0.11	0.03	61.14	0.22		0.04	0.04	0.66	0.06	0.00	0.00	0.00	0.00	0.00		98.73	2010	Pic 06 05B/2
192	100	33.39	0.03	0.00	0.05	0.05	0.03	0.35	0.02	60.99	2.14		0.00	0.18	0.47	0.00	0.00	0.00	0.00	0.09	0.04		97.83	2010	Pic 06 05B/2
193	101	34.28	0.01	0.00	0.00	0.02	0.17	0.40	0.01	61.78	2.20		0.02	0.26	0.56	0.01	0.00	0.05	0.00	0.06	0.00		99.81	2010	Pic 06 05B/2
194	102	32.39	0.00	0.00	0.00	0.00	0.11	0.32	0.00	61.48	2.04		0.00	0.20	0.47	0.07	0.00	0.05	0.00	0.00	0.02		97.24	2010	Pic 06 05B/2
195	103	35.26	0.00	0.00	0.00	0.02	0.14	0.28	0.00	61.78	2.01		0.00	0.20	0.47	0.00	0.00	0.04	0.00	0.00	0.02		100.21	2010	Pic 06 05B/2
196	104	34.78	0.00	0.00	0.06	0.07	0.09	0.28	0.00	61.98	1.99		0.03	0.16	0.50	0.00	0.02	0.05	0.00	0.00	0.02		100.04	2010	Pic 06 05B/2
197	107	34.51	0.02	0.00	0.08	0.12	0.08	0.36	0.01	61.86	2.02		0.00	0.18	0.54	0.08	0.00	0.01	0.00	0.07	0.00		99.92	2010	Pic 06 05B/2
198	108	33.99	0.12	0.00	0.04	0.05	0.17	0.27	0.02	61.73	1.76		0.06	0.14	0.45	0.02	0.06	0.00	0.00	0.00	0.01		98.88	2010	Pic 06 05B/2
199	109	34.31	0.02	0.00	0.00	0.03	0.15	0.29	0.01	61.79	1.87		0.01	0.03	0.49	0.00	0.06	0.03	0.00	0.01	0.02		99.30	2010	Pic 06 05B/2
200	110	34.14	0.04	0.02	0.00	0.05	0.11	0.38	0.00	61.94	2.19		0.02	0.13	0.48	0.02	0.01	0.00	0.00	0.02	0.01		99.55	2010	Pic 06 05B/2
201	111	35.37	0.09	0.02	0.00	0.04	0.01	0.24	0.00	62.35	1.63		0.01	0.11	0.45	0.03	0.08	0.00	0.00	0.01	0.00		100.43	2010	Pic

INDEX	No.	O	Na	K	V	Co	Mg	P	Cr	Fe	Al	S	Ni	Mn	Si	Pb	Cu	Ti	Ca	Zn	Ba	Sr	Total	Year	Sample
300	265	99.36	0.01	0.00	0.16	0.00	0.00	0.19	0.00	57.63	2.99	0.00	0.00	0.27	0.05	0.00	0.09	0.07	0.00	0.00	0.00	0.00	99.95	2010	Pic 06 21 Line 2
301	295	39.10	0.07	0.00	0.03	0.13	0.05	0.11	0.00	56.14	2.02	0.00	0.02	0.00	0.31	0.00	0.02	0.10	0.00	0.00	0.01	0.00	98.11	2010	Pic 06 21 Line 2
302	325	38.82	0.07	0.00	0.00	0.01	0.06	0.16	0.00	57.81	2.22	0.04	0.00	0.20	0.00	0.00	0.16	0.00	0.00	0.00	0.00	0.00	99.54	2010	Pic 06 21 Line 2
303	355	39.51	0.00	0.00	0.00	0.13	0.05	0.08	0.03	56.64	1.86	0.06	0.03	0.36	0.03	0.09	0.02	0.00	0.00	0.00	0.00	0.00	98.89	2010	Pic 06 21 Line 2
304	385	38.41	0.00	0.00	0.08	0.09	0.03	0.11	0.00	58.76	1.70	0.03	0.00	0.26	0.10	0.00	0.10	0.00	0.00	0.00	0.00	0.00	99.66	2010	Pic 06 21 Line 2
305	405	38.94	0.28	0.01	0.00	0.07	0.00	0.11	0.00	58.13	1.35	0.05	0.00	0.28	0.00	0.04	0.13	0.00	0.04	0.00	0.00	0.00	99.44	2010	Pic 06 21 Line 2
306	435	37.59	0.00	0.00	0.05	0.09	0.00	0.05	0.02	60.79	1.08	0.00	0.07	0.41	0.00	0.01	0.07	0.00	0.00	0.00	0.00	0.00	100.22	2010	Pic 06 21 Line 2
307	283	39.01	0.00	0.02	0.00	0.06	0.05	0.15	0.00	56.93	1.86	0.02	0.00	0.28	0.11	0.04	0.09	0.00	0.08	0.01	0.00	0.00	98.70	2010	Pic 06 21 Line 20
308	313	39.62	0.00	0.00	0.01	0.07	0.05	0.16	0.00	57.17	2.43	0.00	0.00	0.27	0.07	0.02	0.09	0.00	0.01	0.00	0.00	0.00	99.96	2010	Pic 06 21 Line 20
309	343	36.99	0.00	0.00	0.02	0.13	0.02	0.01	0.01	61.12	0.03	0.00	0.01	0.42	0.00	0.00	0.00	0.00	0.00	0.00	0.00	0.00	98.76	2010	Pic 06 21 Line 20
310	373	39.43	0.00	0.00	0.05	0.08	0.00	0.09	0.00	56.73	2.28	0.05	0.00	0.38	0.00	0.00	0.01	0.00	0.04	0.00	0.00	0.00	99.13	2010	Pic 06 21 Line 20
311	403	38.40	0.00	0.01	0.04	0.00	0.00	0.11	0.00	59.01	1.82	0.00	0.00	0.23	0.08	0.00	0.12	0.00	0.00	0.06	0.00	0.00	99.87	2010	Pic 06 21 Line 20
312	423	39.43	0.00	0.02	0.09	0.01	0.00	0.13	0.03	58.42	1.78	0.00	0.03	0.28	0.04	0.00	0.19	0.00	0.07	0.00	0.00	0.00	100.52	2010	Pic 06 21 Line 20
313	453	36.99	0.06	0.01	0.00	0.09	0.01	0.01	0.00	61.77	0.39	0.01	0.00	0.40	0.03	0.00	0.05	0.00	0.00	0.02	0.00	0.00	99.83	2010	Pic 06 21 Line 20
314	284	38.96	0.06	0.01	0.01	0.10	0.03	0.13	0.01	56.77	1.53	0.00	0.00	0.26	0.01	0.00	0.13	0.00	0.00	0.00	0.00	0.00	98.83	2010	Pic 06 21 Line 21
315	314	39.76	0.04	0.00	0.00	0.04	0.00	0.12	0.04	56.25	3.48	0.00	0.00	0.00	0.00	0.10	0.00	0.02	0.07	0.00	0.00	100.21	2010	Pic 06 21 Line 21	
316	344	36.95	0.24	0.00	0.00	0.08	0.00	0.02	0.00	60.90	0.00	0.00	0.00	0.52	0.00	0.00	0.06	0.00	0.03	0.00	0.00	0.00	98.80	2010	Pic 06 21 Line 21
317	374	37.77	0.02	0.00	0.06	0.06	0.00	0.09	0.03	57.23	2.07	0.00	0.02	0.45	0.00	0.00	0.12	0.00	0.07	0.00	0.00	0.00	97.96	2010	Pic 06 21 Line 21
318	424	39.43	0.00	0.00	0.06	0.06	0.04	0.14	0.01	58.02	1.88	0.00	0.00	0.25	0.00	0.09	0.19	0.00	0.00	0.00	0.00	0.00	100.17	2010	Pic 06 21 Line 21
319	454	37.14	0.07	0.00	0.00	0.00	0.00	0.02	0.00	60.97	0.00	0.04	0.38	0.00	0.00	0.02	0.00	0.00	0.00	0.00	0.00	0.00	98.29	2010	Pic 06 21 Line 21
320	285	38.90	0.11	0.00	0.00	0.06	0.02	0.15	0.00	57.78	1.62	0.05	0.04	0.32	0.08	0.01	0.13	0.00	0.03	0.02	0.00	0.00	99.33	2010	Pic 06 21 Line 21
321	315	38.88	0.08	0.00	0.05	0.03	0.02	0.10	0.07	56.96	3.48	0.02	0.03	0.22	0.01	0.00	0.04	0.00	0.00	0.00	0.00	0.00	99.96	2010	Pic 06 21 Line 22
322	345	36.69	0.22	0.00	0.00	0.05	0.00	0.01	0.01	61.39	0.00	0.02	0.04	0.47	0.12	0.00	0.04	0.00	0.01	0.00	0.00	0.00	99.08	2010	Pic 06 21 Line 22
323	375	39.43	0.02	0.00	0.08	0.08	0.01	0.04	0.00	55.83	2.37	0.03	0.08	0.43	0.04	0.00	0.12	0.00	0.02	0.04	0.00	0.00	98.61	2010	Pic 06 21 Line 22
324	425	39.17	0.06	0.00	0.00	0.00	0.00	0.16	0.03	58.00	1.80	0.00	0.00	0.24	0.00	0.01	0.00	0.00	0.00	0.00	0.00	0.00	99.86	2010	Pic 06 21 Line 22
325	455	36.75	0.12	0.00	0.01	0.03	0.00	0.02	0.00	61.17	0.09	0.00	0.02	0.38	0.04	0.00	0.00	0.00	0.07	0.00	0.00	0.00	98.69	2010	Pic 06 21 Line 22
326	286	37.83	0.00	0.01	0.00	0.02	0.04	0.14	0.01	57.59	1.50	0.05	0.01	0.32	0.00	0.00	0.15	0.00	0.00	0.03	0.00	0.00	97.71	2010	Pic 06 21 Line 23
327	316	38.41	0.00	0.00	0.08	0.06	0.02	0.03	0.06	58.30	1.09	0.06	0.02	0.44	0.10	0.00	0.00	0.00	0.00	0.00	0.00	0.00	98.57	2010	Pic 06 21 Line 23
328	346	37.25	0.00	0.00	0.00	0.04	0.00	0.02	0.00	60.55	0.01	0.00	0.00	0.53	0.15	0.04	0.03	0.00	0.00	0.00	0.00	0.00	98.60	2010	Pic 06 21 Line 23
329	376	39.53	0.12	0.00	0.00	0.06	0.04	0.09	0.02	55.71	2.78	0.00	0.00	0.38	0.13	0.00	0.06	0.00	0.00	0.00	0.00	0.00	99.11	2010	Pic 06 21 Line 23
330	426	39.53	0.00	0.00	0.07	0.05	0.00	0.15	0.00	57.89	1.87	0.00	0.00	0.26	0.02	0.07	0.18	0.00	0.04	0.02	0.00	0.00	100.14	2010	Pic 06 21 Line 23
331	456	36.55	0.00	0.01	0.01	0.05	0.05	0.00	0.00	61.40	0.09	0.00	0.00	0.35	0.03	0.00	0.02	0.00	0.04	0.05	0.00	0.00	98.64	2010	Pic 06 21 Line 23
332	287	39.00	0.13	0.01	0.00	0.04	0.00	0.16	0.00	56.56	1.90	0.00	0.03	0.33	0.10	0.03	0.11	0.00	0.01	0.00	0.00	0.00	98.39	2010	Pic 06 21 Line 24
333	317	39.60	0.00	0.00	0.00	0.03	0.05	0.16	0.01	56.28	3.63	0.00	0.01	0.26	0.06	0.00	0.01	0.00	0.00	0.05	0.00	0.00	100.13	2010	Pic 06 21 Line 24
334	347	38.03	0.01	0.00	0.00	0.00	0.00	0.00	0.00	60.67	0.00	0.00	0.00	0.25	0.00	0.00	0.00	0.00	0.00	0.00	0.00	0.00	99.68	2010	Pic 06 21 Line 24
335	427	39.58	0.10	0.00	0.03	0.03	0.02	0.14	0.00	58.02	1.88	0.00	0.00	0.27	0.13	0.00	0.11	0.00	0.11	0.00	0.00	0.00	100.43	2010	Pic 06 21 Line 24
336	457	37.27	0.17	0.00	0.00	0.08	0.01	0.05	0.00	61.08	0.04	0.00	0.00	0.39	0.04	0.02	0.00	0.00	0.01	0.02	0.00	0.00	99.18	2010	Pic 06 21 Line 24
337	288	38.79	0.11	0.01	0.10	0.00	0.08	0.15	0.02	57.15	2.18	0.02	0.04	0.28	0.00	0.03	0.16	0.00	0.00	0.03	0.00	0.00	99.13	2010	Pic 06 21 Line 25
338	318	39.49	0.00	0.02	0.02	0.05	0.02	0.10	0.04	56.16	3.75	0.00	0.02	0.26	0.02	0.00	0.07	0.00	0.00	0.00	0.00	0.00	100.01	2010	Pic 06 21 Line 25
339	348	34.46	0.12	0.00	0.00	0.06	0.08	0.09	0.01	51.35	1.58	0.00	0.00	0.54	0.00	0.00	0.43	0.00	0.00	0.00	0.00	0.00	98.77	2010	Pic 06 21 Line 25
340	428	39.47	0.03	0.01	0.01	0.00	0.02	0.13	0.00	58.13	2.02	0.04	0.02	0.29	0.00	0.02	0.08	0.00	0.00	0.03	0.00	0.00	100.30	2010	Pic 06 21 Line 25
341	289	38.00	0.00	0.00	0.08	0.06	0.10	0.10	0.00	58.55	2.13	0.00	0.00	0.28	0.05	0.00	0.08	0.00	0.00	0.00	0.00	0.00	99.34	2010	Pic 06 21 Line 25
342	349	36.11	0.19	0.00	0.05	0.05	0.07	0.02	0.00	60.62	0.00	0.00	0.10	0.44	0.10	0.00	0.00	0.00	0.00	0.00	0.00	0.00	97.74	2010	Pic 06 21 Line 26
343	429	39.63	0.00	0.00	0.00	0.04	0.03	0.14	0.00	57.66	2.10	0.00	0.00	0.25	0.03	0.05	0.15	0.00	0.00	0.00	0.00	0.00	100.08	2010	Pic 06 21 Line 26
344	290	36.02	0.07	0.00	0.00	0.09	0.00	0.19	0.01	59.98	4.27	0.00	0.00	0.17	0.00	0.00	0.00	0.00	0.00	0.00	0.00	0.00	100.20	2010	Pic 06 21 Line 27
345	320	38.70	0.09	0.01	0.00	0.01	0.00	0.08	0.01	56.77	3.44	0.02	0.03	0.32	0.03	0.00	0.04	0.00	0.02	0.00	0.00	0.00	99.57	2010	Pic 06 21 Line 27
346	350	37.98	0.10	0.00	0.00	0.08	0.00	0.00	0.00	61.08	0.07	0.01	0.01	0.42	0.03	0.01	0.05	0.00	0.02	0.02	0.00	0.00	99.88	2010	Pic 06 21 Line 27
347	430	39.65	0.00	0.00	0.00	0.03	0.03	0.14	0.04	57.21	2.37	0.00	0.00	0.29	0.00	0.05	0.09	0.00	0.04	0.01	0.00	0.00	99.88	2010	Pic 06 21 Line 28
348	321	39.48	0.06	0.01	0.00	0.05	0.00	0.16	0.02	56.47	3.68	0.02	0.00	0.28	0.02	0.00	0.07	0.00	0.09	0.00	0.00	0.00	100.40	2010	Pic 06 21 Line 28
349	351	37.43	0.03	0.00	0.00	0.09	0.00	0.02	0.03	61.37	0.00	0.00	0.00	0.31	0.03	0.00									

INDEX	No.	O	Na	K	V	Co	Mg	P	Cr	Fe	Al	S	Ni	Mn	Si	Pb	Cu	Ti	Ca	Zn	Ba	Sr	Total	Year	Sample
450	621	34.89	0.07	0.00	0.00	0.07	0.10	0.10	0.00	60.80	0.82	0.05	0.00	0.05	0.35	0.06	0.00	0.03	0.00	0.09	-	-	9732	2010	Pic 06 22 VYG
451	622	35.08	0.03	0.00	0.00	0.05	0.03	0.10	0.00	61.01	0.84	0.04	0.00	0.04	0.36	0.15	0.02	0.04	0.00	0.09	-	-	9786	2010	Pic 06 22 VYG
452	623	34.93	0.05	0.00	0.00	0.04	0.05	0.13	0.01	60.79	0.89	0.02	0.01	0.00	0.31	0.13	0.01	0.08	0.00	0.00	-	-	9744	2010	Pic 06 22 VYG
453	624	35.00	0.06	0.01	0.00	0.10	0.00	0.08	0.01	60.90	0.80	0.03	0.00	0.00	0.31	0.09	0.02	0.08	0.00	0.00	-	-	9748	2010	Pic 06 22 VYG
454	625	36.05	0.14	0.00	0.03	0.09	0.00	0.11	0.03	59.80	0.81	0.05	0.06	0.05	0.50	0.00	0.00	0.09	0.00	0.00	-	-	9778	2010	Pic 06 22 VYG
455	626	36.57	0.07	0.00	0.00	0.06	0.01	0.08	0.04	58.75	0.83	0.00	0.00	0.00	1.05	0.01	0.03	0.00	0.00	0.00	-	-	9758	2010	Pic 06 22 VYG
456	627	36.07	0.02	0.00	0.00	0.07	0.01	0.07	0.02	59.47	0.61	0.05	0.02	0.00	0.44	0.08	0.01	0.05	0.00	0.07	-	-	9706	2010	Pic 06 22 VYG
457	628	35.22	0.07	0.00	0.06	0.09	0.00	0.11	0.01	59.91	0.77	0.04	0.00	0.06	0.39	0.00	0.02	0.00	0.00	0.03	-	-	9676	2010	Pic 06 22 VYG
458	629	35.59	0.19	0.02	0.02	0.07	0.00	0.12	0.00	60.42	0.91	0.05	0.04	0.00	0.39	0.03	0.05	0.01	0.00	0.00	-	-	9790	2010	Pic 06 22 VYG
459	630	35.21	0.07	0.00	0.03	0.10	0.00	0.12	0.00	60.70	1.04	0.08	0.00	0.03	0.34	0.01	0.01	0.07	0.00	0.00	-	-	9779	2010	Pic 06 22 VYG
460	631	35.78	0.03	0.00	0.02	0.06	0.05	0.17	0.02	60.32	1.00	0.07	0.00	0.04	0.37	0.00	0.00	0.00	0.00	0.02	-	-	9803	2010	Pic 06 22 VYG
461	632	37.46	0.10	0.01	0.00	0.09	0.00	0.04	0.00	57.38	0.14	0.02	0.00	0.00	0.32	0.03	0.00	0.00	0.00	0.02	-	-	9561	2010	Pic 06 22 VYG
462	633	37.12	0.03	0.01	0.00	0.07	0.00	0.07	0.01	57.66	0.19	0.01	0.00	0.00	0.28	0.10	0.05	0.00	0.00	0.00	-	-	9559	2010	Pic 06 22 VYG
463	634	37.23	0.00	0.00	0.10	0.00	0.00	0.00	0.00	57.72	0.12	0.04	0.00	0.00	0.61	0.07	0.00	0.06	0.00	0.00	-	-	9595	2010	Pic 06 22 VYG
464	636	36.23	0.05	0.01	0.01	0.11	0.01	0.14	0.02	60.53	0.81	0.04	0.00	0.00	0.42	0.05	0.00	0.02	0.00	0.00	-	-	9841	2010	Pic 06 22 VYG
465	637	35.99	0.00	0.00	0.12	0.04	0.07	0.03	0.00	59.99	0.73	0.05	0.00	0.07	0.39	0.00	0.00	0.05	0.00	0.00	-	-	9752	2010	Pic 06 22 VYG
466	638	35.63	0.06	0.00	0.03	0.13	0.03	0.12	0.00	60.55	0.75	0.06	0.00	0.02	0.43	0.06	0.09	0.06	0.00	0.07	-	-	9808	2010	Pic 06 22 VYG
467	639	35.19	0.00	0.00	0.05	0.15	0.04	0.08	0.05	60.95	0.74	0.03	0.00	0.01	0.41	0.00	0.05	0.02	0.00	0.06	-	-	9781	2010	Pic 06 22 VYG
468	640	35.79	0.00	0.01	0.01	0.11	0.05	0.13	0.00	60.21	0.65	0.02	0.00	0.04	0.38	0.00	0.06	0.06	0.00	0.00	-	-	9752	2010	Pic 06 22 VYG
469	641	35.17	0.06	0.00	0.00	0.09	0.01	0.13	0.00	60.52	0.75	0.05	0.02	0.00	0.42	0.05	0.00	0.00	0.00	0.06	-	-	9751	2010	Pic 06 22 VYG
470	642	35.34	0.00	0.00	0.05	0.02	0.11	0.01	0.00	59.70	0.82	0.03	0.00	0.04	0.50	0.05	0.00	0.04	0.00	0.00	-	-	9677	2010	Pic 06 22 VYG
471	643	35.05	0.00	0.01	0.09	0.07	0.03	0.12	0.02	60.44	0.78	0.06	0.00	0.01	0.48	0.01	0.07	0.05	0.00	0.00	-	-	9727	2010	Pic 06 22 VYG
472	644	35.58	0.01	0.00	0.03	0.04	0.02	0.10	0.01	60.44	0.73	0.04	0.00	0.09	0.51	0.01	0.06	0.06	0.00	0.00	-	-	9770	2010	Pic 06 22 VYG
473	645	34.61	0.00	0.02	0.00	0.02	0.00	0.11	0.00	61.06	0.81	0.06	0.00	0.03	0.50	0.00	0.03	0.00	0.00	0.00	-	-	9724	2010	Pic 06 22 VYG
474	646	36.22	0.00	0.00	0.00	0.00	0.03	0.13	0.00	59.99	0.80	0.07	0.00	0.00	0.45	0.13	0.02	0.00	0.00	0.10	-	-	9833	2010	Pic 06 22 VYG
475	647	36.52	0.00	0.00	0.00	0.00	0.00	0.08	0.00	60.52	0.47	0.05	0.03	0.01	0.42	0.00	0.13	0.00	0.00	0.00	-	-	9822	2010	Pic 06 22 VYG
476	648	36.59	0.00	0.00	0.00	0.09	0.03	0.08	0.04	59.94	0.60	0.05	0.05	0.01	0.47	0.04	0.05	0.00	0.00	0.00	-	-	9803	2010	Pic 06 22 VYG
477	649	35.82	0.00	0.02	0.00	0.09	0.04	0.11	0.02	59.98	0.73	0.05	0.00	0.06	0.43	0.00	0.00	0.08	0.00	0.04	-	-	9746	2010	Pic 06 22 VYG
478	650	35.95	0.04	0.00	0.04	0.06	0.03	0.08	0.01	60.61	0.58	0.06	0.04	0.05	0.40	0.04	0.00	0.01	0.00	0.00	-	-	9798	2010	Pic 06 22 VYG
479	651	35.65	0.00	0.00	0.00	0.09	0.01	0.12	0.00	60.65	0.69	0.06	0.06	0.00	0.11	0.03	0.03	0.00	0.00	0.00	-	-	9786	2010	Pic 06 22 VYG
480	652	35.03	0.05	0.00	0.03	0.00	0.03	0.08	0.04	60.79	0.70	0.04	0.00	0.05	0.39	0.01	0.05	0.02	0.00	0.00	-	-	9730	2010	Pic 06 22 VYG
481	653	35.28	0.00	0.00	0.00	0.07	0.02	0.10	0.00	61.26	0.74	0.08	0.04	0.00	0.39	0.05	0.00	0.01	0.00	0.00	-	-	9804	2010	Pic 06 22 VYG
482	654	35.18	0.00	0.00	0.00	0.09	0.05	0.11	0.00	60.69	0.69	0.05	0.04	0.02	0.37	0.13	0.00	0.05	0.00	0.05	-	-	9750	2010	Pic 06 22 VYG
483	655	37.17	0.03	0.00	0.00	0.10	0.01	0.03	0.00	59.37	0.31	0.03	0.00	0.03	0.31	0.01	0.00	0.00	0.00	0.00	-	-	9740	2010	Pic 06 22 VYG
484	656	34.66	0.00	0.00	0.00	0.00	0.00	0.09	0.00	61.06	0.89	0.06	0.00	0.00	0.39	0.00	0.00	0.00	0.00	0.00	-	-	9786	2010	Pic 06 22 VYG
485	657	36.20	0.00	0.00	0.02	0.09	0.05	0.09	0.00	60.75	0.64	0.03	0.00	0.00	0.42	0.00	0.01	0.00	0.00	0.09	-	-	9840	2010	Pic 06 22 VYG
486	658	35.40	0.08	0.00	0.00	0.08	0.02	0.13	0.03	60.59	0.77	0.05	0.00	0.05	0.42	0.15	0.05	0.00	0.00	0.00	-	-	9780	2010	Pic 06 22 VYG
487	659	35.02	0.07	0.00	0.01	0.09	0.01	0.10	0.02	60.95	0.79	0.08	0.00	0.04	0.37	0.05	0.00	0.00	0.00	0.11	-	-	9772	2010	Pic 06 22 VYG
488	660	36.17	0.00	0.00	0.00	0.05	0.03	0.06	0.02	60.17	0.61	0.05	0.00	0.00	0.40	0.03	0.05	0.02	0.00	0.00	-	-	9767	2010	Pic 06 22 VYG
489	661	35.11	0.00	0.00	0.00	0.00	0.02	0.01	0.09	0.00	61.40	0.84	0.06	0.06	0.00	0.45	0.13	0.02	0.00	0.00	-	-	9819	2010	Pic 06 22 VYG
490	662	35.45	0.02	0.00	0.00	0.05	0.01	0.10	0.00	60.93	0.72	0.05	0.00	0.01	0.39	0.00	0.00	0.01	0.00	0.00	-	-	9773	2010	Pic 06 22 VYG
491	663	35.59	0.00	0.01	0.01	0.10	0.04	0.09	0.03	61.54	0.71	0.06	0.01	0.07	0.40	0.05	0.00	0.00	0.00	0.00	-	-	9869	2010	Pic 06 22 VYG
492	664	35.49	0.04	0.00	0.02	0.06	0.03	0.08	0.02	61.01	0.66	0.05	0.02	0.06	0.43	0.03	0.02	0.06	0.00	0.01	-	-	9807	2010	Pic 06 22 VYG
493	665	35.45	0.00	0.04	0.04	0.05	0.01	0.12	0.00	60.69	0.71	0.06	0.00	0.01	0.39	0.00	0.00	0.01	0.00	0.00	-	-	9758	2010	Pic 06 22 VYG
494	666	35.12	0.00	0.00	0.00	0.09	0.01	0.11	0.00	61.16	0.69	0.06	0.06	0.00	0.18	0.02	0.00	0.00	0.00	0.00	-	-	9780	2010	Pic 06 22 VYG
495	667	35.61	0.01	0.00	0.00	0.11	0.02	0.07	0.00	61.06	0.58	0.07	0.00	0.01	0.43	0.00	0.00	0.00	0.00	0.06	-	-	9803	2010	Pic 06 22 VYG
496	668	35.41	0.00	0.00	0.00	0.10	0.00	0.10	0.00	60.45	0.78	0.06	0.00	0.00	0.43	0.13	0.00	0.02	0.00	0.00	-	-	9747	2010	Pic 06 22 VYG
497	669	35.67	0.00	0.00	0.04	0.07	0.04	0.07	0.01	61.32	0.63	0.04	0.00	0.00	0.38	0.02	0.03	0.00	0.00	0.06	-	-	9839	2010	Pic 06 22 VYG
498	134	36.50	0.00	0.00	0.00	0.08	0.02	0.07	0.00	61.86	0.98	0.06	0.04	0.01	0.33	0.15	0.01	0.00	0.00	0.06	0.02	0.00	10019	2010	Pic 06 23 dark goe
499	140	36.51	0.00	0.02	0.04	0.06	0.00	0.02	0.02	62.09	0.12	0.04	0.00	0.00	0.19	0.06	0.00	0.00	0.00	0.03	0.02	0.01	9922	2010	Pic 06 23 dark goe
500	133	30.66	0.00	0.00	0.00	0.07	0.15	0.04	0.03	60.41	2.95	0.00	0.03	0.20	0.06	0.07	0.00	0.07	0.02	0.03	-	-	9558	2010	Pic 06 24/2
501	137	39.10	0.00	0.00	0.01	0.05	0.04	0.43	0.01	56.59	2.46	0.00	0.03	0.00	0.34	0.08	0.00	0.03	0.00	0.00	0.00				

INDEX	No.	O	Na	K	V	Co	Mg	P	Cr	Fe	Al	S	Ni	Mn	Si	Pb	Cu	Ti	Ca	Zn	Ba	Sr	Total	Year	Sample
600	36.69	0.06	0.00	0.02	0.01	0.01	0.21	0.01	0.23	0.00	59.54	0.59	0.00	0.02	0.39	0.05	0.00	0.01	0.04	0.00	0.00	0.00	97.60	2010	Pic-06-01A3
601	39.50	0.01	0.00	0.00	0.06	0.01	0.23	0.00	0.23	0.00	59.67	0.93	-	0.00	0.02	0.44	0.11	0.00	0.07	0.00	0.00	0.00	101.04	2010	Pic-06-01A3
602	35.21	0.00	0.00	0.03	0.09	0.02	0.21	0.04	0.04	59.74	0.71	-	0.00	0.02	0.39	0.03	0.00	0.05	0.00	0.00	0.00	0.00	96.54	2010	Pic-06-01A3
603	35.46	0.02	0.00	0.00	0.12	0.02	0.20	0.00	0.00	59.79	0.71	-	0.00	0.05	0.42	0.02	0.01	0.10	0.00	0.00	0.00	0.00	96.92	2010	Pic-06-01A3
604	37.02	0.00	0.00	0.03	0.05	0.00	0.34	0.00	0.04	60.34	1.15	-	0.02	0.00	0.15	0.00	0.02	0.07	0.00	0.00	0.00	0.00	99.18	2010	Pic-06-01A3
605	34.08	0.00	0.00	0.00	0.09	0.03	0.25	0.00	0.00	60.45	0.69	0.00	0.00	0.02	0.36	0.06	0.01	0.09	0.00	0.00	0.00	0.00	96.13	2010	Pic-06-01A3
606	32.09	0.03	0.00	0.00	0.06	0.03	0.26	0.02	0.00	60.55	0.73	-	0.00	0.03	0.37	0.13	0.03	0.04	0.00	0.04	0.01	0.01	94.43	2010	Pic-06-01A3
607	38.13	0.03	0.00	0.00	0.09	0.02	0.25	0.00	0.00	60.69	0.88	-	0.00	0.02	0.44	0.00	0.07	0.02	0.00	0.02	0.00	0.00	100.66	2010	Pic-06-01A3
608	36.49	0.02	0.00	0.04	0.08	0.00	0.48	0.04	0.04	61.24	1.04	-	0.04	0.01	0.16	0.08	0.00	0.21	0.00	0.12	0.01	0.01	100.04	2010	Pic-06-01A3
609	35.68	0.03	0.00	0.01	0.07	0.00	0.34	0.00	0.00	61.96	0.47	-	0.00	0.00	0.20	0.00	0.00	0.09	0.00	0.00	0.00	0.00	98.86	2010	Pic-06-01A3
610	35.64	0.00	0.00	0.04	0.11	0.00	0.37	0.00	0.00	62.92	1.01	0.00	0.00	0.02	0.31	0.00	0.00	0.02	0.00	0.00	0.00	0.00	100.36	2010	Pic-06-01A3
611	33.75	0.03	0.00	0.00	0.04	0.04	0.37	0.00	0.00	63.30	0.89	-	0.00	0.03	0.21	0.00	0.00	0.13	0.00	0.00	0.01	0.01	98.79	2010	Pic-06-01A3
612	32.96	0.07	0.00	0.00	0.06	0.00	0.22	0.00	0.00	66.00	1.34	-	0.00	0.00	0.17	0.09	0.00	0.10	0.00	0.00	0.00	0.00	101.02	2010	Pic-06-01A3
613	33.42	0.06	0.00	0.06	0.11	0.00	0.23	0.01	0.00	66.21	0.50	-	0.00	0.00	0.17	0.08	0.00	0.10	0.00	0.01	0.01	0.01	100.97	2010	Pic-06-01A3
614	31.97	0.00	0.00	0.01	0.04	0.00	0.30	0.00	0.00	66.56	0.70	-	0.00	0.00	0.15	0.00	0.00	0.05	0.00	0.00	0.00	0.00	99.86	2010	Pic-06-01A3
615	32.53	0.04	0.00	0.02	0.10	0.02	0.27	0.00	0.00	66.57	0.60	-	0.00	0.06	0.15	0.00	0.00	0.04	0.02	0.00	0.00	0.00	100.42	2010	Pic-06-01A3
616	32.84	0.00	0.02	0.00	0.10	0.01	0.19	0.00	0.00	66.72	1.34	-	0.00	0.00	0.16	0.03	0.00	0.10	0.00	0.01	0.01	0.01	101.53	2010	Pic-06-01A3
617	33.10	0.11	0.00	0.00	0.06	0.00	0.22	0.01	0.00	66.87	0.64	-	0.00	0.00	0.27	0.07	0.00	0.10	0.00	0.01	0.00	0.00	101.47	2010	Pic-06-01A3
618	32.53	0.00	0.00	0.01	0.08	0.00	0.24	0.00	0.00	67.16	1.29	-	0.00	0.01	0.21	0.00	0.08	0.09	0.00	0.08	0.00	0.00	101.78	2010	Pic-06-01A3
619	32.36	0.05	0.00	0.00	0.06	0.00	0.20	0.02	0.00	67.33	0.91	-	0.00	0.02	0.24	0.06	0.00	0.13	0.00	0.02	0.00	0.00	99.86	2010	Pic-06-01A3
620	32.45	0.00	0.01	0.00	0.08	0.00	0.20	0.02	0.00	67.57	0.75	-	0.00	0.00	0.23	0.00	0.00	0.01	0.02	0.00	0.00	0.06	101.43	2010	Pic-06-01A3
621	32.72	0.00	0.00	0.00	0.09	0.00	0.17	0.00	0.00	67.61	0.97	-	0.00	0.03	0.19	0.09	0.03	0.09	0.00	0.00	0.00	0.00	101.99	2010	Pic-06-01A3
622	32.26	0.04	0.01	0.00	0.07	0.00	0.22	0.00	0.00	67.81	1.32	-	0.01	0.00	0.13	0.00	0.00	0.00	0.00	0.01	0.01	0.01	101.89	2010	Pic-06-01A3
623	31.84	0.00	0.00	0.02	0.08	0.02	0.16	0.00	0.00	68.33	1.17	-	0.02	0.05	0.19	0.05	0.02	0.06	0.00	0.00	0.00	0.00	102.00	2010	Pic-06-01A3
624	32.34	0.00	0.00	0.01	0.11	0.00	0.18	0.04	0.00	68.43	0.51	-	0.00	0.00	0.27	0.12	0.00	0.06	0.00	0.00	0.00	0.00	101.96	2010	Pic-06-01A3
625	31.63	0.03	0.02	0.00	0.11	0.00	0.17	0.01	0.00	69.15	0.26	-	0.00	0.00	0.21	0.00	0.00	0.11	0.00	0.00	0.00	0.01	101.71	2010	Pic-06-01A3
626	36.84	0.00	0.00	0.00	0.04	0.02	0.18	0.01	0.00	59.23	0.50	-	0.00	0.02	0.39	0.00	0.00	0.00	0.00	0.05	0.00	0.00	97.29	2010	Pic-06-01A3
627	38.80	0.00	0.00	0.07	0.11	0.01	0.44	0.00	0.00	56.91	1.25	-	0.01	0.00	0.40	0.08	0.03	0.09	0.00	0.07	0.00	0.00	98.27	2010	Pic-06-01A4
628	36.07	0.00	0.01	0.03	0.07	0.01	0.40	0.01	0.00	57.72	2.49	-	0.00	0.00	0.40	0.02	0.02	0.30	0.00	0.01	0.00	0.00	97.57	2010	Pic-06-01A4
629	33.56	0.00	0.00	0.00	0.08	0.04	0.11	0.00	0.00	57.90	0.84	0.00	0.00	0.00	0.32	0.00	0.00	0.00	0.00	0.00	0.00	0.00	93.42	2010	Pic-06-01A4
630	37.08	0.05	0.00	0.03	0.06	0.03	0.29	0.00	0.00	58.03	0.47	-	0.00	0.04	0.50	0.04	0.00	0.04	0.00	0.01	0.00	0.00	96.65	2010	Pic-06-01A4
631	38.29	0.01	0.00	0.04	0.05	0.00	0.16	0.00	0.00	58.13	0.88	-	0.00	0.03	0.33	0.03	0.02	0.02	0.00	0.00	0.00	0.00	97.98	2010	Pic-06-01A4
632	30.89	0.00	0.00	0.03	0.04	0.03	0.12	0.00	0.00	58.25	0.59	-	0.00	0.00	0.27	0.05	0.00	0.27	0.00	0.01	0.00	0.00	90.56	2010	Pic-06-01A4
633	37.40	0.03	0.00	0.02	0.13	0.00	0.19	0.02	0.00	58.37	0.45	-	0.00	0.00	0.37	0.00	0.00	0.00	0.00	0.00	0.02	0.00	97.01	2010	Pic-06-01A4
634	38.41	0.00	0.00	0.01	0.07	0.00	0.43	0.02	0.00	58.55	0.36	0.00	0.00	0.00	0.00	0.00	0.00	0.00	0.00	0.00	0.00	0.00	98.80	2010	Pic-06-01A4
635	38.06	0.05	0.00	0.05	0.02	0.01	0.43	0.02	0.00	58.56	0.34	-	0.02	0.00	0.36	0.00	0.00	0.01	0.00	0.00	0.00	0.01	97.95	2010	Pic-06-01A4
636	33.70	0.02	0.00	0.00	0.08	0.03	0.15	0.00	0.00	58.60	0.81	-	0.00	0.01	0.31	0.06	0.00	0.18	0.00	0.02	0.00	0.00	93.97	2010	Pic-06-01A4
637	30.29	0.00	0.01	0.03	0.05	0.01	0.10	0.00	0.00	58.64	0.58	-	0.03	0.04	0.26	0.04	0.00	0.13	0.00	0.00	0.00	0.05	90.22	2010	Pic-06-01A4
638	38.56	0.00	0.00	0.04	0.06	0.00	0.40	0.04	0.04	58.69	0.60	-	0.00	0.01	0.28	0.05	0.01	0.06	0.00	0.01	0.00	0.00	98.81	2010	Pic-06-01A4
639	37.08	0.00	0.00	0.00	0.09	0.01	0.12	0.00	0.00	58.74	0.21	0.00	0.01	0.26	0.00	0.00	0.00	0.00	0.00	0.00	0.00	0.00	96.30	2010	Pic-06-01A4
640	38.30	0.01	0.00	0.00	0.08	0.01	0.35	0.04	0.00	58.77	0.81	-	0.00	0.00	0.29	0.05	0.03	0.30	0.00	0.00	0.00	0.00	99.04	2010	Pic-06-01A4
641	36.43	0.03	0.00	0.00	0.07	0.00	0.31	0.00	0.00	58.82	1.27	-	0.00	0.01	0.28	0.03	0.01	0.08	0.00	0.06	0.02	0.00	97.41	2010	Pic-06-01A4
642	34.58	0.00	0.00	0.00	0.09	0.02	0.34	0.00	0.00	59.13	1.46	-	0.00	0.00	0.36	0.00	0.00	0.10	0.00	0.02	0.00	0.00	96.10	2010	Pic-06-01A4
643	37.14	0.04	0.00	0.01	0.10	0.00	0.15	0.02	0.00	59.15	0.24	-	0.00	0.00	0.36	0.00	0.02	0.00	0.05	0.00	0.00	0.00	97.29	2010	Pic-06-01A4
644	35.25	0.01	0.01	0.02	0.01	0.05	0.20	0.00	0.00	59.30	0.92	0.00	0.00	0.29	0.11	0.00	0.15	0.00	0.00	0.00	0.00	0.00	96.61	2010	Pic-06-01A4
645	38.11	0.00	0.00	0.03	0.03	0.00	0.03	0.00	0.00	59.30	0.03	-	0.00	0.00	0.42	0.00	0.00	0.04	0.00	0.00	0.00	0.00	97.99	2010	Pic-06-01A4
646	36.57	0.00	0.02	0.03	0.09	0.02	0.03	0.00	0.00	59.35	0.00	-	0.00	0.00	0.40	0.01	0.00	0.00	0.00	0.01	0.00	0.00	96.52	2010	Pic-06-01A4
647	35.99	0.00	0.01	0.00	0.05	0.01	0.13	0.00	0.00	59.55	0.34	-	0.00	0.00	0.46	0.03	0.01	0.00	0.00	0.02	0.00	0.00	96.60	2010	Pic-06-01A4
648	34.88	0.06	0.02	0.00	0.08	0.01	0.15	0.02	0.00	59.61	0.89	-	0.00	0.01	0.32	0.07	0.00	0.12	0.00	0.10	0.03	0.00	96.36	2010	Pic-06-01A4
649	36.15	0.00	0.00	0.00	0.07	0.02	0.33	0.00	0.00	59.66	0.58	0.00	0.00	0.02	0.49	0.08	0.03	0.02	0.00	0.05	0.03	0.00	97.52	2010	Pic-06-01A4
650	36.02	0.00	0.00	0.03	0.03	0.00	0.28	0.03	0.00	59.89	0.														

INDEX	No.	O	Na	K	V	Co	Mg	P	Cr	Fe	Al	S	Ni	Mn	Si	Pb	Cu	Ti	Ca	Zn	Ba	Sr	Total	Year	Sample
750	35.34	0.01	0.03	0.02	0.03	0.08	0.28	0.03	0.29	0.04	60.36	0.61	0.00	0.04	0.40	0.00	0.03	0.05	0.00	0.00	0.00	0.00	97.31	2010	Pic-06-01A/8
751	34.17	0.00	0.02	0.01	0.08	0.03	0.29	0.04	60.40	0.70	-	0.06	0.05	0.41	0.09	0.00	0.07	0.00	0.00	0.00	0.07	96.47	2010	Pic-06-01A/8	
752	36.13	0.09	0.00	0.00	0.00	0.00	0.35	0.00	60.54	0.73	-	0.04	0.00	0.44	0.27	0.07	0.03	0.00	0.00	0.00	0.01	98.70	2010	Pic-06-01A/8	
753	35.18	0.00	0.00	0.00	0.08	0.04	0.27	0.00	60.56	0.78	-	0.03	0.00	0.43	0.00	0.03	0.00	0.00	0.03	0.01	-	97.44	2010	Pic-06-01A/8	
754	34.93	0.00	0.00	0.00	0.05	0.03	0.29	0.04	60.68	0.75	-	0.00	0.00	0.44	0.00	0.03	0.03	0.00	0.08	0.00	-	97.33	2010	Pic-06-01A/8	
755	34.15	0.00	0.00	0.00	0.06	0.05	0.37	0.00	60.73	0.75	-	0.00	0.00	0.43	0.00	0.00	0.06	0.00	0.09	0.00	-	96.68	2010	Pic-06-01A/8	
756	34.88	0.06	0.02	0.10	0.01	0.00	0.30	0.00	61.05	0.67	-	0.00	0.02	0.42	0.05	0.02	0.09	0.00	0.02	0.07	97.76	2010	Pic-06-01A/8		
757	33.24	0.04	0.01	0.04	0.02	0.01	0.12	0.00	61.88	0.21	-	0.00	0.00	0.41	0.00	0.00	0.04	0.00	0.02	0.01	96.04	2010	Pic-06-01A/8		
758	40.67	0.02	0.00	0.05	0.03	0.00	0.24	0.05	55.61	1.47	-	0.05	0.07	0.29	0.05	0.02	2.14	0.00	0.05	0.00	100.82	2010	Pic-06-01B/3		
759	39.37	0.06	0.00	0.00	0.04	0.00	0.27	0.01	56.26	2.27	-	0.01	0.01	0.24	0.09	0.00	0.40	0.00	0.03	0.01	99.08	2010	Pic-06-01B/3		
760	39.35	0.07	0.01	0.00	0.08	0.00	0.25	0.00	57.07	1.94	-	0.00	0.00	0.26	0.04	0.02	0.15	0.00	0.05	0.06	99.38	2010	Pic-06-01B/3		
761	39.36	0.00	0.01	0.06	0.06	0.00	0.21	0.00	57.16	1.61	-	0.00	0.01	0.29	0.00	0.01	1.06	0.00	0.01	0.00	99.85	2010	Pic-06-01B/3		
762	38.16	0.00	0.00	0.00	0.08	0.00	0.23	0.02	57.47	1.77	-	0.00	0.02	0.23	0.00	0.00	0.30	0.00	0.00	0.00	98.29	2010	Pic-06-01B/3		
763	39.11	0.03	0.00	0.05	0.09	0.01	0.25	0.04	57.57	1.74	-	0.01	0.02	0.28	0.09	0.00	0.18	0.00	0.00	0.01	99.47	2010	Pic-06-01B/3		
764	39.73	0.01	0.00	0.03	0.00	0.02	0.14	0.03	57.85	1.15	-	0.00	0.00	0.25	0.00	0.04	0.14	0.00	0.01	0.00	99.50	2010	Pic-06-01B/3		
765	39.69	0.03	0.00	0.04	0.04	0.00	0.23	0.00	57.95	1.46	-	0.00	0.00	0.26	0.05	0.00	0.19	0.00	0.00	0.07	100.01	2010	Pic-06-01B/3		
766	36.04	0.05	0.00	0.00	0.03	0.03	0.27	0.01	58.00	1.47	-	0.00	0.00	0.34	0.00	0.00	1.08	0.00	0.07	0.00	97.39	2010	Pic-06-01B/3		
767	37.75	0.06	0.00	0.02	0.04	0.00	0.20	0.01	58.12	1.22	-	0.02	0.03	0.35	0.00	0.00	0.21	0.00	0.03	0.03	98.09	2010	Pic-06-01B/3		
768	38.00	0.00	0.01	0.02	0.06	0.02	0.29	0.01	58.16	1.62	-	0.00	0.01	0.36	0.00	0.00	0.17	0.00	0.00	0.00	98.73	2010	Pic-06-01B/3		
769	39.57	0.01	0.00	0.00	0.04	0.00	0.14	0.02	58.18	1.33	-	0.00	0.00	0.25	0.07	0.03	0.23	0.00	0.00	0.00	99.21	2010	Pic-06-01B/3		
770	39.71	0.04	0.00	0.02	0.06	0.00	0.22	0.02	58.28	1.33	-	0.00	0.02	0.26	0.00	0.00	0.18	0.00	0.00	0.00	100.13	2010	Pic-06-01B/3		
771	38.10	0.03	0.00	0.06	0.05	0.03	0.29	0.04	58.32	0.96	-	0.00	0.01	0.36	0.00	0.02	0.89	0.00	0.03	0.01	99.19	2010	Pic-06-01B/3		
772	33.99	0.00	0.01	0.00	0.11	0.02	0.11	0.00	58.50	1.18	-	0.00	0.00	0.50	0.00	0.00	0.00	0.00	0.02	0.00	93.43	2010	Pic-06-01B/3		
773	36.55	0.00	0.01	0.00	0.06	0.00	0.20	0.00	58.53	0.44	-	0.00	0.00	0.33	0.13	0.00	0.10	0.00	0.00	0.00	97.36	2010	Pic-06-01B/3		
774	38.42	0.00	0.01	0.00	0.00	0.00	0.22	0.04	58.62	1.31	-	0.00	0.00	0.43	0.12	0.00	0.13	0.00	0.02	0.05	99.48	2010	Pic-06-01B/3		
775	38.29	0.01	0.02	0.00	0.04	0.00	0.26	0.04	58.62	1.47	-	0.00	0.00	0.39	0.00	0.00	0.44	0.00	0.06	0.01	99.65	2010	Pic-06-01B/3		
776	39.42	0.00	0.01	0.00	0.09	0.00	0.06	0.00	58.73	0.02	-	0.00	0.00	0.54	0.00	0.00	0.00	0.00	0.05	0.00	98.93	2010	Pic-06-01B/3		
777	37.41	0.02	0.00	0.00	0.04	0.03	0.27	0.01	58.80	0.99	-	0.00	0.05	0.35	0.00	0.05	0.58	0.00	0.09	0.01	98.70	2010	Pic-06-01B/3		
778	38.90	0.00	0.00	0.01	0.09	0.00	0.16	0.00	58.80	0.81	-	0.02	0.01	0.17	0.05	0.00	0.14	0.00	0.00	0.00	99.14	2010	Pic-06-01B/3		
779	35.42	0.00	0.01	0.00	0.00	0.00	0.02	0.03	58.85	1.17	-	0.00	0.00	0.67	0.00	0.00	0.00	0.00	0.00	0.00	98.41	2010	Pic-06-01B/3		
780	34.99	0.00	0.01	0.00	0.10	0.03	0.17	0.01	58.89	1.16	-	0.00	0.00	0.40	0.00	0.04	0.07	0.00	0.04	0.01	95.91	2010	Pic-06-01B/3		
781	37.61	0.04	0.01	0.04	0.03	0.03	0.26	0.03	58.93	0.65	-	0.00	0.00	0.40	0.07	0.06	0.23	0.00	0.00	0.00	98.40	2010	Pic-06-01B/3		
782	33.87	0.00	0.00	0.00	0.08	0.02	0.17	0.00	58.95	0.33	-	0.00	0.00	0.29	0.05	0.00	0.02	0.00	0.00	0.08	0.02	93.87	2010	Pic-06-01B/3	
783	39.40	0.00	0.00	0.01	0.03	0.00	0.04	0.00	58.96	0.05	-	0.00	0.00	0.35	0.04	0.00	0.05	0.00	0.00	0.01	98.94	2010	Pic-06-01B/3		
784	39.54	0.00	0.07	0.00	0.04	0.00	0.09	0.02	59.07	0.40	-	0.00	0.00	0.48	0.01	0.00	0.02	0.00	0.00	0.00	99.76	2010	Pic-06-01B/3		
785	36.81	0.02	0.00	0.00	0.07	0.00	0.12	0.00	59.13	0.25	-	0.00	0.00	0.45	0.03	0.00	0.00	0.00	0.07	0.07	97.00	2010	Pic-06-01B/3		
786	40.24	0.00	0.01	0.04	0.10	0.01	0.05	0.00	59.28	0.05	-	0.01	0.00	0.29	0.15	0.00	0.04	0.00	0.00	0.00	100.28	2010	Pic-06-01B/3		
787	37.69	0.00	0.00	0.00	0.09	0.09	0.22	0.38	0.01	59.31	0.34	-	0.00	0.01	0.47	0.00	0.00	0.06	0.00	0.00	0.02	98.41	2010	Pic-06-01B/3	
788	37.08	0.00	0.00	0.00	0.06	0.04	0.24	0.02	59.37	0.08	-	0.00	0.00	0.54	0.10	0.00	0.07	0.07	0.00	0.00	0.01	97.61	2010	Pic-06-01B/3	
789	37.59	0.01	0.01	0.11	0.02	0.01	0.15	0.01	59.40	0.49	-	0.00	0.00	0.41	0.02	0.03	0.10	0.00	0.00	0.00	98.39	2010	Pic-06-01B/3		
790	39.83	0.00	0.01	0.04	0.05	0.00	0.03	0.03	59.50	0.02	-	0.00	0.00	0.25	0.06	0.00	0.04	0.00	0.00	0.00	99.87	2010	Pic-06-01B/3		
791	37.56	0.00	0.01	0.01	0.00	0.02	0.20	0.00	59.55	0.10	-	0.03	0.00	0.46	0.00	0.07	0.00	0.00	0.00	0.00	98.00	2010	Pic-06-01B/3		
792	33.95	0.01	0.00	0.00	0.08	0.01	0.11	0.00	59.57	0.11	-	0.02	0.00	0.45	0.00	0.00	0.04	0.00	0.00	0.00	94.35	2010	Pic-06-01B/3		
793	36.57	0.02	0.00	0.02	0.02	0.04	0.26	0.00	59.59	0.73	-	0.01	0.00	0.43	0.06	0.03	0.03	0.00	0.04	0.02	97.86	2010	Pic-06-01B/3		
794	37.89	0.00	0.00	0.00	0.07	0.00	0.11	0.03	59.61	0.04	-	0.00	0.00	0.40	0.00	0.00	0.00	0.00	0.00	0.00	98.41	2010	Pic-06-01B/3		
795	36.72	0.04	0.00	0.00	0.02	0.01	0.14	0.00	59.68	0.49	-	0.05	0.00	0.37	0.00	0.01	0.11	0.00	0.00	0.00	97.63	2010	Pic-06-01B/3		
796	38.08	0.06	0.00	0.00	0.04	0.00	0.18	0.00	59.79	0.02	-	0.02	0.00	0.49	0.12	0.00	0.00	0.00	0.00	0.00	98.80	2010	Pic-06-01B/3		
797	36.00	0.03	0.00	0.00	0.06	0.02	0.14	0.05	59.79	0.40	-	0.00	0.04	0.43	0.00	0.00	0.18	0.00	0.00	0.00	97.15	2010	Pic-06-01B/3		
798	36.27	0.01	0.00	0.04	0.03	0.02	0.23	0.00	59.92	0.65	-	0.00	0.00	0.51	0.02	0.00	0.04	0.00	0.00	0.01	97.77	2010	Pic-06-01B/3		
799	37.00	0.00	0.00	0.00	0.05	0.00	0.16	0.00	60.00	0.58	-	0.00	0.00	0.40	0.00	0.00	0.01	0.00	0.00	0.00	98.30	2010	Pic-06-01B/3		
800	35.33	0.00	0.00	0.00	0.01	0.02	0.14	0.00	60.03	0.54	-	0.04	0.00	0.40	0.05	0.00	0.05	0.00	0.06	0.00	96.69	2010	Pic-06-01B/3		
801	34.04	0.00	0.01	0.00	0.05	0.05	0.25	0.01	60.06	0.71	-	0.00	0.00	0.52	0.00	0.00	0.05	0.00	0.06	0.00	95.80	2010	Pic-06-01B/3		
802	37.00	0.00	0.00	0.00	0.09	0.03	0.21	0.00	60.08	0.18	-	0.00	0.01	0.49	0.04	0.00	0.07	0.00	0.06	0.03	98.28	2010	Pic-06-01B/3		
803	36.33	0.05	0.01	0.08	0.03	0.04	0.14	0.00	60.11	0.80	-	0.05	0.02	0.38	0.00	0.00	0.00	0.00	0.02	0.00	98.06	2010	Pic-06-01B/3		
804	34.99																								

INDEX	No.	O	Na	K	V	Co	Mg	P	Cr	Fe	Al	S	Ni	Mn	Si	Pb	Cu	Ti	Ca	Zn	Ba	Sr	Total	Year	Sample
900	32.78	0.00	0.00	0.00	0.02	0.20	0.02	0.20	0.01	62.34	2.42	0.00	0.04	0.04	0.12	0.12	0.00	0.89	0.01	0.00	0.00	0.01	98.94	2010	Pic-06-01C/6
901	33.52	0.03	0.00	0.00	0.04	0.07	0.05	0.25	0.01	62.43	2.54	-	0.01	0.00	0.10	0.00	0.00	0.82	0.00	0.00	0.00	0.01	99.87	2010	Pic-06-01C/6
902	33.45	0.00	0.00	0.00	0.00	0.01	0.00	0.19	0.00	62.91	0.68	-	0.00	0.00	0.22	0.00	0.00	0.15	0.00	0.00	0.00	0.00	97.61	2010	Pic-06-01C/6
903	30.54	0.04	0.00	0.00	0.00	0.09	0.18	0.07	0.00	68.18	0.04	-	0.03	0.00	0.81	0.00	0.00	0.10	0.00	0.05	0.07	0.00	100.21	2010	Pic-06-01C/6
904	31.76	0.00	0.00	0.00	0.08	0.03	0.21	0.02	0.03	63.03	1.06	-	0.01	0.00	0.33	0.00	0.00	0.04	0.00	0.00	0.01	0.00	96.56	2010	Pic-06-03/6
905	36.16	0.00	0.01	0.00	0.07	0.00	0.29	0.00	0.00	56.59	1.38	0.07	0.00	0.02	0.31	0.00	0.00	0.00	0.00	0.05	0.05	0.00	94.97	2010	Pic-06-03/6
906	35.70	0.00	0.00	0.00	0.00	0.01	0.02	0.27	0.01	57.06	1.14	-	0.00	0.03	0.31	0.00	0.08	0.00	0.00	0.00	0.00	0.00	94.64	2010	Pic-06-03/6
907	36.30	0.00	0.00	0.00	0.04	0.06	0.01	0.26	0.00	57.30	1.08	-	0.00	0.00	0.27	0.01	0.00	0.00	0.00	0.00	0.00	0.00	95.34	2010	Pic-06-03/6
908	36.03	0.00	0.01	0.01	0.08	0.02	0.33	0.00	0.00	57.41	1.20	-	0.02	0.01	0.32	0.04	0.00	0.00	0.00	0.07	0.05	0.00	95.58	2010	Pic-06-03/6
909	35.84	0.00	0.03	0.00	0.07	0.04	0.26	0.00	0.00	57.43	1.43	-	0.01	0.00	0.30	0.05	0.09	0.00	0.00	0.00	0.00	0.00	95.53	2010	Pic-06-03/6
910	35.65	0.01	0.00	0.03	0.01	0.02	0.27	0.01	0.00	57.47	1.55	0.00	0.00	0.02	0.25	0.00	0.00	0.01	0.00	0.13	0.04	0.00	95.42	2010	Pic-06-03/6
911	36.15	0.02	0.02	0.06	0.05	0.00	0.26	0.00	0.00	57.63	1.39	-	0.03	0.05	0.33	0.00	0.00	0.00	0.00	0.01	0.00	0.00	95.98	2010	Pic-06-03/6
912	33.51	0.00	0.02	0.03	0.04	0.01	0.29	0.05	0.00	57.86	1.92	-	0.00	0.00	0.22	0.01	0.00	0.00	0.00	0.01	0.05	0.00	94.01	2010	Pic-06-03/6
913	35.80	0.00	0.00	0.00	0.00	0.00	0.27	0.00	0.00	57.93	1.28	-	0.02	0.00	0.27	0.00	0.00	0.03	0.00	0.07	0.00	0.00	95.68	2010	Pic-06-03/6
914	35.88	0.00	0.00	0.07	0.01	0.00	0.24	0.00	0.00	57.97	1.13	-	0.00	0.05	0.28	0.10	0.07	0.00	0.00	0.01	0.04	0.00	95.89	2010	Pic-06-03/6
915	33.42	0.00	0.00	0.00	0.00	0.06	0.27	0.00	0.00	58.02	2.14	-	0.02	0.00	0.25	0.02	0.03	0.02	0.00	0.00	0.00	0.00	94.34	2010	Pic-06-03/6
916	35.91	0.00	0.01	0.00	0.08	0.00	0.26	0.05	0.00	58.14	1.08	-	0.03	0.05	0.30	0.22	0.00	0.00	0.00	0.05	0.04	0.00	96.21	2010	Pic-06-03/6
917	34.29	0.00	0.00	0.00	0.06	0.03	0.28	0.04	0.00	58.16	2.14	-	0.00	0.01	0.24	0.09	0.01	0.01	0.00	0.05	0.05	0.00	95.46	2010	Pic-06-03/6
918	33.95	0.02	0.00	0.08	0.03	0.03	0.29	0.00	0.00	58.21	2.25	-	0.00	0.04	0.25	0.00	0.00	0.00	0.00	0.00	0.01	0.00	95.15	2010	Pic-06-03/6
919	33.58	0.00	0.01	0.00	0.06	0.02	0.25	0.00	0.00	58.40	2.08	-	0.00	0.04	0.27	0.00	0.05	0.00	0.00	0.05	0.01	0.00	94.79	2010	Pic-06-03/6
920	36.24	0.00	0.00	0.07	0.10	0.01	0.28	0.00	0.00	58.48	1.31	-	0.03	0.00	0.28	0.00	0.00	0.00	0.00	0.00	0.00	0.00	95.89	2010	Pic-06-03/6
921	35.54	0.00	0.01	0.00	0.05	0.02	0.29	0.00	0.00	58.52	1.02	-	0.03	0.00	0.26	0.10	0.05	0.03	0.00	0.00	0.00	0.00	95.89	2010	Pic-06-03/6
922	33.33	0.00	0.00	0.00	0.05	0.05	0.30	0.03	0.03	58.52	2.42	-	0.00	0.00	0.22	0.09	0.00	0.00	0.00	0.17	0.00	0.00	95.18	2010	Pic-06-03/6
923	35.50	0.05	0.01	0.00	0.08	0.00	0.27	0.00	0.00	58.66	0.99	-	0.00	0.00	0.25	0.00	0.00	0.01	0.00	0.00	0.00	0.00	95.80	2010	Pic-06-03/6
924	33.34	0.00	0.00	0.00	0.00	0.01	0.30	0.02	0.00	58.79	1.83	-	0.00	0.00	0.37	0.00	0.00	0.00	0.00	0.00	0.00	0.00	94.67	2010	Pic-06-03/6
925	33.19	0.00	0.02	0.04	0.08	0.00	0.28	0.05	0.00	58.81	2.10	-	0.00	0.00	0.27	0.07	0.03	0.00	0.00	0.00	0.02	0.00	94.95	2010	Pic-06-03/6
926	33.84	0.04	0.00	0.04	0.07	0.00	0.26	0.03	0.00	59.20	1.70	-	0.00	0.00	0.25	0.06	0.00	0.01	0.00	0.00	0.01	0.00	95.51	2010	Pic-06-03/6
927	33.71	0.00	0.03	0.05	0.06	0.05	0.25	0.00	0.00	59.31	2.00	-	0.00	0.00	0.24	0.06	0.00	0.02	0.00	0.01	0.00	0.00	95.79	2010	Pic-06-03/6
928	33.64	0.00	0.00	0.05	0.09	0.02	0.23	0.00	0.00	59.99	1.89	-	0.00	0.04	0.25	0.06	0.05	0.00	0.00	0.00	0.03	0.00	96.34	2010	Pic-06-03/6
929	32.83	0.00	0.00	0.00	0.00	0.04	0.25	0.02	0.00	60.26	1.83	0.04	0.00	0.00	0.13	0.00	0.00	0.00	0.00	0.00	0.00	0.00	95.89	2010	Pic-06-03/6
930	33.05	0.00	0.01	0.00	0.05	0.04	0.18	0.01	0.00	61.09	1.73	-	0.00	0.00	0.35	0.16	0.01	0.03	0.00	0.00	0.00	0.03	96.71	2010	Pic-06-03/6
931	32.27	0.00	0.01	0.02	0.04	0.02	0.31	0.05	0.00	61.61	1.55	-	0.04	0.03	0.31	0.16	0.00	0.00	0.00	0.03	0.00	0.00	96.43	2010	Pic-06-03/6
932	32.13	0.00	0.01	0.00	0.06	0.04	0.23	0.05	0.00	62.50	1.22	-	0.00	0.00	0.36	0.10	0.01	0.00	0.00	0.00	0.00	0.00	96.71	2010	Pic-06-03/6
933	31.82	0.02	0.00	0.00	0.00	0.00	0.22	0.00	0.00	62.79	0.98	-	0.00	0.00	0.35	0.09	0.08	0.00	0.00	0.00	0.00	0.00	96.36	2010	Pic-06-03/6
934	32.91	0.02	0.00	0.03	0.01	0.00	0.21	0.03	0.00	62.97	0.16	-	0.00	0.00	0.37	0.00	0.00	0.00	0.00	0.00	0.00	0.00	97.77	2010	Pic-06-03/6
935	31.62	0.01	0.00	0.07	0.08	0.01	0.25	0.00	0.00	63.38	0.95	-	0.00	0.00	0.36	0.12	0.02	0.00	0.00	0.00	0.00	0.00	96.86	2010	Pic-06-03/6
936	32.19	0.00	0.00	0.00	0.03	0.03	0.23	0.00	0.00	63.46	0.80	-	0.00	0.06	0.34	0.15	0.00	0.05	0.00	0.00	0.09	0.00	97.44	2010	Pic-06-03/6
937	32.18	0.00	0.00	0.00	0.00	0.00	0.21	0.00	0.00	63.49	0.97	-	0.00	0.00	0.33	0.00	0.12	0.00	0.00	0.00	0.00	0.00	97.31	2010	Pic-06-03/6
938	31.84	0.00	0.00	0.02	0.07	0.00	0.18	0.00	0.00	63.50	0.79	-	0.00	0.01	0.35	0.11	0.07	0.00	0.00	0.08	0.00	0.00	97.02	2010	Pic-06-03/6
939	32.60	0.00	0.04	0.02	0.05	0.02	0.26	0.05	0.00	63.51	0.79	0.00	0.00	0.00	0.37	0.00	0.00	0.00	0.00	0.00	0.00	0.00	96.79	2010	Pic-06-03/6
940	32.26	0.03	0.01	0.00	0.05	0.02	0.20	0.00	0.00	63.65	0.92	-	0.04	0.00	0.37	0.03	0.00	0.03	0.00	0.00	0.02	0.00	97.62	2010	Pic-06-03/6
941	31.15	0.00	0.00	0.02	0.11	0.00	0.19	0.00	0.00	63.68	0.92	-	0.04	0.00	0.38	0.04	0.10	0.00	0.00	0.00	0.00	0.00	96.64	2010	Pic-06-03/6
942	31.34	0.00	0.02	0.00	0.09	0.00	0.20	0.00	0.00	63.86	0.95	-	0.00	0.01	0.33	0.00	0.00	0.02	0.00	0.00	0.02	0.00	96.82	2010	Pic-06-03/6
943	31.27	0.00	0.00	0.00	0.11	0.02	0.25	0.00	0.00	64.44	0.98	-	0.00	0.00	0.36	0.08	0.04	0.00	0.00	0.00	0.00	0.00	97.56	2010	Pic-06-03/6
944	33.98	0.00	0.00	0.05	0.08	0.00	0.09	0.01	0.00	65.78	0.42	-	0.00	0.00	0.34	0.00	0.00	0.06	0.00	0.04	0.00	0.00	96.70	2010	Pic-06-08/8
945	33.46	0.04	0.01	0.00	0.08	0.02	0.05	0.02	0.00	58.09	0.81	-	0.00	0.00	0.36	0.01	0.03	0.07	0.00	0.12	0.02	0.00	93.19	2010	Pic-06-08/8
946	34.41	0.00	0.00	0.05	0.04	0.05	0.08	0.00	0.00	58.10	0.81	-	0.05	0.02	0.34	0.00	0.05	0.04	0.00	0.09	0.10	0.00	94.22	2010	Pic-06-08/8
947	33.67	0.00	0.00	0.01	0.05	0.02	0.07	0.00	0.00	58.12	0.63	-	0.00	0.06	0.32	0.00	0.00	0.14	0.00	0.11	0.00	0.00	93.20	2010	Pic-06-08/8
948	34.48	0.04	0.00	0.04	0.05	0.01	0.05	0.01	0.00	58.45	0.59	-	0.00	0.04	0.35	0.00	0.00	0.01	0.00	0.09	0.00	0.00	94.20	2010	Pic-06-08/8
949	33.74	0.00	0.00	0.00	0.10	0.00	0.06	0.00	0.00	58.48	0.34	-	0.00	0.01	0.34	0.00	0.00	0.00	0.00	0.04	0.00	0.00	93.25	2010	Pic-06-08/8
950	34.97	0.00	0.00	0.05	0.04	0.06	0.05	0.02	0.00	58.59	0.70	-	0.01	0.											

INDEX	No.	O	Na	K	V	Co	Mg	P	Cr	Fe	Al	S	Ni	Mn	Si	Pb	Cu	Ti	Ca	Zn	Ba	Sr	Total	Year	Sample
1050	34.28	0.00	0.00	0.00	0.00	0.00	0.76	0.00	0.00	57.85	3.25	0.00	0.02	0.06	0.00	0.00	0.13	0.00	0.00	0.00	0.00	0.00	96.47	2010	Pic-06-25C/1
1051	34.31	0.00	0.00	0.03	0.05	0.03	0.50	0.01	0.01	57.90	1.93	-	0.01	0.00	0.16	0.03	0.00	0.09	0.00	0.00	0.00	0.00	95.04	2010	Pic-06-25C/1
1052	34.09	0.00	0.00	0.00	0.07	0.03	0.45	0.00	0.00	58.01	2.35	-	0.00	0.00	0.16	0.07	0.01	0.08	0.00	0.00	0.00	0.00	95.33	2010	Pic-06-25C/1
1053	32.37	0.08	0.00	0.01	0.06	0.01	0.43	0.03	0.03	58.01	1.80	-	0.00	0.00	0.15	0.07	0.01	0.08	0.00	0.00	0.00	0.03	93.14	2010	Pic-06-25C/1
1054	33.06	0.04	0.00	0.00	0.04	0.03	0.57	0.00	0.00	58.01	2.82	-	0.00	0.00	0.11	0.08	0.00	0.03	0.00	0.00	0.00	0.00	94.79	2010	Pic-06-25C/1
1055	33.08	0.00	0.00	0.00	0.10	0.04	0.47	0.00	0.00	58.13	2.05	-	0.00	0.00	0.15	0.00	0.05	0.11	0.00	0.00	0.00	0.07	94.21	2010	Pic-06-25C/1
1056	33.57	0.01	0.00	0.00	0.05	0.00	0.46	0.00	0.00	58.13	1.84	-	0.00	0.00	0.15	0.00	0.02	0.07	0.00	0.00	0.00	0.06	94.36	2010	Pic-06-25C/1
1057	33.73	0.00	0.00	0.05	0.08	0.03	0.48	0.00	0.00	58.22	2.19	-	0.00	0.00	0.12	0.02	0.00	0.07	0.00	0.00	0.00	0.01	94.99	2010	Pic-06-25C/1
1058	33.55	0.02	0.00	0.04	0.05	0.07	0.21	0.01	0.01	58.28	0.67	-	0.00	0.02	0.27	0.00	0.00	0.00	0.00	0.00	0.01	0.01	93.19	2010	Pic-06-25C/1
1059	33.34	0.00	0.00	0.08	0.04	0.02	0.43	0.00	0.00	58.34	2.03	-	0.02	0.03	0.17	0.01	0.00	0.10	0.00	0.03	0.00	0.00	94.64	2010	Pic-06-25C/1
1060	32.69	0.06	0.01	0.02	0.02	0.02	0.47	0.00	0.00	58.39	2.42	-	0.00	0.00	0.14	0.04	0.00	0.03	0.00	0.00	0.00	0.00	94.36	2010	Pic-06-25C/1
1061	35.13	0.00	0.01	0.00	0.05	0.00	0.08	0.00	0.00	58.57	0.30	-	0.00	0.03	0.21	0.08	0.00	0.00	0.00	0.00	0.00	0.00	94.45	2010	Pic-06-25C/1
1062	34.46	0.00	0.00	0.02	0.04	0.02	0.34	0.00	0.00	58.63	1.17	-	0.00	0.01	0.21	0.00	0.01	0.05	0.00	0.00	0.00	0.00	94.96	2010	Pic-06-25C/1
1063	32.87	0.04	0.00	0.00	0.04	0.01	0.07	0.00	0.00	58.71	0.25	-	0.00	0.02	0.22	0.00	0.02	0.00	0.00	0.00	0.00	0.00	92.25	2010	Pic-06-25C/1
1064	34.46	0.07	0.01	0.00	0.06	0.00	0.50	0.00	0.00	58.75	0.05	-	0.04	0.03	0.17	0.03	0.03	0.07	0.00	0.00	0.00	0.00	95.82	2010	Pic-06-25C/1
1065	35.03	0.09	0.00	0.00	0.03	0.00	0.24	0.01	0.01	58.89	0.95	-	0.00	0.00	0.06	0.05	0.02	0.00	0.00	0.00	0.00	0.00	95.59	2010	Pic-06-25C/1
1066	35.39	0.02	0.00	0.00	0.04	0.00	0.09	0.00	0.00	58.94	0.22	-	0.00	0.00	0.20	0.05	0.01	0.03	0.00	0.00	0.00	0.00	94.99	2010	Pic-06-25C/1
1067	33.63	0.00	0.01	0.00	0.03	0.05	0.42	0.00	0.00	59.01	1.47	-	0.01	0.03	0.16	0.00	0.00	0.09	0.00	0.00	0.00	0.00	94.91	2010	Pic-06-25C/1
1068	36.97	0.00	0.00	0.01	0.09	0.01	0.14	0.00	0.00	59.06	0.24	-	0.00	0.00	0.22	0.00	0.00	0.00	0.00	0.00	0.02	0.00	96.75	2010	Pic-06-25C/1
1069	34.90	0.00	0.02	0.00	0.00	0.00	0.10	0.00	0.00	59.20	0.24	-	0.00	0.06	0.21	0.00	0.00	0.00	0.00	0.00	0.00	0.03	94.80	2010	Pic-06-25C/1
1070	35.62	0.00	0.00	0.00	0.05	0.00	0.46	0.00	0.00	59.42	1.61	-	0.00	0.03	0.18	0.12	0.02	0.03	0.00	0.00	0.00	0.05	95.79	2010	Pic-06-25C/1
1071	34.72	0.02	0.00	0.00	0.08	0.00	0.14	0.00	0.00	60.02	0.45	-	0.00	0.00	0.23	0.00	0.00	0.00	0.00	0.04	0.00	0.00	95.70	2010	Pic-06-25C/1
1072	36.87	0.00	0.03	0.00	0.00	0.01	0.22	0.34	0.01	56.62	1.57	-	0.00	0.02	0.04	0.16	0.00	0.66	0.00	0.05	0.00	0.00	96.45	2010	Pic-06-27/2
1073	36.48	0.00	0.00	0.05	0.06	0.01	0.44	0.00	0.00	56.85	1.08	-	0.00	0.01	0.05	0.04	0.00	0.20	0.00	0.00	0.00	0.00	95.25	2010	Pic-06-27/2
1074	35.66	0.06	0.00	0.00	0.00	0.00	0.35	0.00	0.00	56.86	1.04	-	0.03	0.03	0.06	0.00	0.00	0.00	0.00	0.00	0.00	0.00	94.73	2010	Pic-06-27/2
1075	35.89	0.02	0.01	0.03	0.10	0.00	0.19	0.01	0.01	56.97	1.12	-	0.07	0.02	0.07	0.06	0.00	0.13	0.00	0.02	0.04	0.00	94.76	2010	Pic-06-27/2
1076	33.32	0.05	0.00	0.00	0.05	0.00	0.44	0.00	0.00	57.09	0.87	-	0.00	0.00	0.09	0.05	0.00	0.01	0.00	0.03	0.00	0.00	92.01	2010	Pic-06-27/2
1077	35.58	0.01	0.00	0.01	0.03	0.03	0.37	0.02	0.02	57.15	0.97	-	0.00	0.00	0.06	0.05	0.00	0.07	0.00	0.02	0.01	0.00	94.37	2010	Pic-06-27/2
1078	35.14	0.00	0.02	0.04	0.09	0.02	0.42	0.00	0.00	57.17	0.93	-	0.00	0.06	0.08	0.00	0.00	0.00	0.05	0.00	0.00	0.00	94.03	2010	Pic-06-27/2
1079	35.53	0.01	0.00	0.00	0.06	0.01	0.47	0.00	0.00	57.17	1.03	-	0.00	0.00	0.02	0.00	0.00	0.00	0.00	0.00	0.00	0.00	94.54	2010	Pic-06-27/2
1080	35.47	0.11	0.00	0.01	0.04	0.01	0.46	0.00	0.00	57.17	1.05	-	0.00	0.03	0.08	0.09	0.04	0.08	0.00	0.01	0.05	0.00	94.68	2010	Pic-06-27/2
1081	36.03	0.02	0.00	0.00	0.04	0.00	0.27	0.00	0.00	57.19	0.75	-	0.00	0.02	0.06	0.00	0.06	0.10	0.00	0.00	0.07	0.00	94.59	2010	Pic-06-27/2
1082	36.19	0.00	0.00	0.01	0.13	0.01	0.32	0.01	0.01	57.19	1.33	-	0.01	0.00	0.03	0.00	0.00	0.47	0.00	0.00	0.00	0.04	95.75	2010	Pic-06-27/2
1083	35.28	0.07	0.00	0.00	0.04	0.04	0.45	0.05	0.05	57.35	0.92	-	0.00	0.00	0.06	0.11	0.00	0.00	0.00	0.02	0.04	0.00	94.42	2010	Pic-06-27/2
1084	35.45	0.07	0.00	0.00	0.06	0.00	0.37	0.00	0.00	57.37	1.07	-	0.00	0.00	0.05	0.09	0.05	0.04	0.00	0.15	0.00	0.00	94.65	2010	Pic-06-27/2
1085	35.07	0.00	0.02	0.00	0.03	0.04	0.41	0.04	0.00	57.38	0.92	-	0.05	0.00	0.09	0.02	0.00	0.00	0.00	0.00	0.00	0.00	94.07	2010	Pic-06-27/2
1086	35.79	0.00	0.00	0.00	0.05	0.00	0.28	0.00	0.00	57.46	0.53	-	0.00	0.00	0.10	0.08	0.05	0.00	0.00	0.10	0.00	0.00	94.44	2010	Pic-06-27/2
1087	35.62	0.00	0.00	0.07	0.09	0.00	0.49	0.00	0.00	57.53	0.78	-	0.00	0.04	0.08	0.02	0.06	0.00	0.00	0.02	0.11	0.00	94.90	2010	Pic-06-27/2
1088	35.53	0.00	0.02	0.02	0.14	0.02	0.44	0.00	0.00	57.53	0.78	-	0.00	0.00	0.09	0.17	0.00	0.07	0.00	0.00	0.00	0.01	94.81	2010	Pic-06-27/2
1089	34.94	0.07	0.00	0.00	0.00	0.00	0.48	0.02	0.00	57.54	0.96	-	0.03	0.01	0.08	0.06	0.00	0.00	0.00	0.00	0.00	0.00	94.29	2010	Pic-06-27/2
1090	35.37	0.08	0.02	0.01	0.01	0.01	0.31	0.02	0.02	57.56	0.40	-	0.00	0.00	0.10	0.07	0.00	0.06	0.00	0.03	0.00	0.00	94.03	2010	Pic-06-27/2
1091	35.99	0.00	0.00	0.00	0.07	0.03	0.62	0.02	0.02	57.58	0.64	-	0.03	0.05	0.07	0.00	0.00	0.00	0.00	0.04	0.01	0.00	95.13	2010	Pic-06-27/2
1092	35.80	0.00	0.01	0.00	0.02	0.03	0.16	0.00	0.00	57.58	0.71	-	0.01	0.00	0.07	0.11	0.01	0.05	0.00	0.05	0.01	0.00	94.63	2010	Pic-06-27/2
1093	35.12	0.00	0.00	0.00	0.07	0.00	0.45	0.00	0.00	57.58	0.89	-	0.04	0.00	0.08	0.01	0.11	0.00	0.00	0.00	0.00	0.00	94.36	2010	Pic-06-27/2
1094	36.13	0.02	0.01	0.00	0.06	0.00	0.60	0.00	0.00	57.63	0.61	-	0.00	0.00	0.05	0.09	0.00	0.04	0.00	0.15	0.00	0.00	95.72	2010	Pic-06-27/2
1095	35.52	0.02	0.00	0.00	0.08	0.02	0.43	0.00	0.00	57.67	0.32	-	0.01	0.06	0.11	0.05	0.00	0.02	0.00	0.06	0.03	0.00	94.39	2010	Pic-06-27/2
1096	35.50	0.00	0.00	0.00	0.11	0.00	0.63	0.00	0.00	57.67	0.62	-	0.00	0.02	0.07	0.00	0.00	0.00	0.00	0.02	0.02	0.00	94.66	2010	Pic-06-27/2
1097	35.13	0.00	0.00	0.04	0.06	0.05	0.36	0.01	0.01	57.71	0.69	-	0.00	0.02	0.11	0.03	0.03	0.00	0.00	0.03	0.03	0.00	94.27	2010	Pic-06-27/2
1098	35.74	0.00	0.00	0.05	0.03	0.03	0.67	0.00	0.00	57.75	0.57	-	0.00	0.00	0.08	0.11	0.04	0.08	0.00	0.02	0.00	0.00	95.16	2010	Pic-06-27/2
1099	36.41	0.01	0.00	0.00	0.04	0.00	0.71	0.00	0.00	57.79	0.50	-	0.00	0.02	0.05	0.09	0.02	0.00	0.00	0.00	0.00	0.00	95.72	2010	Pic-06-27/2
1100	36.05	0																							

INDEX	No.	O	Na	K	V	Co	Mg	P	Cr	Fe	Al	S	Ni	Mn	Si	Pb	Cu	Ti	Ca	Zn	Ba	Sr	Total	Year	Sample
1200	28.77	0.01	0.01	0.06	0.01	0.00	0.00	0.00	0.00	0.00	69.20	0.00	0.00	0.00	0.22	0.00	0.02	0.07	0.01	0.00	0.00	0.00	98.48	2010	Pic-06-27/5
1201	28.82	0.05	0.01	0.03	0.10	0.00	0.04	0.08	69.24	0.00	-	0.00	0.00	0.19	0.01	0.07	0.00	0.00	0.00	0.00	0.00	0.00	98.64	2010	Pic-06-27/5
1202	28.31	0.02	0.00	0.00	0.02	0.02	0.00	0.00	69.34	0.01	-	0.00	0.00	0.13	0.05	0.04	0.06	0.00	0.03	0.00	0.00	0.00	98.03	2010	Pic-06-27/5
1203	29.01	0.02	0.00	0.01	0.03	0.00	0.00	0.00	69.36	0.04	-	0.00	0.00	0.06	0.08	0.01	0.07	0.00	0.03	0.00	0.00	0.00	98.72	2010	Pic-06-27/5
1204	28.66	0.00	0.01	0.00	0.10	0.03	0.00	0.00	69.47	0.04	-	0.01	0.03	0.30	0.04	0.00	0.00	0.00	0.00	0.00	0.00	0.00	98.68	2010	Pic-06-27/5
1205	28.42	0.08	0.01	0.01	0.06	0.00	0.00	0.00	69.47	0.02	-	0.00	0.00	0.15	0.00	0.07	0.00	0.05	0.00	0.00	0.00	0.00	98.37	2010	Pic-06-27/5
1206	28.51	0.00	0.02	0.00	0.06	0.01	0.03	0.03	69.51	0.00	-	0.00	0.00	0.04	0.11	0.00	0.00	0.00	0.00	0.00	0.00	0.00	98.32	2010	Pic-06-27/5
1207	28.43	0.05	0.01	0.05	0.09	0.00	0.03	0.00	69.64	0.06	-	0.00	0.01	0.00	0.01	0.00	0.08	0.00	0.07	0.00	0.00	0.00	98.52	2010	Pic-06-27/5
1208	28.66	0.00	0.00	0.00	0.07	0.04	0.00	0.00	69.68	0.00	-	0.00	0.00	0.20	0.04	0.00	0.00	0.00	0.00	0.02	0.00	0.00	98.71	2010	Pic-06-27/5
1209	28.60	0.00	0.00	0.09	0.00	0.00	0.01	0.07	69.71	0.00	-	0.00	0.00	0.01	0.00	0.00	0.02	0.00	0.09	0.05	0.00	0.00	98.64	2010	Pic-06-27/5
1210	28.78	0.09	0.01	0.02	0.05	0.02	0.00	0.09	69.75	0.06	-	0.01	0.03	0.20	0.10	0.04	0.00	0.00	0.05	0.00	0.00	0.00	99.24	2010	Pic-06-27/5
1211	28.53	0.00	0.02	0.00	0.06	0.04	0.00	0.02	69.90	0.00	-	0.00	0.03	0.00	0.00	0.02	0.00	0.00	0.00	0.04	0.00	0.00	98.66	2010	Pic-06-27/5
1212	28.83	0.09	0.02	0.03	0.07	0.00	0.01	0.06	69.90	0.00	-	0.05	0.00	0.37	0.13	0.04	0.01	0.00	0.07	0.04	0.00	0.00	99.72	2010	Pic-06-27/5
1213	28.73	0.10	0.00	0.02	0.02	0.00	0.01	0.00	69.92	0.00	-	0.00	0.00	0.17	0.00	0.02	0.06	0.00	0.00	0.00	0.00	0.00	99.05	2010	Pic-06-27/5
1214	28.57	0.10	0.01	0.02	0.08	0.00	0.00	0.00	69.97	0.00	-	0.00	0.00	0.06	0.07	0.00	0.01	0.00	0.05	0.11	0.00	0.00	98.98	2010	Pic-06-27/5
1215	28.85	0.01	0.01	0.00	0.09	0.02	0.01	0.04	70.08	0.01	-	0.00	0.00	0.25	0.08	0.00	0.00	0.00	0.05	0.01	0.00	0.00	99.50	2010	Pic-06-27/5
1216	28.50	0.00	0.01	0.00	0.08	0.00	0.00	0.00	70.11	0.00	-	0.01	0.00	0.00	0.09	0.00	0.00	0.00	0.08	0.00	0.00	0.00	98.89	2010	Pic-06-27/5
1217	28.76	0.00	0.01	0.05	0.12	0.01	0.01	0.00	70.13	0.02	-	0.00	0.00	0.00	0.08	0.01	0.00	0.00	0.06	0.04	0.00	0.00	99.30	2010	Pic-06-27/5
1218	28.89	0.12	0.02	0.02	0.06	0.00	0.02	0.02	70.14	0.00	-	0.00	0.02	0.01	0.08	0.01	0.00	0.00	0.00	0.03	0.00	0.00	99.44	2010	Pic-06-27/5
1219	28.62	0.00	0.00	0.04	0.03	0.04	0.02	0.04	70.25	0.00	-	0.00	0.00	0.02	0.00	0.00	0.00	0.00	0.00	0.00	0.00	0.00	99.13	2010	Pic-06-27/5
1220	28.60	0.00	0.00	0.06	0.00	0.00	0.02	0.02	70.30	0.00	-	0.00	0.00	0.01	0.09	0.00	0.04	0.00	0.03	0.00	0.00	0.00	99.18	2010	Pic-06-27/5
1221	35.98	0.00	0.01	0.00	0.06	0.00	0.00	0.00	58.89	0.00	-	0.04	0.01	0.40	0.06	0.00	0.00	0.00	0.09	0.00	0.00	0.00	95.53	2010	Pic06024
1222	36.15	0.00	0.00	0.01	0.07	0.04	0.00	0.02	59.10	0.02	-	0.02	0.00	0.46	0.02	0.00	0.00	0.00	0.00	0.00	0.00	0.00	95.91	2010	Pic06024
1223	35.18	0.00	0.00	0.01	0.05	0.00	0.01	0.01	59.22	0.02	-	0.00	0.00	0.32	0.11	0.00	0.00	0.00	0.00	0.00	0.00	0.00	94.92	2010	Pic06024
1224	36.81	0.00	0.00	0.00	0.00	0.00	0.00	0.00	59.31	0.00	-	0.02	0.00	0.00	0.00	0.00	0.00	0.00	0.00	0.00	0.00	0.00	96.81	2010	Pic06024
1225	34.00	0.02	0.00	0.00	0.08	0.01	0.04	0.00	59.31	0.02	-	0.00	0.04	0.35	0.08	0.01	0.05	0.00	0.00	0.00	0.00	0.00	93.99	2010	Pic06024
1226	35.40	0.04	0.00	0.00	0.11	0.09	0.01	0.01	59.64	0.29	-	0.00	0.00	0.34	0.00	0.00	0.00	0.00	0.00	0.03	0.00	0.00	95.96	2010	Pic06024
1227	34.01	0.04	0.00	0.00	0.05	0.00	0.00	0.00	59.67	0.08	-	0.02	0.03	0.35	0.00	0.00	0.03	0.00	0.00	0.00	0.03	0.00	94.31	2010	Pic06024
1228	34.72	0.01	0.00	0.02	0.07	0.02	0.00	0.00	59.71	0.01	-	0.01	0.00	0.37	0.15	0.00	0.01	0.00	0.00	0.00	0.00	0.00	95.09	2010	Pic06024
1229	28.11	0.02	0.00	0.05	0.00	0.00	0.00	0.05	59.86	0.63	0.05	0.00	0.00	0.00	0.00	0.00	0.00	0.00	0.00	0.00	0.00	0.00	98.02	2010	Pic06024
1230	35.28	0.07	0.00	0.00	0.08	0.03	0.01	0.00	59.81	0.02	-	0.01	0.00	0.42	0.07	0.00	0.01	0.00	0.08	0.00	0.00	0.00	95.86	2010	Pic06024
1231	34.74	0.10	0.00	0.00	0.06	0.00	0.02	0.00	59.83	0.00	-	0.00	0.01	0.45	0.00	0.00	0.00	0.00	0.02	0.00	0.00	0.00	95.23	2010	Pic06024
1232	35.20	0.00	0.00	0.01	0.09	0.02	0.04	0.01	59.89	0.31	-	0.00	0.06	0.30	0.00	0.00	0.00	0.00	0.01	0.02	0.00	0.00	95.95	2010	Pic06024
1233	33.68	0.04	0.00	0.00	0.08	0.02	0.00	0.02	59.89	0.09	-	0.03	0.07	0.34	0.04	0.04	0.00	0.00	0.02	0.02	0.00	0.00	94.35	2010	Pic06024
1234	35.15	0.00	0.00	0.00	0.10	0.05	0.01	0.02	59.92	0.39	0.00	0.00	0.00	0.00	0.00	0.00	0.00	0.00	0.00	0.00	0.00	0.00	96.01	2010	Pic06024
1235	34.55	0.01	0.01	0.00	0.06	0.00	0.07	0.02	60.04	0.44	-	0.01	0.01	0.34	0.01	0.00	0.07	0.00	0.00	0.00	0.00	0.00	95.65	2010	Pic06024
1236	35.35	0.01	0.00	0.06	0.12	0.04	0.00	0.01	60.22	0.37	-	0.00	0.02	0.30	0.00	0.00	0.04	0.00	0.07	0.00	0.00	0.00	96.60	2010	Pic06024
1237	34.41	0.00	0.00	0.00	0.10	0.03	0.03	0.00	60.27	0.56	-	0.00	0.04	0.26	0.04	0.00	0.02	0.00	0.00	0.00	0.00	0.00	95.78	2010	Pic06024
1238	34.49	0.09	0.00	0.00	0.08	0.00	0.00	0.04	60.30	0.35	-	0.06	0.00	0.25	0.00	0.00	0.00	0.00	0.00	0.00	0.00	0.00	95.66	2010	Pic06024
1239	33.71	0.03	0.00	0.00	0.10	0.06	0.02	0.00	60.46	0.51	0.02	0.00	0.00	0.05	0.51	0.00	0.00	0.00	0.00	0.00	0.00	0.00	95.33	2010	Pic06024
1240	34.15	0.05	0.00	0.02	0.10	0.01	0.01	0.00	60.52	0.53	-	0.00	0.00	0.27	0.03	0.02	0.02	0.00	0.01	0.02	0.00	0.00	95.75	2010	Pic06024
1241	36.47	0.04	0.00	0.00	0.05	0.05	0.04	0.00	60.60	0.54	-	0.00	0.00	0.33	0.00	0.00	0.08	0.00	0.00	0.00	0.00	0.00	98.20	2010	Pic06024
1242	33.06	0.03	0.00	0.02	0.00	0.03	0.02	0.00	60.62	0.27	-	0.04	0.00	0.31	0.00	0.07	0.00	0.00	0.00	0.00	0.00	0.00	94.47	2010	Pic06024
1243	33.99	0.02	0.01	0.00	0.04	0.04	0.01	0.01	60.66	0.40	-	0.02	0.04	0.26	0.00	0.00	0.00	0.00	0.01	0.00	0.00	0.00	95.51	2010	Pic06024
1244	33.19	0.03	0.00	0.00	0.05	0.01	0.02	0.01	60.71	0.25	0.00	0.00	0.00	0.00	0.00	0.00	0.00	0.00	0.00	0.00	0.00	0.00	94.65	2010	Pic06024
1245	32.31	0.02	0.00	0.00	0.00	0.03	0.04	0.00	60.71	0.25	-	0.01	0.01	0.28	0.03	0.00	0.04	0.00	0.00	0.00	0.00	0.00	93.70	2010	Pic06024
1246	34.05	0.00	0.00	0.00	0.03	0.03	0.01	0.00	60.83	0.51	-	0.02	0.00	0.27	0.01	0.00	0.04	0.00	0.00	0.00	0.00	0.00	95.80	2010	Pic06024
1247	33.07	0.04	0.00	0.01	0.10	0.03	0.04	0.02	60.83	0.44	-	0.00	0.03	0.30	0.03	0.00	0.00	0.00	0.09	0.08	0.00	0.00	95.10	2010	Pic06024
1248	34.00	0.00	0.00	0.00	0.11	0.00	0.02	0.00	60.88	0.00	-	0.00	0.03	0.34	0.00	0.03	0.00	0.00	0.00	0.00	0.00	0.00	95.41	2010	Pic06024
1249	35.43	0.00	0.00	0.00	0.01	0.02	0.02	0.01	60.90	0.29	0.01	0.02	0.28	0.00	0.06	0.00	0.00	0.00	0.00	0.00	0.00	0.00	97.43	2010	Pic06024
1250	34.36	0.07	0.00	0.00	0.08	0.02	0.01	0.02	60.91	0.47	-	0.00	0.00	0.27	0.06	0.05	0.01	0.0							

INDEX	No.	O	Na	K	V	Co	Mg	P	Cr	Fe	Al	S	Ni	Mn	Si	Pb	Cu	Ti	Ca	Zn	Ba	Sr	Total	Year	Sample
1350		33.79	0.02	0.00	0.02	0.03	0.07	0.07	0.03	0.00	60.99	0.78	0.03	0.00	0.45	0.00	0.00	0.07	0.00	0.04	0.00		96.33	2010	Pic6027
1351		33.19	0.05	0.00	0.00	0.07	0.02	0.03	0.00	60.99	0.47	-	0.00	0.00	0.46	0.04	0.07	0.01	0.00	0.04	0.00		95.44	2010	Pic6027
1352		33.44	0.07	0.00	0.05	0.08	0.05	0.03	0.03	60.99	0.43	-	0.00	0.06	0.43	0.00	0.00	0.08	0.02	0.02	0.00		95.78	2010	Pic6027
1353		31.86	0.06	0.00	0.00	0.08	0.00	0.03	0.00	61.01	0.45	-	0.00	0.00	0.42	0.12	0.00	0.09	0.00	0.01	0.07		94.21	2010	Pic6027
1354		31.21	0.03	0.00	0.02	0.11	0.01	0.05	0.00	61.02	0.72	-	0.03	0.02	0.43	0.00	0.00	0.10	0.00	0.03	0.00		93.78	2010	Pic6027
1355		33.23	0.00	0.00	0.03	0.07	0.02	0.08	0.00	61.04	0.63	0.07	0.04	0.00	0.42	0.00	0.00	0.02	0.11	0.00	0.00		95.36	2010	Pic6027
1356		32.68	0.00	0.00	0.02	0.04	0.05	0.03	0.00	61.09	0.39	-	0.00	0.00	0.41	0.02	0.05	0.03	0.00	0.00	0.00		94.82	2010	Pic6027
1357		33.02	0.03	0.00	0.00	0.06	0.01	0.04	0.01	61.09	0.50	-	0.00	0.03	0.44	0.00	0.06	0.13	0.00	0.00	0.00		95.42	2010	Pic6027
1358		32.36	0.01	0.00	0.02	0.03	0.01	0.05	0.00	61.17	0.38	-	0.00	0.00	0.43	0.12	0.06	0.14	0.00	0.00	0.00		94.77	2010	Pic6027
1359		32.52	0.07	0.00	0.00	0.04	0.07	0.09	0.02	61.35	0.68	-	0.00	0.00	0.42	0.06	0.00	0.07	0.00	0.00	0.00		95.39	2010	Pic6027
1360		33.81	0.00	0.01	0.03	0.05	0.05	0.04	0.02	61.39	0.37	0.04	0.00	0.00	0.44	0.05	0.00	0.00	0.00	0.00	0.03		96.33	2010	Pic6027
1361		31.42	0.00	0.01	0.01	0.05	0.07	0.04	0.00	61.53	0.23	-	0.00	0.00	0.44	0.00	0.00	0.14	0.00	0.00	0.00		93.94	2010	Pic6027
1362		30.73	0.00	0.00	0.00	0.06	0.07	0.06	0.00	61.55	0.21	-	0.00	0.00	0.47	0.00	0.03	0.07	0.00	0.00	0.00		93.24	2010	Pic6027
1363		34.41	0.00	0.00	0.00	0.07	0.05	0.08	0.00	61.60	0.55	-	0.00	0.00	0.52	0.06	0.00	0.13	0.00	0.00	0.01		97.48	2010	Pic6027
1364		32.66	0.04	0.01	0.00	0.00	0.07	0.02	0.00	53.96	0.26	-	0.00	0.03	5.81	0.02	0.00	0.00	0.03	0.01	0.01		92.98	2010	Pic6029
1365		32.66	0.00	0.00	0.04	0.00	0.00	0.00	0.00	58.75	0.01	-	0.00	0.00	0.38	0.02	0.00	0.03	0.00	0.00	0.00		91.90	2010	Pic6029
1366		35.87	0.00	0.01	0.09	0.04	0.04	0.05	0.01	58.80	1.04	-	0.03	0.00	0.24	0.00	0.00	0.11	0.00	0.00	0.00		96.34	2010	Pic6029
1367		34.74	0.03	0.00	0.01	0.00	0.01	0.01	0.02	58.88	0.00	-	0.00	0.07	0.35	0.00	0.06	0.03	0.00	0.02	0.00		94.22	2010	Pic6029
1368		40.87	0.06	0.00	0.00	0.05	0.03	0.04	0.00	59.19	0.00	-	0.01	0.02	0.47	0.00	0.00	0.00	0.00	0.00	0.03		100.77	2010	Pic6029
1369		35.99	0.04	0.00	0.06	0.00	0.00	0.02	0.00	59.21	0.00	-	0.00	0.29	0.01	0.00	0.00	0.01	0.00	0.09	0.00		95.92	2010	Pic6029
1370		35.67	0.10	0.01	0.00	0.08	0.03	0.03	0.00	59.23	0.00	-	0.00	0.03	0.45	0.03	0.00	0.00	0.00	0.00	0.00		95.77	2010	Pic6029
1371		31.40	0.04	0.00	0.00	0.06	0.00	0.01	0.03	59.37	0.07	-	0.00	0.00	0.39	0.12	0.04	0.00	0.00	0.00	0.00		91.52	2010	Pic6029
1372		36.61	0.00	0.00	0.00	0.06	0.01	0.00	0.00	59.39	0.00	-	0.00	0.00	0.40	0.01	0.02	0.05	0.00	0.01	0.04		96.62	2010	Pic6029
1373		31.23	0.00	0.00	0.01	0.00	0.03	0.02	0.00	59.43	0.03	-	0.00	0.00	0.42	0.00	0.01	0.00	0.00	0.00	0.01		91.19	2010	Pic6029
1374		35.41	0.09	0.00	0.00	0.00	0.03	0.03	0.00	59.43	0.98	-	0.00	0.04	0.00	0.03	0.00	0.00	0.00	0.00	0.00		96.51	2010	Pic6029
1375		34.36	0.00	0.01	0.01	0.06	0.04	0.01	0.00	59.54	0.00	-	0.00	0.01	0.16	0.00	0.00	0.00	0.00	0.03	0.00		94.23	2010	Pic6029
1376		36.47	0.09	0.02	0.01	0.07	0.01	0.02	0.00	59.62	0.00	-	0.00	0.00	0.47	0.14	0.01	0.00	0.00	0.00	0.04		96.96	2010	Pic6029
1377		35.09	0.00	0.00	0.00	0.08	0.02	0.00	0.00	59.68	0.00	-	0.00	0.01	0.55	0.06	0.00	0.03	0.01	0.00	0.01		95.54	2010	Pic6029
1378		35.52	0.11	0.00	0.00	0.06	0.03	0.00	0.00	59.69	0.00	-	0.03	0.00	0.40	0.00	0.05	0.00	0.00	0.02	0.00		95.90	2010	Pic6029
1379		34.58	0.00	0.00	0.00	0.00	0.00	0.01	0.02	59.71	0.01	-	0.00	0.00	0.40	0.00	0.00	0.00	0.00	0.00	0.00		94.86	2010	Pic6029
1380		34.84	0.00	0.00	0.00	0.08	0.01	0.00	0.00	59.74	0.00	-	0.01	0.02	0.53	0.10	0.05	0.03	0.00	0.00	0.00		95.40	2010	Pic6029
1381		31.04	0.00	0.00	0.00	0.03	0.01	0.04	0.02	59.77	0.14	-	0.00	0.02	0.42	0.05	0.01	0.01	0.00	0.02	0.00		91.59	2010	Pic6029
1382		35.73	0.02	0.00	0.00	0.12	0.00	0.00	0.00	59.81	0.01	-	0.01	0.05	0.04	0.00	0.00	0.01	0.00	0.01	0.01		95.81	2010	Pic6029
1383		36.57	0.00	0.00	0.00	0.03	0.02	0.03	0.02	59.82	0.00	-	0.02	0.00	0.29	0.06	0.00	0.00	0.00	0.00	0.00		96.87	2010	Pic6029
1384		34.39	0.00	0.00	0.00	0.00	0.00	0.00	0.00	59.90	0.00	-	0.00	0.00	0.29	0.06	0.00	0.00	0.00	0.00	0.00		95.19	2010	Pic6029
1385		35.70	0.04	0.00	0.00	0.12	0.02	0.00	0.01	59.94	0.00	-	0.01	0.04	0.39	0.07	0.01	0.00	0.00	0.05	0.02		96.42	2010	Pic6029
1386		32.65	0.06	0.01	0.00	0.04	0.03	0.01	0.00	59.94	0.01	-	0.00	0.00	0.50	0.02	0.02	0.02	0.00	0.00	0.00		93.29	2010	Pic6029
1387		35.23	0.00	0.00	0.00	0.07	0.00	0.01	0.00	60.14	0.01	-	0.00	0.00	0.37	0.02	0.00	0.02	0.00	0.00	0.00		95.86	2010	Pic6029
1388		34.28	0.03	0.00	0.00	0.08	0.03	0.01	0.03	60.15	0.00	-	0.00	0.03	0.53	0.00	0.06	0.05	0.00	0.00	0.00		95.26	2010	Pic6029
1389		34.17	0.00	0.00	0.00	0.04	0.04	0.01	0.00	60.15	0.00	-	0.00	0.03	0.52	0.02	0.04	0.02	0.00	0.00	0.00		95.14	2010	Pic6029
1390		32.38	0.00	0.00	0.00	0.05	0.06	0.01	0.00	60.15	0.02	-	0.00	0.00	0.39	0.00	0.00	0.00	0.00	0.00	0.02		93.07	2010	Pic6029
1391		34.10	0.02	0.00	0.00	0.03	0.01	0.00	0.00	60.18	0.02	-	0.00	0.00	0.49	0.05	0.00	0.06	0.00	0.07	0.00		95.02	2010	Pic6029
1392		36.22	0.05	0.00	0.04	0.04	0.03	0.01	0.00	60.22	0.01	-	0.00	0.00	0.40	0.00	0.00	0.00	0.00	0.00	0.00		97.03	2010	Pic6029
1393		37.82	0.00	0.01	0.00	0.05	0.02	0.01	0.03	60.27	0.01	-	0.00	0.00	0.54	0.05	0.00	0.03	0.00	0.03	0.00		98.87	2010	Pic6029
1394		34.23	0.00	0.00	0.00	0.00	0.00	0.00	0.00	60.40	0.02	-	0.02	0.00	0.40	0.02	0.00	0.00	0.00	0.00	0.00		95.36	2010	Pic6029
1395		34.64	0.00	0.00	0.00	0.06	0.05	0.03	0.03	60.41	0.01	-	0.00	0.00	0.29	0.04	0.00	0.00	0.02	0.00	0.00		96.49	2010	Pic6029
1396		34.37	0.00	0.02	0.00	0.05	0.04	0.04	0.01	60.49	0.03	-	0.00	0.02	0.38	0.02	0.01	0.00	0.00	0.03	0.00		95.49	2010	Pic6029
1397		33.09	0.02	0.00	0.00	0.08	0.04	0.00	0.00	60.51	0.01	-	0.00	0.02	0.27	0.02	0.00	0.00	0.00	0.03	0.00		94.09	2010	Pic6029
1398		33.82	0.03	0.00	0.02	0.06	0.05	0.05	0.01	60.54	0.88	-	0.00	0.06	0.33	0.00	0.00	0.06	0.00	0.05	0.00		95.94	2010	Pic6029
1399		34.33	0.00	0.00	0.04	0.07	0.02	0.01	0.00	60.55	0.02	-	0.00	0.01	0.42	0.00	0.04	0.01	0.01	0.06	0.00		95.58	2010	Pic6029
1400		36.68	0.08	0.01	0.00	0.07	0.00	0.01	0.00	60.55	0.00	-	0.00	0.05	0.40	0.01	0.02	0.00	0.00	0.00	0.00		97.89	2010	Pic6029
1401		34.82	0.01	0.00	0.00	0.05	0.02	0.02	0.00	60.69	0.00	-	0.00	0.00	0.48	0.04	0.03	0.01	0.00	0.00	0.03		96.22	2010	Pic6029
1402		33.70	0.02	0.00	0.00	0.07	0.01	0.00	0.00	60.72	0.00	-	0.00	0.04	0.42	0.08	0.00	0.06	0.00	0.07	0.03		95.22	2010	Pic6029
1403		32.28	0.01	0.00	0.00</																				

INDEX	No.	O	Na	K	V	Co	Mg	P	Cr	Fe	Al	S	Ni	Mn	Si	Pb	Cu	Ti	Ca	Zn	Ba	Sr	Total	Year	Sample	
1500	201	36.13			0.04	0.04	0.01	1.00	0.04	58.52	0.01	0.00		0.07	0.30	0.00	0.00	0.03						96.21	2014	BAH F282 118.2 grain 4
1501	206	37.20			0.00	0.05	0.00	1.14	0.03	58.51	0.00	0.00		0.05	0.20	0.00	0.01	0.02						97.22	2014	BAH F282 118.2 grain 4
1502	207	37.26			0.02	0.06	0.00	1.25	0.00	58.95	0.00	0.00		0.08	0.17	0.07	0.03	0.00						97.88	2014	BAH F282 118.2 grain 4
1503	208	36.83			0.00	0.09	0.01	1.01	0.00	58.97	0.01	0.02		0.07	0.33	0.00	0.03	0.00						97.36	2014	BAH F282 118.2 grain 4
1504	209	37.34			0.00	0.05	0.04	1.32	0.00	55.71	0.03	0.00		0.11	0.78	0.00	0.01	0.05						96.45	2014	BAH F282 118.2 grain 4
1505	210	36.18			0.03	0.03	0.04	0.94	0.01	58.03	0.16	0.02		0.06	0.59	0.00	0.53	0.01						96.61	2014	BAH F282 118.2 grain 4
1506	211	36.04			0.02	0.05	0.00	0.84	0.00	58.70	0.02	0.01		0.00	0.32	0.05	0.00	0.00						96.04	2014	BAH F282 118.2 grain 4
1507	212	36.58			0.00	0.11	0.00	1.10	0.00	58.12	0.00	0.01		0.05	0.25	0.05	0.00	0.01						96.28	2014	BAH F282 118.2 grain 4
1508	153	35.59			0.00	0.05	0.01	0.47	0.00	59.50	0.01	0.00		0.09	0.31	0.00	0.38	0.00						96.41	2014	BAH F282 118.2
1509	154	35.22			0.00	0.04	0.01	0.52	0.02	59.63	0.00	0.01		0.06	0.26	0.01	0.26	0.00						96.03	2014	BAH F282 118.2
1510	155	35.86			0.03	0.02	0.04	0.49	0.06	59.56	0.00	0.01		0.07	0.28	0.00	0.18	0.05						96.65	2014	BAH F282 118.2
1511	156	35.29			0.00	0.04	0.03	0.51	0.00	59.83	0.00	0.00		0.04	0.29	0.07	0.27	0.00						96.36	2014	BAH F282 118.2
1512	157	35.65			0.00	0.04	0.04	0.48	0.02	59.86	0.00	0.04		0.08	0.28	0.00	0.37	0.00						96.85	2014	BAH F282 118.2
1513	158	35.27			0.02	0.00	0.01	0.49	0.00	59.74	0.00	0.02		0.07	0.28	0.00	0.24	0.02						96.16	2014	BAH F282 118.2
1514	159	35.67			0.00	0.04	0.01	0.53	0.01	60.21	0.00	0.00		0.08	0.29	0.00	0.21	0.02						97.13	2014	BAH F282 118.2
1515	160	35.81			0.01	0.07	0.01	0.53	0.00	59.86	0.00	0.02		0.02	0.25	0.00	0.32	0.03						96.93	2014	BAH F282 118.2
1516	161	35.65			0.06	0.05	0.01	0.59	0.00	59.76	0.00	0.01		0.11	0.25	0.00	0.26	0.03						96.79	2014	BAH F282 118.2
1517	162	35.75			0.05	0.12	0.06	0.52	0.05	59.72	0.02	0.00		0.04	0.30	0.00	0.22	0.01						96.84	2014	BAH F282 118.2
1518	163	35.35			0.02	0.06	0.02	0.51	0.01	59.35	0.00	0.00		0.10	0.27	0.00	0.28	0.00						95.98	2014	BAH F282 118.2
1519	164	34.78			0.00	0.04	0.03	0.50	0.00	59.59	0.02	0.00		0.09	0.26	0.01	0.18	0.05						95.50	2014	BAH F282 118.2
1520	165	35.59			0.00	0.06	0.03	0.51	0.00	59.19	0.01	0.00		0.04	0.26	0.09	0.24	0.00						96.01	2014	BAH F282 118.2
1521	166	35.63			0.02	0.09	0.00	0.57	0.00	59.68	0.00	0.00		0.03	0.25	0.09	0.22	0.00						96.58	2014	BAH F282 118.2
1522	167	35.52			0.00	0.04	0.03	0.52	0.00	59.48	0.01	0.02		0.05	0.28	0.00	0.17	0.00						96.11	2014	BAH F282 118.2
1523	184	37.97	0.00	0.00	0.04	0.04	0.18	0.00	59.76	0.09	0.01	0.00		0.12	0.64	0.09	1.13	0.01	0.08	0.00	0.00	0.06	101.21	2014	BAH F282 118.2	
1524	185	37.84	0.00	0.00	0.00	0.06	0.12	0.01	60.00	0.13	0.00	0.00		0.03	0.14	0.02	0.03	0.05	0.05	0.05	0.00	0.00	101.23	2014	BAH F282 118.2	
1525	186	37.54	0.00	0.00	0.00	0.01	0.03	0.14	0.07	58.39	0.41	0.00		0.09	0.54	0.06	1.05	0.00	0.05	0.05	0.00	0.00	99.81	2014	BAH F282 118.2	
1526	187	36.08	0.00	0.01	0.04	0.04	0.54	0.05	62.64	0.40	0.00	0.00		0.02	0.57	0.00	0.03	0.00	0.04	0.05	0.00	0.00	100.50	2014	BAH F282 118.2	
1527	188	38.32	0.01	0.00	0.02	0.06	0.72	0.00	60.07	0.61	0.04	0.00		0.08	1.20	0.15	0.12	0.00	0.05	0.00	0.00	0.04	101.49	2014	BAH F282 118.2	
1528	189	38.36	0.01	0.00	0.09	0.04	1.46	0.02	59.31	0.36	0.00	0.02	0.12	0.65	0.00	0.97	0.03	0.05	0.07	0.03	0.00	0.01	101.59	2014	BAH F282 118.2	
1529	190	38.02	0.00	0.00	0.02	0.06	1.24	0.00	60.00	0.24	0.00	0.00		0.14	0.00	1.24	0.00	0.00	0.00	0.00	0.00	0.01	101.54	2014	BAH F282 118.2	
1530	191	37.31	0.00	0.00	0.07	0.02	1.21	0.00	60.47	0.11	0.00	0.00		0.12	0.51	0.13	0.82	0.06	0.11	0.06	0.08	0.00	101.06	2014	BAH F282 118.2	
1531	192	36.29	0.03	0.00	0.06	0.06	0.92	0.00	60.46	0.65	0.01	0.00	0.03	0.45	0.06	1.09	0.03	0.00	0.03	0.05	0.02	0.00	100.23	2014	BAH F282 118.2	
1532	193	36.74	0.00	0.00	0.12	0.00	0.72	0.00	62.93	0.12	0.01	0.00	0.01	0.29	0.08	0.00	0.01	0.00	0.00	0.01	0.00	0.01	101.04	2014	BAH F282 118.2	
1533	194	35.77	0.00	0.01	0.11	0.00	0.96	0.02	62.85	0.01	0.00	0.02	0.01	0.30	0.06	0.04	0.00	0.00	0.00	0.01	0.00	0.01	100.16	2014	BAH F282 118.2	
1534	195	36.24	0.00	0.00	0.01	0.07	0.01	0.97	0.00	62.12	0.00	0.00	0.05	0.07	0.12	0.00	0.32	0.03						96.47	2014	BAH F282 118.2
1535	196	37.31	0.00	0.00	0.05	0.00	1.14	0.00	61.69	0.01	0.00	0.05	0.05	0.23	0.02	0.04	0.00	0.00	0.05	0.05	0.04		100.72	2014	BAH F282 118.2	
1536	189	36.23			0.00	0.06	0.00	0.71	0.00	59.42	0.00	0.00		0.04	0.27	0.00	0.11	0.00						96.84	2014	BAH F282 118.2 grain 3
1537	190	37.54			0.00	0.08	0.02	1.12	0.03	58.20	0.01	0.02		0.12	0.24	0.09	0.00	0.00						97.42	2014	BAH F282 118.2 grain 3
1538	191	36.25			0.00	0.06	0.00	0.83	0.08	60.13	0.02	0.00		0.05	0.20	0.09	0.14	0.00						97.85	2014	BAH F282 118.2 grain 3
1539	192	36.62			0.04	0.76	0.01	0.91	0.09	59.30	0.11	0.01		0.09	0.29	0.03	0.11	0.00						97.42	2014	BAH F282 118.2 grain 3
1540	193	36.91			0.01	0.02	0.03	1.13	0.00	57.22	0.02	0.01		0.12	0.50	0.00	0.72	0.00						96.68	2014	BAH F282 118.2 grain 3
1541	194	36.28			0.12	0.03	0.05	0.78	0.07	56.80	0.89	0.03		0.03	0.89	0.08	0.15	0.00						96.19	2014	BAH F282 118.2 grain 3
1542	195	37.19			0.07	0.05	0.06	1.21	0.04	55.85	0.34	0.01		0.18	0.46	0.00	1.18	0.00						96.62	2014	BAH F282 118.2 grain 3
1543	196	37.35			0.00	0.06	0.02	1.11	0.02	56.45	0.01	0.00		0.14	0.63	0.00	0.92	0.00						96.70	2014	BAH F282 118.2 grain 3
1544	197	37.31			0.00	0.09	0.04	1.07	0.00	55.95	0.02	0.00		0.10	0.66	0.00	1.08	0.00						96.14	2014	BAH F282 118.2 grain 3
1545	168	36.85			0.00	0.06	0.02	0.66	0.00	59.10	0.00	0.00		0.03	0.54	0.00	0.04	0.00						97.29	2014	BAH F282 118.2 grain 2
1546	169	36.15			0.00	0.14	0.00	0.73	0.00	58.29	0.03	0.03		0.03	0.41	0.06	1.09	0.00						96.96	2014	BAH F282 118.2 grain 2
1547	170	35.99			0.06	0.04	0.04	0.73	0.02	57.72	0.03	0.00		0.13	0.41	0.00	1.13	0.06						96.36	2014	BAH F282 118.2 grain 2
1548	171	36.14			0.02	0.08	0.01	0.78	0.04	58.04	0.04	0.00		0.09	0.42	0.09	1.21	0.00						96.96	2014	BAH F282 118.2 grain 2
1549	172	35.95			0.04	0.05	0.04	0.84	0.00	57.83	0.05	0.00		0.12	0.45	0.06	1.19	0.05						96.57	2014	BAH F282 118.2 grain 2
1550	173	36.02			0.06	0.13	0.02	0.90	0.03	57.60	0.06	0.00		0.10	0.44	0.03	1.14	0.00						96.52	2014	BAH F282 118.2 grain 2
1551	174	35.98			0.00	0.04	0.03	0.95	0.01	57.60	0.06	0.00		0.10	0.47	0.00	1.38	0.03						96.64	2014	BAH F282 118.2 grain 2
1552	175	36.00			0.01	0.03	0.04	0.89	0.00	57.20	0.05	0.00		0.07	0.46	0.00	1.21	0.00						95.96	2014	BAH F282 118.2 grain 2
1553	176	36.17			0.00	0.03	0.01	0.95	0.01	57.13	0.05	0.03		0.05	0.46	0.09	1.15	0.08						96.20	2014	BAH F282 118.2 grain

INDEX	No.	O	Na	K	V	Co	Mg	P	Cr	Fe	Al	S	Ni	Mn	Si	Pb	Cu	Ti	Ca	Zn	Ba	Sr	Total	Year	Sample
1650	115	99.16	0.00	0.00	0.15	0.00	0.00	0.54	0.00	55.55	3.47	0.04	0.00	0.00	0.06	0.00	0.00	1.06	0.00	0.00	0.00	0.00	100.09	2014	NIP 13 02
1651	116	38.32	0.00	0.00	0.03	0.02	0.01	0.62	0.00	59.89	1.44	0.00	0.02	0.00	0.04	0.02	0.00	0.05	0.00	0.00	0.04	0.00	100.48	2014	NIP 13 02
1652	117	39.52	0.00	0.00	0.17	0.01	0.00	0.56	0.02	54.40	4.42	0.00	0.00	0.00	0.08	0.00	0.01	0.89	0.00	0.00	0.01	0.00	100.08	2014	NIP 13 02
1653	118	37.28	0.01	0.01	0.01	0.04	0.00	0.20	0.00	60.51	1.06	0.00	0.00	0.00	0.18	0.19	0.01	0.02	0.00	0.00	0.07	0.00	99.59	2014	NIP 13 02
1654	119	35.12	0.00	0.00	0.04	0.06	0.02	0.59	0.00	64.07	1.43	0.00	0.03	0.01	0.06	0.01	0.02	0.00	0.00	0.00	0.00	0.00	101.46	2014	NIP 13 03
1655	120	35.99	0.01	0.00	0.06	0.01	0.00	0.56	0.00	63.57	1.30	0.00	0.01	0.00	0.07	0.00	0.00	0.08	0.03	0.19	0.00	0.00	101.90	2014	NIP 13 03
1656	121	35.49	0.00	0.00	0.01	0.06	0.00	0.59	0.02	63.64	1.26	0.00	0.00	0.01	0.09	0.00	0.00	0.08	0.00	0.01	0.04	0.00	101.32	2014	NIP 13 03
1657	123	36.26	0.04	0.01	0.01	0.13	0.02	0.51	0.01	62.37	2.09	0.03	0.01	0.00	0.09	0.00	0.00	0.14	0.00	0.02	0.00	0.00	101.73	2014	NIP 13 03
1658	126	29.91	0.03	0.01	0.01	0.09	0.02	0.58	0.00	61.43	2.12	0.03	0.02	0.00	0.08	0.03	0.04	0.13	0.00	0.00	0.00	0.00	94.54	2014	NIP 13 03
1659	127	35.01	0.00	0.00	0.02	0.01	0.01	0.62	0.00	63.41	1.52	0.01	0.00	0.04	0.05	0.00	0.00	0.10	0.00	0.00	0.00	0.00	100.80	2014	NIP 13 03
1660	129	35.41	0.00	0.00	0.02	0.06	0.01	0.59	0.02	63.64	1.58	0.00	0.00	0.06	0.05	0.07	0.01	0.09	0.00	0.04	0.00	0.00	101.67	2014	NIP 13 03
1661	131	36.08	0.01	0.01	0.02	0.11	0.00	0.52	0.02	62.20	2.15	0.00	0.02	0.00	0.08	0.02	0.00	0.21	0.00	0.00	0.00	0.00	101.43	2014	NIP 13 03
1662	86	36.88	0.00	0.00	0.03	0.06	0.00	1.00	0.01	61.72	1.87	0.02	0.00	0.00	0.06	0.00	0.00	0.11	0.00	0.00	0.02	0.00	101.76	2014	NIP 13 06 Vitreous gt
1663	88	37.30	0.00	0.01	0.08	0.09	0.01	0.53	0.01	59.23	3.05	0.00	0.00	0.05	0.10	0.00	0.02	0.24	0.00	0.00	0.02	0.00	100.74	2014	NIP 13 06 Vitreous gt
1664	90	37.65	0.00	0.02	0.04	0.07	0.00	0.49	0.03	59.12	3.12	0.01	0.01	0.09	0.00	0.02	0.18	0.00	0.02	0.00	0.00	0.00	100.86	2014	NIP 13 06 Vitreous gt
1665	91	37.33	0.00	0.02	0.07	0.10	0.00	0.56	0.04	59.51	3.17	0.00	0.00	0.01	0.11	0.04	0.00	0.19	0.00	0.00	0.02	0.00	101.23	2014	NIP 13 06 Vitreous gt
1666	92	37.71	0.00	0.00	0.09	0.08	0.01	0.49	0.00	58.68	3.04	0.02	0.00	0.03	0.11	0.00	0.00	0.33	0.00	0.00	0.02	0.00	100.59	2014	NIP 13 06 Vitreous gt
1667	135	31.71	0.00	0.00	0.00	0.08	0.02	0.57	0.00	67.41	0.19	0.06	0.00	0.04	0.27	0.01	0.00	0.00	0.00	0.00	0.03	0.00	100.38	2014	NIP 13 09
1668	137	34.10	0.02	0.00	0.01	0.02	0.00	0.60	0.01	66.14	0.15	0.08	0.00	0.00	0.37	0.00	0.00	0.00	0.00	0.00	0.02	0.00	101.53	2014	NIP 13 09
1669	140	35.38	0.00	0.00	0.01	0.06	0.01	0.57	0.00	64.17	0.10	0.06	0.00	0.02	0.19	0.02	0.00	0.02	0.00	0.00	0.00	0.00	100.59	2014	NIP 13 09
1670	141	32.64	0.00	0.01	0.02	0.06	0.00	0.96	0.00	65.69	0.06	0.10	0.00	0.02	0.31	0.00	0.01	0.01	0.00	0.00	0.00	0.00	99.87	2014	NIP 13 09
1671	142	37.50	0.00	0.00	0.00	0.09	0.02	0.36	0.00	62.98	0.09	0.06	0.00	0.04	0.19	0.00	0.04	0.03	0.00	0.03	0.08	0.00	101.50	2014	NIP 13 09
1672	144	37.21	0.00	0.00	0.02	0.10	0.00	0.76	0.00	63.19	0.20	0.01	0.00	0.01	0.12	0.00	0.03	0.00	0.00	0.01	0.03	0.00	101.69	2014	NIP 13 09
1673	145	36.06	0.00	0.01	0.03	0.06	0.02	0.88	0.00	63.81	0.27	0.04	0.01	0.01	0.15	0.00	0.00	0.00	0.00	0.06	0.00	0.00	101.39	2014	NIP 13 09
1674	147	32.78	0.00	0.00	0.00	0.03	0.00	1.18	0.00	65.53	0.49	0.15	0.03	0.00	0.06	0.10	0.03	0.05	0.00	0.00	0.00	0.00	100.94	2014	NIP 13 09
1675	150	37.73	0.00	0.00	0.01	0.06	0.02	0.49	0.01	61.38	1.31	0.02	0.01	0.00	0.09	0.03	0.00	0.00	0.00	0.03	0.04	0.00	101.23	2014	NIP 13 13
1676	151	37.20	0.00	0.02	0.00	0.05	0.00	0.32	0.00	61.04	1.13	0.03	0.00	0.09	0.09	0.03	0.00	0.00	0.00	0.03	0.03	0.00	100.05	2014	NIP 13 13
1677	152	37.36	0.00	0.00	0.04	0.07	0.00	0.29	0.02	61.34	0.72	0.04	0.02	0.02	0.11	0.05	0.00	0.04	0.00	0.03	0.03	0.00	100.18	2014	NIP 13 13
1678	153	37.22	0.01	0.00	0.00	0.12	0.02	0.51	0.01	60.53	1.90	0.02	0.02	0.01	0.09	0.01	0.03	0.05	0.00	0.00	0.00	0.00	100.54	2014	NIP 13 13
1679	154	37.59	0.00	0.00	0.00	0.00	0.00	0.46	0.00	59.55	2.15	0.00	0.00	0.06	0.00	0.00	0.00	0.00	0.00	0.00	0.00	0.00	100.46	2014	NIP 13 13
1680	155	37.93	0.00	0.02	0.05	0.06	0.00	0.47	0.00	57.78	3.17	0.03	0.08	0.00	0.03	0.01	0.00	0.06	0.00	0.00	0.06	0.00	99.75	2014	NIP 13 13
1681	156	38.26	0.00	0.00	0.12	0.04	0.00	0.50	0.00	56.10	4.18	0.04	0.00	0.00	0.10	0.14	0.03	0.67	0.00	0.00	0.02	0.00	100.19	2014	NIP 13 13
1682	157	38.42	0.00	0.01	0.06	0.05	0.00	0.92	0.00	58.47	2.93	0.01	0.01	0.00	0.07	0.07	0.00	0.15	0.00	0.00	0.01	0.00	101.18	2014	NIP 13 13
1683	158	38.41	0.00	0.00	0.05	0.02	0.00	0.94	0.00	58.23	2.56	0.05	0.00	0.00	0.10	0.02	0.00	0.13	0.00	0.00	0.05	0.00	100.57	2014	NIP 13 13
1684	160	35.80	0.00	0.00	0.00	0.00	0.00	0.10	0.00	63.85	0.25	0.00	0.00	0.00	0.00	0.00	0.00	0.00	0.00	0.00	0.00	0.00	101.75	2014	NIP 13 14
1685	162	35.78	0.00	0.02	0.04	0.09	0.02	0.46	0.02	63.68	0.92	0.07	0.00	0.02	0.19	0.00	0.00	0.00	0.00	0.00	0.01	0.00	101.32	2014	NIP 13 14
1686	164	36.65	0.00	0.01	0.09	0.04	0.00	0.48	0.02	63.12	1.17	0.06	0.00	0.02	0.16	0.03	0.00	0.11	0.00	0.00	0.00	0.00	101.98	2014	NIP 13 14
1687	165	37.04	0.00	0.01	0.11	0.07	0.00	0.56	0.00	61.73	1.41	0.08	0.03	0.02	0.14	0.00	0.00	0.00	0.00	0.00	0.00	0.00	101.20	2014	NIP 13 14
1688	166	37.08	0.00	0.07	0.07	0.07	0.02	0.49	0.00	62.13	1.58	0.05	0.03	0.00	0.13	0.15	0.01	0.08	0.00	0.04	0.03	0.00	101.98	2014	NIP 13 14
1689	171	35.44	0.00	0.00	0.00	0.03	0.00	0.24	0.04	59.71	4.90	0.15	0.03	0.00	0.00	0.00	0.00	0.00	0.00	0.00	0.00	0.00	101.93	2014	NIP 13 17 Psilodites lake shore
1690	173	34.21	0.00	0.00	0.11	0.08	0.02	0.23	0.03	55.81	7.27	0.18	0.00	0.05	0.61	0.00	0.00	0.93	0.04	0.00	0.00	0.00	99.62	2014	NIP 13 17 Psilodites lake shore
1691	176	35.06	0.00	0.00	0.05	0.03	0.01	0.21	0.04	60.75	4.34	0.17	0.00	0.02	0.69	0.00	0.00	0.17	0.00	0.02	0.01	0.00	101.55	2014	NIP 13 17 Psilodites lake shore
1692	179	39.88	0.06	0.00	0.02	0.07	0.00	0.26	0.00	54.64	5.18	0.10	0.00	0.03	0.51	0.01	0.00	0.09	0.00	0.00	0.01	0.00	100.86	2014	NIP 13 18 lake
1693	180	35.51	0.00	0.01	0.01	0.05	0.00	0.28	0.01	53.86	5.87	0.12	0.06	0.00	0.46	0.00	0.00	0.00	0.00	0.08	0.00	0.00	100.30	2014	NIP 13 18 lake
1694	181	37.76	0.00	0.00	0.00	0.00	0.00	0.20	0.00	57.26	3.05	0.07	0.00	0.00	0.00	0.00	0.00	0.00	0.00	0.00	0.00	0.00	99.25	2014	NIP 13 18 lake
1695	182	39.47	0.00	0.02	0.04	0.08	0.00	0.23	0.03	55.95	4.98	0.08	0.00	0.03	0.47	0.06	0.02	0.04	0.00	0.00	0.01	0.00	101.50	2014	NIP 13 18 lake
1696	183	39.57	0.01	0.00	0.05	0.13	0.00	0.30	0.05	55.21	5.11	0.13	0.00	0.00	0.49	0.08	0.03	0.09	0.00	0.00	0.05	0.00	101.27	2014	NIP 13 18 lake
1697	184	38.61	0.03	0.01	0.06	0.09	0.02	0.32	0.00	57.23	4.34	0.10	0.00	0.01	0.50	0.02	0.00	0.07	0.00	0.00	0.01	0.00	101.42	2014	NIP 13 18 lake
1698	188	39.23	0.00	0.01	0.10	0.03	0.02	0.38	0.02	55.33	4.38	0.06	0.00	0.00	0.44	0.00	0.04	0.10	0.00	0.09	0.01	0.00	100.30	2014	NIP 13 18 lake
1699	189	38.93	0.01	0.00	0.00	0.00	0.00	0.40	0.00	55.52	5.24	0.09	0.00	0.00	0.00	0.01	0.0								

INDEX	No.	O	Na	K	V	Co	Mg	P	Cr	Fe	Al	S	Ni	Mn	Si	Pb	Cu	Ti	Ca	Zn	Ba	Sr	Total	Year	Sample
1950	118	37.81	0.00	0.00	0.00	0.08	0.08	1.04	0.02	59.97	0.00	0.02	0.04	0.02	0.17	0.03	0.02	0.01	0.01	0.00	0.00	0.00	99.28	2016	BAH F124-1232.6
1951	119	38.22	0.00	0.02	0.00	0.05	0.00	0.83	0.05	59.75	0.00	0.00	0.01	0.07	0.29	0.07	0.10	0.01	0.00	0.04	0.00	0.00	99.52	2016	BAH F124-1232.7
1952	120	38.04	0.00	0.00	0.08	0.09	0.00	0.96	0.02	59.07	0.01	0.00	0.04	0.05	0.32	0.07	0.16	0.00	0.00	0.01	0.00	0.00	98.90	2016	BAH F124-1232.8
1953	121	38.54	0.00	0.00	0.00	0.00	0.01	1.08	0.02	58.78	0.01	0.00	0.02	0.07	0.33	0.10	0.20	0.00	0.00	0.03	0.00	0.00	99.19	2016	BAH F124-1232.9
1954	127	38.33	0.00	0.01	0.00	0.08	0.02	1.13	0.00	58.38	0.34	0.00	0.00	0.06	0.28	0.03	0.20	0.00	0.00	0.02	0.00	0.00	98.88	2016	BAH F124-1237-1
1955	128	36.92	0.00	0.00	0.01	0.08	0.01	0.98	0.02	59.07	0.01	0.00	0.01	0.04	0.34	0.13	0.20	0.00	0.00	0.11	0.00	0.00	97.93	2016	BAH F124-1237-2
1956	129	37.64	0.00	0.00	0.01	0.07	0.00	1.04	0.00	58.57	0.01	0.00	0.05	0.08	0.35	0.01	0.19	0.00	0.00	0.00	0.00	0.00	98.02	2016	BAH F124-1237-3
1957	130	38.23	0.00	0.00	0.02	0.05	0.01	1.06	0.01	58.62	0.00	0.00	0.03	0.04	0.34	0.11	0.06	0.00	0.00	0.01	0.00	0.00	98.58	2016	BAH F124-1237-4
1958	131	36.88	0.00	0.00	0.02	0.08	0.00	0.97	0.00	58.89	0.01	0.01	0.01	0.07	0.31	0.06	0.12	0.00	0.00	0.07	0.00	0.00	97.50	2016	BAH F124-1237-5
1959	132	38.10	0.01	0.00	0.01	0.10	0.00	1.10	0.00	58.65	0.03	0.02	0.05	0.01	0.24	0.00	0.09	0.00	0.00	0.07	0.00	0.00	98.47	2016	BAH F124-1237-6
1960	26	36.19	0.00	0.00	0.00	0.04	0.00	0.85	0.00	59.25	0.00	0.00	0.02	0.04	0.31	0.00	0.04	0.02	0.00	0.00	0.00	0.00	96.78	2016	BAH F226-1822 stalagmite
1961	27	36.14	0.00	0.00	0.02	0.09	0.00	0.94	0.02	59.39	0.01	0.01	0.05	0.05	0.09	0.30	0.04	0.02	0.00	0.00	0.02	0.00	97.14	2016	BAH F226-1822 stalagmite
1962	28	37.22	0.00	0.01	0.04	0.06	0.00	0.82	0.00	60.88	0.00	0.00	0.08	0.05	0.19	0.00	0.00	0.03	0.00	0.08	0.00	0.00	99.46	2016	BAH F226-1822 stalagmite
1963	29	37.48	0.00	0.00	0.02	0.09	0.00	0.94	0.00	59.39	0.00	0.01	0.03	0.02	0.28	0.07	0.05	0.01	0.00	0.07	0.00	0.00	98.47	2016	BAH F226-1822 stalagmite
1964	30	37.47	0.00	0.00	0.00	0.06	0.00	2.00	0.00	57.14	0.01	0.00	0.00	0.12	0.33	0.06	0.30	0.00	0.00	0.00	0.00	0.00	97.62	2016	BAH F226-1822 stalagmite
1965	31	38.06	0.00	0.00	0.00	0.05	0.04	1.77	0.01	56.98	0.00	0.00	0.05	0.15	0.41	0.01	0.34	0.00	0.03	0.04	0.00	0.00	97.88	2016	BAH F226-1822 stalagmite
1966	32	38.18	0.00	0.00	0.02	0.09	0.00	1.84	0.00	56.47	0.00	0.01	0.04	0.14	0.41	0.05	0.28	0.00	0.02	0.08	0.00	0.00	97.62	2016	BAH F226-1822 stalagmite
1967	33	37.36	0.00	0.00	0.02	0.10	0.02	1.55	0.00	57.12	0.00	0.01	0.02	0.25	0.42	0.02	0.66	0.00	0.00	0.03	0.00	0.00	97.58	2016	BAH F226-1822 stalagmite
1968	34	37.94	0.00	0.01	0.00	0.09	0.02	2.03	0.01	57.12	0.00	0.00	0.00	0.14	0.31	0.01	0.30	0.01	0.01	0.09	0.00	0.00	98.07	2016	BAH F226-1822 stalagmite
1969	35	38.26	0.00	0.00	0.03	0.04	0.03	2.25	0.01	57.08	0.00	0.00	0.04	0.11	0.27	0.08	0.53	0.04	0.06	0.08	0.00	0.00	98.57	2016	BAH F226-1822 stalagmite
1970	36	37.08	0.00	0.01	0.02	0.03	0.01	1.95	0.00	57.55	0.00	0.00	0.00	0.07	0.34	0.00	0.23	0.00	0.03	0.10	0.00	0.00	97.40	2016	BAH F226-1822 stalagmite
1971	37	37.99	0.00	0.00	0.00	0.07	0.02	2.05	0.02	56.60	0.00	0.00	0.01	0.11	0.34	0.10	0.33	0.01	0.05	0.08	0.00	0.00	97.78	2016	BAH F226-1822 stalagmite
1972	106	36.15	0.00	0.00	0.01	0.06	0.04	0.80	0.02	61.41	0.00	0.00	0.03	0.07	0.50	0.03	0.99	0.00	0.00	0.05	0.00	0.00	100.17	2016	BAH F282-118-2.brown
1973	107	36.32	0.00	0.00	0.03	0.07	0.03	0.81	0.01	60.82	0.00	0.00	0.01	0.09	0.52	0.08	0.90	0.00	0.00	0.07	0.00	0.00	99.77	2016	BAH F282-118-2.brown
1974	108	36.57	0.00	0.00	0.00	0.00	0.00	0.77	0.00	61.79	0.00	0.00	0.00	0.11	0.40	0.00	0.88	0.00	0.00	0.00	0.00	0.00	100.02	2016	BAH F282-118-2.brown
1975	109	36.48	0.03	0.00	0.00	0.08	0.04	0.80	0.00	61.37	0.00	0.03	0.02	0.06	0.51	0.02	1.01	0.00	0.00	0.06	0.00	0.00	100.51	2016	BAH F282-118-2.brown
1976	110	36.64	0.00	0.00	0.03	0.04	0.03	0.74	0.02	61.78	0.00	0.01	0.00	0.09	0.51	0.00	1.08	0.00	0.00	0.10	0.00	0.00	101.08	2016	BAH F282-118-2.brown
1977	111	36.55	0.00	0.00	0.00	0.10	0.04	0.77	0.00	61.49	0.01	0.01	0.00	0.06	0.51	0.05	1.04	0.00	0.00	0.09	0.00	0.00	100.70	2016	BAH F282-118-2.brown
1978	112	36.36	0.02	0.00	0.01	0.03	0.05	0.77	0.00	61.47	0.01	0.00	0.04	0.07	0.51	0.00	0.96	0.00	0.00	0.07	0.00	0.00	100.37	2016	BAH F282-118-2.brown
1979	100	35.06	0.00	0.00	0.00	0.00	0.00	0.54	0.00	59.67	0.02	0.05	0.02	0.04	0.30	0.00	0.88	0.00	0.00	0.00	0.00	0.00	95.37	2016	BAH F282-118.4_1
1980	101	35.26	0.00	0.00	0.02	0.06	0.02	0.45	0.02	60.73	0.07	0.00	0.06	0.02	0.25	0.00	0.17	0.00	0.00	0.00	0.00	0.00	97.13	2016	BAH F282-118.4_2
1981	102	35.64	0.01	0.01	0.08	0.05	0.03	0.44	0.00	60.82	0.22	0.01	0.11	0.00	0.26	0.05	0.30	0.00	0.00	0.07	0.00	0.00	98.09	2016	BAH F282-118.4_3
1982	103	37.36	0.00	0.00	0.02	0.14	0.02	0.51	0.00	60.25	0.00	0.00	0.03	0.00	0.30	0.05	0.00	0.00	0.00	0.00	0.00	0.00	98.68	2016	BAH F282-118.4_4
1983	104	35.97	0.00	0.00	0.02	0.09	0.01	0.46	0.02	60.89	0.13	0.00	0.02	0.04	0.27	0.07	0.18	0.05	0.00	0.09	0.00	0.00	98.31	2016	BAH F282-118.4_5
1984	105	36.15	0.00	0.00	0.00	0.00	0.00	0.50	0.04	54.54	0.23	0.00	0.00	0.03	0.14	0.00	0.34	0.00	0.00	0.00	0.00	0.00	99.52	2016	BAH F282-118.4_6
1985	38	36.66	0.01	0.00	0.01	0.06	0.00	0.39	0.01	63.03	0.12	0.01	0.02	0.02	0.12	0.00	0.07	0.00	0.00	0.00	0.00	0.00	100.52	2016	BAH F282-120.5_brown
1986	39	35.23	0.01	0.00	0.02	0.08	0.00	0.39	0.05	64.37	0.21	0.03	0.01	0.02	0.14	0.02	0.09	0.00	0.00	0.00	0.00	0.00	100.67	2016	BAH F282-120.5_brown
1987	40	34.70	0.00	0.00	0.00	0.06	0.00	0.42	0.01	63.99	0.22	0.01	0.00	0.02	0.13	0.02	0.06	0.00	0.00	0.00	0.00	0.00	99.65	2016	BAH F282-120.5_brown
1988	41	35.75	0.00	0.00	0.00	0.06	0.00	0.40	0.00	63.75	0.11	0.01	0.03	0.00	0.13	0.11	0.04	0.05	0.00	0.02	0.00	0.00	100.45	2016	BAH F282-120.5_brown
1989	42	35.26	0.07	0.00	0.01	0.00	0.00	0.41	0.02	63.25	0.11	0.01	0.00	0.01	0.12	0.25	0.00	0.00	0.00	0.00	0.00	0.00	99.37	2016	BAH F282-120.5_brown
1990	43	35.46	0.04	0.00	0.00	0.06	0.00	0.47	0.03	63.28	0.13	0.02	0.00	0.00	0.12	0.04	0.08	0.00	0.00	0.00	0.00	0.00	99.73	2016	BAH F282-120.5_brown
1991	44	34.93	0.02	0.00	0.01	0.08	0.02	0.39	0.01	63.61	0.15	0.03	0.06	0.04	0.13	0.04	0.10	0.00	0.00	0.03	0.00	0.00	99.65	2016	BAH F282-120.5_brown
1992	45	35.60	0.02	0.00	0.03	0.08	0.02	0.53	0.03	64.22	0.58	0.06	0.02	0.09	0.23	0.08	0.18	0.01	0.00	0.00	0.00	0.00	101.75	2016	BAH F282-120.5_brown
1993	46	32.37	0.00	0.00	0.00	0.08	0.00	0.48	0.00	64.69	0.53	0.03	0.00	0.06	0.17	0.06	0.15	0.00	0.00	0.01	0.00	0.00	98.63	2016	BAH F282-120.5_brown
1994	47	35.89	0.00	0.00	0.00	0.00	0.00	0.46	0.00	63.90	0.26	0.05	0.00	0.07	0.13	0.00	0.08	0.00	0.00	0.00	0.00	0.00	101.06	2016	BAH F282-120.5_brown
1995	72	37.06	0.00	0.01	0.01	0.08	0.05	0.67	0.00	56.78	0.01	0.00	0.01	0.05	1.49	0.08	0.35	0.05	0.03	0.07	0.00	0.00	96.80	2016	BAH F282-124.9 stalagmite
1996	73	36.92	0.00	0.02	0.03	0.04	0.00	0.75	0.00	57.73	0.01	0.00	0.02	0.04	1.03	0.03	0.34	0.01	0.00	0.03	0.00	0.00	96.96	2016	BAH F282-124.9 stalagmite
1997	74	37.98	0.00	0.00	0.00	0.06	0.08	0.63	0.01	58.02	0.01	0.00	0.01	0.02	1.23	0.11	0.35	0.01	0.00	0.02	0.00	0.00	98.83	2016	BAH F282-124.9 stalagmite
1998	75	37.44	0.01	0.00	0.00	0.06	0.04	0.70	0.00	58.08	0.00	0.02	0.00	0.02	1.15	0.03	0.24	0.00	0.04	0.04	0.00	0.00	97.54	2016	

INDEX	No.	O	Na	K	V	Co	Mg	P	Cr	Fe	Al	S	Ni	Mn	Si	Pb	Cu	Ti	Ca	Zn	Ba	Sr	Total	Year	Sample
2100	5432	40.83	0.01	0.01	0.07	0.00	0.04	0.40	0.03	0.31	38.31	10.31	0.02	0.00	0.08	8.49	0.04	0.07	0.17	0.03	0.99	0.03	19903	2016	BOI-002
2101	5433	41.32	0.00	0.03	0.05	0.00	0.04	0.35	0.11	40.18	9.52	0.04	0.01	0.11	7.55	0.05	0.02	0.30	0.08	0.07			9983	2016	BOI-002
2102	5540	41.60	0.03	0.02	0.04	0.02	0.02	0.23	0.22	37.69	9.19	0.02	0.01	0.03	7.44	0.03	0.03	0.18	0.02	0.03			9685	2016	BOI-002_G2
2103	5541	40.75	0.03	0.02	0.07	0.02	0.01	0.25	0.22	45.47	6.83	0.02	0.00	0.03	5.08	0.04	0.07	0.22	0.04	0.02			9919	2016	BOI-002_G2
2104	5542	40.59	0.00	0.02	0.08	0.02	0.01	0.25	0.21	45.53	7.26	0.01	0.00	0.06	5.42	0.05	0.04	0.19	0.04	0.10			9989	2016	BOI-002_G2
2105	5543	41.96	0.01	0.04	0.04	0.00	0.03	0.23	0.18	39.24	8.76	0.02	0.04	0.02	6.94	0.01	0.06	0.23	0.03	0.08			9732	2016	BOI-002_G2
2106	5544	41.59	0.03	0.03	0.08	0.00	0.01	0.21	0.19	41.46	7.98	0.03	0.00	0.13	6.27	0.04	0.03	0.19	0.03	0.09			9840	2016	BOI-002_G2
2107	5546	40.36	0.05	0.02	0.01	0.02	0.03	0.29	0.03	49.51	5.81	0.01	0.04	0.15	4.83	0.06	0.00	0.16	0.04	0.00			10143	2016	BOI-002_G2
2108	5551	39.35	0.02	0.03	0.02	0.07	0.03	0.33	0.03	50.16	5.06	0.03	0.05	0.16	4.86	0.00	0.05	0.10	0.05	0.06			10044	2016	BOI-002_G2 (continued)
2109	5552	39.50	0.02	0.04	0.03	0.01	0.03	0.36	0.02	47.67	5.83	0.02	0.00	0.15	5.27	0.04	0.06	0.25	0.05	0.07			9944	2016	BOI-002_G2 (continued)
2110	5553	33.69	0.02	0.00	0.10	0.03	0.00	0.36	0.15	59.67	2.10	0.02	0.04	0.06	1.11	0.03	0.08	0.07	0.03	0.04			9762	2016	BOI-002_G2 (continued)
2111	5457	38.39	0.04	0.01	0.11	0.03	0.03	0.19	0.00	51.56	7.00	0.04	0.00	0.29	2.91	0.01	0.02	0.14	0.07	0.02			10057	2016	BOI-004
2112	5459	37.38	0.05	0.01	0.08	0.00	0.07	0.38	0.00	45.69	9.56	0.06	0.00	0.02	5.10	0.00	0.03	0.44	0.17	0.14			9918	2016	BOI-004
2113	5461	35.96	0.06	0.01	0.08	0.00	0.04	0.23	0.03	50.78	7.21	0.05	0.00	0.01	3.45	0.03	0.05	0.19	0.14	0.01			9834	2016	BOI-004
2114	5462	37.32	0.03	0.01	0.06	0.00	0.04	0.15	0.00	55.79	5.30	0.05	0.00	0.01	2.06	0.00	0.03	0.13	0.00	0.00			10107	2016	BOI-004
2115	5463	38.36	0.00	0.02	0.09	0.00	0.04	0.23	0.01	51.82	6.59	0.03	0.00	0.03	2.82	0.04	0.05	0.18	0.09	0.00			10041	2016	BOI-004
2116	5464	39.33	0.02	0.01	0.11	0.00	0.05	0.22	0.00	49.54	8.00	0.02	0.00	0.01	3.53	0.00	0.02	0.33	0.07	0.05			10133	2016	BOI-004
2117	5465	38.81	0.02	0.02	0.12	0.00	0.03	0.15	0.03	50.49	6.94	0.02	0.00	0.00	2.72	0.04	0.00	0.59	0.06	0.04			10008	2016	BOI-004
2118	5467	39.45	0.02	0.01	0.16	0.00	0.02	0.16	0.00	51.97	6.74	0.04	0.00	0.04	2.32	0.00	0.01	0.11	0.07	0.05			10118	2016	BOI-004
2119	5468	38.18	0.00	0.09	0.00	0.00	0.06	0.29	0.00	47.77	8.96	0.08	0.00	0.00	4.79	0.00	0.02	0.21	0.27	0.08			10086	2016	BOI-004
2120	5469	36.30	0.02	0.01	0.09	0.00	0.05	0.29	0.05	55.09	7.78	0.04	0.01	0.00	2.86	0.00	0.03	0.18	0.13	0.10			9497	2016	BOI-004
2121	5434	37.65	0.02	0.02	0.04	0.00	0.01	0.04	0.01	57.12	3.32	0.01	0.02	0.00	1.00	0.00	0.00	0.09	0.01	0.00			9935	2016	BOI-013
2122	5435	38.40	0.00	0.00	0.00	0.01	0.00	0.05	0.00	57.23	3.33	0.01	0.00	0.00	0.75	0.00	0.01	0.03	0.00	0.00			9982	2016	BOI-013
2123	5436	37.83	0.01	0.07	0.04	0.00	0.00	0.10	0.03	58.20	2.73	0.05	0.03	0.01	0.89	0.09	0.02	0.02	0.01	0.05			10017	2016	BOI-013
2124	5437	38.15	0.01	0.07	0.04	0.00	0.00	0.12	0.00	57.09	3.75	0.05	0.00	0.00	0.83	0.06	0.03	0.03	0.03	0.03			10029	2016	BOI-013
2125	5438	32.38	0.00	0.00	0.04	0.00	0.00	0.06	0.02	55.46	1.97	0.06	0.01	0.02	0.83	0.08	0.01	0.00	0.02	0.00			9093	2016	BOI-013
2126	5439	36.80	0.00	0.01	0.00	0.03	0.00	0.06	0.00	57.67	3.54	0.04	0.02	0.04	0.83	0.08	0.00	0.03	0.03	0.00			9917	2016	BOI-013
2127	5440	37.50	0.02	0.00	0.12	0.00	0.00	0.06	0.01	55.88	4.07	0.04	0.00	0.00	0.52	0.00	0.03	0.07	0.02	0.07			9840	2016	BOI-013
2128	5441	38.52	0.01	0.01	0.07	0.00	0.00	0.11	0.01	56.64	3.57	0.04	0.02	0.00	0.72	0.07	0.07	0.06	0.02	0.01			9995	2016	BOI-013
2129	5442	37.80	0.04	0.00	0.03	0.00	0.00	0.13	0.00	56.52	3.55	0.03	0.01	0.01	0.41	0.00	0.02	0.05	0.03	0.01			9914	2016	BOI-013
2130	5443	38.93	0.01	0.01	0.03	0.00	0.00	0.08	0.00	56.73	3.85	0.04	0.00	0.03	0.49	0.00	0.00	0.09	0.01	0.02			10032	2016	BOI-013
2131	5444	37.30	0.02	0.07	0.40	0.00	0.00	0.48	0.01	57.52	4.24	0.03	0.00	0.03	1.46	0.04	0.02	0.05	0.04	0.04			10173	2016	BOI-014
2132	5445	37.24	0.03	0.00	0.36	0.00	0.01	0.45	0.00	56.52	4.21	0.04	0.00	0.00	1.77	0.00	0.00	0.02	0.02	0.02			10070	2016	BOI-014
2133	5446	36.62	0.03	0.02	0.28	0.01	0.00	0.39	0.00	57.03	3.98	0.02	0.00	0.00	1.60	0.09	0.00	0.09	0.03	0.07			10026	2016	BOI-014
2134	5447	37.89	0.06	0.00	0.38	0.00	0.00	0.47	0.01	55.77	4.59	0.04	0.00	0.00	1.20	0.00	0.02	0.05	0.03	0.01			10135	2016	BOI-014
2135	5448	37.89	0.05	0.00	0.25	0.00	0.00	0.38	0.01	52.96	4.84	0.03	0.00	0.01	3.03	0.04	0.01	0.00	0.03	0.03			9955	2016	BOI-014
2136	5449	35.78	0.00	0.00	0.42	0.00	0.01	0.52	0.00	57.61	3.94	0.03	0.00	0.00	0.97	0.00	0.00	0.06	0.02	0.05			9941	2016	BOI-014
2137	5450	35.82	0.03	0.00	0.33	0.00	0.00	0.46	0.00	58.22	3.96	0.03	0.00	0.00	1.63	0.09	0.01	0.01	0.04	0.10			10075	2016	BOI-014
2138	5452	36.91	0.04	0.00	0.33	0.01	0.01	0.39	0.00	57.83	3.89	0.02	0.00	0.00	1.90	0.00	0.04	0.04	0.04	0.05			10146	2016	BOI-014
2139	5453	36.75	0.00	0.01	0.45	0.00	0.01	0.45	0.00	58.44	3.85	0.03	0.00	0.00	1.45	0.00	0.03	0.06	0.03	0.00			10101	2016	BOI-014
2140	5554	36.74	0.02	0.02	0.24	0.02	0.00	0.26	0.01	55.39	3.94	0.02	0.00	0.02	2.19	0.00	0.00	0.04	0.02	0.06			9899	2016	BOI-014
2141	5555	38.38	0.03	0.00	0.22	0.03	0.00	0.22	0.00	52.57	4.92	0.03	0.01	0.01	3.26	0.04	0.00	0.05	0.04	0.06			9989	2016	BOI-014
2142	5556	37.47	0.02	0.01	0.45	0.03	0.00	0.60	0.00	55.53	4.69	0.03	0.01	0.05	1.23	0.21	0.02	0.02	0.04	0.00			10041	2016	BOI-014
2143	5557	36.56	0.05	0.03	0.33	0.04	0.00	0.45	0.00	56.91	4.45	0.02	0.02	0.00	1.33	0.00	0.03	0.05	0.03	0.01			10031	2016	BOI-014
2144	5558	37.07	0.04	0.01	0.37	0.04	0.01	0.47	0.03	56.89	4.40	0.04	0.00	0.00	1.44	0.00	0.02	0.05	0.03	0.01			10003	2016	BOI-014
2145	5559	35.90	0.03	0.00	0.45	0.00	0.01	0.43	0.00	58.20	4.43	0.02	0.00	0.01	0.49	0.04	0.00	0.04	0.04	0.01			10011	2016	BOI-014
2146	5629	29.39	0.04	0.01	0.04	0.03	0.05	0.51	0.00	63.72	1.08	0.00	0.00	0.01	0.05	0.03	0.00	0.64	0.14	0.00	-	-	9574	2016	G-12-01A
2147	5637	31.66	0.05	0.02	0.00	0.00	0.03	0.57	0.02	64.91	0.89	0.00	0.00	0.00	0.10	0.10	0.02	0.42	0.15	0.10	-	-	9904	2016	G-12-01A (continued)
2148	5609	34.01	0.02	0.01	0.07	0.03	0.05	0.65	0.01	61.55	1.67	0.00	0.00	0.06	0.07	0.14	0.02	2.08	0.19	0.03	-	-	10066	2016	G-12-01B
2149	5620	32.07	0.00	0.00	0.04	0.01	0.03	0.51	0.02	65.36	0.98	0.00	0.01	0.00	0.09	0.01	0.00	0.52	0.13	0.00	-	-	9977	2016	G-12-01B
2150	222	37.21	0.00	0.00	0.00	0.05	0.00	0.53	0.00	57.48	0.79	0.05	0.04	0.06	1.30	0.05	0.14	0.00	0.00	0.00			9906	2016	BAH-100-BI-2.1
2151	231	36.40	0.02	0.01	0.04	0.07	0.00	0.41	0.02	58.26	0.86	0.04	0.00	0.09	1.36	0.02	0.14	0.00	0.00	0.03			9903	2016	BAH-100-BI-2.10
2152	232	37.26	0.00	0.00	0.04																				

INDEX	No.	O	Na	K	V	Co	Mg	P	Cr	Fe	Al	S	Ni	Mn	Si	Pb	Cu	Ti	Ca	Zn	Ba	Sr	Total	Year	Sample
2250	219	37.08	0.00	0.00	0.02	0.04	0.01	1.51	0.03	60.07	0.01	0.01	0.04	0.05	0.30	0.01	2.85	0.00	0.00	0.00	0.00	0.00	101.97	2016	BAH-03cm6_13
2251	220	37.09	0.00	0.00	0.00	0.04	0.03	1.56	0.00	59.74	0.02	0.00	0.03	0.07	0.29	0.00	2.78	0.01	0.00	0.04	0.00	0.00	101.70	2016	BAH-03cm6_14
2252	209	37.25	0.00	0.00	0.00	0.10	0.01	1.47	0.00	59.57	0.00	0.01	0.00	0.03	0.27	0.00	2.79	0.00	0.01	0.01	0.00	0.00	101.53	2016	BAH-03cm6_3
2253	210	37.33	0.00	0.01	0.05	0.05	0.03	1.51	0.02	59.60	0.01	0.00	0.05	0.23	0.27	0.05	2.72	0.00	0.00	0.02	0.00	0.00	101.93	2016	BAH-03cm6_4
2254	211	37.31	0.00	0.00	0.00	0.04	0.01	1.52	0.00	59.81	0.01	0.00	0.00	0.06	0.30	0.00	2.77	0.02	0.00	0.00	0.00	0.00	101.85	2016	BAH-03cm6_5
2255	212	37.72	0.01	0.00	0.00	0.06	0.00	1.48	0.00	58.94	0.01	0.03	0.02	0.12	0.31	0.00	2.80	0.00	0.00	0.07	0.00	0.00	101.57	2016	BAH-03cm6_5
2256	214	37.71	0.00	0.00	0.01	0.07	0.02	1.42	0.00	57.29	0.01	0.00	0.00	0.50	0.27	0.03	2.88	0.05	0.00	0.05	0.00	0.00	100.30	2016	BAH-03cm6_8
2257	215	36.95	0.00	0.01	0.00	0.03	0.01	1.50	0.00	60.20	0.00	0.01	0.00	0.04	0.31	0.02	2.84	0.01	0.00	0.06	0.00	0.00	101.99	2016	BAH-03cm6_9
2258	186	36.08	0.04	0.02	0.02	0.07	0.03	0.43	0.03	63.42	0.22	0.01	0.03	0.05	0.13	0.09	0.09	0.00	0.00	0.06	0.00	0.00	100.76	2016	BAH-100_1
2259	195	30.46	0.00	0.00	0.00	0.07	0.00	0.46	0.00	55.90	0.05	0.00	0.04	0.03	0.09	0.00	0.00	0.00	0.00	0.03	0.00	0.00	87.11	2016	BAH-100_10
2260	196	36.42	0.00	0.00	0.00	0.08	0.00	0.49	0.00	60.55	0.00	0.00	0.00	0.00	0.00	0.00	0.10	0.00	0.00	0.00	0.00	0.00	97.68	2016	BAH-100_11
2261	187	36.61	0.00	0.00	0.00	0.10	0.02	0.40	0.00	63.56	0.21	0.02	0.03	0.02	0.13	0.03	0.11	0.00	0.00	0.05	0.00	0.00	101.28	2016	BAH-100_2
2262	188	35.16	0.00	0.00	0.02	0.03	0.01	0.40	0.00	63.54	0.17	0.03	0.01	0.03	0.15	0.09	0.10	0.02	0.00	0.00	0.00	0.00	99.76	2016	BAH-100_3
2263	189	35.34	0.00	0.00	0.00	0.07	0.02	0.41	0.01	63.74	0.21	0.02	0.00	0.04	0.16	0.00	0.09	0.00	0.00	0.00	0.00	0.00	100.11	2016	BAH-100_4
2264	190	35.27	0.00	0.00	0.00	0.08	0.00	0.40	0.00	63.45	0.18	0.02	0.01	0.05	0.14	0.05	0.02	0.00	0.00	0.00	0.00	0.00	99.73	2016	BAH-100_5
2265	191	36.10	0.00	0.00	0.03	0.07	0.00	0.40	0.01	62.85	0.15	0.01	0.05	0.04	0.04	0.09	0.00	0.00	0.07	0.00	0.00	0.00	99.99	2016	BAH-100_6
2266	192	36.51	0.00	0.00	0.00	0.10	0.02	0.38	0.00	62.84	0.10	0.02	0.03	0.01	0.11	0.17	0.11	0.00	0.00	0.00	0.00	0.00	100.40	2016	BAH-100_7
2267	193	33.66	0.00	0.00	0.00	0.06	0.00	0.54	0.02	60.21	0.04	0.00	0.00	0.01	0.10	0.07	0.04	0.00	0.00	0.04	0.00	0.00	94.80	2016	BAH-100_8
2268	194	30.41	0.00	0.00	0.01	0.05	0.01	0.44	0.00	57.44	0.03	0.01	0.05	0.04	0.11	0.03	0.02	0.02	0.00	0.07	0.00	0.00	88.74	2016	BAH-100_9
2269	151	36.23	0.00	0.00	0.00	0.05	0.00	0.50	0.00	58.65	0.09	0.00	0.00	0.28	1.42	0.03	1.60	0.02	0.00	0.06	0.00	0.00	101.07	2016	BAH-F124-1112_10
2270	152	37.35	0.00	0.01	0.05	0.03	0.00	0.30	0.00	58.50	0.12	0.00	0.00	0.00	1.95	0.37	0.02	1.75	0.00	0.01	0.00	0.00	101.40	2016	BAH-F124-1112_11
2271	153	37.70	0.00	0.00	0.02	0.07	0.04	0.85	0.00	59.95	0.13	0.00	0.00	1.04	0.55	0.00	1.49	0.00	0.00	0.04	0.00	0.00	101.88	2016	BAH-F124-1112_12
2272	154	37.72	0.00	0.01	0.04	0.06	0.02	0.87	0.00	58.51	0.12	0.00	0.06	0.93	0.57	0.09	1.60	0.03	0.00	0.02	0.00	0.00	100.63	2016	BAH-F124-1112_13
2273	156	37.10	0.00	0.00	0.00	0.13	0.02	0.82	0.01	59.22	0.15	0.00	0.01	1.10	0.58	0.04	1.57	0.00	0.00	0.00	0.00	0.00	100.75	2016	BAH-F124-1112_15
2274	157	38.84	0.00	0.00	0.00	0.09	0.04	0.84	0.00	59.14	0.14	0.01	0.00	1.33	0.63	0.00	1.62	0.00	0.00	0.00	0.00	0.00	101.89	2016	BAH-F124-1112_16
2275	143	36.37	0.00	0.00	0.00	0.08	0.05	0.60	0.01	60.51	0.17	0.01	0.02	2.08	0.21	0.03	1.55	0.05	0.00	0.07	0.00	0.00	101.80	2016	BAH-F124-1112_2
2276	162	36.62	0.00	0.01	0.01	0.07	0.01	0.59	0.04	59.08	0.16	0.01	0.02	2.93	0.25	0.02	1.86	0.00	0.00	0.00	0.00	0.00	101.66	2016	BAH-F124-1112_21
2277	163	37.88	0.00	0.00	0.02	0.09	0.04	0.31	0.01	59.45	0.00	0.00	0.00	0.04	0.96	0.00	0.02	0.02	0.00	0.00	0.00	0.00	98.84	2016	BAH-F124-1112_22
2278	145	36.10	0.00	0.00	0.00	0.07	0.05	0.46	0.02	59.81	0.14	0.00	0.00	2.75	0.48	0.00	1.46	0.01	0.00	0.01	0.00	0.00	101.36	2016	BAH-F124-1112_24
2279	146	36.75	0.00	0.00	0.00	0.02	0.00	0.49	0.00	59.96	0.11	0.00	0.00	0.27	0.17	0.05	2.50	0.02	0.20	0.10	0.00	0.00	100.75	2016	BAH-F124-1112_5
2280	148	36.53	0.00	0.00	0.00	0.09	0.03	0.57	0.03	61.68	0.04	0.04	0.00	0.82	0.20	0.04	0.70	0.01	0.00	0.06	0.00	0.00	100.86	2016	BAH-F124-1112_7
2281	149	35.95	0.00	0.00	0.00	0.07	0.01	0.61	0.01	60.51	0.15	0.01	0.00	2.47	0.29	0.00	1.64	0.00	0.00	0.02	0.00	0.00	101.73	2016	BAH-F124-1112_8
2282	221	37.82	0.00	0.00	0.01	0.05	0.02	1.65	0.03	49.62	0.10	0.00	0.00	4.91	0.18	0.02	4.13	0.04	0.00	0.00	0.00	0.00	98.56	2016	IBH-13-03 top crust_1
2283	230	37.86	0.00	0.00	0.00	0.07	0.01	1.57	0.02	51.00	0.05	0.00	0.00	5.36	0.17	0.00	4.26	0.01	0.00	0.04	0.00	0.00	100.41	2016	IBH-13-03 top crust_10
2284	231	37.65	0.00	0.00	0.00	0.00	0.00	1.63	0.00	52.66	0.03	0.00	0.00	4.02	0.13	0.00	3.96	0.00	0.00	0.00	0.00	0.00	100.50	2016	IBH-13-03 top crust_11
2285	232	37.89	0.00	0.00	0.02	0.07	0.02	1.88	0.00	53.01	0.03	0.00	0.03	3.14	0.19	0.00	3.95	0.00	0.00	0.07	0.00	0.00	100.28	2016	IBH-13-03 top crust_12
2286	233	37.76	0.00	0.00	0.01	0.07	0.00	1.71	0.00	52.79	0.02	0.00	0.01	3.91	0.18	0.01	3.94	0.00	0.01	0.04	0.00	0.00	100.47	2016	IBH-13-03 top crust_13
2287	234	38.48	0.00	0.00	0.00	0.08	0.02	2.94	0.00	54.16	0.00	0.02	0.00	0.33	0.18	0.08	2.52	0.02	0.20	0.00	0.00	0.00	99.03	2016	IBH-13-03 top crust_14
2288	235	39.58	0.00	0.00	0.01	0.08	0.01	3.07	0.01	54.08	0.00	0.00	0.02	0.34	0.16	0.02	2.51	0.05	0.18	0.08	0.00	0.00	100.20	2016	IBH-13-03 top crust_15
2289	236	38.11	0.00	0.00	0.00	0.00	0.00	2.85	0.11	54.15	0.00	0.00	0.00	0.17	0.05	0.27	2.50	0.02	0.20	0.00	0.00	0.00	98.87	2016	IBH-13-03 top crust_16
2290	237	38.38	0.00	0.00	0.05	0.06	0.00	2.99	0.02	54.61	0.00	0.00	0.00	0.29	0.19	0.00	2.48	0.01	0.18	0.05	0.00	0.00	99.31	2016	IBH-13-03 top crust_17
2291	238	38.12	0.00	0.00	0.01	0.02	0.02	3.20	0.00	54.09	0.00	0.00	0.00	0.29	0.18	0.00	2.64	0.00	0.23	0.11	0.00	0.00	98.90	2016	IBH-13-03 top crust_18
2292	222	38.04	0.00	0.00	0.00	0.07	0.02	1.92	0.00	51.41	0.07	0.02	0.02	2.97	0.22	0.00	4.24	0.00	0.00	0.07	0.00	0.00	98.76	2016	IBH-13-03 top crust_2
2293	223	37.71	0.00	0.00	0.00	0.07	0.00	1.68	0.01	50.15	0.08	0.01	0.00	4.51	0.18	0.00	4.34	0.01	0.03	0.07	0.00	0.00	98.75	2016	IBH-13-03 top crust_3
2294	224	37.64	0.00	0.00	0.00	0.10	0.00	1.73	0.00	53.84	0.03	0.00	0.01	3.49	0.13	0.00	3.18	0.00	0.00	0.13	0.00	0.00	100.27	2016	IBH-13-03 top crust_4
2295	225	37.20	0.00	0.00	0.00	0.07	0.03	1.83	0.00	56.56	0.04	0.00	0.03	2.30	0.16	0.03	3.17	0.00	0.06	0.00	0.00	0.00	101.48	2016	IBH-13-03 top crust_5
2296	226	37.08	0.00	0.00	0.02	0.06	0.03	1.78	0.00	56.35	0.05	0.00	0.03	2.49	0.15	0.12	3.15	0.02	0.02	0.02	0.00	0.00	101.46	2016	IBH-13-03 top crust_6
2297	227	37.52	0.00	0.00	0.02	0.03	0.01	1.78	0.00	53.19	0.05	0.00	0.01	3.18	0.17	0.04	3.29	0.02	0.00	0.10	0.00	0.00	99.40	2016	IBH-13-03 top crust_7
2298	228	37.57	0.00	0.00	0.00	0.05	0.00	1.77	0.04	54.02	0.03	0.02	0.05	3.55	0.14	0.00	3.39	0.00	0.02	0.04	0.00	0.00	100.68	2016	IBH-13-03 top crust_8
2299	229	37.69	0.00	0.00	0.0																				

INDEX	No.	O	Na	K	V	Co	Mg	P	Cr	Fe	Al	S	Ni	Mn	Si	Pb	Cu	Ti	Ca	Zn	Ba	Sr	Total	Year	Sample
2400	147	36.88	0.03	0.00	0.00	0.01	0.01	0.81	0.00	59.46	2.68	0.01	0.04	0.03	0.16	0.00	0.10	0.10	0.00	0.00	-	-	100.29	2016	MAC-61-2-3
2401	148	36.41	0.00	0.02	0.03	0.08	0.04	0.39	0.02	60.52	1.58	0.01	0.01	0.01	0.10	0.02	0.00	0.15	0.00	0.00	-	-	99.38	2016	MAC-61-2-4
2402	149	36.54	0.00	0.00	0.02	0.07	0.02	0.38	0.03	61.28	1.08	0.03	0.00	0.00	0.11	0.03	0.00	0.11	0.00	0.03	-	-	99.83	2016	MAC-61-2-5
2403	181	38.37	0.05	0.00	0.05	0.05	0.06	0.42	0.00	58.02	3.66	0.04	0.00	0.00	0.15	0.00	0.00	0.00	0.00	0.00	0.00	0.00	100.83	2016	Pic 06 242
2404	340	36.98	0.00	0.00	0.03	0.03	0.00	0.05	0.00	57.78	0.46	0.04	0.00	0.01	1.28	0.00	0.00	0.00	0.00	0.00	-	-	96.62	2016	Pic-06-04 gran 3
2405	162	32.56	0.12	0.01	0.00	0.07	0.06	0.13	0.03	65.76	0.78	0.08	0.00	0.00	0.49	0.00	0.00	0.16	0.07	0.00	-	-	100.30	2016	Pic-6-2-850um-4
2406	165	32.46	0.00	0.00	0.00	0.07	0.10	0.19	0.02	65.35	0.52	0.10	0.00	0.00	0.67	0.03	0.00	0.28	0.06	0.00	-	-	99.84	2016	Pic-6-2-850um-7
2407	166	31.86	0.00	0.00	0.00	0.08	0.08	0.21	0.00	65.58	0.54	0.09	0.00	0.00	0.65	0.05	0.00	0.32	0.05	0.00	-	-	99.51	2016	Pic-6-2-850um-8
2408	188	36.00	0.02	0.01	0.00	0.06	0.03	0.08	0.01	62.45	0.46	0.05	0.00	0.01	0.35	0.06	0.05	0.00	0.00	0.06	-	-	99.69	2016	Pic-6-22-Bt-Gt, K50-425um-2-4
2409	118	34.62	0.06	0.01	0.01	0.08	0.03	0.04	0.00	64.89	0.03	0.04	0.00	0.00	0.61	0.05	0.03	0.00	0.04	0.03	-	-	100.55	2016	Pic-6-2-11-Black-Gt-10
2410	119	34.21	0.06	0.00	0.00	0.10	0.04	0.09	0.00	64.76	0.01	0.03	0.00	0.02	0.44	0.06	0.01	0.00	0.01	0.00	-	-	99.82	2016	Pic-6-2-11-Black-Gt-11
2411	111	36.60	0.02	0.02	0.00	0.04	0.06	0.07	0.01	62.82	0.06	0.08	0.00	0.03	0.51	0.08	0.00	0.00	0.01	0.01	-	-	100.40	2016	Pic-6-2-11-Black-Gt-3
2412	114	37.21	0.00	0.03	0.01	0.06	0.02	0.09	0.00	62.51	0.07	0.03	0.00	0.00	0.38	0.05	0.00	0.02	0.00	0.01	-	-	100.47	2016	Pic-6-2-11-Black-Gt-6
2413	115	35.81	0.01	0.01	0.00	0.08	0.09	0.11	0.00	63.44	0.09	0.08	0.01	0.00	0.54	0.06	0.03	0.00	0.02	0.00	-	-	100.39	2016	Pic-6-2-11-Black-Gt-7
2414	116	35.01	0.07	0.00	0.00	0.08	0.07	0.13	0.00	64.06	0.00	0.09	0.00	0.02	0.60	0.00	0.01	0.01	0.06	0.05	-	-	100.34	2016	Pic-6-2-11-Black-Gt-8
2415	120	32.46	0.00	0.01	0.00	0.09	0.08	0.09	0.00	65.88	0.31	0.10	0.00	0.02	0.65	0.00	0.00	0.16	0.00	0.00	-	-	99.86	2016	Pic-6-2-3-Layered-Gt-1
2416	122	31.90	0.04	0.00	0.00	0.07	0.06	0.09	0.00	65.59	0.45	0.09	0.00	0.00	0.63	0.03	0.00	0.02	0.10	0.11	-	-	99.14	2016	Pic-6-2-3-Layered-Gt-3
2417	124	31.95	0.09	0.00	0.00	0.06	0.07	0.21	0.01	64.29	0.67	0.17	0.00	0.00	0.71	0.04	0.00	0.25	0.09	0.00	-	-	98.60	2016	Pic-6-2-3-Layered-Gt-5
2418	125	32.39	0.12	0.00	0.00	0.08	0.06	0.17	0.02	64.82	0.60	0.09	0.00	0.00	0.77	0.00	0.00	0.18	0.04	0.00	-	-	99.33	2016	Pic-6-2-3-Layered-Gt-6
2419	126	31.82	0.06	0.01	0.00	0.07	0.06	0.10	0.00	65.41	0.10	0.08	0.00	0.00	0.72	0.04	0.08	0.08	0.00	0.05	-	-	98.70	2016	Pic-6-2-3-Layered-Gt-7
2420	71	38.01	0.00	0.00	0.00	0.10	0.00	0.01	0.01	59.49	0.00	0.01	0.00	0.00	0.70	0.10	0.00	0.00	0.00	0.00	-	-	98.42	2016	Pic-6-21-6-Alpoor-Gt-1
2421	72	36.70	0.00	0.02	0.00	0.07	0.00	0.04	0.01	59.61	0.01	0.02	0.00	0.00	0.61	0.00	0.00	0.00	0.00	0.00	-	-	97.10	2016	Pic-6-21-6-Alpoor-Gt-2
2422	73	37.28	0.06	0.00	0.01	0.05	0.00	0.03	0.02	60.58	0.00	0.01	0.00	0.00	0.57	0.00	0.02	0.00	0.00	0.00	-	-	98.63	2016	Pic-6-21-6-Alpoor-Gt-3
2423	74	37.53	0.03	0.00	0.00	0.05	0.01	0.00	0.00	62.11	0.02	0.01	0.00	0.00	0.57	0.00	0.00	0.00	0.00	0.04	-	-	100.38	2016	Pic-6-21-6-Alpoor-Gt-4
2424	75	37.07	0.00	0.00	0.00	0.00	0.00	0.00	0.00	59.25	0.00	0.00	0.00	0.00	0.00	0.00	0.00	0.00	0.00	0.00	-	-	97.12	2016	Pic-6-21-6-Alpoor-Gt-5
2425	76	37.51	0.04	0.00	0.02	0.04	0.00	0.00	0.00	61.44	0.02	0.01	0.01	0.02	0.54	0.02	0.00	0.01	0.00	0.02	-	-	99.69	2016	Pic-6-21-6-Alpoor-Gt-6
2426	61	38.72	0.16	0.00	0.04	0.06	0.01	0.16	0.00	57.20	1.84	0.04	0.00	0.00	0.27	0.00	0.01	0.15	0.00	0.00	-	-	98.66	2016	Pic-6-21-6-Black-Dull-Gt
2427	62	38.96	0.03	0.02	0.00	0.06	0.00	0.10	0.01	57.14	1.82	0.02	0.00	0.00	0.26	0.02	0.00	0.15	0.00	0.06	-	-	98.66	2016	Pic-6-21-6-Black-Dull-Gt
2428	63	38.79	0.01	0.00	0.01	0.05	0.00	0.09	0.00	57.27	1.83	0.05	0.03	0.00	0.26	0.00	0.01	0.13	0.05	0.05	-	-	98.59	2016	Pic-6-21-6-Black-Dull-Gt
2429	64	39.24	0.03	0.00	0.02	0.05	0.01	0.14	0.03	57.27	1.78	0.05	0.03	0.00	0.27	0.04	0.00	0.11	0.00	0.05	-	-	99.06	2016	Pic-6-21-6-Black-Dull-Gt
2430	65	38.98	0.01	0.01	0.01	0.04	0.01	0.11	0.00	57.38	1.77	0.04	0.02	0.02	0.27	0.09	0.01	0.12	0.00	0.01	-	-	98.88	2016	Pic-6-21-6-Black-Dull-Gt
2431	66	38.84	0.02	0.01	0.00	0.06	0.01	0.08	0.01	57.40	1.77	0.02	0.06	0.00	0.28	0.00	0.00	0.12	0.00	0.02	-	-	98.71	2016	Pic-6-21-6-Black-Dull-Gt
2432	67	38.81	0.12	0.01	0.00	0.04	0.00	0.13	0.00	57.14	1.83	0.05	0.00	0.00	0.27	0.02	0.01	0.12	0.00	0.02	-	-	98.56	2016	Pic-6-21-6-Black-Dull-Gt
2433	68	38.89	0.13	0.00	0.00	0.09	0.01	0.11	0.00	57.28	1.83	0.02	0.03	0.01	0.28	0.06	0.03	0.13	0.00	0.04	-	-	98.92	2016	Pic-6-21-6-Black-Dull-Gt
2434	69	38.74	0.00	0.01	0.00	0.05	0.01	0.10	0.00	56.99	1.80	0.05	0.00	0.00	0.27	0.01	0.00	0.13	0.00	0.05	-	-	98.37	2016	Pic-6-21-6-Black-Dull-Gt
2435	70	38.91	0.00	0.01	0.01	0.07	0.00	0.13	0.02	57.47	1.80	0.03	0.00	0.00	0.26	0.08	0.00	0.11	0.00	0.03	-	-	98.93	2016	Pic-6-21-6-Black-Dull-Gt
2436	50	38.58	0.00	0.00	0.03	0.06	0.03	0.07	0.02	56.98	2.65	0.05	0.02	0.00	0.33	0.00	0.00	0.01	0.00	0.06	-	-	98.89	2016	Pic-6-21-6-VG-1
2437	59	38.06	0.04	0.00	0.00	0.05	0.00	0.05	0.02	57.78	1.37	0.06	0.00	0.00	0.37	0.00	0.00	0.00	0.00	0.01	-	-	97.81	2016	Pic-6-21-6-VG-2
2438	60	38.49	0.00	0.00	0.03	0.06	0.00	0.01	0.00	57.77	1.77	0.05	0.00	0.00	0.35	0.00	0.04	0.03	0.00	0.00	-	-	98.62	2016	Pic-6-21-6-VG-11
2439	51	39.32	0.02	0.00	0.00	0.03	0.03	0.08	0.03	56.59	3.16	0.07	0.00	0.00	0.26	0.04	0.00	0.01	0.00	0.00	-	-	99.68	2016	Pic-6-21-6-VG-2
2440	52	38.56	0.00	0.00	0.00	0.05	0.03	0.08	0.01	56.71	3.34	0.07	0.01	0.00	0.23	0.01	0.03	0.05	0.00	0.00	-	-	99.18	2016	Pic-6-21-6-VG-3
2441	53	38.61	0.07	0.00	0.02	0.04	0.00	0.07	0.01	58.10	2.02	0.05	0.00	0.00	0.36	0.00	0.00	0.00	0.00	0.06	-	-	99.43	2016	Pic-6-21-6-VG-4
2442	54	38.78	0.00	0.00	0.00	0.07	0.01	0.06	0.02	56.05	3.19	0.05	0.01	0.00	0.28	0.01	0.01	0.00	0.00	0.00	-	-	98.53	2016	Pic-6-21-6-VG-5
2443	55	38.94	0.08	0.01	0.00	0.06	0.01	0.07	0.00	56.00	3.50	0.05	0.00	0.00	0.19	0.02	0.03	0.04	0.00	0.00	-	-	99.00	2016	Pic-6-21-6-VG-6
2444	56	38.04	0.00	0.00	0.00	0.00	0.01	0.06	0.02	56.29	1.53	0.03	0.00	0.00	0.27	0.00	0.00	0.00	0.00	0.00	-	-	98.42	2016	Pic-6-21-6-VG-7
2445	57	38.71	0.02	0.00	0.02	0.01	0.00	0.03	0.00	59.54	1.67	0.03	0.01	0.02	0.38	0.05	0.03	0.04	0.00	0.00	-	-	100.57	2016	Pic-6-21-6-VG-8
2446	301	37.30	0.00	0.02	-	0.06	0.01	0.30	0.00	60.08	2.18	0.14	0.00	0.01	0.17	0.07	0.00	0.13	0.00	0.00	0.02	0.02	100.50	2016	SC 12-22(a)
2447	167	38.19	0.02	0.00	0.00	0.03	0.05	0.12	0.00	56.84	3.61	0.04	0.03	0.04	0.14	0.01	0.06	0.32	0.00	0.07	-	-	99.56	2016	SC-12-06(A)-Bt-Vt-Gt-1
2448	177	35.98	0.03	0.00	0.07	0.02	0.02	0.00	0.00	63.04	0.25	0.00	0.00	0.02	0.07	0.03	0.02	0.04	0.00	0.00	-	-	99.57	2016	SC-12-06(A)-Bt-Vt-Gt-11
2449	168	36.75	0.00	0.00	0.04	0.04	0.13	0.01	0.00	58.04	3.38	0.05	0.01	0.04	0.19	0.01	0.04	0.20	0.00	0.00	-	-	97.73	2016	SC-12-06(A)-Bt-Vt-Gt-2
2450	171	35.74	0.02	0.00	0.05	0.00	0.05	0.05																	

INDEX	No.	O	Na	K	V	Co	Mg	P	Cr	Fe	Al	S	Ni	Mn	Si	Pb	Cu	Ti	Ca	Zn	Ba	Sr	Total	Year	Sample
2550	32.74				0.02	0.12		0.03	0.00	61.74	0.72		0.00	0.03	1.05	0.03	0.00	0.20		0.01			96.72		Yan-02-01-D2 (4)
2551	33.10				0.00	0.10		0.01	0.00	62.43	0.22		0.00	0.00	1.59	0.00	0.04	0.00		0.01			97.51		Yan-02-01-D2 (4)
2552	32.85				0.03	0.11		0.01	0.00	64.25	0.21		0.04	0.02	1.48	0.03	0.02	0.01		0.00			99.09		Yan-02-01-D2 (4)
2553	33.74				0.01	0.13		0.01	0.00	64.75	0.28		0.03	0.01	1.37	0.07	0.00	0.00		0.00			100.41		Yan-02-01-D2 (4)
2554	31.88				0.02	0.11		0.01	0.00	65.41	0.31		0.00	0.03	1.05	0.06	0.00	0.09		0.00			98.97		Yan-02-01-D2 (4)
2555	33.20				0.03	0.11		0.02	0.03	65.95	0.23		0.00	0.03	1.27	0.10	0.06	0.00		0.05			101.11		Yan-02-01-D2 (4)
2556	33.06				0.00	0.10		0.04	0.02	66.30	0.42		0.02	0.03	0.97	0.08	0.00	0.16		0.00			101.22		Yan-02-01-D2 (4)
2557	41.25				0.04	0.07		0.11	0.00	49.03	4.02		0.00	0.00	1.09	0.03	0.00	0.07		0.00			95.70		Yan-02-D1 (1)
2558	41.73				0.06	0.07		0.15	0.01	50.00	4.71		0.05	0.00	1.05	0.01	0.03	0.20		0.02			98.09		Yan-02-D1 (1)
2559	41.39				0.02	0.08		0.11	0.00	51.70	3.22		0.03	0.01	1.03	0.07	0.01	0.05		0.05			97.79		Yan-02-D1 (1)
2560	41.15				0.04	0.12		0.09	0.02	51.75	2.77		0.00	0.01	0.97	0.06	0.00	0.11		0.06			97.15		Yan-02-D1 (1)
2561	41.01				0.04	0.10		0.12	0.02	51.87	3.47		0.00	0.02	0.88	0.15	0.00	0.10		0.01			97.78		Yan-02-D1 (1)
2562	40.91				0.08	0.11		0.10	0.04	53.12	2.29		0.00	0.01	0.95	0.00	0.03	0.07		0.01			97.74		Yan-02-D1 (1)
2563	41.26				0.02	0.06		0.11	0.00	53.65	3.02		0.01	0.02	0.84	0.07	0.03	0.03		0.03			99.15		Yan-02-D1 (1)
2564	41.82				0.04	0.14		0.17	0.03	49.07	3.77		0.02	0.03	2.00	0.00	0.00	0.12		0.00			97.22		Yan-02-D1 (2)
2565	42.30				0.06	0.08		0.12	0.02	51.23	3.74		0.04	0.03	1.39	0.09	0.02	0.12		0.01			99.26		Yan-02-D1 (2)
2566	41.74				0.06	0.06		0.21	0.01	51.44	3.04		0.01	0.01	1.03	0.01	0.06	0.05		0.00			97.78		Yan-02-D1 (2)

Electronic Appendix 3: SHRIMP-SI oxygen isotopic data

SPOUT #	Session	Date	Time	%O ₂	±	δ ^o O ₂ vsocv	rejected	±Internal error (σ 95%)	±External error (1σ)	¹⁸ O (ppm)	¹⁸ O (median)	no. subets.	
MOUNT HM-1													
normalising standard for run 2													
Capita L-1.1	#02	26/10/14	23:50:55	0.0019373	0.0000002	-17.38		0.09	0.13	0.12	2.44E+09	4.65E+06	1.5
Capita L-1.2	#02	26/10/14	23:56:29	0.0019373	0.0000002	-17.22		0.10	0.10	0.10	2.42E+09	4.73E+06	1.5
Capita L-1.3	#02	27/10/14	0:02:02	0.0019377	0.0000003	-17.14		0.14	0.12	0.14E+09	4.73E+06	1.5	
Capita L-1.4	#02	27/10/14	0:07:36	0.0019377	0.0000002	-17.16		0.11	0.11	0.11	2.44E+09	4.66E+06	1.5
#02			average	-17.22	weighted mean	-17.22							
			std dev (1σ)	0.10	error in mean (1σ)	0.05							
			50% variance	0.005	MSWD	0.84							
					no. outliers	0							
MOUNT HM-1													
Capita L-2.1	#02	27/10/14	0:13:12	0.0019310	0.0000002		-20.62	0.12	0.11	0.11	2.34E+09	4.52E+06	1.5
Capita L-2.2	#02	27/10/14	0:18:46	0.0019334	0.0000002	-19.37		0.10	0.10	0.10	2.47E+09	4.78E+06	1.5
Capita L-2.3	#02	27/10/14	0:24:19	0.0019329	0.0000002	-19.83		0.12	0.11	0.11	2.49E+09	4.81E+06	1.5
Capita L-2.4	#02	27/10/14	0:29:53	0.0019325	0.0000002	-19.84		0.13	0.11	0.11	2.48E+09	4.77E+06	1.5
Capita L-2.5	#02	27/10/14	0:36:27	0.0019331	0.0000002	-19.50		0.11	0.11	0.11	2.47E+09	4.77E+06	1.5
Capita L-2.6	#02	27/10/14	0:41:00	0.0019332	0.0000002	-19.44		0.09	0.09	0.09	2.49E+09	4.80E+06	1.5
Capita L-2.7	#02	27/10/14	0:46:34	0.0019331	0.0000002	-19.51		0.12	0.11	0.11	2.48E+09	4.80E+06	1.5
Capita L-2.8	#02	27/10/14	0:52:07	0.0019333	0.0000003	-19.44		0.14	0.14	0.12	2.53E+09	4.90E+06	1.5
Capita L-2.9	#02	27/10/14	0:57:41	0.0019300	0.0000003		-21.10	0.14	0.14	0.12	2.38E+09	4.55E+06	1.5
Capita L-2.10	#02	27/10/14	1:03:14	0.0019299	0.0000002		-21.16	0.12	0.11	0.11	2.34E+09	4.53E+06	1.5
#02			average	-19.53	weighted mean	-19.56							
			std dev (1σ)	0.13	error in mean (1σ)	0.06							
			50% variance	0.013	MSWD	1.56							
					no. outliers	1							
MOUNT HM-1													
Win-9B-1B	#02	27/10/14	3:17:03	0.0019484	0.0000002	-11.65		0.10	0.10	0.10	2.41E+09	4.70E+06	1.5
WIN0010-B-1.1	#02	27/10/14	3:22:39	0.0019489	0.0000003	-11.34		0.13	0.12	0.12	2.39E+09	4.67E+06	1.5
WIN0010-B-1.2	#02	27/10/14	3:28:15	0.0019482	0.0000003	-11.73		0.14	0.12	0.14E+09	4.76E+06	1.5	
WIN0010-B-1.3	#02	27/10/14	3:33:48	0.0019483	0.0000002	-11.65		0.18	0.15	0.15	2.45E+09	4.77E+06	1.5
WIN0010-B-1.5	#02	27/10/14	3:39:22	0.0019488	0.0000003		-10.92	0.14	0.12	0.12	2.44E+09	4.75E+06	1.5
WIN0010-B-1.6	#02	27/10/14	3:44:55	0.0019380	0.0000003		-9.23	0.14	0.12	0.12	2.39E+09	4.65E+06	1.5
WIN0010-B-1.7	#02	27/10/14	3:50:29	0.0019353	0.0000002		-9.10	0.09	0.09	0.09	2.41E+09	4.71E+06	1.5
WIN0010-B-1.8	#02	27/10/14	3:56:02	0.0019481	0.0000002	-11.86							

SPT #	Session	Date	Time	¹⁸ O/ ¹⁶ O	±	δ ¹⁸ O _{SMOW}	rejected	±Internal error (σ 95%)	±External error (1σ)	¹⁸ O cps (median)	¹⁶ O cps (median)	no. sets, subsets
MOUNT HM-11												
Capao L4												
normalising standard for run 3												
CapaoL4_1.1	#03	20/12/14	11:03:58	0.0019227	0.0000004	-17.64		0.19	0.78	2.20E+09	4.22E+06	1,5
CapaoL4_1.2	#03	20/12/14	12:00:00	0.0019234	0.0000003	-17.30		0.16	0.78	2.20E+09	4.24E+06	1,5
CapaoL4_2.1	#03	20/12/14	12:06:10	0.0019280	0.0000004		-14.91	0.21	0.79	2.10E+09	4.04E+06	1,5
CapaoL4_2.2	#03	20/12/14	12:12:12	0.0019257	0.0000003	-16.11		0.17	0.78	2.09E+09	4.02E+06	1,5
CapaoL4_2.4	#03	20/12/14	12:20:21	0.0019231	0.0000004	-17.46		0.23	0.79	2.21E+09	4.22E+06	1,5
CapaoL4_1.6	#03	20/12/14	12:26:32	0.0019214	0.0000005	-18.35		0.27	0.80	2.17E+09	4.16E+06	1,5
CapaoL4_1.3	#03	20/12/14	13:28:16	0.0019230	0.0000005	-17.48		0.24	0.79	2.22E+09	4.28E+06	1,5
CapaoL4_3.1	#03	20/12/14	13:34:26	0.0019229	0.0000004	-17.53		0.21	0.79	2.22E+09	4.29E+06	1,5
CapaoL4_1.4	#03	20/12/14	14:24:17	0.0019223	0.0000004	-17.85		0.20	0.78	2.18E+09	4.15E+06	1,5
CapaoL4_3.2	#03	20/12/14	14:30:28	0.0019228	0.0000003	-17.61		0.16	0.78	2.23E+09	4.28E+06	1,5
CapaoL4_1.5	#03	20/12/14	15:25:40	0.0019199	0.0000004		-19.09	0.22	0.79	2.12E+09	4.07E+06	1,5
CapaoL4_3.3	#03	20/12/14	15:32:27	0.0019215	0.0000003	-18.26		0.16	0.78	2.06E+09	3.96E+06	1,5
CapaoL4_3.3B	#03	20/12/14	15:38:57	0.0019219	0.0000002	-18.08		0.12	0.78	2.12E+09	4.07E+06	1,5
CapaoL4_2.3	#03	20/12/14	15:49:33	0.0019255	0.0000003	-16.19		0.17	0.78	2.01E+09	3.86E+06	1,5
CapaoL4_1.7	#03	20/12/14	16:49:15	0.0019220	0.0000003	-18.02		0.15	0.78	2.11E+09	4.09E+06	1,5
CapaoL4_3.5	#03	20/12/14	19:55:26	0.0019235	0.0000002	-17.24		0.12	0.78	2.10E+09	4.04E+06	1,5
CapaoL4_1.8	#03	20/12/14	21:38:45	0.0019232	0.0000005	-17.37		0.25	0.79	2.13E+09	4.10E+06	1,5
CapaoL4_3.6	#03	20/12/14	21:45:38	0.0019228	0.0000004	-17.59		0.20	0.79	2.09E+09	3.94E+06	1,5
CapaoL4_3.7	#03	20/12/14	23:09:01	0.0019234	0.0000002	-17.29		0.13	0.78	2.03E+09	3.91E+06	1,5
CapaoL4_4.2	#03	21/12/14	0:41:12	0.0019279	0.0000003	-14.92		0.18	0.78	2.02E+09	3.90E+06	1,5
CapaoL4_1.9	#03	21/12/14	0:47:20	0.0019230	0.0000005	-17.49		0.26	0.79	2.08E+09	4.01E+06	1,5
CapaoL4_1.10	#03	21/12/14	2:10:28	0.0019219	0.0000003	-18.05		0.18	0.78	2.08E+09	4.03E+06	1,5
CapaoL4_4.3	#03	21/12/14	2:17:13	0.0019280	0.0000004		-14.87	0.22	0.79	2.05E+09	3.95E+06	1,5
CapaoL4_1.11	#03	21/12/14	3:43:20	0.0019223	0.0000003	-17.87		0.16	0.78	2.09E+09	4.02E+06	1,5
CapaoL4_4.4	#03	21/12/14	3:50:05	0.0019287	0.0000003		-14.52	0.18	0.78	2.07E+09	3.96E+06	1,5
CapaoL4_1.12	#03	21/12/14	5:03:49	0.0019228	0.0000004	-17.58		0.19	0.78	2.03E+09	3.90E+06	1,5
CapaoL4_4.5	#03	21/12/14	5:10:34	0.0019275	0.0000003	-15.15		0.13	0.78	2.03E+09	3.91E+06	1,5
CapaoL4_1.13	#03	21/12/14	6:13:24	0.0019224	0.0000003	-17.79		0.19	0.78	2.02E+09	3.89E+06	1,5
CapaoL4_5.1	#03	21/12/14	6:20:25	0.0019267	0.0000004	-15.57		0.20	0.79	2.01E+09	3.87E+06	1,5
CapaoL4_4.6	#03	21/12/14	7:38:53	0.0019279	0.0000003	-14.97		0.15	0.78	1.95E+09	3.77E+06	1,5
CapaoL4_3.8	#03	21/12/14	7:45:00	0.0019228	0.0000005	-17.61		0.23	0.79	2.06E+09	3.97E+06	1,5
CapaoL4_3.9	#03	21/12/14	8:46:21	0.0019229	0.0000003	-17.53		0.16	0.78	2.04E+09	3.93E+06	1,5
CapaoL4_5.2	#03	21/12/14	8:52:53	0.0019269	0.0000004	-15.48		0.21	0.79	1.95E+09	3.76E+06	1,5
CapaoL4_1.14	#03	21/12/14	11:18:42	0.0019223	0.0000004	-17.87		0.22	0.79	1.99E+09	3.82E+06	1,5
CapaoL4_5.3	#03	21/12/14	11:24:54	0.0019286	0.0000004	-15.69		0.21	0.79	1.93E+09	3.73E+06	1,5
CapaoL4_1.15	#03	21/12/14	13:02:11	0.0019218	0.0000003	-18.12		0.17	0.78	2.00E+09	3.85E+06	1,5
CapaoL4_5.4	#03	21/12/14	13:08:45	0.0019271	0.0000005	-15.37		0.25	0.79	1.94E+09	3.74E+06	1,5
CapaoL4_1.16	#03	21/12/14	15:01:54	0.0019213	0.0000003	-18.38		0.25	0.79	1.96E+09	3.77E+06	1,5
CapaoL4_3.10	#03	21/12/14	15:08:04	0.0019221	0.0000003	-17.99		0.17	0.78	1.97E+09	3.80E+06	1,5
CapaoL4_1.17	#03	21/12/14	16:40:34	0.0019225	0.0000004	-17.77		0.22	0.79	1.98E+09	3.81E+06	1,5
CapaoL4_3.11	#03	21/12/14	16:46:44	0.0019228	0.0000004	-17.58		0.21	0.79	2.02E+09	3.88E+06	1,5
CapaoL4_3.12	#03	21/12/14	16:48:58	0.0019218	0.0000004	-18.10		0.23	0.79	1.97E+09	3.79E+06	1,5
CapaoL4_1.18	#03	21/12/14	18:53:36	0.0019217	0.0000004	-18.15		0.21	0.79	1.93E+09	3.71E+06	1,5
CapaoL4_5.5	#03	21/12/14	19:59:46	0.0019270	0.0000004	-15.42		0.21	0.79	1.86E+09	3.57E+06	1,5
CapaoL4_4.1	#03	21/12/14	20:37:14	0.0019255	0.0000004	-16.21		0.21	0.79	1.83E+09	3.53E+06	1,5
CapaoL4_1.5b	#03	21/12/14	21:14:39	0.0019214	0.0000005	-18.32		0.24	0.79	1.91E+09	3.67E+06	1,5
CapaoL4_3.6b	#03	21/12/14	21:21:02	0.0019205	0.0000003	-18.78		0.17	0.78	1.96E+09	3.76E+06	1,5
CapaoL4_3.7b	#03	21/12/14	21:38:21	0.0019213	0.0000005	-18.37		0.24	0.79	1.96E+09	3.75E+06	1,5
CapaoL4_4.3b	#03	21/12/14	23:21:03	0.0019262	0.0000006	-15.85		0.31	0.80	1.84E+09	3.54E+06	1,5
CapaoL4_4.4b	#03	21/12/14	23:27:07	0.0019260	0.0000005	-15.91		0.24	0.79	1.84E+09	3.54E+06	1,5
CapaoL4_1.19	#03	21/12/14	23:39:21	0.0019210	0.0000005	-18.53		0.26	0.79	1.89E+09	3.64E+06	1,5
STANDARD												
	#03	average		-17.23	weighted mean	-17.22						
		std dev (1σ)		1.09	error in mean (1σ)	0.15	Internal error (σ 95%)	0.31				
		50% variance		0.60	MSWD	38.60						
				no.	51							
				no. outliers	4							
MOUNT HM-11												
Capao L2												
Capao L2_1.1	#02	21/12/14	1:45:50	0.0019249	0.0000004	-16.50		0.23	0.79	2.03E+09	3.89E+06	1,5
Capao L2_1.2	#03	21/12/14	1:51:54	0.0019247	0.0000003	-16.63		0.17	0.78	2.04E+09	3.93E+06	1,5
Capao L2_1.3	#03	21/12/14	1:57:56	0.0019246	0.0000003	-16.66		0.14	0.78	2.02E+09	3.89E+06	1,5
Capao L2_1.4	#03	21/12/14	2:04:22	0.0019249	0.0000003	-16.49		0.17	0.78	2.04E+09	3.92E+06	1,5
Capao L2_2.1	#04	21/12/14	2:34:01	0.0019249	0.0000005	-16.50		0.28	0.80	1.97E+09	3.79E+06	1,5
Capao L2_2.2	#03	21/12/14	2:30:42	0.0019231	0.0000003	-17.42		0.18	0.78	2.04E+09	3.93E+06	1,5
average												
	#03	std dev (1σ)		-16.70	weighted mean	-16.72						
		50% variance		0.36	error in mean (1σ)	0.15	Internal error (σ 95%)	0.35				
				0.07	MSWD	4.04						
				no.	6							
				no. outliers	0							
MOUNT HM-11												
Row L5												
Row L5_1.1	#03	21/12/14	1:14:19	0.0019562	0.0000004		0.81	0.19	0.78	2.02E+09	3.95E+06	1,5
Row L5_1.2	#03	21/12/14	1:21:00	0.0019588	0.0000003	1.11		0.16	0.78	2.09E+09	4.10E+06	1,5
Row L5_1.3	#03	21/12/14	1:27:19	0.0019179	0.0000004	0.66		0.20	0.79	2.09E+09	4.10E+06	1,5
Row L5_1.4	#03	21/12/14	1:33:38	0.0019600	0.0000003	1.75		0.18	0.78	2.08E+09	4.07E+06	1,5
Row L5_1.5	#03	21/12/14	1:39:39	0.0019596	0.0000004	1.51		0.23	0.79	2.06E+09	4.04E+06	1,5
Row L5_1.1b	#03	21/12/14	23:02:59	0.0019590	0.0000005	1.22		0.26	0.79	1.86E+09	3.62E+06	1,5
Row L5_1.2b	#03	21/12/14	23:08:51	0.0019599	0.0000003	1.16		0.17	0.78	1.87E+09	3.67E+06	1,5
Row L5_1.3b	#03	21/12/14	23:14:56	0.0019575	0.0000004	0.47		0.20	0.79	1.88E+09	3.68E+06	1,5
average												
	#03	std dev (1σ)		1.13	weighted mean	1.13						
		50% variance		0.45	error in mean (1σ)	0.16	Internal error (σ 95%)	0.37				
				0.10	MSWD	5.37						
				no.	8							
				no. outliers	1							
MOUNT HM-11												
Row L6												
Row L6_1.1	#03	20/12/14	23:58:56	0.0019624	0.0000004	2.99		0.19	0.78	2.07E+09		

SPOT #	Session	Date	Time	T ₂ /T ₁	z	δ ⁰ Obs _{row}	rejected	±Internal error (σ 95%)	±External error (1σ)	T ₂ cps (median)	T ₁ cps (median)	no. sets, subsets
capaol.4-7.6	#04	14/4/15	2:13:52	0.0019477	0.0000003	-17.05		0.18	0.28	2.06E+09	4.05E+06	1.5
capaol.4-7.7	#04	14/4/15	2:20:25	0.0019473	0.0000004	-17.27		0.30	0.28	2.06E+09	4.06E+06	1.5
capaol.4-7.8	#04	14/4/15	2:26:55	0.0019481	0.0000003	-16.87		0.15	0.27	2.06E+09	4.05E+06	1.5
capaol.4-8.1	#04	13/4/15	19:37:01	0.0019480	0.0000004	-16.90		0.20	0.29	2.07E+09	4.04E+06	1.5
capaol.4-8.2	#04	13/4/15	19:43:30	0.0019485	0.0000004	-16.68		0.19	0.28	2.07E+09	4.03E+06	1.5
capaol.4-8.3	#04	13/4/15	19:50:00	0.0019479	0.0000004	-16.99		0.22	0.29	2.08E+09	4.04E+06	1.5
capaol.4-8.4	#04	13/4/15	19:56:30	0.0019476	0.0000004	-17.11		0.18	0.28	2.06E+09	4.06E+06	1.5
capaol.4-8.5	#04	14/4/15	2:33:26	0.0019476	0.0000005	-17.10		0.24	0.30	2.07E+09	4.03E+06	1.5
capaol.4-8.6	#04	14/4/15	2:39:55	0.0019484	0.0000004	-16.69		0.23	0.30	2.07E+09	4.03E+06	1.5
capaol.4-8.7	#04	14/4/15	2:46:25	0.0019474	0.0000005	-17.23		0.25	0.31	2.09E+09	4.07E+06	1.5
	#04	STANDARD	average	-17.22	weighted mean	-17.22						
			std dev (1σ)	0.35	error in mean (1σ)	0.04	Internal error (σ 95%)	0.09				
			50% variance	0.06	MSWD	4.44						
					no.	63						
					no. outliers	1						
MOUNT JA-1												
Capla L2												
capaol.2-1.1	#04	13/4/15	12:33:39	0.0019462	0.0000005	-17.82		0.26	0.31	2.06E+09	4.01E+06	1.5
capaol.2-1.2	#04	13/4/15	12:40:10	0.0019458	0.0000005	-18.06		0.26	0.31	2.06E+09	4.02E+06	1.5
capaol.2-1.3	#04	13/4/15	12:46:40	0.0019463	0.0000003	-17.78		0.17	0.28	2.06E+09	3.99E+06	1.5
capaol.2-1.4	#04	13/4/15	12:53:09	0.0019470	0.0000004	-17.42		0.19	0.28	2.06E+09	4.01E+06	1.5
capaol.2-1.5	#04	13/4/15	12:59:40	0.0019481	0.0000005	-16.87		0.24	0.30	2.00E+09	3.89E+06	1.5
capaol.2-1.6	#04	13/4/15	21:47:11	0.0019464	0.0000004	-17.76		0.22	0.29	2.07E+09	4.04E+06	1.5
capaol.2-1.7	#04	13/4/15	21:53:41	0.0019457	0.0000004	-18.09		0.21	0.29	2.07E+09	4.02E+06	1.5
capaol.2-1.8	#04	13/4/15	22:00:11	0.0019458	0.0000004	-18.04		0.21	0.29	2.05E+09	3.99E+06	1.5
capaol.2-1.9	#04	13/4/15	22:06:41	0.0019468	0.0000004	-17.53		0.20	0.29	2.06E+09	4.01E+06	1.5
capaol.2-2.1	#04	13/4/15	13:06:10	0.0019468	0.0000004	-18.55		0.23	0.30	2.06E+09	4.01E+06	1.5
capaol.2-2.2	#04	13/4/15	13:12:40	0.0019453	0.0000004	-18.29		0.21	0.29	2.08E+09	4.04E+06	1.5
capaol.2-2.3	#04	13/4/15	13:19:09	0.0019433	0.0000004	-19.33		0.22	0.29	2.09E+09	4.09E+06	1.5
capaol.2-2.4	#04	13/4/15	13:25:39	0.0019444	0.0000004	-18.74		0.19	0.28	2.07E+09	4.02E+06	1.5
capaol.2-2.5	#04	13/4/15	22:13:11	0.0019451	0.0000003	-18.40		0.17	0.28	2.07E+09	4.03E+06	1.5
capaol.2-2.6	#04	13/4/15	22:19:41	0.0019443	0.0000004	-18.82		0.19	0.28	2.08E+09	4.05E+06	1.5
capaol.2-2.7	#04	13/4/15	22:26:11	0.0019438	0.0000005	-19.09		0.25	0.31	2.08E+09	4.03E+06	1.5
capaol.2-2.8	#04	13/4/15	22:32:41	0.0019441	0.0000004	-18.54		0.26	0.31	2.10E+09	4.05E+06	1.5
capaol.2-3.1	#04	13/4/15	14:24:13	0.0019469	0.0000004	-17.46		0.21	0.29	2.10E+09	4.09E+06	1.5
capaol.2-3.2	#04	13/4/15	14:30:42	0.0019454	0.0000004	-18.27		0.21	0.29	2.13E+09	4.13E+06	1.5
capaol.2-3.3	#04	13/4/15	14:37:15	0.0019457	0.0000005	-18.07		0.25	0.31	2.10E+09	4.09E+06	1.5
capaol.2-3.4	#04	13/4/15	14:43:45	0.0019453	0.0000006	-18.28		0.29	0.32	2.11E+09	4.11E+06	1.5
capaol.2-3.5	#04	13/4/15	23:31:13	0.0019468	0.0000004	-17.53		0.23	0.30	2.11E+09	4.12E+06	1.5
capaol.2-3.6	#04	13/4/15	23:37:43	0.0019477	0.0000005	-17.05		0.24	0.30	2.10E+09	4.09E+06	1.5
capaol.2-3.7	#04	13/4/15	23:44:13	0.0019475	0.0000004	-17.17		0.19	0.28	2.11E+09	4.11E+06	1.5
capaol.2-3.8	#04	13/4/15	23:50:43	0.0019463	0.0000004	-17.80		0.20	0.29	2.10E+09	4.10E+06	1.5
capaol.2-4.1	#04	13/4/15	14:50:15	0.0019447	0.0000004	-18.60		0.22	0.29	2.13E+09	4.15E+06	1.5
capaol.2-4.2	#04	13/4/15	14:56:45	0.0019450	0.0000004	-18.46		0.19	0.28	2.13E+09	4.14E+06	1.5
capaol.2-4.3	#04	13/4/15	15:03:15	0.0019443	0.0000005	-18.79		0.24	0.30	2.12E+09	4.13E+06	1.5
capaol.2-4.4	#04	13/4/15	15:09:44	0.0019446	0.0000003	-18.64		0.17	0.28	2.12E+09	4.13E+06	1.5
capaol.2-4.5	#04	13/4/15	15:57:13	0.0019447	0.0000004	-18.63		0.23	0.30	2.12E+09	4.13E+06	1.5
capaol.2-4.6	#04	14/4/15	0:03:43	0.0019444	0.0000004	-18.74		0.23	0.30	2.12E+09	4.13E+06	1.5
capaol.2-4.7	#04	14/4/15	0:10:13	0.0019440	0.0000004	-18.98		0.20	0.29	2.13E+09	4.13E+06	1.5
capaol.2-4.8	#04	14/4/15	0:16:43	0.0019448	0.0000005	-18.26		0.26	0.31	2.11E+09	4.11E+06	1.5
capaol.2-5.1	#04	13/4/15	16:08:20	0.0019467	0.0000004	-17.60		0.20	0.29	2.09E+09	4.07E+06	1.5
capaol.2-6.2	#04	13/4/15	16:14:50	0.0019456	0.0000004	-18.15		0.21	0.29	2.11E+09	4.10E+06	1.5
capaol.2-6.3	#04	13/4/15	16:21:20	0.0019452	0.0000004	-18.34		0.22	0.29	2.09E+09	4.06E+06	1.5
capaol.2-6.4	#04	13/4/15	16:27:50	0.0019454	0.0000004	-18.24		0.20	0.29	2.09E+09	4.04E+06	1.5
capaol.2-6.5	#04	14/4/15	1:15:21	0.0019458	0.0000004	-18.02		0.23	0.30	2.10E+09	4.09E+06	1.5
capaol.2-6.6	#04	14/4/15	1:21:51	0.0019455	0.0000004	-18.20		0.21	0.29	2.11E+09	4.11E+06	1.5
capaol.2-6.7	#04	14/4/15	1:28:21	0.0019454	0.0000004	-18.25		0.22	0.30	2.10E+09	4.09E+06	1.5
capaol.2-6.8	#04	14/4/15	1:34:51	0.0019453	0.0000005	-18.29		0.23	0.30	2.11E+09	4.11E+06	1.5
capaol.2-6.1	#04	13/4/15	16:34:20	0.0019488	0.0000004	-16.49		0.21	0.29	2.11E+09	4.11E+06	1.5
capaol.2-6.2	#04	13/4/15	16:40:50	0.0019471	0.0000004	-17.38		0.18	0.28	2.11E+09	4.12E+06	1.5
capaol.2-6.3	#04	13/4/15	16:47:20	0.0019473	0.0000004	-17.27		0.20	0.28	2.11E+09	4.10E+06	1.5
capaol.2-6.4	#04	13/4/15	17:20:02	0.0019469	0.0000005	-17.49		0.24	0.30	2.14E+09	4.16E+06	1.5
capaol.2-6.5	#04	14/4/15	1:41:20	0.0019481	0.0000004	-17.87		0.20	0.29	2.13E+09	4.15E+06	1.5
capaol.2-6.6	#04	14/4/15	1:47:50	0.0019462	0.0000004	-16.31		0.27	0.31	2.11E+09	4.14E+06	1.5
capaol.2-6.7	#04	14/4/15	1:54:20	0.0019477	0.0000004	-17.06		0.22	0.29	2.11E+09	4.12E+06	1.5
capaol.2-6.8	#04	14/4/15	2:00:50	0.0019462	0.0000004	-17.85		0.21	0.29	2.12E+09	4.13E+06	1.5
capaol.2-7.1	#04	13/4/15	18:18:39	0.0019467	0.0000004	-16.06		0.18	0.28	2.08E+09	4.06E+06	1.5
capaol.2-7.2	#04	13/4/15	18:25:08	0.0019497	0.0000004	-16.05		0.20	0.29	2.07E+09	4.03E+06	1.5
capaol.2-7.3	#04	13/4/15	18:31:38	0.0019506	0.0000005	-16.60		0.26	0.31	2.07E+09	4.03E+06	1.5
capaol.2-7.4	#04	13/4/15	18:38:08	0.0019501	0.0000004	-15.84		0.20	0.29	2.07E+09	4.04E+06	1.5
capaol.2-7.5	#04	14/4/15	2:52:57	0.0019493	0.0000004	-16.27		0.20	0.29	2.07E+09	4.04E+06	1.5
capaol.2-7.6	#04	14/4/15	2:59:26	0.0019492	0.0000003	-16.31		0.17	0.28	2.07E+09	4.04E+06	1.5
capaol.2-7.7	#04	14/4/15	3:05:56	0.0019511	0.0000003	-15.34	-15.34	0.16	0.27	2.08E+09	4.06E+06	1.5
capaol.2-7.8	#04	14/4/15	3:12:27	0.0019507	0.0000004	-15.55		0.18	0.28	2.07E+09	4.05E+06	1.5
capaol.2-8.1	#04	13/4/15	18:44:39	0.0019468	0.0000004	-17.55		0.21	0.29	2.10E+09	4.08E+06	1.5
capaol.2-8.2	#04	13/4/15	18:51:08	0.0019475	0.0000004	-17.16		0.22	0.29	2.07E+09	4.03E+06	1.5
capaol.2-8.3	#04	13/4/15	18:57:38	0.0019465	0.0000004	-17.68		0.21	0.29	2.08E+09	4.06E+06	1.5
capaol.2-8.4	#04	13/4/15	19:04:08	0.0019467	0.0000004	-17.59		0.23	0.30	2.08E+09	4.04E+06	1.5
capaol.2-8.5	#04	14/4/15	3:18:57	0.0019485	0.0000004	-17.70		0.19	0.28	2.10E+09	4.09E+06	1.5
capaol.2-8.6	#04	14/4/15	3:25:27	0.0019467	0.0000004	-17.56		0.21	0.29	2.08E+09	4.06E+06	1.5
capaol.2-9.1	#04	13/4/15	20:03:04	0.0019462	0.0000005	-16.83		0.25	0.30	2.08E+09	4.04E+06	1.5
capaol.2-9.2	#04	13/4/15	20:09:36	0.0019469	0.0000004	-17.46		0.18	0.28	2.09E+09	4.07E+06	1.5
capaol.2-6.3	#04	13/4/15	20:16:08	0.0019473	0.0000004	-17.28		0.20	0.29	2.09E+09	4.07E+06	1.5
capaol.2-9.4	#04	13/4/15	20:22:38	0.0019465	0.0000005	-17.68		0.28	0.32	2.09E+09	4.06E+06	1.5
capaol.2-9.5	#04	14/4/15	3:31:57	0.0019480	0.0000005	-16.93		0.24	0.30	2.07E+09	4.03E+06	1.5
capaol.2-9.6	#04	14/4/15	3:38:27	0.0019471								

SPOT #	Session	Date	Time	T ₂ /T ₁	z	δ ¹⁸ O _{ysw}	rejected	±Internal error (σ 95%)	±External error (1σ)	T ₂ cps (median)	T ₁ cps (median)	no. sets, subsets
CapaoL4.6.1	#05	6/8/15	15:23:24	0.0019536	0.0000003							
CapaoL4.6.6	#05	6/8/15	15:30:06	0.0019500	0.0000004	-17.19	-15.35	0.17	0.27	2.48E+09	4.88E+06	1.5
CapaoL4.6.7	#05	6/8/15	17:16:22	0.0019497	0.0000004	-17.34		0.21	0.29	2.58E+09	5.05E+06	1.5
CapaoL4.7.1	#05	6/8/15	17:25:49	0.0019535	0.0000004		-15.38	0.19	0.28	2.58E+09	5.02E+06	1.5
CapaoL4.6.8	#05	6/8/15	17:33:36	0.0019501	0.0000004	-17.10		0.20	0.29	2.53E+09	4.94E+06	1.5
CapaoL4.6.9	#05	6/8/15	19:35:52	0.0019494	0.0000004	-17.50		0.18	0.28	2.56E+09	4.99E+06	1.5
CapaoL4.4.1	#05	6/8/15	19:41:43	0.0019513	0.0000004	-16.49		0.18	0.28	2.53E+09	4.94E+06	1.5
CapaoL4.6.10	#05	6/8/15	19:46:20	0.0019491	0.0000004	-17.63		0.19	0.28	2.58E+09	5.02E+06	1.5
CapaoL4.4.2	#05	6/8/15	22:07:11	0.0019502	0.0000004	-17.05		0.19	0.28	2.55E+09	4.98E+06	1.5
CapaoL4.7.1	#05	6/8/15	22:16:08	0.0019534	0.0000004		-15.41	0.19	0.28	2.53E+09	4.95E+06	1.5
CapaoL4.6.11	#05	6/8/15	22:22:57	0.0019497	0.0000004	-17.34		0.20	0.28	2.57E+09	5.01E+06	1.5
CapaoL4.4.3	#05	7/8/15	0:08:13	0.0019499	0.0000004	-17.23		0.18	0.28	2.53E+09	4.94E+06	1.5
CapaoL4.6.12	#05	7/8/15	0:15:28	0.0019492	0.0000004	-17.60		0.20	0.28	2.57E+09	5.01E+06	1.5
CapaoL4.4.4	#05	7/8/15	1:23:32	0.0019513	0.0000004	-16.49		0.19	0.28	2.52E+09	4.91E+06	1.5
CapaoL4.6.13	#05	7/8/15	3:21:33	0.0019496	0.0000004	-17.40		0.21	0.29	2.55E+09	4.96E+06	1.5
CapaoL4.6.14	#05	7/8/15	3:27:20	0.0019498	0.0000003	-17.29		0.17	0.27	2.55E+09	4.97E+06	1.5
				STANDARD	average	-17.22	weighted mean	-17.22				
					std dev (1σ)	0.35	error in mean (1σ)	0.08	Internal error (σ 95%)	0.16		
					50% variance	0.06	MSWD	4.53				
							no.	20				
							no. outliers	3				
MOUNT HM-13												
Capao L4												
normalising standard for run 5												
CapaoL4.6.1	#05	7/8/15	3:52:34	0.0019536	0.0000003	-16.74		0.17	0.37	2.46E+09	4.81E+06	1.5
CapaoL4.6.2	#05	7/8/15	3:58:51	0.0019535	0.0000003	-16.80		0.17	0.37	2.47E+09	4.82E+06	1.5
CapaoL4.6.3	#05	7/8/15	4:04:56	0.0019503	0.0000003	-17.09		0.17	0.37	2.47E+09	4.82E+06	1.5
CapaoL4.6.4	#05	7/8/15	5:54:46	0.0019536	0.0000004	-16.78		0.22	0.38	2.45E+09	4.79E+06	1.5
CapaoL4.4.1	#05	7/8/15	6:00:35	0.0019506	0.0000003	-18.31		0.17	0.37	2.44E+09	4.79E+06	1.5
CapaoL4.6.5	#05	7/8/15	6:58:25	0.0019526	0.0000004	-17.28		0.19	0.38	2.46E+09	4.80E+06	1.5
CapaoL4.2.1	#05	7/8/15	7:56:37	0.0019496	0.0000003		-18.82	0.14	0.37	2.56E+09	5.00E+06	1.5
CapaoL4.6.6	#05	7/8/15	8:37:14	0.0019524	0.0000004	-17.39		0.22	0.38	2.46E+09	4.81E+06	1.5
CapaoL4.4.2	#05	7/8/15	10:03:34	0.0019506	0.0000003	-18.32		0.17	0.37	2.44E+09	4.75E+06	1.5
CapaoL4.6.7	#05	7/8/15	10:09:22	0.0019527	0.0000003	-17.24		0.16	0.37	2.46E+09	4.79E+06	1.5
CapaoL4.7.1	#05	7/8/15	11:44:09	0.0019536	0.0000004	-16.76		0.20	0.38	2.46E+09	4.81E+06	1.5
CapaoL4.7.2	#05	7/8/15	11:50:47	0.0019533	0.0000004	-16.82		0.21	0.38	2.47E+09	4.82E+06	1.5
CapaoL4.6.1	#05	7/8/15	11:56:01	0.0019531	0.0000004	-16.88		0.22	0.38	2.44E+09	4.77E+06	1.5
CapaoL4.3.1	#05	7/8/15	13:22:51	0.0019498	0.0000003		-18.71	0.16	0.37	2.40E+09	4.68E+06	1.5
CapaoL4.7.3	#05	7/8/15	13:28:42	0.0019528	0.0000004	-17.15		0.18	0.37	2.46E+09	4.81E+06	1.5
CapaoL4.6.8	#05	7/8/15	13:36:18	0.0019520	0.0000003	-17.58		0.17	0.37	2.46E+09	4.80E+06	1.5
CapaoL4.6.2	#05	7/8/15	14:47:50	0.0019529	0.0000004	-17.10		0.19	0.38	2.43E+09	4.74E+06	1.5
CapaoL4.7.4	#05	7/8/15	14:55:31	0.0019534	0.0000004	-16.88		0.23	0.39	2.46E+09	4.80E+06	1.5
				STANDARD	average	-17.20	weighted mean	-17.22				
					std dev (1σ)	0.50	error in mean (1σ)	0.12	Internal error (σ 95%)	0.25		
					50% variance	0.12	MSWD	18.47				
							no.	18				
							no. outliers	2				
MOUNT HM-13												
Capao L2												
CapaoL2.1.1	#05	7/8/15	12:47:38	0.0019438	0.0000004	-21.78		0.20	0.38	2.35E+09	4.56E+06	1.5
CapaoL2.1.2	#05	7/8/15	12:53:26	0.0019442	0.0000004	-21.55		0.22	0.38	2.36E+09	4.56E+06	1.5
CapaoL2.1.3	#05	7/8/15	12:56:13	0.0019451	0.0000004	-21.12		0.22	0.38	2.35E+09	4.57E+06	1.5
				STANDARD	average	-21.49	weighted mean	-21.54				
					std dev (1σ)	0.33	error in mean (1σ)	0.12	Internal error (σ 95%)	0.38		
					50% variance	0.06	MSWD	2.08				
							no.	3				
							no. outliers	0				
MOUNT HM-13												
Roy L3												
Roy L5.1.1	#05	7/8/15	5:19:33	0.0019876	0.0000004	0.65		0.19	0.38	2.52E+09	5.02E+06	1.5
Roy L5.1.2	#05	7/8/15	5:25:21	0.0019857	0.0000003	-0.31		0.14	0.36	2.54E+09	5.05E+06	1.5
Roy L5.1.3	#05	7/8/15	5:31:08	0.0019863	0.0000003	-0.03		0.15	0.37	2.53E+09	5.03E+06	1.5
Roy L5.2.1	#05	7/8/15	6:06:25	0.0019870	0.0000003	0.35		0.17	0.37	2.56E+09	5.06E+06	1.5
Roy L5.2.2	#05	7/8/15	6:12:12	0.0019869	0.0000005	0.30		0.23	0.39	2.57E+09	5.10E+06	1.5
Roy L5.2.3	#05	7/8/15	6:18:00	0.0019879	0.0000004	0.83		0.18	0.37	2.57E+09	5.11E+06	1.5
Roy L5.3.1	#05	7/8/15	6:22:33	0.0019869	0.0000003	0.27		0.14	0.37	2.51E+09	4.99E+06	1.5
Roy L5.3.2	#05	7/8/15	6:28:20	0.0019881	0.0000003	0.88		0.15	0.37	2.50E+09	4.98E+06	1.5
Roy L5.3.3	#05	7/8/15	9:34:08	0.0019864	0.0000003	0.02		0.17	0.37	2.51E+09	4.99E+06	1.5
Roy L5.1.2b	#05	7/8/15	10:17:30	0.0019864	0.0000003	0.06		0.17	0.37	2.51E+09	4.98E+06	1.5
Roy L5.1.3b	#05	7/8/15	10:25:31	0.0019866	0.0000003	0.14		0.14	0.37	2.53E+09	5.00E+06	1.5
Roy L5.3.2b	#05	7/8/15	10:39:00	0.0019869	0.0000004	0.31		0.21	0.38	2.48E+09	4.93E+06	1.5
				STANDARD	average	0.29	weighted mean	0.28				
					std dev (1σ)	0.35	error in mean (1σ)	0.10	Internal error (σ 95%)	0.22		
					50% variance	0.06	MSWD	7.07				
							no.	12				
							no. outliers	0				
MOUNT HM-13												
Roy L6												
Roy L6.1.1	#05	7/8/15	7:21:48	0.0019886	0.0000004	1.16		0.18	0.37	2.51E+09	4.99E+06	1.5
Roy L6.1.2	#05	7/8/15	7:27:35	0.0019885	0.0000003	1.10		0.17	0.37	2.49E+09	4.96E+06	1.5
Roy L6.1.3	#05	7/8/15	7:33:22	0.0019885	0.0000004	1.10		0.19	0.38	2.52E+09	5.01E+06	1.5
Roy L6.2.1	#05	7/8/15	8:02:26	0.0019884	0.0000004	1.04		0.20	0.38	2.50E+09	4.98E+06	1.5
Roy L6.2.2	#05	7/8/15	8:08:13	0.0019886	0.0000003	1.69		0.16	0.37	2.53E+09	5.01E+06	1.5
Roy L6.2.3	#05	7/8/15	8:14:01	0.0019890	0.0000004	1.38		0.20	0.38	2.52E+09	5.02E+06	1.5
Roy L6.2.1b	#05	7/8/15	13:44:10	0.0019894	0.0000004	1.56		0.19	0.38	2.48E+09	4.95E+06	1.5
Roy L6.2.2b	#05	7/8/15	13:51:32	0.0019873	0.0000004	0.52		0.19	0.38	2.49E+09	4.95E+06	1.5
Roy L6.3.1	#05	7/8/15	14:08:08	0.0019893	0.0000004	1.52		0.19	0.38	2.46E+09	4.89E+06	1.5
Roy L6.3.2	#05	7/8/15	14:14:28	0.0019882</								

SPOT #	Session	Date	Time	T ₀ /T ₀	±	δ ⁰ Oswow	rejected	±Internal error (σ 95%)	±External error (1σ)	T ₀ cps (median)	T ₀ cps (median)	no. sets, subsets
Capao-L4_3,1	#06	16/5/16	12:22.15	0.0019465	0.0000003	-17.16		0.15	0.33	2.50E+09	4.86E+06	1,6
Capao-L4_3,2	#06	16/5/16	12:28.12	0.0019459	0.0000003	-17.47		0.15	0.33	2.47E+09	4.81E+06	1,6
Capao-L4_3,3	#06	16/5/16	13:44.15	0.0019456	0.0000002	-17.63		0.13	0.33	2.47E+09	4.80E+06	1,6
Capao-L4_3,4	#06	16/5/16	13:51.55	0.0019467	0.0000003	-17.04		0.15	0.33	2.45E+09	4.77E+06	1,6
Capao-L4_3,5	#06	16/5/16	14:36.40	0.0019463	0.0000003	-17.27		0.14	0.33	2.46E+09	4.79E+06	1,6
Capao-L4_3,6	#06	16/5/16	14:42.00	0.0019464	0.0000003	-17.21		0.13	0.33	2.43E+09	4.72E+06	1,6
Capao-L4_3,7	#06	16/5/16	15:14.04	0.0019460	0.0000003	-17.42		0.15	0.33	2.42E+09	4.71E+06	1,6
Capao-L4_3,8	#06	16/5/16	15:19.23	0.0019457	0.0000003	-17.57		0.26	0.33	2.44E+09	4.74E+06	1,6
Capao-L4_5,1	#06	16/5/16	16:32.28	0.0019471	0.0000003	-16.86		0.14	0.33	2.33E+09	4.54E+06	1,6
Capao-L4_5,2	#06	16/5/16	16:39.14	0.0019464	0.0000003	-17.22		0.18	0.34	2.32E+09	4.51E+06	1,6
Capao-L4_3,9	#06	16/5/16	16:47.28	0.0019468	0.0000003	-17.02		0.13	0.33	2.36E+09	4.60E+06	1,6
Capao-L4_3,10	#06	16/5/16	16:53.52	0.0019458	0.0000003	-17.50		0.15	0.33	2.37E+09	4.61E+06	1,6
Capao-L4_1,1	#06	16/5/16	18:01.58	0.0019483	0.0000004	-16.23		0.19	0.34	2.26E+09	4.40E+06	1,6
Capao-L4_1,2	#06	16/5/16	18:07.57	0.0019488	0.0000004	-15.97		0.20	0.34	2.28E+09	4.44E+06	1,6
Capao-L4_3,11	#06	16/5/16	18:14.27	0.0019463	0.0000003	-17.53		0.14	0.33	2.39E+09	4.59E+06	1,6
Capao-L4_3,12	#06	16/5/16	18:21.18	0.0019456	0.0000004	-17.61		0.19	0.34	2.31E+09	4.49E+06	1,6
Capao-L4_3,13	#06	16/5/16	19:46.35	0.0019453	0.0000004	-17.77		0.19	0.34	2.28E+09	4.44E+06	1,6
Capao-L4_3,14	#06	16/5/16	19:51.54	0.0019461	0.0000003	-17.38		0.16	0.33	2.25E+09	4.39E+06	1,6
Capao-L4_3,15	#06	16/5/16	20:50.40	0.0019461	0.0000004	-17.35		0.21	0.35	2.21E+09	4.31E+06	1,6
#06	STANDARD	average	-17.21	weighted mean	-17.22							
		std dev (1σ)	0.44	error in mean (1σ)	0.09			Internal error (σ 95%)	0.20			
		50% variance	0.10	MSWD	10.89							
				no. outliers	22							
					0							
MOUNT HM-16A												
Roy L6												
Roy-L6_1,1	#06	16/5/16	14:15.06	0.0019856	0.0000003		2.92	0.17	0.34	2.45E+09	4.87E+06	1,6
Roy-L6_1,3	#06	16/5/16	14:20.40	0.0019836	0.0000004	1.93		0.18	0.34	2.45E+09	4.85E+06	1,6
Roy-L6_1,4	#06	16/5/16	14:26.00	0.0019834	0.0000003	1.79		0.16	0.33	2.50E+09	4.89E+06	1,6
Roy-L6_1,5	#06	16/5/16	14:31.19	0.0019823	0.0000003	1.25		0.15	0.33	2.50E+09	4.89E+06	1,6
Roy-L6_1,2	#06	16/5/16	15:26.30	0.0019842	0.0000003	2.21		0.15	0.33	2.48E+09	4.95E+06	1,6
#06	average	1.80	weighted mean	1.83								
	std dev (1σ)	0.40	error in mean (1σ)	0.26			Internal error (σ 95%)	0.67				
	50% variance	0.08	MSWD	17.69								
			no. outliers	5								
				1								
MOUNT HM-16A												
Roy L6												
Roy-L6_1,1	#06	16/5/16	14:47.21	0.0019845	0.0000003	2.36		0.17	0.34	2.38E+09	4.72E+06	1,6
Roy-L6_1,2	#06	16/5/16	14:52.41	0.0019841	0.0000004	2.18		0.18	0.34	2.37E+09	4.71E+06	1,6
Roy-L6_1,3	#06	16/5/16	14:58.04	0.0019850	0.0000003	2.62		0.14	0.33	2.36E+09	4.68E+06	1,6
Roy-L6_1,4	#06	16/5/16	15:03.23	0.0019860	0.0000004	3.14		0.18	0.34	2.37E+09	4.71E+06	1,6
Roy-L6_1,5	#06	16/5/16	15:08.43	0.0019857	0.0000004	2.99		0.18	0.34	2.35E+09	4.67E+06	1,6
#06	average	2.66	weighted mean	2.62								
	std dev (1σ)	0.41	error in mean (1σ)	0.18			Internal error (σ 95%)	0.47				
	50% variance	0.08	MSWD	6.57								
			no. outliers	5								
				0								
MOUNT HM-16B												
Capao L4												
normalising standard for run 6												
Capao-L4_3,16	#06	16/5/16	20:55.59	0.0019456	0.0000003	-17.76		0.15	0.51	2.19E+09	4.27E+06	1,6
Capao-L4_4,1	#06	16/5/16	21:18.37	0.0019479	0.0000003	-16.58		0.11	0.51	2.14E+09	4.17E+06	1,6
Capao-L4_4,2	#06	16/5/16	21:25.07	0.0019476	0.0000004	-16.69		0.20	0.52	2.14E+09	4.17E+06	1,6
Capao-L4_3,17	#06	16/5/16	21:32.25	0.0019453	0.0000004	-17.87		0.20	0.52	2.16E+09	4.21E+06	1,6
Capao-L4_3,18	#06	17/5/16	0:08.34	0.0019459	0.0000004	-17.61		0.18	0.52	2.04E+09	3.98E+06	1,6
Capao-L4_3,19	#06	17/5/16	0:13.53	0.0019460	0.0000003	-17.51		0.17	0.51	2.01E+09	3.91E+06	1,6
Capao-L4_3,20	#06	17/5/16	1:17.58	0.0019463	0.0000004	-17.38		0.21	0.52	1.95E+09	3.79E+06	1,6
Capao-L4_3,21	#06	17/5/16	1:23.18	0.0019454	0.0000003	-17.83		0.17	0.51	1.95E+09	3.80E+06	1,6
Capao-L4_5,3	#06	17/5/16	2:22.02	0.0019479	0.0000004	-16.57		0.18	0.52	1.84E+09	3.58E+06	1,6
Capao-L4_5,4	#06	17/5/16	2:27.21	0.0019477	0.0000004	-16.68		0.20	0.52	1.81E+09	3.52E+06	1,6
Capao-L4_3,22	#06	17/5/16	2:32.45	0.0019458	0.0000004	-17.63		0.19	0.52	1.87E+09	3.64E+06	1,6
Capao-L4_3,23	#06	17/5/16	2:38.05	0.0019462	0.0000003	-17.44		0.17	0.51	1.86E+09	3.59E+06	1,6
Capao-L4_2,1	#06	17/5/16	3:47.27	0.0019501	0.0000004	-15.43		0.19	0.52	1.75E+09	3.40E+06	1,6
Capao-L4_2,2	#06	17/5/16	3:52.46	0.0019506	0.0000005	-15.15		0.24	0.53	1.74E+09	3.39E+06	1,6
Capao-L4_3,24	#06	17/5/16	3:58.11	0.0019456	0.0000003	-17.45		0.15	0.51	1.79E+09	3.44E+06	1,6
Capao-L4_3,25	#06	17/5/16	4:03.30	0.0019457	0.0000004	-17.70		0.22	0.52	1.74E+09	3.38E+06	1,6
Capao-L4_3,26	#06	17/5/16	5:02.14	0.0019461	0.0000004	-17.48		0.18	0.52	1.72E+09	3.35E+06	1,6
Capao-L4_3,27	#06	17/5/16	5:07.33	0.0019461	0.0000005	-17.48		0.25	0.53	1.68E+09	3.26E+06	1,6
Capao-L4_3,28	#06	17/5/16	6:06.17	0.0019455	0.0000004	-17.80		0.21	0.52	1.63E+09	3.17E+06	1,6
Capao-L4_3,29	#06	17/5/16	6:11.36	0.0019467	0.0000004	-17.17		0.22	0.52	1.62E+09	3.16E+06	1,6
Capao-L4_3,30	#06	17/5/16	7:15.55	0.0019456	0.0000005	-17.73		0.25	0.53	1.55E+09	3.01E+06	1,6
Capao-L4_3,31	#06	17/5/16	7:21.14	0.0019461	0.0000004	-17.46		0.21	0.52	1.53E+09	2.97E+06	1,6
Capao-L4_3,32	#06	17/5/16	8:19.56	0.0019461	0.0000005	-17.49		0.24	0.53	1.45E+09	2.82E+06	1,6
Capao-L4_3,33	#06	17/5/16	8:25.15	0.0019459	0.0000005	-17.58		0.23	0.53	1.46E+09	2.84E+06	1,6
Capao-L4_5,3	#06	17/5/16	8:30.39	0.0019463	0.0000005	-16.51		0.26	0.53	1.45E+09	2.83E+06	1,6
Capao-L4_5,4	#06	17/5/16	8:35.59	0.0019465	0.0000005	-16.25		0.27	0.54	1.45E+09	2.83E+06	1,6
Capao-L4_3,34	#06	17/5/16	8:18.49	0.0019454	0.0000005	-17.85		0.23	0.53	1.43E+09	2.78E+06	1,6
Capao-L4_3,35	#06	17/5/16	9:24.09	0.0019465	0.0000004	-17.27		0.23	0.53	1.42E+09	2.76E+06	1,6
#06	STANDARD	average	-17.20	weighted mean	-17.22							
	std dev (1σ)	0.71	error in mean (1σ)	0.13			Internal error (σ 95%)	0.27				
	50% variance	0.25	MSWD	24.82								
			no. outliers	28								
				0								
MOUNT HM-16C												
Capao L4												
normalising standard for run 6												
Capao-L4_3,36	#06	17/5/16	9:59.52	0.0019463	0.0000004	-17.55		0.18	0.55	2.20E+09	4.29E+06	1,6
Capao-L4_3,37	#06	17/5/16	11:13.50	0.0019459	0.0000003	-17.74		0.17	0.55	2.08E+09	4.04E+06	1,6
Capao-L4_3,38	#06	17/5/16	11:19.13	0.0019440	0.0000003	-18.72		0.16	0.54	2.10E+09	4.08E+06	1,6
Capao-L4_3,39	#06	17/5/16	13:11.02	0.0019457	0.0000004	-17.84		0.20	0.55	2.08E+09	4.05E+06	1,6
Capao-L4_3,40	#06	17/5/16	13:16.21	0.0019456	0.0000003	-17.93		0.14	0.54	2.10E+09	4.06E+06	1,6
Capao-L4_1,3	#06	17/5/16	13:21.45	0.0019462	0.0000004	-17.63		0.19	0.55	2.19E+09	4.27E+06	1,6
Capao-L4_1,4	#06	17/5/16	13:27.05	0.0019459	0.0000003	-17.75		0.17	0.54	2.18E+09	4.25E+06	1,6
Capao-L4_4,5	#06	17/5/16	13:53.49	0.0019464	0.0000003	-16.46		0.16	0.54	2.10E+09	4.06E+06	1,6
Capao-L4_4,6	#06	17/5/16	13:59.08	0.0019463	0.0000003	-16.52		0.17	0.55	2.08E+09	4.04E+06	1,6
Capao-L4_3,41	#06	17/5/16	14:31.12	0.0019459	0.0000004	-17.76		0.21	0.55	2.08E+09		

SPOT #	Session	Date	Time	T ₀ /T ₀	z	δ ⁰ O ₂ avow	rejected	±Internal error (σ 95%)	±External error (1σ)	T ₀ cps (median)	T ₀ cps (median)	no. sets, subsets
	#06	STANDARD	average	-17.28	weighted mean	-17.22						
			std dev (1σ)	0.74	error in mean (1σ)	0.11	Internal error (σ 95%)	0.23				
			50% variance	0.28	MSWD	24.97						
					no.	43						
					no. outliers	2						
MOUNT HM-17A												
RoyL5												
RoyL5_1.1	#06	17/5/16	18:25:46	0.0019872	0.0000003	1.85		0.17	0.54	2.17E+09	4.31E+06	1.6
RoyL5_1.2	#06	17/5/16	18:31:05	0.0019873	0.0000004	1.93		0.19	0.54	2.18E+09	4.34E+06	1.6
RoyL5_1.3	#06	17/5/16	18:36:24	0.0019886	0.0000003	2.58		0.20	0.54	2.14E+09	4.25E+06	1.6
RoyL5_1.4	#06	17/5/16	18:41:43	0.0019874	0.0000003	1.98		0.13	0.53	2.15E+09	4.28E+06	1.6
RoyL5_1.5	#06	17/5/16	18:47:03	0.0019895	0.0000005	3.06		0.24	0.55	2.15E+09	4.28E+06	1.6
RoyL5_1.6	#06	18/5/16	7:40:54	0.0019850	0.0000008		0.75	0.40	0.59	1.75E+09	3.48E+06	1.6
RoyL5_1.7	#06	18/5/16	7:46:13	0.0019853	0.0000005	2.98		0.24	0.55	1.75E+09	3.48E+06	1.6
RoyL5_1.8	#06	18/5/16	7:51:32	0.0019881	0.0000005	2.33		0.25	0.55	1.75E+09	3.48E+06	1.6
RoyL5_1.0B	#06	18/5/16	11:17:54	0.0019864	0.0000005	0.61		0.23	0.55	2.09E+09	4.16E+06	1.6
	#06		average	2.17	weighted mean	2.43						
			std dev (1σ)	0.78	error in mean (1σ)	0.19	Internal error (σ 95%)	0.43				
			50% variance	0.31	MSWD	16.03						
					no.	9						
					no. outliers	1						
MOUNT HM-17B												
RoyL6												
RoyL6_1.1	#06	17/5/16	18:52:25	0.0019880	0.0000004	2.81		0.22	0.55	2.19E+09	4.35E+06	1.6
RoyL6_1.2	#06	17/5/16	18:57:44	0.0019884	0.0000004	2.51		0.22	0.55	2.17E+09	4.32E+06	1.6
RoyL6_1.3	#06	17/5/16	19:03:04	0.0019882	0.0000004	2.39		0.19	0.54	2.18E+09	4.34E+06	1.6
RoyL6_1.4	#06	17/5/16	19:08:23	0.0019900	0.0000004	3.31		0.18	0.54	2.14E+09	4.27E+06	1.6
RoyL6_1.5	#06	17/5/16	19:13:42	0.0019878	0.0000004	2.17		0.19	0.54	2.15E+09	4.27E+06	1.6
RoyL6_1.6	#06	18/5/16	7:24:52	0.0019833	0.0000010		-0.13	0.48	0.63	1.80E+09	3.56E+06	1.6
RoyL6_1.7	#06	18/5/16	7:30:11	0.0019890	0.0000004	2.80		0.19	0.54	1.78E+09	3.54E+06	1.6
RoyL6_1.8	#06	18/5/16	7:35:31	0.0019888	0.0000003	3.22		0.17	0.54	1.77E+09	3.52E+06	1.6
RoyL6_1.0B	#06	18/5/16	11:25:09	0.0019868	0.0000004	2.88		0.19	0.54	2.08E+09	4.13E+06	1.6
RoyL6_1.5B	#06	18/5/16	11:32:24	0.0019891	0.0000004	1.97		0.21	0.54	2.05E+09	4.09E+06	1.6
	#06		average	2.67	weighted mean	2.83						
			std dev (1σ)	0.45	error in mean (1σ)	0.14	Internal error (σ 95%)	0.32				
			50% variance	0.10	MSWD	10.89						
					no.	10						
					no. outliers	1						
MOUNT HM-17B												
Capao-L4												
normalising standard for run 6												
Capao-L4_3.23	#06	18/5/16	9:50:54	0.0019518	0.0000004	-17.13		0.18	0.42	2.15E+09	4.21E+06	1.6
Capao-L4_3.24	#06	18/5/16	9:58:09	0.0019520	0.0000004	-17.05		0.18	0.42	2.16E+09	4.22E+06	1.6
Capao-L4_3.25	#06	18/5/16	10:05:24	0.0019519	0.0000003	-17.10		0.11	0.13	2.16E+09	4.22E+06	1.6
Capao-L4_3.26	#06	18/5/16	10:12:39	0.0019516	0.0000005	-17.23		0.23	0.43	2.16E+09	4.20E+06	1.6
Capao-L4_6.2B	#06	18/5/16	10:19:54	0.0019496	0.0000003	-18.24		0.15	0.41	2.17E+09	4.22E+06	1.6
Capao-L4_6.3	#06	18/5/16	10:27:09	0.0019486	0.0000005	-18.23	-18.77	0.23	0.43	2.17E+09	4.22E+06	1.6
Capao-L4_6.4	#06	18/5/16	10:34:24	0.0019490	0.0000004	-18.56		0.19	0.42	2.15E+09	4.18E+06	1.6
Capao-L4_3.27	#06	18/5/16	11:10:39	0.0019521	0.0000004	-17.00		0.20	0.42	2.12E+09	4.14E+06	1.6
Capao-L4_4.3B	#06	18/5/16	11:39:39	0.0019519	0.0000006	-17.06		0.31	0.46	2.10E+09	4.05E+06	1.6
Capao-L4_4.4B	#06	18/5/16	11:46:54	0.0019521	0.0000004	-16.48		0.18	0.42	2.05E+09	4.07E+06	1.6
Capao-L4_4.7	#06	18/5/16	13:50:10	0.0019510	0.0000005	-17.54		0.24	0.44	2.05E+09	4.00E+06	1.6
Capao-L4_4.8	#06	18/5/16	13:57:25	0.0019523	0.0000004	-16.88		0.21	0.43	2.04E+09	3.98E+06	1.6
Capao-L4_3.28	#06	18/5/16	14:04:40	0.0019517	0.0000004	-17.16		0.21	0.43	2.07E+09	4.04E+06	1.6
Capao-L4_3.29	#06	18/5/16	15:06:55	0.0019517	0.0000003	-17.18		0.14	0.41	2.00E+09	3.90E+06	1.6
Capao-L4_4.9	#06	18/5/16	15:17:10	0.0019533	0.0000004	-16.36		0.22	0.43	1.99E+09	3.88E+06	1.6
Capao-L4_3.30	#06	18/5/16	15:24:25	0.0019512	0.0000004	-17.46		0.21	0.43	2.01E+09	3.92E+06	1.6
Capao-L4_3.31	#06	18/5/16	15:31:40	0.0019512	0.0000005	-17.42		0.23	0.43	2.03E+09	3.97E+06	1.6
Capao-L4_4.10	#06	18/5/16	16:36:55	0.0019528	0.0000003	-16.60		0.17	0.42	2.01E+09	3.93E+06	1.6
Capao-L4_3.32	#06	18/5/16	16:44:10	0.0019523	0.0000004	-16.85		0.20	0.42	2.02E+09	3.94E+06	1.6
Capao-L4_5.3	#06	18/5/16	17:40:25	0.0019498	0.0000003	-18.14		0.16	0.42	2.03E+09	3.93E+06	1.6
Capao-L4_5.4	#06	18/5/16	17:56:40	0.0019490	0.0000003	-18.56		0.15	0.41	2.02E+09	3.93E+06	1.6
Capao-L4_4.11	#06	18/5/16	18:03:55	0.0019523	0.0000004	-16.90		0.21	0.43	1.99E+09	3.88E+06	1.6
Capao-L4_3.33	#06	18/5/16	18:11:10	0.0019519	0.0000004	-17.07		0.20	0.42	2.00E+09	3.95E+06	1.6
Capao-L4_3.34	#06	18/5/16	18:18:25	0.0019520	0.0000003	-17.04		0.17	0.42	1.99E+09	3.88E+06	1.6
Capao-L4_3.35	#06	18/5/16	19:30:55	0.0019518	0.0000003	-17.12		0.18	0.42	1.96E+09	3.83E+06	1.6
Capao-L4_4.10B	#06	18/5/16	20:43:26	0.0019526	0.0000004	-16.72		0.22	0.43	1.94E+09	3.78E+06	1.6
Capao-L4_3.36	#06	18/5/16	20:50:41	0.0019520	0.0000003	-17.03		0.16	0.42	1.96E+09	3.82E+06	1.6
Capao-L4_4.9B	#06	18/5/16	22:17:41	0.0019517	0.0000004	-17.19		0.22	0.43	1.91E+09	3.73E+06	1.6
Capao-L4_3.37	#06	18/5/16	22:24:58	0.0019521	0.0000005	-16.85		0.24	0.44	1.93E+09	3.77E+06	1.6
Capao-L4_3.38	#06	18/5/16	23:44:41	0.0019536	0.0000004	-16.19		0.21	0.43	1.93E+09	3.77E+06	1.6
Capao-L4_3.39	#06	18/5/16	23:51:56	0.0019512	0.0000005	-17.45		0.23	0.43	1.92E+09	3.74E+06	1.6
	#06	STANDARD	average	-17.19	weighted mean	-17.22						
			std dev (1σ)	0.57	error in mean (1σ)	0.10	Internal error (σ 95%)	0.21				
			50% variance	0.16	MSWD	16.15						
					no.	31						
					no. outliers	1						
MOUNT HM-18A												
Capao-L4												
normalising standard for run 6												
Capao-L4_3.1	#06	18/5/16	23:56:11	0.0019531	0.0000004	-17.14		0.23	0.65	1.88E+09	3.69E+06	1.6
Capao-L4_3.2	#06	18/5/16	0:05:10	0.0019527	0.0000004	-17.31		0.22	0.65	1.88E+09	3.68E+06	1.6
Capao-L4_3.31	#06	18/5/16	0:11:45	0.0019541	0.0000005	-16.63		0.25	0.65	1.87E+09	3.66E+06	1.6
Capao-L4_4.1	#06	18/5/16	1:55:13	0.0019521	0.0000004	-17.62		0.22	0.65	1.86E+09	3.63E+06	1.6
Capao-L4_3.4	#06	18/5/16	2:00:34	0.0019535	0.0000004	-16.92		0.22	0.65	1.83E+09	3.57E+06	1.6
Capao-L4_3.5	#06	18/5/16	2:48:34	0.0019562	0.0000004	-16.57		0.19	0.64	1.82E+09	3.55E+06	1.6
Capao-L4_5.1	#06	18/5/16	2:53:55	0.0019510	0.0000004	-18.22		0.21	0.65	1.82E+09	3.55E+06	1.6
Capao-L4_5.2	#06	18/5/16	3:52:35	0.0019496	0.0000004	-18.90		0.23	0.65	1.80E+09	3.51E+06	1.6
Capao-L4_3.6	#06	18/5/16	3:57:56	0.0019511	0.0000005	-17.10		0.26	0.75	1.78E+09	3.47E+06	1.6
Capao-L4_4.2	#06	18/5/16	5:02:01	0.0019516	0.0000005	-17.87		0.28	0.66	1.74E+09	3.40E+06	1.6
Capao-L4_6.1	#06	18/5/16	5:07:22	0.0019558	0.0000005	-15.73		0.27	0.66	1.70E+09	3.33E+06	1.6
Capao-L4_6.2	#06	18/5/16	5:12:41	0.0019560	0.0000005	-15.64		0.25	0.65	1.69E+09	3.31E+06	1.6
Capao-L4_3.7	#06	18/5/16	6:16:44	0.0019522	0.0000004	-17.61		0.21	0.65	1.68E+09	3.28E+06	1.6
Capao-L4_3.8	#06	18/5/16	6:22:03	0.0019523	0.0000005	-17.55		0.24	0.65	1.68E+09	3.28E+06	1.6
	#06	STANDARD	average	-17.20	weighted mean	-17.22						
			std dev (1σ)	0.89	error in mean (1σ)	0.24	Internal error (σ 95%)	0.51				
			50% variance	0.39	MSWD	21.74						
					no.	14						
					no. outliers	0						

SPOT #	Session	Date	Time	T _g /T _a	z	δ°O ₂ norm	rejected	±Internal error (σ 95%)	±External error (1σ)	T _g cps (median)	T _a cps (median)	no. sets, subsets
Capao-L4_1,3	#06	22/5/16	22:14:20	0.0019396	0.0000002	-16.96		0.12	0.85	2.23E+09	4.33E+06	1,6
Capao-L4_1,4	#06	22/5/16	22:19:33	0.0019394	0.0000003	-17.09		0.16	0.85	2.24E+09	4.34E+06	1,6
Capao-L4_2,1	#06	22/5/16	22:24:48	0.0019381	0.0000002	-17.74		0.12	0.85	2.25E+09	4.36E+06	1,6
Capao-L4_3,16	#06	22/5/16	22:30:07	0.0019396	0.0000002	-17.01		0.13	0.85	2.21E+09	4.29E+06	1,6
Capao-L4_2,2	#06	23/5/16	1:14:36	0.0019379	0.0000003	-17.84		0.13	0.85	2.28E+09	4.42E+06	1,6
Capao-L4_2,3	#06	23/5/16	1:20:27	0.0019378	0.0000003	-17.88		0.14	0.85	2.28E+09	4.43E+06	1,6
Capao-L4_1,5	#06	23/5/16	2:02:32	0.0019398	0.0000005	-16.96		0.23	0.86	2.26E+09	4.39E+06	1,6
Capao-L4_1,6	#06	23/5/16	2:07:46	0.0019400	0.0000003	-16.75		0.14	0.85	2.25E+09	4.36E+06	1,6
Capao-L4_8,1	#06	23/5/16	2:13:01	0.0019442	0.0000002	-14.59		0.12	0.85	2.23E+09	4.33E+06	1,6
Capao-L4_3,17	#06	23/5/16	2:34:11	0.0019394	0.0000003	-17.07		0.15	0.85	2.24E+09	4.35E+06	1,6
Capao-L4_9,1	#06	23/5/16	3:31:55	0.0019395	0.0000004	-18.58		0.22	0.86	2.25E+09	4.42E+06	1,6
Capao-L4_9,2	#06	23/5/16	3:37:09	0.0019397	0.0000002	-18.50		0.11	0.85	2.31E+09	4.48E+06	1,6
Capao-L4_4,6	#06	23/5/16	3:42:27	0.0019387	0.0000003	-17.44		0.15	0.85	2.25E+09	4.36E+06	1,6
Capao-L4_5,7	#06	23/5/16	4:03:36	0.0019393	0.0000002	-17.14		0.11	0.85	2.28E+09	4.42E+06	1,6
Capao-L4_8,2	#06	23/5/16	5:01:20	0.0019453	0.0000002	-14.07		0.12	0.85	2.23E+09	4.35E+06	1,6
Capao-L4_8,3	#06	23/5/16	5:06:34	0.0019446	0.0000002	-14.43		0.13	0.85	2.24E+09	4.35E+06	1,6
Capao-L4_1,7	#06	23/5/16	5:11:48	0.0019388	0.0000003	-17.49		0.14	0.85	2.29E+09	4.44E+06	1,6
Capao-L4_2,4	#06	23/5/16	5:17:02	0.0019380	0.0000002	-17.80		0.10	0.84	2.32E+09	4.50E+06	1,6
Capao-L4_2,5	#06	23/5/16	6:30:44	0.0019294	0.0000010	-22.23		0.49	0.91	2.33E+09	4.49E+06	1,6
Capao-L4_4,7	#06	23/5/16	6:36:03	0.0019395	0.0000003	-17.02		0.14	0.85	2.28E+09	4.42E+06	1,6
Capao-L4_7,5	#06	23/5/16	7:49:45	0.0019287	0.0000008	-22.61		0.42	0.89	2.30E+09	4.54E+06	1,6
Capao-L4_7,6	#06	23/5/16	7:54:58	0.0019387	0.0000002	-18.47		0.11	0.84	2.35E+09	4.55E+06	1,6
Capao-L4_9,3	#06	23/5/16	8:08:39	0.0019364	0.0000002	-18.62		0.11	0.84	2.35E+09	4.56E+06	1,6
Capao-L4_9,4	#06	23/5/16	8:13:53	0.0019369	0.0000002	-18.39		0.12	0.85	2.35E+09	4.56E+06	1,6
Capao-L4_10,1	#06	23/5/16	8:19:08	0.0019403	0.0000002	-18.61		0.11	0.85	2.31E+09	4.48E+06	1,6
Capao-L4_10,2	#06	23/5/16	8:24:22	0.0019420	0.0000003	-15.76		0.18	0.85	2.28E+09	4.42E+06	1,6
Capao-L4_4,8	#06	23/5/16	9:29:41	0.0019373	0.0000004	-16.15		0.21	0.85	2.30E+09	4.45E+06	1,6
Capao-L4_4,9	#06	23/5/16	9:34:54	0.0019396	0.0000003	-16.96		0.15	0.85	2.27E+09	4.40E+06	1,6
Capao-L4_2,6	#06	23/5/16	10:11:48	0.0019367	0.0000003	-18.46		0.15	0.85	2.32E+09	4.49E+06	1,6
Capao-L4_2,7	#06	23/5/16	10:17:02	0.0019370	0.0000003	-18.31		0.14	0.85	2.35E+09	4.55E+06	1,6
Capao-L4_8,4	#06	23/5/16	10:22:18	0.0019445	0.0000004	-14.46		0.09	0.84	2.26E+09	4.40E+06	1,6
Capao-L4_8,5	#06	23/5/16	10:27:30	0.0019440	0.0000003	-14.74		0.16	0.85	2.27E+09	4.40E+06	1,6
Capao-L4_7,7	#06	23/5/16	10:32:49	0.0019370	0.0000002	-18.34		0.11	0.84	2.37E+09	4.59E+06	1,6
Capao-L4_7,8	#06	23/5/16	10:38:02	0.0019362	0.0000003	-18.72		0.14	0.85	2.36E+09	4.59E+06	1,6
Capao-L4_4,8	#06	23/5/16	10:43:21	0.0019398	0.0000002	-17.12		0.15	0.85	2.30E+09	4.45E+06	1,6
Capao-L4_4,9	#06	23/5/16	10:48:35	0.0019397	0.0000002	-16.95		0.11	0.84	2.28E+09	4.42E+06	1,6
Capao-L4_3,18	#06	23/5/16	10:53:49	0.0019365	0.0000005	-18.57		0.27	0.86	2.32E+09	4.49E+06	1,6
Capao-L4_3,19	#06	23/5/16	10:59:03	0.0019405	0.0000002	-16.52		0.11	0.85	2.31E+09	4.48E+06	1,6
Capao-L4_2,5B	#06	23/5/16	11:06:52	0.0019375	0.0000002	-18.07		0.11	0.85	2.34E+09	4.54E+06	1,6
Capao-L4_7,5B	#06	23/5/16	11:12:56	0.0019362	0.0000002	-18.73		0.10	0.84	2.39E+09	4.62E+06	1,6
Capao-L4_10,2B	#06	23/5/16	11:53:39	0.0019412	0.0000003	-16.15		0.15	0.85	2.28E+09	4.42E+06	1,6
Capao-L4_10,3	#06	23/5/16	11:58:53	0.0019417	0.0000002	-15.91		0.09	0.84	2.29E+09	4.45E+06	1,6
Capao-L4_10,4	#06	23/5/16	12:04:06	0.0019409	0.0000003	-16.29		0.13	0.85	2.29E+09	4.45E+06	1,6
Capao-L4_3,20	#06	23/5/16	12:09:25	0.0019400	0.0000002	-16.77		0.11	0.85	2.30E+09	4.47E+06	1,6
Capao-L4_7,9	#06	23/5/16	12:46:26	0.0019381	0.0000003	-18.80		0.15	0.85	2.37E+09	4.60E+06	1,6
Capao-L4_9,5	#06	23/5/16	12:51:44	0.0019376	0.0000002	-18.00		0.13	0.85	2.35E+09	4.56E+06	1,6
Capao-L4_4,10	#06	23/5/16	12:57:02	0.0019373	0.0000005	-16.15		0.25	0.86	2.30E+09	4.46E+06	1,6
Capao-L4_3,21	#06	23/5/16	14:31:32	0.0019401	0.0000002	-16.73		0.10	0.84	2.31E+09	4.47E+06	1,6
Capao-L4_10,5	#06	23/5/16	15:03:02	0.0019418	0.0000002	-15.82		0.10	0.84	2.27E+09	4.41E+06	1,6
Capao-L4_10,6	#06	23/5/16	15:06:16	0.0019409	0.0000003	-16.30		0.13	0.85	2.29E+09	4.44E+06	1,6
Capao-L4_9,6	#06	23/5/16	15:13:21	0.0019370	0.0000002	-16.30		0.12	0.85	2.34E+09	4.53E+06	1,6
Capao-L4_9,7	#06	23/5/16	15:18:45	0.0019377	0.0000002	-17.98		0.12	0.85	2.32E+09	4.49E+06	1,6
Capao-L4_11,1	#06	23/5/16	15:23:59	0.0019408	0.0000002	-16.36		0.10	0.84	2.31E+09	4.47E+06	1,6
Capao-L4_11,2	#06	23/5/16	15:28:13	0.0019421	0.0000003	-15.70		0.13	0.85	2.27E+09	4.41E+06	1,6
Capao-L4_3,22	#06	23/5/16	15:34:31	0.0019412	0.0000003	-16.17		0.15	0.85	2.30E+09	4.47E+06	1,6
Capao-L4_3,23	#06	23/5/16	16:03:36	0.0019418	0.0000002	-15.85		0.11	0.85	2.30E+09	4.46E+06	1,6
Capao-L4_11,3	#06	23/5/16	16:09:49	0.0019418	0.0000002	-15.87		0.13	0.85	2.29E+09	4.46E+06	1,6
Capao-L4_9,8	#06	23/5/16	16:16:19	0.0019353	0.0000005	-19.21		0.26	0.86	2.36E+09	4.56E+06	1,6
#06			average	-17.07	weighted mean	-17.22						
			std dev (1σ)	1.19	error in mean (1σ)	0.13		0.27	1.17			
			50% variance	0.71	MSWD	153.21						
				no.		78						
				no. outliers		4						
MOUNT HM-18C												
Row L6												
Row-L5_1,6	#06	22/5/16	13:52:33	0.0019755	0.0000003	1.51		0.17	0.85	2.06E+09	4.06E+06	1,6
Row-L5_1,7	#06	22/5/16	13:57:47	0.0019760	0.0000003	1.79		0.14	0.85	2.08E+09	4.11E+06	1,6
Row-L5_1,8	#06	22/5/16	15:21:46	0.0019763	0.0000003	1.94		0.13	0.85	2.09E+09	4.13E+06	1,6
Row-L5_1,9	#06	22/5/16	17:28:21	0.0019769	0.0000002	2.25		0.13	0.85	2.14E+09	4.23E+06	1,6
Row-L5_1,10	#06	22/5/16	18:48:20	0.0019767	0.0000002	2.16		0.13	0.85	2.17E+09	4.30E+06	1,6
Row-L5_1,11	#06	22/5/16	21:06:05	0.0019739	0.0000004	0.73		0.19	0.85	2.22E+09	4.39E+06	1,6
Row-L5_1,12	#06	22/5/16	22:40:40	0.0019756	0.0000002	1.75		0.12	0.85	2.24E+09	4.42E+06	1,6
Row-L5_1,11B	#06	22/5/16	22:58:52	0.0019760	0.0000003	1.80		0.15	0.85	2.23E+09	4.41E+06	1,6
Row-L5_1,13	#06	23/5/16	2:28:54	0.0019752	0.0000003	1.40		0.15	0.85	2.25E+09	4.45E+06	1,6
Row-L5_1,14	#06	23/5/16	3:53:01	0.0019771	0.0000002	2.38		0.12	0.85	2.24E+09	4.43E+06	1,6
Row-L5_1,15	#06	23/5/16	5:27:38	0.0019775	0.0000002	2.57		0.11	0.85	2.19E+09	4.38E+06	1,6
Row-L5_1,16	#06	23/5/16	6:46:37	0.0019763	0.0000003	1.94		0.13	0.85	2.29E+09	4.52E+06	1,6
Row-L5_1,17	#06	23/5/16	8:05:35	0.0019781	0.0000004	1.31		0.21	0.85	2.29E+09	4.52E+06	1,6
Row-L5_1,18	#06	23/5/16	10:01:15	0.0019767	0.0000002	2.16		0.12	0.85	2.24E+09	4.42E+06	1,6
Row-L5_1,19	#06	23/5/16	10:06:29	0.0019758	0.0000003	1.69		0.16	0.85	2.31E+09	4.56E+06	1,6
Row-L5_1,20	#06	23/5/16	13:02:19	0.0019777	0.0000002	2.65		0.11	0.84	2.33E+09	4.61E+06	1,6
#06			average	1.95	weighted mean	1.96						
			std dev (1σ)	0.41	error in mean (1σ)	0.10		0.21	1.10			
			50% variance	0.08	MSWD	16.40						
				no.		16						
				no. outliers		1						
MOUNT HM-18C												
Row L6												
Row-L6_1,6	#06	22/5/16	13:42:02	0.0019766	0.0000004	2.11		0.20	0.85	2.06E+09	4.06E+06	1,6
Row-L6_1,7	#06	22/5/16	13:47:16	0.0019766	0.0000002	2.10		0.10	0.85	2.06E+09	4.07E+06	1,6
Row-L6_1,8	#06	22/5/16	15:16:28	0.00								

SPOT #	Session	Date	Time	T ₀ /T ₀	z	δ ⁰ O ₂ nom	rejected	±Internal error (σ 95%)	±External error (1σ)	T ₀ cps (median)	T ₀ cps (median)	no. sets subsets										
Capao-L4-19_2.1	#06	23/5/16	22:07:03	0.0019409	0.0000002	-14.771		0.11	1.01	2.33E+09	4.53E+06	1.6										
Capao-L4-19_2.2	#06	23/5/16	22:13:46	0.0019409	0.0000002	-14.70		0.12	1.01	2.31E+09	4.48E+06	1.6										
Capao-L4-19_2.3	#06	23/5/16	23:00:42	0.0019402	0.0000004	-15.11		0.19	1.01	2.30E+09	4.46E+06	1.6										
Capao-L4-19_1.4	#06	23/5/16	23:07:24	0.0019331	0.0000003	-18.78		0.15	1.01	2.38E+09	4.60E+06	1.6										
Capao-L4-19_1.5	#06	23/5/16	23:34:14	0.0019349	0.0000002	-17.89		0.11	1.01	2.39E+09	4.62E+06	1.6										
Capao-L4-19_1.6	#06	23/5/16	23:40:56	0.0019336	0.0000002	-18.51		0.12	1.01	2.38E+09	4.57E+06	1.6										
Capao-L4-19_1.38b	#06	23/5/16	23:47:39	0.0019337	0.0000003	-18.46		0.15	1.01	2.38E+09	4.60E+06	1.6										
Capao-L4-19_1.18b	#06	23/5/16	23:54:21	0.0019349	0.0000003	-17.99		0.14	1.01	2.38E+09	4.60E+06	1.6										
Capao-L4-19_2.18b	#06	24/5/16	0:01:06	0.0019397	0.0000002	-15.37		0.13	1.01	2.33E+09	4.53E+06	1.6										
Capao-L4-19_2.28b	#06	24/5/16	0:08:06	0.0019384	0.0000004		-16.02	0.20	1.01	2.33E+09	4.52E+06	1.6										
Capao-L4-19_2.38b	#06	24/5/16	0:15:07	0.0019407	0.0000002	-14.85		0.12	1.01	2.34E+09	4.53E+06	1.6										
Capao-L4_1.18b	#06	24/5/16	1:18:09	0.0019354	0.0000002	-17.59		0.11	1.01	2.43E+09	4.70E+06	1.6										
Capao-L4_1.28b	#06	24/5/16	1:25:09	0.0019348	0.0000002	-17.87		0.12	1.01	2.45E+09	4.74E+06	1.6										
Capao-L4_1.38b	#06	24/5/16	1:32:09	0.0019347	0.0000004	-17.94		0.19	1.01	2.44E+09	4.72E+06	1.6										
Capao-L4_3.4	#06	24/5/16	1:39:10	0.0019386	0.0000003	-15.99		0.15	1.01	2.37E+09	4.55E+06	1.6										
Capao-L4_3.5	#06	24/5/16	1:46:10	0.0019405	0.0000002	-14.95		0.12	1.01	2.38E+09	4.59E+06	1.6										
Capao-L4_3.6	#06	24/5/16	1:53:10	0.0019395	0.0000004	-15.45		0.20	1.01	2.38E+09	4.62E+06	1.6										
Capao-L4_4.4	#06	24/5/16	2:00:10	0.0019386	0.0000002	-16.93		0.11	1.01	2.42E+09	4.69E+06	1.6										
Capao-L4_4.5	#06	24/5/16	2:07:11	0.0019354	0.0000004	-17.57		0.18	1.01	2.43E+09	4.70E+06	1.6										
Capao-L4_4.6	#06	24/5/16	2:14:11	0.0019374	0.0000003	-16.54		0.14	1.01	2.43E+09	4.70E+06	1.6										
Capao-L4-19_1.7	#06	24/5/16	3:38:14	0.0019335	0.0000003	-18.57		0.14	1.01	2.40E+09	4.65E+06	1.6										
Capao-L4-19_1.8	#06	24/5/16	3:45:14	0.0019338	0.0000003	-18.42		0.14	1.01	2.39E+09	4.62E+06	1.6										
Capao-L4-19_3.1	#06	24/5/16	3:52:14	0.0019368	0.0000003	-16.84		0.16	1.01	2.41E+09	4.68E+06	1.6										
Capao-L4-19_3.2	#06	24/5/16	3:59:15	0.0019349	0.0000004	-17.82		0.18	1.01	2.40E+09	4.65E+06	1.6										
Capao-L4-19_2.4	#06	24/5/16	5:51:19	0.0019401	0.0000002	-15.13		0.09	1.01	2.39E+09	4.57E+06	1.6										
Capao-L4-19_2.5	#06	24/5/16	5:58:19	0.0019388	0.0000003	-15.79		0.15	1.01	2.37E+09	4.59E+06	1.6										
Capao-L4-19_1.9	#06	24/5/16	7:01:21	0.0019340	0.0000002	-18.29		0.13	1.01	2.40E+09	4.64E+06	1.6										
Capao-L4-19_1.10	#06	24/5/16	7:08:21	0.0019350	0.0000002	-17.78		0.10	1.01	2.38E+09	4.57E+06	1.6										
Capao-L4-19_1.11	#06	24/5/16	8:11:24	0.0019354	0.0000002	-17.55		0.13	1.01	2.38E+09	4.57E+06	1.6										
Capao-L4-19_1.12	#06	24/5/16	8:18:24	0.0019333	0.0000002	-18.63		0.13	1.01	2.41E+09	4.66E+06	1.6										
				average	-17.13	weighted mean	-17.22															
				std dev (1σ)	1.42	error in mean (1σ)	0.21	Internal error (σ 95%)	0.43													
				50% variance	1.01	MSWD	190.85															
							no.	49														
							no. outliers	5														
MOUNT HM-19_20A																						
RoyL5																						
RoyL5_1.1	#06	23/5/16	17:58:56	0.0019746	0.0000002	2.70		0.10	1.01	2.39E+09	4.71E+06	1.6										
RoyL5_1.2	#06	23/5/16	18:05:38	0.0019719	0.0000003	1.26		0.24	1.02	2.38E+09	4.69E+06	1.6										
RoyL5_1.3	#06	23/5/16	18:12:20	0.0019740	0.0000002	2.39		0.12	1.01	2.38E+09	4.69E+06	1.6										
RoyL5_1.28b	#06	23/5/16	19:19:24	0.0019736	0.0000003	2.18		0.13	1.01	2.39E+09	4.71E+06	1.6										
RoyL5-19_1.1	#06	23/5/16	19:19:45	0.0019727	0.0000004	1.68		0.19	1.01	2.33E+09	4.58E+06	1.6										
RoyL5-19_1.2	#06	23/5/16	20:26:28	0.0019739	0.0000002	2.33		0.11	1.01	2.32E+09	4.58E+06	1.6										
RoyL5-19_1.3	#06	23/5/16	20:33:10	0.0019681	0.0000004		-0.68	0.21	1.02	2.36E+09	4.65E+06	1.6										
RoyL5-19_1.38b	#06	24/5/16	0:22:07	0.0019728	0.0000002	1.76		0.11	1.02	2.38E+09	4.68E+06	1.6										
RoyL5-19_1.4	#06	24/5/16	5:09:17	0.0019683	0.0000004		-0.57	0.21	1.02	2.39E+09	4.69E+06	1.6										
RoyL5-19_1.5	#06	24/5/16	5:16:17	0.0019736	0.0000002	2.15		0.09	1.01	2.37E+09	4.67E+06	1.6										
RoyL5-19_1.6	#06	24/5/16	5:23:18	0.0019745	0.0000002	2.63		0.11	1.01	2.38E+09	4.71E+06	1.6										
RoyL5-19_1.38b	#06	24/5/16	9:07:26	0.0019759	0.0000002	3.36		0.11	1.01	2.38E+09	4.69E+06	1.6										
RoyL5-Vert_1.1	#06	24/5/16	9:14:26	0.0019742	0.0000003	2.49		0.15	1.01	2.36E+09	4.65E+06	1.6										
RoyL5-Vert_1.2	#06	24/5/16	9:21:26	0.0019752	0.0000005	1.95		0.23	1.02	2.37E+09	4.67E+06	1.6										
RoyL5_2.1	#06	24/5/16	9:49:27	0.0019663	0.0000006		-1.59	0.33	1.03	6.32E+08	1.24E+06	1.6										
RoyL5_2.2	#06	24/5/16	9:56:07	0.0019586	0.0000007		-5.56	0.34	1.03	8.17E+08	1.79E+06	1.6										
RoyL5_2.3	#06	24/5/16	10:03:28	0.0019534	0.0000008		-8.27	0.41	1.05	8.35E+08	1.63E+06	1.6										
RoyL5_1.4	#06	24/5/16	10:10:28	0.0019756	0.0000002	3.21		0.11	1.01	2.38E+09	4.72E+06	1.6										
RoyL5_1.5	#06	24/5/16	10:17:28	0.0019755	0.0000002	3.16		0.12	1.01	2.38E+09	4.73E+06	1.6										
RoyL5_1.6	#06	24/5/16	10:24:28	0.0019745	0.0000002	2.63		0.11	1.01	2.40E+09	4.74E+06	1.6										
RoyL5_1.7	#06	24/5/16	10:31:29	0.0019746	0.0000002	2.69		0.12	1.01	2.39E+09	4.72E+06	1.6										
RoyL5_1.8	#06	24/5/16	10:38:29	0.0019759	0.0000004	2.29		0.21	1.02	2.41E+09	4.75E+06	1.6										
RoyL5-19_1.48b	#06	24/5/16	10:45:29	0.0019745	0.0000002	2.64		0.10	1.01	2.37E+09	4.68E+06	1.6										
RoyL5-19_1.7	#06	24/5/16	10:52:29	0.0019741	0.0000002	2.40		0.11	1.01	2.39E+09	4.72E+06	1.6										
RoyL5-19_1.8	#06	24/5/16	10:56:30	0.0019712	0.0000004	0.93		0.23	1.02	2.38E+09	4.68E+06	1.6										
RoyL5-19_1.9	#06	24/5/16	11:06:30	0.0019725	0.0000003	1.59		0.17	1.01	2.38E+09	4.70E+06	1.6										
RoyL5-19_1.10	#06	24/5/16	11:13:30	0.0019724	0.0000002	1.52		0.12	1.01	2.38E+09	4.69E+06	1.6										
				average	2.27	weighted mean	2.09															
				std dev (1σ)	0.83	error in mean (1σ)	0.22	Internal error (σ 95%)	0.46													
				50% variance	0.20	MSWD	72.31															
							no.	27														
							no. outliers	5														
MOUNT HM-19_20A																						
RoyL6																						
RoyL6_1.1	#06	23/5/16	18:19:03	0.0019761	0.0000003	3.43		0.15	1.01	2.33E+09	4.81E+06	1.6										
RoyL6_1.2	#06	23/5/16	18:25:45	0.0019757	0.0000002	3.28		0.10	1.01	2.36E+09	4.66E+06	1.6										
RoyL6_1.3	#06	23/5/16	18:32:27	0.0019753	0.0000002	3.02		0.09	1.01	2.35E+09	4.64E+06	1.6										
RoyL6-19_1.1	#06	23/5/16	20:39:52	0.0019737	0.0000003	2.22		0.17	1.01	2.34E+09	4.62E+06	1.6										
RoyL6-19_1.2	#06	23/5/16	20:46:35	0.0019703	0.0000005	1.12	0.45	0.11	1.02	2.42E+09	4.73E+06	1.6										
RoyL6-19_1.3	#06	23/5/16	20:53:17	0.0019720	0.0000003	1.36		0.13	1.01	2.38E+09	4.68E+06	1.6										
RoyL6-19_1.18b	#06	24/5/16	0:29:07	0.0019749	0.0000003	2.84		0.13	1.01	2.35E+09	4.64E+06	1.6										
RoyL6-19_1.28b	#06	24/5/16	0:36:07	0.0019743	0.0000002	2.51		0.11	1.02	2.36E+09	4.65E+06	1.6										
RoyL6-19_1.38b	#06	24/5/16	0:43:08	0.0019711	0.0000003		0.85	0.17	1.01	2.38E+09	4.68E+06	1.6										
RoyL6-19_1.4	#06	24/5/16	5:30:18	0.0019723	0.0000002	1.49		0.12	1.01	2.37E+09	4.67E+06	1.6										
RoyL6-19_1.5	#06	24/5/16	5:37:18	0.0019744	0.0000002	2.56		0.11	1.01	2.37E+09	4.68E+06	1.6										
RoyL6-19_1.6	#06	24/5/16	5:44:18	0.0019722	0.0000003	1.43		0.17	1.01	2.38E+09	4.69E+06	1.6										
RoyL6_1.4	#06	24/5/16	8:25:24	0.0019763	0.0000002	3.57		0.10	1.01	2.35E+09	4.64E+06	1.6										
RoyL6_1.5	#06	24/5/16	8:32:24	0.0019754	0.0000003	3.10		0.13	1.01	2.36E+09	4.65E+06	1.6										
RoyL6_1.6	#06	24/5/16	8:39:25	0.0019763	0.0000002	3.54		0.12	1.01	2.37E+09	4.68E+06	1.6										
RoyL6-Vert_1.1	#06	24/5/16	8:46:25	0.0019753	0.0000002	3.05		0.15	1.02	2.41E+09	4.73E+06	1.6										
RoyL6-Vert_1.2	#06	24/5/16	8:53:25	0.0019740	0.0000002	2.37		0.12	1.01	2.38E+09	4.65E+06	1.6										
RoyL6-Vert_1.3	#06	24/5/16	8:59:25	0.0019762	0.0000002	2.35		0.11	1.01	2.37E+09	4.68E+06	1.6										
RoyL6-19_1.7	#06	24/5/16	11:20:30	0.0019721	0.0000003	1.39		0.10	1.01	2.34E+09	4.64E+06	1.6										
RoyL6-19_1.8	#06	24/5/16	11:27:31	0.0019735	0.0000002	2.10		0.09	1.01	2.40E+09	4.73E+06	1.6										
RoyL6-19_1.9	#06	24/5/16	11:34:31	0.0019714																		

SPOT #	Session	Date	Time	T ₀ /T ₀	±	δ ⁰ Obs _{own}	rejected	±Internal error (σ 95%)	±External error (1σ)	T ₀ cps (median)	T ₀ cps (median)	no. sets, subsets
Capao-L4-19_1.13	#06	25/5/16	7:22.10	0.0019480	0.0000004	-19.59		0.18	0.48	2.41E+09	4.70E+06	1.6
Capao-L4-19_1.14	#06	25/5/16	8:37.19	0.0019498	0.0000003	-17.68		0.16	0.48	2.51E+09	4.88E+06	1.6
Capao-L4-19_1.15	#06	25/5/16	8:44.09	0.0019498	0.0000003	-17.67		0.15	0.48	2.51E+09	4.90E+06	1.6
Capao-L4-19_1.16	#06	25/5/16	9:18.19	0.0019497	0.0000004	-17.74		0.18	0.49	2.51E+09	4.89E+06	1.6
Capao-L4_4.8	#06	25/5/16	11:07.39	0.0019519	0.0000003	-16.57		0.16	0.48	2.50E+09	4.87E+06	1.6
Capao-L4_4.9	#06	25/5/16	11:14.29	0.0019516	0.0000003	-16.76		0.13	0.48	2.47E+09	4.81E+06	1.6
Capao-L4_4.10	#06	25/5/16	11:21.19	0.0019520	0.0000004	-16.54		0.19	0.49	2.49E+09	4.85E+06	1.6
Capao-L4_1.7	#06	25/5/16	11:28.09	0.0019522	0.0000003	-16.45		0.18	0.48	2.52E+09	4.91E+06	1.6
Capao-L4_1.8	#06	25/5/16	11:34.59	0.0019520	0.0000003	-16.58		0.16	0.48	2.51E+09	4.89E+06	1.6
Capao-L4-19_1.17B	#06	25/5/16	12:15.59	0.0019497	0.0000003	-17.71		0.17	0.48	2.53E+09	4.92E+06	1.6
Capao-L4-19_1.3.8	#06	25/5/16	13:51.38	0.0019526	0.0000003	-16.22		0.15	0.48	2.50E+09	4.87E+06	1.6
Capao-L4-19_1.21	#06	25/5/16	14:58.58	0.0019504	0.0000003	-17.36		0.14	0.48	2.50E+09	4.88E+06	1.6
Capao-L4-19_1.22	#06	25/5/16	15:06.48	0.0019497	0.0000003	-17.73		0.14	0.48	2.52E+09	4.90E+06	1.6
Capao-L4-19_1.12	#06	25/5/16	15:13.38	0.0019498	0.0000002	-17.65		0.13	0.48	2.49E+09	4.85E+06	1.6
Capao-L4-19_1.24	#06	25/5/16	16:26.48	0.0019510	0.0000003	-17.05		0.16	0.48	2.50E+09	4.89E+06	1.6
Capao-L4-19_1.25	#06	25/5/16	16:35.38	0.0019513	0.0000002	-16.92		0.11	0.47	2.52E+09	4.91E+06	1.6
#06	STANDARD	average		-17.22	weighted mean	-17.22						
		std dev (1σ)		0.66	error in mean (1σ)	0.08	Internal error (σ 95%)	0.17				
		50% variance		0.22	MSWD	24.62						
					no. no. outliers	62 4						
MOUNT HM-19_20B												
RoyL5												
RoyL5_1.1	#06	24/5/16	16:57.16	0.0019885	0.0000003	2.16		0.15	0.48	2.46E+09	4.90E+06	1.6
RoyL5_1.2	#06	24/5/16	17:04.26	0.0019876	0.0000003	1.73		0.15	0.48	2.45E+09	4.89E+06	1.6
RoyL5_1.3	#06	24/5/16	17:11.35	0.0019880	0.0000004	1.89		0.20	0.49	2.47E+09	4.90E+06	1.6
RoyL5_1.4	#06	24/5/16	17:18.44	0.0019888	0.0000003	2.32		0.14	0.48	2.43E+09	4.84E+06	1.6
RoyL5_1.5	#06	24/5/16	17:25.54	0.0019880	0.0000004	1.91		0.18	0.49	2.44E+09	4.85E+06	1.6
RoyL5-19_1.1	#06	24/5/16	23:45.13	0.0019892	0.0000004	2.50		0.18	0.49	2.39E+09	4.79E+06	1.6
RoyL5-19_1.2	#06	24/5/16	23:52.23	0.0019889	0.0000003	2.36		0.15	0.48	2.39E+09	4.79E+06	1.6
RoyL5-19_1.3	#06	24/5/16	23:59.32	0.0019886	0.0000003	2.25		0.13	0.48	2.40E+09	4.79E+06	1.6
RoyL5-19_1.4	#06	25/5/16	6:34.20	0.0019894	0.0000004	2.65		0.19	0.49	2.40E+09	4.79E+06	1.6
RoyL5-19_1.5	#06	25/5/16	6:41.10	0.0019885	0.0000003	2.16		0.18	0.48	2.41E+09	4.79E+06	1.6
RoyL5-19_1.6	#06	25/5/16	6:48.00	0.0019892	0.0000003	2.55		0.14	0.48	2.40E+09	4.77E+06	1.6
RoyL5-Vert_1.1	#06	25/5/16	9:59.19	0.0019916	0.0000003	3.75		0.17	0.48	2.42E+09	4.81E+06	1.6
RoyL5-Vert_1.2	#06	25/5/16	10:06.09	0.0019920	0.0000003	3.98		0.14	0.48	2.42E+09	4.82E+06	1.6
RoyL5-Vert_1.3	#06	25/5/16	10:12.59	0.0019912	0.0000003	3.56		0.16	0.48	2.40E+09	4.79E+06	1.6
RoyL5-Vert_1.4	#06	25/5/16	10:19.49	0.0019917	0.0000003	3.83		0.17	0.48	2.42E+09	4.81E+06	1.6
RoyL5-Vert_1.5	#06	25/5/16	10:26.29	0.0019928	0.0000002	4.35		0.12	0.48	2.42E+09	4.82E+06	1.6
RoyL5-19_1.7	#06	25/5/16	13:10.39	0.0019915	0.0000004	2.07	3.73	0.20	0.49	2.43E+09	4.83E+06	1.6
RoyL5-19_1.8	#06	25/5/16	13:17.29	0.0019895	0.0000003	2.69		0.17	0.48	2.43E+09	4.83E+06	1.6
RoyL5-19_1.7B	#06	25/5/16	13:44.49	0.0019879	0.0000004	1.87		0.21	0.49	2.45E+09	4.86E+06	1.6
#06		average		2.69	weighted mean	2.71						
		std dev (1σ)		0.82	error in mean (1σ)	0.19	Internal error (σ 95%)	0.41				
		50% variance		0.34	MSWD	51.62						
					no. no. outliers	19 1						
MOUNT HM-19_20B												
RoyL6												
RoyL6_1.1	#06	24/5/16	17:35.03	0.0019909	0.0000004	3.38		0.18	0.49	2.37E+09	4.72E+06	1.6
RoyL6_1.2	#06	24/5/16	17:40.13	0.0019905	0.0000003	3.19		0.15	0.48	2.39E+09	4.75E+06	1.6
RoyL6_1.3	#06	24/5/16	17:47.22	0.0019897	0.0000004	2.79		0.18	0.49	2.41E+09	4.79E+06	1.6
RoyL6_1.4	#06	24/5/16	17:54.32	0.0019898	0.0000004	2.83		0.19	0.49	2.40E+09	4.78E+06	1.6
RoyL6_1.6	#06	24/5/16	18:01.41	0.0019915	0.0000004	2.19	3.70	0.19	0.49	2.39E+09	4.78E+06	1.6
RoyL6_1.5	#06	24/5/16	18:20.25	0.0019898	0.0000003	2.82		0.16	0.48	2.42E+09	4.81E+06	1.6
RoyL6_1.6B	#06	24/5/16	18:27.34	0.0019911	0.0000002	3.50		0.11	0.47	2.38E+09	4.73E+06	1.6
RoyL6_1.7	#06	24/5/16	18:34.43	0.0019893	0.0000003	3.09		0.15	0.48	2.40E+09	4.77E+06	1.6
RoyL6-19_1.1	#06	25/5/16	0:04.51	0.0019888	0.0000003	2.32		0.17	0.48	2.45E+09	4.86E+06	1.6
RoyL6-19_1.2	#06	25/5/16	0:11.41	0.0019889	0.0000003	2.39		0.15	0.48	2.45E+09	4.88E+06	1.6
RoyL6-19_1.3	#06	25/5/16	0:18.31	0.0019880	0.0000003	1.90		0.17	0.48	2.47E+09	4.92E+06	1.6
RoyL6-19_1.1B	#06	25/5/16	4:31.20	0.0019885	0.0000003	2.14		0.22	0.49	2.47E+09	4.91E+06	1.6
RoyL6-19_1.2B	#06	25/5/16	4:38.10	0.0019890	0.0000004	2.43		0.21	0.49	2.44E+09	4.88E+06	1.6
RoyL6-19_1.3B	#06	25/5/16	4:45.00	0.0019880	0.0000003	1.92		0.17	0.48	2.47E+09	4.90E+06	1.6
RoyL6-19_1.4	#06	25/5/16	4:51.50	0.0019883	0.0000003	2.07		0.19	0.49	2.46E+09	4.89E+06	1.6
RoyL6-19_1.4	#06	25/5/16	6:54.50	0.0019891	0.0000003	2.48		0.14	0.48	2.47E+09	4.90E+06	1.6
RoyL6-19_1.5	#06	25/5/16	7:01.40	0.0019903	0.0000003	3.11		0.14	0.48	2.45E+09	4.88E+06	1.6
RoyL6-19_1.6	#06	25/5/16	7:08.30	0.0019889	0.0000003	2.86		0.17	0.48	2.47E+09	4.90E+06	1.6
RoyL6-Vert_1.1	#06	25/5/16	9:25.09	0.0019880	0.0000003	1.93		0.13	0.48	2.48E+09	4.93E+06	1.6
RoyL6-Vert_1.2	#06	25/5/16	9:31.59	0.0019901	0.0000003	2.98		0.16	0.48	2.38E+09	4.74E+06	1.6
RoyL6-Vert_1.3	#06	25/5/16	9:38.49	0.0019884	0.0000003	2.10		0.16	0.48	2.45E+09	4.86E+06	1.6
RoyL6-Vert_1.4	#06	25/5/16	9:45.39	0.0019883	0.0000003	2.09		0.14	0.48	2.48E+09	4.89E+06	1.6
RoyL6-Vert_1.5	#06	25/5/16	9:52.29	0.0019886	0.0000003	2.21		0.15	0.48	2.45E+09	4.88E+06	1.6
RoyL6-19_1.7	#06	25/5/16	13:03.49	0.0019888	0.0000003	2.34		0.17	0.48	2.47E+09	4.90E+06	1.6
RoyL6-19_1.6B	#06	25/5/16	13:37.59	0.0019893	0.0000003	2.60		0.14	0.48	2.46E+09	4.94E+06	1.6
#06		average		2.54	weighted mean	2.57						
		std dev (1σ)		0.48	error in mean (1σ)	0.10	Internal error (σ 95%)	0.20				
		50% variance		0.12	MSWD	19.55						
					no. no. outliers	25 1						
MOUNT HM-19_20B												
Step-6-D1												
Step-6-D1_1.1	#06	24/5/16	18:08.50	0.0019919	0.0000004	3.89		0.18	0.48	2.39E+09	4.79E+06	1.6
Step-6-D1_1.2	#06	24/5/16	18:16.00	0.0019917	0.0000003	3.83		0.16	0.48	2.37E+09	4.73E+06	1.6
Step-6-D1_1.3	#06	24/5/16	18:23.09	0.0019922	0.0000003	4.05		0.15	0.48	2.38E+09	4.74E+06	1.6
Step-6-D1_1.4	#06	24/5/16	18:30.19	0.0019912	0.0000003	3.54		0.14	0.48	2.38E+09	4.73E+06	1.6
Step-6-D1_1.5	#06	24/5/16	18:37.28	0.0019917	0.0000003	3.83		0.14	0.48	2.38E+09	4.76E+06	1.6
Step-6-D1_1.6	#06	24/5/16	18:44.38	0.0019913	0.0000003	3.63		0.14	0.48	2.39E+09	4.77E+06	1.6
Step-6-D1-19_1.1	#06	25/5/16	2:21.31	0.0019903	0.0000003	3.10		0.13	0.48	2.46E+09	4.85E+06	1.6
Step-6-D1-19_1.2	#06	25/5/16	2:28.21	0.0019913	0.0000003	3.59		0.15	0.48	2.48E+09	4.85E+06	1.6
Step-6-D1-19_1.3	#06	25/5/16	2:35.11	0.0019913	0.0000003	3.60		0.15	0.48	2.46E+09	4.90E+06	1.6
Step-6-D1-19_1.4	#06	25/5/16	2:42.01	0.0019890	0.0000004	2.40		0.18	0.48	2.45E+09	4.87E+06	1.6
Step-6-D1-19_1.5	#06	25/5/16	2:48.51	0.0019913	0.0000003	3.60		0.13	0.48	2.46E+09	4.89E+06	1.6
Step-6-D1-19_1.4B	#06	25/5/16	4:17.40	0.0019892	0.0000003	2.51		0.14	0.48	2.46E+09	4.88E+06	1.6
Step-6-D1-19_1.1B	#06	25/5/16	4:24.30	0.0019905	0.0000004	3.21		0.20	0.49	2.50E+09	4.97E+06	1.6
Step-6-D1-Vert_1.1	#06	25/5/1										

		Session	Date	Time	T ₀ /T ₀	z	δ ¹⁵ O _{avow}	rejected	±Internal error (σ 95%)	±External error (1σ)	¹⁵ O cps (median)	¹⁵ O cps (median)	no. sets subsets
RoyL5-Vert_4.4	#06		26/5/16	1:54:05	0.001990299	0.000002251	3.02		0.13	0.26	2.45E+09	4.88E+06	1.6
RoyL5-Vert_4.3	#06		26/5/16	3:13:41	0.001990887	0.000000334	3.32		0.17	0.27	2.46E+09	4.91E+06	1.6
RoyL5-Vert_4.5	#06		26/5/16	3:19:48	0.001990649	0.000000295	3.20		0.15	0.27	2.47E+09	4.91E+06	1.6
RoyL5-1.1	#06		26/5/16	7:06:20	0.001990413	0.000000321	3.08		0.16	0.27	2.54E+09	5.06E+06	1.6
RoyL5-1.2	#06		26/5/16	7:12:27	0.001989884	0.000000088	2.20		0.20	0.28	2.53E+09	5.03E+06	1.6
RoyL5-1.3	#06		26/5/16	7:18:35	0.001988875	0.000000328	2.29		0.16	0.27	2.47E+09	4.91E+06	1.6
RoyL5-1.4	#06		26/5/16	7:24:42	0.001988558	0.000000308	1.10		0.15	0.27	2.48E+09	4.93E+06	1.6
RoyL5-1.5	#06		26/5/16	7:30:49	0.001989733	0.000000328	1.19		0.17	0.27	2.49E+09	4.95E+06	1.6
	#06			average	1.92	weighted mean	1.95						
				std dev (1σ)	0.99	error in mean (1σ)	0.23	Internal error (σ 95%)	0.48				
				50% variance	0.49	MSWD	83.76						
					no.		19						
					no. outliers		0						
MOUNT HM-20_BAH													
RoyL6													
RoyL6-2.1	#06		25/5/16	18:17:29	0.001991541	0.000000325	3.66		0.16	0.27	2.41E+09	4.79E+06	1.6
RoyL6-2.2	#06		25/5/16	18:23:28	0.001991213	0.000000313	3.49		0.16	0.27	2.41E+09	4.81E+06	1.6
RoyL6-2.3	#06		25/5/16	19:11:15	0.001991141	0.000000325	3.45		0.16	0.27	2.44E+09	4.89E+06	1.6
RoyL6-2.4	#06		25/5/16	19:17:14	0.001990208	0.000000298	2.97		0.15	0.27	2.43E+09	4.84E+06	1.6
RoyL6-3.1	#06		25/5/16	22:04:30	0.001989293	0.000000338	2.51		0.17	0.27	2.47E+09	4.91E+06	1.6
RoyL6-3.2	#06		25/5/16	22:10:29	0.001989372	0.000000316	2.55		0.16	0.27	2.48E+09	4.95E+06	1.6
RoyL6-3.3	#06		25/5/16	22:16:27	0.001990971	0.000000393	3.37		0.20	0.28	2.46E+09	4.90E+06	1.6
RoyL6-3.4	#06		25/5/16	23:16:12	0.001990201	0.000000298	2.97		0.15	0.27	2.48E+09	4.94E+06	1.6
RoyL6-3.5	#06		25/5/16	23:22:10	0.001991919	0.000000257	3.85		0.13	0.26	2.46E+09	4.91E+06	1.6
RoyL6-3.6	#06		25/5/16	23:28:09	0.001990959	0.000000340	3.12		0.17	0.27	2.49E+09	4.95E+06	1.6
RoyL6-Vert_4.1	#06		26/5/16	2:00:13	0.001988705	0.000000334	2.20		0.17	0.27	2.45E+09	4.87E+06	1.6
RoyL6-Vert_4.2	#06		26/5/16	2:06:20	0.001990092	0.000000263	2.91		0.13	0.26	2.44E+09	4.87E+06	1.6
RoyL6-Vert_4.3	#06		26/5/16	2:12:27	0.001989936	0.000000303	2.16		0.16	0.27	2.46E+09	4.90E+06	1.6
RoyL6-Vert_4.4	#06		26/5/16	3:25:55	0.001990800	0.000000368	2.40		0.18	0.28	2.45E+09	4.87E+06	1.6
RoyL6-Vert_4.5	#06		26/5/16	3:32:03	0.001988415	0.000000317	2.05		0.16	0.27	2.48E+09	4.93E+06	1.6
RoyL6-1.1	#06		26/5/16	7:36:57	0.001991499	0.000000325	3.64		0.16	0.27	2.44E+09	4.86E+06	1.6
RoyL6-1.2	#06		26/5/16	7:43:04	0.001991348	0.000000331	3.56		0.17	0.27	2.47E+09	4.91E+06	1.6
RoyL6-1.3	#06		26/5/16	7:49:11	0.001991857	0.000000345	3.82		0.17	0.27	2.46E+09	4.91E+06	1.6
RoyL6-1.4	#06		26/5/16	7:55:19	0.001989735	0.000000324	2.73		0.16	0.27	2.48E+09	4.96E+06	1.6
RoyL6-1.5	#06		26/5/16	8:01:26	0.001989041	0.000000367	2.38		0.18	0.28	2.49E+09	4.96E+06	1.6
	#06			average	3.02	weighted mean	3.01						
				std dev (1σ)	0.56	error in mean (1σ)	0.13	Internal error (σ 95%)	0.26				
				50% variance	0.16	MSWD	18.30						
					no.		20						
					no. outliers		0						
MOUNT HM-20_BAH													
Stop-6-D1													
Stop-6-D1_2.1	#06		25/5/16	17:53:35	0.001991484	0.000000352	3.63		0.18	0.27	2.49E+09	4.96E+06	1.6
Stop-6-D1_2.2	#06		25/5/16	17:59:34	0.001990980	0.000000287	3.37		0.14	0.26	2.49E+09	4.95E+06	1.6
Stop-6-D1_2.3	#06		25/5/16	18:47:21	0.001990927	0.000000311	3.19		0.16	0.27	2.48E+09	4.94E+06	1.6
Stop-6-D1_2.4	#06		25/5/16	18:53:20	0.001990947	0.000000310	3.35		0.16	0.27	2.46E+09	4.89E+06	1.6
Stop-6-D1_3.1	#06		25/5/16	21:28:40	0.001991624	0.000000325	3.70		0.16	0.27	2.45E+09	4.87E+06	1.6
Stop-6-D1_3.2	#06		25/5/16	21:34:38	0.001990943	0.000000334	3.35		0.17	0.27	2.45E+09	4.87E+06	1.6
Stop-6-D1_3.3	#06		25/5/16	21:40:37	0.001991159	0.000000325	3.46		0.16	0.27	2.41E+09	4.80E+06	1.6
Stop-6-D1_3.4	#06		25/5/16	22:52:18	0.001991082	0.000000310	3.41		0.16	0.27	2.41E+09	4.81E+06	1.6
Stop-6-D1_3.5	#06		25/5/16	22:58:16	0.001991836	0.000000281	3.81		0.15	0.26	2.42E+09	4.82E+06	1.6
Stop-6-D1-Vert_4.1	#06		26/5/16	2:43:04	0.001991987	0.000000293	3.67		0.15	0.27	2.49E+09	4.97E+06	1.6
Stop-6-D1-Vert_4.2	#06		26/5/16	2:49:11	0.001991560	0.000000346	3.67		0.17	0.27	2.49E+09	4.96E+06	1.6
Stop-6-D1-Vert_4.3	#06		26/5/16	2:55:19	0.001992573	0.000000296	4.19		0.15	0.27	2.49E+09	4.95E+06	1.6
Stop-6-D1-Vert_4.4	#06		26/5/16	3:38:10	0.001992076	0.000000328	4.09		0.16	0.28	2.49E+09	4.96E+06	1.6
Stop-6-D1-Vert_4.5	#06		26/5/16	3:44:18	0.001991758	0.000000309	3.77		0.16	0.27	2.49E+09	4.95E+06	1.6
Stop-6-D1_4.1	#06		26/5/16	6:35:43	0.001989509	0.000000338	2.62		0.17	0.27	2.44E+09	4.86E+06	1.6
Stop-6-D1_4.2	#06		26/5/16	6:41:51	0.001990603	0.000000307	3.18		0.15	0.27	2.47E+09	4.91E+06	1.6
Stop-6-D1_4.3	#06		26/5/16	6:47:58	0.001990185	0.000000328	2.96		0.16	0.27	2.48E+09	4.92E+06	1.6
Stop-6-D1_4.4	#06		26/5/16	6:54:05	0.001991220	0.000000327	3.49		0.16	0.27	2.50E+09	4.98E+06	1.6
Stop-6-D1_4.5	#06		26/5/16	7:00:13	0.001989688	0.000000358	2.71		0.18	0.27	2.51E+09	5.00E+06	1.6
	#06			average	3.45	weighted mean	3.41						
				std dev (1σ)	0.41	error in mean (1σ)	0.09	Internal error (σ 95%)	0.20				
				50% variance	0.08	MSWD	11.23						
					no.		19						
					no. outliers		0						
MOUNT HM-16													
CapaoL4													
normalising standard for run 7													
CapaoL4-1.1	#07		28/11/16	13:19:38	0.0019445	0.000000002		-18.95	0.12	0.47	2.38E+09	4.62E+06	1.6
CapaoL4-1.2	#07		28/11/16	13:25:28	0.0019475	0.000000002	-17.37		0.12	0.47	2.41E+09	4.66E+06	1.6
CapaoL4-1.3	#07		28/11/16	13:31:21	0.0019475	0.000000003	-17.37		0.13	0.47	2.41E+09	4.70E+06	1.6
CapaoL4-1.4	#07		28/11/16	13:37:50	0.0019461	0.000000002	-18.11		0.09	0.46	2.42E+09	4.71E+06	1.6
CapaoL4-1.5	#07		28/11/16	13:43:41	0.0019465	0.000000002	-17.84		0.11	0.47	2.44E+09	4.73E+06	1.6
CapaoL4-1.6	#07		28/11/16	15:47:09	0.0019465	0.000000002	-17.92		0.13	0.47	2.39E+09	4.65E+06	1.6
CapaoL4-1.7	#07		28/11/16	15:53:00	0.0019479	0.000000002	-17.16		0.12	0.47	2.43E+09	4.74E+06	1.6
CapaoL4-1.8	#07		28/11/16	16:03:28	0.0019462	0.000000002	-18.58		0.11	0.47	2.41E+09	4.69E+06	1.6
CapaoL4-1.9	#07		28/11/16	16:25:16	0.0019471	0.000000003	-17.59		0.13	0.47	2.41E+09	4.69E+06	1.6
CapaoL4-1.10	#07		28/11/16	16:31:08	0.0019486	0.000000002	-16.81		0.11	0.47	2.44E+09	4.75E+06	1.6
CapaoL4-2.1	#07		28/11/16	16:40:02	0.0019504	0.000000003		-15.90	0.14	0.47	2.37E+09	4.62E+06	1.6
CapaoL4-2.2	#07		28/11/16	16:46:54	0.0019507	0.000000003		-15.74	0.16	0.47	2.41E+09	4.70E+06	1.6
CapaoL4-1.11	#07		28/11/16	18:06:47	0.0019472	0.000000002	-17.53		0.13	0.47	2.46E+09	4.79E+06	1.6
CapaoL4-1.12	#07		28/11/16	18:12:39	0.0019472	0.000000002	-17.53		0.11	0.47	2.46E+09	4.80E+06	1.6
CapaoL4-1.13	#07		28/11/16	18:18:30	0.0019473	0.000000002	-17.48		0.12	0.47	2.47E+09	4.81E+06	1.6
CapaoL4-3.1	#07		28/11/16	19:58:57	0.0019471	0.000000003	-17.57		0.13	0.47	2.39E+09	4.69E+06	1.6
CapaoL4-3.2	#07		28/11/16	20:04:49	0.0019503	0.000000002	-15.96		0.12	0.47	2.41E+09	4.69E+06	1.6
CapaoL4-3.3	#07		28/11/16	20:10:40	0.0019489	0.000000002	-16.17		0.12	0.47	2.44E+09	4.75E+06	1.6
CapaoL4-3.4	#07		28/11/16	20:16:57	0.0019474	0.000000003	-17.46		0.14	0.47	2.43E+09	4.72E+06	1.6

SPOT #	Session	Date	Time	T ₀ /T ₀	±	δ°Oswow	rejected	±Internal error (σ 95%)	±External error (1σ)	T ₀ cps (median)	T ₀ cps (median)	no. sets, subsets
Capaol-L4.6	#07	29/11/16	14:35:42	0.0019508	0.0000002	-17.06		0.13	0.28	2.37E+09	4.63E+06	1.6
Capaol-L4.7	#07	29/11/16	14:41:03	0.0019512	0.0000002	-16.84		0.12	0.28	2.38E+09	4.64E+06	1.6
Capaol-L4.8	#07	29/11/16	14:46:24	0.0019493	0.0000002	-17.79		0.11	0.28	2.39E+09	4.66E+06	1.6
Capaol-L4.15b	#07	29/11/16	15:12:28	0.0019500	0.0000003	-17.45		0.15	0.28	2.34E+09	4.56E+06	1.6
Capaol-L4.15b	#07	29/11/16	15:17:49	0.0019506	0.0000003	-17.12		0.15	0.28	2.36E+09	4.60E+06	1.6
	#07	STANDARD	average	-17.22	weighted mean	-17.22						
			std dev (1σ)	0.37	error in mean (1σ)	0.15	Internal error (σ 95%)	0.31				
			50% variance	0.07	MSWD	16.03						
				no.		23						
				no. outliers		0						
MOUNT HM-18B												
Row L5												
RowL5-1.1	#07	29/11/16	9:13:53	0.0019870	0.0000003	2.52		0.14	0.28	2.40E+09	4.78E+06	1.6
RowL5-1.2	#07	29/11/16	9:19:44	0.0019888	0.0000002		3.41	0.12	0.28	2.38E+09	4.74E+06	1.6
RowL5-1.3	#07	29/11/16	9:25:36	0.0019867	0.0000002	2.34		0.11	0.28	2.40E+09	4.76E+06	1.6
RowL5-1.4	#07	29/11/16	12:43:03	0.0019851	0.0000002	-16.40		0.12	0.28	2.40E+09	4.76E+06	1.6
RowL5-1.5	#07	29/11/16	12:48:24	0.0019863	0.0000002	2.15		0.10	0.27	2.39E+09	4.74E+06	1.6
RowL5-1.6	#07	29/11/16	12:53:46	0.0019874	0.0000003	2.72		0.13	0.28	2.38E+09	4.72E+06	1.6
RowL5-1.4b	#07	29/11/16	15:44:49	0.0019861	0.0000002	1.04		0.11	0.28	2.39E+09	4.73E+06	1.6
RowL5-1.2b	#07	29/11/16	15:55:27	0.0019859	0.0000003	0.94		0.13	0.28	2.34E+09	4.65E+06	1.6
	#07		average	1.95	weighted mean	2.08						
			std dev (1σ)	0.77	error in mean (1σ)	0.15	Internal error (σ 95%)	0.33				
			50% variance	0.30	MSWD	7.09						
				no.		8						
				no. outliers		2						
MOUNT HM-18B												
Row L6												
RowL6-1.1	#07	29/11/16	8:56:14	0.0019849	0.0000004		1.42	0.18	0.29	2.40E+09	4.76E+06	1.6
RowL6-1.2	#07	29/11/16	9:02:06	0.0019868	0.0000002	2.41		0.11	0.28	2.41E+09	4.80E+06	1.6
RowL6-1.3	#07	29/11/16	9:07:57	0.0019868	0.0000002	2.40		0.11	0.28	2.40E+09	4.78E+06	1.6
RowL6-1.4	#07	29/11/16	10:40:23	0.0019849	0.0000002	1.13	1.42	0.13	0.28	2.39E+09	4.75E+06	1.6
RowL6-1.5	#07	29/11/16	10:54:44	0.0019868	0.0000002	2.41		0.12	0.28	2.40E+09	4.77E+06	1.6
RowL6-1.6	#07	29/11/16	11:00:05	0.0019874	0.0000002	2.72		0.11	0.28	2.39E+09	4.75E+06	1.6
RowL6-1.1b	#07	29/11/16	15:34:02	0.0019851	0.0000002	0.56		0.13	0.28	2.39E+09	4.73E+06	1.6
RowL6-1.4b	#07	29/11/16	15:39:23	0.0019867	0.0000002	1.37		0.13	0.28	2.40E+09	4.78E+06	1.6
	#07		average	1.98	weighted mean	2.24						
			std dev (1σ)	0.84	error in mean (1σ)	0.14	Internal error (σ 95%)	0.36				
			50% variance	0.35	MSWD	7.18						
				no.		8						
				no. outliers		2						
MOUNT HM-17												
Capaol-L4	normalising standard for run 7											
Capaol-L4.1	#07	29/11/16	18:16:30	0.0019454	0.0000004		-19.04	0.18	0.35	2.39E+09	4.64E+06	1.6
Capaol-L4.2	#07	29/11/16	18:21:51	0.0019477	0.0000002	-17.86		0.11	0.34	2.42E+09	4.71E+06	1.6
Capaol-L4.1.3	#07	29/11/16	18:27:13	0.0019472	0.0000003	-16.13		0.15	0.34	2.43E+09	4.73E+06	1.6
Capaol-L4.1.4	#07	29/11/16	18:32:34	0.0019468	0.0000003	-17.31		0.13	0.34	2.43E+09	4.73E+06	1.6
Capaol-L4.1.5	#07	29/11/16	18:37:55	0.0019488	0.0000003	-17.29		0.13	0.34	2.45E+09	4.77E+06	1.6
Capaol-L4.2.1	#07	29/11/16	19:53:49	0.0019489	0.0000002	-17.27		0.12	0.34	2.36E+09	4.59E+06	1.6
Capaol-L4.2.2	#07	29/11/16	19:56:10	0.0019506	0.0000002	-16.40		0.13	0.34	2.39E+09	4.67E+06	1.6
Capaol-L4.2.3	#07	29/11/16	20:04:32	0.0019496	0.0000002	-16.92		0.12	0.34	2.40E+09	4.67E+06	1.6
Capaol-L4.2.4	#07	29/11/16	20:09:53	0.0019509	0.0000002	-16.22		0.11	0.34	2.40E+09	4.68E+06	1.6
Capaol-L4.3.1	#07	29/11/16	20:46:27	0.0019473	0.0000002	-18.06		0.12	0.34	2.40E+09	4.68E+06	1.6
Capaol-L4.3.2	#07	29/11/16	20:51:48	0.0019484	0.0000003	-17.51		0.13	0.34	2.42E+09	4.71E+06	1.6
Capaol-L4.3.3	#07	29/11/16	20:57:09	0.0019482	0.0000003	-17.60		0.16	0.35	2.43E+09	4.73E+06	1.6
Capaol-L4.3.4	#07	29/11/16	21:02:31	0.0019487	0.0000003	-17.33		0.15	0.34	2.43E+09	4.73E+06	1.6
Capaol-L4.4.1	#07	29/11/16	22:35:51	0.0019492	0.0000002	-17.08		0.12	0.34	2.39E+09	4.66E+06	1.6
Capaol-L4.4.2	#07	29/11/16	22:41:13	0.0019497	0.0000002	-16.83		0.12	0.34	2.39E+09	4.67E+06	1.6
Capaol-L4.4.3	#07	29/11/16	22:46:34	0.0019488	0.0000002	-17.31		0.13	0.34	2.40E+09	4.68E+06	1.6
Capaol-L4.4.4	#07	29/11/16	22:51:55	0.0019487	0.0000002	-17.37		0.12	0.34	2.39E+09	4.67E+06	1.6
Capaol-L4.4.5	#07	29/11/16	22:57:16	0.0019502	0.0000002	-16.61		0.11	0.34	2.39E+09	4.65E+06	1.6
Capaol-L4.5.1	#07	30/11/16	0:45:13	0.0019459	0.0000002	-18.10		0.13	0.34	2.44E+09	4.75E+06	1.6
Capaol-L4.5.2	#07	30/11/16	0:50:35	0.0019460	0.0000002	-18.07		0.11	0.34	2.43E+09	4.73E+06	1.6
Capaol-L4.5.3	#07	30/11/16	0:55:56	0.0019474	0.0000003	-17.32		0.15	0.34	2.43E+09	4.74E+06	1.6
Capaol-L4.5.4	#07	30/11/16	1:01:17	0.0019469	0.0000002	-17.62		0.12	0.34	2.44E+09	4.76E+06	1.6
Capaol-L4.5.5	#07	30/11/16	1:06:36	0.0019478	0.0000002	-17.21		0.11	0.34	2.44E+09	4.74E+06	1.6
Capaol-L4.1.6	#07	30/11/16	2:11:33	0.0019491	0.0000003	-16.45		0.13	0.34	2.44E+09	4.75E+06	1.6
Capaol-L4.1.7	#07	30/11/16	2:16:54	0.0019482	0.0000002	-16.94		0.12	0.34	2.43E+09	4.74E+06	1.6
Capaol-L4.1.8	#07	30/11/16	2:22:15	0.0019485	0.0000002	-16.79		0.12	0.34	2.43E+09	4.73E+06	1.6
Capaol-L4.1.9	#07	30/11/16	2:27:36	0.0019479	0.0000003	-17.08		0.16	0.35	2.41E+09	4.69E+06	1.6
Capaol-L4.1.10	#07	30/11/16	2:32:57	0.0019486	0.0000002	-16.70		0.12	0.34	2.42E+09	4.71E+06	1.6
Capaol-L4.5.6	#07	30/11/16	3:59:22	0.0019474	0.0000002	-17.35		0.11	0.34	2.45E+09	4.78E+06	1.6
Capaol-L4.5.7	#07	30/11/16	4:04:44	0.0019472	0.0000003	-17.44		0.13	0.34	2.44E+09	4.76E+06	1.6
Capaol-L4.5.8	#07	30/11/16	4:10:05	0.0019476	0.0000002	-17.22		0.12	0.34	2.44E+09	4.76E+06	1.6
Capaol-L4.5.9	#07	30/11/16	4:15:26	0.0019472	0.0000003	-17.44		0.14	0.34	2.46E+09	4.78E+06	1.6
Capaol-L4.5.10	#07	30/11/16	4:20:47	0.0019471	0.0000003	-17.47		0.16	0.35	2.45E+09	4.77E+06	1.6
Capaol-L4.1.11	#07	30/11/16	5:28:01	0.0019471	0.0000003	-17.50		0.13	0.34	2.43E+09	4.73E+06	1.6
Capaol-L4.1.12	#07	30/11/16	5:33:23	0.0019484	0.0000003	-16.84		0.13	0.34	2.42E+09	4.72E+06	1.6
Capaol-L4.1.13	#07	30/11/16	5:38:44	0.0019471	0.0000002	-17.50		0.12	0.34	2.42E+09	4.71E+06	1.6
Capaol-L4.1.14	#07	30/11/16	5:44:05	0.0019467	0.0000002	-16.67		0.12	0.34	2.44E+09	4.75E+06	1.6
Capaol-L4.2.4b	#07	30/11/16	5:54:32	0.0019485	0.0000002	-16.79		0.11	0.34	2.39E+09	4.64E+06	1.6
Capaol-L4.2.3b	#07	30/11/16	5:59:53	0.0019500	0.0000002	-17.52	-16.00	0.12	0.34	2.40E+09	4.68E+06	1.6
Capaol-L4.5.1b	#07	30/11/16	7:20:26	0.0019472	0.0000003	-17.45		0.13	0.34	2.41E+09	4.75E+06	1.6
Capaol-L4.5.2b	#07	30/11/16	7:25:48	0.0019482	0.0000002	-16.93		0.12	0.34	2.42E+09	4.71E+06	1.6
Capaol-L4.4.6	#07	30/11/16	9:44:19	0.0019480	0.0000002	-17.52		0.10	0.33	2.39E+09	4.64E+06	1.6
Capaol-L4.7	#07	30/11/16	9:49:40	0.0019484	0.0000002	-16.80		0.12	0.34	2.42E+09	4.71E+06	1.6
Capaol-L4.8	#07	30/11/16	9:55:01	0.0019500	0.0000002	-16.51		0.13	0.34	2.42E+09	4.71E+06	1.6
Capaol-L4.9	#07	30/11/16	10:00:22	0.0019493	0.0000003	-16.86		0.13	0.34	2.42E+09	4.71E+06	1.6
Capaol-L4.6.1	#07	30/11/16	12:15:53	0.0019484	0.0000002	-17.33		0.15	0.34	2.42E+09	4.71E+06	1.6
Capaol-L4.6.2	#07	30/11/16	12:21:15	0.0019486	0.0000002	-17.23		0.12	0.34	2.43E+09	4.74E+06	1.6
Capaol-L4.6.3	#07	30/11/16	12:26:36	0.0019486	0.0000003							

SPOT #	Session	Date	Time	T ₀ /T ₀	±	δ°O _{vac}	rejected	±Internal error (σ 95%)	±External error (1σ)	T ₀ cps (median)	T ₀ cps (median)	no. sets subsets
CapaoL4-3.1	#07	2/12/16	4:06:40	0.0019478	0.0000002	-16.34		0.13	0.42	2.36E+09	4.65E+06	1,6
CapaoL4-3.2	#07	2/12/16	4:12:31	0.0019460	0.0000003	-17.25		0.14	0.42	2.37E+09	4.61E+06	1,6
CapaoL4-3.3	#07	2/12/16	5:05:30	0.0019470	0.0000003	-16.77		0.14	0.42	2.38E+09	4.62E+06	1,6
CapaoL4-3.4	#07	2/12/16	5:11:22	0.0019455	0.0000003	-17.54		0.16	0.42	2.37E+09	4.62E+06	1,6
CapaoL4-6.1	#07	2/12/16	5:47:19	0.0019455	0.0000003	-17.52		0.15	0.42	2.36E+09	4.58E+06	1,6
CapaoL4-6.2	#07	2/12/16	5:53:11	0.0019452	0.0000003	-17.68		0.13	0.42	2.36E+09	4.60E+06	1,6
CapaoL4-6.3	#07	2/12/16	5:59:03	0.0019464	0.0000002	-17.07		0.12	0.41	2.35E+09	4.58E+06	1,6
CapaoL4-6.4	#07	2/12/16	6:04:55	0.0019447	0.0000002	-17.94		0.13	0.42	2.35E+09	4.58E+06	1,6
CapaoL4-1.4	#07	2/12/16	6:57:52	0.0019454	0.0000002	-17.60		0.12	0.41	2.40E+09	4.67E+06	1,6
CapaoL4-1.5	#07	2/12/16	7:03:44	0.0019456	0.0000002	-17.47		0.09	0.41	2.41E+09	4.69E+06	1,6
CapaoL4-1.6	#07	2/12/16	7:09:36	0.0019455	0.0000003	-17.55		0.15	0.42	2.42E+09	4.71E+06	1,6
CapaoL4-5.1b	#07	2/12/16	8:23:38	0.0019448	0.0000003	-17.91		0.16	0.42	2.42E+09	4.70E+06	1,6
CapaoL4-2.2b	#07	2/12/16	8:30:55	0.0019461	0.0000002	-17.24		0.10	0.41	2.40E+09	4.66E+06	1,6
CapaoL4-2.3b	#07	2/12/16	8:37:31	0.0019478	0.0000003	-16.35		0.13	0.42	2.41E+09	4.66E+06	1,6
CapaoL4-2.3c	#07	2/12/16	8:44:30	0.0019450	0.0000003	-17.79		0.14	0.42	2.40E+09	4.67E+06	1,6
CapaoL4-3.1b	#07	2/12/16	8:51:22	0.0019466	0.0000003	-16.96		0.14	0.42	2.35E+09	4.58E+06	1,6
CapaoL4-6.4b	#07	2/12/16	10:39:12	0.0019469	0.0000003	-16.83		0.16	0.42	2.37E+09	4.62E+06	1,6
CapaoL4-6.5	#07	2/12/16	10:45:04	0.0019451	0.0000003	-17.72		0.13	0.42	2.36E+09	4.58E+06	1,6
CapaoL4-6.6	#07	2/12/16	10:50:56	0.0019465	0.0000003	-17.01		0.13	0.42	2.37E+09	4.61E+06	1,6
CapaoL4-6.7	#07	2/12/16	10:56:47	0.0019458	0.0000002	-17.37		0.10	0.41	2.35E+09	4.58E+06	1,6
CapaoL4-4.1b	#07	2/12/16	11:51:06	0.0019459	0.0000003	-17.32		0.17	0.42	2.37E+09	4.61E+06	1,6
CapaoL4-4.3b	#07	2/12/16	11:56:58	0.0019466	0.0000003	-16.97		0.16	0.42	2.38E+09	4.64E+06	1,6
CapaoL4-4.4b	#07	2/12/16	12:02:51	0.0019470	0.0000003	-16.74		0.13	0.42	2.38E+09	4.63E+06	1,6
CapaoL4-3.3b	#07	2/12/16	12:55:48	0.0019453	0.0000002	-17.61		0.12	0.41	2.37E+09	4.62E+06	1,6
CapaoL4-3.3c	#07	2/12/16	13:01:40	0.0019464	0.0000003	-17.06		0.16	0.42	2.37E+09	4.62E+06	1,6
CapaoL4-5.5	#07	2/12/16	15:00:29	0.0019452	0.0000002	-17.70		0.10	0.41	2.43E+09	4.72E+06	1,6
CapaoL4-5.6	#07	2/12/16	15:06:21	0.0019434	0.0000003	-17.72	-16.60	0.14	0.42	2.43E+09	4.73E+06	1,6
CapaoL4-5.7	#07	2/12/16	15:12:13	0.0019451	0.0000003	-17.72		0.17	0.42	2.43E+09	4.72E+06	1,6
CapaoL4-5.8	#07	2/12/16	15:18:05	0.0019452	0.0000004	-17.70		0.18	0.43	2.43E+09	4.72E+06	1,6
#07	STANDARD	average	-17.20	weighted mean	-17.22							
		std dev (1σ)	0.57	error in mean (1σ)	0.09		Internal error (σ 95%)	0.18				
		50% variance	0.16	MSWD	18.31							
				no. outliers	43							
					2							
MOUNT HM-17D												
RoyL6												
RoyL6-1.1	#07	1/12/16	21:39:23	0.0019817	0.0000003	1.09		0.15	0.42	2.33E+09	4.63E+06	1,6
RoyL6-1.2	#07	1/12/16	21:45:15	0.0019851	0.0000002	2.81		0.11	0.41	2.33E+09	4.63E+06	1,6
RoyL6-1.3	#07	1/12/16	21:51:07	0.0019851	0.0000003	2.81		0.14	0.42	2.34E+09	4.65E+06	1,6
RoyL6-1.4	#07	1/12/16	21:57:51	0.0019830	0.0000003	1.72		0.15	0.42	2.33E+09	4.62E+06	1,6
RoyL6-1.5	#07	2/12/16	3:13:42	0.0019795	0.0000002	-0.34	-0.03	0.12	0.41	2.37E+09	4.66E+06	1,6
RoyL6-1.5	#07	2/12/16	3:19:34	0.0019805	0.0000002	0.48		0.12	0.41	2.37E+09	4.66E+06	1,6
RoyL6-1.6	#07	2/12/16	3:25:26	0.0019818	0.0000003	1.12		0.13	0.42	2.36E+09	4.66E+06	1,6
RoyL6-1.7	#07	2/12/16	7:15:31	0.0019842	0.0000002	2.34		0.12	0.42	2.34E+09	4.65E+06	1,6
RoyL6-1.8	#07	2/12/16	7:21:22	0.0019811	0.0000003	0.75		0.16	0.42	2.38E+09	4.71E+06	1,6
RoyL6-1.9	#07	2/12/16	7:27:14	0.0019817	0.0000003	1.07		0.13	0.42	2.37E+09	4.66E+06	1,6
RoyL6-1.1b	#07	2/12/16	8:00:01	0.0019833	0.0000003	1.77		0.16	0.42	2.36E+09	4.67E+06	1,6
RoyL6-1.2b	#07	2/12/16	8:07:26	0.0019837	0.0000003	2.08		0.14	0.42	2.37E+09	4.70E+06	1,6
RoyL6-1.3b	#07	2/12/16	8:13:47	0.0019809	0.0000003	0.68		0.16	0.42	2.36E+09	4.67E+06	1,6
RoyL6-1.7b	#07	2/12/16	8:22:00	0.0019842	0.0000002	2.36		0.10	0.41	2.36E+09	4.66E+06	1,6
RoyL6-1.7c	#07	2/12/16	8:29:17	0.0019823	0.0000003	1.36		0.14	0.42	2.34E+09	4.64E+06	1,6
#07	average	1.60	weighted mean	1.58								
		std dev (1σ)	0.78	error in mean (1σ)	0.21		Internal error (σ 95%)	0.45				
		50% variance	0.31	MSWD	38.15							
				no. outliers	15							
					1							
MOUNT HM-17D												
RoyL6												
RoyL6-1.1	#07	1/12/16	21:19:41	0.0019843	0.0000003	2.42		0.16	0.42	2.37E+09	4.71E+06	1,6
RoyL6-1.2	#07	1/12/16	21:25:33	0.0019853	0.0000002	2.93		0.12	0.42	2.37E+09	4.71E+06	1,6
RoyL6-1.3	#07	1/12/16	21:31:25	0.0019841	0.0000003	2.29		0.15	0.42	2.36E+09	4.69E+06	1,6
RoyL6-1.4	#07	2/12/16	1:21:31	0.0019809	0.0000003	0.75	0.68	0.17	0.42	2.37E+09	4.70E+06	1,6
RoyL6-1.5	#07	2/12/16	1:27:22	0.0019839	0.0000002	2.04		0.12	0.41	2.36E+09	4.67E+06	1,6
RoyL6-1.6	#07	2/12/16	1:33:14	0.0019848	0.0000003	2.68		0.14	0.42	2.38E+09	4.73E+06	1,6
RoyL6-1.7	#07	2/12/16	5:29:38	0.0019842	0.0000002	2.33		0.10	0.41	2.36E+09	4.67E+06	1,6
RoyL6-1.8	#07	2/12/16	5:35:30	0.0019830	0.0000003	1.74		0.12	0.42	2.36E+09	4.67E+06	1,6
RoyL6-1.9	#07	2/12/16	5:41:22	0.0019844	0.0000003	2.45		0.14	0.42	2.38E+09	4.73E+06	1,6
RoyL6-1.10	#07	2/12/16	14:06:58	0.0019834	0.0000003	1.97		0.14	0.42	2.36E+09	4.72E+06	1,6
RoyL6-1.11	#07	2/12/16	14:12:49	0.0019848	0.0000002	2.66		0.13	0.42	2.40E+09	4.76E+06	1,6
RoyL6-1.12	#07	2/12/16	14:18:42	0.0019825	0.0000003	1.49		0.13	0.42	2.39E+09	4.74E+06	1,6
#07	average	2.27	weighted mean	2.19								
		std dev (1σ)	0.43	error in mean (1σ)	0.12		Internal error (σ 95%)	0.28				
		50% variance	0.09	MSWD	11.30							
				no. outliers	12							
					1							
MOUNT HM-21												
CapaoL6												
CapaoL4-1.1	#07	2/12/16	17:39:17	0.0019454	0.0000003	-17.26		0.18	0.32	2.39E+09	4.64E+06	1,6
CapaoL4-1.2	#07	2/12/16	17:45:09	0.0019457	0.0000002	-17.10		0.12	0.31	2.38E+09	4.65E+06	1,6
CapaoL4-1.3	#07	2/12/16	17:51:00	0.0019443	0.0000002	-17.85		0.13	0.31	2.40E+09	4.66E+06	1,6
CapaoL4-1.4	#07	2/12/16	17:56:52	0.0019462	0.0000003	-16.88		0.15	0.31	2.38E+09	4.66E+06	1,6
CapaoL4-2.1	#07	2/12/16	18:14:23	0.0019462	0.0000003	-16.87		0.14	0.31	2.40E+09	4.67E+06	1,6
CapaoL4-2.2	#07	2/12/16	18:20:15	0.0019449	0.0000004	-17.51		0.19	0.33	2.40E+09	4.67E+06	1,6
CapaoL4-2.3	#07	2/12/16	18:26:07	0.0019458	0.0000003	-17.08		0.15	0.31	2.40E+09	4.68E+06	1,6
CapaoL4-4.1	#07	2/12/16	20:36:06	0.0019445	0.0000002	-17.82		0.11	0.32	2.38E+09	4.64E+06	1,6
CapaoL4-4.2	#07	2/12/16	20:41:58	0.0019454	0.0000002	-17.33		0.11	0.31	2.40E+09	4.69E+06	1,6
CapaoL4-4.3	#07	2/12/16	20:47:50	0.0019455	0.0000002	-17.32		0.11	0.31	2.40E+09	4.67E+06	1,6
CapaoL4-1.5	#07	2/12/16	20:45:27	0.0019450	0.0000003	-17.55		0.17	0.32	2.38E+09	4.65E+06	1,6
CapaoL4-1.6	#07	2/12/16	23:51:19	0.0019458	0.0000002	-17.13		0.09	0.30	2.38E+09	4.64E+06	1,6
CapaoL4-1.7	#07	2/12/16	23:57:10	0.0019447	0.0000003	-17.73		0.15	0.31	2.39E+09	4.65E+06	1,6
CapaoL4-2.4	#07	3/12/16	1:37:45	0.0019467	0.000							

SPOT #	Session	Date	Time	T _g /T _a	z	δ°O _{sw}	rejected	±Internal error (σ 95%)	±External error (1σ)	T _g cps (median)	T _g cps (median)	no. sets, subsets
Stop-6-D1-1.2	#07	3/12/16	19:24:55	0.0019805	0.0000003	2.31		0.13	0.31	2.37E+09	4.70E+06	1.6
Stop-6-D1-1.3	#07	3/12/16	19:30:47	0.0019852	0.0000003	3.18		0.14	0.31	2.39E+09	4.74E+06	1.6
Stop-6-D1-1.4	#07	3/12/16	19:36:39	0.0019828	0.0000002		1.94	0.11	0.31	2.37E+09	4.71E+06	1.6
Stop-6-D1-1.5	#07	3/12/16	4:23.39	0.0019842	0.0000002	2.60		0.13	0.31	2.40E+09	4.76E+06	1.6
Stop-6-D1-1.6	#07	3/12/16	4:29.31	0.0019860	0.0000003	3.53		0.13	0.31	2.39E+09	4.73E+06	1.6
Stop-6-D1-1.7	#07	3/12/16	4:35.23	0.0019839	0.0000003	2.46		0.15	0.31	2.39E+09	4.74E+06	1.6
Stop-6-D1-1.8	#07	3/12/16	9:54.09	0.0019853	0.0000004	3.17		0.19	0.32	2.41E+09	4.78E+06	1.6
Stop-6-D1-1.9	#07	3/12/16	10:00.00	0.0019838	0.0000002	2.36		0.11	0.30	2.41E+09	4.78E+06	1.6
Stop-6-D1-1.10	#07	3/12/16	10:05.52	0.0019839	0.0000003	2.45		0.13	0.31	2.41E+09	4.78E+06	1.6
Stop-6-D1-1.4b	#07	3/12/16	13:56.19	0.0019846	0.0000003	2.73		0.15	0.31	2.40E+09	4.77E+06	1.6
	#07	STANDARD	average	2.72	weighted mean	2.73						
			std dev (1σ)	0.42	error in mean (1σ)	0.13		Internal error (σ 95%)	0.29			
			50% variance	0.09	MSWD	9.23						
					no.	11						
					no. outliers	1						

MOUNT HM-23

Capao-L4

normalising standard for run 7

Capao-L4-1.1	#07	3/12/16	17:34.42	0.0019445	0.0000002	-17.68		0.12	0.40	2.38E+09	4.64E+06	1.6
Capao-L4-1.2	#07	3/12/16	17:40.34	0.0019452	0.0000003	-17.29		0.13	0.40	2.39E+09	4.63E+06	1.6
Capao-L4-1.3	#07	3/12/16	17:46:26	0.0019470	0.0000002	-16.39		0.13	0.40	2.38E+09	4.64E+06	1.6
Capao-L4-1.4	#07	3/12/16	17:52:18	0.0019462	0.0000002	-16.77		0.12	0.40	2.39E+09	4.64E+06	1.6
Capao-L4-1.5	#07	3/12/16	17:58:10	0.0019465	0.0000004	-16.66		0.19	0.41	2.38E+09	4.63E+06	1.6
Capao-L4-2.1	#07	3/12/16	19:27.21	0.0019440	0.0000004	-17.22		0.22	0.42	2.39E+09	4.63E+06	1.6
Capao-L4-2.2	#07	3/12/16	19:33:12	0.0019472	0.0000003	-16.28		0.15	0.40	2.39E+09	4.65E+06	1.6
Capao-L4-2.3	#07	3/12/16	19:39:04	0.0019478	0.0000003		-15.96	0.15	0.40	2.39E+09	4.67E+06	1.6
Capao-L4-2.4	#07	3/12/16	19:45:14	0.0019455	0.0000003	-17.15		0.17	0.41	2.39E+09	4.65E+06	1.6
Capao-L4-2.3b	#07	3/12/16	19:51:53	0.0019455	0.0000002	-17.17		0.12	0.40	2.41E+09	4.68E+06	1.6
Capao-L4-2.2b	#07	3/12/16	20:04.20	0.0019419	0.0000003		-19.00	0.18	0.41	2.41E+09	4.67E+06	1.6
Capao-L4-1.1b	#07	3/12/16	22:35:04	0.0019411	0.0000003	-16.84		0.16	0.40	2.41E+09	4.69E+06	1.6
Capao-L4-1.2b	#07	3/12/16	22:40:56	0.0019458	0.0000003	-17.01		0.15	0.40	2.41E+09	4.70E+06	1.6
Capao-L4-1.6	#07	4/12/16	0:21.51	0.0019447	0.0000003	-17.58		0.14	0.40	2.42E+09	4.70E+06	1.6
Capao-L4-1.7	#07	4/12/16	0:27.43	0.0019436	0.0000002	-18.12		0.13	0.40	2.42E+09	4.70E+06	1.6
Capao-L4-1.8	#07	4/12/16	0:33.35	0.0019444	0.0000003	-17.72		0.13	0.40	2.42E+09	4.71E+06	1.6
Capao-L4-2.5	#07	4/12/16	2:43.35	0.0019451	0.0000003	-17.34		0.16	0.40	2.41E+09	4.68E+06	1.6
Capao-L4-2.6	#07	4/12/16	2:49:26	0.0019453	0.0000004	-17.28		0.18	0.41	2.40E+09	4.67E+06	1.6
Capao-L4-2.7	#07	4/12/16	4:30.04	0.0019451	0.0000003	-17.35		0.16	0.40	2.41E+09	4.68E+06	1.6
Capao-L4-2.8	#07	4/12/16	4:35:56	0.0019459	0.0000002	-16.92		0.13	0.40	2.40E+09	4.67E+06	1.6
Capao-L4-2.9	#07	4/12/16	4:41:47	0.0019476	0.0000003	-16.05		0.13	0.40	2.39E+09	4.69E+06	1.6
Capao-L4-2.10	#07	4/12/16	4:47:29	0.0019455	0.0000003	-16.66		0.13	0.40	2.39E+09	4.63E+06	1.6
Capao-L4-1.9b	#07	4/12/16	8:04.15	0.0019435	0.0000003	-18.18		0.16	0.40	2.40E+09	4.66E+06	1.6
Capao-L4-1.10b	#07	4/12/16	8:10.19	0.0019437	0.0000003	-18.06		0.14	0.40	2.40E+09	4.66E+06	1.6
Capao-L4-1.11b	#07	4/12/16	8:16:35	0.0019437	0.0000004	-18.08		0.18	0.41	2.39E+09	4.65E+06	1.6
Capao-L4-2.2b	#07	4/12/16	8:25:01	0.0019455	0.0000004	-17.15		0.18	0.41	2.39E+09	4.63E+06	1.6
Capao-L4-1.12	#07	4/12/16	8:32:25	0.0019454	0.0000003	-17.21		0.13	0.40	2.40E+09	4.67E+06	1.6
Capao-L4-1.7b	#07	4/12/16	10:37:35	0.0019455	0.0000002	-17.15		0.12	0.40	2.41E+09	4.69E+06	1.6
Capao-L4-2.9b	#07	4/12/16	10:44:10	0.0019454	0.0000004	-17.22		0.21	0.42	2.41E+09	4.68E+06	1.6
Capao-L4-2.11	#07	4/12/16	13:20.44	0.0019456	0.0000003	-17.10		0.15	0.40	2.40E+09	4.68E+06	1.6
Capao-L4-2.12	#07	4/12/16	13:26:36	0.0019475	0.0000003	-16.11		0.14	0.40	2.41E+09	4.69E+06	1.6
Capao-L4-2.13	#07	4/12/16	14:55:33	0.0019456	0.0000003	-17.08		0.17	0.41	2.42E+09	4.70E+06	1.6
Capao-L4-2.14	#07	4/12/16	15:01:25	0.0019453	0.0000003	-17.24		0.15	0.40	2.41E+09	4.69E+06	1.6
Capao-L4-2.12b	#07	4/12/16	15:43.43	0.0019466	0.0000003	-16.59		0.14	0.40	2.41E+09	4.69E+06	1.6
Capao-L4-1.13	#07	4/12/16	16:05:01	0.0019454	0.0000003	-17.20		0.14	0.40	2.43E+09	4.73E+06	1.6
Capao-L4-1.14	#07	4/12/16	18:14.53	0.0019440	0.0000003	-17.90		0.14	0.40	2.43E+09	4.73E+06	1.6
Capao-L4-1.15	#07	4/12/16	20:24.58	0.0019463	0.0000002	-16.72		0.14	0.40	2.43E+09	4.74E+06	1.6
Capao-L4-1.16	#07	4/12/16	20:30:50	0.0019458	0.0000004	-17.02		0.18	0.41	2.43E+09	4.72E+06	1.6
Capao-L4-1.17	#07	4/12/16	21:48:04	0.0019450	0.0000003	-17.41		0.17	0.40	2.45E+09	4.72E+06	1.6
Capao-L4-1.18	#07	4/12/16	21:53:56	0.0019438	0.0000003	-18.01		0.17	0.40	2.45E+09	4.78E+06	1.6
Capao-L4-23-1.1	#07	5/12/16	13:55:36	0.0019439	0.0000003	-17.99		0.17	0.41	2.46E+09	4.78E+06	1.6
Capao-L4-23-1.2	#07	5/12/16	14:01:28	0.0019446	0.0000003	-17.62		0.13	0.40	2.47E+09	4.80E+06	1.6
Capao-L4-23-1.3	#07	5/12/16	14:07:20	0.0019447	0.0000002	-17.54		0.12	0.40	2.47E+09	4.81E+06	1.6
Capao-L4-23-1.4	#07	5/12/16	14:13:12	0.0019438	0.0000003	-18.00		0.13	0.40	2.47E+09	4.80E+06	1.6
Capao-L4-23-2.1	#07	5/12/16	17:20:07	0.0019451	0.0000003	-17.35		0.18	0.41	2.47E+09	4.80E+06	1.6
Capao-L4-23-2.2	#07	5/12/16	17:25:59	0.0019452	0.0000004	-17.28		0.23	0.42	2.47E+09	4.81E+06	1.6
Capao-L4-23-2.3	#07	5/12/16	17:31:51	0.0019458	0.0000003	-17.01		0.13	0.40	2.47E+09	4.82E+06	1.6
Capao-L4-23-2.4	#07	5/12/16	17:37:43	0.0019431	0.0000003	-18.38		0.16	0.40	2.48E+09	4.82E+06	1.6
Capao-L4-23-1.1	#07	5/12/16	22:07:28	0.0019431	0.0000003	-17.43	-18.40	0.27	0.43	2.44E+09	4.73E+06	1.6
Capao-L4-23-1.2	#07	5/12/16	22:13:20	0.0019437	0.0000003	-18.09		0.14	0.40	2.44E+09	4.74E+06	1.6
Capao-L4-23-1.3	#07	5/12/16	22:34:32	0.0019458	0.0000005	-17.01		0.24	0.42	2.39E+09	4.69E+06	1.6
Capao-L4-23-1.4	#07	5/12/16	22:40:23	0.0019461	0.0000004	-16.84		0.11	0.18	2.42E+09	4.71E+06	1.6
Capao-L4-23-1.5	#07	5/12/16	22:51:10	0.0019442	0.0000002	-17.82		0.11	0.40	2.43E+09	4.72E+06	1.6
Capao-L4-23-1.6	#07	5/12/16	22:57:02	0.0019454	0.0000003	-17.20		0.17	0.41	2.44E+09	4.78E+06	1.6
Capao-L4-23-2.1	#07	6/12/16	2:58:52	0.0019464	0.0000003	-16.69		0.15	0.40	2.46E+09	4.82E+06	1.6
Capao-L4-23-2.2	#07	6/12/16	3:04.43	0.0019456	0.0000002	-17.10		0.12	0.40	2.47E+09	4.81E+06	1.6
Capao-L4-23-2.3	#07	6/12/16	3:10:35	0.0019456	0.0000003	-17.08		0.17	0.40	2.47E+09	4.81E+06	1.6
Capao-L4-23-2.4	#07	6/12/16	3:16:27	0.0019464	0.0000004	-16.71		0.19	0.41	2.47E+09	4.80E+06	1.6
Capao-L4-23-1.7	#07	6/12/16	5:26:23	0.0019456	0.0000002	-17.11		0.11	0.40	2.46E+09	4.79E+06	1.6
Capao-L4-23-1.8	#07	6/12/16	5:32:15	0.0019444	0.0000003	-17.70		0.13	0.40	2.44E+09	4.79E+06	1.6
Capao-L4-23-1.9	#07	6/12/16	5:38:06	0.0019452	0.0000003	-17.32		0.16	0.40	2.45E+09	4.77E+06	1.6
Capao-L4-23-1.10	#07	6/12/16	5:43:58	0.0019450	0.0000003	-17.15		0.15	0.40	2.44E+09	4.78E+06	1.6
Capao-L4-23-2.5	#07	6/12/16	8:17:22	0.0019453	0.0000003	-17.23		0.16	0.40	2.46E+09	4.78E+06	1.6
Capao-L4-23-2.6	#07	6/12/16	8:23:14	0.0019469	0.0000003	-16.45		0.14	0.40	2.45E+09	4.78E+06	1.6
Capao-L4-23-2.7	#07	6/12/16	8:29:06	0.0019471	0.0000002	-16.00		0.11	0.40	2.47E+09	4.82E+06	1.6
Capao-L4-23-2.8	#07	6/12/16	8:34:57	0.0019452	0.0000002	-17.33		0.10	0.39	2.47E+09	4.81E+06	1.6
	#07	STANDARD	average	-17.24	weighted mean	-17.22						
			std dev (1σ)	0.55	error in mean (1σ)	0.07		Internal error (σ 95%)	0.13			
			50% variance	0.15	MSWD	18.82						
					no.	66						
					no. outliers	3						

SPOT #	Session	Date	Time	T ₀ /T ₀	±	δ ⁰ Oswow	rejected	±Internal error (σ 95%)	±External error (te)	T ₀ cps (median)	T ₀ cps (median)	no. sets, subsets
RoyL6-23-1.3	#07	5/12/16	14:36:47	0.0019809	0.0000003	2.57			0.13	0.40	2.48E+09	4.76E+06 1.6
RoyL6-23-2.1	#07	5/12/16	17:43:37	0.0019821	0.0000003	1.68			0.17	0.40	2.48E+09	4.85E+06 1.6
RoyL6-23-2.2	#07	5/12/16	17:49:28	0.0019802	0.0000003		0.67		0.16	0.40	2.48E+09	4.92E+06 1.6
RoyL6-23-2.3	#07	5/12/16	17:55:20	0.0019791	0.0000003		0.11		0.15	0.40	2.48E+09	4.90E+06 1.6
RoyL6-23-1.1	#07	5/12/16	23:31:27	0.0019806	0.0000004	0.88			0.18	0.41	2.38E+09	4.71E+06 1.6
RoyL6-23-1.2	#07	5/12/16	23:37:19	0.0019837	0.0000004	2.48			0.20	0.41	2.44E+09	4.84E+06 1.6
RoyL6-23-1.3	#07	5/12/16	23:43:10	0.0019826	0.0000003	1.91			0.16	0.40	2.36E+09	4.86E+06 1.6
RoyL6-23-1.4	#07	5/12/16	23:49:02	0.0019855	0.0000003	1.15	3.42		0.15	0.40	2.38E+09	4.72E+06 1.6
RoyL6-23-2.1	#07	6/12/16	3:22:21	0.0019821	0.0000004	1.68			0.20	0.41	2.41E+09	4.78E+06 1.6
RoyL6-23-2.2	#07	6/12/16	3:28:13	0.0019819	0.0000004	1.54			0.18	0.41	2.48E+09	4.91E+06 1.6
RoyL6-23-2.3	#07	6/12/16	3:34:05	0.0019822	0.0000003	1.69			0.15	0.40	2.42E+09	4.79E+06 1.6
RoyL6-23-1.5	#07	6/12/16	5:49:53	0.0019816	0.0000003	1.41			0.17	0.40	2.38E+09	4.73E+06 1.6
RoyL6-23-1.6	#07	6/12/16	5:55:44	0.0019841	0.0000004	2.67			0.20	0.41	2.38E+09	4.72E+06 1.6
RoyL6-23-1.7	#07	6/12/16	6:01:36	0.0019823	0.0000003	1.76			0.13	0.40	2.37E+09	4.69E+06 1.6
RoyL6-23-1.8	#07	6/12/16	6:07:27	0.0019832	0.0000003	2.24			0.15	0.40	2.41E+09	4.77E+06 1.6

#07	average	1.95	weighted mean	1.97		
	std dev (1σ)	0.64	error in mean (1σ)	0.10	Internal error (σ 95%)	0.21
	50% variance	0.20	MSWD	18.12		
			no. outliers	41		
				4		

MOUNT HM-23

Win-06-03A

Win-06-03A-1.1	#07	3/12/16	19:05:08	0.0019832	0.0000003	2.24			0.16	0.40	2.37E+09	4.70E+06 1.6
Win-06-03A-1.2	#07	3/12/16	19:11:00	0.0019838	0.0000004	2.56			0.18	0.41	2.38E+09	4.72E+06 1.6
Win-06-03A-1.3	#07	3/12/16	19:16:51	0.0019836	0.0000003	2.42			0.13	0.40	2.39E+09	4.74E+06 1.6
Win-06-03A-1.4	#07	3/12/16	19:10:26	0.0019846	0.0000003	2.94			0.13	0.40	2.39E+09	4.74E+06 1.6
Win-06-03A-1.5	#07	3/12/16	23:16:18	0.0019837	0.0000003	2.50			0.13	0.40	2.40E+09	4.75E+06 1.6
Win-06-03A-1.6	#07	4/12/16	1:03:04	0.0019835	0.0000003	2.39			0.14	0.40	2.39E+09	4.75E+06 1.6
Win-06-03A-1.7	#07	4/12/16	1:08:56	0.0019829	0.0000003	2.02			0.14	0.40	2.40E+09	4.76E+06 1.6
Win-06-03A-2.1	#07	4/12/16	3:18:57	0.0019828	0.0000003	2.02			0.13	0.40	2.37E+09	4.70E+06 1.6
Win-06-03A-2.2	#07	4/12/16	3:24:48	0.0019832	0.0000004	2.23			0.18	0.41	2.37E+09	4.71E+06 1.6
Win-06-03A-2.3	#07	4/12/16	5:17:10	0.0019830	0.0000003	2.14			0.14	0.40	2.39E+09	4.75E+06 1.6
Win-06-03A-2.4	#07	4/12/16	5:23:02	0.0019829	0.0000003	2.01			0.12	0.40	2.46E+09	4.75E+06 1.6
Win-06-03A-2.5	#07	4/12/16	8:01:18	0.0019812	0.0000003	2.01	1.23		0.16	0.40	2.37E+09	4.69E+06 1.6
Win-06-03A-2.6	#07	4/12/16	9:07:10	0.0019851	0.0000003	3.20			0.16	0.40	2.39E+09	4.72E+06 1.6
Win-06-03A-2.7	#07	4/12/16	9:13:08	0.0019824	0.0000003	1.82			0.15	0.40	2.37E+09	4.73E+06 1.6
Win-06-03A-2.8	#07	4/12/16	9:19:21	0.0019815	0.0000002	1.33			0.13	0.40	2.38E+09	4.72E+06 1.6
Win-06-03A-1.8	#07	4/12/16	11:21:24	0.0019831	0.0000003	2.15			0.15	0.40	2.40E+09	4.78E+06 1.6
Win-06-03A-1.9	#07	4/12/16	11:27:18	0.0019828	0.0000003	2.14			0.15	0.40	2.43E+09	4.81E+06 1.6
Win-06-03A-2.9	#07	4/12/16	13:56:07	0.0019844	0.0000003	2.86			0.13	0.40	2.40E+09	4.76E+06 1.6
Win-06-03A-2.10	#07	4/12/16	14:01:58	0.0019824	0.0000002	1.83			0.12	0.40	2.39E+09	4.74E+06 1.6
Win-06-03A-2.11	#07	4/12/16	15:30:56	0.0019833	0.0000003	2.26			0.14	0.40	2.40E+09	4.75E+06 1.6
Win-06-03A-2.12	#07	4/12/16	15:36:47	0.0019821	0.0000003	1.67			0.15	0.40	2.39E+09	4.75E+06 1.6
Win-06-03A-1.10	#07	4/12/16	18:44:23	0.0019825	0.0000003	1.87			0.14	0.40	2.42E+09	4.79E+06 1.6
Win-06-03A-1.11	#07	4/12/16	18:50:15	0.0019836	0.0000002	2.43			0.12	0.40	2.41E+09	4.78E+06 1.6
Win-06-03A-1.12	#07	4/12/16	21:00:20	0.0019825	0.0000003	1.98			0.14	0.40	2.41E+09	4.78E+06 1.6
Win-06-03A-1.13	#07	4/12/16	21:06:12	0.0019820	0.0000002	1.62			0.13	0.40	2.40E+09	4.78E+06 1.6
Win-06-03A-1.14	#07	4/12/16	22:23:26	0.0019838	0.0000003	2.55			0.13	0.40	2.41E+09	4.78E+06 1.6
Win-06-03A-1.15	#07	4/12/16	22:29:18	0.0019842	0.0000003	2.74			0.16	0.40	2.42E+09	4.80E+06 1.6
Win-06-03A-1.4b	#07	4/12/16	23:49:06	0.0019819	0.0000003	1.56			0.16	0.40	2.40E+09	4.75E+06 1.6
Win-06-03A-2.3b	#07	4/12/16	23:56:35	0.0019847	0.0000002	3.00			0.11	0.40	2.42E+09	4.80E+06 1.6
Win-06-03A-2.5b	#07	5/12/16	0:04:15	0.0019838	0.0000003	2.52			0.13	0.40	2.41E+09	4.77E+06 1.6
Win-06-03A-1.11	#07	5/12/16	15:02:22	0.0019821	0.0000003	1.67			0.14	0.40	2.41E+09	4.78E+06 1.6
Win-06-03A-1.12	#07	5/12/16	15:08:14	0.0019831	0.0000003	2.16			0.15	0.40	2.44E+09	4.83E+06 1.6
Win-06-03A-1.3	#07	5/12/16	15:14:05	0.0019853	0.0000003	3.28			0.15	0.40	2.43E+09	4.82E+06 1.6
Win-06-03A-2.11	#07	5/12/16	18:18:56	0.0019829	0.0000003	2.03			0.11	0.40	2.42E+09	4.79E+06 1.6
Win-06-03A-2.2	#07	5/12/16	18:24:48	0.0019843	0.0000003	2.80			0.14	0.40	2.44E+09	4.85E+06 1.6
Win-06-03A-2.3	#07	5/12/16	18:30:40	0.0019840	0.0000002	2.63			0.13	0.40	2.43E+09	4.82E+06 1.6
Win-06-03A-1.11	#07	6/12/16	2:20:25	0.0019813	0.0000003	1.25			0.11	0.39	2.44E+09	4.84E+06 1.6
Win-06-03A-1.2	#07	6/12/16	0:26:17	0.0019832	0.0000003	2.22			0.16	0.40	2.44E+09	4.83E+06 1.6
Win-06-03A-1.3	#07	6/12/16	0:32:08	0.0019838	0.0000002	2.54			0.13	0.40	2.43E+09	4.83E+06 1.6
Win-06-03A-1.4	#07	6/12/16	0:38:00	0.0019835	0.0000003	2.37			0.17	0.40	2.44E+09	4.84E+06 1.6
Win-06-03A-2.11	#07	6/12/16	3:57:41	0.0019820	0.0000003	1.60			0.15	0.40	2.44E+09	4.79E+06 1.6
Win-06-03A-2.2	#07	6/12/16	4:03:33	0.0019829	0.0000003	2.06			0.16	0.40	2.41E+09	4.79E+06 1.6
Win-06-03A-2.3	#07	6/12/16	4:09:25	0.0019835	0.0000003	2.36			0.16	0.40	2.44E+09	4.84E+06 1.6
Win-06-03A-1.5	#07	6/12/16	6:36:55	0.0019830	0.0000003	2.12			0.14	0.40	2.44E+09	4.83E+06 1.6
Win-06-03A-1.6	#07	6/12/16	6:42:46	0.0019842	0.0000003	2.77			0.13	0.40	2.44E+09	4.84E+06 1.6
Win-06-03A-1.7	#07	6/12/16	6:48:38	0.0019825	0.0000003	1.87			0.13	0.40	2.45E+09	4.85E+06 1.6
Win-06-03A-1.8	#07	6/12/16	6:54:30	0.0019821	0.0000002	1.66			0.13	0.40	2.48E+09	4.91E+06 1.6
Win-06-03A-2.4	#07	6/12/16	8:40:52	0.0019847	0.0000003	3.02			0.13	0.40	2.42E+09	4.81E+06 1.6
Win-06-03A-2.5	#07	6/12/16	8:46:43	0.0019811	0.0000003		1.15		0.14	0.40	2.43E+09	4.82E+06 1.6
Win-06-03A-2.6	#07	6/12/16	8:52:45	0.0019832	0.0000003	2.25			0.13	0.40	2.44E+09	4.83E+06 1.6
Win-06-03A-2.7	#07	6/12/16	8:58:26	0.0019844	0.0000003	2.87			0.11	0.39	2.45E+09	4.85E+06 1.6

#07	average	2.25	weighted mean	2.25		
	std dev (1σ)	0.48	error in mean (1σ)	0.07	Internal error (σ 95%)	0.14
	50% variance	0.11	MSWD	12.46		
			no. outliers	52		
				3		

MOUNT HM-23_27

Capaol-4.4

normalising standard for run 7

Capaol-4-23-1.1	#07	5/12/16	2:24:27	0.0019449	0.0000003	-17.46			0.15	0.33	2.44E+09	4.75E+06 1.6
Capaol-4-23-1.2	#07	5/12/16	2:30:18	0.0019451	0.0000002	-17.32			0.10	0.32	2.45E+09	4.77E+06 1.6
Capaol-4-23-1.3	#07	5/12/16	2:36:10	0.0019453	0.0000003	-17.22			0.15	0.33	2.45E+09	4.78E+06 1.6
Capaol-4-23-1.4	#07	5/12/16	2:42:02	0.0019442	0.0000002	-17.79			0.14	0.33	2.45E+09	4.78E+06 1.6
Capaol-4-1.1	#07	5/12/16	3:23:38	0.0019469	0.0000004	-16.42			0.19	0.34	2.47E+09	4.80E+06 1.6
Capaol-4-1.2	#07	5/12/16	3:29:30	0.0019448	0.0000003	-17.48			0.14	0.33	2.47E+09	4.80E+06 1.6
Capaol-4-23-2.1	#07	5/12/16	4:46:58	0.0019445	0.0000003	-17.65			0.14	0.33	2.43E+09	4.73E+06 1.6
Capaol-4-23-2.2	#07	5/12/16	4:52:50	0.0019473	0.0000003		-16.24		0.14	0.33	2.45E+09	4.77E+06 1.6
Capaol-4-23-2.3	#07	5/12/16	4:58:42	0.0019444	0.0000003	-17.69			0.14	0.33	2.43E+09	4.72E+06 1.6
Capaol-4-23-2.4	#07	5/12/16	5:04:33	0.0019456	0.0000003	-17.11			0.16	0.33	2.44E+09	4.75E+06 1.6
Capaol-4-1.3	#07	5/12/16	5:46:09	0.0019455	0.0000004	-17.16			0.19	0.34	2.46E+09	4.79E+06 1.6
Capaol-4-1.4	#07	5/12/16	5:52:00	0.0019456	0.0000003	-17.16			0.18	0.33	2.47E+09	4.81E+06 1.6
Capaol-4-23-1.5	#07	5/12/16	7:09:23	0.0019450	0.0000003	-17.63			0.17	0.34	2.46E+09	4.79E+06 1.6
Capaol-4-23-1.6	#07	5/12/16	7:15:15	0.0019449	0.0000002	-17.44			0.13	0.33	2.45E+09	4.77E+06 1.6
Capaol-4-23-1.7	#07	5/12/16	7:21:07	0.0019445	0.0000002	-17.64			0.15	0.33	2.45E+09	4.78E+06 1.6
Capaol-4-23-1.8	#07	5/12/16	7:26:56	0.0019438	0.0000004	-17.65			0.19	0.34	2.45E+09	4.78E+06 1.6
Capaol-4-1.5	#07	5/12/16	8:08:36	0.0019447	0.0000002	-17.55			0.13	0.33	2.48E+09	4.82E+06 1.6
Capaol-4-1.6	#07	5/12/16	8:14:29	0.0019460	0.0000002	-16.88			0.10	0.32	2.47E+09	4.81E+06 1.6
Capaol-4-23-2.5	#07	5/12/16	8:19:46	0.0019445	0.0000003	-17.68			0.18	0.34	2.46E+09	4.79E+06 1.6
Capaol-4-23-2.6	#07	5/12/16	8:37:38	0.0019447	0.0000002	-17.53			0.14	0.33	2.46E+09	4.79E+06 1.6
Capaol-4-23-2.7	#07	5/12/16	8:43:30	0.0019470	0.0000003	-16.36			0.17	0.34	2.46E+09	4.79E+06 1.6
Capaol-4-23-2.8	#07	5/12/16	8:49:31	0.0019450	0.0000003	-17.41			0.18	0.34	2.46E+09	4.80E+06 1.6
Capaol-4-1.7	#07	5/12/16	10:30:57	0.0019451	0.0000003	-16.52			0.15	0.33	2.46E+09	4.81E+06 1.6
Capaol-4-1.8	#07	5/12/16	10:36:49	0.0019464	0.0000005	-16.65			0.24	0.36	2.48E+09	4.82E+06 1.6
Capaol-4-1.9	#07	5/12/16	10:42:41	0.0019472	0.0000005	-16.26			0.24	0.36	2.47E+09	4.81E+06 1.6
Capaol-4-1.10	#07	5/12/16	10:48:03	0.0019454	0.0000004	-17.19			0.23	0.35	2.49E+09	4.85E+06 1.6
Capaol-4-23-2.9	#07	5/12/16	12:50:38	0.0019453	0.0000002	-17.22		0.11	0.32	2.46E+09	4.79E+06 1.6	
Capaol-4-23-2.7b	#07	5/12/16	12:57:32	0.0019461	0.0000002	-16.82			0.11	0.32	2.44E+09	4.75E+06 1.6

SPOT #	Session	Date	Time	¹⁸ O/ ¹⁶ O	±	δ ¹⁸ O _{SWOW}	rejected	±Internal error (σ 95%)	±External error (1σ)	¹⁸ O cps (median)	¹⁶ O cps (median)	no. sets, subsets								
#08			average	-18.88	weighted mean	-19.18	Internal error (σ 95%)	0.27												
			std dev (1σ)	0.43	error in mean (1σ)	0.12														
			50% variance	0.09	MSWD	11.71														
					no.	13														
					no. outliers	1														
MOUNT HM-22&JA																				
Caplo L4 normalising standard for run 8																				
CapaoL4-HM22-1.1	#08	20/6/17	22:03.32	0.0019291	0.0000002	-17.63		0.10	0.27	2.11E+09	4.08E+06	1,6								
CapaoL4-HM22-1.2	#08	20/6/17	22:08.59	0.0019289	0.0000002	-17.72		0.09	0.27	2.12E+09	4.08E+06	1,6								
CapaoL4-HM22-1.3	#08	20/6/17	22:14.25	0.0019298	0.0000002	-17.28		0.08	0.27	2.11E+09	4.07E+06	1,6								
CapaoL4-HM22-1.4	#08	21/6/17	0:21.19	0.0019309	0.0000002	-16.70		0.09	0.27	2.11E+09	4.07E+06	1,6								
CapaoL4-HM22-1.5	#08	21/6/17	0:26.47	0.0019298	0.0000001	-17.26		0.07	0.27	2.11E+09	4.07E+06	1,6								
CapaoL4-HM22-1.6	#08	21/6/17	0:32.13	0.0019310	0.0000002	-16.68		0.08	0.27	2.10E+09	4.06E+06	1,6								
CapaoL4-HM22-1.7	#08	21/6/17	2:33.40	0.0019292	0.0000002	-17.57		0.11	0.27	2.12E+09	4.09E+06	1,6								
CapaoL4-HM22-1.8	#08	21/6/17	2:39.07	0.0019299	0.0000002	-17.23		0.11	0.27	2.11E+09	4.07E+06	1,6								
CapaoL4-HM22-1.9	#08	21/6/17	2:44.33	0.0019312	0.0000002	-16.57		0.08	0.27	2.11E+09	4.08E+06	1,6								
CapaoL4-HM22-1.10	#08	21/6/17	4:18.06	0.0019302	0.0000002	-17.04		0.10	0.27	2.10E+09	4.05E+06	1,6								
CapaoL4-HM22-1.11	#08	21/6/17	4:23.33	0.0019303	0.0000002	-17.02		0.11	0.27	2.09E+09	4.03E+06	1,6								
CapaoL4-HM22-1.12	#08	21/6/17	4:29.00	0.0019307	0.0000002	-16.83		0.09	0.27	2.07E+09	3.99E+06	1,6								
CapaoL4-HM22-1.13	#08	21/6/17	6:05.37	0.0019299	0.0000002	-17.22		0.09	0.27	2.12E+09	4.08E+06	1,6								
CapaoL4-HM22-1.14	#08	21/6/17	6:11.03	0.0019290	0.0000002	-17.67		0.11	0.27	2.11E+09	4.07E+06	1,6								
CapaoL4-HM22-1.15	#08	21/6/17	6:16.30	0.0019293	0.0000003	-17.51		0.13	0.28	2.10E+09	4.06E+06	1,6								
CapaoL4-HM22-1.16	#08	21/6/17	6:28.53	0.0019304	0.0000002	-16.95		0.10	0.27	2.09E+09	4.04E+06	1,6								
CapaoL4-HM22-1.17	#08	21/6/17	8:34.20	0.0019293	0.0000002	-17.53		0.10	0.27	2.09E+09	4.03E+06	1,6								
CapaoL4-HM22-1.18	#08	21/6/17	10:36.23	0.0019293	0.0000002	-17.51		0.08	0.27	2.09E+09	4.03E+06	1,6								
CapaoL4-HM22-1.19	#08	21/6/17	10:41.50	0.0019293	0.0000002	-17.55		0.10	0.27	2.08E+09	4.01E+06	1,6								
#08			average	-17.23	weighted mean	-17.22	Internal error (σ 95%)	0.17												
			std dev (1σ)	0.37	error in mean (1σ)	0.08														
			50% variance	0.07	MSWD	15.78														
					no.	19														
					no. outliers	0														
MOUNT HM-22&JA																				
Caplo L4																				
CapaoL4-JA1-1.1	#08	20/6/17	22:20.14	0.0019298	0.0000002	-17.29		0.10	0.29	2.08E+09	4.01E+06	1,6								
CapaoL4-JA1-1.2	#08	20/6/17	22:25.41	0.0019301	0.0000002	-17.11		0.11	0.29	2.09E+09	4.03E+06	1,6								
CapaoL4-JA1-2.1	#08	20/6/17	22:31.08	0.0019303	0.0000002	-16.99		0.10	0.28	2.11E+09	4.08E+06	1,6								
CapaoL4-JA1-2.2	#08	20/6/17	2:36.35	0.0019303	0.0000002	-17.02		0.12	0.29	2.09E+09	4.04E+06	1,6								
CapaoL4-JA1-3.1	#08	21/6/17	0:38.02	0.0019294	0.0000002	-17.50		0.12	0.29	2.11E+09	4.07E+06	1,6								
CapaoL4-JA1-3.2	#08	21/6/17	0:43.28	0.0019286	0.0000001	-17.88		0.07	0.28	2.09E+09	4.02E+06	1,6								
CapaoL4-JA1-1.3	#08	21/6/17	0:48.57	0.0019307	0.0000002	-16.82		0.10	0.28	2.09E+09	4.04E+06	1,6								
CapaoL4-JA1-1.4	#08	21/6/17	0:54.24	0.0019304	0.0000002	-16.95		0.11	0.29	2.09E+09	4.04E+06	1,6								
CapaoL4-JA1-2.3	#08	21/6/17	2:50.22	0.0019310	0.0000002	-16.65		0.09	0.28	2.12E+09	4.10E+06	1,6								
CapaoL4-JA1-2.4	#08	21/6/17	2:55.49	0.0019313	0.0000002	-16.52		0.10	0.29	2.11E+09	4.08E+06	1,6								
CapaoL4-JA1-3.3	#08	21/6/17	4:34.48	0.0019295	0.0000002	-17.41		0.10	0.29	2.09E+09	4.04E+06	1,6								
CapaoL4-JA1-3.4	#08	21/6/17	4:40.15	0.0019295	0.0000002	-17.42		0.10	0.28	2.09E+09	4.03E+06	1,6								
CapaoL4-JA1-1.5	#08	21/6/17	6:22.19	0.0019309	0.0000002	-16.71		0.09	0.28	2.10E+09	4.08E+06	1,6								
CapaoL4-JA1-1.6	#08	21/6/17	6:27.46	0.0019303	0.0000002	-17.03		0.10	0.29	2.11E+09	4.07E+06	1,6								
CapaoL4-JA1-1.7	#08	21/6/17	6:33.13	0.0019302	0.0000002	-17.04		0.09	0.28	2.10E+09	4.08E+06	1,6								
CapaoL4-JA1-2.5	#08	21/6/17	6:38.40	0.0019308	0.0000002	-16.73		0.10	0.29	2.11E+09	4.08E+06	1,6								
CapaoL4-JA1-2.6	#08	21/6/17	6:44.07	0.0019306	0.0000002	-16.88		0.12	0.29	2.11E+09	4.08E+06	1,6								
CapaoL4-JA1-2.7	#08	21/6/17	6:49.34	0.0019302	0.0000003	-17.05		0.13	0.29	2.12E+09	4.09E+06	1,6								
CapaoL4-JA1-3.5	#08	21/6/17	6:55.01	0.0019286	0.0000002	-17.89		0.11	0.29	2.08E+09	4.01E+06	1,6								
CapaoL4-JA1-3.6	#08	21/6/17	7:00.28	0.0019283	0.0000002	-18.06		0.10	0.29	2.09E+09	4.02E+06	1,6								
CapaoL4-JA1-3.7	#08	21/6/17	7:05.55	0.0019295	0.0000002	-17.43		0.09	0.28	2.11E+09	4.07E+06	1,6								
CapaoL4-JA1-4.1	#08	21/6/17	7:11.23	0.0019298	0.0000002	-17.28		0.10	0.28	2.08E+09	4.02E+06	1,6								
CapaoL4-JA1-4.2	#08	21/6/17	7:16.49	0.0019300	0.0000002	-17.18		0.13	0.29	2.07E+09	4.00E+06	1,6								
CapaoL4-JA1-4.3	#08	21/6/17	7:22.16	0.0019299	0.0000002	-17.06		0.10	0.28	2.08E+09	3.99E+06	1,6								
CapaoL4-JA1-1.8	#08	21/6/17	8:40.09	0.0019308	0.0000002	-16.77		0.11	0.29	2.11E+09	4.08E+06	1,6								
CapaoL4-JA1-1.9	#08	21/6/17	8:45.36	0.0019303	0.0000002	-16.99		0.10	0.29	2.10E+09	4.05E+06	1,6								
CapaoL4-JA1-1.10	#08	21/6/17	8:51.03	0.0019312	0.0000002	-16.54		0.09	0.28	2.12E+09	4.09E+06	1,6								
CapaoL4-JA1-2.8	#08	21/6/17	8:56.31	0.0019294	0.0000002	-17.48		0.12	0.29	2.09E+09	4.04E+06	1,6								
CapaoL4-JA1-2.9	#08	21/6/17	9:01.58	0.0019298	0.0000003	-17.25		0.14	0.29	2.12E+09	4.09E+06	1,6								
CapaoL4-JA1-2.10	#08	21/6/17	9:07.25	0.0019300	0.0000002	-17.18		0.11	0.29	2.10E+09	4.05E+06	1,6								
CapaoL4-JA1-3.8	#08	21/6/17	9:12.53	0.0019297	0.0000002	-17.30		0.11	0.29	2.10E+09	4.05E+06	1,6								
CapaoL4-JA1-3.9	#08	21/6/17	9:18.20	0.0019289	0.0000002	-17.74		0.13	0.29	2.09E+09	4.03E+06	1,6								
CapaoL4-JA1-3.10	#08	21/6/17	9:23.47	0.0019296	0.0000002	-17.39		0.08	0.28	2.08E+09	4.02E+06	1,6								
CapaoL4-JA1-4.4	#08	21/6/17	9:29.15	0.0019303	0.0000002	-17.04		0.10	0.29	2.09E+09	3.99E+06	1,6								
CapaoL4-JA1-4.5	#08	21/6/17	9:34.42	0.0019315	0.0000002	-16.37		0.10	0.28	2.08E+09	4.01E+06	1,6								
CapaoL4-JA1-4.6	#08	21/6/17	9:40.09	0.0019301	0.0000002	-17.10		0.10	0.29	2.08E+09	3.97E+06	1,6								
CapaoL4-JA1-4.7	#08	21/6/17	10:48.49	0.0019302	0.0000002	-17.04		0.11	0.29	2.10E+09	4.05E+06	1,6								
CapaoL4-JA1-4.8	#08	21/6/17	10:54.16	0.0019304	0.0000002	-16.93		0.12	0.29	2.09E+09	3.97E+06	1,6								
#08			average	-17.15	weighted mean	-17.15	Internal error (σ 95%)	0.27												
			std dev (1σ)	0.39	error in mean (1σ)	0.13														
			50% variance	0.08	MSWD	18.85														
					no.	38														
					no. outliers	0														
MOUNT HM-22&JA																				
ROY L6																				
RoyL5-1.1	#08	20/6/17	22:42.23	0.0019633	0.0000002	-0.11		0.10	0.26	2.09E+09	4.11E+06	1,6								
RoyL5-1.2	#08	20/6/17	22:47.50	0.0019618	0.0000002	-0.70		0.12	0.26	2.09E+09	4.10E+06	1,6								
RoyL5-1.3	#08	20/6/17	22:53.16	0.0019622	0.0000002	-0.50		0.08	0.25	2.10E+09	4.11E+06	1,6								
RoyL5-1.4	#08	21/6/17	1:00.13	0.0019630	0.0000002	-0.07		0.09	0.25	2.10E+09	4.12E+06	1,6								
RoyL5-1.5	#08	21/6/17	1:05.39	0.0019616	0.0000002	-0.81		0.12	0.26	2.09E+09	4.09E+06	1,6								
RoyL5-1.6	#08	21/6/17	3:01.38	0.0019622	0.0000001	-0.47		0.07	0.25	2.11E+09	4.13E+06	1,6								
RoyL5-1.7	#08	21/6/17	3:07.94	0.0019625	0.0000002	-0.34		0.11	0.26	2.11E+09	4.13E+06	1,6								
RoyL5-1.8	#08	21/6/17	7:28.04	0.0019625	0.0000002	-0.32		0.08	0.25	2.08E+09	4.08E+06	1,6								
RoyL5-1.9	#08	21/6/17	7:33.31	0.0019614	0.0000002	-0.88		0.08	0.25	2.07E+09	4.07E+06	1,6								
RoyL5-1.10	#08	21/6/17	9:45.57	0.0019617	0.0000003	-0.74		0.14	0.26	2.08E+09	4.08E+06	1,6								
RoyL5-1.11	#08	21/6/17	9:51.24	0.0019612	0.0000002	-1.02		0.10	0.25	2.09E+09	4.09E+06	1,6								
#08			average	-0.52	weighted mean	-0.52	Internal error (σ 95%)	0.56												
			std dev (1σ)	0.35	error in mean (1σ)	0.25														
			50% variance	0.06	MSWD	17.24														
					no.	11														
					no. outliers	0														
MOUNT HM-22&JA																				
ROY L6																				
RoyL6-1.1	#08	20/6/17	22:58.47	0.0019640	0.0000002	0.46		0.12	0.42	2.15E+09	4.22E+06	1,6								
RoyL6-1.2	#08	20/6/17	23:04.14	0.0019633	0.0000002	-0.09	-1.89	0.09	0.42	2.15E+09	4.23E+06	1,6								
RoyL6-1.3	#08	20/6/17	23:09.40	0.0019695	0.0000002	-0.12		0.09	0.42	2.15E+09	4.21E+06	1,6								
RoyL6-1.4	#08	21/6/17	1:11.10	0.0019615	0.0000002	-0.12		0.12	0.42	2.11E+09	4.14E+06	1,6								
RoyL6-1.5	#08	21/6/17	1:16.37	0.0019633	0.0000002	-0.09		0.09	0.42	2.09E+09	4.11E+06	1,6								
RoyL6-1.6	#08	21/6/17	1:32.35	0.0019627	0.0000002	-0.24		0.09	0.42	2.10E+09	4.12E+06	1,6								
RoyL6-1.7	#08	21/6/17	1:39.02	0.0019615	0.0000002	-0.86		0.11	0.42	2.12E+09	4.15E+06	1,6								
RoyL6-1.8	#08	21/6/17	1:56.28	0.0019627	0.0000002	-0.55		0.11	0.42	2.11E										

SPOT #	Session	Date	Time	¹⁸ O/ ¹⁶ O	±	δ ¹⁸ O _{known}	rejected	±Internal error (σ 95%)	±External error (1σ)	¹⁸ O cps (median)	¹⁶ O cps (median)	no. sets, subsets
Capitol-JA1-7.3	#08	22/6/17	10:24:11	0.0019286	0.0000002	-17.72		0.13	0.22	2.08E+09	4.01E+06	1,6
	#08		average	-17.22	weighted mean	-17.22						
			std dev (1σ)	0.28	error in mean (1σ)	0.08	Internal error (σ 95%)	0.18				
			50% variance	0.04	MSWD	6.62						
				no. outliers	48							
					0							
MOUNT BAHJAJA												
Capilo L2							-19.70	0.11	0.44	2.15E+09	4.13E+06	1,6
Capitol-2-JA1-1.1	#08	22/6/17	3:56:18	0.0019248	0.0000002			0.11	0.44	2.15E+09	4.14E+06	1,6
Capitol-2-JA1-1.2	#08	22/6/17	4:01:45	0.0019254	0.0000002	-19.36		0.08	0.43	2.15E+09	4.14E+06	1,6
Capitol-2-JA1-1.3	#08	22/6/17	4:07:12	0.0019257	0.0000002	-19.23		0.11	0.44	2.17E+09	4.17E+06	1,6
Capitol-2-JA1-1.4	#08	22/6/17	4:12:39	0.0019254	0.0000002	-19.37		0.11	0.44	2.14E+09	4.11E+06	1,6
Capitol-2-JA1-1.5	#08	22/6/17	4:18:05	0.0019287	0.0000002	-17.66		0.12	0.44	2.12E+09	4.09E+06	1,6
Capitol-2-JA1-3.1	#08	22/6/17	4:23:34	0.0019284	0.0000002	-17.81		0.08	0.44	2.17E+09	4.18E+06	1,6
Capitol-2-JA1-3.2	#08	22/6/17	4:29:01	0.0019281	0.0000002	-17.97		0.12	0.44	2.16E+09	4.17E+06	1,6
Capitol-2-JA1-3.3	#08	22/6/17	4:34:26	0.0019274	0.0000002	-18.32		0.10	0.44	2.15E+09	4.14E+06	1,6
Capitol-2-JA1-3.4	#08	22/6/17	4:39:54	0.0019283	0.0000002	-17.89		0.11	0.44	2.17E+09	4.18E+06	1,6
Capitol-2-JA1-3.5	#08	22/6/17	4:45:21	0.0019284	0.0000002	-17.84		0.09	0.44	2.16E+09	4.17E+06	1,6
Capitol-2-JA1-1.6	#08	22/6/17	8:50:11	0.0019286	0.0000002	-18.63		0.11	0.44	2.13E+09	4.10E+06	1,6
Capitol-2-JA1-1.7	#08	22/6/17	8:55:37	0.0019285	0.0000002	-18.79		0.11	0.44	2.11E+09	4.08E+06	1,6
Capitol-2-JA1-1.8	#08	22/6/17	9:01:04	0.0019287	0.0000002	-18.69		0.09	0.44	2.14E+09	4.13E+06	1,6
Capitol-2-JA1-1.9	#08	22/6/17	9:06:30	0.0019287	0.0000002	-18.69		0.09	0.44	2.11E+09	4.08E+06	1,6
Capitol-2-JA1-3.6	#08	22/6/17	9:40:32	0.0019292	0.0000002	-17.41		0.09	0.44	2.15E+09	4.16E+06	1,6
Capitol-2-JA1-3.7	#08	22/6/17	9:45:59	0.0019286	0.0000002	-17.70		0.12	0.44	2.12E+09	4.09E+06	1,6
Capitol-2-JA1-3.8	#08	22/6/17	9:51:26	0.0019292	0.0000002	-17.40		0.08	0.43	2.15E+09	4.14E+06	1,6
Capitol-2-JA1-4.1	#08	22/6/17	9:56:53	0.0019271	0.0000002	-17.44		0.13	0.44	2.03E+09	3.92E+06	1,6
Capitol-2-JA1-4.2	#08	22/6/17	10:02:20	0.0019278	0.0000002	-18.14		0.09	0.44	2.06E+09	3.97E+06	1,6
Capitol-2-JA1-4.3	#08	22/6/17	10:07:47	0.0019281	0.0000002	-17.97		0.12	0.44	2.04E+09	3.93E+06	1,6
Capitol-2-JA1-4.4	#08	22/6/17	10:13:13	0.0019278	0.0000002	-18.11		0.10	0.44	2.05E+09	3.95E+06	1,6
	#08		average	-18.27	weighted mean	-18.28						
			std dev (1σ)	0.61	error in mean (1σ)	0.29	Internal error (σ 95%)	0.61				
			50% variance	0.19	MSWD	44.14						
				no. outliers	21							
					1							
MOUNT HM-238JA												
Capilo L4								0.11	0.25	2.12E+09	4.09E+06	1,6
Capitol-4-JA1-1.1	#08	22/6/17	12:27:28	0.0019309	0.0000002	-16.69		0.11	0.25	2.12E+09	4.10E+06	1,6
Capitol-4-JA1-1.2	#08	22/6/17	12:32:55	0.0019302	0.0000002	-17.00		0.11	0.25	2.12E+09	4.10E+06	1,6
Capitol-4-JA1-1.4	#08	22/6/17	12:38:24	0.0019307	0.0000002	-16.76		0.10	0.25	2.14E+09	4.13E+06	1,6
Capitol-4-JA1-1.2	#08	22/6/17	12:43:51	0.0019298	0.0000002	-17.23		0.10	0.25	2.12E+09	4.10E+06	1,6
Capitol-4-JA1-1.3	#08	22/6/17	14:18:01	0.0019297	0.0000002	-17.29		0.10	0.25	2.13E+09	4.12E+06	1,6
Capitol-4-JA1-1.4	#08	22/6/17	14:23:35	0.0019302	0.0000002	-17.03		0.09	0.25	2.13E+09	4.10E+06	1,6
Capitol-4-JA1-4.3	#08	22/6/17	14:29:11	0.0019294	0.0000002	-17.44		0.10	0.25	2.14E+09	4.12E+06	1,6
Capitol-4-JA1-4.4	#08	22/6/17	14:34:45	0.0019294	0.0000002	-17.44		0.09	0.25	2.16E+09	4.16E+06	1,6
Capitol-4-JA1-1.1b	#08	22/6/17	15:16:04	0.0019304	0.0000002	-16.90		0.10	0.25	2.14E+09	4.14E+06	1,6
Capitol-4-JA1-1.10	#08	22/6/17	15:23:46	0.0019305	0.0000002	-16.88		0.09	0.25	2.13E+09	4.11E+06	1,6
Capitol-4-JA1-8.1	#08	22/6/17	16:08:41	0.0019296	0.0000002	-16.93		0.09	0.25	2.18E+09	4.21E+06	1,6
Capitol-4-JA1-8.2	#08	22/6/17	16:12:09	0.0019304	0.0000002	-16.93		0.09	0.25	2.17E+09	4.18E+06	1,6
Capitol-4-JA1-8.3	#08	22/6/17	17:24:42	0.0019289	0.0000002	-17.68		0.08	0.25	2.17E+09	4.18E+06	1,6
Capitol-4-JA1-8.4	#08	22/6/17	17:36:10	0.0019296	0.0000002	-17.32		0.10	0.25	2.16E+09	4.16E+06	1,6
Capitol-4-JA1-7.1	#08	22/6/17	17:35:38	0.0019293	0.0000002	-17.50		0.10	0.25	2.15E+09	4.15E+06	1,6
Capitol-4-JA1-7.2	#08	22/6/17	17:41:07	0.0019299	0.0000002	-17.17		0.10	0.25	2.14E+09	4.13E+06	1,6
Capitol-4-JA1-7.3	#08	22/6/17	18:36:40	0.0019297	0.0000002	-17.31		0.08	0.25	2.14E+09	4.12E+06	1,6
Capitol-4-JA1-7.4	#08	22/6/17	18:42:09	0.0019297	0.0000002	-17.29		0.11	0.25	2.11E+09	4.09E+06	1,6
Capitol-4-JA1-2.1	#08	22/6/17	21:37:24	0.0019301	0.0000002	-17.10		0.09	0.25	2.19E+09	4.23E+06	1,6
Capitol-4-JA1-2.2	#08	22/6/17	21:42:52	0.0019290	0.0000002	-17.65		0.11	0.25	2.17E+09	4.19E+06	1,6
Capitol-4-JA1-2.3	#08	22/6/17	21:48:20	0.0019295	0.0000002	-17.48		0.09	0.25	2.18E+09	4.21E+06	1,6
Capitol-4-JA1-3.1	#08	22/6/17	23:17:27	0.0019298	0.0000002	-17.24		0.11	0.25	2.18E+09	4.21E+06	1,6
Capitol-4-JA1-3.2	#08	22/6/17	23:22:55	0.0019301	0.0000002	-17.06		0.10	0.25	2.18E+09	4.20E+06	1,6
Capitol-4-JA1-4.5	#08	23/6/17	0:46:29	0.0019292	0.0000002	-17.55		0.10	0.25	2.19E+09	4.23E+06	1,6
Capitol-4-JA1-4.6	#08	23/6/17	0:51:57	0.0019292	0.0000002	-17.50	-16.09	0.10	0.25	2.18E+09	4.19E+06	1,6
Capitol-4-JA1-4.7	#08	23/6/17	2:15:30	0.0019293	0.0000002	-17.52		0.09	0.25	2.18E+09	4.20E+06	1,6
Capitol-4-JA1-2.4	#08	23/6/17	2:21:00	0.0019303	0.0000002	-16.99		0.09	0.25	2.18E+09	4.21E+06	1,6
Capitol-4-JA1-2.5	#08	23/6/17	3:44:34	0.0019303	0.0000001	-16.98		0.08	0.25	2.19E+09	4.23E+06	1,6
Capitol-4-JA1-2.6	#08	23/6/17	3:50:02	0.0019294	0.0000002	-17.47		0.11	0.25	2.18E+09	4.20E+06	1,6
Capitol-4-JA1-3.3	#08	23/6/17	5:13:33	0.0019288	0.0000002	-17.78		0.12	0.25	2.18E+09	4.20E+06	1,6
Capitol-4-JA1-3.4	#08	23/6/17	5:19:01	0.0019286	0.0000002	-17.81		0.10	0.25	2.21E+09	4.23E+06	1,6
Capitol-4-JA1-3.5	#08	23/6/17	7:14:44	0.0019296	0.0000002	-17.34		0.11	0.25	2.19E+09	4.23E+06	1,6
Capitol-4-JA1-3.6	#08	23/6/17	7:20:12	0.0019283	0.0000002	-18.00		0.08	0.25	2.18E+09	4.18E+06	1,6
Capitol-4-JA1-7.5	#08	23/6/17	8:49:08	0.0019303	0.0000002	-17.00		0.09	0.25	2.18E+09	4.20E+06	1,6
Capitol-4-JA1-7.6	#08	23/6/17	8:54:36	0.0019309	0.0000002	-16.68		0.09	0.25	2.16E+09	4.17E+06	1,6
Capitol-4-JA1-7.7	#08	23/6/17	10:23:31	0.0019305	0.0000002	-16.85		0.11	0.25	2.15E+09	4.16E+06	1,6
Capitol-4-JA1-7.8	#08	23/6/17	10:28:59	0.0019305	0.0000002	-16.87		0.09	0.25	2.14E+09	4.13E+06	1,6
	#08		average	-17.22	weighted mean	-17.22						
			std dev (1σ)	0.34	error in mean (1σ)	0.12	Internal error (σ 95%)	0.23				
			50% variance	0.06	MSWD	13.27						
				no. outliers	37							
					1							
MOUNT HM-238JA												
Capilo L4							-19.30	0.10	0.29	2.20E+09	4.24E+06	1,6
Capitol-4-HM23-1.1	#08	22/6/17	12:49:39	0.0019258	0.0000002			0.10	0.30	2.17E+09	4.19E+06	1,6
Capitol-4-HM23-1.2	#08	22/6/17	12:55:06	0.0019248	0.0000002	-19.81		0.10	0.30	2.15E+09	4.13E+06	1,6
Capitol-4-HM23-2.1	#08	22/6/17	13:00:36	0.0019251	0.0000002	-19.69		0.10	0.30	2.15E+09	4.13E+06	1,6
Capitol-4-HM23-2.2	#08	22/6/17	13:06:03	0.0019243	0.0000002	-20.07		0.10	0.30	2.12E+09	4.09E+06	1,6
Capitol-4-HM23-1.3	#08	22/6/17	14:40:44	0.0019242	0.0000002	-19.13		0.09	0.29	2.20E+09	4.24E+06	1,6
Capitol-4-HM23-1.4	#08	22/6/17	14:46:12	0.0019245	0.0000002	-19.69		0.08	0.29	2.19E+09	4.21E+06	1,6
Capitol-4-HM23-2.3	#08	22/6/17	14:51:44	0.0019251	0.0000002	-19.98		0.08	0.29	2.13E+09	4.11E+06	1,6
Capitol-4-HM23-2.4	#08	22/6/17	14:57:12	0.0019249	0.0000002	-19.77		0.08	0.29	2.15E+09	4.14E+06	1,6
Capitol-4-HM23-1.5	#08	22/6/17	16:17:58	0.0019236	0.0000002	-20.46		0.11	0.30	2.29E+09	4.41E+06	1,6
Capitol-4-HM23-1.6	#08	22/6/17	16:23:27	0.0019249	0.0000002	-19.78		0.09	0.29	2.27E+09	4.37E+06	1,6
Capitol-4-HM23-1.7	#08	22/6/17	17:46:56	0.0019244	0.0000002	-20.04		0.09	0.29	2.25E+09	4.33E+06	1,6
Capitol-4-HM23-1.8	#08	22/6/17	17:52:24	0.0019238	0.0000002	-20.33		0.09	0.29	2.27E+09	4.36E+06	1,6
Capitol-4-HM23-1.9	#08	22/6/17	18:47:58	0.0019236	0.0000002	-20.46		0.09	0			

SPT #	Session	Date	Time	¹² C/ ¹³ C	±	δ ¹³ C _{org}	rejected	±Internal error (σ 95%)	±External error (1σ)	¹³ C cps (median)	¹³ C cps (median)	no. sets subsets
Win-06-G3A-1.8	#08	22/6/17	13:36:48	0.0018636	0.0000002	0.27						
Win-06-G3A-1.9	#08	22/6/17	13:44:14	0.0018628	0.0000002	-0.14						
Win-06-G3A-1.8	#08	22/6/17	13:49:41	0.0018624	0.0000002	-0.32						
Win-06-G3A-1.9	#08	22/6/17	13:55:07	0.0018630	0.0000003	-0.01						
Win-06-G3A-1.10	#08	22/6/17	14:00:34	0.0018625	0.0000002	-0.29						
Win-06-G3A-2.1	#08	22/6/17	16:28:57	0.0018605	0.0000002	-1.35						
Win-06-G3A-2.2	#08	22/6/17	16:34:25	0.0018600	0.0000002	-1.61						
Win-06-G3A-2.3	#08	22/6/17	17:57:54	0.0018619	0.0000002	-0.58						
Win-06-G3A-2.4	#08	22/6/17	18:03:23	0.0018636	0.0000002		0.26					
Win-06-G3A-2.5	#08	22/6/17	18:58:57	0.0018601	0.0000001	-1.52						
Win-06-G3A-2.6	#08	22/6/17	19:04:25	0.0018621	0.0000002	-0.49						
Win-06-G3A-2.1b	#08	22/6/17	19:25:40	0.0018617	0.0000002	-0.73						
Win-06-G3A-2.2b	#08	22/6/17	19:31:08	0.0018608	0.0000002	-1.20						
	#08											
		average		-0.49	weighted mean	-0.53						
		std dev (1σ)		0.59	error in mean (1σ)	0.31	Internal error (σ 95%)	0.66				
		50% variance		0.17	MSWD	48.52						
					no.	18						
					no. outliers	1						
MOUNT HM-27 HM-16												
Caplo L4 normalising standard for run 9												
Capacol-4-HMZ7-1	#09	17/8/17	10:15:30	0.0019476	0.0000002	-16.94						
Capacol-4-HMZ7-2	#09	17/8/17	10:20:47	0.0019484	0.0000002	-16.52						
Capacol-4-HMZ7-3	#09	17/8/17	10:26:05	0.0019472	0.0000002	-17.18						
Capacol-4-HMZ7-4	#09	17/8/17	10:31:24	0.0019480	0.0000002	-16.75						
Capacol-4-HMZ7-5	#09	17/8/17	10:51:10	0.0019482	0.0000002	-16.65						
Capacol-4-HM16-1	#09	17/8/17	11:51:30	0.0019466	0.0000002	-17.46						
Capacol-4-HM16-2	#09	17/8/17	11:06:48	0.0019464	0.0000002	-17.57						
Capacol-4-HM16-3	#09	17/8/17	11:12:06	0.0019471	0.0000002	-17.20						
Capacol-4-HMZ7-6	#09	17/8/17	13:11:23	0.0019465	0.0000002	-17.11						
Capacol-4-HMZ7-7	#09	17/8/17	13:16:41	0.0019470	0.0000002	-17.26						
Capacol-4-HMZ7-8	#09	17/8/17	13:21:59	0.0019472	0.0000002	-17.17						
Capacol-4-HMZ7-9	#09	17/8/17	13:27:17	0.0019473	0.0000002	-17.12						
Capacol-4-HM16-1.4	#09	17/8/17	13:35:34	0.0019469	0.0000002	-17.33						
Capacol-4-HM16-1.5	#09	17/8/17	13:40:51	0.0019471	0.0000002	-17.22						
Capacol-4-HM16-1.6	#09	17/8/17	13:46:59	0.0019480	0.0000002	-16.73						
Capacol-4-HM16-2.1	#09	17/8/17	14:16:29	0.0019480	0.0000002	-16.77						
Capacol-4-HM16-2.2	#09	17/8/17	14:21:47	0.0019475	0.0000002	-16.99						
Capacol-4-HM16-2.3	#09	17/8/17	14:27:05	0.0019480	0.0000002	-16.77						
Capacol-4-HM16-2.4	#09	17/8/17	15:41:44	0.0019465	0.0000002	-17.52						
Capacol-4-HM16-2.5	#09	17/8/17	15:47:02	0.0019475	0.0000002	-17.01						
Capacol-4-HM16-2.6	#09	17/8/17	15:52:20	0.0019477	0.0000002	-16.93						
Capacol-4-HMZ7-10	#09	17/8/17	16:36:49	0.0019469	0.0000002	-17.30						
Capacol-4-HMZ7-11	#09	17/8/17	16:42:07	0.0019479	0.0000002	-16.79						
Capacol-4-HMZ7-12	#09	17/8/17	16:47:25	0.0019478	0.0000002	-16.84						
Capacol-4-HM16-3.1	#09	17/8/17	18:44:34	0.0019467	0.0000002	-17.41						
Capacol-4-HM16-3.2	#09	17/8/17	18:49:52	0.0019464	0.0000002	-17.57						
Capacol-4-HM16-3.3	#09	17/8/17	18:55:10	0.0019465	0.0000002	-17.50						
Capacol-4-HM16-3.4	#09	17/8/17	20:13:07	0.0019475	0.0000002	-17.03						
Capacol-4-HM16-3.5	#09	17/8/17	20:18:24	0.0019467	0.0000002	-17.44						
Capacol-4-HMZ7-13	#09	17/8/17	22:03:30	0.0019473	0.0000003	-17.13						
Capacol-4-HMZ7-14	#09	17/8/17	22:08:48	0.0019480	0.0000002	-16.73						
Capacol-4-HMZ7-15	#09	17/8/17	22:14:06	0.0019472	0.0000002	-17.14						
Capacol-4-HM16-1.7	#09	17/8/17	23:34:07	0.0019468	0.0000002	-17.38						
Capacol-4-HM16-1.8	#09	17/8/17	23:39:25	0.0019472	0.0000003	-17.14						
Capacol-4-HM16-1.9	#09	17/8/17	23:44:43	0.0019469	0.0000002	-17.33						
Capacol-4-HMZ7-16	#09	18/8/17	0:06:50	0.0019469	0.0000002	-17.29						
Capacol-4-HMZ7-17	#09	18/8/17	0:12:08	0.0019474	0.0000002	-17.05						
Capacol-4-HM16-1.10	#09	18/8/17	1:10:55	0.0019470	0.0000002	-17.24						
Capacol-4-HM16-1.11	#09	18/8/17	1:16:13	0.0019471	0.0000002	-17.24						
Capacol-4-HM16-1.12	#09	18/8/17	1:21:30	0.0019470	0.0000002	-17.28						
Capacol-4-HMZ7-18	#09	18/8/17	1:43:38	0.0019478	0.0000002	-16.84						
Capacol-4-HMZ7-19	#09	18/8/17	1:46:56	0.0019469	0.0000002	-17.31						
Capacol-4-HM16-3.16	#09	18/8/17	2:53:01	0.0019469	0.0000002	-17.34						
Capacol-4-HM16-3.7	#09	18/8/17	2:58:19	0.0019465	0.0000002	-17.51						
Capacol-4-HM16-3.8	#09	18/8/17	3:03:36	0.0019467	0.0000002	-17.43						
Capacol-4-HMZ7-20	#09	18/8/17	3:09:16	0.0019460	0.0000002	-17.78						
Capacol-4-HMZ7-21	#09	18/8/17	3:14:34	0.0019467	0.0000002	-17.42						
Capacol-4-HM16-3.9	#09	18/8/17	4:13:13	0.0019464	0.0000002	-17.55						
Capacol-4-HM16-3.10	#09	18/8/17	4:18:31	0.0019462	0.0000002	-17.12						
Capacol-4-HM16-3.11	#09	18/8/17	4:23:48	0.0019466	0.0000003	-17.48						
Capacol-4-HMZ7-22	#09	18/8/17	4:40:37	0.0019472	0.0000002	-17.17						
Capacol-4-HMZ7-23	#09	18/8/17	4:45:55	0.0019475	0.0000003	-17.01						
Capacol-4-HMZ7-24	#09	18/8/17	4:51:13	0.0019471	0.0000002	-17.19						
Capacol-4-HM16-1.13	#09	18/8/17	5:44:43	0.0019473	0.0000003	-17.12						
Capacol-4-HM16-1.14	#09	18/8/17	5:50:00	0.0019471	0.0000002	-17.21						
Capacol-4-HMZ7-25	#09	18/8/17	6:12:09	0.0019469	0.0000003	-17.30						
Capacol-4-HMZ7-26	#09	18/8/17	6:17:27	0.0019467	0.0000002	-17.41						
Capacol-4-HMZ7-27	#09	18/8/17	6:22:45	0.0019470	0.0000002	-17.24						
Capacol-4-HMZ7-33	#09	18/8/17	7:15:57	0.0019466	0.0000002	-17.48						
Capacol-4-HMZ7-28	#09	18/8/17	7:21:16	0.0019473	0.0000002	-17.10						
Capacol-4-HMZ7-29	#09	18/8/17	7:38:24	0.0019467	0.0000002	-17.43						
Capacol-4-HMZ7-30	#09	18/8/17	7:43:42	0.0019463	0.0000002	-17.63						
Capacol-4-HMZ7-31	#09	18/8/17	8:42:11	0.0019465	0.0000002	-17.54						
Capacol-4-HMZ7-32	#09	18/8/17	8:47:29	0.0019469	0.0000002	-17.29						
	#09		average	-17.22	weighted mean	-17.22						
		std dev (1σ)		0.28	error in mean (1σ)	0.30	Internal error (σ 95%)	0.13				
		50% variance		0.04	MSWD	5.72						
					no.	64						
					no. outliers	1						
MOUNT HM-27 HM-16												
Caplo L2												
Capacol-2-HMZ7-1.1	#09	18/8/17	6:28:10	0.0019450	0.0000002	-18.27						
Capacol-2-HMZ7-1.2	#09	18/8/17	6:33:28	0.0019447	0.0000002	-18.45						
Capacol-2-HMZ7-1.3	#09	18/8/17	6:38:45	0.0019452	0.0000002	-18.09						
Capacol-2-HMZ7-1.4	#09	18/8/17	6:44:03	0.0019453	0.0000003	-18.15						
Capacol-2-HMZ7-1.5	#09	18/8/17	6:49:21	0.0019449	0.0000002	-18.33						
Capacol-2-HMZ7-1.6	#09	18/8/17	6:54:39	0.0019441	0.0000002	-18.74						
Capacol-2-HMZ7-1.7	#09	18/8/17	6:59:57	0.0019443	0.0000002	-18.66						
Capacol-2-HMZ7-1.8	#09	18/8/17	7:05:14	0.0019456	0.0000002	-17.98						
Capacol-2-HMZ7-1.9	#09	18/8/17	7:10:32	0.0019440	0.0000002	-18.82						
	#09		average	-18.40	weighted mean	-18.26						
		std dev (1σ)		0.29	error in mean (1σ)	0.22	Internal error (σ 95%)	0.50				
		50% variance		0.04	MSWD	6.51						
					no.	9						
					no. outliers	0						
MOUNT HM-27 HM-16												
ROY L5												
RoyL5-HM16-1.1	#09	17/8/17	19:09:26	0.0019811	0.0000002	0.27						
RoyL5-HM16-1.2	#09	17/8/17	19:14:44	0.0019809	0.0000002	0.17						
RoyL5-HM16-1												

SPOT #	Session	Date	Time	T ₀ /T ₀	z	δ ^{Obs} Observed	rejected	±Internal error (σ 95%)	±External error (1σ)	T ₀ cps (median)	T ₀ cps (median)	no. sets subsets
MOUNT HM22-1.6												
CapaoL4-HM22-1.6	#09	18/8/17	12:31:44	0.0019461	0.0000002	-17.45		0.12	0.22	2.38E+09	4.68E+06	1.6
CapaoL4-HM27-6	#09	18/8/17	12:49:07	0.0019467	0.0000002	-17.12		0.09	0.21	2.37E+09	4.61E+06	1.6
CapaoL4-HM27-7	#09	18/8/17	12:54:24	0.0019462	0.0000002	-17.39		0.10	0.21	2.37E+09	4.61E+06	1.6
CapaoL4-HM27-8	#09	18/8/17	12:59:42	0.0019465	0.0000002	-17.25		0.10	0.21	2.37E+09	4.61E+06	1.6
CapaoL4-HM22-1.7	#09	18/8/17	13:55:21	0.0019473	0.0000002	-16.82		0.09	0.21	2.37E+09	4.62E+06	1.6
CapaoL4-HM22-1.8	#09	18/8/17	14:00:39	0.0019476	0.0000002	-16.68		0.10	0.21	2.38E+09	4.63E+06	1.6
CapaoL4-HM22-1.9	#09	18/8/17	14:05:56	0.0019477	0.0000002	-16.61		0.11	0.22	2.37E+09	4.61E+06	1.6
CapaoL4-HM22-1.10	#09	18/8/17	15:09:42	0.0019467	0.0000003	-17.13		0.16	0.23	2.41E+09	4.68E+06	1.6
CapaoL4-HM22-1.11	#09	18/8/17	15:15:00	0.0019468	0.0000002	-17.11		0.11	0.22	2.40E+09	4.68E+06	1.6
CapaoL4-HM27-9	#09	18/8/17	15:20:37	0.0019462	0.0000002	-17.38		0.12	0.22	2.37E+09	4.62E+06	1.6
CapaoL4-HM27-10	#09	18/8/17	15:25:55	0.0019469	0.0000002	-17.05		0.12	0.22	2.38E+09	4.64E+06	1.6
CapaoL4-HM27-11	#09	18/8/17	15:31:13	0.0019468	0.0000002	-17.07		0.11	0.22	2.38E+09	4.63E+06	1.6
CapaoL4-HM22-1.12	#09	18/8/17	16:51:41	0.0019474	0.0000002	-16.79		0.10	0.22	2.40E+09	4.68E+06	1.6
CapaoL4-HM22-1.13	#09	18/8/17	16:56:59	0.0019470	0.0000003	-16.97		0.14	0.23	2.40E+09	4.68E+06	1.6
CapaoL4-HM22-1.14	#09	18/8/17	17:02:17	0.0019459	0.0000002	-17.53		0.15	0.23	2.41E+09	4.69E+06	1.6
CapaoL4-HM27-12	#09	18/8/17	17:07:55	0.0019468	0.0000002	-17.07		0.10	0.21	2.37E+09	4.61E+06	1.6
CapaoL4-HM27-13	#09	18/8/17	17:13:13	0.0019470	0.0000002	-17.01		0.09	0.21	2.38E+09	4.64E+06	1.6
CapaoL4-HM27-14	#09	18/8/17	17:18:31	0.0019471	0.0000002	-16.93		0.11	0.22	2.39E+09	4.65E+06	1.6
CapaoL4-HM27-15	#09	18/8/17	18:39:21	0.0019462	0.0000002	-17.39		0.11	0.22	2.35E+09	4.58E+06	1.6
CapaoL4-HM27-16	#09	18/8/17	18:44:38	0.0019465	0.0000002	-17.26		0.12	0.22	2.34E+09	4.55E+06	1.6
CapaoL4-HM27-17	#09	18/8/17	18:49:56	0.0019467	0.0000002	-17.15		0.10	0.21	2.35E+09	4.57E+06	1.6
CapaoL4-HM22-1.15	#09	18/8/17	19:31:22	0.0019454	0.0000002	-17.78		0.10	0.21	2.37E+09	4.61E+06	1.6
CapaoL4-HM22-1.16	#09	18/8/17	19:36:40	0.0019462	0.0000002	-17.41		0.11	0.22	2.37E+09	4.62E+06	1.6
CapaoL4-HM27-17	#09	18/8/17	19:41:57	0.0019470	0.0000002	-16.98		0.10	0.21	2.38E+09	4.63E+06	1.6
CapaoL4-HM27-18	#09	18/8/17	20:31:35	0.0019461	0.0000003	-17.44		0.13	0.22	2.35E+09	4.57E+06	1.6
CapaoL4-HM27-19	#09	18/8/17	20:36:53	0.0019458	0.0000002	-17.61		0.10	0.21	2.35E+09	4.57E+06	1.6
CapaoL4-HM27-20	#09	18/8/17	20:42:11	0.0019466	0.0000002	-17.19		0.11	0.22	2.35E+09	4.58E+06	1.6
CapaoL4-HM22-1.18	#09	18/8/17	20:47:48	0.0019474	0.0000002	-16.76		0.10	0.21	2.38E+09	4.63E+06	1.6
CapaoL4-HM22-1.19	#09	18/8/17	20:53:05	0.0019481	0.0000002		-16.42	0.11	0.22	2.39E+09	4.65E+06	1.6
CapaoL4-HM22-1.20	#09	18/8/17	20:58:23	0.0019466	0.0000002	-17.21		0.10	0.21	2.37E+09	4.61E+06	1.6
CapaoL4-HM27-21	#09	18/8/17	21:22:21	0.0019459	0.0000002	-17.12		0.12	0.22	2.34E+09	4.55E+06	1.6
CapaoL4-HM27-22	#09	18/8/17	21:27:38	0.0019456	0.0000002	-17.71		0.12	0.22	2.35E+09	4.57E+06	1.6
CapaoL4-HM27-23	#09	18/8/17	21:32:56	0.0019463	0.0000002	-17.38		0.11	0.22	2.33E+09	4.54E+06	1.6
#09			average	-17.22	weighted mean	-17.22						
			std dev (10)	0.29	error in mean (1σ)	0.09		Internal error (σ 95%)	0.18			
			50% variance	0.04	MSWD	7.68						
						43						
						no. outliers						
						1						
MOUNT HM-27_HM22												
ROY L5												
RoyL5-HM22-1.1	#09	18/8/17	11:28:02	0.0019815	0.0000003	0.73		0.13	0.30	2.34E+09	4.64E+06	1.6
RoyL5-HM22-1.2	#09	18/8/17	11:33:20	0.0019812	0.0000002	0.59		0.11	0.29	2.34E+09	4.63E+06	1.6
RoyL5-HM22-1.3	#09	18/8/17	12:42:27	0.0019805	0.0000002	0.23		0.13	0.30	2.35E+09	4.66E+06	1.6
RoyL5-HM22-1.4	#09	18/8/17	14:27:14	0.0019802	0.0000002	0.09		0.10	0.29	2.35E+09	4.66E+06	1.6
RoyL5-HM22-1.5	#09	18/8/17	14:32:32	0.0019798	0.0000002	-0.11		0.11	0.29	2.38E+09	4.71E+06	1.6
RoyL5-HM22-1.6	#09	18/8/17	14:37:50	0.0019819	0.0000002	0.92		0.12	0.30	2.34E+09	4.64E+06	1.6
#09			average	0.41	weighted mean	0.38						
			std dev (10)	0.40	error in mean (1σ)	0.42		Internal error (σ 95%)	1.08			
			50% variance	0.08	MSWD	13.67						
						6						
						no. outliers						
						0						
MOUNT HM-27_HM22												
ROY L6												
RoyL6-HM22-1.1	#09	18/8/17	12:10:31	0.0019804	0.0000002	0.17		0.11	0.19	2.40E+09	4.79E+06	1.6
RoyL6-HM22-1.2	#09	18/8/17	12:15:48	0.0019805	0.0000002	0.24		0.13	0.20	2.39E+09	4.74E+06	1.6
RoyL6-HM22-1.3	#09	18/8/17	12:37:05	0.0019817	0.0000002	0.82		0.10	0.19	2.39E+09	4.75E+06	1.6
RoyL6-HM22-1.4	#09	18/8/17	14:11:17	0.0019806	0.0000002	0.29		0.13	0.20	2.38E+09	4.73E+06	1.6
RoyL6-HM22-1.5	#09	18/8/17	14:16:35	0.0019803	0.0000002	0.13		0.09	0.19	2.38E+09	4.71E+06	1.6
RoyL6-HM22-1.6	#09	18/8/17	14:21:53	0.0019806	0.0000002	0.27		0.10	0.19	2.37E+09	4.70E+06	1.6
#09			average	0.32	weighted mean	0.32						
			std dev (10)	0.29	error in mean (1σ)	0.10		Internal error (σ 95%)	0.71			
			50% variance	0.03	MSWD	7.49						
						6						
						no. outliers						
						0						
MOUNT HM-27_HM22												
Capao L4												
normalising standard for run 9												
CapaoL4-HM23-1.7	#09	18/8/17	0:52:26	0.0019422	0.0000002	-17.78		0.09	0.24	2.48E+09	4.81E+06	1.6
CapaoL4-HM23-1.8	#09	18/8/17	0:57:44	0.0019418	0.0000002	-17.99		0.10	0.24	2.42E+09	4.77E+06	1.6
CapaoL4-HM23-1.9	#09	18/8/17	1:03:02	0.0019431	0.0000002	-17.29		0.11	0.24	2.48E+09	4.84E+06	1.6
CapaoL4-HM23-2.4	#09	18/8/17	1:08:23	0.0019439	0.0000002	-16.92		0.10	0.24	2.46E+09	4.78E+06	1.6
CapaoL4-HM23-2.5	#09	18/8/17	1:13:41	0.0019440	0.0000002	-16.84		0.12	0.24	2.45E+09	4.77E+06	1.6
CapaoL4-HM23-2.6	#09	18/8/17	1:18:59	0.0019441	0.0000002	-16.80		0.12	0.24	2.46E+09	4.78E+06	1.6
CapaoL4-HM23-1.10	#09	18/8/17	2:17:23	0.0019427	0.0000002	-17.50		0.13	0.25	2.42E+09	4.71E+06	1.6
CapaoL4-HM23-1.11	#09	18/8/17	2:22:41	0.0019432	0.0000002	-17.24		0.10	0.24	2.42E+09	4.70E+06	1.6
CapaoL4-HM23-1.12	#09	18/8/17	2:27:58	0.0019437	0.0000002	-17.00		0.11	0.24	2.42E+09	4.71E+06	1.6
CapaoL4-HM23-2.7	#09	18/8/17	2:33:19	0.0019441	0.0000002	-16.82		0.10	0.24	2.45E+09	4.77E+06	1.6
CapaoL4-HM23-2.8	#09	18/8/17	2:38:37	0.0019439	0.0000002	-16.90		0.11	0.24	2.46E+09	4.78E+06	1.6
CapaoL4-HM23-2.9	#09	18/8/17	2:43:55	0.0019433	0.0000002	-17.23		0.10	0.24	2.45E+09	4.76E+06	1.6
CapaoL4-HM23-1.13	#09	18/8/17	3:58:51	0.0019426	0.0000002	-17.56		0.13	0.25	2.42E+09	4.73E+06	1.6
CapaoL4-HM23-1.14	#09	18/8/17	4:04:08	0.0019430	0.0000002	-17.35		0.12	0.24	2.43E+09	4.73E+06	1.6
CapaoL4-HM23-1.15	#09	18/8/17	4:09:27	0.0019434	0.0000002	-17.18		0.11	0.24	2.41E+09	4.69E+06	1.6
CapaoL4-HM23-2.10	#09	18/8/17	4:14:48	0.0019437	0.0000002	-17.03		0.10	0.24	2.41E+09	4.69E+06	1.6
CapaoL4-HM23-2.11	#09	18/8/17	4:20:06	0.0019438	0.0000002	-16.97		0.12	0.24	2.45E+09	4.75E+06	1.6
CapaoL4-HM23-2.12	#09	18/8/17	4:25:23	0.0019440	0.0000002	-16.84		0.11	0.24	2.45E+09	4.75E+06	1.6
CapaoL4-HM23-1.16	#09	18/8/17	5:45:43	0.0019434	0.0000002	-17.16		0.10	0.24	2.45E+09	4.76E+06	1.6
CapaoL4-HM23-1.17	#09	18/8/17	5:51:01	0.0019434	0.0000002	-17.17		0.11	0.24	2.46E+09	4.77E+06	1.6
CapaoL4-HM23-1.18	#09	18/8/17	5:56:19	0.0019426	0.0000002	-17.56		0.09	0.24	2.44E+09	4.74E+06	1.6
CapaoL4-HM23-2.13	#09	18/8/17	6:01:40	0.0019431	0.0000002	-17.31		0.13	0.25	2.46E+09	4.78E+06	1.6
CapaoL4-HM23-2.14	#09	18/8/17	6:06:58	0.0019446	0.0000002	-16.55		0.10	0.24	2.45E+09	4.75E+06	1.6
CapaoL4-HM23-2.15	#09	18/8/17	6:12:16	0.0019445	0.0000003	-16.61		0.13	0.25	2.46E+09	4.78E+06	1.6
CapaoL4-HM23-1.19	#09	18/8/17	7:10:43									

SPOT #	Session	Date	Time	T ₀ /T ₀	z	δ ⁰ O ₂ nom	rejected	±Internal error (σ 95%)	±External error (1σ)	T ₀ cps (median)	T ₀ cps (median)	no. sets, subsets
Capao4-HM27-11	#10	4/9/17	14:56:18	0.0019222	0.0000002		-16.07	0.10	0.33	2.24E+09	4.32E+06	1,6
Capao4-HM27-12	#10	4/9/17	15:01:35	0.0019309	0.0000002	-16.69		0.12	0.34	2.26E+09	4.36E+06	1,6
Capao4-HM17-1.4	#10	4/9/17	15:07:13	0.0019283	0.0000002	-18.08		0.09	0.33	2.24E+09	4.32E+06	1,6
Capao4-HM17-1.5	#10	4/9/17	15:12:31	0.0019283	0.0000002	-18.09		0.11	0.33	2.23E+09	4.29E+06	1,6
Capao4-HM27-13	#10	4/9/17	16:22:25	0.0019310	0.0000002	-16.68		0.11	0.33	2.24E+09	4.32E+06	1,6
Capao4-HM27-14	#10	4/9/17	16:27:45	0.0019303	0.0000001	-17.03		0.08	0.33	2.23E+09	4.31E+06	1,6
Capao4-HM27-15	#10	4/9/17	16:33:03	0.0019305	0.0000002	-16.95		0.13	0.34	2.25E+09	4.34E+06	1,6
Capao4-HM17-1.8	#10	4/9/17	16:39:42	0.0019285	0.0000002	-17.98		0.08	0.33	2.22E+09	4.29E+06	1,6
Capao4-HM17-1.7	#10	4/9/17	16:44:00	0.0019285	0.0000002	-17.94		0.09	0.33	2.22E+09	4.29E+06	1,6
Capao4-HM27-16	#10	4/9/17	17:53:47	0.0019304	0.0000002	-16.99		0.11	0.33	2.24E+09	4.32E+06	1,6
Capao4-HM27-17	#10	4/9/17	17:59:04	0.0019306	0.0000002	-16.85		0.08	0.33	2.24E+09	4.33E+06	1,6
Capao4-HM27-18	#10	4/9/17	18:04:21	0.0019304	0.0000002	-16.97		0.09	0.33	2.24E+09	4.32E+06	1,6
Capao4-HM17-2.1	#10	4/9/17	19:00:15	0.0019288	0.0000002	-17.81		0.08	0.33	2.21E+09	4.29E+06	1,6
Capao4-HM17-2.2	#10	4/9/17	19:05:32	0.0019286	0.0000002	-17.89		0.10	0.33	2.20E+09	4.25E+06	1,6
Capao4-HM17-2.3	#10	4/9/17	19:10:50	0.0019289	0.0000002	-17.76		0.09	0.33	2.19E+09	4.23E+06	1,6
Capao4-HM27-19	#10	4/9/17	20:09:28	0.0019308	0.0000002	-16.77		0.11	0.33	2.24E+09	4.33E+06	1,6
Capao4-HM27-20	#10	4/9/17	20:14:45	0.0019307	0.0000002	-16.82		0.09	0.33	2.24E+09	4.33E+06	1,6
Capao4-HM27-21	#10	4/9/17	20:42:58	0.0019304	0.0000002	-16.99		0.10	0.33	2.24E+09	4.32E+06	1,6
Capao4-HM27-22	#10	4/9/17	21:57:37	0.0019301	0.0000002	-17.14		0.10	0.33	2.28E+09	4.40E+06	1,6
Capao4-HM27-23	#10	4/9/17	22:02:55	0.0019306	0.0000002	-16.88		0.11	0.33	2.28E+09	4.40E+06	1,6
Capao4-HM27-24	#10	4/9/17	22:08:12	0.0019302	0.0000002	-17.07		0.09	0.33	2.26E+09	4.37E+06	1,6
Capao4-HM17-2.4	#10	4/9/17	22:13:52	0.0019292	0.0000003	-17.62		0.13	0.34	2.19E+09	4.21E+06	1,6
Capao4-HM17-2.5	#10	4/9/17	22:19:09	0.0019295	0.0000002	-17.48		0.10	0.33	2.21E+09	4.25E+06	1,6
Capao4-HM17-2.6	#10	4/9/17	22:24:27	0.0019295	0.0000002	-17.47		0.10	0.33	2.22E+09	4.26E+06	1,6
Capao4-HM27-25	#10	4/9/17	23:39:32	0.0019305	0.0000002	-16.93		0.08	0.33	2.26E+09	4.40E+06	1,6
Capao4-HM27-26	#10	4/9/17	23:44:49	0.0019302	0.0000002	-17.07		0.09	0.33	2.29E+09	4.42E+06	1,6
Capao4-HM27-27	#10	4/9/17	23:50:07	0.0019300	0.0000002	-17.17		0.08	0.33	2.28E+09	4.40E+06	1,6
Capao4-HM17-2.7	#10	4/9/17	23:55:47	0.0019298	0.0000002	-17.28		0.11	0.33	2.21E+09	4.21E+06	1,6
Capao4-HM17-2.8	#10	4/9/17	0:01:04	0.0019294	0.0000002	-17.28		0.10	0.33	2.24E+09	4.31E+06	1,6
Capao4-HM27-28	#10	5/9/17	1:10:59	0.0019305	0.0000002	-16.93		0.09	0.33	2.30E+09	4.44E+06	1,6
Capao4-HM27-29	#10	5/9/17	1:16:16	0.0019309	0.0000002	-16.73		0.10	0.33	2.29E+09	4.42E+06	1,6
Capao4-HM27-30	#10	5/9/17	1:21:33	0.0019316	0.0000002	-16.36		0.09	0.33	2.29E+09	4.43E+06	1,6
Capao4-HM17-2.9	#10	5/9/17	1:27:13	0.0019299	0.0000002	-17.24		0.10	0.33	2.23E+09	4.30E+06	1,6
Capao4-HM17-2.10	#10	5/9/17	1:32:30	0.0019297	0.0000002	-17.33		0.08	0.33	2.23E+09	4.30E+06	1,6
Capao4-HM27-31	#10	5/9/17	2:42:22	0.0019312	0.0000002	-16.58		0.10	0.33	2.26E+09	4.40E+06	1,6
Capao4-HM27-32	#10	5/9/17	2:47:39	0.0019315	0.0000002	-16.40		0.08	0.33	2.30E+09	4.44E+06	1,6
Capao4-HM17-2.11	#10	5/9/17	2:53:19	0.0019304	0.0000002	-16.96		0.09	0.33	2.21E+09	4.27E+06	1,6
Capao4-HM17-2.12	#10	5/9/17	2:58:37	0.0019302	0.0000002	-17.11		0.09	0.33	2.22E+09	4.27E+06	1,6
Capao4-HM27-33	#10	5/9/17	4:08:31	0.0019310	0.0000002	-16.66		0.10	0.33	2.29E+09	4.42E+06	1,6
Capao4-HM27-34	#10	5/9/17	4:13:48	0.0019300	0.0000002	-17.20		0.10	0.33	2.28E+09	4.41E+06	1,6
Capao4-HM27-35	#10	5/9/17	4:19:06	0.0019302	0.0000002	-17.08		0.10	0.33	2.29E+09	4.41E+06	1,6
Capao4-HM17-2.13	#10	5/9/17	4:24:46	0.0019300	0.0000002	-17.18		0.11	0.33	2.22E+09	4.28E+06	1,6
Capao4-HM17-2.14	#10	5/9/17	4:30:03	0.0019298	0.0000002	-17.30		0.09	0.33	2.22E+09	4.29E+06	1,6
Capao4-HM27-36	#10	5/9/17	5:50:31	0.0019303	0.0000002	-17.01		0.08	0.33	2.30E+09	4.43E+06	1,6
Capao4-HM27-37	#10	5/9/17	5:55:48	0.0019306	0.0000002	-16.89		0.11	0.33	2.30E+09	4.44E+06	1,6
Capao4-HM17-2.15	#10	5/9/17	6:55:23	0.0019306	0.0000002	-16.87		0.08	0.33	2.18E+09	4.21E+06	1,6
Capao4-HM27-38	#10	5/9/17	7:00:40	0.0019305	0.0000002	-16.95		0.12	0.33	2.20E+09	4.24E+06	1,6
Capao4-HM27-39	#10	5/9/17	8:21:07	0.0019315	0.0000002	-16.41		0.12	0.33	2.26E+09	4.42E+06	1,6
Capao4-HM27-40	#10	5/9/17	8:26:25	0.0019318	0.0000002	-16.24		0.09	0.33	2.24E+09	4.33E+06	1,6
Capao4-HM27-41	#10	5/9/17	8:31:42	0.0019317	0.0000002	-16.32		0.09	0.33	2.24E+09	4.33E+06	1,6
Capao4-HM17-2.17	#10	5/9/17	8:37:21	0.0019324	0.0000002	-17.50		0.13	0.34	2.18E+09	4.21E+06	1,6
Capao4-HM17-2.18	#10	5/9/17	8:42:38	0.0019294	0.0000002	-17.48		0.09	0.33	2.19E+09	4.22E+06	1,6
Capao4-HM27-41	#10	5/9/17	9:51:59	0.0019314	0.0000002	-16.47		0.10	0.33	2.25E+09	4.34E+06	1,6
Capao4-HM27-42	#10	5/9/17	9:57:17	0.0019312	0.0000002	-16.54		0.10	0.33	2.24E+09	4.33E+06	1,6
Capao4-HM27-43	#10	5/9/17	10:02:34	0.0019312	0.0000002	-16.59		0.10	0.33	2.25E+09	4.34E+06	1,6
Capao4-HM17-2.19	#10	5/9/17	10:19:26	0.0019294	0.0000002	-17.47		0.09	0.33	2.19E+09	4.22E+06	1,6
Capao4-HM17-2.20	#10	5/9/17	10:24:44	0.0019291	0.0000002	-17.63		0.11	0.33	2.17E+09	4.19E+06	1,6
Capao4-HM27-44	#10	5/9/17	11:14:33	0.0019312	0.0000001	-16.58		0.08	0.33	2.22E+09	4.32E+06	1,6
Capao4-HM27-45	#10	5/9/17	11:19:50	0.0019305	0.0000002	-16.91		0.11	0.33	2.22E+09	4.29E+06	1,6
Capao4-HM27-46	#10	5/9/17	11:25:11	0.0019308	0.0000002	-16.78		0.09	0.33	2.22E+09	4.29E+06	1,6
Capao4-HM27-47	#10	5/9/17	12:24:09	0.0019304	0.0000002	-16.98		0.12	0.33	2.21E+09	4.27E+06	1,6
Capao4-HM27-48	#10	5/9/17	12:29:26	0.0019304	0.0000002	-16.99		0.09	0.33	2.21E+09	4.28E+06	1,6
Capao4-HM27-49	#10	5/9/17	12:34:44	0.0019304	0.0000002	-17.00		0.10	0.33	2.20E+09	4.24E+06	1,6
Capao4-HM17-2.21	#10	5/9/17	12:51:34	0.0019291	0.0000002	-17.65		0.11	0.33	2.15E+09	4.14E+06	1,6
Capao4-HM17-2.22	#10	5/9/17	12:56:52	0.0019298	0.0000002	-17.78		0.08	0.33	2.16E+09	4.16E+06	1,6
Capao4-HM27-50	#10	5/9/17	13:55:34	0.0019304	0.0000002	-16.97		0.12	0.33	2.21E+09	4.26E+06	1,6
Capao4-HM27-51	#10	5/9/17	14:00:51	0.0019304	0.0000002	-17.00		0.09	0.33	2.21E+09	4.26E+06	1,6
Capao4-HM27-52	#10	5/9/17	14:06:09	0.0019305	0.0000002	-16.93		0.08	0.33	2.21E+09	4.27E+06	1,6
Capao4-HM17-3.1	#10	5/9/17	14:23:01	0.0019293	0.0000002	-17.56		0.11	0.33	2.19E+09	4.23E+06	1,6
Capao4-HM17-3.2	#10	5/9/17	14:28:19	0.0019292	0.0000002	-17.58		0.11	0.33	2.18E+09	4.21E+06	1,6
Capao4-HM17-3.3	#10	5/9/17	14:33:36	0.0019303	0.0000002	-17.01		0.11	0.33	2.18E+09	4.22E+06	1,6
Capao4-HM27-53	#10	5/9/17	15:32:20	0.0019293	0.0000002	-17.54		0.09	0.33	2.23E+09	4.31E+06	1,6
Capao4-HM27-54	#10	5/9/17	15:37:37	0.0019298	0.0000002	-17.27		0.09	0.33	2.23E+09	4.31E+06	1,6
Capao4-HM27-55	#10	5/9/17	15:42:54	0.0019296	0.0000002	-17.39		0.10	0.33	2.22E+09	4.29E+06	1,6
Capao4-HM17-3.4	#10	5/9/17	15:59:47	0.0019300	0.0000002	-17.19		0.10	0.33	2.19E+09	4.21E+06	1,6
Capao4-HM17-3.5	#10	5/9/17	16:05:04	0.0019293	0.0000002	-17.56		0.09	0.33	2.18E+09	4.20E+06	1,6
Capao4-HM17-3.6	#10	5/9/17	16:10:22	0.0019285	0.0000002		-17.97	0.10	0.33	2.16E+09	4.16E+06	1,6
Capao4-HM27-56	#10	5/9/17	17:14:43	0.0019297	0.0000002	-17.36		0.08	0.33	2.22E+09	4.30E+06	1,6
Capao4-HM27-57	#10	5/9/17	17:20:00	0.0019295	0.0000002	-17.46		0.10	0.33	2.23E+09	4.30E+06	1,6
Capao4-HM27-58	#10	5/9/17	17:25:18	0.0019298	0.0000002	-17.27		0.11	0.33	2.23E+09	4.31E+06	1,6
Capao4-HM17-3.7	#10	5/9/17	17:31:50	0.0019299	0.0000002	-17.77		0.08	0.33	2.16E+09	4.17E+06	1,6
Capao4-HM17-3.8	#10	5/9/17	17:36:18	0.0019293	0.0000001	-17.57		0.08	0.33	2.19E+09	4.20E+06	1,6
Capao4-HM27-59	#10	5/9/17	19:12:18	0.0019301	0.0000001	-17.14		0.07	0.33	2.23E+09	4.30E+06	1,6
Capao4-HM27-60	#10	5/9/17	19:17:35	0.0019298	0.0000002	-17.31		0.12	0.33	2.22E+09	4.29E+06	1,6

SPOT #	Session	Date	Time	T ₀ /T ₀	z	δ ⁰ Observed	rejected	±Internal error (σ 95%)	±External error (1σ)	T ₀ cps (median)	T ₀ cps (median)	no. sets, subsets
CapsoL4-HM27-9	#10	7/9/17	15:06:26	0.0019320	0.0000002	-17.35		0.11	0.27	2.08E+09	4.04E+06	1,6
CapsoL4-HM27-10	#10	7/9/17	15:11:43	0.0019324	0.0000002	-17.48		0.11	0.27	2.11E+09	4.08E+06	1,6
CapsoL4-HM23-2.4	#10	7/9/17	15:28:40	0.0019331	0.0000002	-17.09		0.12	0.28	2.15E+09	4.15E+06	1,6
CapsoL4-HM23-2.5	#10	7/9/17	15:33:57	0.0019333	0.0000002	-16.99		0.09	0.27	2.14E+09	4.13E+06	1,6
CapsoL4-HM23-2.6	#10	7/9/17	15:39:15	0.0019332	0.0000002	-17.04		0.09	0.27	2.14E+09	4.14E+06	1,6
CapsoL4-HM23-1.6	#10	7/9/17	15:44:36	0.0019335	0.0000002	-16.88		0.11	0.27	2.16E+09	4.18E+06	1,6
CapsoL4-HM23-1.7	#10	7/9/17	15:49:53	0.0019340	0.0000002	-16.63		0.10	0.27	2.14E+09	4.14E+06	1,6
CapsoL4-HM23-1.8	#10	7/9/17	15:55:11	0.0019335	0.0000002	-16.91		0.09	0.27	2.14E+09	4.13E+06	1,6
CapsoL4-HM27-11	#10	7/9/17	16:55:47	0.0019322	0.0000002	-17.58		0.11	0.27	2.11E+09	4.08E+06	1,6
CapsoL4-HM27-12	#10	7/9/17	17:01:05	0.0019318	0.0000002	-17.77		0.09	0.27	2.10E+09	4.05E+06	1,6
CapsoL4-HM27-13	#10	7/9/17	17:06:22	0.0019322	0.0000002	-17.57		0.11	0.27	2.09E+09	4.04E+06	1,6
CapsoL4-HM23-1.9	#10	7/9/17	17:55:29	0.0019332	0.0000002	-17.07		0.10	0.27	2.22E+09	4.29E+06	1,6
CapsoL4-HM23-1.10	#10	7/9/17	18:00:47	0.0019333	0.0000002	-17.02		0.09	0.27	2.20E+09	4.26E+06	1,6
CapsoL4-HM23-1.11	#10	7/9/17	18:06:04	0.0019332	0.0000002	-17.08		0.08	0.27	2.19E+09	4.24E+06	1,6
CapsoL4-HM27-14	#10	7/9/17	19:04:43	0.0019326	0.0000002	-17.34		0.10	0.27	2.14E+09	4.13E+06	1,6
CapsoL4-HM27-15	#10	7/9/17	19:10:01	0.0019326	0.0000002	-17.35		0.09	0.27	2.13E+09	4.12E+06	1,6
CapsoL4-HM27-16	#10	7/9/17	19:15:18	0.0019328	0.0000002	-17.26		0.11	0.27	2.13E+09	4.11E+06	1,6
CapsoL4-HM23-2.7	#10	7/9/17	19:37:26	0.0019305	0.0000002	-16.91		0.11	0.27	2.20E+09	4.25E+06	1,6
CapsoL4-HM23-2.8	#10	7/9/17	19:42:43	0.0019333	0.0000002	-16.99		0.09	0.27	2.19E+09	4.24E+06	1,6
CapsoL4-HM23-2.9	#10	7/9/17	19:48:00	0.0019328	0.0000002	-17.29		0.11	0.27	2.20E+09	4.25E+06	1,6
CapsoL4-HM27-17	#10	7/9/17	20:46:45	0.0019326	0.0000002	-17.37		0.11	0.27	2.09E+09	4.04E+06	1,6
CapsoL4-HM27-18	#10	7/9/17	20:52:02	0.0019325	0.0000002	-17.43		0.08	0.27	2.10E+09	4.05E+06	1,6
CapsoL4-HM27-19	#10	7/9/17	20:57:20	0.0019323	0.0000002	-17.50		0.10	0.27	2.10E+09	4.05E+06	1,6
CapsoL4-HM23-2.10	#10	7/9/17	21:14:10	0.0019330	0.0000002	-17.18		0.11	0.27	2.17E+09	4.19E+06	1,6
CapsoL4-HM23-2.11	#10	7/9/17	21:19:28	0.0019334	0.0000002	-16.96		0.10	0.27	2.16E+09	4.18E+06	1,6
CapsoL4-HM23-2.12	#10	7/9/17	21:24:45	0.0019331	0.0000002	-17.13		0.09	0.27	2.16E+09	4.17E+06	1,6
CapsoL4-HM27-20	#10	7/9/17	23:15:43	0.0019323	0.0000002	-17.52		0.10	0.27	2.10E+09	4.05E+06	1,6
CapsoL4-HM27-21	#10	7/9/17	23:21:00	0.0019320	0.0000002	-17.66		0.12	0.28	2.09E+09	4.02E+06	1,6
CapsoL4-HM27-22	#10	7/9/17	23:26:17	0.0019323	0.0000002	-17.51		0.09	0.27	2.10E+09	4.08E+06	1,6
CapsoL4-HM23-1.12	#10	7/9/17	23:32:05	0.0019333	0.0000002	-17.01		0.09	0.27	2.15E+09	4.15E+06	1,6
CapsoL4-HM23-1.13	#10	7/9/17	23:37:22	0.0019332	0.0000002	-17.04		0.11	0.27	2.13E+09	4.12E+06	1,6
CapsoL4-HM27-23	#10	8/9/17	0:36:00	0.0019327	0.0000002	-17.31		0.11	0.27	2.12E+09	4.11E+06	1,6
CapsoL4-HM27-24	#10	8/9/17	0:41:19	0.0019325	0.0000002	-17.44		0.09	0.27	2.12E+09	4.10E+06	1,6
CapsoL4-HM27-25	#10	8/9/17	0:46:36	0.0019326	0.0000002	-17.37		0.10	0.27	2.12E+09	4.10E+06	1,6
CapsoL4-HM23-1.14	#10	8/9/17	1:03:27	0.0019334	0.0000002	-16.94		0.09	0.27	2.18E+09	4.21E+06	1,6
CapsoL4-HM23-1.15	#10	8/9/17	1:08:44	0.0019338	0.0000003	-16.73		0.14	0.28	2.16E+09	4.18E+06	1,6
CapsoL4-HM23-1.16	#10	8/9/17	1:14:01	0.0019338	0.0000002	-16.77		0.09	0.27	2.17E+09	4.19E+06	1,6
CapsoL4-HM27-26	#10	8/9/17	2:07:22	0.0019304	0.0000002	-17.45		0.11	0.27	2.13E+09	4.13E+06	1,6
CapsoL4-HM27-27	#10	8/9/17	2:12:39	0.0019328	0.0000002	-17.27		0.11	0.27	2.14E+09	4.13E+06	1,6
CapsoL4-HM27-28	#10	8/9/17	2:17:57	0.0019321	0.0000002	-17.65		0.11	0.27	2.14E+09	4.14E+06	1,6
CapsoL4-HM23-1.17	#10	8/9/17	2:34:48	0.0019335	0.0000002	-16.88		0.08	0.27	2.20E+09	4.25E+06	1,6
CapsoL4-HM23-1.18	#10	8/9/17	2:40:06	0.0019334	0.0000002	-16.95		0.10	0.27	2.21E+09	4.27E+06	1,6
CapsoL4-HM27-29	#10	8/9/17	3:38:45	0.0019318	0.0000002	-17.80		0.08	0.27	2.14E+09	4.13E+06	1,6
CapsoL4-HM27-30	#10	8/9/17	3:44:03	0.0019325	0.0000002	-17.44		0.10	0.27	2.13E+09	4.11E+06	1,6
CapsoL4-HM27-31	#10	8/9/17	3:49:20	0.0019326	0.0000002	-17.26		0.10	0.27	2.12E+09	4.10E+06	1,6
CapsoL4-HM23-2.13	#10	8/9/17	4:06:10	0.0019333	0.0000002	-16.99		0.11	0.27	2.12E+09	4.11E+06	1,6
CapsoL4-HM23-2.14	#10	8/9/17	4:11:28	0.0019334	0.0000002	-16.98		0.09	0.27	2.13E+09	4.13E+06	1,6
CapsoL4-HM23-2.15	#10	8/9/17	4:16:45	0.0019337	0.0000002	-16.81		0.09	0.27	2.15E+09	4.15E+06	1,6
CapsoL4-HM27-32	#10	8/9/17	5:20:43	0.0019324	0.0000001	-17.48		0.07	0.27	2.12E+09	4.10E+06	1,6
CapsoL4-HM27-33	#10	8/9/17	5:26:00	0.0019327	0.0000002	-17.31		0.08	0.27	2.13E+09	4.11E+06	1,6
CapsoL4-HM27-34	#10	8/9/17	5:31:18	0.0019324	0.0000002	-17.45		0.10	0.27	2.13E+09	4.12E+06	1,6
CapsoL4-HM23-2.16	#10	8/9/17	5:48:07	0.0019335	0.0000002	-16.89		0.11	0.27	2.19E+09	4.22E+06	1,6
CapsoL4-HM23-2.17	#10	8/9/17	5:53:25	0.0019340	0.0000002	-16.67		0.10	0.27	2.20E+09	4.25E+06	1,6
CapsoL4-HM23-2.18	#10	8/9/17	5:58:42	0.0019337	0.0000002	-16.76		0.12	0.28	2.17E+09	4.21E+06	1,6
CapsoL4-HM27-35	#10	8/9/17	7:03:14	0.0019326	0.0000002	-17.35		0.11	0.27	2.13E+09	4.13E+06	1,6
CapsoL4-HM27-36	#10	8/9/17	7:08:32	0.0019326	0.0000002	-17.38		0.10	0.27	2.13E+09	4.11E+06	1,6
CapsoL4-HM27-37	#10	8/9/17	7:13:49	0.0019326	0.0000002	-17.36		0.12	0.28	2.12E+09	4.10E+06	1,6
CapsoL4-HM23-1.19	#10	7/9/17	7:30:39	0.0019336	0.0000002	-16.84		0.11	0.27	2.15E+09	4.16E+06	1,6
CapsoL4-HM23-1.20	#10	7/9/17	7:35:56	0.0019334	0.0000003	-16.94		0.13	0.28	2.16E+09	4.17E+06	1,6
CapsoL4-HM27-38	#10	8/9/17	8:40:02	0.0019320	0.0000002	-17.66		0.11	0.27	2.08E+09	4.03E+06	1,6
CapsoL4-HM27-39	#10	8/9/17	8:45:19	0.0019323	0.0000002	-17.52		0.09	0.27	2.07E+09	4.02E+06	1,6
CapsoL4-HM27-40	#10	8/9/17	8:50:39	0.0019325	0.0000002	-17.41		0.09	0.27	2.08E+09	4.02E+06	1,6
CapsoL4-HM23-1.21	#10	8/9/17	9:07:28	0.0019333	0.0000003	-16.99		0.13	0.28	2.13E+09	4.12E+06	1,6
CapsoL4-HM23-1.22	#10	8/9/17	9:12:46	0.0019328	0.0000002	-17.26		0.09	0.27	2.12E+09	4.10E+06	1,6
CapsoL4-HM23-2.19	#10	8/9/17	9:18:06	0.0019326	0.0000002	-17.36		0.10	0.27	2.13E+09	4.13E+06	1,6
CapsoL4-HM23-2.20	#10	8/9/17	9:23:23	0.0019332	0.0000002	-17.07		0.10	0.27	2.12E+09	4.09E+06	1,6
CapsoL4-HM27-41	#10	8/9/17	10:16:50	0.0019320	0.0000002	-17.67		0.11	0.27	2.09E+09	4.04E+06	1,6
CapsoL4-HM27-42	#10	8/9/17	10:22:07	0.0019319	0.0000001	-17.72		0.08	0.27	2.07E+09	4.00E+06	1,6
CapsoL4-HM27-43	#10	8/9/17	10:27:25	0.0019317	0.0000002	-17.82		0.10	0.27	2.07E+09	3.99E+06	1,6
CapsoL4-HM23-2.21	#10	8/9/17	10:44:14	0.0019329	0.0000002	-17.20		0.11	0.27	2.11E+09	4.08E+06	1,6
CapsoL4-HM23-2.22	#10	8/9/17	10:49:32	0.0019324	0.0000002	-17.48		0.09	0.27	2.11E+09	4.09E+06	1,6
CapsoL4-HM23-2.23	#10	8/9/17	10:54:50	0.0019329	0.0000002	-17.23		0.11	0.27	2.10E+09	4.05E+06	1,6
CapsoL4-HM27-44	#10	8/9/17	11:37:46	0.0019315	0.0000002	-17.95		0.10	0.27	2.07E+09	4.00E+06	1,6
CapsoL4-HM27-45	#10	8/9/17	11:43:04	0.0019317	0.0000002	-17.85		0.08	0.27	2.05E+09	3.97E+06	1,6
CapsoL4-HM27-46	#10	8/9/17	11:48:21	0.0019326	0.0000002	-17.39		0.09	0.27	2.09E+09	3.98E+06	1,6
#10			average	-17.22	weighted mean	-17.22						
			std dev (1σ)	0.37	error in mean (1σ)	0.08						
			50% variance	0.07	MSWD	15.66			0.16			
					no. outliers	92						
MOUNT HM-27_HM-21												
ROY L5												
RoyL5-1.1	#10	7/9/17	12:12:10	0.0019673	0.0000001	0.58		0.07	0.17	2.16E+09	4.26E+06	1,6
RoyL5-1.2	#10	7/9/17	12:17:27	0.0019674	0.0000002	0.48		0.09	0.17	2.15E+09	4.23E+06	1,6
RoyL5-1.3	#10	7/9/17	12:22:45	0.0019671	0.0000001	0.50		0.07	0.17	2.16E+09	4.25E+06	1,6
RoyL5-1.4	#10	7/9/17	12:28:02	0.0019680	0.0000002	0.94		0.12	0.18	2.13E+09	4.18E+06	1,6
RoyL5-1.5	#10	7/9/17	16:27:35	0.0019665	0.0000002	0.19		0.09	0.17	2.14E+09	4.21E+06	1,6
RoyL5-1.6	#10	7/9/17	16:32:53	0.001								

SPOT #	Session	Date	Time	¹³ C/ ¹² C	z	δ ¹³ O _{VSMOW}	rejected	±Internal error (σ 95%)	±External error (1σ)	¹³ C cps (median)	¹³ C cps (median)	no. sets subsets
Win-06-03A-1.3	#10	7/9/17	18:48:29	0.0019665	0.0000002	0.17		0.10	0.20	2.19E+09	4.31E+06	1.6
Win-06-03A-1.4	#10	7/9/17	18:53:46	0.0019664	0.0000002	0.11		0.11	0.20	2.19E+09	4.31E+06	1.6
Win-06-03A-1.5	#10	7/9/17	18:59:04	0.0019669	0.0000002	0.40		0.10	0.20	2.12E+09	4.17E+06	1.6
Win-06-03A-1.5b	#10	7/9/17	21:33:14	0.0019667	0.0000002	0.26		0.08	0.19	2.20E+09	4.32E+06	1.6
Win-06-03A-1.6	#10	7/9/17	23:42:42	0.0019672	0.0000002	0.53		0.09	0.19	2.14E+09	4.21E+06	1.6
Win-06-03A-1.7	#10	7/9/17	23:47:59	0.0019671	0.0000002	0.46		0.11	0.20	2.14E+09	4.21E+06	1.6
Win-06-03A-1.8	#10	7/9/17	23:53:17	0.0019673	0.0000002	0.57		0.10	0.20	2.15E+09	4.23E+06	1.6
Win-06-03A-1.9	#10	7/9/17	23:58:34	0.0019666	0.0000002	0.25		0.10	0.20	2.11E+09	4.15E+06	1.6
Win-06-03A-1.10	#10	8/9/17	0:03:52	0.0019670	0.0000002	0.45		0.10	0.20	2.12E+09	4.17E+06	1.6
Win-06-03A-1.11	#10	8/9/17	1:19:22	0.0019674	0.0000002	0.61		0.12	0.20	2.20E+09	4.34E+06	1.6
Win-06-03A-1.12	#10	8/9/17	1:24:39	0.0019671	0.0000002	0.50		0.09	0.19	2.17E+09	4.27E+06	1.6
Win-06-03A-1.13	#10	8/9/17	1:29:56	0.0019671	0.0000002	0.50		0.11	0.20	2.19E+09	4.29E+06	1.6
Win-06-03A-1.14	#10	8/9/17	1:35:14	0.0019673	0.0000002	0.60		0.11	0.20	2.17E+09	4.28E+06	1.6
Win-06-03A-2.6	#10	8/9/17	2:45:26	0.0019667	0.0000002	0.29		0.12	0.20	2.23E+09	4.39E+06	1.6
Win-06-03A-2.7	#10	8/9/17	2:50:44	0.0019659	0.0000002	-0.14		0.08	0.19	2.29E+09	4.44E+06	1.6
Win-06-03A-2.8	#10	8/9/17	2:56:01	0.0019662	0.0000002	0.00		0.09	0.19	2.23E+09	4.39E+06	1.6
Win-06-03A-2.9	#10	8/9/17	3:01:19	0.0019657	0.0000002	-0.24		0.11	0.20	2.19E+09	4.25E+06	1.6
Win-06-03A-2.10	#10	8/9/17	3:08:36	0.0019659	0.0000002	-0.13		0.09	0.19	2.15E+09	4.22E+06	1.6
Win-06-03A-2.1	#10	8/9/17	4:22:06	0.0019672	0.0000002	0.54		0.13	0.20	2.19E+09	4.31E+06	1.6
Win-06-03A-2.2	#10	8/9/17	4:27:24	0.0019660	0.0000002	-0.10		0.09	0.19	2.21E+09	4.34E+06	1.6
Win-06-03A-2.3	#10	8/9/17	4:32:41	0.0019664	0.0000002	0.09		0.08	0.19	2.22E+09	4.37E+06	1.6
Win-06-03A-2.4	#10	8/9/17	4:37:58	0.0019668	0.0000002	0.33		0.12	0.20	2.19E+09	4.30E+06	1.6
Win-06-03A-2.5	#10	8/9/17	4:43:15	0.0019644	0.0000002		-0.90	0.10	0.19	2.19E+09	4.30E+06	1.6
#10				average	0.27	weighted mean	0.27					
				std dev (1σ)	0.26	error in mean (1σ)	0.12					
				50% variance	0.03	MSWD	9.74					
							no.					
							no. outliers					
							1					
							25					
							Internal error (σ 95%)					
							0.25					

**Chapter 6: Cenozoic continental paleoclimatic record from combined (U-Th)/He dating
and SHRIMP-SI $\delta^{18}\text{O}$ analysis of goethite**

Appendices

EA1: Electron Microprobe Analysis

EA2: SHRIMP-SI $^{18}\text{O}/^{16}\text{O}$ Analysis (Carajás and QF)

Appendix: Electron Microprobe Analysis of Brazilian Goethites																										
INDEX	Ns	O	Na	K	V	Co	Mg	P	Cr	Fe	Al	S	Ni	Mn	Si	Ph	Cu	Ti	Ca	Zn	Ba	Sr	Total	Year	Sample	
1	150	36.48	0.00	0.01	0.07	0.02	0.44	0.00	61.70	1.09	0.01	0.03	0.00	0.13	0.00	0.01	0.13	0.00	0.06	100.17	2010			MAC-61-2-6		
2	106	37.40	0.00	0.01	0.00	0.12	0.02	0.00	0.00	55.80	0.87	0.06	0.00	0.00	1.33	0.04	0.07	0.01	0.00	0.00			95.72	2010	PIC-2 (a)	
3	107	35.21	0.00	0.01	0.00	0.09	0.02	0.00	0.03	61.76	0.56	0.07	0.06	0.00	1.19	0.04	0.00	0.00	0.00	0.00			99.05	2010	PIC-2 (a)	
4	108	37.03	0.00	0.00	0.00	0.07	0.00	0.02	0.00	58.98	0.33	0.01	0.02	0.01	0.91	0.02	0.06	0.00	0.00	0.03			97.47	2010	PIC-2 (a)	
5	109	36.59	0.02	0.00	0.00	0.10	0.00	0.00	0.03	57.21	0.54	0.05	0.00	0.11	1.14	0.08	0.00	0.04	0.00	0.00			95.91	2010	PIC-2 (a)	
6	110	36.68	0.00	0.01	0.00	0.04	0.01	0.02	0.03	57.68	0.51	0.06	0.00	0.17	1.15	0.01	0.00	0.00	0.00	0.09			96.46	2010	PIC-2 (a)	
7	111	38.58	0.00	0.00	0.00	0.03	0.01	0.01	0.00	57.73	0.63	0.02	0.00	0.08	1.13	0.07	0.00	0.00	0.00	0.00			98.29	2010	PIC-2 (a)	
8	112	38.62	0.00	0.00	0.00	0.01	0.01	0.00	0.00	56.81	0.76	0.06	0.00	0.01	1.23	0.05	0.01	0.00	0.00	0.09			97.65	2010	PIC-2 (a)	
9	113	36.74	0.03	0.00	0.00	0.01	0.00	0.02	0.00	57.24	0.69	0.05	0.00	0.07	1.17	0.00	0.01	0.00	0.00	0.00			96.03	2010	PIC-2 (a)	
10	114	37.66	0.00	0.01	0.00	0.00	0.00	0.02	0.02	56.66	0.82	0.03	0.08	0.10	1.16	0.01	0.00	0.04	0.00	0.00			96.60	2010	PIC-2 (a)	
11	115	38.47	0.00	0.00	0.00	0.05	0.00	0.01	0.00	57.86	0.39	0.04	0.00	0.01	1.18	0.00	0.04	0.00	0.00	0.00			98.06	2010	PIC-2 (a)	
12	117	33.94	0.03	0.01	0.00	0.08	0.00	0.00	0.00	62.34	0.48	0.03	0.00	0.06	1.38	0.06	0.00	0.03	0.00	0.06			98.50	2010	PIC-2 (a)	
13	118	34.23	0.00	0.01	0.00	0.06	0.04	0.01	0.00	62.82	0.54	0.02	0.00	0.08	1.38	0.00	0.00	0.00	0.00	0.00			99.20	2010	PIC-2 (a)	
14	119	34.28	0.00	0.03	0.00	0.09	0.01	0.05	0.00	62.36	0.75	0.05	0.01	0.02	1.38	0.02	0.00	0.00	0.00	0.00			99.02	2010	PIC-2 (a)	
15	120	34.15	0.07	0.02	0.00	0.05	0.04	0.00	0.00	62.40	0.41	0.03	0.00	0.05	1.46	0.01	0.00	0.00	0.00	0.00			98.69	2010	PIC-2 (a)	
16	121	36.73	0.08	0.00	0.00	0.00	0.00	0.00	0.00	61.39	0.67	0.02	0.05	0.00	1.39	0.07	0.00	0.00	0.00	0.02			100.43	2010	PIC-2 (a)	
17	122	33.96	0.00	0.04	0.00	0.06	0.05	0.02	0.02	62.90	0.61	0.04	0.00	0.00	1.49	0.00	0.06	0.00	0.00	0.00			99.23	2010	PIC-2 (a)	
18	123	33.36	0.08	0.07	0.01	0.09	0.00	0.04	0.00	63.33	0.54	0.04	0.01	0.00	1.49	0.03	0.00	0.01	0.00	0.08			99.19	2010	PIC-2 (a)	
19	124	33.31	0.03	0.00	0.00	0.03	0.04	0.02	0.00	62.91	0.59	0.02	0.00	0.01	1.35	0.00	0.00	0.02	0.00	0.00			98.32	2010	PIC-2 (a)	
20	125	35.23	0.03	0.00	0.00	0.09	0.00	0.01	0.00	59.95	1.03	0.00	0.00	0.09	1.23	0.10	0.00	0.00	0.00	0.05			97.80	2010	PIC-2 (a)	
21	126	33.70	0.03	0.00	0.00	0.00	0.02	0.05	0.00	61.38	0.70	0.03	0.00	0.09	1.28	0.05	0.00	0.00	0.00	0.02			97.34	2010	PIC-2 (a)	
22	127	33.98	0.00	0.02	0.05	0.09	0.00	0.02	0.00	62.60	0.63	0.06	0.00	0.08	1.37	0.05	0.10	0.00	0.00	0.00			99.01	2010	PIC-2 (a)	
23	128	36.47	0.00	0.00	0.03	0.03	0.03	0.04	0.00	59.01	0.70	0.04	0.00	0.03	1.30	0.00	0.00	0.02	0.00	0.01			97.70	2010	PIC-2 (a)	
24	129	33.83	0.05	0.00	0.00	0.08	0.00	0.00	0.00	60.81	0.89	0.04	0.00	0.13	1.28	0.00	0.00	0.00	0.00	0.00			97.17	2010	PIC-2 (a)	
25	130	37.46	0.00	0.00	0.01	0.08	0.00	0.00	0.02	57.43	0.77	0.04	0.08	0.13	1.13	0.04	0.10	0.00	0.00	0.02			97.30	2010	PIC-2 (a)	
26	131	36.59	0.01	0.00	0.00	0.01	0.00	0.00	0.00	58.14	0.96	0.04	0.01	0.20	1.12	0.00	0.00	0.00	0.00	0.00			97.09	2010	PIC-2 (a)	
27	132	38.06	0.00	0.00	0.04	0.10	0.01	0.00	0.00	57.09	0.82	0.04	0.00	0.14	1.20	0.04	0.00	0.04	0.00	0.00			97.58	2010	PIC-2 (a)	
28	133	37.82	0.00	0.02	0.00	0.05	0.01	0.00	0.08	57.58	0.71	0.02	0.00	0.11	1.24	0.00	0.00	0.01	0.00	0.00			97.65	2010	PIC-2 (a)	
29	134	37.11	0.01	0.00	0.00	0.08	0.00	0.00	0.00	57.99	0.69	0.05	0.04	0.12	1.15	0.07	0.00	0.00	0.00	0.06			97.35	2010	PIC-2 (a)	
30	135	34.54	0.04	0.00	0.01	0.08	0.01	0.00	0.00	60.47	0.70	0.08	0.03	0.17	1.11	0.00	0.00	0.07	0.00	0.00			97.22	2010	PIC-2 (a)	
31	136	37.46	0.04	0.02	0.00	0.06	0.00	0.01	0.01	58.05	0.48	0.02	0.00	0.21	1.17	0.05	0.00	0.00	0.00	0.00			97.57	2010	PIC-2 (a)	
32	137	37.00	0.07	0.01	0.03	0.06	0.01	0.00	0.00	58.36	0.56	0.06	0.02	0.06	1.12	0.04	0.02	0.01	0.00	0.00			97.45	2010	PIC-2 (a)	
33	138	37.74	0.00	0.00	0.00	0.10	0.00	0.04	0.00	58.46	0.26	0.02	0.01	0.18	1.17	0.10	0.00	0.00	0.00	0.07			98.17	2010	PIC-2 (a)	
34	139	39.63	0.01	0.00	0.00	0.05	0.01	0.00	0.01	58.87	0.20	0.03	0.00	0.08	1.20	0.01	0.01	0.00	0.00	0.00			100.09	2010	PIC-2 (a)	
35	140	36.43	0.00	0.02	0.00	0.08	0.00	0.00	0.02	58.43	0.26	0.06	0.00	0.16	1.11	0.05	0.07	0.00	0.00	0.06			96.76	2010	PIC-2 (a)	
36	141	36.15	0.00	0.00	0.01	0.08	0.00	0.00	0.00	58.78	0.16	0.04	0.00	0.17	1.08	0.00	0.00	0.00	0.00	0.00			96.28	2010	PIC-2 (a)	
37	142	36.25	0.01	0.00	0.00	0.09	0.01	0.00	0.00	58.60	0.14	0.05	0.01	0.10	0.94	0.00	0.00	0.05	0.00	0.00			96.24	2010	PIC-2 (a)	
38	143	37.53	0.03	0.02	0.00	0.02	0.00	0.00	0.00	58.72	0.17	0.03	0.00	0.05	1.01	0.00	0.00	0.01	0.00	0.04			97.62	2010	PIC-2 (a)	
39	144	37.42	0.00	0.00	0.00	0.08	0.00	0.00	0.02	58.10	0.22	0.05	0.00	0.11	1.23	0.03	0.00	0.01	0.00	0.00			97.27	2010	PIC-2 (a)	
40	145	38.31	0.00	0.00	0.00	0.10	0.01	0.00	0.00	57.91	0.29	0.04	0.00	0.07	1.33	0.00	0.02	0.05	0.00	0.04			98.16	2010	PIC-2 (a)	
41	146	37.89	0.00	0.00	0.06	0.04	0.05	0.00	0.00	57.34	0.37	0.06	0.04	0.21	1.36	0.03	0.01	0.00	0.00	0.03			97.48	2010	PIC-2 (a)	
42	147	38.37	0.00	0.00	0.00	0.06	0.00	0.00	0.00	56.77	1.01	0.04	0.01	0.27	1.29	0.00	0.04	0.05	0.00	0.08			97.98	2010	PIC-2 (a)	
43	148	37.67	0.06	0.00	0.00	0.05	0.01	0.00	0.03	55.45	1.63	0.06	0.00	1.80	0.98	0.00	0.02	0.00	0.00	0.01			97.77	2010	PIC-2 (a)	
44	149	38.00	0.01	0.00	0.00	0.04	0.00	0.00	0.00	56.77	1.79	0.06	0.00	0.44	0.98	0.00	0.00	0.00	0.00	0.00			98.09	2010	PIC-2 (a)	
45	150	37.48	0.00	0.00	0.00	0.08	0.01	0.01	0.01	58.02	0.34	0.06	0.00	0.26	1.20	0.00	0.00	0.00	0.00	0.00			97.48	2010	PIC-2 (a)	
46	151	37.75	0.02	0.00	0.00	0.04	0.00	0.02	0.01	58.50	0.35	0.08	0.03	0.26	1.02	0.01	0.00	0.00	0.00	0.00			98.08	2010	PIC-2 (a)	
47	152	37.97	0.00	0.01	0.00	0.07	0.00	0.02	0.00	58.25	0.52	0.08	0.00	0.41	1.04	0.15	0.00	0.04	0.00	0.02			98.36	2010	PIC-2 (a)	
48	153	37.14	0.00	0.00	0.00	0.07	0.01	0.01	0.00	58.14	0.30	0.08	0.00	0.28	0.96	0.06	0.02	0.00	0.00	0.00			97.06	2010	PIC-2 (a)	
49	154	37.62	0.00	0.00	0.00	0.09	0.00	0.00	0.01	57.84	0.37	0.07	0.00	0.34	1.01	0.08	0.05	0.01	0.00	0.00			97.48	2010	PIC-2 (a)	
50	159	36.75	0.00	0.00	0.00	0.02	0.00	0.04	0.00	61.05	0.28	0.02	0.00	0.02	1.42	0.00	0.07	0.00	0.00	0.10	0.06	0.00	99.82	2010	Pic 06 04	
51	346	37.13						0.00	0.05	0.00	57.51	0.52	0.01	0.00	1.34	0.07	0.02	0.01					96.71	2010	Pic 06 04	
52	36	35.68	0.00	0.00	0.03	0.00	0.00	0.09	0.02	60.85	0.75		0.00	0.07	0.62	0.04	0.00	0.04	0.00	0.06	0.06			98.28	2010	Pic 06 04/3
53	37	35.64																								

INDEX	No.	O	Na	K	V	Co	Mg	P	Cr	Fe	Al	S	Ni	Mn	Si	Pb	Cu	Ti	Ca	Zn	Ba	Sr	Total	Year	Sample
144	206	39.21	0.05	0.00	0.05	0.07	0.00	0.08	0.06	59.31	0.15	0.00	0.17	1.49	0.06	0.01	0.02	0.00	0.06	0.00	0.00	0.00	100.79	2010	Pic 06 19/4 Line 25
145	184	38.36	0.00	0.00	0.02	0.06	0.03	0.03	0.02	60.08	0.10	0.00	0.05	0.32	1.65	0.00	0.01	0.00	0.00	0.00	0.02	0.00	100.73	2010	Pic 06 19/4 Line 3
146	189	36.73	0.07	0.02	0.03	0.00	0.04	0.02	0.03	60.39	0.06	0.00	0.36	1.71	0.02	0.00	0.00	0.00	0.00	0.00	0.00	0.00	99.49	2010	Pic 06 19/4 Line 8
147	264	39.02	0.17	0.01	0.00	0.08	0.03	0.05	0.19	0.03	56.74	2.05	0.00	0.24	0.05	0.03	0.03	0.00	0.07	0.01	0.00	0.00	98.76	2010	Pic 06 21 Line 1
148	294	38.98	0.00	0.04	0.00	0.00	0.04	0.13	0.00	56.62	0.10	0.00	0.00	0.21	0.00	0.00	0.13	0.00	0.00	0.00	0.00	0.00	98.42	2010	Pic 06 21 Line 1
149	324	38.37	0.00	0.00	0.01	0.06	0.05	0.16	0.03	58.01	2.21	0.00	0.00	0.24	0.10	0.04	0.10	0.00	0.01	0.00	0.00	0.00	99.39	2010	Pic 06 21 Line 1
150	354	39.26	0.04	0.02	0.07	0.02	0.05	0.11	0.02	57.10	2.30	0.00	0.01	0.34	0.12	0.02	0.10	0.00	0.04	0.08	0.00	0.00	99.68	2010	Pic 06 21 Line 1
151	384	38.26	0.00	0.00	0.05	0.06	0.02	0.13	0.00	58.83	1.86	0.00	0.00	0.25	0.00	0.00	0.11	0.00	0.00	0.00	0.00	0.00	99.57	2010	Pic 06 21 Line 1
152	404	39.11	0.23	0.00	0.00	0.12	0.02	0.11	0.00	58.35	1.46	0.01	0.00	0.29	0.03	0.00	0.11	0.00	0.00	0.00	0.00	0.00	99.83	2010	Pic 06 21 Line 1
153	434	37.16	0.17	0.01	0.00	0.00	0.06	0.00	0.06	60.34	0.07	0.00	0.00	0.43	0.00	0.04	0.02	0.00	0.00	0.00	0.00	0.00	99.40	2010	Pic 06 21 Line 12
154	303	37.05	0.16	0.01	0.00	0.05	0.01	0.00	0.00	61.02	0.01	0.00	0.00	0.45	0.00	0.00	0.00	0.00	0.00	0.00	0.00	0.00	98.76	2010	Pic 06 21 Line 10
155	333	39.00	0.00	0.00	0.00	0.08	0.03	0.13	0.00	57.28	2.30	0.00	0.03	0.28	0.10	0.05	0.18	0.00	0.00	0.05	0.00	0.00	99.52	2010	Pic 06 21 Line 10
156	363	39.54	0.00	0.02	0.00	0.07	0.00	0.08	0.00	55.86	2.58	0.00	0.00	0.44	0.00	0.00	0.10	0.00	0.04	0.01	0.00	0.00	98.74	2010	Pic 06 21 Line 10
157	393	38.84	0.18	0.00	0.13	0.06	0.01	0.09	0.00	58.40	1.52	0.00	0.01	0.29	0.05	0.04	0.12	0.00	0.11	0.00	0.00	0.00	99.85	2010	Pic 06 21 Line 10
158	413	39.15	0.13	0.00	0.02	0.08	0.00	0.11	0.00	58.80	1.32	0.02	0.00	0.29	0.02	0.00	0.12	0.00	0.04	0.00	0.00	0.00	100.10	2010	Pic 06 21 Line 10
159	274	37.15	0.05	0.01	0.08	0.04	0.03	0.17	0.00	58.23	2.15	0.00	0.00	0.26	0.00	0.04	0.04	0.00	0.01	0.00	0.00	0.00	98.26	2010	Pic 06 21 Line 11
160	304	36.33	0.14	0.00	0.08	0.05	0.06	0.02	0.00	60.29	0.02	0.04	0.06	0.61	0.04	0.00	0.02	0.00	0.00	0.00	0.00	0.00	97.75	2010	Pic 06 21 Line 11
161	334	39.27	0.01	0.01	0.10	0.07	0.00	0.15	0.00	56.71	2.67	0.00	0.01	0.27	0.02	0.05	0.11	0.00	0.07	0.00	0.00	0.00	99.51	2010	Pic 06 21 Line 11
162	364	36.08	0.00	0.00	0.00	0.04	0.05	0.10	0.04	56.45	3.04	0.00	0.00	0.34	0.00	0.02	0.11	0.00	0.00	0.00	0.00	0.00	96.28	2010	Pic 06 21 Line 11
163	394	38.66	0.00	0.01	0.02	0.09	0.00	0.14	0.02	58.36	1.64	0.01	0.00	0.31	0.00	0.00	0.16	0.00	0.11	0.03	0.00	0.00	99.56	2010	Pic 06 21 Line 11
164	414	39.14	0.00	0.00	0.00	0.09	0.00	0.13	0.00	58.23	1.42	0.00	0.00	0.29	0.06	0.00	0.16	0.00	0.02	0.00	0.00	0.00	99.54	2010	Pic 06 21 Line 11
165	444	37.38	0.19	0.00	0.02	0.05	0.00	0.07	0.01	61.39	1.07	0.05	0.04	0.40	0.00	0.00	0.01	0.00	0.00	0.00	0.00	0.00	100.67	2010	Pic 06 21 Line 11
166	275	36.40	0.00	0.00	0.00	0.04	0.00	0.05	0.01	61.21	0.03	0.03	0.00	0.38	0.00	0.00	0.00	0.00	0.00	0.00	0.00	0.00	98.35	2010	Pic 06 21 Line 12
167	305	37.17	0.00	0.00	0.04	0.06	0.01	0.00	0.00	60.34	0.02	0.00	0.00	0.55	0.06	0.04	0.01	0.00	0.11	0.00	0.00	0.00	98.38	2010	Pic 06 21 Line 12
168	335	33.09	0.08	0.01	0.07	0.07	0.00	0.07	0.00	64.37	0.50	0.02	0.00	0.84	0.00	0.00	0.00	0.00	0.00	0.02	0.00	0.00	99.13	2010	Pic 06 21 Line 12
169	395	38.65	0.00	0.00	0.00	0.00	0.00	0.13	0.00	58.28	1.63	0.02	0.00	0.31	0.01	0.00	0.17	0.00	0.06	0.00	0.00	0.00	99.26	2010	Pic 06 21 Line 12
170	415	39.00	0.00	0.00	0.01	0.10	0.03	0.14	0.00	58.80	1.37	0.01	0.01	0.22	0.00	0.04	0.16	0.00	0.00	0.03	0.00	0.00	99.91	2010	Pic 06 21 Line 12
171	445	36.81	0.00	0.00	0.00	0.00	0.01	0.01	0.00	61.52	1.11	0.00	0.01	0.41	0.00	0.00	0.11	0.00	0.00	0.00	0.00	0.00	100.05	2010	Pic 06 21 Line 12
172	276	39.00	0.15	0.00	0.03	0.04	0.00	0.22	0.00	57.24	2.42	0.00	0.04	0.29	0.05	0.02	0.10	0.00	0.01	0.00	0.00	0.00	99.60	2010	Pic 06 21 Line 13
173	306	37.88	0.12	0.00	0.12	0.11	0.01	0.04	0.04	60.70	0.00	0.00	0.03	0.50	0.00	0.02	0.00	0.00	0.00	0.00	0.00	0.00	99.55	2010	Pic 06 21 Line 13
174	336	36.82	0.00	0.00	0.11	0.10	0.05	0.02	0.02	60.50	0.10	0.00	0.00	0.43	0.07	0.00	0.02	0.00	0.00	0.00	0.00	0.00	98.23	2010	Pic 06 21 Line 13
175	366	39.55	0.14	0.00	0.02	0.07	0.02	0.09	0.03	55.74	2.20	0.00	0.06	0.41	0.08	0.09	0.19	0.00	0.01	0.00	0.00	0.00	98.70	2010	Pic 06 21 Line 13
176	396	38.64	0.00	0.01	0.14	0.05	0.16	0.02	0.02	59.34	1.68	0.04	0.04	0.31	0.08	0.00	0.08	0.00	0.03	0.04	0.00	0.00	100.65	2010	Pic 06 21 Line 13
177	416	39.00	0.00	0.00	0.02	0.02	0.00	0.00	0.00	58.43	1.33	0.04	0.05	0.31	0.16	0.01	0.16	0.00	0.03	0.00	0.00	0.00	99.64	2010	Pic 06 21 Line 13
178	446	36.63	0.00	0.00	0.00	0.04	0.00	0.04	0.00	61.29	1.12	0.00	0.00	0.41	0.11	0.03	0.06	0.00	0.02	0.01	0.00	0.00	99.76	2010	Pic 06 21 Line 13
179	277	35.98	0.00	0.03	0.00	0.02	0.04	0.07	0.00	59.46	1.48	0.00	0.00	0.41	0.09	0.00	0.01	0.00	0.00	0.00	0.00	0.00	97.58	2010	Pic 06 21 Line 14
180	307	32.22	0.01	0.00	0.00	0.04	0.06	0.11	0.01	59.98	1.20	0.02	0.01	0.58	0.12	0.05	0.00	0.16	0.01	0.05	0.00	0.00	94.61	2010	Pic 06 21 Line 14
181	337	37.46	0.00	0.00	0.00	0.00	0.04	0.03	0.00	62.13	0.06	0.00	0.05	0.42	0.00	0.00	0.00	0.00	0.00	0.00	0.00	0.00	100.19	2010	Pic 06 21 Line 14
182	367	39.10	0.00	0.01	0.00	0.04	0.06	0.09	0.00	56.64	2.27	0.00	0.05	0.40	0.00	0.01	0.14	0.00	0.01	0.00	0.00	0.00	98.81	2010	Pic 06 21 Line 14
183	397	38.48	0.11	0.00	0.04	0.06	0.14	0.00	0.00	58.84	1.68	0.00	0.03	0.26	0.00	0.00	0.16	0.00	0.02	0.05	0.00	0.00	99.92	2010	Pic 06 21 Line 14
184	417	39.00	0.03	0.00	0.00	0.09	0.00	0.14	0.02	58.24	1.35	0.01	0.00	0.28	0.01	0.08	0.15	0.00	0.00	0.00	0.00	0.00	99.39	2010	Pic 06 21 Line 14
185	447	37.36	0.04	0.00	0.01	0.09	0.07	0.07	0.01	61.02	1.53	0.00	0.00	0.41	0.00	0.01	0.15	0.00	0.00	0.02	0.00	0.00	100.78	2010	Pic 06 21 Line 14
186	278	38.98	0.00	0.00	0.00	0.10	0.05	0.17	0.05	57.11	2.30	0.00	0.00	0.26	0.00	0.00	0.06	0.00	0.08	0.04	0.00	0.00	99.21	2010	Pic 06 21 Line 15
187	308	39.03	0.08	0.00	0.00	0.09	0.01	0.13	0.01	56.62	3.52	0.00	0.00	0.19	0.06	0.06	0.08	0.00	0.00	0.00	0.00	0.00	99.87	2010	Pic 06 21 Line 15
188	338	37.85	0.00	0.00	0.00	0.00	0.04	0.04	0.04	60.91	0.11	0.01	0.00	0.49	0.00	0.08	0.07	0.00	0.03	0.00	0.00	0.00	99.63	2010	Pic 06 21 Line 15
189	368	39.16	0.00	0.00	0.00	0.00	0.01	0.10	0.00	57.07	2.51	0.00	0.02	0.39	0.04	0.00	0.08	0.00	0.00	0.00	0.00	0.00	99.41	2010	Pic 06 21 Line 15
190	398	38.42	0.00	0.00	0.07	0.11	0.03	0.12	0.00	58.64	1.74	0.00	0.02	0.28	0.00	0.04	0.16	0.00	0.00	0.01	0.00	0.00	99.64	2010	Pic 06 21 Line 15
191	418	39.12	0.00	0.01	0.00	0.03	0.07	0.16	0.00	58.68	1.40	0.03	0.01	0.25	0.04	0.02	0.11	0.00	0.00	0.00	0.00	0.00	99.92	2010	Pic 06 21 Line 15
192	448	37.49	0.00	0.00	0.00	0.12	0.03	0.04	0.05	60.23	1.14	0.00	0.00	0.42	0.00	0.05	0.00	0.00	0.00	0.00	0.00	0.00	99.57	2010	Pic 06 21 Line 15
193	279	38.74	0.11	0.00	0.00	0.02	0.08	0.14	0.03	57.24	1.93	0.00	0.00	0.27	0.09</										

INDEX	No.	O	Na	K	V	Co	Mg	P	Cr	Fe	Al	S	Ni	Mn	Si	Pb	Cu	Ti	Ca	Zn	Ba	Sr	Total	Year	Sample
288	387	38.59	0.08	0.01	0.00	0.05	0.01	0.12	0.04	58.80	1.64	0.00	0.00	0.26	0.05	0.02	0.11	0.00	0.02	0.04			99.86	2010	Pic 06 21 Line 4
289	407	39.09	0.00	0.00	0.00	0.06	0.01	0.11	0.00	58.05	1.35	0.00	0.00	0.31	0.01	0.00	0.14	0.00	0.04	0.00			99.22	2010	Pic 06 21 Line 4
290	437	36.94	0.00	0.00	0.00	0.04	0.05	0.09	0.03	61.38	1.18	0.00	0.00	0.43	0.09	0.05	0.11	0.00	0.02	0.00			100.40	2010	Pic 06 21 Line 5
291	268	38.91	0.00	0.00	0.06	0.10	0.00	0.15	0.00	57.23	2.41	0.00	0.00	0.25	0.05	0.07	0.00	0.00	0.01	0.00			99.35	2010	Pic 06 21 Line 4
292	338	38.66	0.00	0.00	0.00	0.08	0.03	0.15	0.00	57.18	2.22	0.01	0.00	0.25	0.00	0.05	0.00	0.00	0.00	0.00			98.71	2010	Pic 06 21 Line 5
293	388	38.76	0.03	0.00	0.05	0.07	0.08	0.13	0.03	58.35	1.63	0.00	0.04	0.29	0.04	0.00	0.12	0.00	0.07	0.00			99.68	2010	Pic 06 21 Line 5
294	408	39.28	0.00	0.01	0.02	0.12	0.03	0.09	0.00	59.10	1.32	0.02	0.05	0.35	0.00	0.00	0.13	0.00	0.00	0.02			100.54	2010	Pic 06 21 Line 5
295	436	38.61	0.05	0.00	0.00	0.09	0.00	0.07	0.00	60.80	1.04	0.05	0.04	0.41	0.06	0.00	0.11	0.00	0.00	0.00			99.33	2010	Pic 06 21 Line 6
296	299	39.25	0.00	0.00	0.00	0.08	0.02	0.12	0.00	56.82	2.86	0.00	0.00	0.30	0.08	0.00	0.04	0.00	0.05	0.00			99.59	2010	Pic 06 21 Line 6
297	329	38.93	0.01	0.02	0.01	0.04	0.16	0.00	57.74	2.43	0.00	0.00	0.22	0.04	0.00	0.00	0.00	0.00	0.00	0.00			99.80	2010	Pic 06 21 Line 6
298	359	39.26	0.00	0.01	0.01	0.09	0.04	0.08	0.04	55.97	3.45	0.00	0.03	0.29	0.02	0.00	0.04	0.04	0.00	0.00			99.32	2010	Pic 06 21 Line 6
299	389	38.70	0.00	0.02	0.00	0.04	0.00	0.14	0.00	58.67	1.62	0.00	0.00	0.30	0.10	0.00	0.16	0.00	0.08	0.03			99.86	2010	Pic 06 21 Line 6
300	409	39.06	0.14	0.00	0.03	0.09	0.00	0.13	0.02	58.58	1.33	0.00	0.05	0.27	0.00	0.00	0.13	0.00	0.06	0.00			99.88	2010	Pic 06 21 Line 6
301	300	36.00	0.00	0.01	0.00	0.04	0.02	0.01	0.01	60.67	0.00	0.00	0.00	0.46	0.00	0.00	0.00	0.00	0.10	0.00			97.32	2010	Pic 06 21 Line 7
302	360	39.35	0.16	0.00	0.09	0.04	0.03	0.10	0.00	56.35	3.35	0.02	0.02	0.27	0.00	0.00	0.05	0.00	0.02	0.00			99.84	2010	Pic 06 21 Line 7
303	390	38.57	0.00	0.00	0.00	0.02	0.00	0.13	0.04	58.79	1.69	0.00	0.03	0.25	0.00	0.00	0.14	0.00	0.11	0.00			99.77	2010	Pic 06 21 Line 7
304	410	39.26	0.08	0.01	0.04	0.11	0.00	0.11	0.01	58.06	1.34	0.01	0.00	0.30	0.00	0.02	0.12	0.00	0.03	0.00			99.50	2010	Pic 06 21 Line 7
305	440	36.97	0.00	0.00	0.09	0.02	0.02	0.05	0.01	61.04	1.11	0.06	0.01	0.44	0.07	0.03	0.08	0.00	0.06	0.00			100.06	2010	Pic 06 21 Line 7
306	271	38.89	0.00	0.00	0.00	0.04	0.05	0.13	0.00	57.46	2.22	0.00	0.00	0.29	0.03	0.00	0.00	0.00	0.00	0.01			99.12	2010	Pic 06 21 Line 8
307	301	37.11	0.16	0.01	0.00	0.03	0.03	0.02	0.00	60.09	0.00	0.01	0.00	0.54	0.01	0.00	0.00	0.00	0.01	0.07			98.06	2010	Pic 06 21 Line 8
308	331	38.82	0.00	0.00	0.00	0.08	0.06	0.10	0.00	57.48	2.48	0.01	0.04	0.23	0.00	0.03	0.03	0.00	0.00	0.00			99.35	2010	Pic 06 21 Line 8
309	361	39.28	0.03	0.02	0.00	0.04	0.00	0.10	0.04	56.19	2.84	0.00	0.05	0.35	0.00	0.00	0.21	0.00	0.07	0.00			99.21	2010	Pic 06 21 Line 8
310	391	38.83	0.06	0.00	0.00	0.05	0.02	0.11	0.00	58.25	1.66	0.02	0.00	0.25	0.10	0.00	0.12	0.00	0.00	0.00			99.48	2010	Pic 06 21 Line 8
311	411	39.20	0.08	0.01	0.00	0.08	0.03	0.08	0.00	58.88	1.27	0.00	0.02	0.25	0.00	0.01	0.13	0.00	0.00	0.02			100.06	2010	Pic 06 21 Line 8
312	441	38.05	0.05	0.00	0.00	0.05	0.04	0.02	0.05	60.94	1.08	0.00	0.01	0.42	0.05	0.02	0.11	0.00	0.04	0.05			100.96	2010	Pic 06 21 Line 8
313	272	37.37	0.07	0.00	0.03	0.03	0.00	0.15	0.05	59.67	3.09	0.00	0.00	0.22	0.00	0.00	0.05	0.00	0.00	0.00			100.74	2010	Pic 06 21 Line 9
314	302	36.98	0.00	0.00	0.01	0.07	0.02	0.03	0.00	60.23	0.02	0.00	0.00	0.51	0.04	0.12	0.00	0.00	0.00	0.01			98.03	2010	Pic 06 21 Line 9
315	332	39.12	0.00	0.00	0.00	0.00	0.00	0.11	0.00	57.26	2.43	0.00	0.01	0.26	0.00	0.00	0.00	0.00	0.00	0.00			99.74	2010	Pic 06 21 Line 9
316	392	38.61	0.10	0.02	0.01	0.02	0.02	0.14	0.00	58.90	1.56	0.01	0.00	0.28	0.03	0.00	0.11	0.00	0.00	0.00			99.80	2010	Pic 06 21 Line 9
317	412	39.49	0.04	0.00	0.01	0.08	0.03	0.14	0.03	58.35	1.29	0.00	0.00	0.31	0.00	0.01	0.22	0.00	0.06	0.00			100.05	2010	Pic 06 21 Line 9
318	442	36.82	0.12	0.01	0.06	0.02	0.05	0.11	0.02	61.50	1.02	0.00	0.04	0.47	0.02	0.00	0.00	0.00	0.00	0.00			100.25	2010	Pic 06 21 Line 9
319	571	36.51	0.00	0.00	0.02	0.04	0.04	0.13	0.01	59.13	0.57	0.03	0.02	0.02	0.73	0.04	0.00	0.00	0.00	0.00			97.28	2010	Pic 06 22 BDG
320	572	36.58	0.00	0.00	0.08	0.03	0.03	0.07	0.00	59.28	0.50	0.01	0.00	0.61	0.06	0.02	0.00	0.00	0.00	0.00			97.26	2010	Pic 06 22 BDG
321	573	35.43	0.00	0.00	0.00	0.11	0.02	0.12	0.01	59.75	0.76	0.09	0.02	0.01	0.56	0.07	0.04	0.06	0.00	0.00			97.04	2010	Pic 06 22 BDG
322	574	37.13	0.00	0.00	0.00	0.10	0.01	0.12	0.02	58.75	0.64	0.08	0.00	0.84	0.00	0.00	0.03	0.00	0.07	0.00			97.78	2010	Pic 06 22 BDG
323	575	37.92	0.02	0.01	0.00	0.03	0.00	0.17	0.00	58.24	0.72	0.02	0.06	0.01	0.87	0.00	0.00	0.00	0.00	0.00			98.05	2010	Pic 06 22 BDG
324	576	37.69	0.00	0.00	0.04	0.03	0.01	0.15	0.00	59.14	0.71	0.02	0.00	0.11	0.81	0.08	0.02	0.01	0.00	0.05			98.86	2010	Pic 06 22 BDG
325	577	37.22	0.00	0.00	0.04	0.06	0.02	0.13	0.01	58.69	0.50	0.03	0.00	0.80	0.02	0.05	0.02	0.00	0.00	0.00			97.58	2010	Pic 06 22 BDG
326	578	37.26	0.00	0.00	0.00	0.00	0.00	0.13	0.00	58.08	0.62	0.07	0.00	0.07	0.82	0.02	0.00	0.00	0.00	0.00			97.08	2010	Pic 06 22 BDG
327	579	37.94	0.00	0.00	0.00	0.00	0.00	0.14	0.00	58.67	0.82	0.03	0.00	0.77	0.12	0.00	0.00	0.00	0.00	0.00			98.54	2010	Pic 06 22 BDG
328	580	36.66	0.00	0.00	0.05	0.08	0.01	0.13	0.00	58.96	0.67	0.04	0.00	0.00	0.70	0.07	0.01	0.08	0.00	0.00			97.45	2010	Pic 06 22 BDG
329	581	37.29	0.00	0.00	0.00	0.05	0.00	0.13	0.00	59.63	0.74	0.03	0.00	0.00	0.76	0.00	0.05	0.00	0.00	0.02			98.70	2010	Pic 06 22 BDG
330	582	36.94	0.00	0.00	0.01	0.13	0.05	0.10	0.00	58.93	0.74	0.03	0.02	0.01	0.77	0.00	0.00	0.00	0.00	0.04			97.77	2010	Pic 06 22 BDG
331	583	37.18	0.02	0.00	0.02	0.06	0.00	0.12	0.02	60.11	0.73	0.04	0.00	0.66	0.67	0.08	0.06	0.01	0.00	0.00			99.16	2010	Pic 06 22 BDG
332	584	36.93	0.00	0.00	0.01	0.03	0.00	0.13	0.02	58.94	0.46	0.03	0.00	0.84	0.00	0.02	0.00	0.00	0.07	0.00			97.46	2010	Pic 06 22 BDG
333	585	37.24	0.05	0.00	0.06	0.07	0.02	0.11	0.02	58.79	0.34	0.05	0.00	0.65	0.76	0.03	0.00	0.00	0.00	0.00			97.63	2010	Pic 06 22 BDG
334	586	36.33	0.02	0.00	0.02	0.06	0.00	0.13	0.04	59.16	1.11	0.00	0.00	0.03	0.84	0.00	0.00	0.02	0.00	0.06			97.80	2010	Pic 06 22 BDG
335	587	37.66	0.04	0.00	0.06	0.14	0.00	0.16	0.03	59.48	0.95	0.05	0.00	0.00	0.72	0.00	0.00	0.05	0.00	0.04			99.36	2010	Pic 06 22 BDG
336	588	37.40	0.00	0.00	0.01	0.01	0.00	0.10	0.00	58.71	0.45	0.03	0.00	0.04	0.72	0.11	0.02	0.04	0.00	0.00			97.64	2010	Pic 06 22 BDG
337	589	37.35	0.01	0.00	0.07	0.05	0.00	0.16	0.00	59.25	0.78	0.01	0.00	0.05	0.71	0.07	0.06	0.01	0.00	0.00			98.57	2010	Pic 06 22 BDG
338	590	36.86	0.00	0.00	0.05	0.07	0.04	0.08	0.00	59.08	0.39	0.05	0.00	0.69	0.00	0.01	0.00	0.00	0.04	0.04			97.38 </		

INDEX	No.	O	Na	K	V	Co	Mg	P	Cr	Fe	Al	S	Ni	Mn	Si	Pb	Cu	Ti	Ca	Zn	Ba	Sr	Total	Year	Sample
432	153	38.55	0.00	0.00	0.01	0.04	0.01	0.33	0.04	56.87	2.75		0.03	0.00	0.17	0.05	0.05	0.24	0.00	0.05	0.00		99.19	2010	Pic 06 24/2
433	154	40.06	0.05	0.01	0.05	0.16	0.00	0.41	0.05	56.27	2.87		0.03	0.00	0.15	0.00	0.05	0.45	0.00	0.06	0.03		100.69	2010	Pic 06 24/2
434	155	38.99	0.06	0.00	0.04	0.11	0.00	0.38	0.00	56.98	2.66		0.00	0.03	0.14	0.01	0.00	0.00	0.00	0.00	0.00		99.38	2010	Pic 06 24/2
435	156	39.06	0.04	0.01	0.00	0.08	0.06	0.32	0.00	56.30	2.74		0.00	0.03	0.17	0.00	0.00	0.00	0.00	0.00	0.00		98.85	2010	Pic 06 24/2
436	157	39.05	0.08	0.00	0.08	0.08	0.11	0.34	0.00	56.65	1.31		0.00	0.03	0.14	0.07	0.00	0.00	0.00	0.00	0.00		99.64	2010	Pic 06 24/2
437	158	38.96	0.03	0.00	0.04	0.09	0.07	0.33	0.00	56.30	2.76		0.00	0.02	0.15	0.00	0.05	0.04	0.00	0.07	0.00		98.90	2010	Pic 06 24/2
438	160	38.14	0.00	0.00	0.00	0.07	0.05	0.32	0.00	57.20	2.97		0.00	0.00	0.09	0.00	0.00	0.06	0.00	0.00	0.00		98.91	2010	Pic 06 24/2
439	161	38.15	0.00	0.03	0.07	0.02	0.01	0.42	0.04	56.14	3.40		0.02	0.02	0.26	0.02	0.04	0.05	0.00	0.01	0.00		98.70	2010	Pic 06 24/2
440	162	39.04	0.00	0.02	0.00	0.11	0.00	0.35	0.06	55.93	3.46		0.01	0.05	0.18	0.07	0.08	0.00	0.00	0.05	0.07		99.47	2010	Pic 06 24/2
441	163	39.16	0.02	0.00	0.04	0.10	0.00	0.36	0.00	56.11	3.40		0.00	0.04	0.18	0.04	0.10	0.06	0.00	0.05	0.05		99.75	2010	Pic 06 24/2
442	164	39.19	0.01	0.01	0.00	0.11	0.02	0.38	0.00	56.07	3.43		0.00	0.04	0.17	0.00	0.00	0.02	0.00	0.00	0.00		99.45	2010	Pic 06 24/2
443	165	39.58	0.07	0.00	0.00	0.09	0.00	0.42	0.01	55.48	4.46		0.00	0.04	0.15	0.12	0.05	0.00	0.00	0.02	0.00		100.49	2010	Pic 06 24/2
444	166	39.73	0.00	0.00	0.08	0.07	0.09	0.36	0.04	56.29	3.67		0.00	0.00	0.16	0.11	0.02	0.08	0.00	0.05	0.01		100.74	2010	Pic 06 24/2
445	167	38.87	0.00	0.01	0.00	0.00	0.02	0.39	0.00	55.77	3.87		0.00	0.00	0.16	0.03	0.00	0.01	0.00	0.05	0.04		99.22	2010	Pic 06 24/2
446	168	39.22	0.05	0.00	0.02	0.03	0.00	0.41	0.01	56.33	3.88		0.00	0.00	0.19	0.00	0.00	0.00	0.00	0.00	0.00		100.14	2010	Pic 06 24/2
447	169	35.42	0.00	0.00	0.00	0.05	0.08	0.43	0.04	59.16	4.55		0.02	0.06	0.16	0.04	0.02	0.03	0.00	0.00	0.06		100.14	2010	Pic 06 24/2
448	172	38.05	0.13	0.01	0.00	0.08	0.07	0.43	0.00	57.08	4.79		0.00	0.00	0.17	0.10	0.00	0.02	0.00	0.03	0.01		100.98	2010	Pic 06 24/2
449	173	39.23	0.00	0.00	0.03	0.00	0.07	0.43	0.03	55.51	3.97		0.01	0.01	0.14	0.00	0.00	0.04	0.00	0.00	0.00		99.47	2010	Pic 06 24/2
450	174	39.45	0.09	0.02	0.00	0.03	0.00	0.36	0.01	55.95	3.63		0.02	0.00	0.16	0.00	0.04	0.01	0.00	0.03	0.00		99.78	2010	Pic 06 24/2
451	175	38.69	0.00	0.00	0.01	0.05	0.04	0.34	0.00	56.40	3.33		0.02	0.01	0.15	0.11	0.01	0.04	0.00	0.07	0.00		99.27	2010	Pic 06 24/2
452	176	39.32	0.03	0.00	0.06	0.02	0.02	0.39	0.02	55.68	4.12		0.00	0.00	0.16	0.07	0.06	0.08	0.00	0.07	0.05		100.14	2010	Pic 06 24/2
453	177	39.39	0.07	0.00	0.00	0.10	0.08	0.40	0.00	55.79	4.07		0.03	0.02	0.15	0.07	0.00	0.00	0.00	0.01	0.00		99.73	2010	Pic 06 24/2
454	178	39.14	0.00	0.00	0.00	0.05	0.06	0.37	0.00	56.63	3.37		0.01	0.00	0.17	0.00	0.09	0.06	0.00	0.12	0.02		100.09	2010	Pic 06 24/2
455	179	38.68	0.00	0.00	0.03	0.08	0.03	0.39	0.00	56.18	3.34		0.00	0.00	0.14	0.00	0.03	0.13	0.00	0.00	0.00		99.04	2010	Pic 06 24/2
456	180	38.91	0.12	0.00	0.00	0.07	0.05	0.42	0.01	56.61	3.69		0.00	0.00	0.13	0.11	0.00	0.02	0.00	0.00	0.00		100.13	2010	Pic 06 24/2
457	43.93	0.02	0.00	0.04	0.09	0.00	0.01	0.00	0.00	52.31	0.04		0.00	0.00	0.02	0.08	0.01	1.01	0.00	0.01	0.02		97.59	2010	Pic-06-1A/2
458	39.40	0.00	0.05	0.05	0.05	0.02	0.44	0.04	54.91	2.49		0.00	0.00	0.22	0.06	0.00	0.35	0.00	0.00	0.00	0.00		98.03	2010	Pic-06-1A/2
459	33.29	0.00	0.00	0.00	0.00	0.00	0.00	0.00	55.50	1.31		0.00	0.00	0.29	0.00	0.00	0.00	0.47	0.00	0.05	0.06		91.08	2010	Pic-06-1A/2
460	39.51	0.03	0.01	0.01	0.01	0.02	0.40	0.02	55.92	1.71		0.00	0.00	0.18	0.07	0.00	0.22	0.22	0.00	0.01	0.01		98.11	2010	Pic-06-1A/2
461	39.00	0.00	0.00	0.05	0.03	0.01	0.36	0.00	55.94	1.69		0.00	0.00	0.20	0.05	0.04	0.26	0.00	0.01	0.00	0.00		97.64	2010	Pic-06-1A/2
462	38.15	0.00	0.00	0.00	0.07	0.03	0.46	0.00	56.09	2.05		0.00	0.00	0.24	0.03	0.00	0.37	0.00	0.00	0.03			97.52	2010	Pic-06-1A/2
463	38.40	0.02	0.00	0.05	0.03	0.04	0.28	0.00	56.12	1.46		0.03	0.04	0.20	0.00	0.00	1.20	0.00	0.00	0.02			97.89	2010	Pic-06-1A/2
464	38.64	0.00	0.00	0.05	0.09	0.00	0.35	0.02	56.38	1.57		0.00	0.01	0.22	0.10	0.02	0.50	0.00	0.02	0.02			97.97	2010	Pic-06-1A/2
465	38.49	0.00	0.00	0.04	0.08	0.01	0.35	0.03	56.40	1.70		0.01	0.01	0.18	0.08	0.00	0.43	0.00	0.00	0.00			97.77	2010	Pic-06-1A/2
466	39.85	0.01	0.00	0.07	0.07	0.00	0.44	0.00	56.65	1.60		0.00	0.02	0.24	0.07	0.00	0.09	0.00	0.08	0.00			99.20	2010	Pic-06-1A/2
467	34.96	0.00	0.00	0.02	0.06	0.06	0.46	0.02	56.73	1.04		0.00	0.00	0.35	0.00	0.04	0.14	0.00	0.00	0.00			93.88	2010	Pic-06-1A/2
468	38.83	0.00	0.00	0.00	0.02	0.02	0.34	0.00	56.79	1.26		0.00	0.00	1.02	0.00	0.00	0.46	0.00	0.00	0.00	0.01		98.74	2010	Pic-06-1A/2
469	38.31	0.00	0.00	0.00	0.05	0.02	0.39	0.02	56.85	1.60		0.06	0.01	0.25	0.06	0.03	0.40	0.00	0.00	0.00			98.04	2010	Pic-06-1A/2
470	38.94	0.02	0.00	0.00	0.09	0.00	0.33	0.00	56.94	1.25		0.00	0.00	0.27	0.00	0.03	0.03	0.00	0.00	0.00			97.89	2010	Pic-06-1A/2
471	38.88	0.00	0.01	0.03	0.02	0.01	0.37	0.02	57.01	1.53		0.02	0.02	0.24	0.06	0.06	0.06	0.00	0.03	0.00			98.31	2010	Pic-06-1A/2
472	37.69	0.04	0.00	0.00	0.05	0.01	0.41	0.02	57.06	1.67		0.00	0.01	0.27	0.05	0.02	0.16	0.00	0.00	0.04			97.48	2010	Pic-06-1A/2
473	38.71	0.00	0.00	0.00	0.02	0.00	0.32	0.00	57.32	0.87		0.03	0.00	0.26	0.01	0.00	0.63	0.00	0.00	0.01			98.17	2010	Pic-06-1A/2
474	37.69	0.00	0.00	0.00	0.08	0.03	0.43	0.00	57.41	1.60		0.00	0.02	0.26	0.00	0.01	0.56	0.00	0.00	0.00			98.08	2010	Pic-06-1A/2
475	37.91	0.06	0.00	0.05	0.07	0.04	0.35	0.01	57.64	0.43		0.02	0.01	0.27	0.05	0.03	0.03	0.00	0.00	0.00			96.96	2010	Pic-06-1A/2
476	37.85	0.00	0.00	0.02	0.06	0.02	0.39	0.02	57.65	1.44		0.00	0.01	0.25	0.03	0.05	0.31	0.00	0.00	0.00			98.10	2010	Pic-06-1A/2
477	34.99	0.05	0.00	0.01	0.05	0.01	0.43	0.04	57.78	1.47		0.02	0.02	0.25	0.09	0.00	0.47	0.00	0.05	0.06			95.73	2010	Pic-06-1A/2
478	37.16	0.01	0.00	0.00	0.01	0.03	0.38	0.02	57.84	0.69		0.00	0.00	0.25	0.06	0.00	0.33	0.00	0.02	0.01			96.81	2010	Pic-06-1A/2
479	37.88	0.02	0.01	0.02	0.07	0.02	0.28	0.00	57.85	1.23		0.00	0.00	0.25	0.00	0.03	0.04	0.00	0.02	0.04			97.74	2010	Pic-06-1A/2
480	38.09	0.01	0.00	0.03	0.09	0.03	0.34	0.01	57.90	1.23		0.00	0.01	0.26	0.00	0.00	0.39	0.00	0.03	0.04			98.47	2010	Pic-06-1A/2
481	36.52	0.00	0.03	0.05	0.02	0.38	0.00	57.97	1.42		0.00	0.00	0.26	0.00	0.01	0.25	0.00	0.02	0.01				96.95	2010	Pic-06-1A/2
482	36.57	0.00	0.00	0.00	0.08	0.03	0.35	0.00	58.02	1.20		0.01	0.00	0.27	0.00	0.02	0.28	0.00	0.05	0.00			96.87	2010	Pic-06-1A/2
483	37.68	0.00	0.00	0.05	0.01	0.01	0.40	0.01	58.08	1.04		0.00	0.00	0.20	0										

INDEX	No.	O	Na	K	V	Co	Mg	P	Cr	Fe	Al	S	Ni	Mn	Si	Pb	Cu	Ti	Ca	Zn	Ba	Sr	Total	Year	Sample
576	34.70	0.00	0.00	0.06	0.08	0.05	0.35	0.01	60.36	0.70	0.00	0.01	0.33	0.10	0.00	0.05	0.00	0.00	0.00	0.07			96.85	2010	Pic-06-01A/4
577	35.63	0.00	0.00	0.02	0.05	0.00	0.13	0.00	60.42	0.26	0.00	0.04	0.51	0.12	0.00	0.01	0.00	0.00	0.00	0.00			97.19	2010	Pic-06-01A/4
578	36.34	0.00	0.01	0.01	0.06	0.05	0.17	0.04	60.54	0.36	0.00	0.00	0.42	0.04	0.00	0.17	0.00	0.00	0.00	0.00			98.21	2010	Pic-06-01A/4
579	37.40	0.06	0.01	0.00	0.02	0.01	0.02	0.01	60.54	0.01	0.00	0.00	0.30	0.00	0.00	0.00	0.00	0.00	0.01	0.00			98.44	2010	Pic-06-01A/4
580	35.22	0.00	0.00	0.00	0.05	0.00	0.00	0.17	0.03	60.00	0.54	0.00	0.37	0.02	0.00	0.00	0.00	0.00	0.00	0.00			97.21	2010	Pic-06-01A/3
581	36.29	0.00	0.00	0.00	0.04	0.01	0.20	0.03	60.75	0.28	0.00	0.00	0.45	0.06	0.00	0.00	0.00	0.00	0.00	0.00			98.11	2010	Pic-06-01A/4
582	39.30	0.04	0.01	0.00	0.11	0.01	0.04	0.00	60.83	0.00	0.00	0.00	0.30	0.00	0.00	0.04	0.00	0.00	0.00	0.00			100.68	2010	Pic-06-01A/4
583	34.46	0.03	0.00	0.00	0.10	0.02	0.15	0.00	60.86	0.54	0.00	0.03	0.46	0.01	0.01	0.16	0.00	0.00	0.00	0.00			95.83	2010	Pic-06-01A/4
584	34.87	0.00	0.01	0.00	0.04	0.03	0.13	0.00	60.92	0.15	0.00	0.00	0.53	0.14	0.00	0.04	0.00	0.00	0.00	0.00			96.85	2010	Pic-06-01A/4
585	33.28	0.00	0.00	0.00	0.06	0.01	0.16	0.05	60.94	0.00	0.00	0.00	0.41	0.05	0.00	0.00	0.00	0.00	0.00	0.00			95.17	2010	Pic-06-01A/4
586	33.56	0.01	0.00	0.01	0.08	0.02	0.21	0.04	61.21	0.14	0.00	0.00	0.52	0.00	0.00	0.02	0.00	0.00	0.00	0.01			95.83	2010	Pic-06-01A/4
587	35.19	0.02	0.00	0.03	0.06	0.02	0.17	0.00	60.64	1.18	0.00	0.00	0.38	0.00	0.03	0.48	0.00	0.04	0.04	0.04			98.26	2010	Pic-06-01A/5 G1
588	35.47	0.09	0.00	0.01	0.02	0.00	0.10	0.01	60.68	0.08	0.00	0.06	0.34	0.00	0.00	0.00	0.00	0.00	0.00	0.05			96.90	2010	Pic-06-01A/5 G1
589	35.32	0.00	0.00	0.04	0.04	0.01	0.09	0.02	61.27	0.39	0.00	0.02	0.28	0.11	0.03	0.15	0.00	0.01	0.03				97.82	2010	Pic-06-01A/5 G1
590	35.49	0.01	0.00	0.03	0.12	0.00	0.12	0.00	62.95	0.06	0.00	0.00	0.37	0.01	0.02	0.00	0.00	0.08	0.00				99.26	2010	Pic-06-01A/5 G1
591	35.10	0.08	0.00	0.02	0.08	0.00	0.20	0.02	63.16	0.28	0.00	0.01	0.38	0.00	0.00	0.02	0.00	0.00	0.02				99.37	2010	Pic-06-01A/5 G1
592	35.30	0.00	0.00	0.06	0.15	0.00	0.10	0.00	63.16	0.60	0.00	0.00	0.34	0.00	0.08	0.03	0.00	0.10	0.00				99.91	2010	Pic-06-01A/5 G1
593	33.80	0.09	0.01	0.00	0.01	0.00	0.06	0.00	63.46	0.87	0.00	0.00	0.39	0.06	0.00	0.01	0.00	0.03	0.07				98.85	2010	Pic-06-01A/5 G1
594	35.68	0.06	0.00	0.02	0.09	0.01	0.14	0.05	63.48	0.25	0.00	0.02	0.44	0.06	0.05	0.07	0.00	0.00	0.00				100.40	2010	Pic-06-01A/5 G1
595	31.39	0.01	0.00	0.00	0.07	0.00	0.04	0.00	63.64	0.50	0.00	0.00	0.55	0.07	0.09	0.02	0.00	0.00	0.03				96.41	2010	Pic-06-01A/5 G1
596	33.36	0.00	0.01	0.03	0.07	0.01	0.08	0.01	63.67	0.85	0.00	0.01	0.37	0.00	0.05	0.08	0.00	0.02	0.01				98.62	2010	Pic-06-01A/5 G1
597	32.64	0.00	0.00	0.02	0.15	0.05	0.04	0.05	63.73	0.65	0.00	0.00	0.56	0.01	0.00	0.01	0.00	0.00	0.00				97.93	2010	Pic-06-01A/5 G1
598	32.73	0.00	0.01	0.00	0.06	0.06	0.04	0.00	63.76	0.66	0.00	0.00	0.46	0.00	0.00	0.02	0.02	0.03	0.00				97.83	2010	Pic-06-01A/5 G1
599	31.37	0.05	0.00	0.03	0.10	0.07	0.08	0.04	63.80	0.78	0.00	0.00	0.42	0.07	0.04	0.18	0.00	0.00	0.07				97.10	2010	Pic-06-01A/5 G1
600	29.91	0.00	0.00	0.00	0.01	0.07	0.06	0.00	63.83	0.55	0.00	0.05	0.55	0.04	0.00	0.00	0.04	0.00	0.08				95.18	2010	Pic-06-01A/5 G1
601	35.16	0.17	0.00	0.02	0.14	0.00	0.31	0.04	63.95	0.37	0.00	0.07	0.46	0.07	0.00	0.06	0.00	0.06	0.02				100.90	2010	Pic-06-01A/5 G1
602	34.39	0.07	0.00	0.04	0.11	0.07	0.30	0.03	63.98	0.57	0.00	0.00	0.50	0.00	0.02	0.02	0.00	0.03	0.02				100.14	2010	Pic-06-01A/5 G1
603	31.81	0.07	0.00	0.01	0.08	0.00	0.07	0.01	64.10	0.07	0.00	0.00	0.53	0.06	0.00	0.00	0.00	0.00	0.00				97.41	2010	Pic-06-01A/5 G1
604	34.48	0.00	0.00	0.00	0.09	0.03	0.08	0.00	64.16	0.67	0.03	0.00	0.49	0.00	0.00	0.11	0.00	0.00	0.00				100.13	2010	Pic-06-01A/5 G1
605	34.51	0.03	0.00	0.00	0.11	0.01	0.07	0.01	64.22	0.48	0.00	0.00	0.45	0.00	0.00	0.06	0.00	0.04	0.00				99.99	2010	Pic-06-01A/5 G1
606	34.79	0.00	0.01	0.03	0.09	0.01	0.20	0.00	64.35	0.18	0.00	0.00	0.48	0.03	0.01	0.00	0.00	0.00	0.01				100.20	2010	Pic-06-01A/5 G1
607	34.00	0.04	0.00	0.00	0.14	0.01	0.23	0.01	64.53	0.27	0.00	0.00	0.46	0.00	0.00	0.00	0.00	0.04	0.00				99.72	2010	Pic-06-01A/5 G1
608	32.37	0.00	0.00	0.00	0.11	0.04	0.19	0.00	64.58	0.06	0.00	0.00	0.45	0.00	0.03	0.00	0.01	0.04	0.00				97.87	2010	Pic-06-01A/5 G1
609	34.36	0.09	0.00	0.00	0.04	0.00	0.19	0.05	64.69	0.20	0.00	0.00	0.45	0.04	0.05	0.08	0.00	0.00	0.00				100.24	2010	Pic-06-01A/5 G1
610	34.07	0.11	0.00	0.00	0.03	0.04	0.29	0.00	64.75	0.13	0.00	0.01	0.48	0.13	0.00	0.00	0.00	0.01	0.00				100.04	2010	Pic-06-01A/5 G1
611	34.25	0.00	0.00	0.02	0.04	0.07	0.20	0.00	64.82	0.13	0.00	0.00	0.43	0.01	0.03	0.01	0.00	0.02	0.03				100.06	2010	Pic-06-01A/5 G1
612	34.65	0.00	0.00	0.02	0.15	0.02	0.16	0.00	65.08	0.03	0.00	0.02	0.37	0.07	0.03	0.00	0.00	0.00	0.00				100.61	2010	Pic-06-01A/5 G1
613	34.67	0.19	0.01	0.04	0.03	0.05	0.23	0.02	65.26	0.26	0.00	0.00	0.44	0.10	0.00	0.01	0.00	0.00	0.00				101.28	2010	Pic-06-01A/5 G1
614	30.69	0.04	0.00	0.00	0.12	0.00	0.23	0.00	65.31	0.08	0.00	0.00	0.42	0.04	0.00	0.00	0.00	0.00	0.00				96.92	2010	Pic-06-01A/5 G1
615	35.13	0.03	0.00	0.04	0.08	0.06	0.21	0.00	65.36	0.21	0.00	0.05	0.43	0.00	0.00	0.00	0.00	0.00	0.00				101.72	2010	Pic-06-01A/5 G1
616	31.60	0.00	0.00	0.00	0.10	0.05	0.18	0.00	65.79	0.20	0.00	0.04	0.45	0.11	0.00	0.11	0.00	0.03	0.01				100.27	2010	Pic-06-01A/5 G1
617	34.61	0.00	0.01	0.02	0.01	0.00	0.13	0.01	57.95	1.19	0.00	0.00	0.30	0.00	0.03	3.74	0.00	0.00	0.02				98.02	2010	Pic-06-01A/5 G2
618	34.89	0.00	0.01	0.03	0.08	0.00	0.09	0.00	59.54	0.52	0.00	0.00	0.21	0.00	0.00	0.25	0.00	0.05	0.00				95.66	2010	Pic-06-01A/5 G2
619	35.37	0.00	0.00	0.05	0.05	0.01	0.10	0.01	59.79	0.29	0.00	0.01	0.25	0.15	0.05	0.03	0.00	0.00	0.00				96.15	2010	Pic-06-01A/5 G2
620	34.92	0.00	0.00	0.00	0.08	0.00	0.08	0.04	62.02	1.22	0.00	0.07	0.47	0.03	0.00	0.24	0.00	0.00	0.00				99.17	2010	Pic-06-01A/5 G2
621	34.48	0.00	0.02	0.00	0.09	0.00	0.09	0.01	62.96	1.07	0.00	0.00	0.47	0.03	0.00	0.11	0.00	0.02	0.00				99.24	2010	Pic-06-01A/5 G2
622	34.86	0.00	0.00	0.04	0.01	0.08	0.06	0.03	63.43	1.43	0.00	0.02	0.49	0.06	0.04	0.05	0.00	0.04	0.00				100.63	2010	Pic-06-01A/5 G2
623	35.04	0.04	0.00	0.01	0.03	0.00	0.03	0.00	63.52	1.34	0.00	0.05	0.37	0.00	0.00	0.08	0.00	0.00	0.03				100.54	2010	Pic-06-01A/5 G2
624	33.03	0.22	0.00	0.00	0.11	0.01	0.09	0.03	64.16	0.95	0.00	0.00	0.43	0.07	0.04	0.20	0.00	0.04	0.06				99.43	2010	Pic-06-01A/5 G2
625	32.88	0.10	0.00	0.00	0.07	0.05	0.08	0.02	64.61	0.64	0.00	0.00	0.47	0.01	0.01	0.03	0.00	0.07	0.00				99.03	2010	Pic-06-01A/5 G2
626	32.55	0.00	0.00	0.00	0.03	0.01	0.08	0.00	64.78	0.49	0.00	0.07	0.51	0.00	0.00	0.03	0.00	0.00	0.00				98.55	2010	Pic-06-01A/5 G2
627	31.90	0.02	0.00	0.05	0.14	0																			

INDEX	No.	O	Na	K	V	Co	Mg	P	Cr	Fe	Al	S	Ni	Mn	Si	Pb	Cu	Ti	Ca	Zn	Ba	Sr	Total	Year	Sample
720	34.04	0.00	0.01	0.00	0.05	0.05	0.25	0.01	60.06	0.71		0.00	0.00	0.52	0.00	0.00	0.05	0.00	0.06	0.00			95.80	2010	Pic-06-01B/3
721	37.00	0.00	0.00	0.00	0.09	0.03	0.21	0.00	60.08	0.18		0.00	0.01	0.49	0.04	0.00	0.07	0.00	0.06	0.03			98.28	2010	Pic-06-01B/3
722	36.33	0.05	0.01	0.08	0.03	0.04	0.14	0.00	60.11	0.80		0.05	0.02	0.38	0.00	0.00	0.00	0.00	0.02	0.00			98.06	2010	Pic-06-01B/3
723	34.99	0.01	0.00	0.00	0.05	0.03	0.24	0.01	60.24	0.62		0.00	0.01	0.42	0.00	0.00	0.08	0.00	0.00	0.00			96.69	2010	Pic-06-01B/3
724	37.29	0.00	0.01	0.08	0.14	0.00	0.37	0.00	59.02	1.08		0.03	0.05	0.23	0.00	0.00	0.13	0.00	0.00	0.12			98.59	2010	Pic-06-01B/5
725	34.70	0.01	0.03	0.01	0.09	0.00	0.28	0.00	55.42	0.96		0.01	0.06	0.22	0.04	0.00	0.02	0.00	0.00	0.00	0.02		91.86	2010	Pic-06-01B/5
726	35.45	0.00	0.01	0.02	0.02	0.00	0.26	0.00	57.47	0.93		0.00	0.00	0.23	0.12	0.02	0.01	0.00	0.00	0.00			94.54	2010	Pic-06-01B/5
727	37.31	0.01	0.00	0.00	0.03	0.00	0.25	0.01	57.64	0.75		0.00	0.00	0.30	0.00	0.00	0.02	0.00	0.03	0.03			96.37	2010	Pic-06-01B/5
728	36.86	0.00	0.00	0.00	0.09	0.00	0.26	0.01	57.72	0.81		0.00	0.02	0.24	0.06	0.00	0.06	0.00	0.00	0.00			96.14	2010	Pic-06-01B/5
729	35.59	0.00	0.00	0.07	0.04	0.00	0.27	0.00	57.78	0.69		0.00	0.00	0.28	0.00	0.00	0.07	0.00	0.01	0.00			94.80	2010	Pic-06-01B/5
730	36.35	0.01	0.00	0.00	0.03	0.00	0.28	0.00	57.88	0.86		0.00	0.03	0.24	0.02	0.00	0.05	0.00	0.02	0.01			95.78	2010	Pic-06-01B/5
731	36.19	0.05	0.00	0.01	0.09	0.02	0.32	0.02	58.24	0.90		0.00	0.05	0.25	0.08	0.04	0.04	0.00	0.02	0.03			96.33	2010	Pic-06-01B/5
732	36.33	0.00	0.01	0.00	0.11	0.02	0.28	0.00	58.27	0.95		0.04	0.00	0.25	0.02	0.03	0.04	0.00	0.06	0.00			96.41	2010	Pic-06-01B/5
733	30.53	0.00	0.00	0.05	0.06	0.02	0.42	0.03	58.27	0.47		0.00	0.00	0.30	0.06	0.00	0.04	0.00	0.00	0.02			90.27	2010	Pic-06-01B/5
734	36.73	0.02	0.00	0.00	0.07	0.00	0.21	0.01	58.30	0.65		0.00	0.05	0.30	0.01	0.01	0.03	0.00	0.02	0.00			96.42	2010	Pic-06-01B/5
735	37.22	0.00	0.00	0.00	0.09	0.02	0.21	0.00	58.33	0.62		0.00	0.00	0.28	0.00	0.00	0.07	0.00	0.02	0.00			96.86	2010	Pic-06-01B/5
736	37.18	0.00	0.01	0.00	0.06	0.02	0.22	0.00	58.61	0.63		0.01	0.00	0.31	0.09	0.09	0.03	0.00	0.09	0.00			97.32	2010	Pic-06-01B/5
737	35.69	0.03	0.01	0.00	0.00	0.01	0.24	0.00	58.79	0.71		0.01	0.00	0.36	0.00	0.00	0.14	0.00	0.00	0.01			96.00	2010	Pic-06-01B/5
738	36.34	0.01	0.00	0.02	0.04	0.01	0.21	0.00	58.81	0.47		0.00	0.01	0.35	0.16	0.01	0.12	0.00	0.00	0.05			96.61	2010	Pic-06-01B/5
739	35.60	0.01	0.00	0.00	0.06	0.05	0.35	0.00	58.86	0.81		0.00	0.05	0.28	0.04	0.04	0.26	0.00	0.00	0.07			96.47	2010	Pic-06-01B/5
740	34.52	0.05	0.00	0.05	0.05	0.00	0.16	0.04	58.89	0.60		0.00	0.00	0.31	0.08	0.04	0.01	0.00	0.00	0.00			94.79	2010	Pic-06-01B/5
741	36.51	0.05	0.00	0.00	0.08	0.00	0.20	0.00	58.94	0.59		0.00	0.00	0.28	0.06	0.01	0.01	0.00	0.00	0.02			96.75	2010	Pic-06-01B/5
742	36.44	0.01	0.00	0.00	0.08	0.00	0.37	0.04	58.97	0.91		0.01	0.02	0.25	0.10	0.02	0.13	0.00	0.00	0.00			97.35	2010	Pic-06-01B/5
743	33.14	0.00	0.01	0.04	0.08	0.00	0.28	0.00	58.99	0.88		0.06	0.00	0.26	0.00	0.00	0.00	0.00	0.00	0.00			93.72	2010	Pic-06-01B/5
744	36.77	0.00	0.01	0.04	0.06	0.03	0.34	0.05	59.00	0.63		0.00	0.00	0.28	0.13	0.00	0.15	0.00	0.03	0.00			97.51	2010	Pic-06-01B/5
745	35.10	0.05	0.02	0.00	0.01	0.03	0.28	0.00	59.04	0.49		0.06	0.00	0.38	0.11	0.01	0.04	0.00	0.00	0.00			95.61	2010	Pic-06-01B/5
746	36.53	0.02	0.01	0.03	0.09	0.02	0.21	0.05	59.04	0.55		0.00	0.03	0.37	0.00	0.00	0.00	0.00	0.00	0.00			96.95	2010	Pic-06-01B/5
747	35.22	0.00	0.00	0.00	0.01	0.00	0.29	0.00	59.09	0.61		0.00	0.00	0.28	0.00	0.00	0.00	0.00	0.00	0.00			95.86	2010	Pic-06-01B/5
748	33.96	0.02	0.00	0.00	0.03	0.00	0.17	0.00	59.22	0.50		0.00	0.05	0.31	0.13	0.00	0.06	0.00	0.06	0.00			94.50	2010	Pic-06-01B/5
749	35.80	0.00	0.00	0.00	0.06	0.00	0.21	0.00	59.24	0.63		0.00	0.02	0.34	0.09	0.05	0.00	0.00	0.08	0.00			96.52	2010	Pic-06-01B/5
750	34.76	0.00	0.00	0.00	0.13	0.05	0.20	0.00	59.32	0.64		0.03	0.03	0.32	0.02	0.03	0.14	0.00	0.03	0.02			95.71	2010	Pic-06-01B/5
751	34.65	0.00	0.02	0.03	0.08	0.04	0.25	0.01	59.33	0.78		0.01	0.00	0.36	0.00	0.00	0.01	0.00	0.00	0.03			95.59	2010	Pic-06-01B/5
752	36.08	0.00	0.00	0.00	0.05	0.05	0.35	0.00	59.38	0.67		0.00	0.00	0.32	0.09	0.00	0.12	0.00	0.01	0.00			97.12	2010	Pic-06-01B/5
753	35.73	0.00	0.01	0.00	0.05	0.04	0.21	0.00	59.39	0.54		0.00	0.00	0.35	0.00	0.02	0.04	0.00	0.00	0.00			96.47	2010	Pic-06-01B/5
754	36.04	0.00	0.00	0.03	0.08	0.00	0.21	0.00	59.41	0.69		0.07	0.01	0.34	0.02	0.02	0.01	0.00	0.04	0.00			96.97	2010	Pic-06-01B/5
755	35.93	0.00	0.00	0.00	0.09	0.01	0.21	0.01	59.46	0.62		0.00	0.07	0.35	0.00	0.08	0.03	0.00	0.01	0.04			96.91	2010	Pic-06-01B/5
756	34.83	0.03	0.00	0.00	0.07	0.04	0.24	0.01	59.46	0.72		0.00	0.07	0.37	0.00	0.00	0.01	0.00	0.05	0.04			95.95	2010	Pic-06-01B/5
757	35.40	0.01	0.00	0.00	0.04	0.00	0.25	0.04	59.47	0.67		0.02	0.05	0.33	0.06	0.00	0.04	0.00	0.01	0.02			96.41	2010	Pic-06-01B/5
758	36.60	0.00	0.00	0.00	0.07	0.03	0.24	0.00	59.47	0.49		0.00	0.06	0.35	0.00	0.03	0.05	0.00	0.01	0.04			97.43	2010	Pic-06-01B/5
759	35.94	0.10	0.00	0.00	0.00	0.00	0.17	0.02	59.56	0.61		0.00	0.03	0.35	0.00	0.03	0.00	0.00	0.00	0.00			96.99	2010	Pic-06-01B/5
760	35.35	0.05	0.04	0.00	0.06	0.00	0.20	0.02	59.58	0.66		0.00	0.00	0.35	0.00	0.03	0.04	0.00	0.07	0.00			96.43	2010	Pic-06-01B/5
761	35.45	0.02	0.00	0.00	0.03	0.03	0.21	0.01	59.63	0.65		0.02	0.04	0.34	0.12	0.05	0.00	0.00	0.01	0.00			96.62	2010	Pic-06-01B/5
762	34.54	0.00	0.00	0.04	0.07	0.01	0.21	0.00	59.72	0.46		0.03	0.03	0.36	0.00	0.00	0.14	0.00	0.02	0.00			95.62	2010	Pic-06-01B/5
763	34.49	0.02	0.00	0.00	0.04	0.03	0.17	0.03	59.72	0.64		0.00	0.01	0.34	0.00	0.00	0.05	0.00	0.00	0.01			95.53	2010	Pic-06-01B/5
764	36.52	0.00	0.02	0.11	0.07	0.02	0.20	0.02	59.82	0.62		0.01	0.01	0.37	0.04	0.00	0.00	0.00	0.03	0.03			97.88	2010	Pic-06-01B/5
765	35.27	0.00	0.00	0.00	0.15	0.02	0.27	0.00	59.98	0.49		0.00	0.02	0.37	0.00	0.05	0.17	0.00	0.05	0.04			96.87	2010	Pic-06-01B/5
766	36.24	0.00	0.00	0.01	0.05	0.01	0.25	0.06	59.99	0.53		0.00	0.00	0.40	0.04	0.00	0.10	0.00	0.13	0.00			97.80	2010	Pic-06-01B/5
767	35.44	0.02	0.00	0.00	0.06	0.00	0.20	0.00	60.07	0.42		0.00	0.00	0.37	0.09	0.02	0.09	0.00	0.00	0.03			96.81	2010	Pic-06-01B/5
768	35.45	0.03	0.02	0.00	0.04	0.00	0.26	0.00	60.17	0.82		0.02	0.00	0.35	0.00	0.00	0.08	0.00	0.06	0.07			97.35	2010	Pic-06-01B/5
769	35.85	0.00	0.00	0.00	0.07	0.02	0.22	0.04	60.18	0.75		0.00	0.01	0.34	0.00	0.04	0.01	0.00	0.00	0.00			97.50	2010	Pic-06-01B/5
770	34.45	0.03	0.00	0.00	0.05	0.02	0.28	0.02	60.20	0.47		0.01	0.00	0.34	0.14	0.00	0.22	0.00	0.00	0.00			96.23	2010	Pic-06-01B/5
771	34.96	0.04	0.00	0.00	0.06	0.00	0.22	0.00	60.25	0.50		0.00	0.03	0.38	0.00	0.06	0.15								

INDEX	No.	O	Na	K	V	Co	Mg	P	Cr	Fe	Al	S	Ni	Mn	Si	Pb	Cu	Ti	Ca	Zn	Ba	Sr	Total	Year	Sample
864	33.46	0.04	0.01	0.00	0.08	0.02	0.05	0.02	58.09	0.81			0.00	0.00	0.36	0.01	0.03	0.07	0.00	0.12	0.02		93.19	2010	Pic-06-08/8
865	34.41	0.00	0.00	0.05	0.04	0.05	0.08	0.00	58.10	0.81			0.05	0.02	0.34	0.00	0.05	0.04	0.00	0.09	0.10		94.22	2010	Pic-06-08/8
866	33.67	0.00	0.00	0.01	0.05	0.02	0.07	0.00	58.12	0.63			0.00	0.06	0.32	0.00	0.00	0.14	0.00	0.11	0.00		93.20	2010	Pic-06-08/8
867	34.48	0.04	0.04	0.05	0.01	0.05	0.01	58.45	0.59				0.00	0.03	0.35	0.00	0.00	0.01	0.00	0.09	0.00		94.20	2010	Pic-06-08/8
868	33.74	0.00	0.02	0.00	0.12	0.00	0.06	58.48	0.34				0.00	0.03	0.34	0.00	0.00	0.06	0.00	0.04	0.00		93.22	2010	Pic-06-08/8
869	34.97	0.00	0.00	0.05	0.04	0.06	0.05	58.59	0.70				0.01	0.01	0.34	0.00	0.02	0.25	0.00	0.00	0.00		95.10	2010	Pic-06-08/8
870	32.87	0.02	0.00	0.02	0.03	0.02	0.08	58.68	0.56				0.01	0.03	0.34	0.09	0.02	0.03	0.00	0.01	0.01		92.82	2010	Pic-06-08/8
871	31.92	0.05	0.00	0.00	0.00	0.04	0.08	58.69	0.28				0.00	0.00	0.36	0.07	0.00	0.09	0.00	0.00	0.03		91.63	2010	Pic-06-08/8
872	35.08	0.00	0.00	0.00	0.07	0.02	0.09	58.85	0.62				0.00	0.05	0.31	0.00	0.00	0.00	0.00	0.00	0.00		95.09	2010	Pic-06-08/8
873	31.42	0.00	0.00	0.00	0.03	0.03	0.00	58.99	0.68				0.00	0.03	0.36	0.00	0.03	0.00	0.00	0.00	0.01		91.76	2010	Pic-06-08/8
874	30.43	0.05	0.00	0.05	0.08	0.04	0.07	59.22	0.26				0.00	0.00	0.37	0.00	0.01	0.00	0.01	0.00	0.00		90.64	2010	Pic-06-08/8
875	33.64	0.00	0.00	0.07	0.07	0.02	0.10	59.29	0.52				0.02	0.06	0.35	0.00	0.01	0.00	0.00	0.00	0.00		94.15	2010	Pic-06-08/8
876	32.29	0.01	0.00	0.00	0.05	0.02	0.08	59.37	0.41				0.04	0.00	0.32	0.12	0.00	0.03	0.00	0.00	0.03		92.77	2010	Pic-06-08/8
877	30.83	0.04	0.03	0.03	0.03	0.04	0.09	59.58	0.29				0.00	0.02	0.37	0.00	0.09	0.01	0.00	0.00	0.05		91.49	2010	Pic-06-08/8
878	31.69	0.00	0.00	0.03	0.08	0.01	0.04	59.69	0.16				0.02	0.04	0.32	0.00	0.07	0.04	0.00	0.01	0.13		92.31	2010	Pic-06-08/8
879	29.47	0.03	0.00	0.07	0.07	0.05	0.06	59.82	0.22				0.00	0.00	0.36	0.00	0.00	0.00	0.01	0.01	0.00		90.19	2010	Pic-06-08/8
880	31.42	0.04	0.00	0.00	0.05	0.03	0.09	59.93	0.23				0.00	0.01	0.34	0.03	0.00	0.00	0.00	0.00	0.00		92.17	2010	Pic-06-08/8
881	33.75	0.01	0.00	0.05	0.16	0.02	0.05	59.94	0.15				0.00	0.00	0.41	0.00	0.04	0.08	0.00	0.03	0.00		94.70	2010	Pic-06-08/8
882	29.21	0.00	0.00	0.00	0.07	0.07	0.10	60.00	0.18				0.00	0.00	0.35	0.06	0.00	0.01	0.00	0.00	0.04		90.09	2010	Pic-06-08/8
883	29.63	0.00	0.00	0.00	0.07	0.04	0.06	60.11	0.20				0.00	0.03	0.35	0.04	0.00	0.13	0.00	0.00	0.00		90.65	2010	Pic-06-08/8
884	29.88	0.04	0.00	0.00	0.01	0.05	0.04	60.14	0.25				0.00	0.03	0.36	0.00	0.02	0.02	0.03	0.00	0.00		90.86	2010	Pic-06-08/8
885	30.64	0.08	0.00	0.00	0.04	0.05	0.11	60.43	0.21				0.00	0.00	0.36	0.11	0.00	0.01	0.00	0.00	0.00		92.86	2010	Pic-06-08/8
886	34.42	0.05	0.00	0.00	0.11	0.01	0.03	60.49	0.15				0.00	0.00	0.40	0.00	0.01	0.00	0.00	0.20	0.06		95.94	2010	Pic-06-08/8
887	30.47	0.00	0.00	0.00	0.07	0.06	0.07	60.64	0.23				0.00	0.05	0.33	0.08	0.00	0.00	0.00	0.00	0.06		92.06	2010	Pic-06-08/8
888	30.51	0.02	0.00	0.00	0.08	0.01	0.09	60.96	0.22				0.00	0.02	0.34	0.05	0.00	0.01	0.00	0.04	0.07		92.42	2010	Pic-06-08/8
889	31.01	0.06	0.00	0.00	0.06	0.03	0.08	61.16	0.20				0.02	0.05	0.35	0.00	0.00	0.00	0.00	0.00	0.00		93.04	2010	Pic-06-08/8
890	31.69	0.00	0.02	0.00	0.08	0.06	0.09	62.73	0.22				0.00	0.02	0.39	0.15	0.04	0.01	0.00	0.05	0.00		95.56	2010	Pic-06-08/8
891	35.35	0.01	0.00	0.00	0.00	0.00	0.11	63.40	0.29	0.05			0.00	0.02	0.40	0.00	0.00	0.00	0.00	0.00	0.00		94.52	2010	Pic-06-23/1
892	35.32	0.04	0.02	0.01	0.04	0.03	0.02	60.58	0.11	0.05			0.01	0.00	0.18	0.03	0.00	0.00	0.00	0.06	0.00		94.81	2010	Pic-06-23/1
893	36.38	0.08	0.01	0.06	0.09	0.06	0.02	59.93	0.65	0.00			0.00	0.00	0.28	0.00	0.00	0.00	0.00	0.00	0.00		97.59	2010	Pic-06-23/1
894	35.12	0.00	0.00	0.02	0.02	0.00	0.03	60.18	0.59	0.00			0.00	0.02	0.00	0.24	0.00	0.00	0.00	0.01	0.05		96.28	2010	Pic-06-23/1
895	32.79	0.03	0.00	0.01	0.05	0.04	0.06	60.85	0.88	0.15	0.00		0.00	0.00	0.38	0.04	0.00	0.00	0.00	0.00	0.00		95.28	2010	Pic-06-23/1
896	33.74	0.06	0.01	0.00	0.05	0.04	0.03	60.86	0.62	0.13	0.00		0.00	0.00	0.30	0.04	0.00	0.00	0.00	0.06	0.00		95.94	2010	Pic-06-23/1
897	35.25	0.00	0.00	0.00	0.08	0.01	0.05	61.31	0.77	0.15	0.00		0.00	0.00	0.32	0.03	0.00	0.00	0.00	0.00	0.04		97.76	2010	Pic-06-23/1
898	36.05	0.05	0.00	0.01	0.05	0.00	0.04	61.06	0.75	0.00	0.00		0.00	0.00	0.27	0.00	0.02	0.00	0.00	0.00	0.00		98.30	2010	Pic-06-23/1
899	35.06	0.05	0.01	0.01	0.10	0.06	0.07	61.17	0.60	0.00	0.00		0.00	0.00	0.33	0.06	0.05	0.01	0.00	0.11	0.00		97.70	2010	Pic-06-23/1
900	32.34	0.00	0.00	0.00	0.04	0.00	0.03	61.20	0.77	0.11	0.00		0.00	0.00	0.30	0.06	0.01	0.00	0.00	0.10	0.00		94.96	2010	Pic-06-23/1
901	35.31	0.00	0.00	0.04	0.08	0.04	0.04	61.25	0.53	0.00	0.00		0.00	0.00	0.30	0.00	0.00	0.02	0.00	0.02	0.00		97.65	2010	Pic-06-23/1
902	34.73	0.11	0.01	0.04	0.07	0.00	0.08	61.29	0.70	0.00	0.03	0.00		0.00	0.30	0.02	0.00	0.00	0.00	0.00	0.04		97.40	2010	Pic-06-23/1
903	35.08	0.04	0.12	0.04	0.04	0.04	0.03	61.32	0.68	0.00	0.04		0.00	0.00	0.34	0.17	0.00	0.01	0.01	0.08	0.04		98.08	2010	Pic-06-23/1
904	34.66	0.00	0.01	0.00	0.08	0.00	0.05	61.33	0.81	0.00	0.00		0.00	0.00	0.34	0.04	0.03	0.00	0.00	0.00	0.04		97.39	2010	Pic-06-23/1
905	34.24	0.03	0.01	0.00	0.05	0.04	0.06	61.35	0.61	0.00	0.00		0.00	0.00	0.34	0.15	0.00	0.03	0.00	0.12	0.00		97.02	2010	Pic-06-23/1
906	35.42	0.00	0.00	0.00	0.11	0.00	0.05	61.43	0.75	0.12	0.00		0.00	0.00	0.29	0.06	0.09	0.00	0.00	0.00	0.02		98.34	2010	Pic-06-23/1
907	35.33	0.07	0.01	0.00	0.04	0.00	0.06	61.44	0.63	0.00	0.00		0.00	0.00	0.30	0.00	0.04	0.00	0.00	0.00	0.01		97.95	2010	Pic-06-23/1
908	35.06	0.00	0.00	0.00	0.10	0.07	0.02	61.46	0.61	0.00	0.02	0.00		0.00	0.28	0.05	0.00	0.00	0.00	0.01	0.00		97.71	2010	Pic-06-23/1
909	31.66	0.00	0.00	0.00	0.00	0.00	0.10	61.47	0.82	0.15	0.00		0.00	0.00	0.39	0.06	0.00	0.00	0.00	0.04	0.02		94.83	2010	Pic-06-23/1
910	32.89	0.14	0.00	0.05	0.10	0.04	0.03	61.63	1.14	0.14	0.00		0.00	0.00	0.27	0.00	0.00	0.01	0.00	0.00	0.00		96.45	2010	Pic-06-23/1
911	32.44	0.00	0.00	0.00	0.04	0.00	0.06	61.64	0.92	0.09	0.01	0.00		0.00	0.30	0.00	0.04	0.00	0.00	0.07	0.04		95.67	2010	Pic-06-23/1
912	34.00	0.06	0.00	0.06	0.05	0.03	0.03	61.71	0.82	0.00	0.04		0.00	0.00	0.31	0.01	0.00	0.00	0.00	0.00	0.00		97.15	2010	Pic-06-23/1
913	34.29	0.05	0.01	0.00	0.11	0.07	0.05	61.73	0.73	0.00	0.03	0.00		0.00	0.32	0.07	0.03	0.01	0.00	0.05	0.04		97.59	2010	Pic-06-23/1
914	35.07	0.17	0.00	0.05	0.11	0.00	0.04	61.75	0.76	0.00	0.00		0.00	0.00	0.29	0.06	0.02	0.00	0.00	0.00	0.00		98.32	2010	Pic-06-23/1
915	34.10	0.00	0.00	0.00	0.00	0.00	0.01	61.96	0.91	0.00	0.00		0.00	0.00	0.27	0.00	0.00	0.00	0.00	0.00	0.00		97.33	2010	Pic-06-23/1</

INDEX	No.	O	Na	K	V	Co	Mg	P	Cr	Fe	Al	S	Ni	Mn	Si	Pb	Cu	Ti	Ca	Zn	Ba	Sr	Total	Year	Sample
1008	34.94	0.08	0.01	0.01	0.07	0.00	0.48	0.02	57.54	0.96	0.00	0.03	0.01	0.08	0.06	0.00	0.00	0.00	0.00	0.00	0.00	0.00	94.29	2010	Pic-06-27/2
1009	35.37	0.08	0.02	0.01	0.01	0.01	0.31	0.02	57.56	0.40	0.00	0.00	0.10	0.07	0.00	0.00	0.06	0.00	0.03	0.00	0.00	0.00	94.03	2010	Pic-06-27/2
1010	35.99	0.00	0.00	0.00	0.07	0.03	0.62	0.02	57.58	0.64	0.03	0.05	0.07	0.00	0.00	0.00	0.00	0.04	0.04	0.01	0.00	0.00	95.13	2010	Pic-06-27/2
1011	35.80	0.00	0.01	0.00	0.03	0.01	0.16	0.00	57.58	0.71	0.01	0.00	0.07	0.11	0.00	0.00	0.00	0.00	0.05	0.01	0.00	0.00	94.63	2010	Pic-06-27/2
1012	35.12	0.00	0.00	0.00	0.07	0.00	0.45	0.00	57.58	0.89	0.04	0.00	0.08	0.01	0.11	0.00	0.00	0.00	0.00	0.00	0.00	0.00	94.36	2010	Pic-06-27/2
1013	36.13	0.02	0.01	0.00	0.06	0.00	0.60	0.00	57.63	0.61	0.00	0.00	0.05	0.09	0.00	0.04	0.00	0.15	0.00	0.00	0.00	0.00	95.40	2010	Pic-06-27/2
1014	35.52	0.02	0.00	0.00	0.08	0.02	0.43	0.00	57.67	0.32	0.01	0.06	0.11	0.05	0.00	0.02	0.00	0.06	0.03	0.00	0.00	0.00	94.39	2010	Pic-06-27/2
1015	35.50	0.00	0.00	0.00	0.11	0.00	0.63	0.00	57.67	0.62	0.00	0.02	0.07	0.00	0.00	0.00	0.00	0.02	0.02	0.00	0.00	0.00	94.66	2010	Pic-06-27/2
1016	35.13	0.00	0.00	0.04	0.06	0.05	0.36	0.01	57.71	0.69	0.00	0.02	0.11	0.03	0.03	0.00	0.00	0.03	0.03	0.00	0.00	0.00	94.27	2010	Pic-06-27/2
1017	35.74	0.00	0.00	0.05	0.03	0.03	0.67	0.00	57.75	0.00	0.00	0.00	0.08	0.11	0.00	0.00	0.00	0.57	0.02	0.00	0.00	0.00	95.16	2010	Pic-06-27/2
1018	36.41	0.01	0.00	0.03	0.04	0.00	0.71	0.00	57.79	0.50	0.00	0.02	0.05	0.05	0.09	0.02	0.00	0.00	0.00	0.00	0.00	0.00	95.72	2010	Pic-06-27/2
1019	36.05	0.02	0.01	0.00	0.04	0.00	0.68	0.00	57.81	0.56	0.06	0.00	0.07	0.00	0.04	0.08	0.00	0.00	0.03	0.00	0.00	0.00	95.42	2010	Pic-06-27/2
1020	36.76	0.03	0.01	0.03	0.09	0.00	0.56	0.02	57.82	0.84	0.00	0.05	0.06	0.05	0.00	0.00	0.00	0.06	0.03	0.00	0.00	0.00	96.42	2010	Pic-06-27/2
1021	34.09	0.02	0.00	0.06	0.08	0.02	0.46	0.00	57.83	0.77	0.00	0.00	0.08	0.00	0.08	0.03	0.00	0.00	0.00	0.02	0.00	0.00	93.53	2010	Pic-06-27/2
1022	35.95	0.05	0.01	0.01	0.06	0.00	0.30	0.03	57.86	0.77	0.01	0.03	0.07	0.00	0.09	0.14	0.00	0.00	0.00	0.00	0.00	0.00	95.35	2010	Pic-06-27/2
1023	35.10	0.00	0.00	0.06	0.08	0.02	0.26	0.00	57.91	0.10	0.03	0.00	0.12	0.00	0.00	0.02	0.00	0.04	0.00	0.00	0.00	0.00	92.73	2010	Pic-06-27/2
1024	35.46	0.05	0.00	0.01	0.03	0.00	0.30	0.03	58.11	0.46	0.02	0.00	0.10	0.03	0.00	0.00	0.00	0.04	0.03	0.00	0.00	0.00	94.67	2010	Pic-06-27/2
1025	35.88	0.00	0.01	0.01	0.12	0.00	0.43	0.02	58.12	0.45	0.00	0.03	0.09	0.03	0.02	0.02	0.00	0.04	0.00	0.00	0.00	0.00	95.25	2010	Pic-06-27/2
1026	35.57	0.07	0.00	0.04	0.08	0.02	0.34	0.00	58.13	0.14	0.00	0.04	0.10	0.00	0.00	0.03	0.03	0.01	0.03	0.00	0.00	0.00	94.61	2010	Pic-06-27/2
1027	34.90	0.00	0.01	0.03	0.09	0.00	0.13	0.00	58.28	0.05	0.00	0.00	0.10	0.05	0.01	0.00	0.00	0.04	0.00	0.00	0.00	0.00	93.68	2010	Pic-06-27/2
1028	35.77	0.08	0.00	0.05	0.04	0.00	0.37	0.00	58.30	0.76	0.04	0.00	0.09	0.00	0.05	0.09	0.00	0.12	0.00	0.00	0.00	0.00	95.75	2010	Pic-06-27/2
1029	35.45	0.04	0.00	0.06	0.14	0.00	0.09	0.00	58.33	0.07	0.03	0.08	0.09	0.06	0.00	0.00	0.00	0.03	0.04	0.00	0.00	0.00	94.50	2010	Pic-06-27/2
1030	36.46	0.00	0.00	0.08	0.01	0.01	0.36	0.03	58.34	0.25	0.01	0.00	0.11	0.03	0.05	0.00	0.00	0.03	0.06	0.00	0.00	0.00	95.82	2010	Pic-06-27/2
1031	34.79	0.07	0.00	0.02	0.05	0.06	0.47	0.00	58.42	0.45	0.00	0.01	0.07	0.06	0.01	0.00	0.00	0.00	0.00	0.00	0.00	0.00	94.47	2010	Pic-06-27/2
1032	35.55	0.02	0.00	0.00	0.09	0.00	0.30	0.00	58.45	0.19	0.01	0.07	0.12	0.00	0.01	0.07	0.00	0.00	0.00	0.00	0.00	0.00	94.88	2010	Pic-06-27/2
1033	36.10	0.00	0.00	0.00	0.04	0.02	0.41	0.00	58.56	0.40	0.00	0.09	0.09	0.00	0.00	0.00	0.00	0.00	0.06	0.00	0.00	0.00	95.77	2010	Pic-06-27/2
1034	35.87	0.02	0.01	0.00	0.08	0.01	0.28	0.01	58.69	0.27	0.06	0.00	0.09	0.05	0.10	0.00	0.00	0.00	0.00	0.00	0.00	0.00	95.52	2010	Pic-06-27/2
1035	36.91	0.04	0.00	0.00	0.03	0.01	0.42	0.00	58.78	0.58	0.03	0.00	0.03	0.01	0.02	0.00	0.00	0.00	0.00	0.00	0.00	0.00	97.21	2010	Pic-06-27/2
1036	35.07	0.00	0.00	0.02	0.00	0.01	0.14	0.00	58.79	0.01	0.01	0.00	0.20	0.11	0.00	0.02	0.00	0.00	0.00	0.00	0.00	0.00	94.38	2010	Pic-06-27/2
1037	34.50	0.01	0.01	0.05	0.03	0.00	0.07	0.00	58.93	0.05	0.00	0.00	0.16	0.09	0.00	0.02	0.00	0.00	0.00	0.00	0.00	0.00	93.91	2010	Pic-06-27/2
1038	35.37	0.10	0.00	0.00	0.02	0.01	0.10	0.00	59.00	0.02	0.00	0.00	0.17	0.16	0.03	0.00	0.00	0.03	0.00	0.00	0.00	0.00	95.00	2010	Pic-06-27/2
1039	34.48	0.09	0.00	0.04	0.12	0.00	0.11	0.03	59.11	0.03	0.00	0.11	0.23	0.00	0.08	0.05	0.00	0.04	0.04	0.00	0.00	0.00	94.54	2010	Pic-06-27/2
1040	35.61	0.00	0.03	0.00	0.09	0.00	0.10	0.00	59.32	0.04	0.00	0.00	0.13	0.01	0.06	0.02	0.00	0.03	0.00	0.00	0.00	0.00	95.43	2010	Pic-06-27/2
1041	35.17	0.00	0.00	0.00	0.09	0.44	0.57	0.06	59.00	1.79	0.00	0.01	3.16	0.10	0.00	0.00	0.00	0.02	0.00	0.00	0.00	0.00	94.41	2010	Pic-06-27/4
1042	35.11	0.01	0.00	0.00	0.09	0.00	0.36	0.02	56.61	0.42	0.03	0.00	0.14	0.00	0.00	0.00	0.00	0.00	0.00	0.00	0.00	0.00	92.79	2010	Pic-06-27/4
1043	35.75	0.00	0.00	0.02	0.09	0.01	0.39	0.05	57.01	0.33	0.00	0.00	0.11	0.00	0.01	0.06	0.00	0.01	0.00	0.00	0.00	0.00	93.83	2010	Pic-06-27/4
1044	35.23	0.00	0.00	0.00	0.10	0.03	0.38	0.03	57.22	0.89	0.00	0.06	0.09	0.02	0.00	0.00	0.00	0.05	0.00	0.00	0.00	0.00	94.10	2010	Pic-06-27/4
1045	35.19	0.02	0.02	0.00	0.03	0.01	0.30	0.04	57.37	0.51	0.02	0.00	0.10	0.00	0.02	0.01	0.00	0.00	0.03	0.00	0.00	0.00	93.67	2010	Pic-06-27/4
1046	35.42	0.06	0.00	0.03	0.05	0.00	0.38	0.00	57.38	0.70	0.04	0.00	0.11	0.03	0.00	0.01	0.00	0.00	0.06	0.00	0.00	0.00	94.27	2010	Pic-06-27/4
1047	34.66	0.00	0.00	0.00	0.03	0.01	0.03	0.02	57.42	0.77	0.00	0.00	0.10	0.03	0.00	0.00	0.00	0.08	0.03	0.00	0.00	0.00	93.56	2010	Pic-06-27/4
1048	35.59	0.00	0.00	0.02	0.13	0.00	0.40	0.00	57.49	0.78	0.02	0.00	0.09	0.01	0.00	0.00	0.00	0.02	0.13	0.00	0.00	0.00	94.69	2010	Pic-06-27/4
1049	35.29	0.09	0.00	0.00	0.08	0.02	0.41	0.00	57.62	0.91	0.00	0.05	0.11	0.15	0.01	0.00	0.00	0.05	0.00	0.00	0.00	0.00	94.77	2010	Pic-06-27/4
1050	35.16	0.02	0.01	0.01	0.08	0.01	0.19	0.03	57.63	0.05	0.03	0.00	0.21	0.09	0.02	0.00	0.00	0.10	0.03	0.00	0.00	0.00	93.66	2010	Pic-06-27/4
1051	35.20	0.02	0.00	0.00	0.10	0.01	0.41	0.00	57.74	0.97	0.00	0.01	0.10	0.10	0.00	0.03	0.00	0.01	0.03	0.00	0.00	0.00	94.72	2010	Pic-06-27/4
1052	35.07	0.00	0.00	0.00	0.06	0.08	0.36	0.09	57.88	0.31	0.00	0.00	0.12	0.00	0.00	0.00	0.00	0.00	0.01	0.01	0.00	0.00	93.98	2010	Pic-06-27/4
1053	35.82	0.01	0.00	0.00	0.09	0.00	0.20	0.02	57.90	0.02	0.03	0.00	0.20	0.03	0.00	0.00	0.00	0.00	0.00	0.00	0.00	0.00	94.36	2010	Pic-06-27/4
1054	33.45	0.04	0.00	0.00	0.05	0.00	0.42	0.01	57.90	0.89	0.00	0.00	0.09	0.00	0.00	0.00	0.00	0.00	0.03	0.00	0.00	0.00	92.89	2010	Pic-06-27/4
1055	34.60	0.00	0.00	0.01	0.08	0.00	0.32	0.00	57.91	0.49	0.00	0.00	0.14	0.15	0.04	0.07	0.00	0.06	0.00	0.00	0.00	0.00	93.86	2010	Pic-06-27/4
1056	33.82	0.02	0.01	0.00	0.00	0.02	0.35	0.05	57.95	0.67	0.00	0.01	0.10	0.00	0.03	0.03	0.00	0.03	0.00	0.00	0.00	0.00	93.07	2010	Pic-06-27/4
1057	34.62	0.00	0.01	0.05	0.03	0.05	0.40	0.02	58.03	0.84	0.01	0.02	0.10	0.07	0.00										

INDEX	No.	O	Na	K	V	Co	Mg	P	Cr	Fe	Al	S	Ni	Mn	Si	Pb	Cu	Ti	Ca	Zn	Ba	Sr	Total	Year	Sample
1152	33.68	0.04	0.00	0.00	0.08	0.02	0.00	0.02	59.89	0.09			0.03	0.07	0.34	0.04	0.04	0.00	0.00	0.02	0.02		94.35	2010	Pic602/4
1153	35.15	0.00	0.00	0.00	0.10	0.05	0.01	0.02	59.92	0.39			0.00	0.00	0.32	0.00	0.03	0.00	0.00	0.01	0.00		96.01	2010	Pic602/4
1154	34.55	0.01	0.01	0.00	0.06	0.00	0.07	0.02	60.04	0.44			0.01	0.01	0.34	0.01	0.00	0.07	0.00	0.00	0.00		95.65	2010	Pic602/4
1155	35.35	0.01	0.00	0.06	0.12	0.04	0.00	0.01	60.22	0.37			0.00	0.02	0.30	0.00	0.00	0.00	0.00	0.07	0.00		96.60	2010	Pic602/4
1156	34.41	0.00	0.00	0.03	0.03	0.03	0.00	0.03	60.27	0.56			0.00	0.04	0.26	0.04	0.00	0.02	0.00	0.00	0.00		95.78	2010	Pic602/4
1157	34.49	0.09	0.00	0.00	0.08	0.00	0.00	0.00	60.30	0.35			0.06	0.00	0.25	0.00	0.00	0.00	0.00	0.00	0.00		95.66	2010	Pic602/4
1158	33.71	0.03	0.00	0.00	0.10	0.06	0.02	0.00	60.46	0.51			0.02	0.00	0.27	0.05	0.00	0.00	0.00	0.09	0.00		95.33	2010	Pic602/4
1159	34.15	0.05	0.00	0.02	0.10	0.01	0.01	0.00	60.52	0.53			0.00	0.00	0.27	0.03	0.02	0.02	0.00	0.01	0.02		95.75	2010	Pic602/4
1160	36.47	0.04	0.00	0.00	0.05	0.05	0.04	0.00	60.60	0.54			0.00	0.00	0.33	0.00	0.00	0.08	0.00	0.00	0.00		98.20	2010	Pic602/4
1161	33.06	0.05	0.00	0.02	0.03	0.03	0.02	0.00	60.62	0.57			0.00	0.03	0.31	0.00	0.00	0.04	0.00	0.00	0.00		94.47	2010	Pic602/4
1162	33.99	0.02	0.01	0.00	0.04	0.04	0.01	0.01	60.66	0.40			0.02	0.04	0.26	0.00	0.00	0.00	0.00	0.01	0.00		95.51	2010	Pic602/4
1163	33.19	0.03	0.00	0.00	0.05	0.01	0.02	0.01	60.71	0.25			0.00	0.00	0.27	0.04	0.00	0.03	0.00	0.02	0.03		94.65	2010	Pic602/4
1164	32.31	0.02	0.00	0.00	0.00	0.03	0.04	0.00	60.71	0.25			0.01	0.01	0.28	0.03	0.00	0.00	0.00	0.00	0.00		93.70	2010	Pic602/4
1165	34.05	0.00	0.00	0.00	0.03	0.03	0.01	0.00	60.83	0.51			0.02	0.00	0.27	0.01	0.00	0.04	0.00	0.00	0.00		95.80	2010	Pic602/4
1166	33.07	0.04	0.00	0.01	0.10	0.03	0.04	0.02	60.83	0.44			0.00	0.03	0.30	0.03	0.00	0.00	0.00	0.09	0.08		95.10	2010	Pic602/4
1167	34.00	0.00	0.00	0.11	0.00	0.02	0.00	60.88	0.00				0.00	0.03	0.34	0.00	0.03	0.00	0.00	0.00	0.00		95.41	2010	Pic602/4
1168	35.43	0.00	0.00	0.00	0.01	0.02	0.02	0.01	60.90	0.29			0.01	0.02	0.28	0.00	0.06	0.00	0.00	0.00	0.00		97.03	2010	Pic602/4
1169	34.36	0.07	0.00	0.00	0.08	0.02	0.01	0.02	60.91	0.47			0.00	0.00	0.27	0.06	0.05	0.01	0.00	0.08	0.00		96.40	2010	Pic602/4
1170	33.55	0.09	0.00	0.01	0.06	0.03	0.02	0.00	60.93	0.38			0.01	0.00	0.25	0.00	0.04	0.03	0.00	0.02	0.00		95.43	2010	Pic602/4
1171	33.69	0.08	0.00	0.00	0.04	0.01	0.01	0.01	60.94	0.45			0.00	0.00	0.29	0.00	0.03	0.04	0.00	0.02	0.00		95.61	2010	Pic602/4
1172	34.45	0.05	0.00	0.00	0.06	0.01	0.00	0.00	60.96	0.05			0.00	0.00	0.37	0.00	0.00	0.00	0.00	0.01	0.03		96.01	2010	Pic602/4
1173	33.54	0.04	0.01	0.00	0.07	0.04	0.03	0.01	60.98	0.54			0.03	0.00	0.29	0.00	0.05	0.00	0.00	0.00	0.00		95.62	2010	Pic602/4
1174	33.90	0.00	0.00	0.00	0.05	0.05	0.03	0.01	61.00	0.43			0.01	0.02	0.26	0.02	0.08	0.00	0.00	0.00	0.02		95.88	2010	Pic602/4
1175	33.80	0.01	0.00	0.00	0.06	0.02	0.01	0.00	61.01	0.41			0.00	0.00	0.28	0.05	0.00	0.00	0.00	0.07	0.00		95.71	2010	Pic602/4
1176	33.16	0.00	0.00	0.01	0.02	0.05	0.01	0.00	61.05	0.23			0.02	0.06	0.26	0.02	0.00	0.07	0.00	0.00	0.00		94.96	2010	Pic602/4
1177	33.74	0.00	0.00	0.01	0.08	0.03	0.01	0.02	61.06	0.31			0.00	0.00	0.27	0.08	0.03	0.02	0.00	0.03	0.00		95.69	2010	Pic602/4
1178	34.48	0.00	0.00	0.00	0.04	0.02	0.01	0.01	61.07	0.29			0.00	0.00	0.28	0.05	0.00	0.00	0.00	0.01	0.00		96.26	2010	Pic602/4
1179	32.79	0.03	0.00	0.00	0.00	0.00	0.01	0.02	61.08	0.56			0.00	0.02	0.24	0.00	0.03	0.00	0.00	0.00	0.00		94.83	2010	Pic602/4
1180	31.93	0.02	0.00	0.00	0.08	0.04	0.05	0.00	61.08	0.57			0.00	0.00	0.30	0.02	0.00	0.00	0.00	0.00	0.01		94.11	2010	Pic602/4
1181	32.74	0.00	0.00	0.01	0.04	0.00	0.05	0.00	61.09	0.38			0.00	0.00	0.28	0.03	0.05	0.01	0.00	0.02	0.01		94.71	2010	Pic602/4
1182	33.65	0.03	0.02	0.04	0.04	0.01	0.00	0.02	61.11	0.63			0.00	0.01	0.25	0.00	0.03	0.02	0.00	0.03	0.00		95.89	2010	Pic602/4
1183	33.22	0.00	0.00	0.03	0.04	0.05	0.03	0.00	61.18	0.62			0.00	0.02	0.28	0.00	0.02	0.00	0.00	0.04	0.01		95.54	2010	Pic602/4
1184	33.75	0.00	0.00	0.02	0.03	0.01	0.01	0.01	61.19	0.55			0.00	0.00	0.25	0.05	0.00	0.00	0.00	0.05	0.00		95.92	2010	Pic602/4
1185	34.56	0.08	0.00	0.07	0.00	0.00	0.01	0.00	61.19	0.35			0.01	0.03	0.26	0.04	0.00	0.02	0.00	0.03	0.00		96.61	2010	Pic602/4
1186	34.04	0.12	0.00	0.00	0.09	0.03	0.02	0.00	61.26	0.31			0.00	0.00	0.26	0.03	0.00	0.00	0.00	0.07	0.00		96.23	2010	Pic602/4
1187	38.03	0.05	0.00	0.03	0.07	0.00	0.24	0.00	56.21	2.13			0.00	0.03	0.18	0.00	0.00	0.30	0.00	0.05	0.03		97.36	2010	Pic602/5
1188	37.33	0.03	0.01	0.00	0.07	0.01	0.24	0.02	56.30	2.05			0.00	0.00	0.17	0.02	0.00	0.25	0.00	0.04	0.03		96.57	2010	Pic602/5
1189	35.46	0.02	0.00	0.00	0.10	0.03	0.14	0.00	56.82	1.27			0.01	0.03	0.15	0.10	0.01	0.05	0.00	0.00	0.04		94.23	2010	Pic602/5
1190	36.11	0.05	0.00	0.00	0.02	0.02	0.16	0.00	56.95	1.58			0.00	0.00	0.20	0.01	0.02	0.72	0.00	0.02	0.05		95.92	2010	Pic602/5
1191	35.91	0.00	0.00	0.01	0.00	0.01	0.15	0.00	57.03	1.36			0.00	0.02	0.24	0.05	0.00	0.09	0.00	0.08	0.00		95.01	2010	Pic602/5
1192	35.86	0.00	0.00	0.00	0.04	0.02	0.20	0.00	57.21	1.49			0.00	0.00	0.20	0.00	0.00	0.20	0.00	0.04	0.01		95.26	2010	Pic602/5
1193	37.17	0.02	0.00	0.01	0.06	0.00	0.14	0.00	57.21	1.46			0.00	0.00	0.18	0.00	0.00	0.02	0.00	0.05	0.00		96.32	2010	Pic602/5
1194	37.17	0.05	0.00	0.04	0.08	0.01	0.22	0.00	57.24	1.40			0.00	0.00	0.18	0.00	0.00	0.10	0.00	0.04	0.00		96.54	2010	Pic602/5
1195	37.04	0.00	0.00	0.02	0.06	0.03	0.21	0.03	57.25	1.87			0.00	0.00	0.22	0.03	0.01	0.15	0.00	0.00	0.00		96.93	2010	Pic602/5
1196	35.46	0.03	0.00	0.00	0.02	0.02	0.18	0.00	57.29	1.64			0.03	0.00	0.20	0.00	0.00	0.14	0.00	0.06	0.04		95.10	2010	Pic602/5
1197	36.42	0.02	0.00	0.00	0.00	0.00	0.28	0.02	57.37	1.72			0.00	0.02	0.20	0.05	0.00	0.23	0.00	0.02	0.01		96.40	2010	Pic602/5
1198	37.25	0.02	0.00	0.00	0.06	0.03	0.20	0.02	57.39	1.65			0.00	0.00	0.18	0.02	0.00	0.11	0.00	0.00	0.00		96.94	2010	Pic602/5
1199	37.45	0.00	0.00	0.00	0.04	0.00	0.20	0.02	57.40	1.29			0.00	0.02	0.20	0.00	0.00	0.10	0.00	0.02	0.00		96.73	2010	Pic602/5
1200	35.28	0.03	0.00	0.00	0.10	0.00	0.08	0.00	57.62	1.27			0.00	0.03	0.18	0.00	0.00	0.06	0.00	0.00	0.00		94.65	2010	Pic602/5
1201	36.16	0.00	0.00	0.00	0.11	0.05	0.16	0.04	57.63	1.26			0.00	0.01	0.22	0.03	0.01	0.02	0.00	0.00	0.00		95.69	2010	Pic602/5
1202	35.62	0.00	0.00	0.02	0.04	0.00	0.20	0.01	57.63	1.76			0.00	0.01	0.20	0.00	0.02	0.04	0.00	0.04	0.00		95.60	2010	Pic602/5
1203	35.81	0.00	0.01	0.02	0.09	0.01	0.18	0.00	57.64	1.58			0.01	0.01	0.21	0.05	0.00	0.15	0.00	0.00	0.00		95.81	2010	Pic602/5
1204	36.26	0.02	0.00	0.04	0.10	0.03	0.21	0.00	57.70	1.64			0.05	0.00	0.22	0.04	0.01	0.14	0.00	0.00	0.06		96.54	2010	Pic602/5
1205	35.04	0.00	0.00	0.01	0.08	0.02	0.22	0.01	57.70	1.67			0.00	0.0											

INDEX	No.	O	Na	K	V	Co	Mg	P	Cr	Fe	Al	S	Ni	Mn	Si	Pb	Cu	Ti	Ca	Zn	Ba	Sr	Total	Year	Sample	
1296		35.09	0.00	0.00	0.00	0.08	0.02	0.00	0.00	59.68	0.00	0.00	0.01	0.55	0.06	0.00	0.03	0.01	0.00	0.01			95.54	2010	Pic6602/9	
1297		35.52	0.11	0.00	0.00	0.06	0.03	0.00	0.00	59.69	0.00	0.00	0.03	0.00	0.40	0.00	0.05	0.00	0.00	0.02	0.00		95.90	2010	Pic6602/9	
1298		34.58	0.00	0.00	0.01	0.10	0.04	0.01	0.02	59.71	0.01	0.00	0.00	0.38	0.00	0.00	0.01	0.00	0.00	0.00			94.86	2010	Pic6602/9	
1299		34.84	0.00	0.00	0.00	0.08	0.01	0.00	0.00	59.74	0.00	0.00	0.01	0.53	0.10	0.05	0.00	0.00	0.00	0.00			95.40	2010	Pic6602/9	
1300		31.04	0.00	0.00	0.00	0.01	0.04	0.01	0.02	59.77	0.14	0.00	0.02	0.42	0.05	0.00	0.00	0.02	0.00	0.00			91.59	2010	Pic6602/9	
1301		35.73	0.02	0.00	0.00	0.12	0.00	0.00	0.00	59.81	0.01	0.01	0.05	0.04	0.00	0.00	0.01	0.00	0.01	0.01			95.81	2010	Pic6602/9	
1302		36.57	0.00	0.00	0.00	0.03	0.02	0.03	0.02	59.82	0.00	0.02	0.00	0.29	0.06	0.00	0.00	0.00	0.00	0.00			96.87	2010	Pic6602/9	
1303		34.39	0.05	0.00	0.00	0.09	0.02	0.00	0.00	59.90	0.00	0.00	0.04	0.61	0.00	0.06	0.00	0.00	0.00	0.03			95.19	2010	Pic6602/9	
1304		35.70	0.04	0.00	0.00	0.12	0.02	0.00	0.01	59.94	0.00	0.01	0.04	0.39	0.07	0.01	0.00	0.00	0.05	0.02			96.42	2010	Pic6602/9	
1305		32.65	0.06	0.00	0.00	0.03	0.00	0.05	0.01	59.94	0.00	0.00	0.50	0.02	0.00	0.00	0.00	0.00	0.00	0.00			93.29	2010	Pic6602/9	
1306		35.23	0.00	0.00	0.00	0.07	0.00	0.01	0.00	60.14	0.01	0.00	0.00	0.37	0.02	0.00	0.02	0.00	0.00	0.00			95.86	2010	Pic6602/9	
1307		34.28	0.03	0.00	0.00	0.08	0.03	0.01	0.03	60.15	0.00	0.00	0.03	0.53	0.00	0.06	0.05	0.00	0.00	0.00			95.26	2010	Pic6602/9	
1308		34.17	0.00	0.00	0.00	0.06	0.04	0.04	0.01	60.15	0.00	0.00	0.03	0.52	0.02	0.04	0.02	0.00	0.00	0.04			95.14	2010	Pic6602/9	
1309		32.38	0.00	0.00	0.00	0.05	0.06	0.01	0.00	60.15	0.02	0.00	0.00	0.39	0.00	0.00	0.00	0.00	0.00	0.00			93.07	2010	Pic6602/9	
1310		34.10	0.02	0.00	0.00	0.03	0.01	0.00	0.00	60.18	0.02	0.00	0.00	0.49	0.05	0.00	0.06	0.00	0.07	0.00			95.02	2010	Pic6602/9	
1311		36.22	0.05	0.00	0.04	0.04	0.03	0.01	0.00	60.22	0.01	0.00	0.00	0.00	0.00	0.00	0.00	0.00	0.00	0.00			97.03	2010	Pic6602/9	
1312		37.82	0.00	0.01	0.00	0.05	0.02	0.01	0.03	60.27	0.01	0.00	0.00	0.54	0.05	0.00	0.03	0.05	0.03	0.00			98.87	2010	Pic6602/9	
1313		34.23	0.00	0.00	0.00	0.04	0.03	0.01	0.00	60.40	0.02	0.02	0.04	0.39	0.08	0.06	0.01	0.00	0.03	0.00			95.36	2010	Pic6602/9	
1314		34.64	0.00	0.00	0.00	0.06	0.05	0.03	0.03	60.41	0.91	0.00	0.00	0.29	0.04	0.00	0.00	0.02	0.00	0.00			96.49	2010	Pic6602/9	
1315		34.37	0.00	0.02	0.00	0.05	0.04	0.04	0.01	60.49	0.03	0.00	0.02	0.38	0.02	0.01	0.00	0.00	0.03	0.00			95.49	2010	Pic6602/9	
1316		33.09	0.02	0.00	0.00	0.08	0.04	0.00	0.00	60.51	0.01	0.00	0.02	0.27	0.02	0.00	0.00	0.00	0.03	0.00			94.09	2010	Pic6602/9	
1317		33.82	0.03	0.00	0.02	0.06	0.05	0.05	0.01	60.54	0.88	0.00	0.06	0.23	0.00	0.00	0.06	0.00	0.05	0.00			95.94	2010	Pic6602/9	
1318		34.33	0.00	0.00	0.00	0.07	0.02	0.01	0.00	60.55	0.02	0.00	0.01	0.42	0.00	0.04	0.01	0.01	0.06	0.00			95.58	2010	Pic6602/9	
1319		36.68	0.08	0.01	0.00	0.07	0.00	0.01	0.00	60.55	0.00	0.00	0.05	0.40	0.01	0.02	0.00	0.00	0.00	0.00			97.89	2010	Pic6602/9	
1320		34.82	0.01	0.00	0.00	0.05	0.02	0.02	0.00	60.69	0.00	0.00	0.00	0.48	0.04	0.03	0.01	0.00	0.00	0.03			96.22	2010	Pic6602/9	
1321		33.70	0.02	0.00	0.00	0.07	0.01	0.00	0.00	60.72	0.00	0.00	0.04	0.42	0.08	0.00	0.06	0.00	0.07	0.03			95.22	2010	Pic6602/9	
1322		32.28	0.01	0.00	0.00	0.06	0.04	0.03	0.01	60.74	0.00	0.00	0.02	0.43	0.02	0.03	0.00	0.00	0.00	0.01			93.67	2010	Pic6602/9	
1323		30.50	0.08	0.00	0.00	0.01	0.03	0.01	0.03	60.75	0.26	0.03	0.13	0.03	0.08	0.00	0.04	0.08	0.00	0.00			92.69	2010	Pic6602/9	
1324		33.71	0.04	0.00	0.00	0.06	0.03	0.02	0.01	60.76	0.90	0.00	0.01	0.28	0.01	0.00	0.01	0.01	0.02	0.00			95.86	2010	Pic6602/9	
1325		34.83	0.00	0.01	0.00	0.02	0.04	0.03	0.03	60.81	0.00	0.08	0.00	0.50	0.01	0.00	0.06	0.00	0.04	0.00			96.47	2010	Pic6602/9	
1326		31.85	0.02	0.00	0.00	0.07	0.08	0.03	0.03	60.90	0.00	0.00	0.01	0.48	0.00	0.06	0.02	0.00	0.09	0.01			93.65	2010	Pic6602/9	
1327		34.85	0.08	0.01	0.04	0.02	0.02	0.01	0.01	61.13	0.00	0.01	0.00	0.65	0.03	0.01	0.00	0.00	0.07	0.00			96.94	2010	Pic6602/9	
1328		29.87	0.01	0.01	0.00	0.08	0.06	0.09	0.00	61.21	0.00	0.00	0.03	0.49	0.01	0.00	0.00	0.00	0.00	0.00			91.86	2010	Pic6602/9	
1329		33.15	0.04	0.00	0.02	0.06	0.01	0.00	0.00	61.39	0.00	0.05	0.53	0.06	0.00	0.03	0.00	0.00	0.00	0.00			95.33	2010	Pic6602/9	
1330		33.08	0.04	0.00	0.00	0.05	0.05	0.03	0.01	61.44	0.68	0.00	0.03	0.31	0.00	0.01	0.01	0.00	0.01	0.04			95.77	2010	Pic6602/9	
1331		31.55	0.06	0.00	0.01	0.06	0.05	0.03	0.04	62.27	0.05	0.03	0.00	0.40	0.00	0.04	0.00	0.00	0.05	0.00			94.64	2010	Pic6602/9	
1332		30.15	0.00	0.00	0.00	0.10	0.07	0.03	0.00	62.33	0.11	0.04	0.04	0.48	0.00	0.03	0.00	0.04	0.00	0.00			93.42	2010	Pic6602/9	
1333	9	36.28	0.00	0.01	0.00	0.08	0.26	0.20	0.03	61.83	0.02	0.02	0.12	1.31	0.00	0.02	0.00	0.00	0.04	0.03	0.00			100.33	2014	Acaba mundo
1334	10	37.44	0.00	0.00	0.00	0.22	0.11	0.21	0.00	59.55	0.00	0.00	0.15	1.42	0.03	0.12	0.00	0.00	0.03	0.00			99.29	2014	Acaba mundo	
1335	11	35.80	0.00	0.00	0.00	0.17	0.17	0.18	0.00	61.06	0.04	0.00	0.17	1.07	0.00	0.06	0.00	0.00	0.00	0.00			99.45	2014	Acaba mundo	
1336	12	37.56	0.00	0.00	0.03	0.24	0.08	0.21	0.02	59.49	0.03	0.00	0.11	1.59	0.05	0.06	0.00	0.00	0.00	0.02			99.47	2014	Acaba mundo	
1337	13	36.32	0.01	0.00	0.00	0.24	0.25	0.24	0.00	62.31	0.00	0.02	0.03	1.15	0.05	0.00	0.00	0.00	0.00	0.04			100.65	2014	Acaba mundo	
1338	14	36.92	0.00	0.01	0.00	0.28	0.22	0.08	0.00	60.88	0.04	0.06	0.05	1.11	0.00	0.06	0.00	0.00	0.04	0.03	0.00			99.81	2014	Acaba mundo
1339	15	36.01	0.00	0.00	0.01	0.20	0.11	0.27	0.00	62.67	0.07	0.02	0.04	1.48	0.00	0.00	0.06	0.00	0.00	0.01	0.02			100.97	2014	Acaba mundo
1340	16	37.16	0.00	0.00	0.00	0.16	0.13	0.12	0.04	60.98	0.03	0.00	0.02	1.15	0.06	0.10	0.00	0.00	0.03	0.00			100.16	2014	Acaba mundo	
1341	17	35.65	0.00	0.01	0.01	0.21	0.21	0.21	0.00	61.91	0.15	0.02	0.00	1.16	0.06	0.04	0.00	0.00	0.05	0.00			99.75	2014	Acaba mundo	
1342	48	38.89	0.03	0.00	0.00	0.07	0.00	0.09	0.00	56.54	3.84	0.14	0.00	0.00	0.21	0.00	0.08	0.00	0.00	0.00			99.88	2014	Acaba Mundo	
1343	49	39.18	0.00	0.01	0.00	0.01	0.00	0.12	0.00	57.30	3.68	0.15	0.01	0.00	0.19	0.00	0.00	0.04	0.00	0.01	0.00			100.70	2014	Acaba Mundo
1344	50	39.17	0.00	0.00	0.00	0.02	0.00	0.13	0.00	57.36	3.64	0.13	0.00	0.01	0.23	0.05	0.00	0.00	0.08	0.00	0.01			100.84	2014	Acaba Mundo
1345	51	39.20	0.00	0.00	0.00	0.01	0.00	0.16	0.00	56.98	3.56	0.15	0.00	0.00	0.23	0.00	0.00	0.00	0.00	0.00	0.05			100.33	2014	Acaba Mundo
1346	52	39.66	0.02	0.01	0.00	0.06	0.01	0.09	0.00	56.84	3.71	0.16	0.00	0.05	0.19	0.00	0.00	0.02	0.00	0.08	0.00			100.88	2014	Acaba Mundo
1347	53	39.04	0.00	0.02	0.01	0.06	0.01	0.00	0.03	57.71	3.59	0.15	0.00	0.00	0.18	0.00	0.00	0.00	0.00	0.00	0.01					

INDEX	No.	O	Na	K	V	Co	Mg	P	Cr	Fe	Al	S	Ni	Mn	Si	Pb	Cu	Ti	Ca	Zn	Ba	Sr	Total	Year	Sample	
1440	166	35.63				0.02	0.09	0.00	0.57	0.00	59.68	0.00	0.00	0.03	0.25	0.09	0.22	0.00						96.58	2014	BAH F282 118.2
1441	167	35.52				0.00	0.04	0.03	0.52	0.00	59.48	0.01	0.02	0.05	0.28	0.00	0.17	0.00						96.11	2014	BAH F282 118.2
1442	184	37.97	0.00	0.00		0.04	0.04	1.18	0.00	59.76	0.09	0.01	0.00	0.12	0.64	0.09	1.13	0.01	0.08	0.00	0.00	0.06		101.21	2014	BAH F282 118.2
1443	185	37.84	0.00	0.01		0.03	0.02	1.21	0.00	60.09	0.13	0.02	0.00	0.13	0.61	0.14	1.05	0.00	0.05	0.00	0.03	0.00		101.23	2014	BAH F282 118.2
1444	186	37.54	0.00	0.00		0.01	0.03	1.54	0.07	58.39	0.41	0.00	0.00	0.09	0.54	0.06	1.05	0.00	0.05	0.05	0.00	0.00		99.81	2014	BAH F282 118.2
1445	187	36.08	0.00	0.01		0.04	0.04	0.54	0.05	62.64	0.40	0.00	0.00	0.02	0.57	0.00	0.00	0.03	0.00	0.04	0.05	0.00		100.50	2014	BAH F282 118.2
1446	188	38.32	0.01	0.00		0.02	0.06	0.72	0.00	60.07	0.61	0.04	0.00	0.08	1.20	0.15	0.12	0.00	0.05	0.00	0.00	0.04		101.49	2014	BAH F282 118.2
1447	189	38.36	0.01	0.00		0.09	0.04	1.46	0.02	59.31	0.36	0.00	0.02	0.12	0.65	0.00	0.97	0.03	0.05	0.07	0.03	0.00		101.59	2014	BAH F282 118.2
1448	190	38.02	0.00	0.01		0.08	0.02	1.24	0.00	60.01	0.25	0.01	0.00	0.12	0.58	0.00	0.92	0.01	0.07	0.09	0.11	0.00		101.50	2014	BAH F282 118.2
1449	191	37.31	0.00	0.00		0.07	0.02	1.21	0.00	60.47	0.00	0.00	0.00	0.12	0.51	0.13	1.05	0.00	0.11	0.06	0.08	0.00		101.06	2014	BAH F282 118.2
1450	192	36.29	0.03	0.00		0.06	0.06	0.92	0.00	60.46	0.63	0.01	0.00	0.03	0.45	0.06	1.09	0.03	0.00	0.03	0.05	0.02		100.23	2014	BAH F282 118.2
1451	193	36.74	0.00	0.00		0.12	0.00	0.72	0.00	62.93	0.12	0.01	0.00	0.01	0.29	0.08	0.00	0.01	0.00	0.00	0.01	0.00		101.04	2014	BAH F282 118.2
1452	194	35.77	0.00	0.01		0.11	0.00	0.96	0.02	62.85	0.01	0.00	0.02	0.01	0.30	0.06	0.04	0.00	0.00	0.00	0.01	0.00		100.16	2014	BAH F282 118.2
1453	195	36.24	0.00	0.01		0.07	0.01	0.97	0.00	62.18	0.00	0.02	0.06	0.08	0.28	0.12	0.00	0.00	0.01	0.01	0.07	0.00		100.14	2014	BAH F282 118.2
1454	196	37.31	0.00	0.00		0.05	0.00	1.14	0.00	61.69	0.01	0.00	0.05	0.05	0.23	0.02	0.04	0.00	0.00	0.05	0.05	0.04		100.72	2014	BAH F282 118.2
1455	189	36.23			0.00	0.06	0.00	0.74	0.00	59.42	0.00	0.00	0.00	0.04	0.27	0.00	0.11	0.00						96.84	2014	BAH F282 118.2 grain 3
1456	190	37.54			0.00	0.08	0.02	1.12	0.03	58.20	0.01	0.02		0.12	0.24	0.05	0.00	0.00						97.42	2014	BAH F282 118.2 grain 3
1457	191	36.25			0.00	0.06	0.00	0.83	0.08	60.13	0.02	0.00		0.05	0.20	0.09	0.14	0.00						97.85	2014	BAH F282 118.2 grain 3
1458	192	36.62			0.00	0.06	0.04	0.76	0.01	59.30	0.11	0.01		0.09	0.29	0.03	0.11	0.00						97.42	2014	BAH F282 118.2 grain 3
1459	193	36.91			0.01	0.02	0.03	1.13	0.00	57.22	0.02	0.01		0.12	0.50	0.00	0.72	0.00						96.68	2014	BAH F282 118.2 grain 3
1460	194	36.28			0.12	0.03	0.05	0.78	0.07	56.80	0.89	0.03		0.03	0.89	0.08	0.15	0.00						96.19	2014	BAH F282 118.2 grain 3
1461	195	37.19			0.06	0.06	0.06	1.21	0.04	55.85	0.34	0.01		0.18	0.46	0.00	1.18	0.00						96.62	2014	BAH F282 118.2 grain2
1462	196	37.35			0.00	0.06	0.02	1.11	0.02	56.45	0.01	0.00		0.14	0.63	0.00	0.92	0.00						96.70	2014	BAH F282 118.2 grain2
1463	197	37.31			0.00	0.09	0.04	1.07	0.00	55.95	0.02	0.00		0.10	0.66	0.00	1.08	0.04						96.34	2014	BAH F282 118.2 grain 3
1464	168	36.85			0.00	0.06	0.02	0.66	0.00	59.10	0.00	0.00		0.03	0.54	0.00	0.04	0.00						97.29	2014	BAH F282 118.2 grain2
1465	169	36.15			0.00	0.14	0.00	0.73	0.00	58.29	0.03	0.03		0.03	0.41	0.06	1.09	0.00						96.96	2014	BAH F282 118.2 grain2
1466	170	35.99			0.06	0.04	0.04	0.73	0.02	57.72	0.03	0.00		0.13	0.41	0.00	1.13	0.06						96.36	2014	BAH F282 118.2 grain2
1467	171	36.14			0.08	0.01	0.02	0.55	0.01	58.04	0.07	0.00		0.18	0.46	0.00	1.18	0.00						96.96	2014	BAH F282 118.2 grain2
1468	172	35.95			0.00	0.05	0.04	0.84	0.00	57.83	0.06	0.00		0.12	0.45	0.00	1.19	0.05						96.57	2014	BAH F282 118.2 grain 3
1469	173	36.02			0.06	0.13	0.02	0.90	0.03	57.60	0.06	0.00		0.10	0.44	0.03	1.14	0.00						96.52	2014	BAH F282 118.2 grain2
1470	174	35.98			0.00	0.04	0.03	0.95	0.01	57.60	0.06	0.00		0.10	0.47	0.00	1.38	0.03						96.64	2014	BAH F282 118.2 grain2
1471	175	36.00			0.01	0.03	0.04	0.89	0.00	57.20	0.05	0.00		0.07	0.46	0.00	1.21	0.00						95.96	2014	BAH F282 118.2 grain2
1472	176	36.17			0.00	0.03	0.01	0.95	0.01	57.13	0.05	0.03		0.05	0.46	0.09	1.15	0.08						96.20	2014	BAH F282 118.2 grain2
1473	177	35.76			0.02	0.04	0.00	0.94	0.00	57.16	0.06	0.01		0.00	0.46	0.04	1.12	0.00						95.60	2014	BAH F282 118.2 grain2
1474	178	35.43			0.01	0.10	0.04	1.09	0.04	56.25	0.08	0.01		0.08	0.46	0.02	1.20	0.03						94.84	2014	BAH F282 118.2 grain2
1475	179	36.57			0.00	0.06	0.05	1.12	0.00	56.84	0.00	0.00		0.13	0.64	0.03	0.60	0.03						96.08	2014	BAH F282 118.2 grain2
1476	180	36.69			0.01	0.07	0.02	0.74	0.05	59.04	0.11	0.00		0.04	0.34	0.00	0.01	0.04						97.15	2014	BAH F282 118.2 grain2
1477	181	36.13			0.05	0.05	0.00	0.91	0.00	59.17	0.00	0.01		0.07	0.30	0.10	0.06	0.01						96.84	2014	BAH F282 118.2 grain2
1478	182	36.80			0.00	0.14	0.01	0.97	0.03	58.42	0.01	0.00		0.07	0.30	0.03	0.00	0.00						96.75	2014	BAH F282 118.2 grain2
1479	91	37.48	0.00	0.04		0.00	0.00	1.20	0.00	51.98	0.05	0.02	0.00	5.46	0.34	0.04	0.05	0.00	0.00	0.03	0.05	0.00		99.81	2014	BAH-99-01
1480	92	37.46	0.00	0.00	0.00	0.10	0.02	0.98	0.04	54.22	0.00	0.04		2.79	0.93	0.05	2.60	0.00	0.00	0.00	0.02	0.00		96.27	2014	BAH-99-01
1481	94	38.16	0.00	0.03	0.00	0.01	0.83	0.00	53.47	0.07	0.00	0.00		3.72	0.97	0.03	2.93	0.00	0.00	0.00	0.00	0.00		100.20	2014	BAH-99-01
1482	95	38.00	0.00	0.00	0.11	0.00	0.55	0.02	54.16	0.01	0.01	0.01		2.45	1.37	0.01	2.58	0.00	0.00	0.05	0.00	0.03		99.37	2014	BAH-99-01
1483	96	37.99	0.00	0.00	0.03	0.05	0.04	0.54	0.00	54.91	0.00	0.02	0.00	2.48	1.28	0.00	2.61	0.04	0.00	0.02	0.00	0.00		99.95	2014	BAH-99-01
1484	97	38.04	0.05	0.03	0.00	0.03	0.00	0.57	0.01	54.16	0.00	0.04	0.00	3.22	1.37	0.00	2.71	0.00	0.00	0.00	0.00	0.07		100.29	2014	BAH-99-01
1485	98	37.83	0.00	0.00	0.03	0.00	0.00	1.64	0.00	54.56	0.01	0.00	0.00	2.42	0.33	0.12	2.79	0.01	0.00	0.03	0.00	0.00		99.87	2014	BAH-99-01
1486	99	38.11	0.00	0.03	0.00	0.05	0.00	1.23	0.00	53.61	0.13	0.00	0.00	3.99	0.23	0.00	3.18	0.08	0.00	0.10	0.03	0.00		100.76	2014	BAH-99-01
1487	100	37.99	0.00	0.02	0.01	0.02	0.00	1.37	0.00	53.91	0.09	0.00	0.07	3.43	0.28	0.05	3.29	0.01	0.00	0.15	0.12	0.00		100.81	2014	BAH-99-01
1488	101	37.87	0.00	0.00	0.00	0.00	0.00	1.35	0.00	52.83	0.10	0.00	0.02	3.83	0.28	0.07	3.34	0.05	0.00	0.05	0.03	0.00		99.82	2014	BAH-99-01
1489	102	37.99	0.00	0.03	0.00	0.00	0.01	1.30	0.02	52.83	0.10	0.01	0.02	3.73	0.41	0.12	3.35	0.00	0.00	0.06	0.01	0.00		100.00	2014	BAH-99-01
1490	103	37.75	0.00	0.00	0.10	0.02	0.00	1.27	0.00	53.15	0.05	0.03	0.00	3.52	0.47	0.00	3.31	0.00	0.00	0.00	0.03	0.00		99.72	2014	BAH-99-01
1491	104	37.83	0.00	0.00	0.04	0.02	0.01	1.22	0.01	53.91	0.06	0.01	0.00	3.43	0.46	0.03	3.21	0.02	0.00	0.00	0.01	0.00		100.27	2014	BAH-99-01
1492	105																									

INDEX	No.	O	Na	K	V	Co	Mg	P	Cr	Fe	Al	S	Ni	Mn	Si	Pb	Cu	Ti	Ca	Zn	Ba	Sr	Total	Year	Sample
1584	91	37.33	0.00	0.02	0.07	0.10	0.00	0.56	0.04	59.51	3.17	0.00	0.00	0.07	0.11	0.04	0.00	0.19	0.00	0.00	0.02	0.00	101.23	2014	NIP 13 06 Vitreous gt
1585	92	37.71	0.00	0.00	0.09	0.08	0.01	0.49	0.00	58.68	3.04	0.02	0.00	0.03	0.11	0.00	0.00	0.33	0.00	0.00	0.00	0.00	100.59	2014	NIP 13 06 Vitreous gt
1586	135	31.71	0.00	0.00	0.00	0.08	0.02	0.57	0.00	67.41	0.19	0.06	0.00	0.04	0.27	0.01	0.00	0.00	0.00	0.00	0.03	0.00	100.38	2014	NIP 13 09
1587	137	34.10	0.00	0.00	0.01	0.02	0.00	0.60	0.01	66.14	0.15	0.08	0.00	0.02	0.37	0.00	0.00	0.00	0.00	0.00	0.02	0.00	101.53	2014	NIP 13 09
1588	140	35.38	0.00	0.00	0.01	0.06	0.01	0.49	0.01	61.38	1.31	0.02	0.01	0.02	0.19	0.00	0.00	0.00	0.00	0.00	0.00	0.00	100.59	2014	NIP 13 09
1589	141	32.64	0.00	0.01	0.02	0.06	0.00	0.96	0.00	65.69	0.06	0.10	0.00	0.02	0.31	0.00	0.01	0.01	0.00	0.00	0.00	0.00	99.87	2014	NIP 13 09
1590	142	37.50	0.00	0.00	0.00	0.09	0.02	0.36	0.00	62.98	0.09	0.06	0.00	0.04	0.19	0.00	0.04	0.03	0.00	0.03	0.08	0.00	101.50	2014	NIP 13 09
1591	144	37.21	0.00	0.00	0.02	0.10	0.00	0.76	0.00	63.19	0.20	0.01	0.00	0.00	0.12	0.00	0.03	0.00	0.00	0.01	0.03	0.00	101.69	2014	NIP 13 09
1592	145	36.06	0.00	0.01	0.03	0.06	0.02	0.88	0.00	63.81	0.27	0.04	0.01	0.01	0.15	0.00	0.00	0.00	0.06	0.00	0.00	0.00	101.39	2014	NIP 13 09
1593	147	32.78	0.00	0.00	0.00	0.06	0.00	0.18	0.00	65.53	1.17	0.03	0.00	0.00	0.16	0.00	0.00	0.00	0.00	0.00	0.00	0.00	100.22	2014	NIP 13 09
1594	150	37.73	0.00	0.00	0.00	0.06	0.02	0.49	0.01	61.38	1.31	0.02	0.01	0.00	0.09	0.03	0.00	0.00	0.00	0.00	0.03	0.00	101.23	2014	NIP 13 13
1595	151	37.20	0.00	0.02	0.00	0.05	0.00	0.32	0.00	61.04	1.13	0.03	0.00	0.09	0.09	0.03	0.00	0.00	0.00	0.03	0.03	0.00	100.05	2014	NIP 13 13
1596	152	37.36	0.00	0.00	0.04	0.07	0.00	0.29	0.02	61.34	0.72	0.04	0.02	0.02	0.11	0.05	0.00	0.04	0.00	0.03	0.03	0.00	100.18	2014	NIP 13 13
1597	153	37.22	0.01	0.00	0.00	0.12	0.02	0.51	0.01	60.53	1.90	0.02	0.02	0.01	0.09	0.01	0.03	0.05	0.00	0.00	0.00	0.00	100.54	2014	NIP 13 13
1598	154	37.59	0.01	0.01	0.02	0.03	0.00	0.46	0.00	59.55	2.15	0.04	0.00	0.00	0.06	0.00	0.08	0.01	0.00	0.05	0.00	0.00	100.04	2014	NIP 13 13
1599	155	37.93	0.00	0.02	0.05	0.06	0.00	0.47	0.00	57.78	3.17	0.03	0.08	0.00	0.03	0.01	0.00	0.06	0.00	0.06	0.00	0.00	99.75	2014	NIP 13 13
1600	156	38.26	0.00	0.00	0.12	0.04	0.00	0.50	0.00	56.10	4.18	0.04	0.00	0.00	0.10	0.14	0.03	0.67	0.00	0.00	0.00	0.00	100.19	2014	NIP 13 13
1601	157	38.42	0.00	0.01	0.06	0.05	0.00	0.92	0.00	58.47	2.93	0.01	0.01	0.00	0.07	0.07	0.00	0.15	0.00	0.00	0.01	0.00	101.18	2014	NIP 13 13
1602	158	38.41	0.00	0.00	0.05	0.02	0.00	0.94	0.00	58.23	2.56	0.05	0.00	0.00	0.10	0.02	0.00	0.13	0.00	0.00	0.05	0.00	100.57	2014	NIP 13 13
1603	160	35.80	0.01	0.00	0.08	0.10	0.00	0.47	0.00	63.85	0.95	0.04	0.00	0.04	0.19	0.05	0.05	0.03	0.00	0.06	0.04	0.00	101.75	2014	NIP 13 14
1604	162	35.78	0.00	0.02	0.04	0.09	0.02	0.46	0.02	63.68	0.92	0.07	0.00	0.02	0.19	0.00	0.00	0.00	0.00	0.00	0.01	0.00	101.32	2014	NIP 13 14
1605	164	36.65	0.00	0.01	0.09	0.04	0.00	0.48	0.02	63.12	1.17	0.06	0.00	0.02	0.16	0.03	0.00	0.11	0.00	0.00	0.00	0.00	101.98	2014	NIP 13 14
1606	165	37.04	0.00	0.01	0.11	0.07	0.00	0.56	0.00	61.73	1.41	0.08	0.03	0.02	0.14	0.00	0.00	0.00	0.00	0.00	0.00	0.00	101.20	2014	NIP 13 14
1607	166	37.08	0.00	0.00	0.07	0.07	0.02	0.49	0.00	62.13	1.58	0.05	0.03	0.00	0.13	0.15	0.01	0.08	0.00	0.04	0.03	0.00	101.98	2014	NIP 13 14
1608	171	35.44	0.01	0.00	0.03	0.07	0.03	0.24	0.04	59.71	4.99	0.15	0.03	0.04	0.79	0.00	0.01	0.30	0.00	0.00	0.05	0.00	101.93	2014	NIP 13 17 Pisoliths lake shore
1609	173	34.21	0.00	0.00	0.11	0.08	0.02	0.29	0.03	55.81	7.27	0.18	0.00	0.05	0.61	0.00	0.00	0.93	0.00	0.04	0.00	0.00	99.62	2014	NIP 13 17 Pisoliths lake shore
1610	176	35.06	0.00	0.00	0.05	0.03	0.01	0.21	0.04	60.75	4.34	0.17	0.00	0.02	0.69	0.00	0.00	0.17	0.00	0.02	0.01	0.00	101.55	2014	NIP 13 17 Pisoliths lake shore
1611	179	39.88	0.00	0.00	0.02	0.04	0.00	0.40	0.00	54.15	5.18	0.03	0.00	0.00	0.54	0.00	0.00	0.00	0.00	0.00	0.00	0.00	100.86	2014	NIP 13 18 lake
1612	180	39.51	0.00	0.01	0.01	0.05	0.00	0.28	0.01	53.86	5.87	0.12	0.06	0.00	0.46	0.00	0.00	0.00	0.00	0.08	0.00	0.00	100.30	2014	NIP 13 18 lake
1613	181	37.76	0.00	0.00	0.05	0.06	0.02	0.20	0.00	57.26	3.05	0.07	0.02	0.00	0.62	0.08	0.08	0.00	0.00	0.00	0.00	0.00	99.25	2014	NIP 13 18 lake
1614	182	39.47	0.00	0.02	0.04	0.08	0.00	0.23	0.03	55.95	4.98	0.08	0.00	0.03	0.47	0.06	0.02	0.04	0.00	0.00	0.01	0.00	101.50	2014	NIP 13 18 lake
1615	183	39.57	0.01	0.00	0.05	0.03	0.00	0.30	0.05	55.21	5.11	0.13	0.00	0.00	0.49	0.08	0.03	0.09	0.00	0.00	0.05	0.00	101.27	2014	NIP 13 18 lake
1616	184	38.61	0.03	0.01	0.06	0.09	0.02	0.32	0.00	57.23	4.34	0.10	0.00	0.01	0.50	0.02	0.00	0.07	0.00	0.00	0.01	0.00	101.42	2014	NIP 13 18 lake
1617	188	39.23	0.00	0.01	0.10	0.03	0.02	0.38	0.02	55.33	4.38	0.06	0.06	0.00	0.44	0.00	0.04	0.10	0.00	0.09	0.07	0.00	100.30	2014	NIP 13 18 lake
1618	189	38.93	0.00	0.01	0.04	0.06	0.01	0.40	0.00	55.82	5.24	0.09	0.00	0.00	0.40	0.00	0.01	0.06	0.00	0.00	0.04	0.00	101.10	2014	NIP 13 18 lake
1619	190	38.67	0.00	0.01	0.04	0.05	0.01	0.37	0.00	56.63	4.38	0.09	0.00	0.05	0.46	0.00	0.00	0.07	0.00	0.00	0.00	0.00	100.82	2014	NIP 13 18 lake
1620	192	38.80	0.00	0.01	0.04	0.04	0.00	0.19	0.00	58.17	3.30	0.03	0.01	0.08	0.59	0.00	0.00	0.00	0.03	0.03	0.00	0.00	101.30	2014	NIP 13 18 lake
1621	193	38.15	0.00	0.01	0.04	0.03	0.00	0.17	0.04	60.75	1.44	0.01	0.00	0.02	0.55	0.05	0.00	0.01	0.00	0.00	0.00	0.00	101.26	2014	NIP 13 18 lake
1622	243	41.37	0.01	0.00	0.10	0.01	0.00	0.39	0.00	41.58	15.99	0.03	0.00	0.00	0.14	0.09	0.00	1.68	0.00	0.13	0.12	0.00	101.63	2014	NIP 13 28
1623	244	39.25	0.00	0.00	0.10	0.00	0.00	0.41	0.04	42.83	16.45	0.02	0.00	0.00	0.23	0.00	0.00	0.84	0.00	0.02	0.01	0.00	100.15	2014	NIP 13 28
1624	245	37.30	0.01	0.01	0.02	0.02	0.00	0.28	0.00	44.15	14.30	0.02	0.00	0.00	0.15	0.00	0.00	0.72	0.00	0.01	0.00	0.00	99.67	2014	NIP 13 28
1625	246	36.47	0.00	0.00	0.08	0.02	0.04	0.34	0.00	54.64	6.89	0.03	0.00	0.00	0.14	0.00	0.00	0.41	0.00	0.00	0.03	0.00	99.06	2014	NIP 13 28
1626	247	37.75	0.00	0.01	0.08	0.00	0.02	0.50	0.00	54.73	5.06	0.01	0.01	0.00	0.17	0.02	0.03	1.13	0.00	0.00	0.05	0.00	99.29	2014	NIP 13 28
1627	248	35.80	0.00	0.00	0.08	0.01	0.02	0.50	0.00	57.86	4.10	0.03	0.00	0.00	0.10	0.04	0.00	0.00	0.00	0.00	0.00	0.00	98.25	2014	NIP 13 28
1628	249	37.44	0.01	0.01	0.00	0.00	0.00	0.14	0.03	60.45	2.28	0.02	0.00	0.02	0.13	0.00	0.00	0.03	0.00	0.00	0.05	0.00	100.61	2014	NIP 13 28
1629	250	37.25	0.00	0.00	0.10	0.00	0.00	0.10	0.00	62.38	1.41	0.03	0.00	0.06	0.17	0.01	0.01	0.05	0.00	0.02	0.02	0.01	101.59	2014	NIP 13 28
1630	251	35.14	0.00	0.00	0.06	0.00	0.01	0.13	0.00	61.92	1.64	0.04	0.00	0.01	0.19	0.01	0.02	0.05	0.00	0.00	0.01	0.00	99.21	2014	NIP 13 28
1631	253	37.12	0.00	0.00	0.09	0.00	0.00	0.15	0.00	60.18	2.88	0.03	0.00	0.03	0.17	0.00	0.00	0.04	0.00	0.00	0.00	0.03	100.71	2014	NIP 13 28
1632	254	34.68	0.00	0.00	0.07	0.00	0.00	0.29	0.02	58.03	3.64	0.01	0.00	0.00	0.16	0.00	0.01	0.00	0.00	0.00	0.00	0.05	96.95 </		

INDEX	No.	O	Na	K	V	Co	Mg	P	Cr	Fe	Al	S	Ni	Mn	Si	Pb	Cu	Ti	Ca	Zn	Ba	Sr	Total	Year	Sample
1728	319	37.08			0.07	0.06	0.01	0.06	0.02	57.85	0.51	0.03		0.00	1.30	0.06	0.00	0.03					97.07	2014	Pic 06 04
1729	320	36.77			0.00	0.04	0.00	0.07	0.05	57.71	0.48	0.01		0.00	1.32	0.07	0.00	0.02					96.54	2014	Pic 06 04
1730	321	36.34			0.02	0.09	0.00	0.03	0.00	57.65	0.45	0.02		0.04	1.33	0.00	0.00	0.07					96.04	2014	Pic 06 04
1731	331	36.85			0.01	0.02	0.00	0.03	0.02	57.32	0.43	0.01		0.04	1.68	0.00	0.00	0.02					96.41	2014	Pic 06 04 grain 2
1732	341	37.24			0.00	0.11	0.02	0.02	0.14	0.01	61.13	0.71	0.05	0.04	1.29	0.03	0.00	0.01					97.47	2014	Pic 06 04 grain 3
1733	342	37.54			0.00	0.08	0.00	0.00	0.01	57.65	0.47	0.04		0.06	1.42	0.00	0.04	0.01					97.32	2014	Pic 06 04 grain 3
1734	343	37.28			0.00	0.06	0.01	0.03	0.03	57.43	0.47	0.05		0.00	1.51	0.12	0.05	0.00					97.05	2014	Pic 06 04 grain 3
1735	344	37.53			0.00	0.07	0.00	0.07	0.00	57.69	0.49	0.01		0.04	1.67	0.00	0.00	0.00					97.56	2014	Pic 06 04 grain 3
1736	345	37.39			0.00	0.06	0.01	0.06	0.00	57.51	0.49	0.03		0.02	1.46	0.07	0.02	0.00					97.11	2014	Pic 06 04 grain 3
1737	131	34.32	0.00	0.00	0.12	0.05	0.00	0.05	0.01	63.94	0.00	0.02	0.01	0.57	1.04	0.00	0.00	0.00	0.00	0.00	0.07		98.43	2014	Pic 06 07/1
1738	670	34.97	0.05	0.00	0.02	0.02	0.14	0.01	61.13	0.71	0.05	0.07	0.00	0.37	0.09	0.02	0.00	0.00	0.00	0.04			97.65	2014	Pic 06 22 VYG
1739	126	35.55	0.00	0.00	0.04	0.00	0.00	0.06	0.00	62.39	1.06	0.06	0.02	0.04	0.30	0.03	0.00	0.00	0.00	0.00	0.00	0.00	99.56	2014	Pic 06 23 dark goe
1740	127	35.34	0.00	0.00	0.02	0.07	0.01	0.07	0.00	62.58	0.88	0.04	0.02	0.02	0.28	0.03	0.05	0.01	0.00	0.03	0.00	0.00	99.44	2014	Pic 06 23 dark goe
1741	128	33.56	0.03	0.00	0.02	0.02	0.10	0.00	64.14	1.10	0.07	0.00	0.02	0.30	0.17	0.04	0.04	0.00	0.07	0.00	0.00	0.00	99.68	2014	Pic 06 23 dark goe
1742	129	33.52	0.04	0.01	0.03	0.08	0.01	0.05	0.00	62.46	0.76	0.05	0.02	0.03	0.28	0.06	0.03	0.00	0.00	0.01	0.02	0.00	97.43	2014	Pic 06 23 dark goe
1743	130	34.98	0.02	0.01	0.01	0.08	0.00	0.03	0.00	62.31	0.64	0.05	0.02	0.02	0.31	0.06	0.00	0.03	0.00	0.05	0.01	0.03	98.64	2014	Pic 06 23 dark goe
1744	131	36.12	0.00	0.00	0.04	0.05	0.00	0.04	0.02	62.18	0.57	0.06	0.00	0.02	0.30	0.12	0.00	0.00	0.00	0.04	0.00	0.00	99.56	2014	Pic 06 23 dark goe
1745	132	35.93	0.00	0.00	0.05	0.08	0.00	0.03	0.01	61.88	0.33	0.03	0.00	0.04	0.33	0.00	0.00	0.00	0.00	0.00	0.01	0.01	98.72	2014	Pic 06 23 dark goe
1746	133	36.91	0.00	0.00	0.00	0.08	0.00	0.08	0.01	61.83	1.11	0.08	0.00	0.08	0.33	0.00	0.00	0.00	0.00	0.11	0.06	0.00	100.67	2014	Pic 06 23 dark goe
1747	135	36.66	0.00	0.00	0.01	0.02	0.13	0.14	0.00	62.13	0.97	0.07	0.00	0.03	0.36	0.09	0.00	0.00	0.00	0.00	0.07	0.01	100.58	2014	Pic 06 23 dark goe
1748	136	36.88	0.04	0.01	0.00	0.04	0.00	0.09	0.00	62.29	0.88	0.05	0.02	0.00	0.36	0.02	0.01	0.05	0.00	0.07	0.00	0.00	100.81	2014	Pic 06 23 dark goe
1749	137	35.97	0.00	0.00	0.01	0.02	0.02	0.05	0.01	61.69	0.90	0.01	0.00	0.06	0.34	0.00	0.00	0.00	0.00	0.00	0.00	0.00	99.21	2014	Pic 06 23 dark goe
1750	138	37.28	0.00	0.00	0.00	0.11	0.02	0.05	0.01	61.37	0.65	0.05	0.00	0.05	0.37	0.00	0.00	0.02	0.00	0.05	0.03	0.00	100.03	2014	Pic 06 23 dark goe
1751	139	35.37	0.04	0.00	0.01	0.08	0.02	0.12	0.00	63.44	1.22	0.08	0.00	0.03	0.49	0.02	0.03	0.03	0.00	0.01	0.00	0.03	100.99	2014	Pic 06 23 dark goe
1752	139	37.27	0.02	0.02	0.02	0.09	0.00	0.64	0.01	58.70	2.67	0.04	0.06	0.38	0.10	0.04	0.00	0.00	0.00	0.00	0.10		100.14	2014	Pic 06 24/2
1753	307	37.10			0.02	0.10	0.00	0.08	0.00	57.00	0.59	0.04		0.06	1.26	0.14	0.00	0.00					96.38	2014	Pic-06-04
1754	308	36.61			0.00	0.07	0.01	0.07	0.00	57.29	0.60	0.02		0.00	1.26	0.08	0.00	0.00					96.01	2014	Pic-06-04
1755	309	36.55			0.00	0.07	0.01	0.07	0.00	57.18	0.59	0.02		0.01	1.27	0.15	0.00	0.00					95.85	2014	Pic-06-04
1756	310	36.55			0.03	0.05	0.01	0.06	0.03	57.30	0.55	0.06		0.01	1.43	0.13	0.00	0.01					96.20	2014	Pic-06-04
1757	311	36.48			0.05	0.09	0.00	0.00	0.00	58.19	0.33	0.04		0.00	1.73	0.03	0.02	0.00					96.95	2014	Pic-06-04
1758	312	36.07			0.03	0.07	0.00	0.08	0.00	57.55	0.64	0.04		0.01	1.43	0.00	0.02	0.01					95.96	2014	Pic-06-04
1759	313	36.60			0.00	0.03	0.00	0.04	0.00	57.09	0.60	0.01		0.01	1.39	0.01	0.02	0.01					95.82	2014	Pic-06-04
1760	314	37.64			0.00	0.11	0.00	0.08	0.00	57.44	0.60	0.03		0.00	1.38	0.02	0.03	0.04					97.37	2014	Pic-06-04
1761	315	36.94			0.00	0.04	0.02	0.16	0.02	57.62	0.52	0.07	0.00	0.00	1.37	0.15	0.00	0.01					96.81	2014	Pic-06-04
1762	322	31.99			0.00	0.05	0.01	0.04	0.00	64.69	0.56	0.02		0.00	1.27	0.00	0.00	0.05					98.68	2014	Pic-06-04 grain 2
1763	323	33.61			0.00	0.07	0.00	0.05	0.00	61.45	0.72	0.04		0.00	1.41	0.00	0.03	0.00					97.39	2014	Pic-06-04 grain 2
1764	324	31.84			0.00	0.04	0.00	0.02	0.00	65.53	0.50	0.03		0.00	1.09	0.04	0.00	0.01					99.11	2014	Pic-06-04 grain 2
1765	325	31.84			0.00	0.05	0.00	0.03	0.00	65.32	0.49	0.00		0.00	1.18	0.00	0.01	0.00					98.91	2014	Pic-06-04 grain 2
1766	326	29.17			0.01	0.09	0.01	0.05	0.00	64.49	0.52	0.01		0.00	1.13	0.09	0.01	0.03					95.61	2014	Pic-06-04 grain 2
1767	327	31.78			0.01	0.02	0.01	0.02	0.01	65.54	0.49	0.00		0.00	1.14	0.04	0.00	0.00					99.08	2014	Pic-06-04 grain 2
1768	328	33.66			0.05	0.10	0.00	0.07	0.00	60.00	0.63	0.02		0.04	1.45	0.04	0.03	0.00					98.08	2014	Pic-06-04 grain 2
1769	329	35.84			0.00	0.09	0.00	0.03	0.00	59.04	0.68	0.03		0.00	1.43	0.01	0.00	0.00					97.15	2014	Pic-06-04 grain 2
1770	330	37.08			0.00	0.03	0.00	0.08	0.06	57.53	0.60	0.02		0.00	1.45	0.09	0.05	0.01					96.99	2014	Pic-06-04 grain 2
1771	333	37.96			0.04	0.05	0.02	0.09	0.00	55.71	1.60	0.06		0.04	0.82	0.12	0.06	0.01					96.59	2014	Pic-06-04 grain 3
1772	334	37.83			0.00	0.07	0.00	0.05	0.01	56.08	1.09	0.05		0.00	1.34	0.11	0.00	0.06					96.65	2014	Pic-06-04 grain 3
1773	335	37.95			0.00	0.05	0.10	0.05	0.00	55.89	0.90	0.00		0.00	1.44	0.02	0.00	0.00					96.46	2014	Pic-06-04 grain 3
1774	336	37.71			0.00	0.04	0.01	0.07	0.02	57.19	0.82	0.02		0.00	1.52	0.02	0.00	0.02					97.45	2014	Pic-06-04 grain 3
1775	337	36.92			0.00	0.07	0.03	0.07	0.03	57.89	0.32	0.02		0.01	1.22	0.01	0.04	0.00					96.60	2014	Pic-06-04 grain 3
1776	338	37.25			0.00	0.08	0.01	0.07	0.02	57.52	0.37	0.03		0.00	1.31	0.09	0.00	0.00					96.75	2014	Pic-06-04 grain 3
1777	339	36.31			0.00	0.07	0.00	0.08	0.00	58.14	0.42	0.03		0.08	1.32	0.00	0.00	0.00					96.44	2014	Pic-06-04 grain 3
1778	189	36.02	0.00	0.01	0.00	0.07	0.05	0.22	0.02	62.90	0.85	0.05	0.00	0.01	0.63	0.01	0.00	0.01					100.77	2014	Pic-6-22-BI-Gt, 850-425um-2-5
1779	58	38.46			0.00	0.07	0.00	0.07	0.02	57.04	1.57	0.03	0.01	0.03	0.38	0.04	0.00	0.01					97.72	2014	Pic-21-6-VG-9
1780	15	35.58	0.01	0.00	0.06	0.07	0.01	0.21	0.01	59.82	4.75	0.07	0.00	0.01	0.14	0.00	0.01	0.07	0.00	0.00	0.00	0.00	100.82	2014	SC 12 06 (A) Black Gt
1781	29	34.01	0.07	0.02	0.01	0.06	0.00	0.01	0.04	64.00	0.09	0.05	0.01	0.01	0.22	0.01	0.00								

INDEX	No.	O	Na	K	V	Co	Mg	P	Cr	Fe	Al	S	Ni	Mn	Si	Pb	Cu	Ti	Ca	Zn	Ba	Sr	Total	Year	Sample
1872	121	38.54	0.00	0.00	0.00	0.00	0.01	1.08	0.02	58.78	0.01	0.00	0.02	0.07	0.33	0.10	0.20	0.00	0.00	0.03			99.19	2016	BAH F124 123-2_9
1873	127	38.33	0.00	0.01	0.00	0.08	0.02	1.13	0.00	58.38	0.34	0.00	0.00	0.06	0.28	0.03	0.20	0.00	0.00	0.02			98.88	2016	BAH F124 123-7.1
1874	128	36.92	0.00	0.00	0.01	0.08	0.01	0.98	0.02	59.07	0.01	0.01	0.00	0.04	0.34	0.13	0.20	0.00	0.00	0.11			97.93	2016	BAH F124 123-7.2
1875	129	37.64	0.00	0.00	0.01	0.07	0.00	0.84	0.00	58.57	0.01	0.00	0.05	0.08	0.35	0.01	0.19	0.00	0.00	0.00			98.02	2016	BAH F124 123-7.3
1876	130	38.23	0.00	0.00	0.02	0.09	0.00	0.94	0.00	58.62	0.00	0.00	0.03	0.04	0.11	0.06	0.00	0.00	0.00	0.00			98.58	2016	BAH F124 123-7.4
1877	131	36.88	0.00	0.00	0.02	0.08	0.00	0.97	0.00	58.89	0.01	0.01	0.01	0.07	0.31	0.06	0.12	0.00	0.00	0.07			97.50	2016	BAH F124 123-7.5
1878	132	38.10	0.01	0.00	0.01	0.10	0.00	1.10	0.00	58.65	0.03	0.02	0.05	0.01	0.24	0.00	0.09	0.00	0.00	0.07			98.47	2016	BAH F124 123-7.6
1879	26	36.19	0.00	0.00	0.00	0.04	0.00	0.85	0.00	59.25	0.00	0.00	0.02	0.04	0.31	0.00	0.04	0.02	0.00	0.03			96.78	2016	BAH F226 182.2 stalagmite
1880	27	36.14	0.00	0.00	0.02	0.09	0.00	0.94	0.02	59.39	0.01	0.01	0.05	0.09	0.30	0.04	0.02	0.00	0.00	0.02			97.14	2016	BAH F226 182.2 stalagmite
1881	28	37.22	0.00	0.01	0.00	0.06	0.00	0.82	0.00	60.88	0.00	0.00	0.08	0.09	0.19	0.00	0.00	0.00	0.00	0.08			99.46	2016	BAH F226 182.2 stalagmite
1882	29	37.48	0.00	0.00	0.02	0.09	0.00	0.94	0.00	59.39	0.01	0.03	0.02	0.02	0.28	0.07	0.05	0.01	0.00	0.00			98.47	2016	BAH F226 182.2 stalagmite
1883	30	37.47	0.00	0.00	0.00	0.06	0.00	2.00	0.00	57.14	0.01	0.01	0.00	0.12	0.33	0.06	0.30	0.04	0.07	0.00			97.62	2016	BAH F226 182.2 stalagmite
1884	31	38.06	0.00	0.00	0.00	0.05	0.00	1.77	0.01	56.98	0.00	0.00	0.05	0.15	0.42	0.01	0.34	0.00	0.03	0.04			97.88	2016	BAH F226 182.2 stalagmite
1885	32	38.18	0.00	0.00	0.02	0.09	0.00	1.84	0.00	56.47	0.00	0.01	0.04	0.14	0.41	0.05	0.28	0.00	0.02	0.08			97.62	2016	BAH F226 182.2 stalagmite
1886	33	37.36	0.00	0.02	0.10	0.10	0.02	1.55	0.00	57.12	0.00	0.01	0.02	0.25	0.42	0.02	0.66	0.00	0.00	0.03			97.58	2016	BAH F226 182.2 stalagmite
1887	34	37.94	0.00	0.01	0.00	0.09	0.02	2.05	0.01	57.12	0.00	0.00	0.02	0.14	0.21	0.01	0.30	0.01	0.01	0.09			98.07	2016	BAH F226 182.2 stalagmite
1888	35	38.26	0.00	0.00	0.03	0.04	0.03	2.02	0.00	57.08	0.00	0.00	0.04	0.11	0.37	0.08	0.35	0.04	0.06	0.09			98.57	2016	BAH F226 182.2 stalagmite
1889	36	37.08	0.00	0.01	0.02	0.03	0.01	1.95	0.00	57.55	0.00	0.00	0.00	0.07	0.34	0.00	0.23	0.00	0.03	0.10			97.40	2016	BAH F226 182.2 stalagmite
1890	37	37.99	0.00	0.00	0.00	0.07	0.02	2.05	0.02	56.60	0.00	0.00	0.01	0.11	0.34	0.10	0.33	0.01	0.05	0.08			97.78	2016	BAH F226 182.2 stalagmite
1891	64	37.48	0.00	0.00	0.00	0.09	0.02	0.95	0.03	60.19	0.04	0.03	0.05	0.04	0.24	0.02	0.05	0.02	0.00	0.00			99.24	2016	BAH F226 193.5
1892	65	36.34	0.00	0.00	0.00	0.06	0.00	1.08	0.00	59.10	0.25	0.00	0.00	0.00	0.29	0.09	0.08	0.02	0.00	0.05			97.36	2016	BAH F226 193.5
1893	66	37.56	0.00	0.00	0.01	0.07	0.00	1.17	0.00	59.64	0.00	0.00	0.02	0.13	0.21	0.03	0.06	0.02	0.00	0.07			98.99	2016	BAH F226 193.5
1894	67	36.95	0.00	0.00	0.02	0.07	0.00	1.27	0.00	58.57	0.01	0.00	0.03	0.06	0.28	0.08	0.03	0.01	0.00	0.10			97.47	2016	BAH F226 193.5
1895	68	37.22	0.00	0.00	0.00	0.07	0.01	1.33	0.00	58.24	0.01	0.02	0.00	0.12	0.37	0.00	0.21	0.00	0.02	0.08			97.70	2016	BAH F226 193.5
1896	69	36.89	0.00	0.01	0.00	0.05	0.02	1.28	0.02	58.20	0.00	0.00	0.02	0.09	0.34	0.00	0.09	0.00	0.00	0.09			97.09	2016	BAH F226 193.5
1897	70	36.82	0.00	0.00	0.01	0.03	0.01	1.26	0.01	58.94	0.00	0.00	0.01	0.13	0.25	0.02	0.09	0.01	0.00	0.04			97.61	2016	BAH F226 193.5
1898	71	37.32	0.00	0.00	0.02	0.10	0.00	1.30	0.03	59.07	0.00	0.00	0.00	0.10	0.28	0.12	0.08	0.04	0.01	0.09			98.47	2016	BAH F226 193.5
1899	106	36.15	0.00	0.00	0.00	0.04	0.00	0.80	0.02	61.41	0.00	0.00	0.03	0.04	0.28	0.00	0.00	0.00	0.00	0.05			100.17	2016	BAH F282 118.2-brown
1900	107	36.32	0.00	0.00	0.03	0.07	0.03	0.81	0.04	60.82	0.00	0.00	0.01	0.09	0.52	0.08	0.90	0.00	0.00	0.07			97.77	2016	BAH F282 118.2-brown
1901	108	36.57	0.00	0.00	0.03	0.09	0.03	0.77	0.00	61.79	0.01	0.00	0.05	0.09	0.49	0.00	0.98	0.00	0.00	0.02			100.92	2016	BAH F282 118.2-brown
1902	109	36.48	0.03	0.00	0.00	0.08	0.04	0.80	0.00	61.37	0.00	0.03	0.02	0.06	0.51	0.02	1.01	0.00	0.00	0.06			100.51	2016	BAH F282 118.2-brown
1903	110	36.64	0.00	0.00	0.03	0.04	0.03	0.74	0.02	61.78	0.00	0.01	0.00	0.09	0.51	0.00	1.08	0.00	0.00	0.10			101.08	2016	BAH F282 118.2-brown
1904	111	36.55	0.00	0.00	0.10	0.10	0.04	0.77	0.00	61.49	0.01	0.01	0.00	0.06	0.51	0.05	1.04	0.00	0.00	0.09			100.70	2016	BAH F282 118.2-brown
1905	112	36.36	0.02	0.00	0.01	0.03	0.05	0.77	0.00	61.47	0.00	0.00	0.04	0.07	0.51	0.00	0.96	0.00	0.00	0.07			100.37	2016	BAH F282 118.2-brown
1906	100	35.06	0.00	0.00	0.02	0.05	0.02	0.54	0.00	59.66	0.02	0.01	0.07	0.03	0.30	0.00	0.03	0.00	0.00	0.04			95.86	2016	BAH F282 118.4_1
1907	101	35.26	0.00	0.00	0.02	0.06	0.02	0.45	0.02	60.73	0.07	0.00	0.06	0.02	0.25	0.00	0.17	0.00	0.00	0.00			97.13	2016	BAH F282 118.4_2
1908	102	35.64	0.00	0.01	0.08	0.05	0.03	0.44	0.00	60.82	0.22	0.01	0.11	0.00	0.26	0.05	0.30	0.00	0.00	0.07			98.09	2016	BAH F282 118.4_3
1909	103	37.36	0.00	0.00	0.02	0.14	0.02	0.51	0.00	60.25	0.00	0.00	0.03	0.00	0.30	0.05	0.00	0.00	0.00	0.00			98.68	2016	BAH F282 118.4_4
1910	104	35.97	0.00	0.00	0.02	0.09	0.01	0.46	0.02	60.89	0.03	0.00	0.02	0.04	0.27	0.07	0.18	0.05	0.00	0.09			98.31	2016	BAH F282 118.4_5
1911	105	36.15	0.01	0.00	0.04	0.08	0.03	0.50	0.04	61.54	0.23	0.00	0.00	0.04	0.28	0.00	0.53	0.00	0.00	0.03			99.53	2016	BAH F282 118.4_6
1912	38	36.66	0.01	0.00	0.01	0.06	0.00	0.39	0.01	63.03	0.12	0.01	0.02	0.02	0.12	0.00	0.07	0.00	0.00	0.00			100.52	2016	BAH F282 120.5_brown
1913	39	35.23	0.01	0.00	0.02	0.08	0.00	0.39	0.05	64.37	0.21	0.03	0.01	0.02	0.14	0.02	0.09	0.00	0.00	0.00			100.67	2016	BAH F282 120.5_brown
1914	40	34.70	0.00	0.00	0.00	0.06	0.00	0.42	0.01	63.99	0.22	0.01	0.00	0.02	0.13	0.02	0.06	0.00	0.00	0.00			99.65	2016	BAH F282 120.5_brown
1915	41	35.75	0.00	0.00	0.00	0.06	0.00	0.40	0.00	63.75	0.11	0.01	0.03	0.00	0.13	0.11	0.04	0.00	0.00	0.02			100.45	2016	BAH F282 120.5_brown
1916	42	35.28	0.00	0.01	0.00	0.07	0.00	0.41	0.02	63.25	0.11	0.02	0.00	0.02	0.11	0.01	0.04	0.02	0.00	0.00			99.37	2016	BAH F282 120.5_brown
1917	43	35.46	0.04	0.00	0.00	0.06	0.04	0.47	0.03	63.28	0.13	0.02	0.00	0.06	0.12	0.04	0.08	0.00	0.00	0.03			99.73	2016	BAH F282 120.5_brown
1918	44	34.93	0.02	0.00	0.01	0.08	0.02	0.39	0.01	63.61	0.15	0.03	0.06	0.04	0.13	0.04	0.10	0.00	0.00	0.03			99.65	2016	BAH F282 120.5_brown
1919	45	35.60	0.02	0.00	0.03	0.08	0.02	0.53	0.00	64.22	0.58	0.06	0.02	0.09	0.23	0.08	0.18	0.01	0.00	0.00			101.75	2016	BAH F282 120.5_brown
1920	46	32.37	0.00	0.00	0.00	0.08	0.00	0.48	0.00	64.69	0.53	0.03	0.00	0.06	0.17	0.06	0.15	0.00	0.00	0.01			98.63	2016	BAH F282 120.5_brown
1921	47	35.89	0.03	0.01	0.00	0.04	0.01	0.46	0.00	63.90	0.26	0.05	0.00	0.07	0.18	0.00	0.08	0.00	0.00	0.02			101.00	2016	BAH F282 120.5_brown
1922	72	37.06																							

INDEX	No.	O	Na	K	V	Co	Mg	P	Cr	Fe	Al	S	Ni	Mn	Si	Pb	Cu	Ti	Ca	Zn	Ba	Sr	Total	Year	Sample
2016	169	36.07	0.01	0.03	0.00	0.10	0.04	0.53	0.01	58.61	0.16	0.00	0.05	3.03	0.38	0.00	1.81	0.00	0.00	0.04	0.00		100.87	2016	BAH-F124-111.2
2017	170	37.08	0.01	0.02	0.02	0.05	0.00	0.41	0.00	58.74	0.10	0.01	0.09	1.67	1.19	0.04	1.60	0.00	0.00	0.01	0.00		101.03	2016	BAH-F124-111.2
2018	171	36.99	0.00	0.01	0.10	0.09	0.02	0.49	0.02	58.88	0.12	0.02	0.03	1.71	1.19	0.00	1.55	0.02	0.00	0.08	0.00		101.20	2016	BAH-F124-111.2
2019	172	36.14	0.00	0.00	0.00	0.00	0.02	0.33	0.00	59.31	0.10	0.00	0.00	1.76	1.15	0.01	1.70	0.01	0.00	0.00	0.03		100.73	2016	BAH-F124-111.2
2020	173	36.62	0.00	0.01	0.03	0.07	0.02	0.33	0.01	58.65	0.11	0.02	0.00	1.92	1.28	0.03	1.75	0.00	0.00	0.08	0.02		101.91	2016	BAH-F124-111.2
2021	174	36.49	0.00	0.02	0.00	0.12	0.01	0.85	0.01	58.60	0.12	0.00	0.00	1.06	0.52	0.03	1.64	0.01	0.00	0.05	0.01		99.55	2016	BAH-F124-111.2
2022	175	36.37	0.00	0.03	0.07	0.03	0.02	0.88	0.00	58.25	0.13	0.02	0.07	0.99	0.56	0.04	1.60	0.01	0.00	0.01	0.01		99.08	2016	BAH-F124-111.2
2023	176	36.82	0.00	0.02	0.01	0.06	0.01	0.91	0.00	58.10	0.11	0.00	0.05	1.00	0.61	0.06	1.60	0.00	0.00	0.00	0.00		99.37	2016	BAH-F124-111.2
2024	177	37.47	0.00	0.01	0.00	0.01	0.01	0.90	0.00	58.41	0.14	0.01	0.00	1.22	0.58	0.11	1.73	0.01	0.00	0.01	0.00		100.60	2016	BAH-F124-111.2
2025	151	36.99	0.00	0.00	0.00	0.04	0.00	0.61	0.01	58.44	0.15	0.01	0.00	2.47	0.29	0.00	1.64	0.00	0.00	0.06	0.00		101.07	2016	BAH-F124-111.2
2026	152	37.35	0.00	0.01	0.01	0.05	0.03	0.30	0.00	58.50	0.12	0.00	0.00	1.95	1.32	0.03	1.60	0.00	0.00	0.01	0.00		101.40	2016	BAH-F124-111.2
2027	153	37.70	0.00	0.00	0.02	0.07	0.04	0.85	0.00	59.95	0.13	0.00	0.00	1.04	0.55	0.00	1.49	0.00	0.00	0.00	0.01		101.88	2016	BAH-F124-111.2
2028	154	37.72	0.00	0.01	0.04	0.06	0.02	0.87	0.00	58.51	0.12	0.00	0.06	0.93	0.57	0.09	1.60	0.03	0.00	0.02	0.00		100.63	2016	BAH-F124-111.2
2029	156	37.10	0.00	0.00	0.00	0.13	0.02	0.82	0.01	59.22	0.15	0.00	0.01	1.10	0.58	0.04	1.57	0.00	0.00	0.00	0.00		100.75	2016	BAH-F124-111.2
2030	157	38.22	0.00	0.00	0.00	0.09	0.04	0.84	0.00	59.14	0.11	0.01	0.00	1.13	0.63	0.00	1.62	0.04	0.00	0.00	0.00		101.89	2016	BAH-F124-111.2
2031	143	36.37	0.00	0.00	0.00	0.08	0.05	0.60	0.01	60.03	0.17	0.01	0.02	2.08	1.01	0.03	1.55	0.05	0.00	0.07	0.00		101.80	2016	BAH-F124-111.2
2032	162	36.62	0.00	0.01	0.01	0.07	0.01	0.59	0.04	59.08	0.16	0.01	0.02	2.93	0.25	0.02	1.86	0.00	0.00	0.00	0.00		101.66	2016	BAH-F124-111.2
2033	163	37.88	0.00	0.00	0.02	0.09	0.04	0.31	0.01	59.45	0.00	0.00	0.00	0.04	0.96	0.00	0.02	0.02	0.00	0.00	0.00		98.84	2016	BAH-F124-111.2
2034	145	36.10	0.00	0.00	0.00	0.07	0.05	0.46	0.02	59.81	0.14	0.00	0.00	2.75	0.48	0.00	1.46	0.01	0.00	0.01	0.00		101.36	2016	BAH-F124-111.2
2035	146	36.75	0.00	0.00	0.00	0.02	0.02	0.49	0.00	59.96	0.11	0.01	0.02	1.93	0.30	0.03	1.35	0.00	0.00	0.03	0.00		101.01	2016	BAH-F124-111.2
2036	148	36.53	0.00	0.00	0.00	0.09	0.03	0.57	0.03	61.68	0.04	0.04	0.00	0.82	0.20	0.04	0.70	0.01	0.00	0.06	0.00		100.86	2016	BAH-F124-111.2
2037	149	35.95	0.00	0.00	0.07	0.01	0.01	0.61	0.01	60.51	0.15	0.01	0.00	2.47	0.29	0.00	1.64	0.00	0.00	0.02	0.00		101.73	2016	BAH-F124-111.2
2038	301	36.11	0.00	0.00	0.00	0.08	0.02	1.39	0.01	60.43	0.29	0.00	0.02	0.04	0.26	0.05	2.20	0.00	0.00	0.10	0.00		101.00	2016	BAH-F124-114.1
2039	302	36.76	0.00	0.01	0.01	0.04	0.01	1.38	0.00	60.15	0.41	0.02	0.02	0.03	0.26	0.03	2.21	0.00	0.00	0.01	0.00		101.35	2016	BAH-F124-114.2
2040	308	36.66	0.00	0.03	0.02	0.10	0.01	1.36	0.00	60.45	0.34	0.00	0.04	0.04	0.25	0.00	2.19	0.00	0.00	0.00	0.00		101.47	2016	BAH-F124-114-2.1
2041	309	36.42	0.00	0.00	0.00	0.06	0.01	1.42	0.00	60.11	0.32	0.00	0.05	0.07	0.26	0.00	2.14	0.00	0.00	0.05	0.00		100.89	2016	BAH-F124-114-2.2
2042	310	36.55	0.00	0.01	0.02	0.09	0.00	1.29	0.00	59.76	0.35	0.02	0.00	0.07	0.26	0.00	2.09	0.04	0.00	0.05	0.00		100.58	2016	BAH-F124-114-2.3
2043	303	36.29	0.00	0.00	0.00	0.00	0.01	1.35	0.00	60.53	0.10	0.00	0.00	0.01	0.28	0.03	1.94	0.02	0.00	0.04	0.00		101.24	2016	BAH-F124-114.3
2044	304	36.60	0.00	0.01	0.05	0.06	0.01	1.38	0.00	60.63	0.34	0.00	0.04	0.03	0.27	0.01	2.27	0.02	0.00	0.05	0.00		101.77	2016	BAH-F124-114.4
2045	305	37.01	0.00	0.01	0.01	0.02	0.02	0.74	0.00	60.03	0.01	0.00	0.01	0.03	0.15	0.05	0.05	0.00	0.00	0.02	0.00		98.15	2016	BAH-F124-114.5
2046	306	36.16	0.00	0.01	0.00	0.06	0.00	0.79	0.00	59.74	0.00	0.00	0.03	0.04	0.18	0.02	0.01	0.00	0.00	0.02	0.00		97.05	2016	BAH-F124-114.6
2047	307	35.58	0.00	0.00	0.00	0.08	0.01	0.62	0.00	60.21	0.03	0.01	0.03	0.03	0.15	0.01	0.01	0.00	0.00	0.03	0.00		96.78	2016	BAH-F124-114.7
2048	215	36.98	0.00	0.00	0.00	0.11	0.00	1.20	0.00	59.30	0.02	0.00	0.01	0.06	0.12	0.00	0.05	0.00	0.08	0.08	0.00		97.92	2016	BAH-F124-123.1-0
2049	216	37.49	0.00	0.00	0.02	0.09	0.00	0.87	0.00	59.11	0.10	0.02	0.02	0.01	0.29	0.03	0.04	0.00	0.00	0.02	0.00		98.00	2016	BAH-F124-123.1-1
2050	217	36.63	0.03	0.00	0.00	0.08	0.00	1.05	0.00	59.47	0.00	0.01	0.00	0.04	0.25	0.03	0.03	0.00	0.00	0.01	0.00		97.62	2016	BAH-F124-123.1-2
2051	218	37.44	0.05	0.01	0.02	0.06	0.01	0.86	0.00	58.72	0.00	0.02	0.04	0.03	0.28	0.03	0.08	0.00	0.00	0.06	0.00		97.68	2016	BAH-F124-123.1-3
2052	219	35.81	0.01	0.00	0.00	0.08	0.02	0.93	0.00	59.57	0.00	0.00	0.03	0.06	0.79	0.01	0.28	0.00	0.00	0.00	0.00		97.60	2016	BAH-F124-123.1-4
2053	220	36.98	0.02	0.00	0.00	0.06	0.02	0.89	0.03	56.40	0.00	0.00	0.00	0.01	1.45	0.03	0.44	0.00	0.01	0.00	0.00		96.33	2016	BAH-F124-123.1-5
2054	221	37.42	0.00	0.01	0.00	0.08	0.01	0.91	0.00	56.85	0.00	0.00	0.01	0.01	1.36	0.04	0.39	0.00	0.00	0.00	0.00		97.10	2016	BAH-F124-123.1-6
2055	208	37.02	0.00	0.00	0.02	0.06	0.01	0.79	0.00	59.55	0.05	0.00	0.01	0.01	0.29	0.00	1.94	0.02	0.00	0.05	0.00		99.25	2016	BAH-F124-123.1-7
2056	209	37.12	0.01	0.00	0.00	0.05	0.02	0.32	0.02	59.05	0.06	0.00	0.00	0.11	1.74	0.01	0.54	0.03	0.00	0.03	0.00		97.10	2016	BAH-F124-123.1-8
2057	212	37.35	0.00	0.02	0.09	0.08	0.00	0.28	0.00	59.32	0.06	0.01	0.00	0.08	1.91	0.03	0.92	0.00	0.04	0.00	0.00		100.19	2016	BAH-F124-123.1-9
2058	213	36.74	0.00	0.00	0.01	0.09	0.00	1.22	0.00	58.11	0.01	0.00	0.06	0.06	0.22	0.01	0.06	0.00	0.02	0.05	0.00		96.65	2016	BAH-F124-123.1-8
2059	214	36.55	0.03	0.01	0.00	0.09	0.00	1.15	0.00	59.64	0.00	0.01	0.05	0.01	0.15	0.01	0.08	0.00	0.00	0.00	0.00		97.78	2016	BAH-F124-123.1-9
2060	236	35.53	0.00	0.04	0.03	0.04	0.00	1.59	0.04	58.93	0.91	0.01	0.00	0.07	0.23	0.00	1.53	0.00	0.00	0.00	0.03		98.97	2016	BAH-F177-115 CavityFilling
2061	237	36.12	0.03	0.03	0.05	0.07	0.01	1.58	0.04	58.44	0.91	0.02	0.01	0.07	0.25	0.03	1.59	0.00	0.00	0.00	0.00		99.22	2016	BAH-F177-115 CavityFilling
2062	238	36.07	0.00	0.05	0.04	0.09	0.00	1.53	0.06	58.30	0.93	0.02	0.00	0.05	0.26	0.01	1.61	0.00	0.00	0.00	0.00		99.01	2016	BAH-F177-115 CavityFilling
2063	239	36.04	0.03	0.03	0.05	0.00	0.05	1.55	0.01	58.43	0.90	0.02	0.07	0.02	0.25	0.04	1.57	0.03	0.00	0.00	0.00		99.03	2016	BAH-F177-115 CavityFilling
2064	240	36.14	0.02	0.05	0.04	0.03	0.00	1.61	0.00	58.46	0.96	0.01	0.00	0.05	0.25	0.04	1.62	0.00	0.00	0.01	0.04		99.34	2016	BAH

INDEX	No.	O	Na	K	V	Co	Mg	P	Cr	Fe	Al	S	Ni	Mn	Si	Pb	Cu	Ti	Ca	Zn	Ba	Sr	Total	Year	Sample
2160	5567	35.95	0.01	0.01	0.00	0.03	0.01	0.41	0.01	61.66	0.12	0.02	0.01	0.01	0.08	0.01	0.05	0.00	0.04	0.02			98.45	2016	BAH100_Gibb+Goe
2161	5568	36.07	0.06	0.00	0.02	0.04	0.00	0.42	0.00	61.32	0.09	0.00	0.05	0.04	0.08	0.01	0.05	0.04	0.03	0.01			98.34	2016	BAH100_Gibb+Goe
2162	5424	40.71	0.00	0.01	0.06	0.00	0.04	0.36	0.02	40.61	8.23	0.03	0.00	0.04	6.91	0.00	0.06	0.20	0.04	0.00			97.31	2016	BOI-002
2163	5425	40.75	0.01	0.01	0.06	0.00	0.03	0.40	0.03	44.55	7.54	0.03	0.00	0.06	5.87	0.00	0.00	0.28	0.05	0.00			99.73	2016	BOI-002
2164	5426	41.81	0.00	0.02	0.08	0.01	0.03	0.31	0.02	38.95	8.68	0.02	0.03	0.04	7.01	0.02	0.00	0.13	0.04	0.04			97.28	2016	BOI-002
2165	5427	41.80	0.04	0.02	0.03	0.00	0.01	0.36	0.05	40.41	8.51	0.01	0.01	0.05	6.74	0.00	0.00	0.17	0.05	0.04			98.28	2016	BOI-002
2166	5428	39.93	0.02	0.01	0.06	0.02	0.04	0.39	0.05	42.10	9.40	0.04	0.02	0.05	7.34	0.00	0.04	0.12	0.10	0.09			99.81	2016	BOI-002
2167	5429	42.23	0.02	0.03	0.07	0.00	0.03	0.30	0.04	37.55	8.75	0.02	0.00	0.08	7.88	0.04	0.00	0.23	0.04	0.02			97.32	2016	BOI-002
2168	5430	40.31	0.01	0.02	0.05	0.00	0.01	0.28	0.06	44.81	7.99	0.03	0.00	0.06	5.45	0.00	0.07	0.17	0.05	0.04			99.42	2016	BOI-002
2169	5431	42.07	0.00	0.04	0.06	0.00	0.03	0.39	0.02	34.90	9.55	0.02	0.04	0.06	8.53	0.00	0.03	0.31	0.06	0.09			96.67	2016	BOI-002
2170	5432	40.83	0.02	0.01	0.07	0.00	0.02	0.40	0.03	38.31	10.31	0.02	0.00	0.08	8.49	0.04	0.08	0.17	0.06	0.07			99.83	2016	BOI-002
2171	5433	41.32	0.00	0.03	0.05	0.00	0.04	0.35	0.11	40.18	9.52	0.04	0.01	0.11	7.55	0.05	0.02	0.30	0.08	0.07			99.83	2016	BOI-002
2172	5540	41.60	0.03	0.02	0.04	0.02	0.02	0.23	0.22	37.69	9.19	0.02	0.01	0.03	7.44	0.03	0.03	0.18	0.02	0.03			96.85	2016	BOI-002_G2
2173	5541	40.75	0.03	0.02	0.07	0.02	0.01	0.25	0.22	45.47	6.83	0.02	0.00	0.03	5.08	0.04	0.07	0.22	0.04	0.02			99.19	2016	BOI-002_G2
2174	5542	40.59	0.00	0.02	0.08	0.02	0.01	0.25	0.21	45.53	7.26	0.01	0.00	0.06	5.42	0.05	0.04	0.19	0.04	0.10			99.89	2016	BOI-002_G2
2175	5543	41.96	0.01	0.04	0.04	0.00	0.03	0.23	0.18	39.24	8.76	0.02	0.04	0.02	6.94	0.01	0.06	0.23	0.03	0.08			97.93	2016	BOI-002_G2
2176	5544	41.59	0.03	0.03	0.08	0.00	0.01	0.21	0.19	41.46	7.98	0.03	0.00	0.13	6.27	0.04	0.03	0.19	0.03	0.09			98.40	2016	BOI-002_G2
2177	5546	40.36	0.05	0.02	0.01	0.02	0.03	0.29	0.03	49.51	5.81	0.01	0.04	0.15	4.83	0.06	0.00	0.16	0.04	0.00			101.43	2016	BOI-002_G2
2178	5551	39.35	0.02	0.03	0.02	0.07	0.03	0.33	0.03	50.16	5.06	0.03	0.05	0.16	4.86	0.00	0.05	0.10	0.05	0.06			100.44	2016	BOI-002_G2 (continued)
2179	5552	39.50	0.02	0.04	0.03	0.01	0.03	0.36	0.02	47.67	5.83	0.02	0.00	0.15	5.27	0.04	0.06	0.25	0.05	0.07			99.44	2016	BOI-002_G2 (continued)
2180	5553	33.69	0.02	0.00	0.10	0.03	0.00	0.36	0.15	59.67	2.10	0.02	0.04	0.06	1.11	0.03	0.08	0.07	0.03	0.04			97.62	2016	BOI-002_G2 (continued)
2181	5457	38.39	0.04	0.01	0.11	0.03	0.03	0.19	0.01	51.56	7.00	0.04	0.00	0.00	2.91	0.01	0.02	0.14	0.07	0.02			100.57	2016	BOI-004
2182	5459	37.38	0.05	0.01	0.08	0.07	0.07	0.38	0.00	45.69	9.56	0.06	0.00	0.02	5.10	0.00	0.03	0.44	0.17	0.14			99.18	2016	BOI-004
2183	5461	35.96	0.06	0.01	0.08	0.00	0.04	0.23	0.03	50.78	7.21	0.05	0.00	0.01	3.45	0.03	0.05	0.19	0.14	0.01			98.34	2016	BOI-004
2184	5462	37.32	0.03	0.01	0.06	0.00	0.04	0.15	0.00	55.79	5.30	0.05	0.00	0.00	2.06	0.00	0.03	0.13	0.09	0.00			101.07	2016	BOI-004
2185	5463	38.36	0.00	0.02	0.09	0.00	0.04	0.23	0.01	51.82	6.59	0.03	0.00	0.03	2.82	0.04	0.05	0.18	0.09	0.00			100.41	2016	BOI-004
2186	5464	39.33	0.02	0.01	0.11	0.00	0.05	0.22	0.00	49.54	8.00	0.02	0.00	0.01	3.53	0.00	0.02	0.33	0.07	0.05			101.33	2016	BOI-004
2187	5465	38.81	0.02	0.02	0.05	0.00	0.03	0.18	0.02	50.49	6.12	0.03	0.01	0.01	3.06	0.04	0.01	0.08	0.09	0.04			99.14	2016	BOI-004
2188	5467	39.45	0.02	0.01	0.16	0.00	0.02	0.16	0.00	51.97	6.74	0.04	0.04	0.04	2.32	0.00	0.01	0.11	0.07	0.05			101.18	2016	BOI-004
2189	5468	38.18	0.00	0.04	0.09	0.00	0.06	0.29	0.00	47.77	8.96	0.08	0.00	0.02	4.79	0.00	0.02	0.21	0.27	0.08			100.86	2016	BOI-004
2190	5469	36.30	0.02	0.01	0.09	0.00	0.05	0.29	0.05	47.04	7.78	0.04	0.01	0.00	2.86	0.00	0.03	0.18	0.13	0.10			94.97	2016	BOI-004
2191	5434	37.65	0.02	0.02	0.04	0.00	0.01	0.04	0.01	57.12	3.32	0.01	0.02	0.00	1.00	0.00	0.00	0.09	0.01	0.00			99.35	2016	BOI-013
2192	5435	38.40	0.00	0.00	0.00	0.01	0.00	0.05	0.00	57.23	3.33	0.01	0.00	0.00	0.75	0.00	0.01	0.03	0.00	0.00			99.82	2016	BOI-013
2193	5436	37.83	0.01	0.07	0.04	0.07	0.00	0.10	0.02	58.20	2.73	0.05	0.03	0.01	0.89	0.09	0.02	0.02	0.01	0.05			100.17	2016	BOI-013
2194	5437	38.15	0.02	0.01	0.07	0.01	0.02	0.12	0.00	57.09	3.75	0.05	0.00	0.02	0.78	0.00	0.03	0.07	0.05	0.05			100.29	2016	BOI-013
2195	5438	32.38	0.00	0.00	0.04	0.00	0.00	0.06	0.02	55.46	1.97	0.06	0.01	0.02	0.81	0.08	0.01	0.00	0.02	0.00			90.93	2016	BOI-013
2196	5439	36.80	0.00	0.01	0.00	0.03	0.00	0.06	0.00	57.67	3.54	0.04	0.02	0.04	0.83	0.08	0.00	0.03	0.03	0.00			99.17	2016	BOI-013
2197	5440	37.50	0.02	0.00	0.12	0.00	0.00	0.06	0.01	55.88	4.07	0.04	0.00	0.00	0.52	0.00	0.03	0.07	0.02	0.07			98.40	2016	BOI-013
2198	5441	38.52	0.01	0.01	0.07	0.00	0.00	0.11	0.01	56.64	3.57	0.04	0.02	0.00	0.72	0.07	0.07	0.06	0.02	0.01			99.95	2016	BOI-013
2199	5442	37.80	0.00	0.02	0.05	0.03	0.00	0.13	0.00	56.52	3.55	0.03	0.01	0.01	0.81	0.08	0.02	0.02	0.01	0.02			99.14	2016	BOI-013
2200	5443	38.93	0.01	0.01	0.03	0.00	0.00	0.08	0.00	56.73	3.85	0.04	0.00	0.03	0.49	0.00	0.00	0.09	0.01	0.02			100.32	2016	BOI-013
2201	5444	37.30	0.02	0.07	0.40	0.00	0.00	0.48	0.01	57.52	4.24	0.03	0.00	0.03	1.46	0.04	0.02	0.05	0.04	0.04			101.73	2016	BOI-014
2202	5445	37.24	0.03	0.00	0.36	0.00	0.01	0.45	0.00	56.52	4.21	0.04	0.00	0.00	1.77	0.00	0.00	0.02	0.02	0.02			100.70	2016	BOI-014
2203	5446	36.62	0.03	0.02	0.28	0.01	0.00	0.39	0.00	57.03	3.98	0.02	0.00	0.00	1.60	0.09	0.00	0.09	0.03	0.07			100.26	2016	BOI-014
2204	5447	37.90	0.06	0.00	0.38	0.00	0.00	0.47	0.01	55.77	4.59	0.04	0.00	0.00	2.00	0.00	0.01	0.08	0.02	0.02			101.35	2016	BOI-014
2205	5448	37.89	0.05	0.00	0.25	0.00	0.00	0.38	0.00	52.96	4.84	0.03	0.00	0.01	3.03	0.04	0.01	0.03	0.04	0.06			99.85	2016	BOI-014
2206	5449	35.78	0.00	0.00	0.42	0.00	0.01	0.52	0.00	57.61	3.94	0.03	0.00	0.00	0.97	0.00	0.00	0.06	0.02	0.05			99.41	2016	BOI-014
2207	5450	35.82	0.03	0.00	0.33	0.00	0.00	0.46	0.00	58.22	3.96	0.03	0.00	0.00	1.63	0.09	0.01	0.01	0.04	0.10			100.75	2016	BOI-014
2208	5452	36.91	0.04	0.00	0.31	0.01	0.01	0.39	0.00	57.83	3.89	0.02	0.00	0.00	1.90	0.00	0.04	0.04	0.04	0.05			101.46	2016	BOI-014
2209	5453	36.75	0.03	0.00	0.35	0.00	0.01	0.45	0.00	58.44	3.85	0.03	0.00	0.01	1.45	0.00	0.03	0.06	0.03	0.00			101.48	2016	BOI-014
2210	5554	36.74	0.02	0.02	0.24	0.02	0.00	0.26	0.01	55.39	3.94	0.02	0.00	0.02	2.19	0.00	0.00	0.04	0.02	0.06			98.99	2016	BOI-014
2211</																									

INDEX	No.	O	Na	K	V	Co	Mg	P	Cr	Fe	Al	S	Ni	Mn	Si	Pb	Cu	Ti	Ca	Zn	Ba	Sr	Total	Year	Sample
2304	252	38.83	0.04	0.02	0.05	0.07	0.03	0.15	0.00	54.92	5.88	0.09	0.00	0.00	0.16	0.01	0.03	0.01	0.00	0.02	0.03		100.35	2016	IBH-13-12, Brown&Black Gt
2305	253	37.35	0.00	0.01	0.02	0.09	0.00	0.07	0.04	56.62	5.46	0.06	0.00	0.00	0.12	0.12	0.00	0.00	0.00	0.01	0.00		96.97	2016	IBH-13-12, Brown&Black Gt
2306	254	39.47	0.00	0.02	0.01	0.03	0.01	0.17	0.03	52.96	5.69	0.19	0.00	0.01	0.11	0.16	0.07	0.01	0.00	0.03	0.07		97.69	2016	IBH-13-12, Brown&Black Gt
2307	255	39.91	0.00	0.03	0.06	0.06	0.00	0.00	0.02	53.14	5.18	0.13	0.00	0.00	0.10	0.00	0.04	0.00	0.00	0.06	0.00		99.04	2016	IBH-13-12, Brown&Black Gt
2308	256	36.66	0.00	0.01	0.02	0.04	0.02	0.04	0.00	53.09	5.96	0.05	0.03	0.01	0.05	0.09	0.01	0.00	0.00	0.02	0.03		98.21	2016	IBH-13-12, Brown&Black Gt
2309	257	37.27	0.04	0.02	0.00	0.08	0.01	0.04	0.00	59.43	1.09	0.05	0.00	0.01	0.15	0.08	0.02	0.04	0.00	0.05	0.01		98.37	2016	IBH-13-12, Brown&Black Gt
2310	258	37.05	0.00	0.00	0.01	0.08	0.01	0.04	0.02	60.21	0.83	0.04	0.00	0.00	0.13	0.03	0.00	0.01	0.00	0.00	0.00		98.45	2016	IBH-13-12, Brown&Black Gt
2311	259	37.22	0.07	0.01	0.00	0.01	0.00	0.04	0.00	58.69	1.62	0.05	0.02	0.00	0.14	0.00	0.04	0.00	0.00	0.00	0.04		97.93	2016	IBH-13-12, Brown&Black Gt
2312	260	37.12	0.05	0.00	0.02	0.08	0.00	0.04	0.00	58.59	1.41	0.05	0.00	0.00	0.15	0.07	0.00	0.00	0.00	0.11	0.00		97.69	2016	IBH-13-12, Brown&Black Gt
2313	261	39.29	0.00	0.03	0.08	0.04	0.02	0.10	0.00	52.45	6.25	0.14	0.00	0.00	0.13	0.04	0.00	0.00	0.00	0.00	0.00		98.82	2016	IBH-13-12, Brown&Black Gt
2314	262	39.05	0.00	0.00	0.08	0.04	0.00	0.12	0.02	53.19	5.04	0.00	0.00	0.00	0.13	0.10	0.04	0.00	0.00	0.02	0.04		98.63	2016	IBH-13-12, Brown&Black Gt
2315	263	38.84	0.00	0.03	0.07	0.06	0.02	0.11	0.04	53.63	6.59	0.15	0.01	0.00	0.12	0.07	0.06	0.04	0.00	0.01	0.02		98.85	2016	IBH-13-12, Brown&Black Gt
2316	264	38.72	0.00	0.00	0.06	0.05	0.03	0.08	0.02	53.23	6.91	0.11	0.00	0.04	0.14	0.05	0.01	0.06	0.00	0.05	0.00		99.55	2016	IBH-13-12, Brown&Black Gt
2317	145	37.46	0.00	0.00	0.01	0.06	0.00	0.77	0.01	57.56	3.30	0.01	0.00	0.00	0.15	0.00	0.01	0.05	0.00	0.07			99.45	2016	MAC-61-2-1
2318	146	37.54	0.00	0.00	0.01	0.06	0.03	0.68	0.00	58.72	3.17	0.01	0.00	0.01	0.14	0.01	0.00	0.07	0.00	0.04			100.48	2016	MAC-61-2-2
2319	147	36.88	0.03	0.00	0.00	0.06	0.01	0.81	0.00	59.46	2.68	0.01	0.04	0.03	0.16	0.00	0.00	0.10	0.00	0.04			100.29	2016	MAC-61-2-3
2320	148	36.41	0.00	0.02	0.05	0.08	0.04	0.39	0.02	60.52	1.58	0.01	0.00	0.01	0.10	0.02	0.00	0.15	0.00	0.00			99.38	2016	MAC-61-2-5
2321	149	36.54	0.09	0.00	0.02	0.07	0.02	0.38	0.03	61.28	1.08	0.03	0.00	0.00	0.11	0.03	0.00	0.11	0.00	0.03			99.83	2016	MAC-61-2-5
2322	181	38.37	0.05	0.00	0.05	0.05	0.06	0.42	0.00	58.02	3.66		0.00	0.00	0.15	0.00	0.00	0.00	0.00	0.00	0.00		100.83	2016	Pic-66 24/2
2323	340	36.98				0.00	0.03	0.00	0.05	0.00	57.78	0.46	0.04		0.01	1.28	0.00	0.00	0.00				96.62	2016	Pic-66 04 grain 3
2324	162	32.56	0.12	0.01	0.00	0.07	0.06	0.13	0.03	65.76	0.78	0.08	0.00	0.00	0.49	0.00	0.00	0.16	0.07	0.00			100.30	2016	Pic-6-2-3-850um-4
2325	165	32.46	0.00	0.00	0.00	0.07	0.10	0.19	0.02	65.35	0.52	0.10	0.00	0.00	0.67	0.03	0.00	0.28	0.06	0.00			99.84	2016	Pic-6-2-3-850um-7
2326	166	31.86	0.00	0.00	0.00	0.08	0.08	0.21	0.00	65.58	0.54	0.09	0.00	0.00	0.65	0.05	0.00	0.32	0.05	0.00			99.51	2016	Pic-6-2-3-850um-8
2327	188	36.00	0.02	0.01	0.00	0.06	0.03	0.08	0.01	62.45	0.46	0.05	0.00	0.01	0.35	0.06	0.05	0.00	0.00	0.06			99.69	2016	Pic-6-22-BH-Gt, 850-425um-2-4
2328	118	34.62	0.06	0.01	0.01	0.08	0.03	0.04	0.00	64.89	0.03	0.04	0.00	0.00	0.61	0.05	0.03	0.00	0.04	0.03			100.55	2016	Pic6-2-11-Black-Gt-10
2329	119	34.21	0.06	0.00	0.00	0.10	0.04	0.09	0.00	64.76	0.01	0.03	0.00	0.02	0.44	0.06	0.01	0.00	0.01	0.00			99.82	2016	Pic6-2-11-Black-Gt-11
2330	111	36.60	0.02	0.02	0.00	0.04	0.06	0.07	0.01	62.82	0.06	0.08	0.00	0.03	0.51	0.08	0.00	0.00	0.00	0.01			100.40	2016	Pic6-2-11-Black-Gt-3
2331	114	37.21	0.00	0.00	0.00	0.00	0.00	0.00	0.00	62.51	0.01	0.00	0.00	0.00	0.38	0.05	0.00	0.00	0.00	0.00			100.47	2016	Pic6-2-11-Black-Gt-6
2332	115	35.81	0.01	0.01	0.00	0.08	0.09	0.11	0.00	63.44	0.09	0.08	0.01	0.00	0.54	0.06	0.03	0.00	0.02	0.00			100.39	2016	Pic6-2-11-Black-Gt-7
2333	116	35.01	0.07	0.00	0.00	0.08	0.07	0.13	0.01	64.06	0.07	0.09	0.01	0.02	0.60	0.00	0.01	0.01	0.06	0.05			100.34	2016	Pic6-2-11-Black-Gt-8
2334	120	32.47	0.00	0.01	0.00	0.09	0.08	0.09	0.00	65.88	0.31	0.10	0.00	0.02	0.65	0.00	0.00	0.16	0.00	0.00			99.86	2016	Pic6-2-3-Layered-Gt-1
2335	122	31.90	0.04	0.00	0.00	0.07	0.06	0.09	0.00	65.59	0.45	0.09	0.00	0.00	0.63	0.00	0.02	0.10	0.00	0.11			99.14	2016	Pic6-2-3-Layered-Gt-3
2336	124	31.95	0.09	0.00	0.00	0.06	0.07	0.21	0.01	64.29	0.67	0.17	0.00	0.00	0.71	0.04	0.00	0.25	0.09	0.00			98.60	2016	Pic6-2-3-Layered-Gt-5
2337	125	32.39	0.12	0.00	0.00	0.06	0.17	0.02	64.82	0.39	0.09	0.00	0.00	0.77	0.00	0.00	0.18	0.04	0.00	0.00			99.33	2016	Pic6-2-3-Layered-Gt-6
2338	126	31.82	0.06	0.01	0.00	0.07	0.06	0.10	0.00	65.41	0.10	0.08	0.00	0.00	0.72	0.04	0.08	0.08	0.00	0.05			98.70	2016	Pic6-2-3-Layered-Gt-7
2339	71	38.01	0.00	0.00	0.00	0.10	0.00	0.01	0.01	59.49	0.00	0.01	0.00	0.00	0.70	0.10	0.00	0.00	0.00	0.00			98.42	2016	Pic6-21-6-Alpoor-Gt-1
2340	72	36.70	0.00	0.02	0.00	0.07	0.00	0.04	0.01	59.61	0.01	0.02	0.00	0.00	0.61	0.00	0.00	0.00	0.00	0.00			97.10	2016	Pic6-21-6-Alpoor-Gt-2
2341	73	37.28	0.06	0.00	0.01	0.05	0.00	0.03	0.02	60.58	0.00	0.01	0.00	0.00	0.57	0.00	0.02	0.00	0.00	0.00			98.63	2016	Pic6-21-6-Alpoor-Gt-3
2342	74	37.53	0.03	0.00	0.00	0.05	0.01	0.00	0.00	62.11	0.02	0.01	0.00	0.00	0.57	0.00	0.00	0.00	0.00	0.04			100.38	2016	Pic6-21-6-Alpoor-Gt-4
2343	75	37.03	0.00	0.00	0.00	0.00	0.01	0.00	0.00	59.29	0.00	0.00	0.00	0.00	0.68	0.02	0.00	0.00	0.00	0.00			97.12	2016	Pic6-21-6-Alpoor-Gt-5
2344	76	37.51	0.04	0.00	0.02	0.04	0.00	0.00	0.00	61.44	0.02	0.01	0.01	0.02	0.54	0.02	0.00	0.01	0.00	0.02			99.69	2016	Pic6-21-6-Alpoor-Gt-6
2345	61	38.72	0.16	0.00	0.04	0.06	0.01	0.16	0.00	57.20	1.84	0.04	0.00	0.00	0.27	0.00	0.01	0.15	0.00	0.00			98.66	2016	Pic6-21-6-Black-Dull-Gt
2346	62	38.96	0.03	0.02	0.00	0.06	0.00	0.10	0.01	57.14	1.82	0.02	0.00	0.00	0.26	0.02	0.00	0.15	0.00	0.06			98.66	2016	Pic6-21-6-Black-Dull-Gt
2347	63	38.79	0.01	0.00	0.01	0.05	0.00	0.09	0.00	57.27	1.83	0.05	0.03	0.00	0.26	0.00	0.01	0.13	0.00	0.05			99.59	2016	Pic6-21-6-Black-Dull-Gt
2348	64	39.24	0.00	0.01	0.00	0.05	0.01	0.14	0.03	57.27	1.78	0.03	0.05	0.00	0.27	0.04	0.00	0.13	0.00	0.00			98.96	2016	Pic6-21-6-Black-Dull-Gt
2349	65	38.98	0.01	0.01	0.01	0.00	0.01	0.01	0.01	57.38	1.77	0.04	0.02	0.00	0.28	0.01	0.01	0.12	0.00	0.01			98.88	2016	Pic6-21-6-Black-Dull-Gt
2350	66	38.84	0.02	0.01	0.00	0.06	0.01	0.08	0.01	57.40	1.77	0.02	0.06	0.00	0.28	0.00	0.00	0.12	0.00	0.02			98.71	2016	Pic6-21-6-Black-Dull-Gt
2351	67	38.81	0.12	0.01	0.00	0.04	0.00	0.13	0.00	57.14	1.83	0.05	0.00	0.00	0.27	0.02	0.01	0.12	0.00	0.02			98.56	2016	Pic6-21-6-Black-Dull-Gt
2352	68	38.89	0.13	0.00	0.00	0.09	0.01	0.11	0.00	57.28	1.83	0.02	0.03	0.01	0.28	0.06	0.03	0.13	0.00	0.04			98.92	2016	Pic6-21-6-Black-Dull-Gt
2353	69	38.74	0.00	0.00	0.01	0.08	0.00	0.15	0.00	56.99	1.80	0.04	0.03	0.00	0.27	0.01	0.06	0.13	0.00	0.05					

INDEX	No.	O	Na	K	V	Co	Mg	P	Cr	Fe	Al	S	Ni	Mn	Si	Pb	Cu	Ti	Ca	Zn	Ba	Sr	Total	Year	Sample
2448	1114	35.04	0.00	0.01	0.00	0.00	0.03	0.19	0.00	63.50	1.32	0.04	0.00	0.02	0.41	0.00	0.00	0.08	0.03	0.00			100.68	2017	G-12-04(A) brown HM-21
2449	1115	35.12	0.00	0.01	0.03	0.00	0.01	0.16	0.00	64.04	1.21	0.07	0.03	0.00	0.44	0.00	0.00	0.10	0.00	0.00			101.22	2017	G-12-04(A) brown HM-21
2450	1116	35.25	0.00	0.03	0.01	0.00	0.03	0.15	0.02	63.56	1.13	0.04	0.01	0.00	0.42	0.03	0.00	0.09	0.00	0.00			100.78	2017	G-12-04(A) brown HM-21
2451	1117	35.39	0.05	0.04	0.00	0.00	0.02	0.14	0.00	64.04	1.27	0.05	0.00	0.00	0.44	0.07	0.03	0.11	0.00	0.00			101.64	2017	G-12-04(A) brown HM-21
2452	1118	35.24	0.01	0.00	0.00	0.00	0.04	0.15	0.02	63.56	1.33	0.08	0.00	0.00	0.46	0.00	0.00	0.06	0.00	0.00			100.89	2017	G-12-04(A) brown HM-21
2453	1119	35.69	0.00	0.00	0.02	0.00	0.02	0.14	0.00	63.10	1.06	0.05	0.02	0.00	0.51	0.00	0.00	0.00	0.01	0.00			100.61	2017	G-12-04(A) brown HM-21
2454	1120	35.88	0.00	0.02	0.00	0.00	0.00	0.07	0.00	63.79	1.76	0.09	0.05	0.01	0.26	0.04	0.00	0.00	0.00	0.00			101.98	2017	G-12-04(A) black HM-21
2455	1121	36.77	0.01	0.01	0.05	0.00	0.01	0.06	0.00	60.74	1.58	0.07	0.04	0.00	0.26	0.04	0.01	0.00	0.00	0.00			99.63	2017	G-12-04(A) black HM-21
2456	1122	37.67	0.00	0.01	0.02	0.00	0.00	0.08	0.00	58.92	1.50	0.09	0.00	0.02	0.22	0.05	0.02	0.01	0.00	0.00			98.62	2017	G-12-04(A) black HM-21
2457	1123	37.98	0.00	0.01	0.00	0.00	0.00	0.07	0.01	59.65	1.65	0.07	0.00	0.00	0.29	0.10	0.05	0.01	0.00	0.00			99.82	2017	G-12-04(A) black HM-21
2458	1124	38.53	0.02	0.01	0.00	0.00	0.02	0.03	0.04	58.97	1.55	0.09	0.03	0.05	0.30	0.11	0.00	0.03	0.00	0.00			99.81	2017	G-12-04(A) black HM-21
2459	1125	38.47	0.00	0.03	0.03	0.00	0.00	0.05	0.00	58.81	1.66	0.08	0.04	0.02	0.26	0.06	0.01	0.01	0.00	0.00			99.56	2017	G-12-04(A) black HM-21
2460	1126	39.56	0.00	0.03	0.02	0.00	0.01	1.12	0.00	57.23	3.42	0.03	0.02	0.00	0.06	0.08	0.02	0.01	0.00	0.00			101.60	2017	Pic 06 25A/8 HM-21
2461	1127	39.07	0.00	0.02	0.03	0.00	0.00	1.09	0.00	56.47	3.45	0.02	0.00	0.00	0.07	0.07	0.00	0.00	0.00	0.00			100.31	2017	Pic 06 25A/8 HM-21
2462	1128	38.77	0.00	0.00	0.00	0.00	0.00	1.16	0.00	57.75	3.28	0.03	0.01	0.00	0.05	0.04	0.00	0.05	0.01	0.00			101.16	2017	Pic 06 25A/8 HM-21
2463	1129	36.45	0.00	0.01	0.02	0.00	0.03	1.10	0.04	61.05	3.21	0.05	0.00	0.00	0.05	0.05	0.03	0.03	0.00	0.00			102.11	2017	Pic 06 25A/8 HM-21
2464	1130	37.81	0.00	0.02	0.00	0.00	0.00	1.03	0.00	59.30	2.46	0.02	0.00	0.00	0.07	0.00	0.00	0.03	0.00	0.00			100.75	2017	Pic 06 25A/8 HM-21
2465	1131	38.34	0.00	0.02	0.00	0.00	0.02	0.99	0.00	58.31	2.55	0.05	0.01	0.00	0.08	0.04	0.00	0.08	0.01	0.00			100.51	2017	Pic 06 25A/8 HM-21
2466	1132	36.40	0.00	0.01	0.00	0.00	0.00	0.34	0.01	59.59	0.22	0.01	0.00	0.00	0.25	0.00	0.03	0.03	0.00	0.00			96.89	2017	Pic 06 25A/8 HM-21
2467	1133	38.70	0.00	0.02	0.00	0.00	0.00	0.73	0.00	59.41	2.32	0.02	0.00	0.00	0.05	0.15	0.00	0.04	0.00	0.00			101.46	2017	Pic 06 25A/8 HM-21
2468	1134	38.98	0.01	0.02	0.03	0.00	0.01	0.90	0.00	57.77	3.20	0.03	0.00	0.00	0.03	0.06	0.03	0.02	0.00	0.00			101.11	2017	Pic 06 25A/8 HM-21
2469	1135	38.50	0.00	0.02	0.00	0.00	0.01	0.83	0.01	59.34	2.05	0.04	0.01	0.05	0.06	0.02	0.01	0.02	0.00	0.00			100.96	2017	Pic 06 25A/8 HM-21
2470	1136	35.74	0.00	0.02	0.00	0.00	0.06	1.23	0.00	60.75	3.66	0.02	0.00	0.00	0.07	0.05	0.07	0.09	0.10	0.00			101.86	2017	Pic 06 25B/2+3 HM-21
2471	1137	34.90	0.00	0.03	0.00	0.00	0.08	1.28	0.01	60.92	3.84	0.03	0.00	0.00	0.05	0.06	0.00	0.01	0.17	0.00			101.37	2017	Pic 06 25B/2+3 HM-21
2472	1138	35.40	0.00	0.03	0.02	0.00	0.07	1.22	0.02	60.33	3.85	0.05	0.01	0.00	0.06	0.02	0.00	0.10	0.13	0.00			101.33	2017	Pic 06 25B/2+3 HM-21
2473	1139	38.19	0.00	0.03	0.05	0.00	0.00	1.22	0.01	58.13	3.62	0.06	0.02	0.04	0.05	0.01	0.00	0.20	0.01	0.00			101.63	2017	Pic 06 25B/2+3 HM-21
2474	1140	37.20	0.00	0.03	0.00	0.00	0.01	1.24	0.00	59.06	3.40	0.01	0.00	0.00	0.03	0.02	0.05	0.10	0.05	0.00			101.21	2017	Pic 06 25B/2+3 HM-21
2475	1141	36.92	0.00	0.00	0.00	0.00	0.02	1.23	0.02	59.34	3.31	0.05	0.00	0.00	0.05	0.07	0.02	0.08	0.00	0.00			101.15	2017	Pic 06 25B/2+3 HM-21
2476	1142	35.62	0.00	0.01	0.04	0.00	0.02	1.23	0.00	60.23	3.05	0.03	0.01	0.02	0.04	0.08	0.00	0.01	0.04	0.00			100.44	2017	Pic 06 25B/2+3 HM-21
2477	1143	33.68	0.00	0.03	0.00	0.00	0.02	1.31	0.00	60.45	3.26	0.04	0.00	0.03	0.12	0.05	0.01	0.04	0.15	0.00			99.19	2017	Pic 06 25B/2+3 HM-21
2478	1144	36.48	0.00	0.01	0.00	0.00	0.00	0.34	0.00	62.56	0.48	0.05	0.00	0.00	0.24	0.05	0.00	0.02	0.00	0.00			100.23	2017	Pic 06 25B/2+3 HM-21
2479	1145	36.13	0.00	0.03	0.04	0.00	0.01	1.33	0.00	61.28	2.82	0.03	0.03	0.00	0.05	0.04	0.07	0.08	0.08	0.00			102.02	2017	Pic 06 25B/2+3 HM-21
2480	1156	35.46	0.01	0.02	0.01	0.00	0.02	0.51	0.01	63.60	0.25	0.02	0.03	0.01	0.14	0.00	0.04	0.00	0.00	0.00			100.15	2017	BAH-100 Gr-Gib-HM-17
2481	1157	35.90	0.03	0.00	0.03	0.00	0.03	0.99	0.00	62.32	0.18	0.02	0.04	0.00	0.15	0.05	0.08	0.00	0.00	0.00			100.27	2017	BAH-100 Gr-Gib-HM-17
2482	1158	36.14	0.07	0.01	0.05	0.00	0.01	0.43	0.03	62.90	0.13	0.01	0.00	0.01	0.12	0.03	0.00	0.01	0.00	0.00			99.95	2017	BAH-100 Gr-Gib-HM-17
2483	1159	35.66	0.03	0.00	0.00	0.00	0.00	0.40	0.01	63.05	0.13	0.02	0.06	0.02	0.12	0.01	0.05	0.00	0.00	0.00			99.55	2017	BAH-100 Gr-Gib-HM-17
2484	1160	34.85	0.00	0.02	0.01	0.00	0.00	0.49	0.00	62.21	0.22	0.02	0.05	0.03	0.19	0.00	0.08	0.00	0.00	0.00			98.17	2017	BAH-100 Gr-Gib-HM-17
2485	1163	34.97	0.00	0.02	0.02	0.00	0.00	0.47	0.00	64.73	0.59	0.05	0.00	0.00	0.12	0.00	0.02	0.01	0.01	0.00			101.03	2017	NIP-13-21b-HM17-3b
2486	1164	35.19	0.00	0.02	0.00	0.00	0.00	0.73	0.00	60.99	0.07	0.00	0.07	0.19	0.15	0.02	0.60	0.00	0.00	0.00			98.05	2017	BAH-03cm6 brown-HM17
2487	1165	32.62	0.00	0.03	0.00	0.00	0.00	0.63	0.00	62.00	0.11	0.02	0.06	0.24	0.17	0.08	0.66	0.00	0.00	0.00			95.62	2017	BAH-03cm6 brown-HM17
2488	1166	33.97	0.00	0.00	0.02	0.00	0.01	0.64	0.00	62.34	0.07	0.00	0.06	0.05	0.22	0.08	0.64	0.01	0.00	0.00			98.12	2017	BAH-03cm6 brown-HM17
2489	1167	34.16	0.00	0.02	0.03	0.00	0.00	0.64	0.04	62.69	0.09	0.02	0.02	0.10	0.19	0.07	0.68	0.00	0.01	0.00			98.75	2017	BAH-03cm6 brown-HM17
2490	1168	34.36	0.02	0.00	0.00	0.00	0.01	0.71	0.00	63.54	0.13	0.03	0.07	0.12	0.20	0.04	0.79	0.02	0.00	0.00			100.02	2017	BAH-03cm6 brown-HM17
2491	1169	35.44	0.00	0.01	0.00	0.00	0.05	0.64	0.00	61.98	0.07	0.02	0.06	0.11	0.18	0.00	0.70	0.00	0.00	0.00			99.26	2017	BAH-03cm6 brown-HM17
2492	1170	34.87	0.00	0.03	0.04	0.00	0.00	0.71	0.03	62.95	0.12	0.01	0.05	0.11	0.18	0.12	0.70	0.05	0.00	0.00			99.96	2017	BAH-03cm6 brown-HM17
2493	1171	33.97	0.03	0.03	0.00	0.00	0.00	0.63	0.00	62.00	0.11	0.02	0.06	0.24	0.17	0.06	0.73	0.00	0.00	0.00			97.98	2017	BAH-03cm6 brown-HM17-2b
2494	1172	38.01	0.00	0.00	0.00	0.00	0.01	0.22	0.00	61.56	0.24	0.03	0.00	0.03	1.15	0.00	0.05	0.00	0.00	0.00			101.31	2017	G-12-12 HM-21
2495	1173	38.12	0.00	0.00	0.01	0.00	0.00	0.15	0.00	60.02	0.35	0.02	0.02	0.02	1.34	0.02	0.02	0.00	0.00	0.00			100.10	2017	G-12-12 HM-21
2496	1174	37.69	0.00	0.03	0.02	0.00	0.00	0.21	0.00	60.05	0.05	0.01	0.00	0.00	0.89	0.09	0.02	0.00	0.00	0.00			99.07	2017	G-12-12 HM-21
2497	1175	37.66	0.00	0.00	0.00	0.00	0.00	0.11	0.02	61.61	0.08	0.02	0.00												

EA2: SHRIMP-SI oxygen isotopic data for Carajás.

SPOT #	Session	Date	Time	¹⁸ O/ ¹⁶ O(a)	± (b)	δ ¹⁸ O _{VSMOW} (a)	rejected	±Internal error (σ 95%)	¹⁸ O cps (median)	¹⁶ O cps (median)	(U-Th)/He ages	±	MOUNT
BAH3BL-1.1	#02	26/10/14	14:13:13	0.0019612	0.0000003		-5.02	0.14	2.50E+09	4.90E+06	13.73	2.14	HM 1
BAH3BL-1.2	#02	26/10/14	14:18:49	0.0019623	0.0000002	-4.44		0.11	2.53E+09	4.97E+06	13.73	2.14	
BAH3BL-1.3	#02	26/10/14	14:24:22	0.0019634	0.0000003	-3.89		0.13	2.50E+09	4.91E+06	13.73	2.14	
BAH3BL-1.4	#02	26/10/14	14:29:56	0.0019617	0.0000003	-4.73		0.14	2.52E+09	4.93E+06	13.73	2.14	
	#02			average		-4.35							
				std dev (1σ)		0.43							
BAH3BL-2.1	#02	26/10/14	14:35:30	0.0019640	0.0000004	-3.57		0.20	2.55E+09	5.00E+06	13.73	2.14	HM 1
BAH3BL-2.2	#02	26/10/14	14:41:04	0.0019632	0.0000005	-3.96		0.27	2.54E+09	4.99E+06	13.73	2.14	
BAH3BL-2.3	#02	26/10/14	14:47:17	0.0019654	0.0000004	-2.85		0.18	2.55E+09	5.01E+06	13.73	2.14	
BAH3BL-2.4	#02	26/10/14	14:53:30	0.0019626	0.0000004	-4.31		0.22	2.60E+09	5.10E+06	13.73	2.14	
BAH3BL-2.7	#02	26/10/14	15:10:54	0.0019643	0.0000004	-3.43		0.21	2.59E+09	5.08E+06	13.73	2.14	
	#02			average		-3.62							
				std dev (1σ)		0.55							
BAH3LGB-1.1	#02	26/10/14	15:16:43	0.0019682	0.0000002	-1.39		0.09	2.55E+09	5.01E+06	16.26	0.92	HM 1
BAH3LGB-1.2	#02	26/10/14	15:22:33	0.0019682	0.0000002	-1.42		0.12	2.56E+09	5.05E+06	16.26	0.92	
	#02			average		-1.41							
				std dev (1σ)		0.02							
BAH3LGB-2.1	#02	26/10/14	15:28:25	0.0019688	0.0000002	-1.11		0.11	2.51E+09	4.94E+06	16.26	0.92	HM 1
BAH3LGB-2.2	#02	26/10/14	15:34:15	0.0019686	0.0000004	-1.17		0.19	2.53E+09	4.97E+06	16.26	0.92	
BAH3LGB-2.3	#02	26/10/14	15:40:03	0.0019680	0.0000004	-1.49		0.19	2.53E+09	4.98E+06	16.26	0.92	
BAH3LGB-2.4	#02	26/10/14	15:45:51	0.0019682	0.0000004	-1.42		0.21	2.53E+09	4.98E+06	16.26	0.92	
BAH3LGB-2.5	#02	26/10/14	15:52:19	0.0019681	0.0000003	-1.44		0.15	2.56E+09	5.04E+06	16.26	0.92	
BAH3LGB-2.6	#02	26/10/14	15:58:33	0.0019677	0.0000004	-1.67		0.18	2.46E+09	4.85E+06	16.26	0.92	
BAH3LGB-2.8	#02	26/10/14	16:06:42	0.0019696	0.0000003		-0.68	0.16	2.56E+09	5.03E+06	16.26	0.92	
BAH3LGB-2.9	#02	26/10/14	16:13:10	0.0019695	0.0000004		-0.71	0.19	2.52E+09	4.95E+06	16.26	0.92	
BAH3LGB-2.6B	#02	26/10/14	17:08:22	0.0019681	0.0000003	-1.47		0.17	2.53E+09	4.97E+06	16.26	0.92	
BAH3LGB-2.8B	#02	26/10/14	17:25:51	0.0019676	0.0000004	-1.73		0.21	2.53E+09	4.97E+06	16.26	0.92	
BAH3LGB-2.9B	#02	26/10/14	17:32:48	0.0019688	0.0000005	-1.11		0.24	2.52E+09	4.96E+06	16.26	0.92	
	#02			average		-1.40							
				std dev (1σ)		0.23							
BAH9901-1.1	#02	27/10/14	2:21:16	0.0019773	0.0000003	3.28		0.15	2.45E+09	4.85E+06	25.06	4.40	HM 1
BAH9901-1.2	#02	27/10/14	2:26:49	0.0019771	0.0000003	3.19		0.13	2.42E+09	4.78E+06	25.06	4.40	
BAH9901-1.3	#02	27/10/14	2:32:23	0.0019762	0.0000003	2.74		0.13	2.44E+09	4.82E+06	25.06	4.40	
BAH9901-1.4	#02	27/10/14	2:37:59	0.0019759	0.0000003	2.55		0.13	2.52E+09	4.98E+06	25.06	4.40	
BAH9901-1.6	#02	27/10/14	2:49:11	0.0019759	0.0000002	2.55		0.08	2.51E+09	4.97E+06	25.06	4.40	
BAH9901-1.7	#02	27/10/14	12:14:11	0.0019781	0.0000004	3.68		0.18	2.44E+09	4.83E+06	25.06	4.40	
BAH9901-1.8	#02	27/10/14	12:23:38	0.0019779	0.0000003	3.62		0.13	2.45E+09	4.84E+06	25.06	4.40	
	#02			average		3.09							
				std dev (1σ)		0.48							
BAH9901-2.1	#02	27/10/14	2:54:45	0.0019776	0.0000002	3.43		0.08	2.44E+09	4.83E+06	25.06	4.40	HM 1
BAH9901-2.2	#02	27/10/14	3:00:22	0.0019780	0.0000003	3.66		0.13	2.42E+09	4.78E+06	25.06	4.40	
BAH9901-2.3	#02	27/10/14	3:05:55	0.0019763	0.0000002	2.76		0.09	2.40E+09	4.75E+06	25.06	4.40	
BAH9901-2.4	#02	27/10/14	3:11:28	0.0019759	0.0000003	2.58		0.14	2.39E+09	4.72E+06	25.06	4.40	
	#02			average		3.11							
				std dev (1σ)		0.52							
BAHF252_118.2-1.1_brown	#02	27/10/14	5:19:52	0.0019701	0.0000002	-0.40		0.10	2.41E+09	4.75E+06	37.28	6.34	HM 1
BAHF252_118.2-1.2_brown	#02	27/10/14	5:25:26	0.0019694	0.0000002	-0.76		0.11	2.40E+09	4.72E+06	37.28	6.34	
BAHF252_118.2-1.3_brown	#02	27/10/14	5:31:00	0.0019696	0.0000002	-0.67		0.09	2.40E+09	4.74E+06	37.28	6.34	
BAHF252_118.2-1.4_brown	#02	27/10/14	5:36:33	0.0019698	0.0000003	-0.59		0.16	2.41E+09	4.74E+06	37.28	6.34	
	#02			average		-0.60							
				std dev (1σ)		0.16							
BAHF252_118.2-2.1	#02	27/10/14	5:42:08	0.0019753	0.0000003	2.26		0.14	2.34E+09	4.62E+06			HM 1
BAHF252_118.2-2.2	#02	27/10/14	5:47:42	0.0019757	0.0000002	2.49		0.10	2.34E+09	4.62E+06			
BAHF252_118.2-2.3	#02	27/10/14	5:53:15	0.0019743	0.0000003	1.73		0.13	2.33E+09	4.61E+06			
BAHF252_118.2-2.4	#02	27/10/14	5:58:49	0.0019756	0.0000002	2.41		0.12	2.34E+09	4.61E+06			
BAHF252_118.2-2.5	#02	27/10/14	6:04:22	0.0019758	0.0000002	2.54		0.11	2.34E+09	4.62E+06			
BAHF252_118.2-2.6	#02	27/10/14	6:09:58	0.0019698	0.0000002		-0.57	0.10	2.23E+09	4.39E+06			
BAHF252_118.2-2.7	#02	27/10/14	6:15:32	0.0019656	0.0000002		-2.74	0.13	2.29E+09	4.51E+06			
BAHF252_118.2-2.8	#02	27/10/14	6:21:07	0.0019776	0.0000002	3.45		0.11	2.44E+09	4.83E+06			
BAHF252_118.2-2.9	#02	27/10/14	6:26:41	0.0019760	0.0000003	2.60		0.14	2.36E+09	4.66E+06			
BAHF252_118.2-2.10	#02	27/10/14	6:32:14	0.0019763	0.0000003	2.76		0.15	2.36E+09	4.66E+06			
	#02			average		2.53							
				std dev (1σ)		0.48							
NIP1302-1.1	#02	27/10/14	12:46:11	0.0019786	0.0000003	3.99		0.13	2.44E+09	4.83E+06			HM 1
NIP1302-1.2	#02	27/10/14	12:51:59	0.0019807	0.0000002	5.03		0.11	2.44E+09	4.83E+06			
NIP1302-1.3	#02	27/10/14	12:57:47	0.0019802	0.0000002	4.77		0.11	2.44E+09	4.83E+06			
NIP1302-1.4	#02	27/10/14	13:03:35	0.0019803	0.0000002	4.84		0.12	2.43E+09	4.81E+06			
NIP1302-1.5	#02	27/10/14	13:09:23	0.0019843	0.0000003	6.89		0.13	2.51E+09	4.97E+06			
NIP1302-1.6	#02	27/10/14	13:15:11	0.0019849	0.0000002	7.22		0.10	2.53E+09	5.01E+06			
NIP1302-1.7	#02	27/10/14	13:20:59	0.0019841	0.0000002	6.79		0.08	2.46E+09	4.88E+06			
NIP1302-1.8	#02	27/10/14	13:26:47	0.0019854	0.0000003	7.49		0.13	2.49E+09	4.95E+06			
	#02			average		5.88							
				std dev (1σ)		1.35							
IBH1308C-1.1	#02	27/10/14	13:44:05	0.0019723	0.0000002		0.73	0.12	2.45E+09	4.84E+06	29.57	0.86	HM 1
IBH1308C-1.2	#02	27/10/14	13:49:53	0.0020109	0.0000002	20.63		0.12	2.40E+09	4.83E+06	29.57	0.86	
IBH1308C-1.3	#02	27/10/14	13:55:42	0.0020072	0.0000002	18.71		0.11	2.42E+09	4.86E+06	29.57	0.86	
IBH1308C-1.4	#02	27/10/14	14:01:										

SPOT #	Session	Date	Time	¹⁸ O/ ¹⁶ O ^(a)	± ^(b)	δ ¹⁸ O _{VSMOW} ^(c)	rejected	±Internal error (σ 95%)	¹⁸ O cps (median)	¹⁶ O cps (median)	(U-Th)/He ages	±	MOUNT
BAH3BL-1.10	#03	28/10/14	5:36:54	0.0019673	0.0000002	-1.27		0.12	2.47E+09	4.85E+06	13.73	2.14	
BAH3BL-1.11	#03	28/10/14	5:42:27	0.0019673	0.0000003	-1.26		0.14	2.44E+09	4.81E+06	13.73	2.14	
BAH3BL_1.1	#03	28/10/14	14:30:45	0.0019661	0.0000002	-1.89		0.12	2.47E+09	4.86E+06	13.73	2.14	
BAH3BL_1.2	#03	28/10/14	14:36:18	0.0019656	0.0000002		-2.13	0.10	2.47E+09	4.85E+06	13.73	2.14	
	#03			average		-1.47							
				std dev (1σ)		0.28							
BAH3LGB_1.1	#03	28/10/14	14:07:28	0.0019663	0.0000003	-1.79		0.13	2.52E+09	4.96E+06	16.26	0.92	HM 4
BAH3LGB_1.2	#03	28/10/14	14:13:02	0.0019655	0.0000002	-2.16		0.11	2.46E+09	4.84E+06	16.26	0.92	
BAH3LGB_1.3	#03	28/10/14	14:18:38	0.0019654	0.0000003	-2.21		0.14	2.46E+09	4.84E+06	16.26	0.92	
BAH3LGB_2.1	#03	28/10/14	14:25:10	0.0019685	0.0000002		-0.63	0.12	2.48E+09	4.89E+06	16.26	0.92	
	#03			average		-2.05							
				std dev (1σ)		0.23							
NIP-13-02_1.1	#03	18/12/14	11:57:04	0.0019813	0.0000002		9.19	0.11	2.55E+09	5.05E+06			HM 4
NIP-13-02_1.2	#03	18/12/14	12:16:56	0.0019760	0.0000002	6.45		0.11	2.51E+09	4.96E+06			
NIP-13-02_1.3	#03	18/12/14	12:22:58	0.0019769	0.0000002	6.89		0.12	2.52E+09	4.97E+06			
NIP-13-02_1.4	#03	18/12/14	12:28:59	0.0019747	0.0000002	5.75		0.12	2.43E+09	4.80E+06			
	#03			average		6.36							
				std dev (1σ)		0.57							
NIP-13-02_2.3	#03	18/12/14	12:47:05	0.0019741	0.0000002	5.38		0.08	2.50E+09	4.94E+06			HM 4
NIP-13-02_2.4	#03	18/12/14	12:53:06	0.0019718	0.0000002	4.21		0.09	2.47E+09	4.86E+06			
	#03			average		4.79							
				std dev (1σ)		0.83							
NIP-13-02_3.1	#03	18/12/14	12:59:10	0.0019701	0.0000003	3.29		0.15	2.27E+09	4.48E+06			HM 4
NIP-13-02_3.2	#03	18/12/14	13:05:14	0.0019686	0.0000002	2.51		0.13	2.26E+09	4.44E+06			
NIP-13-02_3.3	#03	18/12/14	13:11:18	0.0019740	0.0000002	5.29		0.09	2.41E+09	4.76E+06			
NIP-13-02_3.4	#03	18/12/14	13:17:20	0.0019772	0.0000002	6.97		0.12	2.55E+09	5.04E+06			
	#03			average		4.52							
				std dev (1σ)		2.01							
NIP-13-14_1.1	#03	18/12/14	13:29:34	0.0019691	0.0000002	2.75		0.12	2.31E+09	4.55E+06	10.53	4.75	HM 4
NIP-13-14_1.2	#03	18/12/14	13:35:36	0.0019702	0.0000003	3.31		0.13	2.31E+09	4.55E+06	10.53	4.75	
NIP-13-14_1.3	#03	18/12/14	13:41:41	0.0019771	0.0000003		6.89	0.17	2.43E+09	4.81E+06	10.53	4.75	
NIP-13-14_1.4	#03	18/12/14	13:47:45	0.0019708	0.0000003	3.61		0.13	2.43E+09	4.80E+06	10.53	4.75	
NIP-13-14_1.5	#03	18/12/14	13:53:46	0.0019682	0.0000002	2.24		0.11	2.38E+09	4.68E+06	10.53	4.75	
	#03			average		2.98							
				std dev (1σ)		0.61							
NIP-13-14_2.1	#03	18/12/14	13:59:48	0.0019794	0.0000002	8.06		0.11	2.52E+09	4.99E+06	10.53	4.75	HM 4
NIP-13-14_2.2	#03	18/12/14	14:05:52	0.0019793	0.0000002	7.96		0.12	2.53E+09	5.01E+06	10.53	4.75	
NIP-13-14_2.3	#03	18/12/14	14:11:54	0.0019822	0.0000002		9.46	0.10	2.57E+09	5.09E+06	10.53	4.75	
NIP-13-14_2.4	#03	18/12/14	14:17:55	0.0019741	0.0000002	5.28		0.12	2.36E+09	4.66E+06	10.53	4.75	
NIP-13-14_2.5	#03	18/12/14	14:23:57	0.0019735	0.0000003	4.93		0.13	2.35E+09	4.64E+06	10.53	4.75	
	#03			average		6.56							
				std dev (1σ)		1.68							
NIP-13-28_1.1	#03	18/12/14	14:44:16	0.0019789	0.0000002	7.70		0.10	2.61E+09	5.17E+06	20.65	3.46	HM 4
NIP-13-28_1.2	#03	18/12/14	14:50:32	0.0019771	0.0000002	6.77		0.10	2.60E+09	5.14E+06	20.65	3.46	
NIP-13-28_1.3	#03	18/12/14	14:56:52	0.0019761	0.0000002	6.24		0.12	2.60E+09	5.13E+06	20.65	3.46	
NIP-13-28_1.4	#03	18/12/14	15:03:13	0.0019832	0.0000002		9.93	0.10	2.60E+09	5.16E+06	20.65	3.46	
	#03			average		6.90							
				std dev (1σ)		0.74							
NIP-13-32_1.4	#03	18/12/14	17:28:51	0.0019875	0.0000002	11.94		0.10	2.58E+09	5.12E+06	3.60	1.63	HM 4
NIP-13-32_1.5	#03	18/12/14	17:34:55	0.0019845	0.0000003	10.37		0.13	2.58E+09	5.11E+06	3.60	1.63	
NIP-13-32_1.6	#03	18/12/14	17:41:00	0.0019863	0.0000002	11.28		0.09	2.60E+09	5.17E+06	3.60	1.63	
	#03			average		11.20							
				std dev (1σ)		0.79							
NIP-13-32_2.1	#03	18/12/14	17:47:27	0.0019868	0.0000002	11.52		0.09	2.60E+09	5.17E+06	3.60	1.63	HM 4
NIP-13-32_2.2	#03	18/12/14	17:53:32	0.0019898	0.0000002	13.07		0.12	2.58E+09	5.14E+06	3.60	1.63	
NIP-13-32_2.3	#03	18/12/14	17:59:36	0.0019951	0.0000002		15.83	0.12	2.61E+09	5.21E+06	3.60	1.63	
NIP-13-32_2.5	#03	18/12/14	18:11:42	0.0019859	0.0000002	11.03		0.09	2.58E+09	5.12E+06	3.60	1.63	
NIP-13-32_2.6	#03	18/12/14	18:17:43	0.0019870	0.0000002	11.61		0.12	2.57E+09	5.11E+06	3.60	1.63	
NIP-13-32_2.7	#03	18/12/14	18:23:45	0.0019890	0.0000002	12.62		0.11	2.56E+09	5.09E+06	3.60	1.63	
NIP-13-32_2.8	#03	18/12/14	18:29:47	0.0019873	0.0000002	11.72		0.11	2.56E+09	5.08E+06	3.60	1.63	
	#03			average		11.93							
				std dev (1σ)		0.76							
NIP-13-03_1.1	#03	18/12/14	19:36:26	0.0019627	0.0000003	-1.10		0.13	2.40E+09	4.71E+06	21.07	0.04	HM 4
NIP-13-03_1.2	#03	18/12/14	19:42:30	0.0019651	0.0000003	0.15		0.13	2.40E+09	4.71E+06	21.07	0.04	
NIP-13-03_1.3	#03	18/12/14	19:48:49	0.0019613	0.0000002	-1.86		0.12	2.40E+09	4.70E+06	21.07	0.04	
NIP-13-03_1.4	#03	18/12/14	19:54:51	0.0019678	0.0000002		1.48	0.10	2.43E+09	4.78E+06	21.07	0.04	
NIP-13-03_1.5	#03	18/12/14	20:00:53	0.0019630	0.0000003	-1.01		0.16	2.36E+09	4.63E+06	21.07	0.04	
NIP-13-03_1.6	#03	18/12/14	20:06:55	0.0019622	0.0000002	-1.43		0.10	2.31E+09	4.53E+06	21.07	0.04	
NIP-13-03_1.7	#03	18/12/14	20:12:56	0.0019610	0.0000002	-2.04		0.10	2.34E+09	4.59E+06	21.07	0.04	
NIP-13-03_1.8	#03	18/12/14	20:19:00	0.0019652	0.0000002	0.14		0.10	2.39E+09	4.71E+06	21.07	0.04	
	#03			average		-1.02							
				std dev (1σ)		0.88							
BAH F124 114_1.3	#03	21/12/14	6:35:57	0.0019557	0.0000003	-0.63		0.16	1.96E+09	3.84E+06	10.96	0.33	HM 4
BAH F124 114_2.1	#03	21/12/14	6:50:06	0.0019567	0.0000004	-0.14		0.23	1.92E+09	3.75E+06	10.96	0.33	
BAH F124 114_2.2	#03	21/12/14	6:56:10	0.0019571	0.0000004	0.08		0.21	1.90E+09	3.72E+06	10.96	0.33	
BAH F124 114_2.3	#03	21/12/14	7:02:12	0.0019565	0.0000003	-0.22		0.16	1.91E+09	3.74E+06	10.96	0.33	
BAH F124 114_2.4	#03	21/12/14	7:08:14	0.0019571	0.0000003	0.08		0.18	1.91E+09	3.74E+06	10.96	0.33	
	#03			average		-0.17							
				std dev (1σ)		0.29							
BAH 3cm17 LGt Lyr YG_1.2	#03	21/12/14	7:59:52	0.0019570	0.0000003	0.03		0.18	1.94E+09	3.80E+06	16.26	0.92	HM 4
BAH 3cm17 LGt Lyr YG_1.3	#03	21/12/14	8:05:56	0.0019575	0.0000004	0.29		0.21	1.91E+09	3.75E+06	16.26	0.92	
BAH 3cm17 LGt Lyr YG_1.4	#03	21/12/14	8:12:00	0.0019576	0.0000004	0.35		0.20	1.94E+09	3.80E+06	16.26	0.92	
BAH 3cm17 LGt Lyr YG_2.1	#03	21/12/14	8:18:02	0.0019559	0.0000004	-0.54		0.18	1.94E+09	3.79E+06	16.26	0.92	
BAH 3cm17 LGt Lyr YG_2.2	#03	21/12/14	8:24:06	0.0019549	0.0000005	-1.05		0.24	1.95E+09	3.81E+06	16.26	0.92	
BAH 3cm17 LGt Lyr YG_2.3	#03	21/12/14	8:30:08	0.0019553	0.0000005	-0.84		0.26	1.95E+09	3.81E+06	16.26	0.92	
	#03			average		-0.29							
				std dev (1σ)		0.60							
BAH F282 120.5_1.1	#03	21/12/14	14:43:42	0.0019619	0.0000005	2.60		0.27	1.87E+09	3.67E+06	41.05	0.12	HM11
BAH F282 120.5_1.2	#03	21/12/14	14:49:44	0.0019610	0.0000005	2.12		0.23	1.89E+09	3.70E+06	41.05	0.12	

SPOT #	Session	Date	Time	¹⁸ O/ ¹⁶ O ^(a)	± ^(b)	δ ¹⁸ O _{VSMOW} ^(c)	rejected	±Internal error (σ 95%)	¹⁸ O cps (median)	¹⁶ O cps (median)	(U-Th)/He ages	±	MOUNT
BAH F282 120.5_1.3	#03	21/12/14	14:55:45	0.0019612	0.0000004	2.23		0.20	1.88E+09	3.68E+06	41.05	0.12	HM11
	#03												
					average	2.32							
					std dev (1σ)	0.25							
BAH F282 120.5_2.1	#03	21/12/14	15:14:12	0.0019614	0.0000003	2.32		0.15	1.86E+09	3.66E+06	41.05	0.12	
BAH F282 120.5_2.2	#03	21/12/14	15:20:14	0.0019603	0.0000004	1.75		0.19	1.86E+09	3.64E+06	41.05	0.12	
BAH F282 120.5_2.3	#03	21/12/14	15:26:16	0.0019604	0.0000004	1.82		0.22	1.86E+09	3.66E+06	41.05	0.12	
	#03				average	1.96							
					std dev (1σ)	0.31							
BAH F282 118.4_1.1	#03	21/12/14	16:10:17	0.0019850	0.0000006	14.57		0.28	1.76E+09	3.49E+06			HM11
BAH F282 118.4_1.2	#03	21/12/14	16:16:19	0.0019815	0.0000004	12.79		0.18	1.78E+09	3.53E+06			
BAH F282 118.4_1.3	#03	21/12/14	16:22:21	0.0019816	0.0000003	12.81		0.17	1.81E+09	3.58E+06			
BAH F282 118.4_1.4	#03	21/12/14	16:28:23	0.0019830	0.0000005	13.55		0.27	1.79E+09	3.56E+06			
BAH F282 118.4_1.5	#03	21/12/14	16:34:24	0.0019810	0.0000005	12.49		0.25	1.84E+09	3.66E+06			
	#03				average	13.24							HM11
					std dev (1σ)	0.84							
BAH F282 118.4_2.1	#03	21/12/14	16:52:54	0.0019601	0.0000005	1.67		0.25	1.86E+09	3.64E+06	34.89	5.76	
BAH F282 118.4_2.2	#03	21/12/14	16:58:59	0.0019586	0.0000003	0.86		0.13	1.86E+09	3.65E+06	34.89	5.76	
BAH F282 118.4_2.3	#03	21/12/14	17:05:00	0.0019592	0.0000004	1.20		0.18	1.84E+09	3.61E+06	34.89	5.76	
	#03				average	1.24							HM11
					std dev (1σ)	0.40							
BAH F124 111.2B_1.1	#03	21/12/14	17:11:31	0.0019651	0.0000005	4.22		0.28	1.84E+09	3.63E+06	39.00	2.90	
BAH F124 111.2B_1.2	#03	21/12/14	17:40:31	0.0019667	0.0000003	5.09		0.17	1.90E+09	3.74E+06	39.00	2.90	
BAH F124 111.2B_1.3	#03	21/12/14	17:46:33	0.0019656	0.0000004	4.48		0.20	1.84E+09	3.62E+06	39.00	2.90	
BAH F124 111.2B_1.4	#03	21/12/14	17:52:37	0.0019651	0.0000005	4.25		0.26	1.84E+09	3.62E+06	39.00	2.90	
BAH F124 111.2B_1.5	#03	21/12/14	17:58:39	0.0019625	0.0000004		2.88	0.21	1.94E+09	3.80E+06	39.00	2.90	
BAH F124 111.2B_1.6	#03	21/12/14	18:04:41	0.0019640	0.0000005	3.66		0.23	1.85E+09	3.64E+06	39.00	2.90	
BAH F124 111.2B_1.7	#03	21/12/14	18:10:45	0.0019652	0.0000004	4.28		0.22	1.82E+09	3.57E+06	39.00	2.90	
BAH F124 111.2B_1.8	#03	21/12/14	18:16:47	0.0019645	0.0000005	3.95		0.27	1.84E+09	3.62E+06	39.00	2.90	
BAH F124 111.2B_1.9	#03	21/12/14	18:22:51	0.0019654	0.0000004	4.41		0.22	1.82E+09	3.58E+06	39.00	2.90	
BAH F124 111.2B_1.10	#03	21/12/14	18:35:06	0.0019653	0.0000004	4.38		0.23	1.89E+09	3.71E+06	39.00	2.90	
BAH F124 111.2B_1.12	#03	21/12/14	18:47:09	0.0019666	0.0000005	5.03		0.23	1.87E+09	3.68E+06	39.00	2.90	
BAH F124 111.2B_1.13	#03	21/12/14	18:53:11	0.0019648	0.0000004	4.10		0.20	1.91E+09	3.76E+06	39.00	2.90	
BAH F124 111.2B_1.14	#03	21/12/14	18:59:13	0.0019641	0.0000003	3.73		0.15	1.84E+09	3.61E+06	39.00	2.90	
BAH F124 111.2B_1.15	#03	21/12/14	19:05:15	0.0019660	0.0000003	4.72		0.17	1.81E+09	3.55E+06	39.00	2.90	
BAH F124 111.2B_1.16	#03	21/12/14	19:11:17	0.0019641	0.0000003	3.73		0.15	1.84E+09	3.61E+06	39.00	2.90	
	#03				average	4.29							HM11
					std dev (1σ)	0.45							
BAH F115 15-16G_1.1	#03	21/12/14	19:17:20	0.0019621	0.0000004		2.70	0.19	1.82E+09	3.58E+06	25.27	0.14	
BAH F115 15-16G_1.2	#03	21/12/14	19:23:22	0.0019656	0.0000005	4.51		0.23	1.86E+09	3.66E+06	25.27	0.14	
BAH F115 15-16G_1.3	#03	21/12/14	19:29:24	0.0019664	0.0000005	4.94		0.24	1.81E+09	3.57E+06	25.27	0.14	
BAH F115 15-16G_1.4	#03	21/12/14	19:35:26	0.0019669	0.0000004	5.16		0.23	1.83E+09	3.59E+06	25.27	0.14	
BAH F115 15-16G_1.5	#03	21/12/14	19:41:27	0.0019667	0.0000004	5.08		0.18	1.84E+09	3.62E+06	25.27	0.14	
BAH F115 15-16G_1.6	#03	21/12/14	19:47:29	0.0019672	0.0000003	5.35		0.14	1.85E+09	3.64E+06	25.27	0.14	
	#03				average	5.01							
					std dev (1σ)	0.31							
BAH-100(BG)-1.1	#05	6/8/15	14:10:56	0.0019956	0.0000004	6.21		0.19	2.58E+09	5.15E+06	38.57	4.31	HM15
BAH-100(BG)-1.2	#05	6/8/15	14:16:43	0.0019952	0.0000004	6.02		0.19	2.56E+09	5.10E+06	38.57	4.31	
BAH-100(BG)-1.3	#05	6/8/15	14:22:31	0.0019952	0.0000004	6.01		0.18	2.56E+09	5.12E+06	38.57	4.31	
BAH-100(BG)-1.4	#05	6/8/15	15:08:26	0.0019951	0.0000005	5.94		0.24	2.48E+09	4.94E+06	38.57	4.31	
	#03				average	6.05							
					std dev (1σ)	0.11							HM15
BAH-F124_114-1.1	#05	6/8/15	15:38:04	0.0019841	0.0000004	0.32		0.18	2.47E+09	4.90E+06	10.96	0.33	
BAH-F124_114-1.2	#05	6/8/15	15:44:41	0.0019838	0.0000003	0.17		0.17	2.46E+09	4.88E+06	10.96	0.33	
BAH-F124_114-1.3	#05	6/8/15	15:51:06	0.0019840	0.0000004	0.25		0.21	2.46E+09	4.88E+06	10.96	0.33	
	#05				average	0.24							
					std dev (1σ)	0.07							HM15
BAH-F124_114-2.2	#05	6/8/15	16:20:45	0.0019819	0.0000004	-0.79		0.18	2.44E+09	4.84E+06	10.96	0.33	
BAH-F124_114-2.3	#05	6/8/15	16:27:01	0.0019824	0.0000004	-0.56		0.19	2.44E+09	4.83E+06	10.96	0.33	
BAH-F124_114-2.4	#05	6/8/15	16:33:08	0.0019833	0.0000003	-0.12		0.15	2.44E+09	4.84E+06	10.96	0.33	
BAH-F124_114-2.1b	#05	6/8/15	17:49:36	0.0019827	0.0000004	-0.41		0.20	2.44E+09	4.83E+06	10.96	0.33	
BAH-F124_114-2.4b	#05	6/8/15	17:57:21	0.0019819	0.0000004	-0.83		0.18	2.43E+09	4.82E+06	10.96	0.33	HM15
	#05				average	-0.54							
					std dev (1σ)	0.29							
BAH-F282_118.4-1.1	#05	6/8/15	16:41:29	0.0019847	0.0000004	0.64		0.18	2.44E+09	4.85E+06	34.89	5.76	
BAH-F282_118.4-1.2	#05	6/8/15	16:47:27	0.0019847	0.0000004	0.64		0.18	2.44E+09	4.84E+06	34.89	5.76	
BAH-F282_118.4-1.3	#05	6/8/15	16:53:49	0.0019847	0.0000004	0.61		0.19	2.44E+09	4.84E+06	34.89	5.76	HM15
BAH-F282_118.4-1.4	#05	6/8/15	16:59:52	0.0019851	0.0000003	0.80		0.17	2.44E+09	4.83E+06	34.89	5.76	
	#05				average	0.68							
					std dev (1σ)	0.09							
BAH-F282_120.5-1.1_brown	#05	6/8/15	18:20:17	0.0019857	0.0000003	1.16		0.16	2.44E+09	4.85E+06	45.29	1.15	HM15
BAH-F282_120.5-1.2_brown	#05	6/8/15	18:26:04	0.0019852	0.0000004	0.88		0.19	2.46E+09	4.87E+06	45.29	1.15	
BAH-F282_120.5-1.3_brown	#05	6/8/15	18:31:51	0.0019856	0.0000004	1.08		0.19	2.46E+09	4.89E+06	45.29	1.15	
BAH-F282_120.5-1.3b_brown	#05	6/8/15	20:39:02	0.0019866	0.0000004	1.58		0.21	2.45E+09	4.88E+06	45.29	1.15	
	#05				average	1.17							
					std dev (1σ)	0.29							HM15
BAH-F282-120.5-1.4_black	#05	6/8/15	18:37:39	0.0019873	0.0000003	1.97		0.17	2.46E+09	4.89E+06	41.05	0.12	
BAH-F282-120.5-1.5_black	#05	7/8/15	0:24:59	0.0019879	0.0000003	2.27		0.14	2.44E+09	4.85E+06	41.05	0.12	
BAH-F282-120.5-1.6_black	#05	7/8/15	0:31:22	0.0019883	0.0000004	2.45		0.20	2.44E+09	4.85E+06	41.05	0.12	
BAH-F282-120.5-1.7_black	#05	7/8/15	0:37:26	0.0019882	0.0000004	2.41		0.19	2.44E+09	4.85E+06	41.05	0.12	
	#05				average	2.28							HM15

SPOT #	Session	Date	Time	¹⁸ O/ ¹⁶ O ^(a)	± ^(b)	δ ¹⁸ O _{VERMOW} ^(c)	rejected	±Internal error (σ 95%)	¹⁶ O cps (median)	¹⁸ O cps (median)	(U-Th)/He ages	±	MOUNT
BAH-3cmL.Glyr-1.1	#05	6/8/15	18:43:27	0.0019851	0.0000004	0.81		0.18	2.53E+09	5.02E+06	16.26	0.92	HM15
BAH-3cmL.Glyr-1.1b	#05	6/8/15	19:58:44	0.0019846	0.0000003	0.56		0.15	2.48E+09	4.93E+06	16.26	0.92	
BAH-3cmL.Glyr-1.2b	#05	6/8/15	20:14:13	0.0019858	0.0000004	1.19		0.19	2.51E+09	4.99E+06	16.26	0.92	
BAH-3cmL.Glyr-1.3b	#05	6/8/15	20:21:32	0.0019867	0.0000003	1.63		0.17	2.52E+09	5.02E+06	16.26	0.92	
	#05			average		1.05							
				std dev (1σ)		0.47							
BAH-100(BrG)-2.1	#05	6/8/15	20:57:51	0.0019845	0.0000003	0.52		0.16	2.47E+09	4.89E+06	53.69	2.27	HM15
BAH-100(BrG)-2.2	#05	6/8/15	21:04:51	0.0019849	0.0000003	0.72		0.17	2.46E+09	4.89E+06	53.69	2.27	
BAH-100(BrG)-2.3	#05	6/8/15	21:10:54	0.0019837	0.0000003	0.09		0.17	2.45E+09	4.87E+06	53.69	2.27	
BAH-100(BrG)-2.4	#05	6/8/15	21:17:34	0.0019842	0.0000004	0.36		0.19	2.47E+09	4.89E+06	53.69	2.27	
	#05			average		0.42							
				std dev (1σ)		0.27							
BAH-F124-111.2B-1.1	#05	6/8/15	21:26:25	0.0019925	0.0000003	4.64		0.17	2.46E+09	4.90E+06	39.00	2.90	HM15
BAH-F124-111.2B-1.2	#05	6/8/15	21:33:07	0.0019920	0.0000004	4.37		0.18	2.45E+09	4.89E+06	39.00	2.90	
BAH-F124-111.2B-1.3	#05	6/8/15	21:39:44	0.0019919	0.0000003	4.32		0.14	2.51E+09	5.00E+06	39.00	2.90	
	#05			average		4.44							
				std dev (1σ)		0.17							
BAH-99-01-1.1	#05	6/8/15	21:47:27	0.0019936	0.0000003	5.19		0.16	2.47E+09	4.93E+06	25.06	4.40	HM15
BAH-99-01-1.2	#05	6/8/15	21:53:48	0.0019935	0.0000005	5.12		0.23	2.48E+09	4.95E+06	25.06	4.40	
BAH-99-01-1.3	#05	6/8/15	21:59:44	0.0019941	0.0000004	5.43		0.19	2.47E+09	4.92E+06	25.06	4.40	
	#05			average		5.25							
				std dev (1σ)		0.16							
BAH-99-01-2.1	#05	6/8/15	22:30:41	0.0019918	0.0000003	4.27		0.16	2.50E+09	4.99E+06	25.06	4.40	HM15
BAH-99-01-2.2	#05	6/8/15	22:36:54	0.0019911	0.0000003	3.91		0.16	2.51E+09	5.01E+06	25.06	4.40	
BAH-99-01-2.3	#05	6/8/15	22:42:52	0.0019925	0.0000003	4.60		0.17	2.51E+09	5.00E+06	25.06	4.40	
	#05			average		4.26							
				std dev (1σ)		0.35							
BAH-F115_15-16-1.1	#05	6/8/15	22:57:52	0.0019948	0.0000004	5.80		0.21	2.43E+09	4.85E+06	25.27	0.14	HM15
BAH-F115_15-16-1.2	#05	6/8/15	23:04:11	0.0019958	0.0000004	6.32		0.20	2.44E+09	4.88E+06	25.27	0.14	
BAH-F115_15-16-1.3	#05	6/8/15	23:11:13	0.0019941	0.0000004	5.44		0.19	2.49E+09	4.97E+06	25.27	0.14	
BAH-F115_15-16-1.4	#05	6/8/15	23:17:48	0.0019935	0.0000004	5.15		0.18	2.47E+09	4.93E+06	25.27	0.14	
BAH-F115_15-16-1.5	#05	6/8/15	23:24:45	0.0019931	0.0000003	4.94		0.16	2.42E+09	4.82E+06	25.27	0.14	
BAH-F115_15-16-1.6	#05	6/8/15	23:32:07	0.0019953	0.0000004	6.06		0.19	2.44E+09	4.87E+06	25.27	0.14	
BAH-F115_15-16-1.7	#05	6/8/15	23:38:48	0.0019962	0.0000004	6.53		0.18	2.43E+09	4.85E+06	25.27	0.14	
BAH-F115_15-16-1.8	#05	6/8/15	23:45:47	0.0019901	0.0000003	3.41		0.18	2.43E+09	4.84E+06	25.27	0.14	
BAH-F115_15-16-1.9	#05	6/8/15	23:53:39	0.0019947	0.0000004	5.74		0.20	2.51E+09	5.01E+06	25.27	0.14	
BAH-F115_15-16-1.10	#05	7/8/15	0:00:43	0.0019893	0.0000003	3.00		0.17	2.41E+09	4.79E+06	25.27	0.14	
	#05			average		5.24							
				std dev (1σ)		1.18							
BAH-100(BG)-2.1	#05	7/8/15	1:46:12	0.0019920	0.0000004	4.36		0.18	2.53E+09	5.04E+06	38.57	4.31	HM15
BAH-100(BG)-2.2	#05	7/8/15	1:52:45	0.0019930	0.0000004	4.87		0.19	2.47E+09	4.93E+06	38.57	4.31	
BAH-100(BG)-2.3	#05	7/8/15	1:59:02	0.0019920	0.0000003	4.38		0.16	2.44E+09	4.87E+06	38.57	4.31	
BAH-100(BG)-2.4	#05	7/8/15	2:08:11	0.0019953	0.0000003	6.08		0.15	2.53E+09	5.04E+06	38.57	4.31	
BAH-100(BG)-2.5	#05	7/8/15	2:15:16	0.0019952	0.0000004	6.01		0.20	2.52E+09	5.02E+06	38.57	4.31	
BAH-100(BG)-2.6	#05	7/8/15	2:22:23	0.0019949	0.0000003	5.87		0.17	2.52E+09	5.03E+06	38.57	4.31	
	#05			average		5.26							
				std dev (1σ)		0.82							
BAH-3cmL-LGt_1.1	#06	16/5/16	11:18:03	0.0019822	0.0000003	1.42		0.16	2.49E+09	4.94E+06	16.26	0.92	HM16
BAH-3cmL-LGt_1.2	#06	16/5/16	11:24:26	0.0019819	0.0000003	1.25		0.16	2.47E+09	4.90E+06	16.26	0.92	
BAH-3cmL-LGt_1.3	#06	16/5/16	11:30:11	0.0019813	0.0000003	0.95		0.13	2.50E+09	4.95E+06	16.26	0.92	
BAH-3cmL-LGt_1.4	#06	16/5/16	15:39:08	0.0019821	0.0000003	1.16		0.17	2.41E+09	4.78E+06	16.26	0.92	
BAH-3cmL-LGt_1.5	#06	16/5/16	15:44:27	0.0019814	0.0000003	0.79		0.15	2.38E+09	4.73E+06	16.26	0.92	
	#06			average		1.11							
				std dev (1σ)		0.25							
BAH-3cmL-3BL_1.1	#06	16/5/16	11:37:17	0.0019792	0.0000002	-0.17		0.13	2.54E+09	5.03E+06	13.73	2.14	HM16
BAH-3cmL-3BL_1.2	#06	16/5/16	11:43:37	0.0019800	0.0000003	0.24		0.17	2.52E+09	4.98E+06	13.73	2.14	
BAH-3cmL-3BL_1.3	#06	16/5/16	11:49:36	0.0019787	0.0000003	-0.43		0.13	2.53E+09	5.01E+06	13.73	2.14	
BAH-3cmL-3BL_1.4	#06	16/5/16	15:49:48	0.0019800	0.0000002	0.03		0.12	2.44E+09	4.82E+06	13.73	2.14	
BAH-3cmL-3BL_1.5	#06	16/5/16	15:55:07	0.0019795	0.0000003	-0.22		0.15	2.42E+09	4.79E+06	13.73	2.14	
	#06			average		-0.11							
				std dev (1σ)		0.25							
B-93-01_1.1	#06	16/5/16	11:58:21	0.0019898	0.0000003	5.31		0.14	2.44E+09	4.86E+06	66.52	6.00	HM16
B-93-01_1.3	#06	16/5/16	12:15:11	0.0019891	0.0000003	4.93		0.17	2.33E+09	4.64E+06	66.52	6.00	
B-93-01_1.4	#06	16/5/16	12:36:51	0.0019886	0.0000004	4.61		0.18	2.28E+09	4.53E+06	66.52	6.00	
B-93-01_1.5	#06	16/5/16	12:43:44	0.0019897	0.0000003	5.20		0.16	2.29E+09	4.55E+06	66.52	6.00	
B-93-01_1.6	#06	16/5/16	12:50:03	0.0019897	0.0000003	5.18		0.16	2.27E+09	4.51E+06	66.52	6.00	
B-93-01_1.7	#06	16/5/16	12:56:22	0.0019892	0.0000003	4.95		0.17	2.23E+09	4.43E+06	66.52	6.00	
B-93-01_1.8	#06	16/5/16	13:02:55	0.0019911	0.0000002	5.91		0.12	2.34E+09	4.66E+06	66.52	6.00	
B-93-01_1.9	#06	16/5/16	13:09:50	0.0019906	0.0000003	5.62		0.13	2.27E+09	4.53E+06	66.52	6.00	
B-93-01_1.2B	#06	16/5/16	13:16:14	0.0019913	0.0000003	6.00		0.15	2.23E+09	4.44E+06	66.52	6.00	
	#06			average		5.30							
				std dev (1σ)		0.46							
BAH-F124-123.1_1.1	#06	16/5/16	13:24:52	0.0019899	0.0000003	5.26		0.15	2.36E+09	4.69E+06	41.58	5.15	HM16
BAH-F124-123.1_1.2	#06	16/5/16	13:31:23	0.0019895	0.0000003	5.05		0.13	2.41E+09	4.79E+06	41.58	5.15	
BAH-F124-123.1_1.4	#06	16/5/16	16:06:19	0.0019908	0.0000003	5.58		0.15	2.31E+09	4.59E+06	41.58	5.15	
BAH-F124-123.1_1.5_botryoidal	#06	16/5/16	16:12:50	0.0019896	0.0000003	4.94		0.16	2.36E+09	4.69E+06	41.58	5.15	
BAH-F124-123.1_1.6_botryoidal	#06	16/5/16	16:19:07	0.0019897	0.0000003	5.01		0.13	2.35E+09	4.67E+06	41.58	5.15	
BAH-F124-123.1_1.7_botryoidal	#06	16/5/16	16:25:28	0.0019894	0.0000004	4.84		0.18	2.35E+09	4.68E+06	41.58	5.15	
	#06			average		5.11							
				std dev (1σ)		0.27							
BA-P010-Surface_1.1	#06	16/5/16	17:02:24	0.0019905	0.0000004	5.38		0.18	2.35E+09	4.67E+06	67.51	0.89	HM16
BA-P010-Surface_1.2	#06	16/5/16	17:09:35	0.0019902	0.0000004	5.23		0.18	2.30E+09	4.59E+06	67.51	0.89	
BA-P010-Surface_1.3	#06	16/5/16	17:15:27	0.0019912	0.0000004	5.75		0.18	2.28E+09	4.54E+06	67.51	0.89	
BA-P010-Surface_1.4	#06	16/5/16	17:22:29	0.0019916	0.0000004	5.95		0.18	2.30E+09	4.57E+06	67.51	0.89	
BA-P010-Surface_1.5	#06	16/5/16	17:28:58	0.0019875	0.0000004	3.81		0.18	2.19E+09	4.36E+06	67.51	0.89	
BA-P010-Surface_1.6	#06	16/5/16	17:34:46	0.0019918	0.0000004	6.03		0.19	2.29E+09	4.56E+06	67.51	0.89	
BA-P010-Surface_1.7	#06	16/5/16	17:40:47	0.0019906	0.0000004	5.40		0.21	2.29E+09	4.57E+06	67.51	0.89	
BA-P010-Surface_1.8	#06	16/5/16	17:46:49	0.0019877	0.0000004	3.93		0.19	2.25E+09	4.48E+06	67.51	0.89	

SPOT #	Session	Date	Time	¹⁸ O/ ¹⁶ O ^(a)	± ^(b)	δ ¹⁸ O _{VSMOW} ^(c)	rejected	±Internal error (σ 95%)	¹⁸ O cps (median)	¹⁶ O cps (median)	(U-Th)/He ages	±	MOUNT
BAH-F124-123.2_2.9_weird	#07	28/11/16	18:43:14	0.0019855	0.0000003	2.13		0.13	2.23E+09	4.43E+06	29.36	2.54	
	#07				average std dev (1σ)	1.83 0.71							
BAH-F282-120.5_brown-1.1	#07	28/11/16	21:23:03	0.0019852	0.0000002	1.98		0.12	2.29E+09	4.55E+06	45.29	1.15	HM16
BAH-F282-120.5_brown-1.2	#07	28/11/16	21:28:55	0.0019855	0.0000003	2.11		0.13	2.30E+09	4.58E+06	45.29	1.15	
BAH-F282-120.5_brown-1.3	#07	28/11/16	21:34:46	0.0019859	0.0000003	2.32		0.16	2.30E+09	4.57E+06	45.29	1.15	
BAH-F282-120.5_brown-1.4	#07	28/11/16	21:40:38	0.0019841	0.0000002	1.42		0.12	2.30E+09	4.56E+06	45.29	1.15	
BAH-F282-120.5_brown-1.5	#07	28/11/16	21:46:29	0.0019844	0.0000003	1.58		0.14	2.30E+09	4.56E+06	45.29	1.15	
BAH-F282-120.5_brown-1.6	#07	28/11/16	21:52:21	0.0019842	0.0000002	1.45		0.12	2.30E+09	4.56E+06	45.29	1.15	
	#07				average std dev (1σ)	1.81 0.38							
BAH-F282-120.5_black-1.1	#07	28/11/16	21:58:16	0.0019891	0.0000003	3.98		0.14	2.33E+09	4.63E+06	41.05	0.12	HM16
BAH-F282-120.5_black-1.3	#07	28/11/16	22:10:00	0.0019891	0.0000003	3.97		0.14	2.30E+09	4.58E+06	41.05	0.12	
BAH-F282-120.5_black-1.4	#07	28/11/16	22:15:51	0.0019901	0.0000002	4.48		0.12	2.31E+09	4.60E+06	41.05	0.12	
BAH-F282-120.5_black-1.5	#07	28/11/16	22:21:44	0.0019904	0.0000002	4.65		0.11	2.30E+09	4.59E+06	41.05	0.12	
BAH-F282-120.5_black-1.6	#07	28/11/16	22:27:35	0.0019893	0.0000002	4.06		0.12	2.31E+09	4.60E+06	41.05	0.12	
	#07				average std dev (1σ)	4.22 0.31							
BAH-F226-142.7_sparkling-1.2	#07	28/11/16	23:02:55	0.0019815	0.0000003	0.05		0.13	2.33E+09	4.61E+06	14.03	0.66	HM16
BAH-F226-142.7_sparkling-1.2b	#07	29/11/16	1:58:50	0.0019800	0.0000003	-0.71		0.13	2.31E+09	4.57E+06	14.03	0.66	
BAH-F226-142.7_sparkling-1.9	#07	29/11/16	2:08:46	0.0019781	0.0000003	-1.67		0.15	2.34E+09	4.64E+06	14.03	0.66	
	#07				average std dev (1σ)	-0.78 0.86							
BAH-F226-142.7_black-1.3 band 1	#07	28/11/16	23:08:47	0.0019870	0.0000003	2.90		0.17	2.28E+09	4.53E+06	4.59	0.31	HM16
BAH-F226-142.7_black-1.4 band 1	#07	28/11/16	23:14:39	0.0019877	0.0000002	3.23		0.11	2.30E+09	4.58E+06	4.59	0.31	
BAH-F226-142.7_black-1.5 band 1	#07	28/11/16	23:20:31	0.0019877	0.0000002	3.23		0.12	2.29E+09	4.56E+06	4.59	0.31	
	#07				average std dev (1σ)	3.12 0.19							
BAH-F226-142.7_black-1.6 band 2	#07	28/11/16	23:26:23	0.0019841	0.0000003	1.40		0.14	2.19E+09	4.35E+06	4.59	0.31	HM16
BAH-F226-142.7_black-1.7 band 2	#07	28/11/16	23:32:15	0.0019849	0.0000003	1.79		0.14	2.21E+09	4.38E+06	4.59	0.31	
BAH-F226-142.7_black-1.8 band 2	#07	28/11/16	23:38:06	0.0019854	0.0000003	2.05		0.15	2.21E+09	4.38E+06	4.59	0.31	
	#07				average std dev (1σ)	1.75 0.33							
BAH-F124-114-1.2	#07	28/11/16	23:49:53	0.0019822	0.0000003	0.43		0.13	2.29E+09	4.54E+06	10.96	0.33	HM16
BAH-F124-114-1.3	#07	28/11/16	23:55:44	0.0019831	0.0000003	0.88		0.14	2.28E+09	4.53E+06	10.96	0.33	
BAH-F124-114-1.4	#07	29/11/16	0:01:36	0.0019817	0.0000002	0.16		0.12	2.29E+09	4.53E+06	10.96	0.33	
BAH-F124-114-1.5	#07	29/11/16	0:07:28	0.0019822	0.0000003	0.43		0.13	2.28E+09	4.53E+06	10.96	0.33	
BAH-F124-114-1.1b	#07	29/11/16	2:18:39	0.0019818	0.0000002	0.22		0.11	2.27E+09	4.50E+06	10.96	0.33	
	#07				average std dev (1σ)	0.42 0.29							
BAH-F226-142.7_brown-1.1	#07	29/11/16	2:28:50	0.0019811	0.0000003	-0.12		0.14	2.30E+09	4.56E+06	14.03	0.66	HM16
BAH-F226-142.7_brown-1.2	#07	29/11/16	2:34:42	0.0019834	0.0000003	1.06		0.13	2.36E+09	4.67E+06	14.03	0.66	
BAH-F226-142.7_brown-1.3	#07	29/11/16	2:40:33	0.0019818	0.0000002	0.24		0.12	2.31E+09	4.58E+06	14.03	0.66	
	#07				average std dev (1σ)	0.40 0.61							
BAH-F124-111.2-1.1b band1	#07	30/11/16	6:45:42	0.0019907	0.0000002	4.90		0.11	2.29E+09	4.57E+06	39.00	2.90	HM17
BAH-F124-111.2-1.1 band1	#07	29/11/16	21:31:28	0.0019889	0.0000003		3.28	0.13	2.27E+09	4.51E+06	39.00	2.90	
BAH-F124-111.2-1.2 band1	#07	29/11/16	21:36:50	0.0019912	0.0000003	4.42		0.16	2.28E+09	4.54E+06	39.00	2.90	
BAH-F124-111.2-1.3 band1	#07	29/11/16	21:42:11	0.0019901	0.0000003	3.88		0.13	2.28E+09	4.55E+06	39.00	2.90	
	#07				average std dev (1σ)	4.40 0.51							
BAH-F124-111.2-1.4 band2	#07	29/11/16	21:47:33	0.0019921	0.0000003	4.91		0.13	2.30E+09	4.59E+06	39.00	2.90	HM17
BAH-F124-111.2-1.5 band2	#07	29/11/16	21:52:54	0.0019916	0.0000003	4.63		0.13	2.31E+09	4.60E+06	39.00	2.90	
BAH-F124-111.2-1.6 band2	#07	29/11/16	21:58:15	0.0019915	0.0000003	4.62		0.13	2.33E+09	4.65E+06	39.00	2.90	
	#07				average std dev (1σ)	4.72 0.16							
BAH-F124-111.2-1.7 band3	#07	29/11/16	22:03:37	0.0019927	0.0000002	5.21		0.09	2.32E+09	4.63E+06	39.00	2.90	HM17
BAH-F124-111.2-1.8 band3	#07	29/11/16	22:08:58	0.0019927	0.0000003	5.19		0.14	2.37E+09	4.72E+06	39.00	2.90	
BAH-F124-111.2-1.9 band3	#07	29/11/16	22:14:19	0.0019917	0.0000002	4.69		0.12	2.35E+09	4.69E+06	39.00	2.90	
BAH-F124-111.2-1.9b band3	#07	30/11/16	6:51:04	0.0019922	0.0000002	5.66		0.12	2.34E+09	4.65E+06	39.00	2.90	
	#07				average std dev (1σ)	5.19 0.40							
BAH-F124-111.2-1.10 band4	#07	29/11/16	22:19:41	0.0019923	0.0000002	5.01		0.12	2.29E+09	4.56E+06	39.00	2.90	HM17
BAH-F124-111.2-1.11 band4	#07	29/11/16	22:25:02	0.0019924	0.0000002	5.07		0.11	2.28E+09	4.54E+06	39.00	2.90	
BAH-F124-111.2-1.12 band4	#07	29/11/16	22:30:23	0.0019910	0.0000003		4.36	0.13	2.30E+09	4.59E+06	39.00	2.90	
BAH-F124-111.2-1.12b band4	#07	30/11/16	6:56:25	0.0019915	0.0000003	5.30		0.17	2.29E+09	4.55E+06	39.00	2.90	
	#07				average std dev (1σ)	5.12 0.16							
BAH-F177-115-1.1	#07	29/11/16	23:30:06	0.0019869	0.0000002	2.93		0.11	2.30E+09	4.58E+06	3.13	0.30	HM17
BAH-F177-115-1.2	#07	29/11/16	23:35:27	0.0019876	0.0000002	3.30		0.11	2.32E+09	4.61E+06	3.13	0.30	
BAH-F177-115-1.3	#07	29/11/16	23:40:48	0.0019870	0.0000003	3.01		0.13	2.31E+09	4.59E+06	3.13	0.30	
BAH-F177-115-1.4	#07	29/11/16	23:46:09	0.0019881	0.0000003	3.53		0.14	2.33E+09	4.63E+06	3.13	0.30	
BAH-F177-115-1.5	#07	29/11/16	23:51:31	0.0019897	0.0000002		4.40	0.10	2.34E+09	4.66E+06	3.13	0.30	
BAH-F177-115-1.5b	#07	30/11/16	7:09:38	0.0019886	0.0000002	3.83		0.10	2.30E+09	4.58E+06	3.13	0.30	
	#07				average std dev (1σ)	3.32 0.37							
IBH-13-03_gt_under_TC-1.1	#07	29/11/16	23:56:54	0.0019875	0.0000002	3.22		0.11	2.27E+09	4.52E+06	5.48	0.01	HM17
IBH-13-03_gt_under_TC-1.2	#07	30/11/16	0:02:15	0.0019900	0.0000002	4.55		0.11	2.30E+09	4.58E+06	5.48	0.01	
IBH-13-03_gt_under_TC-1.3	#07	30/11/16	0:07:37	0.0019858	0.0000002	2.39		0.12	2.29E+09	4.54E+06	5.48	0.01	
IBH-13-03_gt_under_TC-1.4	#07	30/11/16	0:12:58	0.0019898	0.0000003	4.42		0.13	2.29E+09	4.56E+06	5.48	0.01	
IBH-13-03_gt_under_TC-1.5	#07	30/11/16	0:18:20	0.0019874	0.0000003	3.22		0.13	2.32E+09	4.60E+06	5.48	0.01	
IBH-13-03_gt_under_TC-1.6	#07	30/11/16	0:23:41	0.0019883	0.0000002	3.65		0.11	2.32E+09	4.61E+06	5.48	0.01	
IBH-13-03_gt_under_TC-1.3	#07	30/11/16	6:10:38	0.0019885	0.0000002	3.75		0.11	2.31E+09	4.59E+06	5.48	0.01	
IBH-13-03_gt_under_TC-1.2	#07	30/11/16	6:17:07	0.0019860	0.0000002	2.48		0.12	2.30E+09	4.56E+06	5.48	0.01	
IBH-13-03_gt_under_TC-1.2	#07	30/11/16	6:34:52	0.0019858	0.0000002	2.35		0.12	2.23E+09	4.44E+06	5.48	0.01	
	#07				average std dev (1σ)	3.34 0.83							

SPOT #	Session	Date	Time	¹⁸ O/ ¹⁶ O ^(a)	± ^(b)	δ ¹⁸ O _{VERMON} ^(c)	rejected	±Internal error (σ 95%)	¹⁸ O cps (median)	¹⁶ O cps (median)	(U-Th)/He ages	±	MOUNT
BAH-HS-001-1.1 BAH-HS-001-1.2 BAH-HS-001-1.3 BAH-HS-001-1.4 BAH-HS-001-1.5 BAH-HS-001-1.6	#07			average		14.83							
				std dev (1σ)		4.92							
	#07	2/12/16	3:31:22	0.0019928	0.0000002	6.77		0.12	2.43E+09	4.85E+06	173.20	11.78	HM17
	#07	2/12/16	3:37:14	0.0019924	0.0000002	6.59		0.10	2.45E+09	4.88E+06	173.20	11.78	
	#07	2/12/16	3:43:05	0.0019926	0.0000002	6.69		0.12	2.45E+09	4.88E+06	173.20	11.78	
	#07	2/12/16	3:48:57	0.0019937	0.0000003	7.23		0.14	2.41E+09	4.81E+06	173.20	11.78	
	#07	2/12/16	3:54:50	0.0019919	0.0000002	6.30		0.12	2.45E+09	4.89E+06	173.20	11.78	
BAH-F226-186.8-1.1 BAH-F226-186.8-1.2 BAH-F226-186.8-1.3 BAH-F226-186.8-1.4 BAH-F226-186.8-1.5 BAH-F226-186.8-1.6 BAH-F226-186.8-1.7 BAH-F226-186.8-1.8	#07			average		6.73							
				std dev (1σ)		0.31							
	#07	2/12/16	4:18:28	0.0019873	0.0000003	3.93		0.15	2.32E+09	4.62E+06	49.20	0.85	HM17
	#07	2/12/16	4:24:20	0.0019878	0.0000003	4.22		0.14	2.32E+09	4.61E+06	49.20	0.85	
	#07	2/12/16	4:30:13	0.0019896	0.0000003	5.16		0.15	2.31E+09	4.59E+06	49.20	0.85	
	#07	2/12/16	4:36:04	0.0019860	0.0000003	3.30		0.13	2.31E+09	4.58E+06	49.20	0.85	
	#07	2/12/16	4:41:56	0.0019837	0.0000003	2.12		0.15	2.23E+09	4.43E+06	49.20	0.85	
BAH-3-cml7LGB_c-axis-1.1 BAH-3-cml7LGB_c-axis-1.2 BAH-3-cml7LGB_c-axis-1.3 BAH-3-cml7LGB_c-axis-1.4 BAH-3-cml7LGB_c-axis-1.5	#07			average		3.55							
				std dev (1σ)		1.01							
	#07	1/12/16	23:11:45	0.0019780	0.0000003		-0.82	0.13	2.33E+09	4.60E+06	16.26	0.92	HM17
	#07	2/12/16	6:10:52	0.0019805	0.0000003	0.45		0.15	2.31E+09	4.58E+06	16.26	0.92	
	#07	2/12/16	6:16:44	0.0019824	0.0000003	1.45		0.13	2.31E+09	4.59E+06	16.26	0.92	
	#07	2/12/16	6:22:35	0.0019803	0.0000003	0.36		0.14	2.34E+09	4.64E+06	16.26	0.92	
	#07	2/12/16	6:28:27	0.0019799	0.0000002	0.13		0.12	2.33E+09	4.62E+06	16.26	0.92	
BAH-3-cml7LGB_c-axis-2.1 BAH-3-cml7LGB_c-axis-2.2 BAH-3-cml7LGB_c-axis-2.3 BAH-3-cml7LGB_c-axis-2.4	#07			average		0.60							
				std dev (1σ)		0.58							
	#07	2/12/16	6:34:21	0.0019804	0.0000003	0.42		0.14	2.32E+09	4.60E+06	16.26	0.92	HM17
	#07	2/12/16	6:40:12	0.0019819	0.0000003	1.17		0.14	2.32E+09	4.59E+06	16.26	0.92	
	#07	2/12/16	6:46:04	0.0019809	0.0000002	0.68		0.12	2.30E+09	4.55E+06	16.26	0.92	
	#07	2/12/16	6:51:56	0.0019791	0.0000003	-0.28		0.14	2.33E+09	4.61E+06	16.26	0.92	
IBH-13-09h-1.1 IBH-13-09h-1.2 IBH-13-09h-1.3 IBH-13-09h-1.4 IBH-13-09h-1.5 IBH-13-09h-1.6 IBH-13-09h-1.7 IBH-13-09h-1.8	#07			average		0.50							
				std dev (1σ)		0.60							
	#07	2/12/16	12:08:49	0.0020169	0.0000002	19.15		0.09	2.19E+09	4.42E+06	39.62	2.51	HM17
	#07	2/12/16	12:14:40	0.0020184	0.0000002	19.94		0.11	2.15E+09	4.35E+06	39.62	2.51	
	#07	2/12/16	12:20:32	0.0020119	0.0000002	16.60		0.11	2.35E+09	4.72E+06	39.62	2.51	
	#07	2/12/16	12:26:24	0.0020134	0.0000003	17.39		0.15	2.32E+09	4.67E+06	39.62	2.51	
	#07	2/12/16	12:32:16	0.0020130	0.0000003	17.16		0.15	2.27E+09	4.58E+06	39.62	2.51	
IBH-13-09b(1)-1.1 IBH-13-09b(1)-1.2 IBH-13-09b(1)-1.3 IBH-13-09b(1)-1.4	#07			average		17.96							
				std dev (1σ)		1.25							
	#07	2/12/16	13:07:37	0.0020318	0.0000004	26.80		0.18	1.56E+09	3.18E+06	29.45	2.40	HM17
	#07	2/12/16	13:13:28	0.0020312	0.0000003	26.53		0.13	1.65E+09	3.34E+06	29.45	2.40	
	#07	2/12/16	13:19:21	0.0020286	0.0000004	25.17		0.22	1.83E+09	3.71E+06	29.45	2.40	
	#07	2/12/16	13:25:13	0.0020296	0.0000003	25.69		0.14	1.84E+09	3.72E+06	29.45	2.40	
IBH-13-09b(2)-1.1 IBH-13-09b(2)-1.2 IBH-13-09b(2)-1.3 IBH-13-09b(2)-1.4 IBH-13-09b(2)-1.5 IBH-13-09b(2)-1.6	#07			average		26.05							
				std dev (1σ)		0.75							
	#07	2/12/16	14:24:37	0.0020264	0.0000004	24.03		0.18	1.91E+09	3.86E+06	29.45	2.40	HM17
	#07	2/12/16	14:30:29	0.0020285	0.0000003	25.11		0.15	1.83E+09	3.71E+06	29.45	2.40	
	#07	2/12/16	14:36:20	0.0020313	0.0000004	26.54		0.18	1.64E+09	3.33E+06	29.45	2.40	
	#07	2/12/16	14:42:13	0.0020244	0.0000004	23.04		0.17	1.99E+09	4.02E+06	29.45	2.40	
BAH-99-01-1.1 BAH-99-01-1.2 BAH-99-01-1.3 BAH-99-01-1.4	#07			average		23.57							
				std dev (1σ)		2.09							
	#07	2/12/16	15:38:22	0.0019881	0.0000004	4.36		0.19	2.33E+09	4.64E+06	25.06	4.40	HM17
	#07	2/12/16	15:44:31	0.0019855	0.0000003	3.03		0.15	2.34E+09	4.65E+06	25.06	4.40	
	#07	2/12/16	15:50:48	0.0019866	0.0000004	3.60		0.18	2.35E+09	4.67E+06	25.06	4.40	
	#07	2/12/16	15:56:54	0.0019888	0.0000003	4.72		0.14	2.35E+09	4.66E+06	25.06	4.40	
BAH-F115-15-16-1.1 BAH-F115-15-16-1.2 BAH-F115-15-16-1.3 BAH-F115-15-16-1.4 BAH-F115-15-16-1.5 BAH-F115-15-16-1.6 BAH-F115-15-16-1.7 BAH-F115-15-16-1.8 BAH-F115-15-16-1.1b BAH-F115-15-16-1.4b	#07			average		3.93							
				std dev (1σ)		0.76							
	#07	3/12/16	20:47:12	0.0019865	0.0000003	3.94		0.14	2.24E+09	4.45E+06	25.27	0.14	HM23
	#07	3/12/16	20:53:04	0.0019852	0.0000003	3.26		0.17	2.24E+09	4.45E+06	25.27	0.14	
	#07	3/12/16	20:59:57	0.0019867	0.0000003	4.05		0.14	2.24E+09	4.44E+06	25.27	0.14	
	#07	3/12/16	21:05:49	0.0019885	0.0000002		4.97	0.11	2.23E+09	4.44E+06	25.27	0.14	
BAH-F124-123.2-1.1_weird Gth BAH-F124-123.2-1.2_weird Gth BAH-F124-123.2-1.3_weird Gth BAH-F124-123.2-1.4_weird Gth	#07			average		4.16							
				std dev (1σ)		0.55							
	#07	3/12/16	23:34:41	0.0019858	0.0000004	3.57		0.22	1.95E+09	3.87E+06	25.27	0.14	HM23
	#07	3/12/16	23:40:32	0.0019861	0.0000004	3.73		0.19	1.94E+09	3.85E+06	25.27	0.14	
	#07	3/12/16	23:46:24	0.0019866	0.0000003	4.00		0.15	1.92E+09	3.82E+06	25.27	0.14	
	#07	3/12/16	23:52:16	0.0019865	0.0000003	3.93		0.15	1.91E+09	3.79E+06	25.27	0.14	
BAH-F124-111.2B-1.1	#07			average		3.92							
				std dev (1σ)		0.25							
	#07	4/12/16	1:27:10	0.0019813	0.0000003	1.27		0.16	2.20E+09	4.36E+06	29.36	2.54	HM23
	#07	4/12/16	1:33:03	0.0019790	0.0000003	0.08		0.16	2.25E+09	4.46E+06	29.36	2.54	
	#07	4/12/16	1:38:55	0.0019812	0.0000003	1.22		0.14	2.27E+09	4.50E+06	29.36	2.54	
	#07	4/12/16	1:44:47	0.0019823	0.0000004	1.77		0.18	2.22E+09	4.41E+06	29.36	2.54	
BAH-F124-111.2B-1.1	#07			average		1.08							
				std dev (1σ)		0.72							
	#07	4/12/16	1:56:35	0.0019858	0.0000003	3.55		0.16	2.20E+09	4.36E+06	39.00	2.90	HM23

SPOT #	Session	Date	Time	¹⁸ O/ ¹⁶ O ^(a)	± ^(b)	δ ¹⁸ O _{VSMOW} ^(c)	rejected	±Internal error (σ 95%)	¹⁸ O cps (median)	¹⁶ O cps (median)	(U-Th)/He ages	±	MOUNT
BAH-F124-111.2B-1.2	#07	4/12/16	2:02:26	0.0019857	0.0000003	3.52		0.15	2.21E+09	4.39E+06	39.00	2.90	
BAH-F124-111.2B-1.3	#07	4/12/16	2:08:19	0.0019865	0.0000003	3.95		0.15	2.21E+09	4.39E+06	39.00	2.90	
BAH-F124-111.2B-1.4	#07	4/12/16	2:14:10	0.0019862	0.0000003	3.80		0.16	2.21E+09	4.38E+06	39.00	2.90	
	#07				average std dev (1σ)	3.70 0.20							
BAH-F124-111.2B-1.5	#07	4/12/16	2:20:02	0.0019874	0.0000002	4.37		0.12	2.23E+09	4.44E+06	39.00	2.90	HM23
BAH-F124-111.2B-1.6	#07	4/12/16	2:25:54	0.0019869	0.0000003	4.13		0.13	2.21E+09	4.39E+06	39.00	2.90	
BAH-F124-111.2B-1.7	#07	4/12/16	2:31:46	0.0019867	0.0000003	4.03		0.15	2.22E+09	4.41E+06	39.00	2.90	
BAH-F124-111.2B-1.8b	#07	4/12/16	11:35:53	0.0019865	0.0000003	3.92		0.14	2.18E+09	4.33E+06	39.00	2.90	
	#07				average std dev (1σ)	4.11 0.19							
BAH-F124-111.2B-1.9	#07	4/12/16	3:43:03	0.0019854	0.0000003	3.38		0.13	2.23E+09	4.44E+06	39.00	2.90	HM23
BAH-F124-111.2B-1.10b	#07	4/12/16	11:42:22	0.0019862	0.0000003	3.79		0.14	2.22E+09	4.41E+06	39.00	2.90	
BAH-F124-111.2B-1.11	#07	4/12/16	3:54:47	0.0019859	0.0000003	3.59		0.14	2.22E+09	4.40E+06	39.00	2.90	
BAH-F124-111.2B-1.12	#07	4/12/16	4:00:39	0.0019849	0.0000003	3.08		0.14	2.22E+09	4.40E+06	39.00	2.90	
	#07				average std dev (1σ)	3.46 0.30							
BAH-F124-111.2B-1.13	#07	4/12/16	4:06:32	0.0019850	0.0000003	3.17		0.13	2.28E+09	4.53E+06	39.00	2.90	HM23
BAH-F124-111.2B-1.14	#07	4/12/16	4:12:24	0.0019853	0.0000003	3.33		0.16	2.27E+09	4.51E+06	39.00	2.90	
BAH-F124-111.2B-1.15	#07	4/12/16	4:18:15	0.0019856	0.0000003	3.45		0.13	2.27E+09	4.50E+06	39.00	2.90	
BAH-F124-111.2B-1.16b	#07	4/12/16	11:48:51	0.0019860	0.0000003	3.69		0.14	2.26E+09	4.49E+06	39.00	2.90	
	#07				average std dev (1σ)	3.41 0.22							
BAH-F124-123.2-1.2b	#07	4/12/16	8:39:55	0.0019795	0.0000003	0.33		0.17	2.24E+09	4.44E+06	29.36	2.54	HM23
BAH-F124-123.2-1.5b	#07	4/12/16	8:46:03	0.0019768	0.0000003	-1.05		0.13	2.27E+09	4.49E+06	29.36	2.54	
BAH-F124-123.2-1.1b	#07	4/12/16	8:53:02	0.0019819	0.0000003	1.55		0.17	2.28E+09	4.51E+06	29.36	2.54	
	#07				average std dev (1σ)	0.28 1.30							
BAH-F124-123.2_old-1.1b	#07	4/12/16	9:27:45	0.0019867	0.0000002	4.04		0.11	2.35E+09	4.68E+06	38.80	1.04	HM23
BAH-F124-123.2_old-1.2	#07	4/12/16	5:47:15	0.0019871	0.0000003	4.23		0.15	2.36E+09	4.70E+06	38.80	1.04	
BAH-F124-123.2_old-1.2b	#07	4/12/16	9:33:58	0.0019871	0.0000002	4.22		0.11	2.38E+09	4.73E+06	38.80	1.04	
BAH-F124-123.2_old-1.3b	#07	4/12/16	9:40:01	0.0019866	0.0000003	3.98		0.15	2.44E+09	4.85E+06	38.80	1.04	
BAH-F124-123.2_old-1.4b	#07	4/12/16	9:46:09	0.0019867	0.0000002	4.02		0.11	2.48E+09	4.92E+06	38.80	1.04	
BAH-F124-123.2_old-1.5b	#07	4/12/16	9:54:14	0.0019879	0.0000003	4.66		0.13	2.45E+09	4.87E+06	38.80	1.04	
BAH-F124-123.2_old-1.6b	#07	4/12/16	10:00:12	0.0019866	0.0000003	3.98		0.16	2.41E+09	4.79E+06	38.80	1.04	
BAH-F124-123.2_old-1.7b	#07	4/12/16	10:06:14	0.0019852	0.0000002	3.25		0.12	2.42E+09	4.80E+06	38.80	1.04	
BAH-F124-123.2_old-1.8b	#07	4/12/16	10:12:15	0.0019871	0.0000002	4.23		0.12	2.40E+09	4.77E+06	38.80	1.04	
	#07				average std dev (1σ)	4.07 0.37							
BAH-F124-123.7-1.2	#07	4/12/16	12:39:37	0.0019861	0.0000002	3.74		0.12	2.34E+09	4.65E+06	56.44	1.93	HM23
BAH-F124-123.7-1.3	#07	4/12/16	12:45:29	0.0019853	0.0000002	3.29		0.10	2.32E+09	4.61E+06	56.44	1.93	
BAH-F124-123.7-1.4	#07	4/12/16	12:51:21	0.0019852	0.0000002	3.27		0.12	2.39E+09	4.75E+06	56.44	1.93	
BAH-F124-123.7-1.5	#07	4/12/16	12:57:13	0.0019872	0.0000003	4.27		0.13	2.31E+09	4.59E+06	56.44	1.93	
BAH-F124-123.7-1.6	#07	4/12/16	13:03:05	0.0019922	0.0000003	6.85		0.16	2.27E+09	4.52E+06	56.44	1.93	
BAH-F124-123.7-1.7	#07	4/12/16	13:08:57	0.0019918	0.0000003	6.64		0.15	2.28E+09	4.55E+06	56.44	1.93	
BAH-F124-123.7-1.8	#07	4/12/16	13:14:49	0.0019900	0.0000002	5.74		0.12	2.26E+09	4.49E+06	56.44	1.93	
BAH-F124-123.7-1.10	#07	4/12/16	14:26:06	0.0019915	0.0000003		6.51	0.14	2.33E+09	4.63E+06	56.44	1.93	
BAH-F124-123.7-1.11	#07	4/12/16	14:31:58	0.0019883	0.0000003	4.83		0.14	2.31E+09	4.59E+06	56.44	1.93	
BAH-F124-123.7-1.12	#07	4/12/16	14:37:49	0.0019885	0.0000003	4.96		0.15	2.34E+09	4.65E+06	56.44	1.93	
BAH-F124-123.7-1.1b	#07	4/12/16	16:12:12	0.0019881	0.0000003	4.74		0.15	2.34E+09	4.65E+06	56.44	1.93	
BAH-F124-123.7-1.9b	#07	4/12/16	16:25:18	0.0019902	0.0000002	5.84		0.12	2.29E+09	4.56E+06	56.44	1.93	
BAH-F124-123.7-1.10b	#07	4/12/16	16:31:55	0.0019880	0.0000002	4.72		0.13	2.37E+09	4.70E+06	56.44	1.93	
	#07				average std dev (1σ)	4.91 1.19							
BAH-F124-112-1.2	#07	4/12/16	17:27:52	0.0019884	0.0000003	4.93		0.17	2.30E+09	4.58E+06	52.80	1.73	HM23
BAH-F124-112-1.3	#07	4/12/16	17:33:45	0.0019884	0.0000003	4.88		0.14	2.31E+09	4.60E+06	52.80	1.73	
BAH-F124-112-1.4	#07	4/12/16	17:39:36	0.0019881	0.0000003	4.74		0.14	2.34E+09	4.66E+06	52.80	1.73	
BAH-F124-112-1.5	#07	4/12/16	17:45:28	0.0019886	0.0000003	5.01		0.14	2.30E+09	4.58E+06	52.80	1.73	
BAH-F124-112-1.6	#07	4/12/16	17:51:20	0.0019894	0.0000003	5.43		0.14	2.31E+09	4.59E+06	52.80	1.73	
BAH-F124-112-1.7	#07	4/12/16	17:57:12	0.0019900	0.0000003	5.74		0.13	2.33E+09	4.64E+06	52.80	1.73	
BAH-F124-112-1.8	#07	4/12/16	18:03:04	0.0019902	0.0000003	5.83		0.15	2.33E+09	4.65E+06	52.80	1.73	
BAH-F124-112-1.9	#07	4/12/16	19:08:32	0.0019875	0.0000002	4.42		0.10	2.36E+09	4.70E+06	52.80	1.73	
BAH-F124-112-1.10	#07	4/12/16	19:14:25	0.0019894	0.0000003	5.42		0.17	2.38E+09	4.73E+06	52.80	1.73	
BAH-F124-112-1.11	#07	4/12/16	19:20:17	0.0019886	0.0000003	4.99		0.16	2.36E+09	4.69E+06	52.80	1.73	
BAH-F124-112-1.12	#07	4/12/16	19:26:09	0.0019894	0.0000002	5.41		0.11	2.36E+09	4.70E+06	52.80	1.73	
BAH-F124-112-1.1b	#07	4/12/16	23:01:07	0.0019871	0.0000002	4.21		0.12	2.34E+09	4.66E+06	52.80	1.73	
BAH-F124-112-1.9b	#07	4/12/16	23:08:57	0.0019877	0.0000002	4.53		0.12	2.40E+09	4.77E+06	52.80	1.73	
BAH-F124-112-1.1c	#07	4/12/16	23:35:58	0.0019860	0.0000003	3.68		0.14	2.33E+09	4.62E+06	52.80	1.73	
	#07				average std dev (1σ)	4.94 0.60							
BAH-F124-114-1.1	#07	4/12/16	19:32:03	0.0019801	0.0000004	0.62		0.18	2.27E+09	4.50E+06	10.96	0.33	HM23
BAH-F124-114-1.2	#07	4/12/16	19:37:55	0.0019800	0.0000003	0.57		0.14	2.29E+09	4.52E+06	10.96	0.33	
BAH-F124-114-1.3	#07	4/12/16	19:43:47	0.0019817	0.0000003		1.48	0.15	2.29E+09	4.54E+06	10.96	0.33	
BAH-F124-114-1.4	#07	4/12/16	19:49:38	0.0019784	0.0000003	-0.24		0.17	2.28E+09	4.52E+06	10.96	0.33	
BAH-F124-114-1.5	#07	4/12/16	19:55:30	0.0019802	0.0000003	0.71		0.17	2.30E+09	4.55E+06	10.96	0.33	
BAH-F124-114-1.4b	#07	4/12/16	23:15:22	0.0019790	0.0000003	0.08		0.13	2.32E+09	4.59E+06	10.96	0.33	
	#07				average std dev (1σ)	0.35 0.41							
BAH-F124-123.1-1.1sparkling	#07	4/12/16	20:01:25	0.0019777	0.0000003	-0.60		0.15	2.19E+09	4.33E+06	12.26	1.14	HM23
BAH-F124-123.1-1.2sparkling	#07	4/12/16	20:07:18	0.0019803	0.0000003	0.74		0.16	2.20E+09	4.36E+06	12.26	1.14	
BAH-F124-123.1-1.3sparkling	#07	4/12/16	20:13:10	0.0019824	0.0000003	1.80		0.16	2.23E+09	4.42E+06	12.26	1.14	
BAH-F124-123.1-1.4sparkling	#07	4/12/16	20:19:02	0.0019802	0.0000003	0.67		0.15	2.29E+09	4.54E+06	12.26	1.14	
BAH-F124-123.1-1.1csparkling	#07	4/12/16	23:42:25	0.0019794	0.0000002	0.27		0.12	2.30E+09	4.56E+06	12.26	1.14	
	#07				average std dev (1σ)	0.58 0.87							
BAH-F124-123.1-1.5black	#07	4/12/16	21:24:32	0.0019865	0.0000002	3.93		0.12	2.38E+09	4.72E+06	41.58	5.15	HM23
BAH-F124-123.1-1.6black	#07	4/12/16	21:30:23	0.0019877	0.0000002	4.54		0.12	2.38E+09	4.74E+06	41.58	5.15	
BAH-F124-123.1-1.7black	#07	4/12/16	21:36:15	0.0019852	0.0000002	3.25		0.11	2.39E+09	4.75E+06	41.58	5.15	
BAH-F124-123.1-1.8black	#07	4/12/16	21:42:07	0.0019850	0.0000003	3.16		0.13	2.38E+09	4.72E+06	41.58	5.15	
BAH-F124-123.1-1.6black	#07	4/12/16	23:28:23	0.0019870	0.0000003	4.17		0.14	2.38E+09	4.74E+06	41.58	5.15	
	#07				average std dev (1σ)	3.81 0.59							
BAH-F124-123.2_2.1weird goethite	#07	5/12/16	15:38:06	0.0019758	0.0000003	-1.56		0.16	2.28E+09	4.51E+06			

SPOT #	Session	Date	Time	¹⁸ O/ ¹⁶ O ^(a)	± ^(b)	δ ¹⁸ O _{VSMOW} ^(c)	rejected	±Internal error (σ 95%)	¹⁸ O cps (median)	¹⁶ O cps (median)	(U-Th)/He ages	±	MOUNT
BAH-F124-123.2_2_weird goethite	#07	5/12/16	15:44:43	0.0019754	0.0000003	-1.80		0.16	2.29E+09	4.53E+06	29.36	2.54	
BAH-F124-123.2_2_3weird goethite	#07	5/12/16	15:51:00	0.0019748	0.0000002	-2.09		0.12	2.27E+09	4.48E+06	29.36	2.54	
BAH-F124-123.2_2_4weird goethite	#07	5/12/16	15:59:15	0.0019753	0.0000002	-1.82		0.12	2.29E+09	4.52E+06	29.36	2.54	
BAH-F124-123.2_2_5weird goethite	#07	5/12/16	16:05:27	0.0019788	0.0000003	-0.05		0.16	2.24E+09	4.44E+06	29.36	2.54	
BAH-F124-123.2_2_7weird goethite	#07	5/12/16	16:19:59	0.0019769	0.0000003	-1.03		0.16	2.20E+09	4.36E+06	29.36	2.54	
#07				average	-1.39								
				std dev (1σ)	0.75								
BAH-F177-115-1.1	#07	5/12/16	16:30:26	0.0019881	0.0000003	4.75		0.16	2.41E+09	4.78E+06	3.13	0.30	HM23
BAH-F177-115-1.2	#07	5/12/16	16:36:29	0.0019884	0.0000003	4.93		0.14	2.42E+09	4.81E+06	3.13	0.30	
BAH-F177-115-1.3	#07	5/12/16	16:42:38	0.0019893	0.0000003	5.37		0.13	2.43E+09	4.83E+06	3.13	0.30	
BAH-F177-115-1.4	#07	5/12/16	16:49:16	0.0019882	0.0000004	4.81		0.18	2.42E+09	4.80E+06	3.13	0.30	
BAH-F177-115-1.5Botryoidal	#07	5/12/16	18:36:37	0.0019858	0.0000003	3.56		0.13	2.36E+09	4.69E+06	3.13	0.30	
BAH-F177-115-1.6Botryoidal	#07	5/12/16	18:42:29	0.0019874	0.0000003	4.41		0.13	2.37E+09	4.71E+06	3.13	0.30	
BAH-F177-115-1.8Botryoidal	#07	5/12/16	18:54:12	0.0019858	0.0000004	3.55		0.22	2.39E+09	4.74E+06	3.13	0.30	
BAH-F177-115-1.9Botryoidal	#07	5/12/16	19:00:04	0.0019857	0.0000003	3.49		0.16	2.35E+09	4.67E+06	3.13	0.30	
BAH-F177-115-1.10Botryoidal	#07	5/12/16	19:05:56	0.0019864	0.0000003	3.88		0.15	2.36E+09	4.68E+06	3.13	0.30	
BAH-F177-115-1.11Botryoidal	#07	5/12/16	19:11:48	0.0019864	0.0000003	3.86		0.13	2.38E+09	4.72E+06	3.13	0.30	
BAH-F177-115-1.12Botryoidal	#07	5/12/16	19:17:40	0.0019860	0.0000002	3.69		0.12	2.39E+09	4.74E+06	3.13	0.30	
BAH-F177-115-1.7bBotryoidal	#07	5/12/16	20:49:02	0.0019885	0.0000003	4.97		0.16	2.39E+09	4.75E+06	3.13	0.30	
#07				average	4.27								
				std dev (1σ)	0.67								
BAH-F177-115-1.13brown	#07	6/12/16	2:06:01	0.0019783	0.0000003	-0.29		0.15	2.36E+09	4.66E+06	23.44	2.34	HM23
BAH-F177-115-1.14brown	#07	6/12/16	2:11:52	0.0019791	0.0000003	0.14		0.15	2.37E+09	4.68E+06	23.44	2.34	
BAH-F177-115-1.15brown	#07	6/12/16	2:17:44	0.0019771	0.0000003	-0.90		0.18	2.37E+09	4.69E+06	23.44	2.34	
BAH-F177-115-1.16brown	#07	6/12/16	2:23:36	0.0019778	0.0000004	-0.56		0.18	2.37E+09	4.70E+06	23.44	2.34	
BAH-F177-115-1.17brown	#07	6/12/16	2:29:27	0.0019772	0.0000003	-0.84		0.14	2.36E+09	4.67E+06	23.44	2.34	
BAH-F177-115-1.18brown	#07	6/12/16	2:35:19	0.0019793	0.0000004	0.20		0.18	2.38E+09	4.72E+06	23.44	2.34	
#07				average	-0.37								
				std dev (1σ)	0.48								
BAH-F226-142.7-1.1_black	#07	6/12/16	2:41:12	0.0019853	0.0000004	3.32		0.19	2.26E+09	4.48E+06	4.59	0.31	HM23
BAH-F226-142.7-1.2_black	#07	6/12/16	2:47:04	0.0019814	0.0000003	1.29		0.14	2.25E+09	4.46E+06	4.59	0.31	
BAH-F226-142.7-1.3_black	#07	6/12/16	2:52:56	0.0019831	0.0000003	2.18		0.14	2.25E+09	4.47E+06	4.59	0.31	
BAH-F226-142.7-1.4_black	#07	6/12/16	4:27:41	0.0019841	0.0000003	2.70		0.15	2.27E+09	4.50E+06	4.59	0.31	
BAH-F226-142.7-1.5_black	#07	6/12/16	4:33:32	0.0019832	0.0000003	2.22		0.14	2.27E+09	4.51E+06	4.59	0.31	
BAH-F226-142.7-1.6_black	#07	6/12/16	4:39:24	0.0019832	0.0000002	2.21		0.12	2.28E+09	4.52E+06	4.59	0.31	
#07				average	2.32								
				std dev (1σ)	0.67								
BAH-F226-142.7-1.7sparkling	#07	6/12/16	4:45:16	0.0019818	0.0000003	1.49		0.15	2.33E+09	4.62E+06	14.03	0.66	HM23
BAH-F226-142.7-1.8sparkling	#07	6/12/16	4:51:07	0.0019788	0.0000002		-0.05	0.12	2.35E+09	4.65E+06	14.03	0.66	
BAH-F226-142.7-1.9sparkling	#07	6/12/16	4:56:59	0.0019824	0.0000003	1.80		0.17	2.34E+09	4.63E+06	14.03	0.66	
BAH-F226-142.7-1.10_brown	#07	6/12/16	5:02:51	0.0019841	0.0000003	2.68		0.16	2.40E+09	4.77E+06	14.03	0.66	
BAH-F226-142.7-1.11_brown	#07	6/12/16	5:08:42	0.0019851	0.0000003	3.22		0.16	2.42E+09	4.80E+06	14.03	0.66	
BAH-F226-142.7-1.12_brown	#07	6/12/16	5:14:34	0.0019843	0.0000002	2.81		0.10	2.41E+09	4.79E+06	14.03	0.66	
BAH-F226-142.7-1.13_brown	#07	6/12/16	5:20:26	0.0019816	0.0000003	1.43		0.14	2.40E+09	4.75E+06	14.03	0.66	
#07				average	2.24								
				std dev (1σ)	0.76								
BAH-F226-142.7-1.15_botryoidal	#07	6/12/16	7:18:37	0.0019934	0.0000002	7.45		0.12	2.57E+09	5.11E+06			HM23
BAH-F226-142.7-1.16_botryoidal	#07	6/12/16	7:24:28	0.0019929	0.0000003	7.19		0.14	2.58E+09	5.14E+06			
BAH-F226-142.7-1.17_botryoidal	#07	6/12/16	7:30:20	0.0019926	0.0000003	7.04		0.14	2.57E+09	5.13E+06			
#07				average	7.23								
				std dev (1σ)	0.21								
BAH-F226-157.6-1.1brown	#07	6/12/16	7:36:15	0.0019802	0.0000004	0.67		0.18	2.22E+09	4.40E+06	12.40	0.06	HM23
BAH-F226-157.6-1.2brown	#07	6/12/16	7:42:06	0.0019808	0.0000003	0.99		0.16	2.23E+09	4.42E+06	12.40	0.06	
BAH-F226-157.6-1.3brown	#07	6/12/16	7:47:58	0.0019817	0.0000003	1.45		0.15	2.24E+09	4.44E+06	12.40	0.06	
BAH-F226-157.6-1.4brown	#07	6/12/16	7:53:50	0.0019801	0.0000002	0.62		0.12	2.25E+09	4.45E+06	12.40	0.06	
BAH-F226-157.6-1.5brown	#07	6/12/16	7:59:42	0.0019815	0.0000002	1.34		0.11	2.25E+09	4.46E+06	12.40	0.06	
BAH-F226-157.6-1.6brown	#07	6/12/16	8:05:34	0.0019782	0.0000003	-0.34		0.14	2.25E+09	4.46E+06	12.40	0.06	
BAH-F226-157.6-1.7brown	#07	6/12/16	8:11:26	0.0019810	0.0000003	1.09		0.16	2.25E+09	4.46E+06	12.40	0.06	
#07				average	0.83								
				std dev (1σ)	0.60								
BAH-F226-157.6-2.1black	#07	6/12/16	9:16:44	0.0019842	0.0000003	2.72		0.13	2.27E+09	4.50E+06	10.06	1.01	HM23
BAH-F226-157.6-2.2black	#07	6/12/16	9:22:36	0.0019827	0.0000002	1.98		0.09	2.23E+09	4.43E+06	10.06	1.01	
BAH-F226-157.6-2.3black	#07	6/12/16	9:28:28	0.0019862	0.0000002	3.76		0.11	2.29E+09	4.56E+06	10.06	1.01	
BAH-F226-157.6-2.4black	#07	6/12/16	9:34:19	0.0019842	0.0000003	2.72		0.15	2.28E+09	4.53E+06	10.06	1.01	
#07				average	2.79								
				std dev (1σ)	0.73								
BAH-F226-186.8_old-1.1	#07	6/12/16	12:10:45	0.0019841	0.0000003	2.71		0.14	2.15E+09	4.27E+06	49.20	0.85	HM23
BAH-F226-186.8_old-1.2	#07	6/12/16	12:17:09	0.0019847	0.0000003	3.00		0.16	2.15E+09	4.28E+06	49.20	0.85	
BAH-F226-186.8_old-1.4	#07	6/12/16	12:26:17	0.0019832	0.0000004	2.23		0.20	2.14E+09	4.23E+06	49.20	0.85	
BAH-F226-186.8_old-1.3	#07	6/12/16	12:35:48	0.0019815	0.0000003	1.38		0.16	2.12E+09	4.20E+06	49.20	0.85	
BAH-F226-186.8_old-1.5	#07	6/12/16	12:41:43	0.0019817	0.0000003	1.48		0.16	2.05E+09	4.07E+06	49.20	0.85	
BAH-F226-186.8_old-1.6	#07	6/12/16	12:49:39	0.0019819	0.0000002	1.59		0.12	2.14E+09	4.24E+06	49.20	0.85	
#07				average	2.06								
				std dev (1σ)	0.69								
BAH-F226-157.6-3.1black	#07	6/12/16	12:58:35	0.0019849	0.0000003	3.11		0.15	2.12E+09	4.21E+06	10.06	1.01	HM23
BAH-F226-157.6-3.2black	#07	6/12/16	13:04:33	0.0019848	0.0000003	3.06		0.13	2.12E+09	4.22E+06	10.06	1.01	
BAH-F226-157.6-3.3black	#07	6/12/16	13:10:40	0.0019852	0.0000003	3.26		0.15	2.14E+09	4.25E+06	10.06	1.01	
BAH-F226-157.6-3.4black	#07	6/12/16	13:16:53	0.0019847	0.0000003	3.03		0.14	2.16E+09	4.28E+06	10.06	1.01	
#07				average	3.12								
				std dev (1σ)	0.10								
BAH-F282-124.9_stalag-1.1_botryoidal	#07	6/12/16	14:58:33	0.0019845	0.0000003	2.89		0.13	2.17E+09	4.31E+06	41.60	3.29	HM23
BAH-F282-124.9_stalag-1.2_botryoidal	#07	6/12/16	15:04:33	0.0019861	0.0000003	3.75		0.14	2.20E+09	4.37E+06	41.60	3.29	
BAH-F282-124.9_stalag-1.3_botryoidal	#07	6/12/16	15:12:01	0.0019844	0.0000003	2.84		0.16	2.23E+09	4.43E+06	41.60	3.29	
BAH-F282-124.9_stalag-1.4_botryoidal	#07	6/12/16	15:18:46	0.0019860	0.0000003	3.67		0.14	2.21E+09	4.38E+06	41.60	3.29	
BAH-F282-124.9_stalag-1.5_botryoidal	#07	6/12/16	15:27:51	0.0019875	0.0000003	4.47		0.15	2.17E+09	4.32E+06	41.60	3.29	
BAH-F282-124.9_stalag-1.6_botryoidal	#07	6/12/16	15:35:06	0.0019861	0.0000003	3.74		0.14	2.20E+09	4.36E+06	41.60	3.29	
#07				average	3.56								
				std dev (1σ)	0.61								
BAH-F282-124.9_stalag-1.7	#07	6/12/16	15:41:30	0.0019775	0.0000004	-							

SPOT #	Session	Date	Time	¹⁸ O/ ¹⁶ O ^(a)	± ^(b)	δ ¹⁸ O _{VSMOW} ^(c)	rejected	±Internal error (σ 95%)	¹⁶ O cps (median)	¹⁸ O cps (median)	(U-Th)/He ages	±	MOUNT
BAH-F226-142.7-1.18_brown BAH-F226-142.7-1.19_brown BAH-F226-142.7-1.20_brown BAH-F226-142.7-1.21_brown	#07			average std dev (1σ)		-0.42 0.73							
	#07	6/12/16	19:07:34	0.0019822	0.0000003	1.74		0.17	2.25E+09	4.46E+06	14.03	0.66	HM23
	#07	6/12/16	19:13:26	0.0019818	0.0000002	1.50		0.12	2.25E+09	4.46E+06	14.03	0.66	
	#07	6/12/16	19:19:17	0.0019834	0.0000003	2.36		0.13	2.26E+09	4.47E+06	14.03	0.66	
	#07	6/12/16	19:25:10	0.0019813	0.0000003	1.27		0.14	2.26E+09	4.47E+06	14.03	0.66	
BAH-F226-142.7-1.22_botryoidal BAH-F226-142.7-1.23_botryoidal BAH-F226-142.7-1.24_botryoidal	#07			average std dev (1σ)		1.72 0.47							
	#07	6/12/16	19:31:02	0.0019910	0.0000003	6.27		0.17	2.34E+09	4.66E+06			HM23
	#07	6/12/16	19:36:54	0.0019936	0.0000003	7.57		0.15	2.39E+09	4.76E+06			
	#07	6/12/16	19:42:46	0.0019920	0.0000003	6.77		0.13	2.39E+09	4.75E+06			
	#07			average std dev (1σ)		6.87 0.66							
BAH-F226-142.7-2.1_black BAH-F226-142.7-2.2_black BAH-F226-142.7-2.3_black BAH-F226-142.7-2.4_black BAH-F226-142.7-2.5_black BAH-F226-142.7-2.6_black	#07	6/12/16	19:48:41	0.0019813	0.0000003	1.29		0.16	2.17E+09	4.29E+06	4.59	0.31	HM23
	#07	6/12/16	19:54:32	0.0019829	0.0000003	2.08		0.14	2.17E+09	4.30E+06	4.59	0.31	
	#07	6/12/16	20:00:24	0.0019805	0.0000004		0.84	0.22	2.19E+09	4.34E+06	4.59	0.31	
	#07	6/12/16	20:06:16	0.0019823	0.0000003	1.77		0.17	2.20E+09	4.36E+06	4.59	0.31	
	#07	6/12/16	20:12:08	0.0019831	0.0000003	2.18		0.17	2.21E+09	4.38E+06	4.59	0.31	
BAH-F226-157.6-4.1brown BAH-F226-157.6-4.2brown BAH-F226-157.6-4.3brown BAH-F226-157.6-4.4brown BAH-F226-157.6-4.5brown BAH-F226-157.6-4.6brown BAH-F226-157.6-4.7brown BAH-F226-157.6-4.8brown	#07	6/12/16	20:18:00	0.0019835	0.0000003	2.41		0.13	2.22E+09	4.40E+06	4.59	0.31	
	#07			average std dev (1σ)		1.95 0.43							
	#07	6/12/16	22:05:09	0.0019815	0.0000003	1.35		0.17	2.12E+09	4.20E+06	12.40	0.06	HM23
	#07	6/12/16	22:11:01	0.0019802	0.0000004	0.69		0.18	2.14E+09	4.23E+06	12.40	0.06	
	#07	6/12/16	22:16:52	0.0019807	0.0000003	0.97		0.15	2.14E+09	4.25E+06	12.40	0.06	
BAH-F226-157.6-4.9_bright lyr BAH-F226-157.6-4.10_bright lyr BAH-F226-157.6-4.11_bright lyr	#07	6/12/16	22:22:44	0.0019799	0.0000004	0.57		0.19	2.15E+09	4.26E+06	12.40	0.06	
	#07	6/12/16	22:28:36	0.0019793	0.0000005	0.23		0.25	2.16E+09	4.27E+06	12.40	0.06	
	#07	6/12/16	22:34:29	0.0019798	0.0000003	0.51		0.17	2.13E+09	4.22E+06	12.40	0.06	
	#07	6/12/16	22:40:20	0.0019829	0.0000004		2.10	0.21	2.14E+09	4.25E+06	12.40	0.06	
	#07	6/12/16	22:46:12	0.0019810	0.0000005	1.13		0.26	2.16E+09	4.27E+06	12.40	0.06	
BAH-F226-157.6-4.9_bright lyr BAH-F226-157.6-4.10_bright lyr BAH-F226-157.6-4.11_bright lyr	#07			average std dev (1σ)		0.78 0.39							
	#07	6/12/16	22:52:04	0.0019879	0.0000005	4.66		0.24	2.29E+09	4.56E+06			HM23
	#07	6/12/16	22:57:55	0.0019866	0.0000005	4.00		0.23	2.30E+09	4.56E+06			
	#07	6/12/16	23:03:47	0.0019886	0.0000005	5.01		0.23	2.29E+09	4.56E+06			
	#07			average std dev (1σ)		4.56 0.51							
BAH-F282-120.5_brown-1.1 BAH-F282-120.5_brown-1.2 BAH-F282-120.5_brown-1.3 BAH-F282-120.5_brown-1.5	#07	7/12/16	0:03:16	0.0019810	0.0000003	1.13		0.13	2.14E+09	4.23E+06	45.29	1.15	HM23
	#07	7/12/16	0:09:07	0.0019826	0.0000003	1.95		0.14	2.14E+09	4.24E+06	45.29	1.15	
	#07	7/12/16	0:14:59	0.0019829	0.0000003	2.10		0.18	2.14E+09	4.25E+06	45.29	1.15	
	#07	7/12/16	0:26:43	0.0019833	0.0000004	2.28		0.21	2.15E+09	4.26E+06	45.29	1.15	
	#07			average std dev (1σ)		1.86 0.51							
BAH-F282-120.5_brown-2.1 BAH-F282-120.5_brown-2.2 BAH-F282-120.5_brown-2.3 BAH-F282-120.5_brown-2.4 BAH-F282-120.5_brown-2.5 BAH-F282-120.5_brown-2.6 BAH-F282-120.5_brown-2.7	#07	7/12/16	0:32:36	0.0019821	0.0000006	1.70		0.32	2.14E+09	4.24E+06	45.29	1.15	HM23
	#07	7/12/16	0:38:28	0.0019816	0.0000007	1.40		0.33	2.14E+09	4.24E+06	45.29	1.15	
	#07	7/12/16	0:44:19	0.0019825	0.0000005	1.86		0.25	2.14E+09	4.25E+06	45.29	1.15	
	#07	7/12/16	0:50:11	0.0019818	0.0000006	1.51		0.30	2.14E+09	4.25E+06	45.29	1.15	
	#07	7/12/16	0:56:03	0.0019840	0.0000004	2.65		0.19	2.14E+09	4.25E+06	45.29	1.15	
BAH-F124-123.2_old-2.1 BAH-F124-123.2_old-2.2 BAH-F124-123.2_old-2.3 BAH-F124-123.2_old-2.4 BAH-F124-123.2_old-2.5	#07	7/12/16	1:01:55	0.0019842	0.0000003	2.76		0.14	2.15E+09	4.26E+06	45.29	1.15	
	#07	7/12/16	1:07:47	0.0019838	0.0000003	2.56		0.16	2.15E+09	4.26E+06	45.29	1.15	
	#07			average std dev (1σ)		2.06 0.58							
	#07	7/12/16	2:25:07	0.0019882	0.0000003	4.83		0.16	2.28E+09	4.53E+06	38.80	1.04	HM23
	#07	7/12/16	2:30:59	0.0019859	0.0000003	3.63		0.15	2.28E+09	4.53E+06	38.80	1.04	
BAH-F282-120.5_black-1.1 BAH-F282-120.5_black-1.2 BAH-F282-120.5_black-1.3 BAH-F282-120.5_black-1.4 BAH-F282-120.5_black-1.6	#07	7/12/16	2:36:51	0.0019870	0.0000003	4.20		0.15	2.27E+09	4.52E+06	38.80	1.04	
	#07	7/12/16	2:42:43	0.0019881	0.0000003	4.79		0.13	2.27E+09	4.52E+06	38.80	1.04	
	#07	7/12/16	2:48:34	0.0019912	0.0000003		6.38	0.14	2.26E+09	4.49E+06	38.80	1.04	
	#07			average std dev (1σ)		4.36 0.57							
	#07	7/12/16	2:54:30	0.0019876	0.0000003	4.52		0.16	2.18E+09	4.33E+06	41.05	0.12	HM23
BAH-F282-118.4-1.1 BAH-F282-118.4-1.2 BAH-F282-118.4-1.3 BAH-F282-118.4-1.4 BAH-F282-118.4-1.5 BAH-F282-118.4-1.6	#07	7/12/16	3:00:22	0.0019877	0.0000003	4.56		0.16	2.19E+09	4.36E+06	41.05	0.12	
	#07	7/12/16	3:06:14	0.0019860	0.0000003	3.67		0.13	2.19E+09	4.35E+06	41.05	0.12	
	#07	7/12/16	3:12:07	0.0019883	0.0000002	4.86		0.12	2.24E+09	4.45E+06	41.05	0.12	
	#07	7/12/16	3:23:51	0.0019865	0.0000003	3.93		0.14	2.15E+09	4.27E+06	41.05	0.12	
	#07			average std dev (1σ)		4.31 0.49							
BAH-F226-157.6-5.1brown BAH-F226-157.6-5.2brown BAH-F226-157.6-5.3brown BAH-F226-157.6-5.4brown BAH-F226-157.6-5.5brown	#07	7/12/16	4:23:24	0.0019819	0.0000003	1.59		0.15	2.12E+09	4.20E+06	34.89	5.76	HM23
	#07	7/12/16	4:29:16	0.0019825	0.0000003	1.90		0.17	2.12E+09	4.21E+06	34.89	5.76	
	#07	7/12/16	4:35:08	0.0019842	0.0000003	2.74		0.15	2.12E+09	4.20E+06	34.89	5.76	
	#07	7/12/16	4:41:00	0.0019826	0.0000004	1.94		0.20	2.11E+09	4.18E+06	34.89	5.76	
	#07	7/12/16	4:46:52	0.0019837	0.0000003	2.52		0.17	2.09E+09	4.14E+06	34.89	5.76	
BAH-layer2-1.1 BAH-layer2-1.10 BAH-layer2-1.11 BAH-layer2-1.12 BAH-layer2-1.12b BAH-layer2-1.12c BAH-layer2-1.13 BAH-layer2-1.14 BAH-layer2-1.14 BAH-layer2-1.2 BAH-layer2-1.3	#07	7/12/16	4:52:44	0.0019849	0.0000003	3.11		0.13	2.07E+09	4.12E+06	34.89	5.76	
	#07			average std dev (1σ)		2.30 0.58							
	#07	7/12/16	4:58:41	0.0019819	0.0000003	1.58		0.14	2.12E+09	4.20E+06	12.40	0.06	HM23
	#07	7/12/16	5:04:33	0.0019799	0.0000003	0.55		0.13	2.12E+09	4.20E+06	12.40	0.06	
	#07	7/12/16	5:10:25	0.0019807	0.0000002	0.94		0.12	2.12E+09	4.20E+06	12.40	0.06	
BAH-layer2-1.12c BAH-layer2-1.13 BAH-layer2-1.14 BAH-layer2-1.2 BAH-layer2-1.3	#07	7/12/16	5:16:17	0.0019813	0.0000002	1.29		0.13	2.12E+09	4.20E+06	12.40	0.06	
	#07	7/12/16	5:22:08	0.0019811	0.0000003	1.17		0.15	2.12E+09	4.20E+06	12.40	0.06	
	#07			average std dev (1σ)		1.11 0.39							
	#08	21/6/17	14:31:12	0.0019593	0.0000002	-1.81		0.12	2.04E+09	4.00E+06	13.73	2.14	BAH
	#08	21/6/17	18:04:21	0.0019594	0.0								

SPOT #	Session	Date	Time	¹⁸ O/ ¹⁶ O ^(a)	± ^(b)	δ ¹⁸ O _{VERMOM} ^(c)	rejected	±Internal error (σ 95%)	¹⁸ O cps (median)	¹⁶ O cps (median)	(U-Th)/He ages	±	MOUNT
BAH-layer2-1.4	#08	21/6/17	14:47:47	0.0019595	0.0000002	-1.72		0.10	2.08E+09	4.08E+06	13.73	2.14	
BAH-layer2-1.5	#08	21/6/17	14:53:14	0.0019590	0.0000002	-1.94		0.10	2.08E+09	4.07E+06	13.73	2.14	
BAH-layer2-1.6	#08	21/6/17	14:58:42	0.0019581	0.0000002		-2.40	0.09	2.11E+09	4.13E+06	13.73	2.14	
BAH-layer2-1.7	#08	21/6/17	15:04:10	0.0019594	0.0000002	-1.77		0.09	2.08E+09	4.08E+06	13.73	2.14	
BAH-layer2-1.8	#08	21/6/17	15:09:38	0.0019586	0.0000002	-2.18		0.09	2.05E+09	4.01E+06	13.73	2.14	
BAH-layer2-1.9	#08	21/6/17	17:58:54	0.0019588	0.0000002	-2.07		0.13	2.08E+09	4.07E+06	13.73	2.14	
				average		-1.74							
				std dev (1σ)		0.26							
BAH-layer1-1.1	#08	21/6/17	13:18:53	0.0019580	0.0000002	-2.50		0.10	1.90E+09	3.72E+06	13.73	2.14	BAH
BAH-layer1-1.2	#08	21/6/17	13:24:20	0.0019577	0.0000002	-2.63		0.10	1.91E+09	3.73E+06	13.73	2.14	
BAH-layer1-1.3	#08	21/6/17	13:29:48	0.0019574	0.0000002		-2.78	0.12	1.87E+09	3.65E+06	13.73	2.14	
BAH-layer1-1.4	#08	21/6/17	13:35:15	0.0019577	0.0000002	-2.62		0.10	1.86E+09	3.64E+06	13.73	2.14	
BAH-layer1-1.5	#08	21/6/17	13:40:43	0.0019580	0.0000002	-2.48		0.12	1.86E+09	3.64E+06	13.73	2.14	
BAH-layer1-1.6	#08	21/6/17	13:46:10	0.0019572	0.0000002	-2.89		0.12	1.83E+09	3.58E+06	13.73	2.14	
BAH-layer1-1.7	#08	21/6/17	13:51:37	0.0019569	0.0000002	-3.04		0.11	1.79E+09	3.50E+06	13.73	2.14	
BAH-layer1-1.8	#08	21/6/17	13:57:05	0.0019557	0.0000002		-3.68	0.13	1.75E+09	3.41E+06	13.73	2.14	
BAH-layer1-1.8b	#08	21/6/17	15:42:45	0.0019574	0.0000002	-2.79		0.09	1.77E+09	3.47E+06	13.73	2.14	
				average		-2.71							
				std dev (1σ)		0.21							
BAH-layer3-1.1	#08	21/6/17	19:41:30	0.0019595	0.0000002	-1.69		0.11	2.10E+09	4.12E+06	16.26	0.92	BAH
BAH-layer3-1.2	#08	21/6/17	19:46:58	0.0019587	0.0000002	-2.13		0.12	2.10E+09	4.11E+06	16.26	0.92	
BAH-layer3-1.3	#08	21/6/17	19:52:25	0.0019585	0.0000002	-2.24		0.10	2.10E+09	4.11E+06	16.26	0.92	
BAH-layer3-1.4	#08	21/6/17	19:57:52	0.0019587	0.0000002	-2.14		0.11	2.08E+09	4.07E+06	16.26	0.92	
BAH-layer3-1.5	#08	21/6/17	20:03:19	0.0019586	0.0000002	-2.16		0.10	2.10E+09	4.11E+06	16.26	0.92	
				average		-2.07							
				std dev (1σ)		0.22							
BAH-layer4-1.1	#08	21/6/17	22:18:03	0.0019592	0.0000002	-1.84		0.09	2.11E+09	4.14E+06	16.26	0.92	BAH
BAH-layer4-1.2	#08	21/6/17	22:23:30	0.0019584	0.0000002	-2.28		0.09	2.10E+09	4.12E+06	16.26	0.92	
BAH-layer4-1.3	#08	21/6/17	22:28:58	0.0019589	0.0000002	-1.99		0.10	2.13E+09	4.17E+06	16.26	0.92	
BAH-layer4-1.4	#08	21/6/17	22:34:27	0.0019585	0.0000002	-2.20		0.11	2.13E+09	4.18E+06	16.26	0.92	
BAH-layer4-1.5	#08	21/6/17	22:39:55	0.0019588	0.0000002	-2.07		0.08	2.14E+09	4.20E+06	16.26	0.92	
				average		-2.08							
				std dev (1σ)		0.17							
BAH-layer5-1.1	#08	21/6/17	23:46:44	0.0019587	0.0000002	-2.10		0.09	2.14E+09	4.19E+06	16.26	0.92	BAH
BAH-layer5-1.2	#08	21/6/17	23:52:12	0.0019576	0.0000002	-2.68		0.11	2.15E+09	4.21E+06	16.26	0.92	
BAH-layer5-1.3	#08	21/6/17	23:57:39	0.0019582	0.0000002	-2.36		0.11	2.14E+09	4.20E+06	16.26	0.92	
BAH-layer5-1.4	#08	22/6/17	0:03:07	0.0019584	0.0000002	-2.27		0.09	2.18E+09	4.26E+06	16.26	0.92	
BAH-layer5-1.5	#08	22/6/17	0:08:34	0.0019578	0.0000002	-2.60		0.09	2.18E+09	4.26E+06	16.26	0.92	
				average		-2.40							
				std dev (1σ)		0.24							
BAH-layer6-1.1	#08	22/6/17	1:10:06	0.0019591	0.0000002	-1.91		0.12	2.08E+09	4.08E+06	16.26	0.92	BAH
BAH-layer6-1.10	#08	22/6/17	2:55:08	0.0019598	0.0000002	-1.53		0.12	2.14E+09	4.20E+06	16.26	0.92	
BAH-layer6-1.2	#08	22/6/17	1:15:33	0.0019586	0.0000002	-2.19		0.09	2.10E+09	4.12E+06	16.26	0.92	
BAH-layer6-1.3	#08	22/6/17	1:21:00	0.0019588	0.0000002	-2.09		0.11	2.10E+09	4.12E+06	16.26	0.92	
BAH-layer6-1.4	#08	22/6/17	1:26:28	0.0019588	0.0000002	-2.06		0.09	2.09E+09	4.10E+06	16.26	0.92	
BAH-layer6-1.5	#08	22/6/17	1:31:56	0.0019590	0.0000002	-1.95		0.11	2.13E+09	4.18E+06	16.26	0.92	
BAH-layer6-1.6	#08	22/6/17	2:33:19	0.0019593	0.0000002	-1.80		0.10	2.14E+09	4.19E+06	16.26	0.92	
BAH-layer6-1.7	#08	22/6/17	2:38:46	0.0019595	0.0000002	-1.71		0.09	2.14E+09	4.20E+06	16.26	0.92	
BAH-layer6-1.8	#08	22/6/17	2:44:14	0.0019600	0.0000002	-1.43		0.09	2.14E+09	4.20E+06	16.26	0.92	
BAH-layer6-1.9	#08	22/6/17	2:49:41	0.0019595	0.0000002	-1.70		0.10	2.15E+09	4.22E+06	16.26	0.92	
				average		-1.84							
				std dev (1σ)		0.25							
BAH-layer7-1.1	#08	22/6/17	3:00:48	0.0019613	0.0000002	-0.79		0.11	2.14E+09	4.19E+06	16.26	0.92	BAH
BAH-layer7-1.1b	#08	22/6/17	11:00:30	0.0019610	0.0000002	-0.92		0.12	2.13E+09	4.18E+06	16.26	0.92	
BAH-layer7-1.2	#08	22/6/17	3:06:15	0.0019626	0.0000002	-0.08		0.12	2.13E+09	4.18E+06	16.26	0.92	
BAH-layer7-1.3	#08	22/6/17	3:11:43	0.0019635	0.0000002		0.38	0.09	2.10E+09	4.13E+06	16.26	0.92	
BAH-layer7-1.3b	#08	22/6/17	7:14:35	0.0019630	0.0000002	0.14		0.09	2.12E+09	4.15E+06	16.26	0.92	
BAH-layer7-1.4	#08	22/6/17	3:17:10	0.0019602	0.0000002		-1.32	0.10	2.09E+09	4.10E+06	16.26	0.92	
BAH-layer7-1.4b	#08	22/6/17	10:53:18	0.0019621	0.0000002	-0.35		0.10	2.10E+09	4.13E+06	16.26	0.92	
BAH-layer7-1.5	#08	22/6/17	3:22:37	0.0019611	0.0000003	-0.88		0.13	2.08E+09	4.09E+06	16.26	0.92	
BAH-layer7-1.6	#08	22/6/17	7:20:03	0.0019624	0.0000002	-0.18		0.11	2.05E+09	4.02E+06	16.26	0.92	
BAH-layer7-1.7	#08	22/6/17	7:25:31	0.0019620	0.0000002	-0.42		0.08	2.07E+09	4.05E+06	16.26	0.92	
BAH-layer7-1.8	#08	22/6/17	7:30:58	0.0019618	0.0000001	-0.51		0.08	2.07E+09	4.05E+06	16.26	0.92	
BAH-layer7-1.9	#08	22/6/17	7:36:25	0.0019619	0.0000002	-0.46		0.13	2.06E+09	4.04E+06	16.26	0.92	
				average		-0.45							
				std dev (1σ)		0.35							
BAH-layer1-DiffOrient-1.1	#08	21/6/17	16:21:56	0.0019578	0.0000002	-2.58		0.11	2.15E+09	4.20E+06	13.73	2.14	BAH
BAH-layer1-DiffOrient-1.2	#08	21/6/17	16:27:23	0.0019575	0.0000002	-2.73		0.11	2.15E+09	4.21E+06	13.73	2.14	
BAH-layer1-DiffOrient-1.3	#08	21/6/17	16:32:50	0.0019573	0.0000002	-2.85		0.10	2.15E+09	4.20E+06	13.73	2.14	
BAH-layer1-DiffOrient-1.4	#08	21/6/17	16:38:18	0.0019571	0.0000002	-2.93		0.11	2.11E+09	4.14E+06	13.73	2.14	
BAH-layer1-DiffOrient-1.5	#08	21/6/17	16:43:45	0.0019568	0.0000002	-3.12		0.09	2.10E+09	4.10E+06	13.73	2.14	
				average		-2.84							
				std dev (1σ)		0.20							
BAH-layer2-DiffOrient-1.1	#08	21/6/17	16:49:14	0.0019553	0.0000002	-3.88		0.10	2.12E+09	4.15E+06	13.73	2.14	BAH
BAH-layer2-DiffOrient-1.2	#08	21/6/17	16:54:41	0.0019550	0.0000002	-4.04		0.11	2.12E+09	4.15E+06	13.73	2.14	
BAH-layer2-DiffOrient-1.3	#08	21/6/17	17:00:08	0.0019563	0.0000002	-3.38		0.10	2.12E+09	4.15E+06	13.73	2.14	
BAH-layer2-DiffOrient-1.4	#08	21/6/17	17:05:36	0.0019551	0.0000002	-3.98		0.10	2.12E+09	4.14E+06	13.73	2.14	
BAH-layer2-DiffOrient-1.5	#08	21/6/17	17:11:03	0.0019547	0.0000002	-4.18		0.09	2.09E+09	4.08E+06	13.73	2.14	
				average		-3.89							
				std dev (1σ)		0.31							
BAH-layer3-DiffOrient-1.1	#08	21/6/17	20:08:51	0.0019560	0.0000002	-3.50		0.09	2.12E+09	4.15E+06	16.26	0.92	BAH
BAH-layer3-DiffOrient-1.2	#08	21/6/17	20:14:19	0.0019555	0.0000002	-3.79		0.11	2.13E+09	4.17E+06	16.26	0.92	
BAH-layer3-DiffOrient-1.3	#08	21/6/17	20:19:47	0.0019569	0.0000002	-3.07		0.08	2.16E+09	4.23E+06	16.26	0.92	
BAH-layer3-DiffOrient-1.4	#08	21/6/17	20:25:14	0.0019564	0.0000002	-3.33		0.10	2.18E+09	4.26E+06	16.26	0.92	
BAH-layer3-DiffOrient-1.5	#08	21/6/17	20:30:42	0.0019576	0.0000002	-2.67		0.09	2.19E+09	4.29E+06	16.26	0.92	
				average		-3.27							
				std dev (1σ)		0.42							
BAH-layer4-DiffOrient-1.1	#08	21/6/17	22:45:27	0.0019573	0.0000002	-2.82		0.09	2.13E+09	4.17E+06	16.26	0.92	BAH
BAH-layer4-DiffOrient-1.2	#08	21/6/17	22:50:54	0.0019571	0.0000002	-2.93		0.11	2.12E+09	4.15E+06	16.26	0.92	
BAH-layer4-DiffOrient-1.3	#08	21/6/17	22:56:21	0.0019571	0.0000002	-2.95		0.10	2.12E+09	4.14E+06	16.26	0.92	
BAH-layer4-DiffOrient-1.4	#08	21/6/17	23:01:48	0.0019569	0.0000002	-3.05		0.08	2.10E+09	4.11E+06	16.26	0.92	
BAH-layer4-DiffOrient-1.5	#08	21/6/17											

SPOT #	Session	Date	Time	¹⁸ O/ ¹⁶ O ^(a)	± ^(b)	δ ¹⁸ O _{VSMOW} ^(c)	rejected	±Internal error (σ 95%)	¹⁸ O cps (median)	¹⁶ O cps (median)	(U-Th)/He ages	±	MOUNT
BAH-layer5-DiffOrient-1.1	#08	22/6/17	0:14:15	0.0019570	0.0000002		-3.00	0.09	2.09E+09	4.10E+06	16.26	0.92	BAH
BAH-layer5-DiffOrient-1.1	#08	22/6/17	7:03:25	0.0019586	0.0000002	-2.18		0.10	2.14E+09	4.18E+06	16.26	0.92	
BAH-layer5-DiffOrient-1.2	#08	22/6/17	0:19:42	0.0019575	0.0000002	-2.75		0.10	2.10E+09	4.11E+06	16.26	0.92	
BAH-layer5-DiffOrient-1.3	#08	22/6/17	0:25:11	0.0019578	0.0000002	-2.57		0.10	2.11E+09	4.13E+06	16.26	0.92	
BAH-layer5-DiffOrient-1.4	#08	22/6/17	0:30:38	0.0019580	0.0000002	-2.49		0.11	2.10E+09	4.11E+06	16.26	0.92	
BAH-layer5-DiffOrient-1.5	#08	22/6/17	0:36:06	0.0019585	0.0000002	-2.24		0.08	2.09E+09	4.09E+06	16.26	0.92	
				average	-2.44								
				std dev (1σ)	0.23								
BAH-layer6-DiffOrient-1.1	#08	22/6/17	1:37:27	0.0019589	0.0000002	-2.03		0.10	2.13E+09	4.17E+06	16.26	0.92	BAH
BAH-layer6-DiffOrient-1.2	#08	22/6/17	1:42:54	0.0019589	0.0000002	-2.03		0.10	2.12E+09	4.15E+06	16.26	0.92	
BAH-layer6-DiffOrient-1.3	#08	22/6/17	1:48:21	0.0019587	0.0000002	-2.13		0.11	2.12E+09	4.15E+06	16.26	0.92	
BAH-layer6-DiffOrient-1.4	#08	22/6/17	1:53:48	0.0019580	0.0000002		-2.46	0.10	2.12E+09	4.16E+06	16.26	0.92	
BAH-layer6-DiffOrient-1.4	#08	22/6/17	7:08:54	0.0019586	0.0000002	-2.18		0.08	2.16E+09	4.23E+06	16.26	0.92	
BAH-layer6-DiffOrient-1.5	#08	22/6/17	1:59:16	0.0019588	0.0000002	-2.08		0.10	2.11E+09	4.13E+06	16.26	0.92	
				average	-2.09								
				std dev (1σ)	0.06								
NIP-13-33-1.1	#08	20/6/17	16:25:34	0.0019839	0.0000002	10.88		0.10	2.25E+09	4.46E+06			HM-22
NIP-13-33-1.2	#08	20/6/17	16:31:01	0.0019892	0.0000002	13.65		0.09	2.23E+09	4.44E+06			
NIP-13-33-1.3	#08	20/6/17	16:36:27	0.0019907	0.0000002	14.40		0.10	2.23E+09	4.44E+06			
NIP-13-33-1.4	#08	20/6/17	16:41:54	0.0019857	0.0000002	11.83		0.09	2.24E+09	4.45E+06			
NIP-13-33-1.5	#08	20/6/17	16:58:02	0.0019869	0.0000002	12.45		0.10	2.25E+09	4.46E+06			
NIP-13-33-1.6	#08	20/6/17	17:05:51	0.0019852	0.0000002	11.55		0.09	2.24E+09	4.45E+06			
				average	12.46								
				std dev (1σ)	1.34								
NIP-13-35-1.1	#08	20/6/17	23:15:10	0.0019759	0.0000002	6.61		0.09	2.28E+09	4.50E+06			HM-22
NIP-13-35-1.2	#08	20/6/17	23:20:37	0.0019764	0.0000002	6.89		0.11	2.28E+09	4.50E+06			
NIP-13-35-1.3	#08	20/6/17	23:26:03	0.0019761	0.0000002	6.72		0.11	2.29E+09	4.52E+06			
NIP-13-35-1.4	#08	20/6/17	23:31:30	0.0019774	0.0000002	7.38		0.08	2.29E+09	4.53E+06			
NIP-13-35-1.5	#08	20/6/17	23:36:57	0.0019786	0.0000002	8.01		0.09	2.29E+09	4.54E+06			
				average	7.12								
				std dev (1σ)	0.58								
BOI-002-1.1	#08	20/6/17	23:42:29	0.0020021	0.0000003	20.18		0.13	1.97E+09	3.95E+06	3.06	0.93	HM-22
BOI-002-1.2	#08	20/6/17	23:47:56	0.0020015	0.0000002	19.90		0.10	2.00E+09	4.01E+06	3.06	0.93	
BOI-002-1.3	#08	20/6/17	23:53:23	0.0019985	0.0000002	18.32		0.08	2.02E+09	4.04E+06	3.06	0.93	
BOI-002-1.4	#08	20/6/17	23:58:50	0.0019991	0.0000002	18.64		0.10	2.00E+09	3.99E+06	3.06	0.93	
BOI-002-1.5	#08	21/6/17	0:04:17	0.0020003	0.0000002	19.24		0.11	2.00E+09	4.00E+06	3.06	0.93	
BOI-002-2.1	#08	21/6/17	1:22:08	0.0020023	0.0000002	20.28		0.09	2.01E+09	4.02E+06	3.06	0.93	
BOI-002-2.2	#08	21/6/17	1:27:35	0.0020092	0.0000002	23.87		0.11	1.87E+09	3.75E+06	3.06	0.93	
BOI-002-2.3	#08	21/6/17	1:33:02	0.0020046	0.0000002	21.51		0.08	2.01E+09	4.04E+06	3.06	0.93	
BOI-002-2.4	#08	21/6/17	1:38:29	0.0020079	0.0000002	23.20		0.11	1.93E+09	3.87E+06	3.06	0.93	
BOI-002-2.5	#08	21/6/17	1:43:56	0.0020019	0.0000003	20.08		0.13	1.70E+09	3.41E+06	3.06	0.93	
BOI-002-2.6	#08	21/6/17	1:49:22	0.0020014	0.0000003	19.81		0.14	1.79E+09	3.58E+06	3.06	0.93	
				average	20.46								
				std dev (1σ)	1.75								
N4C-300cm-1.1	#08	21/6/17	1:54:56	0.0019716	0.0000002	4.38		0.09	2.14E+09	4.22E+06			HM-22
N4C-300cm-1.2	#08	21/6/17	2:00:23	0.0019712	0.0000002	4.21		0.09	2.15E+09	4.25E+06			
N4C-300cm-1.3	#08	21/6/17	2:05:50	0.0019753	0.0000002	6.29		0.08	2.22E+09	4.39E+06			
N4C-300cm-1.4	#08	21/6/17	2:11:17	0.0019742	0.0000002	5.74		0.09	2.21E+09	4.37E+06			
N4C-300cm-1.5	#08	21/6/17	2:16:43	0.0019721	0.0000002	4.63		0.10	2.15E+09	4.24E+06			
				average	5.05								
				std dev (1σ)	0.91								
BOI-004-1.1	#08	21/6/17	3:23:31	0.0020053	0.0000002	21.87		0.11	2.21E+09	4.43E+06	0.79	0.29	HM-22
BOI-004-1.2	#08	21/6/17	3:28:57	0.0020019	0.0000002	20.10		0.09	2.24E+09	4.49E+06	0.79	0.29	
BOI-004-1.3	#08	21/6/17	3:34:24	0.0020080	0.0000002	23.23		0.09	1.99E+09	4.00E+06	0.79	0.29	
BOI-004-1.4	#08	21/6/17	3:39:50	0.0020090	0.0000003	23.75		0.13	2.01E+09	4.04E+06	0.79	0.29	
BOI-004-1.5	#08	21/6/17	3:45:17	0.0020166	0.0000002	27.69		0.10	1.56E+09	3.14E+06	0.79	0.29	
BOI-004-1.6	#08	21/6/17	7:49:59	0.0020135	0.0000003	26.09		0.13	1.71E+09	3.44E+06	0.79	0.29	
BOI-004-1.7	#08	21/6/17	7:55:26	0.0020179	0.0000002	28.39		0.11	1.62E+09	3.27E+06	0.79	0.29	
BOI-004-1.8	#08	21/6/17	8:00:54	0.0020057	0.0000002	22.05		0.08	2.21E+09	4.42E+06	0.79	0.29	
				average	24.15								
				std dev (1σ)	2.96								
BAH-100-Gib+Grt-1.1	#08	21/6/17	3:50:49	0.0019627	0.0000002	-0.21		0.10	2.01E+09	3.95E+06	53.69	2.27	HM-22
BAH-100-Gib+Grt-1.2	#08	21/6/17	3:56:15	0.0019635	0.0000002	0.19		0.10	2.01E+09	3.95E+06	53.69	2.27	
BAH-100-Gib+Grt-1.3	#08	21/6/17	4:01:42	0.0019630	0.0000002	-0.08		0.10	2.00E+09	3.92E+06	53.69	2.27	
BAH-100-Gib+Grt-1.4	#08	21/6/17	4:07:09	0.0019631	0.0000002	-0.04		0.10	1.99E+09	3.91E+06	53.69	2.27	
BAH-100-Gib+Grt-1.5	#08	21/6/17	4:12:36	0.0019621	0.0000002	-0.53		0.08	2.01E+09	3.95E+06	53.69	2.27	
				average	-0.13								
				std dev (1σ)	0.26								
BOI-002-2.7	#08	21/6/17	8:06:24	0.0020090	0.0000003	23.78		0.13	1.88E+09	3.78E+06	3.06	0.93	HM-22
BOI-002-2.8	#08	21/6/17	8:11:52	0.0020066	0.0000002	22.54		0.12	1.93E+09	3.86E+06	3.06	0.93	
				average	23.16								
				std dev (1σ)	0.88								
BAH-F226-157.6-1.1	#08	22/6/17	16:40:00	0.0019588	0.0000002	-2.22		0.10	2.04E+09	4.00E+06	12.40	0.06	HM-23
BAH-F226-157.6-1.2	#08	22/6/17	16:45:28	0.0019579	0.0000002	-2.69		0.11	2.04E+09	3.99E+06	12.40	0.06	
BAH-F226-157.6-1.3	#08	22/6/17	16:50:56	0.0019586	0.0000002	-2.30		0.12	2.05E+09	4.01E+06	12.40	0.06	
BAH-F226-157.6-1.4	#08	22/6/17	16:56:24	0.0019586	0.0000002	-2.30		0.11	2.04E+09	3.99E+06	12.40	0.06	
BAH-F226-157.6-1.5	#08	22/6/17	17:01:52	0.0019590	0.0000002	-2.12		0.10	2.04E+09	3.99E+06	12.40	0.06	
BAH-F226-157.6-1.6	#08	22/6/17	17:07:20	0.0019583	0.0000002	-2.46		0.08	2.04E+09	3.99E+06	12.40	0.06	
BAH-F226-157.6-1.7	#08	23/6/17	10:45:49	0.0019587	0.0000002	-2.28		0.11	2.06E+09	4.04E+06	12.40	0.06	
BAH-F226-157.6-1.8	#08	23/6/17	10:51:18	0.0019574	0.0000002	-2.94		0.09	2.05E+09	4.00E+06	12.40	0.06	
BAH-F226-157.6-1.9	#08	23/6/17	10:56:46	0.0019586	0.0000002	-2.34		0.09	2.06E+09	4.03E+06	12.40	0.06	
BAH-F226-157.6-1.10	#08	23/6/17	11:02:14	0.0019581	0.0000002	-2.55		0.09	2.05E+09	4.01E+06	12.40	0.06	
BAH-F226-157.6-1.11	#08	23/6/17	11:07:43	0.0019583	0.0000002	-2.48		0.10	2.05E+09	4.01E+06	12.40	0.06	
BAH-F226-157.6-1.12	#08	23/6/17	11:13:12	0.0019586	0.0000002	-2.32		0.11	2.04E+09	3.99E+06	12.40	0.06	
				average	-2.42								
				std dev (1σ)	0.23								
BAH-F226-157.6-2.1	#08	22/6/17	18:08:58	0.0019597	0.0000002	-1.72		0.11	2.06E+09	4.04E+06	12.40	0.06	HM-23
BAH-F226-157.6-2.2	#08	22/6/17	18:14:26	0.0019601	0.0000002	-1.51		0.08	2.06E+09	4.04E+06	12.40	0.06	
BAH-F226-157.6-2.3	#08	22/6/17	18:19:54	0.0019592	0.0000002	-2.00		0.10	2.05E+09	4.02E+06	12.40	0.06	
BAH-F226-157.6-2.4	#08	22/6/17	18:25:22	0.0019599	0.0000002	-1.66		0.08	2.06E+09	4.04E+06	12.40	0.06	
BAH-F226-157.6-2.5	#08	22/6/17	18:30:51	0.0019597	0.0000002	-1.76		0.11	2.06E+09	4.03E+06	12.4		

SPOT #	Session	Date	Time	¹⁸ O/ ¹⁶ O ^(a)	± ^(b)	δ ¹⁸ O _{VERMON} ^(c)	rejected	±Internal error (σ 95%)	¹⁶ O cps (median)	¹⁸ O cps (median)	(U-Th)/He ages	±	MOUNT
BAH-F226-157.6-2.9	#08	23/6/17	11:35:08	0.0019605	0.0000002	-1.32		0.11	2.07E+09	4.06E+06	12.40	0.06	
BAH-F226-157.6-2.10	#08	23/6/17	11:40:37	0.0019604	0.0000002	-1.38		0.10	2.06E+09	4.04E+06	12.40	0.06	
				average		-1.59							
				std dev (1σ)		0.24							
BAH-F124-111.2B-1.1	#08	22/6/17	22:10:48	0.0019660	0.0000002	1.54		0.10	2.13E+09	4.19E+06	52.80	1.73	HM-23
BAH-F124-111.2B-1.2	#08	22/6/17	22:16:16	0.0019661	0.0000002	1.59		0.10	2.13E+09	4.18E+06	52.80	1.73	
BAH-F124-111.2B-1.3	#08	22/6/17	22:21:44	0.0019656	0.0000002	1.33		0.10	2.12E+09	4.17E+06	52.80	1.73	
BAH-F124-111.2B-1.4	#08	22/6/17	22:27:12	0.0019655	0.0000002	1.27		0.12	2.15E+09	4.23E+06	52.80	1.73	
BAH-F124-111.2B-1.5	#08	22/6/17	22:32:40	0.0019677	0.0000002	2.38		0.10	2.19E+09	4.31E+06	52.80	1.73	
BAH-F124-111.2B-1.6	#08	22/6/17	22:38:08	0.0019651	0.0000002	1.08		0.08	2.15E+09	4.22E+06	52.80	1.73	
BAH-F124-111.2B-1.7	#08	22/6/17	22:43:37	0.0019666	0.0000002	1.81		0.10	2.16E+09	4.26E+06	52.80	1.73	
BAH-F124-111.2B-1.8	#08	22/6/17	22:49:05	0.0019651	0.0000002	1.05		0.09	2.17E+09	4.26E+06	52.80	1.73	
BAH-F124-111.2B-1.9	#08	22/6/17	22:54:34	0.0019662	0.0000002	1.61		0.09	2.13E+09	4.19E+06	52.80	1.73	
BAH-F124-111.2B-1.10	#08	22/6/17	23:00:02	0.0019669	0.0000002	1.99		0.08	2.20E+09	4.32E+06	52.80	1.73	
BAH-F124-111.2B-1.11	#08	22/6/17	23:39:47	0.0019664	0.0000002	1.74		0.11	2.09E+09	4.11E+06	52.80	1.73	
BAH-F124-111.2B-1.12	#08	22/6/17	23:45:15	0.0019657	0.0000002	1.37		0.09	2.07E+09	4.07E+06	52.80	1.73	
BAH-F124-111.2B-1.13	#08	22/6/17	23:50:43	0.0019642	0.0000002	0.60		0.09	2.07E+09	4.06E+06	52.80	1.73	
BAH-F124-111.2B-1.14	#08	22/6/17	23:56:11	0.0019652	0.0000002	1.11		0.11	2.09E+09	4.11E+06	52.80	1.73	
BAH-F124-111.2B-1.15	#08	23/6/17	0:01:40	0.0019650	0.0000002	1.01		0.08	2.15E+09	4.23E+06	52.80	1.73	
BAH-F124-111.2B-1.16	#08	23/6/17	0:07:08	0.0019655	0.0000002	1.27		0.09	2.13E+09	4.19E+06	52.80	1.73	
BAH-F124-111.2B-1.17	#08	23/6/17	0:12:38	0.0019646	0.0000003	0.78		0.13	2.08E+09	4.08E+06	52.80	1.73	
BAH-F124-111.2B-1.18	#08	23/6/17	0:18:06	0.0019643	0.0000002	0.63		0.10	2.12E+09	4.17E+06	52.80	1.73	
BAH-F124-111.2B-1.19	#08	23/6/17	0:23:36	0.0019621	0.0000002	-0.49		0.10	2.12E+09	4.16E+06	52.80	1.73	
BAH-F124-111.2B-1.20	#08	23/6/17	0:29:05	0.0019620	0.0000002	-0.56		0.11	2.10E+09	4.13E+06	52.80	1.73	
BAH-F124-111.2B-1.21	#08	23/6/17	1:08:48	0.0019650	0.0000002	1.01		0.10	2.05E+09	4.04E+06	52.80	1.73	
BAH-F124-111.2B-1.22	#08	23/6/17	1:14:16	0.0019656	0.0000002	1.34		0.10	2.04E+09	4.01E+06	52.80	1.73	
BAH-F124-111.2B-1.23	#08	23/6/17	1:19:44	0.0019656	0.0000002	1.29		0.09	2.08E+09	4.08E+06	52.80	1.73	
BAH-F124-111.2B-1.24	#08	23/6/17	1:25:12	0.0019653	0.0000002	1.19		0.09	2.10E+09	4.13E+06	52.80	1.73	
BAH-F124-111.2B-1.25	#08	23/6/17	1:30:41	0.0019652	0.0000002	1.10		0.09	2.12E+09	4.17E+06	52.80	1.73	
BAH-F124-111.2B-1.26	#08	23/6/17	1:36:11	0.0019616	0.0000002		-0.75	0.11	2.08E+09	4.08E+06	52.80	1.73	
BAH-F124-111.2B-1.27	#08	23/6/17	1:41:39	0.0019645	0.0000002	0.74		0.10	2.06E+09	4.05E+06	52.80	1.73	
BAH-F124-111.2B-1.28	#08	23/6/17	1:47:07	0.0019641	0.0000002	0.54		0.09	2.09E+09	4.10E+06	52.80	1.73	
BAH-F124-111.2B-1.29	#08	23/6/17	1:52:36	0.0019648	0.0000002	0.91		0.10	2.08E+09	4.10E+06	52.80	1.73	
BAH-F124-111.2B-1.30	#08	23/6/17	1:58:05	0.0019646	0.0000002	0.78		0.09	2.07E+09	4.07E+06	52.80	1.73	
BAH-F124-111.2B-1.31	#08	23/6/17	2:37:53	0.0019648	0.0000002	0.92		0.10	2.15E+09	4.23E+06	52.80	1.73	
BAH-F124-111.2B-1.32	#08	23/6/17	2:43:21	0.0019667	0.0000002	1.89		0.09	2.14E+09	4.22E+06	52.80	1.73	
BAH-F124-111.2B-1.33	#08	23/6/17	2:48:49	0.0019652	0.0000002	1.13		0.09	2.13E+09	4.19E+06	52.80	1.73	
BAH-F124-111.2B-1.34	#08	23/6/17	2:54:17	0.0019679	0.0000002	2.49		0.09	2.13E+09	4.19E+06	52.80	1.73	
BAH-F124-111.2B-1.35	#08	23/6/17	2:59:46	0.0019676	0.0000002	2.33		0.11	2.12E+09	4.17E+06	52.80	1.73	
BAH-F124-111.2B-1.36	#08	23/6/17	3:05:14	0.0019657	0.0000002	1.35		0.10	2.11E+09	4.15E+06	52.80	1.73	
BAH-F124-111.2B-1.37	#08	23/6/17	3:10:42	0.0019676	0.0000002	2.34		0.12	2.08E+09	4.09E+06	52.80	1.73	
BAH-F124-111.2B-1.38	#08	23/6/17	3:16:11	0.0019691	0.0000002		3.11	0.09	2.08E+09	4.10E+06	52.80	1.73	
BAH-F124-111.2B-1.39	#08	23/6/17	3:21:41	0.0019663	0.0000002	1.65		0.09	2.16E+09	4.25E+06	52.80	1.73	
BAH-F124-111.2B-1.40	#08	23/6/17	3:27:09	0.0019661	0.0000002	1.57		0.10	2.12E+09	4.18E+06	52.80	1.73	
BAH-F124-111.2B-1.41	#08	23/6/17	4:06:53	0.0019664	0.0000002	1.72		0.09	2.13E+09	4.19E+06	52.80	1.73	
BAH-F124-111.2B-1.42	#08	23/6/17	4:12:21	0.0019644	0.0000002	0.72		0.08	2.12E+09	4.16E+06	52.80	1.73	
BAH-F124-111.2B-1.43	#08	23/6/17	4:17:50	0.0019655	0.0000002	1.29		0.10	2.12E+09	4.16E+06	52.80	1.73	
BAH-F124-111.2B-1.44	#08	23/6/17	4:23:18	0.0019645	0.0000002	0.76		0.09	2.13E+09	4.18E+06	52.80	1.73	
BAH-F124-111.2B-1.45	#08	23/6/17	4:28:47	0.0019654	0.0000002	1.19		0.10	2.09E+09	4.11E+06	52.80	1.73	
BAH-F124-111.2B-1.46	#08	23/6/17	4:34:15	0.0019669	0.0000002	2.01		0.08	2.08E+09	4.09E+06	52.80	1.73	
BAH-F124-111.2B-1.47	#08	23/6/17	4:39:44	0.0019665	0.0000002	1.77		0.10	2.10E+09	4.13E+06	52.80	1.73	
BAH-F124-111.2B-1.48	#08	23/6/17	4:45:12	0.0019663	0.0000002	1.70		0.09	2.10E+09	4.13E+06	52.80	1.73	
BAH-F124-111.2B-1.49	#08	23/6/17	4:50:40	0.0019663	0.0000002	1.70		0.10	2.11E+09	4.15E+06	52.80	1.73	
BAH-F124-111.2B-1.50	#08	23/6/17	4:56:08	0.0019655	0.0000002	1.26		0.09	2.10E+09	4.14E+06	52.80	1.73	
BAH-F124-111.2B-1.51	#08	23/6/17	5:35:54	0.0019652	0.0000002	1.09		0.12	2.10E+09	4.12E+06	52.80	1.73	
BAH-F124-111.2B-1.52	#08	23/6/17	5:41:22	0.0019654	0.0000002	1.20		0.10	2.12E+09	4.17E+06	52.80	1.73	
BAH-F124-111.2B-1.53	#08	23/6/17	6:13:31	0.0019649	0.0000002	0.95		0.10	2.13E+09	4.18E+06	52.80	1.73	
BAH-F124-111.2B-1.54	#08	23/6/17	6:18:59	0.0019654	0.0000002	1.23		0.11	2.19E+09	4.30E+06	52.80	1.73	
BAH-F124-111.2B-1.55	#08	23/6/17	6:24:28	0.0019664	0.0000002	1.71		0.11	2.19E+09	4.31E+06	52.80	1.73	
BAH-F124-111.2B-1.56	#08	23/6/17	6:29:57	0.0019661	0.0000002	1.57		0.10	2.14E+09	4.22E+06	52.80	1.73	
BAH-F124-111.2B-1.57	#08	23/6/17	6:35:25	0.0019662	0.0000002	1.64		0.09	2.11E+09	4.15E+06	52.80	1.73	
BAH-F124-111.2B-1.58	#08	23/6/17	6:40:54	0.0019664	0.0000002	1.76		0.08	2.14E+09	4.21E+06	52.80	1.73	
BAH-F124-111.2B-1.59	#08	23/6/17	6:46:22	0.0019641	0.0000002	0.53		0.10	2.18E+09	4.28E+06	52.80	1.73	
BAH-F124-111.2B-1.60	#08	23/6/17	6:51:50	0.0019652	0.0000002	1.12		0.11	2.10E+09	4.13E+06	52.80	1.73	
BAH-F124-111.2B-1.61	#08	23/6/17	6:57:19	0.0019672	0.0000002	2.16		0.11	2.10E+09	4.14E+06	52.80	1.73	
				average		1.30							
				std dev (1σ)		0.59							
BAH-F226-142.7-1.1	#09	20/8/17	19:03:58	0.0019822	0.0000002	0.77		0.11	2.34E+09	4.64E+06			HM-16
BAH-F226-142.7-1.2	#09	20/8/17	19:09:17	0.0019817	0.0000002	0.50		0.10	2.31E+09	4.58E+06			
BAH-F226-142.7-1.3	#09	20/8/17	19:14:34	0.0019820	0.0000002	0.67		0.10	2.33E+09	4.62E+06			
BAH-F226-142.7-1.4	#09	20/8/17	19:19:53	0.0019826	0.0000002	0.95		0.11	2.30E+09	4.56E+06			
BAH-F226-142.7-1.5	#09	20/8/17	19:25:10	0.0019823	0.0000002	0.84		0.09	2.29E+09	4.53E+06			
BAH-F226-142.7-1.6	#09	20/8/17	19:30:28	0.0019814	0.0000002	0.37		0.09	2.32E+09	4.59E+06			
BAH-F226-142.7-1.7	#09	20/8/17	19:35:47	0.0019797	0.0000002	-0.51		0.10	2.26E+09	4.47E+06			
BAH-F226-142.7-1.8	#09	20/8/17	19:41:05	0.0019801	0.0000002	-0.29		0.11	2.26E+09	4.47E+06			
BAH-F226-142.7-1.9	#09	20/8/17	19:46:23	0.0019808	0.0000002	0.04		0.13	2.26E+09	4.47E+06			
BAH-F226-142.7-1.10	#09	20/8/17	19:51:40	0.0019794	0.0000002	-0.65		0.12	2.25E+09	4.45E+06			
				average		0.27							
				std dev (1σ)		0.59							
BAH-F282-94.3-1.1	#09	20/8/17	20:24:46	0.0019783	0.0000002	-1.21		0.12	2.34E+09	4.62E+06	44.67	5.27	HM-16
BAH-F282-94.3-1.2	#09	20/8/17	20:30:04										

SPOT #	Session	Date	Time	¹⁸ O/ ¹⁶ O ^(a)	± ^(b)	δ ¹⁸ O _{VERMOM} ^(c)	rejected	±Internal error (σ 95%)	¹⁶ O cps (median)	¹⁸ O cps (median)	(U-Th)/He ages	±	MOUNT
				average		2.42							
				std dev (1σ)		0.42							
BAH-F124-123.1-1.1	#09	20/8/17	22:12:12	0.0019840	0.0000002	1.70		0.10	2.42E+09	4.80E+06			HM-16
BAH-F124-123.1-1.2	#09	20/8/17	22:17:30	0.0019843	0.0000002	1.87		0.09	2.43E+09	4.82E+06			
BAH-F124-123.1-1.3	#09	20/8/17	22:22:47	0.0019843	0.0000002	1.83		0.10	2.43E+09	4.82E+06			
				average		1.80							
				std dev (1σ)		0.09							
BAH-F124-123.1_spik-1.1	#09	20/8/17	22:28:06	0.0019777	0.0000002	-1.54		0.10	2.35E+09	4.65E+06	12.26	1.14	HM-16
BAH-F124-123.1_spik-1.2	#09	20/8/17	22:33:24	0.0019760	0.0000002	-2.41		0.10	2.28E+09	4.50E+06	12.26	1.14	
BAH-F124-123.1_spik-1.3	#09	20/8/17	22:38:41	0.0019735	0.0000003	-3.71		0.13	2.41E+09	4.76E+06	12.26	1.14	
BAH-F124-123.1_spik-1.4	#09	20/8/17	22:43:59	0.0019754	0.0000002	-2.70		0.09	2.36E+09	4.65E+06	12.26	1.14	
				average		-2.59							
				std dev (1σ)		0.89							
BAH-F226-152.67-HM22-1.1	#09	18/8/17	11:38:40	0.0019849	0.0000002	2.49		0.13	2.34E+09	4.64E+06	53.44	1.86	HM-22
BAH-F226-152.67-HM22-1.2	#09	18/8/17	11:43:58	0.0019823	0.0000002		1.17	0.10	2.29E+09	4.54E+06	53.44	1.86	
BAH-F226-152.67-HM22-1.3	#09	18/8/17	11:49:15	0.0019864	0.0000002	3.26		0.11	2.23E+09	4.43E+06	53.44	1.86	
BAH-F226-152.67-HM22-1.4	#09	18/8/17	11:54:34	0.0019862	0.0000002	3.13		0.10	2.27E+09	4.51E+06	53.44	1.86	
BAH-F226-152.67-HM22-1.5	#09	18/8/17	11:59:52	0.0019848	0.0000002	2.41		0.10	2.24E+09	4.45E+06	53.44	1.86	
BAH-F226-152.67-HM22-1.6	#09	18/8/17	12:05:09	0.0019862	0.0000002	3.13		0.09	2.31E+09	4.59E+06	53.44	1.86	
BAH-F226-152.67-HM22-1.2b	#09	18/8/17	14:43:09	0.0019836	0.0000003	1.83		0.14	2.28E+09	4.53E+06	53.44	1.86	
BAH-F226-152.67-HM22-1.7	#09	18/8/17	14:48:27	0.0019768	0.0000002	-1.69		0.10	2.25E+09	4.45E+06	53.44	1.86	
BAH-F226-152.67-HM22-1.8	#09	18/8/17	14:53:45	0.0019778	0.0000002	-1.15		0.10	2.24E+09	4.42E+06	53.44	1.86	
BAH-F226-152.67-HM22-1.9	#09	18/8/17	14:59:04	0.0019864	0.0000002	3.25		0.10	2.42E+09	4.81E+06	53.44	1.86	
BAH-F226-152.67-HM22-1.10	#09	18/8/17	15:04:22	0.0019866	0.0000002	3.34		0.12	2.29E+09	4.54E+06	53.44	1.86	
				average		2.00							
				std dev (1σ)		1.87							
BAH-F282-118.2-black-1.1	#09	18/8/17	15:53:20	0.0019778	0.0000002	-1.16		0.10	2.26E+09	4.46E+06			HM-22
BAH-F282-118.2-black-1.2	#09	18/8/17	15:58:38	0.0019712	0.0000002		-4.56	0.11	2.29E+09	4.51E+06			
BAH-F282-118.2-black-1.3	#09	18/8/17	16:03:56	0.0019762	0.0000002	-1.98		0.12	2.28E+09	4.50E+06			
BAH-F282-118.2-black-1.4	#09	18/8/17	16:09:14	0.0019776	0.0000002	-1.28		0.09	2.29E+09	4.53E+06			
BAH-F282-118.2-black-1.5	#09	18/8/17	16:14:31	0.0019776	0.0000003	-1.27		0.13	2.28E+09	4.50E+06			
				average		-1.42							
				std dev (1σ)		0.38							
BAH-F282-118.2-brown-1.1	#09	18/8/17	16:19:51	0.0019802	0.0000002	0.09		0.11	2.33E+09	4.61E+06	36.08	5.13	HM-22
BAH-F282-118.2-brown-1.2	#09	18/8/17	16:25:09	0.0019806	0.0000002	0.26		0.12	2.33E+09	4.61E+06	36.08	5.13	
BAH-F282-118.2-brown-1.3	#09	18/8/17	16:30:27	0.0019803	0.0000002	0.12		0.12	2.32E+09	4.60E+06	36.08	5.13	
BAH-F282-118.2-brown-1.4	#09	18/8/17	16:35:44	0.0019800	0.0000002	-0.02		0.08	2.31E+09	4.58E+06	36.08	5.13	
BAH-F282-118.2-brown-1.5	#09	18/8/17	16:41:02	0.0019804	0.0000004	0.16		0.18	2.32E+09	4.60E+06	36.08	5.13	
BAH-F282-118.2-brown-1.6	#09	18/8/17	16:46:20	0.0019805	0.0000002	0.22		0.11	2.30E+09	4.56E+06	36.08	5.13	
BAH-F282-118.2-brown-1.7	#09	18/8/17	17:40:37	0.0019799	0.0000002	-0.11		0.10	2.32E+09	4.59E+06	36.08	5.13	
				average		0.10							
				std dev (1σ)		0.13							
BAH-F282-118.4-1.1	#09	18/8/17	17:46:00	0.0019811	0.0000002	0.52		0.12	2.30E+09	4.56E+06			HM-22
BAH-F282-118.4-1.2	#09	18/8/17	17:51:18	0.0019810	0.0000002	0.49		0.11	2.29E+09	4.53E+06			
BAH-F282-118.4-1.3	#09	18/8/17	17:56:35	0.0019820	0.0000003	1.01		0.14	2.27E+09	4.51E+06			
BAH-F282-118.4-1.4	#09	18/8/17	18:01:53	0.0019821	0.0000002	1.05		0.12	2.26E+09	4.48E+06			
BAH-F282-118.4-1.5	#09	18/8/17	18:07:11	0.0019810	0.0000004	0.47		0.18	2.25E+09	4.45E+06			
				average		0.71							
				std dev (1σ)		0.29							
BAH-F124-114-HM23-1.1	#09	19/8/17	1:24:21	0.0019783	0.0000002	0.78		0.12	2.31E+09	4.57E+06	10.96	0.33	HM-23
BAH-F124-114-HM23-1.2	#09	19/8/17	1:29:39	0.0019781	0.0000002	0.68		0.10	2.30E+09	4.54E+06	10.96	0.33	
BAH-F124-114-HM23-1.3	#09	19/8/17	1:34:56	0.0019780	0.0000002	0.62		0.10	2.29E+09	4.52E+06	10.96	0.33	
BAH-F124-114-HM23-1.4	#09	19/8/17	1:40:14	0.0019782	0.0000002	0.76		0.10	2.29E+09	4.53E+06	10.96	0.33	
BAH-F124-114-HM23-1.5	#09	19/8/17	1:45:32	0.0019781	0.0000002	0.69		0.12	2.30E+09	4.54E+06	10.96	0.33	
BAH-F124-114-HM23-1.6	#09	19/8/17	1:50:49	0.0019794	0.0000002	1.36		0.09	2.29E+09	4.53E+06	10.96	0.33	
BAH-F124-114-HM23-1.7	#09	19/8/17	1:56:07	0.0019780	0.0000003	0.65		0.13	2.28E+09	4.51E+06	10.96	0.33	
BAH-F124-114-HM23-1.8	#09	19/8/17	2:01:25	0.0019787	0.0000002	1.02		0.09	2.26E+09	4.48E+06	10.96	0.33	
BAH-F124-114-HM23-1.9	#09	19/8/17	2:06:43	0.0019789	0.0000003	1.11		0.13	2.30E+09	4.56E+06	10.96	0.33	
BAH-F124-114-HM23-1.10	#09	19/8/17	2:12:01	0.0019788	0.0000002	1.05		0.10	2.30E+09	4.54E+06	10.96	0.33	
				average		0.87							
				std dev (1σ)		0.25							
BAH-F124-112-HM23-1.1	#09	19/8/17	3:05:48	0.0019874	0.0000002	5.48		0.11	2.31E+09	4.58E+06	52.80	1.73	HM-23
BAH-F124-112-HM23-1.2	#09	19/8/17	3:11:05	0.0019866	0.0000002	5.05		0.11	2.36E+09	4.69E+06	52.80	1.73	
BAH-F124-112-HM23-1.3	#09	19/8/17	3:16:23	0.0019862	0.0000002	4.87		0.12	2.33E+09	4.64E+06	52.80	1.73	
BAH-F124-112-HM23-1.4	#09	19/8/17	3:21:41	0.0019866	0.0000002	5.09		0.10	2.40E+09	4.77E+06	52.80	1.73	
BAH-F124-112-HM23-1.5	#09	19/8/17	3:26:59	0.0019822	0.0000003		2.80	0.13	2.26E+09	4.48E+06	52.80	1.73	
BAH-F124-112-HM23-1.6	#09	19/8/17	3:32:17	0.0019876	0.0000002	5.56		0.11	2.24E+09	4.45E+06	52.80	1.73	
BAH-F124-112-HM23-1.7	#09	19/8/17	3:37:35	0.0019862	0.0000002	4.86		0.10	2.18E+09	4.32E+06	52.80	1.73	
BAH-F124-112-HM23-1.8	#09	19/8/17	3:42:53	0.0019861	0.0000002	4.80		0.09	2.28E+09	4.53E+06	52.80	1.73	
BAH-F124-112-HM23-1.9	#09	19/8/17	3:48:11	0.0019847	0.0000003	4.08		0.13	2.26E+09	4.48E+06	52.80	1.73	
BAH-F124-112-HM23-1.10	#09	19/8/17	3:53:28	0.0019886	0.0000002	6.12		0.11	2.23E+09	4.44E+06	52.80	1.73	
BAH-F124-112-HM23-1.5b	#09	19/8/17	8:20:48	0.0019853	0.0000002	4.42		0.11	2.26E+09	4.49E+06	52.80	1.73	
BAH-F124-112-HM23-1.10b	#09	19/8/17	8:29:40	0.0019870	0.0000002	5.29		0.10	2.20E+09	4.38E+06	52.80	1.73	
				average		5.06							
				std dev (1σ)		0.56							
BAH-F115-15-16-1.1	#09	19/8/17	4:47:20	0.0019849	0.0000002	4.21		0.09	2.28E+09	4.52E+06	25.27	0.14	HM-23
BAH-F115-15-16-1.2	#09	19/8/17	4:52:38	0.0019846	0.0000002	4.05		0.12	2.27E+09	4.51E+06	25.27	0.14	
BAH-F115-15-16-1.3	#09	19/8/17	4:57:55	0.0019862	0.0000003	4.88		0.13	2.26E+09	4.49E+06	25.27	0.14	
BAH-F115-15-16-1.4	#09	19/8/17	5:03:13	0.0019859	0.0000002	4.70		0.10	2.24E+09	4.45E+06	25.27	0.14	
BAH-F115-15-16-1.5	#09	19/8/17	5:08:31	0.0019856	0.0000002	4.56		0.11	2.25E+09	4.46E+06	25.27	0.14	
BAH-F115-15-16-1.6	#09	19/8/17	5:13:50	0.0019876	0.0000003	5.60		0.14	2.27E+09	4.52E+06	25.27	0.14	
BAH-F115-15-16-1.7	#09	19/8/17	5:19:08	0.0019871	0.0000002	5.30		0.12	2.27E+09	4.51E+06	25.27	0.14	
BAH-F115-15-16-1.8	#09	19/8/17	5:24:26	0.0019866	0.0000003	5.06		0.14	2.27E+09	4.50E+06	25.27	0.14	
BAH-F115-15-16-1.9	#09	19/8/17	5:29:43	0.0019872	0.0000003	5.35		0.14	2.26E+09	4.50E+06	25.27	0.14	
BAH-F115-15-16-1.10	#09	19/8/17	5:35:01	0.0019877	0.0000003	5.62		0.13	2.32E+09	4.62E+06	25.27	0.14	
BAH-F115-15-16-1.11	#09	19/8/17	5:40:19	0.0019868	0.0000002	5.19		0.10	2.30E+09	4.57E+06	25.27	0.14	
				average		4.96							
				std dev (1σ)		0.53							
BAH-F177													

SPOT #	Session	Date	Time	¹⁸ O/ ¹⁶ O ^(a)	± ^(b)	δ ¹⁸ O _{VERMOR} ^(c)	rejected	±Internal error (σ 95%)	¹⁸ O cps (median)	¹⁶ O cps (median)	(U-Th)/He ages	±	MOUNT
BAH-F177-115-1.8	#09	19/8/17	6:54:43	0.0019853	0.0000003	4.38		0.14	2.32E+09	4.62E+06	3.13	0.30	
BAH-F177-115-1.9	#09	19/8/17	7:00:01	0.0019862	0.0000003	4.86		0.17	2.32E+09	4.61E+06	3.13	0.30	
BAH-F177-115-1.10	#09	19/8/17	7:05:19	0.0019846	0.0000003	4.06		0.13	2.32E+09	4.61E+06	3.13	0.30	
				average		4.74							
				std dev (1σ)		0.48							
BAH-F177-115-2.1	#09	19/8/17	9:27:52	0.0019890	0.0000002	6.32		0.09	2.41E+09	4.79E+06	3.13	0.30	HM-23
BAH-F177-115-2.2	#09	19/8/17	9:33:09	0.0019888	0.0000002	6.21		0.09	2.40E+09	4.78E+06	3.13	0.30	
BAH-F177-115-2.3	#09	19/8/17	9:38:27	0.0019882	0.0000002	5.88		0.10	2.38E+09	4.74E+06	3.13	0.30	
BAH-F177-115-2.4	#09	19/8/17	10:16:18	0.0019855	0.0000002	4.52		0.09	2.31E+09	4.59E+06	3.13	0.30	
BAH-F177-115-2.5	#09	19/8/17	10:21:35	0.0019846	0.0000002	4.05		0.11	2.30E+09	4.56E+06	3.13	0.30	
BAH-F177-115-2.6	#09	19/8/17	10:26:53	0.0019848	0.0000002	4.12		0.12	2.29E+09	4.55E+06	3.13	0.30	
BAH-F177-115-2.7	#09	19/8/17	10:32:10	0.0019847	0.0000002	4.10		0.11	2.33E+09	4.62E+06	3.13	0.30	
BAH-F177-115-2.8	#09	19/8/17	10:37:28	0.0019841	0.0000002	3.80		0.10	2.30E+09	4.56E+06	3.13	0.30	
BAH-F177-115-2.9	#09	19/8/17	10:42:46	0.0019830	0.0000002	3.23		0.10	2.29E+09	4.53E+06	3.13	0.30	
BAH-F177-115-2.10	#09	19/8/17	10:48:04	0.0019832	0.0000002	3.33		0.12	2.28E+09	4.52E+06	3.13	0.30	
BAH-F177-115-1.9b	#09	19/8/17	13:28:26	0.0019847	0.0000002	4.09		0.11	2.29E+09	4.55E+06	3.13	0.30	
BAH-F177-115-1.1b	#09	19/8/17	13:36:39	0.0019877	0.0000002	5.66		0.11	2.34E+09	4.64E+06	3.13	0.30	
				average		4.61							
				std dev (1σ)		1.11							
BAH-F177-115_brown-1.11	#09	19/8/17	9:01:19	0.0019774	0.0000002	0.35		0.12	2.38E+09	4.70E+06	23.44	2.34	HM-23
BAH-F177-115_brown-1.12	#09	19/8/17	9:06:37	0.0019768	0.0000002	0.00		0.10	2.37E+09	4.69E+06	23.44	2.34	
BAH-F177-115_brown-1.13	#09	19/8/17	9:11:55	0.0019767	0.0000002	-0.05		0.10	2.35E+09	4.65E+06	23.44	2.34	
BAH-F177-115_brown-1.14	#09	19/8/17	9:17:13	0.0019759	0.0000002	-0.44		0.11	2.36E+09	4.66E+06	23.44	2.34	
BAH-F177-115_brown-1.15	#09	19/8/17	9:22:31	0.0019772	0.0000002	0.21		0.08	2.36E+09	4.68E+06	23.44	2.34	
BAH-F177-115_brown-1.14b	#09	19/8/17	13:19:05	0.0019762	0.0000002	-0.27		0.12	2.32E+09	4.58E+06	23.44	2.34	
				average		-0.03							
				std dev (1σ)		0.29							
BAH-F177-115_brown-2.11	#09	19/8/17	10:53:24	0.0019777	0.0000002	0.49		0.11	2.29E+09	4.53E+06	23.44	2.34	HM-23
BAH-F177-115_brown-2.12	#09	19/8/17	10:58:41	0.0019781	0.0000002	0.71		0.11	2.27E+09	4.50E+06	23.44	2.34	
BAH-F177-115_brown-2.13	#09	19/8/17	11:03:59	0.0019784	0.0000002	0.84		0.12	2.29E+09	4.53E+06	23.44	2.34	
BAH-F177-115_brown-2.14	#09	19/8/17	11:36:04	0.0019785	0.0000002	0.88		0.10	2.28E+09	4.51E+06	23.44	2.34	
BAH-F177-115_brown-2.15	#09	19/8/17	11:41:22	0.0019784	0.0000002	0.85		0.09	2.27E+09	4.49E+06	23.44	2.34	
				average		0.75							
				std dev (1σ)		0.16							
BAH-F226-142.7-1.1	#09	19/8/17	11:46:42	0.0019802	0.0000002	1.79		0.10	2.23E+09	4.41E+06			HM-23
BAH-F226-142.7-1.2	#09	19/8/17	11:52:00	0.0019813	0.0000002	2.35		0.12	2.23E+09	4.42E+06			
BAH-F226-142.7-1.3	#09	19/8/17	11:57:18	0.0019800	0.0000002	1.65		0.11	2.19E+09	4.34E+06			
BAH-F226-142.7-1.4	#09	19/8/17	12:02:36	0.0019808	0.0000002	2.07		0.10	2.20E+09	4.35E+06			
BAH-F226-142.7-1.5	#09	19/8/17	12:07:54	0.0019807	0.0000002	2.05		0.09	2.22E+09	4.40E+06			
BAH-F226-142.7-1.6	#09	19/8/17	12:13:12	0.0019805	0.0000002	1.91		0.11	2.20E+09	4.36E+06			
BAH-F226-142.7-1.7	#09	19/8/17	12:18:30	0.0019815	0.0000002	2.42		0.11	2.17E+09	4.30E+06			
BAH-F226-142.7-1.8	#09	19/8/17	12:23:47	0.0019821	0.0000002	2.73		0.11	2.18E+09	4.32E+06			
BAH-F226-142.7-1.9	#09	19/8/17	12:29:05	0.0019814	0.0000002	2.38		0.11	2.16E+09	4.29E+06			
				average		2.15							
				std dev (1σ)		0.35							
BAH-F124-123.7-1.1	#09	19/8/17	13:51:50	0.0019886	0.0000003	6.08		0.14	2.23E+09	4.44E+06	56.44	1.93	HM-23
BAH-F124-123.7-1.2	#09	19/8/17	13:57:08	0.0019854	0.0000002	4.43		0.10	2.26E+09	4.49E+06	56.44	1.93	
BAH-F124-123.7-1.3	#09	19/8/17	14:02:25	0.0019882	0.0000002	5.90		0.09	2.20E+09	4.37E+06	56.44	1.93	
BAH-F124-123.7-1.4	#09	19/8/17	14:07:43	0.0019891	0.0000002	6.35		0.09	2.28E+09	4.53E+06	56.44	1.93	
BAH-F124-123.7-1.5	#09	19/8/17	14:13:01	0.0019832	0.0000002	3.30		0.10	2.35E+09	4.66E+06	56.44	1.93	
BAH-F124-123.7-1.6	#09	19/8/17	14:18:19	0.0019885	0.0000002	6.03		0.11	2.26E+09	4.49E+06	56.44	1.93	
BAH-F124-123.7-1.7	#09	19/8/17	14:23:37	0.0019900	0.0000002	6.82		0.11	2.21E+09	4.41E+06	56.44	1.93	
BAH-F124-123.7-1.2b	#09	19/8/17	14:48:06	0.0019837	0.0000002	3.60		0.09	2.31E+09	4.59E+06	56.44	1.93	
BAH-F124-123.7-1.5b	#09	19/8/17	14:55:32	0.0019852	0.0000002	4.37		0.10	2.33E+09	4.62E+06	56.44	1.93	
BAH-F124-123.7-1.2c	#09	19/8/17	15:03:40	0.0019849	0.0000002	4.19		0.11	2.39E+09	4.74E+06	56.44	1.93	
				average		5.11							
				std dev (1σ)		1.26							
BAH-F282-118.4-1.1	#09	19/8/17	15:48:14	0.0019835	0.0000002	3.49		0.11	2.32E+09	4.60E+06			HM-23
BAH-F282-118.4-1.2	#09	19/8/17	15:53:32	0.0019834	0.0000002	3.42		0.12	2.32E+09	4.60E+06			
BAH-F282-118.4-1.3	#09	19/8/17	15:58:49	0.0019827	0.0000002	3.04		0.11	2.30E+09	4.56E+06			
BAH-F282-118.4-1.4	#09	19/8/17	16:04:07	0.0019825	0.0000002	2.98		0.09	2.28E+09	4.52E+06			
BAH-F282-118.4-1.5	#09	19/8/17	16:09:25	0.0019828	0.0000002	3.12		0.11	2.28E+09	4.53E+06			
				average		3.21							
				std dev (1σ)		0.23							
BAH-F226-142.7_black-1.1_sparkling	#09	17/8/17	11:46:31	0.0019777	0.0000002	-1.49		0.09	2.41E+09	4.77E+06	14.30	1.43	HM-16
BAH-F226-142.7_black-1.2_sparkling	#09	17/8/17	11:51:49	0.0019806	0.0000002	0.00		0.10	2.28E+09	4.52E+06	14.30	1.43	
BAH-F226-142.7_black-1.3_sparkling	#09	17/8/17	11:57:07	0.0019765	0.0000003	-0.59	-2.14	0.13	2.36E+09	4.67E+06	14.30	1.43	
BAH-F226-142.7_black-1.4_sparkling	#09	17/8/17	12:04:06	0.0019795	0.0000003	-0.59		0.15	2.25E+09	4.46E+06	14.30	1.43	
				average		-0.69							
				std dev (1σ)		0.75							
BAH-F226-142.7_black-1.5	#09	17/8/17	12:13:07	0.0019818	0.0000002	0.61		0.09	2.30E+09	4.57E+06	4.59	0.31	HM-16
BAH-F226-142.7_black-1.6	#09	17/8/17	12:18:25	0.0019800	0.0000002	-0.33		0.11	2.28E+09	4.52E+06	4.59	0.31	
BAH-F226-142.7_black-1.7	#09	17/8/17	12:23:43	0.0019816	0.0000002	0.51		0.11	2.29E+09	4.53E+06	4.59	0.31	
BAH-F226-142.7_black-1.8	#09	17/8/17	12:30:44	0.0019819	0.0000002	0.64		0.11	2.24E+09	4.44E+06	4.59	0.31	
BAH-F226-142.7_black-1.9	#09	17/8/17	12:36:02	0.0019828	0.0000002	1.13		0.11	2.26E+09	4.48E+06	4.59	0.31	
BAH-F226-142.7_black-1.10	#09	17/8/17	12:41:19	0.0019821	0.0000002	0.76		0.11	2.24E+09	4.44E+06	4.59	0.31	
BAH-F226-142.7_black-1.6b	#09	17/8/17	14:48:38	0.0019815	0.0000002	0.45		0.11	2.26E+09	4.47E+06	4.59	0.31	
BAH-F226-142.7_black-1.11	#09	17/8/17	14:53:56	0.0019815	0.0000002	0.44		0.08	2.24E+09	4.44E+06	4.59	0.31	
BAH-F226-142.7_black-1.12	#09	17/8/17	14:59:14	0.0019808	0.0000002	0.12		0.10	2.23E+09	4.42E+06	4.59	0.31	
BAH-F226-142.7_black-1.13	#09	17/8/17	15:04:32	0.0019815	0.0000002	0.48		0.11	2.20E+09	4.36E+06	4.59	0.31	
BAH-F226-142.7_black-1.14	#09	17/8/17	15:09:51	0.0019821	0.0000002	0.74		0.12	2.21E+09	4.39E+06	4.59	0.31	
BAH-F226-142.7_black-1.15	#09	17/8/17	15:15:09	0.0019820	0.0000003	0.72		0.14	2.22E+09	4.40E+06	4.59	0.31	
BAH-F226-142.7_black-1.16	#09	17/8/17	15:20:27	0.0019813	0.0000003	0.37		0.14	2.20E+09	4.36E+06	4.59	0.31	
BAH-F226-142.7_black-1.17	#09	17/8/17	15:25:45	0.0019812	0.0000002	0.30		0.09	2.18E+09	4.31E+06	4.59	0.31	
BAH-F226-142.7_black-1.18	#09	17/8/17	15:31:03	0.0019809	0.0000002	0.16		0.11	2.18E+09	4.32E+06	4.59	0.31	
BAH-F226-142.7_black-1.19	#09	17/8/17	15:36:21	0.0019809	0.0000002	0.12		0.12	2.18E+09	4.32E+06	4.59	0.31	
BAH-F226-142.7_black-1.16b	#09	17/8/17	17:18:22	0.0019820	0.0000002	0.69							

SPOT #	Session	Date	Time	¹⁸ O/ ¹⁶ O ^(a)	± ^(b)	δ ¹⁸ O _{VERMOW} ^(c)	rejected	±Internal error (σ 95%)	¹⁶ O cps (median)	¹⁸ O cps (median)	(U-Th)/He ages	±	MOUNT
				average		1.99							
				std dev (1σ)		0.15							
BAHLGB-HM16-1.1	#09	17/8/17	19:46:34	0.0019786	0.0000002	-1.02		0.10	2.36E+09	4.68E+06	16.26	0.92	HM-16
BAHLGB-HM16-1.2	#09	17/8/17	19:51:51	0.0019780	0.0000002	-1.33		0.11	2.36E+09	4.66E+06	16.26	0.92	
BAHLGB-HM16-1.3	#09	17/8/17	19:57:09	0.0019780	0.0000002	-1.32		0.10	2.35E+09	4.66E+06	16.26	0.92	
BAHLGB-HM16-1.4	#09	17/8/17	20:02:27	0.0019789	0.0000002	-0.86		0.09	2.36E+09	4.68E+06	16.26	0.92	
BAHLGB-HM16-1.5	#09	17/8/17	20:07:45	0.0019779	0.0000003	-1.41		0.13	2.36E+09	4.67E+06	16.26	0.92	
BAHLGB-HM16-2.1	#09	17/8/17	22:19:43	0.0019783	0.0000002	-1.18		0.08	2.31E+09	4.58E+06	16.26	0.92	
BAHLGB-HM16-2.2	#09	17/8/17	22:25:02	0.0019781	0.0000002	-1.27		0.10	2.33E+09	4.61E+06	16.26	0.92	
BAHLGB-HM16-2.3	#09	17/8/17	22:30:21	0.0019775	0.0000002	-1.62		0.12	2.31E+09	4.57E+06	16.26	0.92	
BAHLGB-HM16-2.4	#09	17/8/17	22:35:38	0.0019774	0.0000002	-1.66		0.10	2.32E+09	4.59E+06	16.26	0.92	
				average		-1.30							
				std dev (1σ)		0.26							
BAH3BL-HM16-1.1	#09	17/8/17	22:40:58	0.0019766	0.0000002	-2.05		0.10	2.28E+09	4.50E+06	13.73	2.14	HM-16
BAH3BL-HM16-1.2	#09	17/8/17	22:46:16	0.0019765	0.0000002	-2.11		0.11	2.28E+09	4.51E+06	13.73	2.14	
BAH3BL-HM16-1.3	#09	17/8/17	22:51:35	0.0019766	0.0000002	-2.07		0.09	2.27E+09	4.49E+06	13.73	2.14	
BAH3BL-HM16-1.4	#09	17/8/17	22:56:53	0.0019767	0.0000002	-2.02		0.10	2.27E+09	4.48E+06	13.73	2.14	
				average		-2.06					13.73	2.14	
				std dev (1σ)		0.04							
BAH-F282-118.4-1.1	#09	18/8/17	0:17:47	0.0019778	0.0000002	-1.42		0.12	2.23E+09	4.41E+06			HM-16
BAH-F282-118.4-1.2	#09	18/8/17	0:23:04	0.0019766	0.0000002	-2.05		0.08	2.23E+09	4.40E+06			
BAH-F282-118.4-1.3	#09	18/8/17	0:28:22	0.0019783	0.0000002	-1.17		0.08	2.23E+09	4.42E+06			
BAH-F282-118.4-1.4	#09	18/8/17	0:33:40	0.0019773	0.0000002	-1.68		0.12	2.22E+09	4.39E+06			
BAH-F282-118.4-1.5	#09	18/8/17	0:38:58	0.0019792	0.0000002	-0.74		0.09	2.23E+09	4.41E+06			
BAH-F282-118.4-1.6	#09	18/8/17	0:44:15	0.0019779	0.0000002	-1.40		0.08	2.23E+09	4.42E+06			
BAH-F282-118.4-1.7	#09	18/8/17	0:49:33	0.0019771	0.0000002	-1.79		0.12	2.22E+09	4.40E+06			
BAH-F282-118.4-1.8	#09	18/8/17	0:54:51	0.0019781	0.0000002	-1.30		0.11	2.23E+09	4.40E+06			
				average		-1.44							
				std dev (1σ)		0.40							
BAH-F226-157.6-1.1_brown	#09	18/8/17	1:00:14	0.0019787	0.0000002	-0.98		0.12	2.23E+09	4.41E+06	12.40	0.06	HM-16
BAH-F226-157.6-1.2_brown	#09	18/8/17	1:05:32	0.0019790	0.0000002	-0.85		0.10	2.23E+09	4.42E+06	12.40	0.06	
BAH-F226-157.6-1.3_brown	#09	18/8/17	1:54:33	0.0019781	0.0000002	-1.31		0.13	2.21E+09	4.37E+06	12.40	0.06	
BAH-F226-157.6-1.4_brown	#09	18/8/17	1:59:50	0.0019790	0.0000002	-0.81		0.10	2.21E+09	4.38E+06	12.40	0.06	
BAH-F226-157.6-1.5_brown	#09	18/8/17	2:05:08	0.0019785	0.0000002	-1.10		0.11	2.21E+09	4.37E+06	12.40	0.06	
BAH-F226-157.6-1.6_brown	#09	18/8/17	2:10:26	0.0019786	0.0000002	-1.05		0.11	2.21E+09	4.38E+06	12.40	0.06	
BAH-F226-157.6-1.7_brown	#09	18/8/17	2:15:44	0.0019784	0.0000002	-1.14		0.08	2.21E+09	4.37E+06	12.40	0.06	
BAH-F226-157.6-1.8_brown	#09	18/8/17	2:21:01	0.0019788	0.0000003	-0.92		0.13	2.21E+09	4.38E+06	12.40	0.06	
BAH-F226-157.6-1.9_brown	#09	18/8/17	2:26:19	0.0019793	0.0000002	-0.66		0.12	2.21E+09	4.38E+06	12.40	0.06	
				average		-0.98							
				std dev (1σ)		0.19							
BAH-100_brown-1.1	#09	18/8/17	3:20:12	0.0019783	0.0000002	-1.20		0.11	2.29E+09	4.53E+06	53.69	2.27	HM-16
BAH-100_brown-1.2	#09	18/8/17	3:25:30	0.0019778	0.0000002	-1.46		0.11	2.28E+09	4.52E+06	53.69	2.27	
BAH-100_brown-1.3	#09	18/8/17	3:30:47	0.0019779	0.0000002	-1.41		0.09	2.31E+09	4.56E+06	53.69	2.27	
BAH-100_brown-1.4	#09	18/8/17	3:36:05	0.0019776	0.0000002	-1.56		0.10	2.30E+09	4.56E+06	53.69	2.27	
BAH-100_brown-1.5	#09	18/8/17	3:41:23	0.0019782	0.0000002	-1.25		0.10	2.31E+09	4.57E+06	53.69	2.27	
BAH-100_brown-1.6	#09	18/8/17	3:46:41	0.0019780	0.0000002	-1.36		0.10	2.31E+09	4.58E+06	53.69	2.27	
BAH-100_brown-1.7	#09	18/8/17	3:51:58	0.0019777	0.0000002	-1.49		0.11	2.31E+09	4.58E+06	53.69	2.27	
BAH-100_brown-1.8	#09	18/8/17	3:57:16	0.0019785	0.0000002	-1.10		0.12	2.32E+09	4.59E+06	53.69	2.27	
BAH-100_brown-1.9	#09	18/8/17	4:02:33	0.0019777	0.0000002	-1.52		0.08	2.32E+09	4.58E+06	53.69	2.27	
BAH-100_brown-1.10	#09	18/8/17	4:07:51	0.0019778	0.0000002	-1.43		0.10	2.32E+09	4.60E+06	53.69	2.27	
				average		-1.38							
				std dev (1σ)		0.15							
BAH-100_black-1.1	#09	18/8/17	4:56:51	0.0019874	0.0000003	3.47		0.13	2.39E+09	4.75E+06	40.26	5.30	HM-16
BAH-100_black-1.2	#09	18/8/17	5:02:09	0.0019858	0.0000003	2.68		0.14	2.37E+09	4.70E+06	40.26	5.30	
BAH-100_black-1.3	#09	18/8/17	5:07:27	0.0019873	0.0000002	3.42		0.12	2.39E+09	4.75E+06	40.26	5.30	
BAH-100_black-1.4	#09	18/8/17	5:12:45	0.0019864	0.0000002	2.95		0.11	2.38E+09	4.74E+06	40.26	5.30	
BAH-100_black-1.5	#09	18/8/17	5:18:02	0.0019867	0.0000002	3.14		0.11	2.38E+09	4.73E+06	40.26	5.30	
				average		3.13							
				std dev (1σ)		0.33							
BAH-99-01-1.1	#10	4/9/17	16:49:22	0.0019699	0.0000002	3.46		0.09	2.24E+09	4.40E+06	25.06	4.40	HM-17
BAH-99-01-1.2	#10	4/9/17	16:54:39	0.0019698	0.0000002	3.45		0.10	2.24E+09	4.41E+06	25.06	4.40	
BAH-99-01-1.3	#10	4/9/17	16:59:56	0.0019693	0.0000002	3.18		0.12	2.21E+09	4.35E+06	25.06	4.40	
BAH-99-01-1.4	#10	4/9/17	17:05:14	0.0019715	0.0000002	4.32		0.10	2.21E+09	4.35E+06	25.06	4.40	
BAH-99-01-1.5	#10	4/9/17	17:10:31	0.0019701	0.0000002	3.57		0.10	2.24E+09	4.41E+06	25.06	4.40	
BAH-99-01-1.6	#10	4/9/17	17:15:49	0.0019694	0.0000002	3.21		0.10	2.21E+09	4.35E+06	25.06	4.40	
BAH-99-01-1.7	#10	4/9/17	17:21:06	0.0019703	0.0000001	3.72		0.07	2.24E+09	4.40E+06	25.06	4.40	
BAH-99-01-1.8	#10	4/9/17	17:26:23	0.0019689	0.0000002	2.95		0.08	2.24E+09	4.40E+06	25.06	4.40	
BAH-99-01-1.9	#10	4/9/17	17:31:41	0.0019691	0.0000001	3.07		0.08	2.25E+09	4.44E+06	25.06	4.40	
BAH-99-01-1.10	#10	4/9/17	17:36:59	0.0019691	0.0000002	3.08		0.10	2.23E+09	4.38E+06	25.06	4.40	
				average		3.40							
				std dev (1σ)		0.40							
BAH-13-03_underTopCr-1.1	#10	4/9/17	19:16:12	0.0019657	0.0000002	1.31		0.09	2.17E+09	4.27E+06	5.48	0.01	HM-17
BAH-13-03_underTopCr-1.2	#10	4/9/17	19:21:29	0.0019666	0.0000002	1.77		0.08	2.18E+09	4.28E+06	5.48	0.01	
BAH-13-03_underTopCr-1.3	#10	4/9/17	19:26:46	0.0019672	0.0000002	2.08		0.09	2.16E+09	4.25E+06	5.48	0.01	
BAH-13-03_underTopCr-1.4	#10	4/9/17	19:32:04	0.0019667	0.0000002	1.83		0.09	2.16E+09	4.25E+06	5.48	0.01	
BAH-13-03_underTopCr-1.5	#10	4/9/17	19:37:21	0.0019650	0.0000003	0.93		0.13	2.13E+09	4.19E+06	5.48	0.01	
BAH-13-03_underTopCr-1.6	#10	4/9/17	19:42:39	0.0019655	0.0000002	1.21		0.09	2.14E+09	4.21E+06	5.48	0.01	
BAH-13-03_underTopCr-1.7	#10	4/9/17	19:47:56	0.0019633	0.0000002	0.06		0.09	2.12E+09	4.16E+06	5.48	0.01	
BAH-13-03_underTopCr-1.8	#10	4/9/17	19:53:13	0.0019616	0.0000002	-0.80		0.09	2.12E+09	4.16E+06	5.48	0.01	
BAH-13-03_underTopCr-1.9	#10	4/9/17	19:58:31	0.0019618	0.0000002	-0.70</							

SPOT #	Session	Date	Time	¹⁸ O/ ¹⁶ O ^(a)	± ^(b)	δ ¹⁸ O _{VERMOW} ^(c)	rejected	±Internal error (σ 95%)	¹⁸ O cps (median)	¹⁶ O cps (median)	(U-Th)/He ages	±	MOUNT
BAH-03-cml6_black-1.1	#10	4/9/17	22:29:47	0.0019659	0.0000002	1.43		0.09	2.14E+09	4.20E+06	4.75	0.00	HM-17
BAH-03-cml6_black-1.2	#10	4/9/17	22:35:04	0.0019663	0.0000002	1.64		0.10	2.13E+09	4.20E+06	4.75	0.00	
BAH-03-cml6_black-1.3	#10	4/9/17	22:40:21	0.0019659	0.0000002	1.44		0.10	2.13E+09	4.19E+06	4.75	0.00	
BAH-03-cml6_black-1.4	#10	4/9/17	22:45:39	0.0019668	0.0000002	1.86		0.08	2.13E+09	4.19E+06	4.75	0.00	
BAH-03-cml6_black-1.5	#10	4/9/17	22:50:56	0.0019666	0.0000002	1.77		0.11	2.13E+09	4.18E+06	4.75	0.00	
BAH-03-cml6_black-1.6	#10	4/9/17	22:56:14	0.0019665	0.0000002	1.71		0.09	2.11E+09	4.15E+06	4.75	0.00	
BAH-03-cml6_black-1.7	#10	4/9/17	23:01:32	0.0019652	0.0000002	1.06		0.08	2.14E+09	4.21E+06	4.75	0.00	
BAH-03-cml6_black-1.8	#10	4/9/17	23:06:49	0.0019654	0.0000002	1.17		0.11	2.13E+09	4.19E+06	4.75	0.00	
BAH-03-cml6_black-1.9	#10	4/9/17	23:12:06	0.0019664	0.0000002	1.67		0.09	2.14E+09	4.21E+06	4.75	0.00	
BAH-03-cml6_black-1.10	#10	4/9/17	23:17:25	0.0019649	0.0000002	0.89		0.09	2.11E+09	4.14E+06	4.75	0.00	
BAH-03-cml6_black-1.11	#10	4/9/17	23:22:42	0.0019644	0.0000002	0.62		0.09	2.09E+09	4.11E+06	4.75	0.00	
				average		1.39							
				std dev (1σ)		0.40							
BAH-03-cml6_brown-1.1	#10	5/9/17	0:06:30	0.0019545	0.0000002	-4.49		0.08	2.15E+09	4.20E+06	7.73	0.03	HM-17
BAH-03-cml6_brown-1.2	#10	5/9/17	0:11:48	0.0019553	0.0000002	-4.06		0.11	2.15E+09	4.20E+06	7.73	0.03	
BAH-03-cml6_brown-1.3	#10	5/9/17	0:17:05	0.0019557	0.0000002	-3.85		0.09	2.14E+09	4.19E+06	7.73	0.03	
BAH-03-cml6_brown-1.4	#10	5/9/17	0:22:22	0.0019555	0.0000002	-3.98		0.11	2.12E+09	4.15E+06	7.73	0.03	
BAH-03-cml6_brown-1.5	#10	5/9/17	0:27:40	0.0019540	0.0000002	-4.74		0.10	2.13E+09	4.17E+06	7.73	0.03	
BAH-03-cml6_brown-1.6	#10	5/9/17	0:32:58	0.0019544	0.0000002	-4.53		0.11	2.14E+09	4.19E+06	7.73	0.03	
BAH-03-cml6_brown-1.7	#10	5/9/17	0:38:15	0.0019545	0.0000002	-4.51		0.10	2.14E+09	4.17E+06	7.73	0.03	
BAH-03-cml6_brown-1.8	#10	5/9/17	0:43:33	0.0019555	0.0000002	-3.98		0.10	2.14E+09	4.17E+06	7.73	0.03	
BAH-03-cml6_brown-1.9	#10	5/9/17	0:48:50	0.0019548	0.0000002	-4.36		0.11	2.15E+09	4.20E+06	7.73	0.03	
BAH-03-cml6_brown-1.10	#10	5/9/17	0:54:07	0.0019547	0.0000002	-4.40		0.09	2.14E+09	4.19E+06	7.73	0.03	
				average		-4.29							
				std dev (1σ)		0.30							
BA-HS-001-1.1	#10	5/9/17	1:37:54	0.0019745	0.0000003	5.85		0.13	2.36E+09	4.67E+06			HM-17
BA-HS-001-1.2	#10	5/9/17	1:43:11	0.0019738	0.0000002	5.51		0.10	2.35E+09	4.65E+06			
BA-HS-001-1.3	#10	5/9/17	1:48:28	0.0019731	0.0000002	5.13		0.12	2.33E+09	4.59E+06			
BA-HS-001-1.4	#10	5/9/17	1:53:46	0.0019746	0.0000002	5.91		0.12	2.35E+09	4.63E+06			
BA-HS-001-1.5	#10	5/9/17	1:59:03	0.0019741	0.0000002	5.65		0.10	2.35E+09	4.64E+06			
BA-HS-001-1.6	#10	5/9/17	2:04:20	0.0019739	0.0000002	5.54		0.09	2.34E+09	4.62E+06			
BA-HS-001-1.7	#10	5/9/17	2:09:38	0.0019738	0.0000002	5.49		0.10	2.37E+09	4.67E+06			
BA-HS-001-1.8	#10	5/9/17	2:14:55	0.0019735	0.0000002	5.36		0.09	2.37E+09	4.67E+06			
BA-HS-001-1.9	#10	5/9/17	2:20:13	0.0019740	0.0000002	5.64		0.10	2.36E+09	4.66E+06			
BA-HS-001-1.10	#10	5/9/17	2:25:31	0.0019738	0.0000002	5.51		0.10	2.36E+09	4.66E+06			
				average		5.56							
				std dev (1σ)		0.22							
IBH-13-09b(1)_FillCav-1.1	#10	5/9/17	11:30:51	0.0020095	0.0000003	24.00		0.15	1.79E+09	3.60E+06	29.45	2.40	HM-17
IBH-13-09b(1)_FillCav-1.2	#10	5/9/17	11:36:08	0.0020036	0.0000003		20.97	0.13	1.88E+09	3.77E+06	29.45	2.40	
IBH-13-09b(1)_FillCav-1.3	#10	5/9/17	11:41:26	0.0020061	0.0000002	22.24		0.10	1.93E+09	3.87E+06	29.45	2.40	
IBH-13-09b(1)_FillCav-1.4	#10	5/9/17	11:46:43	0.0020072	0.0000002	22.83		0.11	1.87E+09	3.74E+06	29.45	2.40	
IBH-13-09b(1)_FillCav-1.5	#10	5/9/17	11:52:00	0.0020070	0.0000002	22.71		0.12	1.91E+09	3.83E+06	29.45	2.40	
IBH-13-09b(1)_FillCav-2.1	#10	5/9/17	11:57:20	0.0020087	0.0000002	23.59		0.12	1.75E+09	3.52E+06	29.45	2.40	
IBH-13-09b(1)_FillCav-2.2	#10	5/9/17	12:02:37	0.0020092	0.0000003	23.86		0.15	1.72E+09	3.45E+06	29.45	2.40	
IBH-13-09b(1)_FillCav-2.3	#10	5/9/17	12:07:54	0.0020106	0.0000003	24.60		0.14	1.70E+09	3.42E+06	29.45	2.40	
IBH-13-09b(1)_FillCav-2.4	#10	5/9/17	12:13:11	0.0020065	0.0000002	22.46		0.12	1.84E+09	3.70E+06	29.45	2.40	
IBH-13-09b(1)_FillCav-2.5	#10	5/9/17	12:18:29	0.0020051	0.0000003	21.73		0.13	1.89E+09	3.80E+06	29.45	2.40	
				average		23.11							
				std dev (1σ)		0.94							
IBH-13-09b(2)_cement-1.1	#10	5/9/17	13:02:16	0.0020082	0.0000003	23.34		0.14	1.84E+09	3.69E+06	29.45	2.40	HM-17
IBH-13-09b(2)_cement-1.2	#10	5/9/17	13:07:34	0.0020028	0.0000003	20.56		0.14	2.01E+09	4.02E+06	29.45	2.40	
IBH-13-09b(2)_cement-1.3	#10	5/9/17	13:12:52	0.0020006	0.0000002	19.37		0.11	2.06E+09	4.12E+06	29.45	2.40	
IBH-13-09b(2)_cement-1.4	#10	5/9/17	13:18:09	0.0020022	0.0000002	20.21		0.10	1.96E+09	3.92E+06	29.45	2.40	
IBH-13-09b(2)_cement-1.5	#10	5/9/17	13:23:26	0.0020070	0.0000004	22.71		0.18	1.84E+09	3.70E+06	29.45	2.40	
IBH-13-09b(2)_cement-1.6	#10	5/9/17	13:28:44	0.0020043	0.0000002	21.31		0.11	2.04E+09	4.09E+06	29.45	2.40	
IBH-13-09b(2)_cement-1.7	#10	5/9/17	13:34:01	0.0020093	0.0000003	23.90		0.14	1.77E+09	3.55E+06	29.45	2.40	
IBH-13-09b(2)_cement-1.8	#10	5/9/17	13:39:19	0.0020081	0.0000003	23.26		0.15	1.83E+09	3.68E+06	29.45	2.40	
IBH-13-09b(2)_cement-1.9	#10	5/9/17	13:44:37	0.0020097	0.0000003	24.12		0.14	1.75E+09	3.51E+06	29.45	2.40	
IBH-13-09b(2)_cement-1.10	#10	5/9/17	13:49:55	0.0020065	0.0000002	22.44		0.12	1.94E+09	3.90E+06	29.45	2.40	
				average		22.12							
				std dev (1σ)		1.66							
IB-03-8_sdbench-1.1	#10	5/9/17	18:18:57	0.0020236	0.0000006	31.31		0.29	3.48E+08	7.05E+05	20.10	4.61	HM-17
IB-03-8_sdbench-1.2	#10	5/9/17	18:24:15	0.0020078	0.0000003	23.12		0.13	1.52E+09	3.06E+06	20.10	4.61	
IB-03-8_sdbench-1.3	#10	5/9/17	18:29:32	0.0020057	0.0000003	22.06		0.13	1.66E+09	3.32E+06	20.10	4.61	
IB-03-8_sdbench-1.4	#10	5/9/17	18:34:50	0.0020032	0.0000002	20.72		0.12	1.84E+09	3.68E+06	20.10	4.61	
IB-03-8_sdbench-1.5	#10	5/9/17	18:40:07	0.0020008	0.0000002	19.50		0.10	1.97E+09	3.95E+06	20.10	4.61	
IB-03-8_sdbench-1.6	#10	5/9/17	18:45:25	0.0019871	0.0000002	12.40		0.10	2.32E+09	4.61E+06	20.10	4.61	
IB-03-8_sdbench-1.7	#10	5/9/17	18:50:43	0.0019654	0.0000002		1.16	0.10	2.20E+09	4.33E+06	20.10	4.61	
IB-03-8_sdbench-1.8	#10	5/9/17	18:56:00	0.0019961	0.0000002	17.04		0.10	2.06E+09	4.11E+06	20.10	4.61	
IB-03-8_sdbench-1.9	#10	5/9/17	19:01:18	0.0019661	0.0000002		1.50	0.10	2.29E+09	4.51E+06	20.10	4.61	
IB-03-8_sdbench-1.10	#10	5/9/17	19:06:36	0.0019980	0.0000002	18.04		0.10	2.06E+09	4.11E+06	20.10	4.61	
				average		20.52							
				std dev (1σ)		5.49							
BAH-177-115_FillCav-1.1	#10	5/9/17	21:02:57	0.0019683	0.0000002	2.65		0.10	2.22E+09	4.37E+06	3.13	0.30	HM-17
BAH-177-115_FillCav-1.2	#10	5/9/17	21:08:14	0.0019673	0.0000002	2.16		0.10	2.19E+09	4.31E+06	3.13	0.30	
BAH-177-115_FillCav-1.3	#10	5/9/17	21:13:31	0.0019671	0.0000002	2.03		0.11	2.19E+09	4.30E+06	3.13	0.30	
BAH-177-115_FillCav-1.4	#10	5/9/17	21:18:48	0.0019665	0.0000002	1.72		0.11	2.18E+09	4.28E+06	3.13	0.30	
BAH-177-115_FillCav-1.5	#10</												

SPOT #	Session	Date	Time	¹⁸ O/ ¹⁶ O ^(a)	± ^(b)	δ ¹⁸ O _{VSMOW} ^(c)	rejected	±Internal error (σ 95%)	¹⁸ O cps (median)	¹⁶ O cps (median)	(U-Th)/He ages	±	MOUNT	
				std dev (1σ)	0.85									
BAH-F177-115-1.1	#10	7/9/17	19:53:22	0.0019732	0.0000002	3.62		0.10	2.24E+09	4.41E+06	3.13	0.30	HM-23	
BAH-F177-115-1.2	#10	7/9/17	19:58:39	0.0019731	0.0000002	3.59		0.09	2.23E+09	4.40E+06	3.13	0.30		
BAH-F177-115-1.3	#10	7/9/17	20:03:57	0.0019731	0.0000002	3.60		0.12	2.22E+09	4.39E+06	3.13	0.30		
BAH-F177-115-1.4	#10	7/9/17	20:09:14	0.0019731	0.0000002	3.56		0.11	2.22E+09	4.37E+06	3.13	0.30		
BAH-F177-115-1.5	#10	7/9/17	20:14:31	0.0019728	0.0000002	3.41		0.09	2.18E+09	4.30E+06	3.13	0.30		
BAH-F177-115-1.6	#10	7/9/17	20:19:49	0.0019702	0.0000002	2.07		0.09	2.14E+09	4.21E+06	3.13	0.30		
BAH-F177-115-1.7	#10	7/9/17	20:25:06	0.0019701	0.0000002	2.04		0.12	2.14E+09	4.22E+06	3.13	0.30		
BAH-F177-115-1.8	#10	7/9/17	20:30:24	0.0019702	0.0000002	2.06		0.10	2.11E+09	4.16E+06	3.13	0.30		
BAH-F177-115-1.9	#10	7/9/17	20:35:41	0.0019692	0.0000002	1.55		0.08	2.13E+09	4.19E+06	3.13	0.30		
BAH-F177-115-1.10	#10	7/9/17	20:40:59	0.0019703	0.0000002	2.13		0.10	2.14E+09	4.21E+06	3.13	0.30		
BAH-F177-115-1.11	#10	8/9/17	6:04:04	0.0019702	0.0000002	2.06		0.08	2.15E+09	4.24E+06	3.13	0.30		
BAH-F177-115-1.12	#10	8/9/17	6:09:22	0.0019702	0.0000002	2.09		0.09	2.14E+09	4.21E+06	3.13	0.30		
BAH-F177-115-1.13	#10	8/9/17	6:14:39	0.0019704	0.0000002	2.17		0.13	2.15E+09	4.23E+06	3.13	0.30		
BAH-F177-115-1.14	#10	8/9/17	6:19:57	0.0019700	0.0000002	2.00		0.11	2.15E+09	4.23E+06	3.13	0.30		
				average	2.57									
				std dev (1σ)	0.78									
BAH-F226-157.6-1.1	#10	8/9/17	8:02:33	0.0019615	0.0000002	-2.44		0.10	2.07E+09	4.05E+06	12.40	0.06	HM-23	
BAH-F226-157.6-1.2	#10	8/9/17	8:07:50	0.0019612	0.0000002	-2.60		0.10	2.04E+09	4.01E+06	12.40	0.06		
BAH-F226-157.6-1.3	#10	8/9/17	8:13:07	0.0019618	0.0000002	-2.28		0.10	2.04E+09	4.01E+06	12.40	0.06		
BAH-F226-157.6-1.4	#10	8/9/17	8:18:25	0.0019619	0.0000002	-2.19		0.11	2.03E+09	3.98E+06	12.40	0.06		
BAH-F226-157.6-1.5	#10	8/9/17	8:23:42	0.0019617	0.0000002	-2.29		0.09	2.02E+09	3.97E+06	12.40	0.06		
BAH-F226-157.6-1.6	#10	8/9/17	8:28:59	0.0019615	0.0000001	-2.43		0.07	2.05E+09	4.02E+06	12.40	0.06		
BAH-F226-157.6-1.7	#10	8/9/17	8:34:17	0.0019618	0.0000002	-2.25		0.12	2.02E+09	3.97E+06	12.40	0.06		
BAH-F226-157.6-1.8	#10	8/9/17	9:44:43	0.0019621	0.0000002	-2.10		0.12	2.02E+09	3.96E+06	12.40	0.06		
BAH-F226-157.6-1.9	#10	8/9/17	9:50:00	0.0019618	0.0000002	-2.25		0.08	2.02E+09	3.96E+06	12.40	0.06		
BAH-F226-157.6-1.10	#10	8/9/17	9:55:18	0.0019612	0.0000002	-2.58		0.09	2.01E+09	3.95E+06	12.40	0.06		
				average	-2.34									
				std dev (1σ)	0.16									
BAH-F226-157.6-2.1	#10	8/9/17	10:00:39	0.0019629	0.0000002	-1.70		0.10	2.02E+09	3.97E+06	12.40	0.06	HM-23	
BAH-F226-157.6-2.2	#10	8/9/17	10:05:56	0.0019641	0.0000002	-1.05		0.10	1.99E+09	3.90E+06	12.40	0.06		
BAH-F226-157.6-2.3	#10	8/9/17	10:11:13	0.0019641	0.0000002	-1.08		0.11	1.99E+09	3.90E+06	12.40	0.06		
BAH-F226-157.6-2.4	#10	8/9/17	11:00:13	0.0019640	0.0000003	-1.11		0.14	1.98E+09	3.89E+06	12.40	0.06		
BAH-F226-157.6-2.5	#10	8/9/17	11:05:30	0.0019633	0.0000002	-1.46		0.10	1.97E+09	3.87E+06	12.40	0.06		
BAH-F226-157.6-2.6	#10	8/9/17	11:10:48	0.0019637	0.0000002	-1.29		0.11	2.01E+09	3.94E+06	12.40	0.06		
BAH-F226-157.6-2.7	#10	8/9/17	11:16:06	0.0019633	0.0000002	-1.47		0.11	1.99E+09	3.91E+06	12.40	0.06		
BAH-F226-157.6-2.8	#10	8/9/17	11:21:23	0.0019635	0.0000002	-1.41		0.10	1.99E+09	3.90E+06	12.40	0.06		
BAH-F226-157.6-2.9	#10	8/9/17	11:26:42	0.0019638	0.0000002	-1.24		0.11	1.98E+09	3.88E+06	12.40	0.06		
BAH-F226-157.6-2.10	#10	8/9/17	11:31:59	0.0019636	0.0000002	-1.35		0.10	2.01E+09	3.94E+06	12.40	0.06		
				average	-1.32									
				std dev (1σ)	0.21									

(a) Raw ¹⁸O/¹⁶O, corrected for background but not instrumental mass fractionation.

(b) Within spot (internal) precision, 95% conf.

(c) δ¹⁸O (permil) = ((¹⁸O/¹⁶O_{corrected})/(¹⁸O/¹⁶O_{reference})-1)*1000, where ¹⁸O/¹⁶O_{corrected} is the background, and IMF corrected ¹⁸O/¹⁶O ratio, and (¹⁸O/¹⁶O)_{reference} is the reference value of the chosen goethite reference material.

Rejected analyses are in *italics*.

EA2: SHRIMP-SI oxygen isotopic data for the Quadrilátero Ferrífero

SPOT #	Session	Date	Time	¹⁸ O/ ¹⁶ O ^(a)	± ^(b)	δ ¹⁸ O _{VSMOW} ^(c)	rejected	±Internal error (σ 95%)	¹⁶ O cps (median)	¹⁸ O cps (median)	(U-Th)/He ages	±	MOUNT
PIC0623-1.1	#02	27/10/14	6:37:49	0.0019722	0.0000002	0.66		0.11	2.41E+09	4.75E+06	13.72	5.73	HM 1
PIC0623-1.2	#02	27/10/14	6:43:23	0.0019716	0.0000003	0.36		0.17	2.47E+09	4.86E+06	13.72	5.73	
PIC0623-1.3	#02	27/10/14	6:48:56	0.0019717	0.0000002	0.41		0.09	2.47E+09	4.87E+06	13.72	5.73	
PIC0623-1.4	#02	27/10/14	6:54:29	0.0019735	0.0000002	1.36		0.12	2.43E+09	4.80E+06	13.72	5.73	
PIC0623-1.5	#02	27/10/14	7:00:03	0.0019745	0.0000003	1.82		0.14	2.45E+09	4.84E+06	13.72	5.73	
PIC0623-1.6	#02	27/10/14	7:05:36	0.0019725	0.0000003	0.81		0.14	2.43E+09	4.79E+06	13.72	5.73	
	#02			average		0.90							
				std dev (1σ)		0.58							
PIC0622-1.1	#02	27/10/14	7:44:48	0.0019783	0.0000002	3.82		0.11	2.40E+09	4.76E+06	19.55	3.74	HM 1
PIC0622-1.2	#02	27/10/14	7:50:21	0.0019793	0.0000002	4.33		0.12	2.42E+09	4.80E+06	19.55	3.74	
PIC0622-1.3	#02	27/10/14	7:55:55	0.0019786	0.0000002	3.98		0.11	2.43E+09	4.81E+06	19.55	3.74	
PIC0622-1.4	#02	27/10/14	8:01:28	0.0019764	0.0000002	2.81		0.09	2.43E+09	4.79E+06	19.55	3.74	
PIC0622-1.5	#02	27/10/14	8:07:02	0.0019785	0.0000003	3.94		0.13	2.43E+09	4.80E+06	19.55	3.74	
PIC0622-1.6	#02	27/10/14	8:12:35	0.0019779	0.0000002	3.61		0.12	2.41E+09	4.77E+06	19.55	3.74	
PIC0622-1.7	#02	27/10/14	8:18:09	0.0019770	0.0000003	3.14		0.14	2.40E+09	4.75E+06	19.55	3.74	
PIC0622-1.8	#02	27/10/14	8:23:42	0.0019781	0.0000003	3.69		0.13	2.40E+09	4.75E+06	19.55	3.74	
	#02			average		3.66							
				std dev (1σ)		0.49							
PIC0621V-1.1	#02	27/10/14	9:36:33	0.0019845	0.0000003	7.02		0.14	2.08E+09	4.13E+06	11.30	1.06	HM 1
PIC0621V-1.2	#02	27/10/14	9:42:07	0.0019829	0.0000002	6.18		0.12	2.19E+09	4.35E+06	11.30	1.06	
PIC0621V-1.3	#02	27/10/14	9:47:40	0.0019836	0.0000002	6.55		0.10	2.24E+09	4.45E+06	11.30	1.06	
PIC0621V-1.4	#02	27/10/14	9:53:14	0.0019783	0.0000002	3.83		0.10	2.46E+09	4.87E+06	11.30	1.06	
	#02			average		5.90							
				std dev (1σ)		1.42							
PIC0602-1.1	#02	27/10/14	10:33:47	0.0019650	0.0000003	-3.05		0.14	2.35E+09	4.62E+06	1.47	0.49	HM 1
PIC0602-1.2	#02	27/10/14	10:39:37	0.0019671	0.0000003	-1.95		0.13	2.46E+09	4.84E+06	1.47	0.49	
PIC0602-1.3	#02	27/10/14	10:45:25	0.0019576	0.0000003	-6.86		0.17	2.04E+09	4.00E+06	1.47	0.49	
PIC0602-1.4	#02	27/10/14	10:51:14	0.0019603	0.0000003	-5.48		0.13	2.23E+09	4.38E+06	1.47	0.49	
PIC0602-1.5	#02	27/10/14	10:57:02	0.0019633	0.0000003	-3.94		0.14	2.29E+09	4.50E+06	1.47	0.49	
PIC0602-1.6	#02	27/10/14	11:02:53	0.0019577	0.0000002	-6.85		0.10	2.15E+09	4.22E+06	1.47	0.49	
PIC0602-1.8	#02	27/10/14	11:14:32	0.0019664	0.0000002	-2.34		0.12	2.47E+09	4.86E+06	1.47	0.49	
	#02			average		-4.35							
				std dev (1σ)		2.06							
PIC0624-1.1	#02	27/10/14	11:20:25	0.0019712	0.0000002	0.14		0.11	2.34E+09	4.62E+06	14.43	6.63	HM 1
PIC0624-1.2	#02	27/10/14	11:26:13	0.0019742	0.0000002	1.71		0.11	2.44E+09	4.82E+06	14.43	6.63	
PIC0624-1.3	#02	27/10/14	11:32:02	0.0019713	0.0000002	0.19		0.11	2.47E+09	4.88E+06	14.43	6.63	
PIC0624-1.4	#02	27/10/14	12:34:32	0.0019716	0.0000003	0.37		0.13	2.42E+09	4.77E+06	14.43	6.63	
PIC0624-1.5	#02	27/10/14	12:40:20	0.0019695	0.0000002	-0.72		0.12	2.38E+09	4.68E+06	14.43	6.63	
	#02			average		0.34							
				std dev (1σ)		0.88							
PIC0604_1.1	#02	28/10/14	12:00:02	0.0019757	0.0000003	3.08		0.13	2.51E+09	4.95E+06	34.24	8.82	HM 4
PIC0604_1.2	#02	28/10/14	12:05:38	0.0019755	0.0000003	2.97		0.15	2.54E+09	5.02E+06	34.24	8.82	
PIC0604_1.3	#02	28/10/14	12:11:14	0.0019755	0.0000003	2.98		0.13	2.57E+09	5.08E+06	34.24	8.82	
PIC0604_1.4	#02	28/10/14	12:16:48	0.0019761	0.0000002	3.28		0.11	2.56E+09	5.05E+06	34.24	8.82	
PIC0604_1.5	#02	28/10/14	12:22:22	0.0019741	0.0000003	2.27		0.13	2.59E+09	5.11E+06	34.24	8.82	
PIC0604_1.6	#02	28/10/14	12:27:56	0.0019769	0.0000002	3.72		0.10	2.54E+09	5.03E+06	34.24	8.82	
	#02			average		3.05							
				std dev (1σ)		0.47							
PIC0604_1.7	#02	28/10/14	12:33:32	0.0019751	0.0000002	2.76		0.10	2.49E+09	4.93E+06	34.24	8.82	HM 4
PIC0604_1.8	#02	28/10/14	12:39:05	0.0019747	0.0000003	2.58		0.13	2.51E+09	4.96E+06	34.24	8.82	
PIC0604_1.9	#02	28/10/14	12:44:39	0.0019744	0.0000002	2.43		0.10	2.49E+09	4.92E+06	34.24	8.82	
PIC0604_1.10	#02	28/10/14	12:50:13	0.0019753	0.0000002	2.90		0.12	2.48E+09	4.90E+06	34.24	8.82	
PIC0604_1.11	#02	28/10/14	12:55:46	0.0019731	0.0000003	1.72		0.13	2.53E+09	4.99E+06	34.24	8.82	
PIC0604_1.12	#02	28/10/14	13:01:20	0.0019745	0.0000002	2.45		0.12	2.53E+09	5.00E+06	34.24	8.82	
	#02			average		2.47							
				std dev (1σ)		0.41							
Pic-06-24_1.1	#03	18/12/14	16:27:59	0.0019735	0.0000002	4.83		0.10	2.52E+09	4.98E+06	14.43	6.63	HM 4
Pic-06-24_1.2	#03	18/12/14	16:34:18	0.0019765	0.0000002	6.42		0.09	2.60E+09	5.13E+06	14.43	6.63	
Pic-06-24_1.3	#03	18/12/14	16:40:22	0.0019786	0.0000003	7.47		0.15	2.59E+09	5.13E+06	14.43	6.63	
Pic-06-24_1.4	#03	18/12/14	16:46:24	0.0019747	0.0000002	5.46		0.11	2.54E+09	5.01E+06	14.43	6.63	
Pic-06-24_1.5	#03	18/12/14	16:52:26	0.0019751	0.0000002	5.68		0.10	2.55E+09	5.04E+06	14.43	6.63	
Pic-06-24_1.6	#03	18/12/14	16:58:28	0.0019745	0.0000003	5.34		0.13	2.55E+09	5.04E+06	14.43	6.63	
	#03			average		5.87							
				std dev (1σ)		0.94							
Pic-06-02-1.1	#05	5/08/15	12:31:32	0.0019726	0.0000005		-7.27	0.26	1.56E+09	3.07E+06	1.47	0.49	HM 14
Pic-06-02-1.2	#05	5/08/15	12:37:52	0.0019798	0.0000005	-3.58		0.26	1.74E+09	3.45E+06	1.47	0.49	
Pic-06-02-1.3	#05	5/08/15	12:43:52	0.0019816	0.0000004	-2.66		0.21	1.75E+09	3.48E+06	1.47	0.49	
Pic-06-02-1.4	#05	5/08/15	12:49:53	0.0019784	0.0000005	-4.31		0.23	1.73E+09	3.43E+06	1.47	0.49	
Pic-06-02-1.5	#05	5/08/15	13:36:05	0.0019752	0.0000004	-4.76		0.22	2.12E+09	4.19E+06	1.47	0.49	
Pic-06-02-1.6	#05	5/08/15	13:42:54	0.0019787	0.0000004	-2.98		0.18	2.27E+09	4.49E+06	1.47	0.49	
Pic-06-02-1.7	#05	5/08/15	13:49:39	0.0019774	0.0000004	-3.64		0.21	2.22E+09	4.39E+06	1.47	0.49	
Pic-06-02-1.8	#05	5/08/15	13:56:30	0.0019762	0.0000004	-4.27		0.21	2.26E+09	4.46E+06	1.47	0.49	
Pic-06-02-1.9	#05	5/08/15	14:03:35	0.0019771	0.0000003	-3.81		0.17	2.22E+09	4.39E+06	1.47	0.49	
Pic-06-02-1.10	#05	5/08/15	14:10:19	0.0019753	0.0000004	-4.75		0.18	2.29E+09	4.53E+06	1.47	0.49	
Pic-06-02-1.11	#05	5/08/15	14:17:18	0.0019769	0.0000005	-3.93		0.27	2.27E+09	4.49E+06	1.47	0.49	
Pic-06-02-1.12	#05	5/08/15	14:23:59	0.0019774	0.0000004	-3.64		0.22	2.25E				

SPOT #	Session	Date	Time	¹⁸ O/ ¹⁶ O ^(a)	± ^(b)	δ ¹⁸ O _{VERMOR} ^(c)	rejected	±Internal error (σ 95%)	¹⁸ O cps (median)	¹⁶ O cps (median)	(U-Th)/He ages	±	MOUNT
Pic-06-04-1.8band3	#05	5/08/15	16:30:27	0.0019942	0.0000004	4.14		0.19	2.42E+09	4.82E+06	31.23	2.53	HM 14
Pic-06-04-1.9band3	#05	5/08/15	16:43:29	0.0019944	0.0000003	4.25		0.17	2.41E+09	4.81E+06	31.23	2.53	
Pic-06-04-1.10band3	#05	5/08/15	16:52:03	0.0019945	0.0000003	4.30		0.16	2.40E+09	4.79E+06	31.23	2.53	
Pic-06-04-1.11band3	#05	5/08/15	17:00:15	0.0019941	0.0000003	4.11		0.17	2.42E+09	4.82E+06	31.23	2.53	
Pic-06-04-1.12band3	#05	6/08/15	2:47:27	0.0019946	0.0000004	4.38		0.21	2.51E+09	5.00E+06	31.23	2.53	
Pic-06-04-1.13band3	#05	6/08/15	2:53:14	0.0019948	0.0000003	4.49		0.17	2.52E+09	5.03E+06	31.23	2.53	
	#05			average		4.28							
				std dev (1σ)		0.14							
Pic-06-04-1.14band4	#05	5/08/15	17:22:11	0.0019924	0.0000003	3.26		0.15	2.41E+09	4.80E+06	31.23	2.53	
Pic-06-04-1.15band4	#05	5/08/15	17:28:38	0.0019926	0.0000004	3.36		0.21	2.39E+09	4.76E+06	31.23	2.53	
Pic-06-04-1.16band4	#05	6/08/15	11:00:20	0.0019930	0.0000004	3.56		0.20	2.47E+09	4.92E+06	31.23	2.53	
	#05			average		3.40							
				std dev (1σ)		0.15							
Pic-06-08_9-1.1	#05	5/08/15	17:47:06	0.0019873	0.0000005	0.62		0.23	2.33E+09	4.63E+06	4.11	1.44	HM 14
Pic-06-08_9-1.2	#05	5/08/15	17:53:05	0.0019871	0.0000003	0.54		0.18	2.33E+09	4.63E+06	4.11	1.44	
Pic-06-08_9-1.3	#05	5/08/15	17:59:05	0.0019886	0.0000005	1.27		0.25	2.30E+09	4.58E+06	4.11	1.44	
Pic-06-08_9-1.5	#05	5/08/15	18:13:25	0.0019898	0.0000004	1.92		0.19	2.26E+09	4.49E+06	4.11	1.44	
Pic-06-08_9-1.6	#05	5/08/15	18:20:55	0.0019889	0.0000003	1.46		0.17	2.30E+09	4.57E+06	4.11	1.44	
Pic-06-08_9-1.4b	#05	6/08/15	11:16:46	0.0019901	0.0000004	2.07		0.19	2.40E+09	4.77E+06	4.11	1.44	
	#05			average		1.31							
				std dev (1σ)		0.64							
Pic-06-02(YOG)-1.1	#05	5/08/15	18:55:07	0.0019770	0.0000004	-4.63		0.20	2.17E+09	4.29E+06	1.47	0.49	HM 14
Pic-06-02(YOG)-1.2	#05	5/08/15	19:01:10	0.0019779	0.0000004	-4.17		0.22	2.22E+09	4.40E+06	1.47	0.49	
Pic-06-02(YOG)-1.3	#05	5/08/15	19:07:01	0.0019809	0.0000003	-2.64		0.17	2.18E+09	4.32E+06	1.47	0.49	
	#05			average		-2.70							
				std dev (1σ)		2.39							
Pic-06-21_6-2.4_A1 poor	#05	5/08/15	20:02:48	0.0019906	0.0000003	2.33		0.18	2.30E+09	4.57E+06	27.05	5.76	HM 14
Pic-06-21_6-2.2b_A1 poor	#05	5/08/15	20:11:06	0.0019902	0.0000004	2.12		0.20	2.30E+09	4.57E+06	27.05	5.76	
Pic-06-21_6-2.3b_A1 poor	#05	6/08/15	2:41:37	0.0019904	0.0000004	2.20		0.22	2.46E+09	4.90E+06	27.05	5.76	
	#05			average		2.22							
				std dev (1σ)		0.10							
Pic-06-21_6-2.5	#05	5/08/15	20:32:24	0.0019945	0.0000003	4.31		0.14	2.57E+09	5.12E+06	11.30	1.06	HM 14
Pic-06-21_6-2.6	#05	5/08/15	20:39:53	0.0019971	0.0000004	5.64		0.22	2.61E+09	5.21E+06	11.30	1.06	
Pic-06-21_6-2.7	#05	5/08/15	20:47:23	0.0019969	0.0000003	5.52		0.17	2.60E+09	5.20E+06	11.30	1.06	
	#05			average		5.16							
				std dev (1σ)		0.74							
Pic-06-21_6-3.1	#05	6/08/15	9:47:35	0.0019950	0.0000004	4.56		0.19	2.55E+09	5.09E+06	31.28	7.67	HM 14
Pic-06-21_6-3.2	#05	6/08/15	9:53:38	0.0019950	0.0000004	4.57		0.21	2.55E+09	5.08E+06	31.28	7.67	
Pic-06-21_6-3.3	#05	6/08/15	9:59:42	0.0019950	0.0000004	4.58		0.19	2.54E+09	5.07E+06	31.28	7.67	
	#05			average		4.57							
				std dev (1σ)		0.01							
Pic-06-01B_3-1.1	#05	5/08/15	21:15:59	0.0019903	0.0000003	2.18		0.17	2.59E+09	5.16E+06	2.63	0.21	HM 14
Pic-06-01B_3-1.2	#05	5/08/15	21:23:18	0.0019923	0.0000003	3.21		0.16	2.59E+09	5.16E+06	2.63	0.21	
Pic-06-01B_3-1.3	#05	5/08/15	21:29:57	0.0019936	0.0000003	3.83		0.14	2.58E+09	5.13E+06	2.63	0.21	
	#05			average		3.07							
				std dev (1σ)		0.83							
Pic-06-01B_3-1.4	#05	5/08/15	21:37:20	0.0019870	0.0000005	0.47		0.23	2.43E+09	4.82E+06	2.63	0.21	HM 14
Pic-06-01B_3-1.5	#05	5/08/15	21:44:11	0.0019872	0.0000004	0.56		0.22	2.40E+09	4.77E+06	2.63	0.21	
Pic-06-01B_3-1.6b	#05	6/08/15	11:58:00	0.0019889	0.0000003	1.46		0.17	2.41E+09	4.80E+06	2.63	0.21	
	#05			average		0.83							
				std dev (1σ)		0.55							
Pic-06-03_6(YG)-1.1	#05	5/08/15	22:11:30	0.0019909	0.0000004	2.45		0.21	2.42E+09	4.82E+06	7.39	0.74	HM 14
Pic-06-03_6(YG)-1.2	#05	5/08/15	22:17:17	0.0019925	0.0000003	3.28		0.16	2.44E+09	4.86E+06	7.39	0.74	
Pic-06-03_6(YG)-1.3	#05	5/08/15	22:23:05	0.0019890	0.0000005	1.47		0.25	2.28E+09	4.53E+06	7.39	0.74	
	#05			average		2.40							
				std dev (1σ)		0.90							
Pic-06-07_5-2.1	#05	5/08/15	22:34:41	0.0019924	0.0000003	3.22		0.17	2.55E+09	5.09E+06	1.77	1.20	HM 14
Pic-06-07_5-2.2	#05	5/08/15	22:40:29	0.0019915	0.0000004	2.78		0.19	2.54E+09	5.07E+06	1.77	1.20	
Pic-06-07_5-2.3	#05	5/08/15	22:46:16	0.0019914	0.0000003	2.75		0.14	2.54E+09	5.05E+06	1.77	1.20	
	#05			average		2.91							
				std dev (1σ)		0.26							
Pic-06-05B_2-1.1	#05	6/08/15	0:04:00	0.0019902	0.0000003	2.10		0.16	2.45E+09	4.88E+06	25.66	2.57	HM 14
Pic-06-05B_2-1.2	#05	6/08/15	0:09:47	0.0019922	0.0000003	3.12		0.16	2.48E+09	4.94E+06	25.66	2.57	
Pic-06-05B_2-1.3	#05	6/08/15	0:15:35	0.0019909	0.0000004	2.46		0.18	2.45E+09	4.88E+06	25.66	2.57	
Pic-06-05B_2-1.5	#05	6/08/15	0:27:10	0.0019891	0.0000003	1.56		0.16	2.51E+09	4.99E+06	25.66	2.57	
	#05			average		2.31							
				std dev (1σ)		0.65							
G-12-04-1.1	#05	6/08/15	0:33:01	0.0019955	0.0000004	4.83		0.20	2.46E+09	4.90E+06	21.40	2.22	HM 14
G-12-04-1.2	#05	6/08/15	0:39:03	0.0019971	0.0000003	5.65		0.16	2.52E+09	5.03E+06	21.40	2.22	
G-12-04-1.3	#05	6/08/15	0:44:51	0.0019967	0.0000002	5.43		0.12	2.50E+09	4.99E+06	21.40	2.22	
	#05			average		5.30							
				std dev (1σ)		0.42							
G-12-04-2.1	#05	6/08/15	0:50:53	0.0019889	0.0000003	1.45		0.17	2.25E+09	4.46E+06	9.54	1.98	HM 14
G-12-04-2.2	#05	6/08/15	0:56:41	0.0019896	0.0000004	1.83		0.19	2.28E+09	4.54E+06	9.54	1.98	
G-12-04-2.3	#05	6/08/15	1:02:28	0.0019902	0.0000005	2.14		0.23	2.32E+09	4.61E+06	9.54	1.98	
	#05			average		1.81							
				std dev (1σ)		0.35							
Pic-06-01A_3-1.1	#05	6/08/15	1:20:00	0.0019895	0.0000003	1.74		0.17	2.44E+09	4.85E+06	2.92	0.29	HM 14
Pic-06-01A_3-1.2	#05	6/08/15	1:25:47	0.0019901	0.0000004	2.05		0.20	2.46E+09	4.89E+06	2.92	0.29	
Pic-06-01A_3-1.3b	#05	6/08/15	10:36:47	0.0019839	0.0000004	-1.13		0.20	2.42E+09	4.80E+06	2.92	0.29	
	#05			average		0.89							
				std dev (1σ)		1.75							
G-12-11-1.1	#05	6/08/15	1:37:27	0.0019910	0.0000004	2.52		0.21	2.44E+09	4.87E+06	35.40	4.70	HM 14
G-12-11-1.2	#05	6/08/15	1:43:14	0.0019922	0.0000004	3.13		0.20	2.47E+09	4.93E+06	35.40	4.70	

SPOT #	Session	Date	Time	¹⁸ O/ ¹⁶ O ^(a)	± ^(b)	δ ¹⁸ O _{VSMOW} ^(c)	rejected	±Internal error (σ 95%)	¹⁶ O cps (median)	¹⁸ O cps (median)	(U-Th)/He ages	±	MOUNT
G-12-11-1.3	#05	6/08/15	1:49:02	0.0019901	0.0000005	2.05		0.24	2.45E+09	4.87E+06	35.40	4.70	
G-12-11-1.4	#05	6/08/15	1:54:49	0.0019896	0.0000003	1.78		0.16	2.41E+09	4.80E+06	35.40	4.70	
G-12-11-1.5	#05	6/08/15	2:00:37	0.0019902	0.0000003	2.10		0.15	2.44E+09	4.85E+06	35.40	4.70	
	#05				average std dev (1σ)	2.32 0.53							
G-12-05-2.2	#05	6/08/15	3:39:36	0.0019931	0.0000003	3.58		0.15	2.56E+09	5.10E+06	1.27	0.61	HM 14
G-12-05-2.3	#05	6/08/15	3:45:24	0.0019926	0.0000004	3.32		0.19	2.53E+09	5.04E+06	1.27	0.61	
	#05				average std dev (1σ)	3.45 0.19							
Pic-06-01C_6-1.1	#05	6/08/15	6:25:31	0.0019875	0.0000004	0.72		0.18	2.51E+09	4.99E+06	4.90	2.54	HM 14
Pic-06-01C_6-1.2	#05	6/08/15	6:31:48	0.0019878	0.0000004	0.90		0.21	2.47E+09	4.90E+06	4.90	2.54	
	#05				average std dev (1σ)	0.81 0.13							
Pic-06-25A-1.1	#05	6/08/15	6:46:51	0.0019973	0.0000004	5.75		0.19	2.56E+09	5.11E+06	8.52	1.19	HM 14
Pic-06-25A-1.2	#05	6/08/15	6:53:23	0.0019975	0.0000003	5.85		0.15	2.56E+09	5.12E+06	8.52	1.19	
Pic-06-25A-1.3	#05	6/08/15	6:59:47	0.0019957	0.0000004	4.93		0.22	2.53E+09	5.05E+06	8.52	1.19	
Pic-06-25A-1.4b	#05	6/08/15	11:08:22	0.0019963	0.0000004	5.24		0.19	2.50E+09	4.99E+06	8.52	1.19	
	#05				average std dev (1σ)	5.44 0.43							
Pic-06-25B-2.2	#05	6/08/15	7:20:00	0.0019965	0.0000003	5.36		0.17	2.56E+09	5.10E+06	9.42	4.14	HM 14
Pic-06-25B-2.3	#05	6/08/15	7:26:00	0.0019944	0.0000004	4.24		0.19	2.52E+09	5.02E+06	9.42	4.14	
Pic-06-25B-2.4	#05	6/08/15	7:32:15	0.0019960	0.0000003	5.06		0.17	2.49E+09	4.97E+06	9.42	4.14	
	#05				average std dev (1σ)	4.89 0.58							
Pic-06-03_6(BG)-1.1	#05	6/08/15	8:17:21	0.0019948	0.0000004	4.49		0.21	2.45E+09	4.89E+06	21.84	3.56	HM 14
Pic-06-03_6(BG)-1.2	#05	6/08/15	8:23:19	0.0019950	0.0000003	4.55		0.17	2.45E+09	4.88E+06	21.84	3.56	
Pic-06-03_6(BG)-1.3	#05	6/08/15	8:29:27	0.0019946	0.0000003	4.38		0.17	2.45E+09	4.88E+06	21.84	3.56	
	#05				average std dev (1σ)	4.47 0.09							
SC-12-06(A)-2.1	#05	6/08/15	8:50:58	0.0019804	0.0000004	-2.88		0.18	2.33E+09	4.62E+06	3.59	0.84	HM 14
SC-12-06(A)-2.2	#05	6/08/15	8:58:00	0.0019808	0.0000004	-2.72		0.20	2.43E+09	4.82E+06	3.59	0.84	
SC-12-06(A)-2.3	#05	6/08/15	9:04:42	0.0019810	0.0000004	-2.62		0.18	2.37E+09	4.69E+06	3.59	0.84	
	#05				average std dev (1σ)	-2.74 0.14							
Pic-06-22-2.1_BG	#05	6/08/15	11:23:38	0.0019965	0.0000004	5.35		0.18	2.49E+09	4.97E+06	19.55	3.74	HM 14
Pic-06-22-2.2_BG	#05	6/08/15	11:29:36	0.0019963	0.0000003	5.24		0.17	2.49E+09	4.98E+06	19.55	3.74	
	#05				average std dev (1σ)	5.29 0.07							
Pic-06-22-1.1_YG	#05	6/08/15	11:36:50	0.0019889	0.0000003	1.45		0.15	2.49E+09	4.95E+06	14.57	2.46	HM 14
Pic-06-22-1.2_YG	#05	6/08/15	11:42:44	0.0019892	0.0000003	1.59		0.17	2.50E+09	4.97E+06	14.57	2.46	
	#05				average std dev (1σ)	1.52 0.10							
Pic-06-05B_2-1.5b	#05	6/08/15	11:50:32	0.0019891	0.0000004	1.57		0.20	2.42E+09	4.81E+06	25.66	2.57	HM 14
Pic-06-05B_2-1.1b	#05	6/08/15	12:18:09	0.0019906	0.0000004	2.32		0.19	2.40E+09	4.77E+06	25.66	2.57	
Pic-06-05B_2-1.4b	#05	6/08/15	12:25:10	0.0019923	0.0000004	3.17		0.18	2.38E+09	4.75E+06	25.66	2.57	
Pic-06-05B_2-1.7	#05	6/08/15	12:33:47	0.0019890	0.0000004	1.52		0.20	2.39E+09	4.76E+06	25.66	2.57	
	#05				average std dev (1σ)	2.15 0.77							
G-12-06-MassGt-Red_1.1	#06	19/05/16	1:12:31	0.0020096	0.0000004	11.78		0.18	2.00E+09	4.02E+06	8.97	0.90	HM 18
G-12-06-MassGt-Red_1.2	#06	19/05/16	1:17:51	0.0020087	0.0000006	11.35		0.28	2.02E+09	4.05E+06	8.97	0.90	
G-12-06-MassGt-Red_1.3	#06	19/05/16	1:23:10	0.0020082	0.0000004	11.11		0.21	2.02E+09	4.06E+06	8.97	0.90	
G-12-06-MassGt-Red_1.4	#06	19/05/16	1:28:30	0.0020054	0.0000009		9.67	0.43	2.02E+09	4.05E+06	8.97	0.90	
G-12-06-MassGt-Red_1.5	#06	19/05/16	1:33:50	0.0020089	0.0000003	11.43		0.16	2.02E+09	4.05E+06	8.97	0.90	
G-12-06-MassGt-Red_1.6	#06	19/05/16	1:39:10	0.0020094	0.0000004	11.71		0.20	2.02E+09	4.05E+06	8.97	0.90	
G-12-06-MassGt-Red_1.4B	#06	23/05/16	1:51:58	0.0019962	0.0000004	12.19		0.18	2.41E+09	4.81E+06	8.97	0.90	
	#06				average std dev (1σ)	11.60 0.38							
G-12-06-MassGt-Black_1.1	#06	19/05/16	1:44:31	0.0020114	0.0000004	12.73		0.20	2.04E+09	4.11E+06	7.87	0.04	HM 18
G-12-06-MassGt-Black_1.2	#06	19/05/16	1:49:51	0.0020026	0.0000006	8.22		0.28	1.95E+09	3.91E+06	7.87	0.04	
G-12-06-MassGt-Black_1.3	#06	19/05/16	2:05:56	0.0020135	0.0000005	13.80		0.23	2.02E+09	4.08E+06	7.87	0.04	
G-12-06-MassGt-Black_1.4	#06	19/05/16	2:11:15	0.0020092	0.0000003	11.62		0.17	2.00E+09	4.02E+06	7.87	0.04	
G-12-06-MassGt-Black_1.2B	#06	23/05/16	1:57:14	0.0019876	0.0000002	7.77		0.11	2.36E+09	4.70E+06	7.87	0.04	
	#06				average std dev (1σ)	10.83 2.70							
G-12-06-MassGt-Black_1.5	#06	19/05/16	2:16:35	0.0020192	0.0000005	16.71		0.23	2.02E+09	4.08E+06	7.87	0.04	HM 18
G-12-06-MassGt-Black_1.6	#06	19/05/16	2:21:55	0.0020168	0.0000004	15.47		0.19	2.02E+09	4.07E+06	7.87	0.04	
G-12-06-MassGt-Black_1.7	#06	19/05/16	2:27:14	0.0020177	0.0000004	15.95		0.18	2.02E+09	4.08E+06	7.87	0.04	
	#06				average std dev (1σ)	16.04 0.63							
G-12-06-MassGt-Black_2.1	#06	19/05/16	2:32:34	0.0020055	0.0000004		9.69	0.21	1.98E+09	3.96E+06	7.87	0.04	HM 18
G-12-06-MassGt-Black_2.2	#06	19/05/16	2:37:53	0.0020088	0.0000004		11.42	0.21	2.01E+09	4.04E+06	7.87	0.04	
G-12-06-MassGt-Black_2.3	#06	19/05/16	2:43:12	0.0019992	0.0000005		6.46	0.24	1.91E+09	3.81E+06	7.87	0.04	
G-12-06-MassGt-Black_2.1B	#06	23/05/16	3:00:26	0.0019945	0.0000002	11.31		0.10	2.40E+09	4.79E+06	7.87	0.04	
G-12-06-MassGt-Black_2.2B	#06	23/05/16	3:05:39	0.0019934	0.0000002	10.77		0.10	2.38E+09	4.75E+06	7.87	0.04	
G-12-06-MassGt-Black_2.3B	#06	23/05/16	3:10:53	0.0019906	0.0000002	9.30		0.12	2.36E+09	4.70E+06	7.87	0.04	
	#06				average std dev (1σ)	10.46 1.04							
G-12-07a_1.1	#06	19/05/16	4:03:18	0.0019990	0.0000004	6.40		0.19	1.91E+09	3.82E+06	0.96	0.61	HM 18
G-12-07a_1.2	#06	19/05/16	4:08:38	0.0019986	0.0000005	6.17		0.26	1.91E+09	3.83E+06	0.96	0.61	
G-12-07a_1.3	#06	19/05/16	4:13:57	0.0019962	0.0000005	4.95		0.24	1.86E+09	3.72E+06	0.96	0.61	
G-12-07a_1.4	#06	19/05/16	4:19:16	0.0019980	0.0000004	5.85		0.21	1.84E+09	3.69E+06	0.96	0.61	
	#06				average std dev (1σ)	5.84 0.63							
G-12-07b-cement_1.1	#06	19/05/16	5:18:03	0.0019899	0.0000005		1.74	0.27	1.64E+09	3.27E+06	0.98	0.98	HM 18
G-12-07b-cement_1.2	#06	19/05/16	5:23:23	0.0019919	0.0000004	2.75		0.19	1.72E+09	3.43E+06	0.98	0.98	

SPOT #	Session	Date	Time	¹⁸ O/ ¹⁶ O ^(a)	± ^(b)	δ ¹⁸ O _{VSMOW} ^(c)	rejected	±Internal error (σ 95%)	¹⁸ O cps (median)	¹⁶ O cps (median)	(U-Th)/He ages	±	MOUNT
G-12-07b-cement_2.3	#06	19/05/16	5:39:22	0.0019924	0.0000005	2.99		0.27	1.76E+09	3.51E+06	0.98	0.98	
G-12-07b-cement_1.2B	#06	23/05/16	2:39:27	0.0019779	0.0000003	2.78		0.13	2.24E+09	4.43E+06	0.98	0.98	
G-12-07b-cement_1.1B	#06	23/05/16	2:44:41	0.0019794	0.0000002	3.52		0.12	2.18E+09	4.31E+06	0.98	0.98	
G-12-07b-cement_2.3B	#06	23/05/16	2:55:09	0.0019792	0.0000006	3.46		0.31	2.33E+09	4.60E+06	0.98	0.98	
	#06			average		3.10							
				std dev (1σ)		0.37							
G-12-07c_1.1	#06	19/05/16	5:44:44	0.0019903	0.0000004	1.90		0.20	1.69E+09	3.36E+06	27.83	5.54	HM 18
G-12-07c_2.1	#06	19/05/16	5:50:04	0.0019914	0.0000005	2.47		0.24	1.69E+09	3.36E+06	27.83	5.54	
G-12-07c_2.2	#06	19/05/16	5:55:24	0.0019922	0.0000005	2.91		0.27	1.67E+09	3.34E+06	27.83	5.54	
G-12-07c_2.3	#06	19/05/16	6:00:43	0.0019912	0.0000004	2.38		0.19	1.69E+09	3.36E+06	27.83	5.54	
G-12-07c_2.4	#06	19/05/16	6:06:02	0.0019915	0.0000005	2.56		0.23	1.69E+09	3.36E+06	27.83	5.54	
G-12-07c_1.2	#06	19/05/16	6:11:23	0.0019910	0.0000005	2.29		0.24	1.68E+09	3.35E+06	27.83	5.54	
	#06			average		2.42							
				std dev (1σ)		0.33							
SC-12-01-dark_1.1	#06	19/05/16	6:27:26	0.0019925	0.0000005	3.07		0.24	1.64E+09	3.27E+06	29.31	1.61	HM 18
SC-12-01-dark_1.2	#06	19/05/16	6:32:45	0.0019920	0.0000005	2.77		0.23	1.64E+09	3.26E+06	29.31	1.61	
SC-12-01-dark_1.3	#06	19/05/16	6:38:05	0.0019913	0.0000005	2.44		0.27	1.64E+09	3.27E+06	29.31	1.61	
SC-12-01-dark_1.1	#06	19/05/16	8:08:07	0.0019914	0.0000003	2.72		0.16	2.05E+09	4.09E+06	29.31	1.61	
SC-12-01-dark_1.2	#06	19/05/16	8:13:26	0.0019926	0.0000005	3.32		0.28	2.07E+09	4.12E+06	29.31	1.61	
SC-12-01-dark_1.3	#06	19/05/16	8:18:45	0.0019919	0.0000004	2.97		0.18	2.06E+09	4.10E+06	29.31	1.61	
	#06			average		2.88							
				std dev (1σ)		0.31							
Sc-12-20(A)_1.1	#06	19/05/16	6:43:27	0.0019931	0.0000004	3.34		0.22	1.63E+09	3.24E+06	22.94	5.15	HM 18
Sc-12-20(A)_1.1	#06	19/05/16	8:24:08	0.0019923	0.0000003	3.20		0.17	2.06E+09	4.11E+06	22.94	5.15	
Sc-12-20(A)_1.3	#06	19/05/16	8:29:48	0.0019922	0.0000004	3.12		0.20	2.07E+09	4.12E+06	22.94	5.15	
Sc-12-20(A)_1.4	#06	19/05/16	8:35:07	0.0019928	0.0000004	3.43		0.21	2.07E+09	4.12E+06	22.94	5.15	
Sc-12-20(A)_1.5	#06	23/05/16	5:53:58	0.0019799	0.0000002	3.78		0.13	2.21E+09	4.38E+06	22.94	5.15	
Sc-12-20(A)_1.6	#06	23/05/16	5:59:13	0.0019787	0.0000004	3.18		0.21	2.23E+09	4.40E+06	22.94	5.15	
Sc-12-20(A)_1.7	#06	23/05/16	6:04:27	0.0019797	0.0000003	3.69		0.13	2.18E+09	4.32E+06	22.94	5.15	
	#06			average		3.39							
				std dev (1σ)		0.26							
Sc-12-20(A)_2.1	#06	19/05/16	8:40:28	0.0019908	0.0000003	2.40		0.17	2.10E+09	4.17E+06	22.94	5.15	HM 18
Sc-12-20(A)_2.2	#06	19/05/16	8:45:48	0.0019895	0.0000004	1.76		0.18	2.12E+09	4.21E+06	22.94	5.15	
Sc-12-20(A)_2.3	#06	19/05/16	8:51:08	0.0019907	0.0000003	2.36		0.16	2.11E+09	4.20E+06	22.94	5.15	
Sc-12-20(A)_2.4	#06	19/05/16	8:56:27	0.0019881	0.0000006		1.05	0.28	2.11E+09	4.19E+06	22.94	5.15	
SC-12-20(A)_2.4B	#06	23/05/16	5:38:15	0.0019770	0.0000003	2.29		0.16	2.28E+09	4.50E+06	22.94	5.15	
SC-12-20(A)_2.5	#06	23/05/16	5:43:29	0.0019760	0.0000002	1.80		0.12	2.22E+09	4.39E+06	22.94	5.15	
SC-12-20(A)_2.7	#06	23/05/16	5:48:44	0.0019779	0.0000003	2.75		0.14	2.24E+09	4.43E+06	22.94	5.15	
SC-12-20(A)_2.6B	#06	23/05/16	11:33:05	0.0019776	0.0000002	2.61		0.12	2.28E+09	4.50E+06	22.94	5.15	
	#06			average		2.28							
				std dev (1σ)		0.38							
SM-13-01_1.1	#06	22/05/16	17:03:11	0.0019857	0.0000003	6.81		0.14	2.19E+09	4.36E+06	30.10	0.36	HM 18
SM-13-01_1.2	#06	22/05/16	17:08:25	0.0019857	0.0000002	6.77		0.12	2.19E+09	4.34E+06	30.10	0.36	
SM-13-01_1.3	#06	22/05/16	17:45:19	0.0019842	0.0000003		6.00	0.16	2.21E+09	4.39E+06	30.10	0.36	
SM-13-01_1.4	#06	22/05/16	17:50:33	0.0019901	0.0000002	9.04		0.11	2.28E+09	4.54E+06	30.10	0.36	
SM-13-01_1.5	#06	22/05/16	17:55:47	0.0019889	0.0000003	8.44		0.13	2.26E+09	4.50E+06	30.10	0.36	
SM-13-01_1.6	#06	22/05/16	18:01:01	0.0019878	0.0000002	7.87		0.12	2.26E+09	4.49E+06	30.10	0.36	
SM-13-01_1.3B	#06	22/05/16	19:51:12	0.0019849	0.0000002	6.40		0.12	2.22E+09	4.40E+06	30.10	0.36	
	#06			average		7.56							
				std dev (1σ)		1.06							
SC-12-05_1.1	#06	22/05/16	18:06:20	0.0019802	0.0000003	3.97		0.15	2.18E+09	4.31E+06	28.23	4.13	HM 18
SC-12-05_1.2	#06	22/05/16	18:11:33	0.0019820	0.0000002	4.87		0.11	2.17E+09	4.31E+06	28.23	4.13	
SC-12-05_1.3	#06	22/05/16	18:16:47	0.0019800	0.0000002	3.83		0.12	2.17E+09	4.29E+06	28.23	4.13	
SC-12-05_1.4	#06	22/05/16	18:22:01	0.0019796	0.0000004	3.62		0.19	2.17E+09	4.29E+06	28.23	4.13	
SC-12-05_1.5	#06	22/05/16	18:27:14	0.0019797	0.0000002	3.70		0.12	2.18E+09	4.32E+06	28.23	4.13	
SC-12-05_1.2B	#06	22/05/16	19:37:29	0.0019818	0.0000002	4.77		0.12	2.19E+09	4.34E+06	28.23	4.13	
	#06			average		4.13							
				std dev (1σ)		0.55							
SM-13-07_1.1	#06	22/05/16	20:23:59	0.0019795	0.0000003	3.58		0.14	2.14E+09	4.23E+06	27.48	2.21	HM 18
SM-13-07_1.2	#06	22/05/16	20:29:13	0.0019800	0.0000002	3.83		0.11	2.12E+09	4.21E+06	27.48	2.21	
SM-13-07_1.3	#06	22/05/16	20:34:26	0.0019805	0.0000003	4.11		0.13	2.14E+09	4.24E+06	27.48	2.21	
SM-13-07_1.4	#06	22/05/16	20:39:40	0.0019790	0.0000003	3.33		0.17	2.18E+09	4.31E+06	27.48	2.21	
SM-13-07_1.5	#06	22/05/16	21:21:54	0.0019799	0.0000003	3.80		0.14	2.17E+09	4.29E+06	27.48	2.21	
SM-13-07_1.6	#06	22/05/16	21:27:08	0.0019801	0.0000002	3.89		0.12	2.14E+09	4.24E+06	27.48	2.21	
SM-13-07_1.7	#06	22/05/16	21:32:22	0.0019776	0.0000003	2.59		0.14	2.21E+09	4.36E+06	27.48	2.21	
SM-13-07_1.8	#06	22/05/16	21:37:36	0.0019789	0.0000003	3.27		0.13	2.20E+09	4.35E+06	27.48	2.21	
SM-13-07_1.9	#06	22/05/16	21:42:50	0.0019781	0.0000003	2.89		0.15	2.15E+09	4.26E+06	27.48	2.21	
SM-13-07_1.10	#06	22/05/16	21:48:05	0.0019779	0.0000002	2.76		0.12	2.18E+09	4.31E+06	27.48	2.21	
	#06			average		3.41							
				std dev (1σ)		0.52							
G-12-10_1.1	#06	22/05/16	21:53:23	0.0019787	0.0000002	3.19		0.10	2.14E+09	4.23E+06	19.43	1.08	HM 18
G-12-10_1.3	#06	22/05/16	22:03:50	0.0019781	0.0000003	2.90		0.14	2.15E+09	4.26E+06	19.43	1.08	
G-12-10_1.2B	#06	22/05/16	23:19:03	0.0019788	0.0000003	3.24		0.13	2.16E+09	4.27E+06	19.43	1.08	
G-12-10_1.4B	#06	22/05/16	23:25:00	0.0019773	0.0000003	2.44		0.16	2.17E+09	4.28E+06	19.43	1.08	
	#06			average		2.94							
				std dev (1σ)		0.37							
G-12-08_1.1	#06	23/05/16	3:16:12	0.0019979	0.0000002	13.10		0.12	2.43E+09	4.86E+06	15.78	0.67	HM 18
G-12-08_1.2	#06	23/05/16	3:21:25	0.0019975	0.0000002	12.90		0.10	2.43E+09	4.84E+06	15.78	0.67	
G-12-08_1.3	#06	23/05/16	3:26:39	0.0019976	0.0000003	12.95		0.15	2.46E+09	4.91E+06	15.78	0.67	
	#06			average		12.98							
				std dev (1σ)		0.11							
G-12-08_2.1	#06	23/05/16	4:08:54	0.0019867	0.0000003	7.29		0.13	2.32E+09	4.61E+06	15.78	0.67	HM 18
G-12-08_2.2	#06	23/05/16	4:14:08	0.0019865	0.0000003	7.20		0.15	2.35E+09	4.67E+06	15.78	0.67	
G-12-08_2.3	#06	23/05/16	4:19:21	0.0019898	0.0000002	8.91		0.10	2.36E+09	4.69E+06	15.78	0.67	
G-12-08_2.4	#06	23/05/16	4:24:35	0.0019927	0.0000002	10.42		0.11	2.42E+09	4.81E+06	15.78	0.67	
G-12-08_2.5	#06	23/05/16	4:29:49	0.0019962	0.0000002	12.18		0.11	2.44E+09	4.88E+06	15.78	0.67	
G-12-08_2.6	#06	23/05/16	4:35:02	0.0019957	0.0000002	11.97		0.12	2.45E+09	4.88E+06	15.78	0.67	
G-12-08_2.3B	#06	23/05/16	12:30:34	0.0019900	0.0000002	9.02		0.12	2.41E+09	4.81E+06	15.78	0.67	
G-12-08_2.4B	#06	23/05/16	12:35:48	0.0019973	0.0000002	12.77		0.09	2.48E+09	4.94E+06	15.78	0.67	
G-12-08_2.1B	#06	23/05/16	13:18:33	0.0019873	0.0								

SPOT #	Session	Date	Time	¹⁸ O/ ¹⁶ O ^(a)	± ^(b)	δ ¹⁸ O _{VSMOW} ^(c)	rejected	±Internal error (σ 95%)	¹⁸ O cps (median)	¹⁶ O cps (median)	(U-Th)/He ages	±	MOUNT
SC-12-04(B)_1.1	#06	23/05/16	4:40:19	0.0019807	0.0000003	4.22		0.17	2.19E+09	4.33E+06	32.56	7.57	HM 18
SC-12-04(B)_1.2	#06	23/05/16	4:45:32	0.0019819	0.0000002	4.81		0.11	2.16E+09	4.27E+06	32.56	7.57	
SC-12-04(B)_1.3	#06	23/05/16	4:50:46	0.0019820	0.0000002	4.87		0.11	2.19E+09	4.34E+06	32.56	7.57	
SC-12-04(B)_1.4	#06	23/05/16	4:56:00	0.0019811	0.0000002	4.39		0.12	2.18E+09	4.33E+06	32.56	7.57	
	#06				average std dev (1σ)	4.57 0.32							
SC-12-20(A)_3.1	#06	23/05/16	6:09:41	0.0019862	0.0000002	7.06		0.11	2.31E+09	4.59E+06	22.94	5.15	HM 18
SC-12-20(A)_3.3	#06	23/05/16	6:14:57	0.0019862	0.0000002	7.03		0.11	2.36E+09	4.68E+06	22.94	5.15	
SC-12-20(A)_3.4	#06	23/05/16	6:20:12	0.0019822	0.0000003	5.00		0.14	2.33E+09	4.61E+06	22.94	5.15	
SC-12-20(A)_3.5	#06	23/05/16	6:25:26	0.0019827	0.0000002	5.26		0.11	2.30E+09	4.56E+06	22.94	5.15	
	#06				average std dev (1σ)	6.09 1.11							
SC-12-16(B)-Br&Bl_1.1	#06	23/05/16	7:13:00	0.0019834	0.0000003	5.62		0.13	2.34E+09	4.63E+06	39.74	0.15	HM 18
SC-12-16(B)-Br&Bl_2.2	#06	23/05/16	7:23:28	0.0019825	0.0000003	5.14		0.15	2.36E+09	4.69E+06	39.74	0.15	
SC-12-16(B)-Br&Bl_3.1	#06	23/05/16	7:28:42	0.0019833	0.0000002	5.57		0.12	2.34E+09	4.65E+06	39.74	0.15	
SC-12-16(B)-Br&Bl_4.1	#06	23/05/16	7:39:10	0.0019815	0.0000002	4.64		0.12	2.35E+09	4.66E+06	39.74	0.15	
SC-12-16(B)-Br&Bl_4.2	#06	23/05/16	7:44:24	0.0019813	0.0000003	4.52		0.14	2.41E+09	4.77E+06	39.74	0.15	
SC-12-16(B)-Br&Bl_5.1	#06	23/05/16	8:16:12	0.0019785	0.0000002	3.06		0.11	2.37E+09	4.69E+06	39.74	0.15	
SC-12-16(B)-Br&Bl_5.2	#06	23/05/16	8:21:26	0.0019801	0.0000004	3.90		0.20	2.35E+09	4.64E+06	39.74	0.15	
SC-12-16(B)-Br&Bl_2.1B	#06	23/05/16	12:14:43	0.0019781	0.0000003	2.89		0.14	2.38E+09	4.72E+06	39.74	0.15	
SC-12-16(B)-Br&Bl_3.2B	#06	23/05/16	12:19:58	0.0019799	0.0000003	3.78		0.15	2.32E+09	4.59E+06	39.74	0.15	
	#06				average std dev (1σ)	4.35 1.01							
SC-12-01-dark_2.1	#06	23/05/16	8:26:41	0.0019834	0.0000002	5.63		0.11	2.31E+09	4.58E+06	29.31	1.61	HM 18
SC-12-01-dark_2.2	#06	23/05/16	8:31:55	0.0019826	0.0000002	5.19		0.10	2.29E+09	4.54E+06	29.31	1.61	
SC-12-01-dark_2.3	#06	23/05/16	8:37:09	0.0019829	0.0000002	5.35		0.11	2.30E+09	4.57E+06	29.31	1.61	
SC-12-01-dark_2.4	#06	23/05/16	8:42:23	0.0019800	0.0000002	3.85		0.11	2.32E+09	4.60E+06	29.31	1.61	
	#06				average std dev (1σ)	5.01 0.79							
SC-1201-brown_1.1	#06	23/05/16	8:47:40	0.0019788	0.0000002	3.25		0.11	2.33E+09	4.60E+06	29.31	1.61	HM 18
SC-1201-brown_1.2	#06	23/05/16	8:52:53	0.0019795	0.0000002	3.61		0.12	2.27E+09	4.49E+06	29.31	1.61	
SC-1201-brown_1.3	#06	23/05/16	8:58:07	0.0019785	0.0000003	3.07		0.17	2.29E+09	4.53E+06	29.31	1.61	
SC-1201-brown_1.4B	#06	23/05/16	12:25:16	0.0019796	0.0000002	3.66		0.10	2.29E+09	4.53E+06	29.31	1.61	
	#06				average std dev (1σ)	3.40 0.29							
SC-12-07-1.1	#06	23/05/16	13:32:22	0.0019977	0.0000003	12.98		0.13	2.52E+09	5.03E+06	23.16	2.32	HM 18
SC-12-07B_1.2	#06	23/05/16	13:38:10	0.0019953	0.0000002	11.73		0.12	2.48E+09	4.95E+06	23.16	2.32	
SC-12-07B_1.3	#06	23/05/16	13:54:51	0.0019932	0.0000002	10.67		0.11	2.44E+09	4.87E+06	23.16	2.32	
SC-12-07B_1.1B	#06	23/05/16	14:06:30	0.0019958	0.0000002	12.00		0.12	2.46E+09	4.91E+06	23.16	2.32	
	#06				average std dev (1σ)	11.85 0.95							
Pic-21-6-Bl-duilIGt_1.1	#06	23/05/16	21:32:24	0.0019828	0.0000002	6.91		0.12	2.49E+09	4.94E+06	31.28	7.67	HM 19
Pic-21-6-Bl-duilIGt_1.2	#06	23/05/16	21:37:43	0.0019840	0.0000002	7.51		0.12	2.49E+09	4.94E+06	31.28	7.67	
Pic-21-6-Bl-duilIGt_1.3	#06	23/05/16	21:43:03	0.0019838	0.0000002	7.44		0.10	2.49E+09	4.93E+06	31.28	7.67	
Pic-21-6-Bl-duilIGt_1.4	#06	23/05/16	21:48:22	0.0019832	0.0000002	7.10		0.10	2.48E+09	4.92E+06	31.28	7.67	
Pic-21-6-Bl-duilIGt_1.5B	#06	24/05/16	0:52:24	0.0019820	0.0000003	6.52		0.15	2.48E+09	4.91E+06	31.28	7.67	
	#06				average std dev (1σ)	7.10 0.40							
Pic-21-6-Vt-Gt_1.2	#06	23/05/16	22:04:26	0.0019894	0.0000002	10.31		0.11	2.57E+09	5.11E+06	11.30	1.06	HM 19
Pic-21-6-Vt-Gt_1.3	#06	23/05/16	22:09:46	0.0019887	0.0000003	9.97		0.13	2.51E+09	4.99E+06	11.30	1.06	
Pic-21-6-Vt-Gt_1.4	#06	23/05/16	22:15:05	0.0019880	0.0000002	9.61		0.10	2.50E+09	4.98E+06	11.30	1.06	
	#06				average std dev (1σ)	9.96 0.35							
Pic-21-6-Vt-Gt_1.5	#06	23/05/16	22:20:25	0.0019774	0.0000002	4.10		0.10	2.44E+09	4.82E+06	11.30	1.06	HM 19
Pic-21-6-Vt-Gt_1.6	#06	23/05/16	22:36:34	0.0019784	0.0000003	4.63		0.14	2.38E+09	4.71E+06	11.30	1.06	
Pic-21-6-Vt-Gt_1.7	#06	23/05/16	22:41:54	0.0019778	0.0000003	4.35		0.15	2.43E+09	4.81E+06	11.30	1.06	
	#06				average std dev (1σ)	4.36 0.27							
SC-12-21(B)_1.1	#06	24/05/16	3:21:38	0.0019967	0.0000002	14.10		0.12	2.61E+09	5.20E+06	10.58	1.51	HM 19
SC-12-21(B)_1.3	#06	24/05/16	3:32:19	0.0019971	0.0000002	14.32		0.10	2.59E+09	5.17E+06	10.58	1.51	
SC-12-21(B)_1.4	#06	24/05/16	4:26:02	0.0019963	0.0000002	13.89		0.10	2.61E+09	5.21E+06	10.58	1.51	
SC-12-21(B)_1.5	#06	24/05/16	4:31:34	0.0019971	0.0000003	14.32		0.14	2.57E+09	5.14E+06	10.58	1.51	
SC-12-21(B)_1.6	#06	24/05/16	4:36:54	0.0019975	0.0000002	14.52		0.11	2.52E+09	5.03E+06	10.58	1.51	
	#06				average std dev (1σ)	14.23 0.24							
SC-12-21(D)_1.2	#06	24/05/16	4:47:40	0.0019967	0.0000003	14.11		0.13	2.59E+09	5.16E+06	15.65	1.49	HM 19
SC-12-21(D)_1.3	#06	24/05/16	4:53:00	0.0019963	0.0000002	13.87		0.12	2.58E+09	5.16E+06	15.65	1.49	
SC-12-21(D)_2.1	#06	24/05/16	4:58:22	0.0019857	0.0000002	8.42		0.12	2.53E+09	5.03E+06	15.65	1.49	
SC-12-21(D)_3.1	#06	24/05/16	5:03:42	0.0019875	0.0000002	9.33		0.12	2.51E+09	4.98E+06	15.65	1.49	
SC-12-21(D)_4.1	#06	24/05/16	5:09:02	0.0019862	0.0000002	8.67		0.11	2.52E+09	5.01E+06	15.65	1.49	
	#06				average std dev (1σ)	10.88 2.86							
SC-12-22(B)_1.1	#06	24/05/16	5:57:40	0.0020009	0.0000002	16.25		0.11	2.59E+09	5.18E+06	4.41	1.40	HM 19
SC-12-22(B)_1.2	#06	24/05/16	6:03:04	0.0019995	0.0000002	15.52		0.10	2.58E+09	5.16E+06	4.41	1.40	
SC-12-22(B)_1.3	#06	24/05/16	6:08:25	0.0019952	0.0000002	13.31		0.11	2.59E+09	5.16E+06	4.41	1.40	
SC-12-22(B)_1.4	#06	24/05/16	6:13:46	0.0019920	0.0000006	11.64		0.31	2.60E+09	5.18E+06	4.41	1.40	
	#06				average std dev (1σ)	14.18 2.10							
Pic-21-6-ALpoor_1.1	#06	24/05/16	6:19:09	0.0019732	0.0000002	1.94		0.11	2.29E+09	4.53E+06	27.05	5.76	HM 19
Pic-21-6-ALpoor_1.2	#06	24/05/16	6:24:29	0.0019725	0.0000002	1.62		0.13	2.28E+09	4.50E+06	27.05	5.76	
Pic-21-6-ALpoor_1.3	#06	24/05/16	6:29:51	0.0019708	0.0000002	0.73		0.10	2.26E+09	4.46E+06	27.05	5.76	
	#06				average std dev (1σ)	1.43 0.62							
Pic-21-6-ALpoor_2.1	#06	24/05/16	6:51:17	0.0019758	0.0000002	3.32		0.12	2.30E+09	4.55E+06	27.05	5.76	HM 19
Pic-21-6-ALpoor_2.2	#06	24/05/16	6:56:38	0.0019764	0.0000003	3.61		0.16	2.28E+09	4.50E+06	27.05	5.76	
	#06				average std dev (1σ)	3.46 0.21							

SPOT #	Session	Date	Time	$^{18}\text{O}/^{16}\text{O}^{(a)}$	$\pm^{(b)}$	$\delta^{18}\text{O}_{\text{VSMOW}}^{(c)}$	rejected	\pm Internal error (α 95%)	^{18}O cps (median)	^{16}O cps (median)	(U-Th)/He ages	\pm	MOUNT
G-12-11-1.5b	#07	3/12/16	11:37:53	0.0019909	0.0000003	6.01		0.16	2.41E+09	4.80E+06	35.40	4.70	HM 21
G-12-11-1.6b	#07	3/12/16	11:44:51	0.0019906	0.0000003	5.82		0.15	2.40E+09	4.78E+06	35.40	4.70	
G-12-11-1.4b	#07	3/12/16	11:52:12	0.0019931	0.0000004	7.12		0.18	2.42E+09	4.82E+06	35.40	4.70	
G-12-11-1.9b	#07	3/12/16	11:58:33	0.0019919	0.0000003	6.49		0.16	2.46E+09	4.89E+06	35.40	4.70	
G-12-11-1.8b	#07	3/12/16	12:08:16	0.0019926	0.0000003	6.88		0.15	2.45E+09	4.89E+06	35.40	4.70	
G-12-11-1.7b	#07	3/12/16	12:15:21	0.0019885	0.0000003	4.76		0.17	2.40E+09	4.78E+06	35.40	4.70	
G-12-11-1.1c	#07	3/12/16	12:23:31	0.0019893	0.0000003	5.18		0.15	2.44E+09	4.85E+06	35.40	4.70	
G-12-11-1.4c	#07	3/12/16	12:31:15	0.0019890	0.0000003	5.03		0.18	2.40E+09	4.78E+06	35.40	4.70	
	#07				average	5.91							
					std dev (1 σ)	0.88							
SC-12-22(B)-1.1	#07	3/12/16	14:04:03	0.0020013	0.0000003	11.35		0.13	2.58E+09	5.17E+06	4.41	1.40	HM 21
SC-12-22(B)-1.2	#07	3/12/16	14:10:02	0.0019997	0.0000003	10.54		0.14	2.60E+09	5.20E+06	4.41	1.40	
	#07				average	10.95							
					std dev (1 σ)	0.57							
SC-12-22(B)-1.4	#07	3/12/16	14:44:21	0.0019936	0.0000002	7.36		0.09	2.52E+09	5.03E+06	4.41	1.40	HM 21
SC-12-22(B)-1.5	#07	3/12/16	14:53:16	0.0019921	0.0000003	6.59		0.14	2.54E+09	5.05E+06	4.41	1.40	
SC-12-22(B)-1.6	#07	3/12/16	14:59:25	0.0019943	0.0000003	7.73		0.16	2.54E+09	5.07E+06	4.41	1.40	
	#07				average	7.23							
					std dev (1 σ)	0.58							
Pic-06-04-1.1	#07	3/12/16	15:27:18	0.0019889	0.0000003	4.98		0.13	2.40E+09	4.78E+06	31.23	2.53	HM 21
Pic-06-04-1.2	#07	3/12/16	15:33:24	0.0019863	0.0000003		3.65	0.16	2.40E+09	4.77E+06	31.23	2.53	
Pic-06-04-1.3	#07	3/12/16	15:39:26	0.0019894	0.0000003	5.21		0.15	2.43E+09	4.84E+06	31.23	2.53	
Pic-06-04-1.4	#07	3/12/16	15:45:28	0.0019892	0.0000004	5.10		0.18	2.47E+09	4.91E+06	31.23	2.53	
	#07				average	5.10							
					std dev (1 σ)	0.11							
Pic-06-04-1.5	#07	3/12/16	15:51:28	0.0019924	0.0000003		6.76	0.14	2.50E+09	4.98E+06	31.23	2.53	HM 21
Pic-06-04-1.6	#07	3/12/16	15:57:29	0.0019906	0.0000002	5.84		0.10	2.50E+09	4.98E+06	31.23	2.53	
Pic-06-04-1.7	#07	3/12/16	16:03:29	0.0019909	0.0000003	5.97		0.13	2.50E+09	4.99E+06	31.23	2.53	
Pic-06-04-1.8	#07	3/12/16	16:09:34	0.0019921	0.0000002	6.61		0.11	2.50E+09	4.97E+06	31.23	2.53	
	#07				average	6.14							
					std dev (1 σ)	0.41							

(a) Raw $^{18}\text{O}/^{16}\text{O}$, corrected for background but not instrumental mass fractionation.

(b) Within spot (internal) precision, 95% conf.

(c) $\delta^{18}\text{O}$ (permil) = $((^{18}\text{O}/^{16}\text{O}_{\text{corrected}})/(^{18}\text{O}/^{16}\text{O}_{\text{reference}})-1)*1000$, where $^{18}\text{O}/^{16}\text{O}_{\text{corrected}}$ is the background, and IMF corrected $^{18}\text{O}/^{16}\text{O}$ ratio, and $(^{18}\text{O}/^{16}\text{O})_{\text{reference}}$ is the reference value of the chosen goethite reference material. Rejected analyses are in italics.